

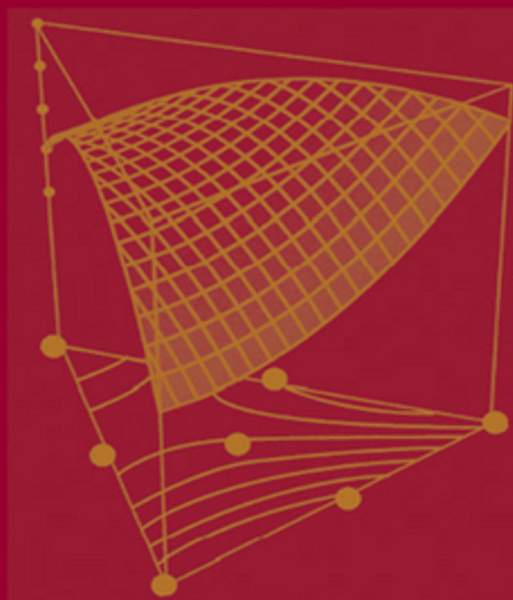
WILEY SERIES IN PROBABILITY AND STATISTICS

# RESPONSE SURFACE METHODOLOGY

---

**Process and Product Optimization  
Using Designed Experiments**

THIRD EDITION



RAYMOND H. MYERS  
DOUGLAS C. MONTGOMERY  
CHRISTINE M. ANDERSON-COOK

 WILEY



# **RESPONSE SURFACE METHODOLOGY**

WILEY SERIES IN PROBABILITY AND STATISTICS

Established by WALTER A. SHEWHART and SAMUEL S. WILKS

Editors: *David J. Balding, Noel A. C. Cressie, Garrett M. Fitzmaurice, Iain M. Johnstone, Geert Molenberghs, David W. Scott, Adrian F. M. Smith, Ruey S. Tsay, Sanford Weisberg*  
Editors Emeriti: *Vic Barnett, J. Stuart Hunter, Jozef L. Teugels*

A complete list of the titles in this series appears at the end of this volume.

# **RESPONSE SURFACE METHODOLOGY**

---

## **Process and Product Optimization Using Designed Experiments**

Third Edition

**RAYMOND H. MYERS**

Virginia Polytechnic University, Department of Statistics, Blacksburg, VA

**DOUGLAS C. MONTGOMERY**

Arizona State University, Department of Industrial Engineering, Tempe, AZ

**CHRISTINE M. ANDERSON-COOK**

Los Alamos National Laboratory, Los Alamos, NM



A JOHN WILEY & SONS, INC., PUBLICATION

Copyright © 2009 by John Wiley & Sons, Inc. All rights reserved

Published by John Wiley & Sons, Inc., Hoboken, New Jersey  
Published simultaneously in Canada

No part of this publication may be reproduced, stored in a retrieval system, or transmitted in any form or by any means, electronic, mechanical, photocopying, recording, scanning, or otherwise, except as permitted under Sections 107 or 108 of the 1976 United States Copyright Act, without either the prior written permission of the Publisher, or authorization through payment of the appropriate per-copy fee to the Copyright Clearance Center, Inc., 222 Rosewood Drive, Danvers, MA 01923, (978) 750-8400, fax (978) 750-4470, or on the web at [www.copyright.com](http://www.copyright.com). Requests to the Publisher for permission should be addressed to the Permissions Department, John Wiley & Sons, Inc., 111 River Street, Hoboken, NJ 07030, (201) 748-6011, fax (201) 748-6008, or online at <http://www.wiley.com/go/permission>.

**Limit of Liability/Disclaimer of Warranty:** While the publisher and author have used their best efforts in preparing this book, they make no representations or warranties with respect to the accuracy or completeness of the contents of this book and specifically disclaim any implied warranties of merchantability or fitness for a particular purpose. No warranty may be created or extended by sales representatives or written sales materials. The advice and strategies contained herein may not be suitable for your situation. You should consult with a professional where appropriate. Neither the publisher nor author shall be liable for any loss of profit or any other commercial damages, including but not limited to special, incidental, consequential, or other damages.

For general information on our other products and services or for technical support, please contact our Customer Care Department within the United States at (800) 762-2974, outside the United States at (317) 572-3993 or fax (317) 572-4002.

Wiley also publishes its books in variety of electronic formats. Some content that appears in print may not be available in electronic format. For more information about Wiley products, visit our web site at [www.wiley.com](http://www.wiley.com).

***Library of Congress Cataloging-in-Publication Data:***

Myers, Raymond H.

Response surface methodology : process and product optimization using designed experiments.

-- 3rd ed. / Raymond H. Myers, Douglas C. Montgomery, Christine M. Anderson-Cook.

p. cm. -- (Wiley series in probability and statistics)

Includes bibliographical references and index.

ISBN 978-0-470-17446-3 (cloth)

1. Experimental design. 2. Response surfaces (Statistics). I. Montgomery, Douglas C.

II. Anderson-Cook, Christine M. III. Title.

QA279.M94 2008

519.5'7 - dc22

2008019012

Printed in the United States of America

10 9 8 7 6 5 4 3 2 1

# CONTENTS

Preface	xi
<b>1 Introduction</b>	<b>1</b>
1.1 Response Surface Methodology, 1	
1.1.1 Approximating Response Functions, 2	
1.1.2 The Sequential Nature of RSM, 6	
1.1.3 Objectives and Typical Applications of RSM, 8	
1.1.4 RSM and the Philosophy of Quality Improvement, 9	
1.2 Product Design and Formulation (Mixture Problems), 10	
1.3 Robust Design and Process Robustness Studies, 10	
1.4 Useful References on RSM, 11	
<b>2 Building Empirical Models</b>	<b>13</b>
2.1 Linear Regression Models, 13	
2.2 Estimation of the Parameters in Linear Regression Models, 14	
2.3 Properties of the Least Squares Estimators and Estimation of $\sigma^2$ , 22	
2.4 Hypothesis Testing in Multiple Regression, 24	
2.4.1 Test for Significance of Regression, 24	
2.4.2 Tests on Individual Regression Coefficients and Groups of Coefficients, 27	
2.5 Confidence Intervals in Multiple Regression, 31	
2.5.1 Confidence Intervals on the Individual Regression Coefficients $\beta$ , 32	
2.5.2 A Joint Confidence Region on the Regression Coefficients $\beta$ , 32	
2.5.3 Confidence Interval on the Mean Response, 33	
2.6 Prediction of New Response Observations, 35	
2.7 Model Adequacy Checking, 36	

2.7.1	Residual Analysis, 37	
2.7.2	Scaling Residuals, 38	
2.7.3	Influence Diagnostics, 42	
2.7.4	Testing for Lack of Fit, 44	
2.8	Fitting a Second-Order Model, 47	
2.9	Qualitative Regressor Variables, 55	
2.10	Transformation of the Response Variable, 58	
	Exercises, 63	
<b>3</b>	<b>Two-Level Factorial Designs</b>	<b>73</b>
3.1	Introduction, 73	
3.2	The $2^2$ Design, 74	
3.3	The $2^3$ Design, 86	
3.4	The General $2^k$ Design, 96	
3.5	A Single Replicate of the $2^k$ Design, 96	
3.6	The Addition of Center Points to the $2^k$ Design, 109	
3.7	Blocking in the $2^k$ Factorial Design, 114	
3.7.1	Blocking in the Replicated Design, 115	
3.7.2	Confounding in the $2^k$ Design, 116	
3.8	Split-Plot Designs, 121	
	Exercises, 124	
<b>4</b>	<b>Two-Level Fractional Factorial Designs</b>	<b>135</b>
4.1	Introduction, 135	
4.2	The One-Half Fraction of the $2^k$ Design, 136	
4.3	The One-Quarter Fraction of the $2^k$ Design, 148	
4.4	The General $2^{k-p}$ Fractional Factorial Design, 154	
4.5	Resolution III Designs, 158	
4.6	Resolution IV and V Designs, 167	
4.7	Fractional Factorial Split-Plot Designs, 168	
4.8	Summary, 172	
	Exercises, 173	
<b>5</b>	<b>Process Improvement with Steepest Ascent</b>	<b>181</b>
5.1	Determining the Path of Steepest Ascent, 182	
5.1.1	Development of the Procedure, 182	
5.1.2	Practical Application of the Method of Steepest Ascent, 184	
5.2	Consideration of Interaction and Curvature, 189	
5.2.1	What About a Second Phase?, 191	
5.2.2	What Happens Following Steepest Ascent?, 192	
5.3	Effect of Scale (Choosing Range of Factors), 193	
5.4	Confidence Region for Direction of Steepest Ascent, 195	
5.5	Steepest Ascent Subject to a Linear Constraint, 198	
5.6	Steepest Ascent in a Split-Plot Experiment, 202	
	Exercises, 210	

<b>6 The Analysis of Second-Order Response Surfaces</b>	<b>219</b>
6.1 Second-Order Response Surface,	219
6.2 Second-Order Approximating Function,	220
6.2.1 The Nature of the Second-Order Function and Second-Order Surface,	220
6.2.2 Illustration of Second-Order Response Surfaces,	222
6.3 A Formal Analytical Approach to the Second-Order Model,	223
6.3.1 Location of the Stationary Point,	223
6.3.2 Nature of the Stationary Point (Canonical Analysis),	224
6.3.3 Ridge Systems,	228
6.3.4 Role of Contour Plots,	232
6.4 Ridge Analysis of the Response Surface,	235
6.4.1 What is the Value of Ridge Analysis?,	236
6.4.2 Mathematical Development of Ridge Analysis,	237
6.5 Sampling Properties of Response Surface Results,	242
6.5.1 Standard Error of Predicted Response,	243
6.5.2 Confidence Region on the Location of the Stationary Point,	245
6.5.3 Use and Computation of the Confidence Region on the Location of the Stationary Point,	246
6.5.4 Confidence Intervals on Eigenvalues in Canonical Analysis,	250
6.6 Multiple Response Optimization,	253
6.7 Further Comments Concerning Response Surface Analysis,	264
Exercises,	265
<b>7 Experimental Designs for Fitting Response Surfaces—I</b>	<b>281</b>
7.1 Desirable Properties of Response Surface Designs,	281
7.2 Operability Region, Region of Interest, and Model Inadequacy,	282
7.2.1 Model Inadequacy and Model Bias,	283
7.3 Design of Experiments for First-Order Models,	285
7.3.1 The First-Order Orthogonal Design,	286
7.3.2 Orthogonal Designs for Models Containing Interaction,	288
7.3.3 Other First-Order Orthogonal Designs—The Simplex Design,	291
7.3.4 Another Variance Property—Prediction Variance,	294
7.4 Designs for Fitting Second-Order Models,	296
7.4.1 The Class of Central Composite Designs,	297
7.4.2 Design Moments and Property of Rotatability,	302
7.4.3 Rotatability and the CCD,	306
7.4.4 More on Prediction Variance—Scaled, Unscaled, and Estimated,	310
7.4.5 The Cuboidal Region and the Face-Centered Cube,	312
7.4.6 When is the Design Region Spherical?,	315
7.4.7 Summary Statements Regarding CCD,	316
7.4.8 The Box–Behnken Design,	317
7.4.9 Other Spherical RSM Designs; Equiradial Designs,	321
7.4.10 Orthogonal Blocking in Second-Order Designs,	325
Exercises,	336

<b>8 Experimental Designs for Fitting Response Surfaces—II</b>	<b>349</b>
8.1 Designs that Require a Relatively Small Run Size, 350	
8.1.1 The Hoke Designs, 350	
8.1.2 Koshal Design, 352	
8.1.3 Hybrid Designs, 354	
8.1.4 The Small Composite Design, 358	
8.1.5 Some Saturated or Near-Saturated Cuboidal Designs, 362	
8.2 General Criteria for Constructing, Evaluating, and Comparing Experimental Designs, 362	
8.2.1 Practical Design Optimality, 365	
8.2.2 Use of Design Efficiencies for Comparison of Standard Second-Order Designs, 371	
8.2.3 Graphical Procedure for Evaluating the Prediction Capability of an RSM Design, 374	
8.3 Computer-Generated Designs in RSM, 386	
8.3.1 Important Relationship between Prediction Variance and Design Augmentation for <i>D</i> -Optimality, 386	
8.3.2 Illustrations Involving Computer-Generated Design, 390	
8.4 Some Final Comments Concerning Design Optimality and Computer-Generated Design, 405	
Exercises, 406	
<b>9 Advanced Topics in Response Surface Methodology</b>	<b>417</b>
9.1 Effects of Model Bias on the Fitted Model and Design, 417	
9.2 A Design Criterion Involving Bias and Variance, 420	
9.2.1 The Case of a First-Order Fitted Model and Cuboidal Region, 423	
9.2.2 Minimum Bias Designs for a Spherical Region of Interest, 429	
9.2.3 Simultaneous Consideration of Bias and Variance, 430	
9.2.4 How Important is Bias?, 431	
9.3 Errors in Control of Design Levels, 432	
9.4 Experiments with Computer Models, 435	
9.5 Minimum Bias Estimation of Response Surface Models, 442	
9.6 Neural Networks, 446	
9.7 RSM for Non-Normal Responses—Generalized Linear Models, 449	
9.7.1 Model Framework: The Link Function, 449	
9.7.2 The Canonical Link Function, 450	
9.7.3 Estimation of Model Coefficients, 451	
9.7.4 Properties of Model Coefficients, 452	
9.7.5 Model Deviance, 453	
9.7.6 Overdispersion, 454	
9.7.7 Examples, 455	
9.7.8 Diagnostic Plots and Other Aspects of the GLM, 462	
9.8 Split-Plot Designs for Second-Order Models, 466	
Exercises, 476	

<b>10 Robust Parameter Design and Process Robustness Studies</b>	<b>483</b>
10.1 Introduction, 483	
10.2 What is Parameter Design?, 483	
10.2.1 Examples of Noise Variables, 484	
10.2.2 An Example of Robust Product Design, 485	
10.3 The Taguchi Approach, 486	
10.3.1 Crossed Array Designs and Signal-to-Noise Ratios, 486	
10.3.2 Analysis Methods, 489	
10.3.3 Further Comments, 494	
10.4 The Response Surface Approach, 495	
10.4.1 The Role of the Control $\times$ Noise Interaction, 495	
10.4.2 A Model Containing Both Control and Noise Variables, 499	
10.4.3 Generalization of Mean and Variance Modeling, 502	
10.4.4 Analysis Procedures Associated with the Two Response Surfaces, 506	
10.4.5 Estimation of the Process Variance, 515	
10.4.6 Direct Variance Modeling, 519	
10.4.7 Use of Generalized Linear Models, 521	
10.5 Experimental Designs for RPD and Process Robustness Studies, 525	
10.5.1 Combined Array Designs, 525	
10.5.2 Second-Order Designs, 527	
10.5.3 Other Aspects of Design, 529	
10.6 Dispersion Effects in Highly Fractionated Designs, 537	
10.6.1 The Use of Residuals, 537	
10.6.2 Further Diagnostic Information from Residuals, 538	
10.6.3 Further Comments Concerning Variance Modeling, 544	
Exercises, 548	
<b>11 Experiments with Mixtures</b>	<b>557</b>
11.1 Introduction, 557	
11.2 Simplex Designs and Canonical Mixture Polynomials, 560	
11.2.1 Simplex Lattice Designs, 560	
11.2.2 The Simplex-Centroid Design and Its Associated Polynomial, 567	
11.2.3 Augmentation of Simplex Designs with Axial Runs, 569	
11.3 Response Trace Plots, 576	
11.4 Reparameterizing Canonical Mixture Models to Contain a Constant Term ( $\beta_0$ ), 577	
Exercises, 581	
<b>12 Other Mixture Design and Analysis Techniques</b>	<b>589</b>
12.1 Constraints on the Component Proportions, 589	
12.1.1 Lower-Bound Constraints on the Component Proportions, 590	
12.1.2 Upper-Bound Constraints on the Component Proportions, 599	

12.1.3	Active Upper- and Lower-Bound Constraints,	602
12.1.4	Multicomponent Constraints,	616
12.2	Mixture Experiments Using Ratios of Components,	617
12.3	Process Variables in Mixture Experiments,	621
12.3.1	Mixture-Process Model and Design Basics,	621
12.3.2	Split-Plot Designs for Mixture-Process Experiments,	629
12.3.3	Robust Parameter Designs for Mixture-Process Experiments,	636
12.4	Screening Mixture Components,	641
	Exercises,	643
<b>Appendix 1</b>	<b>Moment Matrix of a Rotatable Design</b>	<b>655</b>
<b>Appendix 2</b>	<b>Rotatability of a Second-Order Equiradial Design</b>	<b>661</b>
<b>References</b>		<b>665</b>
<b>Index</b>		<b>677</b>

# PREFACE

This book deals with the exploration and optimization of response surfaces. This is a problem faced by experimenters in many technical fields, where, in general, the response variable of interest is  $y$  and there is a set of predictor variables  $x_1, x_2, \dots, x_k$ . For example,  $y$  might be the viscosity of a polymer and  $x_1, x_2$ , and  $x_3$  might be the reaction time, the reactor temperature, and the catalyst feed rate in the process. In some systems the nature of the relationship between  $y$  and the  $x$ 's might be known “exactly,” based on the underlying engineering, chemical, or physical principles. Then we could write a model of the form  $y = g(x_1, x_2, \dots, x_k) + \varepsilon$ , where  $\varepsilon$  represents the “error” in the system. This type of relationship is often called a **mechanistic model**. We consider the more common situation where the underlying mechanism is not fully understood, and the experimenter must approximate the unknown function  $g$  with an appropriate **empirical model**  $y = f(x_1, x_2, \dots, x_k) + \varepsilon$ . Usually the function  $f$  is a first-order or second-order polynomial. This empirical model is called a **response surface model**.

Identifying and fitting an appropriate response surface model from experimental data requires some knowledge of statistical experimental design fundamentals, regression modeling techniques, and elementary optimization methods. This book integrates all three of these topics into what has been popularly called **response surface methodology (RSM)**.

We assume that the reader has some previous exposure to statistical methods and matrix algebra. Formal coursework in basic principles of experimental design and regression analysis would be helpful, but are not essential, because the important elements of these topics are presented early in the text. We have used this book in a graduate-level course on RSM for statisticians, engineers, and chemical/physical scientists. We have also used it in industrial short courses and seminars for individuals with a wide variety of technical backgrounds.

This third edition is a substantial revision of the book. We have rewritten many sections to incorporate new material, ideas, and examples, and to more fully explain some topics that were only briefly mentioned in previous editions. We have also woven the computer more

tightly into the presentation, relying on JMP 7 and Design-Expert Version 7 for much of the computing, but also continuing to employ SAS for a few applications.

Chapters 1 through 4 contain the preliminary material essential to studying RSM. Chapter 1 is an introduction to the general field of RSM, describing typical applications such as (a) finding the levels of process variables that optimize a response of interest or (b) discovering what levels of these process variables will result in a product satisfying certain requirements or specifications on responses such as yield, molecular weight, purity, or viscosity. Chapter 2 is a summary of regression methods useful in response surface work, focusing on the basic ideas of least squares model fitting, diagnostic checking, and inference for the linear regression model. Chapters 3 and 4 describe two-level factorial and fractional factorial designs. These designs are essential for factor screening or identifying the correct set of process variables to use in the RSM study. They are also basic building blocks for many of the response surface designs discussed later in the text. Chapter 5 presents the method of steepest ascent, a simple but powerful optimization procedure used at the early stages of RSM to move the process from a region of relatively poor performance to one of greater potential. Chapter 6 introduces the analysis and optimization of a second-order response surface model. Both graphical and numerical techniques are presented. This chapter also includes techniques for the simultaneous optimization of several responses, a common problem in the application of RSM. Chapters 7 and 8 present detailed information on the choice of experimental designs for fitting response surface models. Chapter 7 is devoted to standard designs, including the central composite and Box–Behnken designs, and the important topic of blocking a response surface design. Chapter 8 covers small response surface designs, design optimality criteria, the use of computer-generated designs in RSM, and methods for evaluation of the prediction properties of response surface models constructed from various designs. We focus on variance dispersion graphs and fraction of design space plots, which are very important ways to summarize prediction properties. Chapter 9 contains more advanced RSM topics, including the use of mean square error as a design criterion, the effect of errors in controllable variables, RSM experiments for computer models, neural networks and RSM, split-plot type designs in a response surface setting, and the use of generalized linear models in the analysis of response surface experiments. Chapter 10 describes how the problem of robust parameter design originally proposed by Taguchi can be efficiently solved in the RSM framework. We show how RSM not only makes the original problem posed by Taguchi easier to solve, but also provides much more information to the analyst about process or system performance. This chapter also contains much information on robust parameter design and process robustness studies. Chapters 11 and 12 present techniques for designing and analyzing experiments that involve mixtures. A mixture experiment is a special type of response surface experiment in which the design factors are the components or ingredients of a mixture, and the response depends on the proportions of the ingredients that are present. Extensive sets of end-of-chapter problems are provided, along with a reference section.

The previous two editions of the text were written to emphasize methods that are useful in industry and that we have found useful in our own consulting experience. We have continued that applied focus in this new edition, though much new material has been added. We develop enough of the underlying theory to allow the reader to gain an understanding of the assumptions and conditions necessary to successfully apply RSM.

We are grateful to many individuals that have contributed meaningfully to this book. In particular, Dr. Bradley Jones, Mr. Pat Whitcomb, Dr. Geoff Vining, Dr. Soren Bisgaard, Dr. Connie Borror, Dr. Scott Kowalski, Dr. Dennis Lin, Dr. George Runger,

and Dr. Enrique Del Castillo made many useful suggestions. Dr. Matt Carlyle and Dr. Enrique Del Castillo also provided some figures that were most helpful. We also thank the many classes of graduate students that have studied from the book and the instructors that have used the book. They have made many helpful comments and suggestions to improve the clarity of the presentation. We have tried to incorporate many of their suggestions. We also thank John Wiley & Sons for permission to use and adapt copyrighted material.

*Blacksburg, Virginia  
Tempe, Arizona  
Los Alamos, New Mexico  
March, 2008*

RAYMOND H. MYERS  
DOUGLAS C. MONTGOMERY  
CHRISTINE M. ANDERSON-COOK



---

# 1

---

## INTRODUCTION

### 1.1 RESPONSE SURFACE METHODOLOGY

Response surface methodology (RSM) is a collection of statistical and mathematical techniques useful for developing, improving, and optimizing processes. It also has important applications in the design, development, and formulation of new products, as well as in the improvement of existing product designs.

The most extensive applications of RSM are in the industrial world, particularly in situations where several input variables potentially influence some performance measure or quality characteristic of the product or process. This performance measure or quality characteristic is called the **response**. It is typically measured on a continuous scale, although attribute responses, ranks, and sensory responses are not unusual. Most real-world applications of RSM will involve more than one response. The input variables are sometimes called **independent variables**, and they are subject to the control of the engineer or scientist, at least for purposes of a test or an experiment.

Figure 1.1 shows graphically the relationship between the response variable yield ( $y$ ) in a chemical process and the two process variables (or independent variables) reaction time ( $\xi_1$ ) and reaction temperature ( $\xi_2$ ). Note that for each value of  $\xi_1$  and  $\xi_2$  there is a corresponding value of yield  $y$ , and that we may view these values of the response yield as a surface lying above the time–temperature plane, as in Fig. 1.1a. It is this graphical perspective of the problem environment that has led to the term **response surface methodology**. It is also convenient to view the response surface in the two-dimensional time–temperature plane, as in Fig. 1.1b. In this presentation we are looking down at the time–temperature plane and connecting all points that have the same yield to produce contour lines of constant response. This type of display is called a **contour plot**.

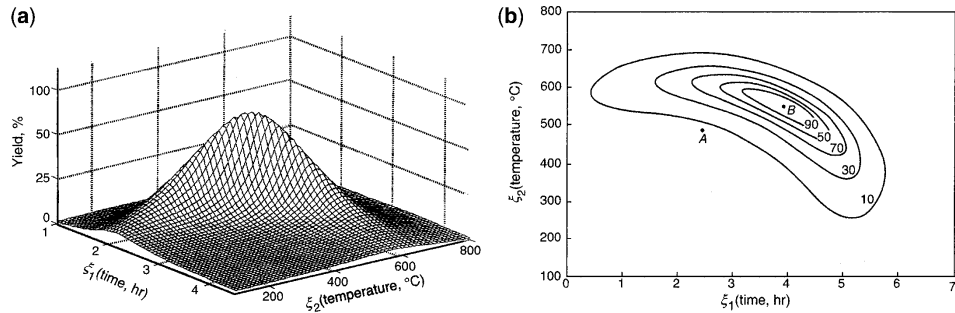


**Figure 1.1** (a) A theoretical response surface showing the relationship between yield of a chemical process and the process variables reaction time ( $\xi_1$ ) and reaction temperature ( $\xi_2$ ). (b) A contour plot of the theoretical response surface.

Clearly, if we could easily construct the graphical displays in Fig. 1.1, optimization of this process would be very straightforward. By inspection of the plot, we note that yield is maximized in the vicinity of time  $\xi_1 = 4$  hr and temperature  $\xi_2 = 525$  °C. Unfortunately, in most practical situations, the true response function in Fig. 1.1 is unknown. The field of response surface methodology consists of the experimental strategy for exploring the space of the process or independent variables (here the variables  $\xi_1$  and  $\xi_2$ ), empirical statistical modeling to develop an appropriate approximating relationship between the yield and the process variables, and optimization methods for finding the levels or values of the process variables  $\xi_1$  and  $\xi_2$  that produce desirable values of the responses (in this case that maximize yield).

### 1.1.1 Approximating Response Functions

In general, suppose that the scientist or engineer (whom we will refer to as the **experimenter**) is concerned with a product, process, or system involving a response  $y$  that depends on the controllable input variables  $\xi_1, \xi_2, \dots, \xi_k$ . The relationship is

$$y = f(\xi_1, \xi_2, \dots, \xi_k) + \varepsilon \quad (1.1)$$

where the form of the true response function  $f$  is unknown and perhaps very complicated, and  $\varepsilon$  is a term that represents other sources of variability not accounted for in  $f$ . Thus  $\varepsilon$  includes effects such as measurement error on the response, other sources of variation that are inherent in the process or system (background noise, or common/special cause variation in the language of statistical process control), the effect of other (possibly unknown) variables, and so on. We will treat  $\varepsilon$  as a **statistical error**, often assuming it to have a normal distribution with mean zero and variance  $\sigma^2$ . If the mean of  $\varepsilon$  is zero, then

$$\begin{aligned} E(y) &\equiv \eta = E[f(\xi_1, \xi_2, \dots, \xi_k)] + E(\varepsilon) \\ &= f(\xi_1, \xi_2, \dots, \xi_k) \end{aligned} \quad (1.2)$$

The variables  $\xi_1, \xi_2, \dots, \xi_k$  in Equation 1.2 are usually called the **natural variables**, because they are expressed in the natural units of measurement, such as degrees Celsius (°C), pounds per square inch (psi), or grams per liter for concentration. In much RSM work it is convenient to transform the natural variables to **coded variables**  $x_1, x_2, \dots, x_k$ ,

which are usually defined to be dimensionless with mean zero and the same spread or standard deviation. In terms of the coded variables, the true response function (1.2) is now written as

$$\eta = f(x_1, x_2, \dots, x_k) \quad (1.3)$$

Because the form of the true response function  $f$  is unknown, we must approximate it. In fact, successful use of RSM is critically dependent upon the experimenter's ability to develop a suitable approximation for  $f$ . Usually, a **low-order polynomial** in some relatively small region of the independent variable space is appropriate. In many cases, either a **first-order** or a **second-order** model is used. For the case of two independent variables, the first-order model in terms of the coded variables is

$$\eta = \beta_0 + \beta_1 x_1 + \beta_2 x_2 \quad (1.4)$$

Figure 1.2 shows the three-dimensional response surface and the two-dimensional contour plot for a particular case of the first-order model, namely,

$$\eta = 50 + 8x_1 + 3x_2$$

In three dimensions, the response surface is a plane lying above the  $x_1, x_2$  space. The contour plot shows that the first-order model can be represented as parallel straight lines of constant response in the  $x_1, x_2$  plane.

The first-order model is likely to be appropriate when the experimenter is interested in approximating the true response surface over a relatively small region of the independent variable space in a location where there is little curvature in  $f$ . For example, consider a small region around the point  $A$  in Fig. 1.1b; the first-order model would likely be appropriate here.

The form of the first-order model in Equation 1.4 is sometimes called a **main effects model**, because it includes only the main effects of the two variables  $x_1$  and  $x_2$ . If there is an **interaction** between these variables, it can be added to the model easily as follows:

$$\eta = \beta_0 + \beta_1 x_1 + \beta_2 x_2 + \beta_{12} x_1 x_2 \quad (1.5)$$

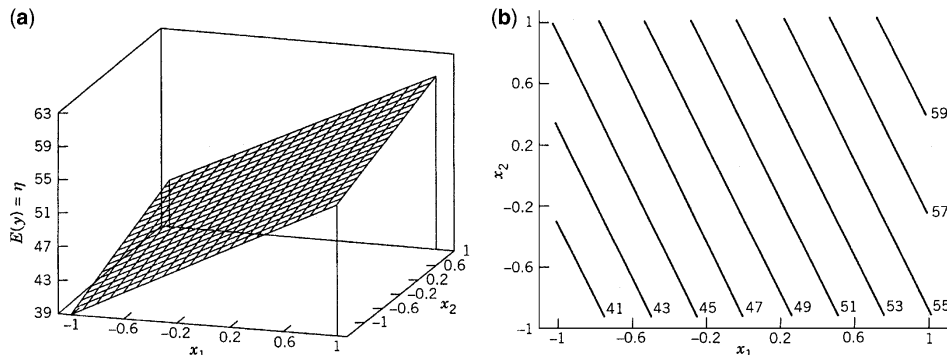


**Figure 1.2** (a) Response surface for the first-order model  $\eta = 50 + 8x_1 + 3x_2$ . (b) Contour plot for the first-order model.

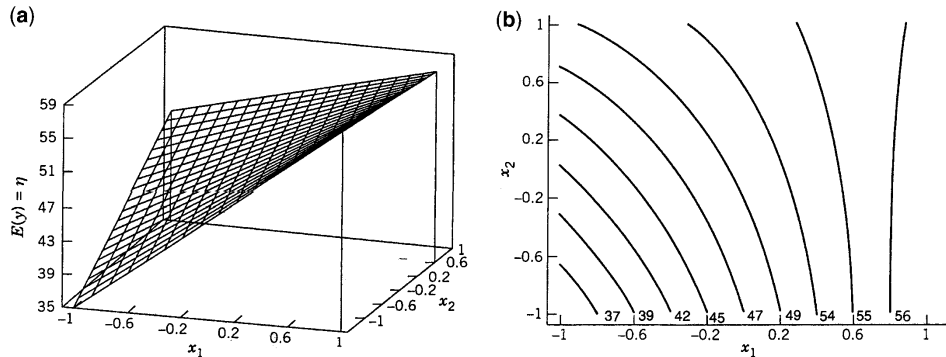


**Figure 1.3** (a) Response surface for the first-order model with interaction  $\eta = 50 + 8x_1 + 3x_2 - 4x_1x_2$ . (b) Contour plot for the first-order model with interaction.

This is the **first-order model with interaction**. Figure 1.3 shows the three-dimensional response surface and the contour plot for the special case

$$\eta = 50 + 8x_1 + 3x_2 - 4x_1x_2$$

Notice that adding the interaction term  $-4x_1x_2$  introduces curvature into the response function.

Often the curvature in the true response surface is strong enough that the first-order model (even with the interaction term included) is inadequate. A **second-order model** will likely be required in these situations. For the case of two variables, the second-order model is

$$\eta = \beta_0 + \beta_1 x_1 + \beta_2 x_2 + \beta_{11} x_1^2 + \beta_{22} x_2^2 + \beta_{12} x_1 x_2 \quad (1.6)$$

This model would likely be useful as an approximation to the true response surface in a relatively small region around the point  $B$  in Fig. 1.1b, where there is substantial curvature in the true response function  $f$ .

Figure 1.4 presents the response surface and contour plot for the special case of the second-order model

$$\eta = 50 + 8x_1 + 3x_2 - 7x_{11}^2 - 3x_{22}^2 - 4x_1x_2$$

Notice the mound-shaped response surface and elliptical contours generated by this model. Such a response surface could arise in approximating a response such as yield, where we would expect to be operating near a maximum point on the surface.

The second-order model is widely used in response surface methodology for several reasons. Among these are the following:

1. The second-order model is very **flexible**. It can take on a wide variety of functional forms, so it will often work well as an approximation to the true response surface. Figure 1.5 shows several different response surfaces and contour plots that can be generated by a second-order model.

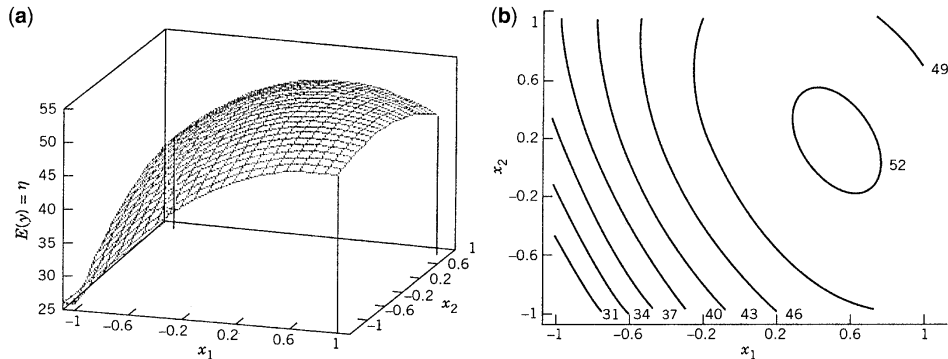


**Figure 1.4** (a) Response surface for the second-order model  $\eta = 50 + 8x_1 + 3x_2 - 7x_1^2 - 3x_2^2 - 4x_1x_2$ . (b) Contour plot for the second-order model.

2. It is **easy to estimate the parameters** (the  $\beta$ 's) in the second-order model. The method of least squares, which is presented in Chapter 2, can be used for this purpose.
3. There is considerable **practical experience** indicating that second-order models work well in solving real response surface problems.

In general, the first-order model is

$$\eta = \beta_0 + \beta_1 x_1 + \beta_2 x_2 + \cdots + \beta_k x_k \quad (1.7)$$

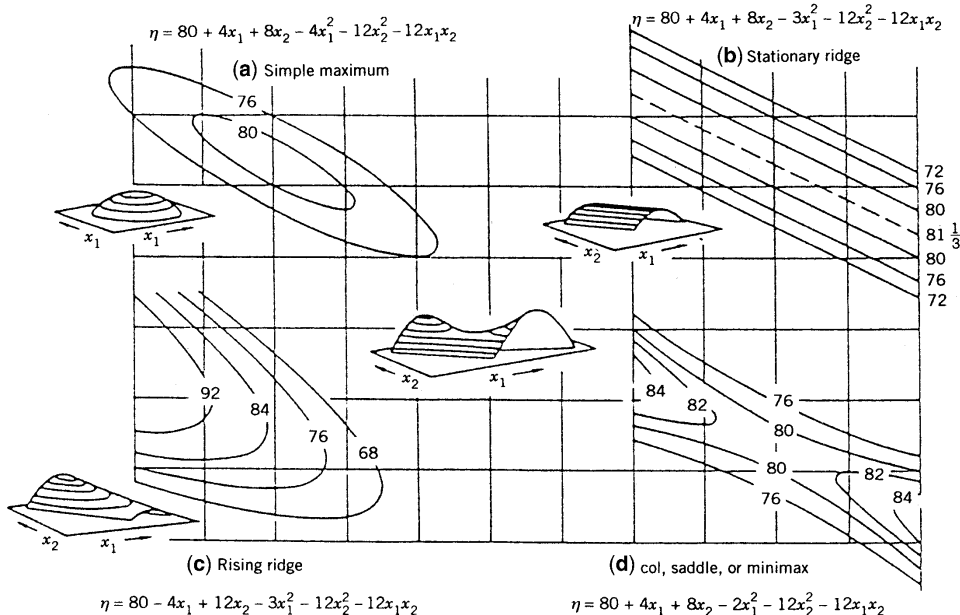


**Figure 1.5** Some examples of types of surfaces defined by the second-order model in two variables  $x_1$  and  $x_2$ . (Adapted with permission from *Empirical Model Building and Response Surfaces*, G. E. P. Box and N. R. Draper, John Wiley & Sons, New York, 1987.)

and the second-order model is

$$\eta = \beta_0 + \sum_{j=1}^k \beta_j x_j + \sum_{j=1}^k \beta_{jj} x_j^2 + \sum_{i < j=2}^k \beta_{ij} x_i x_j \quad (1.8)$$

In some situations, approximating polynomials of order higher than two are used. The general motivation for a polynomial approximation for the true response function  $f$  is based on the **Taylor series expansion** around the point  $x_{10}, x_{20}, \dots, x_{k0}$ . For example, the first-order model is developed from the first-order Taylor series expansion

$$\begin{aligned} f \cong & f(x_{10}, x_{20}, \dots, x_{k0}) + \left. \frac{\partial f}{\partial x_1} \right|_{\mathbf{x}=\mathbf{x}_0} (x_1 - x_{10}) \\ & + \left. \frac{\partial f}{\partial x_2} \right|_{\mathbf{x}=\mathbf{x}_0} (x_2 - x_{20}) + \dots + \left. \frac{\partial f}{\partial x_k} \right|_{\mathbf{x}=\mathbf{x}_0} (x_k - x_{k0}) \end{aligned} \quad (1.9)$$

where  $\mathbf{x}$  refers to the vector of independent variables and  $\mathbf{x}_0$  is the vector of independent variables at the specific point  $x_{10}, x_{20}, \dots, x_{k0}$ . In Equation 1.9 we have only included the first-order terms in the expansion, so if we let  $\beta_0 = f(x_{10}, x_{20}, \dots, x_{k0})$ ,  $\beta_1 = (\partial f / \partial x_1)|_{\mathbf{x}=\mathbf{x}_0}, \dots, \beta_k = (\partial f / \partial x_k)|_{\mathbf{x}=\mathbf{x}_0}$ , we have the first-order approximating model in Equation 1.7. If we were to include second-order terms in Equation 1.9, this would lead to the second-order approximating model in Equation 1.8.

Finally, note that there is a close connection between RSM and **linear regression analysis**. For example, consider the model

$$y = \beta_0 + \beta_1 x_1 + \beta_2 x_2 + \dots + \beta_k x_k + \varepsilon$$

The  $\beta$ 's are a set of unknown parameters. To estimate the values of these parameters, we must collect data on the system we are studying. Regression analysis is a branch of statistical model building that uses these data to estimate the  $\beta$ 's. Because, in general, polynomial models are linear functions of the unknown  $\beta$ 's, we refer to the technique as **linear regression analysis**. We will also see that it is very important to plan the data collection phase of a response surface study carefully. In fact, special types of experimental designs, called **response surface designs**, are valuable in this regard. A substantial part of this book is devoted to response surface designs.

### 1.1.2 The Sequential Nature of RSM

Most applications of RSM are **sequential** in nature. That is, at first some ideas are generated concerning which factors or variables are likely to be important in the response surface study. This usually leads to an experiment designed to investigate these factors with a view toward eliminating the unimportant ones. This type of experiment is usually called a **screening experiment**. Often at the outset of a response surface study there is a rather long list of variables that could be important in explaining the response. The objective of factor screening is to reduce this list of candidate variables to a relative few so that subsequent experiments will be more efficient and require fewer runs or tests. We refer

to a screening experiment as **phase zero** of a response surface study. You should never undertake a response surface analysis until a screening experiment has been performed to identify the important factors.

Once the important independent variables are identified, **phase one** of the response surface study begins. In this phase, the experimenter's objective is to determine if the current levels or settings of the independent variables result in a value of the response that is near the optimum (such as the point *B* in Fig. 1.1b), or if the process is operating in some other region that is (possibly) remote from the optimum (such as the point *A* in Fig. 1.1b). If the current settings or levels of the independent variables are not consistent with optimum performance, then the experimenter must determine a set of adjustments to the process variables that will move the process toward the optimum. This phase of response surface methodology makes considerable use of the first-order model and an optimization technique called the **method of steepest ascent**. These techniques will be discussed and illustrated in Chapter 5.

**Phase two** of a response surface study begins when the process is near the optimum. At this point the experimenter usually wants a model that will accurately approximate the true response function within a relatively small region around the optimum. Because the true response surface usually exhibits curvature near the optimum (refer to Fig. 1.1), a second-order model (or very occasionally some higher-order polynomial) will be used. Once an appropriate approximating model has been obtained, this model may be analyzed to determine the optimum conditions for the process. Chapter 6 will present techniques for the analysis of the second-order model and the determination of optimum conditions.

This sequential experimental process is usually performed within some region of the independent variable space called the **operability region**. For the chemical process illustrated in Fig. 1.1, the operability region is  $0 \text{ hr} < \xi_1 \leq 7 \text{ hr}$  and  $100^\circ\text{C} \leq \xi_2 \leq 800^\circ\text{C}$ .

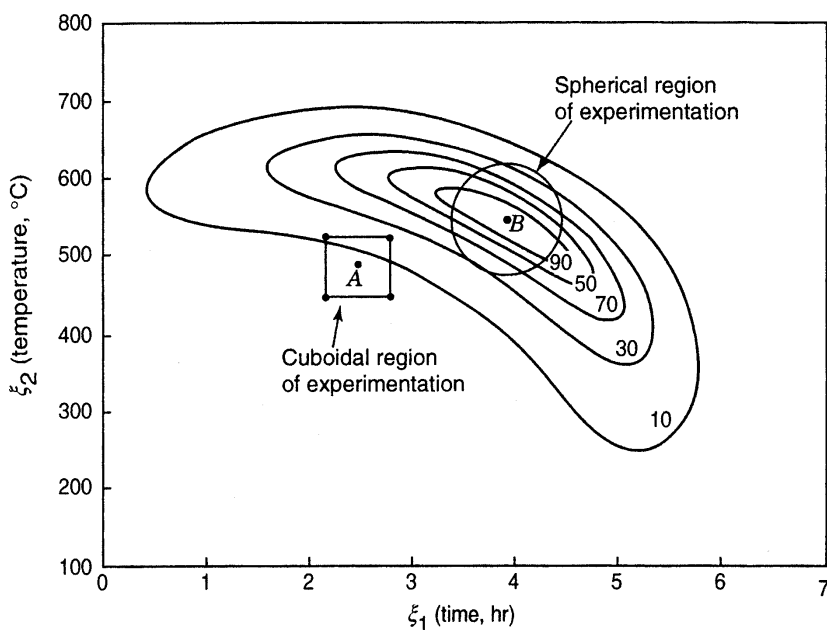


**Figure 1.6** The region of operability and the region of experimentation.

Suppose we are currently operating at the levels  $\xi_1 = 2.5$  hr and  $\xi_2 = 500^\circ\text{C}$ , shown as point *A* in Fig. 1.6. Now it is unlikely that we would want to explore the entire region of operability with a single experiment. Instead, we usually define a smaller **region of interest** or **region of experimentation** around the point *A* within the larger region of operability. Typically, this region of experimentation is either a cuboidal region, as shown around the point *A* in Fig. 1.6, or a spherical region, as shown around point *B*.

The sequential nature of response surface methodology allows the experimenter to learn about the process or system under study as the investigation proceeds. This ensures that over the course of the RSM application the experimenter will learn the answers to questions such as (1) the location of the region of the optimum, (2) the type of approximating function required, (3) the proper choice of experimental designs, (4) how much replication is necessary, and (5) whether or not transformations on the responses or any of the process variables are required. A substantial portion of this book—Chapters 3, 4, 7, and 8—is devoted to designed experiments useful in RSM.

### 1.1.3 Objectives and Typical Applications of RSM

Response surface methodology is useful in the solution of many types of industrial problems. Generally, these problems fall into three categories:

1. *Mapping a Response Surface over a Particular Region of Interest.* Consider the chemical process in Fig. 1.1b. Normally, this process would operate at a particular setting of reaction time and reaction temperature. However, some changes to these normal operating levels might occasionally be necessary, perhaps to produce a product that meets other specific customer requirement. If the true unknown response function has been approximated over a region around the current operating conditions with a suitable fitted response surface (say a second-order surface), then the process engineer can predict in advance the changes in yield that will result from any readjustments to time and temperature.
2. *Optimization of the Response.* In the industrial world, a very important problem is determining the conditions that optimize the process. In the chemical process of Fig. 1.1b, this implies determining the levels of time and temperature that result in maximum yield. An RSM study that began near point *A* in Fig. 1.1b would eventually lead the experimenter to the region near point *B*. A second-order model could then be used to approximate the yield response in a narrow region around point *B*, and from examination of this approximating response surface the optimum levels or condition for time and temperature could be chosen.
3. *Selection of Operating Conditions to Achieve Specifications or Customer Requirements.* In most response surface problems there are several responses that must in some sense be simultaneously considered. For example, in the chemical process of Fig. 1.1, suppose that in addition to yield, there are two other responses: cost and concentration. We would like to maintain yield above 70%, while simultaneously keeping the cost below \$34/pound; however, the customer has imposed specifications for concentration such that this important physical property must be  $65 \pm 3$  g/liter.

One way that we could solve this problem is to obtain response surfaces for all three responses—yield, cost, and concentration—and then superimpose the contours

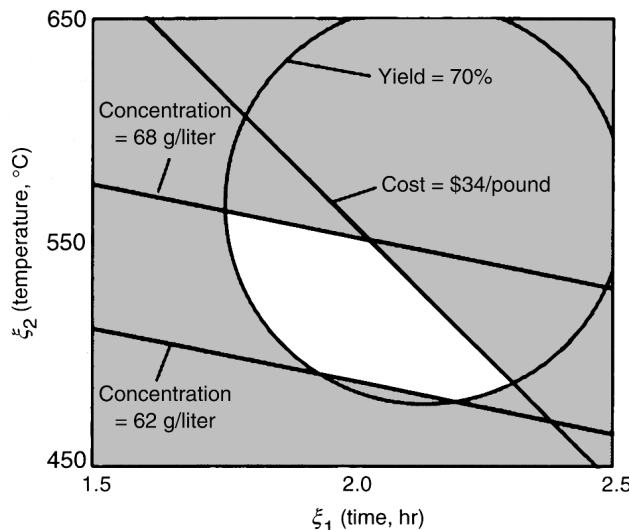


**Figure 1.7** The unshaded region showing the conditions for which yield  $\geq 70\%$ , cost  $\leq \$34/\text{pound}$ , and  $62 \text{ g/liter} \leq \text{concentration} \leq 68 \text{ g/liter}$ .

for these responses in the time–temperature plane, as illustrated in Fig. 1.7. In this figure we have shown the contours for yield = 70%, cost = \$34/pound, concentration = 62 g/liter, and concentration = 68 g/liter. The unshaded region in this figure represents the region containing operating conditions that simultaneously satisfy all requirements on the process.

In practice, complex process optimization problems such as this can often be solved by superimposing appropriate response surface contours. However, it is not unusual to encounter problems with more than two process variables and more complex response requirements to satisfy. In such problems, other optimization methods that are more effective than overlaying contour plots will be necessary. We will discuss methodology for solving these types of problems in Chapter 6.

#### 1.1.4 RSM and the Philosophy of Quality Improvement

During the last few decades, industrial organizations in the United States and Europe have become keenly interested in quality and process improvement. Statistical methods, including statistical process control (SPC) and design of experiments, play a key role in this activity. Quality improvement is most effective when it occurs early in the product and process development cycle. It is very difficult and often expensive to manufacture a poorly designed product. Industries such as semiconductors and electronics, aerospace, automotive, biotechnology and pharmaceuticals, medical devices, chemical, and process industries are all examples where experimental design methodology has resulted in shorter design and development time for new products, as well as products that are easier to manufacture, have higher reliability, have enhanced field performance, and meet or exceed customer requirements.

RSM is an important branch of experimental design in this regard. RSM is a critical technology in developing new processes, optimizing their performance, and improving the design and/or formulation of new products. It is often an important **concurrent**

**engineering tool**, in that product design, process development, quality, manufacturing engineering, and operations personnel often work together in a team environment to apply RSM. The objectives of quality improvement, including reduction of variability and improved product and process performance, can often be accomplished directly using RSM.

## 1.2 PRODUCT DESIGN AND FORMULATION (MIXTURE PROBLEMS)

Many product design and development activities involve formulation problems, in which two or more ingredients are mixed together. For example, suppose we are developing a new household cleaning product. This product is formulated by mixing several chemical surfactants together. The product engineer or scientist would like to find an appropriate blend of the ingredients so that the grease-cutting capability of the cleaner is good, and so that it generates an appropriate level of foam when in use. In this situation the response variables—namely, grease-cutting ability and amount of foam—depend on the percentages or proportions of the individual chemical surfactants (the ingredients) that are present in the product formulation.

There are many industrial problems where the response variables of interest in the product are a function of the proportions of the different ingredients used in its formulation. This is a special type of response surface problem called a **mixture problem**.

While we traditionally think of mixture problems in the product design or formulation environment, they occur in many other settings. Consider plasma etching of silicon wafers, a common manufacturing process in the semiconductor industry. Etching is usually accomplished by introducing a blend of gases inside a chamber containing the wafers. The measured responses include the etch rate, the uniformity of the etch, and the selectivity (a measure of the relative etch rates of the different materials on the wafer). All of these responses are a function of the proportions of the different ingredients blended together in the etching chamber.

There are special experimental design techniques and model-building methods for mixture problems. These techniques are discussed in Chapters 11 and 12.

## 1.3 ROBUST DESIGN AND PROCESS ROBUSTNESS STUDIES

It is well known that variation in key performance characteristics can result in poor product and process quality. During the 1980s, considerable attention was given to this problem, and methodology was developed for using experimental design, specifically for the following:

1. For designing products or processes so that they are robust to environment conditions.
2. For designing or developing products so that they are robust to component variation.
3. For minimizing variability in the output response of a product around a target value.

By **robust**, we mean that the product or process performs consistently on target and is relatively insensitive to factors that are difficult to control.

Professor Genichi Taguchi used the term **robust parameter design** (or RPD) to describe his approach to this important class of industrial problems. Essentially, robust parameter design methodology strives to reduce product or process variation by choosing levels of controllable factors (or parameters) that make the system insensitive (or robust) to changes in a set of uncontrollable factors that represent most of the sources of variability. Taguchi referred to these uncontrollable factors as **noise factors**. These are the environmental factors such as humidity levels, changes in raw material properties, product aging, and component variability referred to in 1 and 2 above. We usually assume that these noise factors are uncontrollable in the field, but can be controlled during product or process development for purposes of a designed experiment.

Considerable attention has been focused on the methodology advocated by Taguchi, and a number of flaws in his approach have been discovered. However, there are many useful concepts in his philosophy, and it is relatively easy to incorporate these within the framework of response surface methodology. In Chapter 10 we will present the response surface approach to robust design and process robustness studies.

## 1.4 USEFUL REFERENCES ON RSM

The origin of RSM is the seminal paper by Box and Wilson (1951). They also describe the application of RSM to chemical processes. This paper had a profound impact on industrial applications of experimental design, and was the motivation of much of the research in the field. Many of the key research and applications papers are cited in this book.

There have also been four review papers published on RSM: Hill and Hunter (1966), Mead and Pike (1975), Myers et al. (1989) and Myers et al. (2004). The paper by Myers (1999) on future directions in RSM offers a view of research needs in the field. There are also two other full-length books on the subject: Box and Draper (1987) and Khuri and Cornell (1996). A second edition of the Box and Draper book was published in 2007 with a slightly different title [Box and Draper (2007)]. The monograph by Myers (1976) was the first book devoted exclusively to RSM.



---

# 2

---

## BUILDING EMPIRICAL MODELS

### 2.1 LINEAR REGRESSION MODELS

The practical application of response surface methodology (RSM) requires developing an approximating model for the true response surface. The underlying true response surface is typically driven by some unknown **physical mechanism**. The approximating model is based on observed data from the process or system and is an **empirical model**. Multiple regression is a collection of statistical techniques useful for building the types of empirical models required in RSM.

As an example, suppose that we wish to develop an empirical model relating the effective life of a cutting tool to the cutting speed and the tool angle. A first-order response surface model that might describe this relationship is

$$y = \beta_0 + \beta_1 x_1 + \beta_2 x_2 + \varepsilon \quad (2.1)$$

where  $y$  represents the tool life,  $x_1$  represents the cutting speed, and  $x_2$  represents the tool angle. This is a **multiple linear regression model** with two independent variables. We often call the independent variables **predictor variables** or **regressors**. The term “linear” is used because Equation 2.1 is a linear function of the unknown parameters  $\beta_0$ ,  $\beta_1$ , and  $\beta_2$ . The model describes a plane in the two-dimensional  $x_1, x_2$  space. The parameter  $\beta_0$  fixes the intercept of the plane. We sometimes call  $\beta_1$  and  $\beta_2$  **partial regression coefficients**, because  $\beta_1$  measures the expected change in  $y$  per unit change in  $x_1$  when  $x_2$  is held constant, and  $\beta_2$  measures the expected change in  $y$  per unit change in  $x_2$  when  $x_1$  is held constant.

In general, the response variable  $y$  may be related to  $k$  regressor variables. The model

$$y = \beta_0 + \beta_1 x_1 + \beta_2 x_2 + \cdots + \beta_k x_k + \varepsilon \quad (2.2)$$

is called a **multiple linear regression model** with  $k$  regressor variables. The parameters  $\beta_j$ ,  $j = 0, 1, \dots, k$ , are called the **regression coefficients**. This model describes a hyperplane in the  $k$ -dimensional space of the regressor variables  $\{x_j\}$ . The parameter  $\beta_j$  represents the expected change in response  $y$  per unit change in  $x_j$  when all the remaining independent variables  $x_i$  ( $i \neq j$ ) are held constant.

Models that are more complex in appearance than Equation 2.2 may often still be analyzed by multiple linear regression techniques. For example, considering adding an **interaction term** to the first-order model in two variables, say

$$y = \beta_0 + \beta_1 x_1 + \beta_2 x_2 + \beta_{12} x_1 x_2 + \varepsilon \quad (2.3)$$

If we let  $x_3 = x_1 x_2$  and  $\beta_3 = \beta_{12}$ , then Equation 2.3 can be written as

$$y = \beta_0 + \beta_1 x_1 + \beta_2 x_2 + \beta_3 x_3 + \varepsilon \quad (2.4)$$

which is a standard multiple linear regression model with three regressors. As another example, consider the **second-order** response surface model in two variables:

$$y = \beta_0 + \beta_1 x_1 + \beta_2 x_2 + \beta_{11} x_1^2 + \beta_{22} x_2^2 + \beta_{12} x_1 x_2 + \varepsilon \quad (2.5)$$

If we let  $x_3 = x_1^2$ ,  $x_4 = x_2^2$ ,  $x_5 = x_1 x_2$ ,  $\beta_3 = \beta_{11}$ ,  $\beta_4 = \beta_{22}$ , and  $\beta_5 = \beta_{12}$ , then this becomes

$$y = \beta_0 + \beta_1 x_1 + \beta_2 x_2 + \beta_3 x_3 + \beta_4 x_4 + \beta_5 x_5 + \varepsilon \quad (2.6)$$

which is a linear regression model. In general, any regression model that is linear in the parameters (the  $\beta$ -values) is a linear regression model, regardless of the shape of the response surface that it generates.

In this chapter we will present and illustrate methods for estimating the parameters in multiple linear regression models. This is often called **model fitting**. We will also discuss methods for testing hypotheses and constructing confidence intervals for these models, as well as for checking the adequacy of the model fit. Our focus is primarily on those aspects of regression analysis useful in RSM. For more complete presentations of regression, refer to Montgomery, Peck, and Vining (2006) and Myers (1990).

## 2.2 ESTIMATION OF THE PARAMETERS IN LINEAR REGRESSION MODELS

The method of least squares is typically used to estimate the regression coefficients in a multiple linear regression model. Suppose that  $n > k$  observations on the response variable are available, say  $y_1, y_2, \dots, y_n$ . Along with each observed response  $y_i$ , we will have an observation on each regressor variable, and let  $x_{ij}$  denote the  $i$ th observation or level of variable  $x_j$ . Table 2.1 shows the data layout. We assume that the error term  $\varepsilon$  in the model has  $E(\varepsilon) = 0$  and  $\text{Var}(\varepsilon) = \sigma^2$  and that the  $\{\varepsilon_i\}$  are uncorrelated random variables.

**TABLE 2.1 Data for Multiple Linear Regression**

$y$	$x_1$	$x_2$	...	$x_k$
$y_1$	$x_{11}$	$x_{12}$	...	$x_{1k}$
$y_2$	$x_{21}$	$x_{22}$	...	$x_{2k}$
$\vdots$	$\vdots$	$\vdots$		$\vdots$
$y_n$	$x_{n1}$	$x_{n2}$	...	$x_{nk}$

We may write the model equation (Eq. 2.2) in terms of the observations in Table 2.1 as

$$\begin{aligned} y_i &= \beta_0 + \beta_1 x_{i1} + \beta_2 x_{i2} + \cdots + \beta_k x_{ik} + \varepsilon_i \\ &= \beta_0 + \sum_{j=1}^k \beta_j x_{ij} + \varepsilon_i, \quad i = 1, 2, \dots, n \end{aligned} \quad (2.7)$$

The method of least squares chooses the  $\beta$ 's in Equation 2.7 so that the sum of the squares of the errors,  $\varepsilon_i$ , are minimized. The least squares function is

$$\begin{aligned} L &= \sum_{i=1}^n \varepsilon_i^2 \\ &= \sum_{i=1}^n \left( y_i - \beta_0 - \sum_{j=1}^k \beta_j x_{ij} \right)^2 \end{aligned} \quad (2.8)$$

The function  $L$  is to be minimized with respect to  $\beta_0, \beta_1, \dots, \beta_k$ . The **least squares estimators**, say  $b_0, b_1, \dots, b_k$ , must satisfy

$$\frac{\partial L}{\partial \beta_0} \Big|_{b_0, b_1, \dots, b_k} = -2 \sum_{i=1}^n \left( y_i - b_0 - \sum_{j=1}^k b_j x_{ij} \right) = 0 \quad (2.9a)$$

and

$$\frac{\partial L}{\partial \beta_j} \Big|_{b_0, b_1, \dots, b_k} = -2 \sum_{i=1}^n \left( y_i - b_0 - \sum_{j=1}^k b_j x_{ij} \right) x_{ij} = 0, \quad (2.9b)$$

where  $j = 1, 2, \dots, k$ . Simplifying Equation 2.9, we obtain

$$\begin{aligned} nb_0 + b_1 \sum_{i=1}^n x_{i1} + b_2 \sum_{i=1}^n x_{i2} + \cdots + b_k \sum_{i=1}^n x_{ik} &= \sum_{i=1}^n y_i \\ b_0 \sum_{i=1}^n x_{i1} + b_1 \sum_{i=1}^n x_{i1}^2 + b_2 \sum_{i=1}^n x_{i1} x_{i2} + \cdots + b_k \sum_{i=1}^n x_{i1} x_{ik} &= \sum_{i=1}^n x_{i1} y_i \\ \vdots &\vdots \\ b_0 \sum_{i=1}^n x_{ik} + b_1 \sum_{i=1}^n x_{ik} x_{i1} + b_2 \sum_{i=1}^n x_{ik} x_{i2} + \cdots + b_k \sum_{i=1}^n x_{ik}^2 &= \sum_{i=1}^n x_{ik} y_i \end{aligned} \quad (2.10)$$

These equations are called the **least squares normal equations**. Note that there are  $p = k + 1$  normal equations, one for each of the unknown regression coefficients. The solution to the normal equations will be the least squares estimators of the regression coefficients  $b_0, b_1, \dots, b_k$ .

It is simpler to solve the normal equations if they are expressed in matrix notation. We now give a matrix development of the normal equations that parallels the development of Equation 2.10. The model in terms of the observations, Equation 2.7, may be written in matrix notation as

$$\mathbf{y} = \mathbf{X}\boldsymbol{\beta} + \boldsymbol{\epsilon}$$

where

$$\mathbf{y} = \begin{bmatrix} y_1 \\ y_2 \\ \vdots \\ y_n \end{bmatrix}, \quad \mathbf{X} = \begin{bmatrix} 1 & x_{11} & x_{12} & \cdots & x_{1k} \\ 1 & x_{21} & x_{22} & \cdots & x_{2k} \\ \vdots & \vdots & \vdots & & \vdots \\ 1 & x_{n1} & x_{n2} & \cdots & x_{nk} \end{bmatrix}, \quad \boldsymbol{\beta} = \begin{bmatrix} \beta_0 \\ \beta_1 \\ \vdots \\ \beta_k \end{bmatrix}, \quad \text{and} \quad \boldsymbol{\epsilon} = \begin{bmatrix} \epsilon_1 \\ \epsilon_2 \\ \vdots \\ \epsilon_n \end{bmatrix}$$

In general,  $\mathbf{y}$  is an  $n \times 1$  vector of the observations,  $\mathbf{X}$  is an  $n \times p$  **model matrix** consisting of the levels of the independent variables expanded to model form,  $\boldsymbol{\beta}$  is a  $p \times 1$  vector of the regression coefficients, and  $\boldsymbol{\epsilon}$  is an  $n \times 1$  vector of random errors. Notice the columns of  $\mathbf{X}$  consist of the independent variables from Table 2.1 plus an additional column of 1s to account for the intercept term in the model.

We wish to find the vector of least squares estimators,  $\mathbf{b}$ , that minimizes

$$L = \sum_{i=1}^n \epsilon_i^2 = \boldsymbol{\epsilon}'\boldsymbol{\epsilon} = (\mathbf{y} - \mathbf{X}\boldsymbol{\beta})'(\mathbf{y} - \mathbf{X}\boldsymbol{\beta})$$

Note that  $L$  may be expressed as

$$\begin{aligned} L &= \mathbf{y}'\mathbf{y} - \boldsymbol{\beta}'\mathbf{X}'\mathbf{y} - \mathbf{y}'\mathbf{X}\boldsymbol{\beta} + \boldsymbol{\beta}'\mathbf{X}'\mathbf{X}\boldsymbol{\beta} \\ &= \mathbf{y}'\mathbf{y} - 2\boldsymbol{\beta}'\mathbf{X}'\mathbf{y} + \boldsymbol{\beta}'\mathbf{X}'\mathbf{X}\boldsymbol{\beta} \end{aligned} \tag{2.11}$$

since  $\boldsymbol{\beta}'\mathbf{X}'\mathbf{y}$  is a  $1 \times 1$  matrix, or a scalar, and its transpose  $(\boldsymbol{\beta}'\mathbf{X}'\mathbf{y})' = \mathbf{y}'\mathbf{X}\boldsymbol{\beta}$  is the same scalar. The least squares estimators must satisfy

$$\frac{\partial L}{\partial \boldsymbol{\beta}} \Big|_{\mathbf{b}} = -2\mathbf{X}'\mathbf{y} + 2\mathbf{X}'\mathbf{X}\mathbf{b} = \mathbf{0}$$

which simplifies to

$$\mathbf{X}'\mathbf{X}\mathbf{b} = \mathbf{X}'\mathbf{y} \tag{2.12}$$

Equation 2.12 is the set of least squares normal equations in matrix form. It is identical to Equation 2.10. To solve the normal equations, multiply both sides of Equation 2.12

by the inverse of  $\mathbf{X}'\mathbf{X}$ . Thus, the least squares estimator of  $\boldsymbol{\beta}$  is

$$\mathbf{b} = (\mathbf{X}'\mathbf{X})^{-1}\mathbf{X}'\mathbf{y} \quad (2.13)$$

It is easy to see that the matrix form of the normal equations is identical to the scalar form. Writing out Equation 2.12 in detail, we obtain

$$\begin{bmatrix} n & \sum_{i=1}^n x_{i1} & \sum_{i=1}^n x_{i2} & \cdots & \sum_{i=1}^n x_{ik} \\ \sum_{i=1}^n x_{i1} & \sum_{i=1}^n x_{i1}^2 & \sum_{i=1}^n x_{i1}x_{i2} & \cdots & \sum_{i=1}^n x_{i1}x_{ik} \\ \vdots & \vdots & \vdots & & \vdots \\ \sum_{i=1}^n x_{ik} & \sum_{i=1}^n x_{ik}x_{i1} & \sum_{i=1}^n x_{ik}x_{i2} & \cdots & \sum_{i=1}^n x_{ik}^2 \end{bmatrix} \begin{bmatrix} b_0 \\ b_1 \\ \vdots \\ b_k \end{bmatrix} = \begin{bmatrix} \sum_{i=1}^n y_i \\ \sum_{i=1}^n x_{i1}y_i \\ \vdots \\ \sum_{i=1}^n x_{ik}y_i \end{bmatrix}$$

If the indicated matrix multiplication is performed, the scalar form of the normal equations (i.e., Eq. 2.10) will result. In this form it is easy to see that  $\mathbf{X}'\mathbf{X}$  is a  $p \times p$  symmetric matrix and  $\mathbf{X}'\mathbf{y}$  is a  $p \times 1$  column vector. Note the special structure of the matrix  $\mathbf{X}'\mathbf{X}$ . The diagonal elements of  $\mathbf{X}'\mathbf{X}$  are the sums of squares of the elements in the columns of  $\mathbf{X}$ , and the off-diagonal elements are the sums of cross-products of the elements in the columns of  $\mathbf{X}$ . Furthermore, note that the elements of  $\mathbf{X}'\mathbf{y}$  are the sums of cross-products of the columns of  $\mathbf{X}$  and the observations  $\{y_i\}$ .

The fitted regression model is

$$\hat{\mathbf{y}} = \mathbf{X}\mathbf{b} \quad (2.14)$$

In scalar notation, the fitted model is

$$\hat{y}_i = b_0 + \sum_{j=1}^k b_j x_{ij}, \quad i = 1, 2, \dots, n$$

The difference between the observation  $y_i$  and the fitted value  $\hat{y}_i$  is a **residual**, say  $e_i = y_i - \hat{y}_i$ . The  $n \times 1$  vector of residuals is denoted by

$$\mathbf{e} = \mathbf{y} - \hat{\mathbf{y}} \quad (2.15)$$

**Example 2.1 The Transistor Gain Data** The transistor gain in an integrated circuit device between emitter and collector ( $hFE$ ) is related to two variables that can be controlled at the deposition process, emitter drive-in time ( $\xi_1$ , in minutes), and emitter dose ( $\xi_2$ , units of  $10^{14}$  ions). Fourteen samples were observed following deposition, and the resulting data are shown in Table 2.2. We will fit a linear regression model using gain as the response and emitter drive-in time and emitter dose as the regressor variables.

Columns 2 and 3 of Table 2.2 show the actual or natural unit values of  $\xi_1$  and  $\xi_2$ , while columns 4 and 5 contain values of the corresponding coded variables  $x_1$  and  $x_2$ , where

**TABLE 2.2 Data on Transistor Gain ( $y$ ) for Example 2.1**

Observation	$\xi_1$ (drive-in time, minutes)	$\xi_2$ (dose, $10^{14}$ ions)	$x_1$	$x_2$	$y$ (gain or $hFE$ )
1	195	4.00	-1	-1	1004
2	255	4.00	1	-1	1636
3	195	4.60	-1	0.6667	852
4	255	4.60	1	0.6667	1506
5	225	4.20	0	-0.4444	1272
6	225	4.10	0	-0.7222	1270
7	225	4.60	0	0.6667	1269
8	195	4.30	-1	-0.1667	903
9	255	4.30	1	-0.1667	1555
10	225	4.00	0	-1	1260
11	225	4.70	0	0.9444	1146
12	225	4.30	0	-0.1667	1276
13	225	4.72	0	1	1225
14	230	4.30	0.1667	-0.1667	1321

$$x_{i1} = \frac{\xi_{i1} - [\max(\xi_{i1}) + \min(\xi_{i1})]/2}{[\max(\xi_{i1}) - \min(\xi_{i1})]/2} = \frac{\xi_{i1} - (255 + 195)/2}{(255 - 195)/2} = \frac{\xi_{i1} - 225}{30}$$

$$x_{i2} = \frac{\xi_{i2} - [\max(\xi_{i2}) + \min(\xi_{i2})]/2}{[\max(\xi_{i2}) - \min(\xi_{i2})]/2} = \frac{\xi_{i2} - (4.72 + 4.00)/2}{(4.72 - 4.00)/2} = \frac{\xi_{i2} - 4.36}{0.36}$$

This coding scheme is widely used in fitting linear regression models, and it results in all the values of  $x_1$  and  $x_2$  falling between  $-1$  and  $+1$ , as shown in Table 2.2.

We will fit the model

$$y = \beta_0 + \beta_1 x_1 + \beta_2 x_2 + \varepsilon$$

using the coded variables. The model matrix  $\mathbf{X}$  and vector  $\mathbf{y}$  are

$$\mathbf{X} = \begin{bmatrix} 1 & -1 & -1 \\ 1 & 1 & -1 \\ 1 & -1 & 0.6667 \\ 1 & 1 & 0.6667 \\ 1 & 0 & -0.4444 \\ 1 & 0 & -0.7222 \\ 1 & 0 & 0.6667 \\ 1 & -1 & -0.1667 \\ 1 & 1 & -0.1667 \\ 1 & 0 & -1 \\ 1 & 0 & 0.9444 \\ 1 & 0 & -0.1667 \\ 1 & 0 & 1 \\ 1 & 0.1667 & -0.1667 \end{bmatrix}, \quad \mathbf{y} = \begin{bmatrix} 1004 \\ 1636 \\ 852 \\ 1506 \\ 1272 \\ 1270 \\ 1269 \\ 903 \\ 1555 \\ 1260 \\ 1146 \\ 1276 \\ 1225 \\ 1321 \end{bmatrix}$$

The matrix  $\mathbf{X}'\mathbf{X}$  is

$$\begin{aligned}\mathbf{X}'\mathbf{X} &= \begin{bmatrix} 1 & 1 & \cdots & 1 \\ -1 & 1 & \cdots & 0.1667 \\ -1 & -1 & \cdots & -0.1667 \end{bmatrix} \begin{bmatrix} 1 & -1 & -1 \\ 1 & 1 & -1 \\ \vdots & \vdots & \vdots \\ 1 & 0.1667 & -0.1667 \end{bmatrix} \\ &= \begin{bmatrix} 14 & 0.1667 & -0.8889 \\ 0.1667 & 6.027789 & -0.02779 \\ -0.8889 & -0.02779 & 7.055578 \end{bmatrix}\end{aligned}$$

and the vector  $\mathbf{X}'\mathbf{y}$  is

$$\begin{aligned}\mathbf{X}'\mathbf{y} &= \begin{bmatrix} 1 & 1 & \cdots & 1 \\ -1 & 1 & \cdots & 0.1667 \\ -1 & -1 & \cdots & -0.1667 \end{bmatrix} \begin{bmatrix} 1004 \\ 1636 \\ \vdots \\ 1321 \end{bmatrix} \\ &= \begin{bmatrix} 17,495 \\ 2158.211 \\ -1499.74 \end{bmatrix}\end{aligned}$$

The least squares estimate of  $\boldsymbol{\beta}$  is

$$\mathbf{b} = (\mathbf{X}'\mathbf{X})^{-1}\mathbf{X}'\mathbf{y}$$

or

$$\begin{aligned}\mathbf{b} &= \begin{bmatrix} 0.072027 & -0.00195 & 0.009067 \\ -0.00195 & 0.165954 & 0.000408 \\ 0.009067 & 0.000408 & 0.142876 \end{bmatrix} \begin{bmatrix} 17,495 \\ 2158.211 \\ -1499.74 \end{bmatrix} \\ &= \begin{bmatrix} 1242.3057 \\ 323.4366 \\ -54.7691 \end{bmatrix}\end{aligned}$$

The least squares fit with the regression coefficients reported to one decimal place is

$$\hat{y} = 1242.3 + 323.4x_1 - 54.8x_2$$

This can be converted into an equation using the natural variables  $\xi_1$  and  $\xi_2$  by substituting the relationships between  $x_1$  and  $\xi_1$  and  $x_2$  and  $\xi_2$  as follows:

$$\hat{y} = 1242.3 + 323.4\left(\frac{\xi_1 - 225}{30}\right) - 54.8\left(\frac{\xi_2 - 4.36}{0.36}\right)$$

**TABLE 2.3 Observations, Fitted Values, Residuals, and Other Summary Information for Example 2.1**

Observation	$y_i$	$\hat{y}_i$	$e_i$	$h_{ii}$	$r_i$	$t_i$	$D_i$
1	1004.0	973.7	30.3	0.367	1.092	1.103	0.231
2	1636.0	1620.5	15.5	0.358	0.553	0.535	0.057
3	852.0	882.4	-30.4	0.317	-1.052	-1.057	0.171
4	1506.0	1529.2	-23.2	0.310	-0.801	-0.787	0.096
5	1272.0	1266.7	5.3	0.092	0.160	0.153	0.001
6	1270.0	1281.9	-11.9	0.133	-0.365	-0.350	0.007
7	1269.0	1205.8	63.2	0.148	1.960	2.316	0.222
8	903.0	928.0	-25.0	0.243	-0.823	-0.810	0.072
9	1555.0	1574.9	-19.9	0.235	-0.651	-0.633	0.043
10	1260.0	1297.1	-37.1	0.197	-1.185	-1.209	0.115
11	1146.0	1190.6	-44.6	0.217	-1.442	-1.527	0.192
12	1276.0	1251.4	24.6	0.073	0.730	0.714	0.014
13	1225.0	1187.5	37.5	0.233	1.225	1.256	0.152
14	1321.0	1305.3	15.7	0.077	0.466	0.449	0.006

or

$$\hat{y} = -520.1 + 10.781\xi_1 - 152.15\xi_2$$

Table 2.3 shows the observed values of  $y_i$ , the corresponding fitted values  $\hat{y}_i$ , and the residuals from this model. There are several other quantities given in this table that will be defined and discussed later. Figure 2.1 shows the fitted response surface and the contour plot for this model. The response surface for gain is a plane lying above the time–dose space.

**Computing** Statistics software is usually employed to fit regression models. Table 2.4 and Fig. 2.2 present some of the output for the transistor gain data in Example 2.1 from JMP, a widely-used software package that supports regression, experimental design, and RSM. This model was fit to the coded variables in Table 2.2. The first portion of the display is

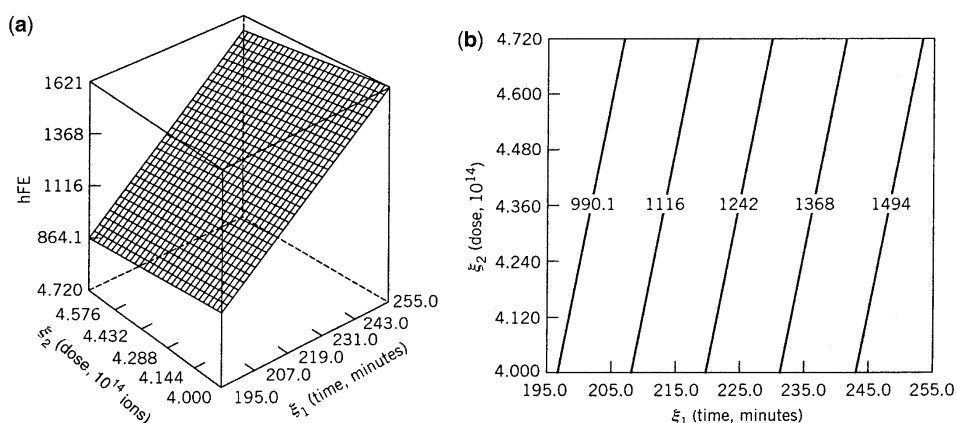


**Figure 2.1** (a) Response surface for gain, Example 2.1. (b) The gain contour plot.

**TABLE 2.4** Regression Output From JMP

Summary of Fit				
R-Square		0.979835		
R-Square Adj		0.976168		
Root Mean Square Error		34.92553		
Mean of Response		1249.643		
Observations (or Sum Wgts)		14		
Analysis of Variance				
Source	DF	Sum of Squares	Mean Square	F-Ratio
Model	2	651969.49	325985	267.2460
Error	11	13417.72	1220	Prob > F
C. Total	13	665387.21		<0.0001
Parameter Estimates				
Term	Estimate	Std Error	t-Ratio	Prob >  t
Intercept	1242.3181	9.373196	132.54	<0.0001
x1	323.4253	14.22778	22.73	<0.0001
x2	-54.77165	13.2001	-4.15	0.0016

a plot of the values of the observed response  $y$  versus the predicted values  $\hat{y}_i$  (see Fig. 2.2a). The pairs  $(y_i, \hat{y}_i)$  lie closely along a straight line (the straight line in the graph is a result of a least squares fit). This is usually a good indication that the model is a satisfactory fit to the data. We will discuss other checks of model adequacy later in this chapter. Notice that the estimates of the regression coefficients closely match those that we have computed manually (it is not unusual to find minor differences between manual and computer software regression calculations because of round-off). In subsequent sections we will show how some of the other quantities in the output are obtained and how to interpret them.

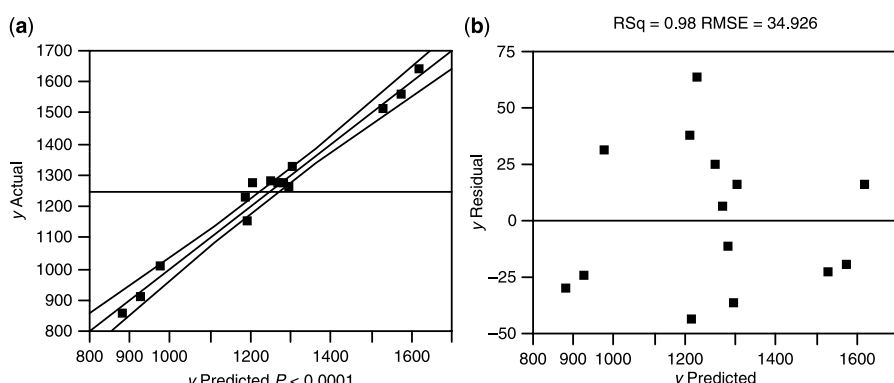


**Figure 2.2** Regression output from JMP. (a) Response  $y$  whole model, actual by predicted plot. (b) Residual by predicted plot.

### 2.3 PROPERTIES OF THE LEAST SQUARES ESTIMATORS AND ESTIMATION OF $\sigma^2$

The method of least squares produces an **unbiased estimator** of the parameter  $\beta$  in the multiple linear regression model. This property may be easily demonstrated by finding the expected value of  $\mathbf{b}$  as follows:

$$\begin{aligned} E(\mathbf{b}) &= E[(\mathbf{X}'\mathbf{X})^{-1}\mathbf{X}'\mathbf{y}] \\ &= E[(\mathbf{X}'\mathbf{X})^{-1}\mathbf{X}'(\mathbf{X}\beta + \mathbf{\epsilon})] \\ &= E[(\mathbf{X}'\mathbf{X})^{-1}\mathbf{X}'\mathbf{X}\beta + (\mathbf{X}'\mathbf{X})^{-1}\mathbf{X}'\mathbf{\epsilon}] \\ &= \beta \end{aligned}$$

because  $E(\mathbf{\epsilon}) = \mathbf{0}$  and  $(\mathbf{X}'\mathbf{X})^{-1}\mathbf{X}'\mathbf{X} = \mathbf{I}$ . Thus  $\mathbf{b}$  is an unbiased estimator of  $\beta$ . The variance property of  $\mathbf{b}$  is expressed by the covariance matrix

$$\text{Cov}(\mathbf{b}) = E\{[\mathbf{b} - E(\mathbf{b})][\mathbf{b} - E(\mathbf{b})]'\}$$

The covariance matrix of  $\mathbf{b}$  is a  $p \times p$  symmetric matrix whose  $(j, j)$ th element is the variance of  $b_j$  and whose  $(i, j)$ th element is the covariance between  $b_i$  and  $b_j$ . The **covariance matrix of  $\mathbf{b}$**  is

$$\text{Cov}(\mathbf{b}) = \sigma^2(\mathbf{X}'\mathbf{X})^{-1} \quad (2.16)$$

It is also usually necessary to estimate  $\sigma^2$ . To develop an estimator of this parameter consider the sum of squares of the residuals, say

$$\begin{aligned} SS_E &= \sum_{i=1}^n (y_i - \hat{y}_i)^2 \\ &= \sum_{i=1}^n e_i^2 \\ &= \mathbf{e}'\mathbf{e} \end{aligned}$$

Substituting  $\mathbf{e} = \mathbf{y} - \hat{\mathbf{y}} = \mathbf{y} - \mathbf{X}\mathbf{b}$ , we have

$$\begin{aligned} SS_E &= (\mathbf{y} - \mathbf{X}\mathbf{b})'(\mathbf{y} - \mathbf{X}\mathbf{b}) \\ &= \mathbf{y}'\mathbf{y} - \mathbf{b}'\mathbf{X}'\mathbf{y} - \mathbf{y}'\mathbf{X}\mathbf{b} + \mathbf{b}'\mathbf{X}'\mathbf{X}\mathbf{b} \\ &= \mathbf{y}'\mathbf{y} - 2\mathbf{b}'\mathbf{X}'\mathbf{y} + \mathbf{b}'\mathbf{X}'\mathbf{X}\mathbf{b} \end{aligned}$$

Because  $\mathbf{X}'\mathbf{X}\mathbf{b} = \mathbf{X}'\mathbf{y}$ , this last equation becomes

$$SS_E = \mathbf{y}'\mathbf{y} - \mathbf{b}'\mathbf{X}'\mathbf{y} \quad (2.17)$$

Equation 2.17 is called the **error or residual sum of squares**, and it has  $n - p$  degrees of freedom associated with it. It can be shown that

$$E(SS_E) = \sigma^2(n - p)$$

so an unbiased estimator of  $\sigma^2$  is given by

$$\hat{\sigma}^2 = \frac{SS_E}{n - p} \quad (2.18)$$

**Example 2.2 The Transistor Gain Data** We will estimate  $\sigma^2$  for the regression model for the transistor gain data from Example 2.1. Because

$$\mathbf{y}'\mathbf{y} = \sum_{i=1}^{14} y_i^2 = 22,527,889.0$$

and

$$\mathbf{b}'\mathbf{X}'\mathbf{y} = [1242.3 \quad 323.4 \quad -54.8] \begin{bmatrix} 17,495 \\ 2158.211 \\ -1499.74 \end{bmatrix} = 22,514,467.9$$

the residual sum of squares is

$$\begin{aligned} SS_E &= \mathbf{y}'\mathbf{y} - \mathbf{b}'\mathbf{X}'\mathbf{y} \\ &= 22,527,889.0 - 22,514,467.9 \\ &= 13,421.1 \end{aligned}$$

Therefore, the estimate of  $\sigma^2$  is computed from Equation 2.18 as follows:

$$\hat{\sigma}^2 = \frac{SS_E}{n - p} = \frac{13,421.1}{14 - 3} = 1220.1$$

Notice that the JMP output in Table 2.4 computes the residual sum of squares (look under the analysis of variance section of the output) as 13,417.72. The difference between the two values is round-off. Both the manual calculations and JMP produce virtually identical estimates of  $\sigma^2$ .

The estimate of  $\sigma^2$  produced by Equation 2.18 is **model-dependent**. That is, it depends on the **form** of the model that is fit to the data. To illustrate this point, suppose that we fit a quadratic model to the gain data, say

$$y = \beta_0 + \beta_1 x_1 + \beta_2 x_2 + \beta_{11} x_1^2 + \beta_{22} x_2^2 + \beta_{12} x_1 x_2 + \varepsilon$$

In this model it can be shown that  $SS_E = 12,479.8$ . Because the number of model parameters,  $p$ , equals 6, the estimate of  $\sigma^2$  based on this model is

$$\hat{\sigma}^2 = \frac{12,479.8}{14 - 6} = 1559.975$$

This estimate of  $\sigma^2$  is actually larger than the estimate obtained from the first-order model, suggesting that the first-order model is superior to the quadratic in that there is less unexplained variability resulting from the first-order fit. If replicate runs are available

(that is, more than one observation on  $y$  at the same  $x$ -levels), then a model-independent estimate of  $\sigma^2$  can be obtained. We will show how to do this in Section 2.7.4.

## 2.4 HYPOTHESIS TESTING IN MULTIPLE REGRESSION

In multiple linear regression problems, certain tests of hypotheses about the model parameters are helpful in measuring the usefulness of the model. In this section, we describe several important hypothesis-testing procedures. These procedures require that the errors  $\varepsilon_i$  in the model be normally and independently distributed with mean zero and variance  $\sigma^2$ , abbreviated  $\varepsilon \sim \text{NID}(0, \sigma^2)$ . As a result of this assumption, the observations  $y_i$  are normally and independently distributed with mean  $\beta_0 + \sum_{j=1}^k \beta_j x_{ij}$  and variance  $\sigma^2$ .

### 2.4.1 Test for Significance of Regression

The test for significance of regression is a test to determine if there is a linear relationship between the response variable  $y$  and a subset of the regressor variables  $x_1, x_2, \dots, x_k$ . The appropriate hypotheses are

$$\begin{aligned} H_0: \beta_1 &= \beta_2 = \dots = \beta_k = 0 \\ H_1: \beta_j &\neq 0 \text{ for at least one } j \end{aligned} \quad (2.19)$$

Rejection of  $H_0$  in Equation 2.19 implies that at least one of the regressor variables  $x_1, x_2, \dots, x_k$  contributes significantly to the model. The test procedure involves partitioning the total sum of squares  $SS_T = \sum_{i=1}^n (y_i - \bar{y})^2$  into a sum of squares due to the model (or to regression) and a sum of squares due to residual (or error), say

$$SS_T = SS_R + SS_E \quad (2.20)$$

Now if the null hypothesis  $H_0: \beta_1 = \beta_2 = \dots = \beta_k = 0$  is true, then  $SS_R/\sigma^2$  is distributed as  $\chi_k^2$ , where the number of degrees of freedom for  $\chi^2$  is equal to the number of regressor variables in the model. Also, we can show that  $SS_E/\sigma^2$  is distributed as  $\chi_{n-k-1}^2$  and that  $SS_E$  and  $SS_R$  are independent. The test procedure for  $H_0: \beta_1 = \beta_2 = \dots = \beta_k = 0$  is to compute

$$F_0 = \frac{SS_R/k}{SS_E/(n-k-1)} = \frac{MS_R}{MS_E} \quad (2.21)$$

and to reject  $H_0$  if  $F_0$  exceeds  $F_{\alpha, k, n-k-1}$ . Alternatively, one could use the  $P$ -value approach to hypothesis testing and, thus, reject  $H_0$  if the  $P$ -value for the statistic  $F_0$  is less than  $\alpha$ . The test is usually summarized in a table such as Table 2.5. This test procedure is called an **analysis of variance (ANOVA)** because it is based on a decomposition of the total variability in the response variable  $y$ .

A computational formula for  $SS_R$  may be found easily. We have derived a computational formula for  $SS_E$  in Equation 2.17—that is,

$$SS_E = \mathbf{y}'\mathbf{y} - \mathbf{b}'\mathbf{X}'\mathbf{y}$$

**TABLE 2.5 Analysis of Variance for Significance of Regression in Multiple Regression**

Source of Variation	Sum of Squares	Degrees of Freedom	Mean Square	$F_0$
Regression	$SS_R$	$k$	$MS_R$	$MS_R/MS_E$
Error or residual	$SS_E$	$n - k - 1$	$MS_E$	
Total	$SS_T$	$n - 1$		

Now because  $SS_T = \sum_{i=1}^n y_i^2 - (\sum_{i=1}^n y_i)^2/n = \mathbf{y}'\mathbf{y} - (\sum_{i=1}^n y_i)^2/n$ , we may rewrite the foregoing equation as

$$SS_E = \mathbf{y}'\mathbf{y} - \frac{\left(\sum_{i=1}^n y_i\right)^2}{n} - \left[ \mathbf{b}'\mathbf{X}'\mathbf{y} - \frac{\left(\sum_{i=1}^n y_i\right)^2}{n} \right]$$

or

$$SS_E = SS_T - SS_R$$

Therefore, the regression sum of squares is

$$SS_R = \mathbf{b}'\mathbf{X}'\mathbf{y} - \frac{\left(\sum_{i=1}^n y_i\right)^2}{n} \quad (2.22)$$

and the error sum of squares is

$$SS_E = \mathbf{y}'\mathbf{y} - \mathbf{b}'\mathbf{X}'\mathbf{y} \quad (2.23)$$

and the total sum of squares is

$$SS_T = \mathbf{y}'\mathbf{y} - \frac{\left(\sum_{i=1}^n y_i\right)^2}{n} \quad (2.24)$$

**Example 2.3 The Transistor Gain Data** We will test for significance of regression using the model fit to the transistor gain data for Example 2.1. Note that

$$\begin{aligned} SS_T &= \mathbf{y}'\mathbf{y} - \frac{\left(\sum_{i=1}^{14} y_i\right)^2}{14} \\ &= 22,527,889.0 - \frac{(17,495)^2}{14} \\ &= 665,387.2 \end{aligned}$$

$$\begin{aligned}
 SS_R &= \mathbf{b}' \mathbf{X}' \mathbf{y} - \frac{\left( \sum_{i=1}^{14} y_i \right)^2}{14} \\
 &= 22,514,467.9 - 21,862,501.8 \\
 &= 651,966.1
 \end{aligned}$$

and

$$\begin{aligned}
 SS_E &= SS_T - SS_R \\
 &= 665,387.2 - 651,966.1 \\
 &= 13,421.1
 \end{aligned}$$

The analysis of variance is shown in Table 2.6. If we select  $\alpha = 0.05$ , then we reject  $H_0: \beta_1 = \beta_2 = 0$  because  $F_0 = 267.2 > F_{0.05,2,11} = 3.98$ . Also, note that the  $P$ -value for  $F_0$  (shown in Table 2.6) is considerably smaller than  $\alpha = 0.05$ . Finally, compare the ANOVA in Table 2.6 to the one in the JMP output in Table 2.4. There is a small difference in the “regression sum of squares” in the two tables. This is due to round-off again.

The coefficient of multiple determination  $R^2$  is defined as

$$R^2 = \frac{SS_R}{SS_T} = 1 - \frac{SS_E}{SS_T} \quad (2.25)$$

$R^2$  is a measure of the amount of reduction in the variability of  $y$  obtained by using the regressor variables  $x_1, x_2, \dots, x_k$  in the model. From inspection of the analysis of the variance identity equation (Eq. 2.20) we see that  $0 \leq R^2 \leq 1$ . However, a large value of  $R^2$  does not necessarily imply that the regression model is good one. Adding a variable to the model will always increase  $R^2$ , regardless of whether the additional variable is statistically significant or not. Thus it is possible for models that have large values of  $R^2$  to yield poor predictions of new observations or estimates of the mean response.

To illustrate, consider the first-order model for the transistor gain data. The value of  $R^2$  for this model is

$$R^2 = \frac{SS_R}{SS_T} = \frac{651,966.1}{665,387.2} = 0.9798$$

That is, the first-order model explains about 97.98% of the variability observed in the gain. Now if we add quadratic terms to this model, we can show that the value of  $R^2$  increases to

TABLE 2.6 Test for Significance of Regression, Example 2.3

Source of Variation	Sum of Squares	Degrees of Freedom	Mean Square	$F_0$	$P$ -Value
Regression	651,996.1	2	325,983.0	267.2	$4.74 \times 10^{-10}$
Error	13,421.1	11	1220.1		
Total	665,387.2	13			

0.9812. This increase in  $R^2$  is relatively small, suggesting that the quadratic terms do not really improve the model. The JMP output in Table 2.4 reports the  $R^2$  statistic.

Because  $R^2$  always increases as we add terms to the model, some regression model builders prefer to use an adjusted  $R^2$  statistic defined as

$$R_{\text{adj}}^2 = 1 - \frac{SS_E/(n-p)}{SS_T/(n-1)} = 1 - \frac{n-1}{n-p}(1-R^2) \quad (2.26)$$

In general, the adjusted  $R^2$  statistic will not always increase as variables are added to the model. In fact, if unnecessary terms are added, the value of  $R_{\text{adj}}^2$  will often decrease.

For example, consider the transistor gain data. The adjusted  $R^2$  for the first-order model is

$$\begin{aligned} R_{\text{adj}}^2 &= 1 - \frac{n-1}{n-p}(1-R^2) \\ &= 1 - \frac{13}{11}(1-0.9798) \\ &= 0.9762 \end{aligned}$$

which is very close to the ordinary  $R^2$  for the first-order model (JMP reports the adjusted  $R^2$  statistic—refer to Table 2.4). When  $R^2$  and  $R_{\text{adj}}^2$  differ dramatically, there is a good chance that nonsignificant terms have been included in the model. Now when the quadratic terms are added to the first-order model, we can show that  $R_{\text{adj}}^2 = 0.9695$ ; that is, the adjusted  $R^2$  actually decreases when the quadratic terms are included in the model. This is a strong indication that the quadratic terms are unnecessary.

## 2.4.2 Tests on Individual Regression Coefficients and Groups of Coefficients

**Individual Regression Coefficients** We are frequently interested in testing hypotheses on the individual regression coefficients. Such tests would be useful in determining the value of each of the regressor variables in the regression model. For example, the model might be more effective with the inclusion of additional variables, or perhaps with the deletion of one or more of the variables already in the model.

Adding a variable to the regression model always causes the sum of squares for regression to increase and the error sum of squares to decrease. We must decide whether the increase in the regression sum of squares is sufficient to warrant using the additional variable in the model. Furthermore, adding an unimportant variable to the model can actually increase the mean square error, thereby decreasing the usefulness of the model.

The hypotheses for testing the significance of any individual regression coefficient, say  $\beta_j$ , are

$$H_0: \beta_j = 0$$

$$H_1: \beta_j \neq 0$$

If  $H_0: \beta_j = 0$  is not rejected, then this indicates that  $x_j$  can be deleted from the model. The test statistic for this hypothesis is

$$t_0 = \frac{b_j}{\sqrt{\hat{\sigma}^2 C_{jj}}} \quad (2.27)$$

where  $C_{jj}$  is the diagonal element of  $(\mathbf{X}'\mathbf{X})^{-1}$  corresponding to  $b_j$ . The null hypothesis  $H_0: \beta_j = 0$  is rejected if  $|t_0| > t_{\alpha/2, n-k-1}$ . A  $P$ -value approach could also be used. See Montgomery et al. (2006) for more details. Note that this is really a partial or marginal test, because the regression coefficient  $b_j$  depends on all the other regressor variables  $x_i$  ( $i \neq j$ ) that are in the model.

The denominator of Equation 2.27,  $\sqrt{\hat{\sigma}^2 C_{jj}}$ , is often called the **standard error** of the regression coefficient  $b_j$ . That is,

$$se(b_j) = \sqrt{\hat{\sigma}^2 C_{jj}} \quad (2.28)$$

Therefore, an equivalent way to write the test statistic in Equation 2.27 is

$$t_0 = \frac{b_j}{se(b_j)} \quad (2.29)$$

#### Example 2.4 Tests on Individual Regression Coefficients for the Transistor Gain

**Data** Consider the regression model for the transistor gain data. We will construct the  $t$ -statistic for the hypotheses  $H_0: \beta_1 = 0$  and  $H_0: \beta_2 = 0$ . The main diagonal elements of  $(\mathbf{X}'\mathbf{X})^{-1}$  corresponding to  $\beta_1$  and  $\beta_2$  are  $C_{11} = 0.165954$  and  $C_{22} = 0.142876$ , respectively, so the two  $t$ -statistics are computed as follows:

$$\begin{aligned} \text{For } H_0: \beta_1 = 0: \quad t_0 &= \frac{b_2}{\sqrt{\hat{\sigma}^2 C_{11}}} \\ &= \frac{323.4}{\sqrt{(1220.1)(0.165954)}} = \frac{323.4}{14.2} = 22.73 \\ \text{For } H_0: \beta_2 = 0: \quad t_0 &= \frac{b_2}{\sqrt{\hat{\sigma}^2 C_{22}}} = \frac{-54.8}{\sqrt{(1220.1)(0.142876)}} \\ &= \frac{-54.8}{13.2} = -4.15 \end{aligned}$$

The absolute values of these  $t$ -statistics are compared with  $t_{0.025, 11} = 2.201$  (assuming that we select  $\alpha = 0.05$ ). Both magnitudes of the  $t$ -statistics are larger than this criterion. Consequently we conclude that  $\beta_1 \neq 0$ , which implies that  $x_1$  contributes significantly to the model given that  $x_2$  is included, and that  $\beta_2 \neq 0$ , which implies that  $x_2$  contributes significantly to the model given that  $x_1$  is included. JMP (refer to Table 2.4) provides the  $t$ -statistics for each regression coefficient. A  $P$ -value approach is used for statistical testing. The  $P$ -values for the two test statistics reported above are small (less than 0.05, say) indicating that both variables contribute significantly to the model.

**Tests as Groups of Coefficients** We may also directly examine the contribution to the regression sum of squares for a particular variable, say  $x_j$ , given that other variables  $x_i$  ( $i \neq j$ ) are included in the model. The procedure used to do this is called the **extra**

**sum of squares method.** This procedure can also be used to investigate the contribution of a *subset* of the regressor variables to the model. Consider the regression model with  $k$  regressor variables:

$$\mathbf{y} = \mathbf{X}\boldsymbol{\beta} + \boldsymbol{\epsilon}$$

where  $\mathbf{y}$  is  $n \times 1$ ,  $\mathbf{X}$  is  $n \times p$ ,  $\boldsymbol{\beta}$  is  $p \times 1$ ,  $\boldsymbol{\epsilon}$  is  $n \times 1$ , and  $p = k + 1$ . We would like to determine if the subset of regressor variables  $x_1, x_2, \dots, x_r$  ( $r < k$ ) contribute significantly to the regression model. Let the vector of regression coefficients be partitioned as follows:

$$\boldsymbol{\beta} = \begin{bmatrix} \boldsymbol{\beta}_1 \\ \boldsymbol{\beta}_2 \end{bmatrix}$$

where  $\boldsymbol{\beta}_1$  is  $r \times 1$ , and  $\boldsymbol{\beta}_2$  is  $(p - r) \times 1$ . We wish to test the hypotheses

$$\begin{aligned} H_0: \boldsymbol{\beta}_1 &= \mathbf{0} \\ H_1: \boldsymbol{\beta}_1 &\neq \mathbf{0} \end{aligned} \tag{2.30}$$

The model may be written as

$$\mathbf{y} = \mathbf{X}\boldsymbol{\beta} + \boldsymbol{\epsilon} = \mathbf{X}_1\boldsymbol{\beta}_1 + \mathbf{X}_2\boldsymbol{\beta}_2 + \boldsymbol{\epsilon} \tag{2.31}$$

where  $\mathbf{X}_1$  represents the columns of  $\mathbf{X}$  associated with  $\boldsymbol{\beta}_1$ , and  $\mathbf{X}_2$  represents the columns of  $\mathbf{X}$  associated with  $\boldsymbol{\beta}_2$ .

For the **full model** (including both  $\boldsymbol{\beta}_1$  and  $\boldsymbol{\beta}_2$ ), we know that  $\mathbf{b} = (\mathbf{X}'\mathbf{X})^{-1}\mathbf{X}'\mathbf{y}$ . Also, the regression sum of squares for all variables including the intercept is

$$SS_R(\boldsymbol{\beta}) = \mathbf{b}'\mathbf{X}'\mathbf{y} \quad (p \text{ degrees of freedom})$$

and

$$MS_E = \frac{\mathbf{y}'\mathbf{y} - \mathbf{b}'\mathbf{X}'\mathbf{y}}{n - p}$$

$SS_R(\boldsymbol{\beta})$  is called the regression sum of squares due to  $\boldsymbol{\beta}$ . To find the contribution of the terms in  $\boldsymbol{\beta}_1$  to the regression, fit the model assuming the null hypothesis  $H_0: \boldsymbol{\beta}_1 = \mathbf{0}$  to be true. The **reduced model** is found from Equation 2.31 with  $\boldsymbol{\beta}_1 = \mathbf{0}$ :

$$\mathbf{y} = \mathbf{X}_2\boldsymbol{\beta}_2 + \boldsymbol{\epsilon} \tag{2.32}$$

The least squares estimator of  $\boldsymbol{\beta}_2$  is  $\mathbf{b}_2 = (\mathbf{X}'_2\mathbf{X}_2)^{-1}\mathbf{X}'_2\mathbf{y}$ , and

$$SS_R(\boldsymbol{\beta}_2) = \mathbf{b}'_2\mathbf{X}'_2\mathbf{y} \quad (p - r \text{ degrees of freedom}) \tag{2.33}$$

The regression sum of squares due to  $\boldsymbol{\beta}_1$  given that  $\boldsymbol{\beta}_2$  is already in the model is

$$SS_R(\boldsymbol{\beta}_1|\boldsymbol{\beta}_2) = SS_R(\boldsymbol{\beta}) - SS_R(\boldsymbol{\beta}_2) \tag{2.34}$$

This sum of squares has  $r$  degrees of freedom. It is often called the **extra sum of squares** due to  $\boldsymbol{\beta}_1$ . Note that  $SS_R(\boldsymbol{\beta}_1|\boldsymbol{\beta}_2)$  is the increase in the regression sum of squares due to

including the variables  $x_1, x_2, \dots, x_r$  in the model. Now  $SS_R(\beta_1 | \beta_2)$  is independent of  $MS_E$ , and the null hypothesis  $\beta_1 = \mathbf{0}$  may be tested by the statistic

$$F_0 = \frac{SS_R(\beta_1 | \beta_2) / r}{MS_E} \quad (2.35)$$

If  $F_0 > F_{\alpha, r, n-p}$ , we reject  $H_0$ , concluding that at least one of the parameters in  $\beta_1$  is not zero and, consequently, at least one of the variables  $x_1, x_2, \dots, x_r$  in  $\mathbf{X}_1$  contributes significantly to the regression model (one could also use the  $P$ -value approach). Some authors call the test in Equation 2.35 a **partial  $F$ -test**.

The partial  $F$ -test is very useful. We can use it to measure the contribution of  $x_j$  as if it were the last variable added to the model by computing

$$SS_R(\beta_j | \beta_0, \beta_1, \dots, \beta_{j-1}, \beta_{j+1}, \dots, \beta_k)$$

This is the increase in the regression sum of squares due to adding  $x_j$  to a model that already includes  $x_1, \dots, x_{j-1}, x_{j+1}, \dots, x_k$ . Note that the partial  $F$ -test on a single variable  $x_j$  is equivalent to the  $t$ -test in Equation 2.27. However, the partial  $F$ -test is a more general procedure in that we can measure the effect of sets of variables. This procedure is used often in response surface work. For example, suppose that we are considering fitting the second-order model

$$y = \beta_0 + \beta_1 x_1 + \beta_2 x_2 + \beta_{11} x_1^2 + \beta_{22} x_2^2 + \beta_{12} x_1 x_2 + \varepsilon$$

and we wish to test the contribution of the second-order terms over and above the contribution from the first-order model. Therefore, the hypotheses of interest are

$$\begin{aligned} H_0: \beta_{11} &= \beta_{22} = \beta_{12} = 0 \\ H_1: \beta_{11} &\neq 0 \quad \text{and/or} \quad \beta_{22} \neq 0 \quad \text{and/or} \quad \beta_{12} \neq 0 \end{aligned}$$

In the notation of this section,  $\beta'_1 = [\beta_{11}, \beta_{22}, \beta_{12}]$  and  $\beta'_2 = [\beta_0, \beta_1, \beta_2]$ , and the columns of  $\mathbf{X}_1$  and  $\mathbf{X}_2$  are the columns of the original  $\mathbf{X}$  matrix associated with the quadratic and linear terms in the model, respectively.

**Example 2.5 Partial  $F$ -tests for the Transistor Gain Data** Consider the transistor gain data in Example 2.1. Suppose that we wish to investigate the contribution of the variable  $x_2$  (dose) to the model. That is, the hypotheses we wish to test are

$$\begin{aligned} H_0: \beta_2 &= 0 \\ H_1: \beta_2 &\neq 0 \end{aligned}$$

This will require the extra sum of squares due to  $\beta_2$ , or

$$\begin{aligned} SS_R(\beta_2 | \beta_1, \beta_0) &= SS_R(\beta_0, \beta_1, \beta_2) - SS_R(\beta_0, \beta_1) \\ &= SS_R(\beta_1, \beta_2 | \beta_0) - SS_R(\beta_1 | \beta_0) \end{aligned}$$

Now from Example 2.3 where we tested for significance of regression, we have (from Table 2.6)

$$SS_R(\beta_1, \beta_2 | \beta_0) = 651,966.1$$

This sum of squares has two degrees of freedom. The reduced model is

$$y = \beta_0 + \beta_1 x_1 + \varepsilon$$

The least squares fit for this model is

$$\hat{y} = 1245.8 + 323.6x_1$$

and the regression sum of squares for this model (with one degree of freedom) is

$$SS_R(\beta_1 | \beta_0) = 630,967.9$$

Therefore,

$$\begin{aligned} SS_R(\beta_2 | \beta_0, \beta_1) &= 651,966.1 - 630,967.9 \\ &= 20,998.2 \end{aligned}$$

with  $2 - 1 = 1$  degree of freedom. This is the increase in the regression sum of squares that results from adding  $x_2$  to a model already containing  $x_1$  (or the extra sum of squares that results from adding  $x_2$  to a model containing  $x_1$ ). To test  $H_0: \beta_2 = 0$ , from the test statistic we obtain

$$F_0 = \frac{SS_R(\beta_2 | \beta_0, \beta_1)/1}{MS_E} = \frac{20,998.2/1}{1220.1} = 17.21$$

Note that  $MS_E$  from the full model (Table 2.6) is used in the denominator of  $F_0$ . Now because  $F_{0.05,1,11} = 4.84$ , we reject  $H_0: \beta_2 = 0$  and conclude that  $x_2$  (dose) contributes significantly to the model.

Because this partial  $F$ -test involves only a single regressor, it is equivalent to the  $t$ -test introduced earlier, because the square of a  $t$  random variable with  $v$  degrees of freedom is an  $F$  random variable with 1 and  $v$  degrees of freedom. To see this, recall that the  $t$ -statistic for  $H_0: \beta_2 = 0$  resulted in  $t_0 = -4.15$  and that  $t_0^2 = (-4.15)^2 = 17.22 \cong F_0$ .

## 2.5 CONFIDENCE INTERVALS IN MULTIPLE REGRESSION

It is often beneficial to construct confidence interval estimates for the regression coefficients  $\{\beta_j\}$  and for other quantities of interest from the regression model. The development of a procedure for obtaining these confidence intervals requires that we assume the errors  $\{\varepsilon_i\}$  to be normally and independently distributed with mean zero and variance  $\sigma^2$ , the same assumption made in the section on hypothesis testing (Section 2.4).

### 2.5.1 Confidence Intervals on the Individual Regression Coefficients $\beta$

Because the least squares estimator  $\mathbf{b}$  is a linear combination of the observations, it follows that  $\mathbf{b}$  is normally distributed with mean vector  $\boldsymbol{\beta}$  and covariance matrix  $\sigma^2(\mathbf{X}'\mathbf{X})^{-1}$ . Then each of the statistics

$$\frac{b_j - \beta_j}{\sqrt{\hat{\sigma}^2 C_{jj}}}, \quad j = 0, 1, \dots, k \quad (2.36)$$

is distributed as  $t$  with  $n - p$  degrees of freedom, where  $C_{jj}$  is the  $(j, j)$ th element of the matrix  $(\mathbf{X}'\mathbf{X})^{-1}$ , and  $\hat{\sigma}^2$  is the estimate of the error variance, obtained from Equation 2.18. Therefore, a  $100(1 - \alpha)\%$  confidence interval for the regression coefficient  $\beta_j, j = 0, 1, \dots, k$ , is

$$b_j - t_{\alpha/2, n-p} \sqrt{\hat{\sigma}^2 C_{jj}} \leq \beta_j \leq b_j + t_{\alpha/2, n-p} \sqrt{\hat{\sigma}^2 C_{jj}} \quad (2.37)$$

Note that this confidence interval can also be written as

$$b_j - t_{\alpha/2, n-p} se(b_j) \leq \beta_j \leq b_j + t_{\alpha/2, n-p} se(b_j)$$

because  $se(b_j) = \sqrt{\hat{\sigma}^2 C_{jj}}$ .

**Example 2.6 The Transistor Gain Data** We will construct a 95% confidence interval for the parameter  $\beta_1$  in Example 2.1. Now  $b_1 = 323.4$ , and because  $\hat{\sigma}^2 = 1220.1$  and  $C_{11} = 0.165954$ , we find that

$$\begin{aligned} b_1 - t_{0.025, 11} \sqrt{\hat{\sigma}^2 C_{11}} &\leq \beta_1 \leq b_1 + t_{0.025, 11} \sqrt{\hat{\sigma}^2 C_{11}} \\ 323.4 - 2.201 \sqrt{(1220.1)(0.165954)} &\leq \beta_1 \leq 323.4 + 2.201 \sqrt{(1220.1)(0.165954)} \\ 323.4 - 2.201(14.2) &\leq \beta_1 \leq 323.4 + 2.201(14.2) \end{aligned}$$

and the 95% confidence interval on  $\beta_1$  is

$$292.1 \leq \beta_1 \leq 354.7$$

### 2.5.2 A Joint Confidence Region on the Regression Coefficients $\beta$

The confidence intervals in the previous subsection should be thought of as one-at-a-time intervals; that is, the confidence coefficient  $1 - \alpha$  applies only to one such interval. Some problems require that several confidence intervals be constructed from the same data. In such cases, the analyst is usually interested in specifying a confidence coefficient that applies to the entire set of confidence intervals. Such intervals are called **simultaneous confidence intervals**.

It is relatively easy to specify a **joint confidence region** for the parameters  $\beta$  in a multiple regression model. We may show that

$$\frac{(\mathbf{b} - \boldsymbol{\beta})' \mathbf{X}' \mathbf{X} (\mathbf{b} - \boldsymbol{\beta})}{pMS_E}$$

has an  $F$ -distribution with  $p$  numerator and  $n - p$  denominator degrees of freedom, and this implies that

$$P\left\{ \frac{(\mathbf{b} - \boldsymbol{\beta})' \mathbf{X}' \mathbf{X} (\mathbf{b} - \boldsymbol{\beta})}{pMS_E} \leq F_{\alpha, p, n-p} \right\} = 1 - \alpha$$

Consequently a  $100(1 - \alpha)\%$  point confidence region for all the parameters in  $\beta$  is

$$\frac{(\mathbf{b} - \boldsymbol{\beta})' \mathbf{X}' \mathbf{X} (\mathbf{b} - \boldsymbol{\beta})}{pMS_E} \leq F_{\alpha, p, n-p} \quad (2.38)$$

This inequality describes an elliptically shaped region, Montgomery, Peck, and Vining (2006) and Myers (1990) demonstrate the construction of this region for  $p = 2$ . When there are only two parameters, finding this region is relatively simple; however, when more than two parameters are involved, the construction problem is considerably harder.

There are other methods for finding joint or simultaneous intervals on regression coefficients, Montgomery, Peck, and Vining (2006) and Myers (1990) discuss and illustrate many of these methods. They also present methods for finding several other types of interval estimates.

### 2.5.3 Confidence Interval on the Mean Response

We may also obtain a confidence interval on the mean response at a particular point, say,  $x_{01}, x_{02}, \dots, x_{0k}$ . Define the vector

$$\mathbf{x}_0 = \begin{bmatrix} 1 \\ x_{01} \\ x_{02} \\ \vdots \\ x_{0k} \end{bmatrix}$$

The mean response at this point is

$$\mu_{y|x_0} = \beta_0 + \beta_1 x_{01} + \beta_2 x_{02} + \dots + \beta_k x_{0k} = \mathbf{x}'_0 \boldsymbol{\beta}$$

The estimated mean response at this point is

$$\hat{y}(\mathbf{x}_0) = \mathbf{x}'_0 \mathbf{b} \quad (2.39)$$

This estimator is unbiased, because  $E[\hat{y}_i(\mathbf{x}_0)] = E(\mathbf{x}'_0 \mathbf{b}) = \mathbf{x}'_0 \boldsymbol{\beta} = \mu_{y|x_0}$ , and the variance of  $\hat{y}_i(\mathbf{x}_0)$  is

$$\text{Var}[\hat{y}(\mathbf{x}_0)] = \sigma^2 \mathbf{x}'_0 (\mathbf{X}' \mathbf{X})^{-1} \mathbf{x}_0 \quad (2.40)$$

Therefore, a  $100(1 - \alpha)\%$  confidence interval on the mean response at the point  $x_{01}, x_{02}, \dots, x_{0k}$  is

$$\begin{aligned}\hat{y}(\mathbf{x}_0) - t_{\alpha/2, n-p} \sqrt{\hat{\sigma}^2 \mathbf{x}'_0 (\mathbf{X}' \mathbf{X})^{-1} \mathbf{x}_0} \\ \leq \mu_{y|\mathbf{x}_0} \leq \hat{y}(\mathbf{x}_0) + t_{\alpha/2, n-p} \sqrt{\hat{\sigma}^2 \mathbf{x}'_0 (\mathbf{X}' \mathbf{X})^{-1} \mathbf{x}_0}\end{aligned}\quad (2.41)$$

**Example 2.7 The Transistor Gain Data** Suppose that we wish to find a 95% confidence interval on the mean response for the transistor gain problem for the point  $\xi_1 = 225$  min and  $\xi_2 = 4.36 \times 10^{14}$  ions. In terms of the coded variables  $x_1$  and  $x_2$ , this point corresponds to

$$\mathbf{x}_0 = \begin{bmatrix} 1 \\ 0 \\ 0 \end{bmatrix}$$

because  $x_{01} = 0$  and  $x_{02} = 0$ . The estimate of the mean response at this point is computed from Equation 2.39 as

$$\hat{y}(\mathbf{x}_0) = \mathbf{x}'_0 \mathbf{b} = [1, 0, 0] \begin{bmatrix} 1242.3 \\ 323.4 \\ -54.8 \end{bmatrix} = 1242.3$$

Now from Equation 2.40, we find  $\text{Var}[\hat{y}(\mathbf{x}_0)]$  as

$$\begin{aligned}\text{Var}[\hat{y}(\mathbf{x}_0)] &= \sigma^2 \mathbf{x}'_0 (\mathbf{X}' \mathbf{X})^{-1} \mathbf{x}_0 \\ &= \sigma^2 [1, 0, 0] \begin{bmatrix} 0.072027 & -0.00195 & 0.009067 \\ -0.00195 & 0.165954 & 0.000408 \\ 0.009067 & 0.000408 & 0.142876 \end{bmatrix} \begin{bmatrix} 1 \\ 0 \\ 0 \end{bmatrix} \\ &= \sigma^2 (0.072027)\end{aligned}$$

Using  $\hat{\sigma}^2 = MS_E = 1220.1$  and Equation 2.41, we find the confidence interval as

$$\begin{aligned}\hat{y}(\mathbf{x}_0) - t_{\alpha/2, n-p} \sqrt{\hat{\sigma}^2 \mathbf{x}'_0 (\mathbf{X}' \mathbf{X})^{-1} \mathbf{x}_0} &\leq \mu_{y|\mathbf{x}_0} \leq \hat{y}(\mathbf{x}_0) \\ + t_{\alpha/2, n-p} \sqrt{\hat{\sigma}^2 \mathbf{x}'_0 (\mathbf{X}' \mathbf{X})^{-1} \mathbf{x}_0} &1242.3 \\ - 2.201 \sqrt{1220.1(0.072027)} &\leq \mu_{y|\mathbf{x}_0} \leq 1242.3 \\ + 2.201 \sqrt{1220.1(0.072027)} &1242.3 \\ - 20.6 &\leq \mu_{y|\mathbf{x}_0} \leq 1242.3 + 20.6\end{aligned}$$

or

$$1221.7 \leq \mu_{y|x_0} \leq 1262.9$$

## 2.6 PREDICTION OF NEW RESPONSE OBSERVATIONS

A regression model can be used to predict future observations on the response  $y$  corresponding to particular values of the regressor variables, say  $x_{01}, x_{02}, \dots, x_{0k}$ . If  $\mathbf{x}'_0 = [1, x_{01}, x_{02}, \dots, x_{0k}]$ , then a point estimate for the future observation  $y_0$  at the point  $x_{01}, x_{02}, \dots, x_{0k}$  is computed from Equation 2.39:

$$\hat{y}(\mathbf{x}_0) = \mathbf{x}'_0 \mathbf{b}$$

A  $100(1 - \alpha)\%$  prediction interval for this future observation is

$$\begin{aligned} & \hat{y}(\mathbf{x}_0) - t_{\alpha/2, n-p} \sqrt{\hat{\sigma}^2(1 + \mathbf{x}'_0 (\mathbf{X}' \mathbf{X})^{-1} \mathbf{x}_0)} \\ & \leq y_0 \leq \hat{y}(\mathbf{x}_0) + t_{\alpha/2, n-p} \sqrt{\hat{\sigma}^2(1 + \mathbf{x}'_0 (\mathbf{X}' \mathbf{X})^{-1} \mathbf{x}_0)} \end{aligned} \quad (2.42)$$

The additional  $\hat{\sigma}^2$  term under the square root sign is due to variability of observations around the predicted mean at that location.

In predicting new observations and in estimating the mean response at a given point  $x_{01}, x_{02}, \dots, x_{0k}$ , one must be careful about extrapolating beyond the region containing the original observations. It is very possible that a model that fits well in the region of the original data will no longer fit well outside of that region. In multiple regression it is often easy to inadvertently extrapolate, since the levels of the variables  $(x_{i1}, x_{i2}, \dots, x_{ik})$ ,

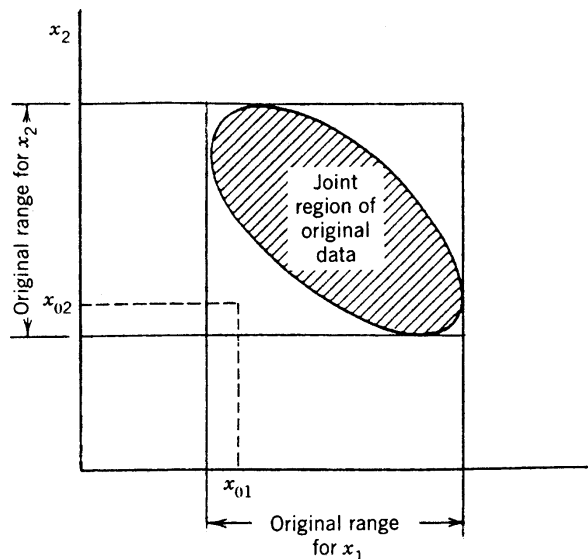


**Figure 2.3** An example of extrapolation in multiple regression.

$i = 1, 2, \dots, n$ , jointly define the region containing the data. As an example, consider Fig. 2.3, which illustrates the region containing the observations for a two-variable regression model. Note that the point  $(x_{01}, x_{02})$  lies within the ranges of both regressor variables  $x_1$  and  $x_2$ , but it is outside the region of the original observations. Thus, either predicting the value of a new observation or estimating the mean response at this point is an extrapolation of the original regression model.

**Example 2.8 A Prediction Interval for the Transistor Gain Data** Suppose that we wish to find a 95% prediction interval on the next observation on the transistor gain at the point  $\xi_1 = 225$  min and  $\xi_2 = 4.36 \times 10^{14}$  ions. In the coded variables, this point is  $x_{01} = 0$  and  $x_{02} = 0$ , so that, as in Example 2.7,  $\mathbf{x}'_0 = [1, 0, 0]$ , and the predicted value of the gain at this point is  $\hat{y}_i(\mathbf{x}_0) = \mathbf{x}'_0 \mathbf{b} = 1242.3$ . From Example 2.7 we know that

$$\mathbf{x}'_0 (\mathbf{X}' \mathbf{X})^{-1} \mathbf{x}_0 = 0.072027$$

Therefore, using Equation 2.42 we can find the 95% prediction interval on  $y_0$  as follows:

$$\begin{aligned} \hat{y}(\mathbf{x}_0) - t_{\alpha/2, n-p} \sqrt{\hat{\sigma}^2(1 + \mathbf{x}'_0 (\mathbf{X}' \mathbf{X})^{-1} \mathbf{x}_0)} &\leq y_0 \leq \hat{y}(\mathbf{x}_0) \\ + t_{\alpha/2, n-p} \sqrt{\hat{\sigma}^2(1 + \mathbf{x}'_0 (\mathbf{X}' \mathbf{X})^{-1} \mathbf{x}_0)} 1242.3 \\ - 2.201 \sqrt{1220.1(1 + 0.072027)} &\leq y_0 \leq 1242.3 \\ + 2.201 \sqrt{1220.1(1 + 0.072027)} 1242.3 \\ - 79.6 &\leq y_0 \leq 1242.3 + 79.6 \end{aligned}$$

or

$$1162.7 \leq y_0 \leq 1321.9$$

If we compare the width of the prediction interval at this point with the width of the confidence interval on the mean gain at the same point from Example 2.7, we observe that the prediction interval is much wider. This reflects the fact that there is more uncertainty in our prediction of an individual future value of a random variable than to estimate the mean of the probability distribution from which that future observation will be drawn.

## 2.7 MODEL ADEQUACY CHECKING

It is always necessary to (a) examine the fitted model to ensure that it provides an adequate approximation to the true system and (b) verify that none of the least squares regression assumptions are violated. Proceeding with exploration and optimization of a fitted response surface will likely give poor or misleading results unless the model provides an adequate fit. In this section we present several techniques for checking model adequacy.

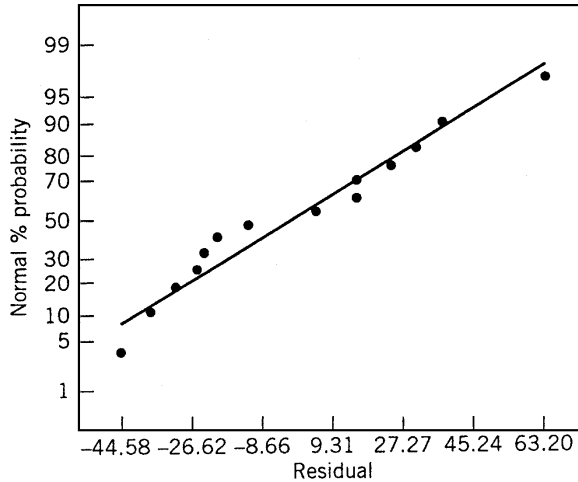


Figure 2.4 Normal probability plot of residuals, Example 2.1.

### 2.7.1 Residual Analysis

The residuals from the least squares fit, defined by  $e_i = y_i - \hat{y}_i$ ,  $i = 1, 2, \dots, n$ , play an important role in judging model adequacy. The residuals from the transistor gain regression model of Example 2.1 are shown in column 3 of Table 2.3.

A check of the normality assumption may be made by constructing a normal probability plot of the residuals, as in Fig. 2.4. If the residuals plot approximately along a straight line, then the normality assumption is satisfied. Figure 2.4 reveals no apparent problem with normality. The straight line in this normal probability plot was determined by eye, concentrating on the central portion of the data. When this plot indicates problems with the normality assumption, we often transform the response variable as a remedial measure. For more details, see Montgomery, Peck, and Vining (2006) and Myers (1990).

Figure 2.5 presents a plot of residuals  $e_i$  versus the predicted response  $\hat{y}_i$  (this plot is also shown in the JMP output in Table 2.4). The general impression is that the residuals

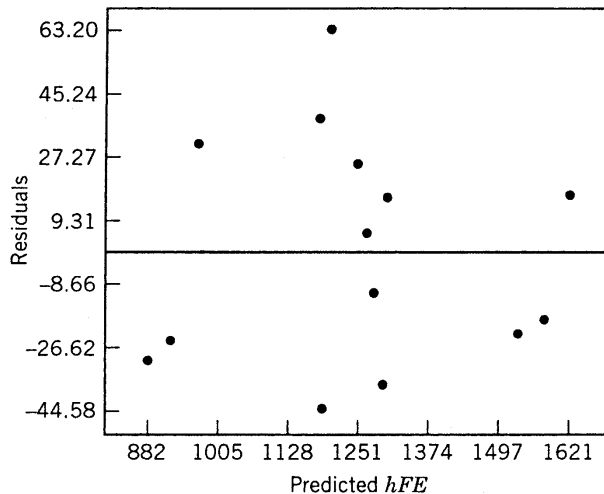


Figure 2.5 Plot of residuals versus predicted response  $\hat{y}_i$ , Example 2.1.

scatter randomly on the display, suggesting that the variance of the original observations is constant for all values of  $y$ . If the variance of the response depends on the mean level of  $y$ , then this plot will often exhibit a funnel-shaped pattern. This is also suggestive of the need for transformation of the response variable  $y$ .

It is also useful to plot the residuals in time or run order and versus each of the individual regressors. Nonrandom patterns on these plots would indicate model inadequacy. In some cases, transformations may stabilize the situation. See Montgomery, Peck, and Vining (2006) and Myers (1990) and Section 2.9 for more details.

## 2.7.2 Scaling Residuals

**Standardized and Studentized Residuals** Many response surface analysts prefer to work with **scaled residuals**, as these scaled residuals often convey more information than do the ordinary least squares residuals.

One type of scaled residual is the **standardized residual**:

$$d_i = \frac{e_i}{\hat{\sigma}}, \quad i = 1, 2, \dots, n \quad (2.43)$$

where we generally use  $\hat{\sigma} = \sqrt{MSE}$  in the computation. These standardized residuals have mean zero and approximately unit variance; consequently, they are useful in looking for **outliers**. Most of the standardized residuals should lie in the interval  $-3 \leq d_i \leq 3$ , and any observation with a standardized residual outside of this interval is potentially unusual with respect to its observed response. These outliers should be carefully examined, because they may represent something as simple as a data recording error or something of more serious concern, such as a region of the regressor variable space where the fitted model is a poor approximation to the true response surface.

The standardizing process in Equation 2.43 scales the residuals by dividing them by their average standard deviation. In some data sets, residuals may have standard deviations that differ greatly. We now present a scaling that takes this into account.

The vector of fitted values  $\hat{y}_i$  corresponding to the observed values  $y_i$  is

$$\begin{aligned} \hat{\mathbf{y}} &= \mathbf{X}\mathbf{b} \\ &= \mathbf{X}(\mathbf{X}'\mathbf{X})^{-1}\mathbf{X}'\mathbf{y} \\ &= \mathbf{H}\mathbf{y} \end{aligned} \quad (2.44)$$

The  $n \times n$  matrix  $\mathbf{H} = \mathbf{X}(\mathbf{X}'\mathbf{X})^{-1}\mathbf{X}'$  is usually called the **hat** matrix because it maps the vector of observed values into a vector of fitted values. The hat matrix and its properties play a central role in regression analysis.

The residuals from the fitted model may be conveniently written in matrix notation as

$$\mathbf{e} = \mathbf{y} - \hat{\mathbf{y}} \quad (2.45)$$

There are several other ways to express the vector of residuals  $\mathbf{e}$  that will prove useful, including

$$\begin{aligned} \mathbf{e} &= \mathbf{y} - \mathbf{X}\mathbf{b} \\ &= \mathbf{y} - \mathbf{H}\mathbf{y} \\ &= (\mathbf{I} - \mathbf{H})\mathbf{y} \end{aligned} \quad (2.46)$$

The hat matrix has several useful properties. It is symmetric ( $\mathbf{H}' = \mathbf{H}$ ) and idempotent ( $\mathbf{H}\mathbf{H} = \mathbf{H}$ ). Similarly the matrix  $\mathbf{I} - \mathbf{H}$  is symmetric and idempotent.

The covariance matrix of the residuals is

$$\begin{aligned}\text{Var}(\mathbf{e}) &= \text{Var}[(\mathbf{I} - \mathbf{H})\mathbf{y}] \\ &= (\mathbf{I} - \mathbf{H})\text{Var}(\mathbf{y})(\mathbf{I} - \mathbf{H})' \\ &= \sigma^2(\mathbf{I} - \mathbf{H})\end{aligned}\tag{2.47}$$

because  $\text{Var}(\mathbf{y}) = \sigma^2\mathbf{I}$  and  $\mathbf{I} - \mathbf{H}$  is symmetric and idempotent. The matrix  $\mathbf{I} - \mathbf{H}$  is generally not diagonal, so the residuals are correlated and have different variances.

The variance of the  $i$ th residual is

$$\text{Var}(e_i) = \sigma^2(1 - h_{ii})\tag{2.48}$$

where  $h_{ii}$  is the  $i$ th diagonal element of  $\mathbf{H}$ . Because  $0 \leq h_{ii} \leq 1$ , using the residual mean square  $MS_E$  to estimate the variance of the residuals actually overestimates  $\text{Var}(e_i)$ . Furthermore, because  $h_{ii}$  is a measure of the location of the  $i$ th point in  $x$ -space, the variance of  $e_i$  depends upon where the point  $\mathbf{x}_i$  lies. Generally, residuals near the center of the  $x$ -space have larger variance than do residuals at more remote locations. Violations of model assumptions are more likely at remote points, and these violations may be hard to detect from inspection of  $e_i$  (or  $d_i$ ) because their residuals will usually be smaller.

We recommend taking this inequality of variance into account when scaling the residuals. We suggest plotting the **studentized residuals**:

$$r_i = \frac{e_i}{\sqrt{\hat{\sigma}^2(1 - h_{ii})}}, \quad i = 1, 2, \dots, n\tag{2.49}$$

with  $\hat{\sigma}^2 = MS_E$  instead of  $e_i$  (or  $d_i$ ). The studentized residuals have constant variance  $\text{Var}(r_i) = 1$  regardless of the location of  $\mathbf{x}_i$  when the form of the model is correct. In many situations the variance of the residuals stabilizes, particularly for large data sets. In these cases there may be little difference between the standardized and studentized residuals. Thus standardized and studentized residuals often convey equivalent information. However, because any point with a large residual and a large  $h_{ii}$  is potentially highly influential on the least squares fit, examination of the studentized residuals is generally recommended.

**PRESS Residuals** The **prediction error sum of squares** (PRESS) proposed by Allen (1971, 1974) provides a useful residual scaling. To calculate PRESS, select an observation—for example,  $i$ . Fit the regression model to the remaining  $n - 1$  observations and use this equation to predict the withheld observation  $y_i$ . Denoting this predicted value by  $\hat{y}_{(i)}$ , we may find the prediction error for point  $i$  as  $e_{(i)} = y_i - \hat{y}_{(i)}$ . The prediction error is often called the  $i$ th PRESS residual. This procedure is repeated for each observation  $i = 1, 2, \dots, n$ , producing a set of  $n$  PRESS residuals  $e_{(1)}, e_{(2)}, \dots, e_{(n)}$ . Then the PRESS statistic is defined as the sum of squares of the  $n$  PRESS residuals as in

$$\text{PRESS} = \sum_{i=1}^n e_{(i)}^2 = \sum_{i=1}^n [y_i - \hat{y}_{(i)}]^2\tag{2.50}$$

Thus PRESS uses each possible subset of  $n - 1$  observations as an estimation data set, and every observation in turn is used to form a prediction data set.

It would initially seem that calculating PRESS requires fitting  $n$  different regressions. However, it is possible to calculate PRESS from the results of a single least squares fit to all  $n$  observations. It turns out that the  $i$ th PRESS residual is

$$e_{(i)} = \frac{e_i}{1 - h_{ii}} \quad (2.51)$$

Thus, because PRESS is just the sum of the squares of the PRESS residuals, a simple computing formula is

$$\text{PRESS} = \sum_{i=1}^n \left( \frac{e_i}{1 - h_{ii}} \right)^2 \quad (2.52)$$

From Equation 2.51 it is easy to see that the PRESS residual is just the ordinary residual weighted according to the diagonal elements of the hat matrix  $h_{ii}$ . Data points for which  $h_{ii}$  are large will have large PRESS residuals. These observations will generally be **high influence** points. Generally, a large difference between the ordinary residual and the PRESS residual will indicate a point where the model fits the data well, but a model built without that point predicts poorly. In the next section we will discuss some other measures of influence.

The variance of the  $i$ th PRESS residual is

$$\begin{aligned} \text{Var}[e_{(i)}] &= \text{Var}\left[\frac{e_i}{1 - h_{ii}}\right] \\ &= \frac{1}{(1 - h_{ii})^2} \sigma^2 (1 - h_{ii}) \\ &= \frac{\sigma^2}{1 - h_{ii}} \end{aligned} \quad (2.53)$$

so that standardized PRESS residual is

$$\begin{aligned} \frac{e_{(i)}}{\sqrt{\text{Var}[e_{(i)}]}} &= \frac{e_i / (1 - h_{ii})}{\sqrt{\sigma^2 / (1 - h_{ii})}} \\ &= \frac{e_i}{\sqrt{\sigma^2 (1 - h_{ii})}} \end{aligned}$$

which, if we use  $MS_E$  to estimate  $\sigma^2$ , is just the studentized residual discussed previously.

Finally, we note that PRESS can be used to compute an approximate  $R^2$  for prediction, say

$$R_{\text{prediction}}^2 = 1 - \frac{\text{PRESS}}{SS_T} \quad (2.54)$$

This statistic gives some indication of the predictive capability of the regression model. For the transistor gain model we can compute the PRESS residuals using the ordinary residuals

and the values of  $h_{ii}$  found in Table 2.3. The corresponding value of the PRESS statistic is  $\text{PRESS} = 22,225.0$ . Then

$$\begin{aligned} R_{\text{prediction}}^2 &= 1 - \frac{\text{PRESS}}{SS_T} \\ &= 1 - \frac{22,225.0}{665,387.2} \\ &= 0.9666 \end{aligned}$$

Therefore we could expect this model to “explain” about 96.66% of the variability in predicting new observations, as compared to the approximately 97.98% of the variability in the original data explained by the least squares fit. The overall predictive capability of the model based on this criterion seems very satisfactory.

**R Student** The studentized residual  $r_i$  discussed above is often considered an outlier diagnostic. It is customary to use  $MS_E$  as an estimate of  $\sigma^2$  in computing  $r_i$ . This is referred to as **internal scaling** of the residual, because  $MS_E$  is an internally generated estimate of  $\sigma^2$  obtained from fitting the model to all  $n$  observations. Another approach would be to use an estimate of  $\sigma^2$  based on a data set with the  $i$ th observation removed. Denote the estimate of  $\sigma^2$  so obtained by  $S_{(i)}^2$ . We can show that

$$S_{(i)}^2 = \frac{(n-p)MS_E - e_i^2/(1-h_{ii})}{n-p-1} \quad (2.55)$$

The estimate of  $\sigma^2$  in Equation 2.55 is used instead of  $MS_E$  to produce an **externally studentized residual**, usually called **R-student**, given by

$$t_i = \frac{e_i}{\sqrt{S_{(i)}^2(1-h_{ii})}}, \quad i = 1, 2, \dots, n \quad (2.56)$$

Some computer packages refer to *R-student* as the outlier  $T$ .

In many situations,  $t_i$  will differ little from the studentized residual  $r_i$ . However, if the  $i$ th observation is influential, then  $S_{(i)}^2$  can differ significantly from  $MS_E$ , and thus *R-student* will be more sensitive to this point. Furthermore, under the standard assumptions,  $t_i$  has a  $t_{n-p-1}$ -distribution. Thus *R-student* offers a more formal procedure for outlier detection via hypothesis testing. One could use a simultaneous inference procedure called the **Bonferroni approach** and compare all  $n$  values of  $[t_i]$  with  $t_{(\alpha/2n),n-p-1}$  to provide guidance regarding outliers. However, it is our view that a formal approach is usually not necessary and that only relatively crude cutoff values need be considered. In general, a diagnostic view as opposed to a strict statistical hypothesis-testing view is best. Furthermore, detection of outliers needs to be considered simultaneously with detection of influential observations.

**Example 2.9 The Transistor Gain Data** Table 2.3 presents the studentized residuals  $r_i$  and the *R-student* values  $t_i$  defined in Equations 2.50 and 2.56 for the transistor

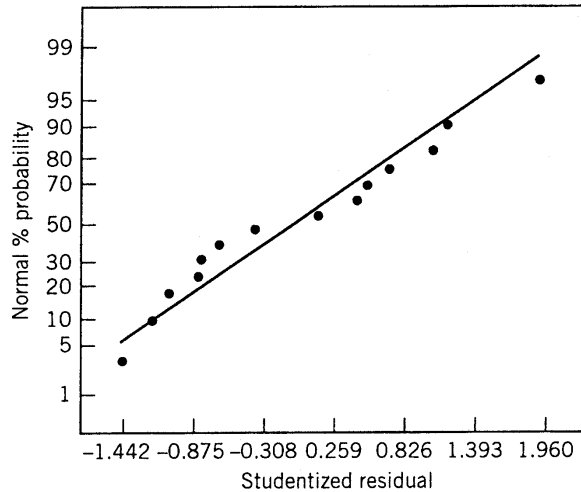


**Figure 2.6** Normal probability plot of the studentized residuals for the transistor gain data.

gain regression model. None of these values are large enough to cause any concern regarding outliers.

Figure 2.6 is a normal probability plot of the studentized residuals. It conveys exactly the same information as the normal probability plot of the ordinary residuals  $e_i$  in Fig. 2.4. This is because most of the  $h_{ii}$ -values are similar and there are no unusually large residuals. In some applications, however, the  $h_{ii}$  can differ considerably, and in those cases plotting the studentized residuals is the best approach.

### 2.7.3 Influence Diagnostics

We occasionally find that a small subset of the data exerts a disproportionate influence on the fitted regression model. That is, parameter estimates or predictions may depend more on the influential subset than on the majority of the data. We would like to locate these influential points and assess their impact on the model. If these influential points are “bad” values, then they should be eliminated. On the other hand, there may be nothing wrong with these points, but if they control key model properties, we would like to know it, because it could affect the use of the model. In this subsection we describe and illustrate several useful measure of influence.

**Leverage Points** The disposition of points in  $x$ -space is important in determining model properties. In particular remote observations potentially have disproportionate leverage on the parameter estimates, the predicted values, and the usual summary statistics.

The hat matrix  $\mathbf{H} = \mathbf{X}(\mathbf{X}'\mathbf{X})^{-1}\mathbf{X}'$  is very useful in identifying influential observations. As noted earlier,  $\mathbf{H}$  determines the variances and covariances of  $\hat{\mathbf{y}}$  and  $\mathbf{e}$ , because  $\text{Var}(\hat{\mathbf{y}}_i) = \sigma^2 \mathbf{H}$  and  $\text{Var}(\mathbf{e}) = \sigma^2(\mathbf{I} - \mathbf{H})$ . The elements  $h_{ij}$  of  $\mathbf{H}$  may be interpreted as the amount of leverage exerted by  $y_j$  on  $\hat{y}_i$ . Thus inspection of the elements of  $\mathbf{H}$  can reveal points that are potentially influential by virtue of their location in  $x$ -space. Attention is usually focused on the diagonal elements  $h_{ii}$ . Because  $\sum_{i=1}^n h_{ii} = \text{rank}(\mathbf{H}) = \text{rank}(\mathbf{X}) = p$ , the average size of the diagonal element of the matrix  $\mathbf{H}$  is  $p/n$ . As a rough guideline, then, if a diagonal element  $h_{ii}$  is greater than  $2p/n$ , observation  $i$  is a

high-leverage point. To apply this to the transistor gain data in Example 2.1, note that  $2p/n = 2(3)/14 = 0.43$ . Table 2.3 gives the hat diagonals  $h_{ii}$  for the first-order model; and because none of the  $h_{ii}$  exceed 0.43, we conclude that there are no leverage points in these data. Further properties and uses of the elements of the hat matrix in regression diagnostics are discussed by Belsley, Kahan, and Welsch (1980).

**Influence on Regression Coefficients** The hat diagonals will identify points that are potentially influential due to their location in  $x$ -space. It is desirable to consider both the location of the point and the response variable in measuring influence. Cook (1977, 1979) has suggested using a measure of the squared distance between the least squares estimate based on all  $n$  points  $\mathbf{b}$  and the estimate obtained by deleting the  $i$ th point, say  $\mathbf{b}_{(i)}$ . This distance measure can be expressed in a general form as

$$D_i(\mathbf{M}, c) = \frac{(\mathbf{b}_{(i)} - \mathbf{b})' \mathbf{M} (\mathbf{b}_{(i)} - \mathbf{b})}{c}, \quad i = 1, 2, \dots, n \quad (2.57)$$

The usual choices of  $\mathbf{M}$  and  $c$  are  $\mathbf{M} = \mathbf{X}'\mathbf{X}$  and  $c = pMS_E$ , so that Equation 2.57 becomes

$$D_i(\mathbf{M}, c) \equiv D_i = \frac{(\mathbf{b}_{(i)} - \mathbf{b})' \mathbf{X}' \mathbf{X} (\mathbf{b}_{(i)} - \mathbf{b})}{pMS_E}, \quad i = 1, 2, \dots, n \quad (2.58)$$

Points with large values of  $D_i$  have considerable influence on the least squares estimates  $\mathbf{b}$ . The magnitude of  $D_i$  may be assessed by comparing it with  $F_{\alpha, p, n-p}$ . If  $D_i \simeq F_{0.5, p, n-p}$ , then deleting point  $i$  would move  $\mathbf{b}$  to the boundary of a 50% confidence region for  $\boldsymbol{\beta}$  based on the complete data set.\* This is a large displacement and indicates that the least squares estimate is sensitive to the  $i$ th data point. Because  $F_{0.5, p, n-p} \simeq 1$ , we usually consider points for which  $D_i > 1$  to be influential. Practical experience has shown the cutoff value of 1 works well in identifying influential points.

The statistic  $D_i$  may be rewritten as

$$D_i = \frac{r_i^2}{p} \frac{\text{Var}[\hat{y}(\mathbf{x}_i)]}{\text{Var}(e_i)} = \frac{r_i^2}{p} \frac{h_{ii}}{1 - h_{ii}}, \quad i = 1, 2, \dots, n \quad (2.59)$$

Thus we see that, apart from the constant  $p$ ,  $D_i$  is the product of the square of the  $i$ th studentized residual and  $h_{ii}/(1 - h_{ii})$ . This ratio can be shown to be the distance from the vector  $\mathbf{x}_i$  to the centroid of the remaining data. Thus  $D_i$  is made up of a component that reflects how well the model fits the  $i$ th observation  $y_i$  and a component that measures how far that point is from the rest of the data. Either component (or both) may contribute to a larger value of  $D_i$ .

Table 2.3 presents the values of  $D_i$  for the first-order model fit to the transistor gain data in Example 2.1. None of these values of  $D_i$  exceed 1, so there is no strong evidence of influential observations in these data.

\*The distance measure  $D_i$  is not an  $F$  random variable, but is compared with an  $F$ -value because of the similarity of  $D_i$  to the normal theory confidence ellipsoid (Eq. 2.38).

### 2.7.4 Testing for Lack of Fit

In RSM, usually we are fitting the regression model to data from a designed experiment. It is frequently useful to obtain two or more observations (replicates) on the response at the same settings of the independent or regressor variables. When this has been done, we may conduct a formal test for the lack of fit on the regression model. For example, consider the data in Fig. 2.7. There is some indication that the straight-line fit is not very satisfactory, and it would be helpful to have a statistical test to determine if there is systematic curvature present.

The lack-of-fit test requires that we have **true replicates** on the response  $y$  for at least one set of levels on the regressors  $x_1, x_2, \dots, x_k$ . These are not just duplicate readings or measurements of  $y$ . For example, suppose that  $y$  is product viscosity and there is only one regressor  $x$  (temperature). True replication consists of running  $n_i$  separate experiments (usually in random order) at  $x = x_i$  and observing viscosity, not just running a single experiment at  $x_i$  and measuring viscosity  $n_i$  times. The readings obtained from the latter procedure provide information mostly on the variability of the method of measuring viscosity. The error variance  $\sigma^2$  includes measurement error, variability in the process over time, and variability associated with reaching and maintaining the same temperature level in different experiments. These replicate points are used to obtain a model-independent estimate of  $\sigma^2$ .

Suppose that we have  $n_i$  observations on the response at the  $i$ th level of the regressors  $\mathbf{x}_i$ ,  $i = 1, 2, \dots, m$ . Let  $y_{ij}$  denote the  $j$ th observation on the response at  $\mathbf{x}_i$ ,  $i = 1, 2, \dots, m$ , and  $j = 1, 2, \dots, n_i$ . There are  $n = \sum_{i=1}^m n_i$  observations altogether. The test procedure involves partitioning the residual sum of squares into two components, say

$$SS_E = SS_{PE} + SS_{LOF}$$

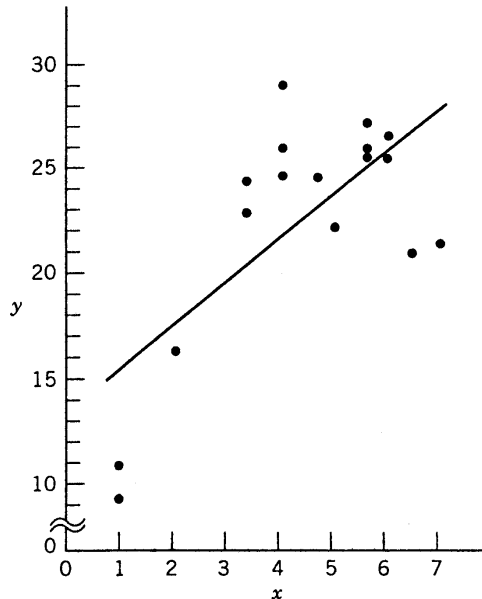


Figure 2.7 Lack of fit of the straight-line model.

where  $SS_{PE}$  is the sum of squares due to pure error and  $SS_{LOF}$  is the sum of squares due to lack of fit.

To develop this partitioning of  $SS_E$ , note that the  $(i, j)$ th residual is

$$y_{ij} - \hat{y}_i = (y_{ij} - \bar{y}_i) + (\bar{y}_i - \hat{y}_i) \quad (2.60)$$

where  $\bar{y}_i$  is the average of the  $n_i$  observations at  $\mathbf{x}_i$ . Squaring both sides of Equation 2.60 and summing over  $i$  and  $j$  yields

$$\sum_{i=1}^m \sum_{j=1}^{n_i} (y_{ij} - \hat{y}_i)^2 = \sum_{i=1}^m \sum_{j=1}^{n_i} (y_{ij} - \bar{y}_i)^2 + \sum_{i=1}^m n_i(\bar{y}_i - \hat{y}_i)^2 \quad (2.61)$$

The left-hand side of Equation 2.61 is the usual residual sum of squares. The two components on the right-hand side measure pure error and lack of fit. We see that the pure error sum of squares

$$SS_{PE} = \sum_{i=1}^m \sum_{j=1}^{n_i} (y_{ij} - \bar{y}_i)^2 \quad (2.62)$$

is obtained by computing the corrected sum of squares of the repeat observations at each level of  $\mathbf{x}$  and then pooling over the  $m$  levels of  $\mathbf{x}$ . If the assumption of constant variance is satisfied, this is a **model-independent** measure of pure error, because only the variability of the ys at each  $\mathbf{x}_i$  level is used to compute  $SS_{PE}$ . Because there are  $n_i - 1$  degrees of freedom for pure error at each level  $\mathbf{x}_i$ , the total number of degrees of freedom associated with the pure error sum of squares is

$$\sum_{i=1}^m (n_i - 1) = n - m \quad (2.63)$$

The sum of squares for lack of fit,

$$SS_{LOF} = \sum_{i=1}^m n_i(\bar{y}_i - \hat{y}_i)^2 \quad (2.64)$$

is a weighted sum of squared deviations between the mean response  $\bar{y}_i$  at each  $\mathbf{x}_i$  level and the corresponding fitted value. If the fitted values  $\hat{y}_i$  are close to the corresponding average responses  $\bar{y}_i$ , then there is a strong indication that the regression function is linear. If the  $\hat{y}_i$  deviate greatly from the  $\bar{y}_i$ , then it is likely that the regression function is not linear. There are  $m - p$  degrees of freedom associated with  $SS_{LOF}$ , because there are  $m$  levels of  $\mathbf{x}$  but  $p$  degrees of freedom are lost because  $p$  parameters must be estimated for the model. Computationally we usually obtain  $SS_{LOF}$  by subtracting  $SS_{PE}$  from  $SS_E$ .

The test statistic for lack of fit is

$$F_0 = \frac{SS_{LOF}/(m-p)}{SS_{PE}/(n-m)} = \frac{MS_{LOF}}{MS_{PE}} \quad (2.65)$$

The expected value of  $MS_{PE}$  is  $\sigma^2$ , and the expected value of  $MS_{LOF}$  is

$$E(MS_{LOF}) = \sigma^2 + \frac{\sum_{i=1}^m n_i \left[ E(y_i) - \beta_0 - \sum_{j=1}^k \beta_j x_{ij} \right]^2}{m-2} \quad (2.66)$$

If the true regression function is linear, then  $E(y_i) = \beta_0 + \sum_{j=1}^k \beta_j x_{ij}$ , and the second term of Equation 2.66 is zero, resulting in  $E(MS_{LOF}) = \sigma^2$ . However, if the true regression function is not linear, then  $E(y_i) \neq \beta_0 + \sum_{j=1}^k \beta_j x_{ij}$ , and  $E(MS_{LOF}) > \sigma^2$ . Furthermore, if the true regression function is linear, then the statistic  $F_0$  follows the  $F_{m-p,n-m}$ -distribution. Therefore, to test for lack of fit, we would compute the test statistic  $F_0$  and conclude that the regression function is not linear if  $F_0 > F_{\alpha,m-p,n-m}$ .

This test procedure may be easily introduced into the analysis of variance conducted for significance of regression. If we conclude that the regression function is not linear, then the tentative model must be abandoned and attempts made to find a more appropriate equation. Alternatively, if  $F_0$  does not exceed  $F_{\alpha,m-p,n-m}$ , there is no strong evidence of lack of fit, and  $MS_{PE}$  and  $MS_{LOF}$  are often combined to estimate  $\sigma^2$ .

Ideally, we find that the  $F$ -ratio for lack of fit is not significant and the hypothesis of significance of regression is rejected. Unfortunately, this does not guarantee that the model will be satisfactory as a prediction equation. Unless the variation of the predicted values is large relative to the random error, the model is not estimated with sufficient precision to yield satisfactory predictions. That is, the model may have been fitted to the errors only. Some analytical work has been done on developing criteria for judging the adequacy of the regression model from a prediction point of view. See Box and Wetz (1973), Ellerton (1978), Gunst and Mason (1979), Hill, Judge, and Fomby (1978), and Suich and Derringer (1977). Box and Wetz's work suggests that the observed  $F$ -ratio must be at least four or five times the critical value from the  $F$ -table if the regression model is to be useful as a predictor—that is, if the spread of predicted values is to be large relative to the noise.

A relatively simple measure of potential prediction performance is found by comparing the range of the fitted values  $\hat{y}$  (i.e.,  $\hat{y}_{\max} - \hat{y}_{\min}$ ) with their average standard error. It can be shown that, regardless of the form of the model, the average variance of the fitted values is

$$\overline{\text{Var}(\hat{y})} = \frac{1}{n} \sum_{i=1}^n \text{Var}[\hat{y}(\mathbf{x}_i)] = \frac{p\sigma^2}{n} \quad (2.67)$$

where  $p$  is the number of parameters in the model. In general, the model is not likely to be a satisfactory predictor unless the range of the fitted values  $\hat{y}_i$  is large relative to their average estimated standard error  $\sqrt{(p\hat{\sigma}^2)/n}$ , where  $\hat{\sigma}^2$  is a model-independent estimate of the error variance.

**TABLE 2.7 Analysis of Variance for Example 2.10**

Source of Variation	Sum of Squares	Degrees of Freedom	Mean Square	$F_0$	P-Value
Regression	234.7087	1	234.7087		
Residual	252.9039	15	16.8603		
Lack of fit	237.3407	8	29.6676	13.34	0.0013
Pure error	15.5632	7	2.2233		
Total	487.6126	16			

**Example 2.10 Testing Lack of Fit** The data in Fig. 2.7 are shown below:

$x$	1.0	1.0	2.0	3.3	3.3	4.0	4.0	4.0	4.7	5.0
$y$	10.84	9.30	16.35	22.88	24.35	24.56	25.86	29.46	24.59	22.25
$x$	5.6	5.6	5.6	6.0	6.0	6.5	6.92			
$y$	25.90	27.20	25.61	25.45	26.56	21.03	21.46			

The straight-line fit is  $\hat{y} = 13.301 + 2.108x$ , with  $SS_T = 487.6126$ ,  $SS_R = 234.7087$ , and  $SS_E = 252.9039$ . Note that there are 10 distinct levels of  $x$ , with repeat points at  $x = 1.0$ ,  $x = 3.3$ ,  $x = 4.0$ ,  $x = 5.6$ , and  $x = 6.0$ . The pure sum of squares is computed using the repeat points as follows:

Level of $x$	$\sum_j (y_{ij} - \bar{y}_i)^2$	Degrees of Freedom
1.0	1.1858	1
3.3	1.0805	1
4.0	11.2467	2
5.6	1.4341	2
6.0	0.6161	1
Total	15.5632	7

The lack-of-fit sum of squares is found by subtraction as

$$\begin{aligned} SS_{LOF} &= SS_E - SS_{PE} \\ &= 252.9039 - 15.5632 = 237.3407 \end{aligned}$$

with  $m - p = 10 - 2 = 8$  degrees of freedom. The analysis of variance incorporating the lack-of-fit test is shown in Table 2.7. The lack-of-fit test statistic is  $F_0 = 13.34$ , and because the  $P$ -value for this test statistic is very small, we reject the hypothesis that the tentative model adequately describes the data.

## 2.8 FITTING A SECOND-ORDER MODEL

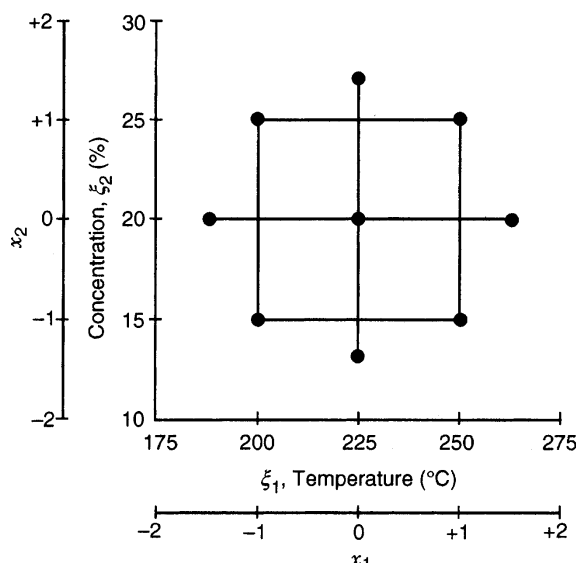
Many applications of response surface methodology involve fitting and checking the adequacy of a second-order model. In this section we present a complete example of this process.

**TABLE 2.8** Central Composite Design for the Chemical Process Example

Observation	Run	A		B		
		Temperature (°C)	Conc. (%)	$x_1$	$x_2$	y
		$\xi_1$	$\xi_2$			
1	4	200	15	-1	-1	43
2	12	250	15	1	-1	78
3	11	200	25	-1	1	69
4	5	250	25	1	1	73
5	6	189.65	20	-1.414	0	48
6	7	260.35	20	1.414	0	78
7	1	225	12.93	0	-1.414	65
8	3	225	27.07	0	1.414	74
9	8	225	20	0	0	76
10	10	225	20	0	0	79
11	9	225	20	0	0	83
12	2	225	20	0	0	81

Table 2.8 presents the data resulting from an investigation into the effect of two variables, reaction temperature ( $\xi_1$ ), and reactant concentration ( $\xi_2$ ), on the percentage conversion of a chemical process (y). The process engineers had used an approach to improving this process based on designed experiments. The first experiment was a screening experiment involving several factors that isolated temperature and concentration as the two most important variables. Because the experimenters thought that the process was operating in the vicinity of the optimum, they elected to fit a quadratic model relating yield to temperature and concentration.

Panel A of Table 2.8 shows the levels used for  $\xi_1$  and  $\xi_2$  in the natural units of measurements. Panel B shows the levels in terms of coded variables  $x_1$  and  $x_2$ . Figure 2.8 shows

**Figure 2.8** Central composite design for the chemical process example.

the experimental design in Table 2.8 graphically. This design is called a **central composite design**, and it is widely used for fitting a second-order response surface. Notice that the design consists of four runs at the corners of a square, plus four runs at the center of this square, plus four **axial runs**. In terms of the coded variables the corners of the square are  $(x_1, x_2) = (-1, -1), (1, -1), (-1, 1), (1, 1)$ ; the center points are at  $(x_1, x_2) = (0, 0)$ ; and the axial runs are at  $(x_1, x_2) = (-1.414, 0), (1.414, 0), (0, -1.414), (0, 1.414)$ .

We will fit the second-order model

$$y = \beta_0 + \beta_1 x_1 + \beta_2 x_2 + \beta_{11} x_1^2 + \beta_{22} x_2^2 + \beta_{12} x_1 x_2 + \varepsilon$$

using the coded variables. The matrix  $\mathbf{X}$  and vector  $\mathbf{y}$  for this model are

$$\mathbf{X} = \begin{array}{cccccc|c} & x_1 & x_2 & x_1^2 & x_2^2 & x_1 x_2 & \\ \begin{matrix} 1 & -1 & -1 & 1 & 1 & 1 \\ 1 & 1 & -1 & 1 & 1 & -1 \\ 1 & -1 & 1 & 1 & 1 & -1 \\ 1 & 1 & 1 & 1 & 1 & 1 \\ 1 & -1.414 & 0 & 2 & 0 & 0 \\ 1 & 1.414 & 0 & 2 & 0 & 0 \\ 1 & 0 & -1.414 & 0 & 2 & 0 \\ 1 & 0 & 1.414 & 0 & 2 & 0 \\ 1 & 0 & 0 & 0 & 0 & 0 \\ 1 & 0 & 0 & 0 & 0 & 0 \\ 1 & 0 & 0 & 0 & 0 & 0 \\ 1 & 0 & 0 & 0 & 0 & 0 \end{matrix} & \left[ \begin{matrix} 43 \\ 78 \\ 69 \\ 73 \\ 48 \\ 76 \\ 65 \\ 74 \\ 76 \\ 79 \\ 83 \\ 81 \end{matrix} \right] & \mathbf{y} = \end{array}$$

Notice that we have shown the variables associated with each column above that column in the matrix  $\mathbf{X}$ . The entries in the columns associated with  $x_1^2$  and  $x_2^2$  are found by squaring the entries in columns  $x_1$  and  $x_2$ , respectively, and the entries in the  $x_1 x_2$  column are found by multiplying each entry from  $x_1$  by the corresponding entry from  $x_2$ . The matrix  $\mathbf{X}'\mathbf{X}$  and vector  $\mathbf{X}'\mathbf{y}$  are

$$\mathbf{X}'\mathbf{X} = \begin{bmatrix} 12 & 0 & 0 & 8 & 8 & 0 \\ 0 & 8 & 0 & 0 & 0 & 0 \\ 0 & 0 & 8 & 0 & 0 & 0 \\ 8 & 0 & 0 & 12 & 4 & 0 \\ 8 & 0 & 0 & 4 & 12 & 0 \\ 0 & 0 & 0 & 0 & 0 & 4 \end{bmatrix}, \mathbf{X}'\mathbf{y} = \begin{bmatrix} 845.000 \\ 78.592 \\ 33.726 \\ 511.000 \\ 541.000 \\ -31.000 \end{bmatrix}$$

and from  $\mathbf{b} = (\mathbf{X}'\mathbf{X})^{-1}\mathbf{X}'\mathbf{y}$  we obtain

$$\mathbf{b} = \begin{bmatrix} 79.75 \\ 10.18 \\ 4.22 \\ -8.50 \\ -5.25 \\ -7.75 \end{bmatrix}$$

Therefore the fitted model for percentage conversion is

$$\hat{y} = 79.75 + 10.18x_1 + 4.22x_2 - 8.50x_1^2 - 5.25x_2^2 - 7.75x_1x_2$$

In terms of the natural variables, the model is

$$\hat{y} = -1080.22 + 7.7671\xi_1 + 23.1932\xi_2 - 0.0136\xi_1^2 - 0.2100\xi_2^2 - 0.0620\xi_1\xi_2$$

Tables 2.9 and 2.10 present some of the output from Design-Expert, a popular statistics software package for experimental design and RSM. In Table 2.9, the model-fitting procedure is presented. Design-Expert attempts to fit a series of models to the data (first-order or linear, first-order with interaction, second-order, and cubic). The significance of

**TABLE 2.9 Model Fitting for the Chemical Process Example (From Design-Expert)**

<i>Sequential Model Sum of Squares [Type I]</i>					
Source	Sum of Squares	df	Mean Square	F-Value	P-value Prob > F
Mean vs Total	59784.08	1	59784.08		
Linear vs Mean	970.98	2	485.49	5.30	0.0301
2FI vs Linear	240.25	1	240.25	3.29	0.1071
Quadratic vs 2FI	546.42	2	273.21	43.98	0.0003 Suggested
Cubic vs Quadratic	10.02	2	5.01	0.74	0.5346 Aliased
Residual	27.25	4	6.81		
Total	61579.00	12	5131.58		
<i>Lack-of-Fit Tests</i>					
Linear	797.19	6	132.86	14.90	0.0246
2FI	556.94	5	111.39	12.49	0.0319
Quadratic	10.52	3	3.51	0.39	0.7682 Suggested
Cubic	0.50	1	0.50	0.056	0.8281 Aliased
Pure Error	26.75	3	8.92		
<i>Model Summary Statistics</i>					
Source	Std. Dev.	R-Squared	Adjusted R-Squared	Predicted R-Squared	PRESS
Linear	9.57	0.5410	0.4390	0.1814	1469.26
2FI	8.54	0.6748	0.5529	0.2901	1274.27
Quadratic	2.49	0.9792	0.9619	0.9318	122.37 Suggested
Cubic	2.61	0.9848	0.9583	0.9557	79.56 Aliased

“*Sequential Model Sum of Squares [Type I]*”: Select the highest order polynomial where the additional terms are significant and the model is not aliased.

“*Lack-of-Fit Tests*”: Want the selected model to have insignificant lack-of-fit.

“*Model Summary Statistics*”: Focus on the model maximizing the “*Adjusted R-Squared*” and the “*Predicted R-Squared*.”

**TABLE 2.10 Design-Expert ANOVA for the Chemical Process Example**

Source	Sum of Squares	df	Mean	F-Value	P-value Prob > F
			Square		
Model	1757.65	5	351.53	56.59	<0.0001
A-Temp	828.78	1	828.78	133.42	<0.0001
B-Conc	142.20	1	142.20	22.89	0.0030
AB	240.25	1	240.25	38.68	0.0008
A <sup>2</sup>	462.40	1	462.40	74.44	0.0001
B <sup>2</sup>	176.40	1	176.40	28.40	0.0018
Residual	37.27	6	6.21		
Lack of Fit	10.52	3	3.51	0.39	0.7682
Pure Error	26.75	3	8.92		
Cor Total	1794.92	11			
Std. Dev.	2.49			R-Squared	0.9792
Mean	70.58			Adj R-Squared	0.9619
C.V. %	3.53			Pred R-Squared	0.9318
PRESS	122.37			Adeq. Precision	20.367

Factor	Coefficient Estimate	Standard df	95% CI		
			Error	Low	High
Intercept	79.75	1	1.25	76.70	82.80
A-Temp	10.18	1	0.88	8.02	12.33
B-Conc	4.22	1	0.88	2.06	6.37
AB	-7.75	1	1.25	-10.80	-4.70
A <sup>2</sup>	-8.50	1	0.99	-10.91	-6.09
B <sup>2</sup>	-5.25	1	0.99	-7.66	-2.84

*Final Equation in Terms of Coded Factors:*

Conversion	=
+79.75	
+10.18	*A
+4.22	*B
-7.75	*A *B
-8.50	*A <sup>2</sup>
-5.25	*B <sup>2</sup>

*Final Equation in Terms of Actual Factors:*

Conversion	=
-1080.21867	
+7.76713	*Temp
+23.19320	*Conc
-0.062000	*Temp *Conc
-0.013600	*Temp <sup>2</sup>
-0.21000	*Conc <sup>2</sup>

each additional group of terms is assessed sequentially using the partial  $F$ -test discussed previously. Lack-of-fit tests and several summary statistics are reported for each of the models considered. Because the central composite design cannot support a full cubic model, the results for that model are accompanied by a statement “aliased,” indicating that not all of the cubic model parameters can be uniquely estimated. The summary statistics strongly support selecting the quadratic model, and this is also the model selected by Design-Expert.

To illustrate the computations in Table 2.9, consider testing the significance of the linear (first-order) terms. The regression sum of squares for this model, that is, the contribution of  $x_1$  and  $x_2$  over the mean (intercept) is  $SS_R(\beta_1, \beta_2 | \beta_0) = 970.98$ . The residual mean square for the linear model can be shown to be  $MS_E = 91.58$ . Therefore, the  $F$ -statistic for testing the contribution of the linear terms beyond the intercept is

$$F_0 = \frac{SS_R(\beta_1, \beta_2 | \beta_0)/2}{MS_E} = \frac{970.98/2}{91.58} = \frac{485.99}{91.58} = 5.30$$

for which the  $P$ -value is  $P = 0.0301$ , so we conclude that the linear terms are significant. The analysis in Table 2.9 indicates that the linear interaction and pure quadratic terms contribute significantly to the model. Table 2.10 summarizes the ANOVA for the quadratic model. In this table, the source of variation labeled “Lack of Fit” contains all of the sums of squares for terms higher-order than quadratic. Table 2.10 also reports 95% confidence intervals for each model parameter. Some of these CIs include zero, indicating that there are no nonsignificant terms in the model. If some of these CIs had included zero, some analysts would drop the nonsignificant variables for the model, resulting in a reduced quadratic model for the process. It is also possible to employ variable selection methods such as step-wise regression to determine the subset of variables to include in the model. Generally, we prefer to fit the full quadratic model whenever possible, unless there are large differences between the full and the reduced model in PRESS and adjusted  $R^2$ . Table 2.10 indicates that the  $R^2$  and adjusted  $R^2$  values for this model are satisfactory. The  $R^2_{\text{prediction}}$  based on PRESS is

$$\begin{aligned} R^2_{\text{prediction}} &= 1 - \frac{\text{PRESS}}{SS_T} \\ &= 1 - \frac{122.37}{1799.92} \\ &= 0.9318 \end{aligned}$$

indicating that the model will probably explain a high percentage (about 93%) of the variability in new data.

Table 2.11 contains the observed and predicted values of percentage conversion, the residuals, and other diagnostic statistics for this model. None of the studentized residuals or the values of  $R$ -student are large enough to indicate any problem with outliers. Notice that the hat diagonals  $h_{ii}$  take on only two values, either 0.625 or 0.250. The values of  $h_{ii} = 0.625$  are associated with the four runs at the corners of the square in the design and the four axial runs. All eight of these points are equidistant from the center of the design; this is why all of the  $h_{ii}$  values are identical. The four center points all have  $h_{ii} = 0.250$ . Figures 2.9, 2.10, and 2.11 show a normal probability plot of the studentized residuals, a

**TABLE 2.11 Observed Values, Predicted Values, Residuals, and Other Diagnostics for the Chemical Process Example**

Obs. Order	Actual Value	Predicted Value	Residual	$h_{ii}$	Student Residual	Cook's $D$	R- Student
1	43.00	43.96	-0.96	0.625	-0.643	0.115	-0.609
2	78.00	79.11	-1.11	0.625	-0.745	0.154	-0.714
3	69.00	67.89	1.11	0.625	0.748	0.155	0.717
4	73.00	72.04	0.96	0.625	0.646	0.116	0.612
5	48.00	48.11	-0.11	0.625	-0.073	0.001	-0.067
6	76.00	75.90	0.10	0.625	-0.073	0.001	-0.067
7	65.00	63.54	1.46	0.625	0.982	0.268	0.979
8	74.00	75.46	-1.46	0.625	-0.985	0.269	-0.982
9	76.00	79.75	-3.75	0.250	-1.784	0.177	-2.377
10	79.00	79.75	-0.75	0.250	-0.357	0.007	-0.329
11	83.00	79.75	3.25	0.250	1.546	0.133	1.820
12	81.00	79.75	1.25	0.250	0.595	0.020	0.560

plot of the studentized residuals versus the predicted values  $\hat{y}_i$ , and a plot of the studentized residuals versus run order. None of these plots reveal any model inadequacy.

Plots of the conversion response surface and the contour plot, respectively, for the fitted model are shown in Fig. 2.12a and b. The response surface plots indicate that the maximum percentage conversion is at about 240°C and 20% concentration.

In many response surface problems the experimenter is interested in predicting the response  $y$  or estimating the mean response at a particular point in the process variable space. The response surface plots in Fig. 2.12 give a graphical display of these quantities. Typically, the variance of the prediction is also of interest, because this is a direct measure of the likely error associated with the point estimate produced by the model. Recall from Equation 2.40 that the variance of the estimate of the mean response at the point  $\mathbf{x}_0$  is given by  $\text{Var}[\hat{y}_i(\mathbf{x}_0)] = \sigma^2 \mathbf{x}'_0 (\mathbf{X}'\mathbf{X})^{-1} \mathbf{x}_0$ . Plots of the estimated standard deviation of the

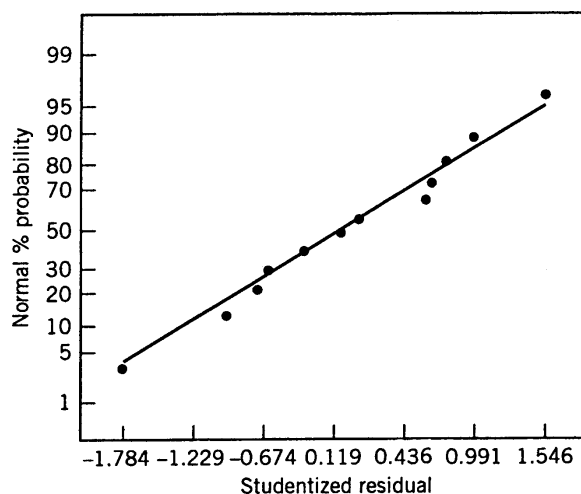


**Figure 2.9** Normal probability plot of the studentized residuals, chemical process example.

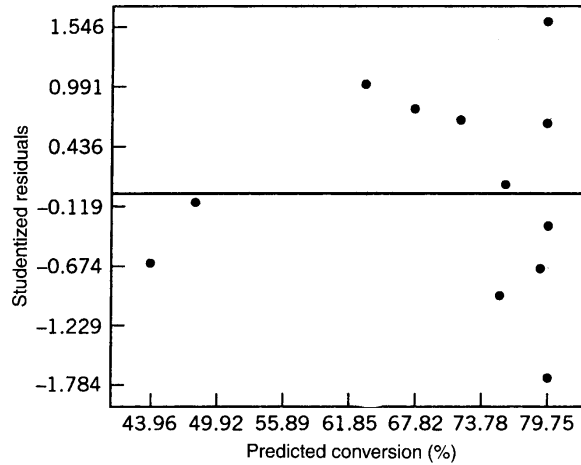


**Figure 2.10** Plot of studentized residuals versus predicted conversion, chemical process example.

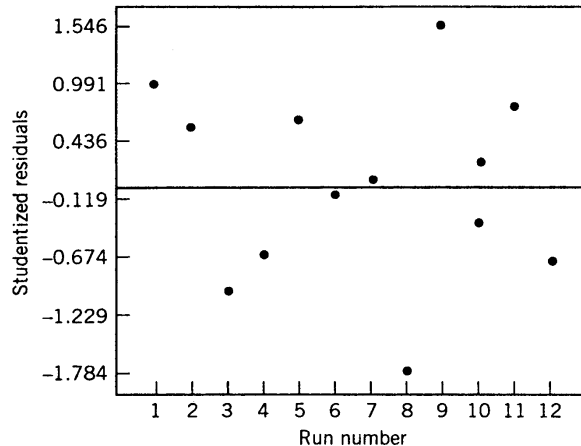


**Figure 2.11** Plot of the studentized residuals versus run order, chemical process example.

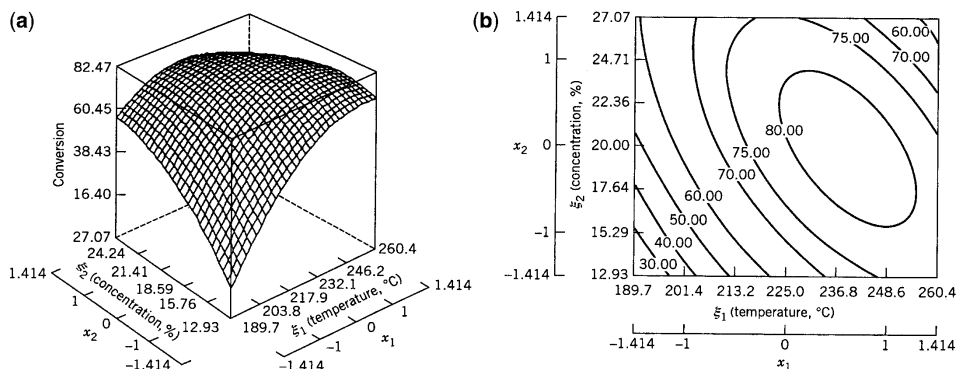


**Figure 2.12** (a) Response surface of predicted conversion. (b) Contour plot of predicted conversion.

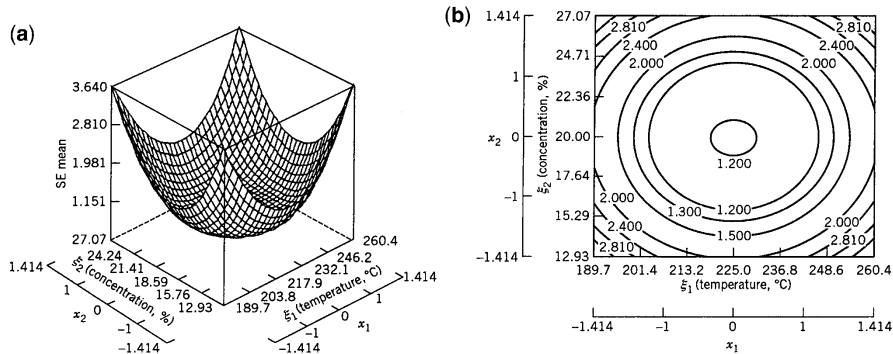


**Figure 2.13** (a) Response surface plot of  $\sqrt{\text{Var}[\hat{y}(x_0)]}$ . (b) Contour plot of  $\sqrt{\text{Var}[\hat{y}(x_0)]}$ .

predicted response,  $\sqrt{\text{Var}[\hat{y}(x_0)]}$ , obtained by estimating  $\sigma^2$  by the mean square error  $MS_E = 5.89$  for this model for all values of  $\mathbf{x}_0$  in the region of experimentation, are presented in Fig. 2.13a and b. Both the response surface in Fig. 2.13a and the contour plot of constant  $\sqrt{\text{Var}[\hat{y}(x_0)]}$  in Fig. 2.13b show that the  $\sqrt{\text{Var}[\hat{y}(x_0)]}$  is the same for all points  $\mathbf{x}_0$  that are the same distance from the center of the design. This is a result of the spacing of the axial runs in the central composite design at 1.414 units from the origin (in the coded variables), and is a design property called **rotatability**. This is an important property for a second-order response surface design, and it will be discussed in more detail in Chapter 7.

## 2.9 QUALITATIVE REGRESSOR VARIABLES

The regression models employed in RSM usually involved **quantitative** variables—that is, variables that are measured on a numerical scale. For example, variables such as temperature, pressure, distance, and age are quantitative variables. Occasionally, we need to incorporate **qualitative** variables in a regression model. For example, suppose that one of the variables in a regression model is the machine from which each observation  $y_i$  is taken. Assume that only two machines are involved. We may wish to assign different levels to the two machines to allow for the possibility that each machine may have a different effect on the response.

The usual method of representing the different levels of a qualitative variable is by using **indicator variables**. For example, to introduce the effect of two different machines into a regression model, we could define an indicator variable as follows:

$$\begin{aligned} x &= 0 && \text{if the observation is from machine 1} \\ x &= 1 && \text{if the observation is from machine 2} \end{aligned}$$

In general, a qualitative variable with  $t$  levels is represented by  $t - 1$  indicator variables, which are assigned the values either 0 or 1. Thus, if there were three machines, the different levels would be accounted for by two indicator variables defined as follows:

$x_1$	$x_2$	
0	0	if the observation is from machine 1
1	0	if the observation is from machine 2
0	1	if the observation is from machine 3

Indicator variables are also referred to as **dummy variables**. The following example illustrates some of the uses of indicator variables. For other applications, see Montgomery, Peck, and Vining (2006) and Myers (1990).

**Example 2.11 The Surface Finish Regression Model** A mechanical engineer is investigating the surface finish of metal parts produced on a lathe and its relationship to the speed [in revolutions per minute (RPM)] of the lathe. The data are shown in Table 2.12. Note that the data have been collected using two different types of cutting tools. Because it is likely that the type of cutting tool affects the surface finish, we will fit the model

$$y = \beta_0 + \beta_1 x_1 + \beta_2 x_2 + \varepsilon$$

where  $y$  is the surface finish,  $x_1$  is the lathe speed in RPM, and  $x_2$  is an indicator variable denoting the type of cutting tool used; that is,

$$x_2 = \begin{cases} 0 & \text{for tool type 302} \\ 1 & \text{for tool type 416} \end{cases}$$

The parameters in this model may be easily interpreted. If  $x_2 = 0$ , then the model becomes

$$y = \beta_0 + \beta_1 x_1 + \varepsilon$$

which is a straight-line model with slope  $\beta_1$  and intercept  $\beta_0$ . However, if  $x_2 = 1$ , the model becomes

$$y = \beta_0 + \beta_1 x_1 + \beta_2(1) + \varepsilon = (\beta_0 + \beta_2) + \beta_1 x_1 + \varepsilon$$

**TABLE 2.12 Surface Finish Data for Example 2.11**

Observation Number, $i$	Surface Finish, $y_i$	RPM	Type of Cutting Tool
1	45.44	225	302
2	42.03	200	302
3	50.10	250	302
4	48.75	245	302
5	47.92	235	302
6	47.79	237	302
7	52.26	265	302
8	50.52	259	302
9	45.58	221	302
10	44.78	218	302
11	33.50	224	416
12	31.23	212	416
13	37.52	248	416
14	37.13	260	416
15	34.70	243	416
16	33.92	238	416
17	32.13	224	416
18	35.47	251	416
19	33.49	232	416
20	32.29	216	416

which is a straight-line model with slope  $\beta_1$  and intercept  $\beta_0 + \beta_2$ . Thus, the model  $y = \beta_0 + \beta_1x_1 + \beta_2x_2 + \epsilon$  implies that surface finish is linearly related to lathe speed and that the slope  $\beta_1$  does not depend on the type of cutting tool used. However, the type of cutting tool does affect the intercept, and  $\beta_2$  indicates the change in the intercept associated with a change in tool type from 302 to 416.

The model matrix  $\mathbf{X}$  and vector  $\mathbf{y}$  for this problem are as follows:

$$\mathbf{X} = \begin{bmatrix} 1 & 225 & 0 \\ 1 & 200 & 0 \\ 1 & 250 & 0 \\ 1 & 245 & 0 \\ 1 & 235 & 0 \\ 1 & 237 & 0 \\ 1 & 265 & 0 \\ 1 & 259 & 0 \\ 1 & 221 & 0 \\ 1 & 218 & 0 \\ 1 & 224 & 0 \\ 1 & 212 & 1 \\ 1 & 248 & 1 \\ 1 & 260 & 1 \\ 1 & 243 & 1 \\ 1 & 238 & 1 \\ 1 & 224 & 1 \\ 1 & 251 & 1 \\ 1 & 232 & 1 \\ 1 & 216 & 1 \end{bmatrix}, \quad \mathbf{y} = \begin{bmatrix} 45.44 \\ 42.03 \\ 50.10 \\ 48.75 \\ 47.92 \\ 47.79 \\ 52.26 \\ 50.52 \\ 45.58 \\ 44.78 \\ 33.50 \\ 31.23 \\ 37.52 \\ 37.13 \\ 34.70 \\ 33.92 \\ 32.13 \\ 35.47 \\ 33.49 \\ 32.29 \end{bmatrix}$$

The fitted model is

$$\hat{y} = 14.27620 + 0.14115x_1 - 13.28020x_2$$

The analysis of variance for this model is shown in Table 2.13. Note that the hypothesis  $H_0: \beta_1 = \beta_2 = 0$  (significance of regression) is rejected. This table also contains the sums of squares

$$\begin{aligned} SS_R &= SS_R(\beta_1, \beta_2 | \beta_0) \\ &= SS_R(\beta_1 | \beta_0) + SS_R(\beta_2 | \beta_1, \beta_0) \end{aligned}$$

so that a test of the hypothesis  $H_0: \beta_2 = 0$  can be made. This hypothesis is also rejected, so we conclude that tool type has an effect on surface finish.

**TABLE 2.13 Analysis of Variance of Example 2.11**

Source of Variation	Sum of Squares	Degrees of Freedom	Mean Square	$F_0$	P-Value
Regression	1012.0595	1	506.0297	1103.69	$1.0175 \times 10^{-18}$
$SS_R(\beta_1   \beta_0)$	(130.6091)	(1)	130.6091	284.87	$4.6980 - 10^{-12}$
$SS_R(\beta_2   \beta_1, \beta_0)$	(881.4504)	(1)	881.4504	1922.52	$6.2439 \times 10^{-19}$
Error	7.7943	17	0.4508		
Total	1019.8538	19			

It is also possible to use indicator variables to investigate whether tool type affects both the slope and intercept. Let the model be reformulated as

$$y = \beta_0 + \beta_1 x_1 + \beta_2 x_2 + \beta_3 x_1 x_2 + \varepsilon$$

where  $x_2$  is the indicator variable. Now if tool type 302 is used, then  $x_2 = 0$ , and the model is

$$y = \beta_0 + \beta_1 x_1 + \varepsilon$$

If tool type 416 is used, then  $x_2 = 1$ , and the model becomes

$$\begin{aligned} y &= \beta_0 + \beta_1 x_1 + \beta_2 + \beta_3 x_1 + \varepsilon \\ &= (\beta_0 + \beta_2) + (\beta_1 + \beta_3) x_1 + \varepsilon \end{aligned}$$

Note that  $\beta_2$  is the change in the intercept, and  $\beta_3$  is the change in slope produced by a change in tool type.

Another method of analyzing this data set is to fit separate regression models to the data for each tool type. However, the indicator variable approach has several advantages. First, only one regression model must be estimated. Second, by pooling the data on both tool types, more degrees of freedom for error are obtained. Third, tests of both hypotheses on the parameters  $\beta_2$  and  $\beta_3$  are just special cases of the extra sum of squares method.

## 2.10 TRANSFORMATION OF THE RESPONSE VARIABLE

We noted in Section 2.7 that often a data transformation can be used when residual analysis indicates some problem with underlying model assumptions, such as nonnormality or nonconstant variance in the response variable. In this section we illustrate the use of data transformation for a classic example from the literature. Following the example, we discuss methods for the choice of the transformation.

**Example 2.12 The Worsted Yarn Data** The data in Table 2.14 [taken from Box and Draper (1987)] show the number of cycles to failure of worsted gain ( $y$ ) and three factors defined as follows:

$$\text{Length of test specimen (mn): } x_1 = \frac{\text{Length} - 300}{50}$$

$$\text{Amplitude of load cycle (MM): } x_2 = \text{Length} - 9$$

$$\text{Load (grams): } x_3 = \frac{\text{Length} - 45}{5}$$

These factors form a  $3^3$  factorial experiment. This experiment will support a complete second-order polynomial. The least squares fit is

$$\begin{aligned} \hat{y} &= 550.7 + 660x_1 - 535.9x_2 - 310.8x_3 + 238.7x_1^2 + 275.7x_2^2 \\ &\quad - 48.3x_3^2 - 456.5x_1 x_2 - 235.7x_1 x_3 + 143x_2 x_3 \end{aligned}$$

**TABLE 2.14** The Worsted Yarn Data

Run Number	Length, $x_1$	Amplitude, $x_2$	Load, $x_3$	Cycles to Failure, $y$
1	-1	-1	-1	674
2	0	-1	-1	1414
3	1	-1	-1	3636
4	-1	0	-1	338
5	0	0	-1	1022
6	1	0	-1	1368
7	-1	1	-1	170
8	0	1	-1	442
9	1	1	-1	1140
10	-1	-1	0	370
11	0	-1	0	1198
12	1	-1	0	3184
13	-1	0	0	266
14	0	0	0	620
15	1	0	0	1070
16	-1	1	0	118
17	0	1	0	332
18	1	1	0	884
19	-1	-1	1	292
20	0	-1	1	634
21	1	-1	1	2000
22	-1	0	1	210
23	0	0	1	438
24	1	0	1	566
25	-1	1	1	90
26	0	1	1	220
27	1	1	1	360

The  $R^2$  value is 0.975. An analysis of variance is given in Table 2.15. The fit appears to be reasonable and both the first- and second-order terms appear to be necessary.

Figure 2.14 is a plot of residuals versus the predicted cycles to failure  $\hat{y}_i$  for this model. There is an indication of an outward-opening funnel in this plot, implying possible inequality of variance.

**TABLE 2.15** Analysis of Variance for the Quadratic Model for the Worsted Yarn Data

Source of Variability	Sum of Squares ( $\times 10^{-3}$ )	Degrees of Freedom	Mean Square ( $\times 10^{-3}$ )	$F_0$
First-order terms	14,748.5	3	4,916.2	70
Added second-order terms	4,224.3	6	704.1	9.5
Residual	1,256.6	17	73.9	
Total	20,229.4	26		

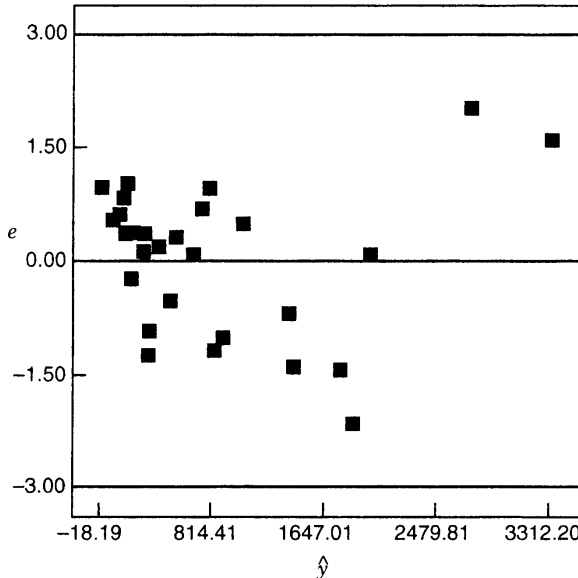


**Figure 2.14** Plot of residuals versus predicted for the worsted yarn, quadratic model.

When a natural log transformation is used for  $y$ , we obtain the following model:

$$\begin{aligned}\ln \hat{y} &= 6.33 + 0.82x_1 - 0.63x_2 - 0.38x_3 \\ \hat{y} &= e^{6.33+0.82x_1-0.63x_2-0.38x_3}\end{aligned}$$

This model has  $R^2 = 0.963$ , and has only three model terms (apart from the intercept). None of the second-order terms are significant. Here, as in most modeling exercises, simplicity is of vital importance. The elimination of the quadratic terms and interaction terms with the change in response metric not only allows a better fit than the second-order model with the natural metric, but the effect of the design variables  $x_1$ ,  $x_2$ , and  $x_3$  on the response is clear.

Figure 2.15 is a plot of residuals versus the predicted response for the log model. There is still some indication of inequality of variance, but the log model, overall, is an improvement on the original quadratic fit.

In the previous example, we illustrated the problem of nonconstant variance in the response variable  $y$  in linear regression and noted that this is a departure from the standard least squares assumptions. This inequality of variance problem occurs fairly often in practice, often in conjunction with a non-normal response variable. Examples include a count of defects or particles, proportion data such as yield or fraction defective, or a response variable that follows some skewed distribution (one tail of the response distribution is longer than the other). We illustrated how **transformation of the response variable** can be used for stabilizing the variance of the response. In our example we selected a log transformation empirically, by noting that it greatly improved the appearance of the residual plots.

Generally, transformations are used for three purposes: stabilizing the response variance, making the distribution of the response variable closer to the normal distribution, and

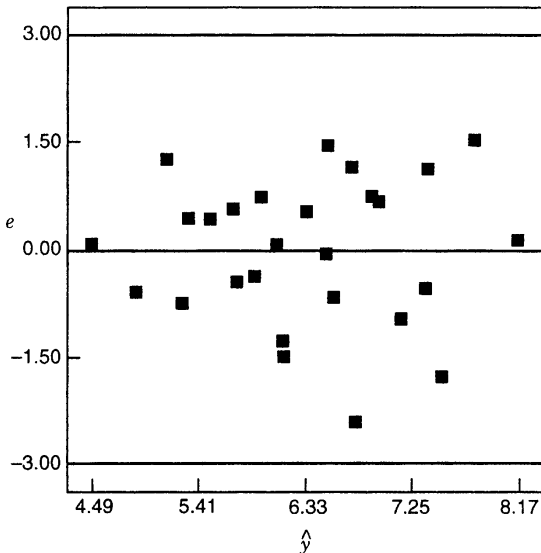


**Figure 2.15** Plot of residuals predicted for the worsted yam data, log model.

improving the fit of the model to the data. This last objective could include model simplification, say by eliminating interaction, or higher-order polynomial terms. Sometimes a transformation will be reasonably effective in simultaneously accomplishing more than one of these objectives.

We often find that the **power family** of transformations  $y^* = y^\lambda$  is very useful, where  $\lambda$  is the parameter of the transformation to be determined (e.g.,  $\lambda = \frac{1}{2}$  means use the square root of the original response). Box and Cox (1964) have shown how the transformation parameter  $\lambda$  may be estimated simultaneously with the other model parameters (overall mean and treatment effects). The theory underlying their method uses the method of maximum likelihood. The actual computational procedure consists of performing, for various values of  $\lambda$ , a standard analysis of variance on

$$y^{(\lambda)} = \begin{cases} \frac{y^{\lambda-1}}{\lambda \dot{y}^{\lambda-1}} & \lambda \neq 0 \\ \dot{y} \ln y & \lambda = 0 \end{cases} \quad (2.68)$$

where  $\dot{y} = \ln^{-1}[(1/n)\sum \ln y]$  is the geometric mean of the observations. The maximum likelihood estimate of  $\lambda$  is the value for which the error sum of squares, say  $SS_E(\lambda)$  is a minimum. This value of  $\lambda$  is usually found by plotting a graph of  $SS_E(\lambda)$  versus  $\lambda$  and then reading the value of  $\lambda$  that minimizes  $SS_E(\lambda)$  from the graph. Usually between 10 and 20 values of  $\lambda$  are sufficient for estimation of the optimum value. A second iteration using a finer mesh of values can be performed if a more accurate estimate of  $\lambda$  is necessary.

Notice that we *cannot* select a value of  $\lambda$  by *directly* comparing the error sums of squares from analyses of variance on  $y^\lambda$ , because for each value of  $\lambda$  the error sum of squares is measured on a different scale. Furthermore, a problem arises in  $y$  when  $\lambda = 0$ ; namely, as  $\lambda$  approaches zero,  $y^\lambda$  approaches unity. That is, when  $\lambda = 0$ , all the response values are a constant. The component  $(y^\lambda - 1)/\lambda$  of Equation 2.68 alleviates this problem because as  $\lambda$  tends to zero,  $(y^\lambda - 1)/\lambda$  goes to a limit of  $\ln y$ . The divisor component

$\hat{y}^{\lambda-1}$  in Equation 2.68 rescales the responses so that the error sums of squares are directly comparable.

In applying the Box–Cox method, we recommend using simple choices for  $\lambda$ , because the practical difference between  $\lambda = 0.5$  and  $\lambda = 0.58$  is likely to be small, but the square root transformation ( $\lambda = 0.5$ ) is much easier to interpret. Obviously, values of  $\lambda$  close to unity would suggest that no transformation is necessary.

Once a value of  $\lambda$  is selected by the Box–Cox method, the experimenter can analyze the data using  $y^\lambda$  as the response, unless of course  $\lambda = 0$ , in which case use  $\ln y$ . It is perfectly acceptable to use  $y^{(\lambda)}$  as the actual response, although the model parameter estimates will have a scale difference and origin shift in comparison with the results obtained using  $y^\lambda$  (or  $\ln y$ ).

An approximate  $100(1 - \alpha)\%$  confidence interval for  $\lambda$  can be found by computing

$$SS^* = SS_E(\lambda) \left( 1 + \frac{t_{\alpha/2, v}^2}{v} \right) \quad (2.69)$$

where  $v$  is the number of degrees of freedom, and plotting a line parallel to the  $\lambda$ -axis at height  $SS^*$  on the graph of  $SS_E(\lambda)$  versus  $\lambda$ . Then by locating the points on the  $\lambda$ -axis where  $SS^*$  cuts the curve  $SS_E(\lambda)$ , we can read confidence limits on  $\lambda$  directly from the graph. If this confidence interval includes the value  $\lambda = 1$ , this implies that the data do not support the need for the transformation.

Several software packages have implemented the Box–Cox procedure. Figure 2.16 shows the output graphics from Design-Expert when the Box–Cox procedure is applied to the worsted yarn data in Table 2.14. The optimum value of  $\lambda$  is  $-0.24$ , and the 95% confidence interval for  $\lambda$  contains zero, so the use of a log transformation is indicated.

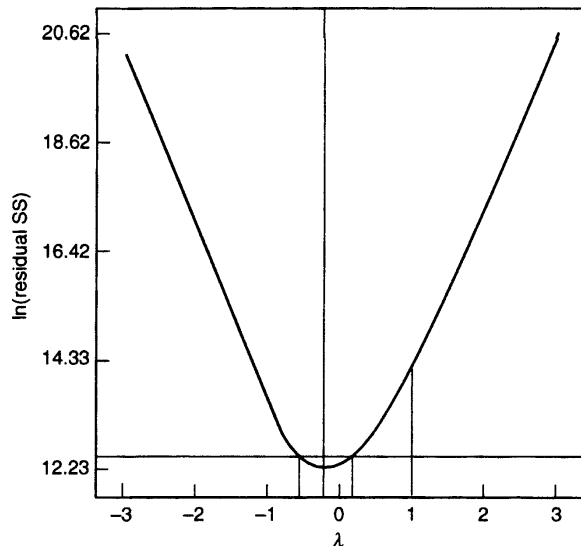


**Figure 2.16** The Box–Cox procedure applied to the worsted yarn data in Table 2.5.

## EXERCISES

- 2.1** A study was performed on wear of a bearing  $y$  and its relationship to  $\xi_1 =$  oil viscosity and  $\xi_2 =$  load. The following data were obtained:

$y$	$\xi_1$	$\xi_2$
193	1.6	851
230	15.5	816
172	22.0	1058
91	43.0	1201
113	33.0	1357
125	40.0	1115

- (a) Fit a multiple linear regression model to these data, using coded variables  $x_1$  and  $x_2$ , defined so that  $-1 \leq x_i \leq 1$ ,  $i = 1, 2$ .
  - (b) Convert the model in part (a) to a model in the natural variables  $\xi_1$  and  $\xi_2$ .
  - (c) Use the model to predict wear when  $\xi_1 = 25$  and  $\xi_2 = 1000$ .
  - (d) Fit a multiple linear regression model with an interaction term to these data. Use the coded variables defined in part (a).
  - (e) Use the model in (d) to predict wear when  $\xi_1 = 25$  and  $\xi_2 = 1000$ . Compare this prediction with the predicted value from part (b) above.
- 2.2** Consider the regression models developed in Exercise 2.1.
- (a) Test for significance of regression from the first-order model in part (a) of Exercise 2.1 using the analysis of variance with  $\alpha = 0.05$ . What are your conclusions?
  - (b) Use the extra sum of squares method to investigate adding the interaction term to the model [part (d) of Exercise 2.1]. With  $\alpha = 0.05$ , what are your conclusions about this term?
- 2.3** The pull strength of a wire bond is an important characteristic. Table E2.1 gives information on pull strength ( $y$ ), die height ( $x_1$ ), post height ( $x_2$ ), loop height ( $x_3$ ), wire length ( $x_4$ ), bond width on the die ( $x_5$ ), and bond width on the post ( $x_6$ ).
- (a) Fit a multiple linear regression model using  $x_2, x_3, x_4$ , and  $x_5$  as the regressors.
  - (b) Test for significance of regression using the analysis of variance with  $\alpha = 0.05$ . What are your conclusions?
  - (c) Use the model from part (a) to predict pull strength when  $x_2 = 20, x_3 = 30, x_4 = 90$ , and  $x_5 = 2.0$ .
- 2.4** An engineer at a semiconductor company wants to model the relationship between the device gain  $hFE(y)$  and three parameters: emitter RS ( $x_1$ ), base RS ( $x_2$ ), and emitter-to-base RS ( $x_3$ ). The data are shown in Table E2.2.
- (a) Fit a multiple linear regression model to the data.
  - (b) Predict  $hFE$  when  $x_1 = 14.5, x_2 = 220$ , and  $x_3 = 5.0$ .
  - (c) Test for significance of regression using the analysis of variance with  $\alpha = 0.05$ . What conclusions can you draw?

**TABLE E2.1** Wire Bond Data for Exercise 2.3

$y$	$x_1$	$x_2$	$x_3$	$x_4$	$x_5$	$x_6$
8.0	5.2	19.6	29.6	94.9	2.1	2.3
8.3	5.2	19.8	32.4	89.7	2.1	1.8
8.5	5.8	19.6	31.0	96.2	2.0	2.0
8.8	6.4	19.4	32.4	95.6	2.2	2.1
9.0	5.8	18.6	28.6	86.5	2.0	1.8
9.3	5.2	18.8	30.6	84.5	2.1	2.1
9.3	5.6	20.4	32.4	88.8	2.2	1.9
9.5	6.0	19.0	32.6	85.7	2.1	1.9
9.8	5.2	20.8	32.2	93.6	2.3	2.1
10.0	5.8	19.9	31.8	86.0	2.1	1.8
10.3	6.4	18.0	32.6	87.1	2.0	1.6
10.5	6.0	20.6	33.4	93.1	2.1	2.1
10.8	6.2	20.2	31.8	83.4	2.2	2.1
11.0	6.2	20.2	32.4	94.5	2.1	1.9
11.3	6.2	19.2	31.4	83.4	1.9	1.8
11.5	5.6	17.0	33.2	85.2	2.1	2.1
11.8	6.0	19.8	35.4	84.1	2.0	1.8
12.3	5.8	18.8	34.0	86.9	2.1	1.8
12.5	5.6	18.6	34.2	83.0	1.9	2.0

**TABLE E2.2** Gain Data for Exercise 2.4

$x_1$ Emitter RS	$x_2$ Base RS	$x_3$ E-to-B RS	$y$ $hFE$
14.620	226.00	7.000	128.40
15.630	220.00	3.375	52.62
14.620	217.40	6.375	113.90
15.000	220.00	6.000	98.01
14.500	226.50	7.625	139.90
15.250	224.10	6.000	102.60
16.120	220.50	3.375	48.14
15.130	223.50	6.125	109.60
15.500	217.60	5.000	82.68
15.130	228.50	6.625	112.60
15.500	230.20	5.750	97.52
16.120	226.50	3.750	59.06
15.130	226.60	6.125	111.80
15.630	225.60	5.375	89.09
15.380	234.00	8.875	171.90
15.500	230.00	4.000	66.80
14.250	224.30	8.000	157.10
14.500	240.50	10.870	208.40
14.620	223.70	7.375	133.40

**TABLE E2.3 Electric Power Consumption Data for Exercise 2.5**

$y$	$x_1$	$x_2$	$x_3$	$x_4$
240	25	24	91	100
236	31	21	90	95
290	45	24	88	110
274	60	25	87	88
301	65	25	91	94
316	72	26	94	99
300	80	25	87	97
296	84	25	86	96
267	75	24	88	110
276	60	25	91	105
288	50	25	90	100
261	38	23	89	98

- 2.5** The electric power consumed each month by a chemical plant is thought to be related to the average ambient temperature ( $x_1$ ), the number of days in the month ( $x_2$ ), the average product purity ( $x_3$ ), and the tons of product produced ( $x_4$ ). The past year's historical data are available and are presented in Table E2.3.
- (a) Fit a multiple linear regression model to the data.
  - (b) Predict power consumption for a month in which  $x_1 = 75^{\circ}\text{F}$ ,  $x_2 = 24$  days,  $x_3 = 90\%$ , and  $x_4 = 98$  tons.
- 2.6** Heat treating is often used to carburize metal parts, such as gears. The thickness of the carburized layer is considered an important feature of the gear, and it contributes to the overall reliability of the part. Because of the critical nature of this feature, two different lab tests are performed on each furnace load. One test is run on a sample pin that accompanies each load. The other test is a destructive test, where an actual part is cross-sectioned. This test involved running a carbon analysis on the surface of both the gear pitch (top of the gear tooth) and the gear root (between the gear teeth). The data in Table E2.4 are the results of the pitch carbon analysis test for 32 parts.
- (a) Fit a linear regression model relating the results of the pitch carbon analysis test (PITCH) to the five regressor variables.
  - (b) Test for significance of regression. Use  $\alpha = 0.05$ .
- 2.7** A regression model  $y = \beta_0 + \beta_1x_1 + \beta_2x_2 + \beta_3x_3 + \varepsilon$  has been fitted to a sample of  $n = 25$  observations. The calculated  $t$ -ratios  $b_j/se(b_j)$ ,  $j = 1, 2, 3$ , are as follows: for  $\beta_1$ ,  $t_0 = 4.82$ ; for  $\beta_2$ ,  $t_0 = 8.21$ ; and for  $\beta_3$ ,  $t_0 = 0.98$ .
- (a) Find  $P$ -values for each of the  $t$ -statistics.
  - (b) Using  $\alpha = 0.05$ , what conclusions can you draw about the regressor  $x_3$ ? Does it seem likely that this regressor contributes significantly to the model?
- 2.8** Consider the electric power consumption data in Exercise 2.5.
- (a) Estimate  $\sigma^2$  for the model fit in Exercise 2.5.
  - (b) Use the  $t$ -test to assess the contribution of each regressor to the model. Using  $\alpha = 0.01$ , what conclusions can you draw?

**TABLE E2.4 Heat Treating Data for Exercise 2.6**

TEMP	SOAKTIME	SOAKPCT	DIFFTIME	DIFFPCT	PITCH
1650	0.58	1.10	0.25	0.90	0.013
1650	0.66	1.10	0.33	0.90	0.016
1650	0.66	1.10	0.33	0.90	0.015
1650	0.66	1.10	0.33	0.95	0.016
1600	0.66	1.15	0.33	1.00	0.015
1600	0.66	1.15	0.33	1.00	0.016
1650	1.00	1.10	0.50	0.80	0.014
1650	1.17	1.10	0.58	0.80	0.021
1650	1.17	1.10	0.58	0.80	0.018
1650	1.17	1.10	0.58	0.80	0.019
1650	1.17	1.10	0.58	0.90	0.021
1650	1.17	1.10	0.58	0.90	0.019
1650	1.17	1.15	0.58	0.90	0.021
1650	1.20	1.15	1.10	0.80	0.025
1650	2.00	1.15	1.00	0.80	0.025
1650	2.00	1.10	1.10	0.80	0.026
1650	2.20	1.10	1.10	0.80	0.024
1650	2.20	1.10	1.10	0.80	0.025
1650	2.20	1.15	1.10	0.80	0.024
1650	2.20	1.10	1.10	0.90	0.025
1650	2.20	1.10	1.10	0.90	0.027
1650	2.20	1.10	1.50	0.90	0.026
1650	3.00	1.15	1.50	0.80	0.029
1650	3.00	1.10	1.50	0.70	0.030
1650	3.00	1.10	1.50	0.75	0.028
1650	3.00	1.15	1.66	0.85	0.032
1650	3.33	1.10	1.50	0.80	0.033
1700	4.00	1.10	1.50	0.70	0.039
1650	4.00	1.10	1.50	0.70	0.040
1650	4.00	1.15	1.50	0.85	0.035
1700	12.50	1.00	1.50	0.70	0.056
1700	18.50	1.00	1.50	0.70	0.068

**2.9** Consider the bearing wear data in Exercise 2.1.

- (a) Estimate  $\sigma^2$  for the no-interaction model.
- (b) Compute the  $t$ -statistic for each regression coefficient. Using  $\alpha = 0.05$ , what conclusions can you draw?
- (c) Use the extra sum of squares method to investigate the usefulness of adding  $x_2 =$  load to the model that already contains  $x_1 =$  oil viscosity. Use  $\alpha = 0.05$ .

**2.10** Consider the wire bond pull strength data in Exercise 2.3.

- (a) Estimate  $\sigma^2$  for this model.
- (b) Find the standard errors for each of the regression coefficients.
- (c) Calculate the  $t$ -test statistic for each regression coefficient. Using  $\alpha = 0.05$ , what conclusions can you draw? Do all variables contribute to the model?

- 2.11** Reconsider the semiconductor data in Exercise 2.4.
- Estimate  $\sigma^2$  for the model you have fitted to the data.
  - Find the standard errors of the regression coefficients.
  - Calculate the  $t$ -test statistic for each regression coefficient. Using  $\alpha = 0.05$ , what conclusions can you draw?
- 2.12** Exercise 2.6 presents data on heat treating gears.
- Estimate  $\sigma^2$  for the model.
  - Find the standard errors of the regression coefficients.
  - Evaluate the contribution of each regressor to the model using the  $t$ -test with  $\alpha = 0.05$ .
  - Fit a new model to the response PITCH using new regressors  $x_1 = \text{SOAKTIME} \times \text{SOAKPCT}$  and  $x_2 = \text{DIFFTIME} \times \text{DIFFPCT}$ .
  - Test the model in part (d) for significance of regression using  $\alpha = 0.05$ . Also calculate the  $t$ -test for each regressor and draw conclusions.
  - Estimate  $\sigma^2$  for the model from part (d), and compare this with the estimate of  $\sigma^2$  obtained in part (b) above. Which estimate is smaller? Does this offer any insight regarding which model might be preferable?
- 2.13** Consider the wire bond pull strength data in Exercise 2.3.
- Find 95% confidence intervals on the regression coefficients.
  - Find a 95% confidence interval on mean pull strength when  $x_2 = 20$ ,  $x_3 = 30$ ,  $x_4 = 90$ , and  $x_5 = 2.0$ .
- 2.14** Consider the semiconductor data in Exercise 2.4.
- Find 99% confidence intervals on the regression coefficients.
  - Find a 99% prediction interval on  $hFE$  when  $x_1 = 14.5$ ,  $x_2 = 220$ , and  $x_3 = 5.0$ .
  - Find a 99% confidence interval on mean  $hFE$  when  $x_1 = 14.5$ ,  $x_2 = 220$ , and  $x_3 = 5.0$ .
- 2.15** Consider the heat-treating data from Exercise 2.6.
- Find 95% confidence intervals on the regression coefficients.
  - Find a 95% interval on mean PITCH on  $\text{TEMP} = 1650$ ,  $\text{SOAKTIME} = 1.00$ ,  $\text{SOAKPCT} = 1.10$ ,  $\text{DIFFTIME} = 1.00$ , and  $\text{DIFFPCT} = 0.80$ .
- 2.16** Reconsider the heat treating in Exercise 2.6 and 2.12, where we fit a model to PITCH using regressors  $x_1 = \text{SOAKTIME} \times \text{SOAKPCT}$  and  $x_2 = \text{DIFFTIME} \times \text{DIFFPCT}$ .
- Using the model with regressors  $x_1$  and  $x_2$ , find a 95% confidence interval on mean PITCH when  $\text{SOAKTIME} = 1.00$ ,  $\text{SOAKPCT} = 1.10$ ,  $\text{DIFFTIME} = 1.00$ , and  $\text{DIFFPCT} = 0.80$ .
  - Compare the length of this confidence interval with the length of the confidence interval on mean PITCH at the same point from Exercise 2.15 part (b), where an additive model in SOAKTIME, SOAKPCT, DIFFTIME, and DIFFPCT was used. Which confidence interval is shorter? Does this tell you anything about which model is preferable?

- 2.17** For the regression model for the wire bond pull strength data in Exercise 2.3.
- Plot the residuals versus  $\hat{y}$  and versus the regressors used in the model. What information is provided by these plots?
  - Construct a normal probability plot of the residuals. Are there reasons to doubt the normality assumption for this model?
  - Are there any indications of influential observations in the data?
- 2.18** Consider the semiconductor  $hFE$  data in Exercise 2.4.
- Plot the residuals from this model versus  $\hat{y}$ . Comment on the information in this plot.
  - What is the value of  $R^2$  for this model?
  - Refit the model using  $\ln hFE$  as the response variable.
  - Plot the residuals versus predicted  $\ln hFE$  for the model in part (c) above. Does this give any information about which model is preferable?
  - Plot the residuals from the model in part (d), versus the regressor  $x_3$ . Comment on this plot.
  - Refit the model to  $\ln hFE$  using  $x_1, x_2$ , and  $1/x_3$  as the regressors. Comment on the effect of this change in the model.
- 2.19** Consider the regression model for the heat-treating data in Exercise 2.6.
- Calculate the percentage of variability explained by this model.
  - Construct a normal probability plot for the residuals. Comment on the normality assumption.
  - Plot the residuals versus  $\hat{y}$ , and interpret the display.
  - Calculate Cook's distance for each observation, and provide an interpretation of this statistic.
- 2.20** In Exercise 2.12 we fitted a model to the response PITCH in the heat treating data of Exercise 2.6 using new regressors  $x_1 = \text{SOAKTIME} \times \text{SOAKPCT}$  and  $x_2 = \text{DIFFTIME} \times \text{DIFFPCT}$ .
- Calculate the  $R^2$  for this model, and compare it with the value of  $R^2$  from the original model in Exercise 2.6. Does this provide some information about which model is preferable?
  - Plot the residuals from this model versus  $\hat{y}$  and on a normal probability scale. Comment on model adequacy.
  - Find the values of Cook's distance measure. Are any observations unusually influential?
- 2.21** An article entitled "A Method for Improving the Accuracy of Polynomial Regression Analysis" in the *Journal of Quality Technology* (1971, pp. 149–155) reported the following data on  $y$  = ultimate shear strength of a rubber compound (psi) and  $x$  = cure temperature ( $^{\circ}\text{F}$ ).

$y$	770	800	840	810	735	640	590	560
$x$	280	284	292	295	298	305	308	315

- (a) Fit a second-order polynomial to these data.
- (b) Test for significance of regression, using  $\alpha = 0.05$ .
- (c) Test the hypothesis that  $\beta_{11} = 0$ , using  $\alpha = 0.05$ .
- (d) Compute the residuals and use them to evaluate model adequacy.
- (e) Suppose that the following additional observations are available:  $(x = 284, y = 815)$ ,  $(x = 295, y = 830)$ ,  $(x = 305, y = 660)$ , and  $(x = 315, y = 545)$ . Test the second-order model for lack of fit.
- 2.22** Consider the following data, which result from an experiment to determine the effect of  $x$  = test time in hours at a particular temperature to  $y$  = change in oil viscosity:
- | $y$ | -4.42 | -1.39 | -1.55 | -1.89 | -2.43 | -3.15 | -4.05 | -5.15 | -6.43 | -7.89 |
|-----|-------|-------|-------|-------|-------|-------|-------|-------|-------|-------|
| $x$ | 0.25  | 0.50  | 0.75  | 1.00  | 1.25  | 1.50  | 1.75  | 2.00  | 2.25  | 2.50  |
- (a) Fit a second-order polynomial to the data.
- (b) Test for significance of regression, using  $\alpha = 0.05$ .
- (c) Test the hypothesis that  $\beta_{11} = 0$ , using  $\alpha = 0.05$ .
- (d) Compute the residuals and use them to evaluate model adequacy.
- 2.23** When fitting polynomial regression models we often subtract  $\bar{x}$  from each  $x$ -value to produce a **centered** regressor  $x' = x - \bar{x}$ . This reduces the effects of dependences among the model terms and often leads to more accurate estimates of the regression coefficients. Using the data from Exercise 2.21, fit the model  $y = \beta_0^* + \beta_1^*x' + \beta_{11}^*(x')^2 + \varepsilon$ . Use the results to estimate the coefficients in the uncentered model  $y = \beta_0 + \beta_1x + \beta_{11}x^2 + \varepsilon$ .
- 2.24** Suppose that we use a standardized variable  $x' = (x - \bar{x})/s_x$ , where  $s_x$  is the standard deviation of  $x$ , in constructing a polynomial regression model. Using the data in Exercise 2.21 and the standardized variable approach, fit the model  $y = \beta_0^* + \beta_1^*x' + \beta_{11}^*(x')^2 + \varepsilon$ .
- (a) What value of  $y$  do you predict when  $x = 285^\circ\text{F}$ ?
- (b) Estimate the regression coefficients in the unstandardized model  $y = \beta_0 + \beta_1x + \beta_{11}x^2 + \varepsilon$ .
- (c) What can you say about the relationship between  $SS_E$  and  $R^2$  for the standardized and unstandardized models?
- (d) Suppose that  $y' = (y - \bar{y})/s_y$  is used in the model along with  $x'$ . Fit the model and comment on the relationship between  $SS_E$  and  $R^2$  in the standardized model and the unstandardized model.
- 2.25** An article in the *Journal of Pharmaceuticals Sciences* (vol. 80, 1991, pp. 971–977) presents data on the observed mole fraction solubility of a solute at a constant temperature to the dispersion, dipolar, and hydrogen bonding Hansen partial solubility parameters. The data are in Table E2.5, where  $y$  is the negative logarithm of the mole fraction solubility,  $x_1$  is the dispersion Hansen partial solubility,  $x_2$  is the dipolar partial solubility, and  $x_3$  is the hydrogen bonding partial solubility.
- (a) Fit the model  $y = \beta_0 + \beta_1x_1 + \beta_2x_2 + \beta_3x_3 + \beta_{12}x_1x_2 + \beta_{13}x_1x_3 + \beta_{23}x_2x_3 + \beta_{11}x_1^2 + \beta_{22}x_2^2 + \beta_{33}x_3^2 + \varepsilon$ .
- (b) Test for significance of regression, using  $\alpha = 0.05$ .

**TABLE E2.5 Data for Exercise 2.25**

Obs	$y$	$x_1$	$x_2$	$x_3$
1	0.22200	7.3	0.0	0.0
2	0.39500	8.7	0.0	0.3
3	0.42200	8.8	0.7	1.0
4	0.43700	8.1	4.0	0.2
5	0.42800	9.0	0.5	1.0
6	0.46700	8.7	1.5	2.8
7	0.44400	9.3	2.1	1.0
8	0.37800	7.6	5.1	3.4
9	0.49400	10.0	0.0	0.3
10	0.45600	8.4	3.7	4.1
11	0.45200	9.3	3.6	2.0
12	0.11200	7.7	2.8	7.1
13	0.43200	9.8	4.2	2.0
14	0.10100	7.3	2.5	6.8
15	0.23200	8.5	2.0	6.6
16	0.30600	9.5	2.5	5.0
17	0.09230	7.4	2.8	7.8
18	0.11600	7.8	2.8	7.7
19	0.07640	7.7	3.0	8.0
20	0.43900	10.3	1.7	4.2
21	0.09440	7.8	3.3	8.5
22	0.11700	7.1	3.9	6.6
23	0.07260	7.7	4.3	9.5
24	0.04120	7.4	6.0	10.9
25	0.25100	7.3	2.0	5.2
26	0.00002	7.6	7.8	20.7

- (c) Plot the residuals, and comment on model adequacy.
- (d) Use the extra sum of squares method to test the contribution of the second-order terms, using  $\alpha = 0.05$ .
- 2.26** Below are data on  $y$  = green liquor concentration (g/liter) and  $x$  = paper machine speed (ft/min) from a kraft paper machine (the data were read from a graph in an article in the *Tappi Journal*, March, 1986).

$y$	16.0	15.8	15.6	15.5	14.8	14.0	13.5	13.0	12.0	11.0
$x$	1700	1720	1730	1740	1750	1760	1770	1780	1790	1795

- (a) Fit the model  $y = \beta_0 + \beta_1 x + \beta_2 x^2 + \varepsilon$  using least squares.
- (b) Test for significance of regression using  $\alpha = 0.05$ . What are your conclusions?
- (c) Test the contribution of the quadratic term to the model, over the contribution of the linear term, using an  $F$ -statistic. If  $\alpha = 0.05$ , what conclusion can you draw?
- (d) Plot the residuals from this model versus  $\hat{y}$ . Does the plot reveal any inadequacies?
- (e) Construct a normal probability plot of the residuals. Comment on the normality assumption.

- 2.27** Consider a multiple regression model with  $k$  regressors. Show that the test statistic for significance of regression can be written as

$$F_k = \frac{R^2/k}{(1 - R^2)/(n - k - 1)}$$

Suppose that  $n = 20$ ,  $k = 4$ , and  $R^2 = 0.90$ . If  $\alpha = 0.05$ , what conclusion would you draw about the relationship between  $y$  and the four regressors?

- 2.28** A regression model is used to relate a response  $y$  to  $k = 4$  regressors. What is the smallest value of  $R^2$  that will result in a significant regression if  $\alpha = 0.05$ ? Use the results of the previous exercise. Are you surprised by how small the value of  $R^2$  is?
- 2.29** Show that we can express the residuals from a multiple regression model as

$$\mathbf{e} = (\mathbf{I} - \mathbf{H})\mathbf{y}$$

where  $\mathbf{H} = \mathbf{X}(\mathbf{X}'\mathbf{X})^{-1}\mathbf{X}'$ .

- 2.30** Show that the variance of the  $i$ th residual  $e_i$  in a multiple regression model is  $\sigma^2(1 - h_{ii})$  and that the covariance between  $e_i$  and  $e_j$  is  $-\sigma^2 h_{ij}$ , where the  $hs$  are the elements of  $\mathbf{H} = \mathbf{X}(\mathbf{X}'\mathbf{X})^{-1}\mathbf{X}'$ .
- 2.31** Consider the multiple linear regression model  $\mathbf{y} = \mathbf{X}\boldsymbol{\beta} + \boldsymbol{\epsilon}$ . If  $\mathbf{b}$  denotes the least squares estimator of  $\boldsymbol{\beta}$ , show that  $\mathbf{b} = \boldsymbol{\beta} + \mathbf{R}\boldsymbol{\epsilon}$  where  $\mathbf{R} = (\mathbf{X}'\mathbf{X})^{-1}\mathbf{X}'$ .
- 2.32** **Constrained least squares:** Suppose we wish to find the least squares estimator of  $\boldsymbol{\beta}$  in the model  $\mathbf{y} = \mathbf{X}\boldsymbol{\beta} + \boldsymbol{\epsilon}$  subject to a set of equality constraints, say  $\mathbf{T}\boldsymbol{\beta} = \mathbf{c}$ . Show that the estimator is

$$\mathbf{b}_c = \mathbf{b}(\mathbf{X}'\mathbf{X})^{-1}\mathbf{T}'[\mathbf{T}(\mathbf{X}'\mathbf{X})^{-1}\mathbf{T}']^{-1}(\mathbf{c} - \mathbf{T}\mathbf{b})$$

where  $\mathbf{b} = (\mathbf{X}'\mathbf{X})^{-1}\mathbf{X}'\mathbf{y}$ .



---

# 3

---

## TWO-LEVEL FACTORIAL DESIGNS

### 3.1 INTRODUCTION

Factorial designs are widely used in experiments involving several factors where it is necessary to investigate the joint effects of the factors on a response variable. By joint factor effects, we typically mean main effects and interactions. A very important special case of the factorial design is that where each of the  $k$  factors of interest has only two levels. Because each replicate of such a design has exactly  $2^k$  experimental trials or runs, these designs are usually called  **$2^k$  factorial designs**. These designs are the subject of this chapter.

The  $2^k$  factorial designs are very important in response surface work. Specifically, they find applications in three areas:

1. A  $2^k$  design (or a fractional version discussed in the next chapter) is useful at the start of a response surface study where **screening experiments** should be performed to identify the important process or system variables.
2. A  $2^k$  design is often used to fit a first-order response surface model and to generate the factor effect estimates required to perform the method of **steepest ascent**.
3. The  $2^k$  design is a basic building block used to create other response surface designs. For example, if you augment a  $2^2$  design with axial runs and center points as in Fig. 2.8 of Chapter 2, then a **central composite design** results. As we will subsequently see, the central composite design is one of the most important designs for fitting second-order response surface models.

### 3.2 THE $2^2$ DESIGN

The simplest design in the  $2^k$  series is one with only two factors, say  $A$  and  $B$ , each run at two levels. This design is called a  **$2^2$  factorial design**. The levels of the factors may be arbitrarily called “low” and “high.” These two levels may be **quantitative**, such as two values of temperature or pressure; or they may be **qualitative**, such as two machines, or two operators. In most response surface studies the factors and their levels are quantitative.

As an example, consider an investigation into the effect of the concentration of the reactant and the feed rate on the viscosity of product from a chemical process. Let the reactant concentration be factor  $A$ , and let the two levels of interest be 15% and 25%. The feed rate is factor  $B$ , with the low level being 20 lb/hr and the high level being 30 lb/hr. The experiment is replicated four times, and the data are as follows:

Factor-Level Combination	Viscosity				
	I	II	III	IV	Total
A low, $B$ low	145	148	147	140	580
A high, $B$ low	158	152	155	152	617
A low, $B$ high	135	138	141	139	553
A high, $B$ high	150	152	146	149	597

The four factor-level or treatment combinations in this design are shown graphically in Fig. 3.1. By convention, we denote the effect of factor by the same capital Latin letter. That is,  $A$  refers to the effect of factor  $A$ ,  $B$  refers to the effect of factor  $B$ , and  $AB$  refers to the  $AB$  interaction. In the  $2^2$  design the low and high levels of  $A$  and  $B$  are denoted by – and +, respectively, on the  $A$ - and  $B$ -axes. Thus, – on the  $A$ -axis represents the low level of concentration (15%), and + represents the high level (25%). Similarly, – on the  $B$ -axis represents the low level of feed rate, and + denotes the high level.

The four factor-level combinations in the design can also be represented by lowercase letters, as shown in Fig. 3.1. We see from the figure that the high level of any factor at a point in the design is denoted by the corresponding lowercase letter and that the low level of a factor at a point in the design is denoted by the absence of the corresponding

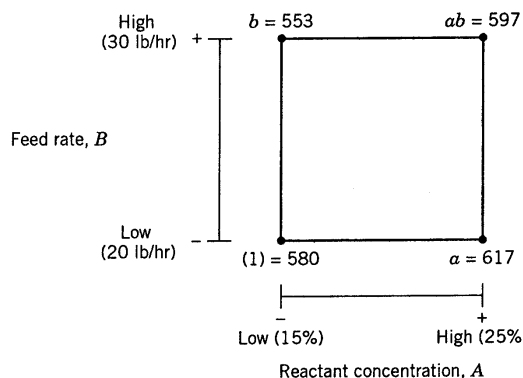


Figure 3.1 The  $2^2$  design.

letter. Thus,  $a$  represents the combination of factor levels with  $A$  at the high level and  $B$  at the low level,  $b$  represents  $A$  at the low level and  $B$  at the high level, and  $ab$  represents both factors at the high level. By convention, (1) is used to denote the run where both factors are at the low level. This notation is used throughout the 2<sup>k</sup> series.

The **average effect of a factor** (or the **main effect**) is defined as the change in response produced by a change in the level on that factor averaged over the levels of the other factor. Also the symbols (1),  $a$ ,  $b$ , and  $ab$  now represent the **totals** of all  $n$  replicates taken at the points in the design, as illustrated in Fig. 3.1. The formulas for the effects of  $A$ ,  $B$ , and  $AB$  may be easily derived. The main effect of  $A$  can be found as the difference in the average response of the two points on the right-hand side of the square in Fig. 3.1 (call this average  $\bar{y}_{A^+}$ , because it is the average response at the points where  $A$  is at the high level) and the two points on the left-hand side (or  $\bar{y}_{A^-}$ ). That is,

$$\begin{aligned} A &= \bar{y}_{A^+} - \bar{y}_{A^-} \\ &= \frac{ab + a}{2n} - \frac{b + (1)}{2n} \\ &= \frac{1}{2n}[ab + a - b - (1)] \end{aligned} \quad (3.1)$$

The main effect of factor  $B$  is found as the difference between the average of the response at the two points on the top of the square ( $\bar{y}_{B^+}$ ) and the average of the response at the two points on the bottom ( $\bar{y}_{B^-}$ ), or

$$\begin{aligned} B &= \bar{y}_{B^+} - \bar{y}_{B^-} \\ &= \frac{ab + b}{2n} - \frac{a + (1)}{2n} \\ &= \frac{1}{2n}[ab + b - a - (1)] \end{aligned} \quad (3.2)$$

Finally, the interaction effect  $AB$  is the average of the responses on the right-to-left diagonal points in the square [ $ab$  and (1)] minus the average of the responses on the left-to-right diagonal points ( $a$  and  $b$ ), or

$$\begin{aligned} AB &= \frac{ab + (1)}{2n} - \frac{a + b}{2n} \\ &= \frac{1}{2n}[ab + (1) - a - b] \end{aligned} \quad (3.3)$$

Using the example data in Fig. 3.1, we may estimate the effects as

$$A = \frac{1}{2(4)}(597 + 617 - 553 - 580) = 10.125$$

$$B = \frac{1}{2(4)}(597 + 553 - 617 - 580) = -5.875$$

$$AB = \frac{1}{2(4)}(597 + 580 - 617 - 553) = 0.875$$

The main effect of  $A$  (reactant concentration) is positive; this suggests that increasing  $A$  from the low level (15%) to the high level (25%) will increase the viscosity. The main effect of  $B$  (feed rate) is negative; this suggests that increasing the feed rate will decrease the viscosity. The interaction effect appears to be small relative to the two main effects.

In many experiments involving  $2^k$  designs, we will examine the magnitude and direction of the factor effects to determine which variables are likely to be important. The analysis of variance can generally be used to confirm this interpretation. In the  $2^k$  design, there are some special, efficient methods for performing the calculations in the analysis of variance.

Consider the sums of squares for  $A$ ,  $B$ , and  $AB$ . Note from Equation 3.1 that a **contrast** is used in estimating  $A$ , namely,

$$\text{Contrast}_A = ab + a - b - (1) \quad (3.4)$$

We usually call this contrast the **total effect** of  $A$ . From Equations 3.2 and 3.3, we see that contrasts are also used to estimate  $B$  and  $AB$ . Furthermore, these three contrasts are orthogonal. The sum of squares for any contrast is equal to the contrast squared divided by the number of observations in each total in the contrast times the sum of the squares of the contrast coefficients. Consequently, we have

$$SS_A = \frac{[ab + a - b - (1)]^2}{n \times 4} \quad (3.5)$$

$$SS_B = \frac{[ab + b - a - (1)]^2}{n \times 4} \quad (3.6)$$

and

$$SS_{AB} = \frac{[ab + (1) - a - b]^2}{n \times 4} \quad (3.7)$$

as the sums of squares for  $A$ ,  $B$ , and  $AB$ .

Using the data in Fig. 3.1, we may find the sums of the squares from Equations 3.5, 3.6, and 3.7 as

$$SS_A = \frac{(81)^2}{4(4)} = 410.0625$$

$$SS_B = \frac{(47)^2}{4(4)} = 138.0625$$

and

$$SS_{AB} = \frac{(7)^2}{4(4)} = 3.0625$$

The total sum of squares is found in the usual way; that is,

$$SS_T = \sum_{i=1}^2 \sum_{j=1}^2 \sum_{k=1}^n y_{ijk}^2 - \frac{y_{...}^2}{4n} \quad (3.8)$$

In general,  $SS_T$  has  $4n - 1$  degrees of freedom. The error sum of squares, with  $4(n - 1)$  degrees of freedom, is usually computed by subtraction as

$$SS_E = SS_T - SS_A - SS_B - SS_{AB} \quad (3.9)$$

For the data in Fig. 3.1, we obtain

$$\begin{aligned} SS_T &= \sum_{i=1}^2 \sum_{j=1}^2 \sum_{k=1}^4 y_{ijk}^2 - \frac{\bar{y}^2}{4(4)} \\ &= 334,527.0000 - 344,275.5625 = 651.4375 \end{aligned}$$

and

$$\begin{aligned} SS_E &= SS_T - SS_A - SS_B - SS_{AB} \\ &= 651.4375 - 410.0625 - 138.0625 - 3.0625 \\ &= 100.2500 \end{aligned}$$

using  $SS_A$ ,  $SS_B$ , and  $SS_{AB}$  computed previously. The complete analysis of variance is summarized in Table 3.1. Both main effects are statistically significant, and the interaction is not significant. This confirms our initial interpretation of the data based on the magnitudes of the factor effects.

It is often convenient to write down the factor level or treatment combinations in the order (1),  $a$ ,  $b$ ,  $ab$ , as in the column labeled “treatment combination” in Table 3.2. This

**TABLE 3.1 Analysis of Variance for Data in Fig. 3.1**

Source of Variation	Sum of Squares	Degrees of Freedom	Mean Square	$F_0$	P-Value
A	410.0625	1	410.0625	49.08	$1.42 \times 10^{-5}$
B	138.0625	1	138.0625	16.53	0.0016
AB	3.0625	1	3.0625	0.37	0.5562
Error	100.2500	12	8.3542		
Total	651.4375	15			

**TABLE 3.2 Signs for Calculating Effects in the  $2^2$  Design**

Treatment Combination	Factorial Effect			
	I	A	B	AB
(1)	+	-	-	+
$a$	+	+	-	-
$b$	+	-	+	-
$ab$	+	+	+	+

is referred to as **standard order**. The columns labeled *A* and *B* in this table contain the + and – signs corresponding to the four runs at the corners of the square in Fig. 3.1. Note that the contrast coefficients for estimating the interaction effect are just the products of the corresponding coefficients for the two main effects. The column labeled *I* in Table 3.2 represents the total or average of all of the observations in the entire experiment. The column corresponding to *I* has only plus signs and is sometimes called the identity column. The row designators are the treatment combinations. To find the contrast for estimating any effect, simply multiply the signs in the appropriate column of the table by the corresponding treatment combination and add. For example, to estimate *A*, the contrast is  $-(1) + a - b + ab$ , which agrees with Equation 3.1.

**The Regression Model** It is easy to convert the effect estimates in a  $2^k$  factorial design into a regression model that can be used to predict the response at any point in the space spanned by the factors in the design. For the chemical process experiment, the first-order regression model is

$$y = \beta_0 + \beta_1 x_1 + \beta_2 x_2 + \varepsilon \quad (3.10)$$

where  $x_1$  is the **coded variable** that represents the reactant concentration,  $x_2$  is the coded variable that represents the feed rate, and the  $\beta$ s are the regression coefficients. The relationship between the natural variables, the reactant concentration and the feed rate, and the coded variables is

$$x_1 = \frac{\text{Conc} - (\text{Conc}_{\text{low}} + \text{Conc}_{\text{high}})/2}{(\text{Conc}_{\text{high}} - \text{Conc}_{\text{low}})/2}$$

and

$$x_2 = \frac{\text{Feed} - (\text{Feed}_{\text{low}} + \text{Feed}_{\text{high}})/2}{(\text{Feed}_{\text{high}} - \text{Feed}_{\text{low}})/2}$$

When the natural variables have only two levels, this coding will produce the  $\pm 1$  notation for the levels of the coded variables. To illustrate this for our example, note that

$$\begin{aligned} x_1 &= \frac{\text{Conc} - (15 + 25)/2}{(25 - 15)/2} \\ &= \frac{\text{Conc} - 20}{5} \end{aligned}$$

Thus, if the concentration is at the high level ( $\text{Conc} = 25\%$ ), then  $x_1 = +1$ , whereas if the concentration is at the low level ( $\text{Conc} = 15\%$ ), then  $x_1 = -1$ . Furthermore,

$$\begin{aligned}x_2 &= \frac{\text{Feed} - (20 + 30)/2}{(30 - 20)/2} \\&= \frac{\text{Feed} - 25}{5}\end{aligned}$$

Thus, if the feed rate is at the high level ( $\text{Feed} = 30 \text{ lb/hr}$ ), then  $x_2 = +1$ , whereas if the feed rate is at the low level ( $\text{Feed} = 20 \text{ lb/hr}$ ), then  $x_2 = -1$ .

The fitted regression model is

$$\begin{aligned}\hat{y} &= 146.6875 + \left(\frac{10.125}{2}\right)x_1 + \left(\frac{-5.875}{2}\right)x_2 \\&= 146.6875 + 5.0625x_1 - 2.9375x_2\end{aligned}$$

where the intercept is the grand average of all 16 observations, and the regression coefficients  $b_1$  and  $b_2$  are one-half the corresponding factor effect estimates. The reason that the regression coefficient is one-half the effect estimate is that a regression coefficient measures the effect of a unit change in  $x$  on the mean of  $y$ , and the effect estimate is based on a two-unit change (from  $-1$  to  $+1$ ). This model explains about 84% of the variability in viscosity, because

$$\begin{aligned}R^2 &= SS_{\text{model}}/SS_T = (SS_A + SS_B)/SS_T \\&= (410.0625 + 138.0625)/651.4375 \\&= 548.1250/651.4375 = 0.8414\end{aligned}$$

This regression model is really a first-order response surface model for the process. If the interaction term in the analysis of variance (Table 3.1) were significant, the regression model would have been

$$y = \beta_0 + \beta_1 x_2 + \beta_2 x_1 + \beta_{12} x_1 x_2 + \epsilon$$

and the estimate of the regression coefficient  $\beta_{12}$  would be one-half the  $AB$  interaction effect, or  $b_{12} = 0.875/2$ . Clearly this coefficient is small relative to  $b_1$  and  $b_2$ , and so this is further evidence that interaction contributes very little to explaining viscosity in this process.

**Regression Coefficients are Least Squares Estimates** The regression coefficient estimates obtained above are **least squares estimates**. To verify this, write out the model in Equation 3.10 in matrix form, that is,

$$\mathbf{y} = \mathbf{X}\boldsymbol{\beta} + \boldsymbol{\epsilon}$$

where

$$\mathbf{y} = \begin{bmatrix} 145 \\ 148 \\ 147 \\ 140 \\ 158 \\ 152 \\ 155 \\ 152 \\ 135 \\ 138 \\ 141 \\ 139 \\ 150 \\ 152 \\ 146 \\ 149 \end{bmatrix}, \quad \mathbf{X} = \begin{bmatrix} 1 & -1 & -1 \\ 1 & -1 & -1 \\ 1 & -1 & -1 \\ 1 & -1 & -1 \\ 1 & 1 & -1 \\ 1 & 1 & -1 \\ 1 & 1 & -1 \\ 1 & 1 & -1 \\ 1 & -1 & 1 \\ 1 & -1 & 1 \\ 1 & -1 & 1 \\ 1 & -1 & 1 \\ 1 & 1 & 1 \\ 1 & 1 & 1 \\ 1 & 1 & 1 \end{bmatrix}, \quad \boldsymbol{\beta} = \begin{bmatrix} \beta_0 \\ \beta_1 \\ \beta_2 \end{bmatrix}, \quad \boldsymbol{\epsilon} = \begin{bmatrix} \varepsilon_1 \\ \varepsilon_2 \\ \varepsilon_3 \\ \varepsilon_4 \\ \varepsilon_5 \\ \varepsilon_6 \\ \varepsilon_7 \\ \varepsilon_8 \\ \varepsilon_9 \\ \varepsilon_{10} \\ \varepsilon_{11} \\ \varepsilon_{12} \\ \varepsilon_{13} \\ \varepsilon_{14} \\ \varepsilon_{15} \\ \varepsilon_{16} \end{bmatrix}$$

The least squares estimates of  $\beta_0$ ,  $\beta_1$ , and  $\beta_2$  are found from

$$\mathbf{b} = (\mathbf{X}'\mathbf{X})^{-1}\mathbf{X}'\mathbf{y}$$

or

$$\begin{bmatrix} b_0 \\ b_1 \\ b_2 \end{bmatrix} = \begin{bmatrix} 16 & 0 & 0 \\ 0 & 16 & 0 \\ 0 & 0 & 16 \end{bmatrix}^{-1} \begin{bmatrix} 2347 \\ 81 \\ -47 \end{bmatrix}$$

$$= \frac{1}{16} \mathbf{I}_3 \begin{bmatrix} 2347 \\ 81 \\ -47 \end{bmatrix}$$

where  $\mathbf{I}_3$  is a  $3 \times 3$  identity matrix. This last expression reduces to

$$\begin{bmatrix} b_0 \\ b_1 \\ b_2 \end{bmatrix} = \begin{bmatrix} 2347/16 \\ 81/16 \\ -47/16 \end{bmatrix}$$

or  $b_0 = 2347/16 = 146.6875$ ,  $b_1 = 5.0625$ , and  $b_2 = -2.9375$ . Therefore, the least squares estimates of  $\beta_1$  and  $\beta_2$  are exactly one-half of the factor effect estimates. This will always be the case in any  $2^k$  factorial design with coded factors between  $-1$  and  $1$ .

**Residual Analysis** It is easy to compute the **residuals** from a  $2^k$  design via the regression model. For the chemical process experiment, the regression model is

$$\hat{y} = 146.6875 + \left(\frac{10.125}{2}\right)x_1 - \left(\frac{5.875}{2}\right)x_2$$

This model can be used to generate the predicted values of  $y$  at the four points in the design. For example, when the reactant concentration is at the low level ( $x_1 = -1$ ) and the feed rate is at the low level ( $x_2 = -1$ ) the predicted viscosity is

$$\begin{aligned}\hat{y} &= 146.6875 + \left(\frac{10.125}{2}\right)(-1) - \left(\frac{5.875}{2}\right)(-1) \\ &= 144.563\end{aligned}$$

There are four observations at this treatment combination, and the residuals are

$$\begin{aligned}e_1 &= 145 - 144.563 = 0.438 \\ e_2 &= 148 - 144.563 = 3.438 \\ e_3 &= 152 - 144.563 = 2.438 \\ e_4 &= 140 - 144.563 = -4.563\end{aligned}$$

The remaining predicted values and residuals are calculated similarly. For the high level of the reactant concentration and the low level of the feed rate:

$$\begin{aligned}\hat{y} &= 146.6875 + \left(\frac{10.125}{2}\right)(+1) + \left(\frac{-5.875}{2}\right)(-1) \\ &= 154.688\end{aligned}$$

and

$$\begin{aligned}e_5 &= 158 - 154.688 = -3.688 \\ e_6 &= 152 - 154.688 = -2.688 \\ e_7 &= 155 - 154.688 = -0.313 \\ e_8 &= 152 - 154.688 = -2.688\end{aligned}$$

For the low level of the reactant concentration and the high level of the feed rate:

$$\begin{aligned}\hat{y} &= 146.6875 + \left(\frac{10.125}{2}\right)(-1) + \left(\frac{-5.875}{2}\right)(+1) \\ &= 138.688\end{aligned}$$

and

$$e_9 = 135 - 138.688 = -3.688$$

$$e_{10} = 138 - 138.688 = -0.688$$

$$e_{11} = 141 - 138.688 = 2.313$$

$$e_{12} = 139 - 138.688 = 0.313$$

Finally, for the high level of both factors:

$$\begin{aligned}\hat{y} &= 146.6875 + \left(\frac{10.125}{2}\right)(+1) + \left(\frac{-5.875}{2}\right)(+1) \\ &= 148.812\end{aligned}$$

and

$$e_{13} = 150 - 148.812 = 1.188$$

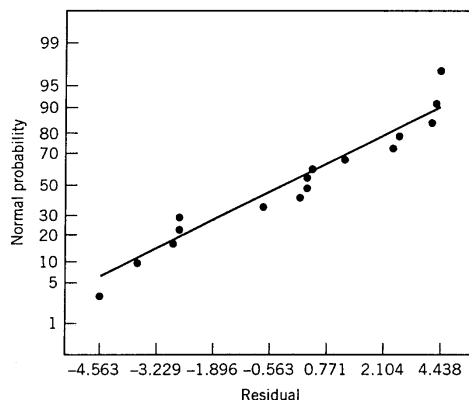
$$e_{14} = 152 - 148.812 = 3.188$$

$$e_{15} = 146 - 148.812 = -2.813$$

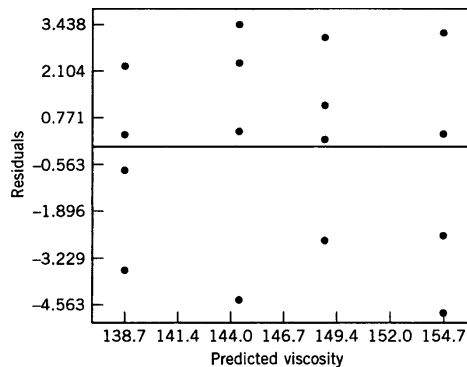
$$e_{16} = 149 - 148.812 = 0.188$$

Figure 3.2 presents a normal probability plot of these residuals, and Fig. 3.3 is a plot of the residuals versus the predicted values  $\hat{y}$ . These plots appear satisfactory, so we have no reason to suspect problems with the validity of our conclusions.

**The Response Surface** Figure 3.4a presents a three-dimensional response surface plot of viscosity, based on the first-order model using reactant concentration and feed rate as the regressors, and Fig. 3.4b is the contour plot. Because the model is first-order, the fitted response surface is a plane. Based on examination of this fitted surface, it is clear that viscosity increases as reactant concentration increases and feed rate decreases. Often a fitted surface such as this can be used to determine an appropriate **direction of potential**



**Figure 3.2** Normal probability plot of the residuals from the chemical process experiment.



**Figure 3.3** Plot of residuals versus predicted viscosity for the chemical process experiment.

**improvement** for a process. A formal method for doing this, called the **method of steepest ascent**, will be introduced in Chapter 5.

**Computer Output** There are several software packages that will construct experimental designs and analyze the resulting data. The output from Design-Expert is shown in Table 3.3. In the upper portion of the table an analysis of variance for the full model is presented. The format of this presentation is slightly different from the analysis of variance in Table 3.1. The source called the “model” is an analysis of variance for the full model using

$$\begin{aligned} SS_{\text{model}} &= SS_A + SS_B + SS_{AB} \\ &= 410.06 + 138.06 + 3.06 \\ &= 551.19 \end{aligned}$$

Thus the statistic

$$F_0 = \frac{MS_{\text{model}}}{MS_E} = \frac{183.73}{8.35} = 21.99$$

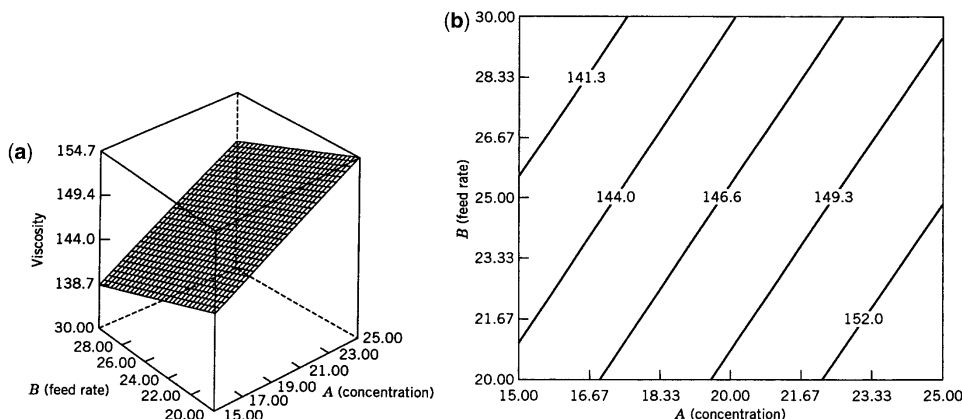


**Figure 3.4** (a) Response surface plot of viscosity from the chemical process experiment. (b) The contour plot.

**TABLE 3.3 Design Expert Output for the  $2^2$  Factorial Example**

Response: Viscosity

ANOVA for Selected Factorial Model

Analysis of variance table [Partial sum of squares]

Source	Sum of Squares	DF	Mean Square	F-Value	Prob > F
Model	551.19	3	183.73	21.99	<0.0001
A	410.06	1	410.06	49.08	<0.0001
B	138.06	1	138.06	16.53	0.0016
AB	3.06	1	3.06	0.37	0.5562
Pure Error	100.25	12	8.35		
Cor Total	651.44	15			
Std. Dev.	2.89	<i>R</i> -Squared		0.8461	
Mean	146.69	Adj <i>R</i> -Squared		0.8076	
C.V.	1.97	Pred <i>R</i> -Squared		0.7264	
PRESS	178.22	Adeq Precision		11.071	
Factor	Coefficient Estimate	DF	Standard Error	95% CI Low	95% CI High
Intercept	146.69	1	0.72	145.11	148.26
A-Reactant C	5.06	1	0.72	3.49	6.64
B-Feed Rate	-2.94	1	0.72	-4.51	-1.36
AB	0.44	1	0.72	-1.14	2.01

Reduced Model:

Response: Viscosity

ANOVA for Selected Factorial Model

Analysis of variance table [Partial sum of squares]

Source	Sum of Squares	DF	Mean Square	F-Value	Prob > F
Model	548.13	2	274.06	34.49	<0.0001
A	410.06	1	410.06	51.60	<0.0001
B	138.06	1	138.06	17.37	0.0011
Residual	103.31	13	7.95		
<i>Lack of Fit</i>	3.06	1	3.06	0.37	0.5562
<i>Pure Error</i>	100.25	12	8.35		
Cor Total	651.44	15			
Std. Dev.	2.82	<i>R</i> -Squared		0.8414	

Mean	146.69	Adj R-Squared	0.8170			
C.V.	1.92	Pred R-Squared	0.7598			
PRESS	156.50	Adeq Precision	13.107			
Factor	Coefficients Estimate	DF	Standard Error	95% CI Low	95% CI High	VIF
Intercept	146.69	1	0.70	145.16	148.21	
A-Reactant C	5.06	1	0.70	3.54	6.59	1.00
B-Feed Rate	-2.94	1	0.70	-4.46	-1.41	1.00

Final Equation in Terms of Coded Factors:

$$\begin{aligned} \text{Viscosity} = \\ +146.69 \\ +5.06 *A \\ -2.94 *B \end{aligned}$$

Final Equation in Terms of Actual Factors:

$$\begin{aligned} \text{Viscosity} = \\ +141.12500 \\ +1.01250 *\text{Reactant C} \\ -0.58750 *\text{Feed Rate} \end{aligned}$$

Run Order	Standard Order	Actual Value	Predicted Value	Diagnostics Case Statistics				
				Residual	Leverage	Student Residual	Cook's Distance	Outlier <i>t</i>
1	1	145.00	144.56	0.44	0.188	0.172	0.002	0.166
16	2	148.00	144.56	3.44	0.188	1.353	0.141	1.402
4	3	147.00	144.56	2.44	0.188	0.959	0.071	0.956
5	4	140.00	144.56	-4.56	0.188	-1.796	0.248	-1.989
3	5	158.00	154.69	3.31	0.188	1.304	0.131	1.343
11	6	152.00	154.69	-2.69	0.188	-1.058	0.086	-1.063
8	7	155.00	154.69	0.31	0.188	0.123	0.001	0.118
12	8	152.00	154.69	-2.69	0.188	-1.058	0.086	-1.063
9	9	135.00	138.69	-3.69	0.188	-1.451	0.162	-1.523
14	10	138.00	138.69	-0.69	0.188	-0.271	0.006	-0.261
7	11	141.00	138.69	2.31	0.188	0.910	0.064	0.904
2	12	139.00	138.69	0.31	0.188	0.123	0.001	0.118
15	13	150.00	148.81	1.19	0.188	0.467	0.017	0.453
13	14	152.00	148.81	3.19	0.188	1.254	0.121	1.285
6	15	146.00	148.81	-2.81	0.188	-1.107	0.094	-1.117
10	16	149.00	148.81	0.19	0.188	0.074	0.000	0.071

is testing the hypotheses

$$H_0: \beta_1 = \beta_2 = \beta_{12} = 0$$

$$H_1: \text{at least one } \beta \neq 0.$$

Because  $F_0$  is large, we conclude that at least one variable has a nonzero effect. Then each individual factorial effect is tested for significance using the  $F$ -statistic (as in Table 3.1).

The lower portion of Table 3.3 shows the analysis of variance summary for the **reduced** model; that is, the model with the nonsignificant  $AB$  interactions removed. The **error** or **residual** sum of squares is now composed of a **pure error** component arising from the replicate runs and a **lack-of-fit** component corresponding to the  $AB$  interaction. The regression model in terms of both actual and coded variables is given, along with confidence intervals on each model coefficient, a summary of several regression diagnostics from Chapter 2, and the model residuals. The column labeled “Outlier  $t$ ” is  $R$ -student.

### 3.3 THE $2^3$ DESIGN

Suppose that three factors,  $A$ ,  $B$ , and  $C$ , each at two levels, are of interest. Then the design is called a  $2^3$  *factorial design*, and the eight treatment combinations can be displayed graphically as a cube, as shown in Fig. 3.5a. Extending the notation discussed in Section 3.2, we write the treatment combinations in standard order as (1),  $a$ ,  $b$ ,  $ab$ ,  $c$ ,  $ac$ ,  $bc$ , and  $abc$ . Remember that these symbols also represent the total of all  $n$  observations taken at that particular treatment combinations.

Using the “+” and “−” notation to represent the high and low levels of each factor, we may list the eight runs in the  $2^3$  design in the tabular format shown in Fig. 3.5b. This is usually called the **design matrix**.

The “+” and “−” notation is often called the **geometric notation**. While other notational schemes could be used, we prefer the geometric notation because it facilitates the translation of the analysis of variance results into a regression model. This notation is widely used in response surface methodology.

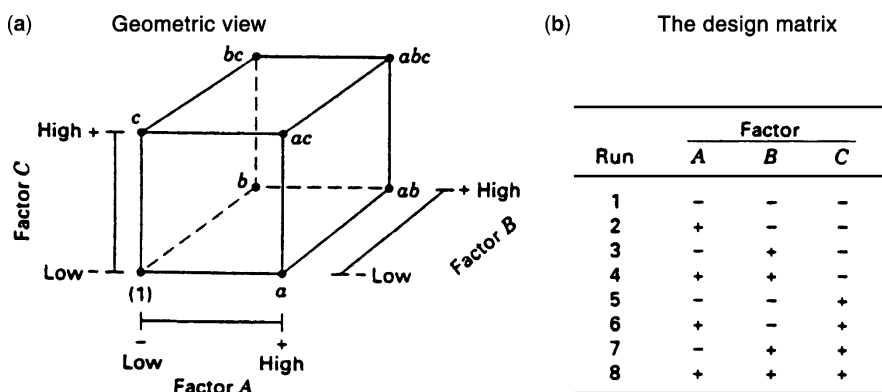


Figure 3.5 The  $2^3$  factorial design.

There are seven degrees of freedom between the eight treatment combinations in the  $2^3$  design. Three degrees of freedom are associated with the main effects of  $A$ ,  $B$ , and  $C$ . Four degrees of freedom are associated with interactions: one each with  $AB$ ,  $AC$ , and  $BC$ , and one with  $ABC$ .

Consider estimating the main effects. First, consider estimating the main effect of  $A$ . This effect estimate can be expressed as a contrast between the four treatment combinations in the right face of the cube in Fig. 3.6a (where  $A$  is at the high level) and the four in the left face (where  $A$  is at the low level). That is, the  $A$  effect is just the average of the four runs where  $A$  is at the high level ( $\bar{y}_{A+}$ ) minus the average of the four runs where  $A$  is at the low level ( $\bar{y}_{A-}$ ), or

$$\begin{aligned} A &= \bar{y}_{A+} - \bar{y}_{A-} \\ &= \frac{a + ab + ac + abc}{4n} - \frac{(1) + b + c + bc}{4n} \end{aligned}$$

This equation can be rearranged as

$$A = \frac{1}{4n} [a + ab + ac + abc - (1) - b - c - bc] \quad (3.11)$$

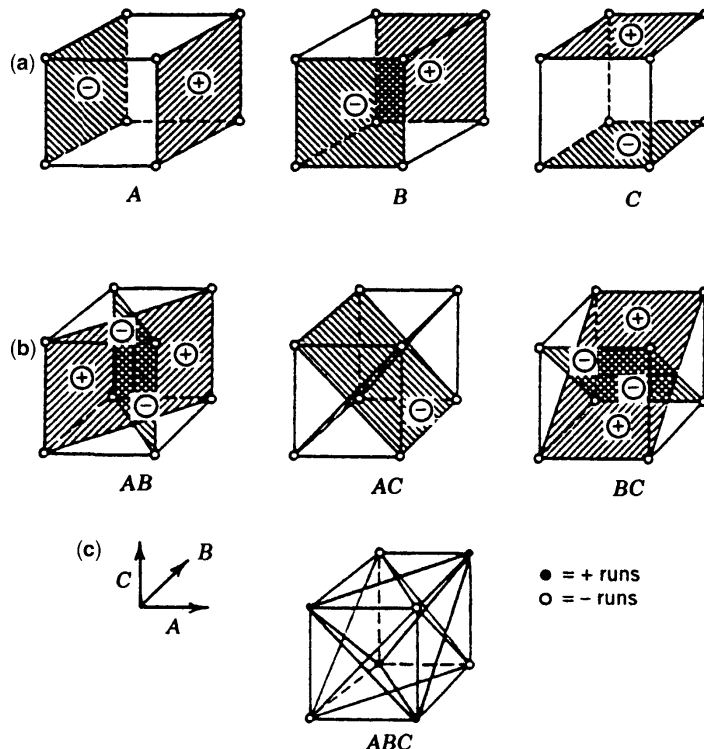


**Figure 3.6** Geometric presentation of contrasts corresponding to the main effects and interaction in the  $2^3$  design, (a) Main effects, (b) Two-factor interactions, (c) Three-factor interaction.

In a similar manner, the effect of  $B$  is the difference in averages between the four treatment combinations in the front face of the cube and the four in the back. This yields

$$\begin{aligned} B &= \bar{y}_{B^+} - \bar{y}_{B^-} \\ &= \frac{1}{4n} [b + ab + bc + abc - (1) - a - c - ac] \end{aligned} \quad (3.12)$$

The effect of  $C$  is the difference in averages between the four treatment combinations in the top face of the cube and the four in the bottom; that is,

$$\begin{aligned} C &= \bar{y}_{C^+} - \bar{y}_{C^-} \\ &= \frac{1}{4n} [c + ac + bc + abc - (1) - a - b - ab] \end{aligned} \quad (3.13)$$

The two-factor interaction effects may be computed easily. A measure of the  $AB$  interaction is the difference between the average  $A$  effects at the two levels of  $B$ . By convention, one-half of this difference is called the  $AB$  interaction. This is expressed symbolically as follows:

$B$	Average $A$ Effect
High (+)	$\frac{(abc - bc) + (ab - b)}{2n}$
Low (-)	$\frac{(ac - c) + [a - (1)]}{2n}$
Difference	$\frac{abc - bc + ab - b - ac + c - a + (1)}{2n}$

Because the  $AB$  interaction is one-half of this difference, we have

$$AB = \frac{[abc - bc + ab - b - ac + c - a + (1)]}{4n} \quad (3.14)$$

We can write Equation 3.14 as follows:

$$AB = \frac{abc + ab + c + (1)}{4n} - \frac{bc + b + ac + a}{4n}$$

In this form, the  $AB$  interaction is easily seen to be the difference in averages between runs on two diagonal planes in the cube in Fig. 3.6b. Using similar logic and referring to Fig. 3.6b, the  $AC$  and  $BC$  interactions are

$$AC = \frac{1}{4n} [(1) - a + b - ab - c + ac - bc + abc] \quad (3.15)$$

and

$$BC = \frac{1}{4n} [(1) + a - b - ab - c - ac + bc + abc] \quad (3.16)$$

The  $ABC$  interaction is defined as the average difference between the  $AB$  interaction for the two different levels of  $C$ . Thus,

$$\begin{aligned} ABC &= \frac{1}{4n} \{ [abc - bc] - [ac - c] - [ab - b] + [a - (1)] \} \\ &= \frac{1}{4n} [abc - bc - ac + c - ab + b + a - (1)] \end{aligned} \quad (3.17)$$

As before, we can think of the  $ABC$  interaction as the difference in two averages. If the runs in the two averages are isolated, they define the vertices of the two tetrahedra that make up the cube in Fig. 3.6c.

In Equations 3.11 through 3.17, the quantities in brackets are contrasts in the treatment combinations. A table of plus and minus signs can be developed for the contrasts and is shown in Table 3.4. Signs for the main effects are determined by associating a plus with the high level and a minus with the low level. Once the signs for the main effects have been established, the signs for the interaction columns can be obtained by multiplying the appropriate preceding columns, row by row. For example, the signs in the  $AB$  column are the products of the  $A$  and  $B$  column signs in each row. The contrast for any effect can be obtained from this table.

Table 3.4 has several interesting properties: (1) Except for column  $I$ , every column has an equal number of plus and minus signs. (2) The sum of the products of the signs in any two columns is zero. (3) Column  $I$  multiplied by any column leaves that column unchanged. That is,  $I$  is an identity element. (4) The product of any two columns yields a column in the table. For example,  $A \times B = AB$ , and

$$AB \times B = AB^2 = A$$

We see that the exponents in the products are formed by using modulus 2 arithmetic. (That is, the exponent can only be zero or one; if it is greater than one, it is reduced by multiples of 2.)

**TABLE 3.4** Algebraic Signs for Calculating Effects in the  $2^3$  Design

two until it is either zero or one.) All of these properties result from the fact that the  $2^3$  (indeed all  $2^k$  designs) is an **orthogonal design**.

Sums of squares for the effects are easily computed, because each effect has a corresponding single-degree-of-freedom contrast. In the  $2^3$  design with  $n$  replicates, the sum of squares for any effect is

$$SS = \frac{(\text{contrast})^2}{8n} \quad (3.18)$$

**Example 3.1 The Plasma Etch Experiment** An electrical engineer is investigating a plasma etching process used in semiconductor manufacturing. He is studying the effects of three factors—anode–cathode gap ( $A$ ),  $\text{C}_2\text{F}_6$  gas flow rate ( $B$ ), and power applied to the cathode ( $C$ )—on the etch rate. Each factor is run at two levels. Two replicates of a  $2^3$  factorial design are shown in Table 3.5, along with the resulting response variable values. The design is shown graphically in Fig. 3.7.

Using the totals shown in Table 3.5 for each of the eight runs in the design, we may calculate the effect estimates as follows:

$$\begin{aligned} A &= \frac{1}{4n}[a - (1) + ab - b + ac - c + abc - bc] \\ &= \frac{1}{8}[916 - 647 + 880 - 834 + 1221 - 1687 + 1190 - 1640] \\ &= \frac{1}{8}[-601] = -75.125 \\ B &= \frac{1}{4n}[b + ab + bc + abc - (1) - a - c - ac] \\ &= \frac{1}{8}[834 + 880 + 1640 + 1190 - 647 - 916 - 1687 - 1221] \\ &= \frac{1}{8}[73] = 9.125 \end{aligned}$$

TABLE 3.5 The  $2^3$  Factorial Design for Example 3.1

$A$ (Gap)	$B$ ( $\text{C}_2\text{F}_6$ Flow)	$C$ (Power)	Etch Rate ( $\text{\AA}/\text{min}$ )		
			Replicate I	Replicate II	Totals
-1	-1	-1	247	400	(1) = 647
1	-1	-1	470	446	$a = 916$
-1	1	-1	429	405	$b = 834$
1	1	-1	435	445	$ab = 880$
-1	-1	1	837	850	$c = 1687$
1	-1	1	551	670	$ac = 1221$
-1	1	1	775	865	$bc = 1640$
1	1	1	660	530	$abc = 1190$

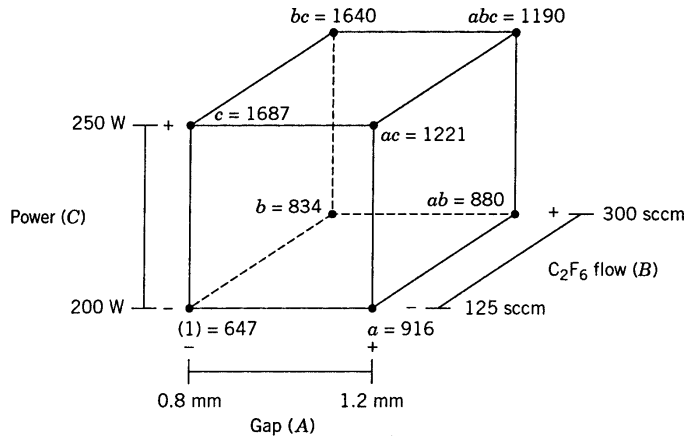


**Figure 3.7** The  $2^3$  design for Example 3.1.

$$\begin{aligned}
 C &= \frac{1}{4n} [c + ac + bc + abc - (1) - a - b - ab] \\
 &= \frac{1}{8} [1687 + 1221 + 1640 + 1190 - 647 - 916 - 834 - 886] \\
 &= \frac{1}{8} [2461] = 307.625 \\
 AB &= \frac{1}{4n} [ab - a - b + (1) + abc - bc - ac + c] \\
 &= \frac{1}{8} [880 - 916 - 834 + 647 + 1190 - 1640 - 1221 + 1687] \\
 &= \frac{1}{8} [-207] = -25.875 \\
 AC &= \frac{1}{4n} [(1) - a + b - ab - c + ac - bc + abc] \\
 &= \frac{1}{8} [647 - 916 + 834 - 880 - 1687 + 1221 - 1640 + 1190] \\
 &= \frac{1}{8} [-1231] = -153.875 \\
 BC &= \frac{1}{4n} [(1) + a - b - ab - c - ac + bc + abc] \\
 &= \frac{1}{8} [647 + 916 - 834 - 880 - 1687 - 1221 + 1640 + 1190] \\
 &= \frac{1}{8} [-229] = -28.625
 \end{aligned}$$

and

$$\begin{aligned}
 ABC &= \frac{1}{4n} [abc - bc - ac + c - ab + b + a - (1)] \\
 &= \frac{1}{8} [1190 - 1640 - 1221 + 1687 - 880 + 834 + 916 - 647] \\
 &= \frac{1}{8} [239] = 29.875
 \end{aligned}$$

The largest effects are for the gap ( $A = -75.125$ ), the power ( $C = 307.625$ ), and the gap-power interaction ( $AC = -153.875$ ).

The analysis of variance may be used to confirm the magnitude of these effects. From Equation 3.18, the sums of squares are

$$\begin{aligned}
 SS_A &= \frac{(-601)^2}{16} = 22,575.1 \\
 SS_B &= \frac{(73)^2}{16} = 333.1 \\
 SS_C &= \frac{(2461)^2}{16} = 378,532.6 \\
 SS_{AB} &= \frac{(-207)^2}{16} = 2678.1 \\
 SS_{AC} &= \frac{(-1231)^2}{16} = 94,710.1 \\
 SS_{BC} &= \frac{(-229)^2}{16} = 3277.6
 \end{aligned}$$

and

$$SS_{ABC} = \frac{(239)^2}{16} = 3570.1$$

The analysis of variance is summarized in Table 3.6. Based on the  $P$ -values shown in this table, we concluded that gap ( $A$ ) and power ( $C$ ) are statistically significant effects, as is the gap-power ( $AC$ ) interaction.

The regression model for this process, based on the above analysis, is

$$\begin{aligned}
 \hat{y} &= b_0 + b_1x_1 + b_3x_3 + b_{13}x_1x_3 \\
 &= 563.438 + \left(\frac{-75.125}{2}\right)x_1 + \left(\frac{307.625}{2}\right)x_3 + \left(\frac{-153.875}{2}\right)x_1x_3 \\
 &= 563.438 - 37.563x_1 + 153.813x_3 - 76.938x_1x_3
 \end{aligned}$$

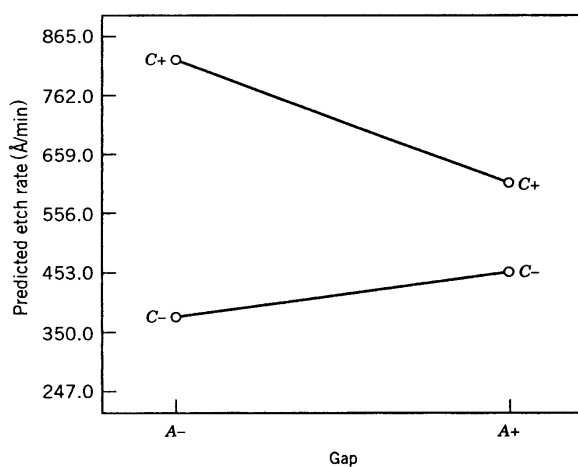
**TABLE 3.6** Analysis of Variance for Example 3.5

Source of Variation	Sum of Squares	Degrees of Freedom	Mean Square	$F_0$	P-Value
<i>A</i>	22,575.1	1	22,575.1	5.64	0.0448
<i>B</i>	333.1	1	333.1	0.08	0.7802
<i>C</i>	378,532.6	1	378,532.6	94.65	$1.04 \times 10^{-5}$
<i>AB</i>	2678.1	1	2678.1	0.67	0.4369
<i>AC</i>	94,710.1	1	94,710.1	23.68	0.0012
<i>BC</i>	3277.6	1	3277.6	0.82	0.3918
<i>ABC</i>	3570.1	1	3570.1	0.89	0.3724
Error	31,995.5	8	3999.4		
Total	537,671.9	15			

where the variables  $x_1$  and  $x_3$  represent the design factors *A* and *C*, respectively, on the coded ( $-1$ ,  $+1$ ) scale. This regression model can be used to generate predicted values at each corner of the design, from which residuals can be obtained. The reader should obtain these residuals and graphically analyze them.

The factor effect estimates (and the regression model) indicate that etch rate increases as the gap (*A*) decreases and as the power (*C*) increases, and that these factors interact. The two-factor interaction graph, shown in Fig. 3.8, is helpful in the practical interpretation of the results. This graph was constructed by plotting average etch rate versus gap (*A*) for each power setting and connecting the points for the low- and high-power settings to give the two lines shown in the figure. Inspection of the interaction graph indicates that changes in the anode–cathode gap produces a much larger change in etch rate at the high-power setting than at the low-power setting.

Figure 3.9 is a response surface plot and contour plot of etch rate as a function of gap and power setting. These plots were obtained from the fitted model. The effect of the strong

**Figure 3.8** Gap–power (*AC*) interaction graph, Example 3.1.

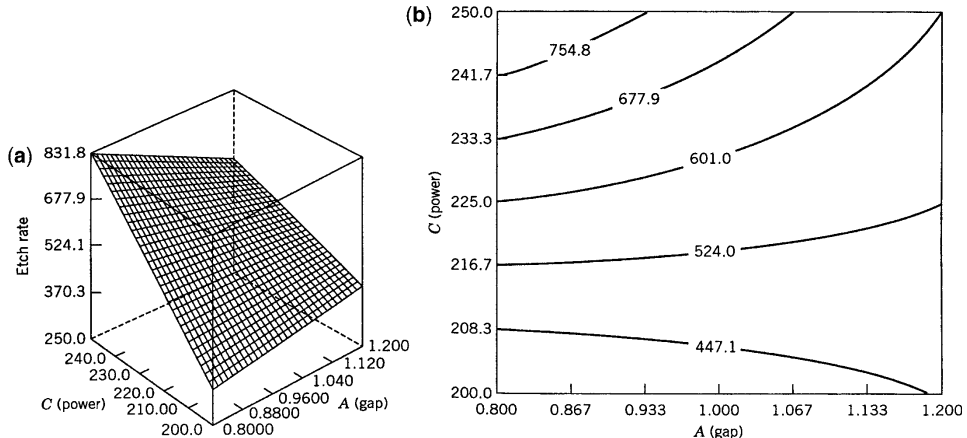


**Figure 3.9** (a) Response surface of etch rate, Example 3.1. (b) The contour plot.

interaction on this process is very clear; notice that the response surface is now a **twisted plane** (that is, the lines in the contour plot are not parallel straight lines). Thus the interaction term in the model is a form of **curvature**. In processes such as this one, the engineer is usually trying to select the appropriate factor settings (in this case gap and power) to obtain a desired etch rate. The response surface and contour plot will be most helpful for this analysis.

**Other Methods for Judging the Significance of Effects** The analysis of variance is a formal way to determine which factor effects are nonzero. There are two other methods that are useful. In the first method, we calculate the **standard error** of the effects and compare the magnitudes of the effects with their standard errors. The second method, which we will illustrate in Section 3.5, uses **normal probability plots** to assess the importance of the effects.

The standard error of an effect is easy to find. If we assume that there are  $n$  replicates at each of the  $2^k$  runs or treatment combinations in the design, and if  $y_{i1}, y_{i2}, \dots, y_{in}$  are the observations at the  $i$ th run, then

$$s_i^2 = \frac{1}{n-1} \sum_{j=1}^n (y_{ij} - \bar{y}_i)^2, \quad i = 1, 2, \dots, 2^k$$

is an estimate of the variance at the  $i$ th run. The  $2^k$  variance estimates can be combined to give an overall variance estimate:

$$s^2 = \frac{1}{2^k(n-1)} \sum_{i=1}^{2^k} \sum_{j=1}^n (y_{ij} - \bar{y}_i)^2$$

This is also the variance estimate given by the error mean square in the analysis of variance. The variance of each effect estimate is

$$\begin{aligned}\text{Var(Effect)} &= \text{Var}\left(\frac{\text{Contrast}}{n2^{k-1}}\right) \\ &= \frac{1}{(n2^{k-1})^2} \text{Var(Contrast)}\end{aligned}$$

Each contrast is a linear combination of  $2^k$  treatment totals, and each total consists of  $n$  observations. Therefore,

$$\text{Var(Contrast)} = n2^k \sigma^2$$

and the variance of an effect is

$$\begin{aligned}\text{Var(Effect)} &= \frac{1}{(n2^{k-1})^2} n2^k \sigma^2 \\ &= \frac{1}{n2^{k-2}} \sigma^2\end{aligned}\tag{3.19}$$

The estimated standard error would be found by replacing  $\sigma^2$  by its estimate  $s^2$  and taking the square root of Equation 3.19.

To illustrate this method, consider the etch rate experiment in Example 3.1. The mean square error is  $MS_E = 3999.4$ . Therefore, the standard error of each effect is (using  $s^2 = MS_E$ )

$$\begin{aligned}\text{se(Effect)} &= \sqrt{\frac{1}{n2^{k-2}} s^2} \\ &= \sqrt{\frac{1}{2(2^{3-2})} 3999.4} \\ &= 31.62\end{aligned}$$

Two standard error limits on the effect estimates are then

$$\begin{aligned}A: &\quad -75.125 \pm 63.24 \\ B: &\quad 9.125 \pm 63.24 \\ C: &\quad 307.625 \pm 63.24 \\ AB: &\quad -25.875 \pm 63.24 \\ AC: &\quad -153.875 \pm 63.24 \\ BC: &\quad -28.625 \pm 63.24 \\ ABC: &\quad 29.875 \pm 63.24\end{aligned}$$

These intervals are approximate 95% **confidence intervals**. This analysis indicates that  $A$ ,  $C$ , and the  $AC$  interaction are important effects, because they are the only factor effect estimates for which the intervals do not include zero.

### 3.4 THE GENERAL $2^k$ DESIGN

The methods of analysis that we have presented thus far may be generalized to the case of a  $2^k$  factorial design; that is, a design with  $k$  factors, each at two levels. The statistical model for a  $2^k$  design will include  $k$  main effects,  $\binom{k}{2}$  two-factor interactions,  $\binom{k}{3}$  three-factor interactions, . . . , and one  $k$ -factor interaction. That is, for a  $2^k$  design the complete model will contain  $2^k - 1$  effects. The notation introduced earlier for treatment combinations is also used here. For example, in a  $2^5$  design  $abd$  denotes the treatment combination with factors  $A$ ,  $B$ , and  $D$  at the high level and factors  $C$  and  $E$  at the low level. The treatment combinations may be written in standard order by introducing the factors, one at a time, with each new factor being successively combined with those that precede it. For example, the standard order for a  $2^4$  design is  $(1)$ ,  $a$ ,  $b$ ,  $ab$ ,  $c$ ,  $ac$ ,  $bc$ ,  $abc$ ,  $d$ ,  $ad$ ,  $bd$ ,  $abd$ ,  $cd$ ,  $acd$ ,  $bcd$ , and  $abcd$ .

To estimate an effect or to compute the sum of squares for an effect, we must first determine the contrast associated with that effect. This can always be done by using a table of plus and minus signs, such as Table 3.2 or Table 3.3. However, for large values of  $k$  this is awkward. Most modern computer programs generate the effect estimates, the regression coefficients, and the sums of squares for the analysis of variance using the method of least squares.

### 3.5 A SINGLE REPLICATE OF THE $2^k$ DESIGN

For even a moderate number of factors, the total number of treatment combinations in a  $2^k$  factorial design is large. For example, a  $2^5$  design has 32 treatment combinations, a  $2^6$  design has 64 treatment combinations, and a  $2^{10}$  design has 1024 treatment combinations. Because resources are usually limited, the number of replicates that the experimenter can employ may be restricted. Frequently, available resources only allow a single replicate of the design to be run, unless the experimenter is willing to omit some of the original factors.

A **single replicate** of a  $2^k$  design is sometimes called an **unreplicated factorial**. With only one replicate, there is no estimate of error. One approach to the analysis of an unreplicated factorial is to assume that certain high-order interactions are negligible and combine their mean squares to estimate the error. This is an appeal to the **sparsity of effects principle**; that is, most systems are dominated by some of the main effects and low-order interactions, and most high-order interactions are negligible.

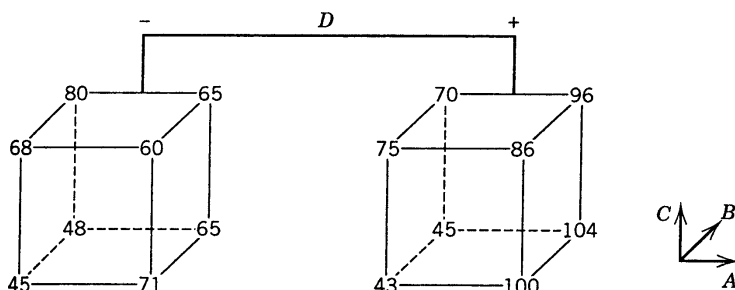
When analyzing data from unreplicate factorial designs, occasionally very high-order interactions occur. The use of an error mean square obtained by pooling high-order interactions is inappropriate in these cases. A method of analysis attributed to Daniel (1959) provides a simple way to overcome this problem. Daniel suggests constructing a normal probability plot of the effect estimates. The effects that are negligible are normally distributed, with mean zero and variance  $\sigma^2$ , and will tend to fall along a straight line on this plot, whereas significant effects will have nonzero means and will not lie along the straight line. We will illustrate this method in the following example.

**TABLE 3.7** Pilot Plant Filtration Rate Experiment

Run Number	Factor				Treatment Combination	Filtration Rate (gal/hr)
	A	B	C	D		
1	-	-	-	-	(1)	45
2	+	-	-	-	a	71
3	-	+	-	-	b	48
4	+	+	-	-	ab	65
5	-	-	+	-	c	68
6	+	-	+	-	ac	60
7	-	+	+	-	bc	80
8	+	+	+	-	abc	65
9	-	-	-	+	d	43
10	+	-	-	+	ad	100
11	-	+	-	+	bd	45
12	+	+	-	+	abd	104
13	-	-	+	+	cd	75
14	+	-	+	+	acd	86
15	-	+	+	+	bcd	70
16	+	+	+	+	abcd	96

**Example 3.2 A Single Replicate of the  $2^4$  Design** Montgomery (2005) describes a factorial experiment carried out in a pilot plant to study the factors thought to influence the filtration rate of a chemical product. The four factors are temperature ( $A$ ), pressure ( $B$ ), concentration of formaldehyde ( $C$ ), and stirring rate ( $D$ ). Each factor is present at two levels, and the data obtained from a single replicate of the  $2^4$  experiment are shown in Table 3.7 and Fig. 3.10. The 16 runs are made in random order. The process engineer is interested in maximizing the filtration rate. Current process conditions give filtration rates of around 75 gal/hr. The process also currently uses the concentration of formaldehyde, factor  $C$ , at the high level. The engineer would like to reduce the formaldehyde concentration as much as possible but has been unable to do so because it always results in lower filtration rates.

We will begin the analysis of this data by constructing a normal probability plot of the effect estimates. The plus and minus signs for the contrast constants for the  $2^4$  design are shown in Table 3.8. From these contrasts, we may estimate the 15 factorial effect estimates

**Figure 3.10** Data from the pilot plant filtration rate experiment for Example 3.2.

**TABLE 3.8 Contrast Constants and Effect Estimates for the  $2^4$  Design, Example 3.2**

Observations	A	B	AB	C	AC	BC	ABC	D	AD	BD	ABD	CD	ACD	BCD	ABCD
(1) = 45	-	-	+	-	+	+	-	-	+	+	-	+	-	-	+
$a = 71$	+	-	-	-	-	+	+	-	-	+	+	+	+	-	-
$b = 48$	-	+	-	-	+	-	+	-	+	-	+	+	-	+	-
$b = 65$	+	+	+	-	-	-	-	-	-	-	-	+	+	+	+
$c = 68$	-	-	+	+	-	-	+	-	+	+	-	-	+	+	-
$ac = 60$	+	-	-	+	+	-	-	-	-	+	+	-	-	+	+
$bc = 80$	-	+	-	+	-	+	-	-	+	-	+	-	+	-	+
$abc = 65$	+	+	+	+	+	+	+	-	-	-	-	-	-	-	-
$d = 43$	-	-	+	-	+	+	-	+	-	-	+	-	+	+	-
$ad = 100$	+	-	-	-	-	+	+	+	+	-	-	-	-	+	+
$bd = 45$	-	+	-	-	+	-	+	+	-	+	-	-	+	-	+
$abd = 104$	+	+	+	-	-	-	+	+	+	+	+	-	-	-	-
$cd = 75$	-	-	+	+	-	-	+	+	-	-	+	+	-	-	+
$acd = 86$	+	-	-	+	+	-	-	+	+	-	-	+	+	-	-
$bcd = 70$	-	+	-	+	-	+	-	+	-	+	-	+	-	+	-
$abcd = 96$	+	+	+	+	+	+	+	+	+	+	+	+	+	+	+
Effect	21.625		0.125		-18.125		1.875		16.625		4.125		-1.625		1.375
Estimates		3.125		9.875		2.375		14.625		-0.375		-1.125		-2.625	

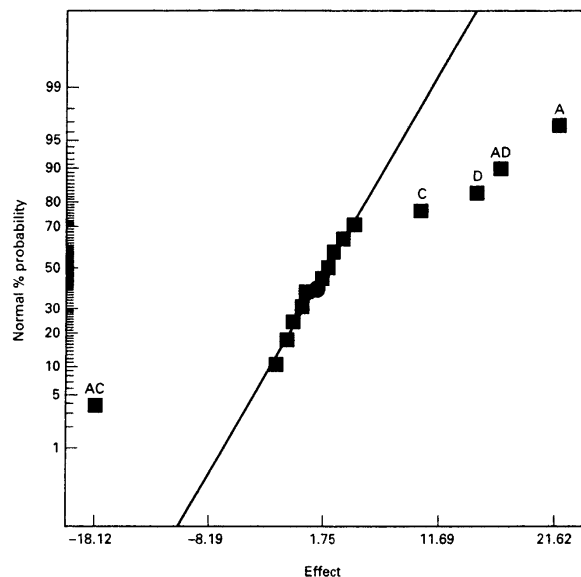


**Figure 3.11** Normal probability plot of effects for the  $2^4$  factorial in Example 3.2.

shown at the foot of each column in Table 3.8. The normal probability plot of these effects is shown in Fig. 3.11. All of the effects that lie along the line are negligible, whereas the large effects are far from the line. The important effects that emerge from this analysis are the main effects of  $A$ ,  $C$ , and  $D$  and the  $AC$  and  $AD$  interactions. Table 3.9 summarizes the analysis of variance for this design. In this analysis we have pooled the nonsignificant effects to form the error term. The  $F$ -tests reveal that the effects of  $A$ ,  $C$ ,  $D$ , and the  $AC$  and  $AD$  interactions are large.

The main effects of  $A$ ,  $C$ , and  $D$  are plotted in Fig. 3.12a. All three effects are positive, and if we considered only these main effects, we would run all three factors at the high level to maximize the filtration rate. However, it is always necessary to examine any interactions that are important. Remember that main effects do not have much meaning when they are involved in significant interactions.

The  $AC$  and  $AD$  interactions are plotted in Fig. 3.12b. These interactions are the key to solving the problem. Note from the  $AC$  interaction that the temperature effect is very small when the concentration is at the high level and very large when the concentration is at the

**TABLE 3.9 Analysis of Variance, Example 3.2**

Source of Variation	Sum of Squares	Degrees of Freedom	Mean Square	$F_0$	P-Value
$A$	1870.563	1	1870.563	95.86	$1.93 \times 10^{-6}$
$C$	390.062	1	390.062	19.99	0.0012
$D$	855.562	1	855.562	43.85	0.0001
$AC$	1314.062	1	1314.062	67.34	$9.42 \times 10^{-6}$
$AD$	1105.563	1	1105.563	56.66	$2.00 \times 10^{-5}$
Error	195.125	10	19.513		
Total	5730.937	15			

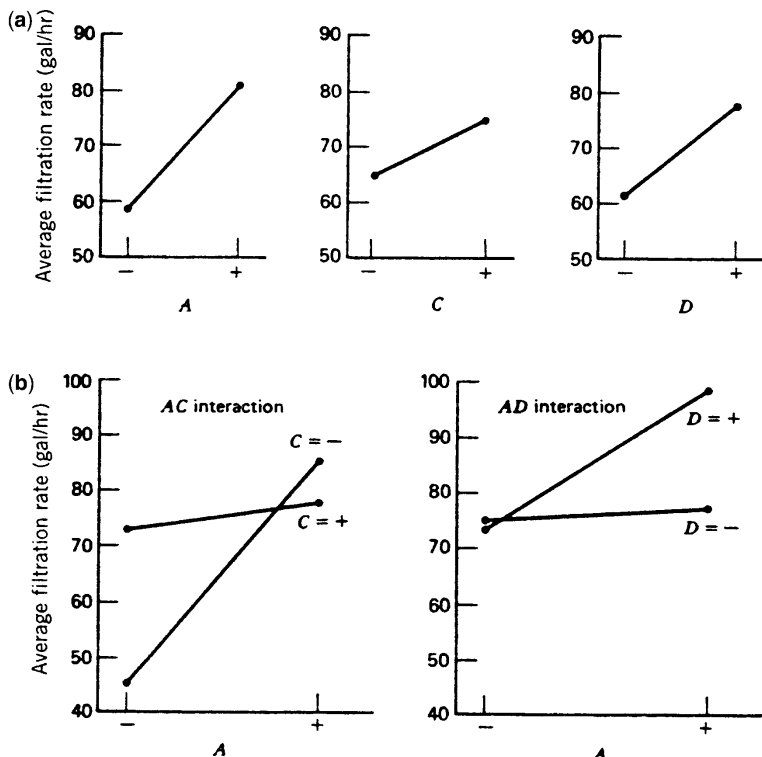


**Figure 3.12** Main effect and interaction plots for Example 3.2. (a) Main effect plots, (b) Interaction plots.

low level, the best results being obtained with low concentration and high temperature. The  $AD$  interaction indicates that stirring rate  $D$  has little effect at low temperature but has a large positive effect at high temperature. Therefore, the best filtration rates would appear to be obtained when  $A$  and  $D$  are at the high level and  $C$  is at the low level. This would allow the reduction of the formaldehyde concentration to a lower level, another objective of the experimenter.

**The Half-Normal Probability Plot of Effects** An alternative to the normal probability plot of the factor effects is the **half-normal plot**. This is a plot of the absolute value of the effect estimates against their cumulative normal probabilities. Fig. 3.13 presents the half-normal plot of the effects for the pilot plant filtration rate experiment. The straight line on the half-normal plot always passes through the origin and should also pass close to the fiftieth percentile data value. Many analysts feel that the half-normal plot is easier to interpret particularly when there are only a few effect estimates, as when the experimenter has used an eight-run design. Some software packages will construct both plots.

**Design Projection** Another interpretation of the data in Fig. 3.11 is possible. Because  $B$  (pressure) is not significant and all interactions involving  $B$  are negligible, we may discard  $B$  from the experiment so that the design becomes a  $2^3$  factorial in  $A$ ,  $C$ , and  $D$  with two replicates. This is easily seen from examining only columns  $A$ ,  $C$ , and  $D$  in

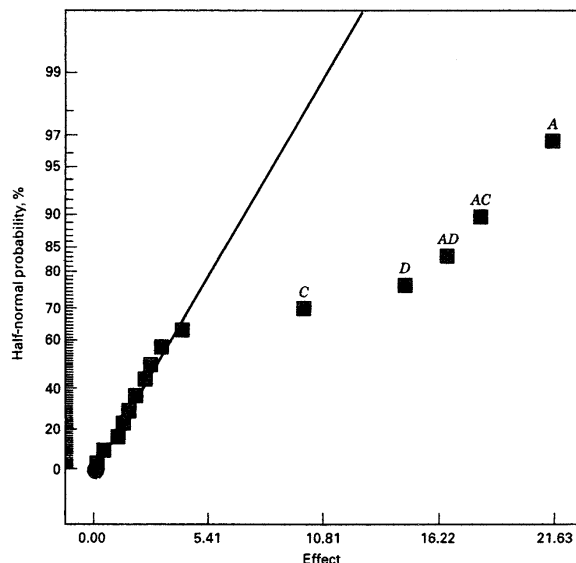


**Figure 3.13** Half-normal plot of the factor effects from the  $2^4$  factorial in Example 3.2.

Table 3.7 and noting that those columns form two replicates of a  $2^3$  design. The analysis of variance for the data using this simplifying assumption is summarized in Table 3.10. The conclusions that we would draw from this analysis are essentially unchanged from those of Example 3.2. Note that by projecting the single replicate of the  $2^4$  into a replicated  $2^3$ , we now have both an estimate of the  $ACD$  interaction and an estimate of error based on replication.

The technique of projecting an unreplicated factorial into a replicated factorial in fewer factors is very useful. In general, if we have a single replicate of a  $2^k$  design and if  $h$  ( $h < k$ ) factors are negligible and can be dropped, then the original data correspond to a full two-level factorial in the remaining  $k - h$  factors with  $2^h$  replicates.

**The Regression Model and Diagnostic Checking** The usual diagnostic checks should be applied to the residuals from a  $2^k$  design. Our analysis indicates that the only significant effect are  $A = 21.625$ ,  $C = 9.875$ ,  $D = 14.625$ ,  $AC = -18.125$ , and  $AD = 16.625$ . If this is

**TABLE 3.10 Analysis of Variance for the Pilot Plant Filtration Rate Experiment in A, C, and D**

Source of Variation	Sum of Squares	Degrees of Freedom	Mean Square	$F_0$	P-Value
A	1870.56	1	1870.56	83.36	$1.67 \times 10^{-5}$
C	390.06	1	390.06	17.38	0.0031
D	855.56	1	855.56	38.13	0.0003
AC	1314.06	1	1314.06	58.56	0.0001
AD	1105.56	1	1105.56	49.27	0.0001
CD	5.06	1	5.06	0.23	0.6476
ACD	10.56	1	10.56	0.47	0.5121
Error	179.52	8	22.44		
Total	5730.94	15			

true, then the predicted values of the filtration rate over the region spanned by the design are given by the regression model

$$\hat{y} = 70.06 + \left(\frac{21.625}{2}\right)x_1 + \left(\frac{9.875}{2}\right)x_3 + \left(\frac{14.625}{2}\right)x_4 \\ - \left(\frac{18.125}{2}\right)x_1x_3 + \left(\frac{16.625}{2}\right)x_1x_4$$

where 70.06 is the average response and the coded variables  $x_1, x_3, x_4$  take on values in the interval from  $-1$  to  $+1$ . For example, the predicted filtration rate at the run where all three factors are at the low level is

$$\hat{y} = 70.06 + \left(\frac{21.625}{2}\right)(-1) + \left(\frac{9.875}{2}\right)(-1) + \left(\frac{14.625}{2}\right)(-1) \\ - \left(\frac{18.125}{2}\right)(-1)(-1) + \left(\frac{16.625}{2}\right)(-1)(-1) \\ = 46.22$$

Because the observed value is 45, the residual is  $e = y - \hat{y} = 45 - 46.22 = -1.22$ . The values of  $y$ ,  $\hat{y}$ , and  $e = y - \hat{y}$  for all 16 observations follow:

	$y$	$\hat{y}$	$e = y - \hat{y}$
(1)	45	46.22	-1.22
$a$	71	69.39	1.61
$b$	48	46.22	1.78
$ab$	65	69.39	-4.39
$c$	68	74.23	-6.23
$ac$	60	61.14	-1.14
$bc$	80	74.23	5.77
$abc$	65	61.14	3.86
$d$	43	44.22	-1.22
$ad$	100	100.65	3.35
$bd$	45	44.22	0.78
$abd$	104	100.65	3.35
$cd$	75	72.23	2.77
$acd$	86	92.40	-6.40
$bcd$	70	72.23	-2.23
$abcd$	96	92.40	3.60

A normal probability plot of these residuals is shown in Fig. 3.14. The points on this plot lie reasonably close to a straight line, lending support to our conclusion that  $A$ ,  $C$ ,  $D$ ,  $AC$ , and  $AD$  are the only significant effects and that the underlying assumptions of the analysis are satisfied.

**Example 3.3 Duplicate Measurements of the Response** A team of engineers at a semiconductor manufacturer ran a  $2^4$  factorial design in a vertical oxidation furnace. The purpose of the experiment was to study the effects of the four factors in oxide

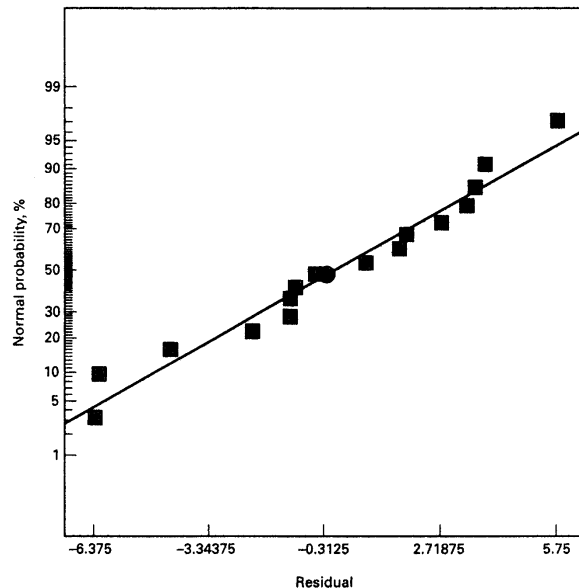


**Figure 3.14** Normal probability plot of residuals of Example 3.2.

thickness. Four wafers are stacked in the furnace, and the response variable of interest is the oxide thickness on the wafers. The four design factors are temperature ( $A$ ), time ( $B$ ), pressure ( $C$ ), and gas flow ( $D$ ). The experiment is conducted by loading four wafers into the furnace, setting the process variables to the test conditions required by the experimental design, processing the wafers, and then measuring the oxide thickness on all four wafers. Table 3.11 presents the design and the resulting thickness measurements. In this table, the four columns labeled “Thickness” contains the oxide thickness measurements on

**TABLE 3.11** The Oxide Thickness Experiment

Standard Order	Run Order	$A$	$B$	$C$	$D$	Thickness			$\bar{y}$	$s^2$
1	10	-1	-1	-1	-1	378	376	379	379	378
2	7	1	-1	-1	-1	415	416	416	417	416
3	3	-1	1	-1	-1	380	379	382	383	381
4	9	1	1	-1	-1	450	446	449	447	448
5	6	-1	-1	1	-1	375	371	373	369	372
6	2	1	-1	1	-1	391	390	388	391	390
7	5	-1	1	1	-1	384	385	386	385	385
8	4	1	1	1	-1	426	433	430	431	430
9	12	-1	-1	-1	1	381	381	375	383	380
10	16	1	-1	-1	1	416	420	412	412	415
11	8	-1	1	-1	1	371	372	371	370	371
12	1	1	1	-1	1	445	448	443	448	446
13	14	-1	-1	1	1	377	377	379	379	378
14	15	1	-1	1	1	391	391	386	400	392
15	11	-1	1	1	1	375	376	376	377	376
16	13	1	1	1	1	430	430	428	428	429

**TABLE 3.12 Effect Estimates for Example 3.3: Response Variable is Average Oxide Thickness**

Model Term	Effect Estimate	Sum of Squares	Percent Contribution
<i>A</i>	43.125	7439.06	67.9339
<i>B</i>	18.125	1314.06	12.0001
<i>C</i>	-10.375	430.562	3.93192
<i>D</i>	-1.625	10.5625	0.0964573
<i>AB</i>	16.875	1139.06	10.402
<i>AC</i>	-10.625	451.563	4.12369
<i>AD</i>	1.125	5.0625	0.046231
<i>BC</i>	3.875	60.0625	0.548494
<i>BD</i>	-3.875	60.0625	0.548494
<i>CD</i>	1.125	5.0625	0.046231
<i>ABC</i>	-0.375	0.5625	0.00513678
<i>ABD</i>	2.875	33.0625	0.301929
<i>ACD</i>	-0.125	0.0625	0.000570752
<i>BCD</i>	-0.625	1.5625	0.0142688
<i>ABCD</i>	0.125	0.0625	0.000570753

each individual wafer, and the last two columns contain the sample average and sample variance of the thickness measurements on the four wafers in each run.

The proper analysis of this experiment is to consider the individual wafer thickness measurements as **duplicate measurements**, and not as replicates. If they were actually replicates, each wafer would have been processed individually on a single run of the furnace. However, because all four wafers were processed together, they received the treatment factors (i.e., the levels of the design variables) *simultaneously*, so there is much less variability in the individual wafer thickness measurements than would have been observed if each wafer had been a replicate. Therefore, the **average** of the thickness measurements is the correct response variable to initially consider.

Table 3.12 presents the effect estimates for this experiment, using the average oxide thickness  $\bar{y}$  as the response variable. Note that factors *A* and *B* and the *AB* interaction have large effects that together account for nearly 90% of the variability in average oxide thickness. Figure 3.15 is a normal probability plot of the effects. From examination of this display, we conclude that factors *A*, *B*, and *C* and the *AB* and *AC* interactions are important. The analysis of variance display for this model is shown in Table 3.13.

The model for predicting the average oxide thickness is

$$\hat{y} = 399.19 + 21.56x_1 + 9.06x_2 - 519x_3 + 8.44x_1x_2 - 5.31x_1x_3$$

The residual analysis of this model is satisfactory.

The experimenters are interested in obtaining an average oxide thickness of 400 Å, and product specifications require that the thickness must lie between 390 and 410 Å. Figure 3.16 presents two contour plots of average thickness, one with factor *C* (or  $x_3$ ), pressure, at the low level (i.e.,  $x_3 = -1$ ) and the other with *C* (or  $x_3$ ) at the high level (i.e.,  $x_3 = +1$ ). From examining these contour plots, it is obvious that there are many combinations of time and temperature (factors *A* and *B*) that will produce acceptable results. However, if pressure is held constant at the low level, the operating window is shifted toward the left, or lower, end of the time axis, indicating that lower cycle times will be required to achieve the desired oxide thickness.

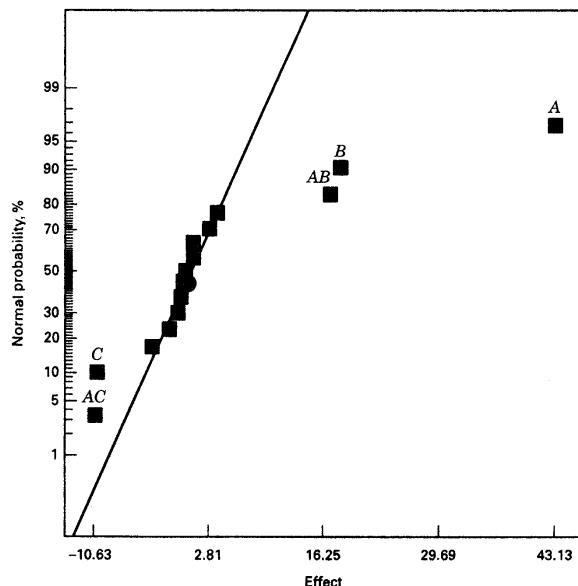


**Figure 3.15** Normal probability plot of the effects for the average oxide thickness response, Example 3.3.

It is interesting to observe the results that would be obtained if we *incorrectly* considered the individual wafer oxide thickness measurements as replicates. Table 3.14 presents a full model analysis of variance based on treating the experiment as a replicated  $2^4$  factorial. Notice that there are many significant factors in this analysis, suggesting a much more complex model than we found when using the average oxide thickness as the response. The reason for this is that the estimate of the error variance in Table 3.14 is too small ( $\hat{\sigma}^2 = 6.12$ ). The residual mean square in Table 3.14 primarily reflects the variability between wafers *within* a run and damps out the variability *between* runs. The estimate of error obtained from Table 3.13 is much larger,  $\hat{\sigma}^2 = 17.61$ , and it is primarily a measure of the between-run variability. This is the best estimate of error to use in judging the significance of process variables that are changed from run to run.

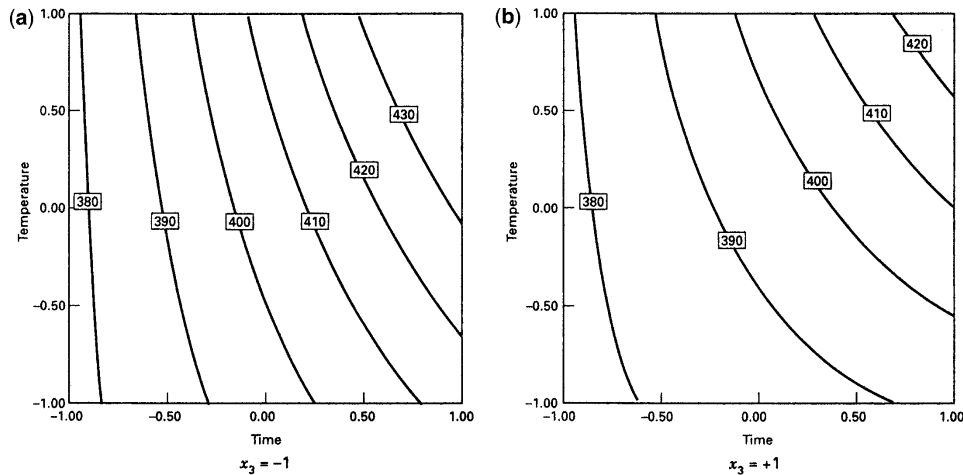
A logical question to ask is: What harm results from identifying too many factors as important?, as the incorrect analysis in Table 3.14 would certainly do. The answer is that trying to manipulate or optimize the unimportant factors would be a waste of resources, and it could result in adding unnecessary variability to *other* responses of interest.

When there are duplicate measurements on the response, there is almost always useful information about some aspect of **process variability** contained in these observations. For example, if the duplicate measurements are multiple tests by a gauge on the same experimental unit; then the duplicate measurements give some insight into **gauge capability**. If the duplicate measurements are made at different locations on an experimental unit, they may give some information about the **uniformity** of the response variable across that unit. In our example, because we have one observation on each of four experimental units that have undergone processing together, we have some information about the **within-run variability** in the process. The information is contained in the variance of the oxide thickness measurements from the four wafers in each run. It would be of interest to determine if any of the process variables influence the within-run variability.

**TABLE 3.13 Analysis of Variance (from Design-Expert) for the Average Oxide Thickness Response, Example 3.3**

Source	Sum of Squares	DF	Mean Square	F Value	Prob > F
<i>Model</i>	10,774.31	5	2154.86	122.35	<0.0000
<i>A</i>	7439.06	1	7439.06	422.37	<0.000
<i>B</i>	1314.96	1	1314.06	74.61	<0.000
<i>C</i>	430.56	1	430.56	24.45	0.0006
<i>AB</i>	1139.06	1	1139.06	64.67	<0.000
<i>AC</i>	451.56	1	451.56	25.64	0.0005
Residual	176.12	10	17.61		
Cor. Total	10,950.44	15			
Std. Dev.	4.20		<i>R</i> -Squared	0.9839	
Mean	399.19		Adj. <i>R</i> -Squared	0.9759	
C.V.	1.05		Pred. <i>R</i> -Squared	0.9588	
PRESS	450.88		Adeq. Precision	27.967	

Factor	Coefficient Estimate	DF	Standard Error	95% CI	
				CI Low	CI High
Intercept	399.19	1	1.05	396.85	401.53
<i>A</i> -Time	21.56	1	1.05	19.22	23.90
<i>B</i> -Temp	9.06	1	1.05	6.72	11.40
<i>C</i> -Pressure	-5.19	1	1.05	-7.53	-2.85
<i>AB</i>	8.44	1	1.05	6.10	10.78
<i>AC</i>	-5.31	1	1.05	-7.65	-2.97



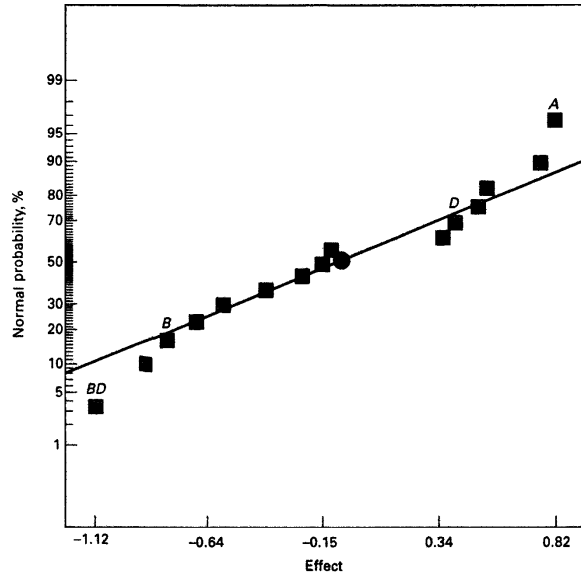
**Figure 3.16** Contour plots of average oxide thickness with pressure ( $x_3$ ) held constant.

Figure 3.17 is a normal probability plot of the effect estimates obtained using  $\ln(s^2)$  as the response. As we will discuss further in Chapter 10, there is historical evidence that the log transformation is generally appropriate for modeling variability. There are not any strong individual effects, but factor *A* and the *BD* interaction are the largest. If we also include the main effects of *B* and *D* to obtain a hierarchical model, then the model for  $\ln(s^2)$  is

$$\ln(s^2) = 1.08 + 0.41x_1 - 0.40x_2 + 0.20x_4 - 0.56x_2x_4$$

**TABLE 3.14** Analysis of Variance (from Design-Expert) of the Individual Wafer Oxide Thickness Response if Duplicates are Incorrectly Treated as Replicates

Source	Sum of Squares	DF	Mean Square	F Value	Prob > F
Model	43,801.75	15	2920.12	476.75	<0.0001
<i>A</i>	29,756.25	1	29,756.25	4858.16	<0.001
<i>B</i>	5256.25	1	5256.25	858.16	<0.001
<i>C</i>	1722.25	1	1722.25	281.18	<0.001
<i>D</i>	42.25	1	42.25	6.90	0.0115
<i>AB</i>	4556.25	1	4556.25	743.88	<0.001
<i>AC</i>	1806.25	1	1806.25	294.90	<0.001
<i>AD</i>	20.25	1	20.25	3.31	0.0753
<i>BC</i>	240.25	1	240.25	39.22	<0.001
<i>BD</i>	240.25	1	240.25	39.22	<0.001
<i>CD</i>	20.25	1	20.25	3.31	0.0753
<i>ABD</i>	132.25	1	132.25	21.59	<0.001
<i>ABC</i>	2.25	1	2.25	0.37	0.5473
<i>ACD</i>	0.25	1	0.25	0.941	0.8407
<i>BCD</i>	6.25	1	6.25	1.02	0.3175
<i>ABCD</i>	0.25	1	0.25	0.041	0.8407
Residual	294.00	48	6.12		
<i>Lack of Fit</i>	0.000	0			
<i>Pure Error</i>	294.00	48	6.13		
Cor. Total	44,095.75	63			



**Figure 3.17** Normal probability plot of the effects using  $\ln(s^2)$  as the response. Example 3.3.

The model accounts for just slightly less than half of the variability in the  $\ln(s^2)$  response, which is certainly not spectacular as empirical models go; but it is often difficult to obtain exceptionally good models of variances.

Figure 3.18 is a contour plot of the predicted variance (not the log of the predicted variance) with pressure  $x_3$  at the low level (recall that this minimizes the cycle time) and gas flow  $x_4$  at the high level. This choice of gas flow gives the lowest values of predicted variance in the region of the contour plot.

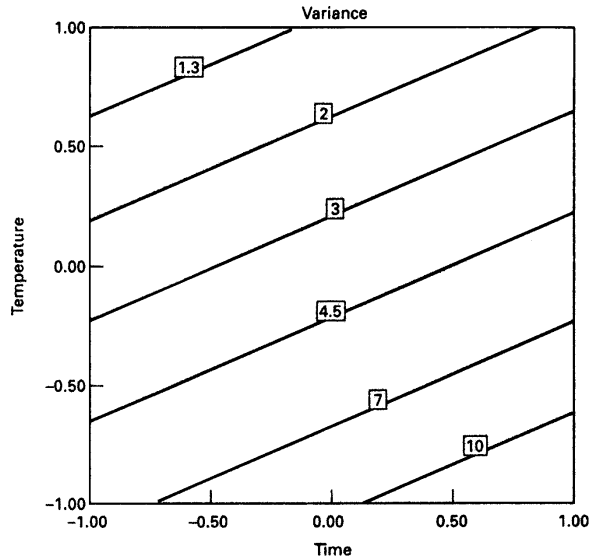


**Figure 3.18** Contour plot of  $s^2$  (within-run variability) with pressure at the low level and gas flow at the high level.

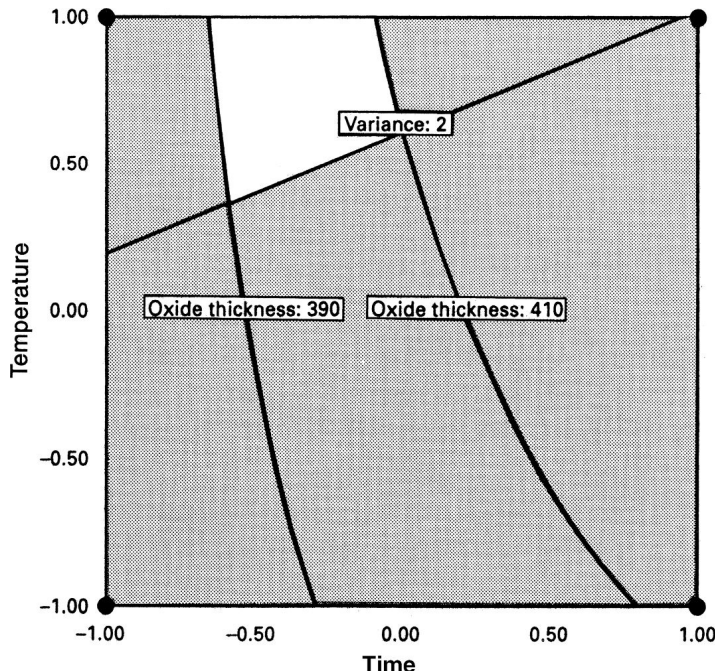


**Figure 3.19** Overlay of the average oxide thickness and  $s^2$  responses with pressure at the low level and gas flow at the high level.

The experimenters here were interested in selecting values of the design variables that gave a mean oxide thickness within the process specifications and as close to 400 Å as possible, while simultaneously making the within-run variability small, say  $s^2 \leq 2$ . One possible way to find a suitable set of conditions is to overlay the contour plots in Figs. 3.17 and 3.18. The overlay plot is shown in Fig. 3.19, with the specifications on mean oxide thickness and the constraint  $s^2 \leq 2$  shown as contours. In this plot, pressure is held constant at the low level and gas flow is held constant at the high level. The open region near the upper left of the graph identifies a feasible region for the variables time and temperature.

This is a simple example of using contour plots to study two responses simultaneously. We will discuss techniques for simultaneously analyzing and optimizing several responses in more detail in Chapter 6.

### 3.6 THE ADDITION OF CENTER POINTS TO THE $2^k$ DESIGN

A potential concern in the use of two-level factorial designs is the assumption of *linearity* in the factor effects. Of course, perfect linearity is unnecessary, and the  $2^k$  system will work quite well even when the linearity assumption holds only very approximately. In fact, we have noted that if **interaction terms** are added to a main effects or first-order model, resulting in

$$y = \beta_0 + \sum_{j=1}^k \beta_j x_j + \sum_{i < j=2}^k \beta_{ij} x_i x_j + \varepsilon \quad (3.20)$$

then we have a model capable of representing some curvature in the response function. This curvature, of course, results from the twisting of the plane induced by the interaction terms  $\beta_{ij}x_i x_j$ .

There are going to be situations where the curvature in the response function is not adequately modeled by Equation 3.20. In such cases, a logical model to consider is the complete **second-order response surface model**:

$$y = \beta_0 + \sum_{j=1}^k \beta_j x_j + \sum_{i < j=2}^k \beta_{ij} x_i x_j + \sum_{j=1}^k \beta_{jj} x_j^2 + \varepsilon \quad (3.21)$$

In running a two-level factorial experiment, we usually anticipate fitting the first-order model in Equation 3.20, but we should be alert to the possibility that the second-order model in Equation 3.21 is really more appropriate. There is a method of replicating certain points in a  $2^k$  factorial that will provide protection against curvature from second-order effects as well as allow an independent estimate of error to be obtained. The method consists of adding **center points** to the  $2^k$  design. These consist of  $n$  replicates run at the points  $x_i = 0$  ( $i = 1, 2, \dots, k$ ). One important reason for adding the replicate runs at the design center is that center points do not effect the usual effect estimates in a  $2^k$  design. When we add center points, we assume that the  $k$  factors are **quantitative**.

To illustrate the approach, consider a  $2^2$  design with one observation at each of the factorial points  $(-, -)$ ,  $(+, -)$ ,  $(-, +)$ , and  $(+, +)$  and  $n_C$  observations at the center point  $(0, 0)$ . Figure 3.20 illustrates the situation. Let  $\bar{y}_F$  be the average of the four runs at the four factorial points, and let  $\bar{y}_C$  be the average of the  $n_C$  runs at the center point. If the difference  $\bar{y}_F - \bar{y}_C$  is small, then the center points lie on or near the plane passing

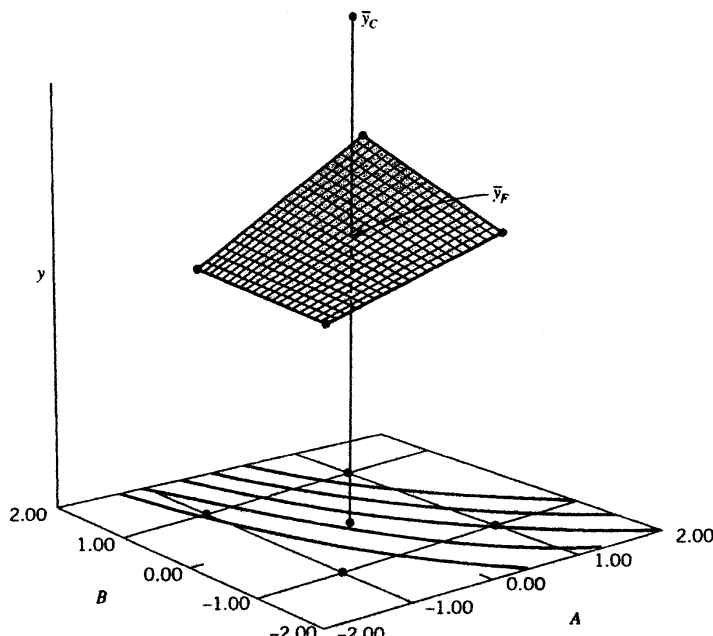


Figure 3.20 A  $2^2$  design with center points.

through the factorial points, and there is no quadratic curvature. On the other hand, if  $\bar{y}_F - \bar{y}_C$  is large, then quadratic curvature is present. A single-degree-of-freedom **sum of squares for pure quadratic curvature** is given by

$$SS_{\text{pure quadratic}} = \frac{n_F n_C (\bar{y}_F - \bar{y}_C)^2}{n_F + n_C} \quad (3.22)$$

where, in general,  $n_F$  is the number of factorial design points. This quantity may be compared with the error mean square to test for pure quadratic curvature. More specifically, when points are added to the center of the  $2^k$  design, then the test for curvature based on Equation 3.22 actually tests the hypothesis

$$\begin{aligned} H_0: \quad & \sum_{j=1}^k \beta_{jj} = 0 \\ H_1: \quad & \sum_{j=1}^k \beta_{jj} \neq 0 \end{aligned}$$

Furthermore, if the factorial points in the design are unreplicated, one may use the  $n_C$  center points to construct an estimate of error with  $n_C - 1$  degrees of freedom.

**Example 3.4 Testing for Curvature** A chemical engineer is studying the yield of a process. There are two variables of interest: reaction time and reaction temperature. Because she is uncertain about the assumption of linearity over the region of exploration, the engineer decides to conduct a  $2^2$  design (with a single replicate of each factorial run) augmented with five center points. The design and the yield data are shown in Fig. 3.21.

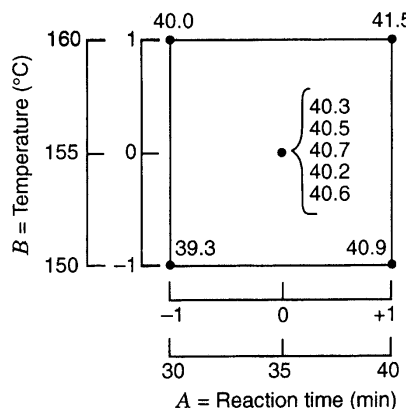


Figure 3.21 The  $2^2$  design with five center points for Example 3.4.

**TABLE 3.15** Analysis of Variance for Example 3.4

Source of Variability	Sum of Squares	Degrees of Freedom	Mean Square	$F_0$	P-Value
A (time)	2.4025	1	2.4025	55.87	0.0017
B (temperature)	0.4225	1	0.4225	9.83	0.0350
AB	0.0025	1	0.0025	0.06	0.8185
Curvature	0.0027	1	0.0027	0.06	0.8185
Error	0.1720	4	0.0430		
Total	3.0022	8			

Table 3.15 summarizes the analysis of variance for this experiment. The mean square error is calculated from the center points as follows:

$$\begin{aligned}
 MS_E &= \frac{SS_E}{n_C - 1} \\
 &= \frac{\sum_{\text{center points}} (y_i - \bar{y}_C)^2}{n_C - 1} \\
 &= \frac{\sum_{i=1}^5 (y_i - 40.46)^2}{4} \\
 &= \frac{0.1720}{4} \\
 &= 0.0430
 \end{aligned}$$

The average of the points in the factorial portion of the design is  $\bar{y}_F = 40.425$ , and the average of the points at the center is  $\bar{y}_C = 40.46$ . The difference  $\bar{y}_F - \bar{y}_C = 40.425 - 40.46 = -0.035$  appears to be small. The curvature sum of squares in the analysis of variance table is computed from Equation 3.22 as follows:

$$\begin{aligned}
 SS_{\text{Curvature}} &= \frac{n_F n_C (\bar{y}_F - \bar{y}_C)^2}{n_F + n_C} \\
 &= \frac{(4)(5)(-0.035)^2}{4 + 5} \\
 &= 0.0027
 \end{aligned}$$

The analysis of variance indicates that both factors exhibit significant main effects, that there is no interaction, and that there is no evidence of curvature in the response over the region of exploration. That is, the null hypothesis  $H_0: \sum_{j=1}^2 \beta_{jj} = 0$  cannot be rejected.

In Example 3.4, we concluded that there was no indication of quadratic effects; that is, a first-order model with interaction

$$y = \beta_0 + \beta_1 x_1 + \beta_2 x_2 + \beta_{12} x_1 x_2 + \varepsilon$$

is appropriate (although we probably don't need the interaction term). There will be situations where the quadratic terms will be required. That is, we will have to assume a

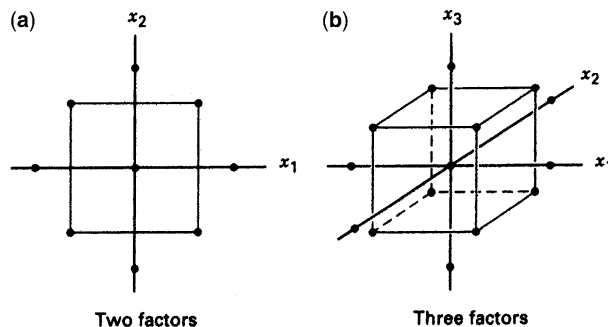


**Figure 3.22** Central composite designs.

second-order model such as

$$y = \beta_0 + \beta_1 x_1 + \beta_2 x_2 + \beta_{12} x_1 x_2 + \beta_{11} x_1^2 + \beta_{22} x_2^2 + \varepsilon$$

Unfortunately, we cannot estimate all of the unknown parameters (the  $\beta$ 's) in this model, because there are six parameters to estimate, and the  $2^2$  design plus center points in Fig. 3.21 only has five independent runs.

A simple and highly effective solution to this problem is to augment the  $2^2$  design with four **axial runs**, as shown in Fig. 3.22a. The resulting design is the **central composite design**. Figure 3.22b shows a central composite design for  $k = 3$  factors. This design has  $14 + n_C$  runs (usually  $3 \leq n_C \leq 5$ ), and is a very efficient design for fitting the 10-parameter second-order model in  $k = 3$  factors.

As we noted in Chapter 2, central composite designs are used extensively in building second-order response surface models. These designs will be illustrated and discussed in more detail in Chapters 6 and 7.

We conclude this section with a few additional useful suggestions and observations concerning the use of center points.

- When a factorial experiment is conducted in an ongoing process, consider using the current operating conditions (or recipe) as the center point in the design. This often assures the operating personnel that at least some of the runs in the experiment are going to be performed under familiar conditions, and so the results obtained (at least for these runs) are unlikely to be any worse than are typically obtained.
  - When the center point in a factorial experiment correspond to the usual operating recipe, the experimenter can use the observed responses at the center point to provide a rough check of whether anything unusual occurred during the experiment. That is, the center point responses should be very similar to responses observed historically in routine process operation. Often operating personnel will maintain a control chart for monitoring process performance. Sometimes the center point responses can be plotted directly on the control chart as a check of the manner in which the process was operating during the experiment.
  - Consider running the replicates at the center point in nonrandom order. Specifically, run one or two center points at or near the beginning of the experiment, one or two near the middle, and one or two near the end. By spreading the center points out in time, the experimenter has a rough check on the stability of the process during the experiment.

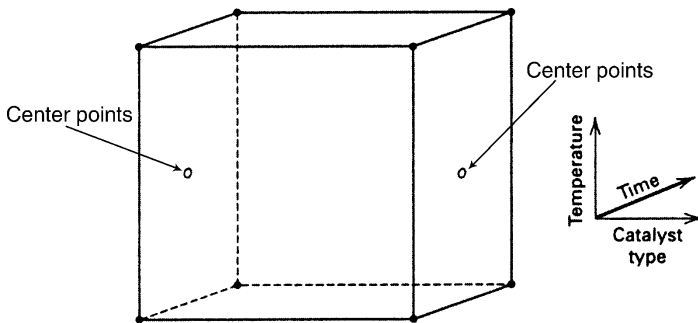


**Figure 3.23** A  $2^3$  factorial design with one qualitative factor and center points.

For example, if a trend has occurred in the response while the experiment was performed, plotting the center point responses versus time order may reveal this.

4. Sometimes experiments must be conducted in situations where there is little or no prior information about process variability. In these cases, running two or three center points as the first few runs in the experiment can be very helpful. These runs can provide a preliminary estimate of variability. If the magnitude of the variability seems reasonable, continue; on the other hand, if larger than anticipated (or reasonable!) variability is observed, stop. Often it will be very profitable to study why the variability is so large before proceeding with the rest of the experiment.
5. Usually, center points are employed when all design factors are **quantitative**. However, sometimes there will be one or more qualitative or categorical variables and several quantitative ones. Center points can still be employed in these cases. To illustrate, consider an experiment with two quantitative factors, time and temperature, each at two levels, and a single qualitative factor, catalyst type, also with two levels (organic and nonorganic). Figure 3.23 shows the  $2^3$  design for these factors. Notice that the center points are placed on the opposed faces of the cube that involve the quantitative factors. In other words, the center points can be run at the high- and low-level treatment combinations of the qualitative factors, just so long as those subspaces involve only quantitative factors.

### 3.7 BLOCKING IN THE $2^k$ FACTORIAL DESIGN

There are many situations in which it is impossible to completely randomize all of the runs in the experiment. For example, we might not be able to perform all of the runs in a factorial experiment under homogeneous conditions. As examples, these conditions might be a single time period (such as one day), a single batch of homogeneous raw material, using only one operator, or the like. In other cases, it might be desirable to deliberately vary the experimental conditions to ensure that the treatments are equally effective (one might say robust) across many situations likely to be encountered in practice. For example, a chemical engineer may run a pilot plant experiment with several batches of raw material because he knows that different raw material batches of different quality grades will be used in the full-scale process. Sometimes the presence of nuisance factors prevents complete randomization.

The design technique used in these situations is called **blocking**. In this section we show how to arrange the  $2^k$  factorial design in blocks.

### 3.7.1 Blocking in the Replicated Design

Suppose that the  $2^k$  factorial design has been replicated  $n$  times. A simple way to incorporate nonhomogeneous conditions or nuisance factors in this situation is to consider each set of these conditions or nuisance factor levels as a block and to run each replicate of the design in a separate block. The runs in each block are to be made in random order. Because each block contains all of the runs from a complete replicate of the experiment, this type of blocking arrangement is called a **randomized complete block design (RCBD)**.

**Example 3.5 The Chemical Process Revisited** Consider the chemical process experiment described in Section 3.2. Suppose that only four experimental trials could be easily be made from a single batch of raw material. Therefore, four batches of raw material will be required in order to run all four replicates. Table 3.16 shows the RCBD for this experiment, assuming that each replicate is run in a single batch of material. Within each material batch, the four runs are made in random order.

The analysis of variance for this design is shown in Table 3.17. All of the sums of squares in this table are calculated as in a standard (unblocked)  $2^k$  factorial, except the sum of squares for blocks. If we let  $B_i$  ( $i = 1, 2, 3, 4$ ) represent the four block totals (see Table 3.16), then

$$\begin{aligned} SS_{\text{Blocks}} &= \sum_{i=1}^4 \frac{B_i^2}{4} - \frac{\bar{y}_{\dots}^2}{16} \\ &= \frac{(588)^2 + (590)^2 + (589)^2 + (580)^2}{4} - \frac{(2347)^2}{16} \\ &= 15.6875 \end{aligned}$$

There are three degrees of freedom among the four blocks. Table 3.17 indicates that the conclusions from this experiment are identical to those in Section 3.2 and that the block effect is relatively small.

**TABLE 3.16 The Chemical Process Experiment in Four Blocks (RCBD)**

	Block 1	Block 2	Block 3	Block 4
(1) = 145	(1) = 148	(1) = 147	(1) = 140	
$a = 158$	$a = 152$	$a = 155$	$a = 152$	
$b = 135$	$b = 138$	$b = 141$	$b = 139$	
$ab = 150$	$ab = 152$	$ab = 146$	$ab = 149$	
Block totals	588	590	589	580

**TABLE 3.17 Analysis of Variance for the Chemical Process Experiment in Four Blocks, Example 3.5**

Source of Variation	Sum of Squares	Degrees of Freedom	Mean Square	$F_0$	P-Value
Blocks	15.6875	3	5.2292		
A	410.0625	1	410.0625	43.64	0.0001
B	138.0625	1	138.0625	14.69	0.0040
AB	3.0625	1	3.0625	0.33	0.5820
Error	84.5625	9	9.3959		
Total	651.4375	15			

### 3.7.2 Confounding in the $2^k$ Design

In many situations, it is impossible to perform a complete replicate of a factorial design in one block. **Confounding** is a design technique for arranging a complete factorial experiment in blocks, where the block size is smaller than the number of treatment combinations in one replicate. The technique causes information about certain treatment effects (usually high-order interactions) to be indistinguishable from, or **confounded** with, blocks. In this section we introduce confounding systems for the  $2^k$  factorial design. Note that even though the designs presented are incomplete block designs because each block does not contain all the treatments or treatment combinations, the special structure of the  $2^k$  factorial system allows a simplified method of design construction and analysis.

We consider the construction and analysis of the  $2^k$  factorial design in  $2^p$  incomplete blocks, where  $p < k$ . Consequently, these designs can be run in two blocks, four blocks, eight blocks, and so on.

**Two Blocks** Suppose that we wish to run a single replicate of the  $2^2$  design. Each of the  $2^2 = 4$  treatment combinations requires some quantity of raw material, for example, and each batch of raw material is only large enough for two treatment combinations to be tested. Thus, two batches of raw material are required. If batches of raw material are considered as blocks, then we must assign two of the four treatment combinations to each block.

Figure 3.24 shows one possible design for this problem. The geometric view, Fig. 3.24a, indicates that treatment combinations on opposing diagonals are assigned to different blocks. Notice from Fig. 3.24b. that block 1 contains the treatment combinations (1) and  $ab$  and that block 2 contains  $a$  and  $b$ . Of course the order in which the treatment combinations are run within a block is randomly determined. We would also randomly decide which block to run first. Suppose we estimate the main effect of  $A$  and  $B$  just as if no blocking had occurred. The effect estimates are

$$A = \frac{1}{2}[ab + a - b - (1)]$$

$$B = \frac{1}{2}[ab + b - a - (1)]$$

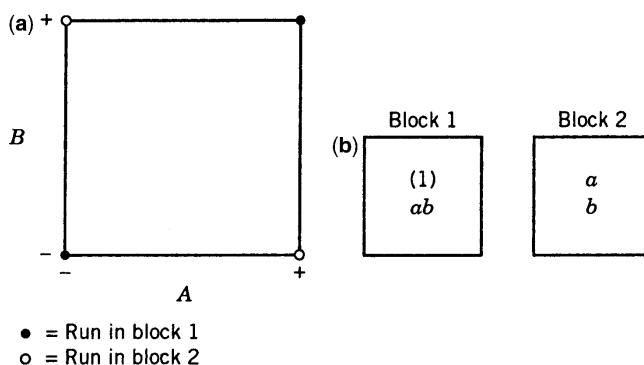


**Figure 3.24** A  $2^2$  design in two blocks. (a) Geometric view. (b) Assignment of the four runs to two blocks.

**TABLE 3.18** Table of Plus and Minus Signs for the  $2^2$  Design

Treatment Combination	Factorial Effect			
	I	A	B	AB
(1)	+	-	-	+
a	+	+	-	-
b	+	-	+	-
ab	+	+	+	+

Note that both of the effect estimates  $A$  and  $B$  are unaffected by blocking because in each estimate there is one plus and one minus treatment combination from each block. That is, any difference between block 1 and block 2 will cancel out.

Now consider the  $AB$  interaction

$$AB = \frac{1}{2}[ab + (1) - a - b]$$

Because the two treatment combinations with the plus sign [ $ab$  and  $(1)$ ] are in block 1 and the two with the minus sign [ $a$  and  $b$ ] are in block 2, the block effect and the  $AB$  interaction are identical. That is,  $AB$  is confounded with blocks.

The reason for this is apparent from the table of plus and minus signs for the  $2^2$  design. This was originally given as Table 3.2, but for convenience it is reproduced as Table 3.18. From this table, we see that all treatment combinations that have a plus on  $AB$  are assigned to block 1, whereas all treatment combinations that have a minus on  $AB$  are assigned to block 2. This approach can be used to confound any effect ( $A$ ,  $B$ , or  $AB$ ) with blocks. For example, if  $(1)$  and  $b$  had been assigned to block 1 and  $a$  and  $ab$  to block 2, then the main effect  $A$  would have been confounded with blocks. The usual practice is to confound the highest-order interaction with blocks.

This scheme can be used to confound any  $2^k$  design in two blocks. As a second example, consider a  $2^3$  design run in two blocks. Suppose we wish to confound the three-factor interaction  $ABC$  with blocks. From the plus and minus signs shown in Table 3.3, we assign the treatment combinations that are minus on  $ABC$  to block 1 and those that are plus on  $ABC$  to block 2. The resulting design is shown in Fig. 3.25. Once again, we emphasize that the treatment combinations within a block are run in random order.

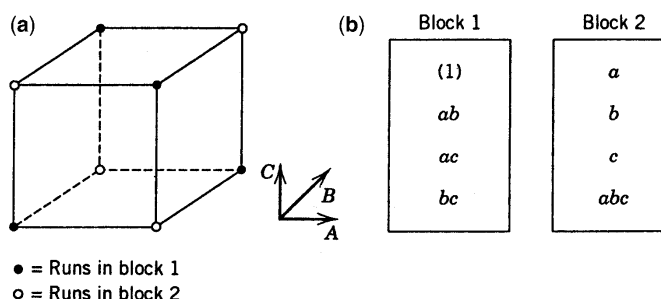


**Figure 3.25** A  $2^3$  design in two blocks. (a) Geometric view. (b) Assignment of the eight runs to two blocks.

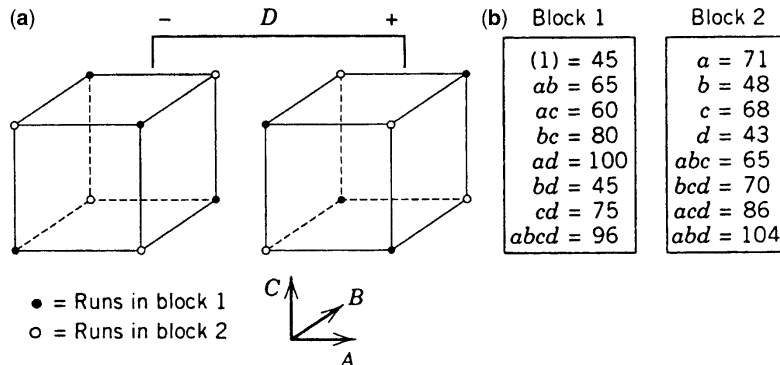


**Figure 3.26** The  $2^4$  design in two blocks for Example 3.6. (a) Geometric view. (b) Assignment of the 16 runs to 2 blocks.

**Example 3.6 A  $2^4$  Factorial in Two Blocks** Consider the situation described in Example 3.2. Recall that four factors—temperature ( $A$ ), pressure ( $B$ ), concentration of formaldehyde ( $C$ ), and stirring rate ( $D$ )—are studied in a pilot plant to determine their effect on product filtration rate. Suppose now that the  $2^4 = 16$  treatment combinations cannot all be run on one day. The experimenter can make eight runs per day, so a  $2^4$  design confounded in two blocks seems appropriate. It is logical to confound the highest-order interaction  $ABCD$  with blocks. The design is shown in Fig. 3.26. Because the block totals are 566 and 555, the sum of squares for blocks is

$$SS_{\text{Blocks}} = \frac{(566)^2 + (555)^2}{8} - \frac{(1121)^2}{16} = 7.5625$$

which is identical to the sum of squares for  $ABCD$ . A normal probability plot of the remaining effects indicates that only factors  $A$ ,  $C$ ,  $D$  and the  $AC$  and  $CD$  interactions are important. Therefore, the error sum of squares is formed by pooling the remaining effects. The resulting analysis of variance is shown in Table 3.19. The practical conclusions are identical to those found in the original Example 3.2.

**TABLE 3.19 Analysis of Variance, Example 3.16**

Source of Variation	Sum of Squares	Degrees of Freedom	Mean Squares	$F_0$	P-Value
Blocks ( $ABCD$ )	7.563	1			
$A$	1870.563	1	1870.563	89.76	$5.60 \times 10^{-6}$
$C$	390.062	1	390.062	18.72	0.0019
$D$	855.562	1	855.562	41.05	0.0001
$AC$	1314.062	1	1314.062	63.05	$2.35 \times 10^{-5}$
$AD$	1105.562	1	1105.563	53.05	$4.65 \times 10^{-5}$
Error	187.562	9	20.840		
Total	5730.937	15			

	Block 1 -	Block 2 +	Block 3 -	Block 4 +
ADE	-	+	-	+
BCE	-	-	+	+
(1)	abc	a bc	b abce	e abcde
ad	ace	d abde	abd ae	ade bd
bc	cde	abc ce	c bcde	bce ac
abcd	bde	bcd acde	acd de	ab cd

**Figure 3.27** The  $2^5$  design in four blocks with  $ADE$ ,  $BCE$ , and  $ABCD$  confounded.

**Four or More Blocks** It is possible to construct  $2^k$  factorial designs confounded in four blocks of  $2^k/4 = 2^{k-2}$  observations each. These designs are particularly useful in situations where the number of factors is moderately large, say  $k \geq 4$ , or block sizes are relatively small.

As an example, consider the  $2^5$  design. If each block will hold only eight runs, then four blocks must be used. The construction of this design is relatively straightforward. Select two effects to be confounded with blocks, say  $ADE$  and  $BCE$ . Then construct a table of plus and minus signs for the  $2^5$  design. If you consider only the  $ADE$  and  $BCE$  columns in such a table, there will be exactly four different sign patterns for the 32 observations in these two columns. The sign patterns are as follows:

ADE	BCE
-	-
+	-
-	+
+	+

The design would be constructed by placing all the runs that are  $(-, -)$  in block 1, those that are  $(+, -)$  in block 2, those that are  $(-, +)$  in block 3, and those that are  $(+, +)$  in block 4. The design is shown in Fig. 3.27.

With a little reflection we realize that another effect in addition to  $ADE$  and  $BCE$  must be confounded with blocks. Because there are four blocks with three degrees of freedom between them, and because  $ADE$  and  $BCE$  have only one degree of freedom each, clearly an additional effect with one degree of freedom must be confounded. This effect is the **generalized interaction** of  $ADE$  and  $BCE$ , which is defined as the product of  $ADE$  and  $BCE$  modulo 2. Thus, in our example the generalized interaction  $(ADE)(BCE) = ABCDE^2 = ABCD$  is also confounded with blocks. It is easy to verify this by referring to a table of plus and minus signs for the  $2^5$  design. Inspection of such a table would reveal that the treatment combinations are assigned to the blocks as follows:

Treatment Combinations in	Sign on ADE	Sign on BCE	Sign on ABCD
Block 1	-	-	+
Block 2	+	-	-
Block 3	-	+	-
Block 4	+	+	+

**TABLE 3.20** Suggested Blocking Arrangements for the  $2^k$  Factorial Design

Number of Factors, $k$	Number of Blocks, $2^p$	Block Size, $2^{k-p}$	Effects Chosen to Generate the Blocks	Interactions Confounded with Blocks
3	2	4	$ABC$	$ABC$
	4	2	$AB, AC$	$AB, AC, BC$
4	2	8	$ABCD$	$ABCD$
	4	4	$ABC, ACD$	$ABC, ACD, BD$
	8	2	$AB, BC, CD$	$AB, BC, CD, AC, BD, AD, ABCD$
5	2	16	$ABCDE$	$ABCDE$
	4	8	$ABC, CDE$	$ABC, CDE, ABDE$
	8	4	$ABE, BCE, CDE$	$ABE, BCE, CDE, AC, ABCD, BD, ADE$
	16	2	$AB, AC, CD, DE$	All 2-factor and 4-factor interactions (15 effects)
	32	1	$ABCDEF$	$ABCDEF$
6	4	16	$ABCF, CDEF$	$ABCF, CDEF, ABDE$
	8	8	$ABEF, ABCD, ACE$	$ABEF, ABCD, ACE, BCF, BDE, CDEF, ADF$
	16	4	$ABF, ACF, BDF, DEF$	$ABE, ACF, BDF, DEF, BC, ABCD, ABDE, AD, ACDE, CE, BDF, BCDEF, ABCEF, AEF, BE$
	32	2	$AB, BC, CD, DE, EF$	All 2-factor, 4-factor, and 6-factor interactions (31 effects)
	64	1	$ABCDEFG$	$ABCDEFG$
7	4	32	$ABCfg, CDEFG$	$ABCfg, CDEFG, ABDE$
	8	16	$ABC, DEF, AFG$	$ABC, DEF, AFG, ABCDEF, DCFG, ADEG, BCDEFG$
	16	8	$ABD, EFG, CDE, ADG$	$ABCD, EFG, CDE, ADG, ABCDEFG, ABE, BCG, CDFG, ADEF, ACEG, ABFG, BCEF, BDEG, ACF, BDF$
	32	4	$ABG, BCG, CDG, DEG, EFG$	$ABG, BCG, CDG, DEG, EFG, AC, BD, DE, DF, AE, BE, ABCD, ABDE, ABEF, BCDE, BCEF, CDEF, ABCDEFG, ADG, ACDEG, ACEFG, ABDFG, ABCEG, BEG, BDEFG, CFG, ADEF, ACDF, ABCF, AFG$
	64	2	$AB, BC, CD, DE, EF, FG$	All 2-factor, 4-factor, and 6-factor interactions (63 effects)

Notice that the product of signs of any two effects for a particular block (e.g.,  $ADE$  and  $BCE$ ) yields the sign of the other effect for that block (in this case  $ABCD$ ). Thus  $ADE$ ,  $BCE$ , and  $ABCD$  are all confounded with blocks.

The general procedure for constructing a  $2^k$  design confounded in four blocks is to choose two effects to generate the blocks, automatically confounding a third effect that is the generalized interaction of the first two. Then, the design is constructed by assigning the treatment combinations that have the sign pattern  $(-, -), (+, +), (+, -), (-, +)$  in the two original

columns to four blocks. In selecting effects to be confounded with blocks, care must be exercised to obtain a design that does not confound effects that may be of interest. For example, in a  $2^5$  design we might choose to confound  $ABCDE$  and  $ABD$ , which automatically confounds  $CE$ , an effect that is probably of interest. A better choice is to confound  $ADE$  and  $BCE$ , which automatically confounds  $ABCD$ . It is preferable to sacrifice information on the three-factor interactions  $ADE$  and  $BCE$  instead of the two-factor interaction  $CE$ .

We can extend this procedure to even larger numbers of blocks. It is possible to construct a  $2^k$  factorial design in  $2^p$  blocks (where  $p < k$ ) of  $2^{k-p}$  treatment combinations each. To do this, select  $p$  independent effects to confound with blocks, where “independent” means that no chosen effect is the generalized interaction of the others. The plus and minus sign patterns on these  $p$  columns are used to assign the treatment combinations to the blocks. In addition, exactly  $2^p - p - 1$  other effects will be confounded with blocks, these effects being the generalized interactions of the  $p$  effects initially chosen. The choice of these  $p$  effects is critical, because the confounding pattern in the design depends on them. Table 3.20, from Montgomery (2005), presents a selection of useful designs for  $k \leq 7$  factors. To illustrate the use of this table, suppose we want to run a  $2^6$  design in  $2^3 = 8$  blocks of  $2^{6-3} = 8$  runs each. Table 3.20 indicates that we should choose  $ABEF$ ,  $ABCD$ , and  $ACE$  as the  $p = 3$  independent effects to construct the blocks. Then  $2^p - p - 1 = 2^3 - 3 - 1 = 4$  other effects are also confounded. These are the generalized interaction of these three, or

$$(ABEF)(ABCD) = A^2B^2CDEF = CDEF$$

$$(ABEF)(ACE) = A^2BCE^2F = BCF$$

$$(ABCD)(ACE) = A^2BC^2DE = BDE$$

$$(ABEF)(ABCD)(ACE) = A^3B^2C^2DE^2F = ADF$$

Notice that this design would confound three four-factor interactions and four three-factor interactions with blocks. This is the best possible blocking arrangement for this design.

There are several computer programs for constructing and analyzing two-level factorial designs. Most of these programs have the capability to generate the confounded versions of these designs discussed in this section. The authors of these programs have typically used Table 3.20, or a similar one, as the basis for their designs.

### 3.8 SPLIT-PLOT DESIGNS

The experimental designs we have considered so far are either **completely randomized designs** (CRDs) or **randomized blocks**, where the randomization is restricted to within different levels of nuisance factors (the blocks). In some experimental situations we may be unable to completely randomize the order of the runs because some of the factors are hard to change. To illustrate, suppose that it is hard to change the level for one of the factors in the experiment. When this happens, practitioners typically fix the level of the hard-to-change factor and run multiple combinations of the other factors at that level of the hard-to-change factor. This results in a generalization of the factorial design called a **split-plot design**.

As an example, consider a paper manufacturer who is interested in two different pulp preparation methods (the methods differ in the amount of hardwood in the pulp mixture) and two different cooking temperatures for the pulp and who wishes to study the effect of these two factors on the tensile strength of the paper. Each replicate of a factorial experiment requires four observations, and the experimenter has decided to run two replicates. Therefore, the complete experiment will require eight runs. Also, the pulp preparation method factor is hard to change in that each batch of pulp is quite large, and making up a separate batch of pulp for each run of the experiment or eight pulp batches is impractical. Therefore, he conducts the experiment as follows. A batch of pulp is produced by one of the two methods under study. Then this batch is divided into two samples, and each sample is cooked at one of the two temperatures. Then a second batch of pulp is made up using the remaining pulp preparation method. This second batch is also divided into two samples that are tested at the two temperatures. Then a third batch is made up using one of the two methods, it is divided into two samples and the samples are tested using the two temperatures. Finally, another batch of pulp is prepared using the remaining method, it is divided into two samples and both temperatures are tested. The data are shown in Table 3.21.

Initially, we might consider this to be a factorial experiment with two levels of preparation method (factor  $A$ ) and two levels of temperature (factor  $B$ ). If this is the case, then the order of experimentation should be completely randomized; that is, within a block, we should randomly select a treatment combination (a preparation method and a temperature) and obtain an observation, and then we should randomly select another treatment combination and obtain a second observation, and so on, until all eight treatment combinations corresponding to the two replicates have been taken. However, the experimenter did not conduct the experiment this way. He made up a batch of pulp and obtained observations for both temperatures from that batch. Because of the size of the batches, this is the only feasible way to run this experiment. A completely randomized factorial experiment would require eight batches of pulp, which is unrealistic. The split-plot design requires only four batches. Obviously, the split-plot design has resulted in a gain in experimental efficiency when compared to the completely randomized design.

Split-plot designs have their origin in the agricultural sciences. Suppose that we have an agricultural field trial with two factors: irrigation method and seed variety. The irrigation method is hard to change, in that it can only be applied over a relatively large section of the test field, called a **whole plot**. The factor associated with this is therefore called a **whole plot factor**. Within the whole plot, the second factor—seed variety—is applied to

TABLE 3.21 Split-Plot Design for the Pulp Preparation Method-Temperature Experiment

Whole Plots	Method	Temperature	y
1	-1	-1	36
1	-1	1	50
2	1	-1	25
2	1	1	30
3	-1	1	46
3	-1	-1	35
4	1	-1	20
4	1	1	27

**TABLE 3.22 JMP Output for the Split-Plot Experiment in Table 3.21**

Response Y Summary of Fit					
R-Square	0.995006				
R-Square Adj	0.991261				
Root Mean Square Error	1.274755				
Mean of Response	33.625				
Observations (or Sum Wgts)	8				
Parameter Estimates					
Term	Estimate	Std Error	DFDen	t-Ratio	Prob >  t
Intercept	33.625	1.179248	2	28.51	0.0012
X1	-8.125	1.179248	2	-6.89	0.0204
X2	4.625	0.450694	2	10.26	0.0094
X1*X2	-1.625	0.450694	2	-3.61	0.0691
REML Variance Component Estimates					
Random Effect	Var Ratio	Var Component	Std Error	95% Lower	95% Upper
Whole Plots	2.9230769	4.75	5.6215267	-6.268192	15.768192
Residual		1.625	1.625	0.4405132	64.184072
Total		6.375			100.000
-2 LogLikelihood = 25.45867972					
Fixed Effect Tests					
Source	Nparm	DF	DFDen	F-Ratio	Prob > F
X1	1	1	2	47.4719	0.0204
X2	1	1	2	105.3077	0.0094
X1*X2	1	1	2	13.0000	0.0691

smaller sections of the field, which are obtained by splitting the larger section of the field into **subplots** or **split plots**. This factor is called the **subplot factor**. In the paper manufacturing example, pulp preparation method is the whole plot factor and temperature is the subplot factor.

The pulp preparation method–temperature experiment is fairly typical of how the split-plot design is used in an industrial setting. Notice that the two factors were essentially “applied” at different times. Consequently, a split-plot design can be viewed as two experiments “combined” or superimposed on each other. One “experiment” has the whole plot factor applied to the large experimental units (or it is a factor whose levels are hard to change) and the other “experiment” has the subplot factor applied to the smaller experimental units (or it is a factor whose levels are easy to change).

The statistical model for a split-plot design can be written as

$$y_{ij} = \mu + \tau_i + \varepsilon_{WP} + \beta_j + (\tau\beta)_{ij} + \varepsilon_{SP}$$

where  $\mu$  is an overall mean,  $\tau_i$  is the whole plot factor (the pulp preparation methods),  $\varepsilon_{WP}$  is the whole plot error,  $\beta_j$  is the subplot factor (the temperature),  $(\tau\beta)_{ij}$  is the methods–temperature interaction, and  $\varepsilon_{SP}$  is the subplot error. Notice that the model has two error terms,  $\varepsilon_{WP}$  and  $\varepsilon_{SP}$ , because there are two different randomizations involved; one for the whole plots, and another for the subplots. Consequently there are two variance components that represent these errors,  $\sigma_{WP}^2$  and  $\sigma_{SP}^2$ . We usually say that the split-plot design has **two different error structures**. All of the whole plot factors are tested against the whole plot error, and all of the subplot factors along with interactions between whole plot and subplot factors are tested against the subplot error. Generally we find that the subplot error variance is less than the whole plot error variance, because the subplots are usually more homogeneous than the whole plots. Because the subplot treatments are compared with greater precision, it is preferable to assign the factor we are most interested in to the subplots, if possible. However, practical or economic considerations of the hard-to-change versus easy-to-change nature of the factors may make this impossible.

JMP will construct and analyze split-plot designs. Some of the JMP output for the pulp preparation method–temperature experiment is shown in Table 3.22. In addition to an ANOVA summary for the model (see the section in Table 3.22 labeled “Fixed Effect Tests”) JMP also obtains estimates of the whole plot and subplot variance components using a maximum likelihood approach (see the section labeled “REML Variance Components Estimates”). Both factors, pulp preparation methods and temperature are significant, and there is reasonable indication of an interaction between these factors (the  $P$ -value is approximately 0.07). Also, we see that the whole plot error estimate  $\hat{\sigma}_{WP}^2 = 4.75$ , is greater than the subplot error estimate  $\hat{\sigma}_{SP}^2 = 1.625$ .

## EXERCISES

- 3.1** A router is used to cut registration notches on a printed circuit board. The vibration at the surface of the board as it is cut is considered to be a major source of dimensional variation in the notches. Two factors are thought to influence vibration: bit size ( $A$ ) and cutting speed ( $B$ ). Two bit sizes ( $\frac{1}{16}$  and  $\frac{1}{8}$  inch) and two speeds (40 and 90 rpm)

are selected, and four boards are cut at each set of conditions as shown in Table E3.1. The response variable is vibration measured as the resultant vector of three accelerometers ( $x$ ,  $y$ , and  $z$ ) on each test circuit board.

**TABLE E3.1 The  $2^2$  Design for Exercise 3.1**

$A$	$B$	Treatment Combination	Replicate			
			I	II	III	IV
–	–	(1)	18.2	18.9	12.9	14.4
+	–	$a$	27.2	24.0	22.4	22.5
–	+	$b$	15.9	14.5	15.1	14.2
+	+	$ab$	41.0	43.9	36.3	39.9

- (a) Analyze the data from this experiment.
  - (b) Construct a normal probability plot of the residuals and a plot of the residuals versus the predicted vibration level. Interpret these plots.
  - (c) Draw the  $AB$  interaction plot. Interpret this plot. What levels of bit size and speed would you recommend for routine operation?
  - (d) Construct a contour plot of vibration as a function of speed and bit size.
- 3.2** An engineer is interested in the effects of cutting speed ( $A$ ), tool geometry ( $B$ ), and cutting angle ( $C$ ) on the life (in hours) of a machine tool. Two levels of each factor are chosen, and two replicates of a  $2^3$  factorial design are run. The results are shown in Table E3.2.

**TABLE E3.2 The  $2^3$  Design for Exercise 3.2**

$A$	$B$	$C$	Treatment Combination	Replicate	
				I	II
–	–	–	(1)	22	31
+	–	–	$a$	32	43
–	+	–	$b$	35	34
+	+	–	$ab$	55	47
–	–	+	$c$	44	45
+	–	+	$ac$	40	37
–	+	+	$bc$	60	50
+	+	+	$abc$	39	41

- (a) Estimate the factor effects. Which effects appear to be large?
- (b) Use the analysis of variance to confirm your conclusions for part (a).
- (c) Analyze the residuals. Are there obvious problems or violations of the assumptions?
- (d) What levels of  $A$ ,  $B$ , and  $C$  would you recommend, based on the data from this experiment?

- 3.3** An industrial engineer employed by a beverage bottler is interested in the effects of two different types of 32-ounce bottles on the time to deliver 12-bottle cases of the product. The two bottle types are glass and plastic. Two workers are used to perform a task consisting of moving 40 cases of the product 50 ft on a standard type of hand truck and stacking the cases in a display. Four replicates of a  $2^2$  factorial design are performed, and the times observed are given in Table E3.3. Analyze the data and draw appropriate conclusions. Analyze the residuals and comment on model adequacy.

**TABLE E3.3** The  $2^2$  Design for Exercise 3.3

Bottle Type	Time	
	Worker 1	Worker 2
Glass	5.12	6.65
	4.98	5.49
	4.89	6.24
	5.00	5.55
	4.95	5.28
Plastic	4.27	4.75
	4.43	4.91
	4.25	4.71

- 3.4** Find the two standard error limits for the factor effects in Exercise 3.1. Does the results of this analysis agree with the conclusions from the analysis of variance?
- 3.5** Find the two standard error limits for the factor effects in Exercise 3.2. Does the result of this analysis agree with the conclusions from the analysis of variance?
- 3.6** An experiment was performed to improve the yield of a chemical process. Four factors were selected, and one replicate of a completely randomized experiment was run. The results are shown in Table E3.4.
- (a) Estimate the factor effects. Construct a normal probability plot of these effects. Which effects appear large?
- (b) Prepare an analysis of variance table using the information obtained in part (a).
- (c) Plot the residuals versus the predicted yield and on normal probability paper. Does the residual analysis appear satisfactory?
- (d) Construct a contour plot of yield as a function of the important process variables.

**TABLE E3.4** The  $2^3$  Design for Exercise 3.6

Treatment Combination	Yield	Treatment Combination	Yield
(1)	90	<i>d</i>	98
<i>a</i>	64	<i>ad</i>	62
<i>b</i>	81	<i>bd</i>	87
<i>ab</i>	63	<i>abd</i>	75
<i>c</i>	77	<i>cd</i>	99
<i>ac</i>	61	<i>acd</i>	69
<i>bc</i>	88	<i>bcd</i>	87
<i>abc</i>	53	<i>abcd</i>	60

- 3.7** Consider the design of Exercise 3.6. Suppose that four additional runs were made at the center of the region of experimentation. The response values at these center points were 94, 90, 99, and 87. Use this additional information to test for curvature in the response function. What are your conclusions?
- 3.8** An article in the *AT&T Technical Journal* (March/April 1986, Vol. 65, pp. 39–50) describes the application of two-level factorial designs to integrated circuit manufacturing. A basic processing step is to grow an epitaxial layer on polished silicon wafers. The wafers mounted on a susceptor are positioned inside a bell jar, and chemical vapors are introduced. The susceptor is rotated and heat is applied until the epitaxial layer is thick enough. An experiment was run using two factors: arsenic flow rate ( $A$ ) and deposition time ( $B$ ). Four replicates were run, and the epitaxial layer thickness (in micrometers) was measured. The data from this experiment are in Table E3.5.
- Estimate the factor effects.
  - Conduct the analysis of variance. Which factors are important?
  - Analyze the residuals. Are there any residuals that should cause concern?
  - Discuss how you might deal with the potential outlier found in part (c).
  - Construct a contour plot of the layer thickness response surface as a function of flow rate and deposition time.

**TABLE E3.5 The Layer Thickness Experiment from Exercise 3.8**

A	B	Replicate				Level		
		I	II	III	IV	Factor	Low (−)	High (+)
−	−	14.037	16.165	13.972	13.907	A	55%	59%
+	−	13.880	13.860	14.032	13.914	B	Short	Long
−	+	14.821	14.757	14.843	14.878			
+	+	14.88	14.921	14.415	14.932			

- 3.9** A nickel–titanium alloy is used to make components for jet turbine aircraft engines. Cracking is a potentially serious problem in the final part, because it can lead to nonrecoverable failure. A test is run at the parts producer to determine the effect of four factors on cracks. The four factors are pouring temperature ( $A$ ), titanium content ( $B$ ), heat treatment method ( $C$ ), and amount of grain refiner used ( $D$ ). A single replicate of a  $2^4$  design is run, and the lengths (in millimeters) of three cracks induced in a sample coupon subjected to a standard test are measured. The data are shown in Table E3.6.
- Use the average crack length as the response. Estimate the factor effects. Which effects appear to be large?
  - Using the results of part (a), form a tentative model and conduct an analysis of variance.
  - Analyze the residuals from this model.
  - Use the logarithm of the variance of crack length as the response. Is there any evidence that any of the design factors affect the variability in crack length?
  - Make recommendations for process operating conditions.

**TABLE E3.6** The Crack Length Experiment from Exercise 3.9

A	B	C	D	Treatment Combination		Crack Length
–	–	–	–	(1)	0.011	0.015
+	–	–	–	<i>a</i>	1.015	1.002
–	+	–	–	<i>b</i>	0.014	0.012
+	+	–	–	<i>ab</i>	1.032	1.020
–	–	+	–	<i>c</i>	0.440	0.444
+	–	+	–	<i>ac</i>	2.388	2.253
–	+	+	–	<i>bc</i>	1.228	1.100
+	+	+	–	<i>abc</i>	2.759	2.560
–	–	–	–	<i>d</i>	0.010	0.013
+	–	–	+	<i>ad</i>	0.593	0.542
–	+	–	+	<i>bd</i>	0.675	0.600
+	+	–	+	<i>abd</i>	1.362	1.215
–	–	+	+	<i>cd</i>	0.544	0.591
+	–	+	+	<i>acd</i>	2.112	2.003
–	+	+	+	<i>bcd</i>	1.553	1.318
+	+	+	+	<i>abcd</i>	2.497	2.220
						2.753

- 3.10** Reconsider the crack length experiment in Exercise 3.9. Factor *C*, type of heat treatment, is a categorical variable. Write down the appropriate models for the mean case length response for each type of heat treatment.
- (a) Construct the contour plots of average crack length for these two models. Comment on any differences in the plots.
  - (b) Is there any evidence that one heat treatment method results in lower variability in crack length than the other?
- 3.11** An article in *Solid State Technology* (“Orthogonal Design for Process Optimization and its Application in Plasma Etching,” May 1987, pp. 127–132) describes the application of factorial designs in developing a nitride etch process on a single-wafer plasma etcher. The process uses  $\text{C}_2\text{F}_6$  as the reactant gas. Four factors are of interest: anode–cathode gap (*A*), pressure in the reactor chamber (*B*)  $\text{C}_2\text{F}_6$  gas flow (*C*), and power applied to the cathode (*D*). The response variable of interest is the etch rate for silicon nitride. A single replicate of a  $2^4$  design is run, and the resulting data are in Table E3.7.
- (a) Estimate the factor effects. Construct a normal probability plot of the factor effects. Which effects appear large?
  - (b) Conduct an analysis of variance to confirm your findings for part (a).
  - (c) Analyze the residuals from this experiment. Comment on the model’s adequacy.
  - (d) If not all the factors are important, project the  $2^4$  design into a  $2^k$  design with  $k < 4$  and conduct the analysis of variance.
  - (e) Draw graphs to interpret any significant interactions.
  - (f) Plot the residuals versus the actual run order. What problems might be revealed by this plot?

**TABLE E3.7** The Etch Rate Experiment from Exercise 3.11

Run Number	Run Order	Actual				Etch Rate (Å/min)	Factor	Level	
		A	B	C	D			Low (-)	High (+)
1	13	—	—	—	—	500	A (cm)	0.8	1.20
2	8	+	—	—	—	669	B (mTorr)	4.5	550
3	12	—	+	—	—	604	C (sccm)	125	200
4	9	+	+	—	—	650	D (W)	275	325
5	4	—	—	+	—	633			
6	15	+	—	+	—	642			
7	16	—	+	+	—	601			
8	3	+	+	+	—	635			
9	1	—	—	—	+	1037			
10	14	+	—	—	+	749			
11	5	—	+	—	+	1052			
12	10	+	+	—	+	868			
13	11	—	—	+	+	1075			
14	2	+	—	+	+	860			
15	7	—	+	+	+	1063			
16	6	+	+	+	+	729			

- 3.12** Consider the single replicate of the  $2^4$  design in Example 3.11. Suppose we had arbitrarily decided to analyze the data assuming that all three- and four-factor interactions were negligible. Conduct this analysis and compare your results with those obtained in the example. Do you think that it is a good idea to arbitrarily assume interactions to be negligible even if they are relatively high-order ones?
- 3.13** An experiment was run in a semiconductor fabrication plant in an effort to increase the number of good chips produced per wafer. Five factors, each at two levels, were studied. The factors (and levels) were  $A$  = aperture setting (small, large),  $B$  = exposure time (20% below nominal),  $C$  = development time (30 sec, 45 sec),  $D$  = mask dimension (small, large), and  $E$  = etch time (14.5 min, 15.5 min). The unreplicated  $2^5$  design shown in Table E3.8 is run.
- (a) Construct a normal probability plot of the effect estimates. Which effects appear to be large?
- (b) Conduct an analysis of variance to confirm your findings for part (a).

**TABLE E3.8** The  $2^5$  Experiment from Exercise 3.13

(1)	15	d	16	e	14	de	12
a	20	ad	21	ae	23	ade	19
b	70	bd	65	be	71	bde	60
ab	112	abd	100	abe	110	abde	106
c	30	cd	35	ce	31	cde	32
ac	40	acd	45	ace	43	acde	39
bc	79	bcd	85	bce	90	bcde	82
abc	125	abcd	120	abce	130	abcde	128

- (c) Plot the residuals on normal probability paper. Is the plot satisfactory?
  - (d) Plot the residuals versus the predicted yields and versus each of the five factors. Comment on the plots.
  - (e) Interpret any significant interactions.
  - (f) What are your recommendations regarding process operating conditions?
  - (g) Project the  $2^5$  design in this problem into a  $2^k$  design in the important factors. Sketch the design, and show the average and range of yields at each run. Does this sketch aid in data interpretation?
  - (h) Construct a contour plot showing how yield changes in terms of the important factors.
- 3.14** After running a  $2^4$  factorial design, an engineer obtained the following factor effect estimates:

$$\begin{array}{lll}
 A = -1.3 & AB = -2.9 & ABC = 0.5 \\
 B = 10.1 & AC = 1.9 & ABD = 1.8 \\
 C = 7.5 & AD = -4.0 & ACD = -2.7 \\
 D = -1.4 & BC = -5.1 & BCD = 2.8 \\
 & BD = 2.2 & ABCD = -0.6 \\
 & CD = -0.2
 \end{array}$$

Use a normal probability plot to interpret these effects.

- 3.15** Consider the data from the experiment in Exercise 3.11. Suppose that the last run made in this experiment (run order number 16) was lost; in fact, the wafer was broken so that no reading on etch rate could be obtained. One logical approach to analyzing these data is to estimate the missing value that makes the highest-order interaction effect estimate zero. Apply this technique to these data, and compare your results with those obtained in the analysis of the full data set in Exercise 3.10.
- 3.16 Continuation of Exercise 3.15.** Reconsider the situation described in Exercise 3.15.
- (a) Analyze the data by fitting a regression model in the main effects to the 15 observations.
  - (b) Investigate the adequacy of this model. What are your conclusions?
  - (c) Build a model for the 15 observations with stepwise regression methods, using the main effects and two-factor interactions as the candidate variables.
  - (d) Comment on the model obtained above, and compare it to those from Exercise 3.11 and 3.15.
- 3.17 Contour Plots for Exercise 3.11.** Reconsider the etch rate experiment in Exercise 3.11. Construct contour plots for the etch rate response. Suppose that it is important to operate this process with a mean etch rate very close to  $800 \text{ \AA/m}$ . What operating conditions do you recommend?
- 3.18** An experiment was conducted on a chemical process that produces a polymer. The four factors studied were temperature ( $A$ ), catalyst concentration ( $B$ ), time ( $C$ ), and pressure ( $D$ ). Two responses, molecular weight and viscosity, were observed. The design matrix and the resulting data are given in Table E3.9.

**TABLE E3.9 The Chemical Process Experiment, Exercise 3.18**

Run Number	Actual Run Order					Molecular Weight	Viscosity	Factor	Level	
		A	B	C	D				Low (-)	High (+)
1	18	-	-	-	-	2400	1400	A (°C)	100	120
2	9	+	-	-	-	2410	1500	B (%)	4	8
3	13	-	+	-	-	2315	1520	C (min)	20	30
4	8	+	+	-	-	2510	1630	D (psi)	60	75
5	3	-	-	+	-	2615	1380			
6	11	+	-	+	-	2625	1525			
7	14	-	+	+	-	2400	1500			
8	17	+	+	+	-	2750	1620			
9	6	-	-	-	+	2400	1400			
10	7	+	-	-	+	2390	1525			
11	2	-	+	-	+	2300	1500			
12	10	+	+	-	+	2520	1500			
13	4	-	-	+	+	2625	1420			
14	19	+	-	+	+	2630	1490			
15	15	-	+	+	+	2500	1500			
16	20	+	+	+	+	2710	1600			
17	1	0	0	0	0	2515	1500			
18	5	0	0	0	0	2500	1460			
19	16	0	0	0	0	2400	1525			
20	12	0	0	0	0	2475	1500			

- (a) Consider only the molecular weight response. Plot the effect estimates on a normal probability scale. What effects appear important?
- (b) Use an analysis of variance to confirm the results from part (a). Is there indication of curvature?
- (c) Write down a regression model to predict molecular weight as a function of the important variables.
- (d) Analyze the residuals and comment on model adequacy.
- (e) Repeat parts (a)–(d) using the viscosity response.
- 3.19 Continuation of Exercise 3.18.** Use the regression models for molecular weight and viscosity to answer the following questions.
- (a) Construct a response surface contour plot for molecular weight. In what direction would you adjust the process variables to increase molecular weight?
- (b) Construct a response surface contour plot for viscosity. In what direction would you adjust the process variables to decrease viscosity?
- (c) What operating conditions would you recommend if it is necessary to produce a product with molecular weight between 2400 and 2500 and with low viscosity?
- 3.20** Consider the experiment described in Exercise 3.1. Suppose that only one replicate (four runs) could be obtained in a single 4-hr time period, and the experimenters were concerned about unknown factors that could vary from one time period to another.
- (a) Set up a design in four blocks that will minimize the time effects.
- (b) Analyze the data assuming that the design had been run as in part (a). Compare the results of your analysis with the original analysis in Exercise 3.1.
- (c) Suppose that the experimenter's concerns were realized and that as a result of the time effect, the observations in replicate IV were  $(1) = 34.4$ ,  $a = 44.5$ ,  $b = 34.2$ , and  $ab = 59.9$  instead of the values shown in Exercise 3.1. Reanalyze these new data, assuming that the blocked design from part (a) had been used. How has the time effect influenced your conclusions?
- 3.21** Consider the experiment described in Exercise 3.2. Suppose that this experiment had been run with each replicate considered as a block. Analyze the data and draw conclusions. How do the results of your analysis compare with the analysis of the original Exercise 3.2?
- 3.22** Consider only the data from the first replicate of Exercise 3.2. Set up a design to run these observations in two blocks of four runs each with  $ABC$  confounded with blocks. Analyze the data.
- 3.23** Consider the data from both replicates of Exercise 3.2. Suppose that only four runs could be made under the same conditions, so that it was necessary to run this design in blocks of four runs.
- (a) Set up a design that confounds  $ABC$  in both replicates. Analyze the data.
- (b) Set up a design that confounds  $ABC$  in the first replicate and  $AB$  in the second replicate. Analyze this design, using the data from replicate I to draw conclusions about the  $AB$  effect, and the data from replicate II to draw conclusions about the  $ABC$  effect (this is a design technique called *partial confounding*).

- 3.24** Consider the data from Exercise 3.6. Construct a design with two blocks of eight runs each, with  $ABCD$  confounded with blocks. Analyze the data.
- 3.25 Continuation of Exercise 3.24.** Reconsider the situation in Exercise 3.24, and assume that the block effect causes all observations in the second block to be reduced by 20. Analyze the data that result. Is the block effect significant? How are the other conclusions affected?
- 3.26** Consider the situation described in Exercise 3.13. Set up a design in two blocks for 16 observations each of this problem. Analyze the data that result.
- 3.27** Consider the situation described in Exercise 3.13. Set up a design in four blocks of eight runs each, with  $ACDE$  and  $BCE$  confounded with blocks. What is the other confounded effect? Analyze the data and draw conclusions.
- 3.28** Construct a  $2^6$  design in eight blocks of eight runs each. Show the complete set of effects that are confounded with blocks.
- 3.29** Suppose that an experimenter has run a  $2^3$  factorial design (eight trials) in random order. He fits the following model to the data:

$$y = \beta_0 + \beta_1 x_1 + \beta_2 x_2 + \beta_3 x_3 + \varepsilon$$

(a) Suppose that the true model is

$$E(y) = \beta_0 + \beta_1 x_1 + \beta_2 x_2 + \beta_3 x_3 + \beta_{12} x_1 x_2$$

Does the interaction term result in biased estimates of  $\beta_0$ ,  $\beta_1$ ,  $\beta_2$ , and  $\beta_3$  in the fitted first-order model?

(b) Suppose that the true model is

$$E(y) = \beta_0 + \beta_1 x_1 + \beta_2 x_2 + \beta_3 x_3 + \beta_{12} x_1 x_2 + \beta_{11} x_1^2$$

Determine the bias induced in the least squares estimates of  $\beta_0$ ,  $\beta_1$ ,  $\beta_2$ , and  $\beta_3$  by the failure to include the terms  $\beta_{12} x_1 x_2$  and  $\beta_{11} x_1^2$  in the fitted model.

- 3.30** An experimenter has run a  $2^3$  design in standard order (no randomization). Unknown to the experimenter, a fourth variable  $x_4$  takes on the values shown in Table E3.10. Suppose that the experimenter fits the first-order model

$$y = \beta_0 + \beta_1 x_1 + \beta_2 x_2 + \beta_3 x_3 + \varepsilon$$

Find the bias in the least squares estimates of  $\beta_0$ ,  $\beta_1$ ,  $\beta_2$ , and  $\beta_3$  that results from not including the term  $\beta_4 x_4$  in the model.

- 3.31** Consider the runs from a  $2^3$  factorial design shown in Table E3.11, in random order. The first four observations are subject to a block effect of 20 units.
- (a) Find the effect of the block effect on the estimates of the main effects of  $A$ ,  $B$ , and  $C$ .

**TABLE E3.10** The  $2^3$  Experiment for Exercise 3.30

Run	$x_1$	$x_2$	$x_3$	$x_4$
1	-1	-1	-1	-4
2	1	-1	-1	-3
3	-1	1	-1	-2
4	1	1	-1	-1
5	-1	-1	1	1
6	1	-1	1	2
7	-1	1	1	3
8	1	1	1	4

**TABLE E3.11** The  $2^3$  Experiment for Exercise 3.31

Run Order	$A$	$B$	$C$	Observation
1	+	+	-	$ab + 20$
2	+	-	-	$a + 20$
3	-	-	-	$(1) + 20$
4	+	+	+	$abc + 20$
5	-	+	-	$b$
6	+	-	+	$ac$
7	-	-	+	$c$
8	-	+	+	$bc$

- (b) Suppose that the design had been set up with  $ABC$  confounded with blocks, and once again, the first 4 runs were subject to a block effect of 20 units. What is the effect of this block effect on the estimates of  $A$ ,  $B$ , and  $C$ ?
- 3.32** Consider a  $2^3$  design with a center point that has been replicated  $n_C$  times. Show that the runs at the center do not affect the estimates of any of the factorial affects. Do the center points affect the estimate of the overall mean? Will these results generalize to any  $2^k$  design?
- 3.33** Consider the  $2^k$  design with  $n_C$  center points. Show that an unbiased estimate of the sum of the pure quadratic coefficients ( $\sum_{i=1}^k \beta_{ij}$ ) in a second-order model can be obtained from the difference between  $\bar{y}_F$  and  $\bar{y}_C$ .
- 3.34** Consider the  $2^k$  design with  $n_C$  center points. We gave an  $F$ -test for pure quadratic curvature. Show that the same hypothesis can be tested using a  $t$ -test.
- 3.35** Consider the plasma etching experiment described in Exercise 3.11. Suppose that factor  $A$ , the anode-cathode gap, is a hard-to-change factor. Set up an appropriate split-plot design for conducting this experiment.
- 3.36** Consider the chemical process experiment described in Exercise 3.18. Suppose that temperature is a hard-to-change factor. Set up an appropriate split-plot design for conducting this experiment.

---

# 4

---

## TWO-LEVEL FRACTIONAL FACTORIAL DESIGNS

### 4.1 INTRODUCTION

As the number of factors in a  $2^k$  factorial design increases, the number of runs required for a complete replicate of the design rapidly outgrows the resources of most experimenters. For example, a complete replicate of the  $2^6$  design requires 64 runs. In this design only 6 of the 63 degrees of freedom are used to estimate the main effects, and only 15 degrees of freedom are used to estimate the two-factor interactions. The remaining 42 degrees of freedom are associated with three-factor and higher interactions.

If the experimenter can reasonably assume that certain high-order interactions are negligible, then information on the main effects and low-order interactions may be obtained by running only a fraction of the complete factorial experiment. These **fractional factorial designs** are among the most widely used types of design in industry.

A major use of fractional factorials is in **screening experiments**. These are experiments in which many factors are considered with the purpose of identifying those factors (if any) that have large effects. Remember that screening experiments are usually performed early in a response surface study when it is likely that many of the factors initially considered have little or no effect on the response. The factors that are identified as important are then investigated more thoroughly in subsequent experiments.

The successful use of fractional factorial designs is based on three key ideas:

1. *The Sparsity-of-Effects Principle.* When there are several variables, the system or process is likely to be driven primarily by some of the main effects and low-order interactions.
2. *The Projection Property.* Fractional factorial designs can be projected into stronger (larger) designs in the subset of significant factors.

3. *Sequential Experimentation.* It is possible to combine the runs of two (or more) fractional factorials to assemble sequentially a larger design to estimate the factor effects and interactions of interest.

We will focus on these principles in this chapter and illustrate them with several examples.

## 4.2 THE ONE-HALF FRACTION OF THE $2^k$ DESIGN

Consider the situation in which three factors, each at two levels, are of interest, but the experimenters do not wish to run all  $2^3 = 8$  treatment combinations. Suppose they consider a design with four runs. This suggests a **one-half fraction** of a  $2^3$  design. Because the design contains  $2^{3-1} = 4$  treatment combinations, a one-half fraction of the  $2^3$  design is often called a  $2^{3-1}$  design.

The table of plus and minus signs for the  $2^3$  design is shown in Table 4.1. Suppose we select the four treatment combinations  $a$ ,  $b$ ,  $c$ , and  $abc$  as our one-half fraction. These runs are shown in the top half of Table 4.1 and in Fig. 4.1a. Notice that the  $2^{3-1}$  design is formed by selecting only those treatment combinations that have a plus in the  $ABC$  column. Thus,  $ABC$  is called the **generator** of this particular fraction. Sometimes we will refer to a generator such as  $ABC$  as a **word**. Furthermore, the identity column  $I$  is also always plus, so we call

$$I = ABC$$

the **defining relation** for our design. In general, the defining relation for a fractional factorial will be the set of all columns that are equal to the identity column  $I$ .

The treatment combinations in the  $2^{3-1}$  design yield three degrees of freedom that we may use to estimate the main effects. Referring to Table 4.1, we note that the linear combinations of the observations used to estimate the main effects of  $A$ ,  $B$ , and  $C$  are

$$\begin{aligned}[A] &= \frac{1}{2}(a - b - c + abc) \\ [B] &= \frac{1}{2}(-a + b - c + abc) \\ [C] &= \frac{1}{2}(-a - b + c + abc)\end{aligned}$$

**TABLE 4.1** Plus and Minus Signs for the  $2^3$  Factorial Design

Treatment Combination	Factorial Effect							
	$I$	$A$	$B$	$C$	$AB$	$AC$	$BC$	$ABC$
$a$	+	+	-	-	-	-	+	+
$b$	+	-	+	-	-	+	-	+
$c$	+	-	-	+	+	-	-	+
$abc$	+	+	+	+	+	+	+	+
$ab$	+	+	+	-	+	-	-	-
$ac$	+	+	-	+	-	+	-	-
$bc$	+	-	+	+	-	-	+	-
(1)	+	-	-	-	+	+	+	-

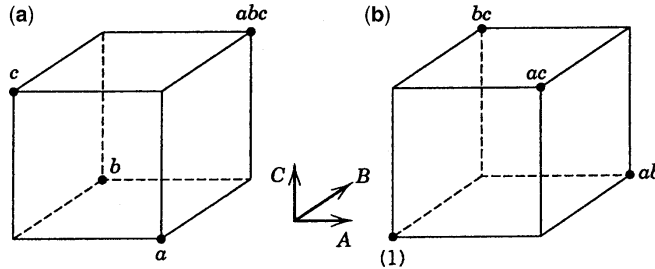


**Figure 4.1** The two one-half fractions of the  $2^3$  design. (a) The principal fraction,  $I = +ABC$ . (b) The alternate fraction,  $I = -ABC$ .

It is also easy to verify that the linear combinations of the observations used to estimate the two-factor interactions are

$$\begin{aligned}[BC] &= \frac{1}{2}(a - b - c + abc) \\ [AC] &= \frac{1}{2}(-a + b - c + abc) \\ [AB] &= \frac{1}{2}(-a - b + c + abc)\end{aligned}$$

Thus,  $[A] = [BC]$ ,  $[B] = [AC]$ , and  $[C] = [AB]$ ; consequently, it is impossible to differentiate between  $A$  and  $BC$ ,  $B$  and  $AC$ , and  $C$  and  $AB$ . In fact, when we estimate  $A$ ,  $B$ , and  $C$  we are really estimating  $A + BC$ ,  $B + AC$ , and  $C + AB$ . Two or more effects that have this property are called **aliases**. In our example,  $A$  and  $BC$  are aliases,  $B$  and  $AC$  are aliases, and  $C$  and  $AB$  are aliases. We indicate this by the notation  $[A] \rightarrow A + BC$ ,  $[B] \rightarrow B + AC$ , and  $[C] \rightarrow C + AB$ .

The alias structure for this design may be easily determined by using the defining relation  $I = ABC$ . Multiplying any column by the defining relation yields the aliases for that effect. In our example, this yields as the alias of  $A$

$$A \cdot I = A \cdot ABC = A^2BC$$

or, because the square of any column is just the identity  $I$ ,

$$A = BC$$

Similarly, we find the aliases of  $B$  and  $C$  as

$$B \cdot I = B \cdot ABC$$

$$B = AB^2C = AC$$

and

$$C \cdot I = C \cdot ABC$$

$$C = ABC^2 = AB$$

This one-half fraction, with  $I = +ABC$ , is usually called the **principal fraction**.

Now suppose that we had selected the other one-half fraction; that is, the treatment combinations in Table 4.1 associated with a minus sign in the *ABC* column. This **alternate** or **complementary fraction** is shown in Fig. 4.1b. Notice that it consists of the runs labeled (1), *ab*, *ac*, and *bc*. The defining relation for this design is

$$I = -ABC$$

The linear combination of the observations, say  $[A]'$ ,  $[B]'$ , and  $[C]'$ , from the alternate fraction gives us the following alias relationships:

$$\begin{aligned}[A]' &\longrightarrow A - BC \\ [B]' &\longrightarrow B - AC \\ [C]' &\longrightarrow C - AB\end{aligned}$$

Thus, when we estimate *A*, *B*, and *C* with this particular fraction, we are really estimating  $A - BC$ ,  $B - AC$ , and  $C - AB$ .

In practice, it does not matter which fraction is actually used. Both fractions belong to the same **family**; that is, the two one-half fractions form a complete  $2^3$  design. This is easily seen by referring to Fig. 4.1a and 4.1b.

Suppose that after running one of the one-half fractions of the  $2^3$  design, the other one was also run. Thus, all eight runs associated with the full  $2^3$  are now available. We may now obtain de-aliased estimates of all the effects by analyzing the eight runs as a full  $2^3$  design in two blocks of four runs each. This could also be done by adding and subtracting the linear combination of effects from the two individual fractions. For example, consider  $[A] \longrightarrow A + BC$  and  $[A]' \longrightarrow A - BC$ . This implies that

$$\frac{1}{2}([A] + [A]') = \frac{1}{2}(A + BC + A - BC) \longrightarrow A$$

and

$$\frac{1}{2}([A] - [A]') = \frac{1}{2}(A + BC - A + BC) \longrightarrow BC$$

Thus, for all three pairs of linear combinations, we would obtain the following:

<i>i</i>	From $\frac{1}{2}([i] + [i]')$	From $\frac{1}{2}([i] - [i]')$
<i>A</i>	<i>A</i>	<i>BC</i>
<i>B</i>	<i>B</i>	<i>AC</i>
<i>C</i>	<i>C</i>	<i>AB</i>

**Design Resolution** The preceding  $2^{3-1}$  design is called a **resolution III design**. In such a design, main effects are aliased with two-factor interactions. A design is of resolution *R* if no *p*-factor effect is aliased with another effect containing less than *R* – *p* factors. We usually employ a Roman numeral subscript to denote design resolution; thus, the one-half fraction of the  $2^3$  design with the defining relation  $I = ABC$  (or  $I = -ABC$ ) is a  $2_{III}^{3-1}$  design.

Designs of resolution III, IV, and V are particularly important. The definitions of these designs and an example of each follow.

1. *Resolution III Designs.* These are designs in which no main effects are aliased with any other main effect, but main effects are aliased with two-factor interactions and two-factor interactions may be aliased with each other. The  $2^{3-1}$  design in Table 4.1 is of resolution III ( $2_{III}^{3-1}$ ).
  2. *Resolution IV Designs.* These are designs in which no main effect is aliased with any other main effect or with any two-factor interaction, but two-factor interactions are aliased with each other. A  $2^{4-1}$  design with  $I = ABCD$  is of resolution IV ( $2_{IV}^{4-1}$ ).
  3. *Resolution V Designs.* These are designs in which no main effect or two-factor interaction is aliased with any other main effect or two-factor interaction, but two-factor interactions are aliased with three-factor interactions. A  $2^{5-1}$  design with  $I = ABCDE$  is of resolution V ( $2_{V}^{5-1}$ ).

In general, the resolution of a two-level fractional factorial design is equal to the smallest number of letters in any word in the defining relation. Consequently, we could call the preceding design types three-letter, four-letter, and five-letter designs, respectively. We usually like to employ fractional designs that have the highest possible resolution consistent with the degree of fractionation required. The higher the resolution, the less restrictive the assumptions that are required regarding which interactions are negligible in order to obtain a unique interpretation of the data.

**Constructing One-Half Fractions** A one-half fraction of the  $2^k$  design of the highest resolution may be constructed by writing down a *basic design* consisting of the runs for a full  $2^{k-1}$  factorial and then adding the  $k$ th factor by identifying its plus and minus levels with the plus and minus signs of the highest-order interaction  $ABC \dots (K - 1)$ . Therefore, the  $2_{III}^{3-1}$  fractional factorial is obtained by writing down the full  $2^2$  factorial as the basic design and then equating factor  $C$  to the  $AB$  interaction. The alternate fraction would be obtained by equating factor  $C$  to the  $-AB$  interaction. This approach is illustrated in Table 4.2. Notice that the basic design always has the right number of runs (rows), but it is missing one column. The generator  $K = ABC \dots (K - 1)$  defines the product of plus and minus signs to use in each row to produce the levels for the  $k$ th factor.

Note that any interaction effect could be used to generate the column for the  $k$ th factor. However, using any effect other than  $ABC \dots (K - 1)$  as the generator will not produce a design of the highest possible resolution.

**TABLE 4.2** The Two One-Half Fractions of the  $2^3$  Design

Another way to view the construction of a one-half fraction is to partition the runs into two blocks with the highest-order interaction  $ABC \dots K$  confounded. Each block is a  $2^{k-1}$  fractional factorial design of the highest resolution.

**Projection of Fractions into Factorials** Any fractional factorial design of resolution  $R$  contains complete factorial designs (possibly replicated factorials) in any subset of  $R - 1$  factors. This is an important and useful concept. For example, if an experimenter has several factors of potential interest but believes that only  $R - 1$  of them have important effects, then a fractional factorial design of resolution  $R$  is the appropriate choice of design. If the experimenter is correct, then the fractional factorial design of resolution  $R$  will project into a full factorial in the  $R - 1$  significant factors. This process is illustrated in Fig. 4.2 for the  $2_{III}^{3-1}$  design, which projects into a  $2^2$  design in every subset of two factors.

Because the maximum possible resolution of a one-half fraction of the  $2^k$  design is  $R = k$ , every  $2^{k-1}$  design will project into a full factorial in any  $k - 1$  of the original  $k$  factors. Furthermore, a  $2^{k-1}$  design may be projected into two replicates of a full factorial in any subset of  $k - 2$  factors, four replicates of a full factorial in any subset of  $k - 3$  factors, and so on.

**Sequences of Fractional Factorials** Using fractional factorial designs often leads to great economy and efficiency in experimentation, particularly if the runs can be made sequentially. For example, suppose that we were investigating  $k = 4$  factors ( $2^4 = 16$  runs). It is almost always preferable to run a  $2_{IV}^{4-1}$  fractional design (8 runs), analyze the results, and then decide on the best set of runs to perform next. If it is necessary to resolve ambiguities, we can always run the alternate fraction and complete the  $2^4$  design. When this method is used to complete the design, both one-half fractions represent blocks of the complete design with the highest-order interaction confounded with blocks (here  $ABCD$ ) would be confounded. Thus, sequential experimentation has the result of losing information only on the highest-order interaction. Alternatively, in many cases we learn enough from the one-half fraction to proceed to the next stage of experimentation, which might involve adding or removing factors, changing responses, or varying some of the factors over new ranges. This potential saving can prove valuable, with additional resources being available for subsequent stages of experimentation.

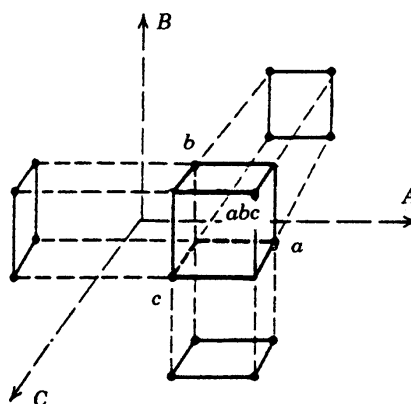


Figure 4.2 Projection of a  $2_{III}^{3-1}$  design into three  $2^2$  designs.

**Example 4.1 The Filtration Rate Experiment** Consider the filtration rate experiment in Example 3.2. The original design, shown in Table 3.6, is a single replicate of the  $2^4$  design. In this example, we found that the main effects  $A$ ,  $C$ , and  $D$  and the interactions  $AC$  and  $AD$  were different from zero. We will now return to this experiment and simulate what would have happened if a half-fraction of the  $2^4$  design had been run instead of the full factorial.

We will use the  $2^{4-1}$  design with  $I = ABCD$ , because this choice of generator will result in a design of the highest possible resolution (IV). To construct the design, we first write down the basic design, which is a  $2^3$  design, as shown in the first three columns of Table 4.3. Because the generator  $ABCD$  is positive, this  $2^{4-1}_{IV}$  design is the principal fraction. The design is shown graphically in Fig. 4.3.

Using the defining relation, we note that each main effect is aliased with a three-factor interaction; that is,  $A = A^2BCD = BCD$ ,  $B = AB^2CD = ACD$ ,  $C = ABC^2D = ABD$ , and  $D = ABCD^2 = ABC$ . Furthermore, every two-factor interaction is aliased with another two-factor interaction. These alias relationships are  $AB = CD$ ,  $AC = BD$ , and  $BC = AD$ . The four main effects plus the three two-factor interaction alias pairs account for the seven degrees of freedom for the design.

At this point, we would normally randomize the eight runs and perform the experiment. Because we have already run the full  $2^4$  design, we will simply select the eight observed filtration rates from Example 3.2 that correspond to the runs in the  $2^{4-1}_{IV}$  design. These observations are shown in the last column of Table 4.3 and are also shown in Fig. 4.3.

TABLE 4.3 The  $2^{4-1}_{IV}$  Design with the Defining Relation  $I = ABCD$

Run	Basic Design			$D = ABC$	Treatment Combination	Filtration Rate
	A	B	C			
1	—	—	—	—	(1)	45
2	+	—	—	+	$ad$	100
3	—	+	—	+	$bd$	45
4	+	+	—	—	$ab$	65
5	—	—	+	+	$cd$	75
6	+	—	+	—	$ac$	60
7	—	+	+	—	$bc$	80
8	+	+	+	+	$abcd$	96

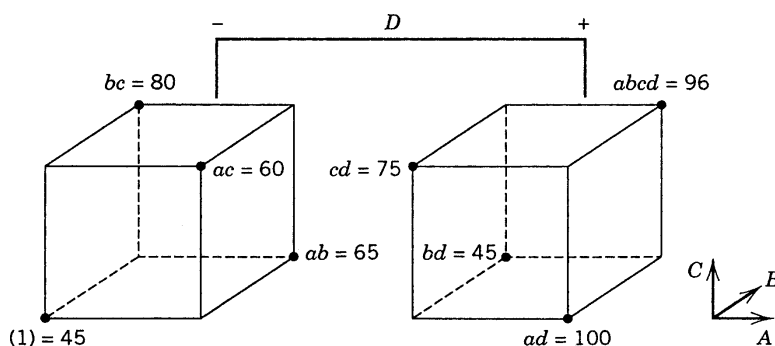


Figure 4.3 The  $2^{4-1}_{IV}$  design for the filtration rate experiment of Example 4.1.

**TABLE 4.4 Estimates of Effects and Aliases from Example 4.1**

Estimate	Alias Structure <sup>a</sup>
$[A] = 19.00$	$[A] \rightarrow \mathbf{A} + BCD$
$[B] = 1.50$	$[B] \rightarrow B + ACD$
$[C] = 14.00$	$[C] \rightarrow \mathbf{C} + ABD$
$[D] = 16.50$	$[D] \rightarrow \mathbf{D} + ABC$
$[AB] = -1.00$	$[AB] \rightarrow AB + CD$
$[AC] = -18.50$	$[AC] \rightarrow \mathbf{AC} + BD$
$[BC] = 19.00$	$[BC] \rightarrow BC + \mathbf{AD}$

<sup>a</sup>Significant effects are shown in boldface type.

The estimates of the effects obtained from this  $2_{IV}^{4-1}$  design are shown in Table 4.4. To illustrate the calculations, the linear combination of observations associated with the  $A$  effect is

$$[A] = \frac{1}{4}(-45 + 100 - 45 + 65 - 75 + 60 - 80 + 96) = 19.00 \rightarrow A + BCD$$

whereas for the  $AB$  effect we obtain

$$[AB] = \frac{1}{4}(45 - 100 - 45 + 65 + 75 - 60 - 80 + 96) = -1.00 \rightarrow AB + CD$$

From inspection of the information in Table 4.4, it is not unreasonable to conclude that the main effects  $A$ ,  $C$ , and  $D$  are large and that the  $AC$  and  $AD$  interactions are also significant. This agrees with the conclusions from the analysis of the complete  $2^4$  design in Example 3.2.

Because factor  $B$  is not significant, we may drop it from consideration. Consequently, we may project this  $2_{IV}^{4-1}$  design into a single replicate of the  $2^3$  design in factors  $A$ ,  $C$ , and  $D$ , as shown in Fig. 4.4. Visual examination of this cube plot makes us more comfortable with the conclusions reached above. Notice that if the temperature ( $A$ ) is at the low level, the concentration ( $C$ ) has a large positive effect, whereas if the temperature is at the high level, the concentration has a very small effect. This is likely due to an  $AC$  interaction. Furthermore, if the temperature is at the low level, the effect of the stirring rate ( $D$ ) is negligible, whereas if the temperature is at the high level, the stirring rate has a large positive effect. This is likely due to the  $AD$  interaction tentatively identified previously.

Now suppose that the experimenter decided to run the alternate fraction, given by  $I = -ABCD$ . It is straightforward to show that the design and the responses are as follows:

Run	$A$	$B$	$C$	$D = -ABC$	Treatment Combination	Filtration Rate
1	-	-	-	+	$d$	43
2	+	-	-	-	$a$	71
3	-	+	-	-	$b$	48
4	+	+	-	+	$abd$	104
5	-	-	+	-	$c$	68
6	+	-	+	+	$acd$	86
7	-	+	+	+	$bcd$	70
8	+	+	+	-	$abc$	65

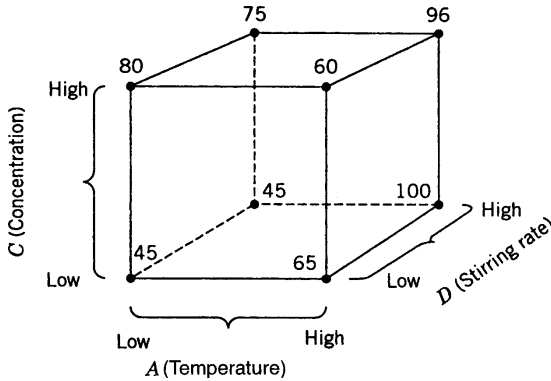


**Figure 4.4** Projection of the  $2^{4-1}_{IV}$  design into  $2^3$  design in  $A$ ,  $C$ , and  $D$  for Example 4.1.

The linear combinations of observations obtained from this alternate fraction are

$$\begin{aligned}[A]' &= 24.25 \rightarrow A - BCD \\ [B]' &= 4.75 \rightarrow B - ACD \\ [C]' &= 5.75 \rightarrow C - ABD \\ [D]' &= 12.75 \rightarrow D - ABC \\ [AB]' &= 1.25 \rightarrow AB - CD \\ [AC]' &= -17.75 \rightarrow AC - BD \\ [BC]' &= -14.25 \rightarrow BC - AD\end{aligned}$$

These estimates may be combined with those obtained from the original one-half fraction to yield the following estimates of the effects:

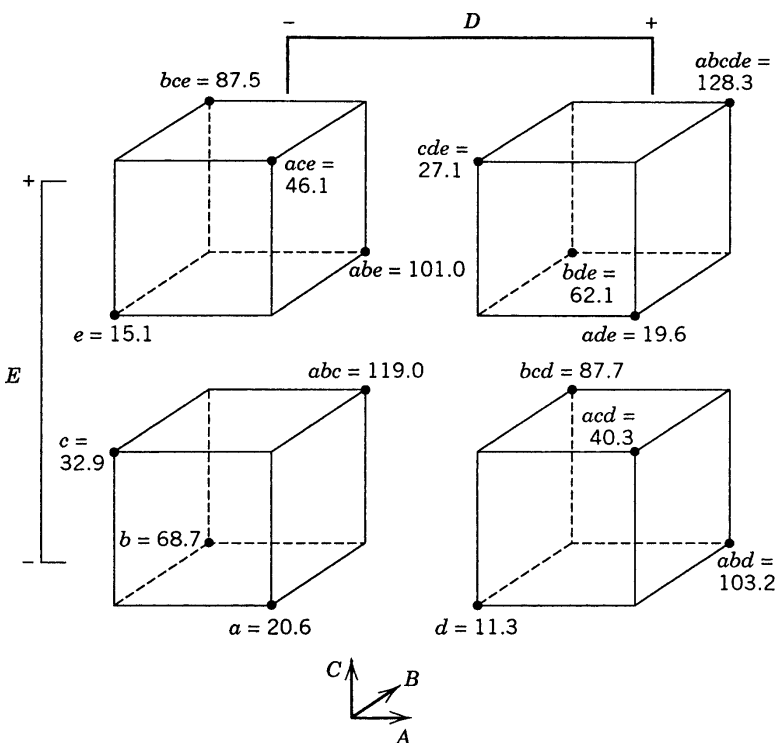
$i$	From $\frac{1}{2}([A] + [A]')$	From $\frac{1}{2}([A] - [A]')$
$A$	21.63 $\rightarrow A$	-2.63 $\rightarrow BCD$
$B$	3.13 $\rightarrow B$	-1.63 $\rightarrow ACD$
$C$	9.88 $\rightarrow C$	4.13 $\rightarrow ABD$
$D$	14.63 $\rightarrow D$	1.88 $\rightarrow ABC$
$AB$	0.13 $\rightarrow AB$	-1.13 $\rightarrow CD$
$AC$	-18.13 $\rightarrow AC$	-0.38 $\rightarrow BD$
$BC$	2.38 $\rightarrow BC$	16.63 $\rightarrow AD$

These estimates agree exactly with those from the original analysis of the data as a single replicate of a  $2^4$  factorial design, as reported in Example 3.2.

**Example 4.2 A  $2^{5-1}$  Design** Five factors in a manufacturing process for an integrated circuit were investigated in a  $2^{5-1}$  design with the objective of learning how these factors affect the resistivity of the wafer. The five factors were  $A$  = implant dose,  $B$  = temperature,  $C$  = time,  $D$  = oxide thickness, and  $E$  = furnace position. Each factor was run at two levels. The construction of the  $2^{5-1}$  design is shown in Table 4.5. Notice that the design was constructed by writing down the basic design having 16 runs (a  $2^4$  design in  $A$ ,  $B$ ,  $C$ , and  $D$ ), selecting  $ABCDE$  as the generator, and then setting the levels of the fifth factor  $E = ABCD$ . Figure 4.5 gives a pictorial representation of the design.

TABLE 4.5 A  $2^{5-1}$  Design for Example 4.2

Run	A	B	C	D	$E = ABCD$	Treatment Combination	Resistivity
1	-	-	-	-	+	e	15.1
2	+	-	-	-	-	a	20.6
3	-	+	-	-	-	b	68.7
4	+	+	-	-	+	abe	101.0
5	-	-	+	-	-	c	32.9
6	+	-	+	-	+	ace	46.1
7	-	+	+	-	+	bce	87.5
8	+	+	+	-	-	abc	119.0
9	-	-	-	+	-	d	11.3
10	+	-	-	+	+	ade	19.6
11	-	+	-	+	+	bde	62.1
12	+	+	-	+	-	abd	103.2
13	-	-	+	+	+	cde	27.1
14	+	-	+	+	-	acd	40.3
15	-	+	+	+	-	bcd	87.7
16	+	+	+	+	+	abcde	128.3

Figure 4.5 The  $2^{5-1}_V$  design for Example 4.2.

The defining relation for the design is  $I = ABCDE$ . Consequently, every main effect is aliased with a four-factor interaction:

$$\begin{aligned}[A] &\rightarrow A + BCDE \\ [B] &\rightarrow B + ACDE \\ [C] &\rightarrow C + ABDE \\ [D] &\rightarrow D + ABCE \\ [E] &\rightarrow E + ABCD\end{aligned}$$

Every two-factor interaction is aliased with a three-factor interaction:

$$\begin{array}{lll} [AB] \rightarrow AB + CDE & [BD] \rightarrow BD + ACE \\ [AC] \rightarrow AC + BDE & [BE] \rightarrow BE + ACD \\ [AD] \rightarrow AD + BCE & [CD] \rightarrow CD + ABE \\ [AE] \rightarrow AE + BCD & [CE] \rightarrow CE + ABD \\ [BC] \rightarrow BC + ADE & [DE] \rightarrow DE + ABC \end{array}$$

This is a resolution V design. We would expect this  $2^{5-1}_V$  design to provide excellent information concerning the main effects and all two-factor interactions.

The estimates of the effects are

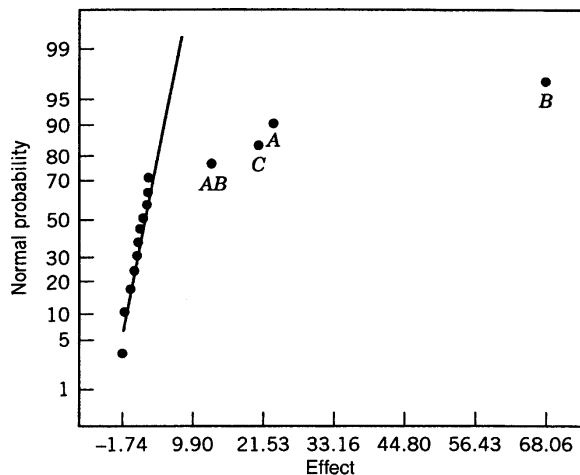
$$\begin{array}{ll} [A] \rightarrow A + BCDE = 23.2125 & \\ [B] \rightarrow B + ACDE = 68.0625 & \\ [C] \rightarrow C + ABDE = 20.9125 & \\ [D] \rightarrow D + ABCE = -1.4125 & \\ [E] \rightarrow E + ABCD = 0.3875 & \\ \\ [AB] \rightarrow AB + CDE = 13.1625 & [BD] \rightarrow BD + ACE = 2.6875 \\ [AC] \rightarrow AC + BDE = 1.4125 & [BD] \rightarrow BE + ACD = -0.3125 \\ [AD] \rightarrow AD + BCE = 2.5875 & [CD] \rightarrow CD + ABE = 0.8875 \\ [AE] \rightarrow AE + BCD = 2.5875 & [CE] \rightarrow CE + ABD = 1.8875 \\ [BC] \rightarrow BC + ADE = 0.9675 & [DE] \rightarrow DE + ABC = -1.7375 \end{array}$$

The effects  $A$ ,  $B$ ,  $C$ , and  $AB$  seem large. Figure 4.6 presents a normal probability plot of the effect estimates from this experiment. This plot confirms that the main effects of  $A$ ,  $B$ , and  $C$ , and the  $AB$  interaction are large. Remember that, because of aliasing, these effects are really  $A + BCDE$ ,  $B + ACDE$ ,  $C + ABDE$ , and  $AB + CDE$ . However, because it seems plausible that three-factor and higher interactions are negligible, we feel safe in concluding that only  $A$ ,  $B$ ,  $C$ , and  $AB$  are important effects.

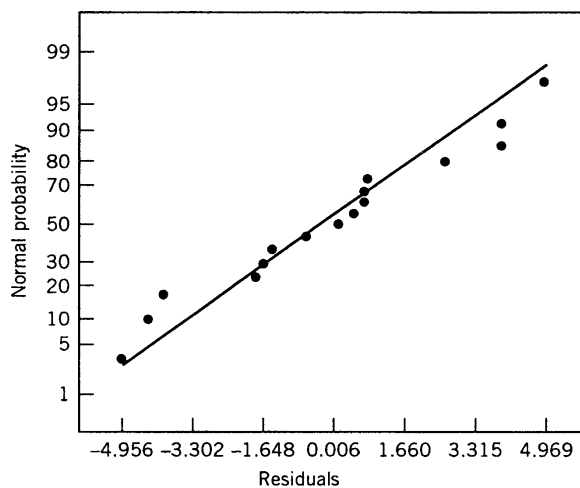
Table 4.6 summarizes the analysis of variance for this experiment. The model sum of squares is  $SS_{\text{model}} = SS_A + SS_B + SS_C + SS_{AB} = 23,127.63$ , and this accounts for over 99% of the total variability in the response. The regression model that would be used to predict resistivity over the space of the three factors  $A$ ,  $B$ , and  $C$  is

$$\hat{y} = 60.65625 + 11.60625x_1 + 34.03125x_2 + 10.45625x_3 + 6.58125x_1x_2$$

where  $x_1$ ,  $x_2$ , and  $x_3$  are coded variables on the interval  $-1$ ,  $+1$  that represent  $A$ ,  $B$ , and  $C$ .

**Figure 4.6** Normal probability plot of effects for Example 4.2.**TABLE 4.6** Analysis of Variance for Example 4.2

Source of Variation	Sum of Squares	Degrees of Freedom	Mean Square	$F_0$
A	2155.28	1	2155.28	193.20
B	18,530.02	1	18,530.02	1791.24
C	1749.33	1	1749.33	184.61
AB	693.01	1	693.01	73.78
Error	132.59	11	12.05	
Total	23,260.22	15		

**Figure 4.7** Normal probability plot of the residuals for Example 4.2.

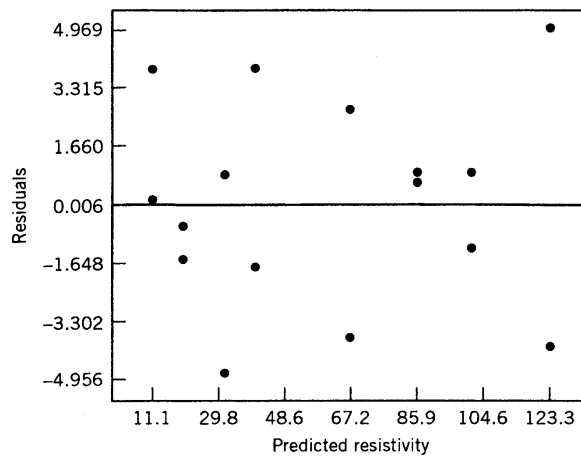


**Figure 4.8** Plot of residuals versus predicted resistivity, Example 4.2.

Figure 4.7 presents a normal probability plot of the residuals from this model, and Fig. 4.8 is a plot of the residuals versus the predicted values. Both plots are satisfactory.

The three factors  $A$ ,  $B$ , and  $C$  have large positive effects. The  $AB$  or implant dose–temperature interaction is plotted in Fig. 4.9. This plot indicates that the implant dose has a much stronger effect on resistivity when temperature is at the high level.

The  $2^{5-1}$  design will collapse into two replicates of a  $2^3$  design in any three of the original five factors. (Looking at Fig. 4.5 will help you visualize this.) Figure 4.10 is a cube plot in the factors  $A$ ,  $B$ , and  $C$  with the average resistivity superimposed on the eight corners. It is clear from inspection of the cube plot that highest resistivity values are achieved with  $A$ ,  $B$ , and  $C$  all at the high level. Factors  $D$  and  $E$  have little effect on resistivity and may be set to values that optimize other objectives (such as cost).

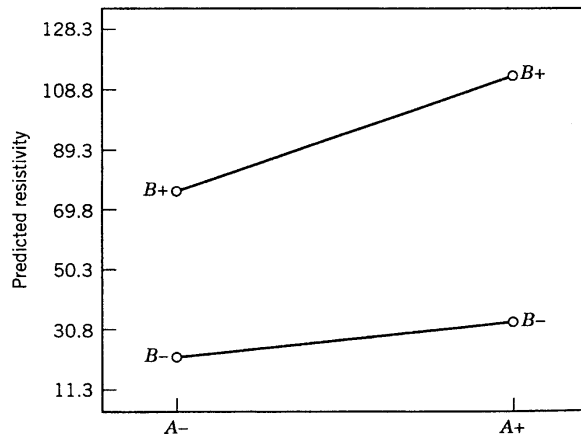


**Figure 4.9** Implant dose–temperature interaction, Example 4.2.

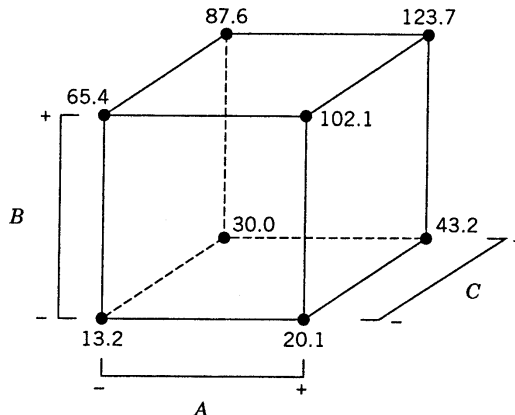


**Figure 4.10** Projection of the  $2^{5-1}$  design in Example 4.2 into two replicates of a  $2^3$  design in the factors  $A$ ,  $B$ , and  $C$ .

### 4.3 THE ONE-QUARTER FRACTION OF THE $2^k$ DESIGN

For a moderately large number of factors, smaller fractions of the  $2^k$  design are frequently useful. Consider a one-quarter fraction of the  $2^k$  design. This design contains  $2^{k-2}$  runs and is usually called a  $2^{k-2}$  fractional factorial.

The  $2^{k-2}$  design may be constructed by first writing down a basic design consisting of the runs associated with a full factorial in  $k-2$  factors and then associating the two additional columns with generators that are appropriately chosen interactions involving the first  $k-2$  factors. Thus, a one-quarter fraction of the  $2^k$  design has two generators. If  $P$  and  $Q$  represent the generators chosen, then  $I = P$  and  $I = Q$  are called **generating relations** for the design. The signs of  $P$  and  $Q$  (either + or -) determine which one of the one-quarter fractions is produced. All four fractions associated with the choice of generators  $\pm P$  and  $\pm Q$  are members of the same family. The fraction for which both  $P$  and  $Q$  are positive is the **principal fraction**.

The **complete defining relation** for the design consists of all the columns that are equal to the identity column  $I$ . These will consist of  $P$ ,  $Q$ , and their **generalized interaction**  $PQ$ ; that is, the defining relation is  $I = P = Q = PQ$ . We call the elements  $P$ ,  $Q$ , and  $PQ$  in the defining relation **words**. The aliases of any effect are produced by the multiplication of the column for that effect by each word in the defining relation. Clearly, each effect has three aliases. The experimenter should be careful in choosing the generators so that potentially important effects are not aliased with each other.

As an example, consider the  $2^{6-2}$  design. Suppose we choose  $I = ABCE$  and  $I = BCDF$  as the design generators. Now the generalized interaction of the generators  $ABCE$  and  $BCDF$  is  $ADEF$ ; therefore, the complete defining relation for this design is

$$I = ABCE = BCDF = ADEF$$

Consequently, this design is of resolution IV. To find the aliases of any effect (e.g.,  $A$ ), multiply that effect by each word in the defining relation. For  $A$ , this produces

$$A = BCE = ABCDF = DEF$$

**TABLE 4.7 Alias Structure for the  $2^{6-2}_{IV}$  Design with  
 $I = ABCE = BCDF = ADEF$**

$A = BCE = DEF = ABCDF$	$AB = CE = ACDF = BDEF$
$B = ACE = CDF = ABDEF$	$AC = BE = ABDF = CDEF$
$C = ABE = BDF = ACDEF$	$AD = EF = ABDF = CDEF$
$D = BCF = AEF = ABCDE$	$AE = BC = DF = ABCDEF$
$E = ABC = ADF = BCDEF$	$AF = DE = BCEF = ABCD$
$F = BCD = ADE = ABCEF$	$BD = CF = ACDE = ABEF$
	$BF = CD = ACEF = ABDE$
$ABD = CDE = ACF = BEF$	
$ACD = BDE = ABF = CEF$	

It is easy to verify that every main effect is aliased by three-factor and five-factor interactions, whereas two-factor interactions are aliased with each other and with higher-order interactions. Thus, when we estimate  $A$ , for example, we are really estimating  $A + BCE + DEF + ABCDF$ . The complete alias structure of this design is shown in Table 4.7. If three-factor and higher interactions are negligible, this design gives clear estimates of the main effects.

To construct the design, first write down the basic design, which consists of the 16 runs for a full  $2^{6-2} = 2^4$  design in  $A$ ,  $B$ ,  $C$ , and  $D$ . Then the two factors  $E$  and  $F$  are added by associating their plus and minus levels with the plus and minus signs of the interactions  $ABC$  and  $BCD$ , respectively. This procedure is shown in Table 4.8.

There are, of course, three alternate fractions of this particular  $2^{6-2}_{IV}$  design. They are the fractions with generating relationships  $I = ABCE$  and  $I = -BCDF$ ;  $I = -ABCE$  and  $I = BCDF$ ; and  $I = -ABCE$  and  $I = -BCDF$ . These fractions may be easily constructed by the method shown in Table 4.8. For example, if we wish to find the fraction for which

**TABLE 4.8 Construction of the  $2^{6-2}_{IV}$  Design with the Generators  
 $I = ABCE$  and  $I = BCDF$**

Run	$A$	$B$	$C$	$D$	$E = ABC$	$F = BCD$
1	-	-	-	-	-	-
2	+	-	-	-	+	-
3	-	+	-	-	+	+
4	+	+	-	-	-	+
5	-	-	+	-	+	+
6	+	-	+	-	-	+
7	-	+	+	-	-	-
8	+	+	+	-	+	-
9	-	-	-	+	-	+
10	+	-	-	+	+	+
11	-	+	-	+	+	-
12	+	+	-	+	-	-
13	-	-	+	+	+	-
14	+	-	+	+	-	-
15	-	+	+	+	-	+
16	+	+	+	+	+	+

$I = ABCE$  and  $I = -BCDF$ , then in the last column of Table 4.8 we set  $F = -BCD$ , and the column of levels for factor  $F$  becomes

$$+ + - - - + + - - + + + + -$$

The complete defining relation for this alternative fraction is  $I = ABCE = -BCDF = -ADEF$ . Certain signs in the alias structure in Table 4.8 are now changed; for instance, the aliases of  $A$  are  $A = BCE = -DEF = -ABCDF$ . Thus, the linear combination of the observations [A] actually estimates  $A + BCE - DEF - ABCDF$ .

Finally, note that the  $2^{6-2}$  fractional factorial collapses to a single replicate of a  $2^4$  design in any subset of four factors that is not a word in the defining relation. It also collapses to a replicated one-half fraction of a  $2^4$  in any subset of four factors that is a word in the defining relation. Thus, the design in Table 4.8 becomes two replicates of a  $2^{4-1}$  in the factors  $ABCE$ ,  $BCDF$ , and  $ABEF$ , because these are the words in the defining relation. There are 12 other combinations of the six factors, such as  $ABCD$ ,  $ABDF$ , and so on, for which the design projects to a single replicate of the  $2^4$ . This design also collapses to two replicates of a  $2^3$  in any subset of three of the six factors or four replicates of a  $2^2$  in any subset of two factors.

In general, any  $2^{k-2}$  fractional factorial design can be collapsed into either a full factorial or a fractional factorial in some subset of  $r \leq k - 2$  of the original factors. Those subsets of variables that form full factorials in  $r = k - 2$  are not words in the complete defining relation. Any subset of  $r = 3$  factors will give a full factorial design.

**Example 4.3 The Injection Molding Experiment** Parts manufactured in an injection molding process are showing excessive shrinkage. This is causing problems in assembly operations downstream from the injection molding area. A quality improvement team has decided to use a designed experiment to study the injection molding process so that shrinkage can be reduced. The team decides to investigate six factors—mold temperature ( $A$ ), screw speed ( $B$ ), holding time ( $C$ ), cycle time ( $D$ ), gate size ( $E$ ), and holding pressure ( $F$ )—each at two levels, with the objective of learning how each factor affects shrinkage and also something about how the factors interact.

The team decides to use the 16-run two-level fractional factorial design in Table 4.8 along with four center points, so that the linearity of the response function can be investigated via a curvature test. The design is shown in Table 4.9, along with the observed shrinkage ( $\times 10$ ) for the test part produced at each of the 20 runs in the design.

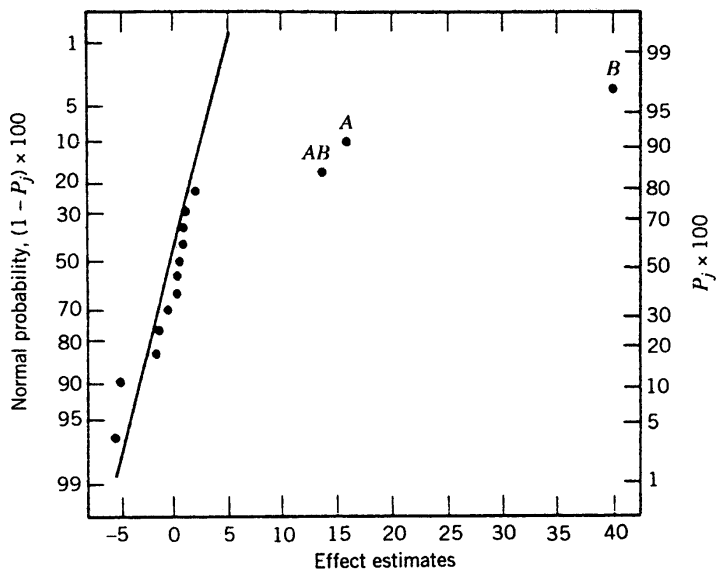
A normal probability plot of the effect estimates from this experiment is shown in Fig. 4.11. The only large effects are  $A$  (mold temperature),  $B$  (screw speed), and the  $AB$  interaction. In light of the alias relationships in Table 4.7, it seems reasonable to adopt these conclusions tentatively. Table 4.10 shows the analysis of variance for this experiment. The pure error sum of squares is computed from the replicate runs at the center, and the lack-of-fit sum of squares is formed by pooling all the effects that appeared small on the normal probability plot. Notice that the lack-of-fit (higher-order interaction) and curvature (quadratic) tests have small  $F$ -ratios, so the model is correctly specified.

The plot of the  $AB$  interaction in Fig. 4.12 shows that the process is insensitive to temperature if the screw speed is at the low level but very sensitive to temperature if the screw speed is at the high level. With the screw speed at the low level, the process should produce an average shrinkage of around 10% regardless of the temperature level chosen.

Based on this initial analysis, the team decides to set both the mold temperature and the screw speed at the low level. This set of conditions will reduce the mean shrinkage of parts to around 10%. However, the variability in shrinkage from part to part is still a potential

**TABLE 4.9** A  $2^{6-2}_{IV}$  Design for the Injection Molding Experiment in Example 4.3

Run	<i>A</i>	<i>B</i>	<i>C</i>	<i>D</i>	<i>E = ABC</i>	<i>F = BCD</i>	Observed Shrinkage ( $\times 10$ )
1	—	—	—	—	—	—	6
2	+	—	—	—	+	—	10
3	—	+	—	—	+	+	32
4	+	+	—	—	—	+	60
5	—	—	+	—	+	+	4
6	+	—	+	—	—	+	15
7	—	+	+	—	—	—	26
8	+	+	+	—	+	—	60
9	—	—	—	+	—	+	8
10	+	—	—	+	+	+	12
11	—	+	—	+	+	—	34
12	+	+	—	+	—	—	60
13	—	—	+	+	+	—	16
14	+	—	+	+	—	—	5
15	—	+	+	+	—	+	37
16	+	+	+	+	+	+	52
17	0	0	0	0	0	0	29
18	0	0	0	0	0	0	34
19	0	0	0	0	0	0	26
20	0	0	0	0	0	0	30

**Figure 4.11** Normal probability plot of effects for Example 4.3.

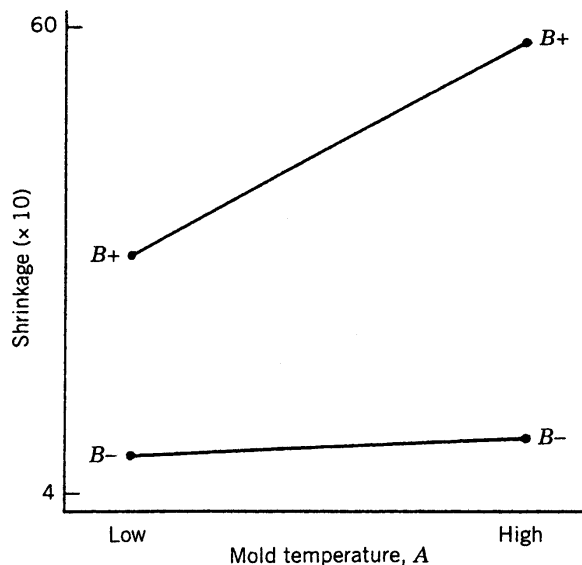
**TABLE 4.10** Analysis of Variance for the Injection Molding Experiment (Example 4.3)

Source of Variation	Sum of Squares	Degrees of Freedom	Mean Squares	$F_0$	P-Value
<i>A</i>	770.063	1	770.063	41.033	$1.18 \times 10^{-5}$
<i>B</i>	5076.563	1	5076.563	270.505	$5.25 \times 10^{-11}$
<i>AB</i>	564.063	1	564.063	30.056	0.0001
Curvature	19.012	1	19.012	1.742	0.2786
Residual	281.500	15	18.767		
Lack-of-fit	(248.750)	(12)	20.729	1.899	0.3277
Pure error	(32.750)	(3)	10.917		
Total	6711.200	19			

problem. In effect, the mean shrinkage can be substantially reduced by the above modifications; however, the part-to-part variability in shrinkage over a production run could still cause problems in assembly. One way to address this issue is to see if any of the process factors affect the variability in parts shrinkage.

Figure 4.13 presents the normal probability plot of the residuals. This plot appears satisfactory. The plots of residuals versus each factor were then constructed. One of these plots, that for residuals versus factor *C* (holding time), is shown in Fig. 4.14. The plot reveals that there is much less scatter in the residuals at the low holding time than at the high holding time. These residuals were obtained in the usual way from the model for predicted shrinkage

$$\hat{y} = b_0 + b_1x_1 + b_2x_2 + b_{12}x_1x_2 \\ = 27.3125 + 6.9375x_1 + 17.8125x_2 + 5.9375x_1x_2$$

**Figure 4.12** Plot of *AB* (mold-temperature–screw-speed) interaction for Example 4.3.

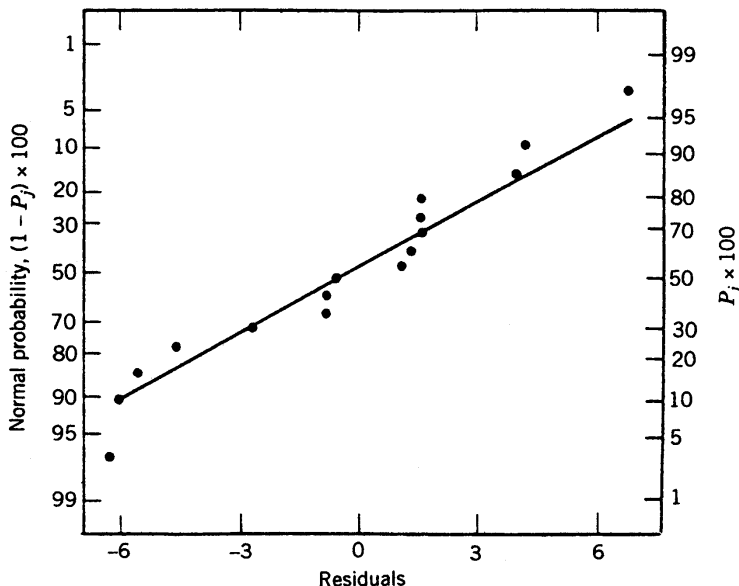


**Figure 4.13** Normal probability plot of residuals for Example 4.3.

where  $x_1$ ,  $x_2$ , and  $x_1x_2$  are the coded variables that correspond to the factors  $A$  and  $B$  and the  $AB$  interaction. The residuals are then

$$e = y - \hat{y}$$

The regression model used to produce the residuals essentially removes the location effects of  $A$ ,  $B$ , and  $AB$  from the data; the residuals therefore contain information about unexplained variability. Figure 4.14 indicates that there is a pattern in the variability and that the variability in shrinkage of parts may be smaller when the holding time is at the low level.

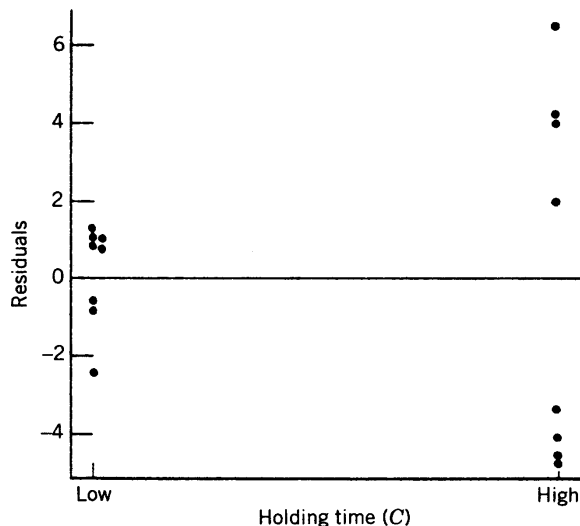


**Figure 4.14** Residuals versus holding time ( $C$ ) for Example 4.4.

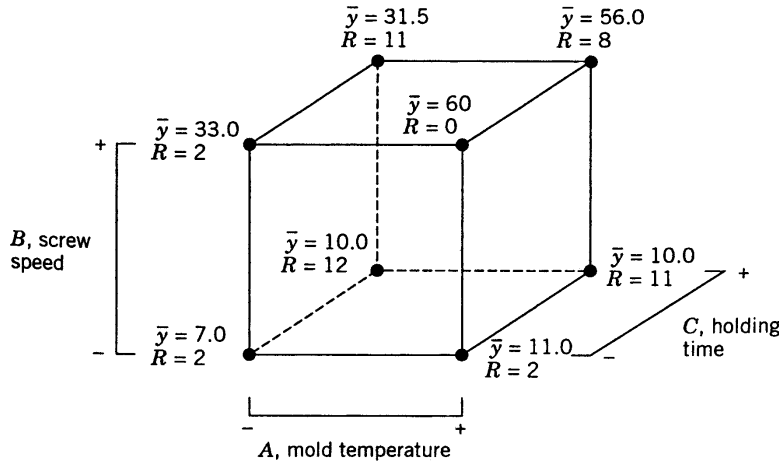


**Figure 4.15** Average shrinkage ( $\bar{y}$ ) and range of shrinkage ( $R$ ) in factors  $A$ ,  $B$ , and  $C$  for Example 4.3.

Figure 4.15 shows the data from this experiment projected onto a cube in the factors  $A$ ,  $B$ , and  $C$ . The average observed shrinkage and the range of observed shrinkage are shown at each corner of the cube. From inspection of this figure, we see that running the process with the screw speed ( $B$ ) at the low level is the key to reducing average parts shrinkage. If  $B$  is low, virtually any combination of temperature ( $A$ ) and holding time ( $C$ ) will result in low values of average part shrinkage. However, from examining the ranges of the shrinkage values at each corner of the cube, it is immediately clear that setting the holding time ( $C$ ) at the low level is the only reasonable choice if we wish to keep the part-to-part variability in shrinkage low during a production run.

In many response surface problems it is useful to actually build a model for both the *mean response* and a measure of the *variability* in response (such as the range, the variance, or the standard deviation). In fact, we illustrated this in Example 3.3. Then the optimization problem is a tradeoff between these two criteria, such as minimizing the variability while simultaneously moving the mean response to a desired or target value. We will present several techniques for doing this in subsequent chapters.

#### 4.4 THE GENERAL $2^{k-p}$ FRACTIONAL FACTORIAL DESIGN

A  $2^k$  fractional factorial design containing  $2^{k-p}$  runs is called a  $1/2^p$  fraction of the  $2^k$  design or, more simply, a  $2^{k-p}$  fractional factorial design. These designs require the selection of  $p$  independent design generators. The defining relation for the design consists of the  $p$  generators initially chosen and their  $2^p - p - 1$  generalized interactions. In this section we discuss the construction and analysis of these designs.

The alias structure may be found by multiplying each effect column by the defining relations. Care should be exercised in choosing the generators so that effects of potential interest are not aliased with each other. Each effect has  $2^p - 1$  aliases. For moderately large values of  $k$ , we usually assume higher-order interactions (say, third- or fourth-order and higher) to be negligible, and this greatly simplifies the alias structure.

It is important to select the  $p$  generators for a  $2^{k-p}$  fractional factorial design in such a way that we obtain the best possible alias relationships. A reasonable criterion is to select the generators such that the resulting  $2^{k-p}$  design has the highest possible resolution. Table 4.11 presents a selection of  $2^{k-p}$  fractional factorial designs for  $k \leq 11$  factors and up to  $n \leq 128$  runs, adapted from Montgomery (2005). The suggested generators in this table will result in a design of the highest possible resolution. The alias relationships for all of the designs in Table 4.11 for which  $n \leq 64$  are given in Appendix Table XII(a-v) of Montgomery (2005).

**Example 4.4 Selection of a Fractional Factorial** To illustrate the use of Table 4.11, suppose that we have seven factors and that we are interested in estimating the seven main effects and getting some insight regarding the two-factor interactions. We are willing to assume that three-factor and higher interactions are negligible. This information suggests that a resolution IV design would be appropriate.

Table 4.11 shows that there are two resolutions IV fractions available: the  $2_{IV}^{7-2}$  design with 32 runs and the  $2_{IV}^{7-3}$  with 16 runs. Consider the 16-run design. This is a one-eighth fraction with generators  $E = \pm ABC$ ,  $F = \pm BCD$ , and  $G = \pm ACD$ , and if we choose the principal fraction the complete defining relation is

$$I = ABCE = BCDF = ADEF = ACDG = BDEG = ABFG = CEFG$$

Now because the design is of resolution IV, it is clear that the main effects will be aliased with at worst a three-factor interaction. So if we can safely ignore these higher-order interactions, this design will give excellent information on the main effects. The two-factor interaction alias chains are

$$\begin{aligned} AB &= CE = FG \\ AC &= BE = DG \\ AD &= EF = CG \\ AE &= BC = DF \\ AF &= DE = BG \\ AG &= CD = BF \\ BD &= CF = EG \end{aligned}$$

when ignoring three-factor and higher interactions. Thus this design would likely be satisfactory to satisfy the experimenter's objectives.

The complete design is shown in Table 4.12. Notice that it was constructed by starting with the 16-run  $2^4$  design in  $A$ ,  $B$ ,  $C$ , and  $D$  as the basic design and then adding the three columns  $E = ABC$ ,  $F = BCD$ , and  $G = ACD$  as suggested in Table 4.11.

**Projection of the  $2^{k-p}$  Fractional Factorial** The  $2^{k-p}$  design collapses into either a full factorial or a fractional factorial in any subset of  $r \leq k - p$  of the original factors. Those subsets of factors providing fractional factorials are subsets appearing as words in the complete defining relation. Furthermore, a design of resolution  $R$  will project into a full factorial in any subset of  $R - 1$  factors. These results are particularly useful in screening experiments when we suspect at the outset of the experiment that most of the original factors will have small effects. The original  $2^{k-p}$  fractional factorial can then be

**TABLE 4.11 Selected  $2^{k-p}$  Fractional Factorial Designs**

Number of Factors, $k$	Fraction	Number of Runs	Design Generators
3	$2_{\text{III}}^{3-1}$	4	$C = \pm AB$
4	$2_{\text{IV}}^{4-1}$	8	$D = \pm ABC$
5	$2_{\text{V}}^{5-1}$ $2_{\text{III}}^{5-2}$	16 8	$E = \pm ABCD$ $D = \pm AB$ $E = \pm AC$
6	$2_{\text{VI}}^{6-1}$ $2_{\text{IV}}^{6-2}$ $2_{\text{III}}^{6-3}$	32 16 8	$F = \pm ABCDE$ $E = \pm ABC$ $F = \pm BCD$ $D = \pm AB$ $E = \pm AC$ $F = \pm BC$
7	$2_{\text{VII}}^{7-1}$ $2_{\text{IV}}^{7-2}$ $2_{\text{IV}}^{7-3}$ $2_{\text{III}}^{7-4}$	64 32 16 8	$G = \pm ABCDEF$ $F = \pm ABCD$ $G = \pm ABDE$ $E = \pm ABC$ $F = \pm BCD$ $G = \pm ACD$ $D = \pm AB$ $E = \pm AC$ $F = \pm BC$ $G = \pm ABC$
8	$2_{\text{V}}^{8-2}$ $2_{\text{IV}}^{8-3}$ $2_{\text{IV}}^{8-4}$	64 32 16	$G = \pm ABCD$ $H = \pm ABEF$ $F = \pm ABC$ $G = \pm ABD$ $H = \pm BCDE$ $E = \pm BCD$ $F = \pm ACD$ $G = \pm ABC$ $H = \pm ABD$
9	$2_{\text{VI}}^{9-2}$ $2_{\text{IV}}^{9-3}$ $2_{\text{IV}}^{9-4}$ $2_{\text{III}}^{9-5}$	128 64 32 16	$H = \pm ACDFG$ $J = \pm BCEFG$ $G = \pm ABCD$ $H = \pm ACEF$ $J = \pm CDEF$ $F = \pm BCDE$ $G = \pm ACDE$ $H = \pm ABDE$ $J = \pm ABCE$ $E = \pm ABC$ $F = \pm BCD$ $G = \pm ACD$ $H = \pm ABD$ $J = \pm ABCD$

(Continued)

**TABLE 4.11** *Continued*

Number of Factors, $k$	Fraction	Number of Runs	Design Generators
10	$2_{\text{IV}}^{10-3}$	128	$H = \pm ABCG$
			$J = \pm ACDE$
			$K = \pm ACDF$
			$G = \pm BCDF$
			$H = \pm ACDF$
	$2_{\text{IV}}^{10-4}$	64	$J = \pm ABDE$
			$K = \pm ABCE$
			$F = \pm ABCD$
			$G = \pm ABCE$
			$H = \pm ABDE$
11	$2_{\text{IV}}^{10-5}$	32	$J = \pm ACDE$
			$K = \pm BCDE$
			$E = \pm ABC$
			$F = \pm BCD$
			$G = \pm ACD$
	$2_{\text{III}}^{10-6}$	16	$H = \pm ABD$
			$J = \pm ABCD$
			$K = \pm AB$
			$G = \pm CDE$
			$H = \pm ABCD$
11	$2_{\text{IV}}^{11-5}$	64	$J = \pm ABF$
			$K = \pm BDEF$
			$L = \pm ADEF$
			$F = \pm ABC$
			$G = \pm BCD$
	$2_{\text{IV}}^{11-6}$	32	$H = \pm CDE$
			$J = \pm ACD$
			$K = \pm ADE$
			$L = \pm BDE$
			$E = \pm ABC$
11	$2_{\text{III}}^{11-7}$	16	$F = \pm BCD$
			$G = \pm ACD$
			$H = \pm ABD$
			$J = \pm ABCD$
			$K = \pm AB$
			$L = \pm AC$

projected into a full factorial, say, in the most interesting factors. Conclusions drawn from designs of this type should be considered tentative and subject to further analysis. It is usually possible to find alternative explanations of the data involving higher-order interactions.

As an example, consider the  $2_{\text{IV}}^{7-3}$  design from Example 4.4. This is a 16-run design involving seven factors. It will project into a full factorial in any four of the original seven factors that is not a word in the complete defining relation (see Table 4.12). Thus, there are 28 subsets of four factors that would form  $2^4$  designs. One combination that is

**TABLE 4.12 A  $2^{7-3}$  Fractional Factorial Design**

Run	Basic Design				$E = ABC$	$F = BCD$	$G = ACD$
	A	B	C	D			
1	-	-	-	-	-	-	-
2	+	-	-	-	+	-	+
3	-	+	-	-	+	+	-
4	+	+	-	-	-	+	+
5	-	-	+	-	+	+	+
6	+	-	+	-	-	+	-
7	-	+	+	-	-	-	+
8	+	+	+	-	+	-	-
9	-	-	-	+	-	+	+
10	+	-	-	+	+	+	-
11	-	+	-	+	+	-	+
12	+	+	-	+	-	-	-
13	-	-	+	+	+	-	-
14	+	-	+	+	-	-	+
15	-	+	+	+	-	+	-
16	+	+	+	+	+	+	+

obvious upon inspecting Table 4.12 is  $A$ ,  $B$ ,  $C$ , and  $D$ . It will also form a replicated full factorial in any subset of three of the original seven factors.

To illustrate the usefulness of this projection properly, suppose that we are conducting an experiment to improve the performance of a chemical process and the seven factors are:

1. Concentration of reactant  $A$
2. Temperature
3. Feed rate
4. Time
5. Agitation rate
6. Concentration of reactant  $B$
7. Catalyst type

We are fairly certain that time, temperature, catalyst type, and concentration of reactant  $A$  will affect performance and that these factors may interact. The role of the other three factors is less well known, but it is likely that they are negligible. A reasonable strategy would be to assign these four factors to columns  $A$ ,  $B$ ,  $C$ , and  $D$ , respectively, in Table 4.12. The remaining three factors would be assigned to columns  $E$ ,  $F$ , and  $G$ , respectively. If we are correct and the “minor variables”  $E$ ,  $F$ , and  $G$  are negligible, we will be left with a full  $2^k$  design in the key process variables.

## 4.5 RESOLUTION III DESIGNS

As indicated earlier, the sequential use of fractional factorial designs is very useful, often leading to great economy and efficiency in experimentation. We now illustrate these

ideas using the class of resolution III designs. Box and Hunter (1961a, b) are excellent references for the technical details.

It is possible to construct resolution III designs for investigating up to  $k = N - 1$  factors in only  $N$  runs, where  $N$  is a multiple of 4. These designs are frequently useful in industrial experimentation. Designs in which  $N$  is a power of 2 can be constructed by the methods presented earlier in this chapter, and these are presented first. Of particular importance are designs requiring 4 runs for up to 3 factors, 8 runs for up to 7 factors, and 16 runs for up to 15 factors. If  $k = N - 1$ , the fractional factorial design is said to be **saturated**.

A design for analyzing up to three factors in four runs is the  $2_{III}^{3-1}$  design, presented in Section 4.2. Another very useful saturated fractional factorial is a design for studying up to seven factors in eight runs; that is, the  $2_{III}^{7-4}$  design. This design is a one-sixteenth fraction of the  $2^7$ . It may be constructed by first writing down as the basic design the plus and minus levels for a full  $2^3$  design in  $A$ ,  $B$ , and  $C$  and then associating the levels of four additional factors with the interactions of the original three as follows:  $D = AB$ ,  $E = AC$ ,  $F = BC$ , and  $G = ABC$ . Thus, the generators for this design are  $I = ABD$ ,  $I = ACE$ ,  $I = BCF$ , and  $I = ABCG$ . The design is shown in Table 4.13.

The complete defining relation for this design is obtained by multiplying the four generators  $ABD$ ,  $ACE$ ,  $BCF$ , and  $ABCG$  together two at a time, three at a time, and four at a time, yielding

$$\begin{aligned} I &= ABD = ACE = BCF = ABCG = BCDE = ACDF = CDG \\ &= ABEF = BEG = AFG = DEF = ADEG = CEFG = BDFG \\ &= ABCDEFG \end{aligned}$$

To find the aliases of any effect, simply multiply the effect by each word in the defining relation. For example, the aliases of  $B$  are

$$\begin{aligned} B &= AD = ABCE = CF = ACG = CDE = ABCDF = BCDG = AEF = EG \\ &= ABFG = BDEF = ABDEG = BCEFG = DFG = ACDEFG \end{aligned}$$

This design is a one-sixteenth fraction; and because the signs chosen for the generators are positive, this is the principal fraction. It is also of resolution III, because the smallest number of letters in any word of the defining contrast is three. Any one of the 16 different

**TABLE 4.13** The Saturated  $2_{III}^{7-4}$  Design with the Generators  $I = ABD$ ,  $I = ACE$ ,  $I = BCF$ , and  $I = ABCG$

Run	$A$	$B$	$C$	$D = AB$	$E = AC$	$F = BC$	$G = ABC$
1	–	–	–	+	+	+	–
2	+	–	–	–	–	+	+
3	–	+	–	–	+	–	+
4	+	+	–	+	–	–	–
5	–	–	+	+	–	–	+
6	+	–	+	–	+	–	–
7	–	+	+	–	–	+	–
8	+	+	+	+	+	+	+

$2^{7-4}$  designs in this family could be constructed by using the generators with one of the 16 possible arrangements of signs in  $I = \pm ABC$ ,  $I = \pm ACE$ ,  $I = \pm BCF$ ,  $I = \pm ABCG$ .

The seven degrees of freedom in this design may be used to estimate the seven main effects. Each of these effects has 15 aliases; however, if we assume that three-factor and higher interactions are negligible, then considerable simplification in the alias structure results. Making this assumption, each of the linear combinations associated with the seven main effects in this design actually estimates the main effect and three two-factor interactions:

$$\begin{aligned}
 [A] &\rightarrow A + BD + CE + FG \\
 [B] &\rightarrow B + AD + CF + EG \\
 [C] &\rightarrow C + AE + BF + DG \\
 [D] &\rightarrow D + AB + CG + EF \\
 [E] &\rightarrow E + AC + BG + DF \\
 [F] &\rightarrow F + BC + AG + DE \\
 [G] &\rightarrow G + CD + BE + AF
 \end{aligned} \tag{4.1}$$

In obtaining these aliases, we have ignored the three-factor and higher-order interactions, assuming that they will be negligible in most practical applications where a design of this type would be considered.

The saturated  $2^{7-4}_{III}$  design in Table 4.13 can be used to obtain resolution III designs for studying fewer than seven factors in eight runs. For example, to generate a design for six factors in eight runs, simply drop any one column in Table 4.13, for example, column *G*. This produces the design shown in Table 4.14.

It is easy to verify that this design is also of resolution III; in fact, it is a  $2_{III}^{6-3}$ , or a one-eighth fraction of the  $2^6$  design. The defining relation for the  $2_{III}^{6-3}$  design is equal to the defining relation for the original  $2_{III}^{7-4}$  design with any words containing the letter  $G$  deleted. Thus, the defining relation for our new design is

$$I = ABD = ACE = BCF = BCDE = ACDF = ABEF = DEF$$

In general, when  $d$  factors are dropped to produce a new design, the new defining relation is obtained as those words in the original defining relation that do not contain any dropped

TABLE 4.14 A  $2^{6-3}_{III}$  Design with the Generators  $I = ABD$ ,  $I = ACE$ , and  $I = BCF$

letters. When constructing designs by this method, care should be exercised to obtain the best arrangement possible. If we drop columns  $B$ ,  $D$ ,  $F$ , and  $G$  from Table 4.13, we obtain a design for three factors in eight runs, yet the treatment combinations correspond to two replicates of a  $2^2$  design. The experimenter would probably prefer to run a full  $2^3$  design in  $A$ ,  $C$ , and  $E$ .

It is also possible to obtain a resolution III design for studying up to 15 factors in 16 runs. This saturated  $2_{\text{III}}^{15-11}$  design can be generated by first writing down the 16 treatment combinations associated with a  $2^4$  design in  $A$ ,  $B$ ,  $C$ , and  $D$  and then equating 11 new factors with the two-, three-, and four-factor interactions of the original four. In this design, each of the 15 main effects is aliased with seven two-factor interactions. A similar procedure can be used for the  $2_{\text{III}}^{31-26}$  design, which allows up to 31 factors to be studied in 32 runs.

**Sequential Use of Fractions to Separate Effects** By combining fractional factorial designs in which certain signs are switched, we can systematically isolate effects of potential interest. The alias structure for any fraction with the signs for one or more factors reversed is obtained by making changes of sign on the appropriate factors in the alias structure of the original fraction. This general procedure is called **fold-over**, and it is used in resolution III designs to break the links between main effects and two-factor interactions. In a **full fold-over**, we add to a resolution III fractional a second fraction in which the signs for all the factors are reversed. We may now use the combined design to estimate all the main effects clear of any two-factor interactions. The following example illustrates the technique.

**Example 4.5 Fold-Over of a Fractional Factorial** A human performance analyst is conducting an experiment to study eye focus time and has built an apparatus in which several factors can be controlled during the test. The factors he initially regards as important are acuity or sharpness of vision ( $A$ ), distance from target to eye ( $B$ ), target shape ( $C$ ), illumination level ( $D$ ), target size ( $E$ ), target density ( $F$ ), and subject ( $G$ ). Two levels of each factor are considered. He suspects that only a few of these seven factors are of major importance and that high-order interactions between the factors can be neglected. On the basis of this assumption, the analyst decides to run a screening experiment to identify the most important factors and then to concentrate further study on those. To screen these seven factors, he runs the treatment combinations from the  $2_{\text{III}}^{7-4}$  design in Table 4.13 in random order, obtaining the focus times in milliseconds, as shown in Table 4.15.

**TABLE 4.15 A  $2_{\text{III}}^{7-4}$  Design for the Eye Focus Time Experiment**

Run	$A$	$B$	$C$	$D = AB$	$E = AC$	$F = BC$	$G = ABC$	Time	
1	–	–	–	+	+	+	–	def	85.5
2	+	–	–	–	–	+	+	afg	75.1
3	–	+	–	–	+	–	+	beg	93.2
4	+	+	–	+	–	–	–	abd	145.4
5	–	–	+	+	–	–	+	cde	83.7
6	+	–	+	–	+	–	–	ace	77.6
7	–	+	+	–	–	+	–	bcf	95.0
8	+	+	+	+	+	+	+	abcdefg	141.8

Seven main effects and their aliases may be estimated from these data. From Equation 4.1, we see that the effects and their aliases are

$$\begin{aligned}[A] &= 20.63 \rightarrow A + BD + CE + FG \\[B] &= 38.38 \rightarrow B + AD + CF + EG \\[C] &= -0.28 \rightarrow C + AE + BF + DG \\[D] &= 28.88 \rightarrow D + AB + CG + EF \\[E] &= -0.28 \rightarrow E + AC + BG + DF \\[F] &= -0.63 \rightarrow F + BC + AG + DE \\[G] &= -2.43 \rightarrow G + CD + BE + AF\end{aligned}$$

For example,

$$\begin{aligned}[A] &= \frac{1}{4}(-85.5 + 75.1 - 93.2 + 145.4 - 83.7 + 77.6 - 95.0 + 141.8) \\&= 20.63\end{aligned}$$

The largest three effects are  $[A]$ ,  $[B]$ , and  $[D]$ . The simplest interpretation of the data is that the main effects of  $A$ ,  $B$ , and  $D$  are all significant. However, this interpretation is not unique, because one could also logically conclude that  $A$ ,  $B$ , and the  $AB$  interaction, or perhaps  $B$ ,  $D$ , and the  $BD$  interaction, or perhaps  $A$ ,  $D$ , and the  $AD$  interaction are the true effects.

Notice that  $ABD$  is a word in the defining relation for this design. Therefore, this  $2_{III}^{7-4}$  design does not project into a full  $2^3$  factorial in  $A$ ,  $B$ , and  $D$ ; instead, it projects into two replicates of a  $2^{3-1}$  design, as shown in Fig. 4.16. Because the  $2^{3-1}$  design is a resolution III design,  $A$  will be aliased with  $BD$ ,  $B$  will be aliased with  $AD$ , and  $D$  will be aliased with  $AB$ , so the interactions cannot be separated from the main effects. The analyst here may have been unlucky. If he had assigned illumination level to column  $C$  in Table 4.13 instead of  $D$ , the design would have projected into a  $2^3$  design.

To separate the main effects and the two-factor interactions, a second fraction is run with all the signs reversed. This fold-over design is shown in Table 4.16 along with the observed

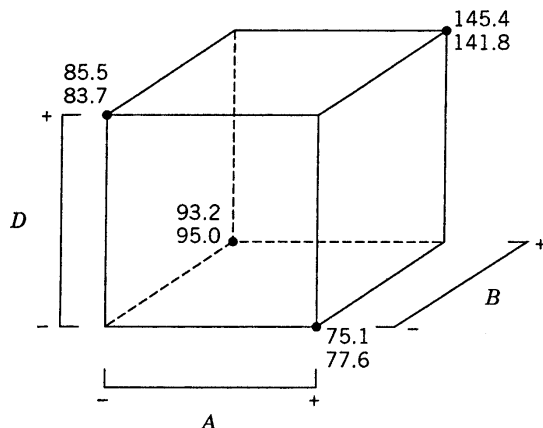


**Figure 4.16** The  $2_{III}^{7-4}$  design projected into two replicates of a  $2^{3-1}$  design in  $A$ ,  $B$ , and  $D$ .

**TABLE 4.16 Fold-over of the  $2^{7-4}_{III}$  Design in Table 4.15**

Run	A	B	C	$D = -AB$	$E = -AC$	$F = -BC$	$G = ABC$	Time
1	+	+	+	-	-	-	+	abcg
2	-	+	+	+	+	-	-	bcd e
3	+	-	+	+	-	+	-	acdf
4	-	-	+	-	+	+	+	cefg
5	+	+	-	-	+	+	-	abef
6	-	+	-	+	-	+	+	bdfg
7	+	-	-	+	+	-	+	a deg
8	-	-	-	-	-	-	-	(1)
								71.9

responses. Notice that when we fold over a resolution III design in this manner, we (in effect) change the signs on the generators that have an odd number of letters. The effects estimated by this fraction are

$$\begin{aligned}[A]' &= -17.68 \rightarrow A - BD - CE - FG \\ [B]' &= 37.73 \rightarrow B - AD - CF - EG \\ [C]' &= -3.33 \rightarrow C - AE - BF - DG \\ [D]' &= 29.88 \rightarrow D - AB - CG - EF \\ [E]' &= 0.53 \rightarrow E - AC - BG - DF \\ [F]' &= 1.63 \rightarrow F - BC - AG - DE \\ [G]' &= 2.68 \rightarrow G - CD - BE - AF\end{aligned}$$

By combining the effect estimates from this second fraction with the effect estimates from the original eight runs, we obtain the following estimates of the effects:

$i$	From $\frac{1}{2}([i] + [i]')$	From $\frac{1}{2}([i] - [i]')$
A	$A = 1.48$	$\mathbf{BD} + CE + FG = 19.15$
B	$\mathbf{B} = 38.05$	$AD + CF + EG = 0.33$
C	$C = -1.80$	$AE + BF + DG = 1.53$
D	$\mathbf{D} = 29.38$	$AB + CG + EF = -0.50$
E	$E = 0.13$	$AC + BG + DF = -0.40$
F	$F = 0.50$	$BC + AG + DE = -1.53$
G	$G = 0.13$	$CD + BE + AF = -2.55$

The largest two effects are  $B$  and  $D$ . Furthermore, the third largest effect is  $BD + CE + FG$ , so it seems reasonable to attribute this to the  $BD$  interaction. The analyst used the two factors distance ( $B$ ) and illumination level ( $D$ ) in subsequent experiments with the other factors  $A$ ,  $C$ ,  $E$ , and  $F$  at standard settings and verified the results obtained here. He decided to use subjects as blocks in these new experiments rather than ignore a potential subject effect, because several different subjects had to be used to complete the experiment.

While the full fold-over strategy illustrated in Example 4.5 is used very frequently, there is another variation of this technique that occasionally proves helpful. In a **single-factor fold-over** we add to a fractional factorial design of resolution III a second fraction of the

same size with the signs for only one of the factors reversed. In the combined design, we will be able to estimate the main effect of the factor for which the signs were reversed as well as all two-factor interactions involving that factor.

To illustrate, consider the  $2^{7-4}_{III}$  design in Table 4.13. Suppose that along with this principal fraction a second fractional design with the signs reversed in the column for factor  $D$  is also run. That is, the column for  $D$  in the second fraction is

$$- + - - + + -$$

The effects that may be estimated from the first fraction are shown in Equation 4.1, and from the second fraction we obtain

$$\begin{aligned}[A]' &\rightarrow A - BD + CE + FG \\ [B]' &\rightarrow B - AD + CF + EG \\ [C]' &\rightarrow C + AE + BF - DG \\ [D]' &\rightarrow D - AB - CG - EF\end{aligned}$$

that is,

$$\begin{aligned}[D]' &\rightarrow -D + AB + CG + EF \\ [E]' &\rightarrow E + AC + BG - DF \\ [F]' &\rightarrow F + BC + AG - DE \\ [G]' &\rightarrow G - CD + BE + AF\end{aligned}$$

assuming that three-factor and higher interactions are insignificant. Now from the two linear combinations of effects  $\frac{1}{2}([i] + [i]')$  and  $\frac{1}{2}([i] - [i]')$  we obtain

$i$	$\frac{1}{2}([i] + [i]')$	$\frac{1}{2}([i] - [i]')$
$A$	$A + CE + FG$	$BD$
$B$	$B + CF + EG$	$AD$
$C$	$C + AE + BF$	$DG$
$D$	$D$	$AB + CG + EF$
$E$	$E + AC + BG$	$DF$
$F$	$F + BC + AG$	$DE$
$G$	$G + BE + AF$	$CD$

Thus, we have isolated the main effect of  $D$  and all of its two-factor interactions.

**The Defining Relation for a Fold-over Design** Combining fractional factorial designs via fold-over as demonstrated in Example 4.5 is a very useful technique. It is often of interest to know the defining relation for the combined design. Fortunately, this can be easily determined. Each separate fraction will have  $L + U$  words used as generators:  $L$  words of like sign and  $U$  words of unlike sign. The combined design will have  $L + U - 1$  words used as generators. These will be the  $L$  words of like sign and the  $U - 1$  words consisting of independent even products of the words of unlike sign. (Even products are words taken two at a time, four at a time, and so forth.)

To illustrate this procedure, consider the design in Example 4.5. For the first fraction, the generators are

$$I = ABD, \quad I = ACE, \quad I = BCF, \quad \text{and } I = ABCG$$

and for the second fraction, they are

$$I = -ABD, \quad I = -ACE, \quad I = -BCF, \quad \text{and } I = ABCG$$

Notice that in the second fraction we have switched the signs on the generators with an odd number of letters. Also, notice that  $L + U = 1 + 3 = 4$ . The combined design will have  $I = ABCG$  (the like-sign word) as a generator, and two words that are independent even products of the words of unlike sign. For example, take  $I = ABD$  and  $I = ACE$ ; then  $I = (ABD)(ACE) = BCDE$  is a generator of the combined design. Also, take  $I = ABD$  and  $I = BCF$ ; then  $I = (ABD)(BCF) = ACDF$  is a generator of the combined design. The complete defining relation for the combined design is

$$I = ABCG = BCDE = ACDF = ADEG = BDFG = ABEG = CEFG$$

Because the defining relation for the combined design contains only four-letter words, the combined design is of resolution IV.

**Plackett–Burman Designs** These designs, attributed to Plackett and Burman (1946), are two-level fractional designs for studying up to  $k = N - 1$  variables in  $N$  runs, where  $N$  is a multiple of 4. If  $N$  is a power of 2, these designs are identical to those presented earlier in this section. However, for  $N = 12, 20, 24, 28$ , and 36, the Plackett–Burman designs are sometimes of interest.

The upper half of Table 4.17 presents rows of plus and minus signs that are used to construct the Plackett–Burman designs for  $N = 12, 20, 24$ , and 36, whereas the lower half of the table presents blocks of plus and minus signs for constructing the design for  $N = 28$ . The designs for  $N = 12, 20, 24$ , and 36 are obtained by writing the appropriate row in Table 4.17 as a column (or row). A second column for (or row) is then generated from this first one by moving the elements of the column (or row) down (or to the right) one position and placing the last element in the first position. A third column (or row) is produced

**TABLE 4.17 Plus and Minus Signs for the Plackett–Burman Designs**

$k = 11, N = 12 + + - + + + - - + -$		
$k = 19, N = 20 + + - - + + + + - + - + - - - + + -$		
$k = 23, N = 24 + + + + + - + - + + - + + - + - + - - -$		
$k = 35, N = 36 - + - + + + - - + + + + + - + + + - + - + + - + - + -$		
$k = 27, N = 28$		
$+ - + + + - - -$	$- + - - + - - +$	$+ + - + - + + - +$
$+ + - + + + - - -$	$- - + + - - + - -$	$- + + + + - + + -$
$- + + + + - - -$	$+ - - - + - - + -$	$+ - + - + + - + +$
$- - - + - + + +$	$- - + - + - - -$	$+ - + + + - + - +$
$- - - + + - + + +$	$+ - - - + + - -$	$+ + - - + + + + -$
$- - - - + + + + +$	$- + - + - - - + -$	$- + + + - + - + +$
$+ + + - - - + - +$	$- - + - - + - + -$	$+ - + + - + + + -$
$+ + + - - - + + -$	$+ - - + - - - - +$	$+ + - + + - - + +$
$+ + + - - - - + +$	$- + - - + - + - -$	$- + + - + + + - +$

**TABLE 4.18 Plackett–Burman Design for  $N = 12$ ,  $k = 11$  Using Generator in Table 4.17**

Run	A	B	C	D	E	F	G	H	I	J	K
1	+	-	+	-	-	-	+	+	+	-	+
2	+	+	-	+	-	-	-	+	+	+	-
3	-	+	+	-	+	-	-	-	+	+	+
4	+	-	+	+	-	+	-	-	-	+	+
5	+	+	-	+	+	-	+	-	-	-	+
6	+	+	+	-	+	+	-	+	-	-	-
7	-	+	+	+	-	+	+	-	+	-	-
8	-	-	+	+	+	-	+	+	-	+	-
9	-	-	-	+	+	+	-	+	+	-	+
10	+	-	-	-	+	+	+	-	+	+	-
11	-	+	-	-	-	+	+	+	-	+	+
12	-	-	-	-	-	-	-	-	-	-	-

from the second similarly, and the process continued until column (or row)  $k$  is generated. A row of minus signs is then added, completing the design. For  $N = 28$ , the three blocks  $X$ ,  $Y$ , and  $Z$  are written down in the order

$$\begin{array}{ccc} X & Y & Z \\ Z & X & Y \\ Y & Z & X \end{array}$$

and a row of minus signs is added to these 27 rows. The design for  $N = 12$  runs and  $k = 11$  factors is shown in Table 4.18, where the generator in Table 4.17 was used as a column.

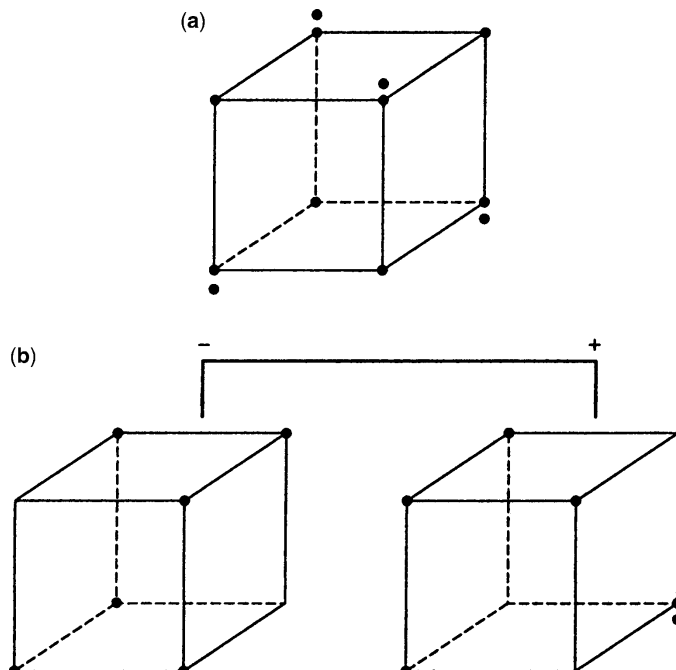


**Figure 4.17** Projection of the 12-run Plackett–Burman design into three- and four-factor designs. (a) Projection into three factors. (b) Projection into four factors.

The Plackett–Burman designs for  $N = 12, 20, 24, 28$ , and  $36$  have very messy alias structures. For example, in the 12-run design every main effect is **partially aliased** with every two-factor interaction not involving itself. Thus, the  $AB$  interaction is partially aliased with the nine main effects  $C, D, \dots, K$ . Furthermore, each main effect is partially aliased with 45 two-factor interactions. In the larger designs, the situation is even more complex. We advise experimenter to use these designs in screening situations very carefully. However, as we will see in subsequent chapters, they can be used in the construction of certain types of second-order response surface designs.

The projection properties of the Plackett–Burman designs are not terribly attractive. For example, consider the 12-run design in Table 4.18. This design will project into three replicates of a full  $2^2$  design in any two of the original 11 factors. However, in three factors, the projected design is a full  $2^3$  factorial plus a  $2^{3-1}_{\text{III}}$  fractional factorial [see Fig. 4.17a]. The four-dimensional projections are shown in Fig. 4.17b. Notice that these three- and four-factor projections are not balanced designs. This would complicate their interpretation. Plackett–Burman designs with  $N = 12, 20, 24, 28$ , and  $36$  are often called **nongeometric** Plackett–Burman designs.

## 4.6 RESOLUTION IV AND V DESIGNS

A  $2^{p-k}$  fractional factorial design is of resolution IV if the main effects are clear of two-factor interactions, but some two-factor interactions are aliased with each other. Thus, if three-factor and higher interactions are assumed negligible and suppressed, the main effects may be estimated directly in a  $2^{k-p}_{\text{IV}}$  design. An example is the  $2^{6-2}_{\text{IV}}$  design in Table 4.9. Furthermore, the two combined fractions of the  $2^{7-4}_{\text{III}}$  design in Example 4.5 yield a  $2^{7-3}_{\text{IV}}$  design.

Any  $2^{k-p}_{\text{IV}}$  design must contain at least  $2k$  runs. Resolution IV designs that contain exactly  $2k$  runs are called **minimal designs**. Resolution IV designs may be obtained from resolution III designs by the process of fold-over. Recall that to fold over a design, one simply adds to the original fraction a second fraction with all the signs reversed. Then the plus signs in the identity column  $I$  in the first fraction can be switched in the second fraction, and a  $(k+1)$ st factor associated with this column. The result is a  $2^{k+1-p}_{\text{IV}}$  fractional factorial design. The process is demonstrated in Table 4.19 for the  $2^{3-1}_{\text{III}}$  design. It is easy to verify that the resulting design is a  $2^{4-1}_{\text{IV}}$  design with defining relation  $I = ABCD$ .

It is also possible to fold over resolution IV designs to separate two-factor interactions that are aliased with each other. One way to fold over a resolution IV design is to run a second fraction in which the sign is reversed on every design generator that has an *even number of letters*. To illustrate, consider the  $2^{6-2}_{\text{IV}}$  design used for the injection molding experiment in Example 4.3. The generators for the design in Table 4.11 are  $I = ABCE$  and  $I = BCDF$ . The second fraction uses the generators  $I = -ABCE$  and  $I = -BCDF$ , and the single generator for the combined design is  $I = ADEF$ . Thus, the combined design is still a resolution IV fractional factorial design. However, the alias relationships will be much simpler than in the original  $2^{6-2}_{\text{IV}}$  fractional. In fact, the only two-factor interactions that will be aliased are  $AD = EF$ ,  $AE = DF$ , and  $AF = DE$ . All the other two-factor interactions can be estimated from the combined design.

Notice that when you start with a resolution III design, the fold-over procedure guarantees that the combined design will be of resolution IV, thereby ensuring that all the main effects can be separated from their two-factor interaction aliases. When folding over a

**TABLE 4.19** A  $2^{4-1}_{\text{IV}}$  Design Obtained by Fold-Over

<i>D</i>	<i>A</i>	<i>B</i>	<i>C</i>
<i>I</i>			
<i>Original</i> $2^{3-1}_{\text{III}}$ <i>with</i> $\text{I} = \text{ABC}$			
+	-	-	+
+	+	-	-
+	-	+	-
+	+	+	+
<i>Second</i> $2^{3-1}_{\text{III}}$ <i>with Signs Switched</i>			
-	+	+	-
-	-	+	+
-	+	-	+
-	-	-	-

resolution IV design, we will not necessarily separate all the two-factor interactions. In fact, if the original fraction has an alias structure with more than two two-factor interactions in any alias chain, folding over will not completely separate all the two-factor interactions. Notice that in the foregoing example, the  $2^{6-2}_{\text{IV}}$  has one such two-factor interaction alias chain. For more information on fold-over of resolution IV designs, see Montgomery and Runger (1996) and Montgomery (2005).

Resolution V designs are fractional factorials in which the main effects and the two-factor interactions do not have other main effects and two-factor interactions as their aliases. These are very powerful designs, allowing the unique estimation of all the main effects and two-factor interactions provided that all the three-factor and higher interactions are negligible. The smallest word in the defining relation of such a design must have five letters. The  $2^{5-1}$  with the generating relation  $\text{I} = \text{ABCDE}$  is of resolution V. Another example is the  $2^{8-2}_{\text{V}}$  design with the generating relations  $\text{I} = \text{ABCDG}$  and  $\text{I} = \text{ABEFH}$ . Further examples of these designs are given by Box and Hunter (1961b).

## 4.7 FRACTIONAL FACTORIAL SPLIT-PLOT DESIGNS

In Chapter 3 we introduced the **split-plot design** as a technique for dealing with hard-to-change versus easy-to-change factors in an experiment. Recall that the hard-to-change variables are changed less frequently in the experiment and placed in the whole plots, while the easy-to-change variables are still reset for each experimental run and are placed in the subplots. Factorial experiments with three or more factors in a split-plot structure often tend to be rather large experiments. On the other hand, the split-plots structure often makes it easier to conduct a larger experiment because we have reduced the number of times the hard-to-change factors need to be reset, and it can be quite easy and inexpensive to change the levels of the subplot variables.

As the number of factors in the experiment grows, the experimenter may consider using a fractional factorial experiment in the split-plot setting. As an illustration, consider an experiment involving five factors that potentially affect uniformity in a single-wafer

plasma etching process. Three of the factors on the etching tool are relatively difficult to change from run to run:  $A$  = electrode gap,  $B$  = gas flow, and  $C$  = pressure. Two other factors are easy to change from run to run:  $D$  = time and  $E$  = RF (radio frequency) power. For subsequent clarity, we have used bold-face letters to represent the easy-to-change factors. The experimenters want to use a fractional factorial split-plot (FFSP) design to investigate these five factors because the number of test wafers available is limited. The hard-to-change factors also indicate that a split-plot design should be considered to reduce the total number of changes required. The experimenters decide to use a  $2^{5-1}$  design with factors  $A$ ,  $B$ , and  $C$  in the whole plots and factors  $D$  and  $E$  in the subplots. The design generator is  $E = ABCD$ . This produces a 16-run fractional factorial with eight whole plots. Every whole plot contains one of the eight treatment combinations from a complete  $2^3$  factorial design in factors  $A$ ,  $B$ , and  $C$ . Each whole plot is divided into two subplots, with one of the treatment combinations for factors  $D$  and  $E$  in each subplot. The resulting FFSP design with measured responses of uniformity is shown in Table 4.20.

We will assume that all three-, four- and five-factor interactions are negligible. If this assumption is reasonable, then with 16 total observations the 15 effects (5 main effect and 10 two-way interactions) can be estimated. In the whole plots all hard-to-change factors,  $A$ ,  $B$ , and  $C$ , and their two-factor interactions,  $AB$ ,  $AC$ , and  $BC$ , can be estimated from the eight whole plots. There are seven degrees of freedom available for estimating whole plot effects, with the remaining degree of freedom from the whole plot terms being assigned to  $ABC = DE$ . There are eight degrees of freedom available for estimating subplot terms, which are for the two main effects,  $D$  and  $E$ , and all of the interactions involving a hard-to-change and easy-to-change factor ( $AD$ ,  $AE$ ,  $BD$ ,  $BE$ ,  $CD$ ,  $CE$ ). This illustrates one of the interesting trade-offs for using a fractional factorial split-plot design: Since we have a reduced number of runs for the experiment, and the defining equation involves both hard-to-change and easy-to-change factors, care needs to be taken to determine which terms can be estimated with which degrees of freedom.

**TABLE 4.20** The Fractional Factorial Split-Plot Design for the Plasma Etching Experiment

Whole Plots	Whole-Plot Factors			Subplot Factors		Uniformity
	<i>A</i>	<i>B</i>	<i>C</i>	<i>D</i>	<i>E</i>	
1	–	–	–	–	+	40.85
				+	–	41.07
2	+	–	–	–	–	35.67
				+	+	51.15
3	–	+	–	–	–	41.80
				+	+	37.01
4	+	+	–	–	+	91.09
				+	–	48.67
5	–	–	+	–	–	40.32
				+	+	43.34
6	+	–	+	–	+	62.46
				+	–	38.08
7	–	+	+	–	+	31.99
				+	–	41.03
8	+	+	+	–	–	70.31
				+	+	81.03

**TABLE 4.21 Effects for Plasma Etching Experiment Separated into Whole Plot and Subplot Effects**

Term	Parameter Estimates	Type of Term
Intercept	49.73875	
Gap ( <i>A</i> )	10.0625	Whole
Gas Flow ( <i>B</i> )	5.6275	Whole
Pressure ( <i>C</i> )	1.325	Whole
Time ( <i>D</i> )	-2.0725	Subplot
RF Power ( <i>E</i> )	5.12625	Subplot
<i>AB</i>	7.34625	Whole
<i>AC</i>	1.83125	Whole
<i>AD</i>	-3.00875	Subplot
<i>AE</i>	6.505	Subplot
<i>BC</i>	-0.60125	Whole
<i>BD</i>	-1.35875	Subplot
<i>BE</i>	-0.2125	Subplot
<i>CD</i>	1.86625	Subplot
<i>CE</i>	-1.485	Subplot
<i>DE</i>	0.34	Whole

Each term in our model is confounded with one other effect. Therefore, both should be examined to determine how the effect will be estimated. If either of the two confounded effects involves only hard-to-change factors, then this term will need to be estimated with a whole-plot degree of freedom. For example, since  $ABC = DE$ , the two-factor interaction involving the two easy-to-change factors,  $DE$ , will be estimated as a whole-plot term.

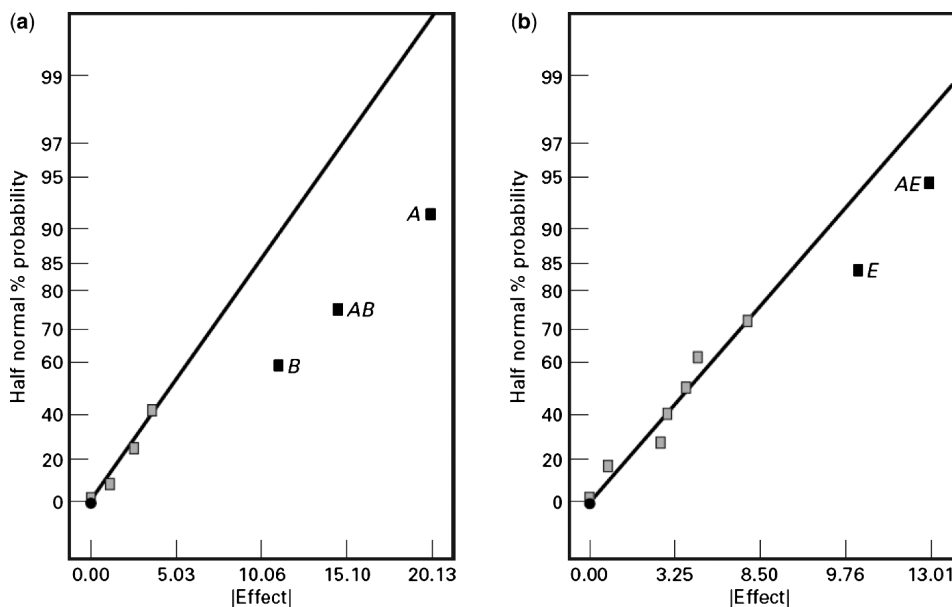


**Figure 4.18** Half-normal plots of the effects from the  $2^{5-1}$  fractional factorial split-plot design for the plasma etching experiment. (a) Whole-plot effects. (b) Subplot effects.

In general, any main effect or interaction that involves only main effects will need to be compared to the whole-plot error. This also includes any terms that are aliased with higher-order terms that involve only whole-plot factors. Terms that involve any combination of factors that include at least one subplot factor in each term of the defining equation should be compared to the subplot error. See Montgomery (2005) for a more thorough discussion.

In this example, all of the two-way interactions involving a hard-to-change and easy-to-change factor are confounded with a three-way interaction involving both hard- and easy-to-change factors, and hence are estimated with subplot terms. For example,  $AD = BCE$  both involve at least one easy-to-change factor. Table 4.21 lists the effects and their estimates, separated into whole- and subplot terms. Since the terms of the model use all of the

**TABLE 4.22 Default 32-Run Design from JMP for the Plasma Etching Experiment**

Whole Plots	Whole-Plot Factors			Subplot Factors	
	A	B	C	D	E
1	–	–	–	–	–
				–	+
				+	–
				+	+
2	–	–	+	–	–
				–	+
				+	–
				+	+
3	–	+	–	–	–
				–	+
				+	–
				+	+
4	–	+	+	–	–
				–	+
				+	–
				+	+
5	+	–	–	–	–
				–	+
				+	–
				+	+
6	+	–	+	–	–
				–	+
				+	–
				+	+
7	+	+	–	–	–
				–	+
				+	–
				+	+
8	+	+	+	–	–
				–	+
				+	–
				+	+

available degrees of freedom, the effects can be assessed via a normal probability plot. Because we have two error terms in the model, one for the whole-plot and one for the subplot, separate normal probability plots are required. Figure 4.18a is a half-normal probability plot of the effects estimates for the whole-plot terms,  $A$ ,  $B$ ,  $C$ ,  $AB$ ,  $AC$ ,  $BC$ , and  $DE$  ( $=ABC$ ). Notice that factors,  $A$ ,  $B$  and the  $AB$  interaction have large effects. Figure 4.18b is the half-normal probability plot of the subplot effects,  $D$ ,  $E$ ,  $AD$ ,  $AE$ ,  $BD$ ,  $BE$ ,  $CD$ , and  $CE$ . Only the main effect of  $E$  and  $AE$  interaction are large.

The design can be constructed using the JMP software package, by specifying the number of whole plots (8) and total observations (16) desired. The default design recommended by the software is the 32-run design shown in Table 4.22. This 32-run design is actually a full factorial split-plot design with eight whole plots and four subplots per whole plot, not a fractional factorial split-plot. It allows estimation of both the whole-plot and subplot error terms. It should be noted that the comparison between the two designs in Tables 4.20 and 4.22 involves considering the relative increase in cost from 16 to 32 runs, but since both designs just involve eight whole plots, they both involve the same number of changes to the hard-to-change factors. Hence the actual cost of running the smaller design might not be much different than the total cost of the full factorial. In this case, the restriction on the number of test wafers available forces the choice of the FFSP.

## 4.8 SUMMARY

This chapter has introduced the  $2^{k-p}$  fractional factorial design. We have emphasized the use of these designs in screening experiments to identify quickly and efficiently the subset of factors that are active and to provide some information on interaction. The projection property of these designs makes it possible in many cases to examine the active factors in more detail. Sequential assembly of these designs via fold-over is a very effective way to gain additional information about interactions that an initial experiment may identify as possibly important.

In practice,  $2^{k-p}$  fractional factorial designs with  $N = 4$ , 8, 16, and 32 runs are highly useful. Table 4.23 summarizes these designs, identifying how many factors can be used with each design to obtain various types of screening experiments. For example, the 16-run design is a full factorial for 4 factors, a one-half fraction for 5 factors, resolution IV fractional design for 6–8 factors, and a resolution III fraction for 9–15 factors. All of these designs may be constructed using the methods discussed in this chapter. Montgomery (2005) gives the alias relationships for many of these designs.

**TABLE 4.23** Useful Factorial and Fractional Factorial Designs from the  $2^{k-p}$  System

Design Type	Number of Factors in Experiment			
	4	8	16	32 runs
Full factorial	2	3	4	5
Half-fraction	3	4	5	6
Resolution IV fraction	—	4	6–8	7–16
Resolution III fraction	3	5–7	9–15	17–31

## EXERCISES

- 4.1** Suppose that in the chemical process development experiment described in Exercise 3.6, it was only possible to run a one-half fraction of the  $2^3$  design. Construct the design and perform the statistical analysis by selecting the relevant runs.
- 4.2** Suppose that in Exercise 3.9, only a one-half fraction of the  $2^4$  design could be run. Construct the design and perform the analysis by selecting the relevant runs.
- 4.3** Consider the plasma etch experiment described in Exercise 3.10. Suppose that only a one-half fraction of the design could be run. Set up the design and analyze the data.
- 4.4** Example 4.2 describes a process improvement study in the manufacture of an integrated circuit. Suppose that only eight runs could be made in this process. Set up an appropriate  $2^{5-2}$  design and find the alias structure. Use the data from Example 4.2 as the observations in this design, and estimate the factor effects. What conclusions can you draw?
- 4.5** **Continuation of Exercise 4.4.** Suppose you have made the eight runs in the  $2^{5-2}$  design in Exercise 4.4. What additional runs would be required to identify the factor effects that are of interest? What are the alias relationships in the combined design?
- 4.6** R. D. Snee ("Experimenting with a Large Number of Variables," in *Experiments in Industry: Design, Analysis and Interpretation of Results*, by R. D. Snee, L. B. Hare, and J. B. Trout, editors, ASQC, 1985) describes an experiment in which a  $2^{5-1}$  design with  $I = ABCDE$  was used to investigate that effects of five factors on the color of a chemical product. The factors are  $A$  = solvent/reactant,  $B$  = catalyst/reactant,  $C$  = temperature,  $D$  = reactant purity, and  $E$  = reactant pH. The results obtained were as follows:

$$\begin{array}{ll}
 e = -0.63 & d = 6.79 \\
 a = 2.51 & ade = 5.47 \\
 b = -2.68 & bde = 3.45 \\
 abe = 1.66 & abd = 5.68 \\
 c = 2.06 & cde = 5.22 \\
 ace = 1.22 & acd = 4.38 \\
 bce = -2.09 & bcd = 4.30 \\
 abc = 1.93 & abcde = 4.05
 \end{array}$$

- (a) Prepare a normal probability plot of the effects. Which effects seem active?
- (b) Calculate the residuals. Construct a normal probability plot of the residuals and plot the residuals versus the fitted values. Comment on the plots.
- (c) If any factors are negligible, collapse the  $2^{5-1}$  design into a full factorial in the active factors. Comment on the resulting design, and interpret the results.
- 4.7** An article in the *Journal of Quality Technology* (Vol. 17, 1985, pp. 198–206) describes the use of a replicated fractional factorial to investigate the effect of five

**TABLE E4.1** The Leot Spring Experiment from Exercise 4.7

A	B	C	D	E	Free Height	
-	-	-	-	-	7.78	7.78
+	-	-	+	-	8.15	8.18
-	+	-	+	-	7.50	7.56
+	+	-	-	-	7.59	7.56
-	-	+	+	-	7.54	8.00
+	-	+	-	-	7.69	8.09
-	+	+	-	-	7.56	7.52
+	+	+	+	-	7.56	7.81
-	-	-	-	+	7.50	7.25
+	-	-	+	+	7.88	7.88
-	+	-	+	+	7.50	7.56
+	+	-	-	+	7.63	7.75
-	-	+	+	+	7.32	7.44
+	-	+	-	+	7.56	7.69
-	+	+	-	+	7.18	7.18
+	+	+	+	+	7.81	7.50

factors on the free height of leaf springs used in a automotive application. The factors are  $A$  = furnace temperature,  $B$  = heating time,  $C$  = transfer time,  $D$  = hold-down time, and  $E$  = quench oil temperature. The data are shown in Table E4.1

- (a) Write out the alias structure for this design. What is the resolution of this design?
  - (b) Analyze the data. What factors influence the mean free height?
  - (c) Calculate the range and standard deviation of the free height for each run. Is there any indication that any of these factors affects variability in the free height?
  - (d) Analyze the residuals from this experiment, and comment on your findings.
  - (e) Is this the best possible design for five factors in 16 runs? Specifically, can you find a fractional design for five factors in 16 runs with a higher resolution than this one?
- 4.8** Reconsider the experiment in Exercise 4.6. Suppose that along with the original 16 runs the experimenter had run four center points with the following observed responses: 5.20, 4.98, 5.26, and 5.40.
- (a) Use the center points to obtain an estimate of pure error.
  - (b) Test for curvature in the response function and lack of fit.
  - (c) What type of model seems appropriate for this purpose?
  - (d) Can you fit the model in part (c) using the data from this experiment?
- 4.9** An article in *Industrial and Engineering Chemistry* ("More on Planning Experiments to Increase Research Efficiency," 1970, pp. 60–65) uses a  $2^{5-2}$  design to investigate the effect of  $A$  = condensation temperature,  $B$  = amount of material 1,  $C$  = solvent volume,  $D$  = condensation time, and  $E$  = amount of

material 2 on yield. The results obtained are as follows:

$$\begin{array}{llll} e = 23.2 & ad = 16.9 & cd = 23.8 & bde = 16.8 \\ ab = 15.5 & bc = 16.2 & ace = 23.4 & abcde = 18.1 \end{array}$$

- (a) Verify that the design generators used were  $I = ACE$  and  $I = BDE$ .
  - (b) Write down the complete defining relation and the aliases for this design.
  - (c) Estimate the main effects.
  - (d) Prepare an analysis of variance table. Verify that the  $AB$  and  $AD$  interactions are available to use as error.
  - (e) Plot the residuals versus the fitted values. Also construct a normal probability plot of the residuals. Comment on the results.
- 4.10** Reconsider the experiment in Exercise 4.9. Suppose that four center points were run, and that the responses are as follows: 20.1, 20.9, 19.8, and 20.4.
- (a) Use the center points to obtain an estimate of pure error.
  - (b) Test for lack of fit and curvature. What conclusions can you draw about the type of model required for yield in this process?
- 4.11** An industrial engineer is conducting an experiment using a Monte Carlo simulation model of an inventory system. The independent variables in her model are the order quantity ( $A$ ), the reorder point ( $B$ ), the setup cost ( $C$ ), the backorder cost ( $D$ ), and the carrying cost rate ( $E$ ). The response variable is average annual cost. To conserve computer time, she decides to investigate these factors using a  $2^{5-2}_{III}$  design with  $I = ABD$  and  $I = BCE$ . The results she obtains are  $de = 95$ ,  $ae = 134$ ,  $b = 158$ ,  $abd = 190$ ,  $cd = 92$ ,  $ac = 187$ ,  $bce = 155$ , and  $abcde = 185$ .
- (a) Verify that the treatment combinations given are correct. Estimate the effects, assuming three-factor and higher interaction are negligible.
  - (b) Suppose that a second fraction is added to the first. The runs in this new design are  $ade = 136$ ,  $e = 93$ ,  $ab = 187$ ,  $bd = 153$ ,  $acd = 139$ ,  $c = 99$ ,  $abce = 191$ , and  $bcde = 150$ . How was this second fraction obtained? Add these runs to the original fraction, and estimate the effects.
  - (c) Suppose that the fraction  $abc = 189$ ,  $ce = 96$ ,  $bcd = 154$ ,  $acde = 135$ ,  $abe = 193$ ,  $bde = 152$ ,  $ad = 137$ , and  $(1) = 98$  was run. How was this fraction obtained? Add these data to the original fraction, and estimate the effects.
- 4.12** Carbon anodes used in a smelting process are baked in a ring furnace. An experiment is run in the furnace to determine which factors influence the weight of packing material that is stuck to the anodes after baking. Six variables are of interest, each at two levels:  $A$  = pitch/fines ratio (0.45, 0.55);  $B$  = packing material type (1, 2);  $C$  = packing material temperature (ambient,  $325^{\circ}\text{C}$ );  $D$  = flue location (inside, outside);  $E$  = pit temperature (ambient,  $195^{\circ}\text{C}$ ); and  $F$  = delay time before packing (zero, 24 hours). A  $2^{6-3}$  design is run, and three replicates are obtained at each of the design points. The weight of packing material stuck to the anodes is measured in grams. The data in run order are as follows:  $abd = (984, 826, 936)$ ;  $abcdef = (1275, 976, 1457)$ ;  $be = (1217, 1201, 890)$ ;  $af = (1474, 1164,$

$1541$ ;  $def = (1320, 1156, 913)$ ;  $cd = (765, 705, 821)$ ;  $ace = (1338, 1254, 1294)$ ; and  $bcd = (1325, 1299, 1253)$ . We wish to minimize the amount of stuck packing material.

- (a) Verify that the eight runs correspond to a  $2^{6-3}_{III}$  design. What is the alias structure?
  - (b) Use the average weight as a response. What factors appear to be influential?
  - (c) Use the range of the weights as a response. What factors appear to be influential?
  - (d) What recommendations would you make to the process engineers?
- 4.13 A 16-run experiment was performed in a semiconductor manufacturing plant to study the effects of six factors on the curvature, or **camber**, of the substrate devices produced. The six variables and their levels are shown in Table E4.2. Each run was replicated four times, and a camber measurement was taken on the substrate. The data are shown in Table E4.3.
- (a) What type of design did the experimenters use?
  - (b) What are the alias relationships in this design?
  - (c) Do any of the process variables affect average camber?
  - (d) Do any of the process variables affect the variability in camber measurements?
  - (e) If it is important to reduce mean camber as much as possible, what recommendations would you make?
  - (f) Fit an appropriate model for both mean camber and the standard deviation of camber. If we would like to reduce the variability in camber while keeping the mean camber as close as possible to  $100 \times 10^{-4}$  in./in., what recommendations would you make?

TABLE E4.2 Factors Levels for the Experiment in Exercise 4.13

Run	Lamination Temperature (°C)	Lamination Time (sec)	Lamination Pressure (ton)	Firing Temperature (°C)	Firing Cycle Time (hr)	Firing Dew Point (°C)
1	55	10	5	1580	17.5	20
2	75	10	5	1580	29	26
3	55	25	5	1580	29	20
4	75	25	5	1580	17.5	26
5	55	10	10	1580	29	26
6	75	10	10	1580	17.5	20
7	55	25	10	1580	17.5	26
8	75	25	10	1580	29	20
9	55	10	5	1620	17.5	26
10	75	10	5	1620	29	20
11	55	25	5	1620	29	26
12	75	25	5	1620	17.5	20
13	55	10	10	1620	29	20
14	75	10	10	1620	17.5	26
15	55	25	10	1620	17.5	20
16	75	25	10	1620	29	26

**TABLE E4.3 Data for the Experiment in Exercise 4.13**

Run	Camber for Replicate (in./in.)				Total ( $10^{-4}$ in./in.)	Mean ( $10^{-4}$ in./in.)	Standard Deviation
	1	2	3	4			
1	0.0167	0.0128	0.0149	0.0185	629	157.25	24.418
2	0.0062	0.0066	0.0044	0.0020	192	48.00	20.976
3	0.0041	0.0043	0.0042	0.0050	176	44.00	4.0825
4	0.0073	0.0071	0.0039	0.0030	223	55.75	25.025
5	0.0047	0.0047	0.0040	0.0089	223	55.75	22.410
6	0.0219	0.0258	0.0147	0.0296	920	230.00	63.639
7	0.0121	0.0090	0.0092	0.0086	389	97.25	16.029
8	0.0255	0.0250	0.0226	0.0169	900	225.00	39.42
9	0.0032	0.0023	0.0077	0.0069	201	50.25	26.725
10	0.0078	0.0158	0.0060	0.0045	341	85.25	50.341
11	0.0043	0.0027	0.0028	0.0028	126	31.50	7.681
12	0.0186	0.0137	0.0158	0.0159	640	160.00	20.083
13	0.0110	0.0086	0.0101	0.0158	455	113.75	31.12
14	0.0065	0.0109	0.0126	0.0071	371	92.75	29.51
15	0.0155	0.0158	0.0145	0.0145	603	150.75	6.75
16	0.0093	0.0124	0.0110	0.0133	460	115.00	17.45

- 4.14** A spin coater is used to apply photoresist to a silicon wafer. This operation usually occurs early in the semiconductor manufacturing process, and the average coating thickness and the variability in the coating thickness have important effects on downstream manufacturing steps. Six variables are used in the experiment. The variables and their high and low levels are shown in Table E4.4. The experimenter decides to use a  $2^{6-1}$  design, and to make three readings on resist thickness on each test wafer. The data are shown in Table E4.5.
- (a) Verify that this is a  $2^{6-1}$  design. Discuss the alias relationships in this design.
  - (b) What factors appear to affect average resist thickness?
  - (c) Since the volume of resist applied has little effect on average thickness, does this have any important practical implications for the process engineers?
  - (d) Project this design into a smaller design involving only significant factors. Display the result graphically. Does this aid in interpretation?
  - (e) Use the range of resist thickness as a response variable. Is there any indication that any of these factors affect the variability in resist thickness?
  - (f) Where would you recommend that the process engineers run the process?

**TABLE E4.4 Factors and Levels for the Experiment in Exercise 4.14**

Factor	Low Level	High Level
Final spin speed	7300 rpm	6650 rpm
Acceleration rate	5	20
Volume of resist applied	3 cc	5 cc
Time of spin	14 s	6 s
Resist batch variation	Batch 1	Batch 2
Exhaust pressure	Cover off	Cover on

**TABLE E4.5** Data for the Experiment in Exercise 4.14

Run	A Volume	B Batch	C Time	D Speed	E Acc.	F Cover	Resist Thickness			
							Left	Center	Right	Average
1	5	Batch 2	14	7350	5	Off	4531	4531	4515	4525.7
2	5	Batch 1	6	7350	5	Off	4446	4464	4428	4446
3	3	Batch 1	6	6650	5	Off	4452	4490	4452	4464.7
4	3	Batch 2	14	7350	20	Off	4316	4328	4308	4317.3
5	3	Batch 1	14	7350	5	Off	4307	4295	4289	4297
6	5	Batch 1	6	6650	20	Off	4470	4492	4495	4485.7
7	3	Batch 1	6	7350	5	On	4496	4502	4482	4493.3
8	5	Batch 2	14	6650	20	Off	4542	4547	4538	4542.3
9	5	Batch 1	14	6650	5	Off	4621	4643	4613	4625.7
10	3	Batch 1	14	6650	5	On	4653	4670	4645	4656
11	3	Batch 2	14	6650	20	On	4480	4486	4470	4478.7
12	3	Batch 1	6	7350	20	Off	4221	4233	4217	4223.7
13	5	Batch 1	6	6650	5	On	4620	4641	4619	4626.7
14	3	Batch 1	6	6650	20	On	4455	4480	4466	4467
15	5	Batch 2	14	7350	20	On	4255	4288	4243	4262
16	5	Batch 2	6	7350	5	On	4490	4534	4523	4515.7
17	3	Batch 2	14	7350	5	On	4514	4551	4540	4535
18	3	Batch 1	14	6650	20	Off	4494	4503	4496	4497.7
19	5	Batch 2	6	7350	20	Off	4293	4306	4302	4300.3
20	3	Batch 2	6	7350	5	Off	4534	4545	4512	4530.3
21	5	Batch 1	14	6650	20	On	4460	4457	4436	4451
22	3	Batch 2	6	6650	5	On	4650	4688	4656	4664.7
23	5	Batch 1	14	7350	20	Off	4231	4244	4230	4235
24	3	Batch 2	6	7350	20	On	4225	4228	4208	4220.3
25	5	Batch 1	14	7350	5	On	4381	4391	4376	4382.7
26	3	Batch 2	6	6650	20	Off	4533	4521	4511	4521.7
27	3	Batch 1	14	7350	20	On	4194	4230	4172	4198.7
28	5	Batch 2	6	6650	5	Off	4666	4695	4672	4677.7
29	5	Batch 1	6	7350	20	On	4180	4213	4197	4196.7
30	5	Batch 2	6	6650	20	On	4465	4496	4463	4474.7
31	5	Batch 2	14	6650	5	On	4653	4685	4665	4667.7
32	3	Batch 2	14	6650	5	Off	4683	4712	4677	4690.7

- 4.15** Consider the leaf spring experiment in Exercise 4.7. Suppose that factor  $E$  (quench oil temperature) is very difficult to control during manufacturing. Where would you set factors  $A$ ,  $B$ ,  $C$ , and  $D$  to reduce variability in the free height as much as possible regardless of the quench oil temperature used?
- 4.16** Construct a  $2^{7-2}$  design by choosing two four-factor interactions as the independent generators. Write down the complete alias structure for this design. Outline the analysis of variance table. What is the resolution of this design?
- 4.17** Consider the  $2^5$  design in Exercise 3.12. Suppose that only a one-half fraction could be run. Furthermore, two days were required to take the 16 observations, and it was necessary to confound the  $2^{5-1}$  design in two blocks. Construct the design and analyze the data.
- 4.18** Analyze the data in the first replicate of Exercise 3.9 as if it came from a  $2_{IV}^{4-1}$  design with  $I = ABCD$ . Project the design into a full factorial in the subset of the original four factors that appear to be significant.

- 4.19** Repeat Exercise 4.18 using  $I = -ABCD$ . Does use of the alternate fraction change your interpretation of the data?
- 4.20** Project the  $2_{\text{IV}}^{4-1}$  design in Example 4.1 into two replicates of a  $2^2$  design in the factors  $A$  and  $B$ . Analyze the data and draw conclusions.
- 4.21** Construct a  $2_{\text{III}}^{6-3}$  design. Determine the effects that may be estimated if a second fraction of this design is run with all signs reversed.
- 4.22** Consider the  $2_{\text{III}}^{6-3}$  design in Exercise 4.21. Determine the effects that may be estimated if a second fraction of this design is run with the signs for factor  $A$  reversed.
- 4.23** Fold over the  $2_{\text{III}}^{7-3}$  design in Table 4.13. Verify that the resulting design is a  $2_{\text{IV}}^{8-4}$  design. Is this a minimal design?
- 4.24** Fold over a  $2_{\text{III}}^{5-2}$  design. Verify that the resulting design is a  $2_{\text{IV}}^{6-2}$  design. Compare this design with the  $2_{\text{IV}}^{6-2}$  design in Table 4.14.
- 4.25** Suppose that you have run a  $2_{\text{IV}}^{4-1}$  design with  $I = ABCD$ , and that you have fit the model  $y = \beta_0 + \beta_1x_1 + \beta_2x_2 + \beta_3x_3 + \beta_4x_4 + \varepsilon$ .
- Assume that the true model for the system is  $E(y) = \beta_0 + \sum_{i=1}^4 \beta_i x_i + \beta_{12}x_1x_2$ . Are the least squares estimates of  $\beta_0$ ,  $\beta_1$ ,  $\beta_2$ ,  $\beta_3$ , and  $\beta_4$  in the fitted model unbiased? Is the result you obtained an “intuitive” one?
  - Assume that the true model is  $E(y) = \beta_0 + \sum_{i=1}^4 \beta_i x_i + \beta_{12}x_1x_2 + \beta_{11}x_1^2 + \beta_{22}x_2^2$ . Are the least squares estimates of  $\beta_0$ ,  $\beta_1$ ,  $\beta_2$ ,  $\beta_3$ , and  $\beta_4$  biased estimates?
- 4.26** Reconsider the experiment described in Exercise 4.13. Suppose that “firing temperature” is hard to change. Construct an appropriate fractional factorial split-plot design for this problem.
- 4.27** Reconsider the spin coating experiment from Exercise 4.14 with the factor “resist batch variation” as hard to change. Construct an appropriate fractional factorial split-plot design for this problem.



---

# 5

---

## PROCESS IMPROVEMENT WITH STEEPEST ASCENT

In previous chapters we dedicated considerable attention to constructing and applying designed experiments with views toward model building. The designs discussed are very efficient for development of empirical equations that relate controllable factors to an important response. Clearly these empirical regression equations serve to provide information about the properties of the system from which the data are taken. Signs and magnitudes of coefficients and the presence or absence of interaction in the system underscore important pieces of information for the user. Often the primary purpose of the model is for interpretations such as these.

There are many other situations in which a model is used for **process optimization** or **process improvement**. The result of a model-building procedure is an equation. A statistical analyst is armed with mathematical and analytical techniques, the purpose of which is to optimize the process. This and other chapters that follow will deal with process optimization for a variety of situations. Here we assume that the practitioner is experimenting with a system (perhaps a new system) in which the goal is not to find a *point of optimum response*, but to search for a new *region* in which the process or product is improved. Perhaps the current working region for designed experiments is only based on an educated guess, or on preliminary experiments on a different manufacturing scale (such as a pilot plant). It is felt that improvement can be found. For example, in a chemical process one seeks to find a new region where improved yields will be experienced.

The experimental design, model-building procedure, and sequential experimentation that are used in searching for a region of improved response constitute the **method of steepest ascent**. The type of designs used are those discussed in Chapters 3 and 4, namely, two-level factorial and fractional factorial designs. One must keep in mind that the strategy involves sequential movement from one region in the factors to another. As a result the total operation may involve more than one experiment. Thus, design

economy and model simplicity may be very important. One begins by assuming that a first-order model (a planar representation) is a reasonable approximation of the system in the initial region of  $x_1, x_2, \dots, x_k$ . Then the method of steepest ascent consists of the following steps:

1. Fit a **first-order model** (a plane or hyperplane) using an orthogonal design. Two-level designs will be quite appropriate, although center runs are often recommended.
2. Compute a path of **steepest ascent** if maximizing the response is required. If minimum response is required, one should compute the path of **steepest descent**. The path of steepest ascent is computed so that one may expect the **maximum increase** in response. Steepest descent produces a path that results in a **maximum decrease** in response.
3. Conduct **experimental runs** along the path. That is, do either single runs or replicated runs, and observe the response value. The results will normally show improving values of the response. At some region along the path the improvement will decline and eventually disappear. This stems from the deterioration of the simple first-order model once one strays too far from the initial experimental region. A good rule of thumb is to continue experimentation along the path of steepest ascent until two consecutive runs result in decreased response values. Often the first experimental run should be taken near the design perimeter (at coordinates corresponding to a value of 1.0 in an important variable) to serve as a confirming experiment.
4. At some point where an approximation of the maximum (or minimum) response is located on the path, a base for a **second experiment** is chosen. The design should again be a first-order design. It is quite likely that center runs for testing curvature, and degrees of freedom for interaction-type lack of fit, are important at this point.
5. A second experiment is conducted, and another first-order model is fitted to the data. A test for lack of fit is made. If the lack of fit is not significant, a second path based on the new model is computed. This is often called a **mid-course correction**. Single or replicated experiments along this second path are conducted. It is quite likely that the improvement will not be as strong as that enjoyed in the first path. After improvement is diminished, one typically has a base for conducting a more elaborate experiment and a more sophisticated process optimization.

This step-by-step procedure is meant to be only a guideline. It is quite possible that only one stage (and hence one path) will be used. Clearly, if interaction or quadratic lack-of-fit contributions are prominent at the second stage, the analyst will likely not conduct experiments along a path that is based on a planar model. Augmentation of the first-order design to allow higher-order models will be discussed in more detail in Chapter 6.

## 5.1 DETERMINING THE PATH OF STEEPEST ASCENT

### 5.1.1 Development of the Procedure

The coordinates along the path of steepest ascent depend on the **signs** and **magnitudes** of the regression coefficients in the fitted first-order model. The following describes the

movement in, say,  $x_j$  ( $j = 1, 2, \dots, k$ ) relative to the movement of the other factors. Remember that the variables are in coded form with the center of the design at  $x_1 = x_2 = \dots = x_k = 0$ .

The movement in  $x_j$  along the path of steepest ascent is proportional to the magnitude of the regression coefficient  $b_j$  with the direction taken matching the sign of the coefficient. Steepest descent requires the direction to be opposite the sign of the coefficient.

For example, if the experiment and the resulting first-order model analysis produces an equation  $\hat{y} = 20 + 3x_1 - 1.5x_2$ , the path of the steepest ascent will result in  $x_1$  moving in a positive direction and  $x_2$  in a negative direction. In addition,  $x_1$  will move twice as fast; that is,  $x_1$  moves two units for every single unit movement in  $x_2$ . Figure 5.1 indicates the nature of the path of steepest ascent for this example. The path is indicated by the arrow. Note that the path is **perpendicular** to lines of constant response. This is clearly the most rapid movement (steepest ascent) toward large response values. For  $k \geq 3$ , these lines become planes (or hyperplanes) and the path of steepest ascent moves perpendicular to these planes.

While a path created by moving  $x_j$  a relative distance that is proportional to the regression coefficient  $b_j$  is a reasonable and intuitive selection, one may appreciate and better understand the procedure through a mathematical development of the procedure. Consider the fitted first-order regression model

$$\hat{y} = b_0 + b_1x_1 + b_2x_2 + \dots + b_kx_k$$

By the path of **steepest ascent** we mean that which produces a maximum estimated response with the constraint that  $\sum_{i=1}^k x_i^2 = r^2$ . Constrained optimization must be used, because maximizing the fitted response  $\hat{y}$  from the first-order model results in all of the  $x$ 's at infinity. In other words, of all points that are a fixed distance  $r$  from the center of the design, we seek that point  $x_1, x_2, x_3, \dots, x_k$  for which  $\hat{y}$  is maximized.

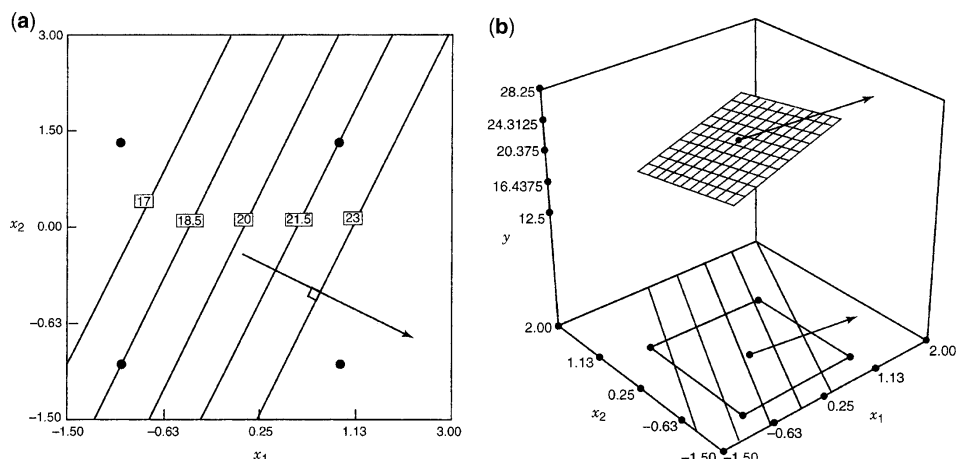


**Figure 5.1** The path of steepest ascent. (a) Contour plot. (b) Three-dimensional response surface view.

Remember that in the metric of the coded design variables the design center is  $(0, 0, \dots, 0)$ . As a result, the constraint given by  $\sum_{i=1}^k x_i^2 = r^2$  is that of a sphere with radius  $r$ .

The solution to this optimization problem involves the use of Lagrange multipliers. Maximization requires the partial derivatives with respect to  $x_j$  ( $j = 1, 2, \dots, k$ ) of

$$L = b_0 + b_1 x_1 + b_2 x_2 + \dots + b_k x_k - \lambda \left( \sum_{i=1}^k x_i^2 - r^2 \right) \quad (5.1)$$

The derivative with respect to  $x_j$  is

$$\frac{\partial L}{\partial x_j} = b_j - 2\lambda x_j \quad (j = 1, 2, \dots, k)$$

Setting  $\partial L / \partial x_j = 0$  gives the following coordinate of  $x_j$  of the path of steepest ascent

$$x_j = \frac{b_j}{2\lambda} \quad (j = 1, 2, \dots, k)$$

Now, the quantity  $1/2\lambda = \rho$  may be viewed as a **constant of proportionality**. That is, the coordinates are given by

$$x_1 = \rho b_1, x_2 = \rho b_2, \dots, x_k = \rho b_k \quad (5.2)$$

where, for **steepest ascent**, the constant  $\rho$  is **positive**. For **steepest descent**,  $\rho$  is taken to be **negative**. Now, this implies that the choice of  $\rho$ , which is related to  $\lambda$ , merely determines the distance from the design center that the resulting point will reside. As a result, of course, the constant  $\rho$  is determined by the practitioner.

One can view the path of steepest ascent as being generated as shown in Fig. 5.2. Suppose again that  $\hat{y} = 20 + 3x_1 - 1.5x_2$ . The points on the path are viewed as locations of maximum values of  $\hat{y}$  at fixed radii. Each point on the path then, is a point of maximum response. Again, note that the path involves a movement in a positive direction for  $x_1$  and a negative direction for  $x_2$ , with a change of two units in  $x_1$  for every single unit change in  $x_2$ .

### 5.1.2 Practical Application of the Method of Steepest Ascent

We now give two examples illustrating the calculations to determine the path of steepest ascent. We also give some practical guidance regarding its use.

**Example 5.1 The Plasma Etch Process** A common processing step in semiconductor manufacture is plasma etching of silicon wafers. The etch rate is the typical response of interest. Table 5.1 presents data from a  $2^2$  factorial design with four center points used to study this process. The process variables of interest are the anode–cathode gap ( $x_1$ ) and the power applied to the cathode ( $x_2$ ). The etch rates observed here are too low, and the experimenter would like to move to a region where the etch rate is around 1000 Å/min.

Table 5.2 shows the condensed analysis of this experiment from Design-Expert. Notice that the interaction term is not significant and there is no indication of lack of fit. Therefore,

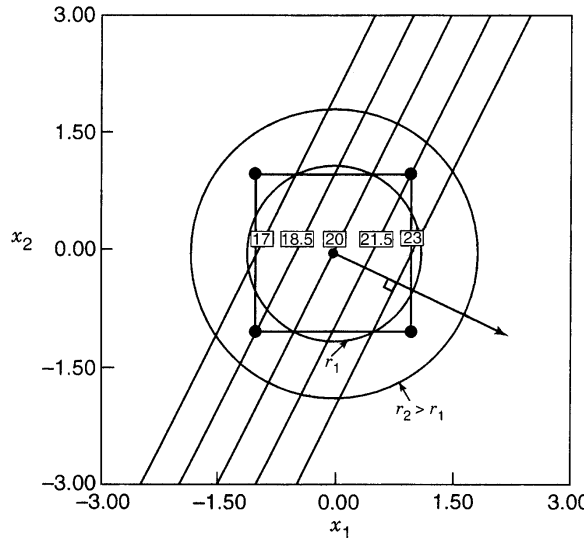


**Figure 5.2** The path of steepest ascent as the path passing through the maximum value of  $y$  at a fixed distance  $r$  from the design center.

we will use the first-order model

$$\hat{y} = 766.25 - 66.25x_1 + 43.75x_2$$

to construct the path of steepest ascent.

Since the sign of  $x_1$  is negative and the sign of  $x_2$  is positive, we will decrease the gap and increase the power in order to increase the etch rate. Furthermore, for every unit of change in the gap ( $x_1$ ), we will change the power by  $43.75/66.25 = 0.66$  units. Consequently, if we choose the gap step size *in coded units* to be  $\Delta x_1 = -1.0$ , then the power step size *in coded units* is  $\Delta x_2 = 0.66$ . In *natural units* the step sizes are  $\Delta \text{gap} = -0.20 \text{ cm}$  and  $\Delta \text{power} = 16.5 \text{ W}$ .

Table 5.3 and Fig. 5.3 show the results of applying steepest ascent to this process. The first point on the path of steepest ascent, denoted Base + $\Delta$  in Table 5.3, has the setting gap = 1.20 cm and power = 316.5 W. The observed response at this point is  $y = 845 \text{ \AA/min}$ . Notice that this is very close to the 840- $\text{\AA}/\text{min}$  contour passing near to this point. It is always a good idea to run the first point on the path near to the original experimental

**TABLE 5.1** The Plasma Etch Experiment

Gap (cm)	Power (W)	$x_1$	$x_2$	$y$ (Etch Rate $\text{\AA}/\text{min}$ )
1.20	275	-1	-1	775
1.60	275	+1	-1	670
1.20	325	-1	+1	890
1.60	325	+1	+1	730
1.40	300	0	0	745
1.40	300	0	0	760
1.40	300	0	0	780
1.40	300	0	0	720

**TABLE 5.2 Analysis of the Etch Rate Experiment**

Response: Etch rate

ANOVA for Selected Factorial Model					
Analysis of Variance Table [Partial sum of squares]					
Source	Sum of Squares	DF	Mean Square	F-Value	Prob > F
Model	25968.75	3	8656.25	13.53	0.0300
A	17556.25	1	17556.25	27.45	0.0135
B	7656.25	1	7656.25	11.97	0.0406
AB	756.25	1	756.25	1.18	0.3564
Curvature	450.00	1	450.00	0.70	0.4632
Pure Error	1918.75	3	639.58		
Cor Total	28337.50	7			
Std. Dev.	25.29	R-Squared		0.9312	
Mean	758.75	Adj R-Squared		0.8624	
C.V.	3.33	Adeq Precision		11.004	
Coefficient		Standard		95% Cl	
Factor	Estimate	DF	Error	95% Cl Low	High
Intercept	766.25	1	12.64	726.01	806.49
A-gap	-66.25	1	12.64	-106.49	-26.01
B-Power	43.75	1	12.64	3.51	83.99
AB	-13.75	1	12.64	-53.99	26.49
Center Point	-15.00	1	17.88	-71.91	41.91
VIF					

Final Equation in Terms of Coded Factors:

$$\begin{aligned} \text{Etch rate} = \\ +766.25 \\ -66.25 * A \\ +43.75 * B \\ -13.75 * A * B \end{aligned}$$

Final Equation in Terms of Actual Factors:

$$\begin{aligned} \text{Etch rate} = \\ -450.00000 \\ +493.75000 * \text{gap} \\ +5.60000 * \text{power} \\ -2.75000 * \text{gap} * \text{power} \end{aligned}$$

region as a **confirmation test**, to ensure that conditions experienced during the original experiment have not changed. At Base  $+2\Delta$  the etch rate response has increased to 950 Å/min, and at base  $+3\Delta$  it has reached 1040 Å/min. Clearly we have arrived at a region close to the desired etch rate of 1000 Å/min.

Because the plasma etch experiment in Example 5.1 has only two process variables, an experimenter could actually implement the method of steepest ascent **graphically**, just by reference to a contour plot such as Fig. 5.3. However, when there are more than  $k = 2$  design factors, a formal procedure can be helpful.

**TABLE 5.3 Computation of the Path of Steepest Ascent for the Plasma Etch Process, Example 5.1**

Point	Coded Variables		Natural Variables		y
	Gap (cm)	Power (W)	$x_1$	$x_2$	
Base (starting point)	1.40	300	0	0	
$\Delta$	-0.20	16.5	-1	0.66	
Base + $\Delta$	1.20	316.5	-1	0.66	845
Base + $2\Delta$	1.00	333	-2	1.32	950
Base + $3\Delta$	0.80	349.5	-3	1.98	1040

It is easy to give a general algorithm for determining the coordinates of a point on the path of steepest ascent. Assume that the point  $x_1 = x_2 = \dots = x_k = 0$  is the base or origin point. Then

1. Choose a step size in one of the process variables, say  $\Delta x_i$ . Usually, we select the variable we know the most about, or we select the variable that has the largest (or nearly the largest) absolute regression coefficient  $|b_i|$ .
2. The step size in the other variables is (from Eq. 5.2)

$$\Delta x_j = \frac{b_j}{b_i/\Delta x_i}, \quad j = 1, 2, \dots, k, \quad i \neq j \quad (5.3)$$

3. Convert the  $\Delta x_j$  from the coded variables to the natural variables.

We will illustrate this procedure with a four-variable example.

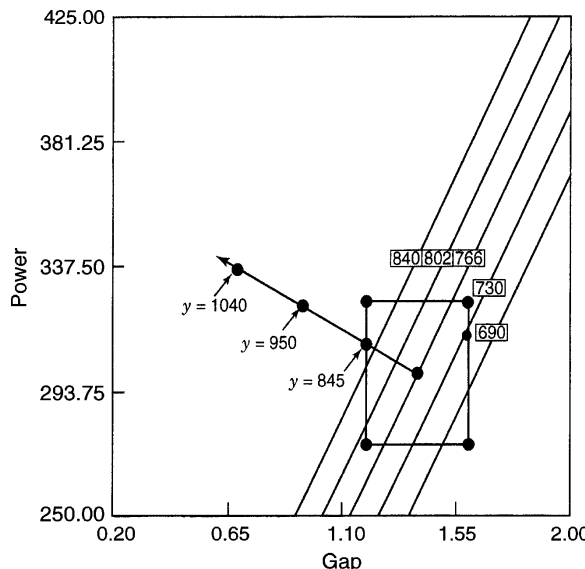


**Figure 5.3** The path of steepest ascent for the plasma etch experiment in Example 5.1.

**Example 5.2 A Four-Variable Illustration of Steepest Descent** Many manufacturing companies use molded parts as components of the process. Shrinkage is often a problem. Often a molded die for a part will be built larger than nominal to allow for part shrinkage. In the following experiment a new die is being produced, and ultimately it is important to find the proper settings to minimize shrinkage. In the following experiment, the response values are deviations from nominal—that is, shrinkage. The factor levels in natural and design units are as follows:

Factor	Design Units	
	-1	+1
$x_1$ : Injection velocity (ft/sec)	1.0	2.0
$x_2$ : Mold temperature (°C)	100	150
$x_3$ : Mold pressure (psi)	500	1000
$x_4$ : Back pressure (psi)	75	120

The design was an unreplicated  $2^4$  factorial. The response is in units of  $10^{-4}$  cm. The actual data are not given, but the first-order model fit to the data is

$$\hat{y} = 80 - 5.28x_1 - 6.22x_2 - 1.21x_3 - 1.07x_4$$

This linear regression model relates predicted shrinkage to the design variables in coded design units. It appears that movement to a region with higher injection velocity and mold temperature will be beneficial. In addition, a slight increase in mold pressure and back pressure may be beneficial. One must keep in mind that we are searching for the path of steepest descent. Then an increase proportional to the regression coefficient in each factor will define the proper path for future experiments.

Suppose that we select  $x_1$  as the variable to define the step size (note that  $x_1$  has one of the two largest regression coefficients). We will let  $\Delta x_1 = 1$ , corresponding to 0.5 ft/sec in injection velocity. Then from Equation 5.3 we have

$$\Delta x_2 = \frac{b_2}{b_1} = \frac{6.22}{5.28} = 1.178 \text{ design units increase in } x_2$$

$$\Delta x_3 = \frac{b_3}{b_1} = \frac{1.21}{5.28} = 0.23 \text{ design units increase in } x_3$$

$$\Delta x_4 = \frac{b_4}{b_1} = \frac{1.07}{5.28} = 0.203 \text{ design units increase in } x_4$$

The corresponding change in terms of the natural units are

$$\Delta(\text{mold temperature}) = (1.178)[(150 - 100)/2] = (1.178)(25) = 29.45$$

$$\Delta(\text{mold pressure}) = (0.23)(250) = 57.5$$

$$\Delta(\text{back pressure}) = (0.203)(22.5) = 4.57$$

Table 5.4 shows the path of steepest descent in terms of both coded (design) units and natural units. The strategy involves making experimental runs along this path until no further improvement in shrinkage is observed.

**TABLE 5.4** The Path of Steepest Descent for Example 5.2

	Coded Units				Natural Units			
	$x_1$	$x_2$	$x_3$	$x_4$	ft/sec	°C	psi	psi
Base	0	0	0	0	1.5	125	750	97.50
Increment = $\Delta$	1.0	1.178	0.23	0.203	0.5	29.45	57.5	4.57
Base + $\Delta$	1.0	1.178	0.23	0.203	2.0	154.45	807.5	102.07
Base + 2 $\Delta$	2.0	2.356	0.46	0.406	2.5	183.90	865.0	106.64
Base + 3 $\Delta$	3.0	3.534	0.69	0.609	3.0	213.35	922.5	111.21
Base + 4 $\Delta$	4.0	4.712	0.92	0.812	3.5	242.80	980.0	115.78

### *Practical Notes Regarding Steepest Ascent*

1. Steepest ascent is a first-order **gradient-based** optimization technique. It works very well when starting a long way from the optimum. When used near an extreme point on the true response surface, steepest ascent will usually result in a very short movement away from the starting point. This could be an indication to consider expanding the model by adding higher-order terms.
2. We have illustrated making **individual observations** at each point on the path. In some cases **replicates**, or **repeat runs**, will be useful. For example, if we are optimizing a process such as chemical vapor deposition, the variability in layer thickness will generally increase with the average thickness of the deposited layer. Using repeat measurements at different sites on the unit or processing several units at the same time and determining both the average and the standard deviation of the response can be very useful.
3. Other first-order optimization techniques can be employed as alternatives to steepest descent. These more automatic **hill-climbing procedures** do not provide the feedback of process information about factor effects obtained from the factorial design.
4. Some experimenters will adjust the step size after the first few steps, depending on the results obtained. For example, if the response is changing slowly, the step size can be lengthened. This should be done very carefully, however, as it is easy to overshoot the region of the optimum if the step size is too big. If no other information is available, choosing the variable with the largest coefficient for setting  $\Delta x$  may be an appropriate conservative choice.

## 5.2 CONSIDERATION OF INTERACTION AND CURVATURE

As we indicated earlier in this chapter, typically that no more than two rounds of the steepest ascent (or descent) procedure will be needed. This general strategy is at its best when the researcher begins experimentation far from the region of optimum conditions. Here one expects the first-order approximation to be quite reasonable. As the experimental region moves near the region of optimum conditions, it is expected that curvature will be more prevalent and, of course, interactions among the factors will become more important. As a result, the experimental design used to carry out the strategy should allow estimation

(and testing) of potentially important interactions. In later stages of the strategy, the design should allow some information regarding model curvature. The use of center runs allows a single-degree-of-freedom estimate of quadratic curvature (see Section 3.6). Clearly, if interactions are found to be important and/or a test for curvature finds significant quadratic terms, the researcher will suspect that the steepest ascent (descent) methodology will become ineffective. Augmentation of the design to allow the fitting of a complete second-order model should then be done.

When second-order terms describing interaction and pure quadratic curvature ( $x_1^2, x_2^2, \dots$ ) begin to **dominate**, then continuing the ascent exercise and experimentation will be self-defeating. However, the question arises, “What do we mean by ‘dominant’?” It is possible that second-order terms can be statistically significant, yet the first-order approximation allows a reasonably successful experimental strategy. One must keep in mind that “statistical significance” only implies that the effects are real in comparison with experimental error. The second-order effects may be small in magnitude compared to their first-order counterparts. As a result, there will certainly be situations where one should compute the path and take experimental trials even though certain second-order effects are significant.

Figure 5.4 shows the contour plot for the plasma etch experiment in Example 5.1 with the interaction term included in the model. The path of steepest ascent is now the curved path shown in the figure. Here the interaction is quite small, so the effect of ignoring it is negligible. Even when interactions are moderately large, ignoring them will usually cause the computed path of steepest ascent to differ only modestly from the true path. In practice, this should have little effect on the final outcome. It can lead to an extra round of steepest ascent to compensate for the errors in estimating the path.

**Example 5.3 Another Four-Variable Illustration of Steepest Ascent** For this example, we consider an illustration of a steepest ascent experiment in which it is of interest to maximize the reaction yield. Four factors,  $A$  (amount of reactant A),  $B$  (reaction time),  $C$  (amount of reactant C), and  $D$  (temperature), are being considered. The natural and coded levels are given as follows:

	Coded Levels	
	-1	+1
Natural Levels	10	15
	1	2
	25	35
	75	85
		(factor A, grams)
		(factor B, minutes)
		(factor C, grams)
		(factor D, °C)

A  $2^{4-1}$  fractional factorial was used as the design, with the yield values given as follows:

$$\begin{array}{ll}
 (1): & 62.0 \quad ad: 61.8 \\
 ab: & 69.0 \quad bc: 64.7 \\
 cd: & 57.0 \quad bd: 62.2 \\
 ac: & 64.5 \quad abcd: 66.3
 \end{array}$$

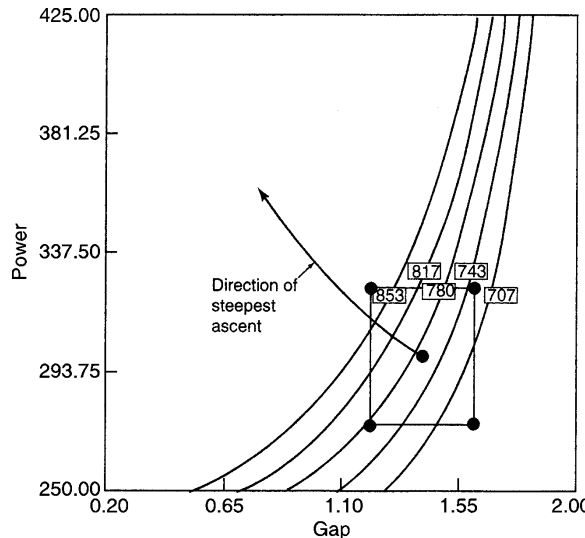


**Figure 5.4** The plasma etch experiment in Example 5.1 with the interaction term included in the model.

The fitted linear regression model is given by

$$\hat{y} = 63.44 + 1.9625x_1 + 2.1125x_2 - 0.3125x_3 - 1.6125x_4$$

The basis for computation of points along the path was chosen to be 1 gram of reactant A. This corresponds to  $1/2.5 = 0.4$  design units. As a result, the corresponding movements in the other design variables are  $(2.1125/1.9625)(0.4) = 0.4306$  design units for  $x_2$ ,  $(-0.3125/1.9625)(0.4) = -0.0637$  design units for  $x_3$ , and  $(-1.6125/1.9625)(0.4) = -0.3287$  design units for  $x_4$ . The movement along the path will be positive for  $x_1$  and  $x_2$ , and negative for  $x_3$  and  $x_4$ . Table 5.5 shows the appropriate coordinates along the path in the natural variables. At some location along the design perimeter, experimental runs should be made. In this case, runs were made at base  $+4\Delta$  (after four increments): Runs 9, 10, 11, and 12 indicate new experimental runs. Theoretically, one expects an increase in response as runs are taken along the path. Eventually, of course, deterioration should occur when the first-order approximation that produced the original path is no longer valid because the true response surface is now influenced by interaction and quadratic curvature. In this case a reduction in yield is experienced after run 11. Any further follow-up experiment should involve an experimental design centered in the vicinity of run 11.

### 5.2.1 What About a Second Phase?

As we indicated earlier, one should expect that the evidence of curvature in the system and interaction among the factors will eventually necessitate an abandonment of steepest ascent. Any additional phases (or mid-course corrections) of the procedure beyond the first will usually not bring about the level of success enjoyed in the initial phase. In addition, one should be careful to use a design in the second phase that allows for testing lack of fit that includes interaction and curvature induced by quadratic terms. In Example 5.3 a reasonable design for the second stage is the other half of the original

**TABLE 5.5 Coordinates on the Path of Steepest Ascent in Natural Variables for Example 5.3**

Run	$x_1$	$x_2$	$x_3$	$x_4$	$y$
Base	12.5	1.5	30	80	
$\Delta$	1.0	(0.4306)(0.5) = 0.215	(−0.0637)(5) = −0.319	(−0.3287)(5) = −1.643	
Base + $\Delta$	13.5	1.715	29.681	78.357	
Base + 2 $\Delta$	14.5	1.930	29.362	76.714	
Base + 3 $\Delta$	15.5	2.145	29.043	75.071	
9 Base + 4 $\Delta$	16.5	2.360	28.724	73.428	74.0
10 Base + 6 $\Delta$	18.5	2.790	28.086	70.142	77.0
11 Base + 8 $\Delta$	20.5	3.220	27.448	73.856	81.0
12 Base + 9 $\Delta$	21.5	3.435	27.129	65.213	78.7

$2^{4-1}$  design (forming a complete  $2^4$ ) augmented by **center runs**. This allows for three degrees of freedom for testing interaction type lack of fit and one degrees of freedom for testing curvature. If the lack of fit is significant, one might expect little or no success with steepest ascent.

### 5.2.2 What Happens Following Steepest Ascent?

It should be emphasized at this point that quality improvement through analysis of designed experiments, when successful, is usually an **iterative** process. This is illustrated quite well in dealing with the strategy of steepest ascent. In our example the investigator may well invest in a  $2^4$  factorial with, say, five center runs for a second phase of steepest ascent. However, if curvature and interaction are found to be quite evident, the steepest ascent procedure will certainly soon be truncated. At this point the investigators will surely be interested in finding optimum conditions through the use of a fitted **second-order model**. This allows computation of estimated optimum conditions. The first-order two-level design with center runs is nicely augmented to allow estimation of second-order terms. For example, a  $2^{4-1}$  fractional factorial (resolution IV) with five center runs is augmented with the alternate fraction and axial runs as shown in Table 5.6.

The complete design allows for efficient estimation of the terms in the model

$$y = \beta_0 + \sum_{i=1}^4 \beta_i x_i + \sum_{i=1}^4 \beta_{ii} x_i^2 + \sum_{i < j=2}^4 \beta_{ij} x_i x_j + \epsilon$$

This is the **second-order response surface model** and it is widely used for process optimization. The design is called the **central composite design**. Process optimization with the second-order model is discussed in Chapter 6. Designs for fitting second-order models, including the central composite design, are discussed in Chapters 7 and 8.

The point made here is that the total strategy of product improvement or optimization can very well involve both steepest ascent (region seeking) and more formal response surface optimization in an iterative procedure. The transition from one to the other can be made quite easily without any waste of experimental effort.

**TABLE 5.6 The Central Composite Design Resulting from Augmenting an Initial  $2^{4-1}$  Design**

$x_1$	$x_2$	$x_3$	$x_4$
-1	-1	-1	-1
1	1	-1	-1
1	-1	1	-1
1	-1	-1	1
-1	1	1	-1
-1	1	-1	1
-1	-1	1	1
1	1	1	1
0	0	0	0
0	0	0	0
0	0	0	0
0	0	0	0
1	-1	-1	-1
-1	1	-1	-1
-1	-1	1	-1
-1	-1	-1	1
1	1	1	-1
1	1	-1	1
-1	1	1	1
1	-1	1	1
-2	0	0	0
2	0	0	0
0	-2	0	0
0	2	0	0
0	0	-2	0
0	0	2	0
0	0	0	-2
0	0	0	2

### 5.3 EFFECT OF SCALE (CHOOSING RANGE OF FACTORS)

The methodology of proceeding along the path of steepest ascent is generally a precursor to a more elaborate experimental effort and optimization involving a more sophisticated model and analysis. In Chapters 3 and 4, considerable attention was paid to two-level designs, with variable screening being an important goal. It was suggested at that point that choosing ranges on the factors is a vital decision and something that the researcher should not take lightly. Clearly, variable screening and steepest ascent are early steps in the process optimization experience. Sloppy decisions with little forethought in these early stages may lead to very inefficient process optimization at a later stage. It should be clear by now to the reader that there is a connection between selection of ranges of the variables and the choice of scale. For example, the coding in Example 5.2 suggests a decision in which one design unit in injection velocity is 0.5 ft/sec. An **equivalent unit** in mold temperature is 25°C. This choice of scale is a decision that is made by the practitioner. Note that the regression coefficient on back pressure ( $x_4$ ) is considerably smaller in magnitude than those of  $x_1$  and  $x_2$ . Perhaps the implication is that the choice of range (and

hence, choice of scale) on back pressure was incorrect. Choosing design factor ranges certainly should improve with increased experience with the system. If variable screening has already been accomplished, then one would expect a more educated choice of scale for the hill-climbing exercise of steepest ascent. One can only use the latest information available.

A change of scale does not change the direction that a factor should move along the path of steepest ascent. However, it changes the relative magnitude of movement of the factor. Suppose now we have an ideal situation with time ( $x_1$ ) and temperature ( $x_2$ ) in which the true regression structure involving yield  $y$  is as follows:

$$E(y) = \beta_0 + \beta x_1 + \beta x_2$$

where  $\beta$  is a coefficient that corresponds to a  $(+1, -1)$  scaling for ranges of temperature of  $50^\circ\text{C}$  and time of 1.0 hr. Suppose researcher A chooses the above ranges with  $(+1, -1)$  scaling while researcher B chooses a  $50^\circ\text{C}$  range of temperature, but a 0.5 range of time, again with  $(+1, -1)$  scaling on the true factors. The model that is relevant to researcher B is given by

$$E(y) = \beta_0 + \beta x_1 + (\beta/2)x_2$$

Thus the expected value of the time regression coefficient  $b_2$  for researcher B is one-half that of the same coefficient for researcher A. As a result, the relative movement in  $x_2$  with respect to  $x_1$  along the path, in design units, will be half as great. As an example, suppose design levels are as follows for the researchers:

Researcher A				
	Natural Levels	Coded Design Units		
Temperature	200°F	250°F	-1	+1
Time	1.0	2.0	-1	+1

Researcher B				
	Natural Levels	Coded Design Units		
Temperature	200°F	250°F	-1	+1
Time	1.25	1.75	-1	+1

Suppose both researchers use  $2^2$  factorial experimental plans. Let us assume that the steepest ascent coordinates are to be based on a change of  $25^\circ\text{F}$  in temperature. The steepest ascent picture is as follows:

	A		B	
Base	225	1.5	225	1.5
$\Delta$	25	0.5	25	0.125
Base + $\Delta$	250	2.0	250	1.625
Base + $2\Delta$	275	2.5	275	1.750

Note that the actual change in time for researcher B is **one-fourth** the change incurred by researcher A. The 0.125 incremental change for researcher B results from the fact that the change per coded unit change in  $x_2$  is only one-half that experienced by researcher A on the average. In addition, the computation of the coordinates for the natural variable must take into account that the design unit described by researcher B is only one-half that described by researcher A. As a result the reader should be able to ascertain the following general rule that reflects the distinction between steepest ascent coordinates in a  $k$ -variable problem.

Suppose researcher A chooses scale factor (range)  $r_1, r_2, \dots, r_k$  and researcher B chooses  $r'_1, r'_2, \dots, r'_k$ , where  $a_j = r_j/r'_j$ . Refer to the relative movements along the path in the natural variables as follows:  $\Delta_1, \Delta_2, \dots, \Delta_k$  and  $\Delta'_1, \Delta'_2, \dots, \Delta'_k$  for researcher A and B, respectively; then  $\Delta_j/\Delta'_j = a_j^2$  for  $j = 1, 2, \dots, k$ .

This does suggest that the user of steepest ascent must use whatever knowledge of the system is at his or her disposal to determine the range of the variable and hence the scale—that is, the definition of a design unit. As we indicated earlier, each experimental experience with a particular system allows for a more educated choice of intervals on the variable being studied. One can view this general procedure as one in which there are truly many paths of steepest ascent (or descent) that will lead to a region where the response is improved. The method itself can be a learning device that will allow for a better choice of ranges in future experiments, particularly those experiments in which the goal is to find optimum process conditions. One should not let that difficulty in choosing ranges prohibit the use of this region-seeking method. The methodology allows the user to be the beneficiary of more appropriate regions and ranges for future experiments.

#### 5.4 CONFIDENCE REGION FOR DIRECTION OF STEEPEST ASCENT

It is useful to take into account sampling variation in assessing the nature of the path of steepest ascent. One must remember that the path is based on the regression coefficients and these coefficients have sampling properties characterized by standard errors. As a result, the path has sampling variation. This sampling variation can lead to a confidence region for the path itself. The value of the confidence region may be derived by plots, say in the case of two or three variables. A graphical analysis may indicate the amount of flexibility the practitioner has in experiments along the path. A tighter region gives the user confidence that the path is being estimated well.

Suppose there are  $k$  design variables and, indeed, coefficients  $b_1, b_2, \dots, b_k$  provide estimates of the relative movement of variables along the path. Assuming that the first-order model is correct, the **true path** is defined by parameters  $\beta_1, \beta_2, \dots, \beta_k$ , and

$$E(b_i) = \beta_i \quad (i = 1, 2, \dots, k)$$

and the true coefficients are proportional to the relative movement along the path (i.e., Eq. 5.2) implies

$$\beta_i = \gamma X_i \quad (i = 1, 2, \dots, k) \tag{5.4}$$

where  $X_i$  are the **direction cosines** of the path. In other words,  $X_1, X_2, \dots, X_k$  are constants that, if known, could be used to compute any coordinates on the true path. We can view the

relationship in Equation 5.4 as a regression model *without an intercept*. The subject of the statistical inference here will be the  $X_i$ . Though the regression structure may appear to be rather unorthodox, we consider the model

$$b_i = \gamma X_i + \varepsilon_i \quad (i = 1, 2, \dots, k) \quad (5.5)$$

The variance of the  $b_i$  is constant across all coefficients if one uses a standard two-level orthogonal design. Call the estimated variance  $s_b^2$ . A second variance,  $s_b^{2*}$ , is found from the error mean square of the regression of Equation 5.5. The quantity  $s_b^{2*}$  is given by

$$s_b^{2*} = \frac{\sum_{i=1}^k (b_i - \hat{\gamma}X_i)^2}{k - 1}$$

where

$$\hat{\gamma} = \frac{\sum_{i=1}^k b_i X_i}{\sum_{i=1}^k X_i^2}$$

Then, of course,  $k - 1$  is the number of error degrees of freedom for the regression. As a result,

$$\frac{s_b^{2*}}{s_b^2} \sim F_{k-1, v_b} \quad (5.6)$$

where  $v_b$  is the number of error degrees of freedom associated with the estimate  $s_b^2$  (from the steepest ascent experiment). Values of  $X_1, X_2, \dots, X_k$  that fall inside the confidence region are those for which the resulting values of  $s_b^{2*}/s_b^2$  do not appear to refute Equation 5.6. In particular, coordinates outside the confidence region are those for which  $s_b^{2*}$  is significantly larger than  $s_b^2$ . As a result, the  $100(1 - \alpha)\%$  confidence region is defined as the set of values  $X_1, X_2, \dots, X_k$  for which

$$\sum_{i=1}^k \frac{(b_i - \hat{\gamma}X_i)^2 / (k - 1)}{s_b^2} \leq F_{\alpha, k-1, v_b} \quad (5.7)$$

where  $F_{\alpha, k-1, v_b}$  is the upper  $100(1 - \alpha)\%$  point of the  $F_{k-1, v_b}$  distribution.

**What Does the Confidence Region Mean?** One must understand that specific coordinates  $X_1, X_2, \dots, X_k$  specify the direction along the path. For example,  $X_1 = \sqrt{0.5}$ ,  $X_2 = \sqrt{0.3}$ , and  $X_3 = \sqrt{0.2}$  specify a direction and also represent coordinates that are a unit distance away from the design origin. (Keep in mind that we remain in design unit scaling.) The confidence region turns out to be a cone (or a hypercone in more than three variables) with the apex at the design origin and all points a unit distance from the origin satisfying

$$\sum_{i=1}^k b_i^2 - \frac{\left(\sum_{i=1}^k b_i X_i\right)^2}{(k-1) \sum_{i=1}^k X_i^2} \leq s_b^2 F_{\alpha, k-1, v_b} \quad (5.8)$$

**Example 5.4 An Example with  $k = 2$**  Consider the path of steepest ascent illustrated in Fig. 5.1. The coefficients are  $b_1 = 3$  and  $b_2 = -1.5$ . Suppose further that the estimates of the variances of the coefficients are both  $\frac{1}{4}$  and there are four error degrees of freedom. The value  $F_{0.05,2,4} = 7.71$ . As a result, the 95% confidence region for the path of steepest ascent at fixed distance  $X_1^2 + X_2^2 = 1.0$  is determined by solutions  $(X_1, X_2)$  to

$$9 + 2.25 - (3X_1 - 1.5X_2)^2 \leq \frac{1}{4}(7.71)$$

or

$$(3X_1 - 1.5X_2)^2 \geq 9.3225 \quad (5.9)$$

As a result, the total confidence region on the path is as illustrated in Fig. 5.5. Similar graphical approaches to the problem are reasonable for  $k = 3$ . See Box and Draper (1987). For  $k > 3$  one cannot display a graphical picture of the confidence region. Of course, one can always substitute any value  $(X_1, X_2, \dots, X_k)$  into Equation 5.7 to determine if the point falls inside the confidence region. In general, it may be rather difficult to determine the relative size of the confidence region, and yet the user needs to have some indication of whether or not it is permissible to continue. Box and Draper describe an interesting analytic procedure for determining what percentage of the possible directions was excluded by the 95% confidence region. This then produces some impression about how “tight” the confidence region is for any specific example. In our simple  $k = 2$  example, this might correspond to the

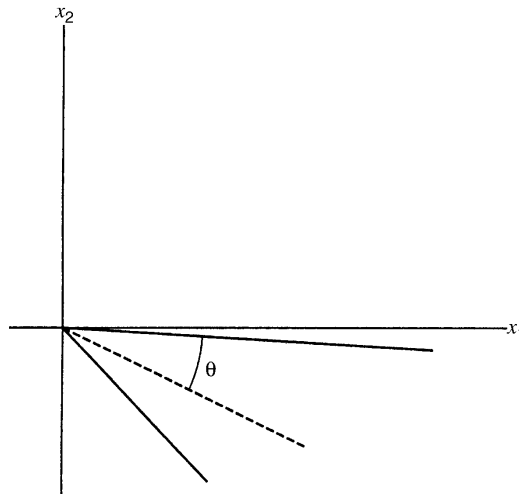
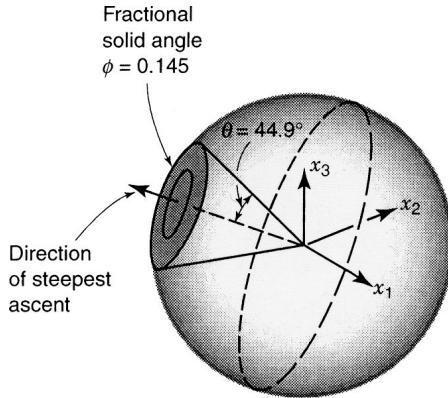


Figure 5.5 Confidence region on path of steepest ascent in Fig. 5.1.



**Figure 5.6** Confidence cone for direction of steepest ascent for  $k = 3$ . [From Box and Draper (1987), with permission.]

determination of the angle  $\theta$  in Fig. 5.5. It turns out that

$$\theta = \arcsin \left\{ \frac{(k-1)s_b^2 F_{\alpha, k-1, v_2}}{\sum_{i=1}^k b_i^2} \right\}^{1/2} \quad (5.10)$$

For our example, we have

$$\begin{aligned} \theta &= \arcsin \left\{ \left[ \left( \frac{1}{4} \right) (7.71) \left( \frac{1}{11.25} \right) \right]^{1/2} \right\} \\ &= \arcsin[0.413] \end{aligned}$$

Thus  $\theta \cong 24.4^\circ$ . As a result, the confidence region illustrated by Fig. 5.5 sweeps an angle of  $2\theta = 48.8^\circ$ . Of interest is the ratio  $48.8/360 = 0.135$ , suggesting that 86.5% of the possible directions taken from the design origin are excluded. Clearly, the larger the percentage excluded, the more accurate the computed path. For  $k = 3$  the confidence region is a cone and the quality of the confidence region depends on the fraction of the area of the total sphere that is taken up by the solid angle created by the confidence cone. Consider, for example, Fig. 5.6. The dashed line represents the computed path. The ratio of the shaded area to the total area of the sphere determines the quality of the computed path.

## 5.5 STEEPEST ASCENT SUBJECT TO A LINEAR CONSTRAINT

Anytime a researcher encounters a task of sequential experimentation that involves considerable movement, there is the possibility that the path will move into an area of the design space where one or more of the variables are not in a permissible range from an engineering or scientific point of view. For example, it is quite possible that an ingredient concentration

may exceed practical limits. As a result, in many situations it becomes necessary to build the path of steepest ascent with a constraint imposed in the design variables. Suppose, in fact, that we view the constraint in the form of a boundary. That is, we are bounded by

$$c_0 + c_1x_1 + c_2x_2 + \cdots + c_kx_k = 0 \quad (5.11)$$

This bound need not involve all  $k$  variables. For example,  $x_j = c_0$  may represent a boundary on a single design variable. One must keep in mind that in practice the constraint must be formulated in terms of the natural (uncoded) variables and then written in the form of coded variables for manipulation.

Figure 5.7 illustrates, for  $k = 2$ , the necessary steepest ascent procedure when a linear constraint is to be applied. The procedure is as follows:

1. Proceed along the usual path of steepest ascent until contact is made with the constraining line (or plane for  $k > 2$ ). Call this point of contact point **O**.
2. Beginning at point **O**, proceed along an adjusted or modified path.
3. Conduct experiments along the modified path, as usual, with the stopping rule based on the same general principles as those discussed in Sections 5.1 and 5.2.

**What is the Modified Path?** Figure 5.7 clearly outlines the modified path for the  $k = 2$  illustration. In general, however, the proper direction vector is one that satisfies the constraint and still makes the greatest possible progress toward maximizing (or minimizing) the response. (Clearly the modified path in our illustration is correct.)

It turns out (and is intuitively reasonable) that the modified path is given by the direction vector

$$b_i - dc_i \quad (i = 1, 2, \dots, k) \quad (5.12)$$

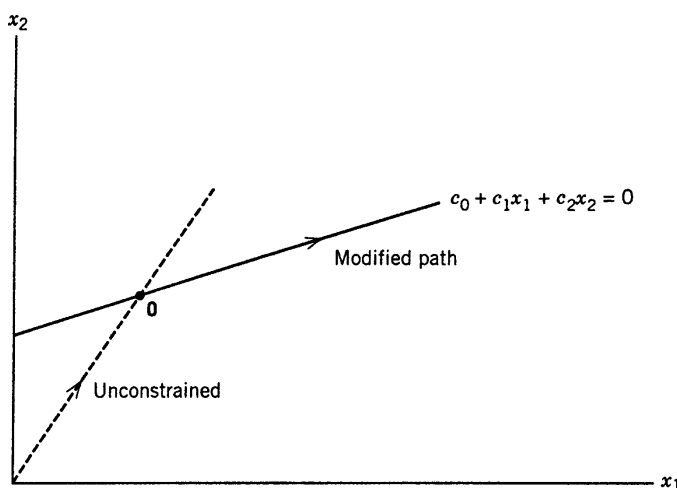


Figure 5.7 Steepest ascent with a linear constraint.

for which

$$\sum_{i=1}^k (b_i - dc_i)^2$$

is minimized. That is, the direction along the constraint line (or plane) is taken so as to be “closest” to the original path. Once again we can consider this to be a simple regression situation in which the  $b_i$  are being regressed against the  $c_i$ . As a result, the quantity  $d$  plays the role of a regression slope, and minimization of the residual sum of squares produces the value

$$d = \frac{\sum_{i=1}^k b_i c_i}{\sum_{i=1}^k c_i^2} \quad (5.13)$$

Thus, the modified path begins at point **O** and proceeds using the direction vector  $b_1 - dc_1$ ,  $b_2 - dc_2, \dots, b_k - dc_k$ .

It remains then to determine the point **O**, that is, the point that lies on the original path but is also on the constraint plane. From Equation 5.2 we know that  $x_j = \rho b_j$  for  $j = 1, 2, \dots, k$ . But we also know that for point **O**, the constraint equation (Eq. 5.10) must hold. As a result, the collision between the original path of steepest ascent and the constraint plane must occur for  $\rho = \rho_0$  satisfying

$$c_0 + (c_1 b_1 + c_2 b_2 + \dots + c_k b_k) \rho_0 = 0$$

Thus,

$$\rho_0 = \frac{-c_0}{\sum_{i=1}^k c_i b_i} \quad (5.14)$$

As a result, the modified path starts at  $x_{j,0} = \rho_0 b_j$  (for  $j = 1, 2, \dots, k$ ) and moves along the modified path, being defined by

$$x_{j,m} = x_{j,0} + \lambda(b_j - dc_j) \quad (j = 1, 2, \dots, k) \quad (5.15)$$

where  $d$  is given by Equation 5.13 and  $\lambda$  is a proportionality constant. Note that the modified path is like the standard path except it does not start at the origin and the regression coefficient  $b_j$  is replaced by  $b_j - dc_j$  in order to accommodate the constraint.

Linear constraints on design variables occur frequently in practice. In the chemical and related fields, constraints are often imposed in situations in which the design variable represents concentrations of components in a system. In a gasoline blending system there will certainly be constraints imposed on the components in the system. General information regarding **designs for mixture problems** will be presented in Chapters 11 and 12. In the example that follows we illustrate steepest ascent in a situation where mixture factors are involved and a linear constraint must be applied to modify the path of steepest ascent.

**Example 5.5 The Fabric Strength Experiment** Consider a situation in which the breaking strength (in grams per square inch) of a certain type of fabric is a function of the amount of three important components in a kilogram of raw material. We will call the components  $\xi_1$ ,  $\xi_2$ , and  $\xi_3$ . The levels used in the experiment are as follows:

Material	Amount in Grams	
	-1	+1
1	100	150
2	50	100
3	20	40

The remaining ingredients in the raw material are known to have no effect on fabric strength. However, it is important that  $\xi_1$  and  $\xi_2$ , the amounts of material 1 and 2 respectively, be constrained by the following equation:

$$\xi_1 + \xi_2 \leq 500$$

The design-factor centering and scaling are given by

$$\begin{aligned}x_1 &= \frac{\xi_1 - 125}{25}, & \xi_1 &= 25x_1 + 125 \\x_2 &= \frac{\xi_2 - 75}{25}, & \xi_2 &= 25x_2 + 75 \\x_3 &= \frac{\xi_3 - 30}{10}, & \xi_3 &= 10x_3 + 30\end{aligned}$$

As a result, the constraint reduces to

$$25x_1 + 25x_2 \leq 300$$

Suppose the fitted regression function is given by

$$\hat{y} = 150 + 1.7x_1 + 0.8x_2 + 0.5x_3$$

Because it is desired to find the condition for increased fabric strength, the unconstrained path of steepest ascent will proceed with increasing values of all three components. The increments along the path are to correspond to changes in  $\xi_1$  of 25 g/in.<sup>2</sup>, or one design unit. This corresponds to changes in  $x_2$  and  $x_3$  of 0.47 and 0.294 units, respectively.

Now, based on the above information, the standard path of steepest ascent can be computed. But at what point does the path make contact with the constraint and with the constraint plane? From Equation 5.14 we obtain

$$\rho_0 = \frac{300}{(25)(1.7) + (25)(0.8)} = \frac{300}{62.5} = 4.8$$

As a result, the modified path starts at

$$x_{j,0} = 4.8b_j \quad (j = 1, 2, 3)$$

**TABLE 5.7 A Constrained Path of Steepest Ascent**

	$x_1$	$x_2$	$x_3$
Base	0	0	0
$\Delta$	1	0.47	0.294
Base + $\Delta$	1	0.47	0.294
Base + $2\Delta$	2	0.94	0.598
:	:	:	:
Base + $5\Delta$	5	2.35	1.470
Point <b>O</b>	8.16	3.84	2.4
	8.61	3.39	2.9
	9.06	2.94	3.4
	9.51	2.49	3.9
	:	:	:

which results in the coordinates (8.16, 3.84, 2.4) in design units. As a result, the coordinates of the modified path are given by Equation 5.14; that is,

$$x_{j,m} = 4.8b_j + \lambda(b_j - dc_j) \quad (j = 1, 2, 3)$$

where

$$d = \frac{(25)(1.7) + (25)(0.8)}{1250} = 0.05$$

As a result, the modified path is given by

$$\begin{aligned} x_{1,m} &= 8.16 + \lambda(0.45) \\ x_{2,m} &= 3.84 + \lambda(-0.45) \\ x_{3,m} &= 2.4 + \lambda(0.5) \end{aligned}$$

Thus, Table 5.7 shows a set of coordinates on the path of steepest ascent, followed by points along the modified path. For the modified path we are using  $\lambda = 1.0$  for convenience. Note that all points on the modified path satisfy the constraint.

## 5.6 STEEPEST ASCENT IN A SPLIT-PLOT EXPERIMENT

In previous sections we have discussed how the method of steepest ascent operates when the experiment used to fit the first-order model is a completely randomized design (CRD). Sometimes in the steepest ascent environment we will encounter easy-to-change and hard-to-change factors. That is, the experimental situation in which the first-order model is fit is a split-plot. The split-plot nature of the experimental situation can necessitate some modification of the steepest ascent procedure. This problem is discussed in detail by Kowalski, Borror and Montgomery (2005). Here we describe their recommendations.

We will let the hard-to-change factors be the whole-plot variables, denoted by  $z_i$ ,  $i = 1, 2, \dots, k_1$  and the easy-to-change factors as the subplot variables, denoted by  $x_j$ ,

$j = 1, 2, \dots, k_2$ . The fitted first-order model is

$$\hat{y} = b_0 + \sum_{i=1}^{k_1} a_i z_i + \sum_{j=1}^{k_2} b_j x_j$$

This model is used to calculate the path of steepest ascent.

Because split-plot experiments contain two types of factors, we let  $\Delta_i$  represent the step size in the whole-plot factors and  $\Delta_j$  to represent the step size in the subplot factors. There are several reasons for the choice of two distinct  $\Delta$ s:

1. It is consistent with the way the experiment was carried out; that is, in a split-plot, which separates the two types of factors.
2. The hard-to-change factors have a different standard error than the easy-to-change factors; therefore, selecting the largest regression coefficient across all factors to define a single step size could be misleading.
3. By their very nature, some factors are hard to change, and so choosing the step size for the path based on the regression coefficient of an easy-to-change factor may lead to a level that is either very difficult or not possible for one of the hard-to-change factors.

For example, it may be easier to change temperature in steps of, say  $10^{\circ}\text{F}$  than to have an easy-to-change factor dictate that temperature be changed in steps of, say,  $6.42^{\circ}\text{F}$ . On the other hand, having a hard-to-change factor dictate the step size in the easy-to-change factors may require the steps to be larger than desired and may force the path to the boundary of the region. Although the experimenter can choose to have a common step size ( $\Delta_i = \Delta_j = \Delta$ ), we will allow for the use of two separate  $\Delta$ s for the reasons mentioned above.

Let  $r_1$  represent the radius for the whole-plot factors,  $\sum_{i=1}^{k_1} z_i^2 = r_1^2$ , and let  $r_2$  represent the radius for the subplot factors,  $\sum_{j=1}^{k_2} x_j^2 = r_2^2$ . Then there are two equations involving Lagrange multipliers:

$$L_1 = b_0 + \sum_{i=1}^{k_1} a_i z_i + \lambda_1 \left( \sum_{i=1}^{k_1} z_i^2 - r_1^2 \right)$$

and

$$L_2 = b_0 + \sum_{i=1}^{k_2} b_i x_i + \lambda_2 \left( \sum_{j=1}^{k_2} x_j^2 - r_2^2 \right)$$

where  $\lambda_1$  and  $\lambda_2$  are the Lagrange multipliers. Because we are assuming a first-order model with no interactions between the whole-plot and subplot factors, these two equations can be solved separately. Therefore, taking partial derivatives of  $L_1$  with respect to each of the  $z_i$  and  $\lambda_1$  will result in the equations

$$\frac{\partial L_1}{\partial z_i} = a_i - 2\lambda_1 z_i = 0$$

and

$$\frac{\partial L_1}{\partial \lambda_1} = - \sum_{i=1}^{k_1} z_i^2 + r_1^2 = 0$$

Likewise, similar equations will result from taking the partial derivatives of  $L_2$  with respect to each  $x_j$  and  $\lambda_2$ . Hence, the solutions will be  $z_i^* = a_i/2\lambda_1$  and  $x_j^* = b_j/2\lambda_2$ . Therefore, two variables,  $z_i^*$ , and  $x_j^*$ , and their amount of change must be chosen to determine the path. There will be two centers or base points; one for the whole-plot factors (Base1) and one for the subplot factors (Base2). Each base point will be  $(0, 0, \dots, 0)$  in the coded variables.

Kowalski et al. (2005) describe an experiment to study the image quality of a printing process. There are five important factors:  $A$  = blanket type (in units of thickness),  $B$  = paper type (in units of thickness),  $C$  = cylinder gap,  $D$  = ink flow, and  $E$  = press speed. Figure 5.8 is a diagram of this part of the printing press. Changing the cylinder gap, ink flow, and press speed is a very simple procedure simply consisting of making an adjustment on a control panel while the printing press is still running. Therefore, these are the easy-to-change factors in the experiment. Changing the blanket type and paper type, on the other hand, requires the press to be stopped and a manual replacement of the blanket and/or paper type. Thus, these two factors are hard-to-change factors. A completely randomized full factorial design would run the 32 treatment combinations in random order, requiring frequent stopping of the press so that the blanket type and/or paper type could be changed. Instead, a split-plot design is used with two whole plot variables,  $z_1$  and  $z_2$  ( $A$  and  $B$ ), and three subplot variables,  $x_1$ ,  $x_2$ , and  $x_3$  ( $C$ ,  $D$ , and  $E$ ). The levels of these factors in the natural units are provided in Table 5.8. Let

$$\hat{y} = 60 + 4.2z_1 + 6.8z_2 + 1.4x_1 - 3.6x_2 + 2.2x_3 \quad (5.16)$$

be the fitted first-order model. Suppose a change of two natural units in  $z_2$  (the whole-plot variable with the largest effect), equivalent to one coded unit, is chosen for determining the path in the whole-plot variables. Then  $\lambda_1 = 6.8/2(1) = 3.4$ , and the corresponding change in  $z_1$  is  $4.2/2(3.4) = 0.618$ . Now suppose that a change of five natural units in  $x_2$  (the subplot variable with the greatest effect), equivalent to one coded unit, is chosen for

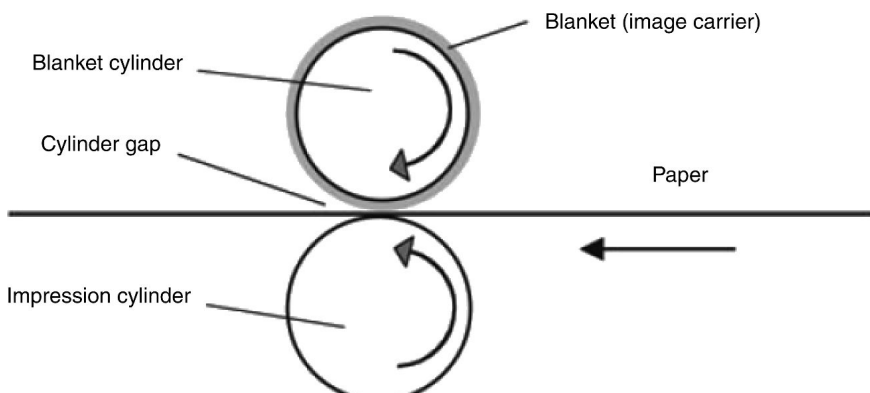


**Figure 5.8** The printing press.

**TABLE 5.8** Printing Press Factor Levels in the Natural Units

	$z_1$	$z_2$	$x_1$	$x_2$	$x_3$
Low	10	4	20	5	2
High	20	8	40	15	6

**TABLE 5.9** Steps in the Coded Variables Along the Path of Steepest Ascent for the Printing Press Example

	$z_1$	$z_2$		$x_1$	$x_2$	$x_3$
Base1	0	0	Base2	0	0	0
$\Delta_i$	0.618	1.0	$\Delta_j$	0.389	-1.0	0.611
Base1 + $\Delta_i$	0.618	1.0	Base2 + $\Delta_j$	0.389	-1.0	0.611
Base1 + 2 $\Delta_i$	1.236	2.0	Base2 + 2 $\Delta_j$	0.778	-2.0	1.222
Base1 + 3 $\Delta_i$	1.854	3.0	Base2 + 3 $\Delta_j$	1.167	-3.0	1.833

determining the path in the subplot variables. Then  $\lambda_2 = -3.6/2(1) = -1.8$  and the change in  $x_j$  is  $b_j/2(|\lambda_2|)$ . So the change in  $x_3$  is  $2.2/2(1.8) = 0.611$  and the change in  $x_1$  is  $1.4/2(1.8) = 0.389$ . Table 5.9 shows the steps for the path of steepest ascent in the coded units.

When the experiment is completely randomized, runs are typically carried out one at a time on the path of steepest ascent. This is not realistic in the split-plot setting. When setting up the order of the split-plot runs, careful consideration has to be given to the restricted randomization. After a setting in the whole-plot factors is determined, several subplots should be run. One must decide how to run the various whole-plot settings as well as which subplot settings will go in each whole plot. Kowalski et al. (2005) propose three methods for carrying out the method of steepest ascent in a split-plot experiment. We will use the model in Equation 5.16 to illustrate the methods. Also, throughout this discussion, we will use  $m = 1$  for the first step along the whole plot and subplot paths. Typically, there are only 4–6 steps along the path before the response starts to drop off.

**Method 1** This method fixes a whole plot setting and carries out the subplot path. Then, using the result from the subplot path it carries out the whole plot path with fixed subplot settings. Using  $m = 1$ , the first whole-plot setting is Base1 +  $\Delta_i$ . Within this setting of the whole-plot factors, many subplots can be used for the subplot path. For example, say we use six subplots: Base2 +  $\Delta_j$ , Base2 + 2 $\Delta_j$ , . . . , Base2 + 6 $\Delta_j$  run in random order. This determines, the subplot setting with the highest response. Now steps are made along the path in the whole-plot factors. The whole-plot path starts with Base1 +  $\Delta_i$  and Base1 + 2 $\Delta_i$ . In each of these whole-plot settings, some replicates, say four, of the highest response setting in the subplot factors from the previous subplot path are run. The average of these four subplot runs serve as the response value for the whole-plot path. Continue running new whole-plot setting along the path until the average response values drop off. This factor setting along the whole-plot path and the previously determined subplot settings from the subplot path could be used as the center for any follow-up experimentation.

Consider the model fit in Equation 5.16. Then, as an example of Method 1, first the runs in Table 5.10 are carried out in random order. The subplot path gives the setting Base2 + 3 $\Delta_j$  because it has the highest response (75). Next, more whole-plot settings are used, all

**TABLE 5.10** First Whole-Plot Run with Setting  $\text{Base1} + \Delta_i$ , Using Method 1

Subplot Runs	$x_1$	$x_2$	$x_3$	Response
$\text{Base2} + \Delta_j$	0.389	-1	0.611	69
$\text{Base2} + 2\Delta_j$	0.778	-2	1.222	73
$\text{Base2} + 3\Delta_j$	1.167	-3	1.833	75
$\text{Base2} + 4\Delta_j$	1.556	-4	2.444	73
$\text{Base2} + 5\Delta_j$	1.945	-5	3.055	70
$\text{Base2} + 6\Delta_j$	2.334	-6	3.666	66

**TABLE 5.11** New Whole-Plot Runs Using Subplot Setting  $\text{Base2} + 3\Delta_j$ , Using Method 1

Subplot Setting	Whole Plot Settings		
	$\text{Base1} + \Delta_i$	$\text{Base1} + 2\Delta_i$	$\text{Base1} + 3\Delta_i$
$\text{Base2} + 3\Delta_j$	76	79	74
$\text{Base2} + 3\Delta_j$	75	77	75
$\text{Base2} + 3\Delta_j$	76	77	74
$\text{Base2} + 3\Delta_j$	75	76	73
Average	75.5	77.25	74.0

with the same subplot setting  $\text{Base2} + 3\Delta_j$ . The average response of the subplots will be the whole-plot response. From Table 5.11, the whole-plot response drops off after  $\text{Base1} + 2\Delta_i$ . Thus, this example produces the setting of  $\text{Base1} + 2\Delta_i$  in the whole-plot variables and the setting of  $\text{Base2} + 3\Delta_j$  in the subplot variables as the center of the follow-up experiment. The design point in coded units for this setting is  $z_1 = 1.236$ ,  $z_2 = 2.0$ ,  $x_1 = 1.167$ ,  $x_2 = -3$ , and  $x_3 = 1.833$ .

The number of steps required in this particular example, using the split-plot Method 1 approach, was five. It is important to keep in mind the split-plot nature in determining the steps to termination of the path. In this example, even though 18 runs were carried out, the path terminates after only two steps in the whole-plot variables and three steps in the subplot variables.

**Method 2** Method 2 essentially reverses the roles of whole and subplots from Method 1. Instead of determining the ideal subplot setting first and then finding the whole-plot setting, method two finds the whole-plot setting first and then determines the subplot setting. Therefore, one would start by running two whole-plot settings,  $\text{Base1} + \Delta_i$  and  $\text{Base1} + 2\Delta_i$ , with each containing, say, four replicates of  $\text{Base2} + \Delta_j$ . Using the average of the subplot runs as the response, continue running whole-plot settings along the whole-plot path until the average response drops off. This will determine the whole-plot setting. Then, in this whole-plot setting, say, six subplots can be run:  $\text{Base2} + \Delta_j$ ,  $\text{Base2} + 2\Delta_j$ , ...,  $\text{Base2} + 6\Delta_j$ . These can be used to determine where the subplot responses drop off. The setting from this subplot path and the previously determined whole-plot setting from the whole-plot path could serve as the center for any follow-up experimentation.

Using Equation 5.16 to provide an example of Method 2, the runs in Table 5.12 are carried out, resulting in  $\text{Base1} + 2\Delta_i$  as the choice for the whole-plot variables. Next, subplot settings are run in random order, all with the same whole-plot setting  $\text{Base1} + 2\Delta_i$  from the whole plot path. From Table 5.13, the subplot response drops off after

**TABLE 5.12 Whole-Plot Runs with setting Base2 +  $\Delta_j$ , Using Method 2**

Subplot Setting	Whole-Plot Settings		
	Base1 + $\Delta_i$	Base1 + 2 $\Delta_i$	Base1 + 3 $\Delta_i$
Base2 + $\Delta_j$	70	73	71
Base2 + 2 $\Delta_j$	72	75	73
Base2 + 3 $\Delta_j$	69	72	70
Base2 + 4 $\Delta_j$	69	72	70
Average	70.0	73.0	71.0

**TABLE 5.13 Subplot Settings at the Best Whole-Plot Setting, Basel + 2 $\Delta_i$ , Using Method 2**

Subplot Runs	$x_1$	$x_2$	$x_3$	Response
Base2 + $\Delta_j$	0.389	-1	0.611	73
Base2 + 2 $\Delta_j$	0.778	-2	1.222	76
Base2 + 3 $\Delta_j$	1.167	-3	1.833	78
Base2 + 4 $\Delta_j$	1.556	-4	2.444	75
Base2 + 5 $\Delta_j$	1.945	-5	3.055	73
Base2 + 6 $\Delta_j$	2.334	-6	3.666	69

Base2 + 3 $\Delta_j$ , so Base1 + 2 $\Delta_i$  in the whole-plot variables and Base2 + 3 $\Delta_j$  in the subplot variables can be used as the center for any follow-up experimentation. The design point for this setting would be  $z_1 = 1.236$ ,  $z_2 = 2.0$ ,  $x_1 = 1.167$ ,  $x_2 = -3$ , and  $x_3 = 1.833$ . In this example, the same termination point is achieved from Methods 1 and 2, although this will not always be the case.

It should be noted that both Methods 1 and 2 rely heavily on the assumption of no interaction between whole-plot and subplot factors. However, when the method of steepest ascent is applied in the usual completely randomized RSM experiments, a strict first-order model is assumed to be adequate. Therefore, the assumption of no interaction between whole-plot and subplot factors is not an additional assumption, and is consistent with typical RSM situations.

**Choosing Between Methods 1 and 2** There is no simple way to choose between Methods 1 and 2 in an optimum fashion, where, by optimum, we mean choosing the method that would result in the most rapid movement to the region of the maximum. The optimum choice depends on the starting point in the true response surface and the shape of this surface. These are, of course, unknown to the experimenter. The authors report examining many types of surfaces and used different starting points to study this question empirically. They report that applying Methods 1 and 2 to these surfaces resulted in very little difference in terms of the total number of runs needed. Figures 5.9 and 5.10 illustrate the two methods on one such surface for one starting point (the bold symbols indicate steps along the whole plot path and the + symbol indicates steps along the subplot path). Figure 5.9 uses Method 1, while Fig. 5.10 illustrates Method 2. Both methods require two steps along the whole plot path and 4–5 steps along the subplot path. From a practical point of view, if the largest standardized regression coefficient (coefficient/standard error of the coefficient) belongs to a hard-to-change factor, Method 2 seems like an obvious choice. This would allow the experimenter to make great leaps in the

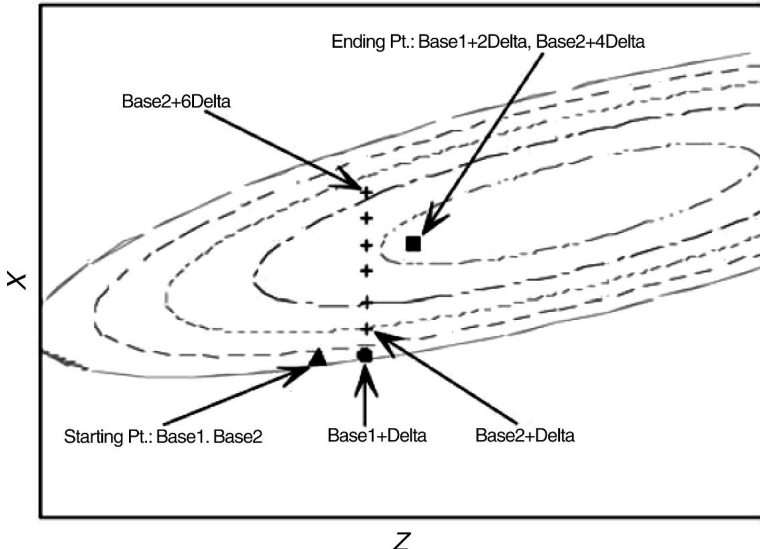


**Figure 5.9** Trajectory using Method 1.

hard-to-change factors toward the optimum and then minor refinements in the easy-to-change factors. On the other hand, if the largest standardized regression coefficient belongs to an easy-to-change factor, Method 1 seems like a better choice because movement in the easy-to-change factors should provide the quicker ascent.

It is possible to combine or switch between the two methods. Suppose while using Method 1 there is very little change in the response as the steps along the path in the

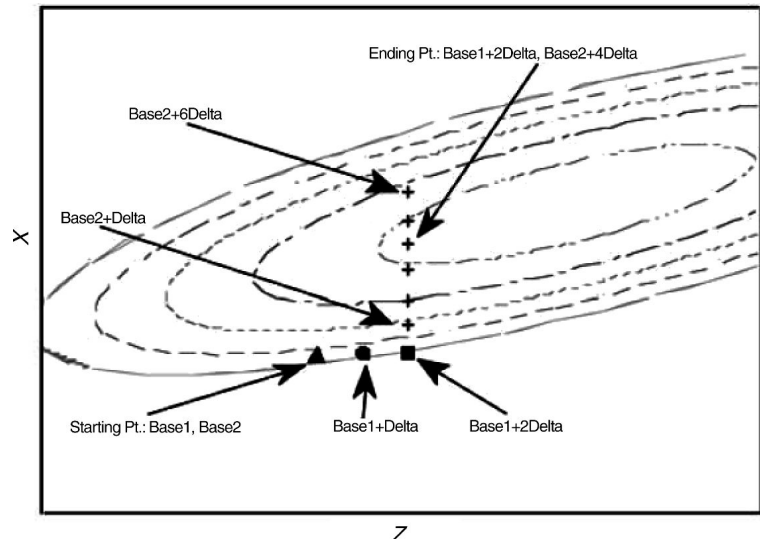


**Figure 5.10** Trajectory using Method 2.

easy-to-change factors are carried out. This may lead the experimenter to switch to Method 2 and implement steps along the path in the hard-to-change factors to move more quickly to an optimum point.

**Method 3** In this method, we propose running a certain number of whole plots, each with the same number of subplots. This can be thought of as one experiment that carries out both paths at the same time. This approach is preferred if the time to obtain responses is lengthy and collecting data in batches is more time- or cost-effective. Suppose it is practical to run four whole plots, each with six subplots. The whole-plot settings of  $\text{Base1} + \Delta_i$ ,  $\text{Base1} + 2\Delta_i$ ,  $\text{Base1} + 3\Delta_i$ , and  $\text{Base1} + 4\Delta_i$  should be randomized. In each of these settings, the subplot settings of  $\text{Base2} + \Delta_j$ ,  $\text{Base2} + 2\Delta_j$ , ...,  $\text{Base2} + 6\Delta_j$  should be separately randomized for each whole-plot setting. We assume there is no whole-plot by subplot interaction, which is consistent with RSM applications and the model in Equation 5.16. There are two ways to determine the response setting that will serve as the center of a follow-up experiment. One approach is to first find the average of the subplot settings for each whole-plot setting. These can be compared to determine the maximum. Next, the average of the same subplot settings across the whole plots can be calculated to determine the maximum in the subplot settings. Combining these two gives an appropriate point. Another approach is to simply take the highest response from the 24 runs and make this the new center for a follow-up experiment.

Using Equation 5.16 as an example, suppose an experiment with four whole plots and six subplots is chosen, with the resulting runs displayed in Table 5.14. In this example, the highest response occurs at  $(\text{Base1} + 2\Delta_i, \text{Base2} + 3\Delta_j)$ . Also, the highest average subplot setting is  $\text{Base2} + 3\Delta_j$ , and the highest average whole-plot setting is  $\text{Base1} + 2\Delta_i$ . The design point at this setting would be  $z_1 = 1.236$ ,  $z_2 = 2.0$ ,  $x_1 = 1.167$ ,  $x_2 = -3$ , and  $x_3 = 1.833$ . This agreement between the highest overall setting and the highest average settings may not occur in all situations. The advantage of Method 3 compared with Methods 1 and 2 is that all the data for the experiment are collected together. This can be important in some industrial settings. For example, in semiconductor manufacturing, multiple runs may be performed on a single-wafer tool during one time period. These runs involve changing both hard-to-change and easy-to-change factors on the tool. The wafers are then sent to a lab for processing, and it may take up to a week to get the response values back. Therefore, it is important to collect all of the data at one time, and it would be impractical to attempt to collect the measurements sequentially, as is required with Methods 1 and 2.

One possible disadvantage of Method 3 is that the response may not drop off after, say, four steps in the hard-to-change factors and/or six steps in the easy-to-change factors.

**TABLE 5.14 Experimental Runs for Method 3 (Bold Numbers Indicate Highest Responses)**

Subplots	$\text{Base1} + \Delta_i$	$\text{Base1} + 2\Delta_i$	$\text{Base1} + 3\Delta_i$	$\text{Base1} + 4\Delta_i$	Average
$\text{Base2} + \Delta_j$	70	72	72	60	70.25
$\text{Base2} + 2\Delta_j$	74	75	73	71	73.25
$\text{Base2} + 3\Delta_j$	74	<b>79</b>	76	75	<b>76.00</b>
$\text{Base2} + 4\Delta_j$	73	75	75	71	73.50
$\text{Base2} + 5\Delta_j$	70	74	73	70	71.75
$\text{Base2} + 6\Delta_j$	67	70	70	67	68.50
Average	71.33	<b>74.16</b>	73.16	70.50	

When using any of these methods, it is useful to have a rule for deciding when to stop conducting experiments along the path. The rule of thumb that we have suggested previously is to continue experimenting along the path of steepest ascent until two consecutive runs have resulted in a decrease in the response.

## EXERCISES

- 5.1** Given the fitted response function

$$\hat{y} = 72.0 + 3.6x_1 - 2.5x_2$$

which is found to fit well in a localized region of  $(x_1, x_2)$ .

- (a) Plot contours of constant response,  $y$ , in the  $(x_1, x_2)$  plane.
- (b) Calculate and plot the path of steepest ascent generated from this response function. Use  $x_1$  to determine the path, with  $\Delta x_1 = 1$ .

- 5.2** Suppose a fitted first-order model is given by

$$y = 25 + 4x_1 + 3x_2 - 2.5x_3$$

Suppose that we wish to maximize the response. Calculate several points along the path of steepest ascent.

- 5.3** Reconsider the model in Exercise 5.1. Construct a path of steepest ascent, using  $x_2$  to define the path, with  $\Delta x_2 = 1$ .
  - (a) Plot this path as the same graph that you constructed in Example 5.1.
  - (b) How different are the two paths that you have constructed?
- 5.4** Consider the injection molding experiment in Example 5.2.
  - (a) Use the coded design units to determine how far the point Base +  $4\Delta$  is from the design center.
  - (b) Suppose that we had selected  $x_2$  to express the points on the path of steepest descent with  $\Delta x_2 = 1$ . Recompute the points in Table E5.4. Use the point Base +  $4\Delta$ , and compute the distance of this point from the design center.
  - (c) How different are the two points you have computed?
- 5.5** In a metallurgy experiment it is desired to test the effect of four factors and their interactions on the concentration (percent by weight) of a particular phosphorus compound in costing material. The variables are:  $A$ , percent phosphorus in the refinement;  $B$ , percent remelted material;  $C$ , fluxing time, and  $D$ , holding time. The four factors are varied in a  $2^4$  factorial experiment with two castings taken at each factor combination. The 32 castings were made in random order, and the data are shown in Table E5.1.
  - (a) Build a first-order response function.
  - (b) Construct a table of the path of steepest ascent in the coded design variables.

**TABLE E5.1 Data for Exercise 5.5**

Treatment Combination	Weight % of Phosphorus Compound		
	Replication 1	Replication 2	Total
(1)	30.3	28.6	58.9
<i>a</i>	28.5	31.4	59.9
<i>b</i>	24.5	25.6	50.1
<i>ab</i>	25.9	27.2	53.1
<i>c</i>	24.8	23.4	48.2
<i>ac</i>	26.9	23.8	50.7
<i>bc</i>	24.8	27.8	52.6
<i>abc</i>	22.2	24.9	47.1
<i>d</i>	31.7	33.5	65.2
<i>ad</i>	24.6	26.2	50.8
<i>bd</i>	27.6	30.6	58.2
<i>abd</i>	26.3	27.8	54.1
<i>cd</i>	29.9	27.7	57.6
<i>acd</i>	26.8	24.2	51.0
<i>bcd</i>	26.4	24.9	51.3
<i>abcd</i>	26.9	29.3	56.2
Total	428.1	436.9	865.0

- (c) It is important to constrain the percentage of phosphorus and the percentage of remelted material. In fact, in the metric of the coded variables we obtain

$$x_1 + x_2 = 2.7$$

where  $x_1$  is percent phosphorus and  $x_2$  is percent remelted material. Recalculate the path of steepest ascent subject to the above constraint.

- 5.6** Consider the  $2^2$  factorial design featured in the illustration in Figure 3.1 in Chapter 3. Factor *A* is the concentration of a reactant, factor *B* is the feed rate, and the response is the viscosity of the output material. As one can tell by the computed effects and the analysis of variance shown, the main effects dominate in the analysis.
- (a) Fit a first-order model.
  - (b) Compute and plot the path of steepest ascent.
  - (c) Suppose that in the metric of the coded variables, the concentration cannot exceed 3.5 and the feed rate cannot go below  $-2.7$ . Show the **practical** path of steepest ascent—that is, the path that takes account of these constraints.
- 5.7** It is stated in the text that the development of the path of steepest ascent makes use of the assumption that the model is truly first-order in nature. However, even if there is a modest amount of curvature or interaction in the system, the use of steepest ascent can be extremely useful in determining a future experimental region. Suppose that in a system involving  $x_1$  and  $x_2$  the actual model is given by

$$E(y) = 14 + 5x_1 - 10x_2 + 3x_1x_2$$

Assume that  $x_1$  and  $x_2$  are in coded form.

- (a) Show a plot of the path of steepest ascent (based on actual parameters) if the interaction is ignored.
  - (b) Show a plot of the path of steepest ascent for the model with interaction. Note that this path is not linear.
  - (c) Comment on the difference in the two paths.
- 5.8** If the first-order model regression coefficients are scaled to a unit vector ( $\sum_{j=1}^k b_j^2 = 1$ ), then any point on the path of steepest ascent is just a multiple of that unit vector. Use this to answer the following questions regarding the model in Exercise 5.1.
- (a) Is the point  $x_1 = 1.23$  and  $x_2 = -3.75$  on the path of steepest ascent?
  - (b) Is the point  $x_1 = 1.75$  and  $x_2 = -4.0$  on the path of steepest ascent?
  - (c) Is the point  $x_1 = 1.44$  and  $x_2 = -1.0$  on the path of steepest ascent?
  - (d) Is the point  $x_1 = 2.0$  and  $x_2 = -1.5$  on the path of steepest ascent?
- 5.9** Consider Example 3.3 in Chapter 3.
- (a) Using a first-order regression model plot the path of steepest ascent.
  - (b) Indicate expected responses in a table for various points on the path.
  - (c) The test for curvature indicated that no quadratic terms are significant. Suppose that, instead of having center runs, four additional runs were placed on the factorial points (one at each point). Will the steepest ascent be improved? Explain.
  - (d) Refer to part (c) above. Give an argument for improvement that takes the confidence region on the path of steepest ascent into account.
- 5.10** Consider Example 3.5 in Chapter 3. There are two design variables and four blocks. The experiment involves complete blocks, and it is assumed that there is no interaction between blocks and the design variables.
- (a) Write the linear regression model for this experiment. Assume blocks are a part of the model. Assume no interaction between the design variables.
  - (b) Show that the path of steepest ascent is the same whether or not blocking is involved in the experiment.
  - (c) Suppose the block effects are extremely important. Explain how blocking will improve the precision of the path of steepest ascent.
- 5.11** Consider the fractional factorial experiment illustrated in Exercise 4.9.
- (a) From the analysis, write out a first-order regression model. All factors are quantitative. Assume that the levels are centered and scaled to  $\pm 1$  levels.
  - (b) Construct a table giving the path of steepest ascent for achieving maximum yield.
  - (c) Suppose, for example, that the  $CE$  interaction is extremely important but the analyst does not realize it. How does this effect the computed path in part (b)? Give a qualitative explanation.
- 5.12** Consider the data in Table E5.2. Apply the method of steepest ascent and create an appropriate path.

**TABLE E5.2** Data for Exercise 5.12

Natural Variables		Coded Variables		Response
$\xi_1$	$\xi_2$	$x_1$	$x_2$	
80	40	-1	-1	15
100	40	1	-1	32
80	60	-1	1	25
100	60	1	1	40
90	50	0	0	33
90	50	0	0	27
90	50	0	0	30

**5.13** Suppose the model you fitted in Exercise 5.12 was the following:

$$\hat{y} = 28 + 8x_1 - 4.5x_2$$

(Note that this is not necessarily the model *you* actually found when you worked this problem. It's just one that we will use in *this* question, under the assumption that it is the correct model.)

- (a) Which variable would you use to define the step size along the path of steepest ascent in this model, and why?
  - (b) Using the variable you selected in part (a), choose a step size that is large enough to take you to the boundary of the experimental region in that particular direction. Find and show the coordinates of this point on the path of steepest ascent in the coded variables  $x_1$  and  $x_2$ .
  - (c) Find and show the coordinates of the point from part (c) in terms of the natural variables.
  - (d) Are the points  $\xi_1 = 107.4$  and  $\xi_2 = 59.8$  on the path of steepest ascent?
- 5.14** Consider the data in Table E5.3, which were observed during an experiment conducted to apply the method of steepest ascent (or descent) to a process.
- (a) Fit a first-order model (without interaction) to these data. Show the model in terms of the coded variables.

**TABLE E5.3** Data for Exercise 5.14

Natural Variables			Coded Variables			Response
$\xi_1$	$\xi_2$	$\xi_3$	$x_1$	$x_2$	$x_3$	
40	10	80	-1	-1	-1	20
60	10	80	1	-1	-1	29
40	30	80	-1	1	-1	18
60	30	80	1	1	-1	32
40	10	120	-1	-1	1	29
60	10	120	1	-1	1	28
40	30	120	-1	1	1	17
60	30	120	1	1	1	25

- (b) Which variables would you retain in your model as being important? Justify your answer.
- 5.15** This problem refers to the design used in Exercise 5.14. Assume that the experimenter also included the center runs shown in Table E5.4 in his/her design.
- Find an estimate of  $\sigma$ , the standard deviation of the process.
  - Use the new observations to test for lack of fit of the first-order model. Specifically, does there seem to be an indication of curvature (either interaction or pure second-order effects) present?
- 5.16** Suppose that you have fit the following model
- $$\hat{y} = 20 + 10x_1 - 4x_2 + 12x_3$$
- The experimenter decides to choose  $x_1$  as the variable to define the step size for steepest ascent. Do you think that this is a good choice for defining step size? Explain why or why not.
  - The experimenter decides to make the step size exactly one coded unit in the  $x_1$  direction. Find the coordinates of this point from the design center on the path of steepest ascent.
  - Suppose that you had used  $x_3$  as the variable to define the direction of steepest ascent. Assuming a step size of one coded unit, find the coordinates of the first step in this direction away from the design center.
  - Find the distance between the two points found in parts (b) and (c), respectively.
- 5.17** Suppose that you have fit the following response surface model in terms of coded design variables:

$$\hat{y} = 100 + 10x_1 + 15x_2 - 4x_3$$

The design used to fit this model was a  $2^3$  factorial.

- The experimenter is going to use the method of steepest ascent. He/she decides to make the step size exactly one coded unit in the  $x_2$  direction. Find the coordinates of this point from the design center on the path of steepest ascent in terms of the *coded* variables.

**TABLE E5.4 Center Runs for the Experiment in Table E5.3**

Natural Variables			Coded Variables			Response
$\xi_1$	$\xi_2$	$\xi_3$	$x_1$	$x_2$	$x_3$	$y$
50	20	100	0	0	0	32
50	20	100	0	0	0	36
50	20	100	0	0	0	39
50	20	100	0	0	0	33

- (b) Suppose that the experimenter had chosen  $x_3$  as the variable to define the step size for steepest ascent. Do you think that this is a good choice for defining step size? Explain why or why not.
- (c) Suppose that the levels of the natural variables  $\xi_1$ ,  $\xi_2$ , and  $\xi_3$  used in the  $2^3$  design were (100, 200), (10, 20), and (50, 80), respectively. What are the coordinates of the point on the path of steepest ascent from part (a) in terms of the *natural* variables?
- (d) Find the coordinates of the unit vector defining the path of steepest ascent.
- (e) Suppose that the experimenters want to run the process at the point (in the natural variables)  $\xi_1 = 204$ ,  $\xi_2 = 23.1$ , and  $\xi_3 = 71.6$ . Assuming that the base point is the design center, is this point on the path of steepest ascent?
- 5.18** Suppose that you have fit the following response surface model in terms of coded design variables:

$$\hat{y} = 250 + 20x_1 + 25x_2 - 8x_3$$

The design used to fit this model was a  $2^3$  factorial.

- (a) The experimenter is using the method of steepest ascent. He/she decides to make the step size exactly one coded unit in the  $x_1$  direction. Find the coordinates of this point from the design center on the path of steepest ascent in terms of *coded* design variables.
- (b) Suppose that the experimenter had chosen  $x_2$  as the variable to define the step size for steepest ascent. Once again, the length of the step is one coded unit. Do you think that this is a better choice for defining step size than was used in part (a)? Explain why or why not.
- (c) Suppose that the levels of the natural variables  $\xi_1$ ,  $\xi_2$ , and  $\xi_3$  used in the  $2^3$  design were (100, 150), (10, 20), and (60, 80), respectively. What are the coordinates of the point on the path of steepest ascent from part (b) in terms of the *natural* variables?
- (d) Find the distance separating the two points that you found in parts (a) and (b).
- 5.19** Suppose that you have fit the following response surface model in terms of coded design variables:

$$\hat{y} = 200 + 25x_1 + 30x_2 - 12x_3$$

The design used to fit this model was a  $2^3$  factorial.

- (a) The experimenter is using the method of steepest ascent. He/she decides to make the step size exactly one coded unit in the  $x_1$  direction. Find the coordinates of this point from the design center on the path of steepest ascent in terms of *coded* design variables.
- (b) Suppose that the experimenter had chosen  $x_2$  as the variable to define the step size for steepest ascent. Once again, the length of the step is one coded unit. Do you think that this is a better choice for defining step size than was used in part (a)? Explain why or why not.
- (c) Suppose that the levels of the natural variables  $\xi_1$ ,  $\xi_2$ , and  $\xi_3$  used in the  $2^3$  design were (100, 200), (10, 12), and (60, 100), respectively. What are the coordinates

of the point on the path of steepest ascent from part (b) in terms of the *natural* variables?

- (d) Find the distance separating the two points that you found in parts (a) and (b).
- 5.20** Consider Example 5.2 in the textbook. In this example, the variable with the second-largest coefficient (in absolute value) was used to define the path of steepest ascent. Rework this example using the factor with the largest absolute value regression coefficient ( $x_2$ ).
- (a) Construct a table similar to Table 5.4 in the textbook that shows the first four steps taken along the path, assuming that the step size in coded units is  $\Delta x_2 = 1$ .
- (b) Find the distance separating the point that you have found after the fourth step from part (a) above and the fourth step from Table 5.4 in the text. Use coded units.
- 5.21** Consider the first-order model

$$\hat{y} = 100 + 5x_1 + 8x_2 - 3x_3$$

This model was fit using a  $2^3$  design in the coded variables  $-1 \leq x_i \leq +1$ ,  $i = 1, 2, 3$ . The model fit was adequate. The region of exploration on the natural variables was

$$\begin{aligned}\xi_1 &= \text{temperature } (100, 110^\circ\text{C}) & \xi_2 &= \text{time } (1, 2 \text{ hr}) \\ \xi_3 &= \text{pressure } (50, 75 \text{ psi})\end{aligned}$$

- (a) Which variable would you choose to define the step size along the path of steepest ascent, and why?
- (b) Using the variable in part (a), choose a step size large enough to take you to the boundary of the experimental region in that particular direction. Find and show the coordinates of this point on the path of steepest ascent in the coded variables  $x_i$ .
- (c) Find and show the coordinates of this point on the path of steepest ascent from part (b) using the natural variables.
- (d) Find a unit vector that defines the path of steepest ascent.
- (e) What step size multiplier for the unit vector in (d) above would give the same point on the path of steepest ascent you found in parts (b) and (c)?

- 5.22** Consider the fitted first-order model

$$\hat{y} = 15.96 + 1.02x_1 + 3.4x_2 - 2.4x_3$$

where  $x_i$  is a coded variable such that  $-1 \leq x_i \leq 1$ , and the natural variables are

Pressure( $x_1$ )	24–30 psig
Time( $x_2$ )	1–2 min
Amount of caustic( $x_3$ )	2–4 lb

If the step size in terms of the natural variable time is 1.5 min, find the coordinates of a point on the path of steepest ascent.

- 5.23** Reconsider the model in Exercise 5.22. Are the following points on the path of steepest ascent?
- (a)  $x_1 = 1.5, x_2 = 3.9, x_3 = -1.8$ .
  - (b)  $x_2 = 3.0, x_2 = 7.5, x_3 = -1.0$ .
  - (c) Pressure = 22 psig, time = 1 min, amount of caustic = 2.2 points.
- 5.24** Consider the data of Exercise 5.12. Show graphically a confidence region for the path of steepest ascent.
- 5.25** Reconsider the data of Exercise 5.12. Perform tests for interaction and curvature. From these tests, do you feel comfortable doing the method of steepest ascent? Explain why or why not.
- 5.26** Reconsider the situation described in Exercise 5.1. Suppose that the variance of the regression coefficients is 0.5 and that there are four error degrees of freedom. Find the 95% confidence region on the path of steepest ascent. What fraction of the possible directions from the design origin are excluded by the path of steepest ascent that you have computed?
- 5.27** Rework Exercise 5.26 assuming that the variance of the regression coefficients is 0.25 with four error degrees of freedom. Compare your new results with those obtained previously. What impact does the improved precision of estimation have on the results?



---

# 6

---

## THE ANALYSIS OF SECOND-ORDER RESPONSE SURFACES

### 6.1 SECOND-ORDER RESPONSE SURFACE

In previous discussions we have confined ourselves to models that either are *first-order* in the design variables or contain first-order plus *interaction* terms. In Chapters 3 and 4, attention was focused on two-level designs. These designs are natural choices for fitting models containing first-order main effects and low-order interactions. Indeed, the material in Chapter 5 dealing with steepest ascent made use of first-order models only. Nevertheless, we have often mentioned the need for fitting second-order response surface models. For example, in Chapter 3 we discussed the use of multiple center runs as, an augmentation of the standard two-level design. Interest centered on the detection of model curvature, that is, the detection of pure quadratic terms  $\beta_{11}x_1^2, \beta_{22}x_2^2, \dots, \beta_{kk}x_k^2$ . Recall that the use of center runs to augment a standard two-level design allows only a single degree of freedom for estimation of (and thus testing of) these second-order coefficients. As a result, efficient estimates of  $\beta_{11}, \beta_{22}, \dots, \beta_{kk}$  separately require additional design points.

In Chapter 5, we indicated that in most attempts at product improvement through the gradient technique, called steepest ascent, the investigator will encounter situations where the lack of fit attributable to curvature from these pure second-order terms is found to be quite significant. In these cases it is likely that the model containing first-order terms and, say, two-factor interaction terms  $\beta_{12}, \beta_{13}, \dots, \beta_{k-1,k}$  is woefully inadequate. As a result, a **second-order response surface model**, discussed in the next section, is a reasonable choice.

## 6.2 SECOND-ORDER APPROXIMATING FUNCTION

In Chapter 1 the notion of approximating polynomial functions was discussed. In response surface methodology (RSM) work it is assumed that the true functional relationship

$$y = f(\mathbf{x}, \boldsymbol{\theta}) + \varepsilon \quad (6.1)$$

is, in fact, unknown. Here the variables  $x_1, x_2, \dots, x_k$  are in centered and scaled **design units**. The genesis of the first-order approximating model or the model that contains first-order terms and low-order interaction terms is the Taylor series approximation of Equation 6.1. Clearly, a Taylor series expansion of Equation 6.1 through second-order terms would result in a model of the type

$$\begin{aligned} y &= \beta_0 + \beta_1 x_1 + \beta_2 x_2 + \cdots + \beta_k x_k + \beta_{11} x_1^2 + \cdots + \beta_{kk} x_k^2 + \beta_{12} x_1 x_2 \\ &\quad + \beta_{13} x_1 x_3 + \cdots + \beta_{k-1, k} x_{k-1} x_k + \varepsilon \\ &= \beta_0 + \sum_{i=1}^k \beta_i x_i + \sum_{i=1}^k \beta_{ii} x_i^2 + \sum_{i < j=2}^k \beta_{ij} x_i x_j + \varepsilon \end{aligned} \quad (6.2)$$

The model of Equation 6.2 is the **second-order response surface model**. Note that it contains all model terms through order two. The term  $\varepsilon$  is the usual random error component. The assumptions on the random error are those discussed in Chapters 2, 3, and 4.

### 6.2.1 The Nature of the Second-Order Function and Second-Order Surface

The model of Equation 6.2 is an interesting and very flexible model to describe experimental data in which there is curvature. We do not mean to imply here that all systems containing curvature are well accommodated by this model. There are often times in which a model nonlinear in the parameters is necessary. In some cases one may even require the use of cubic terms (say  $x_1^2 x_2, x_1^3$ , and so on) to achieve an adequate fit. In other cases the curvature may be quite easily handled through the use of transformation on the response itself; for example, in the case where  $k = 2$ ,

$$\ln y = \beta_0 + \beta_1 x_1 + \beta_2 x_2 + \beta_{12} x_1 x_2 + \varepsilon$$

In other situations, transformation of the design variables may lead to a satisfactory approximating function—for example,

$$y = \beta_0 + \beta_1 \ln x_1 + \beta_2 \ln x_2 + \varepsilon$$

At times transformation of both response and design variables may be needed.

The second-order model described in Equation 6.2 is quite useful and is easily accommodated via the use of a wide variety of experimental designs. Families of designs for fitting the second-order model are discussed in Chapters 7 and 8. Note from Equation 6.2 that the model contains  $1 + 2k + k(k - 1)/2$  parameters. As a result, the experimental design used must contain at least  $1 + 2k + k(k - 1)/2$  distinct design points. In addition, of course, the design must involve at least three levels of each design variable to estimate the pure quadratic terms.

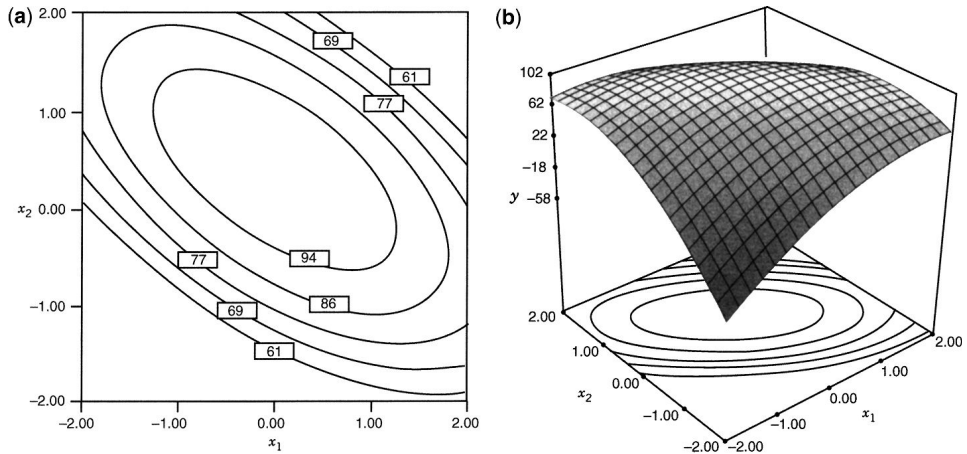


**Figure 6.1** Second-order system displaying a maximum. (a) Contour plot. (b) Response surface.

The geometric nature of the second-order function is displayed in Figs. 6.1, 6.2, and 6.3. This will become vital in Section 6.3 as we discuss the location of estimated optimum conditions. Figures 6.1 and 6.2 show contours of constant response for a hypothetical situation with  $k = 2$  variables. In Fig. 6.1 the center of the system, or **stationary point**, is a point of *maximum response*. In Fig. 6.2 the stationary point is a point of *minimum response*. In both cases the response picture displays concentric ellipses. In Fig. 6.3, a hyperbolic system of contours is displayed. Note that the center is neither a maximum nor a minimum point. In this case, the stationary point is called a **saddle point** and the system of contours is called a **saddle or minimax system**. The detection of the nature of the system and the location of the stationary point are an important part of the second-order analysis. Modern computer graphics blend nicely with this type of analysis. Three-dimensional graphics can be very helpful to the data analyst in the determination and understanding of the nature of a response surface.

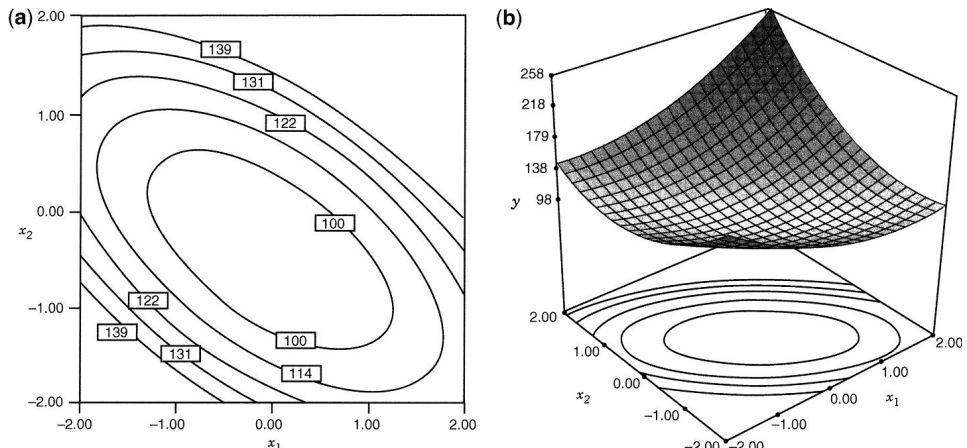


**Figure 6.2** Second-order system displaying a minimum. (a) Contour plot. (b) Response surface.

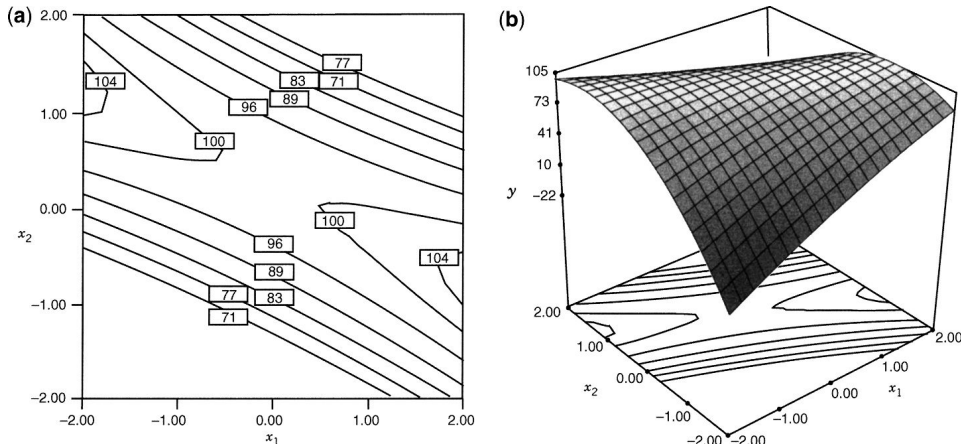


**Figure 6.3** Second-order system displaying a saddle point. (a) Contour plot. (b) Response surface.

### 6.2.2 Illustration of Second-Order Response Surfaces

The nature of the response surface system (maximum, minimum, or saddle point) depends on the signs and magnitudes of the coefficients in the model of Equation 6.2. The second-order coefficients (interaction and pure quadratic terms) play a vital role. One must keep in mind that the coefficients used are *estimates* of the  $\beta$ 's of Equation 6.2. As a result the contours (or surfaces) represent contours of the *estimated response*. Thus, even the system itself (saddle, maximum, or minimum points) is part of the estimation process. The stationary point and the general nature of the system arise as a result of a fitted model, not the true structure.

Consider the example in Fig. 6.1, for which the fitted second-order model is given by

$$\hat{y} = 100 + 5x_1 + 10x_2 - 8x_1^2 - 12x_2^2 - 12x_1x_2$$

An analysis of this response function would determine the location of the stationary point and the nature of the response system. Because  $k = 2$  in this case, some simple graphics deals with both issues. Figure 6.1 shows the response surface with contours of constant  $\hat{y}$  plotted against  $x_1$  and  $x_2$ . It shows that the system produces a stationary point that has maximum estimated response. The stationary point is the solution to

$$\frac{\partial \hat{y}}{\partial x_1} = \frac{\partial \hat{y}}{\partial x_2} = 0$$

This results in the system of *linear* equations

$$\begin{aligned} 16x_1 + 12x_2 &= 5 \\ 12x_1 + 24x_2 &= 10 \end{aligned}$$

yielding the solution for the stationary point

$$x_1 = 0, \quad x_2 = \frac{5}{12}$$

The estimated response at the stationary point is given by  $\hat{y} = 102.08$ .

In the following sections we deal in a general way with the determination of the nature of the response surface contours and the stationary point. Graphical analysis, including contour plotting, plays an important role. However, there are many times when the formal analysis is very helpful. This is particularly true when several ( $k > 2$ ) design variables are involved. The formal analysis can shed much light on the nature of the response surface. Often the nature of the system is elucidated through a combination of analytical techniques and graphical displays. In addition, it is often necessary for the scientist or engineer to use constrained optimization to arrive at potential operating conditions. This is particularly true when the stationary point is a saddle point or point of maximum or minimum response that resides well outside the experimental region, or where several response variables must be simultaneously considered. It turns out that the strategy that results in process and quality improvement simultaneously is profoundly dependent on the nature of the response system.

### 6.3 A FORMAL ANALYTICAL APPROACH TO THE SECOND-ORDER MODEL

Consider again the second-order response surface model of Equation 6.2. However, let us consider the **fitted model** in matrix notation as

$$\hat{y} = b_0 + \mathbf{x}'\mathbf{b} + \mathbf{x}'\hat{\mathbf{B}}\mathbf{x} \quad (6.3)$$

where  $b_0$ ,  $\mathbf{b}$ , and  $\hat{\mathbf{B}}$  are the estimates of the intercept, linear, and second-order coefficients, respectively. In fact  $\mathbf{x}' = [x_1, x_2, \dots, x_k]$ ,  $\mathbf{b}' = [b_1, b_2, \dots, b_k]$ , and  $\hat{\mathbf{B}}$  is the  $k \times k$  symmetric matrix

$$\hat{\mathbf{B}} = \begin{bmatrix} b_{11} & b_{12}/2 & \cdots & b_{1k}/2 \\ b_{21} & b_{22} & \cdots & b_{2k}/2 \\ \vdots & \ddots & \ddots & \vdots \\ b_{k1} & b_{k2}/2 & \cdots & b_{kk} \end{bmatrix} \quad (6.4)$$

Note that the term  $\mathbf{x}'\hat{\mathbf{B}}\mathbf{x}$  contributes the pure quadratics from the diagonals and the two-way interactions from the sum of two off-diagonal elements  $2(\frac{1}{2}b_{ij}x_i x_j)$ .

#### 6.3.1 Location of the Stationary Point

It is straightforward to give a general expression for the location of the stationary point, say  $\mathbf{x}_s$ . One can differentiate  $\hat{y}$  in Equation 6.3 with respect to  $\mathbf{x}$  and obtain

$$\partial\hat{y}/\partial\mathbf{x} = \mathbf{b} + 2\hat{\mathbf{B}}\mathbf{x}$$

Setting the derivative equal to  $\mathbf{0}$ , one can solve for the stationary point of the system:

$$\mathbf{x}_s = -\frac{1}{2}\hat{\mathbf{B}}^{-1}\mathbf{b} \quad (6.5)$$

The **predicted response** at the stationary point is

$$\begin{aligned}\hat{y}_s &= b_0 + \mathbf{x}'_s \mathbf{b} + \mathbf{x}'_s \hat{\mathbf{B}} \mathbf{x}_s \\ &= b_0 + \mathbf{x}'_s \mathbf{b} + (-\frac{1}{2} \mathbf{b}' \hat{\mathbf{B}}^{-1}) \hat{\mathbf{B}} \mathbf{x}_s \\ &= b_0 + \frac{1}{2} \mathbf{x}'_s \mathbf{b}\end{aligned}$$

### 6.3.2 Nature of the Stationary Point (Canonical Analysis)

The nature of the stationary point is determined from the signs of the eigenvalues of the matrix  $\hat{\mathbf{B}}$ . The relative magnitudes of these eigenvalues can be helpful in the total interpretation. For example, let the  $k \times k$  matrix  $\mathbf{P}$  be the matrix whose columns are the normalized eigenvectors associated with the eigenvalues of  $\hat{\mathbf{B}}$ . We know that

$$\mathbf{P}' \hat{\mathbf{B}} \mathbf{P} = \Lambda \quad (6.6)$$

where  $\Lambda$  is a diagonal matrix containing the eigenvalues of  $\hat{\mathbf{B}}$  as main diagonal elements. Now if we translate the model of Equation 6.3 to a new center, namely the stationary point, and rotate the axes corresponding to the principal axes of the contour system, we have

$$\begin{aligned}\mathbf{z} &= \mathbf{x} - \mathbf{x}_s \\ \mathbf{w} &= \mathbf{P}' \mathbf{z}\end{aligned} \quad (6.7)$$

The process is illustrated graphically in Fig. 6.4. The translation gives

$$\begin{aligned}\hat{y} &= b_0 + (\mathbf{z} + \mathbf{x}_s)' \mathbf{b} + (\mathbf{z} + \mathbf{x}_s)' \hat{\mathbf{B}} (\mathbf{z} + \mathbf{x}_s) \\ &= [b_0 + \mathbf{x}'_s \mathbf{b} + \mathbf{x}'_s \hat{\mathbf{B}} \mathbf{x}_s] + \mathbf{z}' \mathbf{b} + \mathbf{z}' \hat{\mathbf{B}} \mathbf{z} + 2\mathbf{x}'_s \hat{\mathbf{B}} \mathbf{z} \\ &= \hat{y}_s + \mathbf{z}' \hat{\mathbf{B}} \mathbf{z}\end{aligned}$$

because  $2\mathbf{x}'_s \hat{\mathbf{B}} \mathbf{z} = -\mathbf{z}' \mathbf{b}$  from Equation 6.5. The rotation gives

$$\begin{aligned}\hat{y} &= \hat{y}_s + \mathbf{w}' \mathbf{P}' \hat{\mathbf{B}} \mathbf{P} \mathbf{w} \\ &= \hat{y}_s + \mathbf{w}' \Lambda \mathbf{w}\end{aligned} \quad (6.8)$$

The  $w$ -axes are the principal axes of the contour system. Equation 6.8 can be written

$$\hat{y} = \hat{y}_s + \sum_{i=1}^k \lambda_i w_i^2 \quad (6.9)$$

where  $\hat{y}_s$  is the estimated response at the stationary point and  $\lambda_1, \lambda_2, \dots, \lambda_k$  are the eigenvalues of  $\hat{\mathbf{B}}$ . The variables  $w_1, w_2, \dots, w_k$  are called **canonical variables**.

The translation and rotation described above leads to Equation 6.9. This equation nicely describes the nature of the stationary point and the nature of the system around the stationary point. The *signs* of the  $\lambda$ 's determine the nature of  $\mathbf{x}_s$ , and the relative magnitude of the eigenvalues help the user gain a better understanding of the response system:

1. If  $\lambda_1, \lambda_2, \dots, \lambda_k$  are all *negative*, the stationary point is a point of *maximum* response.
2. If  $\lambda_1, \lambda_2, \dots, \lambda_k$  are all *positive*, the stationary point is a point of *minimum* response.
3. If  $\lambda_1, \lambda_2, \dots, \lambda_k$  are *mixed* in sign, the stationary point is a *saddle* point.

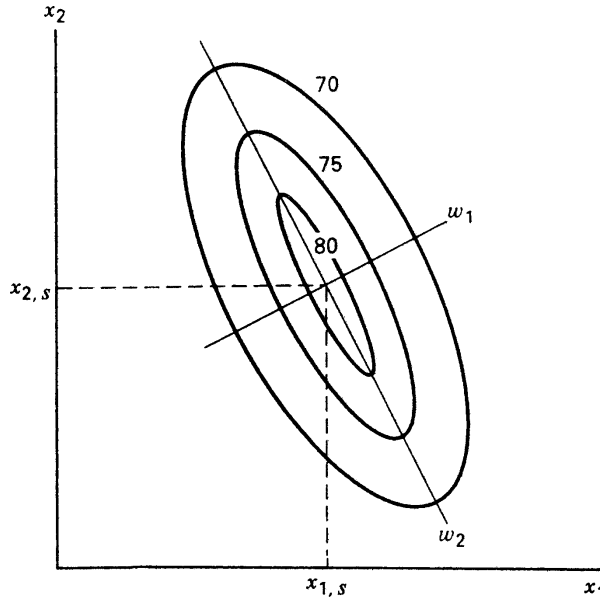


**Figure 6.4** Canonical form of the second-order model.

This entire translation and rotation of axes described here is called a **canonical analysis** of the response system. Obviously, if a saddle system occurs, the experimenter will often be led to an alternative type of analysis. However, even if a maximum or minimum resides at  $\mathbf{x}_s$ , the canonical analysis can be helpful. This is true even when one is dealing with a relatively small number of design variables. For example, suppose  $k = 3$  and one seeks a large value for the response. Suppose also that  $\mathbf{x}_s$  is a point of maximum response (all three eigenvalues are negative) but  $|\lambda_1| \cong 0$  and  $|\lambda_2| \cong 0$ . The implication here is that there is considerable flexibility in locating an acceptable set of operating conditions. In fact, there is essentially an entire plane rather than merely a point where the response is approximately at its maximum value. In fact, it is simple to see that the conditions described by

$$w_3 = 0$$

may in fact describe a rich set of conditions for nearly maximum response. Now, of course,  $w_3 = 0$  describes the plane

$$w_3 = \mathbf{p}'_3 \begin{bmatrix} x_1 - x_{1,s} \\ x_2 - x_{2,s} \\ x_3 - x_{3,s} \end{bmatrix} = 0$$

where the vector  $\mathbf{p}_3$  is the normalized eigenvector associated with the negative eigenvalue  $\lambda_3$ .

**Example 6.1 Canonical Analysis** In Section 2.8 we presented a complete example of fitting a second-order response surface model. The example involved a chemical process in which temperature and concentration were studied, and the response variable was conversion. We used a **central composite design**, originally shown in Table 2.8, but repeated for

**TABLE 6.1** Central Composite Design for Chemical Process Example

Observation	A		B		
	Temperature (°C) $\xi_1$	Conc. (%) $\xi_2$	$x_1$	$x_2$	$y$
1	200	15	-1	-1	43
2	250	15	1	-1	78
3	200	25	-1	1	69
4	250	25	1	1	73
5	189.65	20	-1.414	0	48
6	260.35	20	1.414	0	76
7	225	12.93	0	-1.414	65
8	225	27.07	0	1.414	74
9	225	20	0	0	76
10	225	20	0	0	79
11	225	20	0	0	83
12	225	20	0	0	81

convenience in Table 6.1. The fitted model is

$$\hat{y} = 79.75 + 10.18x_1 + 4.22x_2 - 8.50x_1^2 - 5.25x_2^2 - 7.75x_1x_2$$

and the contour plot for this model is in Fig. 6.5.

*The Central Composite Design.* Before we embark on a discussion of the analysis, we should make a few comments about the experimental design. Notice that there are five levels in an experimental design that involves three components. They are: (i) a  $2^2$  factorial, at levels  $\pm 1$ ; (ii) a one-factor-at-a-time array given by

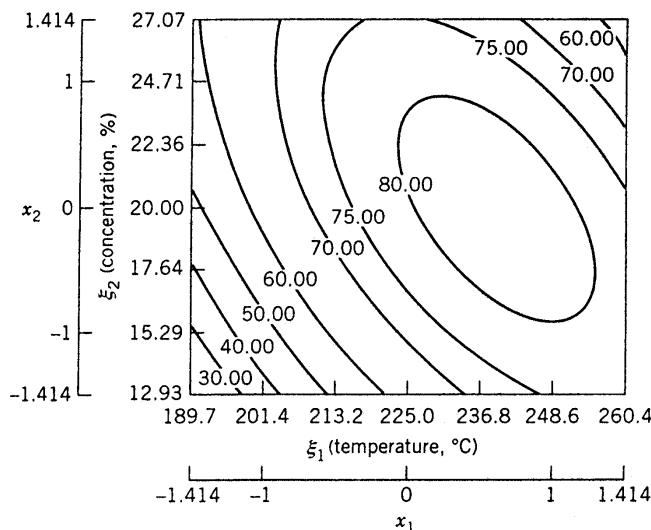


**Figure 6.5** Contour plot of predicted conversion for Example 6.1.

$x_1$	$x_2$
−1.414	0
1.414	0
0	−1.414
0	1.414

and (iii) four center runs. A graphical depiction of this design was given in Fig. 2.7. The design essentially consists of eight equally spaced points on a circle of radius  $\sqrt{2}$  and four runs at the design center. The four design points of type (ii) displayed above are called **axial points**. This terminology stems from the fact that the points lie on the  $x_1$  or the  $x_2$  axis. Note also that in the axial portion of the design the factors are not varying simultaneously but rather in a one-factor-at-a-time array. As a result, no information regarding the  $x_1x_2$  interaction is provided by this portion of the design. However, the axial portion allows for efficient estimation of pure quadratic terms, that is,  $x_1^2$  and  $x_2^2$ . In Chapter 7, we will discuss the central composite design and several other design families in a more thorough way.

*Canonical Analysis.* We begin the canonical analysis by determining the location of the stationary point. Note that

$$\hat{\mathbf{B}} = \begin{bmatrix} -8.50 & -3.875 \\ -3.875 & -5.25 \end{bmatrix}, \quad \mathbf{b} = \begin{bmatrix} 10.12 \\ 4.22 \end{bmatrix}$$

and from Equation 6.6

$$\begin{aligned} \mathbf{x}_s &= -\frac{1}{2}\mathbf{B}^{-1}\mathbf{b} \\ &= -\frac{1}{2} \begin{bmatrix} -0.1773 & 0.1309 \\ 0.1309 & -0.2871 \end{bmatrix} \begin{bmatrix} 10.12 \\ 4.22 \end{bmatrix} \\ &= \begin{bmatrix} 0.6264 \\ -0.0604 \end{bmatrix} \end{aligned}$$

The predicted response at the stationary point  $(x_1, x_2) = (0.6263, -0.0604)$  is  $\hat{y}_s = 82.81$ . In the natural units, the stationary point is

$$\begin{aligned} \text{Temperature} &= 225 + 25x_{1,s} = 225 + 25(0.6263) = 240.7^\circ\text{C} \\ \text{Concentration} &= 20 + 5x_{2,s} = 20 + 5(-0.0604) = 19.7\% \end{aligned}$$

This is in close agreement with the location of the optimum that would be obtained by visual inspection of Fig. 6.5.

The eigenvalues of the matrix  $\hat{\mathbf{B}}$  are the solutions to the equation

$$|\mathbf{B} - \lambda\mathbf{I}| = 0$$

or

$$\left| \begin{bmatrix} -8.50 - \lambda & -3.875 \\ -3.875 & -5.25 - \lambda \end{bmatrix} \right| = 0$$

This reduces to the quadratic equation

$$\lambda^2 + 13.75\lambda + 29.61 = 0$$

The roots of this equation,  $\lambda_1 = -11.0769$  and  $\lambda_2 = -2.6731$ , are the eigenvalues. Thus the canonical form of the second-order model is

$$\begin{aligned}\hat{y} &= \hat{y}_s + \lambda_1 w_1^2 + \lambda_2 w_2^2 \\ &= 82.81 - 11.0769w_1^2 - 2.6731w_2^2\end{aligned}$$

Since both eigenvalues are negative, the stationary point is a maximum (as is obvious from inspection of Fig. 6.5). Furthermore, since  $|\lambda_1| > |\lambda_2|$ , the response changes more quickly as we move along the  $w_1$  canonical direction. The surface is somewhat elongated in the  $w_2$  canonical direction with greater distance between the contour lines.

### 6.3.3 Ridge Systems

Variations of the pure minimum, pure maximum, and saddle point surfaces are fairly common. In fact, we suggested such a situation at the conclusion of the previous section, where there were  $k = 3$  variables and two of the eigenvalues were approximately zero ( $|\lambda_1| \cong 0$ ,  $|\lambda_2| \cong 0$ ). A very small (essentially zero) eigenvalue implies considerable elongation of the response surface in that canonical direction, resulting in a **ridge system**.

**Stationary Ridge** Consider the situation shown in Fig. 6.6 for  $k = 2$ , where  $\lambda_1 < 0$  and  $\lambda_2 < 0$  with  $|\lambda_1| \cong 0$ . The canonical model for this surface is

$$\hat{y} = \hat{y}_s + \lambda_2 w_2^2.$$

The stationary point is in the region of the experimental design. This type of response surface is a **stationary ridge system**. The stationary point is a maximum, and yet there is an approximate maximum on a line *within the design region*. That is, there is essentially a **line maximum**. Consider locations in the design region where  $w_2 = 0$ ; the insensitivity of the response to movement along the  $w_1$ -axis results in little change in response as we move away from the stationary point. The contours of constant response are concentric ellipses that are greatly elongated along  $w_1$ -axis. Sizable changes in response are experienced along the  $w_2$ -axis.

**Rising Ridge** There are other ridge systems that signal certain changes in strategy by the analyst. While the stationary ridge suggests flexibility in choice of operating conditions, the **rising** (or **falling**) ridge suggests that movement outside the experimental region for additional experimentation might warrant consideration. For example, consider a  $k = 2$  situation in which the stationary point is remote from the experimental region. Assume also that one needs to maximize the response. Consider the case where  $\lambda_1$  and  $\lambda_2$  are both negative, but  $\lambda_1$  is near zero. This condition is displayed in Fig. 6.7. The remoteness of the stationary point from the experimental region might suggest here that a movement (experimentally) along the  $w_1$ -axis may well result in an increase in response values. Indeed the rising (or falling) ridge often is a signal to the researcher that he or she has perhaps made a

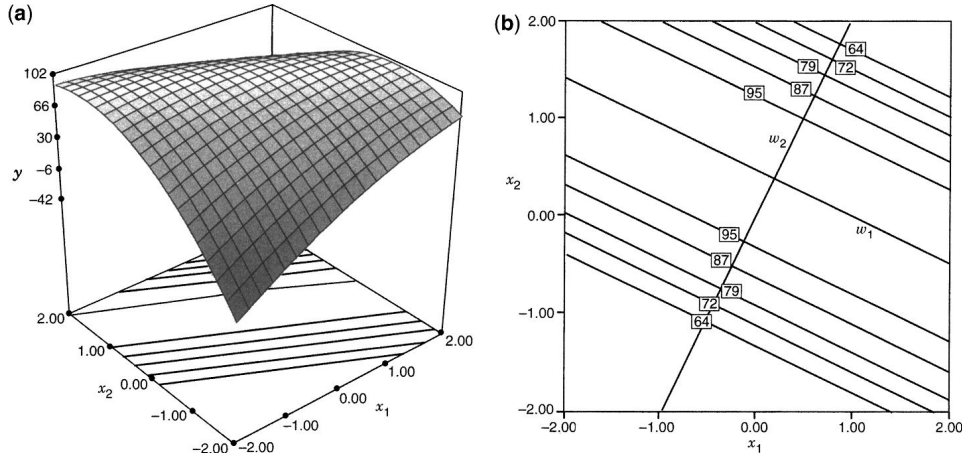


**Figure 6.6** Stationary ridge system for  $k = 2$ . (a) Response surface. (b) Contour plot.

faulty or premature selection of the experimental design region. This is not at all uncommon in applications of RSM.

The rising ridge is signaled by a *stationary point* that is *remote* from the design region. In addition, one of the eigenvalues is near zero. The limiting condition for three variables is displayed in the illustration in Fig. 6.8. Here the eigenvalues for  $w_1$ ,  $w_2$ , and  $w_3$  are  $(-, -, \approx 0)$ . Experimentation along the  $w_3$ -axis toward the stationary point is certainly suggested if these represent feasible operating conditions.

Consider the data in Table 6.2 from an experiment on a square region with two factors,  $A$  and  $B$ , using a central composite design ( $2^2$  factorial, four axial runs) with three center runs. The output from Design-Expert is shown in Table 6.3 with the estimated predicted response of

$$\hat{y} = 50.27 - 12.42A + 8.28B - 4.11A^2 - 9.11B^2 + 11.13AB.$$

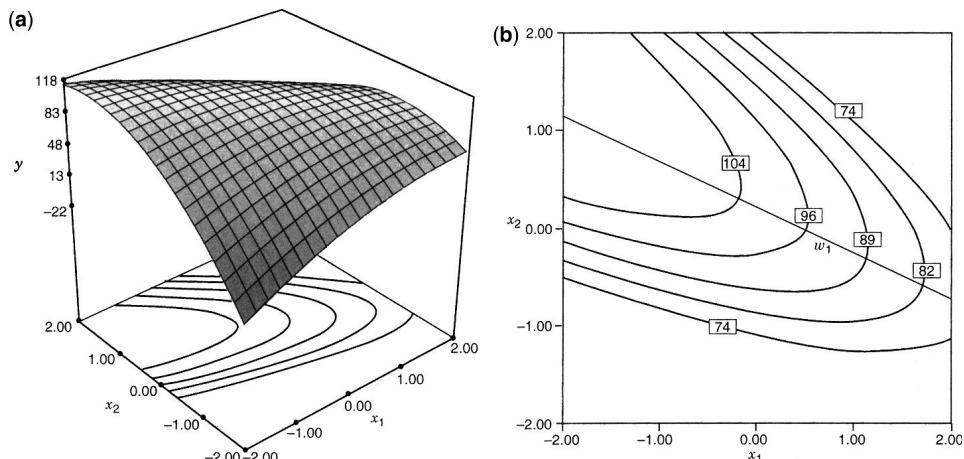


**Figure 6.7** Rising ridge system for  $k = 2$ . (a) Response surface. (b) Contour plot.

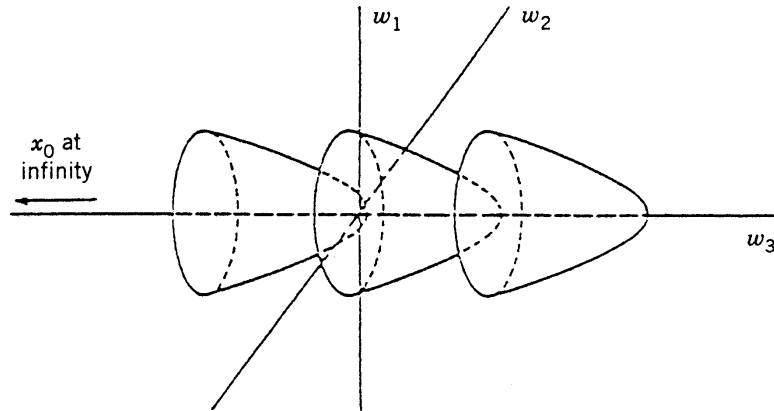


**Figure 6.8** Rising ridge conditions in  $k = 3$  variables.

Solving for the canonical form, we find that the response can be re-expressed as

$$\hat{y} = \hat{y}_s - 0.509w_1^2 - 12.71w_2^2$$

where  $x_s = (-5.18, -2.71)$  and the  $w_1$  and  $w_2$  directions are shown in Fig. 6.9b.

In this case the maximum of the system is located well outside the experimental region, and so it may be helpful to examine both the contour plot of the response for the region where data were observed in Fig. 6.9a and extending the region to include the stationary point in Fig. 6.9b. Note that for each unit moved in the  $w_1$  direction, a 0.509 unit change in the response is observed, while moving a single unit in the  $w_2$  direction results in a 12.71 unit change.

Examples of ridge systems will be seen in illustrations in other portions of this text. In Section 6.3.4 we discuss the role of contour plots in the practical analysis of the second-order fitted surface.

**TABLE 6.2 Design and Data for Rising Ridge System**

Standard Order	Observation #	A	B	Response
1	1	-1	-1	52.3
2	8	1	-1	5.3
3	3	-1	1	46.7
4	7	1	1	44.2
5	9	-1	0	58.5
6	11	1	0	33.5
7	2	0	-1	32.8
8	6	0	1	49.2
9	10	0	0	49.3
10	4	0	0	50.2
11	5	0	0	51.6

**TABLE 6.3** Design-Expert Output for Rising Ridge System

Source	Sum of Squares	DF	Mean Square	F-Value	Prob > F
<i>ANOVA for Response Surface Quadratic Model</i>					
Model	2159.04	5	431.81	750.41	<0.0001
Residual	2.88	5	0.58		
<i>Lack of fit</i>	0.20	3	0.068	0.051	0.9813
<i>Pure Error</i>	2.67	2	1.34		
Cor Total	2161.92	10			
Root MSE	0.76	<i>R-Squared</i>		0.9987	
Dep Mean	43.06	<i>Adj R-Squared</i>		0.9873	
C.V.	1.76	<i>Pred R-Squared</i>		0.9970	
PRESS	6.45	<i>Adeq Precision</i>		95.237	Desire > 4
Factor	Coefficient Estimate	DF	Standard Error	<i>t</i> for $H_0$ Coeff = 0	Prob >   <i>t</i>
Factor	Estimate	DF	Error		VIF
Intercept	50.27	1	0.39		
<i>A-A</i>	-12.42	1	0.31	-40.09	<0.0001
<i>B-B</i>	8.28	1	0.31	26.75	<0.0001
$A^2$	-4.11	1	0.48	-8.63	0.0003
$B^2$	-9.11	1	0.48	-19.12	<0.0001
<i>AB</i>	11.13	1	0.38	29.33	<0.0001

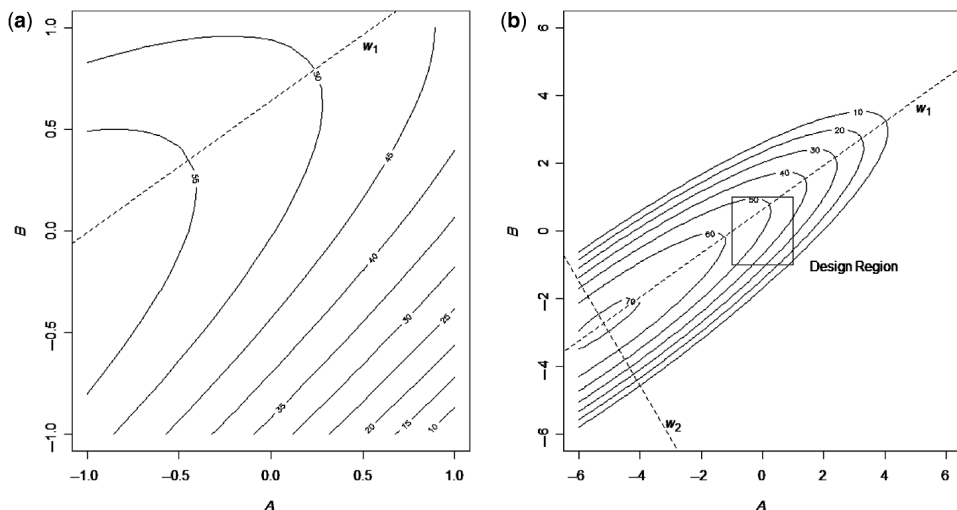


**Figure 6.9** Contour plot of rising ridge system for  $k = 2$  for data in Table 6.2. (a) Experimental region. (b) Expanded region to include stationary point.

**An Alternate Canonical Form** The canonical form of the second-order model given in Equation 6.8 is usually called the **B-canonical form**. It is very useful for determining the nature of the fitted response surface, particularly in identifying saddle systems and ridges. When the fitted surface is a **rising ridge**, it can be useful to use a slightly different canonical form, namely

$$\hat{y} = a_0 + \mathbf{u}'\mathbf{a} + \mathbf{u}'\boldsymbol{\Lambda}\mathbf{u} \quad (6.10)$$

This is usually called the **A-canonical form**. It basically assumes that the axes have been rotated exactly as in the B-form, but not first translated to the stationary point. In the A-canonical form, the first-order coefficients are

$$\mathbf{a} = \mathbf{P}'\mathbf{b}$$

The first-order terms are useful in determining the direction of movement along the rising ridge towards the optimum.

### 6.3.4 Role of Contour Plots

**Contour plots**, or contour maps, provide one of the most revealing ways of illustrating and interpreting the response surface system. The contour plots are merely two-dimensional (or sometimes three-dimensional) graphs that show contours of constant response with the axis system being a specific pair of the design variables, say  $x_i$  and  $x_j$ , while the other design variables are held constant. Modern graphics allow interesting interpretations that can be of benefit to the user. In fact, in almost all practical response surface situations, the analysis should be followed with a display of contour plotting. The reader should recall the contour plot in Example 6.1. The plots are particularly necessary when the stationary point is not of practical significance (a saddle point, or, say, a maximum point when one seeks a point of minimum response) or when the stationary point is remote from the design region. Clearly, ridge systems can only be interpreted when one can observe two-dimensional systems as a set of “snapshots” of the design region. Of course, if there are a large number of design variables, contour plotting is more difficult, since many factors need to be held constant. The method of ridge analysis (Section 6.4) can often aid the user in an understanding of the system.

The prediction profiler in JMP is a dynamic alternative to contour plots. Figure 6.10 illustrates a single view of the slices of the response surface which can be explored using this tool for Example 6.1. Here we have selected scaled temperature = 0 and scaled concentration = 0, but by moving the vertical lines, any combination of temperature and concentration can be examined.

Each plot shows the response surface line conditioned on the other input factor being held constant.

One cautionary note regarding contour plots must be made at this point. The investigator must bear in mind that the contours are only estimates, and if repeated data sets were observed using the same design, the complexion of the response system may change slightly or drastically. In other words, the *contours are not generated by deterministic equations*. Every point on a contour has a standard error. The prediction profiler includes uncertainty bounds on the surface which are helpful reminders that the response surface line is an estimate. This will be illustrated in a more technical way in a subsequent section.

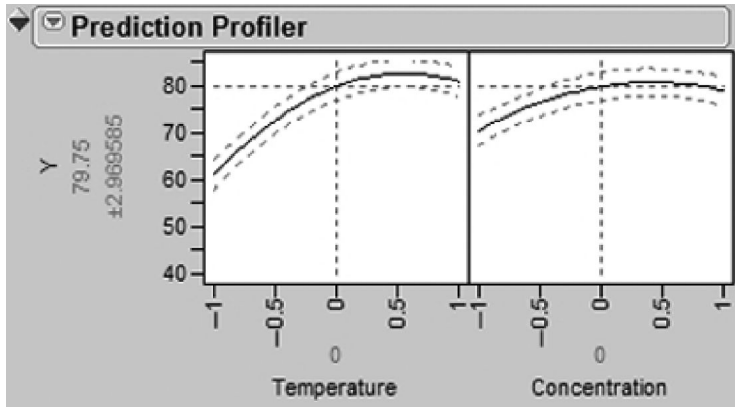


**Figure 6.10** Prediction Profiler in JMP for Example 6.1 response surface.

**Example 6.2 Contour Plotting of Survival Data** The following data are adapted from an experiment designed for estimating optimum conditions for storing bovine semen to obtain maximum survival. The variables under study are percent sodium citrate, percent glycerol, and the equilibration time in hours. The response observed is percent survival of motile spermatozoa. The data with the design levels in coded design units are shown in Table 6.4.

The design levels relate to the natural levels in the following way:

	-2	-1	0	1	2
Sodium citrate	1.6	2.3	3.0	3.7	4.4
Glycerol	2.0	5.0	8.0	11.0	14.0
Equilibration time	4.0	10.0	16.0	22.0	28.0

Note that the design consists of a  $2^3$  factorial component, four center runs and six axial or one-factor-at-a-time experimental runs in which each factor is set at level +2 and -2. The 18 experimental runs, involving three factors at five evenly spaced levels, is another example of a central composite design. The fitted second-order response function is given by

$$\hat{y} = 66.73 - 1.31x_1 - 2.31x_2 - 1.06x_3 - 11.44x_1^2 - 13.82x_2^2 - 3.57x_3^2 + 9.13x_1x_2 + 0.63x_1x_3 + 0.87x_2x_3$$

From Equation 6.6 the stationary point is given by

$$\mathbf{x}_s = \begin{bmatrix} x_{1,s} \\ x_{2,s} \\ x_{3,s} \end{bmatrix} = \begin{bmatrix} -0.112 \\ -0.126 \\ -0.174 \end{bmatrix}$$

and the eigenvalues of the matrix  $\hat{\mathbf{B}}$  are

$$\lambda_1 = -3.508, \quad \lambda_2 = -7.973, \quad \lambda_3 = -17.349$$

**TABLE 6.4 Survival Data for Example 6.2**

Treatment Combination	Percent Sodium Citrate	Percent Glycerol	Equilibrium Time (hr)	Percent Survival
1	-1	-1	-1	57
2	1	-1	-1	40
3	-1	1	-1	19
4	1	1	-1	40
5	-1	-1	1	54
6	1	-1	1	41
7	-1	1	1	21
8	1	1	1	43
9	0	0	0	60
10	0	0	0	70
11	0	0	0	62
12	0	0	0	72
13	-2	0	0	28
14	2	0	0	11
15	0	-2	0	2
16	0	2	0	18
17	0	0	-2	56
18	0	0	2	46

The canonical and stationary point analysis indicates that the stationary point is a point of maximum estimated response—that is, *maximum estimated percent survival*. The estimated response at the maximum is  $\hat{y} = 67.041$ . As a result, the estimated condition sought by the experimenters is found inside the experimental design region at the stationary point. Figure 6.11a shows the response surface contours in the vicinity of the optimum with equilibration time 14.96 hr.

Clearly, in this case, the researcher may be quite satisfied to operate at the conditions of the computed stationary point. However, because of economic considerations and scientific constraints of the problem, it is often of interest to determine how sensitive the estimated response is to movement away from the stationary point. In this regard, contour plotting can be very useful. For example, in this case, the stationary point  $\mathbf{x}_s$  corresponds to 2.9% sodium citrate, 7.61 glycerol, and 14.96 hr equilibration time. The equilibration time may be viewed as being somewhat long from a practical point of view, even though the optimum level is inside the experimental design region. Scientific curiosity suggests the need to determine how much is lost in estimated percent survival if equilibration time is set at 14, 12, and 10 hr. An analytical procedure would answer the question, but one gains considerably more information from the set of pictures produced from contour plotting. Figures 6.11b–d reveal the two-dimensional plots giving contours of constant estimated percent survival for fixed values of equilibration times of 14, 12, and 10 hr, respectively. For 14-hr equilibration time, the maximum estimated survival time is over 66%. In fact, Fig. 6.11d reveals that an equilibration time as low as 10 hr can result in an estimated survival time that exceeds 64%. As a result, one could recommend using values of the equilibration time considerably below the optimum and still not sacrifice much in percent survival.

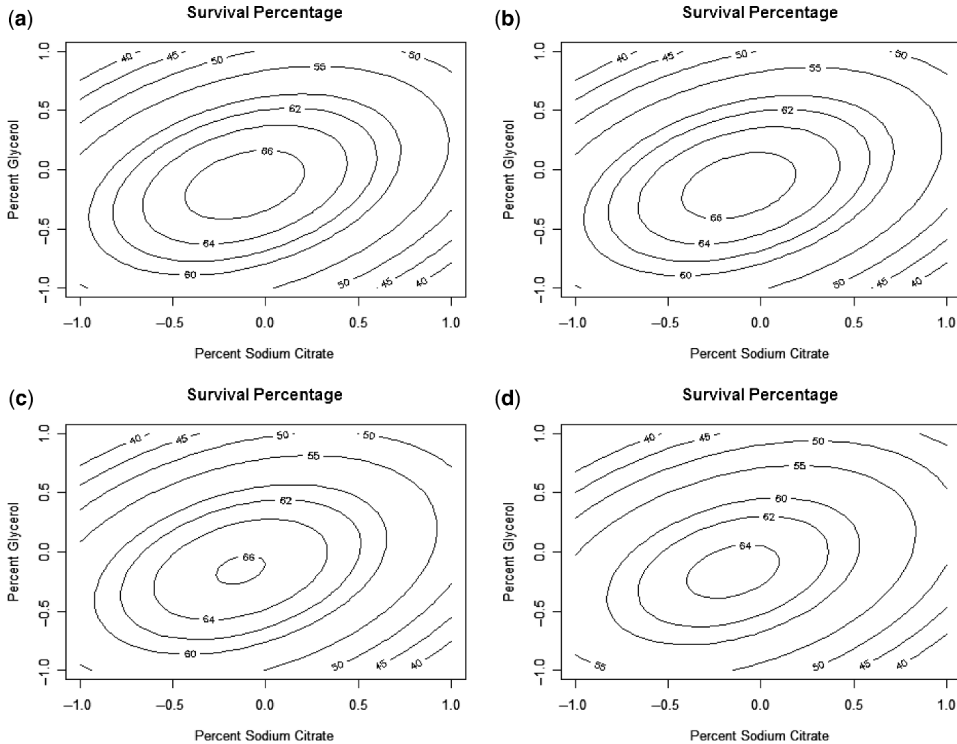


**Figure 6.11** Contours of constant percent survival for Example 6.2. (a) Equilibrium time 14.96 hours. (b) Equilibrium time 14 hours. (c) Equilibrium time 12 hours. (d) Equilibrium time 10 hours.

## 6.4 RIDGE ANALYSIS OF THE RESPONSE SURFACE

Often the analyst is confronted with a situation in which the stationary point itself is essentially of no value. For example, the stationary point may be a saddle point, which of course is neither a point of estimated maximum nor minimum response. In fact, even if one encounters a stationary point that is a point of maximum or minimum response, if the point is outside the experimental region, it would not be advisable to suggest it as a candidate for operating conditions, because the fitted model is not reliable outside the region of the experiment. Certainly the use of contour plotting can be beneficial in these situations. Of course, the goal of the analysis is to determine the nature of the system inside or on the perimeter of the experimental region. As a result, a useful procedure involves a **constrained optimization** algorithm. It is particularly useful when several design variables are in the response surface model. The methodology, called **ridge analysis**, produces a locus of points, each of which is a point of maximum response, with a constraint that the point resides on a sphere of a certain radius. For example, for  $k = 2$  design variables a typical ridge analysis might produce the locus of points as in Fig. 6.12. The origin is  $x_1 = x_2 = 0$ , the design center; a given point, say  $\mathbf{x}_p$ , is a point of maximum (or minimum) estimated response, with the constraint being that the point must be on a sphere of radius  $(\mathbf{x}'_p \mathbf{x}_p)^{1/2} = r_p$ . In other words, *all points are constrained stationary points*. Indeed, if the stationary point of the system is not a maximum (or minimum) inside the experimental

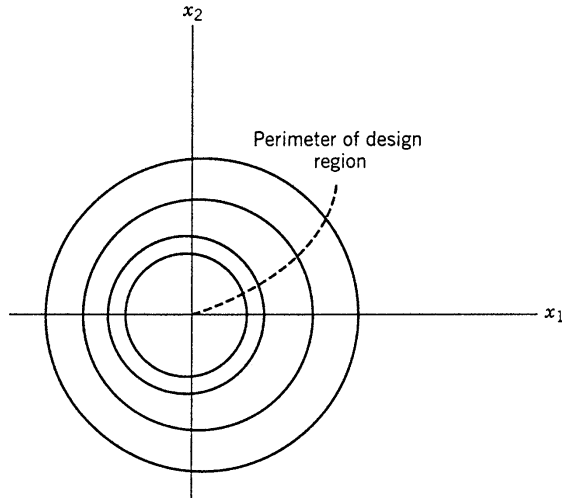


**Figure 6.12** A ridge analysis locus of points for  $k = 2$ .

region, then the point on the path at the design perimeter is the point of maximum (minimum) estimated response over all points on the path. This, then, may be viewed as a reasonable candidate for recommended operating conditions.

#### 6.4.1 What is the Value of Ridge Analysis?

The purpose of ridge analysis is to *anchor* the stationary point inside the experimental region. The output of the analysis is the set of coordinates of the maxima (or minima) along with the predicted response,  $\hat{y}$ , at each computed point on the path. From this, the analyst gains useful information regarding the roles of the design variables inside the experimental region. He or she is also given some candidate locations for suggested improved operating conditions. This is not to infer that additional information would not come from the contour plots. However, when one is faced with a large number of design variables, many contour plots may be required. Typical output of ridge analysis might simply be a set of two-dimensional plots, despite the value of  $k$ . For example, consider Figs. 6.13a and b.

In this case there are three design variables; let us assume that the perimeter of the experimental design is at radius  $\sqrt{3}$ . If one seeks to maximize response, a candidate set of conditions is given by  $x_1 \cong 1.5$ ,  $x_2 \cong 0.4$ ,  $x_3 \cong -0.7$ . The estimated maximum response achieved is given by  $\hat{y} \cong 60$ . Another useful feature of ridge analysis is that one obtains some guidelines regarding where future experiments should be made in order to achieve conditions that are more desirable than those experienced in the current experiment.

One must keep in mind that while ridge analysis as a formal tool is closest to ideal when the design region is spherical, often the design that has been used is not spherical but rather cuboidal in nature. In the latter case, one can still gain important practical information about the behavior of the response system inside the experimental region, particularly when one encounters several important design variables.

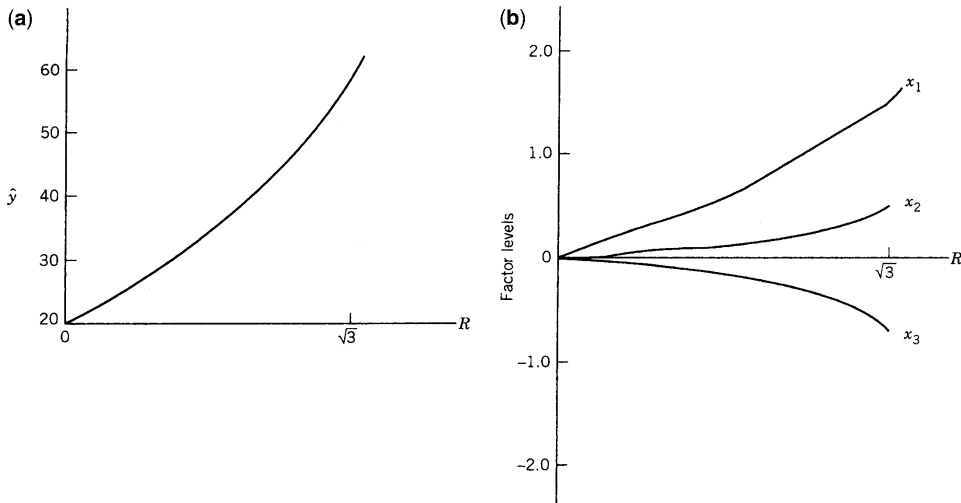


**Figure 6.13** Maximum response (a) and constrained optimum conditions (b) plotted against radius.

### 6.4.2 Mathematical Development of Ridge Analysis

In this section we sketch the development of ridge analysis. Many of the details are similar to those of steepest ascent. In fact, *ridge analysis is steepest ascent applied to second-order models*. The reader should recall that the intent of steepest ascent was to provide a path to an improved product in the case of a system that had not been well studied. A rather inexpensive first-order experiment is the usual vehicle for steepest ascent. However, ridge analysis is generally used when the practitioner feels that he or she is in or quite near the region of the optimum. Nevertheless, both are constrained optimization procedures.

Consider the fitted second-order response surface model of Equation 6.3:

$$\hat{y} = b_0 + \mathbf{x}'\mathbf{b} + \mathbf{x}'\hat{\mathbf{B}}\mathbf{x}$$

We maximize  $\hat{y}$  subject to the constraint

$$\mathbf{x}'\mathbf{x} = R^2$$

where  $\mathbf{x}' = [x_1, x_2, \dots, x_k]$  and the center of the design region is taken to be  $x_1 = x_2 = \dots = x_k = 0$ . Using Lagrange multipliers, we need to differentiate

$$L = b_0 + \mathbf{x}'\mathbf{b} + \mathbf{x}'\hat{\mathbf{B}}\mathbf{x} - \mu(\mathbf{x}'\mathbf{x} - R^2) \quad (6.11)$$

with respect to the vector  $\mathbf{x}$ . The derivative  $\partial L / \partial \mathbf{x}$  is given by

$$\frac{\partial L}{\partial \mathbf{x}} = \mathbf{b} + 2\hat{\mathbf{B}}\mathbf{x} - 2\mu\mathbf{x}$$

To determine constrained stationary points we set  $\partial L / \partial \mathbf{x} = \mathbf{0}$ . This results in

$$(\hat{\mathbf{B}} - \mu\mathbf{I})\mathbf{x} = -\frac{1}{2}\mathbf{b} \quad (6.12)$$

As a result, for a fixed  $\mu$ , a solution  $\mathbf{x}$  of Equation 6.12 is a stationary point on  $R = (\mathbf{x}'\mathbf{x})^{1/2}$ . However, the appropriate solution  $\mathbf{x}$  is that which results in a maximum  $\hat{y}$  on  $R$  or a minimum  $\hat{y}$  on  $R$ , depending on which is desired. It turns out that the appropriate choice of  $\mu$  depends on the eigenvalues of  $\hat{\mathbf{B}}$ . The reader should recall the important role of these eigenvalues in the determination of the nature of the stationary point of the response system (see Section 6.3.2). The following are rules for selection of values of  $\mu$ :

1. If  $\mu$  exceeds the largest eigenvalue of  $\hat{\mathbf{B}}$ , the solution  $\mathbf{x}$  in Equation 6.12 will result in an absolute maximum for  $\hat{y}$  on  $R = (\mathbf{x}'\mathbf{x})^{1/2}$ .
2. If  $\mu$  is smaller than the smallest eigenvalue of  $\hat{\mathbf{B}}$ , the solution in Equation 6.12 will result in an absolute minimum for  $\hat{y}$  on  $R = (\mathbf{x}'\mathbf{x})^{1/2}$ .

Consider the orthogonal matrix  $\mathbf{P}$  that diagonalizes  $\mathbf{B}$ . That is,

$$\mathbf{P}'\mathbf{B}\mathbf{P} = \Lambda$$

$$= \begin{bmatrix} \lambda_1 & & 0 \\ & \lambda_2 & \\ & & \ddots \\ 0 & & \lambda_k \end{bmatrix}$$

where the  $\lambda_i$  are the eigenvalues of  $\mathbf{B}$ . The solution  $\mathbf{x}$  that produces locations where  $\partial L/\partial \mathbf{x} = \mathbf{0}$  is given by

$$(\mathbf{B} - \mu\mathbf{I})\mathbf{x} = -\frac{1}{2}\mathbf{b}$$

If we premultiply  $\mathbf{B} - \mu\mathbf{I}$  by  $\mathbf{P}'$  and postmultiply by  $\mathbf{P}$ , we obtain

$$\mathbf{P}'(\mathbf{B} - \mu\mathbf{I})\mathbf{P} = \Lambda - \mu\mathbf{I}$$

because  $\mathbf{P}'\mathbf{P} = \mathbf{I}_k$ . If  $\mathbf{B} - \mu\mathbf{I}$  is negative definite, the resulting solution  $\mathbf{x}$  is at least a local maximum on the radius  $R = (\mathbf{x}'\mathbf{x})^{1/2}$ . On the other hand, if  $\mathbf{B} - \mu\mathbf{I}$  is positive definite, the result is a local minimum. Because

$$\begin{aligned} (\mathbf{B} - \mu\mathbf{I}) &= \Lambda - \mu\mathbf{I} \\ &= \begin{bmatrix} \lambda_1 - \mu & & 0 \\ & \lambda_2 - \mu & \\ & & \ddots \\ 0 & & \lambda_k - \mu \end{bmatrix} \end{aligned}$$

we see that if  $\mu > \lambda_{\max}$ , then  $\mathbf{B} - \mu\mathbf{I}$  is negative definite, and if  $\mu < \lambda_{\min}$ , then  $\mathbf{B} - \mu\mathbf{I}$  is positive definite.

The above development does not prove that the solutions  $\mathbf{x}$  are absolute maxima or minima. For further details see Draper (1963) or Myers (1976).

We should also reflect at this point on the relationship between  $R$  and  $\mu$ . The analyst desires to observe results on a locus of points like that depicted in Fig. 6.14. As a result,

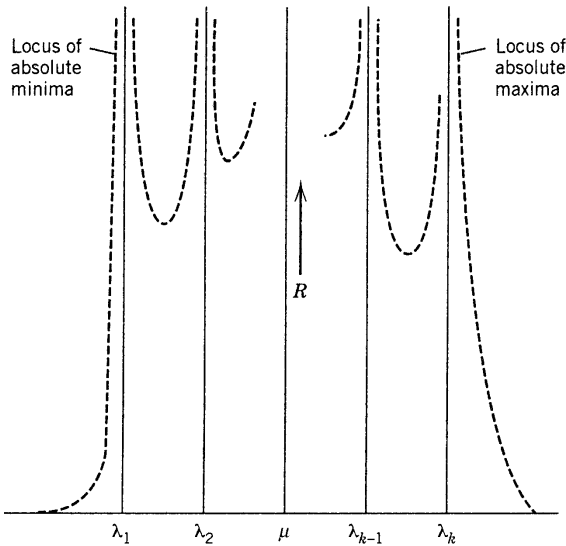


**Figure 6.14** Relationship between  $R$  and  $\mu$  in ridge analysis.

of course, the radii of the solution to Equation 6.12 should fall in the interval  $[0, R_b]$ , where  $R_b$  is a radius approximately representing the boundary of the experimental region. The value  $R$  is actually controlled through the choice of  $\mu$ . In the **working regions** of  $\mu$ , namely  $\mu > \lambda_k$  or  $\mu < \lambda_1$ , where  $\lambda_1$  is the smallest eigenvalue of  $\hat{\mathbf{B}}$  and  $\lambda_k$  is the largest eigenvalue of  $\hat{\mathbf{B}}$ ,  $R$  is a monotonic function of  $\mu$ . In fact, Fig. 6.14 gives the relationship between  $R$  and  $\mu$  throughout the spectrum of the eigenvalues.

As a result, a computer algorithm for ridge analysis involves the substitution of  $\mu > \lambda_k$  (for a designed maximum response) and increases  $\mu$  until radii near the design perimeter are encountered. Future increases in  $\mu$  results in coordinates that are closer to the design center. The same applies for  $\mu < \lambda_1$  (for desired minimum response), with decreasing values of  $\mu$  being required.

**Example 6.3 Ridge Analysis of a Saddle Point Surface** A chemical process that converts 1,2-propanediol to 2,5-dimethylpiperazine is the object of an experiment to determine optimum process conditions—that is, conditions for maximum conversion [see Myers (1976)]. The following factors were studied:

$$\begin{aligned}x_1 &= \frac{\text{amount of NH}_3 - 102}{51} \\x_2 &= \frac{\text{temperature} - 250}{20} \\x_3 &= \frac{\text{amount of H}_2\text{O} - 300}{200} \\x_4 &= \frac{\text{hydrogen pressure} - 850}{350}\end{aligned}$$

As in previous examples, the type of design used for fitting the second-order model was a central composite design. The design matrix and observation vector are as follows:

	$x_1$	$x_2$	$x_3$	$x_4$	
$\mathbf{D} =$	-1	-1	-1	-1	58.2
	+1	-1	-1	-1	23.4
	-1	+1	-1	-1	21.9
	+1	+1	-1	-1	21.8
	-1	-1	+1	-1	14.3
	+1	-1	+1	-1	6.3
	-1	+1	+1	-1	4.5
	+1	+1	+1	-1	21.8
	-1	-1	-1	+1	46.7
	+1	-1	-1	+1	53.2
	-1	+1	-1	+1	23.7
	+1	+1	-1	+1	40.3
	-1	-1	+1	+1	7.5
	+1	-1	+1	+1	13.3
	-1	+1	+1	+1	49.3
	+1	+1	+1	+1	20.1
	0	0	0	0	32.8
	-1.4	0	0	0	31.1
	+1.4	0	0	0	28.1
	0	-1.4	0	0	17.5
	0	+1.4	0	0	49.7
	0	0	-1.4	0	49.9
	0	0	+1.4	0	34.2
	0	0	0	-1.4	31.1
	0	0	0	+1.4	43.1

The fitted second-order model is given by

$$\begin{aligned}\hat{y} = & 40.198 - 1.511x_1 + 1.284x_2 - 8.739x_3 + 4.955x_4 - 6.332x_1^2 \\ & + 2.194x_1x_2 - 4.292x_2^2 - 0.144x_1x_3 + 8.006x_2x_3 + 0.0196x_3^2 \\ & + 1.581x_1x_4 + 2.806x_2x_4 + 0.294x_3x_4 - 2.506x_4^2\end{aligned}$$

Table 6.5 shows a computer printout of the ridge analysis of maximum response. The accompanying plot of the response versus radius is shown in Fig. 6.15. The stationary point (in design units) is given by  $x_{1,s} = 0.265$ ,  $x_{2,s} = 1.034$ ,  $x_{3,s} = 0.291$ , and  $x_{4,s} = 1.668$ . The response at the stationary point is  $\hat{y}_s = 43.52$ , but the eigenvalues of the matrix  $\hat{\mathbf{B}}$  are  $-7.55$ ,  $-6.01$ ,  $-2.16$ , and  $+2.60$ , indicating a saddle point. They indicate that a ridge analysis might reveal reasonable candidates for operating conditions, with

**TABLE 6.5** Ridge Analysis of Data in Example 6.3

Radius	Estimated Response	Standard Error of Prediction	Design Factor Levels			
			$x_1$	$x_2$	$x_3$	$x_4$
0	40.198	8.321	0	0	0	0
0.10	41.207	8.304	-0.0125	0.0063	-0.0870	0.0470
0.20	42.195	8.254	-0.0217	-0.0012	-0.1772	0.0900
0.30	43.175	8.175	-0.0287	-0.0141	-0.2698	0.1270
0.40	44.159	8.073	-0.0345	-0.0379	-0.3640	0.1575
0.50	45.157	7.960	-0.0398	-0.0685	-0.4591	0.1814
0.60	46.176	7.848	-0.0450	-0.1044	-0.5543	0.1993
0.70	47.222	7.757	-0.0502	-0.1443	-0.6493	0.2120
0.80	48.301	7.707	-0.0556	-0.1873	-0.7438	0.2202
0.90	49.416	7.724	-0.0611	-0.2324	-0.8376	0.2247
1.00	50.571	7.832	-0.0668	-0.2793	-0.9307	0.2262
1.10	51.767	8.055	-0.0727	-0.3274	-1.0231	0.2251
1.20	53.007	8.414	-0.0787	-0.3765	-1.1147	0.2219
1.30	54.291	8.920	-0.0849	-0.4263	-1.2057	0.2170
1.40	55.621	9.581	-0.0912	-0.4767	-1.2961	0.2106
1.50	56.998	10.394	-0.0976	-0.5276	-1.3859	0.2029
1.60	58.423	11.357	-0.1041	-0.5788	-1.4752	0.1942
1.70	59.896	12.461	-0.1107	-0.6303	-1.5640	0.1846
1.80	61.418	13.698	-0.1173	-0.6820	-1.6524	0.1742
1.90	62.989	15.061	-0.1240	-0.7340	-1.7404	0.1631
2.00	64.610	16.543	-0.1308	-0.7860	-1.8281	0.1514

the implied constraint that the candidates lie inside or on the boundary of the experimental design. In this case the factorial points are at a distance of two units from the design center. Note that among the reasonable candidates for coordinates, we have

$$x_1 = -0.1308, \quad x_2 = -0.7861, \quad x_3 = -1.8281, \quad x_4 = 0.1514$$

at a radius of two units. The estimated response is given by  $\hat{y}_s = 64.61$ . Note also that the estimated standard error of prediction at this location is given by

$$s_{\hat{y}} = 16.543$$

This, of course, reflects the variability in  $\hat{y}$  conditioned on the given set of coordinates; that is, given that prediction is desired at the location indicated in  $x_1, x_2, x_3$ , and  $x_4$ . Note how this standard error begins to grow rather rapidly after a radius of 1.4. Recall that the axial distance in the design is 1.4, and the factorial points are at a distance of 2.0. It turns out that a better choice of axial distance would have been 2.0. This would have prevented the quick acceleration of the standard error of prediction as one approaches the design perimeter. In fact, in this case one might feel obliged to recommend conditions at radius 1.4 or 1.5, where the predicted response is smaller but the standard error is considerably smaller. We will shed more light on the standard error of prediction in the next section and in future chapters. This criterion plays a critical role in discussions that relate to the choice of experimental design and comparisons among designs.

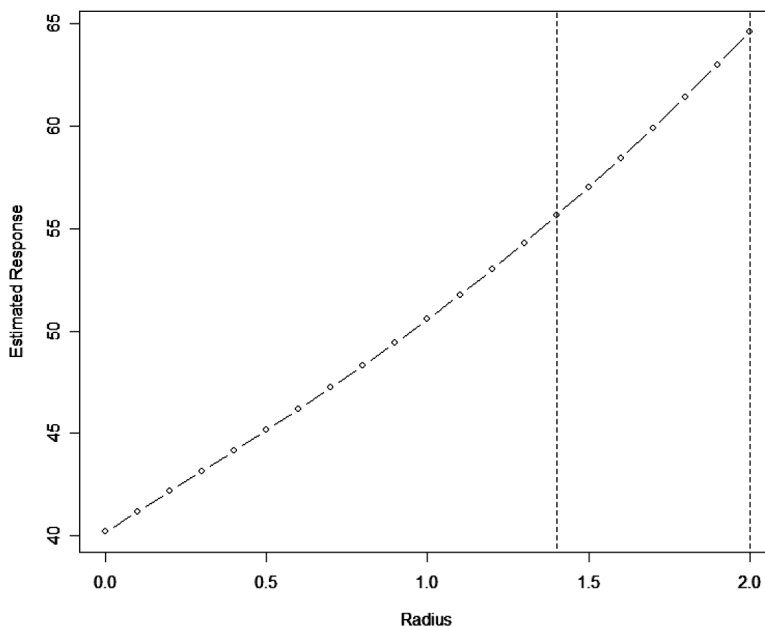


**Figure 6.15** Maximum predicted response versus radius for data in Example 6.3.

For further discussion and developments related to ridge analysis the reader is referred to Hoerl (1959, 1964), who originated the concept, and Draper (1963), who developed the mathematical ideas behind the concept. The paper by Hoerl (1985) and the book by Box and Draper (2007) provide additional insights into this technique.

## 6.5 SAMPLING PROPERTIES OF RESPONSE SURFACE RESULTS

In response surface analysis there is considerable attention given to the use of contour plots and the estimation of optimum conditions—either absolute ones, or constrained ones as in the case of ridge analysis. It is always a temptation to offer interpretations that treat these optimum conditions or observed contours of constant response as if the values were scientifically exact. One must bear in mind that in any RSM analysis the computed stationary point is only an estimate, and any point on any contour (and, indeed, the contour itself) possesses sampling variability. Thus, standard errors and, at times, confidence regions afford the analyst a more realistic assessment of the quality of the point estimate. In addition, it forces the researcher to properly “tone down” or temper interpretations in many cases. Interpretations that are made as if the results were deterministic can be erroneous and highly misleading. It is our impression that too often in practice the randomness and resulting noise associated with an RSM result are completely ignored.

The first type of sampling property we shall introduce deals with the standard error of predicted response, or standard error of estimated mean response. This concept was discussed briefly in the development of standard regression analysis in Chapter 2. It was also discussed in the previous section.

### 6.5.1 Standard Error of Predicted Response

The most fundamental sampling property in any model building exercise is the standard error of the predicted response at some point of interest  $\mathbf{x}$ , often denoted  $s_{\hat{y}(\mathbf{x})}$ , where in the most general framework

$$\hat{y}(\mathbf{x}) = \mathbf{x}^{(m)\prime} \mathbf{b}$$

and  $\mathbf{b} = (\mathbf{X}'\mathbf{X})^{-1}\mathbf{X}'\mathbf{y}$ . Here, of course, the model matrix  $\mathbf{X}$  is as discussed in Chapter 2. The vector  $\mathbf{x}^{(m)}$  is a function of the location at which one is predicting the response; the  $(m)$  indicates that  $\mathbf{x}^{(m)}$  is just  $\mathbf{x}$  expanded to **model space**; that is, the vector reflects the form of the model as  $\mathbf{X}$  does. For example, for  $k = 2$  design variables and a second-order model we have

$$\begin{aligned}\mathbf{x}^{(2)\prime} &= [1, x_1, x_2, x_1^2, x_2^2, x_1x_2] \\ \mathbf{b}' &= [b_0, b_1, b_2, b_{11}, b_{22}, b_{12}]\end{aligned}$$

Under the usual i.i.d. error assumptions for first- and second-order models and, of course, with the assumption of constant error variance  $\sigma^2$ , we have

$$\text{Var}[\hat{y}(\mathbf{x})] = \mathbf{x}^{(m)\prime}(\mathbf{X}'\mathbf{X})^{-1}\mathbf{x}^{(m)}\sigma^2$$

As a result, an **estimated standard error** of  $\hat{y}(\mathbf{x})$  is given by

$$s_{\hat{y}(\mathbf{x})} = s\sqrt{\mathbf{x}^{(m)\prime}(\mathbf{X}'\mathbf{X})^{-1}\mathbf{x}^{(m)}} \quad (6.13)$$

where  $s = \sqrt{MS_E}$  is the square root of the mean square error of the fitted response surface—that is, for a fitted model with  $p$  parameters,

$$s = \sqrt{\sum_{i=1}^k (y_i - \hat{y}_i)^2 / (n - p)}$$

The standard error  $s_{\hat{y}(\mathbf{x})}$  is used in constructing confidence limits around a predicted response. That is, for  $\hat{y}(\mathbf{x}) = \mathbf{x}^{(m)\prime} \mathbf{b}$ , a prediction at some location  $\mathbf{x}$ , the  $100(1 - \alpha)\%$  confidence interval on the mean response  $E(y|\mathbf{x})$  is given by

$$\hat{y}(\mathbf{x}) \pm t_{\alpha/2, n-p} s \sqrt{\mathbf{x}^{(m)\prime}(\mathbf{X}'\mathbf{X})^{-1}\mathbf{x}^{(m)}} \quad (6.14)$$

The standard error  $s_{\hat{y}(\mathbf{x})}$  of predicted value and the corresponding confidence intervals are the simplest form of sampling properties associated with an RSM analysis. The standard error can provide the user with a rough idea about the relative quality of predicted response values in various locations in the design region. For example, Fig. 6.16 and Table 6.5 show how the standard error of prediction value changes as a function of where we wish to predict in the design space for the ridge system of Example 6.3. Figure 6.16 shows three slices of the design space for fixed values of  $x_3$  and  $x_4$ . Because of the symmetry of the central composite design, the roles of  $x_1, x_2, x_3$ , and  $x_4$  are interchangeable in terms of the standard error

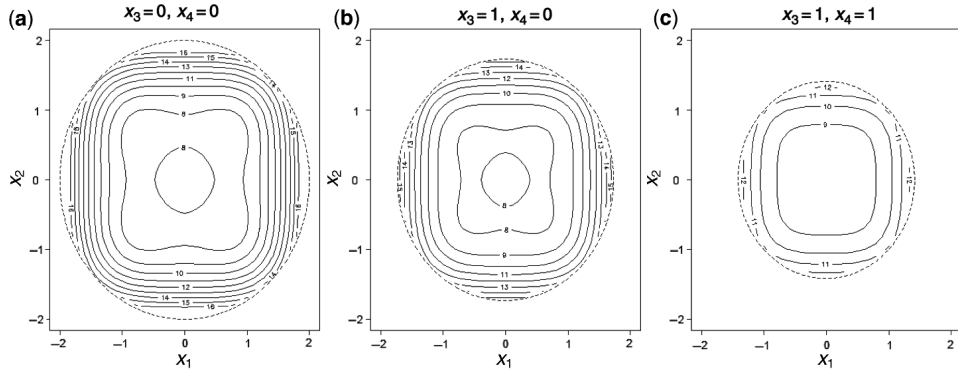


**Figure 6.16** Contour plots of standard error of predicted value for different  $x_3$  and  $x_4$  values for Example 6.3.

of prediction. The dotted lines on each plot indicate a radius of 2 from the center of the design space. Note how prediction with this second-order response surface becomes worse as one gets near the design perimeter. This may very well lead, in some cases, to the conclusion that a reasonable choice of recommended operating conditions might be further inside the perimeter when the predicted value at the optimum on the boundary has a relatively large standard error. The standard error of prediction should be computed at any point that the investigator considers a potentially useful location in the design region.

**Standard Error of Prediction as a Function of Design** Because of the prominent role of  $(\mathbf{X}'\mathbf{X})^{-1}$  in Equation 6.13, it should be apparent that  $s_{\hat{y}(\mathbf{x})}$  is very much dependent on the experimental design. In Table 6.5, the larger standard error that is experienced close to the design perimeter is a result of the choice of design. In the case of the central composite design, the choice of the **axial distance** ( $\pm 1.4$  in this case) and the number of center runs have an important influence on the quality of  $\hat{y}(\mathbf{x})$  as a predictor. In Chapter 7 we deal with properties of first- and second-order designs. Much attention is devoted to  $\text{Var}[\hat{y}(\mathbf{x})]/\sigma^2 = \mathbf{x}^{(m)'}(\mathbf{X}'\mathbf{X})^{-1}\mathbf{x}^{(m)}$ . In fact, designs are compared on the basis of relative distribution of values of  $\mathbf{x}^{(m)'}(\mathbf{X}'\mathbf{X})^{-1}\mathbf{x}^{(m)}$  in the design space.

**What Are the Restrictions on the Standard Error of Prediction?** The user of RSM can learn a great deal about relative quality of prediction using the fitted response surface in various locations in the design space. The prediction standard error—a function of the model, the design, and the location  $\mathbf{x}$ —is quite fundamental. However, it is important for the reader to understand what the standard error of prediction is *not* as well as what it is.

The value  $s_{\hat{y}(\mathbf{x})}$  in Equation 6.13 is an estimate of the standard deviation of  $\hat{y}(\mathbf{x})$  over repeated experiments in which the same design and model are employed, and thus repeated values of  $\hat{y}$  are calculated at the same location  $\mathbf{x}$ .

As a result, if the analyst calculates a stationary point  $\mathbf{x}_s$  (a point of maximum estimated response) and determines the standard error of prediction at  $\mathbf{x}_s$ , it cannot be said that the resulting confidence interval is a proper confidence interval on the maximum response. One must keep in mind that repeated experiments would not produce  $\mathbf{x}_s$ -coordinates at

the same location. Indeed, repeated experiments may not all result in stationary points that are maxima. The computed confidence interval here is a confidence interval *conditional on* prediction at the point  $\mathbf{x}_s$ , which only happens to be a stationary point in the present experiment. The confidence region on the location of the stationary point and the confidence interval on the maximum response are considerably more complicated.

### 6.5.2 Confidence Region on the Location of the Stationary Point

There are instances where the computed stationary point is of considerable interest to the user. It may be the location in the space of the design variables that represents recommended operating conditions for the process. However, there remains the obvious question, “How good are the estimates of these coordinates?” Perhaps there is sufficient noise in the estimator that a secondary, less costly set of conditions results in a mean response that is not significantly different from that produced by the location of the stationary point. These issues can be dealt with nicely through the construction of a confidence region on the location of the stationary point.

Suppose we again consider the fitted second-order response surface model

$$\begin{aligned}\hat{y}(\mathbf{x}) &= b_0 + \sum_{i=1}^k b_i x_i + \sum_{i=1}^k b_{ii} x_i^2 + \sum_{i < j = 2}^k b_{ij} x_i x_j \\ &= b_0 + \mathbf{x}' \mathbf{b} + \mathbf{x}' \hat{\mathbf{B}} \mathbf{x}\end{aligned}$$

One should recall from Section 6.3 that the stationary point is computed from setting the derivatives  $\partial\hat{y}(\mathbf{x})/\partial\mathbf{x}$  to zero. We have

$$\partial\hat{y}(\mathbf{x})/\partial\mathbf{x} = \mathbf{b} + 2\hat{\mathbf{B}}\mathbf{x}$$

The  $j$ th derivative,  $d_j(\mathbf{x})$ , can be written  $d_j(\mathbf{x}) = b_j + 2\hat{\mathbf{B}}'_j \mathbf{x}$ , where the vector  $\hat{\mathbf{B}}'_j$  is the  $j$ th row of  $\hat{\mathbf{B}}$ , the matrix of quadratic coefficients described by Equation 6.5. These derivatives are simple linear functions of  $x_1, x_2, \dots, x_k$ . We denote the vector of derivatives as the  $k$ -dimensional vector  $\mathbf{d}(\mathbf{x})$ . Now, suppose we consider the derivatives evaluated at  $\mathbf{t}$ , where the coordinates of  $\mathbf{t}$  are the coordinates of the *true stationary point of the system* (which of course are unknown). If the errors around the model of Equation 6.2 are i.i.d. normal,  $N(0, \sigma)$ , then

$$\mathbf{d}(\mathbf{t}) \sim N(\mathbf{0}, \text{Var}[\mathbf{d}(\mathbf{t})])$$

where  $\text{Var}[\mathbf{d}(\mathbf{t})]$  is the variance–covariance matrix of  $\mathbf{d}(\mathbf{t})$ . As a result [see Graybill (1976), Myers and Milton (1991)],

$$\frac{\mathbf{d}'(\mathbf{t}) [\widehat{\text{Var}}[\mathbf{d}(\mathbf{t})]]^{-1} \mathbf{d}(\mathbf{t})}{k} \sim F_{k, n-p} \quad (6.15)$$

where  $F_{k, n-p}$  is the  $F$ -distribution with  $k$  and  $n - p$  degrees of freedom. It is important to note that  $\text{Var}[\mathbf{d}(\mathbf{t})]$  is a  $k \times k$  matrix that contains the error variance  $\sigma^2$  as a multiplier. In addition,  $\text{Var}[\mathbf{d}(\mathbf{t})]$  is clearly a function of  $\mathbf{t}$ . For example, in the case of two

design variables,

$$d_1(\mathbf{t}) = b_1 + 2\left(b_{11}t_1 + \frac{b_{12}}{2}t_2\right)$$

$$d_2(\mathbf{t}) = b_2 + 2\left(\frac{b_{12}}{2}t_1 + b_{22}t_2\right)$$

and

$$\text{Var}[\mathbf{d}(\mathbf{t})] = \begin{bmatrix} \text{Var}[d_1(\mathbf{t})] & \text{Cov}[d_1(\mathbf{t}), d_2(\mathbf{t})] \\ \text{Cov}[d_1(\mathbf{t}), d_2(\mathbf{t})] & \text{Var}[d_2(\mathbf{t})] \end{bmatrix}$$

One can easily observe that elements in this matrix came from  $(\mathbf{X}'\mathbf{X})^{-1}\sigma^2$ , the variance–covariance matrix of regression coefficients. The role of  $t_1$  and  $t_2$  should also be apparent. In Equation 6.15 the “ $\widehat{\text{Var}}$ ” in  $\{\widehat{\text{Var}}[d(\mathbf{t})]\}$  merely implies that  $\sigma^2$  is replaced by the familiar  $s^2$ , the model error mean square. Now, based on Equation 6.15 we have

$$\Pr\left\{\mathbf{d}'(\mathbf{t})\left\{\widehat{\text{Var}}[\mathbf{d}(\mathbf{t})]\right\}^{-1}\mathbf{d}(\mathbf{t}) \leq kF_{\alpha,k,n-p}\right\} = 1 - \alpha \quad (6.16)$$

where  $F_{\alpha,k,n-p}$  is the upper  $\alpha$ th percentile point of the  $F$ -distribution for  $k$  and  $n - p$  degrees of freedom. Note that while  $\mathbf{t}$  is truly unknown, all other quantities in Equation 6.16 are known. As a result, values  $t_1, t_2, \dots, t_k$  that fall inside the  $100(1 - \alpha)\%$  confidence region for the stationary point are those that satisfy the following inequality:

$$\mathbf{d}'(\mathbf{t})\left\{\widehat{\text{Var}}[\mathbf{d}(\mathbf{t})]\right\}^{-1}\mathbf{d}(\mathbf{t}) \leq kF_{\alpha,k,n-p} \quad (6.17)$$

This useful and important approach was developed by Box and Hunter (1954).

### 6.5.3 Use and Computation of the Confidence Region on the Location of the Stationary Point

As one can easily observe from Equation 6.17, the computation of the confidence region is quite simple. However, the display of the confidence region carries with it a clumsiness that is similar to that of the response surface display, particularly when several design variables are involved. For two or three design variables a graphical approach can be very informative. The general size (or volume) of the confidence region can be visualized and the analyst can gain some insight regarding how much flexibility is available in the recommendation of optimum conditions.

**Example 6.4 A Chemical Process with  $k = 2$**  A central composite design was used to develop a response surface relating yield ( $y$ ) to temperature and reaction time. The experimental results are shown in Table 6.6.

The fitted second-order model is

$$\hat{y} = 90.790 - 1.095x_1 - 1.045x_2 - 2.781x_1^2 - 2.524x_2^2 - 0.775x_1x_2$$

with the stationary point at  $\mathbf{x}_s' = [-0.1716, -0.1806]$ . As shown in Fig. 6.17, this is a point of maximum response with the predicted response at the stationary point  $\hat{y}_s = 90.978\%$ . The  $R^2$ -value for this model is approximately 0.84.

**TABLE 6.6** The Central Composite Design for Example 6.4

$x_1$ (Temp.)	$x_2$ (Time)	$y$
-1	-1	88.55
1	-1	85.80
-1	1	86.29
1	1	80.44
-1.414	0	85.50
1.414	0	85.39
0	-1.414	86.22
0	1.414	85.70
0	0	90.21
0	0	90.85
0	0	91.31
Coded levels	-1.414 -1 0 1 1.414	
Temperature (°C)	110.86 115 125 135 139.14	
Time (sec)	257.58 270 300 330 342.42	

The major components in the inequality of Equation 6.17 are quite simple to determine. There are  $p = 6$  parameters in the second-order system, and

$$d_1(\mathbf{t}) = -1.095 - 5.562t_1 - 0.775t_2$$

$$d_2(\mathbf{t}) = -1.045 - 0.775t_1 - 5.048t_2$$

The variances and covariances are obtained from the matrix  $(\mathbf{X}'\mathbf{X})^{-1}$  with

$$\mathbf{X}'\mathbf{X} = \begin{bmatrix} b_0 & b_1 & b_2 & b_{11} & b_{22} & b_{12} \\ 1 & 0 & 0 & 8 & 8 & 0 \\ 8 & 0 & 0 & 0 & 0 & 0 \\ 8 & 0 & 0 & 0 & 0 & 0 \\ 12 & 4 & 0 & 0 & 0 & 0 \\ 12 & 0 & 0 & 0 & 0 & 4 \end{bmatrix}_{\text{sym.}}$$

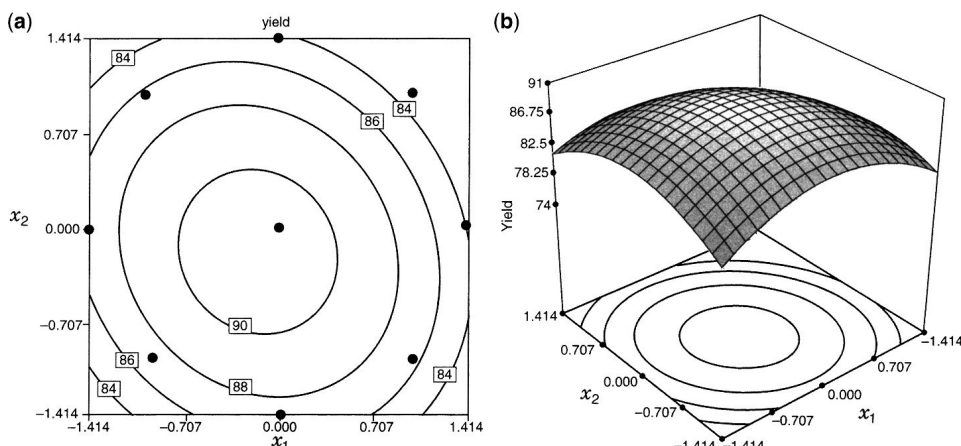


**Figure 6.17** The second-order model for Example 6.4. (a) Contour plot. (b) Response surface.

and

$$(\mathbf{X}'\mathbf{X})^{-1} = \begin{bmatrix} \frac{1}{3} & 0 & 0 & -\frac{1}{6} & -\frac{1}{6} & 0 \\ 0 & \frac{1}{8} & 0 & 0 & 0 & 0 \\ 0 & 0 & \frac{1}{8} & 0 & 0 & 0 \\ 0 & 0 & 0 & 0.1772 & 0.0521 & 0 \\ 0 & 0 & 0 & 0.1772 & 0.1772 & 0 \\ \text{sym.} & & & & & \frac{1}{4} \end{bmatrix}$$

The error mean square from the fitted response surface is  $s^2 = 3.1635$  (five degrees of freedom). Apart from  $s^2$ , the variances and covariances of the coefficients of the fitted response surface are the elements of  $(\mathbf{X}'\mathbf{X})^{-1}$  above.

As a result, elements of  $\widehat{\text{Var}}[\mathbf{d}(t)]$  are easily determined. For example,

$$\widehat{\text{Var}}[d_1(\mathbf{t})] = \frac{s^2}{\sigma^2} \{ \text{Var}b_1 + 4t_1^2 \text{Var}b_{11} + t_2^2 \text{Var}b_{12} \}$$

Note that the covariances involving  $b_1$  are zero and  $\text{Cov}(b_{11}, b_{12}) = \text{Cov}(b_{12}, b_{22}) = 0$ . Thus

$$\begin{aligned} \widehat{\text{Var}}[d_2(\mathbf{t})] &= \frac{s^2}{\sigma^2} \{ \text{Var}b_2 + t_1^2 \text{Var}b_{12} + 4t_2^2 \text{Var}b_{22} \} \\ \widehat{\text{Cov}}[d_1(\mathbf{t}), d_2(\mathbf{t})] &= \frac{s^2}{\sigma^2} \{ 4t_1 t_2 \text{Cov}(b_{11}, b_{22}) + t_1 t_2 \text{Var}b_{12} \} \end{aligned}$$

As a result, we have

$$\begin{aligned} \widehat{\text{Var}}[d_1(\mathbf{t})] &= 3.1635 \left\{ \frac{1}{8} + 4t_1^2(0.1772) + \frac{1}{4}t_2^2 \right\} \\ \widehat{\text{Var}}[d_2(\mathbf{t})] &= 3.1635 \left\{ \frac{1}{8} + \frac{1}{4}t_1^2 + 4t_2^2(0.1772) \right\} \\ \widehat{\text{Cov}}[d_1(\mathbf{t}), d_2(\mathbf{t})] &= 3.1635 \left\{ 4(0.0521)t_1 t_2 + \frac{1}{4}t_1 t_2 \right\} \end{aligned}$$

Equation 6.17 can now be used to plot the confidence region. The reader should note how the design has a profound influence on the important elements of  $(\mathbf{X}'\mathbf{X})^{-1}$ . The confidence region is displayed in Fig. 6.18. This graph was obtained from a Maple program written under the supervision of Dr. Enrique Del Castillo (available at <http://lb350e.ie.psu.edu/software.htm>).

The display in Fig. 6.18 presents a rather bleak picture concerning the quality of estimation of the stationary point. The larger, cross-hatched region is the 95% confidence region on the location of the stationary point, while the smaller, solid region is the 90% confidence region. One must not forget the interpretation, which is that a true response surface maximum at any location inside the 95% contour could readily have produced the data that were observed. The 95% interval does not close inside the experimental design region.

Confidence regions on the location of optima like those shown in Fig. 6.18 are not unusual. The quality of the confidence region depends a great deal on the nature of the design and the fit of the model to the data. Recall that  $R^2$  is approximately 84%. One

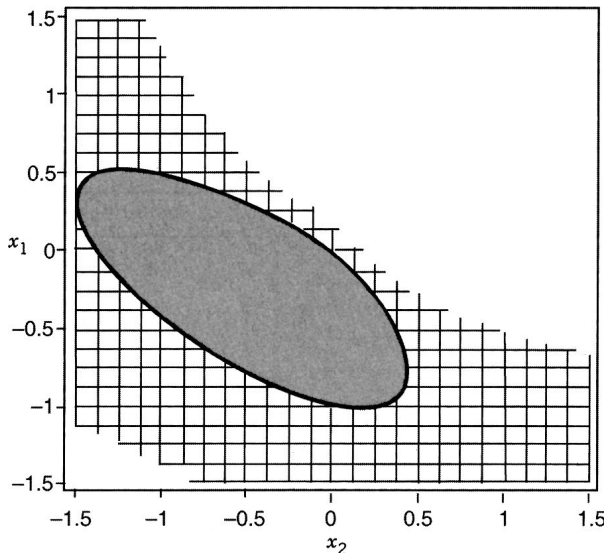


**Figure 6.18** Confidence regions on location of stationary point for data of Example 6.4. The solid region is a 90% confidence region while the cross-hatched region corresponds to a 95% confidence region.

can note the role of the variances (and covariances of coefficients (and, of course, the error mean square) in the analysis. The appearance of the confidence region shown in Fig. 6.18 should serve as a lesson regarding the emphasis that is put on a *point estimate* of optimum conditions. As we have indicated (and will continue to expound), process improvement should be regarded as a continuing, iterative process, and any optimum found in any given experiment should perhaps not be considered as important as what one clearly gains in process improvement and what one learns about the process in general.

Consider now a second data set with the same design as the one in the previous example. One will notice that the fit is considerably better. The data are in Table 6.7. The

**TABLE 6.7 Data for Second Example Showing Confidence Region on Location of Stationary Point**

$x_1$	$x_2$	$y$
-1	-1	87.6
-1	1	85.7
1	-1	86.5
1	1	86.9
$-\sqrt{2}$	0	86.7
$\sqrt{2}$	0	86.8
0	$-\sqrt{2}$	87.4
0	$\sqrt{2}$	86.7
0	0	90.3
0	0	91.0
0	0	90.8

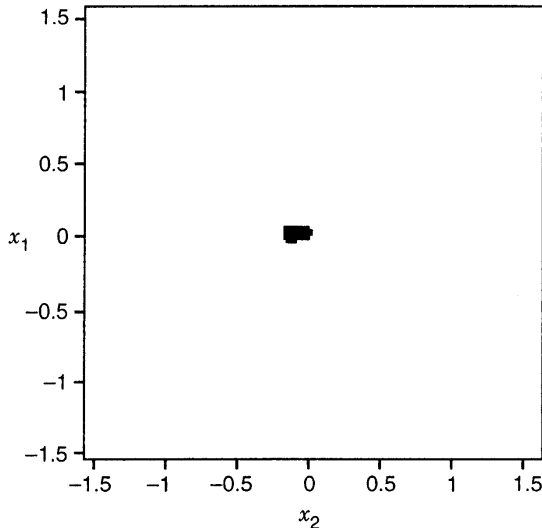


**Figure 6.19** Confidence region on location of stationary point for data of Table 6.7.

second-order model is given by

$$\hat{y} = 90.7000 + 0.0302x_1 - 0.3112x_2 - 2.0316x_1^2 - 1.8816x_2^2 + 0.5750x_1x_2$$

The value of  $R^2$  is 0.9891.

The stationary point (maximum) is at  $(-0.004373, -0.08339)$  with  $\hat{y}_s = 90.7130$ . One would certainly expect the confidence region to be considerably tighter in this case. Figure 6.19 shows the 95% confidence region around the estimated stationary point. We show the graph using the same scale as in the previous example in order to emphasize the contrast. Clearly, the stationary point in this example is estimated very well. It should be emphasized that a large confidence region is not necessarily bad news. A model that fits quite well yet generates a large confidence region on the stationary point may produce a “flat” surface, which implies flexibility in choosing the optimum. This is clearly of interest to the engineer or scientist.

The two examples in this section illustrate contrasting situations. One should not get the feeling that the RSM in the first example will not produce important and interesting results about the process. However, in many RSM situations, *estimation of optimum conditions is very difficult*.

#### 6.5.4 Confidence Intervals on Eigenvalues in Canonical Analysis

In our discussion of the canonical analysis, we noted that if one or more eigenvalues of the matrix  $\hat{\mathbf{B}}$  are close to zero, a ridge system of some type is present. In judging the size of an eigenvalue it can be helpful to have a *confidence interval* estimate of this parameter. Carter, Chinchilli, and Campbell (1990) and Bisgaard and Ankenman (1996) have described procedures for doing this. Because Bisgaard and Ankenman’s procedure is simpler to implement and is equivalent to that of Carter, Chinchilli, and Campbell, we will concentrate on it.

Bisgaard and Ankenman's procedure is usually called the **double linear regression (DLR)** method, because it involves fitting an initial second-order model to the data, finding the matrix  $\hat{\mathbf{B}}$  and its eigenvalues and eigenvectors, and then fitting the canonical model in Equation 6.10:

$$\hat{y} = \hat{a}_0 + \sum_{i=1}^k \hat{a}_i u_i + \sum_{i=2}^k \hat{\lambda}_i u_i^2 \quad (6.18)$$

where the variables  $u_1, u_2, \dots, u_k$  are the canonical variables obtained by rotation of the variables  $x_1, x_{21}, \dots, x_k$ :

$$\mathbf{u} = \mathbf{x}' \mathbf{P} \quad (6.19)$$

Because Equation 6.18 is just a standard linear regression model, we can find the standard errors of the  $\hat{\lambda}_i$  directly and obtain a  $100(1-\alpha)\%$  confidence interval on them using the methods described in Chapter 2, namely,

$$\hat{\lambda}_i \pm t_{\alpha/2, n-p} se(\hat{\lambda}_i)$$

when the model is assumed to have  $p$  parameters.

**Example 6.5 The DLR Method** In Example 6.1 we performed a complete canonical analysis of a second-order model fitted to the chemical process data first introduced in Section 2.8. We found that the eigenvalues of the matrix  $\hat{\mathbf{B}}$  were  $\lambda_1 = -11.0782$  and  $\lambda_2 = -2.6740$ , indicating that the response surface contains a maximum, but it is at least moderately elongated in one direction. We will find 95% confidence intervals on the eigenvalues, using the DLR method.

The first step in the DLR procedure is to find the levels of the original coded design variables in the new rotated canonical variables. For Example 6.1 the original design matrix is

$$\mathbf{D} = \begin{bmatrix} -1 & -1 \\ 1 & -1 \\ -1 & 1 \\ 1 & 1 \\ -1.414 & 0 \\ 1.414 & 0 \\ 0 & -1.414 \\ 0 & 1.414 \\ 0 & 0 \\ 0 & 0 \\ 0 & 0 \end{bmatrix}$$

and from the estimated fitted model

$$\hat{y} = 79.75 + 10.12x_1 + 4.22x_2 - 8.50x_1^2 - 5.25x_2^2 - 7.75x_1x_2$$

we obtain the matrix containing the corresponding eigenvectors

$$\mathbf{P} = \begin{bmatrix} 0.8327 & 0.5538 \\ 0.5538 & -0.8327 \end{bmatrix}$$

Hence, the new canonical-variable design matrix using Equation 6.19 gives

$$\mathbf{U} = \mathbf{DP} = \begin{bmatrix} -1.3864 & -0.2789 \\ 0.2789 & -1.3864 \\ -0.2789 & 1.3864 \\ 1.3864 & 0.2789 \\ -1.1774 & 0.7830 \\ 1.1774 & -0.7830 \\ -0.7830 & -1.1774 \\ 0.7830 & 1.1774 \\ 0 & 0 \\ 0 & 0 \\ 0 & 0 \\ 0 & 0 \end{bmatrix}$$

The first-order terms of the fitted canonical model are obtained by calculating

$$\mathbf{b}'\mathbf{P} = (10.12, 4.22) \begin{bmatrix} 0.8327 & 0.5538 \\ 0.5538 & -0.8327 \end{bmatrix} = (10.8135, -2.1232)$$

and then fitting Equation 6.18 to obtain

$$\hat{y} = 79.75 + 10.8135u_1 - 2.1232u_2 - 11.0769u_1^2 - 2.6731u_2^2$$

Notice that  $\hat{\lambda}_1$  and  $\hat{\lambda}_2$  are identical to the original eigenvalues of  $\hat{\mathbf{B}}$  (to two decimal places). The standard errors of these estimates are

$$se(\hat{\lambda}_1) = se(\hat{\lambda}_2) = 0.9852$$

and  $t_{0.025,7} = 2.365$ . Therefore the 95% confidence intervals on the eigenvalues are

$$\begin{aligned} -11.0769 - 2.365(0.9852) &\leq \lambda_1 \leq -11.0769 + 2.365(0.9852) \\ -13.4069 &\leq \lambda_1 \leq -8.7469 \end{aligned}$$

and

$$\begin{aligned} -2.6731 - 2.365(0.9852) &\leq \lambda_2 \leq -2.6731 + 2.365(0.9852) \\ -5.003 &\leq \lambda_2 \leq -0.3431 \end{aligned}$$

Because neither confidence interval includes zero, we conclude that both  $\lambda_1$  and  $\lambda_2$  are indeed negative, so the true response surface is a maximum. However, note that the

upper confidence limit for  $\lambda_2$  is very close to zero, implying that there is potentially more elongation in the surface in the  $w_2$ -direction than is visually apparent from Fig. 6.5, and the true response surface could actually be fairly close to a stationary ridge system.

## 6.6 MULTIPLE RESPONSE OPTIMIZATION

Up to this point we have emphasized the use of response surface analyses for improvement of the quality of products and processes. We have focused on modeling a measured response or a function of design variables and letting the analysis indicate areas in the design region where the process is likely to give *desirable results*, the term “desirable” being a function of the predicted response. However, in many instances the term “desirable” is a function of more than one response. In a chemical process there are almost always *several properties* of the product output that must be considered in the definition of “desirable.” In many consumer products (food or beverages), the scientist must deal with taste as a response but also must consider other responses such as color and texture, as well as undesirable by-products. In the pharmaceutical or biomedical area, the clinician is primarily concerned with the efficacy of the drug or remedy but must not ignore the possibility of serious side-effects. In a tool life problem, cutting speed ( $x_1$ ) and depth of cut ( $x_2$ ) influence the primary response, the life of the tool. However, a secondary response, rate of metal removed, may also be important in the study.

As an illustration, consider the experiment shown in Table 6.8 This is a central composite design in  $k = 2$  variables, conducted in a chemical process [see Montgomery (2005) for more details]. The two process variables are time and temperature, and there are three responses of interest:  $y_1$  = yield,  $y_2$  = viscosity, and  $y_3$  = number-average molecular weight.

Simultaneous consideration of multiple responses involves first building an appropriate response surface model for each response and then trying to find a set of operating conditions that in some sense optimizes all responses or at least keeps them in desired ranges. We focus initially on the yield response  $y_1$ . Table 6.9 presents the output from

**TABLE 6.8 Central Composite Design with Three Responses**

Natural Variables		Coded Variables		Responses		
$\xi_1$	$\xi_2$	$x_1$	$x_2$	$y_1$ (yield)	$y_2$ (viscosity)	$y_3$ (molecular weight)
80	170	-1	-1	76.5	62	2940
80	180	-1	1	77.0	60	3470
90	170	1	-1	78.0	66	3680
90	180	1	1	79.5	59	3890
85	175	0	0	79.9	72	3480
85	175	0	0	80.3	69	3200
85	175	0	0	80.0	68	3410
85	175	0	0	79.7	70	3290
85	175	0	0	79.8	71	3500
92.07	175	1.414	0	78.4	68	3360
77.93	175	-1.414	0	75.6	71	3020
85	182.07	0	1.414	78.5	58	3630
85	167.93	0	-1.414	77.0	57	3150

**TABLE 6.9 Computer Output from Design-Expert for Fitting a Model to the Yield Response in Table 6.8**

Response: yield

\*\*\*WARNING: The Cubic Model is Aliased!\*\*\*

## Sequential Model Sum of Squares

Source	Sum of Squares	DF	Mean Square	F-Value	Prob > F
Mean	80062.16	1	80062.16		
Linear	10.04	2	5.02	2.69	0.1166
2FI	0.25	1	0.25	0.12	0.7350
<i>Quadratic</i>	<i>17.95</i>	<i>2</i>	<i>8.98</i>	<i>126.888</i>	<i>&lt;0.0001</i> <i>Suggested</i>
Cubic	2.042E-003	2	1.021E-003	0.010	0.9897 <i>Aliased</i>
Residual	0.49	5	0.099		
Total	80090.90	13	6160.84		

## Lack of Fit Tests

Source	Sum of Squares	DF	Mean Square	F-Value	Prob > F
Linear	18.89	6	3.08	58.14	0.0008
2FI	18.24	5	3.65	68.82	0.0006
<i>Quadratic</i>	<i>0.28</i>	<i>3</i>	<i>0.094</i>	<i>1.78</i>	<i>0.2897</i> <i>Suggested</i>
Cubic	0.28	1	0.28	5.31	0.0826 <i>Aliased</i>
Pure Error	0.21	4	0.053		

## Model Summary Statistics

Source	Std. Dev.	R-Squared	Adjusted R-Squared	Predicted R-Squared	Press
Linear	1.37	0.3494	0.2193	-0.0435	29.99
2FI	1.43	0.3561	0.1441	-0.2730	36.59

<i>Quadratic</i>	0.27	0.9828	0.9705	0.9184	2.35	<i>Suggested</i>
Cubic	0.31	0.9828	0.9588	0.3622	18.33	<i>Aliased</i>

Response: Yield

ANOVA for Response Surface Quadratic Model Analysis of variance table [Partial sum of squares]

Source	Sum of Squares	DF	Mean Square	F-Value	Prob > F
Model	28.25	5	5.65	79.85	<0.0001
A	7.92	1	7.92	111.93	<0.0001
B	2.12	1	2.12	30.01	0.0009
$A^2$	13.18	1	13.18	186.22	<0.0001
$B^2$	6.97	1	6.97	98.56	<0.0001
AB	0.25	1	0.25	3.53	0.1022
Residual	0.50	7	0.071		
Lack of Fit	0.28	3	0.094	1.78	0.2897
Pure Error	0.21	4	0.053		
Cor Total	28.74	12			

Std. Dev.	0.27	R-Squared	0.9828
Mean	78.48	Adj R-Squared	0.9705
C.V.	0.34	Pred R-Squared	0.9184
PRESS	2.35	Adeq Precision	23.018

Factor	Coefficient Estimate	DF	Standard Error	95% CI Low	95% CI High	VIF
Intercept	79.94	1	0.12	79.66	80.22	
A-time	0.99	1	0.094	0.77	1.22	1.00
B-temp	0.52	1	0.094	0.29	0.74	1.00
$A^2$	-1.38	1	0.10	-1.61	-1.14	1.02
$B^2$	-1.00	1	0.10	-1.24	-0.76	1.02
AB	0.25	1	0.13	-0.064	0.56	1.00

(Continued)

**TABLE 6.9** (*Continued*)

---

Final Equation in Terms of Coded Factors:

$$\begin{aligned}\text{yield} = \\ +79.94 \\ +0.99 * A \\ +0.52 * B \\ -1.38 * A^2 \\ -1.00 * B^2 \\ +0.25 * A * B\end{aligned}$$

Final Equation in Terms of Actual Factors:

$$\begin{aligned}\text{yield} = \\ -1430.52285 \\ +7.80749 * \text{time} \\ +13.27053 * \text{temp} \\ -0.055050 * \text{time}^2 \\ -0.040050 * \text{temp}^2 \\ + 0.010000 * \text{time} * \text{temp}\end{aligned}$$

Run Order	Standard Order	Actual Value	Diagnostics Case Statistics					
			Predicted Value	Residual	Leverage	Student Residual	Cook's Distance	Outlier <i>t</i>
8	1	76.50	76.30	0.20	0.625	1.213	0.409	1.264
6	2	78.00	77.79	0.21	0.625	1.275	0.452	1.347
9	3	77.00	76.83	0.17	0.625	1.027	0.293	1.032
11	4	79.50	79.32	0.18	0.625	1.089	0.329	1.106
12	5	75.60	75.78	-0.18	0.625	-1.107	0.341	-1.129
10	6	78.40	78.59	-0.19	0.625	-1.195	0.396	-1.240
7	7	77.00	77.21	-0.21	0.625	-1.283	0.457	-1.358
1	8	78.50	78.67	-0.17	0.625	-1.019	0.289	-1.023
5	9	79.90	79.94	-0.040	0.200	-0.168	0.001	-0.156
3	10	80.30	79.94	0.36	0.200	1.513	0.095	1.708
13	11	80.00	79.94	0.060	0.200	0.252	0.003	0.235
2	12	79.70	79.94	-0.24	0.200	-1.009	0.042	-1.010
4	13	79.80	79.94	-0.14	0.200	-0.588	0.014	-0.559

“Sequential Model Sum of Squares”: Select the highest order polynomial where the additional terms are significant.

“Lack of Fit Test”: Want the selected model to have insignificant lack-of-fit.

“Model Summary Statistics”: Focus on the model minimizing the “PRESS,” or equivalently maximizing the “PRED R-SOR.”

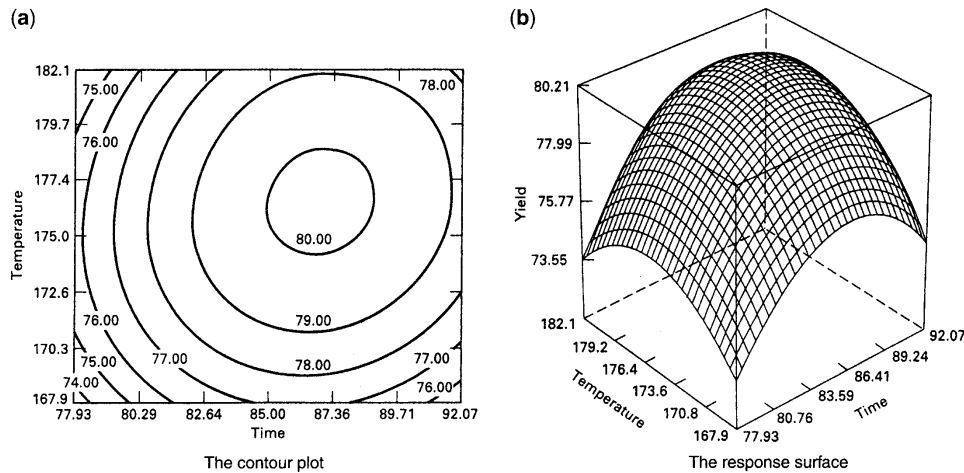


**Figure 6.20** Contour and response surface plots of the yield response in Table 6.8.

Design-Expert for this response. From examining this table we notice that the software package first computes the sequential or extra sums of squares for the linear, quadratic, and cubic terms in the model (there is a warning message concerning aliasing in the cubic model because the CCD does not contain enough runs to support a full cubic model). Based on the small *P*-value for the quadratic term, we decided to fit the second-order model to the yield response. The computer output shows the final model in terms of both the coded variables and the natural or actual factor levels.

Figure 6.20 shows the three-dimensional response surface plot and the contour plot for the yield response in terms of the process variables time and temperature. It is relatively easy to see from examining these figures that the optimum is very near 176°F and 87 min of reaction time and that the response is at a maximum at this point. From examination of the contour plot, we note that the process may be slightly more sensitive to change in reaction time than to changes in temperature.

We obtain models for the viscosity and molecular weight responses ( $y_2$  and  $y_3$ , respectively) as follows:

$$\begin{aligned}\hat{y}_2 &= 70.00 - 0.16x_1 - 0.95x_2 - 0.69x_1^2 - 6.69x_2^2 - 1.25x_1x_2 \\ \hat{y}_3 &= 3386.2 + 205.1x_1 + 177.4x_2\end{aligned}$$

In terms of the natural levels of time ( $\xi_1$ ) and temperature ( $\xi_2$ ), these models are

$$\begin{aligned}\hat{y}_2 &= -9028.79 + 13.394\xi_1 + 97.685\xi_2 \\ &\quad - 2.75 \times 10^{-2}\xi_1^2 - 0.26750\xi_2^2 - 5 \times 10^{-2}\xi_1\xi_2\end{aligned}$$

and

$$\hat{y}_3 = -6308.0 + 41.021\xi_1 + 35.47\xi_2$$

Figures 6.21 and 6.22 present the contour and response surface plots for these models.

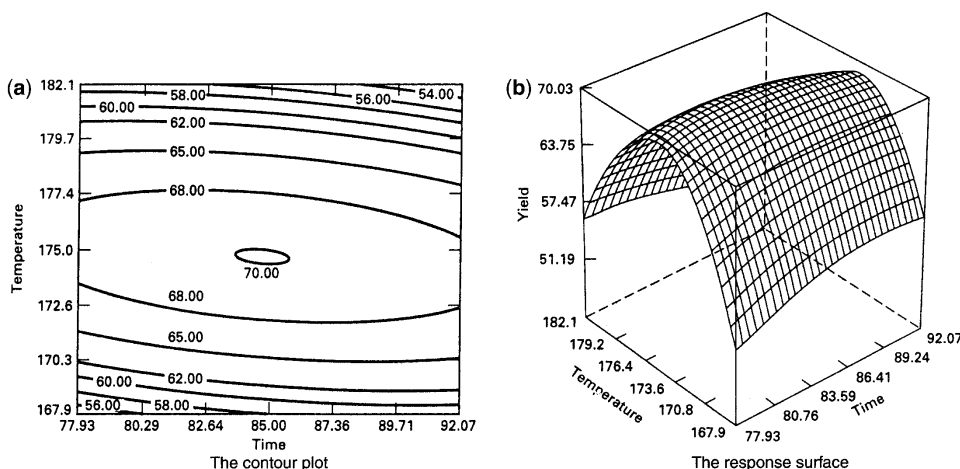


**Figure 6.21** Contour plot and response surface plot of viscosity in Table 6.8.

A relatively straightforward approach to optimizing several responses that works well when there are only a few process variables is to **overlay the contour plots** for each response. [For an early illustration of this approach, see Lind, Goldin, and Hickman (1960).] Figure 6.23 shows an overlay plot for the three responses in Table 6.8, with contours for which  $y_1$  (yield)  $\geq 78.5$ ,  $62 \leq y_2$  (viscosity)  $\leq 68$ , and  $y_3$  (molecular weight Mn)  $\leq 3400$ . If these boundaries represent important conditions that must be met by the process, then as the unshaded portion of Fig. 6.23 shows, there are a number of combinations of time and temperature that will result in a satisfactory process. The experimenter can visually examine the contour plot to determine appropriate operating conditions. For example, it is likely that the experimenter would be most interested in the larger of the two feasible operating regions shown in Fig. 6.23.

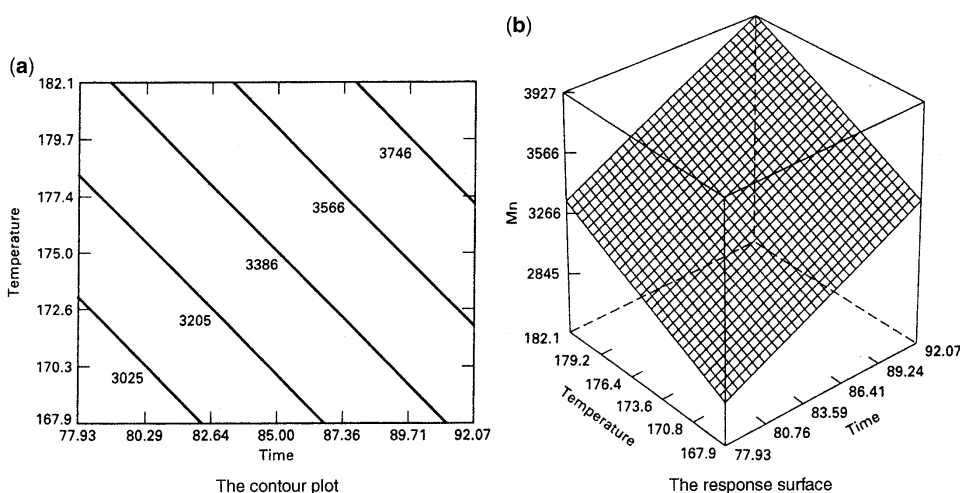


**Figure 6.22** Contour and response surface plot of molecular weight in Table 6.8.

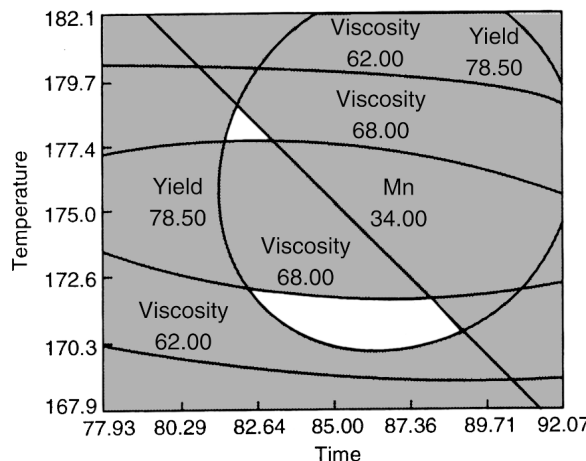


**Figure 6.23** Region of the optimum found by overlaying yield, viscosity, and molecular weight response surfaces in Table 6.8.

When there are more than three design variables, overlaying contour plots becomes awkward, because the contour plot is two-dimensional, and  $k - 2$  of the design variables must be held constant to construct the graph. Often a lot of trial and error is required to determine which factors to hold constant and what levels to select to obtain the best view of the surface. Therefore, there is practical interest in more formal optimization methods for multiple responses.

A popular approach is to formulate and solve the problem as a **constrained optimization problem**. To illustrate, we might formulate the problem as

$$\begin{aligned} & \text{Max } y_1 \\ & \text{subject to} \\ & 62 \leq y_2 \leq 68 \\ & y_3 \leq 3400 \end{aligned}$$

There are many numerical techniques that can be used to solve this problem. Sometimes these techniques are referred to as **nonlinear programming methods**. The Design-Expert software package solves this version of the problem using a direct search procedure. The two solutions found are

$$\text{time} = 83.5 \quad \text{temp} = 177.1 \quad \hat{y}_1 = 79.5$$

and

$$\text{time} = 86.6 \quad \text{temp} = 172.25 \quad \hat{y}_1 = 79.5$$

Notice that the first solution is in the upper (smaller) feasible region of the design space (refer to Fig. 6.23), whereas the second solution is in the larger region. Both solutions are very near to the boundary of the constraints.

In addition to direct search solutions, numerical optimization algorithms can be employed to find the optimum. Del Castillo and Montgomery (1993) describe this approach using the

generalized reduced gradient (GRG) method. Carlyle et al. (2000) overview both direct search and numerical optimization techniques.

There are many ways to use nonlinear programming techniques to formulate and solve the multiple response optimization problem. Del Castillo (1996) describes an interesting approach involving constrained confidence regions. Optimal solutions are found that simultaneously satisfy confidence regions for the responses.

Another useful approach to optimization of multiple responses is to use the simultaneous optimization technique popularized by Derringer and Suich (1980). Their procedure makes use of **desirability functions**. The general approach is to first convert each response  $y_i$  into an individual desirability function  $d_i$  that varies over the range

$$0 \leq d_i \leq 1$$

where if the response  $y_i$  is at its goal or target, then  $d_i = 1$ , and if the response is outside an acceptable region,  $d_i = 0$ . Then the design variables are chosen to maximize the overall desirability

$$D = (d_1 d_2 \cdots d_m)^{1/m}$$

where there are  $m$  responses.

The individual desirability functions are structured as shown in Fig. 6.24. If the objective or target  $T$  for the response  $y$  is a maximum value,

$$d = \begin{cases} 0 & y < L \\ \left(\frac{y-L}{T-L}\right)^r & L \leq y \leq T \\ 1, & y > T \end{cases} \quad (6.20)$$

when the weight  $r = 1$ , the desirability function is linear. Choosing  $r > 1$  places more emphasis on being close to the target value, and choosing  $0 < r < 1$  makes this less important. If the target for the response is a minimum value,

$$d = \begin{cases} 1 & y < T \\ \left(\frac{U-y}{U-T}\right)^r & T \leq y \leq U \\ 0 & y > U \end{cases} \quad (6.21)$$

The two-sided desirability shown in Fig. 6.24c assumes that the target is located between the lower ( $L$ ) and upper ( $U$ ) limits, and is defined as

$$d = \begin{cases} 0 & y < L \\ \left(\frac{y-L}{T-L}\right)^{r_1} & L \leq y \leq T \\ \left(\frac{U-y}{U-T}\right)^{r_2} & T \leq y \leq U \\ 0 & y > U \end{cases} \quad (6.22)$$

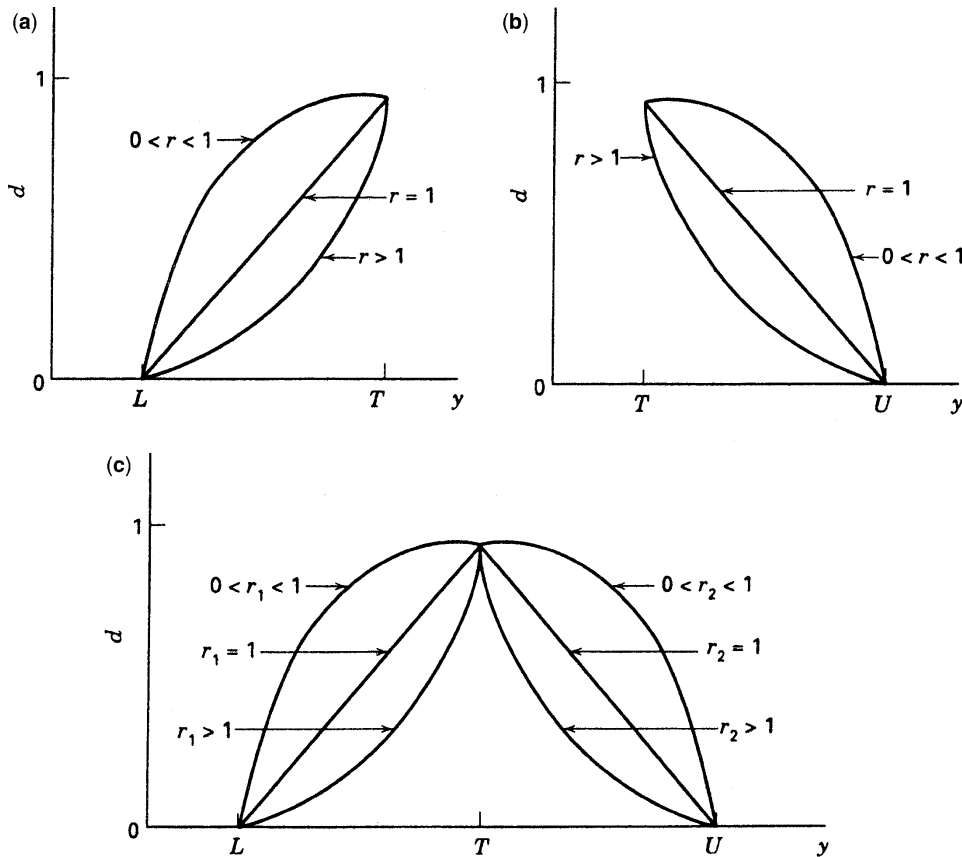


**Figure 6.24** Individual desirability functions for simultaneous optimization  $y$ . (a) Objective (target) is to maximize  $y$ . (b) Objective (target) is to minimize  $y$ . (c) Objective is for  $y$  to be as close as possible to the target.

The Design-Expert software package was used to apply the desirability function approach to the problem in Table 6.8. We chose  $T = 80$  as the target for the yield response, chose  $L = 70$ , and set the weight for this individual desirability equal to unity. We set  $T = 65$  for the viscosity response with  $L = 62$  and  $U = 68$  (to be consistent with specifications), with both weights  $r_1 = r_2 = 1$ . Finally, we indicated that any molecular weight between 3200 and 3400 was acceptable. Two solutions were found.

**Solution 1:**

$$\begin{aligned} \text{Time} &= 86.1 & \text{Temp} &= 170.3 & D &= 0.929 \\ \hat{y}_1 &= 78.6 & \hat{y}_2 &= 65 & \hat{y}_3 &= 3319 \end{aligned}$$

**Solution 2:**

$$\begin{aligned} \text{Time} &= 80.3 & \text{Temp} &= 179.2 & D &= 0.855 \\ \hat{y}_1 &= 77.3 & \hat{y}_2 &= 65 & \hat{y}_3 &= 3400 \end{aligned}$$

Solution 1 has the highest overall desirability. Notice that it results in on-target viscosity and acceptable molecular weight. This solution is in the larger of the two operating

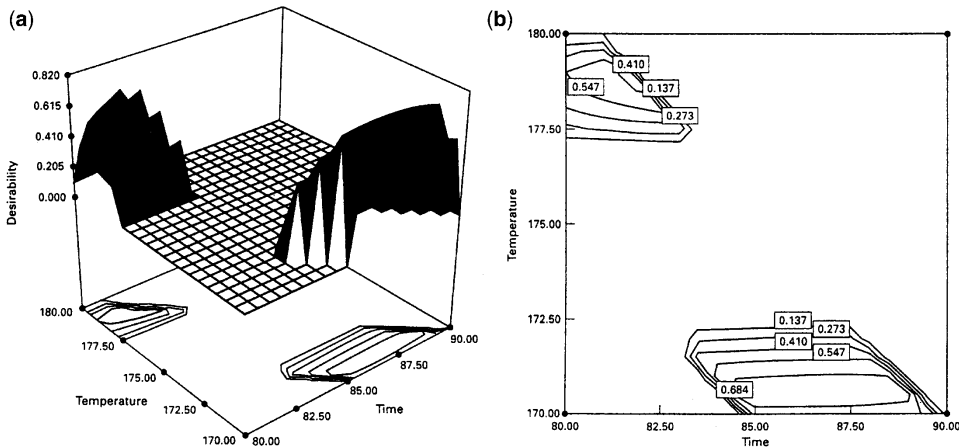


**Figure 6.25** Desirability function response surface and contour plot for the problem in Table 6.8. (a) Response surface. (b) Contour plot.

regions in Fig. 6.23, whereas the second solution is in the smaller region. Figure 6.25 shows a response surface and contour plot of the overall desirability function  $D$ .

Design-Expert uses direct search methods to maximize the desirability function  $D$ . Because the individual desirability functions are not differentiable, numerical optimization methods such as the GRG cannot be used directly. However, Del Castillo, Montgomery, and McCarville (1996) show how the individual desirability functions can be replaced with polynomial approximations that are everywhere differentiable so that the GRG and other derivative-based optimization algorithms can be employed.

As we indicated earlier, multiple response procedures will typically involve compromise between important responses. In addition to the approaches illustrated above, several creative ideas have been put forth in the literature, and some enjoy considerable use in industry. We now give a brief overview of these other methods.

**Dual Response Approach** In the case of two responses, a useful technique termed the **dual response approach** was introduced by Myers and Carter (1973). It is assumed that the two responses can be categorized as **primary** and **secondary**. The goal then involves the determination of conditions  $\mathbf{x}$  on the design variables that produces  $\max \hat{y}_p(\mathbf{x})$  [or  $\min \hat{y}_s(\mathbf{x})$ ] subject to a constraint on  $\hat{y}_s(\mathbf{x})$ . Here  $\hat{y}_p(\mathbf{x})$  is the primary response function and  $\hat{y}_s(\mathbf{x})$  is the secondary response function. The methodology, which is not unlike ridge analysis discussed earlier in this chapter, produces a locus of coordinates in which various values of  $\hat{y}_s(\mathbf{x})$  are considered. For example, in a yield-cost scenario one might let the secondary response be yield and determine conditions on  $\mathbf{x}$  that minimize cost for fixed satisfactory levels of yield. This approach was the forerunner of more sophisticated nonlinear programming procedures. Biles (1975) and Del Castillo and Montgomery (1993) discuss the extension of this concept to more than two responses. Del Castillo, Fan, and Semple (1997) discuss computing global optima in dual-response systems, and Fan (2000) gives a Fortran program. Also see Lin and Tu (1995).

**Khuri–Conlon Approach** Khuri and Conlon (1981) introduced a procedure that is based on a **distance** function that computes the overall closeness of the response functions to their

respective optima at the same set of conditions. That is, it gives a measure of closeness to the *ideal optimum*. One then finds conditions on  $\mathbf{x}$  that minimize this distance function over all  $\mathbf{x}$  in the experimental region. The distance function they use is

$$[\hat{\mathbf{y}}(\mathbf{x}) - \boldsymbol{\theta}]' \Sigma_{\hat{\mathbf{y}}(\mathbf{x})}^{-1} [\hat{\mathbf{y}}(\mathbf{x}) - \boldsymbol{\theta}]$$

where  $\hat{\mathbf{y}}(\mathbf{x})$  is the vector of estimated responses at the point  $\mathbf{x}$ ,  $\Sigma_{\hat{\mathbf{y}}(\mathbf{x})}$  is the covariance matrix for the estimated responses at this location, and  $\boldsymbol{\theta}$  is the vector of target values or ideal optimal values for the responses. The optimum value of  $\mathbf{x}$  would minimize this distance function. A very nice aspect of this approach is that it considers directly the correlation structure of the responses and the quality of the response predictions. However, it does not allow the analyst to create appropriate priorities for the individual responses.

**Squared Error Loss Approaches** Several authors have recommended approaches based on squared error loss (indeed, the Khuri–Conlon method is a squared error loss procedure). For example, see Pignatiello (1993), Ames et al. (1997), and Vining (1998). In Vining's approach the squared error loss function is

$$L = [\hat{\mathbf{y}}(\mathbf{x}) - \boldsymbol{\theta}]' \mathbf{C} [\hat{\mathbf{y}}(\mathbf{x}) - \boldsymbol{\theta}]$$

where  $\mathbf{C}$  is a positive definite matrix of weights or costs. He minimizes the expected loss

$$E(L) = \{E[\hat{\mathbf{y}}(\mathbf{x})] - \boldsymbol{\theta}\}' \mathbf{C} \{E[\hat{\mathbf{y}}(\mathbf{x})] - \boldsymbol{\theta}\} + \text{Trace}[\mathbf{C} \Sigma_{\hat{\mathbf{y}}(\mathbf{x})}]$$

The estimated expected loss is

$$\widehat{E(L)} = [\hat{\mathbf{y}}(\mathbf{x}) - \boldsymbol{\theta}]' \mathbf{C} [\hat{\mathbf{y}}(\mathbf{x}) - \boldsymbol{\theta}] + \text{Trace}[\mathbf{C} \Sigma_{\hat{\mathbf{y}}(\mathbf{x})}]$$

There are several different choices for the matrix  $\mathbf{C}$ .

## 6.7 FURTHER COMMENTS CONCERNING RESPONSE SURFACE ANALYSIS

There are several important aspects of RSM that only become apparent after one gains a certain level of experience. In a textbook presentation of RSM, a great deal is taken for granted—the model, the experimental region, the proper choice of response, and, of course, the goal of the study. All, however, need to be handled with care, and each one needs to be a topic of discussion between statistician and scientist or engineer.

The choice of experimental region needs to be made very carefully. Choice of range in the natural variable levels cannot be taken lightly. Ranges that are too small may result in an important factor becoming insignificant in the analysis. This is particularly crucial in the phase of the analysis when variable screening is being done. Often the natural sequential deployment of RSM allows the user to make intelligent choices of variable ranges after preliminary phases of the study have been analyzed. For example, following variable screening, the user should have better choices of ranges for a steepest ascent procedure. After steepest ascent is accomplished, choice of variable ranges to be used for a second-order analysis should be easier to make.

Let us consider briefly the issue of the goal of the experiment. This textbook develops and emphasizes the need to find optimum conditions. However, one should keep in mind that the estimated optimum conditions from one experiment are indeed only estimates. The next experiment may well find the estimated optimum conditions to be at a different set of coordinates. Also, process technology changes from time to time, and a computed set of optimum conditions may well be fleeting. What is often more important is for the analysis to reveal important information about the process and information about the roles of the variables. The computation of a stationary point, a canonical analysis, or a ridge analysis may well lead to important information about the process. This in the long run will often be more valuable than a single set of coordinates representing an estimate of optimum conditions.

## EXERCISES

- 6.1** In a study to determine the nature of a response system that relates dry modulus of rupture (psi) in a certain ceramic material with three important independent variables, the following quadratic regression equation was determined [see Hackney and Jones (1969)]:

$$\begin{aligned}\hat{y} \times 10^{-2} = & 6.88 - 0.1466x_1^2 + 0.1875x_1x_2 + 0.2050x_1x_3 + 0.0325x_1 \\ & - 0.0053x_2^2 - 0.1450x_2x_3 + 0.2588x_2 + 0.1359x_3^2 - 0.1363x_3\end{aligned}$$

The independent variables represent ratios of concentration of various ingredients in the material.

- (a) Determine the stationary point.
  - (b) Put the response surface into canonical form, and determine the nature of the stationary point.
  - (c) Find the appropriate expressions relating the canonical variables to the independent variables  $x_1$ ,  $x_2$ , and  $x_3$ .
  - (d) Generate two-dimensional graphs showing contours of constant estimated modulus of rupture. Use  $x_3 = -1, 0, 1$ .
- 6.2** In a chemical engineering experiment dealing with heat transfer in a shallow fluidized bed, data are collected on the following four regressor variables: fluidizing gas flow rate, lb/hr ( $x_1$ ); supernatant gas flow rate, lb/hr ( $x_2$ ); supernatant gas inlet nozzle opening, mm ( $x_3$ ); supernatant gas inlet temperature, °F ( $x_4$ ). The responses measured are heat transfer efficiency ( $y_1$ ) and thermal efficiency ( $y_2$ ). The data are given in Table E6.1.

This is a good example of what often happens in practice. An attempt was made to use a particular second-order design. However, errors in controlling the variables produced a design that is only an approximation of the standard design.

- (a) Center and scale the design variables. That is, create the design matrix in coded form.
- (b) Fit a second-order model for both responses.

**TABLE E6.1 Data for Exercise 6.2**

Observation	$y_1$	$y_2$	$x_1$	$x_2$	$x_3$	$x_4$
1	41.852	38.75	69.69	170.83	45	219.74
2	155.329	51.87	113.46	230.06	25	181.22
3	99.628	53.79	113.54	228.19	65	179.06
4	49.409	53.84	118.75	117.73	65	281.30
5	72.958	49.17	119.72	117.69	25	282.20
6	107.702	47.61	168.38	173.46	45	216.14
7	97.239	64.19	169.85	169.85	45	223.88
8	105.856	52.73	169.85	170.86	45	222.80
9	99.438	51.00	170.89	173.92	80	218.84
10	111.907	47.37	171.31	173.34	25	218.12
11	100.008	43.18	171.43	171.43	45	219.20
12	175.380	71.23	171.59	263.49	45	168.62
13	117.800	49.30	171.63	171.63	45	217.58
14	217.409	50.87	171.93	170.91	10	219.92
15	41.725	54.44	173.92	71.73	45	296.60
16	151.139	47.93	221.44	217.39	65	189.14
17	220.630	42.91	222.74	221.73	25	186.08
18	131.666	66.60	228.90	114.40	25	285.80
19	80.537	64.94	231.19	113.52	65	286.34
20	152.966	43.18	236.84	167.77	45	221.72

- (c) In the case of transfer efficiency ( $y_1$ ), do a canonical analysis and determine the nature of the stationary point. Do the same for thermal efficiency ( $y_2$ ).
- (d) For the case of transfer efficiency, what levels (natural levels) of the design variables would you recommend if maximum transfer efficiency is sought?
- (e) Do the same for thermal efficiency; that is, find levels of the design variables that you recommend for maximization of thermal efficiency.
- (f) The chemical engineer requires that  $y_2$  exceed 60. Find levels (natural) of  $x_1$ ,  $x_2$ , and  $x_3$  that maximize  $y_1$  subject to the constraint  $y_2 > 60$ .
- 6.3** A chemical extraction process was studied using a central composite design in an effort to find operating conditions on three variables that maximize yield. The results are shown in Table E6.2.
- (a) Fit a second-order response surface model to these data.  
 (b) Use contour plots to find conditions that maximize yield.  
 (c) Perform the canonical analysis, including finding the location of the stationary point. Interpret the fitted surface.
- 6.4** Rayon whiteness is an important factor for scientists dealing with fabric quality. Whiteness is affected by pulp quality and other processing variables. Some of the variables include: acid bath temperature, °C ( $x_1$ ); cascade acid concentration, % ( $x_2$ ); water temperature, °C ( $x_3$ ); sulfide concentration, % ( $x_4$ ); amount of chlorine bleach, lb/min ( $x_5$ ). Table E6.3 shows an experimental design involving these five design variables. The response is a measure of whiteness.

**TABLE E6.2 Data for Exercise 6.3**

$x_1$	$x_2$	$x_3$	$y$
-1	-1	-1	56.6
1	-1	-1	58.5
-1	1	-1	48.9
1	1	-1	55.2
-1	-1	1	61.8
1	-1	1	63.3
-1	1	1	61.5
1	1	1	64.0
-1	0	0	61.3
1	0	0	65.5
0	-1	0	64.6
0	1	0	65.9
0	0	-1	63.6
0	0	1	65.0
0	0	0	62.9
0	0	0	63.8

The coding of the design variables is as follows:

$$x_1 = \frac{\text{temp} - 45}{10}; \quad x_2 = \frac{\text{conc} - 0.5}{0.2}, \quad x_3 = \frac{\text{temp} - 85}{3};$$

$$x_4 = \frac{\text{conc} - 0.25}{0.05}, \quad x_5 = \frac{\text{amt} - 0.4}{0.1}$$

- (a) Fit an appropriate second-order model in the metric of the coded variables.
- (b) Find the stationary point, and describe the nature of the surface.
- (c) Give a recommendation for operating conditions on the design variables. It is important to maximize whiteness.
- (d) Compute the standard error of prediction at the following design locations:
  - i. Design center (0,0,0,0,0)
  - ii. All factorial points
  - iii. All axial points

Comment on the relative stability of the standard error of prediction.

- 6.5 A client from the Department of Mechanical Engineering at Virginia Polytechnic Institute and State University asked for help in analyzing an experiment dealing with gas turbine generators. The voltage output of a generator was measured at various combinations of blade speed and voltage measuring sensor extension. The data are given in Table E6.4.
- (a) Write the design matrix in coded form.
  - (b) What type of design has been used?
  - (c) Fit an appropriate model.
  - (d) Find the stationary point, and interpret the fitted surface.

**TABLE E6.3 Data for Exercises 6.4**

$x_1$	$x_2$	$x_3$	$x_4$	$x_5$	$y$
-1	-1	-1	-1	-1	71.5
1	1	-1	-1	-1	76.0
1	-1	1	-1	-1	79.9
1	-1	-1	1	-1	83.5
1	-1	-1	-1	1	89.5
-1	1	1	-1	-1	84.2
-1	1	-1	1	-1	85.7
-1	1	-1	-1	1	94.5
-1	-1	1	1	-1	89.4
-1	-1	1	-1	1	97.5
-1	-1	-1	1	1	103.2
1	1	1	1	-1	108.7
1	1	1	-1	1	115.2
1	1	-1	1	1	111.5
1	-1	1	1	1	102.3
-1	1	1	1	1	108.1
-2	0	0	0	0	80.2
2	0	0	0	0	84.1
0	-2	0	0	0	77.2
0	2	0	0	0	85.1
0	0	-2	0	0	71.5
0	0	2	0	0	84.5
0	0	0	-2	0	77.5
0	0	0	2	0	79.2
0	0	0	0	-2	71.0
0	0	0	0	2	90.2
0	0	0	0	0	72.1
0	0	0	0	0	72.0
0	0	0	0	0	72.4
0	0	0	0	0	71.7
0	0	0	0	0	72.8

**TABLE E6.4 Data for Exercise 6.5**

$y$ (volts)	Speed $x_1$ (in./sec)	Extension $x_2$ (in.)
1.23	5300	0.000
3.13	8300	0.000
1.22	5300	0.012
1.92	8300	0.012
2.02	6800	0.000
1.51	6800	0.012
1.32	5300	0.006
2.62	8300	0.006
1.65	6800	0.006
1.62	6800	0.006
1.59	6800	0.006

- (e) It is important to determine what value of speed and extension results in a response that exceeds 2.8 volts. Describe where in the design region this voltage can be achieved. Use a two-dimensional contour plot to answer the question.
- 6.6** In Exercise 3.9 we discussed an application dealing with effects on cracking of a titanium alloy. An additional study was made in which the same factors were studied except the heat treatment method. The “high” or “+” method was used and held constant. However, in this case, a second-order design was used so the analyst could fit a second-order model involving curvature. The three factors are pouring temperature  $x_1$ ; titanium content  $x_2$ ; and amount of grain refiner,  $x_3$ . Table E6.5 gives the design points and the response data. The response is the crack length (in millimeters) induced in a sample of the alloy.
- (a) Fit an appropriate model with the data of the above central composite design.
  - (b) From the fitted model in (a), estimate the conditions that give rise to minimum shrinkage. Be sure that these estimated conditions are not remote from the current experimental design.
  - (c) Compute the predicted value and its standard error at your recommended set of conditions.
  - (d) Does this experiment give rise to suggestions for future experimental runs? Explain.
- 6.7** Consider the reaction yield data shown in Table E6.6.
- (a) Fit a second-order model to the data.
  - (b) Construct contour plots, and comment on the fitted response surface.
  - (c) Perform the canonical analysis.

**TABLE E6.5 Data for Exercise 6.6**

$x_1$	$x_2$	$x_3$	$y$
-1	-1	-1	0.5269
+1	-1	-1	2.6680
-1	+1	-1	1.0310
+1	+1	-1	2.3380
-1	-1	+1	3.2220
+1	-1	+1	4.0060
-1	+1	+1	3.3640
+1	+1	+1	3.2200
0	0	0	2.0280
0	0	0	1.9670
0	0	0	1.9300
0	0	0	2.0130
-1.732	0	0	1.6200
1.732	0	0	3.4510
0	-1.732	0	2.9590
0	1.732	0	2.6990
0	0	-1.732	0.9414
0	0	1.732	3.7880

**TABLE E6.6 Data for Exercise 6.7**

$x_1$	$x_2$	$y$
-1	-1	88.55
-1	1	86.29
1	-1	85.80
1	1	80.40
0	0	91.21
0	0	91.85
-1.414	0	85.50
1.414	0	85.39
0	-1.414	86.22
0	1.414	85.70
0	0	91.31
0	0	91.94

- 6.8** In the computer industry, it is important to use experimental design and response surface methods to analyze performance data from integrated circuit/packet-switched computer networks. Here, the design variables are network input variables that affect network size, traffic load, link capacity, and so on. The response measures represent the network performance. In this experiment [Schmidt and Launsby (1990)] the design variables are:

CS: Circuit switch arrival rate (voice calls/min)  
 PS: Packet switch arrival rate (packets/sec)  
 SERV: Voice call service rate (sec)  
 SLOTS: Number of time slots per link (a capacity indicator)

Two responses were measured. They were:

ALU: Average link utilization  
 BLK: Fraction of voice calls blocked

The data are given in Table E6.7.

- (a)** Write the design in coded form. Use the coding

$$\begin{aligned}x_1 &= (\text{CS} - 4)/2 \\x_2 &= (\text{PS} - 300)/150 \\x_3 &= (\text{SERV} - 180)/60 \\x_4 &= (\text{SLOTS} - 40)/6\end{aligned}$$

- (b)** Fit two second-order models for the two responses.  
**(c)** Consider the response surface for the BLK response. Can the model be improved by a power transformation? Discuss.  
**(d)** Use the two models above to determine optimum conditions for the two responses *separately*. We need to maximize ALU and minimize BLK.

**TABLE E6.7** Data for Exercise 6.8

OBS	CS	PS	SERV	SLOTS	ALU	BLK
1	2	150	120	34	0.282	0.000
2	2	150	120	46	0.194	0.000
3	2	150	240	34	0.372	0.000
4	2	150	240	46	0.275	0.000
5	2	450	120	34	0.553	0.016
6	2	450	120	46	0.396	0.000
7	2	450	240	34	0.676	0.031
8	2	450	240	46	0.481	0.003
9	6	150	120	34	0.520	0.012
10	6	150	120	46	0.386	0.000
11	6	450	120	46	0.594	0.016
12	6	300	180	40	0.231	0.000
13	4	300	180	40	0.325	0.000
14	4	300	180	52	0.427	0.000
15	4	300	180	40	0.561	0.016
16	4	300	180	40	0.571	0.005
17	4	300	180	40	0.561	0.011
18	4	300	180	40	0.581	0.020
19	4	300	180	40	0.562	0.017
20	4	300	180	40	0.608	0.036
21	4	300	180	40	0.560	0.007
22	5	400	210	43	0.739	0.070
23	5	400	210	43	0.746	0.082
24	5	400	150	37	0.725	0.067
25	5	400	150	37	0.725	0.084
26	5	400	150	43	0.615	0.027
27	5	400	210	40	0.785	0.106
28	5	400	210	40	0.782	0.125
29	4	400	210	37	0.747	0.084
30	4	400	210	37	0.745	0.101
31	4	400	210	40	0.695	0.063
32	4	400	210	40	0.667	0.057
33	4	400	180	40	0.648	0.035
34	5	400	180	40	0.722	0.074
35	5	400	180	40	0.731	0.077
36	5	400	180	37	0.775	0.110
37	5	400	180	37	0.779	0.139
38	4	400	180	37	0.712	0.057
39	4	400	180	37	0.701	0.065
40	3	400	210	37	0.652	0.017
41	3	400	210	43	0.541	0.003
42	3	400	150	37	0.570	0.003
43	3	400	150	43	0.476	0.005

- (e) Use appropriate software to find conditions that

$$\max \widehat{\text{ALU}}|\widehat{\text{BLK}} < 0.005$$

- (f) Use the Derringer–Suich procedure to find optimum conditions. Use the conditions that ALU cannot be less than 0.5 and BLK cannot exceed 0.10.
- 6.9** In Schmidt and Launsby (1990), a simulation program was given that simulates an auto-bumper plating process using thickness as the response with time, temperature, and pH as the design variables. An experiment was conducted in order that a response surface optimization could be accomplished. The coding for the design variables is given by
- $$x_1 = \frac{\text{time} - 8}{4}$$
- $$x_2 = \frac{\text{temp} - 24}{8}$$
- $$x_3 = \frac{\text{nickel} - 14}{4}$$
- The design in the natural units is given in Table E6.8 along with the thickness values.
- (a) Write the design in coded form. Name the type of design.  
 (b) Fit a complete second-order model in the coded metric.  
 (c) Edit the model by eliminating obviously insignificant terms.  
 (d) Check model assumptions by plotting residuals against the design variables separately.  
 (e) The purpose of this experiment was not to merely find optimum conditions (conditions that maximize thickness) but to gain an impression about the role of the three design variables. Show contour plots, fixing levels of nickel at 10, 14, and 18.  
 (f) Use the plots to produce a recommended set of conditions that maximize thickness.  
 (g) Compute the standard error of prediction at the location of maximum thickness.
- 6.10** Refer to Exercise 6.9. The same simulation model was used to construct another response surface using a different experimental design. This second design, in natural units, is given in Table E6.9 along with the thickness data:
- (a) Using the same coding as in Exercise 6.9, write out the design matrix in coded form.  
 (b) Is this a central composite design?  
 (c) Fit and edit a second-order response surface model. That is, fit and eliminate insignificant terms.  
 (d) Find conditions that maximize thickness, with the constraint that the condition falls inside the design region. Use an appropriate software package. In addition, compute the standard error of prediction at the location of optimum conditions.

**TABLE E6.8 Data for Exercise 6.9**

Run Number	Time	Temperature	Nickel	Thickness
1	4	16	10	113
2	12	16	10	756
3	4	32	10	78
4	12	32	10	686
5	4	16	18	87
6	12	16	18	788
7	4	32	18	115
8	12	32	18	696
9	4	16	10	99
10	12	16	10	739
11	4	32	10	10
12	12	32	10	712
13	4	16	18	159
14	12	16	18	776
15	4	32	18	162
16	12	32	18	759
17	8	24	14	351
18	8	24	14	373
19	8	24	14	353
20	8	24	14	321
21	12	24	14	736.1
22	4	24	14	96.0
23	8	32	14	328.9
24	8	16	14	303.5
25	8	24	18	358.2
26	8	24	10	347.7

**TABLE E6.9 Data for Exercise 6.10**

Run Number	Time	Temperature	Nickel	Thickness
1	4	16	14	122
2	12	16	14	790
3	4	32	14	100
4	12	32	14	695
5	4	24	10	50
6	12	24	10	720
7	4	24	18	118
8	12	24	18	650
9	8	16	10	330
10	8	32	10	314
11	8	16	18	302
12	8	32	18	340
13	8	24	14	364
14	8	24	14	342
15	8	24	14	404

- 6.11** Reconsider Exercises 6.9 and 6.10. In addition to the designs in these exercises, a *D-optimal* design was used to generate data on thickness from the simulation model. The notion of **D-optimality** will be discussed at length in Chapter 8. The design and data are given in Table E6.10.
- Using the same coding scheme as in Exercises 6.9 and 6.10, write the design in coded units.
  - Fit a second-order model, and edit it—that is, eliminate insignificant terms.
  - Find conditions of estimated maximum thickness. Can this be done with a two-dimensional contour plot? Explain. Compute the standard error of prediction at the set of optimum conditions.
- 6.12** Exercises 6.9, 6.10, and 6.11 illustrate the use of three different types of designs for modeling the same system. All three designs are used because of their capability to efficiently fit a *complete* second-order model, even if the edited model contains no interactions. Another type of design that allows for estimation of linear and pure quadratic effects is the **Taguchi  $L_{27}$** . The Taguchi approach to quality improvement will be discussed in detail in Chapter 10. The  $L_{27}$  was also used to generate data on thickness as in the previous exercises. The design and response data are given in Table E6.11.
- Code the design factors as in previous exercises.
  - Form the complete matrix  $\mathbf{X}$  for the  $L_{27}$  (using coded design levels).
  - Comment on whether or not this design is adequate for a *complete* second-order model (including interactions).
- 6.13** In this exercise we will make comparisons among the central composite, Box–Behnken, and *D*-optimal designs used in Exercises 6.9, 6.10, and 6.11. We will not deal with any particular edited model, but rather with a complete

**TABLE E6.10 Data for Exercise 6.11**

Run Number	Time	Temperature	Nickel	Thickness
1	12	32	10	717
2	4	16	10	136
3	12	16	18	787
4	4	32	18	78
5	4	16	18	87
6	4	32	10	80
7	12	16	10	760
8	8	24	10	282
9	8	32	14	318
10	4	24	14	96
11	12	32	18	682
12	12	24	14	747
13	12	24	14	764
14	12	24	14	742

**TABLE E6.11 Data for Exercise 6.12**

Run Number	Time	Temperature	Nickel	Thickness
1	4	16	10	113
2	4	16	14	152
3	4	16	18	147
4	4	24	10	65
5	4	24	14	53
6	4	24	18	130
7	4	32	10	83
8	4	32	14	40
9	4	32	18	94
10	8	16	10	339
11	8	16	14	303
12	8	16	18	381
13	8	24	10	348
14	8	24	14	342
15	8	24	18	420
16	8	32	10	327
17	8	32	14	255
18	8	32	18	322
19	12	16	10	745
20	12	16	14	780
21	12	16	18	740
22	12	24	10	772
23	12	24	14	769
24	12	24	18	755
25	12	32	10	735
26	12	32	14	726
27	12	32	18	757

second-order model. Compute the *scaled* standard error of prediction

$$\sqrt{\frac{N \text{Var}[\hat{y}(\mathbf{x})]}{\sigma^2}} = \sqrt{N[\mathbf{x}^{(2)\prime}(\mathbf{X}'\mathbf{X})^{-1}\mathbf{X}^{(2)}]}$$

at the locations given in Table E6.12 in coded design units.  $N$  is the size of the design.

Comment on comparisons among the three designs.

- 6.14** In their paper Derringer and Suich (1980) illustrate their multiple-response procedure with an interesting data set. The central composite design given in Table E6.13 shows data obtained in the development of a tire tread compound on four responses: PICO Abrasion Index,  $y_1$ ; 200% modulus,  $y_2$ ; elongation at break,  $y_3$ ; hardness,  $y_4$ . Each column was taken at the 20 sets of conditions shown, where  $x_1$ ,  $x_2$ ,  $x_3$  are coded levels of the variables  $x_1$  = hydrated silica level,  $x_2$  = silane coupling agent level, and  $x_3$  = sulfur. The following inequalities represent

**TABLE E6.12 Design Location for Exercise 6.13**

$x_1$	$x_2$	$x_3$
-1	-1	-1
1	-1	-1
-1	1	-1
-1	-1	1
1	1	-1
1	-1	1
-1	1	1
1	1	1
-1	0	0
1	0	0
0	-1	0
0	1	0
0	0	-1
0	0	1
0	0	0

desirable conditions on the responses:

$$\begin{aligned}y_1 &> 120 \\y_2 &> 1,000 \\400 < y_3 < 600 \\60 < y_4 < 75\end{aligned}$$

- (a) Fit appropriate response surface models for all responses.
  - (b) Develop two-dimensional contours (at  $x_3 = -1.6, -1, 0, 1, 1.6$ ) of constant response for all four responses. Can you determine sets of conditions on  $x_1$ ,  $x_2$ , and  $x_3$  that meet the above requirements? If so, list them.
  - (c) Use the desirability function procedure to determine other competing conditions.
- 6.15** The experiment given in Table E6.14 uses a central composite design to study three variables in a chemical process.
- (a) Fit a second-order model to the conversion response  $y_1$ .
  - (b) Investigate the fitted surface using contour plots.
  - (c) Find the stationary point, and perform the canonical analysis.
- 6.16** Reconsider the chemical process experiment in Exercise 6.15. Find appropriate response surface models for both responses.
- (a) Use contour plots to find conditions where the conversion  $y_1$  is maximized and the thermal activity  $y_2$  is between 55 and 60.
  - (b) Rework part (a) using a constrained optimization formulation.
  - (c) Rework part (a) using the desirability function approach, but assume that it is necessary to make the thermal activity as close to 57.5 as possible.
- 6.17** Reconsider the experiment in Exercise 6.14. Formulate and solve the optimization problem using:
- (a)  $y_1$ , as the objective function (maximize  $y_1$ ).

**TABLE E6.13 Data for Exercises 6.14, 6.17**

Compound Number	$x_1$	$x_2$	$x_3$	$y_1$	$y_2$	$y_3$	$y_4$
1	-1	-1	1	102	900	470	67.5
2	1	-1	-1	120	860	410	65
3	-1	1	-1	117	800	570	77.5
4	1	1	1	198	2294	240	74.5
5	-1	-1	-1	103	490	640	62.5
6	1	-1	1	132	1289	270	67
7	-1	1	1	132	1270	410	78
8	1	1	-1	139	1090	380	70
9	-1.633	0	0	102	770	590	76
10	1.633	0	0	154	1690	260	70
11	0	-1.633	0	96	700	520	63
12	0	1.633	0	163	1540	380	75
13	0	0	-1.633	116	2184	520	65
14	0	0	1.633	153	1784	290	71
15	0	0	0	133	1300	380	70
16	0	0	0	133	1300	380	68.5
17	0	0	0	140	1145	430	68
18	0	0	0	142	1090	430	68
19	0	0	0	145	1260	390	69
20	0	0	0	142	1344	390	70

**TABLE E6.14 Data for Exercises 6.15, 6.16**

$x_1$ Time	$x_2$ Temperature	$x_3$ Catalyst	$y_1$ Conversion	$y_2$ Activity
-1	-1	-1	74.00	53.20
1	-1	-1	51.00	62.90
-1	1	-1	88.00	53.40
1	1	-1	70.00	62.60
-1	-1	1	71.00	57.30
1	-1	1	90.00	67.90
-1	1	1	66.00	59.80
1	1	1	97.00	67.80
-1.682	0	0	76.00	59.10
1.682	0	0	79.00	65.90
0	-1.682	0	85.00	60.00
0	1.682	0	97.00	60.70
0	0	1.682	55.00	57.40
0	0	1.682	81.00	63.20
0	0	0	81.00	59.20
0	0	0	75.00	60.40
0	0	0	76.00	59.10
0	0	0	83.00	60.60
0	0	0	80.00	60.80
0	0	0	91.00	58.90

- (b)  $y_2$  as the objective function (maximize  $y_2$ ).  
 (c) Compare the answers obtained in parts (a) and (b) with the answer from the desirability function approach in Exercise 6.14.
- 6.18** Consider the viscosity response data in Table 6.8.  
 (a) Perform a canonical analysis on the second-order model for these data.  
 (b) Use the double linear regression method to find confidence intervals on the eigenvalues. The design in terms of the canonical variables is

$$\mathbf{U} = \begin{bmatrix} 0.8922 & 1.0972 \\ -1.0972 & 0.8922 \\ 1.0972 & -0.8922 \\ -0.8922 & -1.0972 \\ 1.4066 & 0.1449 \\ -1.4066 & -0.1449 \\ -0.1449 & 1.4066 \\ 0.1449 & -1.4066 \\ 0 & 0 \\ 0 & 0 \\ 0 & 0 \\ 0 & 0 \end{bmatrix}$$

- (c) Interpret the fitted surface. Can you suggest a procedure for making the fitted model more closely approximate the true response surface?
- 6.19** The method given in the text is only one possible way to implement the desirability function procedure. Below are two variations of the procedure.
- Fit a separate response surface for each of the  $m$  responses. Create  $d_1, d_2, \dots, d_m$  and then  $D = (\prod_{i=1}^m d_i)^{1/m}$  at each design point according to values of the fitted response (the  $\hat{y}_i$ ). Then build a response surface with
 
$$D = f(x_1, x_2, \dots, x_k)$$
 and find conditions on  $\mathbf{x}$  that maximize  $D$ . One could then make use of canonical analysis, possibly ridge analysis, and so on.
  - Compute  $d_1, d_2, \dots, d_m$  and  $D$  at each design point according to the individual observations—that is, the values  $y_1, y_2, \dots, y_m$ . Then build a response surface with the computed response  $D$ , and use appropriate methodology for finding  $\mathbf{x}$  that maximizes  $D$ .
- How do you think these two methods will perform as multiple-response optimization techniques?

**6.20** For the estimated response surface listed below, answer the following questions:

$$\hat{y} = 35 + 1.02x_1 + 1.76x_2 - 0.59x_3 - 2.66x_1x_2 + 3.02x_1x_3 - 0.62x_2x_3 \\ + 5.04x_1^2 + 2.63x_2^2 + 5.33x_3^2$$

- (a) Write the model in the canonical form.
  - (b) Describe what kind of stationary point the response surface has and where it is located.
  - (c) If all the coded variables have range  $[-1, 1]$  and the range of the actual variables are as follows:  $X_1^* \in [10, 30]$   $X_2^* \in [150, 200]$   $X_3^* \in [1.0, 2.0]$ 
    - (i) Where is the global minimum located in terms of the original variables?
    - (ii) Where is the maximum located within the observed range of the actual variables (stay in the cube design space)?
- 6.21** For a given problem we obtain a second-order model, which we describe in terms of its canonical parameterization. We obtain the following pieces for the model in the form  $\hat{y} = 10.5 + \mathbf{x}\mathbf{b} + \mathbf{x}\hat{\mathbf{B}}\mathbf{x}$

$$\mathbf{b} = \begin{pmatrix} 1 \\ 0 \\ 1 \end{pmatrix} \quad \hat{\mathbf{B}} = \begin{pmatrix} 2.04 & -0.1 & -0.075 \\ -0.1 & 0.160 & 0.25 \\ -0.075 & 0.25 & 1.15 \end{pmatrix} \quad \mathbf{x}_s = \begin{pmatrix} -0.23 \\ 0.85 \\ -0.63 \end{pmatrix}$$

with eigenvalues and eigenvectors:

```
$ values:
[1]      2.05420808   1.19864128   0.09715064
$ vectors:
           [, 1]           [, 2]           [, 3]
[1, ]    0.99276672  -0.1127446  -0.04126621
[2, ]   -0.06567526  -0.2222498  -0.97277530
[3, ]   -0.10050377  -0.9684491   0.22804674
```

- (a) Write the model in standard form ( $y = \hat{\beta}_0 + \hat{\beta}_1X_1 + \dots$ ) with the actual coefficients listed for all main, interaction and quadratic effects.
- (b) Describe the kind of surface we have for the response.
- (c) If we are using a standard cuboidal region, is the stationary point located inside the region of study? Explain.

If the value of the function at the stationary point is 11.91, give the equation for the model in the canonical form,  $\hat{y} = \hat{y}_s + \sum \lambda_i w_i$ .



---

# 7

---

## EXPERIMENTAL DESIGNS FOR FITTING RESPONSE SURFACES—I

Many of our examples in Chapter 6 displayed the fitting of second-order response surfaces with data taken from real-life applications of response surface methodology (RSM). In those examples, the experimental design possesses properties required to fit a second-order response surface—that is,

1. at least three levels of each design variable
2. at least  $1 + 2k + k(k - 1)/2$  distinct design points

The above represent minimum conditions for fitting a second-order model. The reader has also noticed the reference to the **central composite design** in Chapter 6. This second-order design class was represented in almost all of the illustrations. The composite design is the most popular second-order design in use by practitioners. As a result, it will receive considerable attention in sections that follow. First, however, some general commentary should be presented regarding the choice of designs for response surface analysis.

### 7.1 DESIRABLE PROPERTIES OF RESPONSE SURFACE DESIGNS

There are many classes of experimental designs in the literature, and there are many criteria on which experimental designs are based. Indeed, there are many computer packages that give optimal designs based on special criteria and input from the user. Special design criteria and important issues associated with computer-generated design of experiments will be discussed in a later section and in Chapter 8. However, it is important for the reader to first review a set of properties that should be taken into account when the

choice of a response surface design is made. Some of the important characteristics are as follows:

1. Result in a good fit of the model to the data.
2. Give sufficient information to allow a test for lack of fit.
3. Allow models of increasing order to be constructed sequentially.
4. Provide an estimate of “pure” experimental error.
5. Be insensitive (robust) to the presence of outliers in the data.
6. Be robust to errors in control of design levels.
7. Be cost-effective.
8. Allow for experiments to be done in blocks.
9. Provide a check on the homogeneous variance assumption.
10. Provide a good distribution of  $\text{Var}[\hat{y}(\mathbf{x})]/\sigma^2$ .

As one can readily see, not all of the above properties are required in every RSM application. However, most of them should be given serious consideration on each occasion in which one designs experiments. Most of the properties are self-explanatory. We have already made reference to item 3. Item 5 is important if one expects outliers to occur. Though we have not discussed blocking in the context of fitting second-order models, we will consider the concept in detail later in this chapter. Item 10 is very important. The reader has been exposed to the notion of prediction variance in Chapters 2 and 6. In later sections we shall discuss the importance of stability of prediction variance.

There are several purposes behind the introduction of the list of 10 characteristics at this point in the text. Of primary importance is a reminder to the reader that designing an experiment is not necessarily easy and should involve balancing multiple objectives, not just focusing on a single characteristic. Indeed, a few of the 10 items may be important and yet the researcher may not be aware of the magnitude of their importance. Some items do conflict with each other. As a result, there are tradeoffs that almost always exist when one chooses an appropriate design. An excellent discourse on the many considerations that one must consider in choosing a response surface design is given by Box and Draper (1975).

## 7.2 OPERABILITY REGION, REGION OF INTEREST, AND MODEL INADEQUACY

At the end of the previous chapter we discussed the choice of ranges on the design variables; this naturally leads to an introduction of the notion of the **region of interest** in the design variables. As we indicated in Chapter 6, we are assuming that the true function relating  $y$  to the design variables is unknown. In fact,

$$E(y) = f(\mathbf{x}, \boldsymbol{\theta})$$

and we are assuming that in the region of interest,  $R(\mathbf{x})$ ,  $f$  is well approximated by a low-order polynomial. This, of course, brings on the notion of the first-order or second-order response functions. They are approximations (justified by a Taylor series expansion of  $f$ ) in the confined region  $R$ .

It is important for the reader to understand that while the experimental design may be confined to  $R$ , the region  $R$  may change from experiment to experiment (say, for

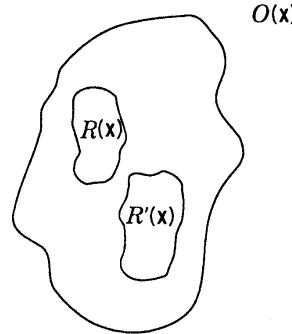


**Figure 7.1** Region of operability and region of interest.

example, in a steepest ascent experiment). However, there is a secondary region called the **region of operability**  $O(\mathbf{x})$ . This is the region in which the equipment, electronic system, chemical process, drug, or the like, works, and it is theoretically possible to do the experiment and observe response values. In some cases, data points in the design may be taken outside  $R(\mathbf{x})$ . Obviously, if one takes data too far outside  $R(\mathbf{x})$ , then the adequacy of our response surface representation (polynomial model) may be in question. Though the framework of the regions of interest and operability is important for the reader to understand, assuming knowledge of  $R(\mathbf{x})$  or  $O(\mathbf{x})$  in a given situation may be too idealistic. The region  $R$  changes, and at times  $O$  is not truly known until much is known about the process.

Figure 7.1 gives the reader a pictorial depiction of  $O$  and  $R$ . In this case, with two different experiments we have  $R$  and  $R'$ , both being considerably more confined than  $O$ . The region  $R$  is the current best guess at where the optimum is. It is also the region in which we feel that  $\hat{y}(\mathbf{x})$  should be a good predictor or, say, a good estimator of  $f(\mathbf{x}, \boldsymbol{\theta})$ . However, the user should constantly be aware of potential model inadequacy in cases where  $\hat{y}(\mathbf{x})$  is not a good approximation of  $f(\mathbf{x}, \boldsymbol{\theta})$ .

### 7.2.1 Model Inadequacy and Model Bias

In this section, we provide details concerning the impact of specifying a response surface model incorrectly. This is particularly important since one is almost always making use of empirical models. Thus, in many instances, more than one empirical model may be reasonable and some are better than others.

Consider a situation in which we assume a model of the form  $\mathbf{y} = \mathbf{X}_1 \boldsymbol{\beta}_1 + \boldsymbol{\varepsilon}$ . After the data are collected and fit, we have a vector of fitted values,

$$\hat{\mathbf{y}} = \mathbf{X}_1 \mathbf{b}_1 \quad (7.1)$$

where

$$\mathbf{b}_1 = (\mathbf{X}'_1 \mathbf{X}_1)^{-1} \mathbf{X}_1 \mathbf{y}$$

Here we implicitly make the assumption that

$$E(\mathbf{y}) = \mathbf{X}_1 \boldsymbol{\beta}_1$$

However, there may be a better approximation of  $E(y)$  given by

$$E(\mathbf{y}) = \mathbf{X}_1 \boldsymbol{\beta}_1 + \mathbf{X}_2 \boldsymbol{\beta}_2 \quad (7.2)$$

where, say,  $\mathbf{X}_1$  is an  $N \times p_1$  matrix, and  $\mathbf{X}_2$  is  $N \times p_2$ . The additional term in Equation 7.2,  $\mathbf{X}_2\beta_2$  contains additional linear model terms which provide more flexibility in the modeling of the response. Examples of this would be higher order terms or additional interaction terms. Then the expected value of  $\mathbf{b}_1$  is given by

$$\begin{aligned} E(\mathbf{b}_1) &= (\mathbf{X}'_1 \mathbf{X}_1)^{-1} \mathbf{X}'_1 E[\mathbf{y}] \\ &= (\mathbf{X}'_1 \mathbf{X}_1)^{-1} \mathbf{X}'_1 E[\mathbf{X}_1 \beta_1 + \mathbf{X}_2 \beta_2 + \boldsymbol{\epsilon}] \\ &= (\mathbf{X}'_1 \mathbf{X}_1)^{-1} \mathbf{X}'_1 \mathbf{X}_1 \beta_1 + (\mathbf{X}'_1 \mathbf{X}_1)^{-1} \mathbf{X}'_1 \mathbf{X}_2 \beta_2 \\ &= \beta_1 + (\mathbf{X}'_1 \mathbf{X}_1)^{-1} \mathbf{X}'_1 \mathbf{X}_2 \beta_2 \\ &= \beta_1 + \mathbf{A} \beta_2 \end{aligned}$$

Here  $\boldsymbol{\epsilon}$  is the usual random error, and  $\mathbf{A} = (\mathbf{X}'_1 \mathbf{X}_1)^{-1} \mathbf{X}'_1 \mathbf{X}_2$  is called the **alias matrix**. The alias matrix transmits bias errors to the estimate  $\mathbf{b}_1$ . Understanding the effect of bias on the estimates of the model is applicable for many types of models. There is considerable direct application to first order models, such as fractional factorials discussed in Chapter 4 (see Exercises 7.7, 7.8, and 7.9).

As one might expect, if there is appreciable model misspecification, bias errors also appear in the fitted values. For, in the above scenario, the expected value of the vector of fitted values is given by

$$\begin{aligned} E(\hat{\mathbf{y}}) &= \mathbf{X}_1 E(\mathbf{b}_1) \\ &= \mathbf{X}_1 (\beta_1 + \mathbf{A} \beta_2) \\ &= \mathbf{X}_1 \beta_1 + \mathbf{X}_1 \mathbf{A} \beta_2 \end{aligned}$$

and thus

$$\begin{aligned} E(\hat{\mathbf{y}}) - E(\mathbf{y}) &= [\mathbf{X}_1 \beta_1 + \mathbf{X}_1 \mathbf{A} \beta_2] - [\mathbf{X}_1 \beta_1 + \mathbf{X}_2 \beta_2] \\ &= (\mathbf{X}_1 \mathbf{A} - \mathbf{X}_2) \beta_2 \end{aligned} \tag{7.3}$$

When the true model is best approximated by Equation 7.2, bias is transmitted to both model coefficients and fitted values. Equation 7.3 is important in that it plays a role in the lack-of-fit test described in Chapter 6. If the model is misspecified as we have described here, the residual mean square,  $s^2$ , in the analysis of variance is also biased. Instead of estimating  $\sigma^2$  as expected, it has expectation

$$E(s^2) = \sigma^2 + \frac{1}{p_1} \{ \beta'_2 [\mathbf{X}_1 \mathbf{A} - \mathbf{X}_2]' [\mathbf{X}_1 \mathbf{A} - \mathbf{X}_2] \beta_2 \}$$

The bias in  $s^2$  described above is intuitive. It is simply proportional to the sum of squares of the biases in the fitted values. This is reasonable since the lower mean square is itself proportional to the sum of squares of deviations between  $y$  observations and fitted values. If we call the bias in  $s^2$

$$\frac{1}{p_1} \{ \beta'_2 \mathbf{R}' \mathbf{R} \beta_2 \} \tag{7.4}$$

where  $\mathbf{R} = \mathbf{X}_1 \mathbf{A} - \mathbf{X}_2$ , then it becomes clear that the lack-of-fit test, when significant, is detecting the existence of a non-zero  $\beta_2$  through the quadratic form  $\beta'_2 \mathbf{R}' \mathbf{R} \beta_2$ .

In addition to lack-of-fit the vector of biases in fitted value given in Equation 7.3 may play an important role in the choice of an experimental design. One point of view is to determine the design based on control of two types of error, **variance error** and **bias error**. Thus, we have a loss function type criterion. For each observation,  $y_j$ , we want to make small the loss

$$\begin{aligned} E[\hat{y}_j - f(\mathbf{x}_j, \boldsymbol{\beta})]^2 &= E[\hat{y}_j - E(\hat{y}_j) + E(\hat{y}_j) - f(\mathbf{x}_j, \boldsymbol{\beta})]^2 \\ &= E[\hat{y}_j - E(\hat{y}_j)]^2 + [E(\hat{y}_j) - f(\mathbf{x}_j, \boldsymbol{\beta})]^2 \\ &= \text{Var}(\hat{y}_j) + [\text{Bias}(\hat{y}_j)]^2 \end{aligned} \quad (7.5)$$

The term  $\text{Var}(\hat{y}_j)$  is clear. It has been discussed in Chapter 6 and will receive further attention in this chapter. The term  $[\text{Bias}(\hat{y}_j)]^2$  is the squared bias in the fitted values if indeed  $E(\mathbf{y}) \neq \mathbf{X}_1\boldsymbol{\beta}_1$ . The bias term is related to Equation 7.4 as

$$\frac{1}{p_1}\{\boldsymbol{\beta}'_2 \mathbf{R}' \mathbf{R} \boldsymbol{\beta}_2\} = \sum_{j=1}^N [\text{Bias}(\hat{y}_j)]^2$$

The statistics literature contains a considerable amount of information on experimental design for regression or response surface modeling. However, the majority of this technical or theoretical information deals with variance-oriented design criteria—that is, the type of design criteria that ignores model misspecification. In other words, these criteria essentially assume that the model specified by the user is correct. In what follows, we shall initially focus on variance-type criteria. More recently, work has been considered where designs are evaluated not only by assessing the variance error, but also considering potential bias error. Because the bias term contains  $\boldsymbol{\beta}_2$ , some additional assumptions for the magnitude of these missing terms is needed to quantify the size of the bias. See Draper and Sanders (1988), Vining and Myers (1991), Allen et al. (2003) and Anderson-Cook et al. (2008) for a variety of approaches to considering bias error. However, the errors associated with model misspecification will be revisited in Chapter 9. In what follows, we begin with experimental designs for first-order response models.

### 7.3 DESIGN OF EXPERIMENTS FOR FIRST-ORDER MODELS

Consider a situation in which  $N$  experimental runs are conducted on  $k$  design variables  $x_1, x_2, \dots, x_k$  and a single response  $y$ . A model is postulated of the type

$$y_i = \beta_0 + \beta_1 x_{i1} + \beta_2 x_{i2} + \cdots + \beta_k x_{ik} + \varepsilon_i \quad (i = 1, 2, \dots, N)$$

As a result a fitted model is given by

$$\hat{y}_i = b_0 + b_1 x_{i1} + b_2 x_{i2} + \cdots + b_k x_{ik}$$

Here, of course, the  $b_j$  are found by the method of least squares. Obviously, the most intuitive variance-based criterion involves the variance of the regression coefficients—that is,  $\text{Var}(b_i)$  ( $i = 0, 1, 2, \dots, k$ ). Let us assume that each design variable is in coded design units and that the ranges for the design levels are such that  $x_j \in [-1, +1]$ . A key ingredient in choosing a design that minimizes the variances is the concept of **orthogonality**.

### 7.3.1 The First-Order Orthogonal Design

The terms **orthogonal design**, **orthogonal array**, and **orthogonal main effect plan** received considerable attention in the 1950s and 1960s. A first-order orthogonal design is one for which  $\mathbf{X}'\mathbf{X}$  is a diagonal matrix. The above definition implies, of course, that the columns of  $\mathbf{X}$  are mutually orthogonal. In other words, if we write

$$\mathbf{X} = [\mathbf{1}, \mathbf{x}_1, \mathbf{x}_2, \dots, \mathbf{x}_k]$$

where  $\mathbf{x}_j$  is the  $j$ th column of  $\mathbf{X}$ , then a first-order orthogonal design is such that  $\mathbf{x}_i' \mathbf{x}_j = 0$  for all  $i \neq j$ , and, of course,  $\mathbf{1}' \mathbf{x}_j = 0$  for  $j = 1, 2, \dots, k$ . It should be clear that if two columns are orthogonal, the levels of the two corresponding variables are linearly independent. The implication is that the roles of the two variables are being assessed independent of each other. This underscores the virtues of orthogonality. In the first-order situations, an orthogonal design in which the ranges on these variables are taken to extremes results in minimizing  $\text{Var}(b_i)$  on a per observation basis. In other words:

For the first-order model and a fixed sample  $N$ , if  $X_j \in [-1, +1]$  for  $j = 1, 2, \dots, k$ , then  $\text{Var}(b_i)/\sigma^2$  for  $i = 1, 2, \dots, k$  is minimized if the design is orthogonal and all  $x_i$  levels in the design are  $\pm 1$  for  $i = 1, 2, \dots, k$ .

Thus, the elements on the diagonals of  $(\mathbf{X}'\mathbf{X})^{-1}$  are minimized [recall that  $\text{Var}(\mathbf{b}) = \sigma^2(\mathbf{X}'\mathbf{X})^{-1}$ ] by making off-diagonals of  $\mathbf{X}'\mathbf{X}$  zero and by forcing the diagonals of  $\mathbf{X}'\mathbf{X}$  to be as large as possible. The notion of **linear independence** and **variable levels at  $\pm 1$  extremes** as a desirable set of conditions should certainly be intuitive to the reader.

**Example 7.1 Variance-Optimal First-Order Designs I** Two-level factorial plans and fractions of resolution III and higher do, in fact, minimize the variances of all coefficients (variances scaled by  $\sigma^2$ ) on a per observation basis. To illustrate this, consider the following  $2^{4-1}$  fractional factorial (resolution IV) with the defining relation  $I = ABCD$ . The matrix  $\mathbf{X}$  is given by

$$\mathbf{X} = \begin{array}{ccccc} & x_1 & x_2 & x_3 & x_4 \\ \begin{bmatrix} 1 & -1 & -1 & -1 & -1 \\ 1 & 1 & 1 & -1 & -1 \\ 1 & 1 & -1 & 1 & -1 \\ 1 & 1 & -1 & -1 & 1 \\ 1 & -1 & 1 & 1 & -1 \\ 1 & -1 & 1 & -1 & 1 \\ 1 & -1 & -1 & 1 & 1 \\ 1 & 1 & 1 & 1 & 1 \end{bmatrix} \end{array}$$

One can easily determine that  $\mathbf{X}'\mathbf{X} = 8\mathbf{I}_5$  and  $(\mathbf{X}'\mathbf{X})^{-1} = \frac{1}{8}\mathbf{I}_5$ . Indeed, one can say that *no other design with eight experimental runs in this region can result in variances smaller than  $\sigma^2/8$* . It should be apparent to the reader that a full  $2^4$  factorial results in all coefficient variances being  $\sigma^2/16$ . In other words, if the size of the design is doubled, the variances of coefficients are cut in half. However, both are considered optimal designs on a per observation basis.

**Example 7.2 Variance-Optimal First-Order Designs II** Consider a situation in which there are three design variables and the user wishes to use eight experimental runs but also to have design replication. A  $2^{3-1}$  fractional factorial (resolution III) is used with each design point replicated. The matrix  $\mathbf{X}$  for the design is as follows (defining relation  $I = ABC$ ):

$$\mathbf{X} = \begin{array}{c} \begin{matrix} & x_1 & x_2 & x_3 \end{matrix} \\ \left[ \begin{matrix} 1 & 1 & -1 & -1 \\ 1 & 1 & -1 & -1 \\ 1 & -1 & 1 & -1 \\ 1 & -1 & 1 & -1 \\ 1 & -1 & -1 & 1 \\ 1 & -1 & -1 & 1 \\ 1 & 1 & 1 & 1 \\ 1 & 1 & 1 & 1 \end{matrix} \right] \end{array}$$

Note that the columns are orthogonal and all levels are at  $\pm 1$  extremes. Thus the design is **variance optimal** for the model

$$\hat{y} = b_0 + b_1x_1 + b_2x_2 + b_3x_3$$

That is, all coefficients in the above model have minimum variance over all designs with sample size  $N = 8$ . In fact, the variance–covariance matrix is given by

$$\text{Var}(\mathbf{b}) = (\sigma^2/8)\mathbf{I}_4$$

It is interesting that for this situation a full  $2^3$  factorial results in the same variance–covariance matrix. Though the two designs are quite different, from a variance point of view they are equivalent for the first-order model in three design variables. Obviously, in the case of the  $2^{3-1}$  fraction (replicated) there are no degrees of freedom for lack of fit, whereas the  $2^3$  factorial enjoys four lack-of-fit degrees of freedom that are attributable to  $x_1x_2$ ,  $x_1x_3$ ,  $x_2x_3$ , and  $x_1x_2x_3$ . On the other hand, the replicated one-half fraction allows four degrees of freedom for replication error (pure error), and, of course, the full  $2^3$  possesses no degrees of freedom for replication error. As a result, even though they are variance-equivalent, the two orthogonal designs would find use in somewhat different circumstances.

It should be apparent to the reader that for the use of two-level factorials or fractions for a first-order model, orthogonality (and hence variance optimality) is obtained with resolution at least III. In the case of resolution III, the  $\mathbf{x}_i$  columns in  $\mathbf{X}$  will be aliased with the  $\mathbf{x}_j\mathbf{x}_k$  columns. However, no  $\mathbf{x}_i$  column will be aliased with any  $\mathbf{x}_j$  column. In the case of  $2^k$  factorials or *regular fractions*, *any two columns in  $\mathbf{X}$  that are not aliased are, indeed, orthogonal*.

The notion of orthogonality and its relationship to design resolution clearly suggests that variance-optimal designs should also be available if the fitted response model contains first-order terms and one or more interaction terms. The following subsection addresses this topic.

### 7.3.2 Orthogonal Designs for Models Containing Interaction

As we indicated earlier, it is not uncommon for the process or system to require one or more interaction terms to accompany the linear main effect terms in a first-order model. The two-level factorials and fractions are quite appropriate. As in the case of the first-order model, the orthogonal design is variance-optimal—the sense again being that variances of all coefficients are minimized on a per observation basis. Based on the discussion earlier in Section 7.3, it should be apparent that the two-level full factorial is orthogonal for models containing main effects and any (or all) interactions involving cross products of linear terms. If a fraction is to be used, one must have sufficient resolution to ensure that no model terms are aliased. For example, if two factor interaction terms appear in the model, a resolution of at least V is appropriate.

As an illustration, suppose for  $k = 4$  the analyst postulates a model

$$y_i = \beta_0 + \sum_{i=1}^4 \beta_i x_i + \sum_{i < j = 2}^4 \beta_{ij} x_i x_j + \varepsilon$$

Then clearly no fractional factorial will be orthogonal, because a resolution IV fraction will result in aliasing two factor interactions with each other. In fact, a one-half fraction in this case would involve only eight design points, and the above model contains 11 model terms. A full  $2^4$  factorial is an orthogonal design for the above model.

Consider a second illustration in which five design variables are varied in a study in which the model can be written as

$$y = \beta_0 + \sum_{i=1}^5 \beta_i x_i + \sum_{i \leq j=2}^5 \beta_{ij} x_i x_j + \varepsilon$$

In this case a complete  $2^5$  or a resolution V  $2^{5-1}$  serves as an orthogonal design. In this case, linear main effects are orthogonal to each other and orthogonal to two-factor interactions, while two-factor interactions are orthogonal to each other. The following matrix  $\mathbf{X}$  illustrates the concept of orthogonality in the case of the one-half fraction:

$$\mathbf{X} = \begin{bmatrix} x_1 & x_2 & x_3 & x_4 & x_5 & x_1x_2 & x_1x_3 & x_1x_4 & x_1x_5 & x_2x_3 & x_2x_4 & x_2x_5 & x_3x_4 & x_3x_5 & x_4x_5 \end{bmatrix}$$

The defining contrast  $I = ABCDE$  was used to construct the one-half fraction. It is clear that the columns of  $\mathbf{X}$  are orthogonal to each other and that

$$\mathbf{X}'\mathbf{X} = 16\mathbf{I}_{16} \quad \text{with } (\mathbf{X}'\mathbf{X})^{-1} = \frac{1}{16}\mathbf{I}_{16}$$

and thus the variances of the coefficients are given by

$$\text{Var}(b_0) = \text{Var}(b_i) = \text{Var}(b_{ij}) = \frac{\sigma^2}{16} \quad (i, j = 1, 2, 3, 4, 5; i \neq j)$$

**The Saturated Design** The reader should note that in the previous illustration there are 16 design points and 16 model terms. The result is that there are *zero residual degrees of freedom*. This type of scenario deserves special attention. The absence of any lack-of-fit degrees of freedom implies, of course, that no test can be made for lack of fit; that is, there is no information to test for model inadequacy. In fact, this type of design will by definition fit the data perfectly with  $R^2 = 100\%$ . In this situation the design is said to be **saturated**. While this type of situation should be avoided, there certainly are practical situations in which cost constraints only allow a saturated design. The saturated design will continue to receive attention in future chapters. The discussion of the saturated design invites a question regarding what form the analysis takes. Can any inferences be made regarding model terms? The reader should recall the discussion in Chapter 3 regarding use of normal probability plots for effects. For an orthogonal design with a first-order model or a first-order-with-interaction model the model coefficients are simple functions of the **computed effects** discussed in Chapter 3. As a result, the use of normal probability plots for detection of **active effects** can be used to detect **active regression coefficients**. However, the reader should understand that when at all possible, saturated designs should be avoided in favor of designs that contain degrees of freedom for pure error and degrees of freedom for lack of fit.

**Effect of Center Runs** In Chapters 3 and 4 we discussed the utility of center runs as an important augmentation of the two-level factorial and fraction. This was discussed again and illustrated in Chapter 5. The addition of center runs to an orthogonal design does not alter the orthogonality property. However, the design is no longer a variance-optimal design; that is, the variances of regression coefficients are no longer minimized on a per observation basis. Obviously, the requirement that all levels be at  $\pm 1$  extremes is not met. Indeed, the center runs (runs at the zero coordinates in design units) add nothing to information about linear effects and interactions. However, let us not forget the importance of the detection of quadratic effects (see Chapter 3), a task that is handled very effectively and efficiently with the use of center runs.

**What Design Should Be Used?** The discussion of center runs and saturated designs in the context of orthogonal designs underscores a very important point. The design that is used in a given situation depends a great deal on the goal of the experiment and the assumptions that one is willing to make. It should also be clear that an optimal (i.e., variance-optimal) design is not always appropriate. Consider an example in which one is interested in fitting the model

$$y_i = \beta_0 + \beta_1 x_{i1} + \beta_2 x_{i2} + \beta_3 x_{i3} + \varepsilon_i \quad (i = 1, 2, 3, \dots, 8)$$

that is, a first-order model in three design variables. Among the candidate designs are three orthogonal designs that we will discuss and compare. All three of these designs involve eight

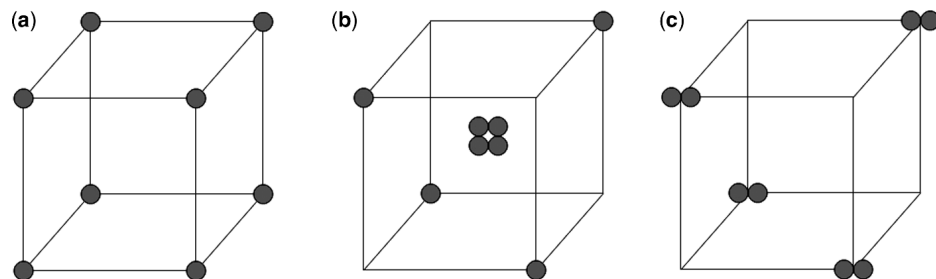


**Figure 7.2** Three designs for a first-order model in three design variables. (a)  $2^3$  factorial. (b)  $2^{3-1}$  fractional factorial with 4 center runs. (c) Replicated  $2^{3-1}$  fractional factorial.

experimental runs. Consider the following designs illustrated in Fig. 7.2:

**Design 1.** The  $2^3$  factorial

**Design 2.** Resolution III fraction of the  $2^3$  augmented with four center runs

**Design 3.** Resolution III fraction of the  $2^3$  with replicate runs at each design point

Designs 1 and 3 are both variance-optimal designs. The variances of regression coefficients will be  $\sigma^2/8$  for Designs 1 and 3. For Design 2, the variance of the intercept term will be  $\sigma^2/8$  but the variances of the linear coefficients will be  $\sigma^2/4$ . Comments concerning all three designs follow:

**Design 1.** It does not allow for estimation of replication error (pure error). There are four lack-of-fit degrees of freedom, but no error degrees of freedom are available to test lack of fit. The design is appropriate if there is strong prior information that there is no model inadequacy.

**Design 2.** Pure error degrees of freedom (3 df) are available for testing linear effects. One can also test for curvature (1 df for pure quadratic terms). The linear terms in the model are not estimated as precisely as for Designs 1 and 2. It should be used when one accepts the possibility of quadratic terms but can absolutely rule out interaction (the presence of pure quadratic terms with no interaction is not particularly likely).

**Design 3.** The design contains four pure error degrees of freedom but no lack-of-fit degrees of freedom associated with interaction terms or pure quadratic terms. Tests of significance can be made on model coefficients for the first-order model, but the design should not be used if either quadratic effects or interaction may be present. There is no model adequacy check of any kind.

From the above description it would seem that all these candidates possess disadvantages. However, one must keep in mind that with a sample size of eight and four model terms there is not much room for an efficient check for model inadequacy, because both lack-of-fit and pure error information is needed. Incidentally, a full  $2^3$  augmented with, say, three or more center runs would provide pure error degrees of freedom that could be used to test pure quadratic curvature and the presence of interaction.

### 7.3.3 Other First-Order Orthogonal Designs—The Simplex Design

The majority of applications of orthogonal designs for first-order models should suggest the use of the two-level designs that we have discussed here and in Chapters 3 and 4. However, it is important for the reader to be aware of a special class of first-order orthogonal designs that are saturated. This class is called the class of **simplex designs**. Let it be clear that these designs are saturated for a *first-order model*—a fact that implies that no information is available at all to study interactions.

The main feature of the simplex design is that it requires  $N = k + 1$  observations to fit a first-order model in  $k$  variables. Geometrically, the design points represent the vertices of a regular sided figure. That is, the design points, given by the rows of the design matrix

$$\mathbf{D} = \begin{bmatrix} x_{11} & x_{21} & \cdots & x_{k1} \\ x_{12} & x_{22} & \cdots & x_{k2} \\ \vdots & \vdots & & \vdots \\ x_{1,N} & x_{2,N} & \cdots & x_{k,N} \end{bmatrix}$$

are points in  $k$  dimensions such that the angle that any two points make with the origin is  $\theta$ , where

$$\cos \theta = -\frac{1}{N-1} = -\frac{1}{k}$$

For  $k = 2, N = 3$ ,  $\cos \theta = -\frac{1}{2}$ , and thus  $\theta = 120^\circ$ . Thus, for this case, the points are coordinates of an *equilateral triangle*. For  $k = 3$  and  $N = 4$ , the design points are the vertices of a *tetrahedron*. For  $k = 2$ , the design matrix is given by

$$\mathbf{D} = \begin{bmatrix} x_1 & x_2 \\ \sqrt{3}/2 & -1/\sqrt{2} \\ -\sqrt{3}/2 & -1/\sqrt{2} \\ 0 & 2/\sqrt{2} \end{bmatrix} \quad (7.6)$$

Figure 7.3 reveals that the design for  $k = 2$  contains points on the vertices of an equilateral triangle. The three rows in the design matrix correspond to points 1, 2, and 3, respectively.

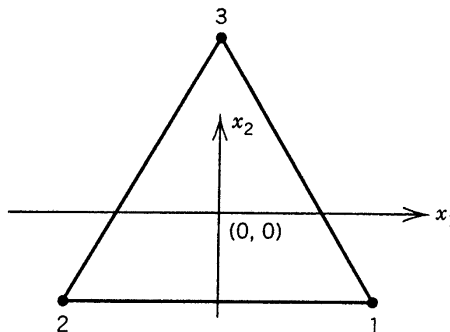


**Figure 7.3** Design points for the simplex in two variables.

The matrix  $\mathbf{X}$  is the design matrix augmented by a column of ones. Thus

$$\mathbf{X} = \begin{bmatrix} 1 & \sqrt{3}/2 & -1/\sqrt{2} \\ 1 & -\sqrt{3}/2 & -1/\sqrt{2} \\ 1 & 0 & 2/\sqrt{2} \end{bmatrix} \quad (7.7)$$

As a result, one can readily observe the orthogonality from

$$\mathbf{X}'\mathbf{X} = \begin{bmatrix} 3 & 0 & 0 \\ 0 & 3 & 0 \\ 0 & 0 & 3 \end{bmatrix}$$

For  $k = 3$ , the design involves the use of  $N = 4$  points and any two points make an angle  $\theta$  with the origin, where  $\cos \theta = -\frac{1}{3}$ . The appropriate design is given by

$$\mathbf{D} = \begin{bmatrix} x_1 & x_2 & x_3 \\ 1 & -1 & -1 \\ -1 & 1 & -1 \\ -1 & -1 & 1 \\ 1 & 1 & 1 \end{bmatrix} \quad (7.8)$$

If we use  $\mathbf{X} = [\mathbf{1}|\mathbf{D}]$ , it is clear that

$$\mathbf{X}'\mathbf{X} = 4\mathbf{I}_4$$

and hence the design is orthogonal for fitting the first-order model. Figure 7.4 shows the coordinates displayed in three dimensions. Note that any two points form the same angle with the origin  $(0, 0, 0)$ . Also note that in this special case the simplex is a one-half fraction of a  $2^3$ . The one we have chosen to display is the resolution III fraction with  $I = ABC$  as the defining relation. Indeed, the fraction formed from  $I = -ABC$  also is a simplex.

**Rotation and Construction of the Simplex** For a specific value of  $k$  there are numerous simplex designs that can be constructed. In fact, if one rotates the rows of the design matrix

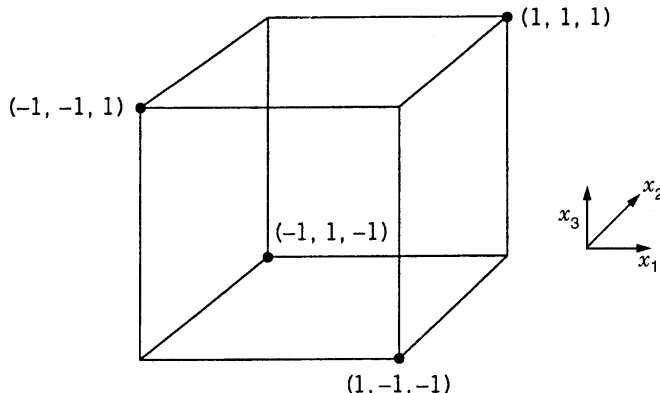


Figure 7.4 Simplex in three design variables.

through an angle, say  $\phi$ , the resulting design is still a simplex and thus still possesses the property of being first-order orthogonal. For example, a change in the orientation of the equilateral triangle of the design in Equation 7.6 will result in a second simplex. For  $k = 3$ , a design that is an alternative to that shown in Equation 7.8 is given by

$$\mathbf{D} = \begin{bmatrix} x_1 & x_2 & x_3 \\ 0 & \sqrt{2} & -1 \\ -\sqrt{2} & 0 & 1 \\ 0 & -\sqrt{2} & -1 \\ \sqrt{2} & 0 & 1 \end{bmatrix} \quad (7.9)$$

It is easily seen that this design is also first-order orthogonal, although from a pragmatic point of view the design in Equation 7.8 is usually preferable.

The construction of the matrix  $\mathbf{X}$  for the general  $k$ -dimensional simplex is quite simple. One merely starts with an orthogonal matrix  $\mathbf{O}$  of order  $N \times N$  with the elements of the first column being equal. The matrix  $\mathbf{X}$  is then

$$\mathbf{X} = \mathbf{O} \cdot N^{1/2}$$

Thus, it is easily seen that  $\mathbf{X}'\mathbf{X} = N(\mathbf{O}'\mathbf{O}) = N\mathbf{I}_N$ . For example, the  $k = 2$  simplex in Equation 7.7 can be constructed from the orthogonal matrix

$$\mathbf{O} = \begin{bmatrix} 1 & 1 & -1 \\ 1 & -1 & -1 \\ 1 & 0 & 2 \\ 1/\sqrt{3} & 1/\sqrt{2} & 1/\sqrt{6} \end{bmatrix}$$

The values at the bottom of each column are to be multiplied by each element in the column. We have

$$\mathbf{X} = \mathbf{O} \cdot \sqrt{3} = \begin{bmatrix} 1 & \sqrt{3/2} & -1/\sqrt{2} \\ 1 & -\sqrt{3/2} & -1/\sqrt{2} \\ 1 & 0 & 2/\sqrt{2} \end{bmatrix}$$

which is the matrix  $\mathbf{X}$  in Equation 7.7. The matrix  $\mathbf{X}$  given in the design of Equation 7.8 can be constructed from the simple orthogonal matrix

$$\mathbf{O} = \begin{bmatrix} 1 & 1 & -1 & -1 \\ 1 & -1 & 1 & -1 \\ 1 & -1 & -1 & 1 \\ 1 & 1 & 1 & 1 \\ 1/2 & 1/2 & 1/2 & 1/2 \end{bmatrix}$$

The reader should keep in mind that the simplex design is first-order saturated, which implies that there is no information available for lack of fit. If the analyst expects system interaction or pure quadratic curvature might be possible, the simplex is not an appropriate design.

**Example 7.3 Use of a Simplex Design** A simplex design is used in a laboratory experiment designed to build a first-order relationship between the growth ( $y$ ) of a particular organism and the percentage of glucose ( $x_1$ ), the percentage of yeast extract ( $x_2$ ), and the

**TABLE 7.1 Experimental Data for Organism Growth Experiment Using Simplex Design**

Run Number	Glucose $x_1$ (%)		Yeast $x_2$ (%)		Time, $x_3$ (hr)		Growth (g/liter)
	Uncoded	Coded	Uncoded	Coded	Uncoded	Coded	
1	3.0	0	0.641	$\sqrt{2}$	30	-1	8.52
2	1.586	$-\sqrt{2}$	0.500	0	60	1	9.76
3	3.0	0	0.359	$-\sqrt{2}$	30	-1	7.38
4	4.414	$\sqrt{2}$	0.500	0	60	1	12.50

time in hours ( $x_3$ ) allowed for organism growth. In coded form the design variables are

$$x_1 = \frac{\text{glucose} - 30\%}{1.0}$$

$$x_2 = \frac{\text{yeast} - 0.5\%}{0.10}$$

$$x_3 = \frac{\text{time} - 45 \text{ hr}}{15}$$

Table 7.1 gives the design in terms of the original and coded variables and indicates the observed response.

The fitted equation is given by

$$\hat{y} = 9.54 + 0.97x_1 + 0.40x_2 + 1.59x_3$$

### 7.3.4 Another Variance Property—Prediction Variance

We earlier indicated that two-level orthogonal first-order designs with levels at  $\pm 1$  extremes result in variances of coefficients that are minimized on a per observation basis. This provided the inspiration for the term “variance optimal” that we used consistently as we discussed examples and applied the concept to models that involve interaction terms. Criteria involving variances of coefficients are certainly important. In fact, in Chapter 8 we explain the notion of special norms on  $(\mathbf{X}'\mathbf{X})^{-1}$  as we more formally deal with design optimality. However, we should also be attentive to the criterion of **prediction variance**. This concept was discussed in Chapter 2 in dealing with confidence intervals around  $\hat{y}(\mathbf{x})$  in regression problems, and again in Chapter 6 as a part of the total RSM analysis. However, the prediction variance concept is a very important aspect of the study of experimental design. It is important for the reader to become familiar with it in what is the simplest scenario—namely, the first-order model.

**Prediction Variance for the First-Order Model** Recall that the prediction variance, or variance of a predicted value, is given by

$$PV(\mathbf{x}) = \text{Var}[\hat{y}(\mathbf{x})] = \sigma^2 \mathbf{x}^{(m)\prime} (\mathbf{X}'\mathbf{X})^{-1} \mathbf{x}^{(m)}$$

where  $\mathbf{x}^{(m)}$  is a function of the location in the design variables at which one predicts and also a function of the model. In fact, the  $(m)$  in  $\mathbf{x}^{(m)}$  reflects the **model**. In the case of a strictly first-order model, we obtain

$$\mathbf{x}^{(1)\prime} = [1, x_1, x_2, \dots, x_k]$$

For a  $k = 2$  model containing  $x_1, x_2$  and their interaction, we obtain

$$\mathbf{x}^{(1)'} = [1, x_1, x_2, x_1 x_2]$$

One can easily see that  $\text{Var}[\hat{y}(\mathbf{x})]$  varies from location to location in the design space. In addition, the presence of  $(\mathbf{X}'\mathbf{X})^{-1}$  attests to the fact that the criterion is very much a function of the experimental design. The reader should view the prediction variance as a reflection of how well one predicts with the model.

In studies that are done to compare designs, it is often convenient to **scale** the prediction variance, that is, work with the **scaled prediction variance**

$$\text{SPV}(\mathbf{x}) = \frac{N \text{Var}[\hat{y}(\mathbf{x})]}{\sigma^2} = N \mathbf{x}^{(m)'} (\mathbf{X}'\mathbf{X})^{-1} \mathbf{x}^{(m)} \quad (7.10)$$

The division by  $\sigma^2$  makes the quantity scale-free, and the multiplication by  $N$  allows the quantity to reflect variance on a *per observation basis*. That is, if two designs are being compared, the scaling by  $N$  automatically “punishes” the design with the larger sample size. It forces a premium on efficiency.

The scaled prediction variance in Equation 7.10 is quite simple for the case of a variance optimal first-order orthogonal design. In fact, because  $(\mathbf{X}'\mathbf{X})^{-1} = (1/N)\mathbf{I}_p$ , we have

$$\begin{aligned} \text{SPV}(\mathbf{x}) &= [1, x_1, x_2, \dots, x_k] \begin{bmatrix} 1 \\ x_1 \\ x_2 \\ \vdots \\ x_k \end{bmatrix} = 1 + \sum_{i=1}^k x_i^2 \\ &= 1 + \rho_{\mathbf{x}}^2 \end{aligned} \quad (7.11)$$

where  $\rho_{\mathbf{x}}$  is the distance that the point  $\mathbf{x}' = [x_1, x_2, \dots, x_k]$  is away from the design origin. As a result, the SPV on  $N \text{Var}[\hat{y}(\mathbf{x})]/\sigma^2 = 1$  at the design center and becomes larger as one moves toward the design perimeter. Anyone who recalls confidence intervals on  $E[y(\mathbf{x})]$  in linear regression should not be surprised at this result. As an illustration, for a  $2^3$  factorial, the following are values of  $N \text{Var}[\hat{y}(\mathbf{x})]/\sigma^2$  at different locations where one may wish to predict:

Location	$N \text{Var}[\hat{y}(\mathbf{x})]/\sigma^2$
0, 0, 0	1
$\frac{1}{2}, \frac{1}{2}, \frac{1}{2}$	1.75
$\frac{1}{2}, \frac{1}{2}, 1$	2.50
$\frac{1}{2}, 1, 1$	3.25
1, 1, 1	4

Thus, the scaled prediction variance increases *fourfold* as one moves from the design center to the design perimeter. For, say, a  $2^5$  factorial at the perimeter [i.e.,  $(\pm 1, \pm 1, \pm 1, +1, \pm 1)$ ],  $N \text{Var}[\hat{y}(\mathbf{x})]/\sigma^2 = 6$  and hence the variance increases *sixfold*.

In the case of a lesser design, (i.e., one that is not variance-optimal, or even orthogonal), this change in prediction variance is even more pronounced. For example, consider a one-half fraction (resolution III) of a  $2^3$  factorial with four center runs as an alternative to a  $2^3$ . We know that

this design is orthogonal but not variance-optimal. Recall this design as Design 2 in the comparisons we made in Section 7.3.2. The  $2^3$  was Design 1. For Design 2 the model matrix is

$$\mathbf{X} = \begin{bmatrix} 1 & 1 & -1 & -1 \\ 1 & -1 & 1 & -1 \\ 1 & -1 & -1 & 1 \\ 1 & 1 & 1 & 1 \\ 1 & 0 & 0 & 0 \\ 1 & 0 & 0 & 0 \\ 1 & 0 & 0 & 0 \\ 1 & 0 & 0 & 0 \end{bmatrix}, \text{ and } \mathbf{X}'\mathbf{X} = \begin{bmatrix} 8 & 0 & 0 & 0 \\ 0 & 4 & 0 & 0 \\ 0 & 0 & 4 & 0 \\ 0 & 0 & 0 & 4 \end{bmatrix}$$

with the variance–covariance matrix (apart from  $\sigma^2$ ) being

$$(\mathbf{X}'\mathbf{X})^{-1} = \begin{bmatrix} \frac{1}{8} & 0 & 0 & 0 \\ 0 & \frac{1}{4} & 0 & 0 \\ 0 & 0 & \frac{1}{4} & 0 \\ 0 & 0 & 0 & \frac{1}{4} \end{bmatrix}$$

Consequently,

$$\begin{aligned} \text{SPV}(\mathbf{x}) &= 8[1, x_1, x_2, x_3] \begin{bmatrix} \frac{1}{8} & 0 & 0 & 0 \\ 0 & \frac{1}{4} & 0 & 0 \\ 0 & 0 & \frac{1}{4} & 0 \\ 0 & 0 & 0 & \frac{1}{4} \end{bmatrix} \begin{bmatrix} 1 \\ x_1 \\ x_2 \\ x_k \end{bmatrix} \\ &= 1 + 2(x_1^2 + x_2^2 + x_3^2) \\ &= 1 + 2\rho_x^2 \end{aligned}$$

As a result, it is apparent that  $\text{SPV}(\mathbf{x})$  for Design 2 increases much faster as one approaches the design perimeter than does Design 1. In fact, at  $(\pm 1, \pm 1, \pm 1)$ ,  $\text{SPV}(\mathbf{x}) = 4$  for Design 1 and  $\text{SPV}(\mathbf{x}) = 7$  for Design 2. Incidentally, Design 3, which is a resolution III fraction of a  $2^3$  with replicate runs, has prediction variance properties identical to that of Design 1; they are both variance-optimal designs.

The reader should view prediction variance as another variance-type criterion by which comparisons among designs can be made. It is different than merely comparing variances of individual coefficients. Much more attention will be given to  $\text{SPV}(\mathbf{x}) = \text{Var}[\hat{y}(\mathbf{x})]/\sigma^2$  later in this chapter and in future chapters.

## 7.4 DESIGNS FOR FITTING SECOND-ORDER MODELS

Before we embark on the huge topic of experimental designs for second-order models, we should review for the reader some minimum design requirements and the RSM philosophy that motivates one or two of the classes of designs that we will subsequently present in detail. Variable screening is an essential phase of RSM that was presented at length in Chapter 1. Here, of course, the two-level factorial designs and fractions play a major role. Any sequential movement (region seeking) that is necessary is also accomplished with a first-order design. Of course, there may be instances where region-seeking via steepest ascent (or descent) and/or variable screening are not required. However, the possibility

of either or both should be included in the total sequential plan. At some point the researcher will be interested in fitting a second-order response surface in the design variables  $x_1, x_2, \dots, x_k$ . This response surface analysis may involve optimization as discussed in Chapter 6. It may lead to even more sequential movement through the use of canonical or ridge analysis. But, regardless of the form of the analysis, the purpose of the experimental design is one that should allow the user to fit the second-order model

$$y = \beta_0 + \sum_{i=1}^k \beta_i x_i + \sum_{i=1}^k \beta_{ii} x_i^2 + \sum_{i < j=2}^k \beta_{ij} x_i x_j + \varepsilon \quad (7.12)$$

The model of Equation 7.12 contains  $1 + 2k + k(k - 1)/2$  parameters. There must be at least this number of distinct design points and at least three levels of each design variable. Now, of course, these represent minimum conditions, and one should keep in mind the 10 desirable design characteristics listed at the beginning of this chapter. In what follows in this chapter and in Chapter 8 we discuss important design properties for the second-order model and specific classes of second-order designs. The reader will recall from the previous section that in the case of first-order designs (or first-order-with-interaction designs), the dominant property is orthogonality. In the case of second-order designs, orthogonality ceases to be such an important issue, and estimation of individual coefficients, while still important, becomes secondary to the scaled prediction variance  $N \text{Var}[\hat{y}(\mathbf{x})]/\sigma^2$ . This stems from the fact that there is often less concern with what variables belong in the model than with the quality of  $\hat{y}(\mathbf{x})$  as a prediction or, rather, an estimator for  $E[y(\mathbf{x})]$ . We now introduce, formally, the class of central composite designs.

### 7.4.1 The Class of Central Composite Designs

The **central composite designs** (CCDs) were introduced in an informal way in Chapter 6. Some of the examples used for illustrative purposes involved the use of the CCD. The CCD is without a doubt the most popular class of second-order designs. It was introduced by Box and Wilson (1951).

Much of the motivation of the CCD evolves from its use in **sequential experimentation**. It involves the use of a **two-level factorial** or fraction (resolution V) combined with the following  $2k$  **axial** or **star** points:

$x_1$	$x_2$	...	$x_k$
$-\alpha$	0	...	0
$\alpha$	0	...	0
0	$-\alpha$	...	0
0	$\alpha$	...	0
$\vdots$	$\vdots$		$\vdots$
0	0	...	$-\alpha$
0	0	...	$\alpha$

As a result, the design involves, say,  $F$  factorial points,  $2k$  axial points, and  $n_c$  center runs. The sequential nature of the design becomes very obvious. The factorial points represent a variance-optimal design for a first-order model or a first-order + two-factor interaction model. Center runs clearly provide information about the existence of curvature in the system. If curvature is found in the system, the addition of axial points allow for efficient estimation of the pure quadratic terms.

While the genesis of this design is derived from sequential experimentation, the CCD is a very efficient design in situations that call for a nonsequential batch response surface experiment. In effect, the three components of the design play important and somewhat different roles.

1. The resolution V fraction contributes substantially to the estimation of linear terms and two-factor interactions. It is variance-optimal for these terms. The factorial points are the only points that contribute to the estimation of the interaction terms.
2. The axial points contribute in a large way to estimation of quadratic terms. Without the axial points, only the sum of the quadratic terms,  $\sum_{i=1}^k \beta_{ii}$ , can be estimated. The axial points do not contribute to the estimation of interaction terms.
3. The center runs provide an internal estimate of error (pure error) and contribute toward the estimation of quadratic terms.

The areas of flexibility in the use of the central composite design reside in the selection of  $\alpha$ , the axial distance, and  $n_c$ , the number of center runs. The choice of these two parameters can be very important. The choice of  $\alpha$  depends to a great extent on the region of operability and region of interest. The choice of  $n_c$  often has an influence on the distribution of  $N \text{Var}[\hat{y}(\mathbf{x})]/\sigma^2$  in the region of interest. More will be said about the choice of  $\alpha$  and  $n_c$  in subsequent sections. Figures 7.5 and 7.6 show the CCD for  $k = 2$  and  $k = 3$ . For the  $k = 2$  case the value of  $\alpha$ , the axial distance is  $\sqrt{2}$ . For  $k = 3$ , the value of  $\alpha$  is  $\sqrt{3}$ . Note that for  $k = 3$  the axial points come through the six faces at a distance  $\sqrt{3}$  from the origin. For  $k = 2$  the design represents eight points equally spaced on a circle, plus the center runs. For  $k = 3$  the design represents 14 points all on a common sphere, plus center runs.

The value of the axial distance generally varies from 1.0 to  $\sqrt{k}$ , the former placing all axial points on the face of the cube or hypercube, the latter resulting in all points being placed on a common sphere. There are times when two or more center runs are needed and times when one or two will suffice. We will allocate considerable space in Chapter 8 to comparison of the CCD with other types of designs. We will discuss the choice of  $\alpha$  and  $n_c$  following a numerical example of the use of a CCD.

In the example that follows we use a real life numerical example to gain insight into the structure of the  $\mathbf{X}$  and  $\mathbf{X}'$  matrices for the general case of a CCD.

**Example 7.4 The Breadwrapper Experiment** An experiment was conducted to study the response surface relating the strength of breadwrapper stock in grams per square inch to

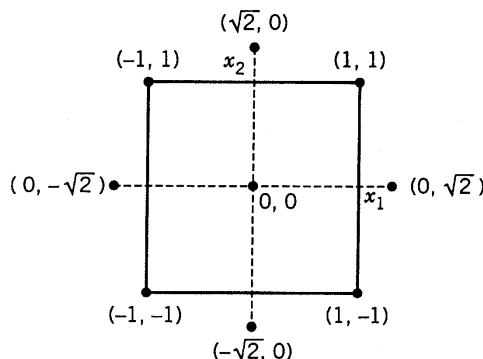


**Figure 7.5** Central composite design for  $k = 2$  and  $\alpha = \sqrt{2}$ .

sealing temperature ( $x_1$ ), cooling bar temperature ( $x_2$ ), and percent polyethylene additive ( $x_3$ ). The definition of the design levels are [see Myers (1976)]:

$$x_1 = \frac{\text{temp.} - 255^{\circ}\text{F}}{30}$$

$$x_2 = \frac{\text{temp.} - 55^{\circ}\text{F}}{9}$$

$$x_3 = \frac{\text{polyethylene} - 1.1\%}{0.6}$$

Five levels of each factor are involved in this design. The coded and natural levels are given by the following:

	-1.682	-1.000	0.000	1.000	1.682
$x_1$	204.5	225	255	285	305.5
$x_2$	39.9	46	55	64	70.1
$x_3$	0.09	0.5	1.1	1.7	2.11

The design matrix  $\mathbf{D}$  and the vector  $\mathbf{y}$  of responses are

$$\mathbf{D} = \begin{bmatrix} x_1 & x_2 & x_3 \\ -1 & -1 & -1 \\ 1 & -1 & -1 \\ -1 & 1 & -1 \\ 1 & 1 & -1 \\ -1 & -1 & 1 \\ 1 & -1 & 1 \\ -1 & 1 & 1 \\ 1 & 1 & 1 \\ -1.682 & 0 & 0 \\ 1.682 & 0 & 0 \\ 0 & -1.682 & 0 \\ 0 & 1.682 & 0 \\ 0 & 0 & -1.682 \\ 0 & 0 & 1.682 \\ 0 & 0 & 0 \\ 0 & 0 & 0 \\ 0 & 0 & 0 \\ 0 & 0 & 0 \\ 0 & 0 & 0 \end{bmatrix}, \quad \mathbf{y} = \begin{bmatrix} 6.6 \\ 6.9 \\ 7.9 \\ 6.1 \\ 9.2 \\ 6.8 \\ 10.4 \\ 7.3 \\ 9.8 \\ 5.0 \\ 6.9 \\ 6.3 \\ 4.0 \\ 8.6 \\ 10.1 \\ 9.9 \\ 12.2 \\ 9.7 \\ 9.7 \\ 9.6 \end{bmatrix}$$

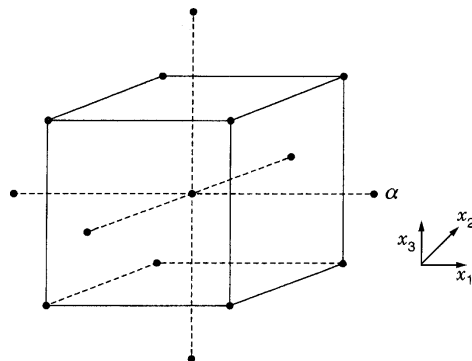


**Figure 7.6** Central composite design for  $k = 3$  and  $\alpha \sqrt{3}$ .

Note that the  $k = 3$  CCD for this example uses  $\alpha = 1.682$  with  $n = 6$  center runs. While this is not the axial distance that stretches to the faces of the cube it is a value to which some importance is attached. It allows the design to possess the property of rotatability and thus the derivation of the value  $\alpha = 1.682$  for the  $k = 3$  breadwrapper design will be discussed in 7.4.2 and 7.4.3. We shall use the breadwrapper design to highlight the structure of  $\mathbf{X}$  and  $\mathbf{X}'\mathbf{X}$ . For the design matrix  $\mathbf{D}$  and the second-order model:

$$\mathbf{X}'\mathbf{X} = \begin{bmatrix} b_0 & b_1 & b_2 & b_3 & b_{11} & b_{22} & b_{33} & b_{12} & b_{13} & b_{23} \\ 20 & 0 & 0 & 0 & 13.658 & 13.658 & 13.658 & 0 & 0 & 0 \\ & 13.658 & 0 & 0 & 0 & 0 & 0 & 0 & 0 & 0 \\ & & 13.658 & 0 & 0 & 0 & 0 & 0 & 0 & 0 \\ & & & 13.658 & 0 & 0 & 0 & 0 & 0 & 0 \\ & & & & 24 & 8 & 8 & 0 & 0 & 0 \\ & & & & & 24 & 8 & 0 & 0 & 0 \\ & & & & & & 24 & 0 & 0 & 0 \\ & & & & & & & 8 & 0 & 0 \\ & & & & & & & & 8 & 0 \\ & & & & & & & & & 8 \\ \text{Symmetric} & & & & & & & & & \end{bmatrix} \quad (7.13b)$$

Note that in the  $\mathbf{X}$  matrix the first four columns involving the column of ones and the linear term columns are mutually orthogonal as one would expect since they jointly represent columns of an orthogonal design. The same is true with the last three columns containing the columns that reflect presence of interaction terms. In addition, these two sets of columns are mutually orthogonal to one another. This is a result of the presence of the factorial portion of the CCD and the fact that that axial are chosen such that orthogonality is maintained among the linear columns. This produces a large number of zeros on the off diagonal elements of  $\mathbf{X}'\mathbf{X}$ . In fact the only non-zero entries on the off diagonals, the values of 8, exist because the “pure” quadratic terms are, of course, not mutually orthogonal. [The non-zeros in the first row and column (i.e., 13.658) could be made zero by centering the  $\mathbf{x}_i^2$  values in the model.] The presence of many zeros on the off diagonals contribute to making the CCD a very efficient design. In addition, we will observe in later sections that the value of  $n_c$ , the number of center runs can be a very important design parameter.

The  $\mathbf{X}'\mathbf{X}$  matrix in Equation 7.13b is certainly specific to the conditions of the breadwrapper problem. However, it is important to understand that the zeros appear in the corresponding positions for any CCD for the reasons described above. In sections that follow we will revisit the general form of  $\mathbf{X}'\mathbf{X}$  as discussed for the CCD here with regard to how it effects the variance of prediction, that is, specifically  $N \text{Var}[\hat{y}(\mathbf{x})]/\sigma^2$ . Indeed certain values of the diagonals and the off-diagonal elements can dramatically influence the distribution of this scaled prediction variance quantity inside the design region of the CCD.

The least squares procedure gives the second-order response function:

$$\begin{aligned} \hat{y} = & 10.165 - 1.1036x_1 + 0.0872x_2 + 1.020x_3 - 0.760x_1^2 \\ & - 1.042x_2^2 - 1.148x_3^2 - 0.350x_1x_2 - 0.500x_1x_3 + 0.150x_2x_3 \end{aligned}$$

An analysis of variance is shown in Table 7.2. Note that there are five degrees of freedom for lack of fit, representing contribution from third-order terms. The  $F$ -test for lack of fit is not significant.

**TABLE 7.2 Analysis of Variance for Breadwrapper Stock Data**

Source of Variation	Sum of Squares	Degrees of Freedom	Mean Square	F
Regression (linear and quadratic)	70.3056	9	7.8117	7.87
Lack of fit	6.9044	5	1.3809	1.39
Error	4.9600	5	0.9920	
Total	82.1700	19		

The stationary point is computed based on the methodology discussed in Chapter 6:

$$\begin{aligned}\mathbf{x}_s &= -\frac{1}{2}\hat{\mathbf{B}}^{-1}\mathbf{b} \\ &= \begin{bmatrix} -1.011 \\ 0.260 \\ 0.681 \end{bmatrix}\end{aligned}$$

with the predicted response at the stationary point given by  $\hat{y}(\mathbf{x}_s) = 11.08$ .

The eigenvalues of the matrix  $\hat{\mathbf{B}}$  are found to be

$$\lambda_1 = -0.562, \quad \lambda_2 = -1.271, \quad \lambda_3 = -1.117$$

Thus the canonical form is given by

$$\hat{y} = 11.08 - 0.562w_1^2 - 1.271w_2^2 - 1.117w_3^2$$

As a result, the stationary point is a point of estimated maximum mean strength of the bread-wrapper. Figure 7.7 displays contour graphs that show the flexibility available around the estimated optimum. Contours of constant response are shown for  $x_3$  (percent polyethylene) values of  $-0.5, 0.00, 0.25$ , and  $0.5$ . The purpose is to determine how much strength is lost by moving percent polyethylene  $x_3$  off the optimum value of 0.681 (coded). From the contour plots it becomes apparent that even if the polyethylene content is reduced to a value as low as 0.25 (coded), the estimated maximum strength is reduced to only slightly less than 10.9 psi. A reduction to 0.500 in polyethylene will still produce a maximum that exceeds 11.0 psi.

The objective of this section is to formally introduce the user to the CCD and to allow more insight into its properties. However, the CCD is such an important part of the heritage and practical use of RSM that it will be revisited frequently in the text. In the next section we reintroduce the notion of **prediction variance**—that is,  $N \text{Var}[\hat{y}(\mathbf{x})]/\sigma^2$  in the case of second-order models. Simultaneously, we discuss the notion of the property of **rotatability**. This will allow the discussion of the choice of  $\alpha$  and  $n_c$  to be brought to focus.

#### 7.4.2 Design Moments and Property of Rotatability

Many of the properties of experimental designs are connected to the manner in which the points are *distributed in the region* of experimentation. Specifically, this distribution of points in space has a profound effect on the distribution of  $N \text{Var}[\hat{y}(\mathbf{x})]/\sigma^2$ , the scaled prediction variance. The distribution of design points is nicely quantified by its **design**

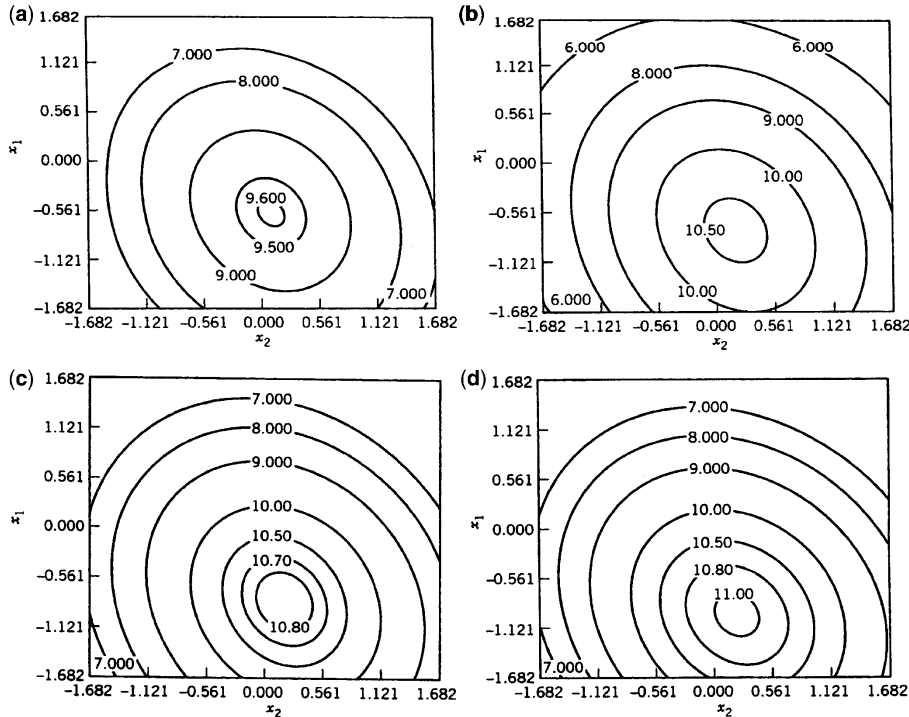


**Figure 7.7** Contours of constant strength at different levels of the percentage of polyethylene,  $x_3$ .  
**(a)**  $x_3 = -0.5$ . **(b)**  $x_3 = 0$ . **(c)**  $x_3 = 0.25$ . **(d)**  $x_3 = 0.5$ .

**moments.** The term moments has the same conceptual meaning as the term sample moments that is taught in elementary statistics. We learn early in our training that the nature of the sample of the data is well characterized by its moments; for example, sample mean (first moment), sample variance (second moment). We also recall that symmetry in a sample is quantified by the third moment. In the case of RSM, the moments that reflect important geometry in the design must also be a function of the model being fit.

Indeed the important moments come from the **moment matrix**

$$\mathbf{M} = \frac{\mathbf{X}'\mathbf{X}}{N}$$

For example, a  $2^k$  factorial or fractional factorial design for a first-order model is orthogonal and its moment matrix is easily seen to be

$$\mathbf{M} = \frac{\mathbf{X}'\mathbf{X}}{N} = \begin{bmatrix} 1 & 0 & \cdots & 0 \\ 0 & 1 & & \\ \vdots & & \ddots & \\ 0 & & & 1 \end{bmatrix} = \mathbf{I}_k$$

The off-diagonal moments are zero due to the orthogonality of the columns of the  $\mathbf{X}$  matrix, and the diagonal moments are all equal to 1, since the  $\mathbf{X}$  matrix is given by

$$\mathbf{X} = \begin{bmatrix} 1 & x_{11} & x_{21} & \cdots & x_{k1} \\ 1 & x_{12} & x_{22} & \cdots & x_{k2} \\ \vdots & \vdots & \vdots & \ddots & \vdots \\ 1 & x_{1N} & x_{2N} & \cdots & x_{kN} \end{bmatrix}$$

where each of the  $x_{ij}$  entries are  $\pm 1$ . We then define the moments as *first moments*; that is,  $\frac{1}{N} \sum_{u=1}^N x_{iu}$ , the *second mixed moments*  $\frac{1}{N} \sum_{u=1}^N x_{iu}x_{ju}$  for  $i \neq j$  and the *second pure moments*  $\frac{1}{N} \sum_{u=1}^N x_{iu}^2$ . The first and second mixed moments are called **odd moments**, since they have at least one variable with an odd power. These are clearly zero for this design. The  $k$  second pure moments are then **even moments** and, of course, are equal to 1 in this case. It should be clear that the second mixed moments are analogous to a sample covariance for the sample moments case in basic statistics, where the first moment can be viewed like a sample mean, and the second pure moments as sample variances.

The design moments that carry importance in characterizing variance properties of a design are clearly a function of the order of the model. In the case of the  $2^k$  factorial or fractional factorial design illustrated above, the moments through order 2 are important since  $\mathbf{M} = \mathbf{X}'\mathbf{X}/N$  contains moments through order 2. However, in the case of the CCD with the corresponding second order design,  $\mathbf{M}$  contains moments through order 4. This is evident when we observe  $\mathbf{X}$  and  $\mathbf{X}'\mathbf{X}$  in Equations 7.13a and 7.13b, respectively. In fact from (7.13b), the relevant moments are

$$\begin{aligned} [i] &= \frac{1}{N} \sum_{u=1}^N x_{iu} && \text{first moments} \\ [ii] &= \frac{1}{N} \sum_{u=1}^N x_{iu}^2 && \text{second pure moments} \\ [ij] &= \frac{1}{N} \sum_{u=1}^N x_{iu}x_{ju} && \text{second mixed moments} \\ [iii] &= \frac{1}{N} \sum_{u=1}^N x_{iu}^3 && \text{third pure moments} \\ [iij] &= \frac{1}{N} \sum_{u=1}^N x_{iu}^2 x_{ju}, \quad [ijk] = \frac{1}{N} \sum_{u=1}^N x_{iu}x_{ju}x_{ku}, && \text{third mixed moments} \\ [iiii] &= \frac{1}{N} \sum_{u=1}^N x_{iu} && \text{fourth pure moments} \\ [iiij] &= \frac{1}{N} \sum_{u=1}^N x_{iu}^4, \quad [iiji] = \frac{1}{N} \sum_{u=1}^N x_{iu}^2 x_{ju}^2, && \text{fourth mixed moments} \\ [iijk] &= \frac{1}{N} \sum_{u=1}^N x_{iu}^2 x_{ju}x_{ku}, \quad [ijkl] = \frac{1}{N} \sum_{u=1}^N x_{iu}x_{ju}x_{ku}x_{lu} \end{aligned}$$

It is clear that for the CCD all odd moments through order four; that is, moments that contain at least one odd power, that is  $[i]$ ,  $[ij]$ ,  $[iii]$ ,  $[iij]$ ,  $[ijk]$ ,  $[iiij]$ , and  $[iijk]$  are zero

for  $i \neq j \neq k$ . Values of zero for odd moments suggest a certain design symmetry which is certainly apparent when one observes the design matrix in Figs. 7.5 and 7.6. In fact from the  $\mathbf{X}'\mathbf{X}$  matrix in Equation 7.13b, the only non-zero moments for the  $k = 3$  CCD are  $[ii]$ ,  $[iij]$ , and  $[iji]$  for all  $i \neq j$ .

The important variance properties of an experimental design are determined by the nature of the moment matrix. This should be evident because the matrix  $(\mathbf{X}'\mathbf{X})^{-1}$  and hence  $\mathbf{X}'\mathbf{X}$  are so important in characterizing variance properties—that is, variances and covariances of regression coefficients as well as prediction variance.

The importance of design moments and hence the moment matrix in characterizing the scaled prediction variance, SPV, is easily seen by observing the definition of SPV in Equation 7.10.

$$\begin{aligned} \text{SPV}(\mathbf{x}) &= N\mathbf{x}^{(m)'}(\mathbf{X}'\mathbf{X})^{-1}\mathbf{x}^{(m)} \\ &= \mathbf{x}^{(m)'} \left( \frac{\mathbf{X}'\mathbf{X}}{N} \right)^{-1} \mathbf{x}^{(m)} \\ &= \mathbf{x}^{(m)'} \mathbf{M}^{-1} \mathbf{x}^{(m)} \end{aligned}$$

So the SPV is a quadratic form of the moment matrix,  $\mathbf{M}$ . Thus the nature of the design moments has a profound effect on the SPV and its distribution in the design space.

It is important for a second-order design to possess a reasonably stable distribution of the scaled prediction variance  $N \text{Var}[\hat{y}(\mathbf{x})]/\sigma^2$  throughout the experimental design region. It must be clearly understood that the experimenter does not know at the outset where in the design space he or she may wish to predict, or where in the design space the optimum may lie. Thus, a reasonably stable scaled prediction variance  $N \text{Var}[\hat{y}(\mathbf{x})]/\sigma^2$  provides insurance that the quality of the  $\hat{y}(\mathbf{x})$  as a prediction of future response values is similar throughout the region of interest. To this end, Box and Hunter (1957) developed the notion of **design rotatability**.

A **rotatable** design is one for which  $N \text{Var}[\hat{y}(\mathbf{x})]/\sigma^2$  has the same value at any two locations that are the same distance from the design center. In other words,  $N \text{Var}[\hat{y}(\mathbf{x})]/\sigma^2$  is constant on spheres.

The purpose of the idea of design rotatability was, in part, to impose a type of stability on  $N \text{Var}[\hat{y}(\mathbf{x})]/\sigma^2$ . The rationale of rotatability is that at two locations in the design space  $\mathbf{x}_1$  and  $\mathbf{x}_2$  for which the distances from the origin are the same [i.e.,  $(\mathbf{x}_1'\mathbf{x}_1)^{1/2} = (\mathbf{x}_2'\mathbf{x}_2)^{1/2}$ ], the predicted values  $\hat{y}(\mathbf{x}_1)$  and  $\hat{y}(\mathbf{x}_2)$  should be equally good—that is, have equal variance. While rotatability itself does not ensure stability or even near-stability throughout the design region, in many cases it provides some useful guidelines for the choice of design parameters—for example, the choice of  $\alpha$  and  $n_c$  in the CCD. The importance of rotatability as a design property depends on many things, not the least of which is the nature of the region of interest and region of operability. It is important to note that rotatability or near-rotatability is often very easy to achieve without the sacrifice of other important design properties. In what follows, we present the foundation that will allow the determination of necessary and sufficient conditions for design rotatability.

**Moment Matrix for a Rotatable Design (First and Second Order)** In this section we give the moment matrix for a rotatable design for both first- and second-order models. Additional theoretical development regarding the general case is given in Appendix 1. For the case of a **first-order model**, a design is rotatable if and only if *odd moments through order two are zero and the pure second moments are all equal*. In other words,

$$\begin{aligned}[i] &= 0 \quad (i = 1, 2, \dots, k) \\ [ij] &= 0 \quad (i \neq j, i, j = 1, 2, \dots, k) \\ [ii] &= \lambda_2 \quad (i = 1, 2, \dots, k)\end{aligned}$$

The quantity  $\lambda_2$  is determined by the scaling of the design. As a result in the first-order case, the moment conditions for a rotatable design are equivalent to the moment conditions for a variance-optimal design. Indeed, with scaling that allows levels at  $\pm 1$  in a two-level design of resolution III or higher, we have

$$[i] = 0, \quad [ij] = 0, \quad [ii] = 1.0 \quad (i = 1, 2, \dots, k, i \neq j)$$

In other words,  $\lambda_2$  is set at 1.0 due to the standard  $\pm 1$  scaling. The equivalence of rotatability to variance optimality in the first-order case should not be surprising. The reader should recall the result of Equation 7.11. We showed that

$$\text{SPV}(\mathbf{x}) = 1 + \rho_{\mathbf{x}}^2$$

for a first-order variance optimal design. Thus, the scaled prediction variance  $N \text{Var}[\hat{y}(\mathbf{x})]/\sigma^2$  is a function of  $\mathbf{x}$  only through  $\rho_{\mathbf{x}}$ , the distance of  $\mathbf{x}$  from the design origin. This implies that  $N \text{Var}[\hat{y}(\mathbf{x})]/\sigma^2$  is the same at any two locations that are the same distance from the origin.

In the case of a **second-order model**, the moments that affect rotatability (or any variance property) are moments through order four. Necessary and sufficient conditions for rotatability are as follows:

1. All odd moments through order four are zero.
  2. The ratio of moments  $[iiii]/[iiji] = 3$  ( $i \neq j$ ).
- (7.14)

The conditions are not only simple, but relatively easy to achieve, particularly with a CCD.

### 7.4.3 Rotatability and the CCD

The conditions given in Equation 7.14 are achieved, at least approximately, by several classes of designs. In the case of the CCD, rotatability is achieved by making a proper choice of  $\alpha$ , the axial distance. Condition 1 above will hold as long as the factorial portion is a full  $2^k$  or a fraction with resolution V or higher. The balance between  $+1$  and  $-1$  in the factorial columns and the orthogonality among certain columns in the matrix  $\mathbf{X}$  for the CCD will result in all odd moments being zero. For condition 2, one

**TABLE 7.3** Values of  $\alpha$  for a Rotatable Central Composite Design

$k$	$F$	$N$	$\alpha$
2	4	$8 + n_c$	1.414
3	8	$14 + n_c$	1.682
4	16	$24 + n_c$	2.000
5	32	$42 + n_c$	2.378
5 ( $\frac{1}{2}$ rep)	16	$26 + n_c$	2.000
6	64	$76 + n_c$	2.828
6 ( $\frac{1}{2}$ rep)	32	$44 + n_c$	2.378
7	128	$142 + n_c$	3.364
7 ( $\frac{1}{2}$ rep)	64	$78 + n_c$	2.828

merely seeks  $\alpha$  for which

$$\frac{[iiii]}{[iiji]} = \frac{F + 2\alpha^4}{F} = 3$$

which results in

$$\alpha = \sqrt[4]{F} \quad (7.15)$$

where, of course,  $F$  is the number of factorial points ( $F = 2^k$  if it is a full factorial). It is important to note that rotatability is achieved by using  $\alpha$  as in Equation 7.15 *regardless of the number of center runs*. Table 7.3 gives value of  $\alpha$  for a rotatable design for various numbers of design variables.

Note that for  $k = 2$  and  $k = 4$  the rotatable CCD contains 8 and 24 points (apart from center runs), respectively, that are equidistant from the design center. For  $k = 3$ , the value  $\alpha = 1.682$  corresponds to the CCD used in the breadwrapper example in Section 7.4.1. For  $k = 2, 3$ , and 4 the rotatable CCD is either exactly or very nearly a spherical design; that is, all points (apart from center runs) are exactly (or approximately for  $k = 3$ ) a distance  $\sqrt{k}$  from the design center.

**Center Runs for the Rotatable CCD** The property of rotatability is an attempt at producing **stability**, in a certain sense, of  $\text{SPV}(\mathbf{x})$ . The “sense” is, of course, constant  $\text{SPV}(\mathbf{x})$  on spheres. However, the presence of a rotatable design does not imply stability throughout the design region. In fact it turns out that a spherical design (all points on a common radius) used for fitting a second-order model has an infinite  $\text{SPV}(\mathbf{x})$ , since the design is **singular**; that is,  $\mathbf{X}'\mathbf{X}$  is a singular matrix [see Box and Hunter (1957), Box and Draper (1975), and Myers (1976)]. The use of center runs does provide reasonable *stability* of  $\text{SPV}(\mathbf{x})$  in the design region; as a result, some center runs for a rotatable CCD are very beneficial. The use of a rotatable or near-rotatable CCD with only a small number of center runs is not a good practice. An illustration of this point is given through Figs. 7.8 and 7.9. Figure 7.8 shows contours of  $\text{SPV}(\mathbf{x})$  for a  $k = 2$  CCD ( $\alpha = \sqrt{2}$ ) and one center run. (For zero center runs the design is singular.) Figure 7.9 gives the contours with  $\alpha = \sqrt{2}$  and five center runs. Note that the design in Fig. 7.9 is preferable. Also note that the criterion involves weighting by  $N$ , which means that the design in

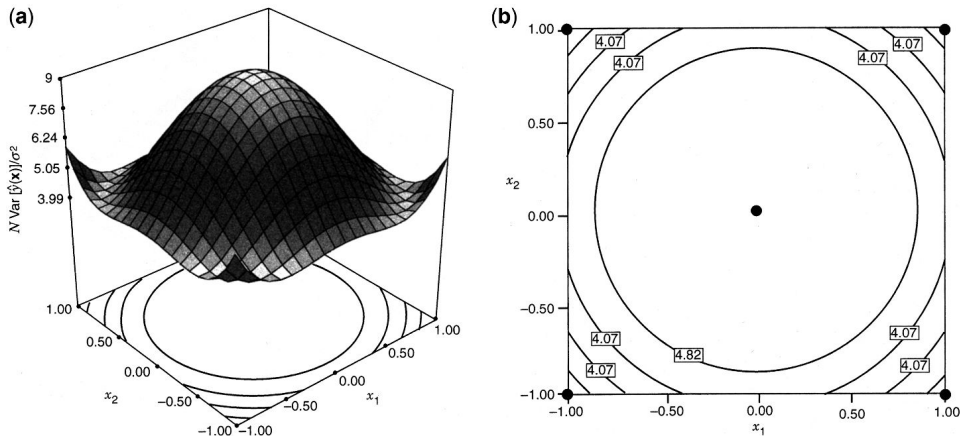


**Figure 7.8** Scaled prediction variance  $N \text{Var}[\hat{y}(\mathbf{x})]/\sigma^2$  for  $k = 2$  CCD,  $\alpha = \sqrt{2}$ ,  $n_c = 1$ .  
**(a)** Response surface. **(b)** Contour plot.

Fig. 7.9 has a larger weight. In spite of this, the  $n_c = 1$  design has a scaled prediction variance at the design center that is 3.5 times as large as that of the  $n_c = 5$  design.

Guidelines regarding the use of center runs with the CCD will be given in the next section; suffice it to say at this point that spherical or nearly spherical designs require three to five center runs in order to avoid a severe imbalance in  $\text{SPV}(\mathbf{x})$  through the design region. The message communicated by Figs. 7.8 and 7.9 extends to larger values of  $k$ . Draper (1982), Giovanetti-Jensen and Myers (1989), and Myers et al. (1992b) supply information regarding center runs in the use of the CCD.

Achieving near rotatability for a design can have the desired effect of producing good stability of prediction variance throughout the design region, even if the conditions for rotatability were not met exactly. Consider the experiment for finding the optimal conditions for

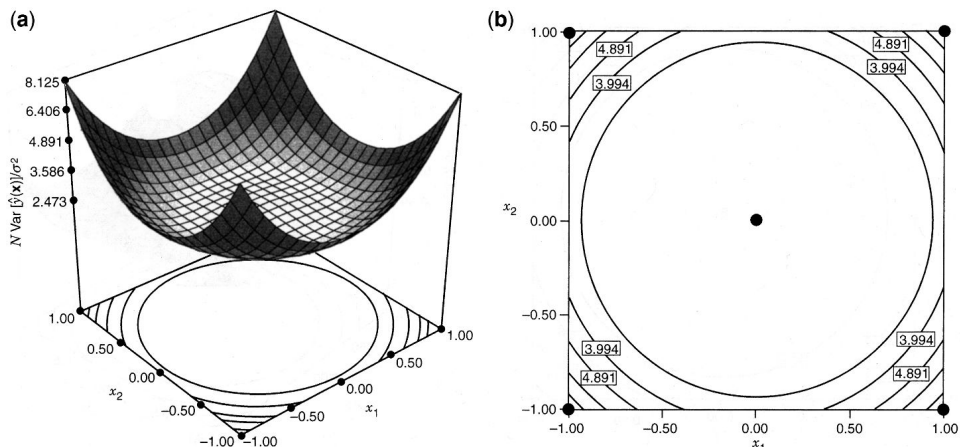


**Figure 7.9** Scaled prediction variance  $N \text{Var}[\hat{y}(\mathbf{x})]/\sigma^2$  for  $k = 2$  CCD,  $\alpha = \sqrt{2}$ ,  $n_c = 5$ .  
**(a)** Response surface. **(b)** Contour plot.

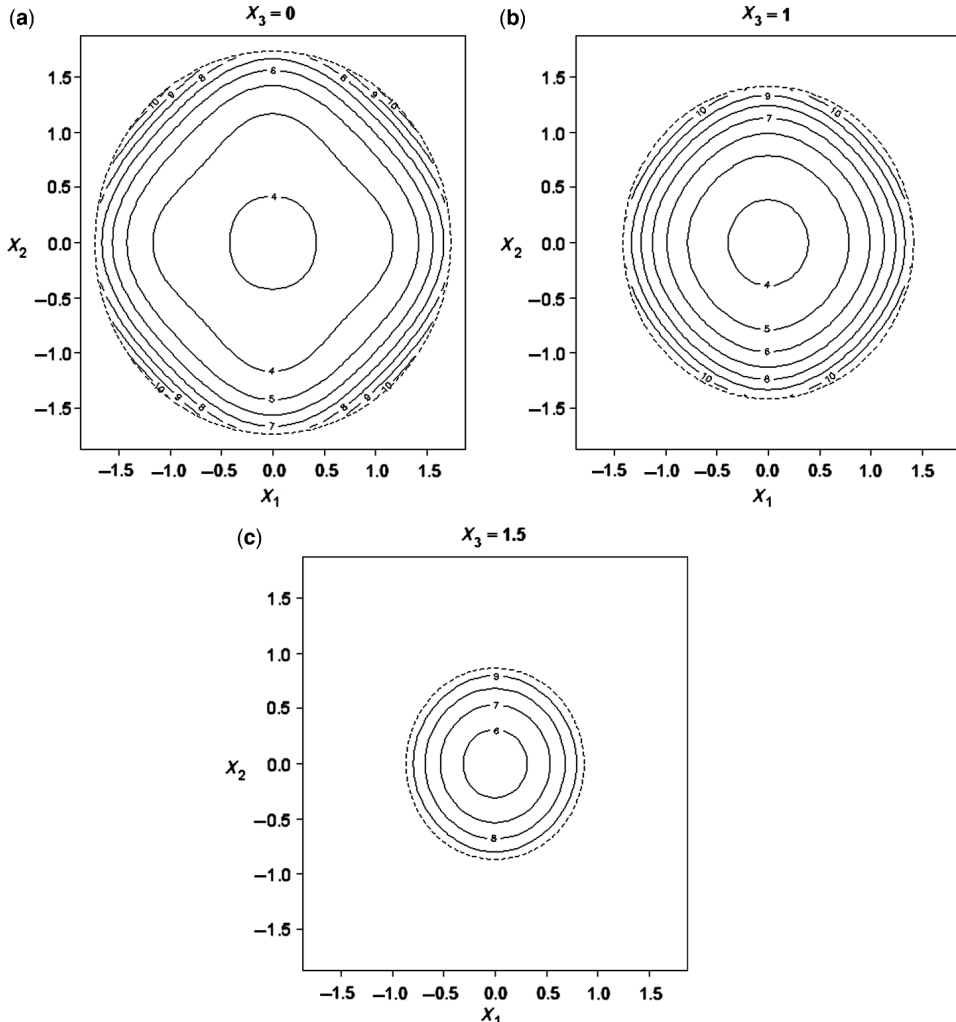


**Figure 7.10** Contour plot of scaled prediction variance for  $k = 3$  CCD,  $\alpha = 2$ ,  $n_c = 4$  for Example 6.2. (a)  $X_3 = 0$ , (b)  $X_3 = 1$ , (c)  $X_3 = 1.5$ .

storing bovine semen given in Example 6.2 with data shown in Table 6.4. In this example, three factors were considered, and the design selected was a CCD with four center runs and  $\alpha = 2$ . Figure 7.10 shows three slices of the spherical design region, based on fixed values of factor  $X_3$ . The dashed line on the plot shows the region of the design space that lies within the sphere of radius  $\sqrt{3}$  from the center. Note that this changes depending on the value of  $X_3$  considered. In this case the axial design points lie outside of the spherical region, still within the region of operability, but outside the region of interest.

Although the axial distance was not 1.682 as recommended for a rotatable design, we can see from Fig. 7.10 that the contours for this design are nearly circular, and hence the design is very close to rotatable. This illustrates that the changes in the axial distance affect the stability of the scaled prediction variance as measured by rotatability relatively slowly.

**How Important is Rotatability?** The rotatable CCD plays an important role in RSM, from both a historical and an operational point of view. However, it is important for the analyst to understand that it is not necessary to have exact rotatability in a second-order design. In fact:

If the desired region of the design is spherical, the CCD that is most effective from a variance point of view is to use  $\alpha = \sqrt{k}$  and three to five center runs.

This design is not necessarily rotatable, but is near-rotatable. The recommendation is based on the stability and size of  $\text{SPV}(\mathbf{x})$  in the spherical design region. For example, for  $k = 3$ ,  $\alpha = \sqrt{3}$  does not produce a rotatable design. However, the loss in rotatability is actually trivial, and the larger value of  $\alpha$  (then the rotatable value  $\alpha = 1.682$ ), results in a design that is slightly preferable. Numerical evidence regarding this recommendation will be given later in this chapter and in Chapter 8. The reader is also referred to Box and Draper (1987), Khuri and Cornell (1996), Lucas (1976), Giovannitti-Jensen and Myers (1989), and Myers et al. (1992b) for information regarding the practical use of the CCD.

#### 7.4.4 More on Prediction Variance—Scaled, Unscaled, and Estimated

The importance of the **prediction variance** or the **variance of a predicted value**, as defined by

$$PV(\mathbf{x}) = \text{Var}[\hat{y}(\mathbf{x})] = \sigma^2 \mathbf{x}^{(m)\prime} (\mathbf{X}'\mathbf{X})^{-1} \mathbf{x}^{(m)}$$

has importance in several phases of the design and analysis of an experiment. The presence of the unknown quantity,  $\sigma^2$ , needs special consideration and different treatment depending on whether data have been collected.

During the design selection stage, no value of  $\sigma^2$  is available. In addition, its value is not informative to the quality of the designs being compared or assessed. Hence, the scaled prediction variance,  $\text{SPV}(\mathbf{x}) = N \text{Var}[\hat{y}(\mathbf{x})]/\sigma^2$ , as defined in Equation 7.10 is a common choice in this stage. In their epic paper in 1957, Box and Hunter used it in graphics to compare competing designs with considerable work attached to the central composite design and other spherical designs. In fact the term “scaled” prediction was not used in their 1957 paper. Rather they used the term “information” to describe the concept. We now describe the origin and reasonableness of this term.

Cost and general design efficiency are important, and it is often helpful to weigh these relative to each other. As we discussed in Section 7.3.4, the SPV works through the use of the *information matrix*,  $\mathbf{X}'\mathbf{X}/N$ , also called the *moment matrix*. This quantity considers quality on a per *observation basis*. Thus many reasonable comparisons between designs take cost (choice of  $N$ ) into account, and balance cost with efficiency. For the SPV can be written

$$\begin{aligned} \text{SPV} &= \mathbf{x}^{(m)\prime} \left( \frac{\mathbf{X}'\mathbf{X}}{N} \right)^{-1} \mathbf{x}^{(m)} \\ &= N \mathbf{x}^{(m)\prime} (\mathbf{X}'\mathbf{X})^{-1} \mathbf{x}^{(m)} \end{aligned}$$

In fact, as will be demonstrated in Chapter 8, an entire spectrum of optimality criteria, such as *D*-optimality, *I*-optimality, *G*-optimality, and *A*-optimality, involve criteria that are norms on  $\mathbf{X}'\mathbf{X}/N$ , and hence use scaling as in the case of SPV.

However, the assumption that the cost of the design is proportional to its size,  $N$ , may not be appropriate for all situations. For example, consider the situation where setting up the general conditions for the experiment are more expensive than the incremental cost of performing runs of the experiment. In this case, we are more likely to want to run an experiment as large as possible given practical constraints, to maximize the benefit of our set-up. Here we might choose to compare designs of different sizes without the penalty term of  $N$  in SPV. Here the quantity, called **unscaled prediction variance**

$$\text{UPV} = \text{Var}[\hat{y}(\mathbf{x})]/\sigma^2 = \mathbf{x}^{(m)'}(\mathbf{X}'\mathbf{X})^{-1}\mathbf{x}^{(m)}$$

may be more appropriate. There is considerable discussion among statisticians about the relative merits of the quantities, SPV and UPV. On the theoretical ground outlined above, SPV is a useful metric for assessing the quality of prediction in the design region taking account of the size of the design. If cost as quantified by the size of the design is not a consideration for selecting between designs, or if the incremental cost of increasing the design size is not appropriately approximated by the scaling  $N$ , then UPV is a good alternative. It gives an absolute measure of the precision of a design. From a practical perspective, the SPV approach is similar to the Derringer-Suich (1980) desirability function approach described in Chapter 6, which seeks to balance good prediction quality with cost considerations. If it is more beneficial to consider these aspects of a design separately, then the UPV may be preferred. See Anderson-Cook et al. (2008) with discussion for different perspectives on the merits of scaling or not.

To summarize, we can use SPV or UPV during the design selection phase. The division by  $\sigma^2$  means that these quantities are a function of only the design matrix and do not require data to have been collected. However, there are certainly many applications of the use of prediction variance in which the scaling of  $N/\sigma^2$  for the SPV or  $1/\sigma^2$  for the UPV should not be used. After the experiment has been run, and data have been collected, the estimate MSE for  $\sigma^2$  should be multiplied by the unscaled quantity  $\mathbf{x}^{(m)'}(\mathbf{X}'\mathbf{X})^{-1}\mathbf{x}^{(m)}$  with the result being the **estimated prediction variance**,

$$\text{EPV} = \text{MSE } \mathbf{x}^{(m)'}(\mathbf{X}'\mathbf{X})^{-1}\mathbf{x}^{(m)}$$

Here the square root of this quantity is the familiar standard error of the estimated mean,  $\hat{y}(\mathbf{x})$ , at a given location in the design space. Students are taught that at a location,  $\mathbf{x}_0$  (in the model space), the  $100(1 - \alpha)\%$  confidence interval on a mean response is given by the familiar expression

$$\hat{y}(\mathbf{x}_0) \pm t_{\alpha/2, \text{df(error)}} \sqrt{\text{MSE } \mathbf{x}_0^{(m)'}(\mathbf{X}'\mathbf{X})^{-1}\mathbf{x}_0^{(m)}}$$

Of course it would make no sense to scale the quantity inside the square root by a factor of  $N$ . In fact, the confidence region would not be correct with such scaling. Plots of this quantity for the variance at  $\mathbf{x}_0$  in the design region are available in several commercial software packages including Design-Expert. For example, plots in Figs. 2.12a and b for the data of Table 2.7 show illustrations of these plots.

From the foregoing, it should be surmised that if an experimental design has been implemented with the data collected, the EPV should be applied for inferences to be drawn concerning the use of the fitted model. In fact, under these conditions, the cost involved and the efficiency (compared to other designs) is no longer an issue. The questions that are now being answered center around “How good is the fitted model that was generated from this design?” Thus there is no need for scaling and using the estimated value of  $\sigma^2$  provides information about prediction that is specific to the experiment.

#### 7.4.5 The Cuboidal Region and the Face-Centered Cube

There are many practical situations in which the scientist or engineer specifies ranges on the design variables, and these ranges are strict. That is, the region of interest and the region of operability are the same, and the obvious region for the design is a **cube**.

For example, in an experimental study designed to study organism growth, the design variables and their ranges are percent glucose [2%, 4%], percent yeast [0.4%, 0.6%], and time [30 hr, 60 hr]. Suppose it is of interest to build a second-order response surface model and the biologist is interested in predicting growth of the organism inside and on the perimeter of the cuboidal region produced by the cube. In addition, for biological reasons, one cannot experiment outside the cube, though experimentation at the extremes in the region is permissible and, in fact, desirable. This scenario, which occurs frequently in many scientific areas, suggests a central composite design in which the eight corners of the cube are centered and scaled to  $(\pm 1, \pm 1, \pm 1)$  and  $\alpha = 1$ . The final design is given (in coded form) by

$$\mathbf{D} = \begin{array}{c} x_1 \quad x_2 \quad x_3 \\ \hline 1 & -1 & -1 \\ -1 & 1 & -1 \\ -1 & -1 & 1 \\ 1 & 1 & -1 \\ 1 & -1 & 1 \\ -1 & 1 & 1 \\ 1 & 1 & 1 \\ -1 & 0 & 0 \\ 1 & 0 & 0 \\ 0 & -1 & 0 \\ 0 & 1 & 0 \\ 0 & 0 & -1 \\ 0 & 0 & 1 \\ \mathbf{0} & \mathbf{0} & \mathbf{0} \end{array}$$

where the  $(\mathbf{0}, \mathbf{0}, \mathbf{0})$  at the design center indicates a vector of  $n_c$  center runs. Figure 7.11 shows the design, often called the **face-centered cube** (or FCD) because the axial points occur at the centers of the faces, rather than outside the faces as in the case of a spherical region.

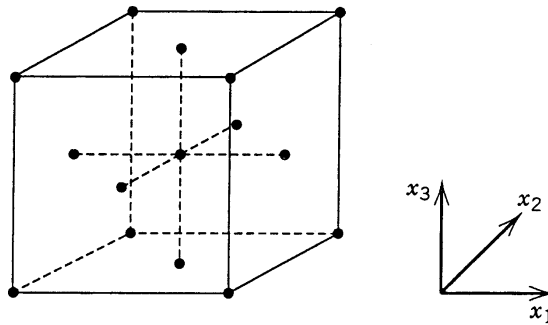


**Figure 7.11** Face-centered cube (FCD with \$\alpha = 1.0\$) for \$k = 3\$.

In the case of a **cuboidal design region**, the face-centered cube is an effective second-order design. When one encounters what is a natural cuboidal region, it is important that the points be pushed to the extreme of the experimental region. This results in the most attractive distribution of \$N \text{Var}[\hat{y}(\mathbf{x})]/\sigma^2\$. It is important for the region to be covered in a symmetric fashion. The face-centered cube accomplishes this. Of course, the design is not rotatable. However, rotatability or near-rotatability is not an important priority when the region of interest is clearly cuboidal. It is a useful option that comes from spherical or near-spherical designs; these designs are certainly appropriate for spherical regions of interest or regions of operability, but are less appropriate with cuboidal regions.

The face-centered cube is a useful design for any number of design variables. Again, a resolution V fraction is used for the factorial portion. The recommendation for center runs is quite different from that of the spherical designs. In the case of spherical designs, center runs are a necessity in order to achieve a reasonable distribution of \$N \text{Var}[\hat{y}(\mathbf{x})]/\sigma^2\$, with \$n\_c = 3 - 5\$ giving good results. In the *cuboidal* case (i.e., with \$\alpha = 1.0\$), one or two center runs are sufficient to produce reasonable stability of \$N \text{Var}[\hat{y}(\mathbf{x})]/\sigma^2\$. The sensitivity of \$N \text{Var}[\hat{y}(\mathbf{x})]/\sigma^2\$ to the number of center runs for the spherical design is seen in Figs. 7.8

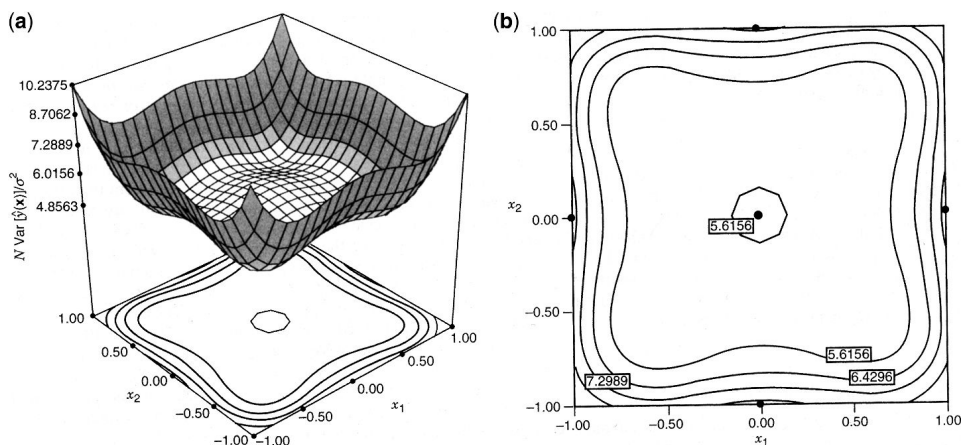


**Figure 7.12** Scaled prediction variance \$N \text{Var}[\hat{y}(\mathbf{x})]/\sigma^2\$: \$\alpha = 1.0\$, \$k = 3\$, \$n\_c = 0\$ with \$x\_2 = 0\$.  
**(a)** Response surface. **(b)** Contour plot.

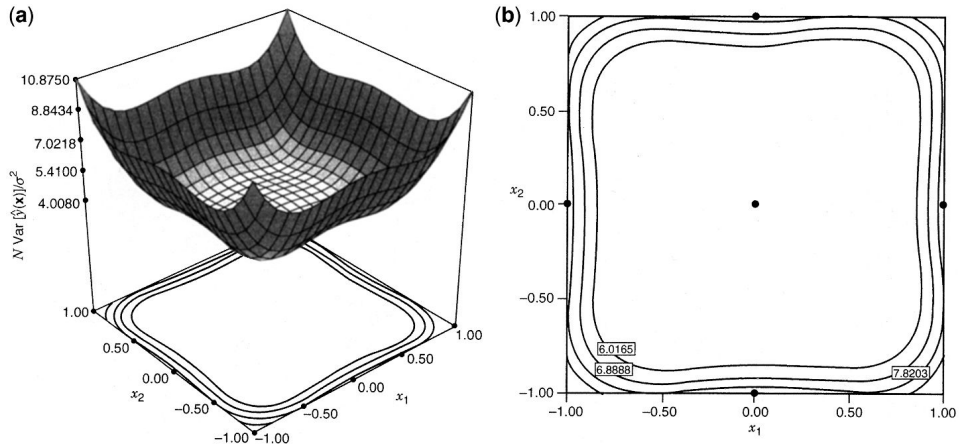


**Figure 7.13** Scaled prediction variance  $N \text{Var}[\hat{y}(\mathbf{x})]/\sigma^2$ :  $\alpha = 1.0$ ,  $k = 3$ ,  $n_c = 1$  with  $x_3 = 0$ . **(a)** Response surface. **(b)** Contour plot.

and 7.9. The insensitivity to center runs for the face-centered cube is illustrated in Figs. 7.12, 7.13, and 7.14. Contours of values of  $N \text{Var}[\hat{y}(\mathbf{x})]/\sigma^2$  are given for  $n_c = 0$ ,  $n_c = 1$ , and  $n_c = 2$  for the  $k = 3$  face-centered cube when  $x_3$  is fixed at 0. It is clear that many center runs are not needed to stabilize the prediction variance. In fact, one center run is quite sufficient for stability, though  $n_c = 2$  is slightly preferable. No further improvement is achieved beyond  $n_c = 2$ .

Though much has been said here about the effect of center runs on the scaled prediction variance  $N \text{Var}[\hat{y}(\mathbf{x})]/\sigma^2$  for both spherical and cuboidal designs, it should be noted that multiple center runs or replication of exterior points may, in many cases, be desirable in order to have a sufficient number of degrees of freedom for pure error.

**Other Three-Level Designs on Cubes** There are other approaches to obtaining three-level designs on cubes for fitting the second-order model. While the complete  $3^k$  requires too many

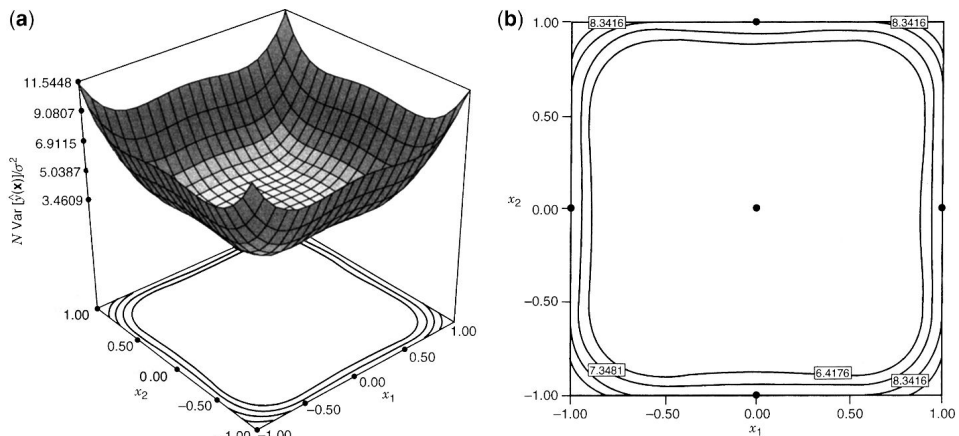


**Figure 7.14** Scaled prediction variance  $N \text{Var}[\hat{y}(\mathbf{x})]/\sigma^2$ :  $\alpha = 1.0$ ,  $k = 3$ ,  $n_c = 2$  with  $x_3 = 0$ . **(a)** Response surface. **(b)** Contour plot.

runs, an experimenter can either use a suitable fraction of the  $3^k$  or construct a computer-generated design based on some **alphabetic optimality criterion** (see Chapter 8). See Hoke (1974) and Mitchell and Bayne (1978) for examples of these approaches. Recently, Morris (2000) has proposed a new class of second-order three level designs called augmented pairs designs, which are based on minimax and maximin distance criteria. Li et al. (2003) and Park et al. (2005) consider various designs on the cuboidal region for different numbers of factors, with graphical summaries to compare their prediction quality.

#### 7.4.6 When is the Design Region Spherical?

As we have indicated in the previous section, the cuboidal CCD is appropriate when a cuboidal region of interest and cuboidal region of operability are apparent to the practitioner. Clearly the problem may suggest ranges on the factors which may define the **corners** where the factorial points should reside. Then the question regarding the design region should hinge on whether axial points outside the ranges are scientifically permissible and should be included in the region of interest. For example, consider Fig. 7.15. The shaded area forms the cube, but after some deliberation it is determined not only that the nonshaded area is within the region of operability but also that the researcher is interested in predicting response in the unshaded area as well as the shaded area. The region of interest is a sphere circumscribed around a cube. A spherical design (CCD with  $\alpha = \sqrt{k}$ ) is certainly appropriate.

A second situation can occur, very much like that in Fig. 7.16. Ranges are chosen on design variable, but as the planning of the experiment evolves, it is determined that several (and perhaps all) of the vertices on the cube defined by the ranges are not scientifically permissible; that is, they are outside both regions of operability, and the region of interest (e.g., in the case of a food product, high levels of flour, shortening, and baking time) is known to produce an unacceptable product. As a result, the corners, shaded in Fig. 7.16, are shaved off, and the design region is formed from the unshaded region. Here, the sphere is inscribed inside the cuboidal region formed from the selection of ranges.

Sometimes the region of operability and the region of interest are not identical. In the case where it is possible to operate slightly outside of a cuboidal region, but primary interest lies in the cube, it is possible to adjust the axial distance of the CCD to take advantage of this. Li et al. (2008) show how “*practical  $\alpha$  values*” (first suggested by Oehlert and Whitcomb 2002) can

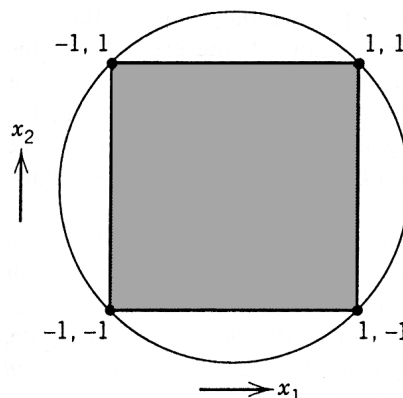


**Figure 7.15** Spherical region (sphere circumscribed).

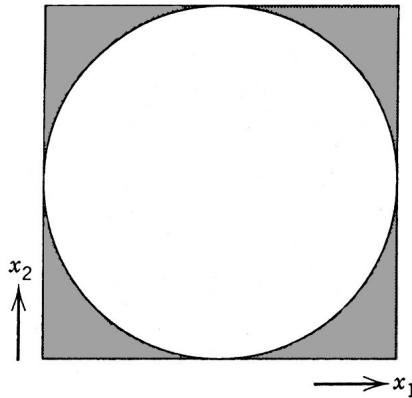


**Figure 7.16** Spherical region (sphere inscribed).

be selected to substantially improve prediction performance in the cuboidal region. These practical  $\alpha$  values are larger than 1, and hence fall outside of the region of interest.

For larger numbers of factors, another class of potential designs to consider are called **minimum-run resolution (MinRes) V designs**. They are equireplicated two-level irregular fractions of resolution V. An equireplicated design is one in which each factor has an equal number of high and low levels. For a complete description of the construction of these designs, see Oehlert and Whitcomb (2002).

It is important to understand that in many situations the region of interest (or perhaps even the region of operability) is not clear cut. It is often difficult enough to get a commitment from a scientist or engineer on what are the interesting and permissible ranges of the factors. Mistakes are often made, and adjustments adopted in future experiments. *Confusion regarding type of design should never be an excuse for not using designed experiments.* Using a spherical region when it is more naturally cuboidal, for example, will still provide important information that will, among other things, lead to more educated selection of regions for future experiments.

#### 7.4.7 Summary Statements Regarding CCD

The CCD is an efficient design that is ideal for sequential experimentation and allows a reasonable amount of information for testing lack of fit while not involving an unusually large number of design points. The design accommodates a spherical region with five levels of each factor and a choice of  $\alpha = \sqrt{k}$ . The design can be a three-level design to accommodate a cuboidal region with the choice of  $\alpha = \sqrt{1.0}$ . In the spherical case, the design is either rotatable or very near rotatable, and three to five center runs should be used. In the cuboidal case, one or two center runs will suffice. Though the cuboidal and spherical designs are natural choices depending on the region of interest, the reader should not get the impression that the use of the CCD must be confined to those choices of  $\alpha$ . There will be practical situations for which  $\alpha = 1.0$  or  $\alpha = \sqrt{k}$  cannot be used. The CCD should not be ruled out in these situations.

The natural competitor for the CCD is, of course, the three-level factorial, that is, the  $3^k$  factorial. The  $3^2$  design is, in fact, the face-centered cube and is thus a CCD. But when  $k$  becomes moderately large, the  $3^k$  factorial design involves an excessive number

of design points. In the case of three factors and a natural cuboidal region, the  $3^3$  factorial is an efficient design if the researcher can afford to use the required 27 design points. However, for  $k > 3$  the number of design points for the  $3^k$  is usually considered impracticable for most applications. A comparison of the  $3^3$  with the face-centered cube and other designs via the consideration of prediction variance is given in Chapter 8.

#### 7.4.8 The Box–Behnken Design

Box and Behnken (1960) developed a family of efficient **three-level designs** for fitting second-order response surfaces. The methodology for design construction is interesting and quite creative. The class of designs is based on the construction of **balanced incomplete block designs**. For example, a balanced incomplete block design with three treatments and three blocks is given by

	Treatment		
	1	2	3
Block 1	X	X	
Block 2	X		X
Block 3		X	X

The pairing together of treatments 1 and 2 symbolically implies, in the response surface setting, that design variables  $x_1$  and  $x_2$  are paired together in a  $2^2$  factorial (scaling  $\pm 1$ ) while  $x_3$  remains fixed at the center ( $x_3 = 0$ ). The same applies for blocks 2 and 3, with a  $2^2$  factorial being represented by each pair of treatments while the third factor remains fixed at 0. As a result, the  $k = 3$  Box–Behnken design is given by

$$\mathbf{D} = \begin{bmatrix} x_1 & x_2 & x_3 \\ -1 & -1 & 0 \\ -1 & 1 & 0 \\ 1 & -1 & 0 \\ 1 & 1 & 0 \\ -1 & 0 & -1 \\ -1 & 0 & 1 \\ 1 & 0 & -1 \\ 1 & 0 & 1 \\ 0 & -1 & -1 \\ 0 & -1 & 1 \\ 0 & 1 & -1 \\ 0 & 1 & 1 \\ \mathbf{0} & \mathbf{0} & \mathbf{0} \end{bmatrix}$$

The last row in the design matrix implies a *vector* of center runs. In the case of  $k = 4$  the same methodology applies. Each pair of factors are linked in a  $2^2$  factorial. The design

matrix is given by

$$\mathbf{D} = \begin{bmatrix} x_1 & x_2 & x_3 & x_4 \\ -1 & -1 & 0 & 0 \\ -1 & 1 & 0 & 0 \\ 1 & -1 & 0 & 0 \\ 1 & 1 & 0 & 0 \\ -1 & 0 & -1 & 0 \\ -1 & 0 & 1 & 0 \\ 1 & 0 & -1 & 0 \\ 1 & 0 & 1 & 0 \\ -1 & 0 & 0 & -1 \\ -1 & 0 & 0 & 1 \\ 1 & 0 & 0 & -1 \\ 1 & 0 & 0 & 1 \\ 0 & -1 & -1 & 0 \\ 0 & -1 & 1 & 0 \\ 0 & 1 & -1 & 0 \\ 0 & 1 & 1 & 0 \\ 0 & -1 & 0 & -1 \\ 0 & -1 & 0 & 1 \\ 0 & 1 & 0 & -1 \\ 0 & 1 & 0 & 1 \\ 0 & 0 & -1 & -1 \\ 0 & 0 & -1 & 1 \\ 0 & 0 & 1 & -1 \\ 0 & 0 & 1 & 1 \\ \mathbf{0} & \mathbf{0} & \mathbf{0} & \mathbf{0} \end{bmatrix} \quad (7.16)$$

Note that the Box–Behnken design (BBD) is quite comparable in number of design points to the CCD for  $k = 3$  and  $k = 4$ . (There is no BBD for  $k = 2$ .) For  $k = 3$ , the CCD contains  $14 + n_c$  runs while the BBD contains  $12 + n_c$  runs. For  $k = 4$  the CCD and BBD both contain  $24 + n_c$  design points. For  $k = 5$  we have the following  $40 + n_c$  experimental runs:

$$\mathbf{D} = \begin{bmatrix} x_1 & x_2 & x_3 & x_4 & x_5 \\ \pm 1 & \pm 1 & 0 & 0 & 0 \\ \pm 1 & 0 & \pm 1 & 0 & 0 \\ \pm 1 & 0 & 0 & \pm 1 & 0 \\ \pm 1 & 0 & 0 & 0 & \pm 1 \\ 0 & \pm 1 & \pm 1 & 0 & 0 \\ 0 & \pm 1 & 0 & \pm 1 & 0 \\ 0 & \pm 1 & 0 & 0 & \pm 1 \\ 0 & 0 & \pm 1 & \pm 1 & 0 \\ 0 & 0 & \pm 1 & 0 & \pm 1 \\ 0 & 0 & 0 & \pm 1 & \pm 1 \\ 0 & 0 & 0 & 0 & 0 \end{bmatrix} \quad (7.17)$$

The CCD for  $k = 5$  involves  $26 + n_c$  runs when the  $\frac{1}{2}$  fraction is used in the factorial portion. When the full factorial is used, the CCD makes use of  $42 + n_c$  runs. Each row in the BBD symbolizes four design points with  $(\pm 1, \pm 1)$  representing a  $2^2$  factorial.

For  $k = 6$  the construction of the design is based on partially balanced incomplete block designs. Thus, each treatment does not occur with every other treatment the same number of times. In the Box–Behnken construction, this means that each factor does not occur in a two-level factorial structure the same number of times with every factor. The design matrix, involving  $N = 48 + n_c$  runs, is given by

$$\mathbf{D} = \begin{bmatrix} x_1 & x_2 & x_3 & x_4 & x_5 & x_6 \\ \pm 1 & \pm 1 & 0 & \pm 1 & 0 & 0 \\ 0 & \pm 1 & \pm 1 & 0 & \pm 1 & 0 \\ 0 & 0 & \pm 1 & \pm 1 & 0 & \pm 1 \\ \pm 1 & 0 & 0 & \pm 1 & \pm 1 & 0 \\ 0 & \pm 1 & 0 & 0 & \pm 1 & \pm 1 \\ \pm 1 & 0 & \pm 1 & 0 & 0 & \pm 1 \\ 0 & 0 & 0 & 0 & 0 & 0 \end{bmatrix} \quad (7.18)$$

The CCD requires  $44 + n_c$  runs when the one-half fraction is used in the factorial portion.

Unlike the  $k = 3, 4$ , and  $5$  cases, the factorial structures in the BBD for  $k = 6$  are  $2^3$  factorials involving three factors. Thus each row of the above matrix involves eight design points.

For  $k = 7$ , the factorial structures again involve combinations of three design factors. The  $N = 56 + n_c$  design runs are given by the following design matrix:

$$\mathbf{D} = \begin{bmatrix} x_1 & x_2 & x_3 & x_4 & x_5 & x_6 & x_7 \\ 0 & 0 & 0 & \pm 1 & \pm 1 & \pm 1 & 0 \\ \pm 1 & 0 & 0 & 0 & 0 & \pm 1 & \pm 1 \\ 0 & \pm 1 & 0 & 0 & \pm 1 & 0 & \pm 1 \\ \pm 1 & \pm 1 & 0 & \pm 1 & 0 & 0 & 0 \\ 0 & 0 & \pm 1 & \pm 1 & 0 & 0 & \pm 1 \\ \pm 1 & 0 & \pm 1 & 0 & \pm 1 & 0 & 0 \\ 0 & \pm 1 & \pm 1 & 0 & 0 & \pm 1 & 0 \\ 0 & 0 & 0 & 0 & 0 & 0 & 0 \end{bmatrix} \quad (7.19)$$

**Characteristics of the Box–Behnken Design** In many scientific studies that require RSM, researchers are inclined to require three evenly spaced levels. Thus, the Box–Behnken design is an efficient option and indeed an important alternative to the central composite design. As we can observe from the sample sizes, there is sufficient information available for testing lack of fit. For example, for  $k = 6$  the use of, say,  $n_c = 5$  would allow four degrees of freedom for pure error and 21 degrees of freedom for lack of fit. The Box–Behnken design does not substantially deviate from rotatability, and, in fact, for  $k = 4$  and  $k = 7$  the design is exactly rotatable. Verification of rotatability in both cases should be quite simple for the reader. From the design matrix in Equation 7.16, it is easy to see that all odd moments are zero. This is a result of the prominence of the sets of  $2^2$  factorial

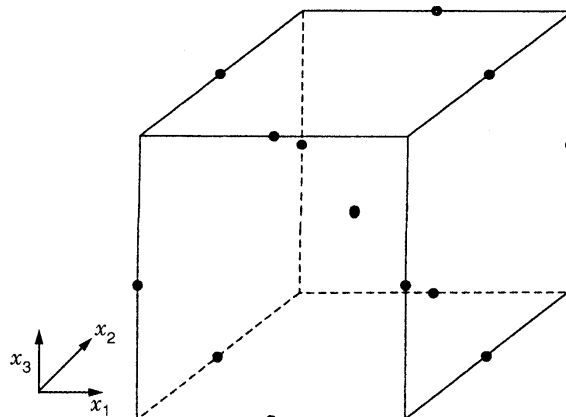


**Figure 7.17** The  $k = 3$  BBD with a center point.

arrays. For the second condition required for rotatability, note from Equation 7.16 that  $(iii) = \frac{12}{24}$  and  $(iijj) = \frac{4}{24}$ , for  $i \neq j$ . As a result,  $(iii)/(iijj) = 3$ . An investigation of Equation 7.19 suggests that the rotatability conditions hold for the  $k = 7$  BBD as well.

Another important characteristic of the BBD is that it is a **spherical design**. Note, for example, in the  $k = 3$  case that all of the points are so-called “edge points” (i.e., points that are on the edges of the cube); in this case, all edge points are a distance  $\sqrt{2}$  from the design center. There are no factorial points or face points. Figure 7.17 displays the BBD for  $k = 3$ . Contrast this design to that depicted in Fig. 7.11 with the face-centered cube. The latter displays face points and factorial points that are not the same distance from the design center, though they all reside on the cube and provide good coverage of the cube. The BBD involves all edge points, but the entire cube is not covered. In fact, there are no points on the corner of the cube or even a distance  $\sqrt{3}$  from the design center. The analyst should not view the lack of coverage of the cube as a reason not to use the BBD. It is not meant to be a cuboidal design. However, the use of the BBD should be confined to situations in which one is *not interested in predicting response at the extremes*; that is, at the corners of the cube. A quick inspection of the design matrices in Equations 7.16–7.19 further underscores the fact that the BBD is not a cuboidal design. For example, for  $k = 7$ , the design points are at a radius of  $\sqrt{3}$ , which is considerably smaller than the radius  $\sqrt{7}$  of the corner of the cube. If three levels are required and coverage of the cube is necessary, one should use a face-centered cube rather than the BBD.

The spherical nature of the BBD, combined with the fact that the designs are rotatable or near-rotatable, suggests that ample center runs should be used. In fact, for  $k = 4$  and 7, center runs are necessary to avoid singularity. The use of three to five center runs is recommended for the BBD.

**Example 7.5 A BBD for Optimizing Viscosity** One step in the production of a particular polyamide resin is the addition of amines. It was felt that the manner of addition has a profound effect on the molecular weight distribution of the resin. Three variables are thought to play a major role: temperature at the time of addition ( $x_1$ , °C), agitation ( $x_2$ , rpm), and rate of addition ( $x_3$ , min $^{-1}$ ). Because it was difficult to physically set the levels of addition and agitation, three levels were chosen and a BBD was used. The

**TABLE 7.4 Data for Resin Viscosity in Example 7.5 Using Box–Behnken Design**

Level	Temperature	Agitation	Rate	$x_1$	$x_2$	$x_3$
High	200	10.0	25	+ 1	+ 1	+ 1
Center	175	7.5	20	0	0	0
Low	150	5.0	15	- 1	- 1	- 1
Standard Order		$x_1$	$x_2$	$x_3$	$y$	
1		- 1	- 1	0	53	
2		+ 1	- 1	0	58	
3		- 1	+ 1	0	59	
4		+ 1	+ 1	0	56	
5		- 1	0	- 1	64	
6		+ 1	0	- 1	45	
7		- 1	0	+ 1	35	
8		+ 1	0	+ 1	60	
9		0	- 1	- 1	59	
10		0	+ 1	- 1	64	
11		0	- 1	+ 1	53	
12		0	+ 1	+ 1	65	
13		0	0	0	65	
14		0	0	0	59	
15		0	0	0	62	

viscosity of the resin was recorded as an indirect measure of molecular weight. The data, including natural levels, design, and response values, are shown in Table 7.4. Figure 7.18 shows an analysis using the package JMP. Three contour plots of constant viscosity (shown in Fig. 7.19) are given in order to illustrate what combination of the factors produce high- and low-molecular-weight resins. Agitation was fixed at the low, medium, and high levels. It is clear that high-molecular-weight resins are produced with low values of agitation, whereas low-molecular-weight resins are potentially available when one uses high values of agitation. In fact, the extremes of low rates, low temperature, and high agitation produces low-molecular-weight resins, whereas low agitation, low temperature, and high rate results in high-molecular-weight resins.

#### 7.4.9 Other Spherical RSM Designs; Equiradial Designs

There are some special and interesting two-factor designs that serve as alternatives to the central composite design. They are the class of **equiradial designs**, beginning with a pentagon (five equally spaced points on a circle); the pentagon, hexagon, heptagon, and so on, do require center runs because they are designs on a common sphere and, as we shall show, are rotatable.

The design matrix for the equiradial design can be written

$$\begin{array}{ll} x_1 & x_2 \\ [\rho \cos(\theta + 2\pi u/n_1), \quad \rho \sin(\theta + 2\pi u/n_1)], u = 0, 1, 2, \dots, n_1 - 1 \end{array} \quad (7.20)$$

where  $\rho$  is the design radius. Here,  $n_1$  is the number of points on the sphere, say, 5, 6, 7, 8, ... . In addition to the  $n_1$  points indicated by Equation 7.20, we will assume  $n_c$  center runs. The value that one chooses for  $\rho$  merely determines the nature of the scaling. It turns

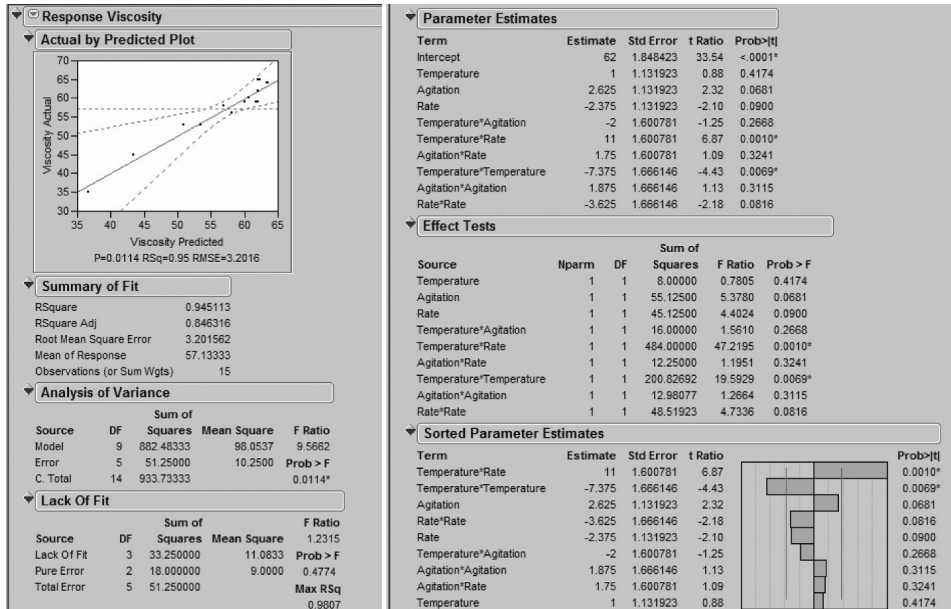
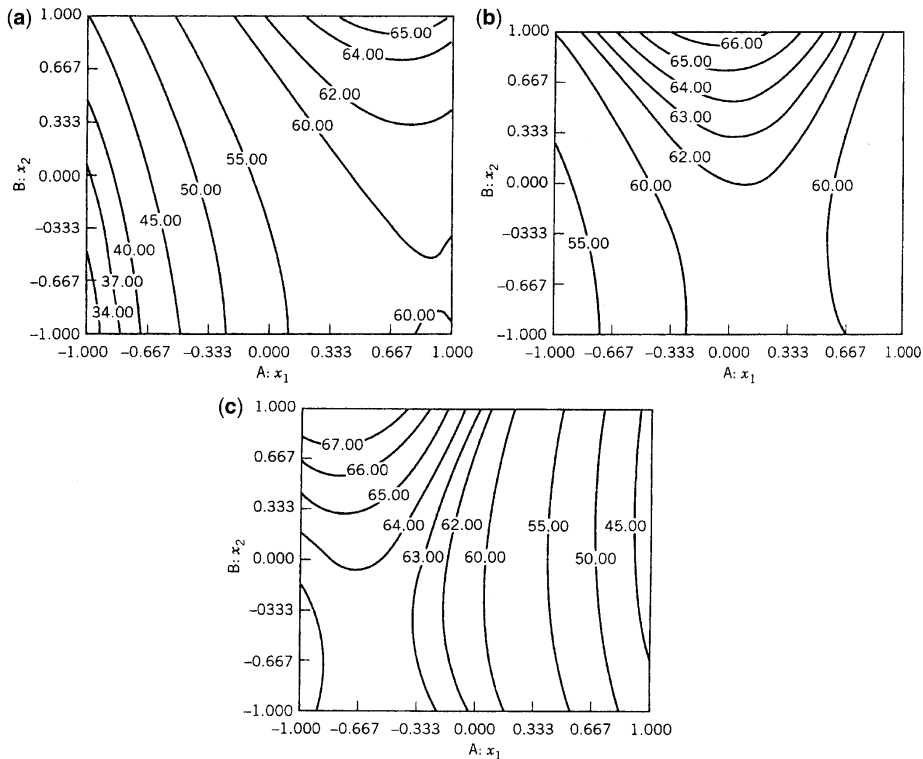


Figure 7.18 JMP analysis of resin viscosity data of Example 7.5.

Figure 7.19 Contour plots of viscosity from Example 7.5. (a) Addition rate  $x_3 = 1$ . (b) Addition rate  $x_3 = 0$ . (c) Addition rate  $x_3 = -1$ .

out that the choice of  $\theta$  has no effect on  $\mathbf{X}'\mathbf{X}$ ; that is, it has no effect on the design as far as the variance structure is concerned. As a result, all of the equiradial second-order designs (i.e., using  $n_1 = 5, 6, 7, 8, \dots$ ) are such that the matrix  $\mathbf{X}'\mathbf{X}$  is *invariant to design rotation*.

A very useful and interesting special case is the **hexagon**—that is, six equally spaced points on a circle. Thus  $n_1 = 6$ ; setting  $\theta = 0$  and  $\rho = 1$ , we have the following design matrix using  $n_c = 3$ :

$$\mathbf{D} = \begin{bmatrix} & x_1 & x_2 \\ & 1 & 0 \\ & 0.5 & \sqrt{0.75} \\ & -0.5 & \sqrt{0.75} \\ & -1 & 0 \\ & -0.5 & -\sqrt{0.75} \\ & 0.5 & -\sqrt{0.75} \\ & 0 & 0 \\ & 0 & 0 \\ & 0 & 0 \end{bmatrix} \quad (7.21)$$

Note that  $x_1$  is at five levels and  $x_2$  is at three levels for this particular rotation. Figure 7.20 shows the design. Note the six evenly spaced points.

It is of interest to consider the important design moments for the hexagon—that is, the moments through order four. From Equation 7.21 we have, for the hexagon,

$$[i] = [ij] = [iij] = [iii] = [iiij] = 0, \quad i \neq j = 1, 2 \text{ (odd moments zero)}$$

$$[iiii] = \frac{9/4}{N}, \quad [iiji] = \frac{3/4}{N}, \quad i \neq j = 1, 2$$

Because all design moments through order four are zero and  $[iiii]/[iiji] = 3$ , the hexagon is indeed rotatable. The reader should also note that these conditions are independent of  $\rho$  and  $\theta$ .

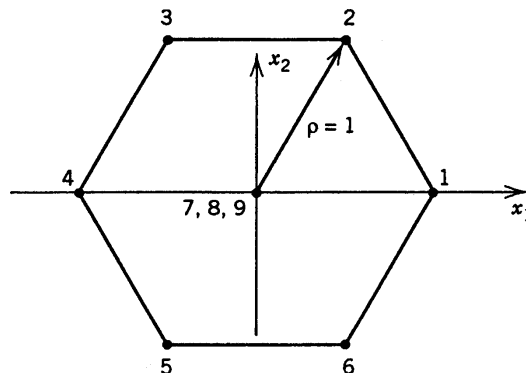


Figure 7.20 Design points for the hexagon.

It turns out that all equiradial designs for  $n_1 \geq 5$  are rotatable. Appendix 2 shows a development of the moment conditions. The relevant moments for the equiradial designs are as follows:

1. All odd moments through order four are zero.
2. The key even moments are

$$[ii] = \frac{\rho^2 n_1}{2N}, \quad i = 1, 2$$

$$[iiii] = \frac{3\rho^4 n_1}{8N}, \quad i = 1, 2$$

$$[iijj] = \frac{\rho^4 n_1}{8N}, \quad i \neq j = 1, 2$$

Of course, these conditions imply that all equiradial designs for  $n_1 \geq 5$  are rotatable.

**Special Case of The Equiradial Design—The CCD for  $k = 2$**  For  $n_1 = 8$ , the equiradial design is the **octagon**. As one might expect, the use of Equation 7.20 for  $n_1 = 8$  produces (using  $\rho = \sqrt{2}$ )

$x_1$	$x_2$
-1	-1
-1	1
1	-1
1	1
$\sqrt{2}$	0
$-\sqrt{2}$	0
0	$-\sqrt{2}$
0	$\sqrt{2}$
<b>0</b>	<b>0</b>

which, of course, is the  $k = 2$  rotatable CCD.

**Summary Comments on the Equiradial Designs** The equiradial designs are an interesting family of designs that enjoy some usage in the case where only two design variables are involved. One should use the CCD (the octagon) whenever possible. However, there are situations when cost constraints do not allow the use of the octagon. The pentagon (plus center runs) is a saturated design and thus should not be used unless absolutely necessary. The hexagon is a nice design that allows one degree of freedom for lack of fit. The heptagon also has its place in some applications. The octagon, hexagon, and nonagon (nine equally spaced points) possess the added property of *orthogonal blocking*, which will be discussed in the next section.

We have already indicated that the equiradial designs require the use of center runs. Reasonable stability of  $N \text{Var}[\hat{y}(\mathbf{x})]/\sigma^2$  is achieved with two to four center runs.

### 7.4.10 Orthogonal Blocking in Second-Order Designs

In many RSM situations the study is too large to allow all runs to be made under homogeneous conditions. As a result, it is important and interesting to consider second-order designs that facilitate *blocking*—that is, the inclusion of block effects. It is important that the assignment of the design points to blocks be done so as to minimize the effect on the model coefficients. The property of the experimental design that we seek is that of **orthogonal blocking**. To say that a design admits orthogonal blocking implies that the block effects in the model are orthogonal to model coefficients. A simple first-order example serves as an illustration. Consider a  $2^2$  factorial to be used for the fitting of a first-order model. Suppose we use  $I = AB$  as the defining relation to form two one-half fractions, which are placed in separate blocks. As a result, we have the model

$$y_i = \beta_0 + \beta_1 x_{i1} + \beta_2 x_{i2} + \delta_1 z_{i1} + \delta_2 z_{i2} + \varepsilon_i \quad (7.22)$$

where  $\delta_1$  and  $\delta_2$  are **block effect** coefficients. Here  $z_{i1}$  and  $z_{i2}$  are **dummy** or indicator variables; that is,  $z_{i1} = 1$  if  $y_i$  is in block 1 and  $z_{i1} = 0$  otherwise. The variable  $z_{i2} = 1$  if  $y_i$  is in block 2 and  $z_{i2} = 0$  otherwise. The  $X$  matrix is then

$$\mathbf{X} = \begin{array}{ccccc} & x_1 & x_2 & z_1 & z_2 \\ & \left[ \begin{array}{ccccc} 1 & -1 & -1 & 1 & 0 \\ 1 & 1 & 1 & 1 & 0 \\ \dots & \dots & \dots & \dots & \dots \\ 1 & -1 & 1 & 0 & 1 \\ 1 & 1 & -1 & 0 & 1 \end{array} \right] & \left. \right\} & \text{Block 1} \\ & & & & \left. \right\} \text{Block 2} \end{array} \quad (7.23)$$

Note that block 1 contains the design points  $\{(1), ab\}$ , whereas block 2 contains  $\{a, b\}$ . Now, in Equation 7.23, the matrix  $\mathbf{X}$  is singular; the last two columns add to the first column. This underscores the fact that the parameters  $\delta_1$  and  $\delta_2$  are not estimable. As a result, one of the indicator variables should not be included. We shall eliminate the  $z_2$  column and center  $z_1$ . As a result, the model Equation 7.22 can be rewritten

$$y_i = \beta_0^* + \beta_1 x_{i1} + \beta_2 x_{i2} + \delta_1(z_{i1} - \bar{z}_1) + \varepsilon_i \quad (7.24)$$

and thus  $\mathbf{X}$  is written

$$\mathbf{X} = \begin{array}{ccccc} & \beta_1 & \beta_2 & \delta_1 & \\ & \left[ \begin{array}{ccccc} 1 & -1 & -1 & 1/2 \\ 1 & 1 & 1 & 1/2 \\ \dots & \dots & \dots & \dots \\ 1 & -1 & 1 & -1/2 \\ 1 & 1 & -1 & -1/2 \end{array} \right] & \left. \right\} & \text{Block 1} \\ & & & & \left. \right\} \text{Block 2} \end{array} \quad (7.25)$$

Now, the concept of orthogonal blocking is nicely illustrated through the use of Equations 7.24 and 7.25. In this example the block effect is orthogonal to the regression coefficients if

$$\begin{aligned} \sum_{u=1}^4 (z_{u1} - \bar{z}_1)x_{1u} &= 0 \\ \sum_{u=1}^4 (z_{u1} - \bar{z}_1)x_{2u} &= 0 \end{aligned} \quad (7.26)$$

Thus, as the reader might have expected, the assignment of design points to blocks in this example provides an array in which the block factor has no effect on the regression coefficients. In fact, if one considers the least squares estimator  $\mathbf{b} = (\mathbf{X}'\mathbf{X})^{-1}\mathbf{X}'\mathbf{y}$ , the regression coefficients  $\beta_0^*$ ,  $\beta_1$ , and  $\beta_2$  are estimated *as if the blocks were not in the experiment*. The variances of the estimates of  $\beta_1$  and  $\beta_2$  in this variance optimal design are not changed in the presence of blocks.

The above example serves two purposes. First, it reinforces the material in Chapter 3 regarding blocking in two-level designs. In the above illustration, the  $x_1x_2$  interaction is **confounded with blocks**. If one augments the matrix  $\mathbf{X}$  with the  $x_1x_2$  column, this confounding becomes evident. The linear effects, or linear coefficients, are independent of block effects, and this is reinforced by the fact that Equations 7.26 hold. Secondly, the example allows us a foundation for setting up conditions for orthogonal blocking for second-order designs.

Though we now move on to the second-order case, there are several exercises at the end of this chapter that deal with blocking for first-order models and first-order-plus-interaction models.

**Conditions for Orthogonal Blocking in Second-Order Designs** Consider a second-order model with  $k$  design variables and  $b$  blocks. The model, then, can be written as

$$\begin{aligned} y_u &= \beta_0 + \sum_{i=1}^k \beta_i x_{ui} + \sum_{i=1}^k \beta_{ii} x_{ui}^2 + \sum_{i < j=2}^k \beta_{ij} x_{ui} x_{uj} \\ &\quad + \sum_{m=1}^b \delta_m (z_{um} - \bar{z}_m), \quad u = 1, 2, \dots, N \end{aligned} \quad (7.27)$$

Here we have used the indicator variable again, with  $z_{mu} = 1$  if the  $u$ th observation is in the  $m$ th block. We have centered the indicator variables as in our earlier example. In addition, we have included all of the block effects in the model even though it results in a singular model. This will not affect the conditions for orthogonal blocking. From Equation 7.27, block effects are orthogonal to regression coefficients if

$$\sum_{u=1}^N x_{ui} (z_{um} - \bar{z}_m) = 0, \quad i = 1, 2, \dots, k, \quad m = 1, 2, \dots, b \quad (7.28)$$

$$\sum_{u=1}^N x_{ui} x_{uj} (z_{um} - \bar{z}_m) = 0, \quad i \neq j, \quad m = 1, 2, \dots, b \quad (7.29)$$

$$\sum_{u=1}^N x_{ui}^2 (z_{um} - \bar{z}_m) = 0, \quad i = 1, 2, \dots, k, \quad m = 1, 2, \dots, b \quad (7.30)$$

In what follows we will assume that we are dealing with designs in which  $[i] = 0$  and  $[ij] = 0$  for all  $i \neq j$ ,  $i, j = 1, 2, \dots, k$ . That is, the first moments and mixed second moments are all zero. Recall that these conditions hold for all central composite designs, Box–Behnken designs, and two-level factorial designs. Now, if we consider Equations 7.28 and 7.29 for a specific value of  $m$  (i.e., for a specific block), we have

$$\sum_{\text{block } m} x_{ui} = \sum_{\text{block } m} x_{ui}x_{uj} = 0, \quad i, j = 1, 2, \dots, k, \quad i \neq j \quad (7.31)$$

But, of course, Equation 7.30 must hold for all blocks. Equation 7.31 implies, then, that in each block the first and second mixed moments are zero, implying that *each block must itself be a first-order orthogonal design* (condition 1).

Now consider Equation 7.30. For say the  $m$ th block, this equation implies that  $\sum_{u=1}^N x_{ui}^2 z_{um} = \bar{z}_m \sum_{u=1}^N x_{ui}^2$  for  $i = 1, 2, \dots, k$ . The quantity  $\bar{z}_m$  is the fraction of the total runs that are in the  $m$ th block. As a result, Equation 7.30 implies that *for each design variable, the sum of squares contribution from each block is proportional to the block size* (condition 2).

An **orthogonal block design for a second order model** requires the following conditions:

1. Each block must consist of a first-order orthogonal design
2. For each design variable, the sum of squares contribution from each block is proportional to the size of the block.

Designs that fulfill conditions 1 and 2 above are not difficult to find. Once again, the central composite design is prominent in that respect due to flexibility involved in the choice of  $\alpha$  and  $n_c$ .

**Orthogonal Blocking in the CCD** It may be instructive to discuss an example CCD that does block orthogonally. Consider a  $k = 2$  rotatable CCD in two blocks with two center points per block. Consider the assignment of design points to blocks as follows:

Block 1		Block 2	
$x_1$	$x_2$	$x_1$	$x_2$
-1	-1	$-\sqrt{2}$	0
-1	1	$-\sqrt{2}$	0
1	-1	0	$-\sqrt{2}$
1	1	0	$\sqrt{2}$
0	0	0	0
0	0	0	0

The above design does block orthogonally. Each block is a first-order orthogonal design; the first moments and mixed second moments are both zero for the design in each block, and thus condition 1 holds. Also, the sum of squares for each design variable is 4.0, and the block sizes are equal. Hence condition 2 regarding the proportionality relationship also holds. In this example, notice that any even number of center runs with half assigned

to block 1 and the other half to block 2 results in orthogonal blocking. In the example, the factorial design points are assigned to one block and the axial points to the other block. In this case, condition 1 will hold automatically. The values for  $\alpha$  and  $n_c$  are chosen to achieve condition 2.

As a second example let us consider, again, a CCD but assume  $k = 3$  and suppose that three blocks are required. The design is as follows:

Block 1			Block 2			Block 3		
$x_1$	$x_2$	$x_3$	$x_1$	$x_2$	$x_3$	$x_1$	$x_2$	$x_3$
-1	-1	-1	1	-1	-1	$-\alpha$	0	0
1	1	-1	-1	1	-1	$\alpha$	0	0
1	-1	1	-1	-1	1	0	$-\alpha$	0
-1	1	1	1	1	1	0	$\alpha$	0
0	0	0	0	0	0	0	0	$-\alpha$
0	0	0	0	0	0	0	0	$\alpha$
						0	0	0
						0	0	0
						0	0	0

Here we have divided the  $2^3 = 8$  factorial points into two blocks with  $I = ABC$  as the defining relation. The reader can again verify that condition 1 for orthogonal blocking holds. We can solve for  $\alpha$  that allows condition 2 to hold:

$$\frac{2\alpha^2}{9} = \frac{4}{6}$$

which result in  $\alpha = \sqrt{3}$ . As a result, we have a spherical CCD with  $\alpha = \sqrt{3}$  (the recommended choice for  $\alpha$  in Section 7.4.3), which blocks orthogonally in three blocks.

As the reader studies these two examples and the use of conditions 1 and 2, two principles obviously emerge: When one requires two blocks, there should be a factorial block and an axial block. In the case of three blocks, the factorial portion is divided into two blocks and the axial portion remains a single block. The partitioning into blocks of the factorial portion must result in a guaranteed orthogonality between blocks and the two factor interaction terms and, of course, orthogonality between blocks and linear coefficients. The numbers of blocks with the CCD are 2, 3, 5, 9, 17, .... There is never a subdivision of the axial block. The axial points are always a single block. Table 7.5 provides more details of the blocking options for the CCD with different numbers of factors. The flexibility in the choice of center runs and the value of  $\alpha$  allows us to achieve orthogonal blocking or near-orthogonal blocking in many situations. At this point, we will deal briefly in the special case of two blocks to give the reader further insight into the choice of  $\alpha$  and the assignment of center runs to blocks.

**Orthogonal Blocking in Two Blocks with the CCD** Suppose we denote by  $F_0$  the number of center runs in the factorial block, and by  $a_0$  the number of center runs in the

**TABLE 7.5 Design Details for Some Useful Central Composite Designs that Block Orthogonally**

$k$	2	3	4	5	5 ( $\frac{1}{2}$ rep)	6	6 ( $\frac{1}{2}$ rep)	7	7 ( $\frac{1}{2}$ rep)
Total # of blocks	2	3	3	5	2	9	3	17	9
Total # of points in design	14	20	30	54	33	90	54	169	90
<i>Factorial block(s)</i>									
$F$ : # of points in factorial portion	4	8	16	32	16	64	32	128	64
# of blocks in factorial portion	1	2	2	4	1	8	2	16	8
# points in each block from factorial	4	4	8	8	16	8	16	8	8
$F_0$ : Number of added center points per block	3	2	2	2	6	1	4	1	1
Total # of points per block	7	6	10	10	22	9	20	9	9
<i>Axial block</i>									
$2k$ : # of axial points	4	6	8	10	10	12	12	14	14
$\alpha_0$ : # of added center points	3	2	2	4	1	6	2	11	4
Total # of points in block	7	8	10	14	11	18	14	25	18

Source: G. E. P. Box and J. S. Hunter (1957).

axial block. Condition 1 holds when we assign the factorial and axial points as the two blocks. Condition 2 holds if

$$\frac{\sum_{\text{ax.bl.}} x_{iu}^2}{\sum_{\text{fac.bl.}} x_{iu}^2} = \frac{2k + a_0}{F + F_0}, \quad i = 1, 2, \dots, k \quad (7.32)$$

where, of course,  $F = 2^k$  or  $F = 2^{k-1}$  (resolution V fraction). The value for  $\alpha$  that results in orthogonal blocking is developed from Equation 7.32. From Equation 7.32 we have

$$\frac{2\alpha^2}{F} = \frac{2k + a_0}{F + F_0}$$

and the solution for  $\alpha$  is given by

$$\alpha = \sqrt{\frac{F(2k + a_0)}{2(F + F_0)}} \quad (7.33)$$

**General Recommendations for Blocking with the CCD** There are many instances in which the practitioner using RSM can achieve orthogonal blocking and still have designs that contain design parameters near those recommended in Section 7.4.3 when the region is spherical. We have already seen this to be the case with the  $k = 2$  and  $k = 3$  CCD. A value of  $\alpha = \sqrt{2}$  for the case of two blocks produces orthogonal blocking as long as center runs are evenly divided between the two blocks.

The case of the cuboidal region deserves special attention. In order to achieve orthogonal blocking for (say) a face-centered cube, one must resort to badly disproportionate

block sizes, which may often be a problem. For example, the following face-centered cube blocks orthogonally for  $k = 2$ :

$$\mathbf{D} = \begin{array}{cc} x_1 & x_2 \\ \begin{bmatrix} -1 & -1 \\ -1 & 1 \\ 1 & -1 \\ 1 & 1 \\ 0 & 0 \\ 0 & 0 \\ 0 & 0 \\ \dots\dots\dots \\ -1 & 0 \\ 1 & 0 \\ 0 & -1 \\ 0 & 1 \end{bmatrix} & \left. \begin{array}{l} \\ \\ \\ \\ \\ \\ \\ \\ \\ \\ \\ \\ \\ \\ \end{array} \right\} \text{Block 1} \\ \left. \begin{array}{l} \\ \\ \\ \\ \\ \\ \\ \\ \\ \\ \\ \\ \\ \\ \end{array} \right\} \text{Block 2} \end{array}$$

For three variables, if one requires say three blocks, the two factorial blocks require eight center runs apiece if one requires that  $\alpha = 1.0$  in a cuboidal region. As a result, when ranges for the experiment seem to suggest the need for a cuboidal design region and orthogonal blocking is required, one might need to consider a spherical design in order that blocking be better accommodated.

In the case of spherical designs, many practical designs exist. Table 7.5 shows a working table of useful second-order designs that block orthogonally. For designs in which “ $\frac{1}{2}$  rep” is indicated, the factorial portion is a one-half fraction of the  $2^k$ . In all cases with multiple blocks from the factorial portion, defining contrasts are chosen so that three-factor interactions or higher are confounded with blocks.

**Blocking with the Box–Behnken Design** The flexibility of the CCD makes it an attractive choice when blocking is required in an RSM analysis. However, there are other second-order designs that do block orthogonally. Included among these is the class of BBDs for  $k = 4$  and  $k = 5$ . Consider first the design matrix in Equation 7.16 for the  $k = 4$  BBD. Using  $\pm 1$  notation to indicate the  $2^2$  factorial structure among pairs of variables, we have

$$\mathbf{D} = \begin{array}{cccc} x_1 & x_2 & x_3 & x_4 \\ \begin{bmatrix} \pm 1 & \pm 1 & 0 & 0 \\ 0 & 0 & \pm 1 & \pm 1 \\ 0 & 0 & 0 & 0 \\ \dots\dots\dots \\ \pm 1 & 0 & 0 & \pm 1 \\ 0 & \pm 1 & \pm 1 & 0 \\ 0 & 0 & 0 & 0 \\ \dots\dots\dots \\ \pm 1 & 0 & \pm 1 & 0 \\ 0 & \pm 1 & 0 & \pm 1 \\ 0 & 0 & 0 & 0 \end{bmatrix} & \left. \begin{array}{l} \\ \\ \\ \\ \\ \\ \\ \\ \\ \\ \\ \\ \\ \end{array} \right\} \text{Block 1} \\ \left. \begin{array}{l} \\ \\ \\ \\ \\ \\ \\ \\ \\ \\ \\ \\ \\ \end{array} \right\} \text{Block 2} \\ \left. \begin{array}{l} \\ \\ \\ \\ \\ \\ \\ \\ \\ \\ \\ \\ \\ \end{array} \right\} \text{Block 3} \end{array}$$

The requirement on the vectors of center runs is that each block contain the same number of center runs. This, of course, results in equal block sizes, a requirement that results from the equal sum of squares for each factor in each block.

The  $k = 5$  BBD blocks orthogonally in two blocks. Consider the design of Equation 7.17. This design can be partitioned into two parts so that conditions for orthogonal blocking hold. Again, the center runs should be even in number, and half of them should be assigned to each block. The reader can easily verify that conditions 1 and 2 for orthogonal blocking both hold (see Exercise 7.28).

**Orthogonal Blocking with Equiradial Designs** It has already been established that the CCD for  $k = 2$  and  $\alpha = \sqrt{2}$  involves eight points equally spaced on a circle—that is, an octagon. Much has already been said about orthogonal blocking with this design. The use of an even value for  $n_c$  and  $n_c/2$  in the factorial block and  $n_c/2$  assigned to the axial block results in a very efficient design for  $k = 2$  that blocks orthogonality. But other equiradial designs block orthogonally too. For example, consider the hexagon. Figure 7.20 shows the hexagonal design. The hexagon is a combination of two equilateral triangles. For example, in the figure, points 1, 3, and 5 form one equilateral triangle and points 2, 4, and 6 form another. The reader should recall that an equilateral triangle is a simplex design that is first-order orthogonal; thus if one assigns points 1, 3, and 5 to one block and points 2, 4, and 6 to a second block, condition 1 for orthogonal blocking will hold. For condition 2 recall the design matrix of the simplex from Equation 7.21. The order of the points are in the matrix are 1 through 6. Note

$$\sum_{\text{block 1}} x_{ui}^2 = \sum_{\text{block 2}} x_{ui}^2 = 1.5, \quad i = 1, 2$$

and thus the assignment of points 1, 3, and 5 to block 1 and 2, 4, and 6 to block 2 with  $n_c$  even and  $n_c/2$  assigned to each block will result in a design that blocks orthogonally in two blocks.

The nonagon (nine equally spaced points on a circle) blocks orthogonally in three blocks. The nonagon combines *three* equilateral triangles, and thus  $n_c > 3$ ,  $n_c$  is divisible by three, and  $n_c/3$  assigned to each block gives a design that blocks orthogonally. Actually, there are other equiradial designs that block orthogonally, but the plans described here are the more practical ones.

**Form of Analysis with a Blocked Experiment** The first and foremost topic of discussion in this area should be the model. It is important to understand that we are assuming that blocks enter the model as additive effects. This was outlined in the model form in Equation 7.27. It is assumed that there is no interaction between blocks and other model terms. This concept should be thoroughly discussed among the practitioners involved. If it is clear that blocks interact with the factors, then it means that the analysis should involve the fitting of a separate response surface for each block. This often results in difficulty regarding interpretation of results. Another important issue centers around what is truly meant by orthogonal blocking. As we indicated earlier, orthogonal means that block effects are orthogonal to model coefficients. However, the final fitted model will obviously include estimates of block effects. The fitted model is not at all unlike an analysis of covariance (ANCOVA) model where blocks play the role of treatments and one is assuming that for each block the model coefficients are the same (quite like assuming equal slopes

in ANCOVA). But, of course, the presence of block effects implies that we have multiple intercepts, one for each block. Thus, for, say, three blocks we have

$$\hat{y}_{\text{block } 1} = \hat{\beta}_{0,1} + f(\mathbf{x})$$

$$\hat{y}_{\text{block } 2} = \hat{\beta}_{0,2} + f(\mathbf{x})$$

$$\hat{y}_{\text{block } 3} = \hat{\beta}_{0,3} + f(\mathbf{x})$$

where  $f(\mathbf{x})$  is a second-order function containing linear quadratic, and interaction terms, all of which are the same for each block. Now, the coefficients (apart from the intercepts) can be computed as if there were no blocking. As a result, the stationary point, canonical analysis, and ridge analysis path are computed by ignoring blocking, because none of these computations involves the intercepts. Then for the purpose of computing the predicted response, separate intercepts are merely found from the overall intercept and block effects. One must understand that the essence of the RSM analysis is intended to be a description of the system *in spite of* blocking; and blocks are assumed to have no effect on the nature and shape of the response surface. The following example should be beneficial.

**Example 7.6 The Analysis of a Blocked CCD** In a chemical process it is important to fit a response surface and find conditions on time ( $x_1$ ) and temperature ( $x_2$ ) that give a high yield. It is important that a yield of at least 80% be achieved. A list of natural and coded variables appears in Table 7.6. The design requires 14 experimental runs. However, two batches of raw materials must be used, so seven experimental runs were made for each batch. The experiment was run in two blocks, and the order of the runs was randomized in each block. The factorial runs plus three center runs were made in one block (batch), and the axial runs plus three center runs were made in the second block (batch). The resulting design does block orthogonally.

**TABLE 7.6 Natural and Design Levels for Chemical Reaction Experiment**

Natural Variables		Design Units		Block	Yield Response
Time	Temperature	$x_1$	$x_2$		
80	170	-1	-1	1	80.5
80	180	-1	1	1	81.5
90	170	1	-1	1	82.0
90	180	1	1	1	83.5
85	175	0	0	1	83.9
85	175	0	0	1	84.3
85	175	0	0	1	84.0
85	175	0	0	2	79.7
85	175	0	0	2	79.8
85	175	0	0	2	79.5
92.070	175	1.414	0	2	78.4
77.930	175	-1.414	0	2	75.6
85	182.07	0	1.414	2	78.5
85	167.93	0	-1.414	2	77.0

**TABLE 7.7 Design-Expert Analysis of the Blocked CCD in Example 7.6 Using Design-Expert**

Response	Yield									
***WARNING: The Cubic Model is Aliased!***										
<i>Sequential Model Sum of Squares</i>										
Source	Sum of Squares	DF	Mean Square	F-Value	Prob > F					
Mean	90916.80	1	90916.80							
Block	69.53	1	69.53							
Linear	9.63	2	4.81	2.67	0.1179					
2FI	0.063	1	0.063	0.031	0.8635					
Quadratic	17.79	2	8.90	334.32	<0.0001					
Cubic	0.044	2	0.022	0.78	0.5067					
Residual	0.14	5	0.028							
Total	91014.00	14	6501.00							
<i>Lack of Fit Tests</i>										
Linear	17.91	6	2.98	89.53	0.0003					
2FI	17.84	5	3.57	107.07	0.0002					
Quadratic	0.053	3	0.018	0.53	0.6859					
Cubic	8.571E-003	1	8.571E-003	0.26	0.6388					
Pure Error	0.13	2	0.033							
<i>Model Summary Statistics</i>										
Source	Std. Dev.	R-Squared	Adjusted R-Squared	Predicted R-Squared	PRESS					
Linear	1.34	0.3479	0.2175	-0.2812	35.44					
2FI	1.41	0.3502	0.1336	-0.9332	53.48					
Quadratic	0.16	0.9933	0.9885	0.9726	0.76					
Cubic	0.17	0.9949	0.9877	0.9451	1.52					

**Table 7.7** *Continued*

Response Yield  
ANOVA for Response Surface Quadratic Model

*Analysis of Variance Table [Partial sum of squares]*

Source	Sum of Squares	DF	Mean Square	F-Value	Prob > F
Block	69.53	1	69.53		
Model	27.48	5	5.50	206.55	<0.0001
A	6.96	1	6.96	261.43	<0.001
B	2.67	1	2.67	100.33	<0.0001
A <sup>2</sup>	12.64	1	12.64	475.06	<0.0001
B <sup>2</sup>	6.43	1	6.43	241.76	<0.0001
AB	0.063	1	0.063	2.35	0.1692
Residual	0.19	7	0.027		
Lack of Fit	0.053	3	0.018	0.53	0.6859
Pure Error	0.13	4	0.033		
Cor total	97.20	13			
Std. Dev.	0.16			R-Squared	0.9933
Mean	80.59			Adj R-Squared	0.9885
C.V.	0.20			Pred R-Squared	0.9726
PRESS	0.76			Adeq Precision	72.761

Factor	Coefficient Estimate	DF	Standard Error	95% CI		
				Low	High	VIF
Intercept	81.87	1	0.067	81.71	82.02	
Block 1	2.23	1				
Block 2	-2.23					
A-Temp	0.93	1	0.058	0.80	1.07	1.00

B-Temp	0.58	1	0.058	0.44	0.71	1.00
$A^2$	-1.31	1	0.060	-1.45	-1.17	1.01
$B^2$	-0.93	1	0.060	-1.08	-0.79	1.01
$AB$	0.13	1	0.082	-0.068	0.32	1.00

Final Equation in Terms of Coded Factors:

---

$$\begin{aligned} \text{Yield} &= \\ +81.87 & \\ +0.93 & *A \\ +0.58 & *B \\ -1.31 & *A^2 \\ -0.93 & *B^2 \\ +0.13 & *A*B \end{aligned}$$

Final Equation in Terms of Actual Factors:

---

$$\begin{aligned} \text{Yield} &= \\ -1401.27035 & \\ +8.20816 & *Time \\ +12.75720 & *Temp \\ -0.052333 & *Time^2 \\ -0.037333 & *Temp^2 \\ +5.00000E-003 & *Time*Temp \end{aligned}$$


---

“Sequential Model Sum of Squares”: Select the highest order polynomial where the additional terms are significant.

“Lack of Fit Test”: Want the selected model to have insignificant lack-of-fit.

“Model Summary Statistics”: Focus on the model maximizing the “Adjusted R-Squared” and the “Predicted R-Squared.”

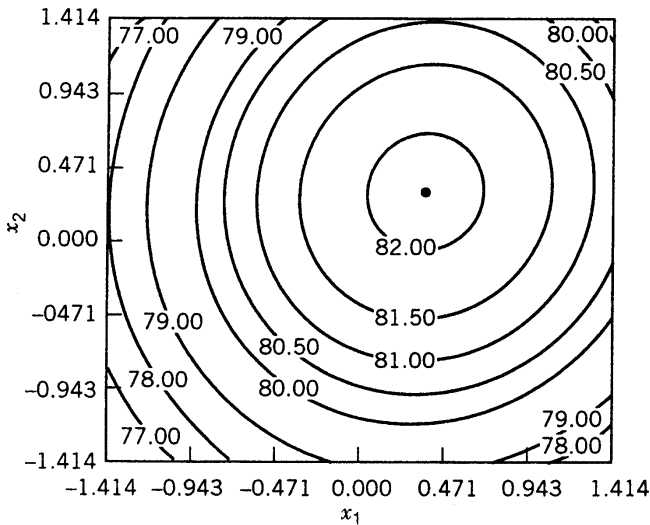


**Figure 7.21** Contour plot of yield for Example 7.6.

A second-order analysis was performed. Table 7.7 shows the analysis produced by Design-Expert, and Fig. 7.21 is a contour plot in the coded units. The stationary point is a maximum. The fitted model is

$$\hat{y} = 81.87 + 0.93x_1 + 0.58x_2 - 1.31x_1^2 - 0.93x_2^2 + 0.13x_1x_2$$

Note that the *P*-values indicate that one model term ( $x_1x_2$ ) is insignificant. The data were analyzed *as if no blocking had been done*. This renders coefficients (and canonical analysis, if one is performed) correct, but standard errors are inflated because of variability due to blocks. The appropriate location of the maximum response is given by

$$x_{1,s} = 0.372$$

$$x_{2,s} = 0.335$$

in our design units. The predicted value at the stationary point is 82.136.

Further examination of the Design-Expert output can determine the block effects. Note that while the overall intercept is 81.87, the estimates of block effects are 2.23 and  $-2.23$  for block 1 and block 2, respectively. As a result, the two separate intercepts are  $81.867 \pm 2.23 = 84.097$  and  $79.637$ , respectively.

## EXERCISES

- 7.1** Consider the design of an experiment to fit the first-order response model

$$y = \beta_0 + \beta_1x_1 + \beta_2x_2 + \beta_3x_3 + \beta_4x_4 + \beta_5x_5 + \varepsilon$$

The design used is a  $2^{5-2}$  fractional factorial with defining relations

$$\begin{aligned} I &= ABC = x_1x_2x_3 \\ I &= CDE = x_3x_4x_5 \end{aligned}$$

The factors are quantitative, and thus we use the notation  $x_1, x_2, x_3, \dots$  rather than  $A, B, C, \dots$

- (a) Construct the matrix  $\mathbf{X}$  for the first-order model using the design described above.
  - (b) Is the design orthogonal? Explain why or why not.
  - (c) Is the design a variance-optimal design—that is, one that results in minimum values of  $N \text{Var}(b_i)/\sigma^2$ . Note that the weight  $N$  is used in order to take sample size into account.
- 7.2 Consider the situation of Exercise 7.1. Suppose we use four center runs to augment the  $2^{5-2}$  design constructed.
- (a) What is the advantage of using the center runs?
  - (b) Will the resulting 12-run design be orthogonal? Explain.
  - (c) Will the resulting design be variance-optimal?
  - (d) If your answer to (c) is no, give a 12-run first-order design with values of  $\text{Var}(b_i)/\sigma^2$  smaller than the 12-run design with center runs.
  - (e) Give the variances of regression coefficients for both designs—that is, the  $2_{III}^{5-2}$  with four center runs and your design in (d).
- 7.3 Consider again the design constructed in Exercise 7.1. Suppose the fitted model is first-order and the analysis reveals significant lack of fit and a large effect for the interaction  $x_1x_4 = x_2x_5$ . As a result, a second phase would suggest an augmentation of the design. Suppose the second phase is a fold-over of the design in Exercise 7.1. Is the resulting design orthogonal and thus variance-optimal for the model

$$y_u = \beta_0 + \sum_{i=1}^5 \beta_i x_{ui} + \sum \sum_{i < j=2}^5 \beta_{ij} x_{ui} x_{uj} + \varepsilon_u,$$

$$u = 1, 2, 3, \dots, 16$$

Explain why or why not.

- 7.4 Consider the  $L_{27}$  design (in coded form) discussed in Exercise 6.12. Suppose we consider this design for fitting the first-order model

$$y_u = \beta_0 + \sum_{i=1}^3 \beta_i x_{ui} + \varepsilon_u, \quad u = 1, 2, \dots, 27$$

- (a) Is the design first-order orthogonal? Explain.
- (b) Is the design variance-optimal? Explain.
- (c) Compare the  $N \text{Var}(b_i)/\sigma^2$  using the  $L_{27}$  with a  $2^3$ . Compare with a Plackett–Burman 12-run design. Compare with a Plackett–Burman 28-run design.

- (d) Your answer to (c) above should be that the Plackett–Burman 12-run design and  $2^3$  design for a first-order model are *variance-equivalent on a per observation basis*. What are extra advantages enjoyed by the  $2^3$  over the Plackett–Burman 12-run design?
- 7.5 Consider a situation involving seven design variables when, in fact, a first-order model is required but only eight runs can be used. Design a saturated eight-run design that is variance-optimal.
- 7.6 Consider a situation in which five factors are to be studied and a first-order model is postulated though it is not quite clear that this is the correct model. Sixteen design runs are to be used. The designs to be considered are as follows:
- $2_{\text{III}}^{5-2}$  replicated
  - $2_{\text{V}}^{5-1}$
  - A Plackett–Burman 12-run design augmented with four center runs.

Discuss the advantages and disadvantages of the three designs. Use the terms *variance-optimal* and *model misspecification* in your discussion.

- 7.7 Consider the “model inadequacy” material in Section 7.2. The material can be used to nicely illustrate the aliasing ideas discussed in Chapter 4. Aliasing plays an important role when one deals with fractional factorials for fitting first-order and first-order-plus-interaction response surface models. Suppose one fits a first-order model using a  $2_{\text{III}}^{3-1}$  with defining relation

$$I = x_1 x_2 x_3$$

However, suppose the true model is

$$E(y) = \beta_0 + \beta_1 x_1 + \beta_2 x_2 + \beta_3 x_3 + \beta_{12} x_1 x_2 + \beta_{13} x_1 x_3 + \beta_{23} x_2 x_3$$

Using Equation 7.2, we obtain

$$\mathbf{X}_1 = \begin{bmatrix} x_1 & x_2 & x_3 \\ 1 & -1 & 1 & 1 \\ 1 & 1 & -1 & 1 \\ 1 & 1 & 1 & -1 \\ 1 & -1 & -1 & 1 \end{bmatrix} \quad \mathbf{X}_2 = \begin{bmatrix} x_1 x_2 & x_1 x_3 & x_2 x_3 \\ -1 & -1 & 1 \\ -1 & 1 & -1 \\ 1 & -1 & -1 \\ 1 & 1 & 1 \end{bmatrix}$$

$$\boldsymbol{\beta}_1 = \begin{bmatrix} \beta_0 \\ \beta_1 \\ \beta_2 \\ \beta_3 \end{bmatrix} \quad \boldsymbol{\beta}_2 = \begin{bmatrix} \beta_{12} \\ \beta_{13} \\ \beta_{23} \end{bmatrix}$$

Use the expression

$$\begin{aligned} E(\mathbf{b}_1) &= \boldsymbol{\beta}_1 + (\mathbf{X}'_1 \mathbf{X})^{-1} \mathbf{X}'_1 \mathbf{X}_2 \mathbf{y} \\ &= \boldsymbol{\beta}_1 + \mathbf{A} \mathbf{y} \end{aligned}$$

to verify the following expected values:

$$\begin{aligned} E(b_0) &= \beta_0 \\ E(b_1) &= \beta_1 - \beta_{23} \\ E(b_2) &= \beta_2 - \beta_{13} \\ E(b_3) &= \beta_3 - \beta_{12} \end{aligned}$$

- 7.8** In Exercise 7.7, if the true model is given by

$$E(y) = \beta_0 + \beta_1 x_1 + \beta_2 x_2 + \beta_3 x_3 + \beta_{12} x_1 x_2 + \beta_{13} x_1 x_3 + \beta_{23} x_2 x_3 + \beta_{123} x_1 x_2 x_3$$

show that the expected values are given by

$$\begin{aligned} E(b_0) &= \beta_0 - \beta_{123} \\ E(b_1), E(b_2), E(b_3) &\text{ as in Exercise 7.7} \end{aligned}$$

Exercises 7.7 and 7.8 illustrate the effect of aliasing in the sense of a regression model. Thus, in the case of these two exercises, the aliasing of  $x_1$  with  $x_2 x_3$  implies that the coefficient  $b_1$  is not an unbiased estimator of  $\beta_1$  but is biased by  $\beta_{23}$ , the coefficient of  $x_2 x_3$ . Indeed, the coefficient of the interaction described by the defining contrast, namely  $\beta_{123}$ , biases the estimated intercept  $\beta_0$ .

- 7.9** Consider the same situation as in Exercise 7.7. However, the *other fraction* given by  $I = x_1 x_2 x_3$  is used. If the fitted first-order model is incorrect and the true model is as stated in Exercise 7.8, show that the biases in the coefficients are indicated by

$$\begin{aligned} E(b_0) &= \beta_0 + \beta_{123} \\ E(b_1) &= \beta_1 + \beta_{23} \\ E(b_2) &= \beta_2 + \beta_{13} \\ E(b_3) &= \beta_3 + \beta_{12} \end{aligned}$$

- 7.10** Consider a  $2^{5-2}$  fractional factorial with defining relations

$$\begin{aligned} I &= x_1 x_2 x_3 \\ I &= x_3 x_4 x_5 \end{aligned}$$

Suppose a first-order model is fitted to the data and the true model includes, additionally, all two-factor interactions. Use the expression

$$E(\mathbf{b}_1) = \boldsymbol{\beta}_1 + \mathbf{A} \boldsymbol{\beta}_2$$

to develop,  $E(b_1)$ ,  $E(b_2)$ ,  $E(b_3)$ ,  $E(b_4)$ , and  $E(b_5)$  where the fitted first-order model is

$$\hat{y} = b_0 + b_1x_1 + b_2x_2 + b_3x_3 + b_4x_4 + b_5x_5$$

- 7.11** Consider Example 4.2 in Chapter 4. The strong effects are those for the factors  $A$ ,  $B$ ,  $C$ , and  $AB$ , and the fitted regression is given by

$$\hat{y} = 60.65625 + 11.60625x_1 + 34.03125x_2 + 10.45625x_3 + 6.58125x_1x_2$$

- (a) Verify the above coefficients by considering this five-parameter model in the form

$$\mathbf{y} = \mathbf{X}\boldsymbol{\beta} + \boldsymbol{\epsilon}$$

and by using

$$\mathbf{b} = (\mathbf{X}'\mathbf{X})^{-1}\mathbf{X}'\mathbf{y}$$

- (b) Is the design in Table 4.5 orthogonal for the model that was fitted? If so, verify it. Is the design variance-optimal?  
 (c) Is the design orthogonal for a model containing  $x_1$ ,  $x_2$ ,  $x_3$ ,  $x_4$ ,  $x_5$ ,  $x_1x_2$ ,  $x_1x_3$ ,  $x_1x_4$ ,  $x_1x_5$ ,  $x_2x_3$ ,  $x_2x_4$ ,  $x_2x_5$ ,  $x_3x_4$ ,  $x_3x_5$ , and  $x_4x_5$ ?  
**7.12** Consider the design listed in Table 4.9 with the injection molding data. Answer the following questions.

- (a) For the model that is fitted, namely

$$\hat{y} = b_0 + b_1x_1 + b_2x_2 + b_{12}x_{12}$$

give the variance of each coefficient, assuming common error variance  $\sigma^2$ .

- (b) Using the error mean square from Table 4.10, give the estimated standard errors of all four coefficients.  
 (c) In light of the plot in Figure 4.14, why are the results in (b) somewhat precarious?  
 (d) Is this design orthogonal for a model containing all linear terms and the two-factor interactions  $x_1x_2$ ,  $x_1x_3$ ,  $x_1x_4$ ,  $x_1x_5$ , and  $x_1x_6$ ? If so, justify it; if not, explain why not.  
**7.13** In Section 4.5 of Chapter 4 the  $2^{7-4}_{III}$  design is discussed. Here we may be interested in building a regression model for studying seven factors. The design is given in Table 4.13. Suppose one fits a first-order model but, in fact, all two factor interactions are in the true model. Write out  $E(b_1)$ ,  $E(b_2)$ ,  $E(b_3)$ ,  $E(b_4)$ ,  $E(b_5)$ ,  $E(b_6)$ , and  $E(b_7)$ . Explain all your terms.

- 7.14** Consider Exercise 4.7 in Chapter 4.
- Is the design first-order orthogonal?
  - From your answer in Exercise 4.7b, write a response surface model.
  - Give estimated standard errors of all coefficients.
  - From your model in Exercise 7.14b estimate the standard error of prediction at all design locations.
  - Compute the estimated standard error of prediction at the design center.
- 7.15** Consider Exercise 4.8 in which four center runs were added to the design in Exercise 4.7. Answer the questions asked in Exercise 7.14d and 7.14e again. Use the replication error variability (3 df) in computing your mean square error.
- 7.16** (a) Consider Exercise 4.11 in Chapter 4. For the data in Exercise 4.11a develop a first-order regression model. Estimate the standard error of prediction at each design point.  
 (b) Do all the work in (a) again after the second fraction in Exercise 4.11b is added. Comment on what was gained with the addition of the second fraction.
- 7.17** Suppose we are interested in fitting a response surface model in five design variables. The analyst is quite sure that the form of the model should be

$$\begin{aligned}y_i = & \beta_0 + \beta_1 x_{i1} + \beta_2 x_{i2} + \beta_3 x_{i3} + \beta_4 x_{i4} + \beta_5 x_{i5} \\& + \beta_{12} x_{i1} x_{i2} + \beta_{13} x_{i1} x_{i3} + \varepsilon_i\end{aligned}$$

The analyst can use 12 experimental runs in the design. Discuss and compare the following candidate designs. Use the variances of individual coefficients in your discussion. However, do not let your discussion be confined to this criterion. The candidate designs are as follows:

$$\begin{aligned}\mathbf{D}_1: & 2^{5-2}_{III} \text{ with four center runs} \\ \mathbf{D}_2: & \text{Plackett–Burman with 12 runs}\end{aligned}$$

- 7.18** Equation 7.11 is a very important expression. It gives the scaled prediction variance for a first-order orthogonal design in which all design points are at the  $\pm 1$  extremes. It also implies that this class of designs give equal prediction variance at any two locations that are on the same sphere. This implies that this class of designs is rotatable. Does the same property hold for orthogonal designs used to accommodate a model containing interaction? Illustrate with a  $2^2$  factorial and the model

$$y_i = \beta_0 + \beta_1 x_{i1} + \beta_2 x_{i2} + \beta_{12} x_{i1} x_{i2}$$

Compute  $N \text{Var}[\hat{y}(\mathbf{x})]/\sigma^2$  at the following locations on the same sphere:

- 1, 1
- 1, 1

- (iii)  $1, -1$
- (iv)  $1, 1$
- (v)  $\sqrt{2}, 0$
- (vi)  $-\sqrt{2}, 0$
- (vii)  $0, -\sqrt{2}$
- (viii)  $0, \sqrt{2}$

Comment on your results.

- 7.19** A first-order orthogonal design with all points at  $\pm 1$  extremes remains rotatable for a first-order model if all points are replicated the same number of times. True or false? Justify your answer.
- 7.20** A second-order rotatable design with  $\alpha = \sqrt[4]{F}$  remains rotatable for the second-order model if all factorial and axial runs are replicated the same number of times. True or false? Justify your answer.
- 7.21** Consider the model in Exercise 7.17 along with designs  $\mathbf{D}_1$  and  $\mathbf{D}_2$ . Which design is superior using the scaled prediction variance criterion? Use as illustrations the following locations:

$$\begin{aligned} & (1, 1, 1, 1, 1) \\ & (-1, -1, -1, -1, -1) \\ & (1, 1, -1, -1, -1) \\ & (1, -1, -1, 1, 1) \\ & (1, -1, -1, -1, -1) \\ & (-1, 1, 1, 1, 1) \end{aligned}$$

- 7.22** Consider a central composite design with  $\alpha = \sqrt{F}$ . Use the result in Equation 7.14 to show that the number of center runs has no effect on the rotatability property.
- 7.23** Consider a situation in which there are two design variables and one is interested in fitting a second-order model. A curious and interesting comparison surfaces when one considers the central composite design (octagon) and a design with points placed at the vertices of a hexagon. Both are equiradial designs. The beauty of the hexagon (plus center runs)—or even the pentagon (plus center runs)—lies in its high relative efficiency in spite of its small design size. One should always choose the octagon unless it is too costly. However, it is interesting to compare the two *on a per observation basis*. Consider a comparison between a hexagon and a rotatable CCD. To make a valid comparison, one should scale the designs so they are comparable, that is, reside on the same radius (keep in mind that scaling is really arbitrary). The factorial points on the CCD are at radius  $\sqrt{2}$ . As scaled in Equation 7.21, the hexagon lies on a circle of radius 1. As a result, for proper comparison the hexagon

should be multiplied by  $\sqrt{2}$ . Thus we have

$$\mathbf{D}_1 = \begin{bmatrix} x_1 & x_2 \\ \hline \sqrt{2} & 0 \\ \sqrt{2}/2 & \sqrt{3}/2 \\ -\sqrt{2}/2 & \sqrt{3}/2 \\ -\sqrt{2} & 0 \\ -\sqrt{2}/2 & -\sqrt{3}/2 \\ \sqrt{2}/2 & -\sqrt{3}/2 \\ 0 & 0 \\ 0 & 0 \\ 0 & 0 \end{bmatrix} \quad (\text{hexagon})$$

and, of course,

$$\mathbf{D}_1 = \begin{bmatrix} x_1 & x_2 \\ \hline -1 & -1 \\ -1 & 1 \\ 1 & -1 \\ 1 & 1 \\ -\sqrt{2} & 0 \\ \sqrt{2} & 0 \\ 0 & -\sqrt{2} \\ 0 & \sqrt{2} \\ 0 & 0 \\ 0 & 0 \\ 0 & 0 \end{bmatrix} \quad (\text{CCD})$$

Use  $\mathbf{D}_1$  and  $\mathbf{D}_2$  to construct scaled prediction variances. Both designs are rotatable, so a rather complete comparison can be made by filling in the following table:

$\rho$	$N \text{Var}[\hat{y}(\mathbf{x})]/\sigma^2$ for $\mathbf{D}_1$	$N \text{Var}[\hat{y}(\mathbf{x})]/\sigma^2$ for $\mathbf{D}_2$
0		
0.5		
1.0		
1.5		
$\sqrt{3}$		

Comment on your study.

- 7.24 It is stated in Section 7.4.10 that for second-order models, orthogonal blocking is much more easily accommodated with the use of the spherical CCD than with use of the face-centered cube (cuboidal CCD). However, orthogonal blocking is accommodated with the face-centered cube when *axial points are replicated*. Show that the following design blocks orthogonally in two blocks:

$$\mathbf{D}_1 = \left[ \begin{array}{cc} x_1 & x_2 \\ -1 & -1 \\ -1 & 1 \\ 1 & -1 \\ 1 & 1 \\ 0 & 0 \\ 0 & 0 \\ 0 & 0 \\ 0 & 0 \\ \dots & \dots \\ -1 & 0 \\ -1 & 0 \\ 1 & 0 \\ 1 & 0 \\ 0 & -1 \\ 0 & -1 \\ 0 & 1 \\ 0 & 1 \end{array} \right] \quad \left. \right\} \text{Block 1}$$

- 7.25** Consider Table 7.5. The designs suggested in the table are those that block orthogonally and are rotatable or near-rotatable. For example, consider the design under the column headed  $k = 5(\frac{1}{2}\text{rep})$ . Construct the design completely, and verify that it meets both conditions for orthogonal blocking.

**7.26** Answer the same question as in Exercise 7.24, but use the  $k = 5$  line with four blocks from the factorial portion and one block from the axial portion.

**7.27** The designs given in Table 7.5 are not the only ones that block orthogonally and are practical. The values for  $\alpha$  and  $n_c$  can be altered in a very flexible manner. Suppose,

for example, that for  $k = 4$  the run size does not allow a design that is shown in the table. Rather, we must use

$$\mathbf{D} = \begin{bmatrix} x_1 & x_2 & x_3 & x_4 \\ -1 & -1 & -1 & -1 \\ 1 & 1 & -1 & -1 \\ 1 & -1 & 1 & -1 \\ 1 & -1 & -1 & 1 \\ -1 & 1 & 1 & -1 \\ -1 & 1 & -1 & 1 \\ -1 & -1 & 1 & 1 \\ 1 & 1 & 1 & 1 \\ 0 & 0 & 0 & 0 \\ \dots & & & \\ 1 & -1 & -1 & -1 \\ -1 & 1 & -1 & -1 \\ -1 & -1 & 1 & -1 \\ -1 & -1 & -1 & 1 \\ 1 & 1 & 1 & -1 \\ 1 & 1 & -1 & 1 \\ 1 & -1 & 1 & 1 \\ -1 & 1 & 1 & 1 \\ 0 & 0 & 0 & 0 \\ \dots & & & \\ -\alpha & 0 & 0 & 0 \\ \alpha & 0 & 0 & 0 \\ 0 & -\alpha & 0 & 0 \\ 0 & \alpha & 0 & 0 \\ 0 & 0 & -\alpha & 0 \\ 0 & 0 & \alpha & 0 \\ 0 & 0 & 0 & -\alpha \\ 0 & 0 & 0 & \alpha \end{bmatrix}$$

This design can be made to block orthogonally. What value of  $\alpha$  results in orthogonal blocking?

- 7.28** Construct a Box–Behnken design in five variables that blocks orthogonally for a second-order model. Show the assignment of design points to blocks.
- 7.29** Compare a  $2^{6-3}$  fractional factorial design ( $I = ABD = ACE = BCF$ ) with four center runs (total of 12 runs), or a Plackett–Burman design with 12 runs for estimating the model

$$y = \beta_0 + \beta_1 A + \beta_2 B + \beta_3 C + \beta_4 D + \beta_5 E + \beta_6 F + \beta_{12} AB$$

Which is better for

- (a) estimating effects independently?
- (b) smallest variance for coefficient estimates?
- (c) testing lack of fit?
- (d) testing curvature?
- (e) estimating pure error?

Based on (a)–(e), which design do you prefer? Explain.

- 7.30** We are interested in studying the main effects ( $A, B, C, D, E$ ) and some two-way interactions ( $AB, AC$ ) for five factors by running a half fraction of a fractional factorial. We also have the restriction that we can only have eight observations per block.
- (a) Suggest a suitable design that will allow all effects to be estimated independently of each other. Give the defining equation, as well as what effect would be aliased with the block.
  - (b) List the combinations of  $A, B, C, D, E$  would be run in each of the blocks.
  - (c) If we assume a model with terms for  $A, B, C, D, E, AB, AC$ , and *Block*, what would the ANOVA table for this design look like? (Source, d.f.)
  - (d) Give the equation (using combinations of  $A, B, C, D, E$ ) for how you would calculate the effect for the  $AB$  interaction.
  - (e) If the true model had terms  $A, B, C, D, E, AB, AC$ , and *Block* as well as  $BC$  and  $CD$ , would your model be adequate to estimate all of the effects? Explain.
- 7.31** For a full  $2^3$  factorial with two center runs, we assume a first-order model with all two-way interactions is the correct model. If the correct model is actually, the first-order model with two-way interactions and a quadratic effect for factor  $A$ , find which estimates are unbiased?
- 7.32** For the following designs and specified models, give the appropriate design matrix, and show whether or not they are rotatable (work with design moments where convenient).
- (a) Plackett–Burman design (12 runs) for a first-order model for effects  $A, B, C, D, E$
  - (b) Factorial design for a first-order model with interactions for effects  $A, B, C$
  - (c) CCD design with half-fraction for the factorial portion,  $\alpha = 2$  and  $n_c = 3$  for a second-order model for effects  $A, B, C, D, E$
  - (d) BBD design with  $n_c = 3$  for a second-order model for effects  $A, B, C, D, E$

- (e) An equiradial design with seven points for a second-order model for effects  $A$  and  $B$ .
- 7.33** Assume a second-order model with three factors ( $A, B, C$ ) is the model of interest. For the following designs, calculate the scaled predicted variance,  $\text{SPV} = (N\text{Var}[\hat{y}(\mathbf{x})]/\sigma^2)$  along the lines  $(a, 0, 0)$ ,  $(a, a, 0)$ ,  $(a, -a, 0)$ ,  $(a, a, a)$ , and  $(a, -a, a)$  for different values of  $a$ . Select an appropriate range to consider and plot the results on a graph of distance from center versus SPV. Comment on your results, referring to rotatability and desirability of the design.
- (a) CCD with  $\alpha = 1, n_c = 2$
  - (b) CCD with  $\alpha = 1, n_c = 4$
  - (c) BBD with  $n_c = 2$
  - (d) BBD with  $n_c = 4$
- 7.34** For a  $2^{4-1}$  fractional factorial design with defining equation  $I = ABCD$  and assumed first order model with interactions  $AB$ ,  $AC$ , and  $BC$ :
- (a) What is the “alias matrix” if a better model for the relationship between factors and response has all of the above terms as well as the interactions  $AD$  and  $ABC$ ? What coefficient estimates will not be unbiased?
  - (b) Now assume that the run order of the experiment was as follows:

$$ab, cd, ad, ac, (1), abcd, bc, bd.$$

If (unknown to the experimenter) conditions changed after the first four runs (treat this as two “self-imposed” blocks), what will the “alias matrix” look like (assume the initial model is otherwise correct)? What coefficient estimates will be unbiased?

- 7.35** An experimenter wants to run a screening experiment with six factors of interest and 16 runs. She *thinks* a first-order model is adequate for any effects that are present. Consider the following four designs:
- D<sub>1</sub>**: A  $2_{\text{IV}}^{6-2}$  fractional factorial.
  - D<sub>2</sub>**: A  $2_{\text{III}}^{6-3}$  fractional factorial two reps at each location.
  - D<sub>3</sub>**: A Plackett–Burman design with  $n = 12$  and four center runs.
  - D<sub>4</sub>**: A Plackett–Burman design with  $n = 12$  and four reps chosen at random locations.

Which is better for

- (a) estimating effects independently?
- (b) smallest variance for coefficient estimates?
- (c) testing lack of fit?
- (d) testing curvature?
- (e) estimating pure error?

Based on (a)–(e), which design do you prefer? Explain.

- 7.36** For an experiment with four factors ( $A, B, C, D$ ) in a spherical region, a CCD with  $\alpha = 2$  and  $n_c = 3$  is selected. It is assumed that a second-order model is adequate. Find the “alias matrix” if a better model for the relationship between factors and response includes the cubic terms  $A^3, B^3, C^3, D^3$ . Which terms in the second-order model will be unbiased?
- 7.37** For an experiment with four factors ( $A, B, C, D$ ) in a spherical region, a CCD with  $\alpha = 2$  and  $n_c = 3$  is selected. It is assumed that a second-order model is adequate. Find the “alias matrix” if a better model for the relationship between factors and response includes the third-order terms  $ABC, ABD, ACD, BCD$ . Which terms in the second-order model will be unbiased?
- 7.38** An experiment involving three factors in a spherical region can be run in blocks as large as eight runs. Three competing designs with orthogonal blocking are being considered:
- D<sub>1</sub>**: A three block design given in Table 7.5 with two factorial blocks of size 6 and the axial block of size 8.
- D<sub>2</sub>**: A three block design with two factorial blocks and an axial block, all of size 8.
- D<sub>3</sub>**: A two block design with one factorial block (of size 8) and an axial block of size 8.
- (a) For design **D<sub>2</sub>**, find the axial distance that makes the blocks orthogonal.
  - (b) For design **D<sub>3</sub>**, find the axial distance that makes the blocks orthogonal.
  - (c) Based on a comparison of estimation of pure error, location of the axial runs, and overall size of the designs, rank the different designs.
  - (d) Which design would you recommend for the experiment?
- 7.39** An experiment involving four factors in a spherical region can be run in blocks as large as 12 runs. Three competing designs with orthogonal blocking are being considered:
- D<sub>1</sub>**: A three block design given in Table 7.5 with two factorial blocks of size 10 and the axial block of size 10.
- D<sub>2</sub>**: A three block design with two factorial blocks and an axial block, all of size 12.
- D<sub>3</sub>**: A three block design with two factorial blocks of size 12 and an axial block of size 10.
- (a) For design **D<sub>2</sub>**, find the axial distance that makes the blocks orthogonal.
  - (b) For design **D<sub>3</sub>**, find the axial distance that makes the blocks orthogonal.
  - (c) Based on a comparison of estimation of pure error, location of the axial runs, and overall size of the designs, rank the different designs.
  - (d) Which design would you recommend for the experiment?

---

# 8

---

## EXPERIMENTAL DESIGNS FOR FITTING RESPONSE SURFACES—II

In Chapter 7 we dealt with standard second-order response surface designs. The central composite designs (CCDs) and Box-Behnken designs (BBDs) are extremely popular with practitioners, and some of the equiradial designs enjoy usage for the special case of two design variables. The popularity of these standard designs is linked to the list of 10 important properties of response surface designs presented in Section 7.1. The CCD and BBD rate quite well for the 10 properties listed, particularly when they are augmented with center runs as recommended. One of the most important features associated with these two designs deals with run size. The run size is large enough to provide a comfortable margin for lack of fit, but not so large as to involve wasted degrees of freedom or unnecessary experimental expense.

Despite the importance of the CCD and the BBD, there are instances in which the researcher cannot afford the required number of runs. As a result, there is certainly a need for design classes that are either **saturated** or **near-saturated**, in other words, second-order designs that contain close to (but not less than)  $p$  design points where

$$p = 1 + 2k + \frac{k(k - 1)}{2} \quad (8.1)$$

Note that  $p$  is the number of terms in the second-order model with 1 intercept,  $k$  first-order,  $k$  pure quadratic, and  $k(k - 1)/2$  interaction terms. There are several design classes that allow saturated or near-saturated second-order designs. These are designs that should not be used

unless cost prohibits the use of one of the standard designs. In a later section we will make some comparisons that will shed light on this point. In the section that follows we will introduce a few of these design classes and make reference to others.

## 8.1 DESIGNS THAT REQUIRE A RELATIVELY SMALL RUN SIZE

### 8.1.1 The Hoke Designs

The Hoke designs are a class of economical designs based on subsets of all combinations of three levels ( $-1$ ,  $0$ , and  $1$ ) for a given number of factors, and are irregular fractions of the  $3^k$  factorial. They consist of factorial, axial and edge points that create efficient second-order arrays for  $k = 3$ ,  $4$ ,  $5$ , and  $6$ . Among very small designs, several in this class perform remarkably well and should be considered if there are restrictions on the design size which require the experimenter to consider saturated or near-saturated designs. Developed by Hoke (1974), the designs are suitable for a cuboidal region of interest.

For each number of factors, several versions of the Hoke designs exist and have been labeled as  $\mathbf{D}_1$ ,  $\mathbf{D}_2$ ,  $\dots$ ,  $\mathbf{D}_7$ . A good characteristic of all of the versions is symmetry of the designs across all factors. Two popular choices are  $\mathbf{D}_2$  and  $\mathbf{D}_6$ , since they perform well with small variances for model parameters and prediction of new observations among the Hoke design choices. For  $k = 3$ , we have

$$\mathbf{D}_2 = \begin{matrix} & x_1 & x_2 & x_3 \\ \begin{matrix} x_1 & x_2 & x_3 \end{matrix} & \left[ \begin{matrix} -1 & -1 & -1 \\ 1 & 1 & -1 \\ 1 & -1 & 1 \\ -1 & 1 & 1 \\ 1 & -1 & -1 \\ -1 & 1 & -1 \\ -1 & -1 & 1 \\ -1 & 0 & 0 \\ 0 & -1 & 0 \\ 0 & 0 & -1 \end{matrix} \right] \end{matrix} \quad \text{and} \quad \mathbf{D}_6 = \begin{matrix} & x_1 & x_2 & x_3 \\ \left[ \begin{matrix} -1 & -1 & -1 \\ 1 & 1 & -1 \\ 1 & -1 & 1 \\ -1 & 1 & 1 \\ 1 & -1 & -1 \\ -1 & 1 & -1 \\ -1 & -1 & 1 \\ -1 & 0 & 0 \\ 0 & -1 & 0 \\ 0 & 0 & -1 \\ 1 & 1 & 0 \\ 1 & 0 & 1 \\ 0 & 1 & 1 \end{matrix} \right] \end{matrix}$$

The  $\mathbf{D}_2$  design is saturated with 10 observations to estimate the 10 model parameters, while the  $\mathbf{D}_6$  design is near-saturated with a total of 13 observations. We can gain some

understanding about the estimation capability of the designs by observing the  $\mathbf{X}'\mathbf{X}$  for the two designs. For the  $\mathbf{D}_2$  design, all of the terms have non-zero correlations, which have a strong effect on the variance of the regression coefficients. By comparison, many more of the terms of the  $\mathbf{D}_6$  design are mutually orthogonal, leading to improved estimation for the terms of the model.

$$\mathbf{X}'\mathbf{X}_{\mathbf{D}_2} = \begin{bmatrix} x_1 & x_2 & x_3 & x_1^2 & x_2^2 & x_3^2 & x_1x_2 & x_1x_3 & x_2x_3 \\ 10 & -2 & -2 & -2 & 8 & 8 & 8 & -1 & -1 & -1 \\ & 8 & -1 & -1 & -2 & -1 & -1 & -1 & -1 & -1 \\ & & 8 & -1 & -1 & -2 & -1 & -1 & -1 & -1 \\ & & & 8 & -1 & -1 & -2 & -1 & -1 & -1 \\ & & & & 8 & 7 & 7 & -1 & -1 & -1 \\ & & & & & 8 & 7 & -1 & -1 & -1 \\ & & & & & & 8 & -1 & -1 & -1 \\ & & & & & & & 7 & -1 & -1 \\ & & & & & & & & 7 & \\ & & & & & & & & & 7 \end{bmatrix}$$

$$\mathbf{X}'\mathbf{X}_{\mathbf{D}_6} = \begin{bmatrix} x_1 & x_2 & x_3 & x_1^2 & x_2^2 & x_3^2 & x_1x_2 & x_1x_3 & x_2x_3 \\ 13 & 0 & 0 & 0 & 10 & 10 & 10 & 0 & 0 & 0 \\ 10 & 0 & 0 & 0 & 0 & 0 & 0 & 0 & 0 & -1 \\ & 10 & 0 & 0 & 0 & 0 & 0 & 0 & -1 & 0 \\ & & 10 & 0 & 0 & 0 & -1 & 0 & 0 & 0 \\ & & & 10 & 8 & 8 & 0 & 0 & -1 \\ & & & & 10 & 8 & 0 & -1 & 0 \\ & & & & & 10 & -1 & 0 & 0 \\ & & & & & & 8 & -1 & -1 \\ & & & & & & & 8 & -1 \\ & & & & & & & & 8 \end{bmatrix}$$

**Hoke Designs for  $k > 3$**  The Hoke designs exist for any number of factors, with the  $\mathbf{D}_1$  to  $\mathbf{D}_3$  designs being saturated, and the  $\mathbf{D}_4$  to  $\mathbf{D}_7$  designs near-saturated. We can construct the designs using symmetry for a given patterns of levels. For example, for  $k = 4$  the saturated  $\mathbf{D}_2$  design is constructed by taking all combinations of the following combinations of the three levels:  $(-1, -1, -1, -1)$ ,  $(1, 1, 1, -1)$ ,  $(1, 1, -1, -1)$  and  $(-1, 0, 0, 0)$ . This gives 1,

4, 6, and 4 rows for the design matrix, respectively. The  $\mathbf{D}_6$  design is the same as the  $\mathbf{D}_2$  design but with the four combinations of (1,1,1,0) added.

$$\mathbf{D}_2 = \begin{bmatrix} x_1 & x_2 & x_3 & x_4 \\ -1 & -1 & -1 & -1 \\ 1 & 1 & 1 & -1 \\ 1 & 1 & -1 & 1 \\ 1 & -1 & 1 & 1 \\ -1 & 1 & 1 & 1 \\ 1 & 1 & -1 & -1 \\ 1 & -1 & 1 & -1 \\ 1 & -1 & -1 & 1 \\ -1 & -1 & 1 & 1 \\ -1 & 1 & -1 & 1 \\ -1 & 1 & 1 & -1 \\ -1 & 0 & 0 & 0 \\ 0 & -1 & 0 & 0 \\ 0 & 0 & -1 & 0 \\ 0 & 0 & 0 & -1 \end{bmatrix}$$

The Hoke designs are an important class of designs, which offer a good option if a saturated or near-saturated design is required. In general, the use of saturated designs can be potentially risky as no degrees of freedom are available to estimate pure error or lack-of-fit. However, it is inevitable that these designs will be used where cost constraints are a major obstacle. In these cases, the Hoke designs are a good choice, and can typically be easily implemented since only three levels for each factor are required.

### 8.1.2 Koshal Design

Another class of design requiring a small run size is the family of **Koshal designs**. Koshal (1933) introduced this type of design for use in an effort to solve a set of likelihood equations. The designs are saturated for modeling of any response surface of order  $d$  ( $d = 1, 2, \dots$ ). We will not supply general details but will list Koshal designs for  $d = 1$  and 2.

**Koshal Design for First-Order Model** For the first-order model the Koshal design is simply the *one-factor-at-a-time* design. For  $k$  design variables we simply have

$$\mathbf{D} = \begin{bmatrix} x_1 & x_2 & \dots & x_k \\ \mathbf{0} & \mathbf{0} & \cdots & \mathbf{0} \\ 1 & 0 & \cdots & 0 \\ 0 & 1 & \cdots & 0 \\ \vdots & \vdots & & \vdots \\ 0 & 0 & \cdots & 1 \end{bmatrix}$$

Thus, for the special case in which three variables are of interest we have

$$\mathbf{D} = \begin{bmatrix} x_1 & x_2 & x_3 \\ \mathbf{0} & \mathbf{0} & \mathbf{0} \\ 1 & 0 & 0 \\ 0 & 1 & 0 \\ 0 & 0 & 1 \end{bmatrix}$$

As a result, four coefficients can be estimated in the model

$$y_i = \beta_0 + \beta_1 x_{1i} + \beta_2 x_{2i} + \beta_3 x_{3i} + \varepsilon_i$$

It is important to note that the Koshal design for the first-order model does not allow estimation of any interaction terms.

**First-Order Plus Interaction** The Koshal family can be nicely extended to accommodate the first-order model with interaction. One simply augments the first-order Koshal design with **interaction rows**. For example, the appropriate design for  $k = 3$  is given by

$$\mathbf{D} = \begin{bmatrix} x_1 & x_2 & x_3 \\ \mathbf{0} & \mathbf{0} & \mathbf{0} \\ 1 & 0 & 0 \\ 0 & 1 & 0 \\ 0 & 0 & 1 \\ 1 & 1 & 0 \\ 1 & 0 & 1 \\ 0 & 1 & 1 \end{bmatrix}$$

**Second-Order Koshal Design** The Koshal design for fitting a second-order model must, of course, include at least three levels. The one-factor-at-a-time idea remains the basis for the design. For  $k = 3$ , the design is given by

$$\mathbf{D} = \begin{bmatrix} x_1 & x_2 & x_3 \\ \mathbf{0} & \mathbf{0} & \mathbf{0} \\ 1 & 0 & 0 \\ 0 & 1 & 0 \\ 0 & 0 & 1 \\ 2 & 0 & 0 \\ 0 & 2 & 0 \\ 0 & 0 & 2 \\ 1 & 1 & 0 \\ 1 & 0 & 1 \\ 0 & 1 & 1 \end{bmatrix}$$

The design contains three levels and 10 design points. Another form of the second order Koshal design is given by

$$\mathbf{D} = \begin{bmatrix} x_1 & x_2 & x_3 \\ \mathbf{0} & \mathbf{0} & \mathbf{0} \\ 1 & 0 & 0 \\ 0 & 1 & 0 \\ 0 & 0 & 1 \\ -1 & 0 & 0 \\ 0 & -1 & 0 \\ 0 & 0 & -1 \\ 1 & 1 & 0 \\ 1 & 0 & 1 \\ 0 & 1 & 1 \end{bmatrix}$$

It should be quite clear to the reader how to extend the Koshal designs to more than three variables.

### 8.1.3 Hybrid Designs

Roquemore (1976) developed a set of saturated or near-saturated second-order designs called **hybrid designs**. These hybrid designs are very efficient. They were created via an imaginative idea that involves the use of a central composite design for  $k - 1$  variables, and the levels of the  $k$ th variable are determined in such a way as to create certain symmetries in the design. The result is a class of designs that are economical and either rotatable or near-rotatable for  $k = 3, 4, 6$ , and 7. For example, for  $k = 3$  and  $N = 10$  we have the **hybrid 310** with design matrix

$$\mathbf{D}_{310} = \begin{bmatrix} x_1 & x_2 & x_3 \\ 0 & 0 & 1.2906 \\ 0 & 0 & -0.1360 \\ -1 & -1 & 0.6386 \\ 1 & -1 & 0.6386 \\ -1 & 1 & 0.6386 \\ 1 & 1 & 0.6386 \\ 1.736 & 0 & -0.9273 \\ -1.736 & 0 & -0.9273 \\ 0 & 1.736 & -0.9273 \\ 0 & -1.736 & -0.9273 \end{bmatrix}$$

It is important to note that the efficiency of the hybrid is based to a large extent on the fact that eight of the ten design points and two center runs on  $x_1$  and  $x_2$  are a central composite in these two variables. Then four levels are chosen on the remaining variable,  $x_3$ , with these levels chosen to *make odd moments zero, all second pure moments equal, and a near-rotatable design*. The design name, 310, comes from  $k = 3$  and 10 distinct design points.

Roquemore developed two additional  $k = 3$  hybrid designs. The design matrices are given by

$$\mathbf{D}_{311A} = \begin{bmatrix} x_1 & x_2 & x_3 \\ 0 & 0 & \sqrt{2} \\ 0 & 0 & -\sqrt{2} \\ -1 & -1 & 1/\sqrt{2} \\ 1 & -1 & 1/\sqrt{2} \\ -1 & 1 & 1/\sqrt{2} \\ 1 & 1 & 1/\sqrt{2} \\ \sqrt{2} & 0 & -1/\sqrt{2} \\ -\sqrt{2} & 0 & -1/\sqrt{2} \\ 0 & \sqrt{2} & -1/\sqrt{2} \\ 0 & \sqrt{2} & -1/\sqrt{2} \\ \mathbf{0} & \mathbf{0} & \mathbf{0} \end{bmatrix}$$

$$\mathbf{D}_{311B} = \begin{bmatrix} x_1 & x_2 & x_3 \\ 0 & 0 & \sqrt{6} \\ 0 & 0 & -\sqrt{6} \\ -0.7507 & 2.1063 & 1 \\ 2.1063 & 0.7507 & 1 \\ 0.7507 & -2.1063 & 1 \\ -2.1063 & -0.7507 & 1 \\ 0.7507 & 2.1063 & -1 \\ 2.1063 & -0.7507 & -1 \\ -0.7507 & -2.1063 & -1 \\ -2.1063 & 0.7507 & -1 \\ \mathbf{0} & \mathbf{0} & \mathbf{0} \end{bmatrix}$$

Both the 311A and 311B are near-rotatable. Eleven design points include a center run to avoid near-singularity.

There are three hybrid designs for  $k = 4$ . They are given by

$$\mathbf{D}_{416A} = \begin{bmatrix} x_1 & x_2 & x_3 & x_4 \\ 0 & 0 & 0 & 1.7844 \\ 0 & 0 & 0 & -1.4945 \\ -1 & -1 & -1 & 0.6444 \\ 1 & -1 & -1 & 0.6444 \\ -1 & 1 & -1 & 0.6444 \\ 1 & 1 & -1 & 0.6444 \\ -1 & -1 & 1 & 0.6444 \\ 1 & -1 & 1 & 0.6444 \\ -1 & 1 & 1 & 0.6444 \\ 1 & 1 & 1 & 0.6444 \\ 1.6853 & 0 & 0 & -0.9075 \\ -1.6853 & 0 & 0 & -0.9075 \\ 0 & 1.6853 & 0 & -0.9075 \\ 0 & -1.6553 & 0 & -0.9075 \\ 0 & 0 & 1.6853 & -0.9075 \\ 0 & 0 & -1.6853 & -0.9075 \end{bmatrix}$$

$$\mathbf{D}_{416B} = \begin{bmatrix} x_1 & x_2 & x_3 & x_4 \\ 0 & 0 & 0 & 1.7317 \\ 0 & 0 & 0 & -0.2692 \\ \pm 1 & \pm 1 & \pm 1 & \mathbf{0.6045} \\ \pm 1.5177 & 0 & 0 & -1.0498 \\ 0 & \pm 1.5177 & 0 & -1.0498 \\ 0 & 0 & \pm 1.5177 & -1.0498 \end{bmatrix}$$

$$\mathbf{D}_{416C} = \begin{bmatrix} x_1 & x_2 & x_3 & x_4 \\ 0 & 0 & 0 & 1.7658 \\ 0 & 0 & 0 & 0 \\ \pm 1 & \pm 1 & \pm 1 & \mathbf{0.5675} \\ \pm 1.4697 & 0 & 0 & -1.0509 \\ 0 & \pm 1.4697 & 0 & -1.0509 \\ 0 & 0 & \pm 1.4697 & -1.0509 \end{bmatrix}$$

We have condensed the notation for 416B and 416C. The notation  $\pm 1$  indicates a  $2^3$  factorial in  $x_1$ ,  $x_2$ , and  $x_3$  with  $x_4$  fixed. The design points following the  $2^3$  factorial are axial points in  $x_1$ ,  $x_2$ , and  $x_3$  with  $x_4$  fixed. A center run is used in 416C to avoid near-similarity. The notation  $\pm 1.4697$  or  $\pm 1.5177$  implies two axial points. When possible, one or two more center runs should be added to the hybrid design.

There are two hybrid designs for six design variables. Both include 28 runs, and thus both are saturated. The 628A design is as follows:

$$\mathbf{D}_{628A} = \begin{bmatrix} x_1 & x_2 & x_3 & x_4 & x_5 & x_6 \\ 0 & 0 & 0 & 0 & 0 & 4/\sqrt{3} \\ \pm 1 & 1/\sqrt{3} \\ \pm 2 & 0 & 0 & 0 & 0 & -2/\sqrt{3} \\ 0 & \pm 2 & 0 & 0 & 0 & -2/\sqrt{3} \\ 0 & 0 & \pm 2 & 0 & 0 & -2/\sqrt{3} \\ 0 & 0 & 0 & \pm 2 & 0 & -2/\sqrt{3} \\ 0 & 0 & 0 & 0 & \pm 2 & -2/\sqrt{3} \\ 0 & 0 & 0 & 0 & 0 & 0 \end{bmatrix}$$

The notation  $\pm 1$  indicates a resolution V  $2^{5-1}$  in  $x_1$ ,  $x_2$ ,  $x_3$ ,  $x_4$ , and  $x_5$ , while  $x_6$  is held at  $4/\sqrt{3}$ . The  $\pm 2$  implies two axial points A second six-variable design, the 628B, is constructed in a manner similar to that of 628A. The components of the design are as follows:

1. Resolution V  $2^{5-1}$  in  $x_1 - x_5$  with  $x_6 = 0.6096$
2. Axial points in  $x_1 - x_5$  with  $\alpha = 2.1749$  and  $x_6 = -1.0310$
3. Two additional center points with  $x_6 = 2.397$  and  $-1.8110$

**General Comments Concerning the Hybrid Designs** As we indicated earlier, the hybrid designs represent a very efficient class of saturated or near-saturated second-order designs. The hybrid designs are quite competitive with central composite designs *when the criteria for comparison takes design size into account*—for example, when one makes comparisons using  $N \text{Var}[\hat{y}(\mathbf{x})]/\sigma^2$ . Further discussion of design comparisons is in Sections 8.2 and 8.3.

It has been our experience that hybrid designs are not used as much in industrial applications as they should be. As previously discussed, the use of saturated or near-saturated response surface designs should be avoided. However, where cost constraints are major obstacles, the hybrid design is a good choice. It is likely that potential users are reluctant to use the hybrid designs because of the “messy levels” required of the extra design variable—that is, the variable not involved in the central composite structure. One must remember that the levels reported in the design matrices in this text are those solved for by Roquemore in order to achieve certain ideal design conditions. An efficient design will still result if one merely approximates these levels. Minor *errors in control* do not alter the efficiencies of these designs. One should assign the extra design variable to a

factor that is easiest to alter and thus accommodates these levels. Of course, many practitioners are attracted to designs that involve three evenly spaced levels or levels that provide little difficulty when the experiment is conducted.

### 8.1.4 The Small Composite Design

The small composite design is commonly available in some software packages, and is present here because of its popularity. However, we would like to discourage the use of this design because of its poor estimation and prediction performance. More details about its performance are given in Section 8.2. The small composite design gets its name from the ideas of the central composite, but the factorial portion is neither a complete  $2^k$  nor a resolution V fraction, but, rather, a special resolution III fraction in which no four-letter word is among the defining relations. This type of fraction is often called *resolution III\**. As a result, the total run size is reduced from that of the CCD—hence the term **small** composite design. For  $k = 3$ , we have

$$\mathbf{D} = \begin{bmatrix} x_1 & x_2 & x_3 \\ -1 & -1 & -1 \\ 1 & 1 & -1 \\ 1 & -1 & 1 \\ -1 & 1 & 1 \\ -\alpha & 0 & 0 \\ \alpha & 0 & 0 \\ 0 & -\alpha & 0 \\ 0 & \alpha & 0 \\ 0 & 0 & -\alpha \\ 0 & 0 & \alpha \\ \mathbf{0} & \mathbf{0} & \mathbf{0} \end{bmatrix} \quad (8.2)$$

The factorial portion is the fraction generated using  $I = -ABC$ . Obviously, the alternative fraction would be equally satisfactory in the construction of the small composite design. In this case,  $p$ , the number of second-order parameters, is 10, and thus the design is one degree of freedom above saturation. Multiple center runs allow degrees of freedom for pure error but if the fitted model is second order, there will be one degree of freedom for lack of fit.

If we focus on the example design in Equation 8.2, it becomes obvious that in the factorial portion linear main effect terms are aliased with two-factor interaction terms. Hartley (1959) observed that in spite of this, all coefficients in the second-order model are estimable because the linear coefficients benefit from the axial points, though axial points provide no information on the estimation of interaction coefficients. One may gain some additional

insight into this by observing the matrix  $\mathbf{X}'\mathbf{X}$  for the  $k = 3$  small composite design (SCD) contrasted with that for the  $k = 3$  full central composite (assume a single center run for both designs):

$$\mathbf{X}'\mathbf{X}_{\text{SCD}} = \begin{bmatrix} x_1 & x_2 & x_3 & x_1^2 & x_2^2 & x_3^2 & x_1x_2 & x_1x_3 & x_2x_3 \\ 11 & 0 & 0 & 0 & 4+2\alpha^2 & 4+2\alpha^2 & 4+2\alpha^2 & 0 & 0 & 0 \\ 4+2\alpha^2 & 0 & 0 & 0 & 0 & 0 & 0 & 0 & 0 & -4 \\ 4+2\alpha^2 & 0 & 0 & 0 & 0 & 0 & 0 & -4 & 0 & 0 \\ 4+2\alpha^2 & 0 & 0 & 0 & 0 & 0 & -4 & 0 & 0 & 0 \\ 4+2\alpha^4 & 4 & 4 & 0 & 0 & 0 & 0 & 0 & 0 & 0 \\ 4+2\alpha^4 & 4 & 4 & 0 & 0 & 0 & 0 & 0 & 0 & 0 \\ 4+2\alpha^4 & 0 & 0 & 0 & 0 & 0 & 0 & 0 & 0 & 0 \\ 4 & 0 & 0 & 0 & 0 & 0 & 0 & 0 & 0 & 0 \\ 4 & 0 & 0 & 0 & 0 & 0 & 0 & 0 & 0 & 0 \\ 4 \end{bmatrix} \quad (8.3)$$

$$\mathbf{X}'\mathbf{X}_{\text{CCD}} = \begin{bmatrix} x_1 & x_2 & x_3 & x_1^2 & x_2^2 & x_3^2 & x_1x_2 & x_1x_3 & x_2x_3 \\ 15 & 0 & 0 & 0 & 8+2\alpha^2 & 8+2\alpha^2 & 8+2\alpha^2 & 0 & 0 & 0 \\ 8+2\alpha^2 & 0 & 0 & 0 & 0 & 0 & 0 & 0 & 0 & 0 \\ 8+2\alpha^2 & 0 & 0 & 0 & 0 & 0 & 0 & 0 & 0 & 0 \\ 8+2\alpha^2 & 0 & 0 & 0 & 0 & 0 & 0 & 0 & 0 & 0 \\ 8+2\alpha^4 & 8 & 8 & 0 & 0 & 0 & 0 & 0 & 0 & 0 \\ 8+2\alpha^4 & 8 & 8 & 0 & 0 & 0 & 0 & 0 & 0 & 0 \\ 8+2\alpha^4 & 0 & 0 & 0 & 0 & 0 & 0 & 0 & 0 & 0 \\ 8 & 0 & 0 & 0 & 0 & 0 & 0 & 0 & 0 & 0 \\ 8 & 0 & 0 & 0 & 0 & 0 & 0 & 0 & 0 & 0 \\ 8 \end{bmatrix} \quad (8.4)$$

The distinction between the two designs stems from the fact that in the CCD all linear main effects and two-factor interactions are mutually orthogonal, whereas in the SCD the  $-4$  values reflect the nonorthogonality of  $x_1$  with  $x_2x_3$ ,  $x_2$  with  $x_1x_3$ , and  $x_3$  with  $x_1x_2$ . The correlation among these model terms has a strong effect on the variance of the regression coefficients of  $x_1$ ,  $x_2$ ,  $x_3$ ,  $x_1x_2$ ,  $x_1x_3$ , and  $x_2x_3$ . In fact, a comparison can be made by creating scaled variances for the two designs, that is,  $N \text{Var}(b_i)/\sigma^2$  for  $i = 1, 2, 3$  and  $N \text{Var}(b_{ij})/\sigma^2$

**TABLE 8.1** Scaled Variances of Model Coefficients for CCD and SCD

	$b_0$	$b_i$	$b_{ii}$	$b_{ij}$
CCD ( $N = 17$ )	5.6666	1.2143	1.3942	2.125
SCD (AC = 13)	4.3333	2.1666	1.1074	5.4166

for  $i, j = 1, 2, 3; i \neq j$ . Table 8.1 shows these values taken from appropriate diagonals of the matrix  $N(\mathbf{X}'\mathbf{X})^{-1}$ . In our illustration,  $\alpha$  was taken to be  $\sqrt{3}$  and  $n_c = 3$  for each design. Notice that the designs are nearly identical for estimation of pure quadratic coefficients. However, the small composite design suffers considerably in efficiency for estimation of linear and interaction coefficients.

The efficiencies of model coefficients certainly suggest that the small composite design should not be used, as several of the other designs, such as the Hoke and hybrid designs have similar size and perform much better. Coefficient by coefficient comparisons of variances is certainly not the only, nor necessarily even the best, method for comparing designs. Graphical methods for comparing designs in terms of scaled prediction variance (i.e.,  $N \text{Var}[\hat{y}(\mathbf{x})]/\sigma^2$ ) can be used. These methods are presented later in this chapter, and the comparison between the CCD and SCD will be displayed prominently.

**Small Composite Design for  $k = 2$**  For  $k = 2$  there is a small composite design in which the factorial portion is the one-half fraction of a  $2^2$ . The design is given by

$$\mathbf{D} = \begin{bmatrix} & x_1 & x_2 \\ & -1 & -1 \\ & 1 & 1 \\ -\alpha & 0 & \\ \alpha & 0 & \\ 0 & -\alpha & \\ 0 & \alpha & \\ \mathbf{0} & \mathbf{0} & \end{bmatrix}$$

The defining relation for the factorial portion is given by  $I = AB$ . With six parameters to estimate, this design affords one degree of freedom for lack of fit. For  $k = 2$  the hexagon is a more efficient design. This SCD design may find some use if the design region is cuboidal, in which case  $\alpha$  must be 1.0.

**Small Composite Designs for  $k > 3$**  The general SCD is a resolution III\* fraction of a  $2^k$  augmented with axial points and runs in the center of the design. This structure applies for all  $k > 2$ . For example, for  $k = 4$  a SCD is given by

$$\mathbf{D} = \begin{array}{cccc} & x_1 & x_2 & x_3 & x_4 \\ \left[ \begin{array}{cccc} -1 & -1 & -1 & +1 \\ 1 & -1 & -1 & -1 \\ -1 & 1 & -1 & -1 \\ -1 & -1 & 1 & 1 \\ 1 & 1 & -1 & 1 \\ 1 & -1 & 1 & -1 \\ -1 & 1 & 1 & -1 \\ 1 & 1 & 1 & 1 \\ -\alpha & 0 & 0 & 0 \\ \alpha & 0 & 0 & 0 \\ 0 & -\alpha & 0 & 0 \\ 0 & \alpha & 0 & 0 \\ 0 & 0 & -\alpha & 0 \\ 0 & 0 & \alpha & 0 \\ 0 & 0 & 0 & -\alpha \\ 0 & 0 & 0 & -\alpha \\ \mathbf{0} & \mathbf{0} & \mathbf{0} & \mathbf{0} \end{array} \right] \end{array} \quad (8.5)$$

The factorial portion of the design in Equation 8.5 is a one-half fraction of a  $2^4$  with  $I = ABD$  as the defining relation. The design points yield 17 degrees of freedom for parameter estimation. Thus, the design is not saturated but results in only two degrees of freedom for lack of fit. In comparison, the CCD for  $k = 4$  allows 10 degrees of freedom for lack of fit. Comparisons between scaled variances of coefficients of the linear and interaction coefficients of the SCD with that of the CCD essentially tell the same story as in the  $k = 3$  case. The superiority of the CCD is quite apparent, and indeed other small designs also outperform the SCD substantially.

An additional important point should be made regarding the  $k = 4$  case. One is tempted to use a resolution IV fraction rather than resolution III\* for  $k = 4$  and possibly for larger values of  $k$  where higher fractions might be exploited. For example, for  $k = 6$  a resolution IV  $2^{6-2}$  fraction is available. This allows 16 factorial points plus 12 axial points plus center runs, and the result is one degree of freedom over saturation. However, the design *cannot* involve a resolution IV fraction: the result would be complete aliasing among two-factor interactions. One must be mindful of the fact that unlike linear or pure quadratic coefficients, all information on interaction coefficients is derived from the factorial portion. Thus, aliasing among two-factor interaction terms in the factorial portion results in aliasing of two-factor interactions for the entire design.

**Further Comments on the Small Composite Design** Despite its availability in software packages, the small composite design is typically not the best choice when cost constraints restrict the design size to substantially smaller than that required by the central composite or Box–Behnken designs. If the primary goal of the experiment is to understand the second-order model, other alternatives such as the Hoke or hybrid designs provide better estimation and prediction with a similar small sample size.

One potential virtue of the SCD may arise in sequential experimentation. Most of the discussion regarding sequential experimentation has centered on the transition from the first-order fitted model to the second-order model. One should regard response surface methodology (RSM) as nearly always involving iterative experimentation and iterative decision-making. A first-stage experiment with an SCD may suggest that the current region is, indeed, the proper one. That is, there are no ridge conditions and no need to move to an alternative region. Then a second-stage augmentation of the factorial portion is conducted; the result is now either a full factorial or resolution V fraction that accompanies the axial points. As a result, the second stage is more efficient than what was used in the first stage. Further information about the SCD and comparisons with other designs will be given later in the chapter.

### 8.1.5 Some Saturated or Near-Saturated Cuboidal Designs

During the 1970s and early 1980s, considerable attention was given to the development of efficient second-order designs on a cube. This movement settled down considerably in the 1980s, and attention shifted to developments that led to general computer-generated experimental designs. Computer-generated design will be discussed in general in Section 8.3. However, there remain several interesting design classes for a cube that have potential use. Designs developed by Notz (1982), and Box and Draper (1974) are particularly noteworthy. As an example, the Notz three-variable design involves seven design points from a  $2^3$  factorial plus three one-factor-at-a-time axial points. Specifically, this design is given by

$$\mathbf{D} = \begin{array}{c} x_1 \quad x_2 \quad x_3 \\ \hline -1 & -1 & -1 \\ 1 & -1 & -1 \\ -1 & 1 & -1 \\ -1 & -1 & 1 \\ 1 & 1 & -1 \\ 1 & -1 & 1 \\ -1 & 1 & 1 \\ 1 & 0 & 0 \\ 0 & 1 & 0 \\ 0 & 0 & 1 \end{array}$$

A design consisting of one additional point, namely  $(+1, +1, +1)$  to complete the  $2^3$  factorial, resulting in 11 design points, is a nice augmentation of the three-factor Notz design. The four-variable Notz design is constructed in a similar manner, with 11 points from the  $2^4$  factorial plus four axial points.

## 8.2 GENERAL CRITERIA FOR CONSTRUCTING, EVALUATING, AND COMPARING EXPERIMENTAL DESIGNS

As we indicated in the previous section, the 1980s began the era of using the computer for design construction. This period brought many new users into the experimental design

arena, simply because it became easier to find an appropriate design. While the virtues of computer-generated designs are considerable in number, there are also negative aspects. Often users treat the computer package like a black box without really understanding what criteria are being used for constructing the design. There certainly are practical situations in which the computer is a vital tool for design construction in spite of the fact that many of the standard RSM designs discussed in this chapter and Chapter 7 are extremely useful designs.

Much of what is available in evaluation and comparison of RSM designs as well as computer-generated design were results of the work of Kiefer (1959, 1961) and Kiefer and Wolfowitz (1959) in **optimal design theory**. Their work is couched in a measure theoretic approach in which an experimental design is viewed in terms of design measure. Design optimality moved into the practical arena in the 1970s and 1980s as designs were put forth as being efficient in terms of criteria inspired by Kiefer and his coworkers. Computer algorithms were developed that allowed “best” designs to be generated by a computer package based on the practitioner’s choice of sample size, model, ranges on variables, and other constraints. The notion of reducing the “goodness” of a design to a single number is perhaps too ambitious, and so optimality should most often be considered as one of many aspects to be balanced.

There are three situations where some type of computer-generated design may be appropriate.

1. *An irregular experimental region.* If the region of interest for the experiment is not a cube or a sphere, standard designs may not be the best choice. Irregular regions of interest occur fairly often. For example, an experimenter is investigating the properties of a particular adhesive. The adhesive is applied to two parts and then cured at an elevated temperature. The two factors of interest are the amount of adhesive applied and the cure temperature. Over the ranges of these two factors, taken as  $-1$  to  $+1$  on the usual coded variable scale, the experimenter knows that if too little adhesive is applied and the cure temperature is too low, the parts will not bond satisfactorily. In terms of the coded variables, this leads to a **constraint** on the design variables, say

$$-1.5 \leq x_1 + x_2$$

where  $x_1$  represents the application amount of adhesive and  $x_2$  represents the temperature. Furthermore, if the temperature is too high and too much adhesive is applied, either the parts will be damaged by heat stress or an inadequate bond will result. Thus, there is another constraint on the factor levels:

$$x_1 + x_2 \leq 1$$

Figure 8.1 shows the experimental region that results from applying these constraints. Notice that the constraints effectively remove two corners of the square, producing an irregular experimental region. There is no standard response surface design that will fit exactly into this region.

2. *A nonstandard model.* Usually an experimenter elects a first- or second-order response surface model, realizing that this **empirical model** is an approximation to the true underlying mechanism. However, sometimes the experimenter may

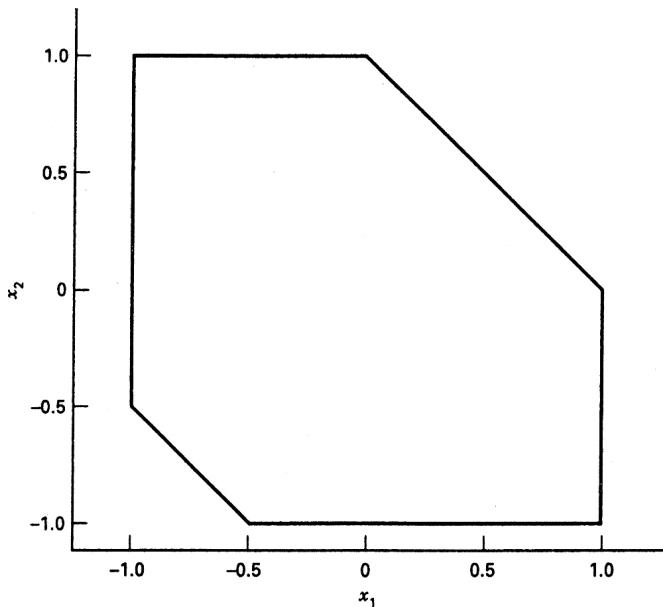


**Figure 8.1** A constrained design region in two variables.

have some special knowledge or insight about the process being studied that may suggest a nonstandard model. For example, the model

$$\begin{aligned} y = & \beta_0 + \beta_1 x_1 + \beta_2 x_2 + \beta_{12} x_1 x_2 + \beta_{11} x_1^2 + \beta_{22} x_2^2 \\ & + \beta_{112} x_1^2 x_2 + \beta_{1112} x_1^3 x_2 + \varepsilon \end{aligned}$$

may be of interest. The experimenter would be interested in obtaining an efficient design for fitting this reduced quartic model. As another illustration, sometimes we encounter response surface problems where some of the, design factors are categorical variables. There are no standard response surface designs for this situation. We will discuss this further in Section 8.3.2.

3. *Unusual sample size or block size requirements.* Occasionally an experimenter may need to reduce the number of runs required by a standard response surface design. For example, suppose we intend to fit a second-order model in four variables. The central composite design for this situation requires between 28 and 30 runs, depending on the number of center points selected. However, the model has only 15 terms. If the runs are extremely expensive or time-consuming, the experimenter may want a design with fewer trials. Although computer-generated designs can be used for this purpose, there may be better approaches. For example, the Hoke D6 design uses only 19 runs, has very good properties, and a hybrid design with as few as 16 runs is also available. These can be superior choices to using a computer-generated design to reduce the number of trials. Unusual requirements concerning either the number of blocks or the block size can also lean to the use of a computer-generated design.

### 8.2.1 Practical Design Optimality

Design optimality criteria are characterized by letters of the alphabet and as a result, are often called **alphabetic optimality criteria**. Some criteria focus on good estimation of model parameters, while others focus on good prediction in the design region. The best-known and most often used criterion is *D*-optimality.

**D-Optimality and D-Efficiency** *D*-optimality, which focuses on good model parameter estimation, is based on the notion that the experimental design should be chosen so as to achieve certain properties in the **moment matrix**

$$\mathbf{M} = \frac{\mathbf{X}'\mathbf{X}}{N} \quad (8.6)$$

The reader recalls the importance of the elements of the moment matrix in the determination of rotatability. Also, the inverse of  $\mathbf{M}$ , namely

$$\mathbf{M}^{-1} = N(\mathbf{X}'\mathbf{X})^{-1} \quad (8.7)$$

(the **scaled dispersion matrix**), contains variances and covariances of the regression coefficients, scaled by  $N/\sigma^2$ . As a result, control of the moment matrix by design implies control of the variances and covariances.

It turns out that an important norm on the moment matrix is the **determinant**, that is,

$$|\mathbf{M}| = \frac{|\mathbf{X}'\mathbf{X}|}{N^p} \quad (8.8)$$

where  $p$  is the number of parameters in the model. Under the assumption of independent normal model errors with constant variance, the *determinant of  $\mathbf{X}'\mathbf{X}$  is inversely proportional to the square of the volume of the confidence region on the regression coefficients*. The volume of the confidence region is relevant because it reflects how well the set of coefficients are estimated. A small  $|\mathbf{X}'\mathbf{X}|$  and hence large  $|(\mathbf{X}'\mathbf{X})^{-1}| = 1/|\mathbf{X}'\mathbf{X}|$  implies poor estimation of  $\boldsymbol{\beta}$  in the model. For the response surface model which is a special case of the general linear model

$$\mathbf{y} = \mathbf{X}\boldsymbol{\beta} + \boldsymbol{\epsilon}$$

the  $100(1 - \alpha)\%$  confidence ellipsoid on  $\boldsymbol{\beta}$  under the assumption  $\boldsymbol{\epsilon} \sim N(\mathbf{0}, \sigma^2\mathbf{I})$  is given by solutions to  $\boldsymbol{\beta}$  in

$$\frac{(\mathbf{b} - \boldsymbol{\beta})'(\mathbf{X}'\mathbf{X})(\mathbf{b} - \boldsymbol{\beta})}{ps^2} \leq F_{\alpha,p,n-p}$$

or

$$(\mathbf{b} - \boldsymbol{\beta})'(\mathbf{X}'\mathbf{X})(\mathbf{b} - \boldsymbol{\beta}) \leq C$$

where  $C = ps^2F_{\alpha,p,n-p}$ . As a result, the volume of the confidence region is the volume of the ellipsoid

$$(\mathbf{b} - \boldsymbol{\beta})'(\mathbf{X}'\mathbf{X})(\mathbf{b} - \boldsymbol{\beta}) = C$$

Suppose we consider the orthogonal matrix  $\mathbf{Q}$  such that

$$\mathbf{Q}'(\mathbf{X}'\mathbf{X})\mathbf{Q} = \begin{bmatrix} \lambda_1^* & & 0 \\ & \lambda_2^* & \\ & & \ddots \\ 0 & & \lambda_p^* \end{bmatrix}$$

where the  $\lambda_i^*$  are the eigenvalues of  $\mathbf{X}'\mathbf{X}$ . We can write

$$\mathbf{X}'\mathbf{X} = \mathbf{Q} \begin{bmatrix} \lambda_1^* & & 0 \\ & \ddots & \\ 0 & & \lambda_p^* \end{bmatrix} \mathbf{Q}'$$

As a result, we can write

$$(\mathbf{b} - \boldsymbol{\beta})'(\mathbf{X}'\mathbf{X})(\mathbf{b} - \boldsymbol{\beta}) = \sum_{i=1}^p (b_i - \beta_i)^2 \lambda_i^* = C$$

The volume of this ellipsoid is proportional to  $[\prod_{i=1}^p (1/\lambda_i^*)]^{1/2}$ . The quantity  $[\prod_{i=1}^p (1/\lambda_i^*)]^{1/2} = 1/|\mathbf{X}'\mathbf{X}|^{1/2}$ . As a result, the volume of the ellipsoid is inversely proportional to the square root of the determinant of  $\mathbf{X}'\mathbf{X}$ .

A *D-optimal design* is one in which  $|\mathbf{M}| = |\mathbf{X}'\mathbf{X}|/N^p$  is maximized<sup>†</sup>; that is,

$$\text{Max}_{\zeta} |\mathbf{M}(\zeta)| \quad (8.9)$$

where Max implies that the maximum is taken over all designs  $\zeta$ . As a result, it is natural to define the *D*-efficiency of a design  $\zeta^*$  as

$$D_{\text{eff}} = \left( |\mathbf{M}(\zeta^*)| / \text{Max}_{\zeta} |\mathbf{M}(\zeta)| \right)^{1/p} \quad (8.10)$$

Here, the  $1/p$  power takes account of the  $p$  parameter estimates being assessed when one computes the determinant of the variance–covariance matrix. The definition of *D*-efficiency in Equation (8.10) allows for comparing designs that have different sample sizes by comparing *D*-efficiencies. Since it is helpful to balance the multiple objectives of a good design outlined in Section 7.1, *D*-efficiency can be a useful tool for quantifying the quality of our estimation of model parameters.

There have been many studies that have been conducted to compare standard experimental designs through the use of *D*-efficiency. Readers are referred to Lucas (1976) for comparisons among some of the designs that we have discussed in this chapter and in Chapter 7. St. John and Draper (1975) give an excellent review of *D*-optimality and provide much insight into pragmatic use of design optimality. One should also read Box and Draper (1971), Myers et al. (1989), and the text by Pukelsheim (1995).

<sup>†</sup>Equivalently, one may minimize  $N^p |(\mathbf{X}'\mathbf{X})^{-1}|$ .

Recall that in Chapter 7 we discussed the notion of variance-optimal designs in the first-order and first-order-plus-interaction case. While our main objective in this chapter is to continue dealing with second-order designs, it is natural to consider  $D$ -optimality and  $D$ -efficiency in the case of simpler models. Consider the variance-optimal design, namely the orthogonal design with all levels at the  $\pm 1$  extremes of the experimental region. The moment matrix is given by

$$\mathbf{M} = \frac{\mathbf{X}'\mathbf{X}}{N} = \mathbf{I}_p$$

It is not difficult to show that for the first-order and first-order-plus-interaction cases, optimality extends to the determinant, that is,

$$\max_{\zeta} |\mathbf{M}(\zeta)| = 1,$$

and thus for these simpler models, the so-called variance-optimal design is also optimal in the determinant sense—that is,  $D$ -optimal.

Before we embark on some comparisons among standard designs and discussion of how  $D$ -optimality affects practical tools in the use of computer-generated design, we offer a few other important optimality criteria and methods of comparison.

**A-Optimality** The concept of **A-optimality**, which also aims to estimate model parameters well, deals with the individual variances of the regression coefficients. Unlike  $D$ -optimality, it does not consider the covariances among coefficients; recall that the variances of regression coefficients appear on the diagonals of  $(\mathbf{X}'\mathbf{X})^{-1}$ . A-optimality is defined as

$$\min_{\zeta} \text{tr}[\mathbf{M}(\zeta)]^{-1} \quad (8.11)$$

where  $\text{tr}$  represents trace, that is, the sum of the variances of the coefficients (weighted by  $N$ ). Some computer-generated design packages make use of A-optimality.

**Criteria Associated with Prediction Variance (G-, V-, and I-Optimality)** Throughout Chapter 7, we consistently made reference to the use of the scaled prediction variance  $N \text{Var}[\hat{y}(\mathbf{x})]/\sigma^2 = v(\mathbf{x})$  as an important measure of performance. The primary goal of many designed experiments is to allow for good prediction throughout the design space. Hence, focusing on  $v(\mathbf{x})$  makes direct assessment possible. Our feeling is that practical designers of experiments don't make use of this measure as they should. One clear disadvantage, of course, is that, unlike  $\text{tr}(\mathbf{M}^{-1})$  or  $|\mathbf{M}|$ ,  $v(\mathbf{x})$  is not a single number but rather depends on the location  $\mathbf{x}$  at which one is predicting. In fact, recall that

$$v(\mathbf{x}) = \frac{N \text{Var}[\hat{y}(\mathbf{x})]}{\sigma^2} = N \mathbf{x}^{(m)'} (\mathbf{X}'\mathbf{X})^{-1} \mathbf{x}^m$$

where  $\mathbf{x}^{(m)}$  reflects location in the design space as well as the nature of the model. In previous discussions in Chapter 7, we focused on attempts to stabilize  $v(\mathbf{x})$  by proper design (choice of center runs).

One interesting design optimality criterion that focuses on  $v(\mathbf{x})$  is *G-optimality*. ***G-optimality*** and the corresponding ***G-efficiency*** emphasize the use of designs for which the *maximum  $v(\mathbf{x})$  in the region of the design is not too large*. It seeks to protect against the worst case prediction variance, since when we use the results of our analysis we may wish to predict new response values anywhere in the design region. A *G-optimal* design  $\zeta$  is one in which we have

$$\min_{\zeta} \left[ \max_{\mathbf{x} \in R} v(\mathbf{x}) \right]$$

Note that this is equivalent to

$$\min_{\zeta} \left[ \max_{\mathbf{x} \in R} \{ \mathbf{x}^{(m)\prime} [\mathbf{M}(\zeta)]^{-1} \mathbf{x}^{(m)} \} \right]$$

because  $N \text{Var}[\hat{y}(\mathbf{x})]/\sigma^2$  is a quadratic form in  $[\mathbf{M}(\zeta)]^{-1}$ . Of course, the natural choices of regions for  $R$  are the cube and sphere. The resulting *G-efficiency* is conceptually quite simple to grasp. It turns out that under the standard independence and homogeneous variance on the model errors, there is a natural lower bound for the maximum prediction variance of

$$\max_{\mathbf{x} \in R} [v(\mathbf{x})] \geq p \quad (8.12)$$

To understand this bound, consider the expression for hat diagonals discussed in Chapter 2. Given the linear model

$$y_i = \mathbf{x}_i^{(m)\prime} \mathbf{b} \quad (i = 1, 2, \dots, n)$$

the  $i$ th hat diagonal is given by

$$h_{ii} = \mathbf{x}_i^{(m)\prime} (\mathbf{X}' \mathbf{X})^{-1} \mathbf{x}_i^{(m)} \quad (i = 1, 2, \dots, n)$$

and, indeed,

$$\sum_{i=1}^n h_{ii} = \sum_{i=1}^n \mathbf{x}_i^{(m)\prime} (\mathbf{X}' \mathbf{X})^{-1} \mathbf{x}_i^{(m)} = p \text{ (number of parameters)}$$

See Myers (1990) or Montgomery, Peck, and Vining (2006). Consider an experimental design and the corresponding scaled prediction variance

$$v(\mathbf{x}) = N \mathbf{x}^{(m)\prime} (\mathbf{X}' \mathbf{X})^{-1} \mathbf{x}^{(m)}$$

Suppose we consider the maximum value of  $v(\mathbf{x})$  in some region  $R$ . The *average value* of  $v(\mathbf{x})$  at the data points is  $p$ . Obviously then

$$\max_{\mathbf{x} \in R} v(\mathbf{x}) \geq p$$

In addition, if a design is *G-optimal*, all hat diagonals are equal, thus implying that  $v(\mathbf{x}) = p$  at all hat diagonals and

$$v(\mathbf{x}) \leq p$$

at all other locations in  $R$ . The result in Equation 8.12 is very important and usually very surprising to practitioners. One must keep in mind that  $v(\mathbf{x}) = N \text{Var}[\hat{y}(\mathbf{x})]/\sigma^2$  is a scale-free quantity. The  $G$ -efficiency is very easily determined for a design, say  $\zeta$ , as

$$G_{\text{eff}} = \frac{p}{\underset{\mathbf{x} \in R}{\text{Max}} v(\mathbf{x})} \quad (8.13)$$

It is always instructive to investigate efficiencies of our two-level designs of Chapters 4 and 6 with regard to first-order and first-order-plus-interaction models. Consider, for example, a  $2^2$  factorial in the case of the first-order model

$$y = \beta_0 + \beta_1 x_1 + \beta_2 x_2 + \varepsilon$$

with the region  $R$  being described by  $-1 \leq x_1 \leq 1$  and  $-1 \leq x_2 \leq 1$ . We know that

$$\mathbf{M} = \mathbf{X}'\mathbf{X}/N = \mathbf{I}_3$$

and

$$\begin{aligned} v(\mathbf{x}) &= [1, x_1, x_2] \mathbf{I}_3 \begin{bmatrix} 1 \\ x_1 \\ x_2 \end{bmatrix} \\ &= 1 + x_1^2 + x_2^2 \end{aligned}$$

As a result, the maximum of  $v(\mathbf{x})$  occurs at the extremes of the cube, namely at  $x_1 = \pm 1$ ,  $x_2 = \pm 1$ . In addition, it is obvious that for the  $2^2$  factorial,

$$\underset{\mathbf{x} \in R}{\text{Max}} [v(\mathbf{x})] = 3 = p$$

Thus, the  $G$ -efficiency of the  $2^2$  design is 1.0. As a result, the design is  $G$ -optimal. In fact, it is simple to show that for the first-order model in  $k$  design variables for the cuboidal region, a two-level design of resolution  $\geq III$  with levels at  $\pm 1$  results in

$$\underset{\mathbf{x} \in R}{\text{Max}} [v(\mathbf{x})] = p$$

Thus all these designs are  $G$ -optimal for the first-order model.

Another prediction-oriented optimality is  **$V$ -optimality**. The  $V$ -criterion considers the prediction variance at a specific *set* of points of interest in the design region, say  $\mathbf{x}_1, \mathbf{x}_2, \dots, \mathbf{x}_m$ . The set of points could be the candidate set from which the design was selected, or it could be some other collection of points that have specific meaning to the experimenter. A design that minimizes the *average* prediction variance over this set of  $m$  points is a  **$V$ -optimal design**.

An important design-optimality criterion that addresses prediction variance is  **$I$ -optimality**, or  **$IV$**  (integrated variance) optimality. The attempt here is to generate a single measure of prediction performance through an averaging process; that is,  $v(\mathbf{x})$  is averaged over some *region of interest*  $R$ . The averaging is accomplished via the integration

over  $R$ . The corresponding division by the volume of  $R$  produces an average. Thus, the  $I$ -criterion is clearly related to the  $V$ -criterion. The  $I$ -optimal design is given by

$$\min_{\zeta} \frac{1}{K} \int_R v(\mathbf{x}) d\mathbf{x} = \max_{\zeta} I(\zeta) \quad (8.14)$$

where  $K = \int_R d\mathbf{x}$ . Notice, then, that we can write the criterion for a design  $\zeta$  as

$$\min_{\zeta} \left\{ \frac{1}{K} \int_R \mathbf{x}^{(m)\prime} [\mathbf{M}(\zeta)]^{-1} \mathbf{x}^{(m)} d\mathbf{x} \right\} = \min_{\zeta} I(\zeta) \quad (8.15)$$

In this way the  $I$ -optimal, or  $IV$ -optimal, design is that in which the *average scaled prediction variance* is minimized. Strictly speaking, the  $I$ -criterion given in Equation 8.15 is a special case of a more general criterion in which the scaled prediction variance is multiplied by a weight function  $w(\mathbf{x})$ . The utility of the weight function is to weight more heavily certain parts of  $R$ . Of course, in most practical situations  $w(\mathbf{x}) = 1.0$ .

The  $I$ -optimality criterion is conceptually a very reasonable device to use for choosing experimental designs, since selecting a design with good average prediction variance should produce satisfactory results throughout the design space. The concept in Equation 8.15 in a different form does enjoy some use in computer-generated designs. However, neither  $G$  nor  $I$  is used as much as  $D$ -optimality. We will shed more light on this in the next section. The  $I$ -criterion leads nicely to a  $I$ -efficiency for design  $\zeta^*$  as

$$I_{\text{eff}} = \min_{\zeta} [I(\zeta)] / I(\zeta^*)$$

As in previous cases, it is instructive to apply the  $I$ -criterion to a simple case, namely a first-order model. Consider, again, the model

$$y = \beta_0 + \sum_{j=1}^k \beta_j x_j + \varepsilon$$

Let us assume that the region is once again given by the cuboidal region  $-1 \leq x_j \leq 1$ . The  $I$ -criterion can be written

$$\begin{aligned} I(\zeta) &= \frac{1}{K} \int_R v(\mathbf{x}) d\mathbf{x} \\ &= \frac{N}{K} \int_R \mathbf{x}^{(m)\prime} (\mathbf{X}' \mathbf{X})^{-1} \mathbf{x}^{(m)} d\mathbf{x} \end{aligned} \quad (8.16)$$

where  $\mathbf{x}^{(m)\prime} = [1, x_1, x_2, \dots, x_k]$ . Here, of course,  $\int_R$  implies  $\int_{-1}^1 \int_{-1}^1 \cdots \int_{-1}^1$ . Because  $\mathbf{x}^{(m)\prime} (\mathbf{X}' \mathbf{X})^{-1} \mathbf{x}^{(m)}$  is a scalar, we can write

$$\begin{aligned} I(\zeta) &= \frac{N}{K} \int_R \text{tr}[\mathbf{x}^{(m)\prime} (\mathbf{X}' \mathbf{X})^{-1} \mathbf{x}^{(m)}] d\mathbf{x} \\ &= \frac{N}{K} \int_R \text{tr}[\mathbf{x}^{(m)} \mathbf{x}^{(m)\prime} (\mathbf{X}' \mathbf{X})^{-1}] d\mathbf{x} \\ &= \text{tr} \left\{ [\mathbf{X}' \mathbf{X}]^{-1} \left[ \frac{1}{K} \int_R \mathbf{x}^{(m)} \mathbf{x}^{(m)\prime} d\mathbf{x} \right] \right\} \end{aligned} \quad (8.17)$$

Now, the matrix  $(1/K) \int_R \mathbf{x}^{(m)} \mathbf{x}^{(m)'} d\mathbf{x}$  is a  $(k+1) \times (k+1)$  matrix of **region moments**, that is, the diagonal elements (apart from the initial diagonal element, which is 1.0) are the  $(1/K) \int_R x_i^2 d\mathbf{x}$ . For the off-diagonals, we have  $(1/K) \int_R x_i d\mathbf{x}$  in the first row and first column and  $(1/K) \int_R x_i x_j d\mathbf{x}$  for  $i \neq j$  as the other off-diagonal elements. Because the region  $R$  is symmetric,  $\int_R x_i d\mathbf{x}$  and  $\int_R x_i x_j d\mathbf{x}$  are both zero. As a result, Equation 8.17 becomes

$$I(\zeta) = \text{tr}\{[\mathbf{M}(\zeta)]^{-1} [\mathbf{D}_R]\} \quad (8.18)$$

where  $\mathbf{D}_R$  is a diagonal matrix given by

$$\mathbf{D}_R = \begin{bmatrix} 1 & 0 & \cdots & 0 \\ 0 & & & \\ \vdots & & \frac{1}{3} I_k & \\ 0 & & & \end{bmatrix}$$

because  $(1/K) \int_R x_i^2 d\mathbf{x} = (1/2^k)(2^k)(\frac{1}{3}) = \frac{1}{3}$ .

Now, Equation 8.18 can be written as a simple function of the variances of the least squares estimators  $b_0, b_1, b_1, \dots, b_k$  of the coefficients in the first-order model. In fact, we have

$$I(\zeta) = N \left[ \text{Var}(b_0) + \frac{1}{3} \sum_{i=1}^k \text{Var}(b_i) \right] \quad (8.19)$$

The value of  $I(\zeta)$ , the scaled prediction variance, averaged over the cuboidal region, is minimized by a design for which the variances of all coefficients are simultaneously minimized. This, as we learned in Chapter 7, is accomplished by the **variance-optimal** design, namely the two-level first-order orthogonal design (resolution  $\geq III$ ) with levels set at the  $\pm 1$  extremes.

If we change the region  $R$  from the cuboidal region to a spherical region, the two-level resolution  $\geq III$  design is both  $D$ - and  $I$ -optimal. Again, the requirement remains that the design be first-order orthogonal with two levels set at the perimeter of the experimental region (see Exercise 8.8).

### 8.2.2 Use of Design Efficiencies for Comparison of Standard Second-Order Designs

Design optimality is an extremely interesting and useful concept. Considerable interest has been drawn to design of experiments and RSM because of the existence of computer packages that allow the user to generate designs with the use of the notion of alphabetic optimality.  $D$ -optimality in particular has received much usage and attention, primarily because it lends itself to relatively simple computation and because algorithms were developed early to implement it. Both Design-Expert and JMP can generate  $D$ -optimal designs, and JMP can generate  $I$ -optimal designs.

The reader should bear in mind the 10 or more desirable properties of an RSM experimental design, listed in Section 7.1. They suggest that what is required in practice, if they can be obtained, are designs that reflect several important properties, not designs

that are optimal with respect to a single criterion. They suggest that what one desires are **good designs**—that is, designs that will produce reliable results under a wide variety of possible circumstances, not designs that are optimal under a fairly restrictive and idealized set of conditions and assumptions. In the case of first-order models and first-order-plus-interaction models, standard designs are optimal designs. We have seen some evidence of this in this chapter; but, in the second-order case, standard RSM designs that we discussed in Chapter 7 are rarely optimal designs, and yet we know that they can be constructed to achieve many desirable properties listed among the 10 given in Chapter 7.

For purposes of an RSM analysis, the standard central composite or Box-Behnken designs should be used whenever possible. When economical designs are needed (near-saturated), the Hoke or hybrid designs should be used whenever possible. *This does not imply that optimal designs obtained through computer-generated designs have no value.* They can be extremely useful and perhaps necessary in many circumstances. There are many conditions encountered by the user under which the use of a CCD or BBD is impossible. In particular, we shall see in Chapter 12 than the use of **mixture designs** often necessitates the use of computer-generated designs due to restrictions on the factor levels and design sizes. Even in nonmixture situations, constraints or unusual design size will often rule out the use of a standard design. We will focus on optimal designs in the context of computer-generated designs later in this chapter. But, it seems reasonable that the reader may gain some further insight into the virtues of standard designs if we discuss the performance of these designs in the context of design efficiencies. In what follows, we investigate the CCD, BBD, hybrid, and certain other saturated or near-saturated designs.

It should be emphasized that because the notion of design optimality as introduced by Kiefer considers an experimental design as a probability measure, most finite designs (i.e.,  $N$ -point designs) will naturally have design efficiencies less than 1.0. As a result, it is natural that designs with small design size will have small efficiencies. The information in Table 8.2 give  $D$ - and  $G$ -efficiencies for various CCD, BBD, and hybrid designs for a spherical region. The table includes values of  $k$  from 2 through 5. For the CCD,  $\alpha = \sqrt{k}$ . [Further information regarding these design efficiencies can be found in Lucas (1974, 1976) and in Nalimov, Golikova, and Nikeshina (1970).] Several facts are noteworthy.

The **central composite and Box–Behnken designs are quite efficient**. For example, note that a CCD for  $k = 3$  with three center points has an efficiency of 97.63%. This means that if the design were replicated  $1/0.9763 \cong 1.02$  times, it would be equivalent to a  $D$ -optimal design. Obviously, this design is nearly  $D$ -optimal. Note that while the design efficiencies are highest for  $n_c = 2$ , one should not view these results as an indication that there is no advantage in using additional center runs. The use of three to five center runs, according to our recommendation in Chapter 7, brings stability in  $v(\mathbf{x})$  and provides important pure error degrees of freedom. Note that for  $k = 4$ , the CCD and BBD have identical efficiencies. This stems from the fact that the BBD is merely a rotation of the CCD for  $k = 4$ . The CCD is rotatable, and the variance properties do not change with rotation of the design.

The lack of  $G$ -efficiency in the CCD for a single center run should not be surprising. Recall that for  $n_c = 0$  and a spherical region,  $\mathbf{X}'\mathbf{X}$  is either singular or near-singular. The use of only one center run results in a large value of  $v(\mathbf{x})$  at the design center. As additional

**TABLE 8.2 D- and G-Efficiencies for Some Standard Second-Order Designs for a Spherical Region**

Number of Factors	Sample Size	Design	D <sub>eff</sub> (%)	G <sub>eff</sub> (%)
2	9	CCD ( $n_c = 1$ )	98.62	66.67
2	10	CCD ( $n_c = 2$ )	99.64	96.0
2	11	CCD ( $n_c = 3$ )	96.91	87.27
3	15	CCD ( $n_c = 1$ )	99.14	66.67
3	16	CCD ( $n_c = 2$ )	99.61	94.59
3	17	CCD ( $n_c = 3$ )	97.63	89.03
3	13	BBD ( $n_c = 1$ )	97.0	76.92
3	14	BBD ( $n_c = 2$ )	96.53	71.43
3	15	BBD ( $n_c = 3$ )	93.82	66.67
3	10	310	72.8	47.4
3	11	311A	79.1	78.6
3	11	311B	83.1	90.9
4	25	CCD ( $n_c = 1$ )	99.23	60.0
4	26	CCD ( $n_c = 2$ )	99.92	98.90
4	27	CCD ( $n_c = 3$ )	98.86	95.24
4	25	BBD ( $n_c = 1$ )	99.23	60.0
4	26	BBD ( $n_c = 2$ )	99.92	98.90
4	27	BBD ( $n_c = 3$ )	98.86	95.24
4	16	416A	81.7	88.0
4	17	416A ( $n_c = 1$ )	90.6	74.3
4	16	416B	96.3	63.1
4	17	416B ( $n_c = 1$ )	95.1	70.1
4	16	416C	96.9	78.0
5	43	CCD ( $n_c = 1$ )	98.6	48.84
5	44	CCD ( $n_c = 2$ )	99.60	87.63
5	45	CCD ( $n_c = 3$ )	99.28	85.56
5	27	CCD ( $\frac{1}{2}$ rep) ( $n_c = 1$ )	98.43	77.78
5	28	CCD ( $\frac{1}{2}$ rep) ( $n_c = 2$ )	98.10	87.64
5	29	CCD ( $\frac{1}{2}$ rep) ( $n_c = 3$ )	96.57	84.62
5	41	BBD ( $n_c = 1$ )	97.93	51.22
5	42	BBD ( $n_c = 2$ )	98.83	90.91
5	43	BED ( $n_c = 3$ )	98.41	88.79

center runs are added, values of  $v(\mathbf{x})$  grow nearer to a condition of stability; it is the nature of the G- and D-criteria to react adversely to the use of center runs in most cases.

It is natural to expect saturated or near-saturated designs to have low efficiencies. As a result, the results for some of the hybrid designs are quite impressive, especially in the case of the 311B and 416A, 416B, and 416C. Though we only included results for  $k$  from 2 through 5, it should be noted that the D-efficiencies and G-efficiencies for the 628A are both 100%, while the corresponding efficiencies for the 628B with a single center run are 90.6% and 84.4%. Further comparisons of hybrid designs with other economical designs such as the small composite design will be illustrated later. While we will not show tables of design efficiencies for the case of the cuboidal region, the following represent a synopsis of results for the CCD, Hoke, and Box–Draper designs. Again, for specific

construction of the Hoke or Box–Draper design, one should consult Hoke (1974) or Box and Draper (1974).

1. The CCD for  $\alpha = 1.0$  is quite efficient, particularly in the  $D$  sense. For  $k = 3, 4$ , and  $5$ , this design has  $D$ -efficiency from approximately 87% to 97% *without center runs*. Center runs reduce  $D$ -efficiency and change  $G$ -efficiency very little.
2. The Hoke  $D_2$  and  $D_6$  designs have  $D$ -efficiencies that range from 80% to 97%. This is quite good given the small design size. The  $G$ -efficiencies are considerably lower, but this is not unexpected with small designs. In general, the Hoke designs perform better than the Box–Draper designs.

In the next section we focus once again on design comparison. We make use of graphical methods in order to gain some perspective about the distribution of  $v(\mathbf{x})$  in the design region. Our purpose is to compare standard designs and also point the reader toward graphical methodology that can be used to evaluate designs in practice.

### 8.2.3 Graphical Procedure for Evaluating the Prediction Capability of an RSM Design

Design efficiencies are single numbers that purport to evaluate the capabilities of an experimental design. In cases of interest here, the designs are RSM designs. Design efficiencies can be beneficial. Indeed, they were of benefit to us in the previous section. They enabled the reader to understand that standard RSM designs are often fairly close to the “best possible” design in the  $D$ -optimality or  $G$ -optimality sense. One must remember that in almost all cases (hybrid 628A being an exception) the best finite-sample-size designs have efficiencies less than 100%.

When one is interested in stability of  $v(\mathbf{x})$  over the design region, a single-number criterion such as a design efficiency may not capture the true design capability, which is actually a multidimensional concept. There is very useful information in a methodology that allows the user to know values of  $v(\mathbf{x})$  throughout the design region. Obviously, for  $k = 2$  two-dimensional plots of  $v(\mathbf{x})$  can easily be constructed. This type of plot can be used to compare designs. In addition, for a specific RSM analysis, if data have been collected, a plot showing contours of constant  $\widehat{\text{Var}[\hat{y}(\mathbf{x})]}$  or  $\{\widehat{\text{Var}[\hat{y}(\mathbf{x})]}\}^{1/2}$  can aid the practitioner in visualizing confidence limits on the mean response at interesting locations in the design region. The following example provides an illustration.

**Example 8.2 Contour Plots of Prediction Variance** Consider the  $k = 2$  illustration of Example 6.4. The design used is a second-order rotatable CCD. Contours of constant response are shown in Fig. 6.14. Figure 8.2 is a two-dimensional plot showing the estimated prediction standard deviation or estimated standard error of prediction

$$\left\{ \widehat{\text{Var}[\hat{y}(\mathbf{x})]} \right\}^{1/2} = s \sqrt{\mathbf{x}^{(m)\prime} (\mathbf{X}' \mathbf{X})^{-1} \mathbf{x}^{(m)}}$$

where  $s$  is the square root of the mean square error. Note the stability of the prediction standard error on spheres. Note also that the prediction begins to break down as one moves outside the design region. For example, for  $x_1 = x_2 = 1.414$ , we are outside the design region and beyond where any data have been collected.

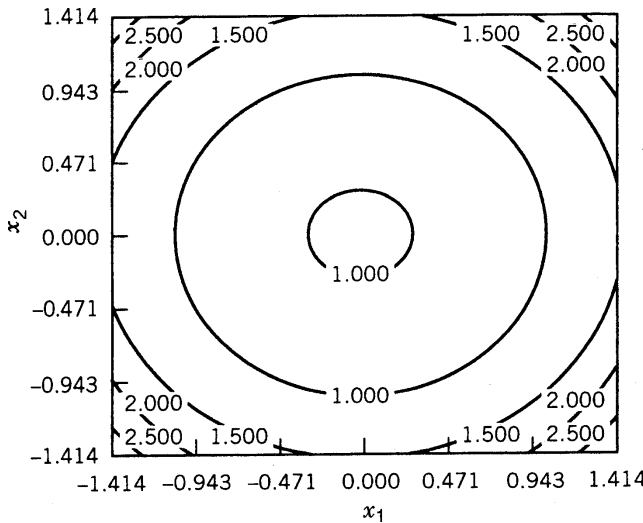


**Figure 8.2** Contours of constant standard error of prediction.

For values of  $k > 2$ , contours of prediction variance are, of course, considerably more awkward. However, there are other graphical procedures that allow comparison of the distribution of  $v(\mathbf{x})$  among RSM designs for any number of design variables. These graphical procedures make use of **variance dispersion graphs** and **fraction of design space plots**. The following sub-subsections define both types of plots and illustrate their use.

**Variance Dispersion Graphs (VDGs)** Giovannitti-Jensen and Myers (1989) and Myers et al. (1992b) developed the variance dispersion graph and produced case studies that allowed for interesting comparisons between standard designs. Rozum (1990) and Rozum and Myers (1991) extended the work from spherical to cuboidal regions.

A variance dispersion graph for an RSM design displays a “snapshot” that allows the practitioner to gain an impression regarding the stability of  $v(\mathbf{x}) = N \text{Var}[\hat{y}(\mathbf{x})]/\sigma^2$  and how the design compares to an ideal. Let us first assume a spherical design. The VDG contains three graphical components:

1. A plot of the **spherical variance**  $V^r$  against the radius  $r$ . The spherical variance is essentially  $v(\mathbf{x})$  averaged over the surface of a sphere of radius  $r$ , namely,

$$V^r = \frac{N\psi}{\sigma^2} \int_{U_r} \text{Var}[\hat{y}(\mathbf{x})] d\mathbf{x} \quad (8.20)$$

where  $U_r$  implies integration over the surface of a sphere of radius  $r$  and  $\psi = (\int_{U_r} d\mathbf{x})^{-1}$ .

2. A plot of the **maximum**  $v(\mathbf{x})$  on a radius  $r$  against  $r$ . That is,

$$\max_{\mathbf{x} \in U_r} \left[ \frac{N \text{Var}[\hat{y}(\mathbf{x})]}{\sigma^2} \right] = \max_{\mathbf{x} \in U_r} [v(\mathbf{x})]$$

3. A plot of the **minimum**  $v(\mathbf{x})$  on a radius  $r$  against  $r$ .

In addition to the above three plots, which offer information about  $v(\mathbf{x})$  for the design being evaluated, the result of Equation 8.12 is used to provide some sense of closeness to ideal. A horizontal line at  $v(\mathbf{x}) = p$  is added. Obviously, if the design is rotatable, the entire VDG will involve only the spherical variance and the horizontal line, since the maximum, minimum, and average  $v(\mathbf{x})$  will be identical at any radius  $r$ .

It is of interest to discuss briefly the computations associated with the spherical variance. It turns out that the integral in Equation 8.20 can be written as

$$\begin{aligned}
 V^r &= \frac{N\psi}{\sigma^2} \int_{U_r} \text{Var}\hat{y}(\mathbf{x}) d\mathbf{x} \\
 &= \frac{N\psi}{\sigma^2} \int_{U_r} \mathbf{x}^{(m)\prime} (\mathbf{X}'\mathbf{X})^{-1} \mathbf{x}^{(m)} d\mathbf{x} \\
 &= \frac{N\psi}{\sigma^2} \int_{U_r} \text{tr}[\mathbf{x}^{(m)\prime} (\mathbf{X}'\mathbf{X})^{-1} \mathbf{x}^{(m)}] d\mathbf{x} \\
 &= \frac{N\psi}{\sigma^2} \int_{U_r} \text{tr}[(\mathbf{X}'\mathbf{X})^{-1} \mathbf{x}^{(m)} \mathbf{x}^{(m)\prime}] d\mathbf{x} \\
 &= \text{tr}(\mathbf{X}'\mathbf{X})^{-1} \left[ \frac{N\psi}{\sigma^2} \int_{U_r} \mathbf{x}^{(m)} \mathbf{x}^{(m)\prime} d\mathbf{x} \right] \\
 &= \text{tr}(\mathbf{X}'\mathbf{X})^{-1} \mathbf{S}
 \end{aligned} \tag{8.21}$$

where  $\mathbf{S}$  is the  $p \times p$  matrix of region moments, with the region being the hypersphere given by  $U_r$ .

**Fraction of Design Space (FDS) Plots** Zahran et al. (2003) developed the fraction of design space plots as a complement to the variance dispersion graph. While the variance dispersion plot shows where in the design space various values of  $v(\mathbf{x})$  are observed, the fraction of design space plots summarizes the prediction performance for the entire design space with a single curve. The stability of  $v(\mathbf{x})$ , its minimum, maximum, and quantiles can all be extracted from the summary curve, allowing for easy assessment of the prediction of a design or comparisons between competing designs. The FDS for an ideal design will have a large fraction of the design space with small  $v(\mathbf{x})$  values and be relatively flat, which corresponds to stability of  $v(\mathbf{x})$  throughout the region.

The curve of an FDS plots matches the value of  $v(\mathbf{x})$  against the fraction of the design space that has prediction variance less than or equal to the given value. A graph of the cumulative fraction provides the user with a sketch of the prediction variance throughout the appropriate design region. The plot can be constructed by taking a random sample of design locations throughout the design space, and calculating  $v(\mathbf{x})$  at these locations. These values are then sorted and plotted against the quantiles from 0 to 1, in a manner similar to a cumulative distribution function for a statistical distribution. Both JMP and Design-Expert can construct FDS plots for a given design.

By using VDGs and FDS plots in combination, we can make comparisons between different potential designs before any data are collected. It is important when we compare competing designs to make sure that the same design regions are being compared, and that these represent the area of interest for the experiment. The FDS plot allows for direct comparisons of which design has a larger proportion of the design space at or below a particular value, or for a fixed fraction, which design has the smaller  $v(\mathbf{x})$  value. Each design is summarized with

a single curve, which helps make comparisons straightforward. The maximum  $v(\mathbf{x})$  value is shown in both VDG and FDS plots allowing for easy observation of the  $G$ -efficiency. The VDGs allow us to see where the good and bad regions of prediction are relative to the distance from the center of the design, as well as assess if the design is rotatable or near-rotatable. One disadvantage of the VDGs is that the relative emphasis of different regions of the design space are not proportionate to the fraction of the design space that they represent. Small values of the radius (namely those close to zero) where only a small proportion of the design space is located are given greater visual emphasis than the edge of the region. This effect becomes increasingly dramatic as the number of factors,  $k$ , increases.

The goal of using graphical summaries to compare different designs is to gain better understanding of where the designs predict well or poorly in the design space of interest, as well as to see how well we might expect to predict future observations based on the experiment that we will have run.

In the following example we illustrate the use of the VDG and FDS plots in a study to determine the utility of center runs with a rotatable CCD for  $k = 5$ .

**Example 8.3 Choosing the Number of Center Runs in a CCD** Consider a central composite design in five design variables with the factorial portion being the resolution V fraction of a  $2^5$ . The value of  $\alpha$  is 2.0, so that the design is rotatable. As a result,  $v(\mathbf{x})$  is constant on spheres, and hence  $\max_{\mathbf{x} \in R}[v(\mathbf{x})] = \min_{\mathbf{x} \in R}[v(\mathbf{x})] = V^r$ . The plot in Fig. 8.3a shows five VDGs for the number of center runs  $n_c = 1$  through  $n_c = 5$ . The horizontal line is at  $p = 21$ . Recall that the maximum value of  $v(\mathbf{x})$  in the design region can be no smaller than  $p$ , and if this value is attained, we have a  $G$ -optimal design. Figure 8.3b shows the corresponding FDS plot for the same five designs.

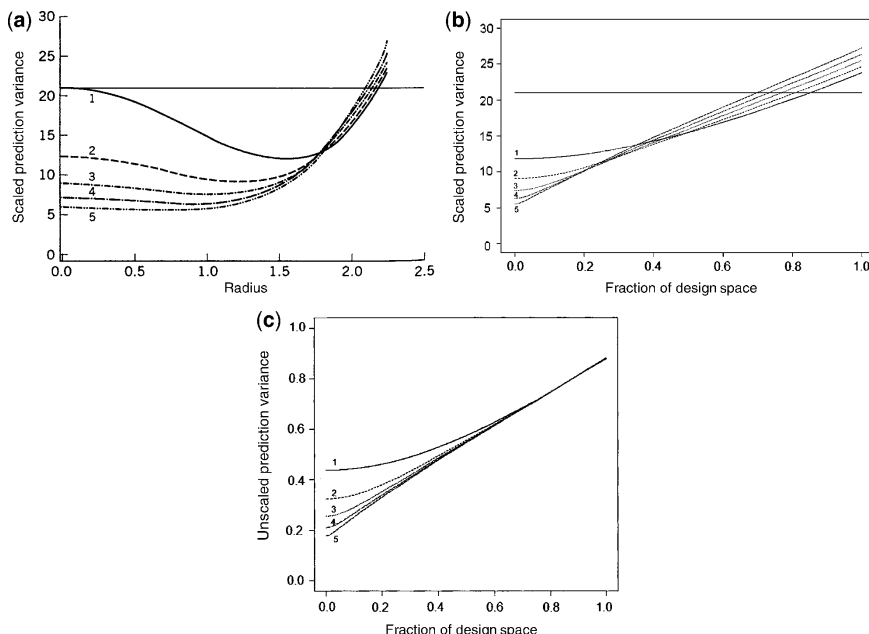


**Figure 8.3** Plots showing the effect of center runs for a  $k = 5$  rotatable CCD with a  $2^{5-1}$  as the factorial portion (a), VDG (b) FDS plot with SPV, (c) FDS plot with UPV.

The plot in Fig. 8.3a reflects values in the region  $0 \leq r \leq \sqrt{5}$  because the factorial points are at radius  $\sqrt{5}$ . The VDG shows how additional center runs lower  $v(\mathbf{x})$  at the center of the design space at the cost of slightly worsening prediction at the edge of the design space. This worsening is a function of  $v(\mathbf{x})$  penalizing larger designs. The rate of improvement at the center is diminishing and becomes marginal for additional center runs after  $n_c = 4$ . The FDS shows the same information in a different way, with the minimum  $v(\mathbf{x})$  shown at the left of the plot, and the maximum  $v(\mathbf{x})$  at the right for each design. In terms of  $G$ -efficiency, the best design is the CCD with  $n_c = 1$ , but this has the largest minimum  $v(\mathbf{x})$  value. Notice how the VDG accentuates the improvement at the center of the design space, even though this is proportionately a much smaller fraction of the design region than at the edge of the design space.

In Fig. 8.3c, a FDS plot is shown for the unscaled prediction variance. As discussed in Chapter 7, the unscaled prediction variance is useful to consider when we are interested in the raw improvement in prediction variance for additional runs of our experiment. In this plot, we see the effect of the additional center runs on the overall prediction performance. With the scaled prediction variance, there was a trade-off in prediction performance on a per observation basis, with improvements at the center of the design space resulting in a slightly worse  $v(\mathbf{x})$  at the edge of the design space. With the unscaled prediction variance, we see that the additional center runs (and corresponding increase in design size) can only improve the prediction. There are slight gains throughout a majority of the design space, but the maximum unscaled prediction variance at the edge of the design space is unaffected by additional observations at the center of the design space.

**Example 8.4 Comparison of the CCD and the BBD** In this illustration we use the variance dispersion graph and fraction of design space plot to show a comparison of the distribution of  $v(\mathbf{x})$  in the design region between a CCD and a BBD. The reader should recall that both of these very popular designs are spherical designs. Both designs involve three design variables, with the CCD having  $\alpha = \sqrt{3}$  and  $n_c = 3$ , while the BBD also contains three center runs. One must keep in mind that the total sample sizes are 17 and 15 for the CCD and BBD, respectively. A plot with both VDGs is in Fig. 8.4a. Note that both designs contain three lines in the VDG; the min  $v(\mathbf{x})$ , average  $v(\mathbf{x})$ , and max  $v(\mathbf{x})$  are shown because neither design is rotatable. The plots stop at radius  $\sqrt{3}$ . Both designs have been scaled so that points are at a radius  $\sqrt{3}$  from the design center. Figure 8.4b shows the FDS plot for the same two designs.

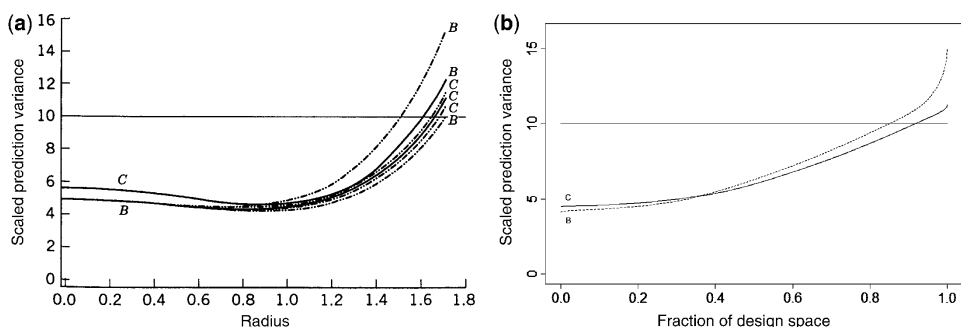


**Figure 8.4** Variance dispersion graphs (a) and fraction of design space plots (b) for CCD (C) and Box–Behnken design (B) for  $k = 3$ . Both designs contain three center runs.

The following represent obvious conclusions from the plots.

1. The combination of the VDG and FDS plots provide a wealth of information about the two designs being compared. From the FDS plot it is easy to see that the BBD has better minimum prediction than the CCD, but at the cost of worse maximum prediction at the edge of the design space. The minimum  $v(\mathbf{x})$  for both designs occurs at a radius between 0.8 and 1.0.
2. The values of  $v(\mathbf{x})$  become much larger for the BBD at the very edge of the region, but only a very small proportion of the region has these very large  $v(\mathbf{x})$  values. Hence  $G$ -efficiency, which considers only the maximum  $v(\mathbf{x})$  can be somewhat deceptive about what is happening with the majority of the design space.
3. Comparison with the ideal design is readily seen for both designs. The maximum  $v(\mathbf{x})$  in the design region is roughly 15 for the BBD and 11.2 for the CCD. Thus the  $G$ -efficiencies for the two designs are  $(10/11.2) \times 100 = 89\%$  for the CCD and  $(10/15) \times 100 = 67\%$  for the BBD. These numbers correspond to those given in Table 8.2.
4. Comparing the two designs is somewhat easier using the FDS plot since each design is summarized with a single curve, while the non-rotatability of the designs makes comparing using the three curves with the VDG a bit more difficult. However, being able to see where the good and bad  $v(\mathbf{x})$  values occur is only available using the VDGs.
5. The  $\alpha = \sqrt{3}$  CCD is nearly rotatable. This is not surprising because  $\alpha = 1.682$  results in exact rotatability. The slight deviation from rotatability occurs close to the design perimeter. The BBD shows a more pronounced deviation from rotatability that becomes greater as one nears the edge of the design space.
6. The values of  $v(\mathbf{x})$  are very close for the two designs near the design center. In fact the difference at the center is accounted for by the difference in the sample sizes.
7. For prediction from radius 1.0 to  $\sqrt{3}$  the CCD is the better design. The stability in  $v(\mathbf{x})$  is greater with the CCD, and the max  $v(\mathbf{x})$  is smaller than that of the BBD. This is also reflected in the FDS plot where for all fractions along the  $x$ -axis greater than 0.4, the CCD has the smaller  $v(\mathbf{x})$  value.

The illustration in this example nicely underscores the usefulness of graphical methods for comparing competing designs. It also illustrates how a single-number efficiency, while useful, cannot capture design performance. For example, the clear distinction between the two designs in terms of prediction errors is not captured in the comparison of  $D$ -efficiencies (97.63% and 93.82%) from Table 8.2. In addition, the  $G$ -efficiencies accurately reflect the differences that exist in  $v(\mathbf{x})$ , *but only at the design perimeter*. Almost without exception (completely without exception in the first-order case), max  $v(\mathbf{x})$  in a design region for a second-order design occurs at the design perimeter. Thus  $G$ -efficiency reflects what is occurring at the design perimeter.

**Example 8.5 Comparison of Different Axial Values of the CCD** In Fig. 8.5 we show the graphical summaries for three CCDs with  $k = 5$  in a spherical region with maximum radius  $\sqrt{5}$ . The  $\alpha$ -values are 1.5, 2.0, and  $\sqrt{5}$ . In each case the factorial portion is a resolution V fraction. Each design contains three center runs, and thus the total design size is  $N = 29$ . The  $\alpha = 1.5$  design is not expected to predict as well near the edge of the design space, because the axial points are not placed at or near the region perimeter. The  $\alpha = 2.0$  design is rotatable because  $\alpha = \sqrt[4]{16} = \sqrt[4]{F} = 2.0$ .

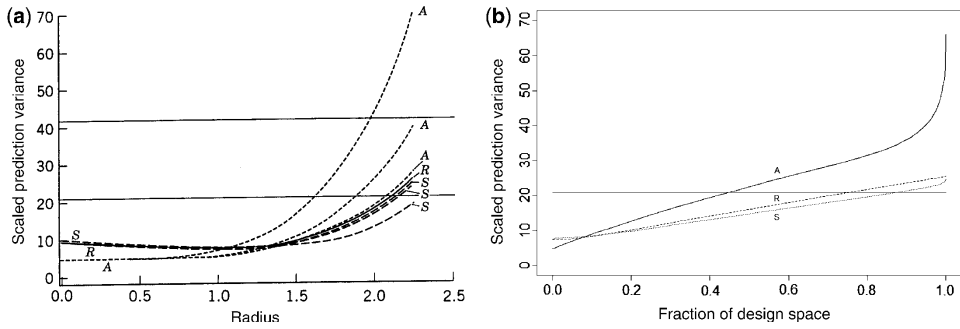


**Figure 8.5** VDG and FDS for three CCDs for  $k = 5$ . Design A contains  $\alpha = 1.5$ , design R contains  $\alpha = 2.0$ , and design S contains  $\alpha = \sqrt{5}$ . Each contains a  $2^{5-1}$  and three center runs.

The following are conclusions drawn from Fig. 8.5.

1. The use of  $\alpha = 1.5$  does result in a loss in efficiency compared to the other two designs. While the prediction is better in the design center, it suffers at the perimeter. The FDS plot shows that this benefit occurs for less than 10% of the total design space. In fact, one gains some insight into how much efficiency is lost with  $\alpha = 1.5$  by observing that the value of  $\max v(\mathbf{x})$  at the design perimeter is roughly 65. The two horizontal lines in the VDG are at  $p$  and  $2p$ , representing  $G$ -efficiencies of 100% and 50%. The  $G$ -efficiency for the  $\alpha = 1.5$  design is roughly  $(21/65) \times 100 \cong 32\%$ .
2. While  $\alpha = 2.0$  is the rotatable value, the use of  $\alpha = \sqrt{5}$  and the resulting loss of rotatability do not produce severe instability in  $v(\mathbf{x})$ . The same appeared to be true for the  $\alpha = \sqrt{3}$  CCD in Fig. 8.4. Again, this VDG reflects the fact that for the CCD, allowing the value of  $\alpha$  to be pushed to the edge of the design perimeter, namely to  $\sqrt{k}$ , is preferable, even if rotatability is compromised. Clearly the loss in rotatability is a trivial matter here and for the CCD in Fig. 8.4. The  $\max v(\mathbf{x})$  plot for design S or design R reflects a  $G$ -efficiency of roughly 85%, which is consistent with the results in Table 8.2.
3. The choice of  $\alpha = \sqrt{5}$  improves estimation not only at the edge of the design space, but also throughout most of the region. By comparing the lines of the FDS plot, we can see that the lower line for the  $\alpha = \sqrt{5}$  CCD represents a helpful improvement in reducing  $v(\mathbf{x})$ .

One pragmatic point needs to be made here regarding design S in Fig. 8.5. For  $k = 5$  and other large values, the “best” CCD requires  $\alpha = \sqrt{k}$ . This requires the levels set by the investigator to be  $-2.236, -1, 0, 1, 2.236$ . This design may, in fact, produce practical problems because the axial level is much larger than the factorial level. Indeed, the evenly spaced levels of design R may be more reasonable. For  $k = 2, 3$ , and  $4$ , this is not a serious problem.

**Example 8.6 Hybrid Designs and SCDs** In previous sections we mentioned the importance of the class of hybrid designs in cases where the researcher requires the use of a small design size. The efficiencies of the hybrid design in Table 8.2 are quite good for saturated or near-saturated designs, though this may not be apparent, because we showed no comparisons with other designs of small sample size. In Fig. 8.6a we show overlaid VDGs of a hybrid 416B with four center runs and a  $k = 4$  SCD with three center runs. The small composite contains a resolution III  $2^{4-1}$  with axial value  $\alpha = 2.0$ . Figure 8.6b shows the corresponding FDS plot for the two designs.

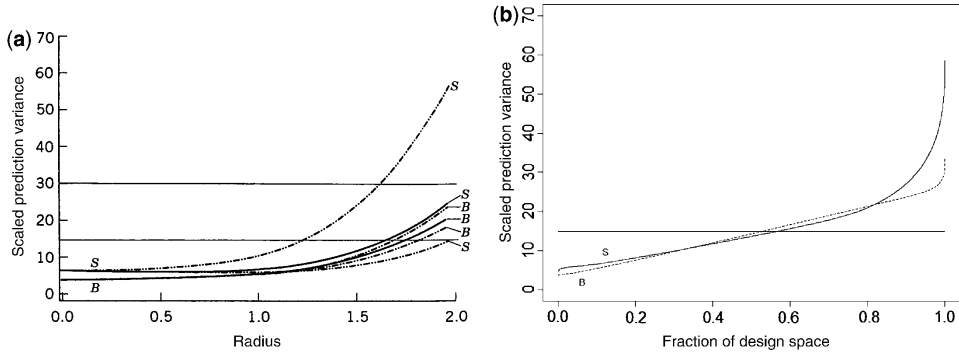


**Figure 8.6** Variance dispersion graphs and fraction of design space plots for hybrid 416B and SCD. Design  $B$  is hybrid 416B.  $N = 19$  for the SCD and  $N = 20$  for 416B.

From the  $p$  and  $2p$  lines it is clear that the 416B is considerably more efficient. The  $G$ -efficiency of the 416B is roughly 60%, while the  $G$ -efficiency for the SCD is only slightly above 25%. More importantly, the max  $v(\mathbf{x})$  for the SCD becomes large very quickly. The discrepancy between the designs is not only at the design perimeter. The FDS plot shows that the 416B design has a smaller minimum  $v(\mathbf{x})$ , is competitive with the SCD for most fraction of the design, and far superior with a much smaller maximum  $v(\mathbf{x})$ . As the number of factors increases, the maximum  $v(\mathbf{x})$  of the SCD rises very rapidly making this a poor choice of design for good prediction.

**Example 8.7 Adding Center Runs to Hybrid Designs** Figure 8.7 gives overlaid VDGs for the hybrid 310 with a center run added and for the hybrid 311B. One should note from the efficiency table (Table 8.2) that both the  $D$ - and  $G$ -efficiency for the 311B are quite good compared to the 310. Indeed, from Fig. 8.7a it is clear that the 311B is nearly rotatable with high  $G$ -efficiency. However, what the efficiency figures do not reflect is that the prediction variance is much smaller for the 310 near the design center. The FDS plot of Fig. 8.7b helps clarify the relative proportion of the design space affected by the poorer prediction at the center by 311B. The apparent advantage of better prediction by 310 represents only a small fraction of the total volume of the design space. The better prediction of the 311B at the perimeter is much more dominant than is highlighted by the

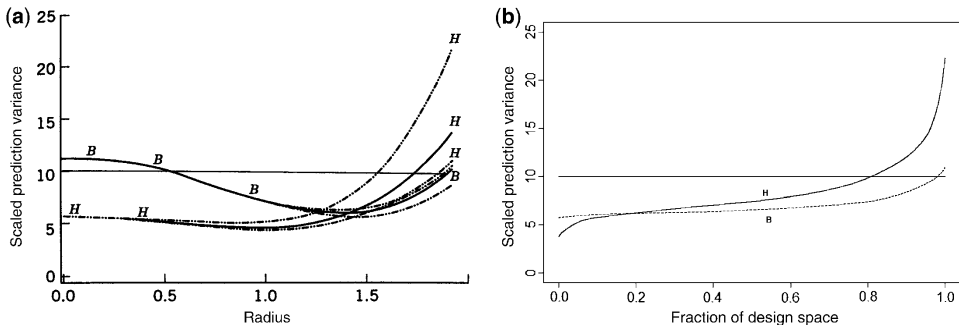


**Figure 8.7** VDGs and FDS for 310 plus one center run and for 311B. Design  $B$  is hybrid 311B, and design  $H$  is hybrid 310.

VDG. Again, the combination of the VDG and FDS plot allows for improved understanding of  $v(\mathbf{x})$  throughout the design region.

Incidentally, the picture suggests that an additional center run for the 311B would substantially reduce  $v(\mathbf{x})$  at the center. This, in fact, is the case. An additional run in the center reduces  $v(\mathbf{x})$  to approximately the value achieved by the 310. Interestingly, this increases  $v(\mathbf{x})$  at the perimeter slightly, *thereby reducing the G-efficiency*. Thus, we have often seen situations of a design (311B + one center run) that has a smaller *G*-efficiency (and *D*-efficiency in this case) than does a clearly inferior design (311B). Figure 8.8 shows a VDG to compare the same two designs as in Fig. 8.7 with the additional center run given to the 311B.

**VDGs for Cuboidal Designs** All of the preceding discussion and illustration deal with variance dispersion graphs for spherical regions. In this case it is natural to observe values of  $v(\mathbf{x})$  averaging over the surfaces of spheres. Then the minimum and maximum of  $v(\mathbf{x})$  is taken over the surfaces of spheres. However, it is not natural to deal with surfaces of spheres when the design is cuboidal, and hence the natural region of interest is a cube. As a result, the variance dispersion graph contains the following components:

1. A plot of the **cuboidal variance**  $V^{r*}$  against  $r$ , the half edge of a cube:  $V^{r*}$  is defined as

$$V^{r*} = \frac{N\psi^*}{\sigma^2} \int_{U_r^*} \left[ \frac{\text{Var}[\hat{y}(\mathbf{x})]}{\sigma^2} \right] d\mathbf{x}$$

where  $U_r^*$  is the surface area of the cube with half edge  $r$  and  $\int_{U_r^*}$  implies integration over the surface area of the same cube. In our illustrations  $r$  is called the **radius**. We define  $\psi^* = (\int_{U_r^*} d\mathbf{x})^{-1}$ .

2.  $\max_{\mathbf{x} \in U_r^*} [v(\mathbf{x})]$ .
3.  $\min_{\mathbf{x} \in U_r^*} [v(\mathbf{x})]$ .

As a result, the average and range of  $v(\mathbf{x})$  are depicted over the surface of cubes that are nested inside the cube defined by the design region. Figure 8.9 gives the reader an impression of what

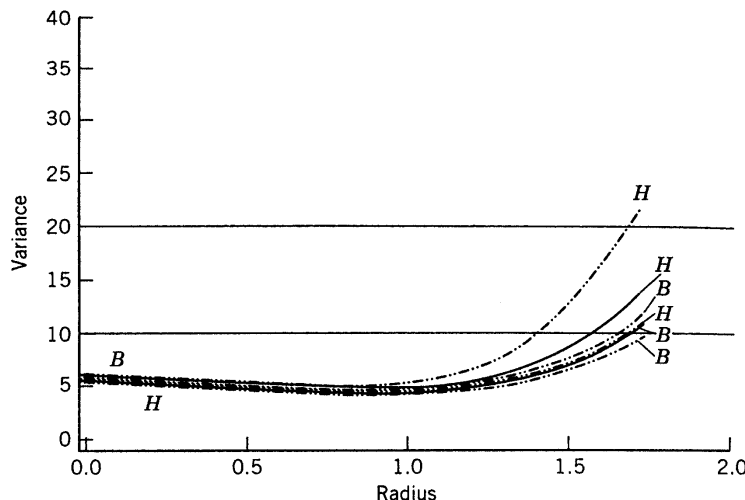
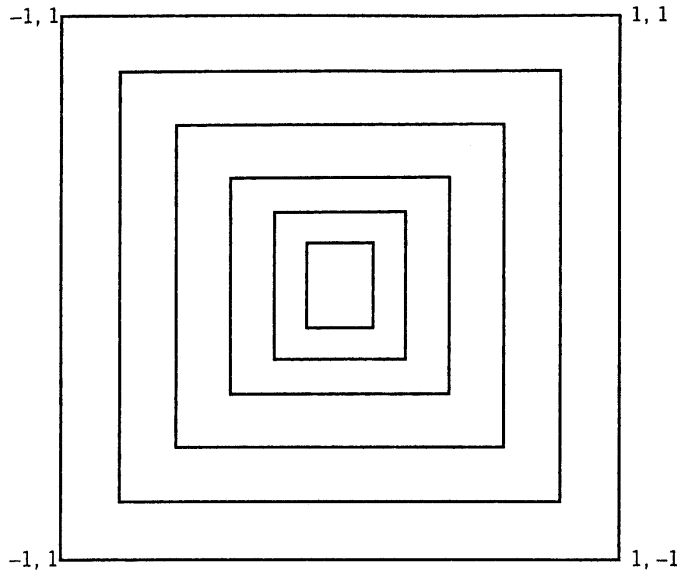


Figure 8.8 VDGs for 310 plus one center run and for 311B plus one center run.



**Figure 8.9** Nested cubes of the VDG for cuboidal designs.

is displayed by the VDG. Averages, maxima, and minima are computed for half edges from 0 to 1.0. These values are plotted in a two-dimensional graph. Spheres nested inside the design cube can be used as the media for the graphs. See Myers et al. (1992b). However, cubes nested inside the design cube are more natural, just as rotatability [i.e., constant  $v(\mathbf{x})$  on spheres] is a more important criterion for spherical regions of interest than for cuboidal regions.

**FDS Plots for Cuboidal Regions** The adaption of the FDS plot needed for cuboidal regions is much simpler than for the VDGs. Indeed for any shaped design region, the FDS plot remains unchanged. The  $x$ -axis still is from 0 to 1, and the interpretation of the quantiles is the same. For calculating the values of  $v(\mathbf{x})$ , we sample uniformly from our newly shaped region, calculate  $v(\mathbf{x})$ , and plot the sorted values against the appropriate quantiles.

**Comparison of  $3^3$  Factorial with Face-Centred Cube** Although the CCD involves considerably fewer design points than the three-level factorial design for  $k = 3$ , they are natural rival designs when the design region is a cube. Of course, the scaled prediction variance will involve a sample size weighting of  $N = 27$  for the factorial design and  $N = 15$  for the  $\alpha = 1$  CCD, that is the face-centered cube (FCC). Figure 8.10 shows the VDGs for the two designs, and Fig. 8.11 shows the corresponding FDS plot. The FCC design predicts considerably better near the center of the design space, and has very stable prediction for points of radius 0.6 or less. From the FDS plot we can see that the  $3^3$  factorial design is being heavily penalized for its large design size with poorer performance at both the minimum and maximum  $v(\mathbf{x})$  values. The stability of prediction for the  $3^3$  factorial design is quite good for most of the region, with only a small fraction of the region (less than 2%) having much larger  $v(\mathbf{x})$  values. The  $G$ -efficiency of the FCC is better than that of the  $3^3$  factorial design. Certainly the face-centered cube is an important design for cuboidal regions. However, if cost-considerations allow for a design of size  $N = 27$ , the full  $3^3$  factorial design is a good alternative.

Variance dispersion graphs for cuboidal regions are no less important than those for spherical regions. Both are useful tools for comparing competing designs. The VDG will

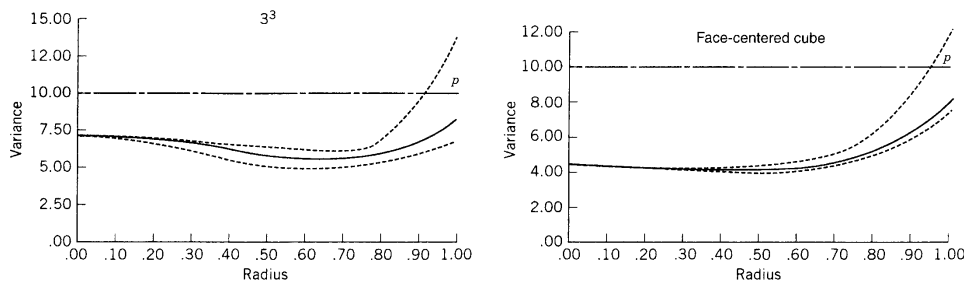


**Figure 8.10** Variance dispersion graphs for the  $3^3$  factorial and the face-centered cube (FCC).

surface again later in this chapter as we focus on computer-generated designs. Information regarding software for construction of VDGs can be found in Vining (1993), Rozum and Myers (1991), and Borror (1998).

**Extensions and Alternatives to the VDG and FDS Plots** There have been a number of very useful extensions of the VDG. Trinca and Gilmour (1998) extend the VDG to situations where the response surface design has been run in **blocks**. They point out that allocation of runs to the blocks can have serious effects on the prediction properties of a design. Vining and Myers (1991) extend the VDG to plots of the **average mean square error**, which is the sum of prediction variance and squared bias (use of mean square error and bias in design selection is discussed in Chapter 9). Borror, Montgomery, and Myers (2002) construct VDGs for experiments containing **noise variables**. These designs are used extensively in process robustness studies (see Chapter 10). Vining, Cornell, and Myers (1993) show how to develop VDGs for mixture designs (see Chapters 11 and 12 for an introduction to experiments with mixtures).

Goldfarb et al. (2004a) developed three-dimensional VDGs for mixture-process experiments, where interest lies in understanding differences in  $v(\mathbf{x})$  separately for the mixture and process variables. Goldfarb et al. (2004b) also adapted FDS plots for mixture and mixture-process experiments. Liang et al. (2006a, 2006b) created VDGs and FDS plots for

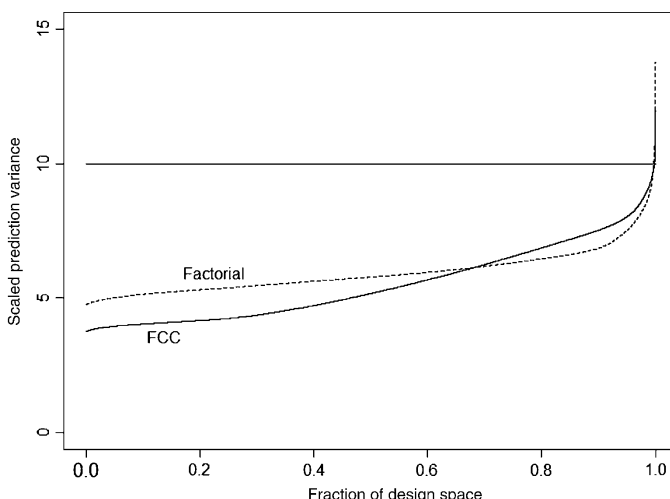


**Figure 8.11** Fraction of design space plot for comparing  $3^3$  factorial and the face-centered cube (FCC).

split-plot designs, where the whole plot and split-plot characteristics could be examined separately. Ozol-Godfrey et al. (2005) and Anderson-Cook et al. (2009) adapted FDS plots to prediction when the assumed model may not be correct. Liang et al. (2007) consider alternative FDS plots which adjust for different cost-structures for split-plot designs, which allow for flexible comparison of quality of prediction versus the cost of running the experiment.

Khuri et al. (1996) describe a method for describing the entire distribution of prediction variance over the design region. They do this by plotting **quantiles** of the prediction variance distribution. They note that quantile plots give more information than VDGs and present an example where the VDGs of the competing designs are quite similar yet the quantile plots of prediction variance are very different. Khuri, Harrison, and Cornell (1999) extend this technique to experiments with mixtures.

A dynamic graphical tool for visualizing the prediction variance is available in JMP. This allows the user to interactively examine the unscaled prediction variance of a design. Figure 8.12 shows the prediction variance for the face-centered cube for  $k = 3$  at both the center (0,0,0) and corner (1,1,1) of the design region. When used in JMP, any combination of factor levels in the design region can be explored. Note that the maximum unscaled prediction variance value of 0.797222 obtained at any corner of the design space, matches with the maximum values of  $0.797222 \times 15 = 11.958$  in the VDG and FDS plots of Figs. 8.10 and 8.11.

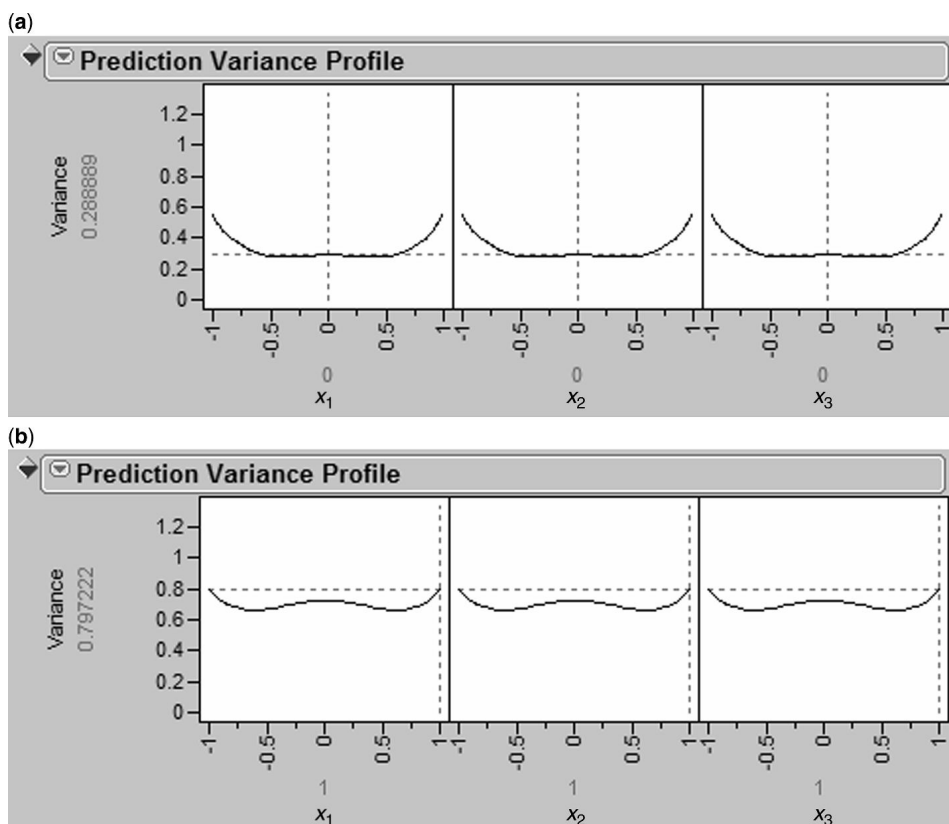


**Figure 8.12** Prediction profiler from JMP to show the prediction variance for the face-centered cube for  $k = 3$  at the center (a) and corner (b) of the design region.

### 8.3 COMPUTER-GENERATED DESIGNS IN RSM

Computer-generated design of experiments was the natural extension of design optimality as the computer era in statistics unfolded in the late 1960s and early 1970s. Today many computer packages generate designs for the user. While many criteria are available, the criterion most often used is  $D$ -optimality or, rather,  $D$ -efficiency. In addition, some computer packages offer a criterion that involves the use of  $v(\mathbf{x})$ , the scaled prediction variance. There were many important papers that provided the fundamental theory that led to the current state of technology in computer-generated design. The work of Dykstra (1966), Covey-Crump and Silvey (1970), and Hebble and Mitchell (1972) represent but a few important contributions.

The computer is used to aid the researcher in designing RSM experiments in several ways. Some of these are as follows:

1. *To design an experiment from scratch.* The user inputs a model, required sample size, set of candidate points, ranges on the design variables, and other possible constraints (e.g., blocking information).
2. *To augment or repair a current experimental design.* The input information is often the same as in item 1.
3. *To replace points in a current experimental design.* Often input information is as in item 1.
4. *To construct the “ideal” standard experimental design for a particular region of interest or to satisfy certain restrictions.*

One should notice the reference to a list of candidate points. The implication is that the computer picks from this list for design augmentation or constructing a design from scratch. If the candidate list is not supplied, often the package will select as a default a grid of points of its choice. Thus, the design chosen certainly is a discrete design, and the goal is to select the design with the highest efficiency, say  $D$ -efficiency. With increased computer power, finding optimal designs has become more tractible.

#### 8.3.1 Important Relationship between Prediction Variance and Design Augmentation for $D$ -Optimality

An important relationship exists between the coordinates of points that augment an existing design via  $D$ -optimality and the concept of prediction variance. In fact, it is this relationship that is the foundation of computer-aided design of experiments. The result has to do with the selection of the  $(r + 1)$ th point in an existing design containing  $r$  points. The coordinates to be chosen will be those such that  $|M|$  is maximized. As a result, the  $(r + 1)$ th point chosen is that which produces a **conditional  $D$ -optimality**—that is, that which gives  $D$ -optimality given the initial  $r$ -point design. The result is as follows:

Given an  $r$ -point design with design and model characterized by  $\mathbf{X}_r$ , the point  $\mathbf{x}_{r+1}$  that maximizes  $|\mathbf{X}'_{r+1}\mathbf{X}_{r+1}|$  is that for which  $\mathbf{x}_{r+1}^{(m)\prime}(\mathbf{X}'_r\mathbf{X}_r)^{-1}\mathbf{x}_{r+1}^{(m)}$  is maximized. Hence  $\mathbf{X}_{r+1}$  is the  $\mathbf{X}$ -matrix containing the  $(r + 1)$ th point.

To understand this result, let us begin with a well-known result dealing with the determinant of a matrix. Given a square matrix

$$\mathbf{A} = \begin{bmatrix} \mathbf{A}_{11} & \mathbf{A}_{12} \\ \mathbf{A}_{21} & \mathbf{A}_{22} \end{bmatrix}$$

then if  $\mathbf{A}_{22}$  is nonsingular,

$$|\mathbf{A}| = |\mathbf{A}_{22}| |\mathbf{A}_{11} - \mathbf{A}_{12}\mathbf{A}_{22}^{-1}\mathbf{A}_{21}|$$

and if  $\mathbf{A}_{11}$  is nonsingular,

$$|\mathbf{A}| = |\mathbf{A}_{11}| |\mathbf{A}_{22} - \mathbf{A}_{21}\mathbf{A}_{11}^{-1}\mathbf{A}_{12}|$$

Now let

$$\mathbf{X}_{r+1} = \begin{bmatrix} \mathbf{X} \\ \vdots \\ \mathbf{x}'_{r+1} \end{bmatrix}$$

denote the  $\mathbf{X}$ -matrix after  $\mathbf{x}_{r+1}$  has been selected. Obviously,  $\mathbf{X}$  is  $\mathbf{X}_{r+1}$  apart from the selected point. It is easy to show that

$$(\mathbf{X}'\mathbf{X}) = \mathbf{X}'_{r+1}\mathbf{X}_{r+1} - \mathbf{x}_{r+1}\mathbf{x}'_{r+1}$$

and hence

$$\begin{aligned} |\mathbf{X}'_{r+1}\mathbf{X}_{r+1} - \mathbf{x}_{r+1}\mathbf{x}'_{r+1}| &= \begin{vmatrix} \mathbf{X}'_{r+1}\mathbf{X}_{r+1} & \mathbf{x}_{r+1} \\ \mathbf{x}'_{r+1} & 1 \end{vmatrix} \\ &= |\mathbf{X}'_{r+1}\mathbf{X}_{r+1}| |1 - \mathbf{x}'_{r+1}(\mathbf{X}'_{r+1}\mathbf{X}_{r+1})^{-1}\mathbf{x}_{r+1}| \end{aligned}$$

Now the above implies that

$$|\mathbf{X}'\mathbf{X}| = |\mathbf{X}'_{r+1}\mathbf{X}_{r+1}| |1 - \mathbf{x}'_{r+1}(\mathbf{X}'_{r+1}\mathbf{X}_{r+1})^{-1}\mathbf{x}_{r+1}|$$

Thus, because  $1 - \mathbf{x}'_{r+1}(\mathbf{X}'_{r+1}\mathbf{X}_{r+1})^{-1}\mathbf{x}_{r+1}$  is a scalar, we have

$$\frac{|\mathbf{X}'_{r+1}\mathbf{X}_{r+1}|}{|\mathbf{X}'\mathbf{X}|} = \frac{1}{1 - \mathbf{x}'_{r+1}(\mathbf{X}'_{r+1}\mathbf{X}_{r+1})^{-1}\mathbf{x}_{r+1}}$$

A well-known result for regression analysis relates  $\mathbf{x}'_{r+1}(\mathbf{X}'_{r+1}\mathbf{X}_{r+1})^{-1}\mathbf{x}_{r+1}$  to  $\mathbf{x}'_{r+1}(\mathbf{X}'\mathbf{X})^{-1}\mathbf{x}_{r+1}$ . Keep in mind that the former relates to the variance of a predicted value at the location defined by  $\mathbf{x}_{r+1}$ , whereas the latter relates to the prediction variance at  $\mathbf{x}_{r+1}$  for a fitted model *before the new point was placed in the data set*. From Myers (1990) or Montgomery et al. (2006) we have

$$\mathbf{x}'_{r+1}(\mathbf{X}'\mathbf{X})^{-1}\mathbf{x}_{r+1} = \frac{\mathbf{x}'_{r+1}(\mathbf{X}'_{r+1}\mathbf{X}_{r+1})^{-1}\mathbf{x}_{r+1}}{1 - \mathbf{x}'_{r+1}(\mathbf{X}'_{r+1}\mathbf{X}_{r+1})^{-1}\mathbf{x}_{r+1}}$$

One desires to select  $\mathbf{x}_{r+1}$  in order to maximize  $|\mathbf{X}'_{r+1}\mathbf{X}_{r+1}|$  for *D*-optimality. Because  $\mathbf{x}'_{r+1}(\mathbf{X}'_{r+1}\mathbf{X}_{r+1})^{-1}\mathbf{x}_{r+1}$  is a hat diagonal, we obtain  $\mathbf{x}'_{r+1}(\mathbf{X}'_{r+1}\mathbf{X}_{r+1})^{-1}\mathbf{x}_{r+1} \leq 1$ . One then must choose  $\mathbf{x}_{r+1}$  so that  $\mathbf{x}'_{r+1}(\mathbf{X}'_{r+1}\mathbf{X}_{r+1})^{-1}\mathbf{x}_{r+1}$  is maximized. From the above Equation,

maximizing  $\mathbf{x}'_{r+1}(\mathbf{X}'_{r+1}\mathbf{X}_{r+1})^{-1}\mathbf{x}_{r+1}$  is equivalent to maximizing  $\mathbf{x}'_{r+1}(\mathbf{X}'\mathbf{X})^{-1}\mathbf{x}_{r+1}$ . Thus one should choose the next point  $\mathbf{x}_{r+1}$  at which the prediction variance (i.e.,  $\text{Var}[\hat{y}(\mathbf{x}_{r+1})]/\sigma^2$ ) is maximized.

The above result is not only interesting but also very useful. It essentially says that for design augmentation, the *next point* that is most appropriate in a *D*-optimality sense is that for which the prediction is worse when one uses the current design for prediction. In other words,  $\mathbf{x}_{r+1}$  is a type of “soft spot,” and putting this spot in the design produces the design that is conditionally *D*-optimal.

**Example 8.8 An Example with  $k = 2$**  Consider an initial design containing a  $2^2$  factorial:

$x_1$	$x_2$
-1	-1
-1	1
1	-1
1	1

The model is a first-order model in two design variables. Now, suppose the candidate list of points are those of a  $3^2$  factorial design. The next point to be chosen is that for which  $\mathbf{x}^{(1)'}(\mathbf{X}'\mathbf{X})^{-1}\mathbf{x}^{(1)}$  is largest. Here, of course,  $\mathbf{x}^{(1)'} = [1, x_1, x_2]$  and  $(\mathbf{X}'\mathbf{X})^{-1} = \frac{1}{4}\mathbf{I}_3$ , reflecting the fact that the initial design is first-order orthogonal. As a result, the expression  $\text{Var}[\hat{y}(\mathbf{x})]/\sigma^2 = \mathbf{x}^{(1)'}(\mathbf{X}'\mathbf{X})^{-1}\mathbf{x}^{(1)}$  is given by

$$\begin{aligned} [1, x_1, x_2] & \begin{bmatrix} \frac{1}{4} & 0 & 0 \\ 0 & \frac{1}{4} & 0 \\ 0 & 0 & \frac{1}{4} \end{bmatrix} \begin{bmatrix} 1 \\ x_1 \\ x_2 \end{bmatrix} \\ &= \frac{1}{4} [1 + x_1^2 + x_2^2] \end{aligned}$$

As a result, the values of  $\text{Var}[\hat{y}(\mathbf{x})]/\sigma^2$  for the candidate list are

$x_1$	$x_2$	$\text{Var}[\hat{y}(\mathbf{x})]/\sigma^2$
-1	-1	$\frac{3}{4}$
-1	1	$\frac{3}{4}$
1	-1	$\frac{3}{4}$
1	1	$\frac{3}{4}$
0	-1	$\frac{1}{2}$
0	1	$\frac{1}{2}$
-1	0	$\frac{1}{2}$
1	0	$\frac{1}{2}$
0	0	$\frac{1}{4}$

Thus the best augmentation of the  $2^2$  factorial is another factorial point, and it makes no difference which one of the four is added. An interesting point here is that if the center run is added, the design remains orthogonal; but a five-run nonorthogonal design is

preferable (in the  $D$ -optimal sense). This is an example that points out a shortcoming of a  $D$ -optimal design. Many experimenters would prefer to add the center run to provide some information about lack of fit. However, the optimal design will never include the center point, because the assumption is that the model is correct.

**Example 8.9 An Irregular Fraction with  $k = 3$**  Consider a situation in which one wishes to fit the model

$$y = \beta_0 + \beta_1 x_1 + \beta_2 x_2 + \beta_3 x_3 + \beta_{12} x_1 x_2 + \varepsilon$$

The initial design is the irregular fraction

$x_1$	$x_2$	$x_3$
-1	-1	-1
1	1	-1
1	-1	1
-1	1	1
1	1	1

This is a five-point design and all parameters are estimable. Suppose the list of candidate points includes the complete  $2^3$  design. Computation of  $\text{Var}[\hat{y}(\mathbf{x})]/\sigma^2$  is given below for the candidate list:

$x_1$	$x_2$	$x_3$	$\text{Var}[\hat{y}(\mathbf{x})]/\sigma^2$
-1	-1	-1	1.0
-1	-1	1	3.0
-1	1	-1	3.0
-1	1	1	1.0
1	-1	-1	3.0
1	-1	1	1.0
1	1	-1	1.0
1	1	1	1.0

As a result, the best augmentation of the initial design involves the use of any one of the points  $(-1, -1, 1)$ ,  $(-1, 1, -1)$ , and  $(1, -1, -1)$ . Nearly all of the software algorithms make use of conditional optimization gives the existing points. It is obvious how it is used for design augmentation. In this regard, one must keep in mind that a candidate list of points is used; as a result, the augmentation is chosen, sequentially one at a time, from points in the candidates list. When a design is chosen from scratch, the same result applies.

Two types of exchange algorithms are common: **point exchange** and **coordinate exchange**. In the point exchange algorithm, a random design of the appropriate size is created from the set of candidate points. Then new designs are created by iteratively replacing individual points with the best replacement available from the candidates, conditional on the other points in the design. This is repeated for all points in the design until no improvements are possible. The entire process is repeated multiple times for different random initial designs, and the best overall design from all the starts is selected.

Coordinate exchange is a candidate-free approach, which begins with a random design of the appropriate size. Each coordinate for each factor for each design point is sequentially

adjusted to its optimal value within the range of that factor, conditional on all other coordinates and points in the design. This is repeated for all coordinates in the design until no further improvements exist. As with the point exchange algorithm, multiple random initial designs are considered and the best overall design from all starts is chosen.

If *D*- or *I*-optimality are the selected criteria for the above algorithms, there are computationally efficient methods for updating the effect on the determinant from changing a single point within a design. Hence, these algorithms can be used quickly and easily, and can consider a large number of initial designs in a timely manner. If *G*-optimality is considered, the search for best designs can be more time-consuming and requires more computational effort.

Because construction of an alphabetically optimal design is essentially a combinatorial optimization problem, methods for solving these types of problems could also be employed. Indeed, some authors have used **branch and bound techniques** (Welch, 1982) to construct optimal designs. **Simulated annealing** (Meyers and Nachtsheim, 1998) and **genetic algorithms** (Heredia-Langner et al., 2003) have also been used.

It should be strongly emphasized that the goal of the computer-generated design algorithms is to produce a design that gives *approximately* the highest *D*-efficiency. Different packages may, indeed, produce different designs with the same input information.

### 8.3.2 Illustrations Involving Computer-Generated Design

In this section we focus on a few illustrations of computer-generated designs with emphasis on the use of JMP and Design-Expert. This does not mean to imply that these are the only or even the best computer packages. Following the illustrations, the appropriateness, advantage, and disadvantages of computer-generated design will be addressed. Our first example is a fairly simple one where, based on our discussions in this and other chapters, the reader likely could have correctly conjectured the most appropriate design.

**Example 8.10 *D*- and *I*-Optimal Designs for a Nonstandard Model** Suppose there are  $k = 3$  design variables, and an intelligent “guess” gives the appropriate model as

$$y = \beta_0 + \beta_1 x_1 + \beta_2 x_2 + \beta_3 x_3 + \beta_{11} x_1^2 + \varepsilon$$

The ranges being considered by the researcher are  $[-1, +1]$  (coded) for all three variables. Using the “Custom Design” option under “DOE” in JMP, we specify the model with three continuous factors and the model given above. Figure 8.13 shows the dialog boxes for creating the design, while Fig. 8.14 shows the created design. Under the red arrow for Custom Design show in Fig. 8.13, the “Optimality Criterion” selected was “Make *D*-Optimal Design.”

Note that the design in the output is a  $3 \times 2 \times 2$  factorial. As the reader might expect, three levels were selected for  $x_1$ , while only two levels were selected for each of  $x_2$  and  $x_3$ . The design chosen is *D*-optimal. It turns out that the *G*-efficiency of the design is 100%. In fact, the maximum value of  $N \text{Var}[\hat{y}(\mathbf{x})]/\sigma^2$  is five, the total number of model parameters. This can be evaluated by using the FDS plot or the Prediction Variance Profiler to find that the maximum value of  $v(\mathbf{x}) = \text{Var}[\hat{y}(\mathbf{x})]/\sigma^2$  is 0.4167. Note that JMP gives the prediction variance in the output which is not scaled by the sample size, and  $5 = 12 \times 0.4167$ .

As a result the design is *G*-optimal. Note that the *I*-efficiency of the design is difficult to assess, since this value is not provided in the output. By looking at the 0.5 fraction of the FDS plot, we can estimate the median value of the prediction variance, but this value is likely not a good approximation of the average prediction variance since the distribution of the prediction variance throughout the design space is skewed.

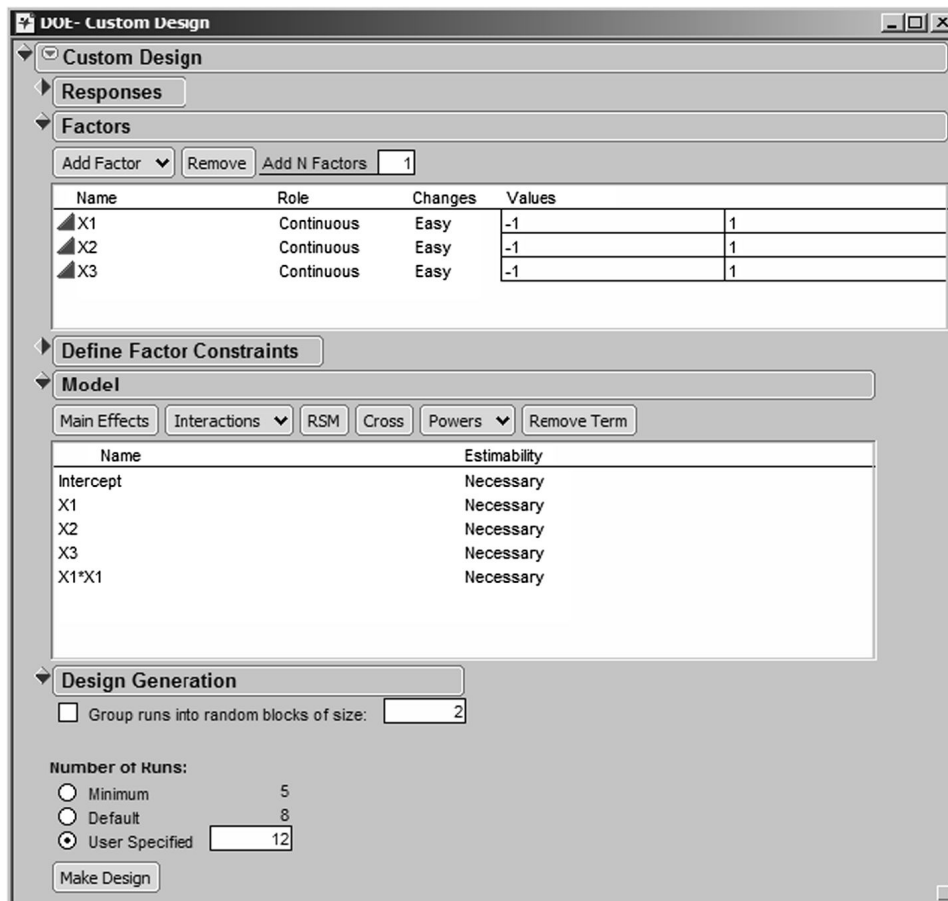


**Figure 8.13** Custom Design dialog box from JMP to create design with 12 runs for the nonstandard model.

If instead of focusing on *D*-optimality, we had been interested in using the *I*-optimality criterion, we could specify this option in JMP with the “Optimality Criterion” selected as “Make *I*-Optimal Design.” The design obtained is as follows:

$x_1$	$x_2$	$x_3$
-1	-1	1
-1	1	1
-1	1	-1
0	1	1
0	1	1
0	-1	-1
0	-1	-1
0	1	-1
0	1	-1
1	1	1
1	1	-1
1	-1	1

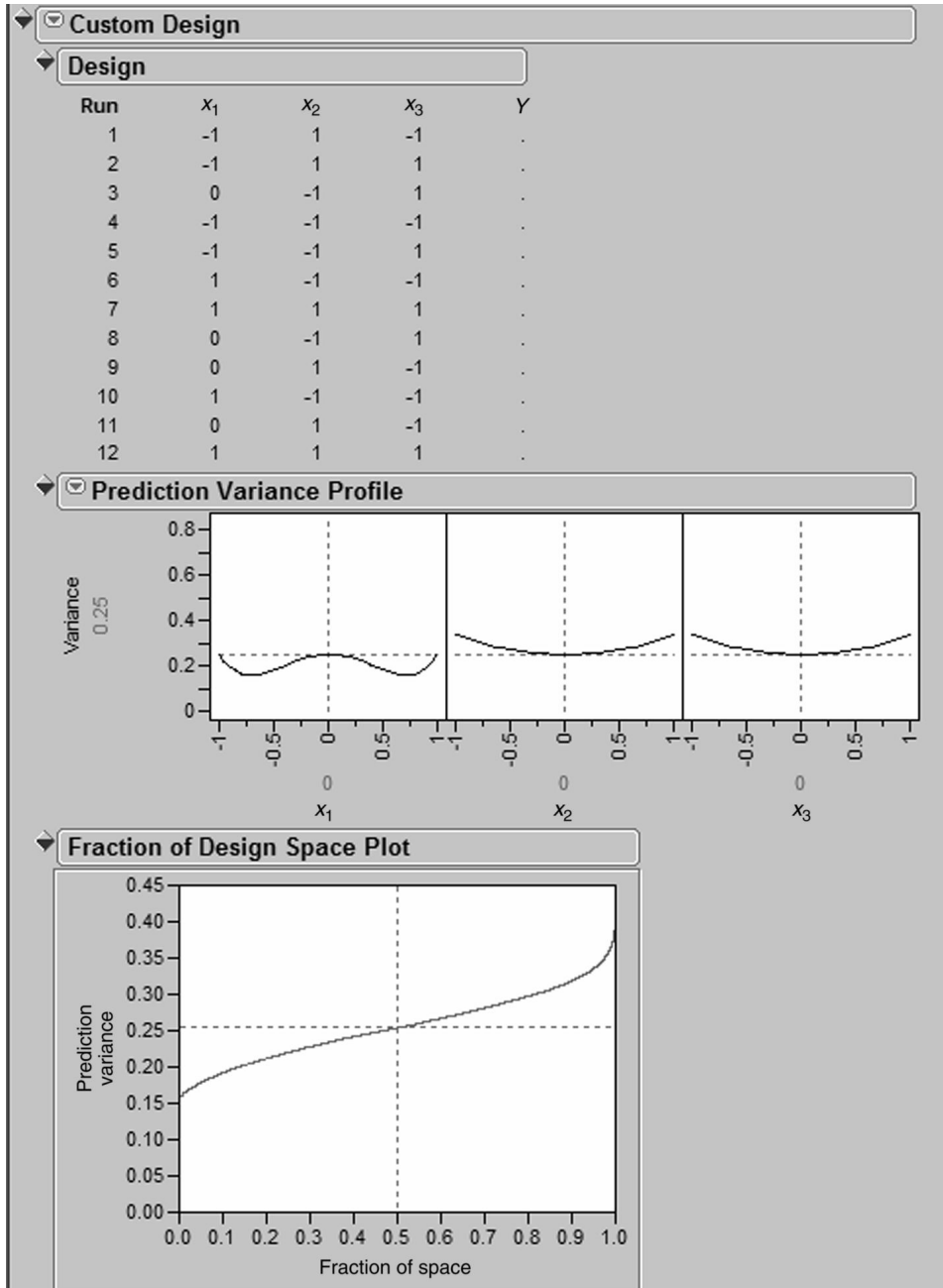


**Figure 8.14** Result of Custom Design for  $D$ -optimal design for the nonstandard model, with table of design points, Prediction Variance Profiler and FDS plot.

This design places more emphasis on good prediction at the center of the design space with additional points allocated for  $x_1 = 0$ . This comes at the expense of the worst prediction in the region being inflated to 0.6667, which would lead to a  $G$ -efficiency of  $5/(12 \times 0.6667) = 62.5\%$ . This result is relatively typical for designs involving second

order terms in the model: optimizing good average prediction in the entire region often comes at the cost of making the worst prediction variance somewhere in the region larger.

**Example 8.11 Use of Additional Runs** Consider the same scenario as in the previous example except that the user can afford to use  $N = 15$  runs. Using the “Augment Design” option under “DOE” in JMP, we can add three additional runs to the design created in Example 8.10. Figure 8.15 shows the dialog box used to create the new design.

Figure 8.16 shows the resulting design, with the three additional runs. Note that we have adjusted the Prediction Variance Profiler to show the maximum prediction variance value at one of the corners of the design space. This design has a lower maximum  $v(\mathbf{x})$  value of 0.375, which makes this a better design for prediction. However, if we are using scaled prediction variance, then the maximum  $N \text{Var}[\hat{y}(\mathbf{x})]/\sigma^2 = 15 \times 0.375 = 5.625$ . This gives a

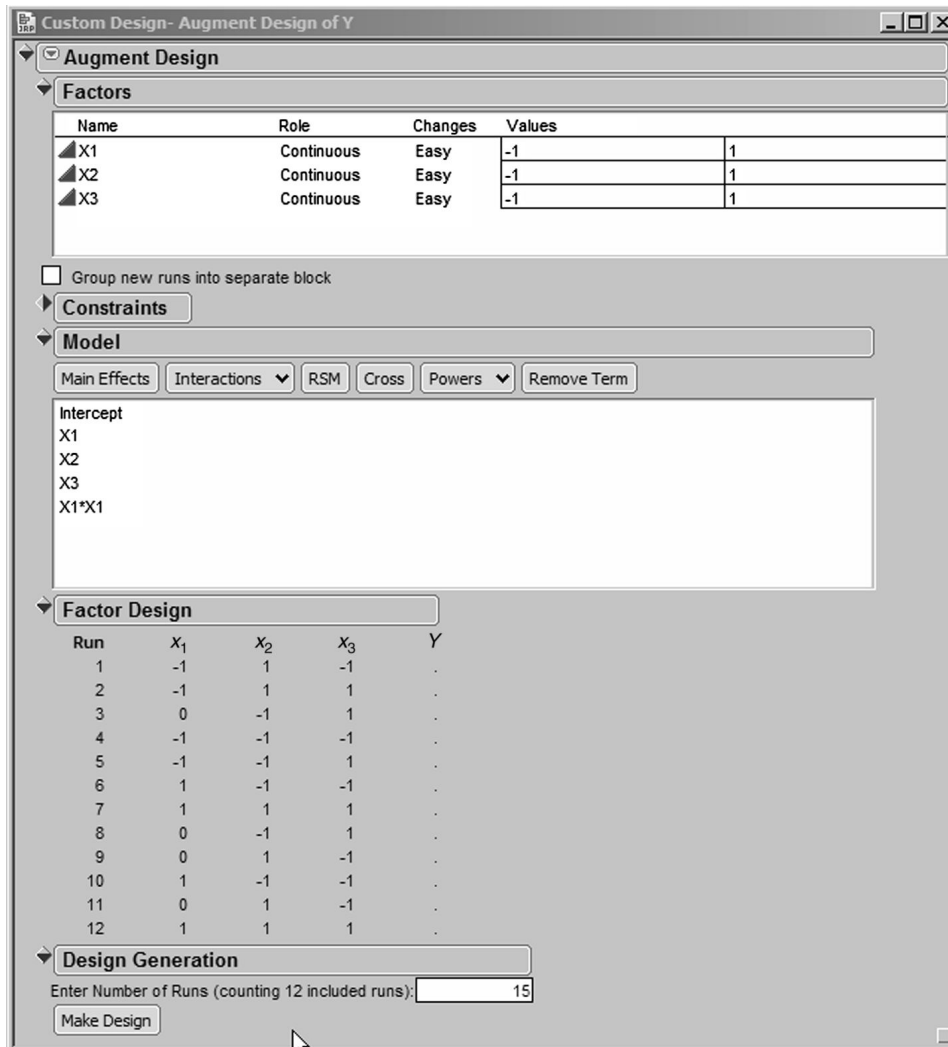


Figure 8.15 Dialog box to augment the 12 run design of Example 8.10 to a 15 run design.

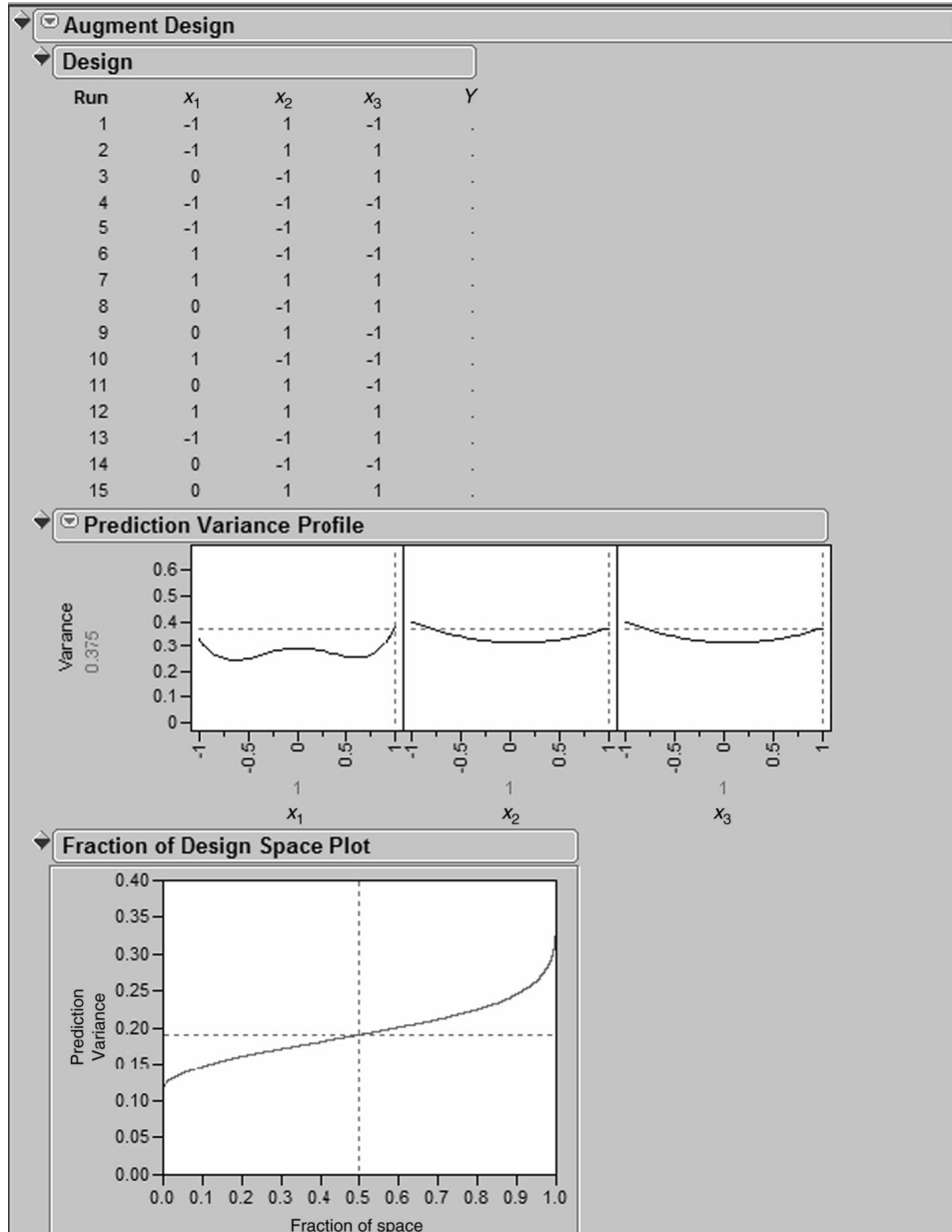


Figure 8.16 Augmented design for nonstandard model with  $N = 15$ .

$G$ -efficiency of  $5/5.625 = 89\%$ . Hence this design is not superior to the 12-run design on a per observation basis, but will improve prediction if we consider the unscaled prediction variance.

Use of  $D$ -efficiency under constraints on lack-of-fit and pure error degrees of freedom via computer packages is a continuing attempt to make the “automated design” concept

**TABLE 8.3 Output from Design-Expert for  $D$ -Optimal Design with  $k = 3$ , Two Lack-of-Fit Degrees of Freedom, and Two Pure Error Degrees of Freedom**

$x_1$	$x_2$	$x_3$
-1.0	-1.0	-1.0
1.0	-1.0	-1.0
1.0	-1.0	-1.0
0.0	0.0	-1.0
-1.0	1.0	-1.0
-1.0	1.0	-1.0
1.0	1.0	-1.0
-1.0	0.0	0.0
0.0	0.0	0.0
0.0	1.0	0.0
-1.0	-1.0	1.0
-1.0	-1.0	1.0
-1.0	1.0	1.0
1.0	1.0	1.0
-0.5	-0.5	-0.5

practical. Quite often the constraints revolve around total sample size, levels, and so on. However, there are algorithms that generate a most  $D$ -efficient design where the constraints are built around pure error and lack-of-fit degrees of freedom. For example, suppose that in a  $k = 3$  situation it is of interest to design an experiment with two lack-of-fit degrees of freedom and two pure error degrees of freedom. For a second-order model this corresponds to 12 distinct design points and 15 total runs. The resulting design, produced by Design-Expert, is given in Table 8.3.

Note from Table 8.3 that the design allows a single center run and has replication at two distinct factorial points. While we are accustomed to seeing designs with center runs replicated, there are certainly advantages to having replication at *different points* so some checking on the homogeneous variance assumption can be made.

**Example 8.12 A Nonstandard Model with  $k = 4$  Variables** In this example we provide another illustration of the use of computer-generated designs. This example serves as an illustration of some of the *disadvantages* of computer-generated design and design optimality in general.

Suppose we have four design variables and the input involves three levels on each, coded to  $-1$ ,  $0$ ,  $+1$ . Thus, the candidate list will be the  $3^4 = 81$  design points. Suppose the practitioner has difficulty choosing a model for purpose of design construction but decides on

$$\begin{aligned} E(y) = & \beta_0 + \beta_1 x_1 + \beta_2 x_2 + \beta_3 x_3 + \beta_4 x_4 \\ & + \beta_{12} x_1 x_2 + \beta_{23} x_2 x_3 + \beta_{11} x_1^2 + \beta_{44} x_4^2 \end{aligned} \quad (8.22)$$

The practitioner can afford  $N = 25$  runs. The  $D$ -optimal design is

Observation	$x_1$	$x_2$	$x_3$	$x_4$
1	-1	-1	-1	-1
2	-1	-1	-1	0
3	-1	-1	-1	0
4	-1	-1	1	-1
5	-1	-1	1	1
6	-1	1	-1	-1
7	-1	1	-1	0
8	-1	1	1	1
9	-1	1	1	1
10	0	-1	-1	1
11	0	-1	1	0
12	0	-1	1	1
13	0	1	-1	-1
14	0	1	-1	0
15	0	1	1	-1
16	0	1	1	0
17	1	-1	-1	-1
18	1	-1	-1	0
19	1	-1	-1	1
20	1	-1	1	-1
21	1	-1	1	0
22	1	1	-1	1
23	1	1	-1	1
24	1	1	1	-1
25	1	1	1	0

The  $D$ -efficiency is 62.35%, and the  $G$ -efficiency is 94.13%.

It is of interest to compare this design with a standard design. In fact, a CCD with  $\alpha = 1.0$  and one center run satisfies the  $N = 25$  requirements. Of course, the CCD is totally symmetric, requires three levels of each variable, and estimates coefficients for all six two-factor interactions equally well. In addition, all pure quadratic coefficients are estimated equally well. As one would expect, the CCD is not as efficient for the incomplete second-order model listed above. In fact, the efficiencies are

$$\begin{aligned} D_{\text{eff}} &= 52.13\% \\ G_{\text{eff}} &= 94.09\% \end{aligned}$$

How often, however, is the practitioner certain of the model prior to designing an experiment, particularly in an RSM scenario when most (or all) factors are continuous? Suppose we consider a situation in which, after the data are collected, the model that is fitted to the data is given by

$$\begin{aligned} E(y) &= \beta_0 + \beta_1 x_1 + \beta_2 x_2 + \beta_3 x_3 + \beta_4 x_4 \\ &\quad + \beta_{12} x_1 x_2 + \beta_{34} x_3 x_4 \end{aligned} \tag{8.23}$$

Of course, the constructed design is no longer  $D$ -optimal. In fact, a highly efficient two-level design could be constructed with the computer. However, one must live with the design chosen. Now, the CCD is also not designed for the model of Equation 8.23, particularly because there are no quadratic terms. The efficiencies are:

	$D$	$A$	$G$
Computer-generated	75.88	67.86	82.07
CCD	72.96	72.31	85.04

As a result, the CCD is just as efficient as (if not more so than) the computer-generated design. Now, suppose the actual model, unknown to the practitioner, involves a quadratic term in either  $x_2$  or  $x_3$ . Here, the computer-generated design of Equation 8.22 is a **singular design**; that is, the coefficients of  $x_2^2$  and  $x_3^2$  are not estimable. The point here is that the CCD has a high  $D$ -efficiency and  $G$ -efficiency for the full second-order model and is often reasonably robust to model mis-specification, in contrast with a computer-generated design. One cannot always be certain that a computer-generated  $D$ -optimal design will allow estimation of all coefficients if the model that is eventually fitted differs from that used in the input information.

**Example 8.13 The Adhesive Bonding Experiment** Consider the adhesive bonding experiment described in Section 8.2 that led to the constrained region of interest in Fig. 8.1. Recall that the two variables are  $x_1$  = amount of adhesive and  $x_2$  = cure temperature, and that the feasible design region is

$$-1.5 \leq x_1 + x_2 \leq 1.0$$

Suppose that the response of interest is the pulloff force and we want to fit a second-order model to this response. Table 8.4 and Fig. 8.17a show a 12-run  $D$ -optimal design for this problem, generated with Design-Expert. We required that  $N = 12$ , and that there would be three replicated runs to provide an estimate of pure error. Notice that one of the replicates is at the center of the region, and two are at corners, or **vertices**. Figure 8.17a shows the contours of  $\sqrt{\text{Var}[\hat{y}(\mathbf{x})]/\sigma^2}$  for this design, and Fig. 8.17b shows the corresponding response surface.

**TABLE 8.4 A  $D$ -Optimal Design for the Constrained Region in Fig. 8.1**

Standard Order	$x_1$	$x_2$	$y$
1	-0.50	-1.00	173.9
2	1.00	0.00	195.9
3	-0.08	-0.08	201.2
4	-1.00	1.00	199.3
5	1.00	-1.00	190.3
6	0.00	1.00	198.5
7	-1.00	0.25	190.5
8	0.25	-1.00	179.5
9	-1.00	-0.50	176.7
10	1.00	0.00	198.1
11	0.00	1.00	200.5
12	-0.08	-0.08	197.1

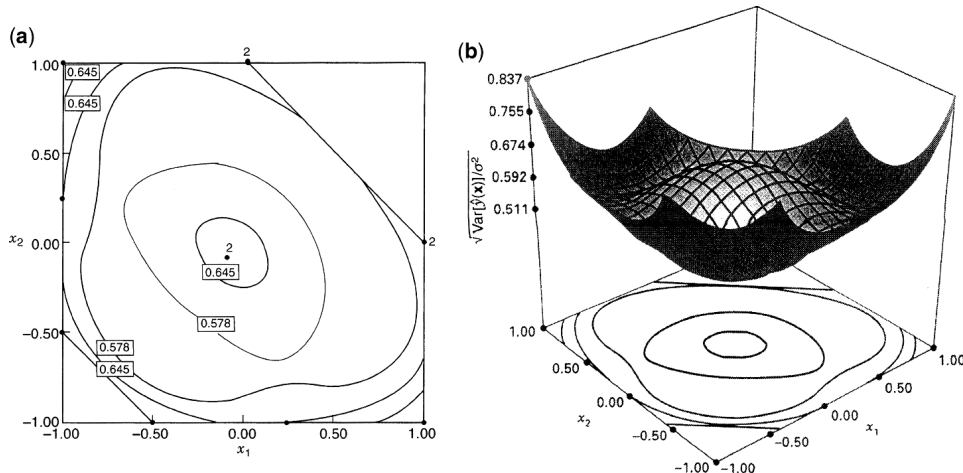


**Figure 8.17** A *D*-optimal design for the constrained design region in Fig. 8.1. **(a)** The design and contours of constant  $\sqrt{\text{Var}[\hat{y}(\mathbf{x})]/\sigma^2}$ . **(b)** The response surface plot.

Table 8.5 is a summary of the fit of a second-order model to the data in Table 8.4 using Design-Expert. The model is

$$\hat{y} = 199.10 + 4.51x_1 + 9.56x_2 - 9.57x_1x_2 - 6.19x_1^2 - 9.00x_2^2$$

Figure 8.18 shows the contour plot and the response surface for the estimated response for this model. The point giving the maximum pulloff force is  $x_1 = 0.08$  and  $x_2 = 0.52$ .

**Example 8.14 Use of Qualitative Variables** Quite often in practice, response surface studies need to be conducted even though at least one factor is **qualitative** in nature. In a RSM study involving qualitative variables, it stands to reason that the goal of the experiment for these variables is no different from that of the quantitative variables. That is, they must be included in the model and designs, and they must be involved in any response prediction or optimization using the model. The reader should bear in mind that *qualitative variances in an RSM study are not like blocks*. They are not nuisance factors. Indeed one must allow for possible interaction between qualitative factors and standard RSM terms involving quantitative factors.

For example, in an extraction experiment an engineer may wish to model the amount of extraction against temperature and time. The eventual goal may be to determine temperature and time values that maximize extraction. However, it is natural to consider a third factor: type of extraction solvent. One may view this qualitative factor as having three levels, because three potential candidate solvents exist, each with a distinctive chemical composition.

Computer-generated designs are a powerful tool when one encounters qualitative variables that must be modeled with the usual continuous quantitative design variables. Here, of course, the user must be concerned about the interaction that exists between continuous and qualitative factors. In the extraction example, the effect of temperature or time may change depending on which of the solvents is being considered.

Consider the situation in which we would like to model the amount of extraction as a function of type of solvent (with solvents *A*, *B*, and *C*) in addition to temperature and time, two standard continuous design variables. The model assumed is second order in

**TABLE 8.5** The Second-Order Model for the Pulloff Force

Response: Force

\*\*\*WARNING: The Cubic Model is Aliased!\*\*\*

<i>Sequential Model Sum of Squares</i>					
Source	Sum of Squares	DF	Mean Square	F-Value	Prob > F
Mean	4.414E + 005	1	4.414E + 005		
Linear	809.80	2	404.90	14.96	0.0014
2FI	30.83	1	30.83	1.16	0.3130
Quadratic	165.87	2	82.94	10.61	0.0107
Cubic	34.10	3	11.37	2.66	0.2216
Residual	12.83	3	4.28		
Total	4.425E + 005	12	36871.83		
<i>Lack of Fit Tests</i>					
Source	Sum of Squares	DF	Mean Square	F-Value	Prob > F
Linear	230.80	6	38.47	9.06	0.0496
2FI	199.97	5	39.99	9.36	0.0475
Quadratic	34.10	3	11.37	2.66	0.2216
Cubic	0.000	0			
Pure Error	12.82	3	4.27		
<i>Model Summary Statistics</i>					
Source	Std. Dev.	R-Squared	Adjusted R-Squared	Predicted R-Squared	PRESS
Linear	5.20	0.7687	0.7173	0.6494	369.32
2FI	5.16	0.7980	0.7222	0.6982	317.96
Quadratic	2.80	0.9555	0.9183	0.8260	183.32
Cubic	2.07	0.9878	0.9554	+	Aliased

+Cases(s) with leverage of 1.0000: PRESS statistic not defined

**TABLE 8.5** *Continued*

Response Force

*ANOVA for Response Surface Quadratic Model*  
*Analysis of variance table [Partial sum of squares]*

Source	Sum of Squares	DF	Mean Square	F-Value	Prob > F
Model	1006.51	5	201.30	25.74	0.0006
A	110.69	1	110.69	14.15	0.0094
B	496.83	1	496.83	63.53	0.0002
$A^2$	72.86	1	72.86	9.32	0.0224
$B^2$	154.39	1	154.39	19.74	0.0044
AB	137.55	1	137.55	17.59	0.0057
Residual	46.92	6	7.82		
<i>Lack of Fit</i>	34.10	3	11.37	2.66	0.2216
<i>Pure Error</i>	12.82	3	4.27		
Cor Total	1053.43	11			
Std. Dev.	2.80		R-Squared	0.9555	
Mean	191.79		Adj R-Squared	0.9183	
C.V.	1.46		Pred R-Squared	0.8260	
PRESS	183.32		Adeq Precision	14.01	
					95% CI
Factor	Coefficient Estimate	DF	Standard Error	Low	High
Intercept	199.10	1	1.84	194.61	203.60
A-Amount	4.51	1	1.20	1.58	7.45
B-Temp	9.56	1	1.20	6.62	12.49
$A^2$	-6.19	1	2.03	-11.14	-1.23
$B^2$	-9.00	1	2.03	-13.96	4.05
AB	-9.570	1	2.28	-15.16	-3.99

---

Final Equation in Terms of Coded Factors:

$$\begin{array}{ll} \text{Force} & = \\ +199.10 & \\ +4.51 & *A \\ +9.56 & *B \\ -6.19 & *A^2 \\ -9.00 & *B^2 \\ -9.57 & *A*B \end{array}$$

---

“*Sequential Model Sum of Squares*”: Select the highest order polynomial where the additional terms are significant.

“*Lack of Fit Test*”: Want the selected model to have insignificant lack-of-fit.

“*Model Summary Statistics*”: Focus on the model maximizing the “Adjusted R-squared”; and the “Predicted R-Squared.”

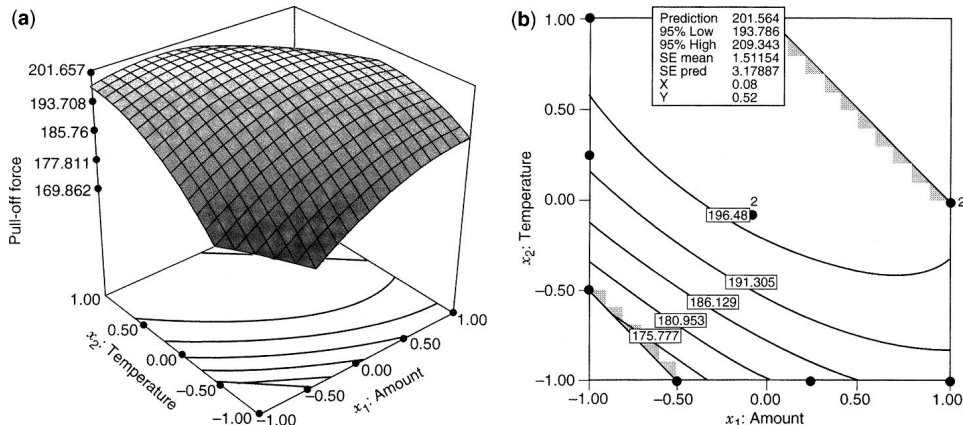


**Figure 8.18** Plots of predicted pulloff force, Example 8.13. (a) Response surface. (b) Contour plot, showing location of the stationary point.

$x_1$  (temperature) and  $x_2$  (time) and the qualitative variable (solvent) interacts with  $x_1$  and  $x_2$ . The required design size is  $N = 15$ . Formally, the model is written

$$y = \beta_0 + \beta_1 x_1 + \beta_2 x_2 + \beta_{12} x_1 x_2 + \beta_{11} x_1^2 + \beta_{22} x_2^2 + \gamma_1 z_1 + \gamma_2 z_2 + \delta_{11} z_1 x_1 + \delta_{21} z_2 x_1 + \delta_{12} z_1 x_2 + \delta_{22} z_2 x_2 + \varepsilon$$

Here

$$z_1 = \begin{cases} 1 & \text{if } A \text{ is the discrete level} \\ 0 & \text{elsewhere} \end{cases}$$

$$z_2 = \begin{cases} 1 & \text{if } B \text{ is the discrete level} \\ 0 & \text{elsewhere} \end{cases}$$

Notice that indicator variables are used to represent the qualitative factor, type of solvent. The  $N = 15$  computer generated design using  $D$ -optimality is given by

$$\mathbf{D} = \begin{array}{c|ccc} & x_1 & x_2 & x_3 \\ \hline & -1 & -1 & C \\ & -1 & -1 & B \\ & -1 & -1 & A \\ & -1 & 1 & C \\ & -1 & 1 & B \\ & -1 & 1 & A \\ & 1 & -1 & C \\ & 1 & -1 & B \\ & 1 & -1 & A \\ & 1 & 1 & C \\ & 1 & 1 & B \\ & 1 & 1 & A \\ & 0 & 0 & A \\ & 0 & 1 & B \\ & -1 & 0 & B \end{array}$$

Note the **crossing** of the  $2^2$  factorial points with the three levels  $A$ ,  $B$ , and  $C$  in order to capture the interactions  $x_1z_1$ ,  $x_1z_2$ ,  $x_2z_1$ ,  $x_2z_2$ , and  $x_1x_2$ . The center and two axial points in  $x_1$  and  $x_2$  allow further information for estimation of  $x_1^2$  and  $x_2^2$  terms.

**Example 8.15 Designs for Three Quantitative and Two Qualitative Variables**

Consider a situation in which there are three quantitative variables  $x_1$ ,  $x_2$ , and  $x_3$  and two qualitative variables  $z_1$  and  $z_2$ , each at two levels. Assume that the practitioner wishes to fit a full second-order model in the three quantitative variables as well as the terms  $z_1$ ,  $z_2$ ,  $z_1x_j$ ,  $z_2x_j$ ,  $z_1x_j^2$ , and  $z_2x_j^2$  for  $j = 1, 2, 3$ . There are 24 model terms to be fitted, including  $\beta_0$ . Using Design-Expert, a  $D$ -optimal design was created with 30 runs, specifying that the additional six degrees of freedom should be allocated with three degrees of freedom for lack of fit and three replicates. Table 8.6 shows the design.

The reader should note that in this example we are not assuming a separate response surface for all four combinations of the qualitative variables. We are in fact assuming that the  $x_i x_j$  ( $i \neq j$ ) terms are the same at the four combinations. Indeed, a model assuming

**TABLE 8.6 Design Expert  $D$ -Optimal Design for Three Quantitative and Two Qualitative Variables**

Obs	$x_1$	$x_2$	$x_3$	$z_1$	$z_2$
1	-1	-1	1	L1	L1
2	-0.5	0	0	L1	L1
3	1	1	1	L1	L1
4	1	1	1	L1	L1
5	1	1	-1	L1	L1
6	1	-1	1	L1	L1
7	1	-1	-1	L1	L1
8	-1	1	-0.33	L1	L2
9	-1	0.33	-1	L1	L2
10	-1	0.33	-1	L1	L2
11	-1	0.33	1	L1	L2
12	0	-1	0	L1	L2
13	0.33	1	-1	L1	L2
14	1	0	0	L1	L2
15	1	-1	-1	L1	L2
16	-1	-1	-1	L1	L2
17	-1	1	1	L2	L1
18	-1	1	-0.33	L2	L1
19	-1	0.33	1	L2	L1
20	-0.33	1	-1	L2	L1
21	0	-1	0	L2	L1
22	1	1	-1	L2	L1
23	1	1	-1	L2	L1
24	-1	1	0	L2	L2
25	-1	-1	0	L2	L2
26	0	-1	1	L2	L2
27	0	0	0	L2	L2
28	1	1	0	L2	L2
29	1	0	1	L2	L2
30	1	-1	-0.33	L2	L2

separate response surfaces would require 16 additional model terms containing  $x_i x_j z_k$  terms ( $i \neq j$ ),  $z_1 z_2 x_i$  terms,  $z_1 z_2 x_i^2$  terms and  $z_1 z_2 x_i x_j$  terms ( $i \neq j$ ). Thus, in our model we assume stability of  $x_i x_j$  across  $z_1$  and  $z_2$  and no interaction among  $z_1$  and  $z_2$ .

Note some of the symmetry in the design: all four of the combinations of the qualitative variables have seven or eight observations, and the three replicates are spread with one pair in three of the four combinations.

Table 8.7 shows the *I*-optimal design generated by JMP, with no restrictions placed on the degrees of fit allocated for lack of fit or replication. This design also has seven or eight observations for each of the qualitative variables. Note how more of the continuous variable levels are selected with a value of 0 to give better prediction near the center and to lower the average prediction variance value. When no degrees of freedom are allocated for estimating lack of fit, then only three levels of each of the quantitative variables are selected. In addition, no replicates are selected if they are not requested.

**TABLE 8.7 JMP *I*-Optimal Design for Three Quantitative and Two Qualitative Variables**

Obs	$x_1$	$x_2$	$x_3$	$z_1$	$z_2$
1	-1	0	0	L1	L1
2	-1	-1	1	L1	L1
3	0	0	-1	L1	L1
4	0	-1	0	L1	L1
5	1	-1	-1	L1	L1
6	1	1	-1	L1	L1
7	1	1	1	L1	L1
8	-1	1	1	L1	L2
9	-1	1	-1	L1	L2
10	0	1	0	L1	L2
11	0	0	1	L1	L2
12	1	1	-1	L1	L2
13	1	0	0	L1	L2
14	1	-1	1	L1	L2
15	-1	-1	-1	L2	L1
16	-1	1	1	L2	L1
17	0	0	1	L2	L1
18	0	0	0	L2	L1
19	0	-1	0	L2	L1
20	1	-1	1	L2	L1
21	1	1	-1	L2	L1
22	1	0	0	L2	L1
23	-1	-1	0	L2	L2
24	-1	1	-1	L2	L2
25	0	-1	-1	L2	L2
26	0	0	0	L2	L2
27	0	1	0	L2	L2
28	0	0	1	L2	L2
29	1	1	1	L2	L2
30	1	0	0	L2	L2

Computer-generated designs are particularly useful for situations with a combination of qualitative and quantitative variables, as they provide great flexibility for accommodating the model structure required.

#### **8.4 SOME FINAL COMMENTS CONCERNING DESIGN OPTIMALITY AND COMPUTER-GENERATED DESIGN**

As we indicated earlier in this chapter, the current status of computer generated design is a result of the theoretical work of Keifer and coworkers and decades of work by many who made the concept usable by practitioners. There is no question that computer-aided design of experiments can be of value. However, in RSM work there are several reasons to proceed with caution. Those who successfully use design computer packages to aid in constructing RSM designs are those who do not use it as a “black box.” Computer-aided designs can be useful if the user allows it to complement the available arsenal of standard RSM designs. The user who is likely to fail with computer-aided designs is the one who is not armed with important knowledge about design optimality and standard RSM designs.

The development of optimal design theory is based on the use of a continuous design measure that determines the proportion of runs that should be made at a number of points in a predetermined design space. In practice, of course, the concept of continuous designs is impractical. However, the idea is to determine discrete designs that approximate the optimal continuous designs. The ideas of candidate lists and sequential formation of the design according to the important augmentation relationship of Section 8.3.1 provide computational ease and make computer-aided design practical. However, perhaps because of this useful relationship, *D*-optimality or, rather, the maximization of *D*-efficiency has become the criterion that is used more than any other. One must keep in mind that the *D*-criterion is necessarily quite narrow, based on crucial and often unrealistic assumptions, and does not address many of the 10 important goals of RSM designs discussed in Chapter 7. Many of these 10 goals address the notion of *design robustness*—that is, robustness to model misspecification, robustness to errors in control, and so on. In addition, they address the distribution of  $\text{Var}[\hat{y}(\mathbf{x})]/\sigma^2$ , which is very important in RSM studies. The idea of maximization of *D*-efficiency does not directly deal with the prediction variance, and, indeed, often computer-generated design based on the *D*-criterion does not result in an attractive distribution of  $\text{Var}[\hat{y}(\mathbf{x})]/\sigma^2$ . The availability of *I*-optimal computer-generated designs can be very beneficial if the primary focus of the study is to predict or optimize the response.

The following are, formally, some items that should breed caution among practitioners in the use of computer-generated *D*-efficient designs:

1. The user must indicate a model. Model editing is part of any modeling strategy. Often the model is not known. If the fitted model is not that which is input to the computer, the computer-generated design is *not* that which maximizes *D*-efficiency, and, indeed, it may not be a good design at all. Heredia-Langner et al. (2004) present strategies for generating designs that are robust to model choice, while Ozol-Godfrey et al. (2005) present graphical tools to evaluate prediction variance for different edited models.
2. Designs generated from the *D*-criterion do not address prediction variance. In some cases, a *D*-efficient design may not have ideal properties for prediction.

3. For second-order models, the  $D$ -criterion often does not allow any (or many) center runs. This often results in large values of  $\text{Var}[\hat{y}(\mathbf{x})]/\sigma^2$  in the design center. Hence, augmenting  $D$ -efficient designs with additional center runs can yield considerably better prediction performance. Both JMP and Design-Expert provide an option for adding center runs after an optimal design has been created.

In RSM analyses, the user should search for an appropriate standard design discussed in Chapter 7 and 8. Nevertheless, there will be circumstances under which a computer-generated design will be helpful. Constraints regarding sample sizes, the use of qualitative variables, and cases where the user must deal with an unusual combination of ranges or constraints are situations where computer-aided design may be helpful. Augmenting computer-generated designs with additional runs can help make designs perform better in many of the 10 criteria listed in Chapter 7. Drain et al. (2004) present general methodology for constructing optimal RSM designs using a genetic algorithm. However, the user should be cautious regarding the input model and should be aware of the pitfalls we have discussed here.

## EXERCISES

- 8.1** There is considerable interest in the use of saturated or near saturated second-order designs. One interesting comparison involves the hexagon ( $k = 2$ ) and the small composite design. Both involve six design points (plus center runs). In this exercise, we make comparisons that take into account variances of coefficients and prediction variance. However, before any two designs can be compared, they must be adjusted so they have the same scale. Consider the hexagon of Equation 7.22 and the  $k = 2$  small composite design listed in Section 8.1. For proper comparisons we have

$$\mathbf{D}_{\text{SCD}} = \begin{bmatrix} x_1 & x_2 \\ -1 & -1 \\ 1 & 1 \\ -\sqrt{2} & 0 \\ \sqrt{2} & 0 \\ 0 & -\sqrt{2} \\ 0 & \sqrt{2} \\ 0 & 0 \\ 0 & 0 \end{bmatrix} \quad \mathbf{D}_{\text{HEX}} = \begin{bmatrix} x_1 & x_2 \\ \sqrt{2} & 0 \\ \sqrt{2}/2 & \sqrt{3}/2 \\ -\sqrt{2}/2 & \sqrt{3}/2 \\ \sqrt{2} & 0 \\ -\sqrt{2}/2 & -\sqrt{3}/2 \\ \sqrt{2}/2 & -\sqrt{3}/2 \\ 0 & 0 \\ 0 & 0 \end{bmatrix}$$

For this scaling, both designs are on spheres of radius  $\sqrt{2}$  (apart from center runs).

- (a) Compute  $N\text{Var}(b_0)/\sigma^2$ ,  $N\text{Var}(b_{ii})/\sigma^2$ ,  $N\text{Var}(b_{ii})/\sigma^2$ ,  $N\text{Var}(b_{ij})/\sigma^2$  for both designs. Comment.
- (b) Compute  $N\text{Var}[\hat{y}(\mathbf{x})]/\sigma^2$  at the design center and at all design points for both designs. Is this an illustration of rotatability?
- (c) Construct FDS plots and VDGs for both designs. Comment on which design you prefer and why.

- (d) From part (b), is there an illustration of the rotatability of the hexagon?
- (e) Is the small composite design rotatable? Explain.
- 8.2** Consider a comparison between the  $k = 4$  SCD of Equation 8.5 with the  $k = 4$  CCD ( $N = 24 + n_c$ ). Use  $n_c = 4$  center runs for each design, and use  $\alpha = 2$  for both designs.
- (a) Do the designs need to be rescaled? Explain.
- (b) Make the same type of comparisons as in Exercise 8.1.
- 8.3** Perhaps you noticed some evidence in Exercise 8.1 that the  $k = 2$  SCD was not rotatable. Actually the conditions required for rotatability cannot be met for any SCD that involves a resolution III\* fraction of a  $2^k$ . Prove this result. *Hint:* Look at odd moments.
- 8.4** Create FDS and VDG plots for the Hoke  $\mathbf{D}_2$  and  $\mathbf{D}_6$  designs for  $k = 3$ . Compare their prediction variance to the CCD with two center runs on a cuboidal region. Which design seems preferable? Explain.
- 8.5** The SCD that involves the PBD represents a nice alternative to the CCD for  $k \geq 4$ . It produces a nice design size that is quite economical compared to what is usually recommended. Because the design size is considerably above saturation, the design enjoys efficiency that is higher than that of the *smaller* SCD listed in Table E8.2.
- (a) Consider the case of  $k = 6$ . Construct a SCD by using a 24-run PBD combined with axial points at  $\alpha = \sqrt{6}$  plus  $n_c = 4$  center runs. Compare, in terms of the scaled variances of regression coefficients, with the SCD in Table E8.2 with  $n_c = 2$ . Be sure that the design from Table E8.2 contains a resolution III fraction and  $\alpha = \sqrt{6}$ .
- (b) Compare the larger SCD in (a) with a CCD containing
- (i)  $2_{VI}^{6-1}$
  - (ii) axial points at  $\alpha = \sqrt{6}$
  - (iii)  $n_c = 4$
- 8.6** The Koshal design is an interesting experimental plan that was not derived with statistical analysis in mind. Analysts are often surprised at the applicability and the efficiency of the design, particularly when information regarding interaction is either known or considered to be unimportant. The Koshal design is a natural competitor of the saturated or near-saturated SCD. Compare the  $k = 3$  Koshal design with the  $k = 3$  ( $N = 10 + n_c$ ) SCD. Again, use scaled variances of regression coefficients. In addition, use  $N\text{Var}[\hat{y}(\mathbf{x})]/\sigma^2$  at the following locations in the *scaled design units*:

$$\begin{aligned} & (0, 0, 0) \\ & (1, 0, 0) \\ & (-1, 0, 0) \\ & (1.5, 0, 0) \\ & (-1.5, 0, 0) \\ & (1, 1, 1) \\ & (-1, -1, -1) \end{aligned}$$

The design scaling should be as follows:

$$\mathbf{D}_{\text{SCD}} = \begin{bmatrix} x_1 & x_2 & x_3 \\ 1 & -1 & -1 \\ 1 & 1 & -1 \\ 1 & -1 & 1 \\ -1 & 1 & 1 \\ -\sqrt{3} & 0 & 0 \\ \sqrt{3} & 0 & 0 \\ 0 & -\sqrt{3} & 0 \\ 0 & \sqrt{3} & 0 \\ 0 & 0 & -\sqrt{3} \\ 0 & 0 & \sqrt{3} \\ 0 & 0 & 0 \\ 0 & 0 & 0 \end{bmatrix} \quad \mathbf{D}_{\text{Kosh}} = \begin{bmatrix} x_1 & x_2 & x_3 \\ \sqrt{3}/2 & 0 & 0 \\ 0 & \sqrt{3}/2 & 0 \\ 0 & 0 & \sqrt{3}/2 \\ -\sqrt{3}/2 & 0 & 0 \\ 0 & -\sqrt{3}/2 & 0 \\ 0 & 0 & -\sqrt{3}/2 \\ \sqrt{3}/2 & \sqrt{3}/2 & 0 \\ \sqrt{3}/2 & 0 & \sqrt{3}/2 \\ 0 & \sqrt{3}/2 & \sqrt{3}/2 \end{bmatrix}$$

Comment on your results.

- 8.7** Compare, in terms of scaled regression coefficients, the  $k = 3$  311B (use  $n_c = 3$ ) with the CCD and SCD values in Table 8.1. The 311B must, of course, be scaled properly. Thus, divide it by  $\sqrt{2}$ . Comment on your results.
- 8.8** Consider the following first-order design

$$\mathbf{D} = \begin{bmatrix} x_1 & x_2 & x_3 \\ -1 & -1 & -1 \\ 1 & 1 & -1 \\ 1 & 1 & -1 \\ 1 & -1 & 1 \\ -1 & -1 & 1 \\ -1 & 1 & -1 \\ 1 & 1 & 1 \\ -1 & -1 & 1 \end{bmatrix}$$

- (a) Is the design first-order orthogonal? Explain?
- (b) Give the  $D$ -efficiency of this design.
- (c) Give the  $I$ -efficiency of the design.
- (d) Give the  $A$ -efficiency of the design. *Hint:* The  $A$ -efficiency of a design is given by

$$\frac{\min_{\zeta} \text{tr}[\mathbf{M}(\zeta)]^{-1}}{N \text{tr}(\mathbf{X}'\mathbf{X})^{-1}}$$

Now, of course, for a first-order model with range  $[-1, +1]$  on each design variable we have

$$\underset{\zeta}{\text{Min}} \text{tr}[\mathbf{M}(\zeta)]^{-1} = p$$

- 8.9** Consider a model containing first-order and two-factor interaction terms in three design variables—that is,

$$\hat{y} = b_0 + b_1x_1 + b_2x_2 + b_3x_3 + b_{12}x_1x_2 + b_{13}x_1x_3 + b_{23}x_2x_3$$

In Section 8.2.1 we demonstrated that a resolution III two-level design is  $D$ -,  $A$ -,  $G$ -, and  $I$ -optimal for a first-order model. The levels must be at  $\pm 1$  extremes.

- (a) Show that all variances of coefficients are minimized with a resolution IV two-level design with levels at  $\pm 1$  extremes.
- (b) Using the result in (a), show that the members of the same resolution IV class are  $I$ -optimal.
- (c) Show that these designs are also  $G$ -optimal. The region  $R$  is, of course, the unit cube. Make use of the result [Equation (8.12)]

$$\underset{\mathbf{x} \in R}{\text{Max}} [\nu(\mathbf{x})] \geq p$$

and show that, for the class of designs in question,

$$\underset{\mathbf{x} \in R}{\text{Max}} [\nu(\mathbf{x})] = p$$

where, of course,  $p = 7$ .

- 8.10** Consider the Hoke  $\mathbf{D}_2$  design for  $k = 4$  assuming a second order model.
- (a) Calculate the  $\mathbf{X}'\mathbf{X}$  matrix for this design.
  - (b) Is the design rotatable? Explain.
  - (c) Generate an FDS plot for the design.
  - (d) Is the design  $G$ -optimal? If not, what is its  $G$ -efficiency?
- 8.11** Consider the following Koshal design for  $k = 3$ :

$$\mathbf{D} = \begin{array}{c} x_1 \quad x_2 \quad x_3 \\ \hline \end{array} \begin{bmatrix} 0 & 0 & 0 \\ 1 & 0 & 0 \\ 0 & 1 & 0 \\ 0 & 0 & 1 \\ 1 & 1 & 0 \\ 1 & 0 & 1 \\ 0 & 1 & 1 \end{bmatrix}$$

Assume that the region of design operability is  $[-1, +1]$  on each design variable. Consider the model

$$\hat{y} = b_0 + b_1x_1 + b_2x_2 + b_3x_3 + b_{12}x_1x_2 + b_{13}x_1x_3 + b_{23}x_2x_3$$

- (a) Compute the  $D$ -efficiency for this design for the above model.
  - (b) Compute the  $A$ -efficiency.
  - (c) Compute the  $G$ -efficiency.
- 8.12** Often a standard second-order design is planned because the practitioner expects that the fitted model will, indeed, be second-order. However, when the analysis is conducted, it is determined that the model is considerably less than order 2. As an example, suppose a  $k = 2$  CCD with  $\alpha = 1.0$  and two center runs is used and all second-order effects (quadratic and interaction) are very insignificant. The design is used eventually for a first-order model.
- (a) What is the  $D$ -efficiency for a  $k = 2$  CCD with  $\alpha = 1.0$  and two center runs for a first-order model? Comment.
  - (b) How does the  $D$ -efficiency change if there are no center runs?
  - (c) Is the difference between the results in (a) and (b) expected?
  - (d) Give the  $A$ -efficiency for both designs.
- 8.13** Refer to Exercise 8.12. Give the  $D$ -efficiency of a  $k = 3$  BBD for the model
- $$\hat{y} = b_0 + b_1x_1 + b_2x_2 + b_3x_3 + b_{12}x_1x_2 + b_{13}x_1x_3 + b_{23}x_2x_3$$
- 8.14** Consider the following experimental design:
- |                | $x_1$   | $x_2$ | $x_3$ |
|----------------|---|-------|-------|
| $\mathbf{D} =$ | $\begin{bmatrix} -1 & -1 & -1 \\ 1 & -1 & -1 \\ -1 & 1 & -1 \\ -1 & -1 & 1 \\ 1 & 1 & -1 \\ 1 & -1 & 1 \\ -1 & 1 & 1 \\ 0 & 0 & 0 \\ 0 & 0 & 0 \end{bmatrix}$ |       |       |
- A second stage is used, as it becomes obvious that the model is quadratic. Use a computer-generated design package to augment the above design with six more design points in order to accommodate a complete second-order model.
- 8.15** Consider a first-order orthogonal design with  $\pm 1$  levels. Show that the addition of center runs *must* lower the  $D$ -efficiency. Show that the same is true for  $A$ -efficiency and for  $G$ -efficiency.
  - 8.16** Consider a  $k = 4$  scenario. The practitioner plans to use 20 design points in order to accommodate a complete second-order model. However, it is not clear what the true

model is prior to conducting the experiment. As a result, the design selected should be one that is fairly **robust**—that is, one that will be reasonably efficient even if the model on which the design is based is not correct.

- (a) Using the  $3^4$  factorial as the candidate list, construct the  $D$ -optimal design using a second-order model as the basis.
  - (b) Suppose the edited model contains all linear terms and the interactions  $x_1x_2$  and  $x_1x_3$ . Give the  $D$ -efficiency of the design for this model.
  - (c) Suppose, rather than use the computer-generated design, the practitioner uses a SCD containing
    - (i) A PBD with 12 design points
    - (ii) Eight axial points with  $\alpha = 1.0$
 Give the  $D$ -efficiency of this design for a second-order model.
  - (d) Give the  $D$ -efficiency of this design for the reduced model given in (b).
  - (e) Comment on the above.
- 8.17** Consider Table 8.2. Notice that the CCD has high  $D$ -efficiencies but low  $G$ -efficiencies when the design has small numbers of center runs. Then when the number of center runs increases, the  $G$ -efficiency increases substantially. Explain why this is happening. Look at the variance dispersion graphs.
- 8.18** Consider a second-order model with four design variables and levels  $-2, -1, 0, 1, 2$  for each design variable. However, due to experimental constraints the candidate list should include:
  - (i) A  $3^4$  factorial with levels  $-1, 0, 1$
  - (ii) Eight axial points at  $\alpha = 2$
  - (iii) A center point
 Suppose 30 runs are to be used.
  - (a) Using a computer-generated design package, give the  $D$ -optimal design.
  - (b) Compare your design in (a) with a CCD with  $\alpha = 2$  and  $n_c = 6$ . Use  $N \text{Var}[\hat{y}(\mathbf{x})]/\sigma^2$  at the center of the design for your comparison.
  - (c) Compare again, using the variances of the predicted values averaged over all of the candidate points.
  - (d) Using VDG and FDS plots, compare where prediction is best and worst in each region, and determine which design is preferable.

**8.19** Consider again the two designs compared in Exercise 8.18. Suppose that the “true” model involves all linear main effects and two-factor interactions only. Compare the  $D$ -efficiencies and the  $A$ -efficiencies.

**8.20** Consider a hybrid 311B with three center runs. As an alternative, consider a BBD for  $k = 3$  with  $n_0 = 3$  center runs. Answer the following questions:
 
  - (a) Which has the higher  $D$ -efficiency for a second-order model?
  - (b) Which has the higher  $D$ -efficiency if, in fact, the true model is first-order? First-order with two-factor interactions?

- 8.21** Show that for the case of a first-order model in  $k$  variables and spherical region of interest, a resolution III design with levels at  $\pm 1$  extremes is a  $I$ -optimal design. *Hint:* For this region,  $(1/K) \int_R x_i d\mathbf{x}$  and  $(1/K) \int_R x_i x_j d\mathbf{x}$  are both zero.
- 8.22** Consider the  $D$ -optimal design in Table 8.4 for the constrained region shown in Fig. 8.1. Suppose that you were to move all three replicates to the center of the design.
- Generate a graph of prediction standard errors similar to those in Fig. 8.17. What effect has moving the replicates to the center on those quantities?
  - Compute the  $D$ -efficiency of this new design relative to the one used in Example 8.13 (Table 8.4).
- 8.23** Reconsider the adhesive force experiment in Example 8.13. Find a  $D$ -optimal design with  $N = 10$  runs. Use two runs as replicates. Compare the  $D$ -efficiency of this design with that of 12-run design in Table 8.4.
- 8.24** Consider a response surface design problem in  $k = 3$  factors where the region is constrained so that  $x_1 + x_2 + x_3 \leq 2$ . Find a  $D$ -optimal design for fitting a second-order model with  $N = 15$  runs, assuming that two runs are to be used as replicates. Generate plots of the standard deviation of the predicted response.
- 8.25** Rework Exercise 8.24 assuming that the constrained region is defined by  $-1.5 \leq x_1 + x_2 + x_3 \leq 2$ .
- 8.26** Consider the three experimental designs considered in Exercises 6.9, 6.10, and 6.11 for the auto-bumper plating process, assuming a full second-order model.
- Find the relative  $D$ -efficiencies of the designs in 6.10 and 6.11 relative to that in 6.9. Which design is best?
  - Find the  $G$ -efficiencies of the three designs.
  - Construct FDS plots for the three designs.
  - Based on the results of parts (a), (b), and (c), which design would you recommend?
- 8.27** Consider three competitors to the  $2^2$  factorial design, all operating on the same design space (using coded variables:  $x_1$  and  $x_2$  in  $[-1, 1]$ )

$$\mathbf{X}_A = \begin{bmatrix} 1 & 0.5 & 1 \\ 1 & -0.5 & 1 \\ 1 & 1 & -1 \\ 1 & -1 & -1 \end{bmatrix} \quad \mathbf{X}_B = \begin{bmatrix} 1 & 0.5 & 0.5 \\ 1 & -0.5 & 0.5 \\ 1 & 1 & -0.5 \\ 1 & -1 & -0.5 \end{bmatrix} \quad \mathbf{X}_C = \begin{bmatrix} 1 & 0.5 & 0.5 \\ 1 & -0.5 & 1 \\ 1 & 1 & -1 \\ 1 & -1 & -0.5 \end{bmatrix}$$

For a first-order model,  $y = \beta_0 + \beta_1 x_1 + \beta_2 x_2 + \epsilon$ , compare the three models and the  $2^2$  factorial design based on

- orthogonality
- variance of the model coefficients
- scaled predicted variance (using some graphical summary)

Based on your findings in (a)–(c) rank them for each of the criteria.

- 8.28** Consider the comparison of the CCD and BBD shown in Fig. 8.4. Suppose that the total cost of the experiment is not critical to the decision of which design to select. Construct the VDG and FDS plots for the 17 run CCD and the 15 run BBD using the unscaled prediction variance  $UPV = \mathbf{x}^{(m)\prime}(\mathbf{X}'\mathbf{X})^{-1}\mathbf{x}^{(m)}/\sigma^2$  to compare the designs. Which design would be preferred now?
- 8.29** Consider the hybrid designs 310 and 311B. By plotting FDS plots of both SPV and UPV for different numbers of center runs, determine what a suitable number of center runs would be for each design.
- 8.30** Consider the comparison of the  $3^3$  factorial design ( $N = 27$ ) and the face-centered cube ( $N = 15$ ) shown in Figs. 8.10 and 8.11. Construct the VDG and FDS plots for these designs using the unscaled prediction variance  $UPV = \mathbf{x}^{(m)\prime}(\mathbf{X}'\mathbf{X})^{-1}\mathbf{x}^{(m)}/\sigma^2$  which does not penalize for design size to compare the designs. Which design would be preferred now? When would it be appropriate to use this comparison rather than the one based on the SPV?
- 8.31** Consider the comparison of the five-factor CCD on a cuboidal region using either the full factorial or the  $\frac{1}{2}$  fraction. Based on their relative  $D$ -,  $G$ -, and  $I$ -efficiencies, and the FDS plot for scaled prediction variance, which design is better?
- 8.32** Consider the hybrid designs 416A, 416B and 416C, each with one center run. By plotting FDS plots of SPV, which design seems preferable?
- 8.33** Consider the Hoke **D2** ( $N = 15$ ) and **D6** ( $N = 19$ ) designs for four factors in a cuboidal region described in 8.1.1. Based on their relative  $D$ -,  $G$ -, and  $I$ -efficiencies, and the FDS plot for scaled prediction variance, which design is better?
- 8.34** For the same four factor cuboidal region described in Exercise 8.33, find  $I$ -optimal optimal designs of size  $N = 15$  and  $N = 19$  using a statistical software package. Based on their relative  $D$ -,  $G$ -, and  $I$ -efficiencies, and the FDS plot for scaled prediction variance, which design do you prefer? How do these designs compare to the Hoke **D2** and **D6** designs of Example 8.33?
- 8.35** An experiment was conducted to study the effect of temperature and type of oven on the life of a particular component being tested. Four types of ovens and three temperature levels were used in the experiment. Twenty-four pieces were assigned randomly, two to each combination of treatments, and the results in Table E8.1 were recorded:
- Fit an appropriate response surface model using  $-1, 0, 1$  coding for temperature. Be sure to determine if interaction exists among ovens and the response surface terms in temperature.
  - Find the estimated optimum temperature—that is, that which maximizes oven life. Does it depend on oven type?
- 8.36** To estimate the degree of a suspension polyethylene, we extract polyethylene by using a solvent, and we compare the gel contents (gel proportion). This method is called the **gel proportion estimation method**. In the book *Design of Experiments for Quality Improvement* published by the Japanese

**TABLE E8.1** The Experiment Design for Exercise 8.35

Temperature (degrees)	Life			
	Oven O <sub>1</sub>	O <sub>2</sub>	O <sub>3</sub>	O <sub>4</sub>
500	227	214	225	260
	221	259	236	229
550	187	181	232	246
	208	179	198	273
600	174	198	178	206
	202	194	213	219

Standards Association (1989), a study is reported on the relationship between the amount of gel generated and three factors (solvent, extraction temperature, and extraction time) that influence amount of gel. The data are provided in Table E8.2.

- (a) Build (and state) an appropriate response surface model in terms of coded temperature and time. Write a separate model for each solvent if necessary.
- (b) Give an estimate of the conditions that maximize the amount of gel generated. Is there any indication of conditions for future experiments?
- 8.37** Consider a situation in which one is interested in three levels of each of two quantitative design variables. These levels are  $-1, 0, 1$ . In addition, there are three levels of a single qualitative factor. It is felt that the design should accommodate a second-order model in the quantitative variables and interaction between the linear terms and the qualitative variable.
- (a) Write out the model to be fitted.
- (b) Using 18 experimental runs, construct, using a computer-generated design package, an appropriate design.

**TABLE E8.2** The Experiment Design for Exercise 8.36

Solvent	Temperature	Amount of Gel		
		Time: 4	8	16
Ethanol	120	94.0	93.8	91.1
		94.0	94.2	90.5
	80	95.3	94.9	92.5
		95.1	95.3	92.4
Toluene	120	94.6	93.6	91.1
		94.5	94.1	91.0
	80	95.4	95.6	92.1
		95.4	96.0	92.1

- 8.38** The following data was taken on two quantitative design variables and one two-level qualitative variable:

$x_1$	$x_2$	$z$	$y$
-1	1	-1	17.5
1	1	-1	22.1
0	0	-1	25.2
0	0	-1	26.5
0	0	+1	29.4
0	0	+1	31.3
-1	-1	+1	19.2
1	-1	+1	13.4

- (a) Fit a model of the type

$$\hat{y} = b_0 + c_1 z + b_1 x_1 + b_2 x_2 + b_{12} x_1 x_2$$

- (b) Edit the model, and give recommendations on levels of  $x_1$  and  $x_2$  that maximize the response.

- 8.39** In Section 6.3.3, the method of ridge analysis is used to optimize a process that is designed to convert 1,2-propanediol to 2,5-dimethyl-piperazine. The design is a

**TABLE E8.3 The Experiment in Exercise 8.39**

$x_1$	$x_2$	$x_3$	$x_4$	$z$	$y$
-1	-1	-1	-1	-1	68.4
1	-1	-1	-1	1	28.5
-1	1	-1	-1	1	22.0
-1	-1	1	-1	1	15.7
-1	-1	-1	1	1	48.5
1	1	-1	-1	-1	28.5
1	-1	1	-1	-1	18.7
1	-1	-1	1	-1	65.8
-1	1	1	-1	-1	9.2
-1	1	-1	1	-1	32.9
-1	-1	1	1	-1	12.5
-1	1	1	1	1	49.8
1	-1	1	1	1	12.9
1	1	-1	1	1	30.9
1	1	1	-1	1	22.9
1	1	1	1	-1	28.2
-1.4	0	0	0	-1	32.1
1.4	0	0	0	-1	18.2
0	-1.4	0	0	-1	19.2
0	1.4	0	0	-1	50.5
0	0	-1.4	0	1	52.1
0	0	1.4	0	1	39.2
0	0	0	-1.4	1	30.7
0	0	0	1.4	1	40.7
0	0	0	0	1	39.5
0	0	0	0	1	38.2

central composite design with  $k = 4$  and  $\alpha = 1.4$ . Suppose, in addition, that two different catalysts are being used. The design and response values are in Table E8.3.

- (a) Construct an appropriate response surface model taking into account the two catalysts ( $z = +1, -1$ ).
  - (b) Obtain a separate response surface model for each catalyst.
- 8.40** Consider Exercise 3.9 in Chapter 3. Four factors were varied, and their effects were measured on alloy cracking. One of the factors is the type of heat treatment method (factor  $C$ ) at two levels. This is a good example of a mix of qualitative and quantitative variables. Use the coding  $-1$  and  $+1$  for all factors, including factor  $C$ .
- (a) Write out an appropriate model for relating the design variables to the response. Be sure the model is edited if necessary.
  - (b) Use your result in (a) to develop two response surface models, one for each heat treatment method.
- 8.41** Consider Exercise 4.12. A  $2^{6-3}$  fractional factorial is used to fit a first-order model
- (a) Write out the first-order model using  $-1, +1$  coding on the material type as the qualitative variable.
  - (b) Write out separate models for material type 1 and material type 2.
  - (c) What assumptions are you making in your developments in (b) above?
- 8.42** Consider the data in Exercise 4.14. Two qualitative variables appear.
- (a) Fit a model containing all main effects and two-factor interactions.
  - (b) Edit the model to contain only significant terms.
  - (c) Use your model in (b) to write separate models for each combination of the qualitative variables.

---

# 9

---

## ADVANCED TOPICS IN RESPONSE SURFACE METHODOLOGY

In this chapter we deal with several more advanced response surface topics. This chapter focuses on the effects of bias in the fitting of response surface models, the effects of errors in the design variables, experiments with computer models, minimum-bias estimation as an alternative to the method of least squares, the role of artificial neural networks in RSM, how to deal with non-normal responses through the use of generalized linear models, and response surface designs in a split-plot structure.

### 9.1 EFFECTS OF MODEL BIAS ON THE FITTED MODEL AND DESIGN

In Chapter 7 we discussed the role of model bias on the test of lack of fit and the estimate of the error variance  $\sigma^2$ . We learned that if the fitted polynomial approximation is given by

$$\hat{y} = \mathbf{X}_1 \mathbf{b}_1 \quad (9.1)$$

and the true model for the expected response  $E(y)$  is better approximated by

$$E(y) = \mathbf{X}_1 \boldsymbol{\beta}_1 + \mathbf{X}_2 \boldsymbol{\beta}_2 \quad (9.2)$$

then the estimator  $\mathbf{b}_1$  is biased, and the estimator of  $\sigma^2$ , the error mean square in the analysis of variance, is biased upward. In fact, it is the bias in the mean squared error that one is detecting in a standard lack-of-fit test.

The important point here is that there are two types of model errors. In the postulated model

$$\mathbf{y} = \mathbf{X}_1 \boldsymbol{\beta}_1 + \boldsymbol{\varepsilon}$$

$\mathbf{X}_1 \boldsymbol{\beta}_1$  is merely an approximation; errors associated with the model can be put into two categories:

1. Random errors—that is, elements in  $\boldsymbol{\varepsilon}$  (with variance  $\sigma^2$ )
2. Systematic errors—that is, bias errors of the type  $\mathbf{X}_1 \boldsymbol{\beta}_1 - E(\mathbf{y})$

Apart from the simple lack-of-fit test, the entire emphasis in design and analysis has been placed on variability produced by random variation. In particular, all experimental design criteria in Chapter 8 deal with variance oriented criteria; that is,  $D$ ,  $G$ ,  $A$ ,  $V$ , and  $I$  (or  $IV$ ) optimality all deal with criteria that relate to  $\mathbf{X}'\mathbf{X}$  or the moment matrix  $\mathbf{X}'\mathbf{X}/N$ . In what follows we will link the  $I$ -optimality-criterion with another involving model bias.

**What Effect Does Design Have on Variance and Bias?** The most effective way to demonstrate the effect of design on variance and bias is to illustrate with a simple scenario. Suppose that  $k = 1$  and the **true model**  $f(x)$  is given by

$$f(x) = \beta_0 + \beta_1 x + \beta_{11} x^2 = 1 + x + x^2 \quad (9.3)$$

and it is approximated by a straight line with the formal fitted model

$$\hat{y}(x) = b_0 + b_1 x$$

For simplicity we assume that the region of interest and region of operability are the same, namely, the interval  $[-1, +1]$ . In addition, suppose the design contains a single run at each of the endpoints,  $-1$  and  $+1$ . As a result, the variance transmitted to the predicted value, namely  $v(x) = N \text{Var}[\hat{y}(x)]$ , is given by (assume  $\sigma = 1$ )

$$\begin{aligned} v(x) &= 2[\text{Var}(b_0) + x^2 \text{Var}(b_1)] \\ &= 2\left[\frac{1}{2} + x^2 \text{Var}(b_1)\right] \\ &= 2\left[\frac{1}{2} + \frac{x^2}{2}\right] \end{aligned} \quad (9.4)$$

because  $\text{Var}(b_1) = \sigma^2 / \sum_{i=1}^2 (x_i)^2 = \frac{1}{2}$ . As a result,

$$v(x) = 1 + x^2 \quad (9.5)$$

The measure of bias that is consistent in units with  $v(x)$  is given by

$$d(x) = N[E\hat{y}(x) - f(x)]^2 \quad (9.6)$$

We have  $E[\hat{y}(x)] = E(b_0) + xE(b_1)$ . Recall from Chapter 7 that if one fits an incomplete model  $\hat{\mathbf{y}} = \mathbf{X}_1 \boldsymbol{\beta}_1$ , when in fact  $E(\mathbf{y}) = \mathbf{X}_1 \boldsymbol{\beta}_1 + \mathbf{X}_2 \boldsymbol{\beta}_2$ , then

$$E(\boldsymbol{\beta}_1) = \boldsymbol{\beta}_1 + (\mathbf{X}'_1 \mathbf{X}_1)^{-1} \mathbf{X}'_1 \mathbf{X}_2 \boldsymbol{\beta}_2$$

Indeed, in our case

$$\boldsymbol{\beta} = \begin{bmatrix} 1 \\ 1 \end{bmatrix}, \quad (\mathbf{X}'_1 \mathbf{X}_1)^{-1} = \begin{bmatrix} \frac{1}{2} & 0 \\ 0 & \frac{1}{2} \end{bmatrix}, \quad \text{and}$$

$$\mathbf{X}'_1 \mathbf{X}_2 = \begin{bmatrix} 1 & -1 \\ 1 & -1 \end{bmatrix} \begin{bmatrix} (1)^2 \\ (-1)^2 \end{bmatrix} = \begin{bmatrix} 2 \\ 0 \end{bmatrix}$$

Thus, because  $\beta_2 = \beta_{11} = 1$ , we obtain

$$E \begin{bmatrix} b_0 \\ b_1 \end{bmatrix} = \begin{bmatrix} \beta_0 + 1 \\ \beta_1 \end{bmatrix}$$

As a result, in this case the bias is transmitted only to the intercept estimate. Thus  $E[\hat{y}(x)] = \beta_0 + 1 + \beta_1 x = 2 + x$ . From Equation 9.6 we obtain

$$\begin{aligned} d(x) &= 2[\beta_0 + 1 + \beta_1 x - (\beta_0 + \beta_1 x + x^2)]^2 \\ &= 2[1 - x^2]^2 \end{aligned} \tag{9.7}$$

The results in Equations 9.5 and 9.7 represent the two components that contribute to error in predicted values  $\hat{y}(x)$  in the region  $[-1, +1]$ . Now, consider Fig. 9.1. The actual function  $f(x)$  is plotted along with  $E[\hat{y}(x)] = 2 + x$ . The differences, or vertical deviations, represent **model bias** values that are incurred with this endpoint design, namely, the two-point design at  $-1$  and  $+1$ .

Now, suppose we consider an alternative design, namely, a two-point design at the points  $-0.6$  and  $+0.6$ . Again, in the fitted model  $\hat{y}(x) = b_0 + b_1 x$ ,  $b_1$  is found to be unbiased for  $\beta_1$ , but  $b_0$  is biased. Following the same route as before, we have

$$E \begin{bmatrix} b_0 \\ b_1 \end{bmatrix} = \begin{bmatrix} \beta_0 \\ \beta_1 \end{bmatrix} + \begin{bmatrix} \frac{1}{2} & 0 \\ 0 & \frac{0.5}{(0.6)^2} \end{bmatrix} \begin{bmatrix} 1 & 1 \\ -0.6 & 0.6 \end{bmatrix} \begin{bmatrix} (-0.6)^2 \\ (0.6)^2 \end{bmatrix} \beta_{11} = \begin{bmatrix} \beta_0 + 0.36 \\ \beta_1 \end{bmatrix}$$

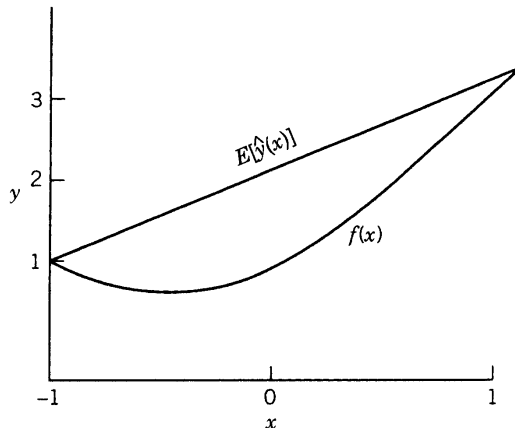


**Figure 9.1** True function  $f(x)$  and  $E[\hat{y}(x)]$  for design with points at  $-1, +1$ .

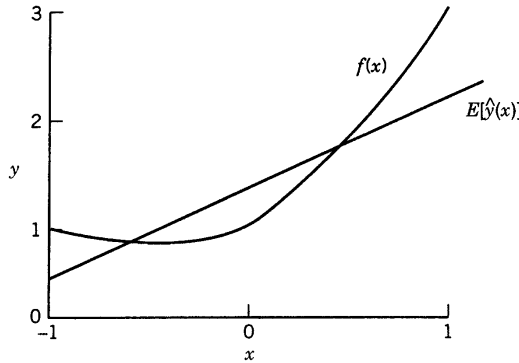


**Figure 9.2** True function  $f(x)$  and  $E[\hat{y}(x)]$  for design at points  $-0.6, 0.6$ .

Note that the bias in the intercept is not as great as in the case of the previous endpoint design. Thus the squared bias  $d(x)$  is given by

$$\begin{aligned} d(x) &= 2[E(b_0 + b_1x) - (\beta_0 + \beta_1x + \beta_{11}x^2)]^2 \\ &= 2[\beta_0 + 0.36 + \beta_1x - \beta_0 - \beta_1x - \beta_{11}x^2]^2 \\ &= 2[0.36 - x^2]^2 \end{aligned}$$

The expected value of the fitted approximation, namely  $E[\hat{y}(x)]$ , is given by

$$E[\hat{y}(x)] = 1.36 + x$$

Figure 9.2 displays  $f(x)$  and  $E[\hat{y}(x)]$  in the case of the second two-point design.

Figures 9.1 and 9.2 reveal how the structure of the bias values  $E[\hat{y}(x)] - f(x)$  are affected by the two designs in different ways. In the case discussed here the endpoint design results in rather small bias errors only near the endpoints where the design points are located. Near the design center very large bias errors occur because there are no data there. As a result, it would appear reasonable that if design points are taken closer to the center, as in the case of the second design, the bias errors should be smaller. In the case of the second design, very small errors occur near the design points and moderate errors are experienced near the design center and at the design perimeter. Clearly, designs with points that are pushed closer to the center of the design afford considerably more protection against bias errors than does the endpoint design, though of course the latter is a minimum variance design. This suggests that when one fears model inadequacy, perhaps there is a need to consider some type of compromise design, because a strategy involving protection against bias errors works counter to a strategy designed to minimize variance.

## 9.2 A DESIGN CRITERION INVOLVING BIAS AND VARIANCE

The scientist or engineer who applies RSM is not always aware when he or she should fit a second-order model. However, very often only a moderate amount of model inadequacy (in magnitude less than is detectable by a lack-of-fit test) will lead to errors that are as serious as variation due to random errors.

It is natural to consider combining bias and variance through the **mean squared error** criterion

$$E[\hat{y}(\mathbf{x}) - f(\mathbf{x})]^2 \quad (9.8)$$

Here  $\mathbf{x}$  is a vector to allow for multiple design variables. Box and Draper (1959, 1963) introduced an average mean squared error criterion in which the mean squared error in Equation 9.8 is averaged over a region of interest in the design variables. They also showed some compelling evidence that bias due to model misspecification should not be ignored when one chooses an experimental design for response surface exploration. Indeed, there are situations when model bias is the dominant component in the mean squared error formulation. As we saw in the development in Section 9.1, it often occurs that the minimum variance approach applies a premium to pushing points to the edge of the region of interest (much as in a  $D$ -optimal approach), whereas a minimum bias approach calls for more placement of points that are at an intermediate distance from the design center. The details depend a great deal on (a) the model that one is fitting and (b) the model that one chooses to protect against. The latter model usually involves model terms that are of order higher than that of the fitted model.

**Generalization of the Average Mean Squared Error** Consider the mean squared error of Equation 9.8. This **average squared error loss criterion** is written so as to be a function of  $\mathbf{x}$ , the location at which one is predicting the response with  $\hat{y}(\mathbf{x})$ . Now, the mean squared error in Equation 9.8 can be partitioned as

$$\begin{aligned} E[\hat{y}(\mathbf{x}) - f(\mathbf{x})]^2 &= E\{[\hat{y}(\mathbf{x}) - E[\hat{y}(\mathbf{x})]] + [E[\hat{y}(\mathbf{x})] - f(\mathbf{x})]\}^2 \\ &= E\{\hat{y}(\mathbf{x}) - E[\hat{y}(\mathbf{x})]\} + \{E[\hat{y}(\mathbf{x})] - f(\mathbf{x})\}^2 \end{aligned} \quad (9.9)$$

The cross-product term in the above squaring operation is zero. The two terms on the right-hand side of Equation 9.9 are, respectively, the variance and the squared bias of  $\hat{y}(\mathbf{x})$ .

It should be clear from the foregoing and other developments in this text that there is a tradeoff in dealing with variance and bias. It should also be apparent that Equation 9.9 does not afford the user a single-number criterion, because the mean squared error depends on  $\mathbf{x}$ , the point at which one predicts. However, Box and Draper suggested the use of an **average mean squared error** (AMSE), where the quantity  $E[\hat{y}(\mathbf{x}) - f(\mathbf{x})]^2$  in Equation 9.9 is averaged over  $\mathbf{x}$  in a preselected region of interest. In other words, a quantity

$$\text{AMSE} = \frac{NK}{\sigma^2} \int_R E[\hat{y}(\mathbf{x}) - f(\mathbf{x})]^2 d\mathbf{x} \quad (9.10)$$

was offered as a single-number criterion. The integral  $\int_R$ , along with the multiplication by  $K = 1/\int_R d\mathbf{x}$ , the reciprocal of the volume of the region, implies that the quantity AMSE is an average of the MSE over  $R$ . The quantity  $N/\sigma^2$  is a scale factor in the same spirit as that provided by the scaled prediction variance  $N \text{Var}[\hat{y}(\mathbf{x})]/\sigma^2$ , which has been used throughout the text. The AMSE can be subdivided as follows:

$$\begin{aligned} \text{AMSE} &= \frac{NK}{\sigma^2} \int_R E\{\hat{y}(\mathbf{x}) - E[\hat{y}(\mathbf{x})]\}^2 d\mathbf{x} + \frac{NK}{\sigma^2} \int_R \{E[\hat{y}(\mathbf{x})] - f(\mathbf{x})\}^2 d\mathbf{x} \\ &= \text{APV} + \text{ASB} \end{aligned} \quad (9.11)$$

where APV stands for **average prediction variance** and ASB stands for **average squared bias**. Here, of course, the averaging is done over the region of interest  $R$ . In what follows we focus heavily on designs that minimize APV and ASB, with strong emphasis on the latter. Note that minimization of APV is equivalent to the  $I$ -optimality criterion discussed in Chapter 8.

The partition of mean squared error into variance and squared bias should bring to mind the material in Chapter 7 dealing with lack of fit. The structure of bias stems from the assumption that the model

$$\hat{\mathbf{y}} = \mathbf{X}_1 \mathbf{b}_1$$

is fitted and the true model is a polynomial of a higher degree. The matrix  $\mathbf{X}_1$  contains model terms of a low-order approximation of the true structure, and the matrix  $\mathbf{X}_2$  contains additional higher-order terms that one wishes to protect against in designing the experiment. Thus

$$\mathbf{f} = E(\mathbf{y}) = \mathbf{X}_1 \boldsymbol{\beta}_1 + \mathbf{X}_2 \boldsymbol{\beta}_2$$

Here, of course,  $\mathbf{y}$  is the  $N \times 1$  vector of observations. From material in Chapter 7, we know that the estimator  $\mathbf{b}_1$  is biased, namely,

$$E(\mathbf{b}_1) = \boldsymbol{\beta}_1 + \mathbf{A} \boldsymbol{\beta}_2 \quad (9.12)$$

where

$$\mathbf{A} = (\mathbf{X}'_1 \mathbf{X}_1)^{-1} \mathbf{X}'_1 \mathbf{X}_2$$

As a result, the bias portion of AMSE, namely ASB, can be written

$$ASB = \frac{NK}{\sigma^2} \int_R \{ \mathbf{x}'_1 E(\mathbf{b}_1) - [(\mathbf{x}'_1 \boldsymbol{\beta}_1 + \mathbf{x}'_2 \boldsymbol{\beta}_2)] \}^2 d\mathbf{x} \quad (9.13)$$

where  $\mathbf{x}_1$  contains the  $p_1$  model terms that are fitted, and  $\mathbf{x}_2$  contains the  $p_2$  terms that are ignored. On invoking Equation 9.12, Equation 9.13 reduces to

$$\begin{aligned} ASB &= \frac{NK}{\sigma^2} \int_R [(\mathbf{x}'_1 \mathbf{A} - \mathbf{x}'_2) \boldsymbol{\beta}_2]^2 d\mathbf{x} \\ &= \frac{NK}{\sigma^2} \int_R \boldsymbol{\beta}'_2 [\mathbf{A}' \mathbf{x}_1 - \mathbf{x}_2] [\mathbf{x}'_1 \mathbf{A} - \mathbf{x}'_2] \boldsymbol{\beta}_2 d\mathbf{x} \\ &= \frac{NK}{\sigma^2} \int_R [\boldsymbol{\beta}'_2 \mathbf{A}' \mathbf{x}_1 \mathbf{x}'_1 \mathbf{A} \boldsymbol{\beta}_2 - 2\boldsymbol{\beta}'_2 \mathbf{x}_2 \mathbf{x}'_1 \mathbf{A} \boldsymbol{\beta}_2 + \boldsymbol{\beta}'_2 \mathbf{x}_2 \mathbf{x}'_2 \boldsymbol{\beta}_2] d\mathbf{x} \end{aligned}$$

For the case of APV we have

$$APV = \frac{NK}{\sigma^2} \int_R \mathbf{x}'_1 (\mathbf{X}'_1 \mathbf{X}_1)^{-1} \mathbf{x}_1 d\mathbf{x}$$

### 9.2.1 The Case of a First-Order Fitted Model and Cuboidal Region

For the situation where the fitted model is first-order, we have

$$\hat{y}(\mathbf{x}) = b_0 + \sum_{i=1}^k b_i x_i$$

and hence  $\mathbf{x}'_1 = [1, x_1, \dots, x_k]$ . If we further assume that we are interested in protecting against a true model that is of second order, then

$$\mathbf{X}_1 = \begin{bmatrix} 1 & x_{11} & \cdots & x_{1k} \\ 1 & x_{21} & \cdots & x_{2k} \\ \vdots & \vdots & & \vdots \\ 1 & x_{N,1} & \cdots & x_{N,k} \end{bmatrix}$$

and

$$\mathbf{X}_2 = \begin{bmatrix} x_{11}^2 & \cdots & x_{1k}^2 & x_{11}x_{12} & \cdots & x_{1,k-1} & x_{1,k} \\ \vdots & & \vdots & & & \vdots & \vdots \\ \vdots & & \vdots & & & \vdots & \vdots \\ x_{N,1}^2 & \cdots & x_{N,k}^2 & x_{N,1}x_{N,2} & \cdots & x_{N,k-1} & x_{N,k} \end{bmatrix} \quad (9.15)$$

Assume that both the region of interest and the region of operability on the design variables is  $-1 \leq x_i \leq 1$  for  $i = 1, 2, \dots, k$ . If we consider variance alone, we can borrow from Chapter 8, where we learned that the  $I$ -optimal design is an orthogonal design in which all levels are set at the  $\pm 1$  extremes. However, for the case of bias, one would expect from the discussion in Section 9.1 that levels should be placed inward from the  $\pm 1$  extremes.

Suppose we consider the minimization of ASB in Equation 9.14 by choice of design. Using the fact that  $\mathbf{A} = (\mathbf{X}'_1 \mathbf{X}_1)^{-1} (\mathbf{X}'_1 \mathbf{X}_2) = \mathbf{M}_{11}^{-1} \mathbf{M}_{12}$ , where  $\mathbf{M}_{11} = \mathbf{X}'_1 \mathbf{X}_1 / N$  and  $\mathbf{M}_{12} = \mathbf{X}'_1 \mathbf{X}_2 / N$  are **moment matrices**. We have

$$\text{ASB} = \frac{NK}{\sigma^2} \int_R \mathbf{\beta}'_2 [\mathbf{M}'_{12} \mathbf{M}_{11}^{-1} \mathbf{x}_1 \mathbf{x}'_1 \mathbf{M}_{11}^{-1} \mathbf{M}_{12} - 2\mathbf{x}_2 \mathbf{x}'_1 \mathbf{M}_{11}^{-1} \mathbf{M}_{12} + \mathbf{x}_2 \mathbf{x}'_2] \mathbf{\beta}_2 d\mathbf{x}$$

At this point it is convenient to introduce the concept of **region moments**. Letting  $\boldsymbol{\alpha}_2 = \sqrt{N} \mathbf{\beta}_2 / \sigma$ , ASB can be written as

$$\text{ASB} = \boldsymbol{\alpha}'_2 [\mathbf{M}'_{12} \mathbf{M}_{11}^{-1} \boldsymbol{\mu}_{11} \mathbf{M}_{11}^{-1} \mathbf{M}_{12} - 2\boldsymbol{\mu}'_2 \mathbf{M}_{11}^{-1} \mathbf{M}_{12} + \boldsymbol{\mu}_{22}] \boldsymbol{\alpha}_2 \quad (9.16)$$

where

$$\boldsymbol{\mu}_{11} = K \int_R \mathbf{x}_1 \mathbf{x}'_1 d\mathbf{x}, \quad \boldsymbol{\mu}_{22} = K \int_R \mathbf{x}_2 \mathbf{x}'_2 d\mathbf{x}, \quad \text{and} \quad \boldsymbol{\mu}_{12} = K \int_R \mathbf{x}_1 \mathbf{x}'_2 d\mathbf{x}.$$

The quantities  $\mu_{11}$ ,  $\mu_{22}$ , and  $\mu_{12}$  are **region moment matrices**. The matrix  $\mu_{11}$  contains first and second moments. In fact,

$$\mu_{11} = K \int_R \mathbf{x}_1 \mathbf{x}'_1 = K \int_R \begin{bmatrix} 1 \\ x_1 \\ x_2 \\ \vdots \\ x_k \end{bmatrix} [1, x_1, x_2, \dots, x_k] d\mathbf{x}$$

Because  $\int_R$  implies  $\int_{-1}^1 \int_{-1}^1 \cdots \int_{-1}^1$ , this first- and second-order region moment matrix  $\mu_{11}$  is given by

$$\mu_{11} = \left[ \begin{array}{c|cccc} 1 & 0 & \cdots & 0 \\ \hline 0 & & & & \\ 0 & & & & \\ \vdots & & & \frac{1}{3} I_k & \\ 0 & & & & \end{array} \right]$$

The matrix  $\mu_{22}$ , in a similar fashion, displays region moments through order four, while  $\mu_{12}$  contains region moments through order three.

An easy prescription for the form of the design that minimizes ASB is obtained by writing the average squared bias in Equation 9.15 as

$$ASB = \boldsymbol{\alpha}'_2 [(\mu_{22} - \mu'_{12} \mu_{11}^{-1} \mu_{12}) + (\mathbf{M}_{11}^{-1} \mathbf{M}_{12} - \mu_{11}^{-1} \mu_{12})' \mu_{11} (\mathbf{M}_{11}^{-1} \mathbf{M}_{12} - \mu_{11}^{-1} \mu_{12})] \boldsymbol{\alpha}_2 \quad (9.17)$$

In the second term in Equation 9.17 the matrix  $\mu_{11}$  is positive definite. [see Box and Draper (1987) and Myers (1976)]. As a result, a sufficient condition for a **minimum bias design** (i.e., a design that minimizes ASB) is to let

$$\mathbf{M}_{11} = \mu_{11} \text{ and } \mathbf{M}_{12} = \mu_{12} \quad (9.18)$$

that is, the design moment matrices  $\mathbf{M}_{11}$  and  $\mathbf{M}_{12}$  should be equal to the corresponding region moment matrices  $\mu_{11}$  and  $\mu_{12}$ . As a result, the minimum bias design is one in which  $ASB = \boldsymbol{\alpha}'_2 [\mu_{22} - \mu'_{12} \mu_{11}^{-1} \mu_{12}] \boldsymbol{\alpha}_2$ . Note that selection of an appropriate design reduces to the selection of design moment matrices  $\mathbf{M}_{11}$  and  $\mathbf{M}_{12}$ . In the case where a first-order model is being fitted and one seeks to protect against a second-order model,  $\mathbf{M}_{11}$  contains moments through order two and  $\mathbf{M}_{12}$  contains moments through order three. However, note that Equation 9.17 allows for the minimum ASB in general—that is, if one fits a model with the form  $\hat{y} = \mathbf{X}_1 \boldsymbol{\beta}_1$  and protection is sought against a model  $\mathbf{y} = \mathbf{X}_1 \boldsymbol{\beta}_1 + \mathbf{X}_2 \boldsymbol{\beta}_2$ .

**Single Design Variable—Minimum Bias Design** It is useful to write one of the general expressions in Equation 9.18 for the special case of a single design variable. Here, of course, the design becomes the selection of the spacing of points in the interval  $[-1, +1]$  in the design variable. As a result, we assume a fitted first-order model

$$\hat{y}(x) = b_0 + b_1 x$$

when the true structure is best approximated by

$$E[y(x)] = \beta_0 + \beta_1 x + \beta_{11} x^2$$

We have an experiment that results in

$$\mathbf{X}_1 = \begin{bmatrix} 1 & x_1 \\ 1 & x_2 \\ \vdots & \vdots \\ 1 & x_N \end{bmatrix}$$

with

$$\mathbf{X}_2 = \begin{bmatrix} x_1^2 \\ x_2^2 \\ \vdots \\ x_N^2 \end{bmatrix}.$$

The relevant moment matrices are

$$\mathbf{M}_{11} = \frac{\mathbf{X}'_1 \mathbf{X}_1}{N} = \begin{bmatrix} 1 & [1] \\ [1] & [11] \end{bmatrix}$$

and

$$\mathbf{M}_{12} = \begin{bmatrix} [11] \\ [111] \end{bmatrix}$$

where  $[11] = (1/N) \sum_u x_u^2$ ,  $[1] = (1/N) \sum_u x_u$ , and  $[111] = (1/N) \sum_u x_u^3$ . Now, the region moment matrices  $\boldsymbol{\mu}_{11}$  and  $\boldsymbol{\mu}_{12}$  are of the same dimension and structure as their design moment counterparts  $\mathbf{M}_{11}$  and  $\mathbf{M}_{12}$ . In fact,

$$\boldsymbol{\mu}_{11} = \frac{1}{2} \int_{-1}^1 \begin{bmatrix} 1 \\ x \end{bmatrix} \begin{bmatrix} 1 & x \end{bmatrix} dx = \begin{bmatrix} 1 & 0 \\ 0 & \frac{1}{3} \end{bmatrix}$$

and

$$\boldsymbol{\mu}_{12} = \frac{1}{2} \int_{-1}^1 \begin{bmatrix} 1 \\ x \end{bmatrix} [x^2] dx = \begin{bmatrix} \frac{1}{3} \\ 0 \end{bmatrix}$$

For the interval  $[-1, +1]$ , which represents the region of interest in  $x$ , *the odd region moments are all zero*. The quantity  $\frac{1}{3}$  in  $\boldsymbol{\mu}_{11}$  and  $\boldsymbol{\mu}_{12}$  is the value of the second pure region moment  $\frac{1}{2} \int_{-1}^1 x^2 dx$ . As a result, a very simple application of the results in Equation 9.18 suggests:

A *minimum bias* (minimum ASB) design for a fitted first-order model with protection against a model of second order can be achieved by having  $[1] = 0$ ,  $[11] = \frac{1}{3}$  and  $[111] = 0$ .

The above result is not at all counterintuitive and, in fact, is certainly the kind of result one expects from the discussion in Section 9.1. Clearly the **minimum variance design** (i.e., the design that minimizes APV for this case) will have  $[1] = 0$  and  $[11] = 1.0$  (all points pushed to the  $\pm 1$  levels). The minimum bias design requires levels to be placed inward from the  $\pm 1$  extremes.

For the case of the single design variable, there are many designs that meet the moment conditions that result in minimum bias—that is, minimum average squared bias. The requirement of zero first and third moments requires only an equal sample size design with levels spaced symmetrically around the center of the design interval. It is interesting, then, that the design that best protects against the quadratic model can take many forms. For example, a *two-level design* with, say,  $N$  observations ( $N$  even) requires

$$N/2 \text{ observations at } x = \sqrt{\frac{1}{3}} = 0.58$$

$$N/2 \text{ observations at } x = -\sqrt{\frac{1}{3}} = -0.58$$

Of course there are obvious advantages in using more than two levels. The extra degrees of freedom for lack of fit are certainly useful. Thus, for three levels and  $N/3$  runs at each level, the design is given by

$$\frac{N}{3} \text{ at } x = a, \quad \frac{N}{3} \text{ at } x = 0, \quad \frac{N}{3} \text{ at } x = -a$$

where, to allow  $[11] = \frac{1}{3}$ , we have

$$\frac{2}{3}a^2 = \frac{1}{3}$$

and thus

$$a = \sqrt{\frac{1}{2}} \cong 0.707$$

This demonstrates the considerable flexibility in constructing the minimum bias design. One can have various numbers of center runs and divide the remaining runs between two levels symmetric around  $x = 0$ . For example, suppose 15 runs are allowed. Suppose, also, that three runs are to be used in the center. The remaining 12 runs are then evenly divided between  $-a$  and  $a$ , where

$$\left(\frac{4}{5}\right)a^2 = \frac{1}{3}$$

and thus

$$a = \sqrt{\frac{5}{12}} \cong 0.644$$

Thus, it is important to be sure that all three moment conditions hold. The minimum bias design need not have equally spaced levels. For example, consider the design with levels  $-a_2$ ,  $-a_1$ ,  $a_1$ , and  $a_2$  (no center runs) with  $N/4$  runs at each level. The values  $a_1$  and  $a_2$  are such that

$$\frac{a_1^2 + a_2^2}{2} = \frac{1}{3}$$

There are many choices for  $a_1$  and  $a_2$  and thus many four-level designs. One example is  $a_1 = \sqrt{\frac{1}{6}}$  and  $a_2 = \sqrt{\frac{1}{2}}$  and another is  $a_1 = \frac{1}{2}$  and  $a_2 = \sqrt{\frac{5}{12}}$ .

**Multiple Design Variables—Minimum Bias Design** The use of Equation 9.18 is general and applies in the case of the fitted model

$$\hat{y}(\mathbf{x}) = b_0 + b_1x_1 + b_2x_2 + \cdots + b_kx_k$$

Suppose we wish to protect against a full second-order model characterized by  $\mathbf{X}_2$  in Equation 9.15. Suppose the region of interest is a cuboidal region with  $-1 < x_i \leq 1$  for  $i = 1, 2, \dots, k$ . The pertinent region moments are

$$\begin{aligned}\boldsymbol{\mu}_{11} &= \left[ \begin{array}{c|cccc} 1 & 0 & \cdots & 0 \\ \hline 0 & & \frac{1}{3}\mathbf{I}_k \\ \vdots & & & \\ 0 & & & \end{array} \right] \\ \boldsymbol{\mu}_{12} &= \left[ \begin{array}{c} \frac{1}{3}\frac{1}{3}\cdots\frac{1}{3}00\cdots0 \\ \hline \mathbf{0} \end{array} \right]\end{aligned}$$

As a result, if we again accomplish minimum ASB by equating design moments to region moments through order three, we require  $\mathbf{M}_{11} = \boldsymbol{\mu}_{11}$  and  $\mathbf{M}_{12} = \boldsymbol{\mu}_{12}$ . This results in setting all odd moments through order three equal to zero. It should be noted that

$$\boldsymbol{\mu}_{12} = \frac{1}{K} \int_R \begin{bmatrix} 1 \\ x_1 \\ x_2 \\ \vdots \\ x_k \end{bmatrix} [x_1^2, x_2^2, \dots, x_k^2, x_1x_2, \dots, x_kx_{k-1}] d\mathbf{x}$$

and thus  $\boldsymbol{\mu}_{12}$  is a  $k+1$  by  $k(k-1)/2$  matrix containing second and third moments. The moment matrix  $\mathbf{M}_{12}$  has the same dimension and structure. As a result, the minimum ASB can be obtained by setting

$$\begin{aligned}[i] &= 0, \quad i = 1, 2, \dots, k \\ [ii] &= \frac{1}{3}, \quad i = 1, 2, \dots, k \\ [iii] &= 0, \quad i = 1, 2, \dots, k \\ [ij] &= 0, \quad i \neq j \\ [ij] &= 0, \quad i \neq j \\ [ijk] &= 0, \quad i \neq j \neq k\end{aligned} \tag{9.19}$$

The two-level full factorial design in  $k$  variables contains the type of symmetries that result in the above odd moments being zero. In order to achieve a design with each second pure moment equal to  $\frac{1}{3}$ , the level of the factorial points must be  $\pm g$ , where  $g = \sqrt{\frac{1}{3}} = 0.58$ .

**What About Fractional Factorials and Center Runs?** It is clear that complete  $2^k$  factorials with levels brought in considerably from the  $\pm 1$  extremes in the case of a cuboidal region satisfy the moment conditions given in Equation 9.19 for a minimum bias design. But will fractional factorials suffice? For the case of odd design moments, the regular  $2^{k-p}$  fractional factorial of resolution  $\geq III$ , or even the Plackett–Burman designs, produce moments  $[i]$ ,  $[iii]$ ,  $[ij]$ , and  $[ij]$  that are zero. However, the resolution III design *does not result in*  $[ijk] = 0$ . This should be obvious, because all  $x_i$  will not be orthogonal to all  $x_j x_k$  ( $i \neq j \neq k$ ) for the case of resolution III. However, the following statement can be made:

A minimum bias design in a cuboidal region for a first-order model with protection against a model of second order is achieved with a  $2^k$  factorial design or a  $2^{k-p}$  fraction with resolution  $\geq IV$ . If the extremes of the cuboidal region are scaled to  $\pm 1$ , the design levels will be at  $\pm 0.58$ .

Center runs are very useful when one desires to afford protection against curvature. The conditions in Equation 9.19 on the odd moments are not altered by the use of center runs, and the condition on the second pure moment is achieved with the intuitively appealing result that the design levels can be moved closer to the  $\pm 1$  extremes. This will likely be an attractive alternative. For example, suppose one uses a  $\frac{1}{2}$  fraction of a  $2^4$  factorial with  $n_0 = 4$  center runs. The extremes for the region of interest are scaled to  $\pm 1$ , and a minimum bias design is given by

$$\mathbf{D} = \begin{bmatrix} x_1 & x_2 & x_3 & x_4 \\ -g & -g & -g & -g \\ g & g & -g & -g \\ g & -g & g & -g \\ g & -g & -g & g \\ -g & g & g & -g \\ -g & g & -g & g \\ -g & -g & g & g \\ g & g & g & g \\ 0 & 0 & 0 & 0 \\ 0 & 0 & 0 & 0 \\ 0 & 0 & 0 & 0 \\ 0 & 0 & 0 & 0 \end{bmatrix}$$

with  $g$  determined so that  $[ii] = \frac{1}{3}$ . In fact,

$$g = \sqrt{\left(\frac{12}{8}\right)\left(\frac{1}{3}\right)} = 0.707$$

As a second example consider a  $\frac{1}{2}$  fraction of a  $2^5$  factorial with  $n_c = 8$  center runs. Using  $\pm g$  notation to indicate design levels, a minimum bias design is produced for a cuboidal region of interest scaled to  $\pm 1$  by using a resolution V fraction with

$$g = \sqrt{\left(\frac{24}{16}\right)\left(\frac{1}{3}\right)} = 0.707$$

It should be clear that the selection of the region of interest is important. Minimizing the bias due to an underspecification of the model requires that points be placed inward from

the extremes of that region, but the criterion (i.e., squared bias) is integrated, or **averaged**, over the entire region. Anderson-Cook et al. (2009) consider several examples of comparing designs on cuboidal regions for protecting against higher order models. While the cuboidal region of interest is certainly quite common in practice, there are still instances in which a spherical region is the operative region of interest. In the next section we discuss the protection against bias due to the presence of a second-order model when the region of interest is spherical.

### 9.2.2 Minimum Bias Designs for a Spherical Region of Interest

Consider again a fitted first-order model with protection against a second-order model, but the squared bias in prediction is average over a **spherical region**. That is, there are ranges in the variables that aid in structuring the region of interest, but locations that represent simultaneous extremes in the variables are not included. As we discussed at length in Chapter 7, this condition suggests a region not unlike a sphere. For simplicity in what follows, we will assume that the region of interest is a unit sphere—that is, the region

$$\sum_{i=1}^k x_i^2 \leq 1 \quad (9.20)$$

Thus the variables are centered so that the center of the region is  $(0, 0, \dots, 0)$  and the radius of the sphere is 1.0.

As in the case of the cuboidal region, the minimum bias design for the spherical region can be obtained by achieving moment conditions that are governed by Equation 9.18. Again this involves equating design moments to region moments through order three. For the region given by Equation 9.20, all odd region moments are zero and the second pure region moment is given by  $K \int_R x_i^2 d\mathbf{x} = 1/(k+2)$ . Notice that for the special case in which  $k = 1$ , the value is  $\frac{1}{3}$ . The minimum bias design for the spherical region of Equation 9.20 is achieved by a design with moment conditions:

$$\begin{aligned} [i] &= [ij] = [iii] = [iji] = [ijk] = 0 \quad (i \neq j \neq k) \\ [ii] &= \frac{1}{k+2} \quad (i = 1, 2, \dots, k) \end{aligned} \quad (9.21)$$

Again it becomes clear that the points that produce the minimum bias design are set in from the perimeter of the sphere. In addition, the symmetry of the region, like that of the cube, requires a design symmetry that forces odd design moments through order three to be zero. Once again the two-level factorial meets all design requirements, with the  $[ii] = 1/(k+2)$  produced by the choice of the specific factorial levels  $\pm g$ .

**Example 9.1** It is important to understand the importance of the scaling specified by the region  $\sum_{i=1}^k x_i^2 = 1.0$ . This implies that the factorial points that are placed at the perimeter of the region reside at  $\pm 1/\sqrt{k}$ . The points  $\pm 1$  are outside the region of interest in the metric invoked by the region. Suppose then that  $k = 4$  and a  $2^4$  factorial with  $n_c = 5$  center runs is employed. The zero odd moments satisfy the requirements of a minimum

bias design according to Equation 9.21. The second pure moment [ii] should be

$$[ii] = \frac{1}{k+2} = \frac{1}{6}$$

As a result, with  $n_c = 5$  center runs, the  $2^4$  factorial contains the design levels  $\pm g$  at

$$\begin{aligned} g &= \sqrt{\left(\frac{1}{6}\right)\frac{21}{16}} \\ &= \sqrt{0.21} \\ &\cong 0.46 \end{aligned}$$

Therefore, the minimum bias design requires factorial points that are placed at 0.46, whereas the factorial points at the perimeter of the design region are scaled to  $1/\sqrt{4} = 0.5$ .

### 9.2.3 Simultaneous Consideration of Bias and Variance

Early in Section 9.2 we introduced the notion of average mean squared error (AMSE) and the partition of Equation 9.11 into APV and ASB. From that point on we have focused strictly on bias and thus the minimization of ASB. At this point let us consider the use of the entire AMSE. From Equations 9.11 and 9.16 we have

$$\begin{aligned} \text{AMSE} &= \boldsymbol{\alpha}'_2[(\boldsymbol{\mu}_{22} - \boldsymbol{\mu}'_{12}\boldsymbol{\mu}_{11}^{-1}\boldsymbol{\mu}_{12}) \\ &\quad + (\boldsymbol{M}_{11}^{-1}\boldsymbol{M}_{12} - \boldsymbol{\mu}_{11}^{-1}\boldsymbol{\mu}_{12})'\boldsymbol{\mu}_{11}(\boldsymbol{M}_{11}^{-1}\boldsymbol{M}_{12} - \boldsymbol{\mu}_{11}^{-1}\boldsymbol{\mu}_{12})]\boldsymbol{\alpha}_2 \\ &\quad + \frac{NK}{\sigma^2} \int_R \text{Var}[\hat{y}(\mathbf{x})]d\mathbf{x} \end{aligned} \quad (9.22)$$

As before, we are assuming, in this general formulation, that we are fitting a model  $\hat{y} = \mathbf{x}'_1\mathbf{b}_1$  and the true model is given by  $E(y) = \mathbf{x}'_1\mathbf{b}_1 + \mathbf{x}'_2\mathbf{b}_2$ . Of course our emphasis will be focused on  $\mathbf{x}'_1\mathbf{b}_1$  representing a first-order model, while  $\mathbf{x}'_2\mathbf{b}_2$  contains second-order terms. The average prediction variance can be written

$$\frac{NK}{\sigma^2} \int_R \text{Var}[\hat{y}(\mathbf{x})]d\mathbf{x} = K \int_R \mathbf{x}'_1 \boldsymbol{M}_{11}^{-1} \mathbf{x}_1 d\mathbf{x} = \text{tr}[\boldsymbol{M}_{11}^{-1} \boldsymbol{\mu}_{11}] \quad (9.23)$$

Clearly a desirable design criterion is to select the design that minimizes AMSE. AMSE is a function of design moments, region moments, and  $\boldsymbol{\alpha}_2$ , a standardized vector of parameters. It was clear in the previous section that the bias component can be minimized in spite of  $\boldsymbol{\alpha}_2$ . However, *AMSE cannot be minimized with respect to design moments without knowledge of  $\boldsymbol{\alpha}_2$* .

As a result, the practical use of AMSE is difficult at best. However, it is of interest to determine what role bias plays in the AMSE and, in particular, how effective the minimum bias design is in controlling AMSE. The following subsection deals with these matters and discusses the use of compromise designs—that is, designs that are not minimum AMSE but are approximately minimum AMSE.

### 9.2.4 How Important is Bias?

Let us consider the relative performance of the minimum variance and minimum bias designs for  $k = 1$  for various magnitudes of bias. In other words, let us ask which design is able to more closely emulate the performance of the optimal design; that is, the design that minimizes AMSE. In Table 9.1, various degrees of bias are listed in the form of  $\sqrt{N}\beta_{11}/\sigma$ , the standardized regression coefficient of the quadratic term. Here we are assuming a fitted model

$$\hat{y} = b_0 + b_1x$$

and a true model

$$E(y) = \beta_0 + \beta_1x + \beta_{11}x^2$$

with  $R$  scaled to  $[-1, +1]$ . For each value of  $\sqrt{N}\beta_{11}/\sigma$ , the optimal design (minimizing AMSE) was computed and thus the minimum value of AMSE was also computed. In addition, the AMSE for the minimum bias ( $[11] = \frac{1}{3}$ ) design and the AMSE for the minimum variance design ( $[11] = 1.0$ ) were computed. These quantities are listed as well as  $\sqrt{N}\beta_{11}/\sigma$ . The degree of bias is quantified by the ratio APV/ASB—that is, the ratio of the variance portion of the AMSE to the bias contribution in the case of the optimal design.

Study of Table 9.1 makes it clear that bias is an important consideration. Even when the bias makes a relatively small contribution—for example, when APV/ASB = 5 or APV/ASB = 3.7—the minimum bias design results in a smaller AMSE than that which results from the minimum variance design. In addition, it is clear that the minimum bias approach is considerably more robust than the minimum variance design. The minimum bias design is never far from optimal (in terms of mean squared error), whereas the minimum variance design performs quite poorly when the bias present is such that APV/ASB < 5.

Table 9.1 suggests that perhaps a compromise design for which  $[11]$  is slightly larger than the minimum bias value of  $\frac{1}{3}$  might be appropriate, because it should be extremely

**TABLE 9.1 Values of Optimal [11] and AMSE for Optimal Design, Minimum Variance Design, and Minimum Bias Design**

$\sqrt{N}\beta_{11}/\sigma$	APV/ASB	[11] (Optimum)	AMSE (Optimum)	AMSE ([11] = 1.0)	AMSE ([11] = $\frac{1}{3}$ )
0		1.0	1.333	1.333	2.0
0.50	10	0.999	1.466	1.466	2.022
1.0	7	0.687	1.699	1.867	2.088
1.5	5	0.565	1.910	2.533	2.205
2.0	3.7	0.500	2.133	3.466	2.352
2.5	3	0.462	2.382	4.672	2.551
3.0	2	0.432	2.666	6.135	2.805
4.0	1.5	0.399	3.333	9.872	3.422
4.5	1.0	0.388	3.718	11.521	3.798
5.0	0.9	0.379	4.153	14.677	4.222
7.0	0.4	0.359	6.316	27.465	6.355

**TABLE 9.2 AMSE Values for the Optimal Design and Compromise Design of [11] = 0.4**

$\sqrt{N}\beta_{11}/\sigma$	AMSE (Optimal)	AMSE ([11] = 0.40)
0	1.33	1.833
0.5	1.467	1.86
1.0	1.699	1.927
1.5	1.910	2.043
2.0	2.133	2.206
2.5	2.382	2.416
3.0	2.666	2.67
4.0	3.333	3.327
5.0	4.153	4.167
7.0	6.316	6.406

robust—that is, very close in AMSE to that of the optimal design. A design with a second moment [11] of 0.40–0.45 is in fact extremely robust. An impression can be obtained from Table 9.2, which shows the performance of the design with [11] = 0.40. Obviously, the use of [11] = 0.45 or 0.5 would produce even better performance for very small values of the bias parameter  $\sqrt{N}\beta_{11}/\sigma$ .

Tables similar to Tables 9.1 and 9.2 for  $k > 1$  design variables can be constructed. The results teach essentially the same lesson: if there is any suspicion at all that there is curvature in the system, the minimum variance design is very likely to be counterproductive. In fact, a reasonable rule of thumb to allow for possible model bias is to use a design with zero moments through order three and second pure moments [*ii*] that are 20–25% higher than that suggested by the minimum bias design. This design prescription serves as a reasonable compromise and will provide a design that will not be far away in performance from the optimal (minimum mean squared error) design over a wide range of bias in the system.

The above design moment recommendations can sometimes be a bit difficult to implement in practice. The problem often stems from uncertainty regarding what is truly the region of interest. Even in the case of what might be perceived to be a cuboidal region, the exact locations, in the design variables, of the corners of the region are not always known. Certainly in preliminary studies where variable screening is involved, choices of ranges of variables often require much thought. As a result, the recommendations made here should be confined to situations in which the researcher is not engaged in variable screening but is reasonably certain regarding the relative importance of design variables and the region in which prediction or predicted values are sought. Thus, of course, protection is achieved by designing an experiment that has resolution at least IV, and the design levels are brought in from the perimeter of the region in which one is required to predict response.

### 9.3 ERRORS IN CONTROL OF DESIGN LEVELS

In practical situations one plans to design experiments according to some master plan that entails the choice of a combination of design levels and a random assignment of these design levels to experimental units. However, it is often difficult to *control* design levels.

This is true even in laboratory situations. This suggests a need to determine how one can assess the effects of **errors in control** of design levels. For an excellent account see Box (1963).

The approach to assessment of errors in design levels in an RSM setting depends on the structure of the error. In some (perhaps most) instances there is a chosen level according to the design plan. This **aimed at** level is reported and used in the analysis even though it is known that it is subject to error. The actual level that is experienced by the process is not known. We call this the **fixed design level** case.

**Fixed Design Level Case** One must keep in mind that the actual levels are not observed in this case. The deviation between the actual and the planned level is a random variable. That is, for the  $u$ th run of the  $j$ th design variable we have

$$w_{ju} = x_{ju} + \theta_{ju} \quad (u = 1, 2, \dots, N, j = 1, 2, \dots, k) \quad (9.24)$$

where  $w_{ju}$  is the actual level,  $x_{ju}$  is the fixed and planned level, and  $\theta_{ju}$  is a random error in control. It may be assumed that

$$E(\theta_{ju}) = 0$$

$$\text{Var}(\theta_{ju}) = \sigma_j^2 \quad (u = 1, 2, \dots, N, j = 1, 2, \dots, k)$$

For the case of multiple design levels, the variances of,  $\sigma_1^2, \sigma_2^2, \dots, \sigma_k^2$  are the variances of the errors in control.

**First-Order Model** Consider the fixed level case when one fits a first-order model. The model, in terms of the true (yet unknown) levels, is given by

$$y = \beta_0 + \beta_1 w_1 + \beta_2 w_2 + \dots + \beta_k w_k + \varepsilon \quad (9.25)$$

Because the analysis will be done on the planned levels, it is instructive to write the model in Equation 9.25 as

$$\begin{aligned} y &= \beta_0 + \beta_1(x_1 + \theta_1) + \beta_2(x_2 + \theta_2) + \dots + \beta_k(x_k + \theta_k) + \varepsilon \\ &= \beta_0 + \sum_{j=1}^k \beta_j x_j + \left\{ \varepsilon + \sum_{j=1}^k \beta_j \theta_j \right\} \\ &= \beta_0 + \sum_{j=1}^k \beta_j x_j + \varepsilon^* \end{aligned} \quad (9.26)$$

The  $\theta_j$  are random variables as described by Equation 9.24, but the  $x_j$  are fixed (predetermined by the design choice). As a result, Equation 9.26 represents an almost standard RSM model with model error

$$\varepsilon^* = \varepsilon + \sum_{j=1}^k \beta_j \theta_j \quad (9.27)$$

It becomes obvious from Equation 9.27 that the errors associated with controlling design variables are transmitted to the model error and the result is an inflated error variance.

As a result, if the model in Equation 9.26 is used and least squares is used to estimate  $\beta_0, \beta_1, \beta_2, \dots, \beta_k$  with ordinary least squares, we have the following:

1. The regression coefficients are unbiased.
2. The variance–covariance matrix of  $\mathbf{b} = (\mathbf{X}'\mathbf{X})^{-1}\mathbf{X}'\mathbf{y}$  is given by  $(\mathbf{X}'\mathbf{X})^{-1}\sigma^2$ , where  $\sigma^2 = \sigma^2 + \sum_{j=1}^k \beta_j^2 \sigma_j^2$ , assuming that the  $\theta_j$  are independent. This results in inflated error variances. Depending on the magnitude of the  $\sigma_j^2$ , the inflation may be severe.
3. Standard RSM (e.g., variable screening) and steepest ascent are valid, although they may be rendered considerably less effective if the  $\sigma_j^2$  are large. Of course, if the  $\sigma_j^2$  are extremely small compared to the model variance  $\sigma^2$ , these errors will not result in major difficulties.

We emphasized that the conclusions drawn in 1 and 2 above do depend on the assumptions made regarding the  $\theta_j$ . Of particular interest is the assumption that the  $\theta_j$  are unbiased—that is,  $E(\theta_j) = 0$ . This assumption is certainly a reasonable one in most cases. However, if it does not hold, the least squares estimator of  $\beta_0$  becomes biased.

**Second-Order Model** In the case of the second-order model, errors in control result in more difficulties than one experiences in the first-order case if the error variances are not negligible. Consider again Equation 9.24 and the second-order model given by

$$\begin{aligned}
 y &= \beta_0 + \sum_{j=1}^k \beta_j w_j + \sum_{j=1}^k \beta_{jj} w_j^2 + \sum_{i < j=2}^k \beta_{ij} w_i w_j + \varepsilon \\
 &= \beta_0 + \sum_{j=1}^k \beta_j (x_j + \theta_j) + \sum_{j=1}^k \beta_{jj} (x_j + \theta_j)^2 + \sum_{i < j=2}^k \beta_{ij} (x_i + \theta_i)(x_j + \theta_j) + \varepsilon \\
 &= \beta_0 + \sum_{j=1}^k \beta_j x_j + \sum_{j=1}^k \beta_{jj} x_j^2 + \sum_{i < j=2}^k \beta_{ij} x_i x_j \\
 &\quad + \left\{ \varepsilon + \sum_{j=1}^k \beta_j \theta_j + \sum_{j=1}^k \beta_{jj} \theta_j (2x_j + \theta_j) + \sum_{i < j=2}^k \beta_{ij} [\theta_i x_j + x_i \theta_j + \theta_i \theta_j] \right\} \\
 &= \beta_0 + \sum_{j=1}^k \beta_j x_j + \sum_{j=1}^k \beta_{jj} x_j^2 + \sum_{i < j=2}^k \beta_{ij} x_i x_j + \varepsilon^* \tag{9.28}
 \end{aligned}$$

The model in Equation 9.28 is best analyzed by considering the expectation and variance of  $\varepsilon^*$ . Once again we have a standard RSM model with error  $\varepsilon^*$ . However, in this case the properties of  $\varepsilon^*$  are more complicated. The expected value of  $\varepsilon^*$  is given by

$$E(\varepsilon^*) = \sum_{j=1}^k \beta_{jj} \sigma_j^2$$

Because  $E(\varepsilon^*) \neq 0$  and the **error bias**  $\sum_{j=1}^k \beta_{jj} \sigma_j^2$  is independent of the  $x_j$ , the least squares estimator of  $\beta_0$  is biased by  $\sum_{j=1}^k \beta_{jj} \sigma_j^2$ .

In order to better illustrate the result in the case of the second-order model, we rewrite  $\varepsilon^*$  in Equation 9.28 as

$$\begin{aligned}\varepsilon^* = \varepsilon + \sum_{i < j=2}^k \theta_i(\beta_{ij}x_j) + \sum_{i < j=2}^k \theta_j\beta_{ij}x_i + \sum_{i < j=2}^k \beta_{ij}\theta_i\theta_j \\ + \sum_{j=1}^k \theta_j\beta_j + 2 \sum_{j=1}^k \beta_{jj}\theta_jx_j + \sum_{j=1}^k \beta_{jj}\theta_j^2\end{aligned}\quad (9.29)$$

If one considers the variance of  $\varepsilon^*$  in Equation 9.29, it becomes apparent that:

1. The error variance is inflated by errors in control transmitted to  $\varepsilon^*$  just as in the first-order case.
2. The error variance will no longer be homogeneous. Rather,  $\text{Var}(\varepsilon^*)$  depends on design levels.

While we will not display  $\sigma^{*2} = \text{Var } \varepsilon^*$ , it should be apparent that terms such as  $\sum_{j=1}^k \beta_j^2\sigma_j^2$ ,  $\sum_{j=1}^k \beta_{ij}^2[E(\theta_j^4) - \sigma_j^4]$ , and  $\sum \sum_{i < j} \beta_{ij}^2\sigma_i^2\sigma_j^2$  inflate the error variance, whereas terms such as  $4 \sum_{j=1}^k \beta_{ij}^2x_j^2\sigma_j^2$ ,  $\sum \sum_{i < j} \beta_{ij}^2x_j^2\sigma_i^2$ , and  $\sum \sum_{i < j} \beta_{ij}^2x_i^2\sigma_j^2$  render the error variance nonhomogeneous.

**Further Comments** The degree of difficulty caused by errors in control obviously depends on the model complexity and on the size of the error variances  $\sigma_1^2, \sigma_2^2, \dots, \sigma_k^2$ . If the latter are dominated by the model error variance  $\sigma^2$ , then the effect of errors in control is negligible.

## 9.4 EXPERIMENTS WITH COMPUTER MODELS

We customarily think of applying RSM to a *physical* process, such as chemical vapor deposition in semiconductor manufacturing, wave soldering, or machining. However, RSM can also be successfully applied to *computer simulation models* of physical systems. In such applications, RSM is used to build a model of the system being modeled by the computer simulation—a **metamodel**—and optimization is carried out on the metamodel. The assumption is that if the computer simulation model is a faithful representation of the real system, then the RSM optimization will result in adequate determination of the optimum conditions for the real system.

Generally, there are two types of simulation models, **stochastic** and **deterministic**. In a stochastic simulation model, the output responses are random variables. Examples include systems simulations such as the factory planning and scheduling models used in the semiconductor industry and traffic flow simulators employed by civil engineers, and Monte Carlo simulations that sample from probability distributions to study complex mathematical phenomena that do not have direct analytical solutions. Sometimes the output from a stochastic simulation model will be in the form of a time series. Often standard experimental design and RSM techniques can be applied to the output from a stochastic simulation model, although a number of specialized techniques have been developed. Sometimes polynomials of higher-order than the usual quadratic response surface model are used.

In a **deterministic simulation** model the output responses are not random variables; they are entirely deterministic quantities whose values are determined by the (often highly complex) mathematical models upon which the computer model is based. Deterministic simulation models are often used by engineers and scientists as computer-based design tools. Typical examples are circuit simulators used for designing electronic circuits and semiconductor devices, finite element analysis models for mechanical and structural design and computational models for physical phenomena such as fluid dynamics. These are often very complex models, requiring considerable computer resources and time to run.

As an example of a situation where a finite element analysis model may be employed, consider the problem of designing a turbine engine to contain a failed compressor rotor. Many factors may influence the design, such as engine operating conditions as well as the location, size, and material properties of surrounding parts. Figure 9.3 shows a cutaway view of a typical compressor containment model. Many parameters for each component are potentially important. The thickness, material type, and geometric feature (bend radius, bolt hole size and location, stiffening ribs or gussets, etc.) are engineering design parameters and, potentially, experimental factors that could be included in a response surface model. One can see that large numbers of factors are potentially important in the design of such a product. Furthermore, the sign or direction of the effect of many of these factors is unknown. For instance, setting factors that increase the axial stiffness of a backface (such as increasing the thickness of the transition duct) may help align a rotor fragment, centering the impact on the containment structure. On the other hand, the increased stiffness may nudge the fragment too much, causing it to miss the primary containment structure. From experience the design engineers may confidently assume that only a small number of these potentially important factors have a significant effect on the performance of the design in containing a failed part. Detailed analysis or testing of the turbine engine is needed to understand

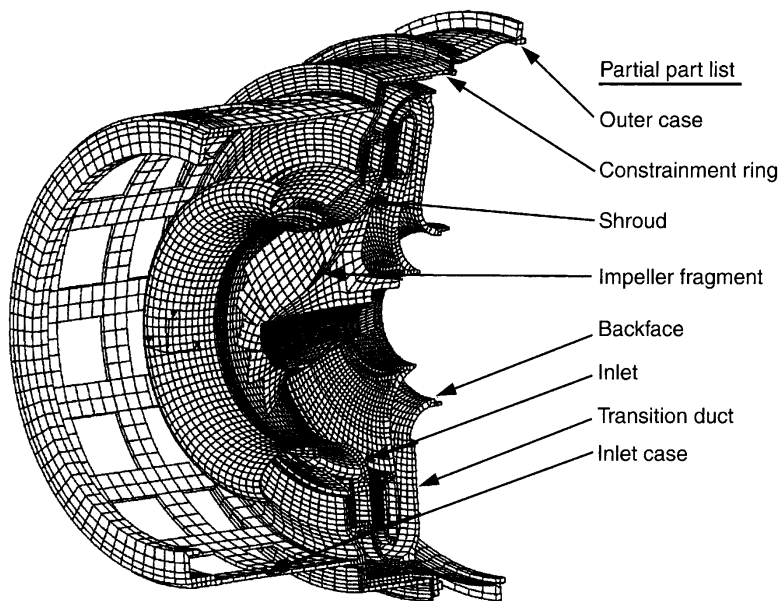


**Figure 9.3** Finite element model for compressor containment analysis of a turbine engine and partial parts list.

which factors are important and to quantify their effect on the design. The cost of building a prototype turbine engine frequently exceeds one million dollars, so studying the effects of these factors using a computer model is very attractive. The type of model used is called a **finite element analysis** model. Simulating a containment event with a finite element analysis model is very computationally intensive. The model shown in Fig. 9.3 has over 100,000 elements and takes about 90 hr of computer time to model 2 ms of event time. Frequently as much as 10 ms of event time must be modeled. Clearly the need to limit experimentation or simulation is great. Therefore the typical RSM approach of factor screening followed by optimization might well be applied to this scenario.

Remember that the RSM approach is based on a philosophy of **sequential experimentation**, with the objective of approximating the response with a low-order polynomial in a relatively small region of interest that contains the optimum solution. Some computer experimenters advocate a somewhat different philosophy. They seek to find a model that approximates the true response surface over a much wider range of the design variables, sometimes extending over the entire region of operability. As mentioned earlier in this section, this can lead to situations where the model considered is much more complex than the first- and second-order polynomials typically employed in RSM [see, for example, Barton (1992, 1994), Mitchell and Morris (1992), and Simpson and Peplinski (1997)].

The choice of a design for a computer simulation experiment presents some interesting alternatives. If the experimenter is considering a polynomial model, then an optimal design such as a *D*-optimal or *I*-optimal design is a possible choice. In recent years, various types of **space-filling designs** have been suggested for computer experiments. Space-filling designs are often thought to be particularly appropriate for deterministic computer models because in general they spread the design points out nearly evenly or uniformly (in some sense) throughout the region of experimentation. This is a desirable feature if the experimenter doesn't know the form of the model that is required, and believes that interesting phenomena are likely to be found in different regions of the experimental space. Furthermore, most space-filling designs do not contain any replicate runs. For a **deterministic** computer model this is desirable, because a single run of the computer model at a design point provides all of the information about the response at that point. Many space-filling designs do not contain replicates even if some factors are dropped and they are projected into lower dimensions.

The first space-filling design proposed was the Latin hypercube design [McKay, Conover, and Beckman (1979)]. A Latin hypercube in  $n$  runs for  $k$  factors is an  $n \times k$  matrix where each column is a random permutation of the levels 1, 2, ...,  $n$ . JMP can create Latin hypercube designs. An example of a 10-run Latin hypercube design in two factors from JMP on the interval  $-1$  to  $+1$  is shown in Fig. 9.4.

The sphere-packing design is chosen so that the minimum distance between pairs of points is minimized. These designs were proposed by Johnson et al. (1990) and are also called maximin designs. An example of a 10-run sphere-packing design in two factors constructed using JMP is shown in Fig. 9.5.

Uniform designs were proposed by Fang (1980). These designs attempt to place the design points so that they are uniformly scattered through the regions as would a sample from a uniform distribution. There are a number of algorithms for creating these designs and several measures of uniformity. See the book by Fang et al. (2006). An example of a 10-run uniform design in two factors constructed using JMP is in Fig. 9.6.

Maximum entropy designs were proposed by Shewry and Wynn (1987). Entropy can be thought of as a measure of the amount of information contained in the distribution of a data

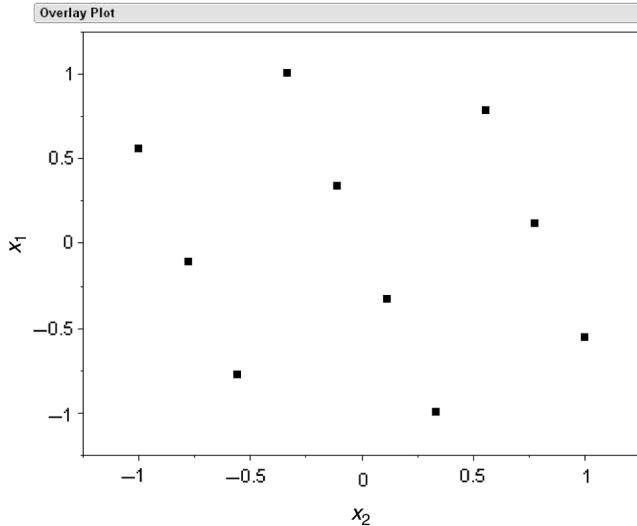


**Figure 9.4** A 10-run Latin hypercube design.

set. Suppose that the data comes from a normal distribution with mean vector  $\mu$  and covariance matrix  $\sigma^2\mathbf{R}(\theta)$ , where  $\mathbf{R}(\theta)$  is a correlation matrix having elements

$$r_{ij} = e^{-\sum_{s=1}^k \theta_s (x_{is} - x_{js})^2} \quad (9.30)$$

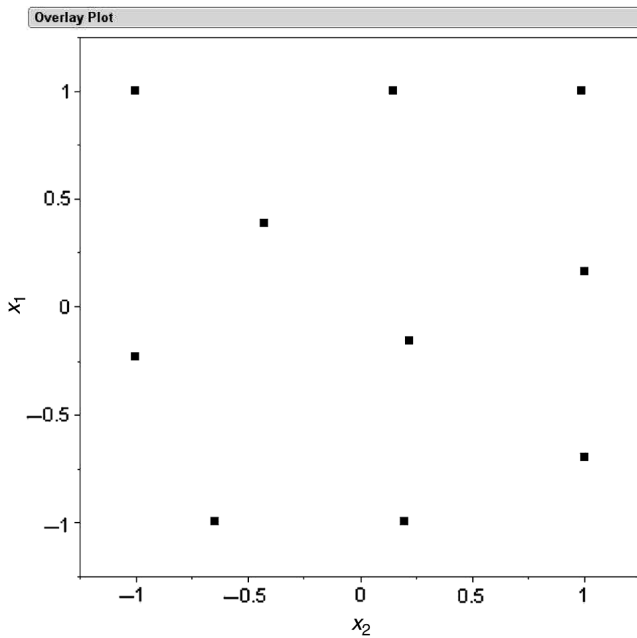


**Figure 9.5** A 10-run sphere-packing design.

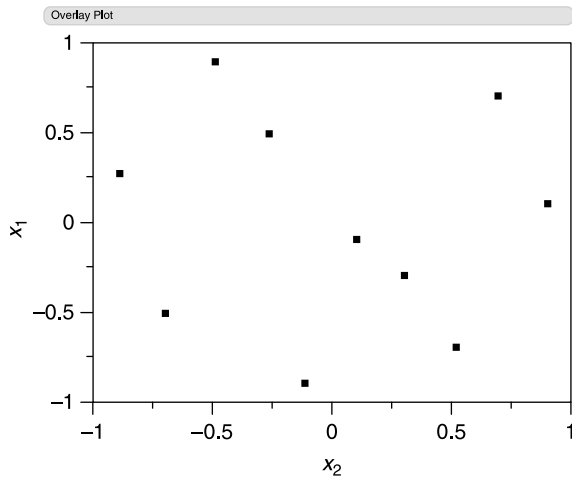


**Figure 9.6** A 10-run uniform design.

The quantities  $r_{ij}$  are the correlations between the responses at two design points. The maximum entropy design maximizes the determinant of  $\mathbf{R}(\boldsymbol{\theta})$ . Figure 9.7 shows a 10-run maximum entropy design in two factors created using JMP.

The **Gaussian process model** is often used to fit the data from a deterministic computer experiment. These models were introduced as models for computer experiments by Sacks et al. (1989). They are desirable because they provide an exact fit to the observations from the experiment. Now this is no assurance that they will interpolate well at locations in the region of interest where there is no data, and no one seriously believes that the Gaussian process model is the correct model for the relationship between the response and the

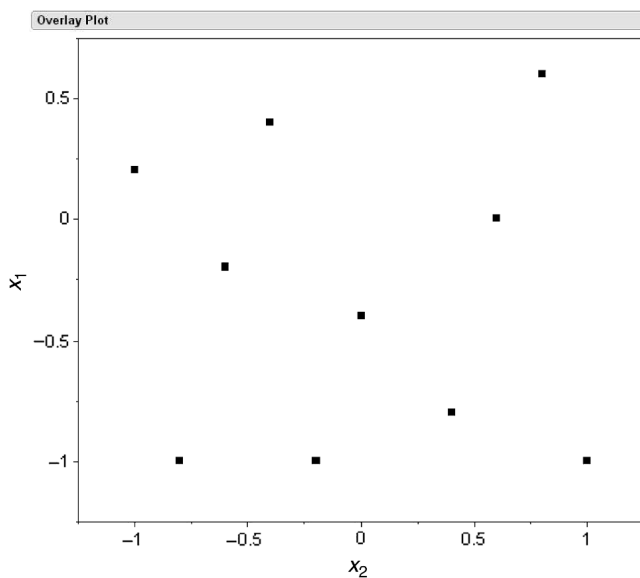


**Figure 9.7** A 10-run maximum entropy design.

design variables. However, the “exact fit” nature of the model and the fact that it only requires one parameter for each factor considered in the experiment has made it quite popular. The Gaussian process model is

$$y = \mu + z(\mathbf{x})$$

where  $z(\mathbf{x})$  is a Gaussian stochastic process with covariance matrix  $\sigma^2 \mathbf{R}(\boldsymbol{\theta})$ , and the elements of  $\mathbf{R}(\boldsymbol{\theta})$  are defined in Equation 9.30. The Gaussian process model is essentially a spatial correlation model, where the correlation of the response between two observations decreases as the values of the design factors become further apart. When design points are close together, this causes ill-conditioning in the data for the Gaussian process model, much like multicollinearity resulting from predictors that are nearly linearly dependent in linear regression models. The parameters  $\mu$  and  $\theta_s$ ,  $s = 1, 2, \dots, k$  are estimated using the method of maximum likelihood. Predicted values of the response at the point  $\mathbf{x}$  are computed from

$$\hat{y}(\mathbf{x}) = \hat{\mu} + \mathbf{r}'(\mathbf{x}) \mathbf{R}(\hat{\boldsymbol{\theta}})^{-1} (\mathbf{y} - \mathbf{j}\hat{\mu}) \quad (9.31)$$

where  $\hat{\mu}$  and  $\hat{\boldsymbol{\theta}}$  are the maximum likelihood estimates of the model parameters  $\mu$  and  $\boldsymbol{\theta}$ , and  $\mathbf{r}'(\mathbf{x}) = [\mathbf{r}(\mathbf{x}_1, \mathbf{x}), \mathbf{r}(\mathbf{x}_2, \mathbf{x}), \dots, \mathbf{r}(\mathbf{x}_n, \mathbf{x})]$ . The prediction equation contains one model term for each design point in the original experiment. JMP will fit and provide predictions from the Gaussian process model.

**Example 9.2** The temperature in the exhaust from a jet turbine engine at different locations in the plume was studied using a computational fluid dynamics (CFD) model. The two design factors of interest were the locations in the plume ( $x$  and  $y$  coordinates, however the  $y$  axis was referred to by the experimenters as the  $R$ -axis or radial axis). Both location axes were coded to the  $-1, +1$  interval. The experimenters used a 10-run sphere-packing design. The experimental design and the output obtained at these test conditions from the CFD model are shown in Table 9.3. Figure 9.8 shows the design.

JMP was used to fit the Gaussian process model to the temperature data. Some of the output is shown in Table 9.4 and Fig. 9.9. The plot of actual by predicted is obtained by “jack-knifing” the predicted values; that is, each predicted value is obtained from a

**TABLE 9.3 Sphere-Packing Design and the Temperature Responses in the CFD Experiment**

$x$ -axis	$R$ -axis	Temperature
0.056	0.062	338.07
0.095	0.013	1613.04
0.077	0.062	335.91
0.095	0.061	327.82
0.090	0.037	449.23
0.072	0.038	440.58
0.064	0.015	1173.82
0.050	0.000	1140.36
0.050	0.035	453.83
0.079	0.000	1261.39

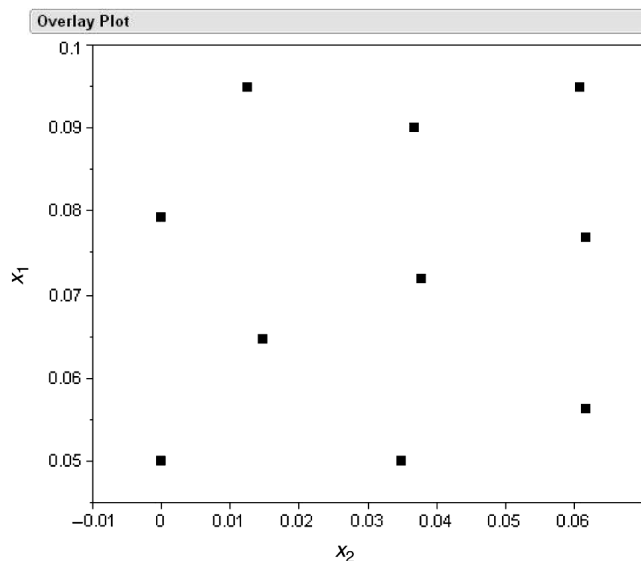


**Figure 9.8** The sphere-packing design for the CFD experiment.

**TABLE 9.4 JMP Output for the Gaussian Process Model for the CFD Experiment in Table 9.3**

Column	Theta	Total Sensitivity	Main Effect	X-axis Interaction	R-axis Interaction
X-axis	65.40254	0.0349982	0.0141129		0.0208852
R-axis	3603.2483	0.9858871	0.9650018	0.0208852	
Mu					
Sigma					
734.54584	212205.18				
-2*Loglikelihood					
132.98004					

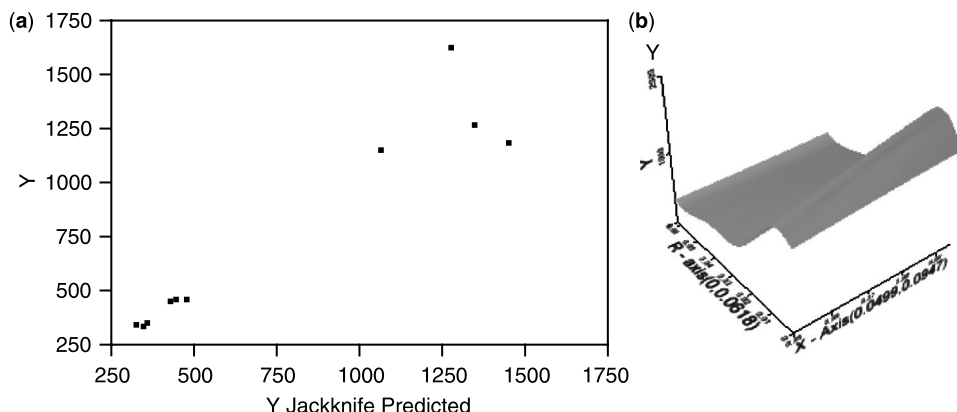


**Figure 9.9** JMP output for the Gaussian process model for the CFD experiment in Table 9.3. (a) Gaussian process, actual by predicted plot. (b) Contour profiler.

**TABLE 9.5** The JMP Gaussian Process Prediction Model for the CFD Experiment

---


$$\hat{y} = 734.545842514493 +$$

$$(-1943.3447961328 * \text{Exp}(-(65.4025404276544 * ((\text{"X-axis"}) - 0.0560573769818389) ^ 2 +$$

$$3603.24827558717 * (\text{"R-axis"} - 0.0618) ^ 2)) +$$

$$3941.7888206788 * \text{Exp}(-(65.4025404276544 * ((\text{"X-axis"}) - 0.0947) ^ 2 + 3603.24827558717 * (\text{"R-axis"} - 0.0126487944665913) ^ 2)) +$$

$$3488.57543918861 * \text{Exp}(-(65.4025404276544 * ((\text{"X-axis"}) - 0.0765974898313444) ^ 2 +$$

$$3603.24827558717 * (\text{"R-axis"} - 0.0618) ^ 2)) +$$

$$2040.39522592773 * \text{Exp}(-(65.4025404276544 * ((\text{"X-axis"}) - 0.0947) ^ 2 + 3603.24827558717 * (\text{"R-axis"} - 0.0608005210868486) ^ 2)) +$$

$$-742.642897583584 * \text{Exp}(-(65.4025404276544 * ((\text{"X-axis"}) - 0.0898402482375096) ^ 2 +$$

$$3603.24827558717 * (\text{"R-axis"} - 0.0367246615426894) ^ 2)) +$$

$$519.918719208163 * \text{Exp}(-(65.4025404276544 * ((\text{"X-axis"}) - 0.0717377150616494) ^ 2 +$$

$$3603.24827558717 * (\text{"R-axis"} - 0.0377241897055609) ^ 2)) +$$

$$-3082.85411601115 * \text{Exp}(-(65.4025404276544 * ((\text{"X-axis"}) - 0.0644873310121405) ^ 2 +$$

$$3603.24827558717 * (\text{"R-axis"} - 0.0148210408248663) ^ 2)) +$$

$$958.926988711818 * \text{Exp}(-(65.4025404276544 * ((\text{"X-axis"}) - 0.0499) ^ 2 + 3603.24827558717 * (\text{"R-axis"} ^ 2)) +$$

$$80.468182554262 * \text{Exp}(-(65.4025404276544 * ((\text{"X-axis"}) - 0.0499) ^ 2 + 3603.24827558717 * (\text{"R-axis"} - 0.0347687447931648) ^ 2)) +$$

$$-1180.44117607546 * \text{Exp}(-(65.4025404276544 * ((\text{"X-axis"}) - 0.0790747191607881) ^ 2 +$$

$$3603.24827558717 * (\text{"R-axis"} ^ 2)))$$


---

model that doesn't contain that observation when the model parameters are estimated. The prediction model obtained from JMP is shown in Table 9.5. In this table, "X-axis" and "R-axis" refer to the coordinates in  $x$  and  $R$  where predictions are to be made.

Other useful references for designs for computer experiments include Bettonvil and Kleijnen (1996), Donohue (1994), Montgomery and Weatherby (1979), Sacks et al. (1989), Sacks and Welch (1989), Slaagame and Barton (1997), and the book by Santner et al. (2003).

## 9.5 MINIMUM BIAS ESTIMATION OF RESPONSE SURFACE MODELS

In Section 9.2 we considered a situation where the experimenter fits a model, say

$$\hat{\mathbf{y}} = \mathbf{X}_1 \mathbf{b} \quad (9.32)$$

that is of lower order than the true system model

$$\mathbf{f}(\mathbf{x}) = E(\mathbf{y}) = \mathbf{X}_1 \boldsymbol{\beta}_1 + \mathbf{X}_2 \boldsymbol{\beta}_2 \quad (9.33)$$

This leads to the AMSE criterion in Equation 9.11, which can be written as

$$\text{AMSE} = \text{APV} + \text{ASB} \quad (9.34)$$

where APV is the average prediction variance and ASB is the average squared bias. We discussed how to minimize the ASB portion of AMSE by properly selecting the experimental

design. We also discussed the important role that the bias plays in the AMSE criterion, noting that often a design that is close to the minimum bias design will come very close to the design that minimizes the AMSE.

Karson, Manson, and Hader (1969) proposed minimizing the average squared bias not by design, but by **estimation**. Their **minimum bias estimation** procedure achieves the minimum value of ASB, leaving the experimenter to select the design to satisfy other objectives such as the minimization of average prediction variance. We now describe their procedure. The true model is a polynomial of degree  $d_2$ ,

$$f(\mathbf{x}) = \mathbf{x}'_1 \boldsymbol{\beta}_1 + \mathbf{x}'_2 \boldsymbol{\beta}_2 \quad (9.35)$$

and the fitted model is a polynomial of degree  $d_1 < d_2$ ,

$$\hat{y}(\mathbf{x}) = \mathbf{x}'_1 \boldsymbol{\alpha}_1 \quad (9.36)$$

Recall from Equation 9.11 that the average squared bias is

$$\text{ASB} = \frac{NK}{\sigma^2} \int_R \{E[\hat{y}(\mathbf{x}) - f(\mathbf{x})]\}^2 d\mathbf{x} \quad (9.37)$$

Now  $E[\hat{y}(\mathbf{x})]$  is a polynomial of degree  $d_1$ , which we may write as

$$E[\hat{y}(\mathbf{x})] = \mathbf{x}'_1 \boldsymbol{\alpha}_1$$

Consequently, the average squared bias is

$$\begin{aligned} \text{ASB} &= \frac{NK}{\sigma^2} \int_R \{E[\hat{y}(\mathbf{x}) - f(\mathbf{x})]\}^2 d\mathbf{x} \\ &= \frac{NK}{\sigma^2} \int_R [\mathbf{x}'_1 (\boldsymbol{\alpha}_1 - \boldsymbol{\beta}_1) - \mathbf{x}'_2 \boldsymbol{\beta}_2]^2 d\mathbf{x} \\ &= \frac{NK}{\sigma^2} \int_R \{(\boldsymbol{\alpha}_1 - \boldsymbol{\beta}_1)' \mathbf{x}_1 \mathbf{x}'_1 (\boldsymbol{\alpha}_1 - \boldsymbol{\beta}_1) - 2(\boldsymbol{\alpha}_1 - \boldsymbol{\beta}_1) \mathbf{x}_1 \mathbf{x}'_2 \boldsymbol{\beta}_2 + \boldsymbol{\beta}'_2 \mathbf{x}_2 \mathbf{x}'_2 \boldsymbol{\beta}_2\} d\mathbf{x} \\ &= \frac{N}{\sigma^2} [(\boldsymbol{\alpha}_1 - \boldsymbol{\beta}_1)' \boldsymbol{\mu}_{11} - 2(\boldsymbol{\alpha}_1 - \boldsymbol{\beta}_1) \boldsymbol{\mu}_{12} \boldsymbol{\beta}_2 + \boldsymbol{\beta}'_2 \boldsymbol{\mu}_{22} \boldsymbol{\beta}_2] \end{aligned} \quad (9.38)$$

where  $\boldsymbol{\mu}_{11}$ ,  $\boldsymbol{\mu}_{12}$ , and  $\boldsymbol{\mu}_{22}$  are the region moment matrices defined earlier. Now to minimize the ASB with respect to  $\boldsymbol{\alpha}_1$ , differentiate Equation 9.38 with respect to  $\boldsymbol{\alpha}_1$ , equate the result to  $\mathbf{0}$ , and solve:

$$\frac{\partial \text{ASB}}{\partial \boldsymbol{\alpha}_1} = 2\boldsymbol{\mu}_{11}(\boldsymbol{\alpha}_1 - \boldsymbol{\beta}_1) - 2\boldsymbol{\mu}_{12}\boldsymbol{\beta}_2 = \mathbf{0}$$

which results in

$$\begin{aligned} \boldsymbol{\alpha}_1 &= \boldsymbol{\beta}_1 + \boldsymbol{\mu}_{11}^{-1} \boldsymbol{\mu}_{12} \boldsymbol{\beta}_2 \\ &= \mathbf{A} \boldsymbol{\beta} \end{aligned} \quad (9.39)$$

where  $\mathbf{A} = [\mathbf{I} \mid \boldsymbol{\mu}_{11}^{-1} \boldsymbol{\mu}_{12}]$  and  $[\boldsymbol{\beta}'_1 \mid \boldsymbol{\beta}'_2]$ . So a necessary and sufficient condition for minimization of average squared bias is that

$$E[\hat{y}(\mathbf{x})] = \mathbf{x}'_1 \mathbf{A} \boldsymbol{\beta} \quad (9.40)$$

or

$$E(\mathbf{b}_1) = \mathbf{A} \boldsymbol{\beta}. \quad (9.41)$$

Now  $\mathbf{b}_1$  is just a linear combination of the observations, say

$$\mathbf{b}_1 = \mathbf{T}' \mathbf{y} \quad (9.42)$$

Because  $E(\mathbf{y}) = \mathbf{X} \boldsymbol{\beta}$ , the requirement that  $E(\mathbf{b}_1) = \mathbf{A} \boldsymbol{\beta}$  means that  $\mathbf{T}'$  must satisfy

$$\mathbf{T}' \mathbf{X} = \mathbf{A} \quad (9.43)$$

where  $\mathbf{X} = [\mathbf{X}_1 : \mathbf{X}_2]$ . The minimum value of the average squared bias is

$$\min \text{ASB} = \frac{N}{\sigma^2} \boldsymbol{\beta}'_2 [\boldsymbol{\mu}_{22} - \boldsymbol{\mu}'_{12} \boldsymbol{\mu}_{11}^{-1} \boldsymbol{\mu}_{12}] \boldsymbol{\beta}_2. \quad (9.44)$$

In addition to achieving the minimum value of ASB, we also want to minimize the average prediction variance (APV) in Equation 9.11. Now the minimum variance estimator of  $\mathbf{x}'_1 \mathbf{A} \boldsymbol{\beta}$  is

$$\hat{y}(\mathbf{x}) = \mathbf{x}'_1 \mathbf{A} (\mathbf{X}' \mathbf{X})^{-1} \mathbf{X}' \mathbf{y} \quad (9.45)$$

The APV is minimized when Equation 9.45 is satisfied, or when

$$\mathbf{T}' = \mathbf{A} (\mathbf{X}' \mathbf{X})^{-1} \mathbf{X}' \quad (9.46)$$

The variance of the fitted model is

$$\text{Var}[\hat{y}(\mathbf{x})] = \sigma^2 \mathbf{x}'_1 \mathbf{T}' \mathbf{T} \mathbf{x}_1 \quad (9.47)$$

**Example 9.3 One Design Variable** Suppose we have one design variable and we wish to fit a first-order model using three observations taken at the points  $x = 0$  and  $x = \pm 1$ . The region of interest is  $R = [-1, 1]$ , and, unknown to us, the true model is quadratic. Therefore,

$$\begin{aligned} \hat{y}(\mathbf{x}) &= \mathbf{x}'_1 \mathbf{b}_1 = b_0 + b_1 x \\ f(\mathbf{x}) &= \mathbf{x}'_1 \boldsymbol{\beta}_1 + \mathbf{x}'_2 \boldsymbol{\beta}_2 = (\beta_0 + \beta_1 x) + \beta_2 x^2 \end{aligned}$$

with  $\mathbf{x}'_1 = [1, x]$ ,  $\mathbf{x}'_2 = [x^2]$ ,  $\boldsymbol{\beta}'_1 = [\beta_0, \beta_1]$ ,  $\boldsymbol{\beta}'_2 = [\beta_2]$ , and  $\mathbf{b}'_1 = [b_0, b_1]$ . Also, note that

$$\begin{aligned}\mathbf{X} &= \begin{bmatrix} \mathbf{x}_1 & \mathbf{x}_2 \end{bmatrix} = \begin{bmatrix} 1 & -l & \vdots & l^2 \\ 1 & 0 & \vdots & 0 \\ 1 & l & \vdots & l^2 \end{bmatrix}, \quad \mathbf{y} = \begin{bmatrix} y_1 \\ y_2 \\ y_3 \end{bmatrix} \\ (\mathbf{X}'\mathbf{X})^{-1} &= \begin{bmatrix} 1 & 0 & -l^{-2} \\ 0 & \frac{1}{2}l^{-2} & 0 \\ -l^{-2} & 0 & \frac{3}{2}l^{-4} \end{bmatrix} \\ k &= \frac{1}{2}, \quad \boldsymbol{\mu}_{11} = \begin{bmatrix} 1 & 0 \\ 0 & \frac{1}{3} \end{bmatrix}, \quad \boldsymbol{\mu}_{12} = \begin{bmatrix} \frac{1}{3} \\ 0 \end{bmatrix}, \quad \boldsymbol{\mu}_{22} = \begin{bmatrix} 1 \\ 5 \end{bmatrix},\end{aligned}$$

and

$$\mathbf{A} = \begin{bmatrix} \mathbf{I}_2 & \boldsymbol{\mu}_{11}^{-1} \boldsymbol{\mu}_{12} \end{bmatrix} = \begin{bmatrix} 1 & 0 & \vdots & \frac{1}{3} \\ 0 & 1 & \vdots & 0 \end{bmatrix}$$

Therefore the minimum bias estimate of  $\mathbf{b}_1$  is

$$\begin{aligned}\mathbf{b}_1 &= \mathbf{T}'\mathbf{y} \\ &= \mathbf{A}(\mathbf{X}'\mathbf{X})^{-1}\mathbf{X}'\mathbf{y} \\ &= \frac{1}{6l^2} \begin{bmatrix} 1 & 2(3l^2 - 1) & 1 \\ -3l & 0 & 3l \end{bmatrix} \begin{bmatrix} y_1 \\ y_2 \\ y_3 \end{bmatrix}\end{aligned}$$

The minimum bias estimator is biased, since

$$E(\mathbf{b}_1) = \mathbf{A}\boldsymbol{\beta} = \begin{bmatrix} \beta_0 + \frac{1}{3}\beta_2 \\ \beta_1 \end{bmatrix}$$

and the predicted values are also biased, because

$$E[\hat{y}(\mathbf{x})] = \beta_0 + \frac{1}{3}\beta_2 + \beta_1 x$$

The minimum value of the ASB is computed from Equation 9.44 as

$$\begin{aligned}\text{Min ASB} &= \frac{N}{\sigma^2} \boldsymbol{\beta}'_2 [\boldsymbol{\mu}_{22} - \boldsymbol{\mu}'_{12} \boldsymbol{\mu}_{11}^{-1} \boldsymbol{\mu}_{12}] \boldsymbol{\beta}_2 \\ &= \left(\frac{3}{\sigma^2}\right) \frac{4}{45} \beta_2^2\end{aligned}$$

Notice that the minimum bias is independent of where the design points  $-l, +l$  are placed in the region  $-1 \leq x \leq +1$ .

The variance of the fitted model is

$$\begin{aligned}\text{Var}[\hat{y}(\mathbf{x})] &= \sigma^2 \mathbf{x}_1' \mathbf{T}' \mathbf{T} \mathbf{x}_1 \\ &= \sigma^2 \mathbf{x}_1' \mathbf{A} (\mathbf{X}' \mathbf{X})^{-1} \mathbf{A} \mathbf{x}_1\end{aligned}$$

and we can show that the APV is

$$\text{APV} = \frac{Nk}{\sigma^2} \int_{-1}^1 \text{Var}[\hat{y}(\mathbf{x})] d\mathbf{x} = 3 - \frac{3}{2l^2} + \frac{1}{2l^4}$$

The APV is minimized at  $l = \sqrt{\frac{2}{3}}$ , for which value the minimum APV is  $\frac{15}{8}$ .

We can compare this with the usual least squares results. It is not difficult to show that

$$\text{ASB}_{\text{LS}} = \frac{3\beta_2^2}{\sigma^2} \left( \frac{4l^4}{9} - \frac{4l^2}{9} + \frac{1}{5} \right)$$

and

$$\text{APV}_{\text{LS}} = 1 + \frac{1}{2l^2}$$

Now it turns out that  $\text{APV}_{\text{LS}}$  is less than APV for minimum bias estimation except at  $l = \sqrt{\frac{1}{2}}$ , where they are identical. The minimum  $\text{ASB}_{\text{LS}}$  is achieved at  $l = \sqrt{\frac{2}{3}}$ , while the ASB is minimized for *any*  $l$  for minimum bias estimation. However, for any value of  $l$  satisfying  $\sqrt{\frac{1}{2}} \leq l \leq 1$  we have  $\text{APV} \leq \text{APV}_{\text{LS}} = 2$ . Therefore, if we use minimum bias estimation, the average mean squared error is less than or equal to the average mean squared error for least squares for *any* design with  $\sqrt{\frac{1}{2}} \leq l \leq 1$ .

## 9.6 NEURAL NETWORKS

Some researchers have suggested using **neural networks** as an alternative to RSM; for example, see Hon et al. (1994), Himmel and May (1991), Carpenter and Barthelemy (1993), and Hussain, Yu, and Johnson (1991). The development of neural networks, or more accurately, **artificial neural networks**, has been motivated by the recognition that the human brain processes information in a way that is fundamentally different from the typical digital computer. The neuron is the basic structural element and information-processing module of the brain. A typical human brain has an enormous number of them (approximately 10 billion neurons in the cortex and 60 trillion synapses or connections between them) arranged in a highly complex, nonlinear, and parallel structure. Consequently, the human brain is a very efficient structure for information processing, learning, and reasoning.

An artificial neural network is a structure that is designed to solve certain types of problems by attempting to emulate the way the human brain would solve the problem. The general form of a neural network is a “black box” model of a type that is often used to model high-dimensional, nonlinear data. Typically, most neural networks are used to solve prediction problems for some system, as opposed to formal model-building or development of underlying knowledge of how the system works. For example, a computer

company might want to develop a procedure for automatically reading handwriting and converting it to typescript. If the procedure can do this quickly and accurately, the company may have little interest in the specific model used to do it.

Multilayer feedforward artificial neural networks are multivariate statistical models used to relate  $p$  predictor variables  $x_1, x_2, \dots, x_p$  to  $q$  response variables  $y_1, y_2, \dots, y_q$ . The model has several layers, each consisting of either the original or some constructed variables. The most common structure involves three layers: the **inputs**, which are the original predictors; the **hidden layer**, consisting of a set of constructed variables; and the **output layer**, made up of the responses. Each variable in a layer is called a **node**. Figure 9.10 shows a typical three-layer artificial neural network.

A node takes as its input a transformed linear combination of the outputs from the nodes in the layer below it. Then it sends as an output a transformation of itself that becomes one of the inputs to one or more nodes on the next layer. The transformation functions are usually either sigmoidal (S-shaped) or linear, and are usually called **activation functions** or **transfer functions**. Let each of the  $k$  hidden layer nodes  $a_u$  be a linear combination of the input variables:

$$a_u = \sum_{j=1}^p \mathbf{w}_{1ju} x_j + \theta_u$$

where the  $\mathbf{w}_{1ju}$  are unknown parameters that must be estimated (called **weights**) and  $\theta_u$  is a parameter that plays the role of an intercept in linear regression (this parameter is sometimes called the **bias node**).

Each node is transformed by the activation function  $g(\cdot)$ . Much of the neural networks literature refers to these activation functions notationally as  $\sigma(\cdot)$  because of their S-shape (this is an unfortunate choice of notation so far as statisticians are concerned).

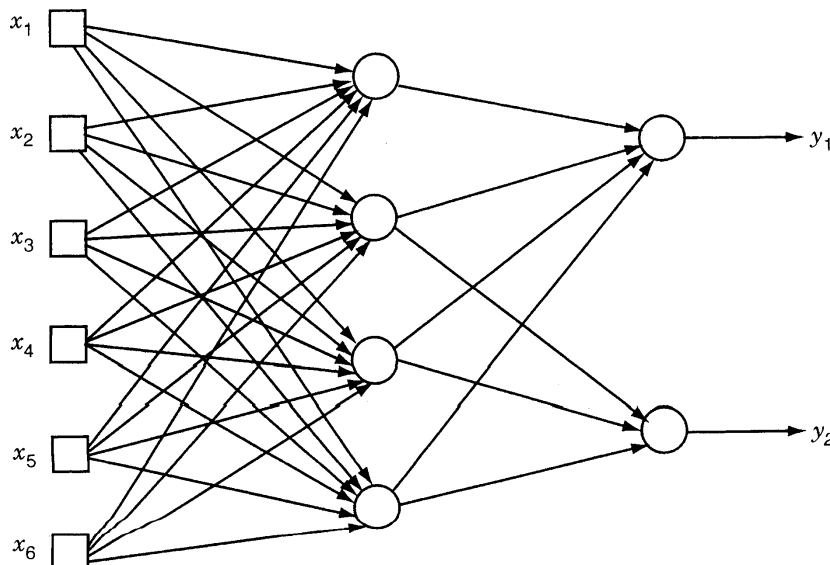


**Figure 9.10** Artificial neural network with one hidden layer.

Let the output of node  $a_u$  be denoted by  $z_u = g(a_u)$ . Now we form a linear combination of these outputs, say  $b_v = \sum_{u=0}^k w_{2uv} z_u$ , where  $z_0 = 1$ . Finally, the  $v$ th response  $y_v$  is a transformation of the  $b_v$ , say  $y_v = \tilde{g}(b_v)$ , where  $\tilde{g}(\cdot)$  is the activation function for the response. This can all be combined to give

$$y_v = \tilde{g} \left[ \sum_{k=1}^u w_{2uv} g \left( \sum_{j=1}^p w_{1ju} x_j + \theta_{1j} \right) + \theta_{2u} \right] \quad (9.48)$$

The response  $y_v$  is a transformed linear combination of transformed linear combinations of the original predictors. For the hidden layer, the activation function is often chosen to be either the logistic function  $g(x) = 1/(1 + e^{-x})$  or the hyperbolic tangent function  $g(x) = \tanh(x) = (e^x - e^{-x})/(e^x + e^{-x})$ . The choice of activation function for the output layer depends on the nature of the response. If the response is bounded or dichotomous the output activation function is usually taken to be sigmoidal, while if it is continuous an identity function is often used.

The model in Equation 9.48 is a very flexible form containing many parameters, and it is this feature that gives a neural network a nearly universal approximation property. That is, it will fit many naturally occurring functions. However, the parameters in 9.48 must be estimated, and there are a lot of them. The usual approach is to estimate the parameters by minimizing the overall residual sum of squares taken over all responses and all observations. This is a nonlinear least squares problem, and a variety of algorithms can be used to solve it. Often a procedure called **backpropagation** (which is a variation of steepest descent) is used, although derivative-based gradient methods have also been employed. As in any nonlinear estimation procedure, starting values for the parameters must be specified in order to use these algorithms. It is customary to standardize all the input variables so that small, essentially random values are chosen for the starting values.

With so many parameters involved in a complex nonlinear function, there is considerable danger of **overfitting**. That is, a neural network will provide a nearly perfect fit to a set of historical or **training** data, but it will often predict new data very poorly. Overfitting is a familiar problem to statisticians trained in empirical model building. The neural network community has developed various methods for dealing with this problem, such as reducing the number of unknown parameters (this is called **optimal brain surgery**), stopping the parameter estimation process before complete convergence and using cross-validation to determine the number of iterations to use, and adding a penalty function to the residual sum of squares that increases as a function of the sum of the squares of the parameter estimates. There are also many different strategies for choosing the number of layers and number of neurons and the form of the activation functions. This is usually referred to as choosing the **network architecture**. Cross-validation can be used to select the number of nodes in the hidden layer. Good references on artificial neural networks are Cheng and Titterington (1994), Bishop (1995), Haykin (1994), and Ripley (1994a, 1994b).

Artificial neural networks are an active area of research and application, particularly for the analysis of large, complex, highly nonlinear problems. The overfitting issue is frequently overlooked by many users and advocates of neural networks, and because many members of the neural network community do not have sound training in empirical model building, they often do not appreciate the difficulties overfitting may cause. Furthermore, many computer programs for implementing neural networks do not handle

the overfitting problem particularly well. Our view is that neural networks are a complement to the familiar statistical tools of regression analysis, RSM, and designed experiments, but certainly not a replacement for them, because a neural network can at best only give a prediction model and not fundamental insight into the underlying process mechanism that produced the data. Furthermore, there is no reason to believe that the prediction properties of these models are superior to those that would be obtained from a well-designed RSM study.

## 9.7 RSM FOR NON-NORMAL RESPONSES—GENERALIZED LINEAR MODELS

Generalized Linear Models are a unified collection of models that accommodate response distributions that obey the **exponential family**. These response distributions include the normal, Poisson, binomial, exponential, and gamma. The collection of models encompassed by the GLMs include both linear and nonlinear models. The common thread is the use of a **linear predictor**  $\mathbf{x}'\boldsymbol{\beta}$ , where the vector  $\mathbf{x}$  is in model form. For example, important members of the class of GLMs are given by the **exponential model**

$$E(y) = e^{\mathbf{x}'\boldsymbol{\beta}} \quad (9.49)$$

and the **inverse polynomial model**

$$E(y) = \frac{1}{\mathbf{x}'\boldsymbol{\beta}} \quad (9.50)$$

While both models are nonlinear in the parameters, they contain a linear component and a linear predictor, hence the word “linear” in their name. As one would expect, GLM applications involve using the response surface model (first-order interactive model, second-order model, etc.) as the linear predictor. As we shall illustrate, certain models are appropriate for certain distributions. For example, a special member of the **GLM** family is the standard linear model

$$E(y) = \mathbf{x}'\boldsymbol{\beta} \quad (9.51)$$

which is particularly appropriate for the case where the response is normal.

Many of the theoretical aspects of GLMs will not be presented in this text. For further details the reader is referred to McCullagh and Nelder (1989), Myers and Montgomery (1997), and Myers, Montgomery, and Vining (2002).

### 9.7.1 Model Framework: The Link Function

The characterization of the model is in terms of what is called a **link function**. The link function describes the transformation on the response mean  $E(y)$  or  $\mu_y$ , which is equated to the linear predictor. In other words, it is the function that *links the mean to the linear predictor*. As examples, consider the linear model, exponential model, and inverse polynomial model mentioned in the introduction to this section.

The exponential model is derived from the log link, that is,

$$\ln \mu_y = \mathbf{x}'\boldsymbol{\beta} \quad (9.52)$$

and thus the model for the mean is

$$\mu_y = e^{\mathbf{x}'\boldsymbol{\beta}} \quad (9.53)$$

The inverse polynomial model comes from the use of the reciprocal link,

$$\mu_y^{-1} = \mathbf{x}'\boldsymbol{\beta} \quad (9.54)$$

and thus the model for the mean is given by

$$\mu_y = \frac{1}{\mathbf{x}'\boldsymbol{\beta}} \quad (9.55)$$

The linear model is derived from the identity link,  $\mu_y = \mathbf{x}'\boldsymbol{\beta}$ , which of course leads to the same expression for the model itself.

We can say then that if we use a link function

$$g(\mu_y) = \mathbf{x}'\boldsymbol{\beta} \quad (9.56)$$

then the model for the mean  $\mu_y$  is given by

$$\mu_y = g^{-1}(\mathbf{x}'\boldsymbol{\beta}) \quad (9.57)$$

One very important link that will be used subsequently is the **logit link** defined by  $g(\mu_y) = \ln[\mu_y/(1 - \mu_y)]$ , resulting in the model

$$\mu_y = g^{-1}(\mathbf{x}'\boldsymbol{\beta}) = \frac{1}{1 + e^{-\mathbf{x}'\boldsymbol{\beta}}}.$$

### 9.7.2 The Canonical Link Function

For each of the members of the exponential family there is a natural **canonical link function**. This does not imply that one is confined to that canonical link. But the reader should understand that this natural link does enjoy certain theoretical as well as practical advantages. At this point we shall give the canonical links for the binomial, Poisson, exponential, gamma, and normal distributions. For the Poisson case the canonical link function is the log link, giving the exponential model. This model is commonly called the **Poisson regression model**. For the binomial case, the canonical link is the **logit link** with the resulting model given by

$$\mu_y = \frac{1}{1 + e^{-\mathbf{x}'\boldsymbol{\beta}}} \quad (9.58)$$

often referred to as the **logistic regression model**. In the case of the logistic regression model,  $\mu_y$  is often the probability  $P$  of an event, say a defective item. Note that the right-hand side of (9.58) is bounded between 0 and 1. If the experiment involves say  $n$

runs at each design point, and the response is the number out of the  $n$  that are defective, then the mean is  $nP$  and the logistic model becomes

$$\mu_y = \frac{n}{1 + e^{-\mathbf{x}'\boldsymbol{\beta}}}.$$

In the Poisson case note that the exponential model  $\mu_y = e^{\mathbf{x}'\boldsymbol{\beta}}$  does not allow negative values for prediction of Poisson counts.

In the use of both the exponential and gamma distributions the canonical link is the **reciprocal link**  $\mu_y^{-1} = \mathbf{x}'\boldsymbol{\beta}$ , resulting in the inverse polynomial model  $\mu_y = 1/(\mathbf{x}'\boldsymbol{\beta})$ .

### 9.7.3 Estimation of Model Coefficients

When we consider the distributions in the exponential family, it becomes apparent that, apart from the normal distribution, the variance is a function of the mean. Since the mean is subject to change through changes in levels of the design variables or regressor levels, the variance of the response will be nonconstant. Thus we have the nonideal conditions described earlier in this chapter. While the observations on the responses are still assumed to be independent, the nonconstant variance and nonlinearity necessitate consideration of an alternative estimation procedure.

The standard operating procedure for estimation of model coefficients in the GLM scenario is the **method of maximum likelihood**. We will not deal with the details of the likelihood for the exponential family; the reader again is referred to McCullagh and Nelder (1989) and Myers, Montgomery, and Vining (2002). The methodology used is easily motivated through a discussion of weighted least squares. Consider, for example, the model

$$y_i = \mu(\mathbf{x}_i, \boldsymbol{\beta}) + \varepsilon_i \quad (i = 1, 2, \dots, n) \quad (9.59)$$

or simply

$$y_i = \mu_i + \varepsilon_i \quad (i = 1, 2, \dots, n) \quad (9.60)$$

Here  $\mu_i$  may be either linear or nonlinear in the parameters. Now if  $\text{Var}(y_i)$  is nonconstant and is denoted by

$$\text{Var}(y_i) = v_i \quad (i = 1, 2, \dots, n)$$

and in fact the  $v_i$  are *known*, then the method of weighted least squares involves finding the coefficient vector  $\boldsymbol{\beta}$  that satisfies

$$\text{Min} \sum_{i=1}^n \left[ \frac{y_i - \mu(\mathbf{x}_i, \boldsymbol{\beta})}{\sqrt{v_i}} \right]^2 \quad (9.61)$$

Here, the  $v_i$  are assumed known, and thus independent of the model coefficients themselves. This is a reasonably straightforward nonlinear weighted least squares procedure and is discussed in detail in Carroll and Ruppert (1988) and Myers, Montgomery, and Vining (2002). However, in GLMs the variance  $v_i$  is a function of the mean and hence a function of model parameters. Thus, the one-step use of weighted least squares cannot be accomplished.

Rather the procedure is iterative in nature. The resulting procedure, termed **iterative reweighted least squares** (IRWLS), is described below.

A good illustration of the method of iterative reweighted least squares is provided by the case of the Poisson distribution with the log link. The model is given by

$$\mu_i = e^{\mathbf{x}'\beta} \quad (9.62)$$

and the variance  $v_i$  is also  $e^{\mathbf{x}'\beta}$ . As a result, a weighted least squares with known  $\beta$  in  $v_i$  implies that the differentiation involves the numerator but the denominator remains fixed. Thus the weighted least squares procedure is to solve (after differentiating Equation 9.61 with respect to  $\beta$ )

$$\sum_i (y_i - e^{\mathbf{x}'\beta}) \mathbf{x}_i = \mathbf{0}$$

for  $\beta$ . The left side of the above equation is referred to as the **score function**. Solution of this equation for  $\beta$  is certainly not difficult. However, keep in mind that the procedure described can only be viewed from a conceptual point of view, because  $\beta$  is not known. Thus the IRWLS is required to accomplish what is described above in an iterative fashion.

Suppose we denote the variance of the  $i$ th observation as  $v_i(\beta)$ . The procedure is as follows:

- (i) Begin with a starting value  $\mathbf{b}_0$ .
- (ii) Substitute  $\mathbf{b}_0$  into  $v_i(\beta)$ , forming  $v_{i,0}$ .
- (iii) Do weighted least squares with fixed weights  $v_{i,0}$ .
- (iv) Use the estimate  $\mathbf{b}_1$  from (iii), and recalculate the weights, thus forming  $v_{i,1}$ .
- (v) Go back to (iii), using  $v_{i,1}$ .
- (vi) Continue until convergence.

The above method converges to the maximum likelihood estimator for the coefficient vector  $\beta$ . See McCullagh and Nelder (1989) and Myers, Montgomery, and Vining (2002) for details.

#### 9.7.4 Properties of Model Coefficients

As in any maximum likelihood procedure, the model coefficients are asymptotically unbiased. The variance–covariance matrix, which is used for tests on coefficients and thus is of primary importance in variable screening, is not generally free of parameters in  $\beta$ . For example, in the case of logistic and Poisson regression with canonical links, asymptotically

$$\text{Var}(\mathbf{b}) = (\mathbf{X}'\mathbf{V}\mathbf{X})^{-1} \quad (9.63)$$

where  $\mathbf{V}$  is the diagonal variance–covariance matrix of the response observations,

$$\mathbf{V} = \text{diag}\{v_i(\beta)\}$$

Thus for logistic regression and Poisson regression with the log link, we have respectively,  $v_i(\beta) = n_i P_i(1 - P_i)$  with  $P_i = 1/(1 + e^{-\mathbf{x}'\beta})$  and  $v_i(\beta) = e^{\mathbf{x}'\beta}$ . Thus any statistical inference that involves standard errors of coefficients makes use of estimated standard errors

with  $\mathbf{b}$  substituted for  $\boldsymbol{\beta}$ . Variable screening through tests on single coefficients makes use of so-called **Wald inference**. The ratio

$$\left[ \frac{b_j}{se(b_j)} \right]^2$$

is asymptotically  $\chi^2_1$ , where  $se(b_j)$  is the standard error of  $j$ th model parameter. Thus the  $\chi^2$  test statistic replaces the  $t$ -statistic used in standard least squares methodology. These Wald  $\chi^2$  statistics will be illustrated in examples.

### 9.7.5 Model Deviance

In certain facets of RSM, tests for lack of fit are important, and residual plots can also be beneficial in evaluating a fitted model. In the case of classical RSM, employed with linear models with constant variance, standard  $F$ -tests are used for lack of fit. In the GLM these  $F$ -tests are not applicable. In classical RSM either ordinary residuals or studentized residuals are plotted. These residuals do not enjoy the same usefulness in a GLM situation, because their values depend critically on the assumption of constant variance. In fact, the broad notion of sums of squares (including regression and residual sums of squares) plays no role of substance in the GLM except in the special case of a normal response with an identity link. For the most part they are replaced by quantities that relate to the concept of **model deviance**. Model deviance is an important component of **likelihood inference**. Likelihood inference is rooted in the fact that, in general, a model is evaluated on the basis of the value of the log likelihood, **computed as a function of model estimates**. For example, likelihood ratio inference allows the use of the likelihood ratio

$$-2 \ln \left[ \frac{L(\mathbf{b}_r)}{L(\mathbf{b}_f)} \right]$$

where  $L(\mathbf{b}_r)$  is the likelihood computed for a restricted model whereas  $L(\mathbf{b}_f)$  is the likelihood computed for the full model. The above likelihood ratio statistic is asymptotically  $\chi^2_\Delta$ , where  $\Delta$  is the difference in the number of model parameters for the two models. Note that this test statistic essentially determines whether the full model results in significantly higher log likelihood. In the case of a linear model with normal responses, the log likelihood is, in fact, apart from constants, the residual sum of squares.

The model deviance is technically a lack-of-fit test in which the model in question is compared with the **saturated model**. The saturated model is that which has zero degrees of freedom for residual. That is, we write the saturated model as  $y_i = \mu_i + \varepsilon_i$ , where  $\mu_i$  contains no regressors. Rather there are  $N$  distinct means and thus there are  $N$  parameters to be estimated. In fact, in the case of a binomial response, the  $i$ th binomial observation  $y_i$  is the estimator of the binomial parameter  $P_i$ . In the case of a nongrouped, or **Bernoulli**, scenario, the estimator of  $P_i$  is a zero or one. Formally, then, the calculated model deviance is given by

$$\lambda(\mathbf{b}) = -2 \ln \left[ \frac{L(\mathbf{b})}{L(\hat{\mathbf{\mu}})} \right] \quad (9.64)$$

where  $L(\mathbf{b})$  is the maximum value of the likelihood for the model in question and  $L(\hat{\mathbf{\mu}})$  is the maximum value of the likelihood for the saturated model. Asymptotically  $\lambda(\mathbf{b})$  is  $\chi^2_{N-p}$ ,

where  $p$  is the number of parameters in the fitted model in question. Formally, an insignificant value of  $\lambda(\mathbf{b})$  in an upper-tail one-tailed test implies that the fit of the model is not significantly worse than that of the saturated model. Thus, a relatively small value of deviance is favorable for the fitted model. More discussion will be given later regarding the deviance value as a goodness-of-fit statistic. Often the rule of thumb is applied that the quality of the fit is reasonable if  $\lambda(\mathbf{b})/(N - p)$  is not appreciably larger than 1. This rule is prompted by the fact that  $N - p$  is the mean of the  $\chi^2_{N-p}$  distribution.

There are instances in which the asymptotic result here is not satisfactory for small samples. For details, see Myers, Montgomery, and Vining (2002).

Tests of nested hypotheses using the likelihood ratio criterion can be accomplished with *differences in deviance*, much like the use of error sums of squares for the case of linear models. Note that from the definition of deviance in Equation 9.64 a likelihood ratio test statistic  $-2 \ln[L(\text{reduced})/L(\text{full})]$  can be written as  $\lambda(\text{reduced}) - \lambda(\text{full})$ , since  $L(\hat{\mathbf{p}})$  in Equation (10.15) cancels out in the difference in deviances. For example, in a case with four parameters  $\beta_0, \beta_1, \beta_2, \beta_3$  where there is interest in testing  $H_0: \beta_1 = \beta_2 = 0$ , the likelihood ratio statistic can be written

$$2 \ln L(b_0, b_1, b_2, b_3) - 2 \ln L(b_0^*, b_3^*) = \lambda(b_0^*, b_3^*) - \lambda(b_0, b_1, b_2, b_3).$$

In fact, deviance can be used quite simply in a stepwise algorithm. The use of deviance and thus log likelihood in nested hypotheses is not as fragile in small samples as the use of deviance as a goodness-of-fit test.

### 9.7.6 Overdispersion

The concept of overdispersion is extremely important for complete understanding of the practical aspects of the fitting of generalized linear models. The term **overdispersion** implies that variability exists over and above the natural variability associated with the distribution in question. Even if the distributional assumption is correct, there may be **extra binomial variability** or extra Poisson variability. In other words, we say that the **scale parameter**  $\sigma^2 > 1$  is such that the variance of an individual observation is  $\sigma^2 np(1 - p)$  rather than  $np(1 - p)$ . In the Poisson case with mean  $\lambda$ , this means that the variance is  $\lambda \cdot \sigma^2$ .

There are reasonable explanations for overdispersion. Details regarding its possible sources appear in Myers, Montgomery, and Vining (2002). One may view the overdispersion scale parameter  $\sigma^2$  as playing the same role as the error variance in standard linear models. Certainly, sloppy or inadequate modeling in linear models increases the estimate of the error variance, since bias due to lack of fit inflates the estimate. The same is true in the case of the estimator of  $\sigma^2$  in the GLM. Here the **mean deviance**, that is,  $\text{deviance}/(N - p)$ , plays the role of the mean square error in linear models. Overdispersion often is a result of nonhomogeneity of experimental units. For example, a Poisson-distributed response may be subject to overdispersion when the experimental materials used are from different sources.

**Effect of Overdispersion on Results** The effect of overdispersion matches very closely the effect of nonhomogeneous experimental units in linear models on the error variance. The result is to increase the standard errors of estimates of model coefficients. For

example, in the case of models using the canonical link (e.g., logistic regression or Poisson regression with an exponential model), the variance–covariance matrix of coefficients is given by

$$\text{Var}(\mathbf{b}) = (\mathbf{X}'\mathbf{V}\mathbf{X})^{-1}\sigma^2 \quad (9.65)$$

and thus the standard errors are underestimated, since the parameter  $\sigma^2 > 1$  will be ignored in the computations. Obviously, in biological applications involving the use of animals as experimental units, some overdispersion is expected. Whether or not overdispersion is expected in an industrial application depends on the nature of the process.

**Adjustments for Overdispersion** It is standard procedure to adjust estimated standard errors to allow for overdispersion. As one might expect, an estimate of the scale parameter is given by

$$\hat{\sigma}^2 = \frac{\text{deviance}}{N - p} \quad (9.66)$$

which is analogous to the error mean square in standard linear models. A second estimate is given by the mean square of the **Pearson  $\chi^2$  residuals**. This statistic is given by

$$\frac{1}{N - p} \sum_{i=1}^N \left[ \frac{(y_i - \hat{y}_i)^2}{\hat{v}_i} \right] = \frac{\chi^2}{N - p} \quad (9.67)$$

The intuition here is quite clear. The  $v_i$  reflects the natural variance that comes from the type of distribution based on the analysis. Clearly then the quantity inside brackets above is the square of a standardized residual. The expression  $\chi^2/(N - p)$  estimates unity in a non-overdispersion scenario. It should be clear then that when overdispersion exists, an adjustment to the computed standard error is made by multiplying the ordinary standard errors by the factor  $\sqrt{\chi^2/(N - p)}$ , or  $\sqrt{\text{deviance}/(N - p)}$ . SAS PROC GENMOD, a software package widely used in fitting the GLM, allows for the adjustment and will be illustrated with an example in Section 9.7.7.

### 9.7.7 Examples

In this section we present two examples, the first representing a designed experiment containing a binomial response, and the second involving a Poisson response. For the binomial example a logistic regression model is fitted to the data, while for the Poisson example the canonical or log link is used, implying an exponential model.

**Example 9.4 Survival of Spermatozoa** This example is a spermatozoa survival study. The endpoint, or response variable in the experiment is survival or nonsurvival. The spermatozoa are stored in sodium citrate and glycerol. The amounts of these substances were varied along with a third factor, equilibration time, in a  $2^3$  factorial design. Fifty samples of the material were subjected to the conditions of each of the eight design points. Interpretation of the effects of the factors was sought. The data appear in Table 9.6.

**TABLE 9.6 Spermatozoa Survival Data**

Sodium Citrate $x_1$	Glycerol $x_2$	Equilibrium Time $x_3$	Number Surviving $y$
-1	-1	-1	34
1	-1	-1	20
-1	1	-1	8
1	1	-1	21
-1	-1	1	30
1	-1	1	20
-1	1	1	10
1	1	1	25

The full model to be fitted to the data contains three linear main effects and all two-factor interactions. The binomial random variable  $y$  is the response. The logit link results in the logistic regression model

$$E(y) = P = \frac{1}{1 + e^{-(\beta_0 + \beta_1 x_1 + \beta_2 x_2 + \beta_3 x_3 + \beta_{12} x_1 x_2 + \beta_{13} x_1 x_3 + \beta_{23} x_2 x_3)}}$$

where  $P$  is the probability of survival.

At this point we will give the likelihood inference designed to test the adequacy of the entire model. This is analogous to the  $F$ -test used in standard linear models. For the intercept-only model

$$P = \frac{1}{1 + e^{-\beta_0}}$$

we have (from PROC GENMOD)

$$-2 \ln L(\text{reduced}) = 544.234$$

whereas for the full model containing seven parameters,

$$-2 \ln L(\text{full}) = 496.055$$

Thus the appropriate likelihood ratio test statistic is

$$\begin{aligned} \chi^2 &= 2 \ln \left[ \frac{L(\text{reduced})}{L(\text{full})} \right] \\ &= 544.234 - 496.055 \\ &= 48.179 \end{aligned}$$

with  $7 - 1 = 6$  degrees of freedom. The value is significant at  $P < 0.0001$ . This implies that the use of the full model significantly *increases* the log likelihood over that of the

**TABLE 9.7 Maximum Likelihood Estimates and Wald Inference on Individual Coefficients for Data of Example 9.4**

Model Term	df	Parameter Estimate	Standard Error	Wald $\chi^2$	P-Value
Intercept	1	-0.3770	0.1101	11.7198	0.0006
$x_1$	1	0.0933	0.1101	0.7175	0.3970
$x_2$	1	-0.4632	0.1101	17.7104	0.0001
$x_3$	1	0.0259	0.1092	0.0563	0.8124
$x_1x_2$	1	0.5851	0.1101	28.2603	0.0001
$x_1x_3$	1	0.0544	0.1093	0.2474	0.6189
$x_2x_3$	1	0.1122	0.1088	1.0624	0.3027

intercept-only model. The maximum likelihood estimates, standard errors, and Wald  $\chi^2$  values for each coefficient appear in Table 9.7.

Note that  $\beta_0$ ,  $\beta_2$ , and  $\beta_{12}$  appear to be important model terms. Any type of stepwise algorithm using log likelihood results in the choice of the same model terms. The reduced model was fitted to the data, and the results are shown in Table 9.8. Thus the fitted model for estimating probability of survival is given by

$$\hat{P} = \frac{1}{1 + e^{(-0.3637 - 0.4505x_2 + 0.5747x_1x_2)}}.$$

Note that fitting the reduced model results in different coefficients than those that appeared in the full model. This is traced to the fact that, unlike the case of *linear* response surface models, for this model the  $2^3$  factorial does not enjoy the property of orthogonality. Also note that the standard errors are not equal as they would be in the case of a linear model with standard assumptions. The contour plot and response surface plot of this model are shown in Fig. 9.11.

From the above fitted model and the plots in Fig. 9.11 it is easily established that when the sodium citrate is at the low level, the amount of glycerol has a negative effect on the probability of survival. By that we mean that a low level of glycerol produces the desired result ( $\hat{P}$  close to 1.0). On the other hand, if the sodium citrate level is high, the amount of glycerol has very little effect. The most desirable result occurs when both  $x_1$  and  $x_2$  are simultaneously at the low level, whereas the worst case in terms of survival occurs when sodium citrate is low and glycerol is high.

One must keep in mind that, as in any designed experiment, the conclusions drawn here depend greatly on the chosen ranges of the design variables. In addition, standard

**TABLE 9.8 The Reduced Model for Example 9.4**

Model Term	df	Parameter Estimate	Standard Error	$\chi^2$	P-Value
Intercept	1	-0.3637	0.1081	11.3116	0.0008
$x_2$	1	-0.4505	0.1084	17.2677	0.0001
$x_1x_2$	1	0.5747	0.1086	27.9923	0.0001

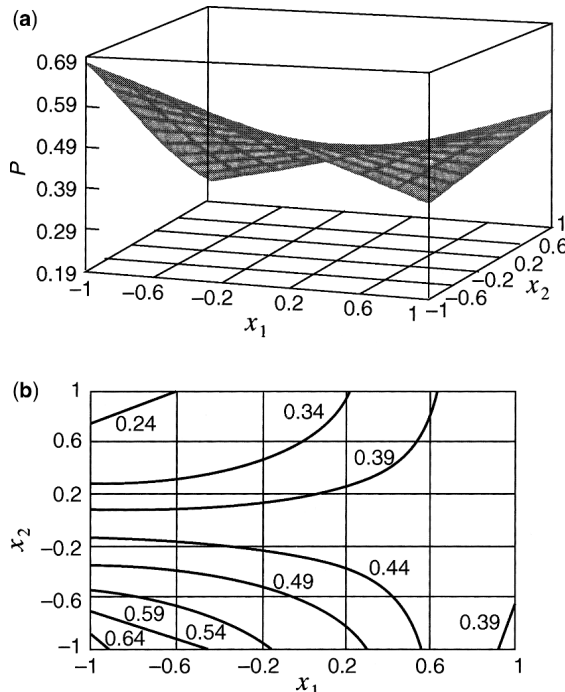


**Figure 9.11** Response surface and contour plot for Example 9.4. (a) Response surface. (b) Contour plot.

techniques such as residual analysis and the use of other diagnostic information should be considered. We will discuss this later.

We now consider **odds ratios** and what they mean in the context of Example 9.4. For the case where a logistic regression model is fitted, the type of interpretation that one obtains from the factor effects that are used for linear models are replaced by odds ratios. In the case of linear models, effect calculations discussed in Chapters 3 and 4 as the difference between the mean response at the high level and that at the low level of a factor are quite natural, simply because the model is in fact linear. In the case of the logistic model the type of interpretation that is natural exploits the *multiplicative* component of the model. In this example we define the **odds** of survival as  $P/(1 - P)$ , where, of course,  $P$  is the probability of survival.

From the logistic model in Equation 9.58 we can write

$$\frac{P}{1 - P} = e^{x'\beta}$$

The multiplicative nature of the above equation leads to a natural interpretation of the effect of a factor as the *ratio* (rather than the difference) of the odds when a factor is at  $x = +1$  to the odds when the factor is, say, at the midpoint of the range, i.e.,  $x = 0$ —that is, the computation of the ratio of change in the odds of survival as the factor increases one unit. If there is no interaction in the model,  $e^{\beta_2}$  becomes the ratio of the odds of survival at

$x_2 = 1$  to the odds of survival at  $x_2 = 0$ . So the interpretation is quite straightforward in the no-interaction model. In fact,  $(e^{\beta_2})^2 = e^{2\beta_2}$  is the ratio of the odds of survival at  $x_2 = 1$  to the odds at  $x_2 = -1$ . However, when there is interaction in the model, as in Example 9.4,  $e^{\beta_2}$  is the ratio of the odds of survival at  $x_2 = 1$  to the odds at  $x_2 = 0$  when  $x_1 = 0$ . Here  $e^{\beta_2} = 0.637$ , which makes a strong case for not storing the sperm with glycerol at its high value, particularly when  $x_1 = 0$ . For  $x_1 = -1$  the relevant calculated odds ratio for  $x_2$  is  $e^{\beta_2 - \beta_{12}} = 0.36$ . This number illustrates how operating at the high level is even more destructive as far as survival is concerned if sodium citrate, is at the low level. On the other hand, if sodium citrate is at the high level, that is,  $x_1 = +1$ , the calculated odds ratio effect of glycerol is  $e^{\beta_2 + \beta_{12}} = e^{0.125} = 1.136$ . This odds ratio near one implies that the effect of  $x_2$  (glycerol) is rendered very small when sodium citrate is used at the high level. So, while the maximum estimated probability of survival is achieved with both factors simultaneously at the low level, the use of sodium citrate at the high level negates the effect of glycerol.

It turns out that for all GLMs there is a connection to the effects used in standard linear models. This will be evident in the next example.

**Example 9.5 Solder Defects** Consider an electronic circuit card assembly by a wave-soldering process. The response is the number of defects in the solder joint. The process involves baking and preheating the circuit card and passing it through a solder wave by conveyor. Condra (1993) originally presented the results shown in Table 9.9, and Hamada and Nelder (1997) reanalyzed them. The seven factors are (A) prebake condition, (B) flux density, (C) conveyor speed, (D) preheat condition, (E) cooling time, (F) ultrasonic solder agitator, and (G) solder temperature. Each factor is at two levels, and the experimental design is a replicated  $2^{7-3}$  fractional factorial. Note that data point 11 has only two

TABLE 9.9 Wave Solder Data

Run	Factor							$y$		
	A	B	C	D	E	F	G	1	2	3
1	-1	-1	-1	-1	-1	-1	-1	13	30	26
2	-1	-1	-1	+1	+1	+1	+1	4	16	11
3	-1	-1	+1	-1	-1	+1	+1	20	15	20
4	-1	-1	+1	+1	+1	-1	-1	42	43	64
5	-1	+1	-1	-1	+1	-1	+1	14	15	17
6	-1	+1	-1	+1	-1	+1	-1	10	17	16
7	-1	+1	+1	-1	+1	+1	-1	36	29	53
8	-1	+1	+1	+1	-1	-1	+1	5	9	16
9	+1	-1	-1	-1	+1	+1	-1	29	0	14
10	+1	-1	-1	+1	-1	-1	+1	10	26	9
11	+1	-1	+1	-1	+1	+1	+1	28		19
12	+1	-1	+1	+1	-1	+1	-1	100	129	151
13	+1	+1	-1	-1	-1	+1	+1	11	15	11
14	+1	+1	-1	+1	+1	-1	-1	17	2	17
15	+1	+1	+1	-1	-1	-1	-1	53	70	89
16	+1	+1	+1	+1	+1	+1	+1	23	22	7

observations. A third observation was reported, but strong evidence suggested that it was an outlier. See Hamada and Nelder (1997).

Table 9.10 displays a SAS GENMOD output for the wave solder data. The response is assumed to obey a Poisson distribution. The log link is used, and thus the model is the exponential model

$$\mu = e^{\mathbf{x}'\boldsymbol{\beta}}$$

with the linear predictor  $\mathbf{x}'\boldsymbol{\beta}$  containing seven main effects and six interaction terms. Note from this output that the mean deviance, deviance/( $N - p$ ), exceeds unity considerably.

**TABLE 9.10 GENMOD Output for Full Model, Wave Solder Data, Example 9.5**

The GENMOD Procedure					
Model Information					
Description	Value				
Data Set	WORK, DEFECT				
Distribution	POISSON				
Link Function	LOG				
Dependent Variable	Y				
Observations Used	47				
Criteria For Assessing Goodness of Fit					
Criterion	DF	Value	Value/DF		
Deviance	33	139.7227	4.2340		
Scaled Deviance	33	139.7227	4.2340		
Pearson Chi-Square	33	122.9190	3.7248		
Scaled Pearson $\chi^2$	33	122.9190	3.7248		
Log Likelihood		3837.9339			
Analysis of Parameter Estimates					
Parameter	DF	Estimate	Std Err	Chi Square	Pr > Chi
INTERCEPT	1	3.0721	0.0344	7981.4934	0.0001
A	1	0.1126	0.0332	11.4710	0.0007
B	1	-0.1349	0.0344	15.3837	0.0001
C	1	0.4168	0.0345	146.1672	0.0001
D	1	-0.0577	0.0344	2.8118	0.0936
E	1	-0.0942	0.0334	7.9508	0.0048
F	1	-0.0176	0.0339	0.2696	0.6036
G	1	-0.3803	0.0343	122.9944	0.0001
AB	1	-0.0175	0.0334	0.2760	0.5993
AC	1	0.1741	0.0339	26.3925	0.0001
AD	1	0.0919	0.0332	7.6421	0.0057
BC	1	-0.0788	0.0343	5.2798	0.0216
BC	1	-0.2996	0.0344	75.8633	0.0001
CD	1	0.0446	0.0345	1.8275	0.1764
SCALE	0	1.0000	0.0000		

**TABLE 9.11 Final Model for Wave Solder Data, Example 9.5**

Link Function	LOG			
Dependent Variable	Y			
Observations Used	47			
<i>Criteria For Assessing Goodness of Fit</i>				
Criterion	DF	Value	Value/DF	
Deviance	42	241.7755	5.7566	
Scaled Deviance	42	42.0000	1.0000	
Pearson Chi-Square	42	237.3981	5.6523	
Scaled Pearson $\chi^2$	42	41.2396	0.9819	
Log Likelihood		657.8421		
<i>Analysis of Parameter Estimates</i>				
Parameter	DF	Estimate	Std Err	Chi Square
INTERCEPT	1	3.0769	0.0825	1391.0260
C	1	0.4405	0.0808	29.7429
G	1	-0.4030	0.0808	24.8954
AC	1	0.2821	0.0667	17.9039
BD	1	-0.3113	0.0808	14.8557
SCALE	0	2.3993	0.0000	

NOTE: The scale parameter was estimated by the square root of DEVIANC/DOF.

This signals the condition of overdispersion. The danger is the underestimation of standard errors of coefficients. Also, we see that the mean squared error of the Pearson  $\chi^2$  residuals exceeds unity considerably. Note from the “Analysis of Parameter Estimates” in the output that all main effects are significant apart from  $D$  and  $F$ . The interactions  $AC$ ,  $AD$ ,  $BC$ , and  $BD$  are also statistically significant according to the Wald  $\chi^2$  values.

The GENMOD output in Table 9.11 contains results in which the standard errors of the estimated coefficients are adjusted for overdispersion. The standard errors are larger by a factor of  $\sqrt{\text{dev}/(N - p)} = \sqrt{4.234}$ . After the adjustment the model terms that appear significant are now  $C$ ,  $G$ ,  $AC$ , and  $BD$ . The conclusions concerning the results are quite different when overdispersion is taken into account.

Finally let us consider the reduced model containing the significant model terms that appear in Table 9.11. The fitted model is given by

$$\hat{\mu} = e^{3.0769 + 0.4405 C - 0.4030 G + 0.2821 AC - 0.3113 BD}$$

where  $\hat{\mu}$  is the estimated mean number of defects. Once again, as in the case of logistic regression, the effects that allow interpretations of the roles of the variables must take into account the multiplicative nature of the model. For example, consider factor  $G$ , solder temperature. The effect  $e^{-0.4030} = 0.65$  is the *factor* by which the number of defects is reduced when solder temperature is changed from (coded level)  $G = 0$  to  $G = 1$ , the high level. Now consider factor  $C$ , conveyor speed. The effect of  $C$  obviously depends on the level of  $A$ , the prebake condition. If  $A$  is at the high level, an increase of conveyor speed from coded level 0 to 1 (one unit) increases the

number of defects by a factor of

$$\begin{aligned} e^{0.4405+0.2821} &= e^{0.7226} \\ &= 2.05 \end{aligned}$$

On the other hand, if the prebake condition is at the low level, an increase in  $C$  from 0 to 1 will increase the number of defects by a factor of 1.17, since

$$e^{0.4405+0.2821} = 1.17$$

Thus the destructive effect of conveyor speed is rendered negligible if the prebake condition is at the low level. The optimum conditions on the factors, i.e., those that result in minimum number of defects, are given by

$$\begin{aligned} C &= -1 \\ G &= +1 \\ A &= +1 \end{aligned}$$

while factors  $B$  and  $D$  are at the extremes, as long as  $B$  and  $D$  take opposite signs. The estimated mean number of defects under these conditions is given by  $e^{1.64} = 5.16$ .

### 9.7.8 Diagnostic Plots and Other Aspects of the GLM

As we have previously emphasized, much of the success of RSM centers around graphics. These graphical displays include diagnostic plots of residuals, effect plots, and contour plots. They are described in detail with illustrations, throughout this text, for RSM under standard conditions, that is, normally distributed responses and independent errors with constant variances. In the case of generalized linear models, similar diagnostic plots involving residuals and effects are available, though they require some separate discussion here.

There are two types of residuals that are available in the GLM: the Pearson  $\chi^2$  residual, which has been introduced briefly in Section 9.7.6, and the **deviance residual**. Both the Pearson residual and the deviance residual have as their roots a goodness-of-fit statistic. The Pearson  $\chi^2$  residual is an ordinary residual  $y_i - \mu_i$ , standardized according to the variance  $\hat{\nu}_i$  at the  $i$ th data point. The sum of squares of these residuals is the **Pearson  $\chi^2$** , which is the basis for a goodness-of-fit statistic in SAS PROC GENMOD. The Pearson  $\chi^2$  is asymptotically  $\chi^2_{N-p}$  like the deviance statistic. However, like the mean deviance, the Pearson  $\chi^2/(N-p)$  is interpreted with the rule of thumb that a value substantially exceeding unity implies that lack of fit is no concern.

In order to gain a sound understanding of the concept of deviance residuals, we should review the basic structure of the deviance calculation with an example. The definition is given in Equation 9.64. Note from this equation that the deviance is a difference in log likelihood. In fact, apart from the factor of 2, we have

$$\lambda(\mathbf{b}) = \ln L(\hat{\mathbf{\mu}}) - \ln L(\mathbf{b})$$

where, of course,  $L(\hat{\mathbf{\mu}})$  is the likelihood for the saturated model and  $L(\mathbf{b})$  is the likelihood for the model in question. Let us consider an example with a Poisson response. The log likelihood is the log of the joint probability function of  $y_1, y_2, \dots, y_N$ , which is given

by the log of

$$P(y_1, y_2, \dots, y_N, \boldsymbol{\mu}) = \frac{e^{-\sum_{i=1}^N \mu_i} \prod_{i=1}^N \mu_i^{y_i}}{\prod_{i=1}^N y_i}$$

Thus

$$\ln L(\hat{\boldsymbol{\mu}}) = -\sum_{i=1}^N \hat{\mu}_i + \sum_{i=1}^N y_i \ln \hat{\mu}_i - \sum_{i=1}^N \ln h_i \quad (9.68)$$

where  $\hat{\mu}_i$  replaces  $\mu_i$  in the log likelihood. For the saturated model  $\hat{\mu}_i$  is replaced by  $y_i$ , the  $i$ th observation, whereas for the Poisson regression model in question,  $\hat{\mu}_i$  is replaced by the maximum likelihood estimator of the mean from the regression model. As a result, for the Poisson deviance we have

$$\begin{aligned} \lambda(\mathbf{b}) &= 2 \sum_{i=1}^N [(\hat{\mu}_i - y_i) - y_i \ln \hat{\mu}_i + y_i \ln y_i] \\ &= 2 \sum_{i=1}^N [y_i \ln (y_i/\hat{\mu}_i) - (y_i/\hat{\mu}_i)] \end{aligned} \quad (9.69)$$

It can be shown (see Exercise 9.3) that for this case  $\sum_{i=1}^N (y_i - \hat{\mu}_i) = 0$  for the canonical link. However, in general the deviance is of the form  $\sum_{i=1}^N d_i$ , where  $d_i$  is the portion in brackets in Equation 9.69. This  $d_i$  is called the *i*th **deviance residual**. It is not exactly what one plots, however. In order to give the residuals the characteristics that more closely resemble those of the residuals in standard linear models, we define the **adjusted deviance residual** ( $r_D$ )<sub>*i*</sub> as

$$(r_D)_i = \text{sgn}(y_i - \hat{\mu}_i) \sqrt{d_i}.$$

This is for most cases the type of residual that is more appropriate to use for plotting purposes. The sum of squares of the  $(r_D)_i$  is the deviance  $\lambda(\beta)$ .

With regard to effect plots, we saw in discussions in our examples that effects are quite often multiplicative in nature, and the interpretations are no less difficult to understand than the linear effects that are generally observed and plotted in the case of linear models. However, these effects often take the form  $e^b$ , where  $b$  is either a regression coefficient or a linear combination of regression coefficients. Since maximum likelihood estimators are known to be asymptotically normal, the best results for normal probability plotting are expected when **standardized coefficients** are plotted, i.e., coefficients divided by their standard errors. It is interesting that when a two-level factorial design or regular fraction is employed, model coefficients are often nearly asymptotically independent when a GLM is used. This depends a great deal on the distribution and link. Indeed, if the so-called **variance-stabilizing link** is used, the coefficients will have covariances that are asymptotically zero. See Myers, Montgomery, and Vining (2002). These links include the square root link for the Poisson case, the log link for the exponential distribution, and the log link for the gamma distribution.

**Example 9.6 The Drill Experiment** We consider a  $2^4$  unreplicated factorial that was used to investigate the advance rate of a drill. This response exhibits a nonconstant variance that depends on the level of the response. Daniel (1976) used this experiment to illustrate the usefulness of normal probability plotting. The model fitted to the data here makes use of a log link with an assumed gamma-distributed response. The data appears in Table 9.12.

The use of the log link results in an exponential model. The estimated model coefficients are as follows:

Term	Coefficient
Intercept	1.598
$x_1$	0.065
$x_2$	0.290
$x_3$	0.577
$x_4$	0.163
$x_1x_2$	-0.017
$x_1x_3$	0.005
$x_1x_4$	0.034
$x_2x_3$	-0.025
$x_2x_4$	-0.008
$x_3x_4$	0.049
$x_1x_2x_3$	0.005
$x_1x_2x_4$	0.025
$x_1x_3x_4$	0.027
$x_2x_3x_4$	-0.017
$x_1x_2x_3x_4$	0.019

TABLE 9.12 The Drill Experiment, Example 9.6

Run	$x_1$	$x_2$	$x_3$	$x_4$	Advance Rate (Original Data)
1	-	-	-	-	1.68
2	+	-	-	-	1.98
3	-	+	-	-	3.28
4	+	+	-	-	3.44
5	-	-	+	-	4.98
6	+	-	+	-	5.70
7	-	+	+	-	9.97
8	+	+	+	-	9.07
9	-	-	-	+	2.07
10	+	-	-	+	2.44
11	-	+	-	+	4.09
12	+	+	-	+	4.53
13	-	-	+	+	7.77
14	+	-	+	+	9.43
15	-	+	+	+	11.75
16	+	+	+	+	16.30

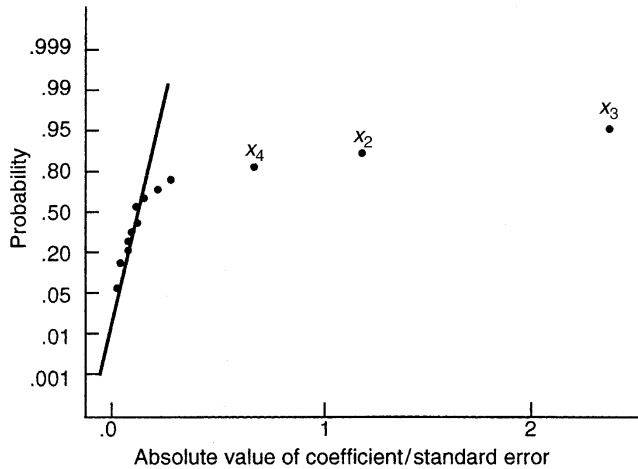


**Figure 9.12** Half normal probability plot of effects for the drill data.

The coefficients divided by their standard errors were plotted on a half normal probability plot. The plot is shown in Fig. 9.12. In this figure  $A = x_1$ ,  $B = x_2$ , and so on.

From the normal probability plot it appears that coefficients for factors  $x_2$ ,  $x_3$ , and  $x_4$  are significantly different from zero. The reduced model was fitted with the resulting estimated response function

$$\hat{y} = e^{1.6032 + 0.2895x_2 + 0.5772x_3 + 0.1656x_4}$$

Lewis, Montgomery, and Myers (2001a) conduct a more extensive analysis of this experiment. They illustrate that the use of the GLM is preferable to performing a log transformation and using ordinary least squares, because the GLM produces shorter confidence intervals on the mean response. Lewis, Montgomery, and Myers (2001b) show that this is a reasonable criterion for selecting between a GLM and a standard linear least squares model following a data transformation. Lewis (1998) is also a useful reference.

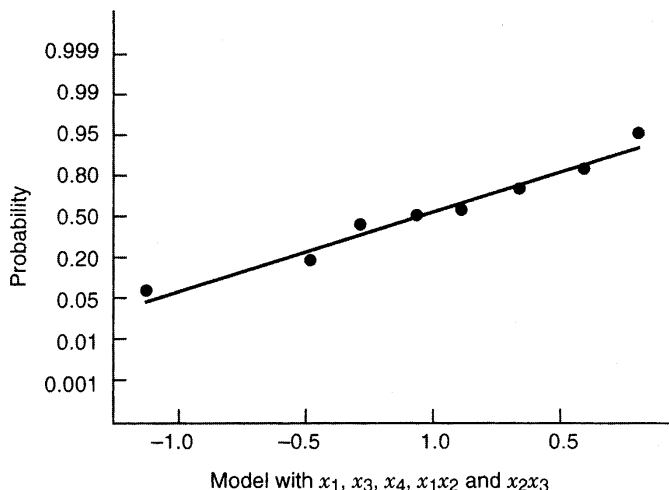
**Example 9.7 Windshield Slugging** This experiment involves the use of a  $2^{4-1}$  fractional factorial in a study of windshield molding. During the operation debris carried into the die appears as dents, or **slugs**, in the product. Martin, Parker, and Zenick (1987) originally presented and analyzed the data. The purpose of the experiment is to improve slugging performance. The response is the number of good parts out of 1000. The binomial distribution is assumed, and the logit link is used. Table 9.13 gives the data.

The reduced logistic regression model includes the terms  $x_1$ ,  $x_3$ ,  $x_4$ ,  $x_2x_3$ , and  $x_1x_2$ . The reader is asked to verify this in Exercise 9.13. The deviance residuals were plotted for model diagnostic checking and appear in Fig. 9.13. They indicate that the logistic model with the logit link is satisfactory.

Generalized linear models represent a useful set of techniques for conducting response surface analysis when the response variables are clearly nonnormal and ordinary least squares estimation is not efficient. Modern software packages, including SAS and S-PLUS, have good GLM capability, and JMP can analyze GLMs for the binomial, Poisson, and exponential distributions. Ozol-Godfrey et al. (2008) show how fraction of

**TABLE 9.13** The Windshield Molding Slugging Experiment

Run	$x_1$	$x_2$	$x_3$	$x_4$	Good Parts (Original Data)
1	+	+	+	+	338
2	+	+	-	-	826
3	+	-	+	+	350
4	+	-	-	-	647
5	-	+	+	-	917
6	-	+	-	+	977
7	-	-	+	-	953
8	-	-	-	+	972

**Figure 9.13** Normal probability plots of deviance residuals for logistic model windshield data.

design space plots introduced in Chapter 8, can be adapted to evaluate designs for GLMs. This is a useful tool to add to the kit of a practitioner who wishes to conduct these types of analysis.

## 9.8 SPLIT-PLOT DESIGNS FOR SECOND-ORDER MODELS

In Chapters 3 and 4 we introduced the split-plot design (SPD) as a technique for running experiments more economically if some of the factors are hard to change. Time or cost constraints lead to considering a split-plot structure rather than a completely randomized design. For response surface models involving second-order models, practical constraints may often dictate that a split-plot design and model be considered to accommodate some hard-to-change factors. Recall that SPDs involve two randomizations. The hard-to-change factor combinations are randomly assigned to whole-plot units based on the whole plot design. Within each whole plot, the easy-to-change factors are assigned to

the subplot units with a separate randomization for each whole plot. These two levels of randomization lead to two error terms, a whole plot error and a subplot error. Care should be taken to ensure that both types of error can be estimated, and that the terms of the model are assessed relative to the appropriate error term. Typically, the main, interaction, and quadratic effects involving whole plot factors are whole-plot effects. Terms of the model involving just subplot factors or combinations of whole and subplot factors are generally subplot effects.

Split-plot designs have practical advantages for running the experiment since the hard-to-change factors are only reset for each whole plot, while the easy-to-change factors are reset for each observation. Not only are these designs more economical to run, but as Goos and Vanderbroek (2004) show, they can also sometimes be more *D*- and *G*-efficient than a similar sized completely randomized design.

The central composite and Box–Behnken designs presented in Chapter 7 can be easily adapted to become split-plot designs with good properties. One simple approach to adapting these designs is to group all experimental runs with common whole-plot levels into a single whole plot. These **restricted split-plot designs** have the minimal allowable number of whole plots, with just a single whole plot for each combination of whole plot levels. Table 9.14 shows an example of a restricted central composite design for two hard-to-change ( $z_1$  and  $z_2$ ) and two easy-to-change ( $x_1$  and  $x_2$ ) factors. Table 9.15 shows an example of a restricted Box–Behnken design for the same set of factors. If the hard-to-change factors are prohibitively expensive, then this approach allows us to minimize the cost of changing these factors. One obvious weakness of this type of design is that there are no replicated whole plots to estimate the whole-plot error term.

In Section 7.1, some important characteristics for a good response surface design are given. With the new structure for a split-plot design, some adaptation and expansion of the criteria are needed to consider the presence of two types of experimental units, namely the whole-plot and subplot experimental units. A *good* SPD should seek to balance and simultaneously optimize a number of varied criteria:

1. Result in a good fit of the model to the data.
2. Allow good estimation of model parameters.

**TABLE 9.14 A Restricted Central Composite Split-Plot Design With Nine Whole Plots for Two Hard-to-Change and Two Easy-to-Change Factors**

Whole Plot #	$z_1$	$z_2$	$x_1$	$x_2$	# Runs
1	−1	−1	±1	±1	4
2	−1	+1	±1	±1	4
3	+1	−1	±1	±1	4
4	+1	+1	±1	±1	4
5	− $\alpha$	0	0	0	1
6	+ $\alpha$	0	0	0	1
7	0	− $\alpha$	0	0	1
8	0	+ $\alpha$	0	0	1
9	0	0	$\pm\alpha$	0	4 + #CR
			0	$\pm\alpha$	
			0	0	

3. Allow good prediction throughout the design space.
4. Provide estimates of “pure” error at both the whole plot and subplot levels.
5. Give sufficient information to allow a test for lack-of-fit.
6. Provide a check on the homogeneity of variance in both the whole plot and subplot portions of the design space.
7. Consider the relative cost in setting the hard-to-change and easy-to-change factors.
8. Consider simplicity and symmetry of the design.
9. Consider the required complexity of analysis.
10. Be robust to errors in control of design levels.
11. Be insensitive to the presence of outliers in the data.

As with completely randomized designs, not all of these properties are required in every split-plot application and no single design is capable of performing best in all of these properties simultaneously. However, it is beneficial when choosing a designed experiment to give serious consideration to the relative importance of these criteria. Often a good design can do quite well for several of these properties. Item 4 has been expanded to note that the two error terms now need to both be estimated. Frequently obtaining a good estimate of the sub-plot error term is relatively easy, but because of the nature of hard-to-change factors, many designs do not place adequate emphasis of estimating the whole plot error term. Similarly for Item 6, it may be difficult to obtain sufficient information about homogeneity of variance in the whole plot space. Item 7 deserves special emphasis as the relative cost of setting the hard-to-change and easy-to-change factors will typically dictate what designs can be considered. Some additional discussion of this is presented in subsequently. Finally, Item 9 has added importance in the split plot setting as some alternatives exist for the estimation and analysis, depending on the type of design selected. Parker et al. (2008) present a thorough discussion about how to balance several criteria in the split-plot design case.

**TABLE 9.15 A Restricted Box–Behnken Split-Plot Design With Nine Whole Plots for Two Hard-to-Change and Two Easy-to-Change Factors**

Whole Plot #	$z_1$	$z_2$	$x_1$	$x_2$	# Runs
1	-1	-1	0	0	1
2	-1	+1	0	0	1
3	+1	-1	0	0	1
4	+1	+1	0	0	1
5	-1	0	$\pm 1$	0	4
			0	$\pm 1$	
6	+1	0	$\pm 1$	0	4
			0	$\pm 1$	
7	0	-1	$\pm 1$	0	4
			0	$\pm 1$	
8	0	+1	$\pm 1$	0	4
			0	$\pm 1$	
9	0	0	$\pm 1$	$\pm 1$	$4 + \#CR$
			<b>0</b>	<b>0</b>	

**Example 9.8 The Adhesive Strength Experiment** Consider an experiment involving four factors that potentially affect the strength of an adhesive intended for application in a medical device application. Two of the factors ( $A$  = cure temperature and  $B$  = percent of resin in the adhesive) are relatively hard to change from run to run, while the other two ( $C$  = amount of adhesive applied and  $D$  = cure time) are easy to change. A second-order model is thought to be appropriate for the underlying relationship between strength and the input factors. The form of the model is

$$\begin{aligned} \text{Strength} = & \beta_0 + \beta_1 A + \beta_2 B + \beta_{12} AB + \beta_{11} A^2 + \beta_{22} B^2 + \gamma_1 C + \gamma_2 D \\ & + \gamma_{12} CD + \gamma_{11} C^2 + \gamma_{22} D^2 + \alpha_{11} AC + \alpha_{12} AD + \alpha_{21} BC \\ & + \alpha_{22} BD + \delta + \varepsilon \end{aligned}$$

where the  $\beta$  terms involve hard-to-change factors, the  $\gamma$  terms involve easy-to-change factors and the  $\alpha$  terms involve both hard- and easy-to-change factors. Written in matrix form, we have a model

$$\mathbf{y} = \mathbf{X}\boldsymbol{\beta} + \mathbf{Z}\boldsymbol{\delta} + \boldsymbol{\varepsilon}.$$

with  $\mathbf{X}$  is the  $N \times p$  design matrix expanded to model form for the  $p$  model parameters which include the intercept;  $\mathbf{Z}$  is an  $N \times a$  classification matrix of ones and zeros where the  $ij$ th entry is 1 if the  $i$ th observation ( $i = 1, \dots, N$ ) belongs to the  $j$ th whole plot ( $j = 1, \dots, a$ ). Note the two errors terms:  $\boldsymbol{\delta} \sim N(0, \sigma_{WP}^2)$  for the whole plot and  $\boldsymbol{\varepsilon} \sim N(0, \sigma^2)$  for the subplot error. We also assume  $\boldsymbol{\delta}$  and  $\boldsymbol{\varepsilon}$  are mutually independent.

The covariance matrix of the responses in a split-plot design is

$$\begin{aligned} \text{Var}(\mathbf{y}) &= \sum = \sigma_{WP}^2 \mathbf{Z} \mathbf{Z}' + \sigma^2 \mathbf{I}_N \\ &= \sigma^2 [d \mathbf{Z} \mathbf{Z}' + \mathbf{I}_N] \end{aligned}$$

where  $\mathbf{I}_N$  is an  $N \times N$  identity matrix and  $d = \sigma_{WP}^2 / \sigma^2$  represents the variance component ratio. This type of error structure is called compound symmetric. If we sort the observations by whole plots, we can write  $\sum = \text{diag}(\sum_1, \dots, \sum_a)$  where each  $n_j \times n_j$  matrix  $\sum_j$  is given by

$$\sum_j = \begin{bmatrix} \sigma_{WP}^2 + \sigma^2 & \cdots & \sigma_{WP}^2 \\ \vdots & \ddots & \vdots \\ \sigma_{WP}^2 & \cdots & \sigma_{WP}^2 + \sigma^2 \end{bmatrix}$$

and  $\sum_j$  denotes the covariance matrix of responses for the  $j$ th whole plot. Note that the variance of an individual observation is the sum of the sub-plot and whole plot error variances,  $\sigma_{WP}^2 + \sigma^2$ .

The experimenters have a budget that will allow them to reset the hard-to-change factors 12 times, with 2 runs of different levels of the easy-to-change factors within each whole plot. Table 9.16 shows the  $I$ -optimal design satisfying the experimenters logistical constraints generated in JMP with the resulting data obtained from the experiment. As with completely randomized designs it is beneficial to explore the prediction variance properties

**TABLE 9.16 The Response Surface Design and Data for the Adhesive Strength Example**

Whole Plot #	A	B	C	D	Strength
1	1	-1	1	-1	15.7
			-1	1	27.0
2	-1	1	-1	1	46.8
			1	-1	29.9
3	-1	-1	-1	1	17.6
			1	-1	45.9
4	-1	1	1	1	36.8
			-1	-1	32.1
5	-1	-1	1	1	30.7
			-1	-1	53.7
6	1	1	1	-1	8.1
			-1	1	45.2
7	1	0	-1	-1	19.4
			0	0	33.6
8	1	-1	-1	-1	18.3
			1	1	19.6
9	0	-1	0	-1	42.9
			-1	0	42.3
10	1	1	1	1	59.1
			-1	-1	16.1
11	0	1	0	0	45.3
			1	-1	31.6
12	0	0	0	1	46.7
			1	0	46.2

of the constructed design for the assumed model. Figure 9.14 shows the range of prediction variance values throughout the design region in the fraction of design space plot generated in JMP. Liang et al. (2006a) provide additional alternatives to this plot to allow for more detailed examination of the prediction performance throughout the design space. For interactive exploration of the prediction variance, the prediction profiler described in Chapter 8 and shown in Fig. 9.15 allows for better understanding.

Because the observations are not independent and have a compound symmetric error structure generalized least squares (GLS) is required to obtain estimates of the model parameters. The software package JMP uses the REML (REstricted or REsidual Maximum Likelihood) method of fitting mixed models (those which contain both fixed effects—the factor effects, and random effects—the whole-plot error terms). See Wolfinger et al. (1994) and Searle et al. (1992) for more details on this estimation approach.

Table 9.17 shows the output generated by JMP for the adhesive strength data. Notice that the whole plot variance component is much larger than the subplot variance component, as is typically the case in split-plot designs. The whole plot variance component accounts for about 70% of the total variability.

**Design Considerations for Split-Plot Experiments** Because of the more complex structure for split-plot designs, there are some additional considerations for selecting a design. Adaptations of the central composite and Box–Behnken designs described in Chapter 7

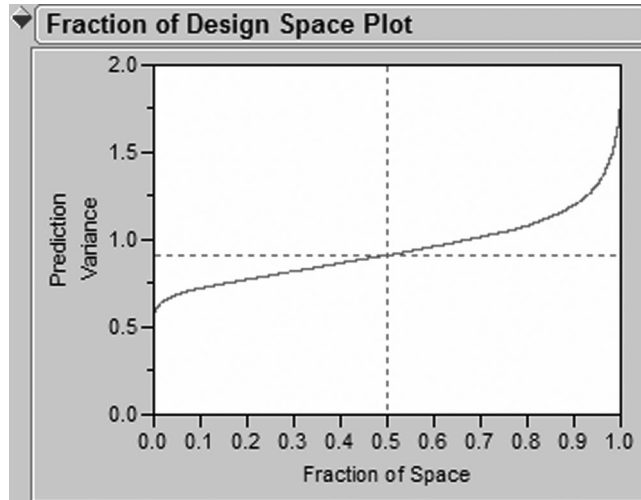


**Figure 9.14** The fraction of design space plot for the adhesive strength example.

are a popular choice for this setting, since many of their desirable properties continue to exist. Much depends on the experiment constraints as in the split-plot there are many aspects to consider.

**Optimality** As with completely randomized designs, computer generated designs are available to optimize based on various criteria. If interest lies primarily in estimating the model parameters, then the  $D$ -optimal criterion described in Section 8.2 can be adapted to the split-plot setting. The optimal design is strictly dependent on the ratio of the two variance components,  $d = \sigma_{WP}^2/\sigma^2$ , although in many situations the design performance is quite robust to a wide range of values of this ratio. Typically this ratio ranges from close to zero, if there is little additional variability associated with the whole plots, to values as large as 10 or 20. Goos (2002) developed methods for generating designs for a variety of specified constraints. The total number of runs, the number of whole plots, or a combination of both can be specified for a particular experiment. The statistical software, JMP, can generate  $D$ -optimal designs for specified numbers of run and whole plots.

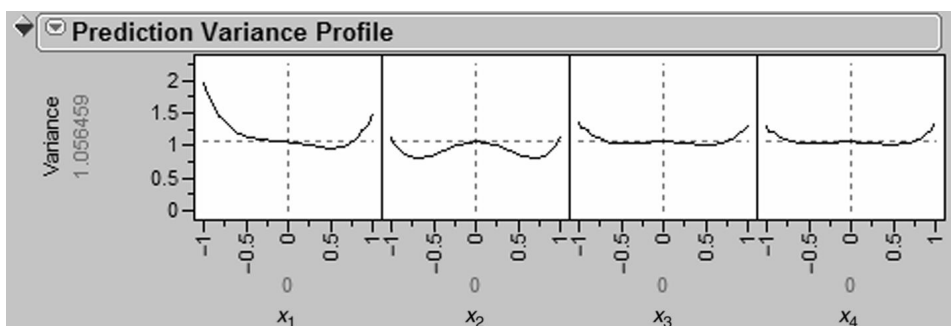


**Figure 9.15** The prediction profiler for the adhesive strength example.

**TABLE 9.17 Output from JMP for Adhesive Strength Example**

## Response Strength Summary of Fit

R-Square	0.969691
R-Square Adj	0.922543
Root Mean Square Error	4.369115
Mean of Response	44.1125
Observations (or Sum Wgts)	24

*Parameter Estimates*

Term	Estimate	Std Error	DFDen	t-Ratio	Prob >  t
Intercept	46.630773	6.134175	5.275	7.60	0.0005
A	-5.202121	2.582063	4.743	-2.01	0.1031
B	3.2464223	2.366201	4.752	1.37	0.2313
C	0.7165934	1.051328	3.605	0.68	0.5367
D	3.4042293	1.0762	3.635	3.16	0.0389
A*A	2.7031269	5.595789	6.018	0.48	0.6461
A*B	3.125	2.637179	4.708	1.18	0.2924
B*B	-1.594711	6.387644	5.214	-0.25	0.8124
A*C	-0.180581	1.089195	3.464	-0.17	0.8775
B*C	0.6198131	1.081642	3.473	0.57	0.6017
C*C	-0.881511	3.294511	3.627	-0.27	0.8035
A*D	1.0819185	1.089195	3.464	0.99	0.3848
B*D	8.4263892	1.085298	3.504	7.76	0.0025
C*D	3.4088539	2.70862	7.694	1.26	0.2450
D*D	-2.134799	3.192447	3.597	-0.67	0.5441

*REML Variance Component Estimates*

Random Effect	Var Ratio	Var Component	Std Error	95% Lower	95% Upper	Pct of Total
Whole Plots	2.4146228	46.093136	37.686598	-27.7726	119.95887	70.714
Residual		19.089166	14.600518	6.451241	205.70398	29.286
Total		65.182302				100.000
-2 LogLikelihood	= 96.742353034					

If the primary goal of the experiment is to obtain good prediction throughout the design space, then *G*- and *I*-optimality can be considered. *G*-optimality minimizes the worst prediction in the design space, while *I*-optimality minimizes the average prediction. While both criteria are possible, recent work has focused more on *I*-optimality since it focuses on the central tendency of prediction variance, rather than just its extreme. As with *D*-optimal designs, the choice of an *I*-optimal design is related to the choice of  $\sigma_{WP}^2/\sigma^2$ , but generally quite robust over a range of values. The statistical software, JMP, can also generate *I*-optimal designs for specified numbers of run and whole plots.

Using either *D*-optimality or *I*-optimality, it is possible to generate flexible designs that meet the needs of particular experimental design situations. Alternately, it is possible to adapt the levels of a central composite design to optimize it for a split-plot design. For the restricted design of Table 9.12, different values of the factorial portion of the design are appropriate for the hard-to-change and easy-to-change factors to optimize design performance based on *D*-, *G*-, or *I*-optimality. The choice of which values should be selected is dependent on the criteria considered as well as the ratio of the two variance components. For more details on this approach, see Liang et al. (2006b).

**Balance** If changing the hard-to-change factors settings is cost- or time-intensive relative to the easy-to-change factors settings, it may be sensible to run as many subplot runs per whole plot as possible. This will allow for maximum use to be made of each reset of the hard-to-change factors. For example, in the polyamide resin example (Example 7.5), consider the scenario where the temperature at the time of addition required considerable time to reset since this temperature was required to stabilize before experimental units could be run. The other two factors, agitation and rate of addition, could be quickly and easily reset. In this case, it may be sensible to consider a balanced split-plot design. A **balanced** split-plot design is one that has equal number of subplot runs for each whole plot.

The restricted central composite design of Table 9.14 and the restricted Box–Behnken design of Table 9.15 are extreme examples of unbalanced split-plot designs, since several of the whole plots have just a single run. Vining et al. (2005) and Parker et al. (2007) give several examples of balanced adaptations of central composite and Box–Behnken designs for different numbers of hard-to-change and easy-to-change factors.

**Cost** The total cost of a split-plot experiment is a function of whole plot costs as well as subplot costs. Bisgaard (2000) and Liang et al. (2007) formulate the cost of a split-plot experiment as

$$C = C_{WP}a + C_{SP}N$$

where  $C$  denotes the total cost of the experiment,  $a$  denotes the number of whole plot units,  $N$  is the total number of observations.  $C_{WP}$  and  $C_{SP}$  are the costs associated with the individual whole plots and subplots, respectively. Note that the cost incurred for measuring the response for each observation is considered a part of subplot costs.

In practice, it may be difficult to estimate the exact costs associated with whole plots or subplots (i.e., precise values for  $C_{WP}$  and  $C_{SP}$ ). It may be more feasible to specify the relative cost of these quantities (i.e.,  $r = C_{SP}/C_{WP}$ ). Hence, the cost of the experiment is

proportional to  $a + rN$  with

$$C \propto a + rN.$$

Typically we might expect  $C_{WP}$  to be greater than  $C_{SP}$  since this involves the hard-to-change factors where more time/effort is required to change levels of the whole plot factors. As  $C_{WP}$  increases relative to  $C_{SP}$ ,  $r$  approaches zero. On the other hand, if obtaining the measurement of the response for each observation is expensive, then  $C_{SP}$  may become larger compared to  $C_{WP}$  and  $r$  will increase.

The  $D$ -,  $G$ -, and  $I$ -optimality criteria from Chapter 7 can be adapted for the split-plot setting using this cost structure. For  $D$ -optimality, the moment matrix for split-plot designs is  $(\mathbf{X}'\sum^{-1}\mathbf{X})$ . We can define the cost-adjusted moment matrix for split-plot designs as

$$M = \frac{(\sigma_{WP}^2 + \sigma^2)(\mathbf{X}'\sum^{-1}\mathbf{X})}{C}.$$

For  $G$ - and  $I$ -optimality, cost-adjusted prediction variance (CPV) is defined as

$$\text{CPV} = \frac{C \text{Var}(\hat{y}(x_0))}{\sigma_{WP}^2 + \sigma^2}.$$

It is noteworthy that we can think of the completely randomized design as a special case of a split-plot design where each observation can be treated as a separate whole plot (in this case,  $a = N$ ). In CRDs the number of whole plots and subplots are equal and the total cost of the experiment is given by

$$C = (C_{WP} + C_{SP})N = C_{WP}(1 + r)N.$$

This expression is proportional then to the standard penalty of  $N$  commonly used for the  $D$ -,  $G$ -, and  $I$ -optimality criteria in completely randomized design. Parker et al. (2008) give a detailed comparison of several designs and the trade-offs between different criteria for a variety of cost and variance component ratios.

**Equivalent Estimation** Split-plot designs can also be constructed such that ordinary least squares (OLS) is equivalent to generalized least squares (GLS) for estimation. Initially this may seem like an unintuitive goal for constructing a design, since the correct analysis approach based on the model is GLS. However, the benefits of this class of design are substantial.

- Design performance is independent of the variance components. As a result, no estimate of the ratio of  $\sigma_{WP}^2/\sigma^2$  is required when selecting a design.
- Model parameter estimates are independent of the variance component estimates. Using REML, the model parameter estimates are typically dependent on the variance

components, which may not be well estimated if few degrees of freedom are available for their estimation.

- The designs can be constructed so the equivalence property holds for any model nested in the complete second-order model. When the data are collected and the model parameters estimated, some terms of the model may not be significant and we wish to reduce the model. In this case, the estimates of the new reduced model can still be estimated using OLS.
- The model parameter estimates are the best linear unbiased estimate (BLUE), and this property is robust to the assumption of normality of the error terms.

For more discussion on the advantages of equivalent estimation designs see Parker et al. (2007).

Several construction techniques exist for creating these designs based on the type of response surface design that is used for the starting point, restrictions on numbers of whole plots, size of whole plots and the ability to select different axial values. Table 9.18 shows an adapted balanced Central Composite design for two hard-to-change and two easy-to-change factors with twelve whole plots and four runs per whole plot. It uses the Vining et al. (2005) (VKM) approach which allows for flexible axial values for both the whole and subplot factors. Table 9.19 shows an adapted Box–Behnken design with the same number and type of factors with the minimum number of allowable whole plots. This design uses the minimum whole plot (MWP) method which allows for subplot center runs to be added to achieve the required conditions for equivalence. Parker et al. (2006, 2007) provide examples and details on the construction for a large number of cases.

The replication of subplot combinations within whole plots reflects the assumption that the cost of setting the hard-to-change factors dominates the cost of setting the easy-to-change factors. It has the added benefit that there are many degrees of freedom available for a pure error estimate of the subplot error,  $\sigma^2$ .

**TABLE 9.18 A Balanced Equivalent Estimation Central Composite Design Using the VKM Construction Method for Two Hard-to-Change and Two Easy-to-Change Factors With Ten Whole Plots and Four Runs Per Whole Plot**

Whole Plot #	$z_1$	$z_2$	$x_1$	$x_2$	# Runs
1	−1	−1	±1	±1	4
2	−1	+1	±1	±1	4
3	+1	−1	±1	±1	4
4	+1	+1	±1	±1	4
5	− $\beta$	0	0	0	4
6	+ $\beta$	0	0	0	4
7	0	− $\beta$	0	0	4
8	0	+ $\beta$	0	0	4
9	0	0	$\pm\alpha$	0	4
			0	$\pm\alpha$	
10	0	0	0	0	4

**TABLE 9.19 A Balanced Equivalent Estimation Box–Behnken Design Using the MWP Construction Method for Two Hard-to-Change and Two Easy-to-Change Factors with Nine Whole Plots and Five Runs Per Whole Plot**

Whole Plot #	$z_1$	$z_2$	$x_1$	$x_2$	# Runs
1	-1	-1	0	0	5
2	-1	+1	0	0	5
3	+1	-1	0	0	5
4	+1	+1	0	0	5
5	-1	0	$\pm 1$	0	5
			0	$\pm 1$	
			0	0	
6	+1	0	$\pm 1$	0	5
			0	$\pm 1$	
			0	0	
7	0	-1	$\pm 1$	0	5
			0	$\pm 1$	
			0	0	
8	0	+1	$\pm 1$	0	5
			0	$\pm 1$	
			0	0	
9	0	0	$\pm 1$	$\pm 1$	5
			0	0	

## EXERCISES

- 9.1** Consider the two simple designs discussed in Section 9.1 namely, the following two-point designs for fitting a first-order model:
- (i)  $N/2$  runs at  $x = -1$ ;  $N/2$  runs at  $x = +1$
  - (ii)  $N/2$  runs at  $x = -0.6$ ;  $N/2$  runs at  $x = +0.6$

The region of interest  $[-1, +1]$  in the design variable  $x$ .

- (a) Suppose the first-order model is correct. Compute

$$\frac{N}{2\sigma^2} \int_{-1}^1 \text{Var}[\hat{y}(\mathbf{x})]dx$$

for both designs.

- (b) Suppose the true model is

$$y = \beta_0 + \beta_1 x + \beta_2 x^2$$

with  $\sqrt{N}\beta_2/\sigma = 2.0$ . Compute  $(N/2\sigma^2) \int_{-1}^1 \{\text{Var}[\hat{y}(\mathbf{x})] + [\text{Bias } \hat{y}(\mathbf{x})]^2\}dx$  for both designs.

- 9.2** Consider a fitted first-order model in four design variables:

$$\hat{y} = b_0 + b_1x_1 + b_2x_2 + b_3x_3 + b_4x_4$$

Suppose the region of interest in the natural variables is given by the following ranges:

- $\xi_1$ : [100, 150]
- $\xi_1$ : [1, 2]
- $\xi_1$ : [1000, 2000]
- $\xi_1$ : [0, 1]

The region is cuboidal. Suppose that the experimenter is interested in protecting against a complete second-order model. A total of 10 runs are to be used.

- (a) Give a minimum bias design in the natural variables.
  - (b) Suppose, instead of using the minimum variance design, the analyst achieves protection against model mis-specification by using a scaled second moment of 0.45. Again, two center runs are used in addition to the eight factorial points. Give the appropriate design in the natural variables.
- 9.3** Consider Exercise 9.2. Suppose that a first-order model is fitted, but the practitioner is interested in protection against the model

$$E(y) = \beta_0 + \sum_{i=1}^4 \beta_i x_i + \sum_{i < j=2}^4 \beta_{ij} x_i x_j$$

In other words, there is no fear of pure quadratic effects in this design region; the protection is sought against *interaction terms only*. Consider the use of Equation 9.18 for the determination of a minimum bias design.

- (a) What are the moment requirements for the minimum bias design in this case?
  - (b) Give a minimum bias design with 10 runs for this case (coded levels).
  - (c) Give the same design in the natural variables.
- 9.4** Refer to Exercise 9.3. With the suggested alternative model, is there any restriction on the second pure design moment for achieving a minimum bias design? Explain.
- 9.5** Consider the following general formulation: If the fitted model is first order, and one is interested in protection against a model that contains first-order terms plus two-factor interactions, the minimum bias design is one in which all odd moments through order three are zero. This means that the two-level design for minimum bias must have resolution at least IV. Prove that this statement is correct.
- 9.6** Prove the following statement: If the fitted model is first-order in  $k$  variables and one is interested in protecting against a model containing linear terms and two-factor interactions, a minimum mean squared error design is a two-level resolution  $\geq$ IV design with pure second moments ( $ii$ ) as large as possible. As a result, the levels are to be placed at  $\pm 1$  extremes.

- 9.7** Reconsider Example 9.2. Show that

$$\text{ASB}_{\text{LS}} = \frac{3\beta_2^2}{\sigma^2} \left( \frac{4l^4}{9} - \frac{4l^2}{9} + \frac{1}{5} \right)$$

and that

$$\text{APV}_{\text{LS}} = 1 + \frac{1}{2l^2}$$

What value of  $l$  results in minimum  $\text{APV}_{\text{LS}}$ ? What is the value of  $\text{ASB}_{\text{LS}}$  at this point? Does this design make sense if you worried about protecting against the quadratic model?

- 9.8** Reconsider Example 9.2. Draw a graph of:

- (a) ASB and  $\text{ASB}_{\text{LS}}$  versus  $l$  in the range  $0 \leq l \leq 1$ .
- (b) APV and  $\text{APV}_{\text{LS}}$  versus  $l$  in the range  $0 \leq l \leq 1$ .
- (c) AMSE and  $\text{AMSE}_{\text{LS}}$  versus  $l$  in the range  $0 \leq l \leq 1$ .

Discuss the graphs you have drawn and the potential utility of minimum bias estimation if you are concerned about fitting the wrong model.

- 9.9** Consider the same situation described in Example 9.2; now, however, suppose that you wish to use a design with one run at  $\pm l_1$ , and  $\pm l_2$ , with  $l_1 < l_2$ , so that  $N = 4$ .

- (a) Find the minimum bias estimator.
- (b) Find ASB for the minimum bias estimator. Note that this will not be a function of  $l_1$  and  $l_2$ .
- (c) Find APV for the minimum bias estimator as a function of  $l_1$  and  $l_2$ . Prepare a graph that shows how APV changes as  $l_1$  and  $l_2$  change.
- (d) Suppose an experimenter uses the method of least squares with  $l_1 = \pm 0.5$  and  $l_2 = \pm 1$ . Find  $\text{APV}_{\text{LS}}$  and  $\text{PSB}_{\text{LS}}$  for this design. Can you find a design that performs better if you use minimum bias estimation?

- 9.10** Consider the case of Poisson response with a log link. Show that  $\sum_{i=1}^N (y_i - \hat{\mu}_i) = 0$ .

- 9.11** Table 9.10 shows data from an experiment used to study the advance rate of a drill.

- (a) Verify that the model coefficient estimates are as given in Example 9.6. Use a gamma response with a log link.
- (b) What are the standard errors of the model parameters?
- (c) Find a 95% confidence interval on the mean response at each of the 16 design points. **Hint:** SAS PROC GENMOD will produce these confidence intervals.

- 9.12** Analyze the drill experiment in Example 9.5 by ordinary least squares, following a log transformation on the response.

- (a) Does the prediction equation look similar to the one found using the GLM?

- (b) Construct contour plots for the least squares model and the GLM model, with  $x_4 = +1$  and  $x_4 = -1$ . Compare the plots.
- (c) Find a 95% confidence interval on the mean response at each of the 16 design points. Express the interval in terms of the original response.
- (d) Compare the lengths of the confidence intervals from (c) with the lengths of the intervals in Exercise 9.11(c). Which modeling approach would you prefer if response prediction was the objective of the experimenter?
- 9.13** Consider the windshield slugging experiment in Example 9.6. Fit the GLM using a binomial response and the logit link. Verify that the correct model includes the factors  $x_1$ ,  $x_3$ ,  $x_4$ ,  $x_1x_2$ , and  $x_2x_3$ .
- 9.14** The experiment shown in the table below is a  $2^{7-4}$  fractional factorial conducted to study the effect of the seven factors on nonconforming tiles. The response variable is the percentage (out of 1000, say) of tiles that are nonconforming. Analyze this experiment, assuming the binomial distribution and the logit link.

Run	$x_1$	$x_2$	$x_3$	$x_4$	$x_5$	$x_6$	$x_7$	% Nonconforming (Original Data)
1	+	+	+	+	+	+	+	0.16
2	+	+	+	-	-	-	-	0.17
3	+	-	-	+	+	-	-	0.12
4	+	-	-	-	-	+	+	0.06
5	-	+	-	+	-	+	-	0.06
6	-	+	-	-	+	-	+	0.68
7	-	-	+	+	-	-	+	0.42
8	-	-	+	-	+	+	-	0.26

- 9.15** Example 2.12 presented the worsted yarn experiment, a  $3^3$  factorial design in which the response variable was the number of cycles to failure of the yarn. A least squares model was fitted to the data after a log transformation.
- (a) Find a GLM for the data, assuming a gamma distribution and the log link.
- (b) Compare the form of this model with the one obtained in Example 2.12. Are they very similar?
- (c) Construct 95% confidence intervals on the mean response at each of the 27 design points. (**Hint:** Use PROC GENMOD to do this for the GLM.) Compare the lengths of the confidence intervals for the two modeling approaches. Based on this comparison, which model would you prefer?
- 9.16** Reconsider the situation described in Exercise 9.15. Use the reciprocal link function, and repeat parts (a) and (b). How does the reciprocal link work in this experiment?
- 9.17** Lewis, Montgomery, and Myers (2001a) present an experiment in a semiconductor manufacturing process involving a CCD where the response variable is the observed number of defects. The data are shown in the following table.

	$x_1$	$x_2$	$x_3$	Number of Defects, $y$	$\sqrt{y}$
1	-1	-1	-1	1	1.000
2	1	-1	-1	15	3.873
3	-1	1	-1	24	4.899
4	1	1	-1	35	5.916
5	-1	-1	1	0	0.000
6	1	-1	1	13	3.606
7	-1	1	1	16	4.000
8	1	1	1	13	3.606
9	-1.732	0	0	1	1.000
10	1.732	0	0	17	4.123
11	0	-1.732	0	7	2.646
12	0	1.732	0	43	6.557
13	0	0	-1.732	14	3.742
14	0	0	1.732	3	1.732
15	0	0	0	4	2.000
16	0	0	0	7	2.646
17	0	0	0	8	2.828
18	0	0	0	6	2.450

- (a) Fit a second-order model to the square root of the number of defects. Construct contour plots of the predicted response. The objective is to find a set of operating conditions that minimize the number of defects.
- (b) How well does the least squares model perform as a predictor in the region of interest?
- (c) Repeat part (a) using a Poisson response and the log link.
- (d) Is the GLM in part (c) a better model? Explain.
- 9.18** Repeat Exercise 9.17 using the square root link.
- 9.19** Reconsider the GLM from the windshield slugging experiment in Example 9.7. Obtain the deviance residuals for the model. Construct a normal probability plot of these residuals. Comment on your findings.
- 9.20** Reconsider the GLM for the worsted yarn experiment in Exercise 9.15. Obtain the deviance residuals for the model. Construct a normal probability plot of these residuals. Is there any indication of model inadequacy?
- 9.21** Reconsider the GLM for the defects experiment in Exercise 9.17. Obtain the deviance residuals for the model. Construct a normal probability plot of the residuals, and comment on the model's adequacy.
- 9.22** Consider the experiment described in Exercise 4.7. Suppose that this experiment had been conducted as a split plot, with factor  $A$  the whole plot variable. Analyze the data, and draw appropriate conclusions.
- 9.23** Consider the experiment described in Example 4.2. Suppose that this experiment had been conducted as a split plot, with factor  $B$  the whole plot variable. Analyze the data, and draw appropriate conclusions.

- 9.24** Consider the experiment described in Example 7.5. Suppose that this experiment had been conducted as a split plot, with temperature as the whole plot variable. Analyze the data, and draw appropriate conclusions.
- 9.25** Suppose that you plan to fit a second-order model in three factors. Factor  $A$  is hard to change, but factors  $B$  and  $C$  are easy to change. Suggest an appropriate experimental design for this problem, if the experimenter wants to minimize the total number of runs.
- 9.26** An experimenter wants to fit a second-order model in five factors; factors  $A$  and  $B$  are hard to change, and the other three factors are easy to change.
- (a) Find a design with the minimum number of runs ( $N = 21$ ).
  - (b) Find a design with  $N = 32$  runs.
  - (c) Compare these two designs.
- 9.27** Reconsider the adhesive strength experiment in Example 9.7. What is the minimum number of runs that could be used to investigate the four factors in this problem? Find the design and compare it to the one actually used in Example 9.7.
- 9.28** Construct a fraction of design space plot for the equivalent estimation design in Table 9.16 using  $\alpha = \beta = 2$ . How does the prediction variance change if the values of these two parameters change to  $\alpha = \beta = 1.5$ ?



---

# 10

---

## ROBUST PARAMETER DESIGN AND PROCESS ROBUSTNESS STUDIES

### 10.1 INTRODUCTION

In the 1980s, Genichi Taguchi [Taguchi and Wu (1980), Taguchi (1986, 1987)] introduced new ideas on quality improvement in the United States. He proposed an approach he called **parameter design** for reducing variation in products and processes. His methods and philosophy generated considerable interest among quality engineers and statisticians. During the 1980s his methodology gained usage at AT&T Bell Laboratories, Ford Motor Company, Xerox, and many other prominent organizations. These techniques generated much debate and controversy in the statistical community—not about Taguchi's philosophy, but rather about its implementation and the technical nature of data analysis. As a result, a response surface approach evolved and has become a collection of tools that allow one to adopt Taguchi's robust design concept while providing a more statistically sound and efficient approach to analysis. This RSM approach to parameter design is the subject of this chapter.

### 10.2 WHAT IS PARAMETER DESIGN?

Parameter design, or **robust parameter design** (RPD), is essentially a principle that emphasizes proper choice of levels of controllable factors (**parameters** in Taguchi's terminology) in a system. The system can be a process or a product. The principle of choice of levels focuses to a great extent on variability around a prechosen target for the output response. These controllable factors are called **control factors**. It is assumed that the majority of variability around target is caused by the presence of a second set of factors called noise factors or **noise variables**. Noise factors are **uncontrollable** in the design of

the product or in the normal operation of the process. In fact, it is this lack of control that transmits variability to the process response. As a result, the term **robust parameter design** entails designing (not in the sense of experimental design) the system (selecting the levels of the controllable variables) so as to achieve **robustness** (insensitively) to inevitable changes in the noise variables. Often an RPD study in a manufacturing process is called a **process robustness study**.

A significant difference between Taguchi's view of process optimization and the traditional viewpoint centers around the notion of *reducing process variability* by involving factors that cause process variability in the experimental design, modeling, and optimization exercise. These factors, the noise factors, are often functions of environmental conditions—for example, humidity, properties of raw materials, and product aging. In certain applications they may involve the way the consumer handles or uses the product. Noise variables may be, and often are, controlled at the research or development level, but of course they cannot be controlled at the production or product use level.

### 10.2.1 Examples of Noise Variables

It should not be inferred that Taguchi discovered the notion of noise variables. Prior to Taguchi, researchers certainly were aware that certain uncontrollable factors provide major sources of variability. However, Taguchi encouraged the formal use of noise variables in the experimental design and, as a result, allowed the subject of the analysis to involve process variability. Table 10.1 presents some examples of noise variables and control variables in several scenarios.

Table 10.1 gives only a few examples where the noise variables involved clearly cannot be controlled in the process, but could be controlled in an experimental

**TABLE 10.1 Some Examples of Control Variables and Noise Variables**

Application	Control Variables	Noise Variables
Development of a cake mix	Amount of sugar, flour, and other dry ingredients	Oven temperature, baking time, amount of milk added
Development of a gasoline	Ingredients in the blend; other processing conditions	Type of driver, driving conditions, engine type
Development of a tobacco product	Ingredient types and concentrations; other processing conditions	Moisture conditions; storage conditions on tobacco
Large-scale chemical process	Processing conditions, including nominal ambient temperature	Deviations from nominal ambient temperature; deviations from other processing conditions
Production of a box-filling machine for filling boxes of detergent	Surface area; geometry of the machine (rectangular, circular)	Particle size of detergent
Manufacturing a dry detergent	Chemical formulation, processing variables	Temperature and relative humidity during manufacture

situation—that is, in a designed experiment. One important point should be made about the “large-scale chemical process” example. Many times the most important noise variables are tolerances in the control variables. In the chemical and some other industries, so-called controllable variables are not controlled at all. In fact, if there is a nominal temperature of, say, 250°F during the large-scale production process, the temperature may vary between 235 and 265°F, and the inability to control the process temperature produces unwanted variability in the product. As a result, nominal temperature (or nominal pressure) becomes a control variable, and the tolerance on temperature at levels  $\pm 15^{\circ}\text{F}$  (say) is a noise variable.

### 10.2.2 An Example of Robust Product Design

Consider a situation in which one is interested in establishing the geometry and surface area of a box-filling machine that achieves a rate of filling that is “closest” to 14 g/sec. We will call surface area *factor A* (two levels) and geometry *factor B* (two levels). The single noise variable is the particle size of the detergent product. Three levels of the noise variable were used. The data are as follows:

Particle Size 1			Particle Size 2			Particle Size 3		
			<i>B</i>					
<i>A</i>	<i>B</i>		<i>A</i>	<i>B</i>		<i>A</i>	<i>B</i>	
–1	13.7	13.7	–1	14.9	14.2	–1	17.4	14.4
+1	14.0	11.9	+1	16.0	11.8	+1	12.0	11.7

Clearly the product that is most insensitive to the noise factor, particle size, is given by (+1, +1). The sample standard deviation of fill rate is  $s = 0.1\text{ g/sec}$ . However, the mean filling rate across particle size is 11.8, and the target is 14.0. On the other hand, the product (+1, –1) results in an average of 14.0, but the variability around the target is relatively large ( $s = 2.0$ ) and thus the product is *not a robust product*. Consider the product (–1, +1). The average filling rate is 14.1, and the variability around the target is quite small ( $s = 0.36$ ). Thus, the optimum design among the four is (–1, +1). It produces the best combination of bias error and variance error.

Strictly speaking, the most robust parameter design is the one that is insensitive to changes in the noise variables. The implication of this definition is that the robust product minimizes variance transmitted by the noise variables. However, one cannot ignore the process mean. In this illustration one might consider the squared error loss criterion; that is, choose the product that minimizes

$$L = \sum (y - 14)^2$$

where the summation is taken over the levels of the particle size. In later sections where we deal with the response surface approach to robust parameter design and process robustness studies, the process mean and variance will be considered simultaneously.

### 10.3 THE TAGUCHI APPROACH

#### 10.3.1 Crossed Array Designs and Signal-to-Noise Ratios

Taguchi's methodology for the RPD problem revolves around the use of orthogonal designs where an **orthogonal array** involving control variables is crossed with an orthogonal array for the noise variables. For example, in a  $2^2 \times 2^2$ , the  $2^2$  for the control variables is called the **inner array** and the  $2^2$  for the noise variables is called the **outer array**. The result is a 16-run design called the **crossed array**. Figure 10.1 gives a graphical representation.

The corners of the inner array are represented by  $(-1, -1)$ ,  $(-1, +1)$ ,  $(+1, -1)$ , and  $(+1, +1)$  for the control variables. Each outer array is a  $2^2$  factorial in the noise variables. The dots in the outer arrays represent the locations of observations. Figure 10.2 shows another crossed array with 32 observations. The design is a  $2^{4-1}$  as the inner array, crossed with a  $2^{3-1}$  as the outer array.

Taguchi suggested that one may summarize the observations in each outer array with a summary statistic that provides information about the mean and variance. For example, in Figs 10.1 and 10.2, the summary statistic is computed across four observations. Thus, in Fig. 10.2 there will be eight summary statistics. The summary statistic is called a **signal-to-noise ratio** (SNR), and the statistical analysis is done using the SNR as the response variable. There are many different SNRs. However, there are four primary ones suggested by Taguchi. The choice depends on the goal of the experiment. As in the case of response surface work, there are three specific goals:

1. *The smaller the better.* The experimenter wishes to minimize the response.
2. *The larger the better.* The experimenter wishes to maximize the response.
3. *The target is best.* The experimenter wishes to achieve a particular target value.

**The Smaller the Better** Taguchi treats the smaller-the-better case as if there were a target value of zero for the response. Thus, the quadratic- loss function  $E_z(y - 0)^2$  leads to the performance criterion

$$\text{SNR}_s = -10 \log \sum_{i=1}^n \frac{y_i^2}{n} \quad (10.1)$$

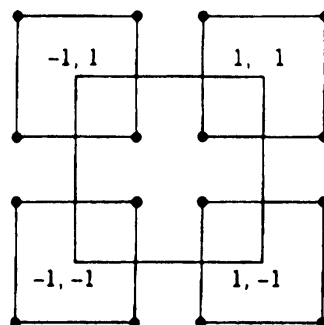


Figure 10.1 The  $2^2 \times 2^2$  crossed array.

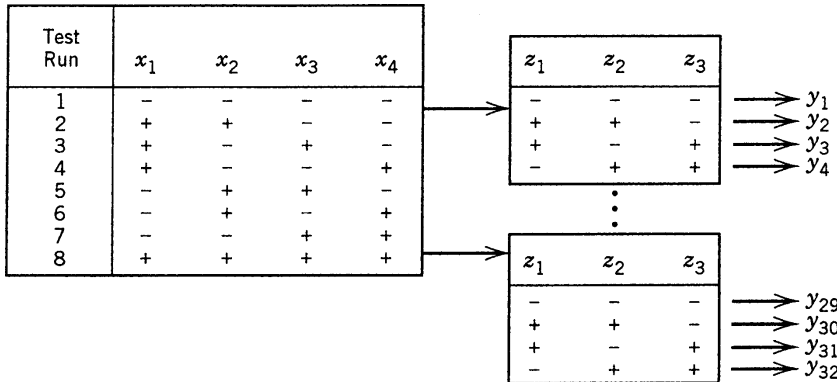


Figure 10.2 The  $2^{4-1} \times 2^{3-1}$  crossed array.

The rationale comes from the need to find  $\mathbf{x}$ , whose elements are the levels of the control variables that minimize the expected squared error  $E_z y^2$ , where  $E_z$  implies expectation across the distribution of the noise variables  $\mathbf{z}$ . In the SNR calculation,  $\sum_{i=1}^n$  implies summation over  $n$  response values at the outer array points. Thus, an SNR value will be present at each inner array design point. Because the  $-10 \log$  transformation is used, one seeks to maximize SNRs.

**The Larger the Better** This case is treated in the same fashion as the smaller-the-better case, but  $y_i$  in Equation 10.1 is replaced by  $1/y_i$ . Thus, the SNR is motivated by the squared error criterion  $E_z(1/y)^2$ . As a result, the SNR is given by

$$\text{SNR}_l = -10 \log \sum_{i=1}^n \frac{1/y_i^2}{n} \quad (10.2)$$

Again, values of the control variables are sought that maximize SNR.

**The Target is Best** In this case, we are attempting to determine values of  $\mathbf{x}$  that achieve a target value for the response, namely  $y = t$ . Deviations in either direction are undesirable. Two different SNRs are considered. The appropriate one depends on the nature of the system. If the response mean and variance can be altered independently, Taguchi suggests that one or more **tuning factors** be used to eliminate bias—that is, provide an adjustment that results in  $E_z(y) = t$ . These tuning factors allow the analyst to alter the mean but leave the variance unchanged. As a result, the analysis is a two-step process: Select the tuning factors that render  $y = t$ , and then select levels of other control factors that maximize an SNR. Assuming that this can be accomplished, the obvious squared error loss function,  $E_z(y - t)^2$ , reduces to  $\text{Var}(y)$ . Thus, the SNR used by Taguchi is given by

$$\text{SNR}_{T_1} = -10 \log s^2 \quad (10.3)$$

where  $s^2 = \sum_{i=1}^n (y_i - \bar{y})^2 / (n - 1)$ . Thus,  $s^2$  is the sample variance over the outer array design points. Again, values of  $\mathbf{x}$  are chosen so that SNR is maximized.

A SNR is suggested by Taguchi for cases in which the response standard deviation is related to the mean. It nicely accommodates situations in which the relationship is linear. In this case adjustment or tuning factors are sought that, again, eliminate bias but leave the coefficient of variation  $\sigma_y/\mu_y$  relatively unaffected. As a result, the natural SNR involves the sample coefficient of variation  $s/\bar{y}$ . In fact, Taguchi's SNR for this case is given by

$$\text{SNR}_{T_2} = -10 \log \left( \frac{\bar{y}^2}{s^2} \right) \quad (10.4)$$

where the SNR is to be maximized. So, again, the two-step procedure is used. Values of the tuning factor (or factors) are chosen that render  $y = t$ . These tuning factors have an effect on the mean response but little or none on the SNR.

**What Is the Utility of the SNR?** The purpose of the SNR in Taguchi's approach to robust parameter design is to provide an easy-to-use performance criterion that takes the process mean and variance into account. The terminology itself is open to criticism. Of the four major SNR formulations, only the one in Equation 10.4 involves a true signal-to-noise ratio (because it is the only one that is dimensionless). There is a wealth of literature in which SNRs are criticized. See, for example, Box (1988) and Welch et al. (1990). A panel discussion, edited by Nair (1992), provides opinions by several researchers regarding the use of SNR. We would like to focus on one interesting characteristic of the SNRs here. While the intention is to use them as performance characteristics that take both response mean and variance into account, many authors have suggested the use of *separate models* for the process mean and variance as a way of achieving better understanding of the process itself. More details will be provided on this approach in a later section.

The use of a SNR does not guarantee that the subject matter scientist will secure valuable information regarding the roles of the process mean and process variance. This **uncoupling** of those control factors that affect mean (location effects) and control factors that affect variance (dispersion effects) is very important in the understanding of the process. For example, the SNR in Equation 10.4 can be written

$$\text{SNR}_{T_2} = -10 \log \bar{y}^2 + 10 \log s^2$$

So, of course, the maximization of this SNR does not distinguish which control factors are location effects and which are dispersion effects. As another example, consider  $\text{SNR}_s$  in Equation 10.1

$$\text{SNR}_s = -10 \log \left( \sum y_i^2 / n \right)$$

While  $\sum y_i^2 / n$  does deal with variability around the target of zero, it is clear that an analysis using this SNR cannot separate the location effects from dispersion effects. It is easy to see that

$$\frac{\sum y_i^2}{n} = \bar{y}^2 + \left( 1 - \frac{1}{n} \right) s^2$$

so again, the mean and variance contributions in  $\text{SNR}_s$  are confounded.

Because the SNRs generally confound location and dispersion, they are not necessarily unique. That is, there can be many different samples of data that will result in exactly the same value of the SNR. Thus, it is not necessarily clear how one should interpret a particular value of a SNR.

**Crossed Array Designs** A final point should be made about crossed array designs. When they were executed it seems that many of these designs were actually run as split plots. That is, a run (or treatment combination) in the inner array was fixed, and all outer array runs were conducted at that setting of the control factors. Another possibility is to fix the settings of the noise variables at a particular run in the outer array and then conduct all runs in the inner array at that configuration of the noise variables. Either approach will produce a split-plot structure. The latter approach is generally preferable, because the control factors and their interactions with the noise factors would be more precisely estimated as they reside in the subplot. For more discussion, see Box and Jones (1992, 2000). No split-plot structure is considered in Taguchi's analysis, which we now describe.

### 10.3.2 Analysis Methods

Taguchi's notion of quality improvement places emphasis on variance reduction. His approach to variance reduction is widely acknowledged as a very important contribution to statistics and engineering. While others had suggested the use of noise variables before Taguchi, his idea of linking their use to variance reduction is original and has had a profound impact. Details of his analysis ideas can be found in Taguchi (1987).

To understand the rationale behind the Taguchi analysis, one must be reminded that the purpose of parameter design is to find the settings on the control variables that produce a robust product or process. The control variables may be quantitative or qualitative. As a result, the Taguchi analysis reduces to process optimization when the performance criterion is the SNR.

The analysis method is simple and is very much linked to the crossed array concept. There is an attempt to **maximize** the SNR. The modeling that is done essentially relates the SNR to the control variables in a main-effects-only scenario. Taguchi rarely considers interactions among the control variables. In fact, many of the designs advocated by Taguchi do not allow estimation of these interactions. Standard ANOVA techniques are used to identify the control factors that affect the SNR. In addition, ANOVA is done on the average response  $\bar{y}$  in order to ascertain possible adjustment factors. The latter are set to levels that bring the mean to target (in the target-is-best case), while the factors that affect the SNR are set to levels that maximize it. This completes the two-step process where it is appropriate. The setting of levels is accomplished by a **pick-the-winner** analysis in which a marginal means approach is accomplished. To gain further insight, consider the following example.

**Example 10.1 Wave Soldering Optimization** In an experiment described by Schmidt and Launsby (1990), solder process optimization is accomplished by robust parameter design in a printed circuit board assembly plant. After the components are inserted into a bare board, the board is put through a wave solder machine, which mechanically and electrically connects all the components into the circuit. Boards are placed on a conveyor and then put through the following steps: bathing in a flux mixture to remove oxide, preheating to minimize warpage, and soldering. An experiment is designed to determine the conditions

that give minimum numbers of solder defects per million joints. The control factors and levels are as follows:

Factor	(-1)	(+1)
A, solder pot temperature (°F)	480	510
B, conveyor speed (ft/min)	7.2	10
C, flux density	0.9	1.0
D, preheat temperature (°F)	150	200
E, wave height (in.)	0.5	0.6

In this illustration, three noise factors are difficult to control in the process. These are the solder pot temperature, the conveyor speed, and the assembly type. Often in such processes, the natural noise factors are *tolerances in the control variables*. In other words, as these factors vary off their nominal values, variability is transmitted to the response. It is known that the control of temperature is within  $\pm 5^{\circ}\text{F}$  and that the control of conveyor speed is within  $\pm 0.2 \text{ ft/min}$ . Thus, it is conceivable that variability is increased substantially because of the inability to control these two factors at nominal levels. The third noise factor is the assembly type. One of the two types of assembly will be used. Thus, the noise factors are as follows:

Factor	(+1)	(-1)
F, solder temp. (°F)	5	-5
G, conveyor speed (ft/min)	+0.2	-0.2
H, assembly type	1	2

Both the control array (inner array) and the noise array (outer array) were chosen to be fractional factorials. The inner array is a  $2^{5-2}$  design, and the outer array is a  $2^{3-1}$ . The *crossed array* and the response values are shown in Table 10.2.

TABLE 10.2 The Wave Solder Experiment

Inner Array					Outer Array					(SNR) <sub>s</sub>
A	B	C	D	E	F	-1	1	1	-1	
					G	-1	1	-1	1	
H	-1	-1	1	1	-1	-1	1	1	1	
1	1	1	-1	-1	194	197	193	275	-46.75	
1	1	-1	1	1	136	136	132	136	-42.61	
1	-1	1	-1	1	185	261	264	264	-47.81	
1	-1	-1	1	-1	47	125	127	42	-39.51	
-1	1	1	1	-1	295	216	204	293	-48.15	
-1	1	-1	-1	1	234	159	231	157	-45.97	
-1	-1	1	1	1	328	326	247	322	-45.76	
-1	-1	-1	-1	-1	186	187	105	104	-43.59	

**Analysis** The analysis in this example involves a marginal means modeling of the SNR of Equation 10.1, namely  $\text{SNR}_s$ , because it is of interest to minimize the number of solder defects. One analytical device used frequently by Taguchi is to depict a main-effects-only analysis through the graphs in Fig. 10.3. The mean  $\text{SNR}_s$  is plotted against levels of each control factor. The means are taken across levels of the other factors. In addition to the mean  $\text{SNR}_s$  plot, a plot of  $\bar{y}$  against the levels of the control variables is also made and appears in Fig. 10.4.

It is clear from Figs 10.3 and 10.4 that temperature and flux density are critical control factors that have a profound effect on  $\text{SNR}_s$  and  $\bar{y}$ . It also appears that wave height has an effect on  $\text{SNR}_s$  but little or no effect on  $\bar{y}$ . Because it is of interest to maximize  $\text{SNR}_s$  and minimize  $\bar{y}$ , the following represent suggested operating conditions:

$$\begin{aligned} \text{Solder temperature} &= 510^{\circ}\text{F} \\ \text{Flux density} &= 0.9 \\ \text{Wave height} &= 0.5 \text{ in.} \end{aligned} \quad (10.5)$$

The conveyor speed and preheat temperature can be placed at the most economical settings, presumably at low levels. The effect of wave height is marginal compared to the impact of solder temperature and flux density. The analysis suggests that the conditions given by Equation 10.5 are the most **robust conditions**, that is, in the context of this example, those conditions that are most insensitive to changes in the noise variables.

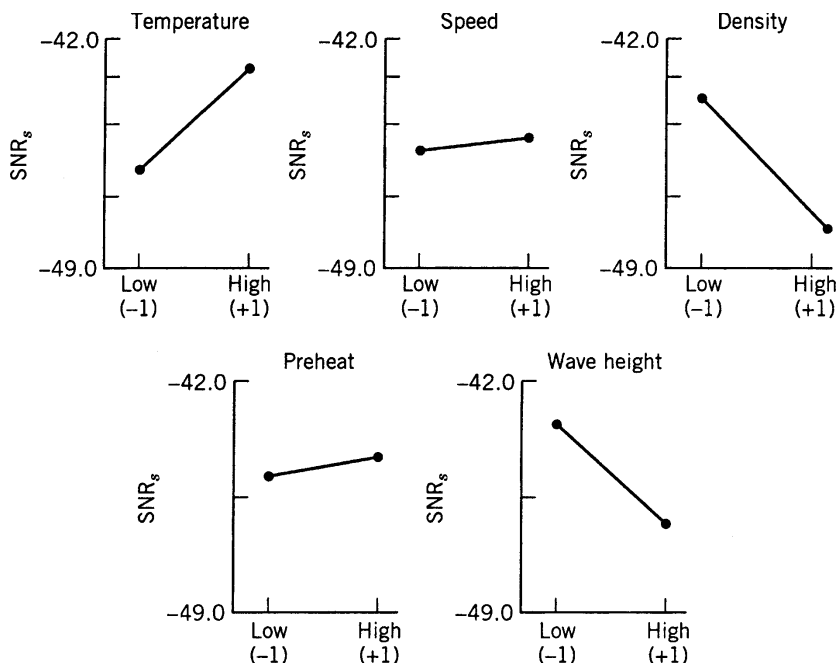
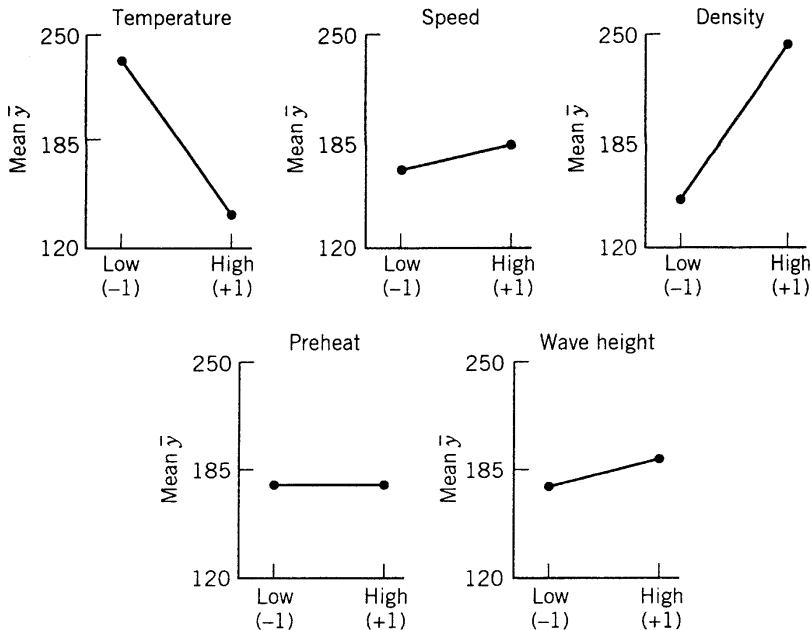


Figure 10.3 Plot of  $\text{SNR}_s$  against level for each control factor.



**Figure 10.4** A plot of  $\bar{y}$  against the levels of control factors.

**Further Comments on the Analysis** In addition to earlier concerns regarding the appropriateness of the SNR, other comments concerning the analysis are in order. The plots in Figs 10.3 and 10.4 are appropriate for selecting optimum (most robust) conditions *if one is willing to assume no interaction among the control variables*. Obviously, in many areas of application this is a safe assumption, and certainly Taguchi's success bears this out. However, there are many areas in which interactions have a very large contribution to process or product performance. This renders the plots of main effect means highly misleading. For example, in Fig. 10.3, consider the temperature plot. High positive slope reveals that across levels of the other factors an increase in temperature increases SNRs. But suppose when the density is low (which is an important level to maintain) the effect of temperature is negligible or even negative. Then, there will be little need to use high temperature when one operates with low density.

Many of the designs employed by Taguchi for inner arrays, where control factors reside, do not accommodate interactions. In addition to the apparent difficulty with SNRs, this has led to criticism of the methodology suggested by Taguchi. Many of the designs suggested by Taguchi are saturated or near-saturated Plackett–Burman designs and thus do not allow the experimenter to estimate interaction effects among the control variables.

A major component of the methodology of Taguchi's robust design is to use **confirmatory trials** at the recommended operating conditions. Indeed, this recommendation is quite appropriate for any statistical procedure in which optimum operating conditions are estimated.

**Example 10.2 The Connector Pulloff Force Experiment** An experiment was conducted in order that a method could be found to assemble an elastometric connector to a nylon tube that would deliver the required pulloff information for use in an automotive

**TABLE 10.3** Factors and Levels on the Connector Pulloff Force Experiment

	Levels		
<i>Controllable Factors</i>			
<i>A</i> = Interference	Low	Medium	High
<i>B</i> = Connector wall thickness	Thin	Medium	Thick
<i>C</i> = Insertion depth	Shallow	Medium	Deep
<i>D</i> = Percent adhesive in connector pre-dip	Low	Medium	High
<i>Uncontrollable Factors</i>			
<i>E</i> = Conditioning time	24 hr	120 hr	
<i>F</i> = Conditioning temperature	72°F	150°F	
<i>G</i> = Conditioning relative humidity	25%	75%	

engine application. The objective is to maximize the pulloff force [see Byrne and Taguchi (1987)]. Four variables were used as control variables. They are interference (*A*), connector wall thickness (*B*), insertion depth (*C*), and percent adhesive in connector pre-dip (*D*). Three factors were chosen as noise variables because they are difficult to control in the process and make a major contribution to variability in the pulloff force. They are conditioning time (*E*), conditioning temperature (*F*), and conditioning relative humidity (*G*). The levels are shown in Table 10.3.

Note that the control factors are at three levels, while the noise factors are at two levels. The experimental design and measured pulloff force are given in Table 10.4. Notice that the inner array is a  $3^{4-2}$  fractional factorial design. (Taguchi refers to this as an  $L_9$ .) The outer array in the noise variables is a  $2^3$ . The levels for the control variables are  $-1$ ,  $0$ , and  $+1$ —representing low, medium, and high, respectively. The usual  $-1$ ,  $+1$  notation is used for low and high as the noise variables. Note also that the design is a crossed array, giving a total of  $9 \times 8 = 72$  observations. The  $\text{SNR}_i$  and  $\bar{y}$  values are given. If formal modeling were to be done, then the fraction of the  $3^4$  could accommodate linear and quadratic terms in each control variable. However, *there are no degrees of freedom left for interaction among the control variables*. The analysis pursued is, once again, the marginal means plots for  $\text{SNR}_i$  and  $\bar{y}$ . Figures 10.5 and 10.6 present the marginal means plots for  $\bar{y}$  and  $\text{SNR}_i$ ,

**TABLE 10.4** Inner and Outer Array for Example 10.2

Run	Inner Array ( $L_9$ )				Outer array ( $L_8$ )								Responses	
					<i>E</i>	-1	-1	-1	-1	+1	+1	+1		
	<i>A</i>	<i>B</i>	<i>C</i>	<i>D</i>	<i>F</i>	-1	-1	+1	+1	-1	-1	+1	$\bar{y}$	$\text{SNR}_i$
1	-1	-1	-1	-1	15.6	9.5	16.9	19.9	19.6	19.6	20.0	19.1	17.525	24.025
2	-1	0	0	0	15.0	16.2	19.4	19.2	19.7	19.8	24.2	21.9	19.475	25.522
3	-1	+1	+1	+1	16.3	16.7	19.1	15.6	22.6	18.2	23.3	20.4	19.025	25.335
4	0	-1	0	+1	18.3	17.4	18.9	18.6	21.0	18.9	23.2	24.7	20.125	25.904
5	0	0	+1	1	19.7	18.6	19.4	25.1	25.6	21.4	27.5	25.3	22.825	26.908
6	0	+1	-1	0	16.2	16.3	20.0	19.8	14.7	19.6	22.5	24.7	19.225	25.326
7	+1	-1	+1	0	16.4	19.1	18.4	23.6	16.8	18.6	24.3	21.6	19.850	25.711
8	+1	0	-1	+1	14.2	15.6	15.1	16.8	17.8	19.6	23.2	24.2	18.338	24.852
9	+1	+1	0	-1	16.1	19.9	19.3	17.3	23.1	22.7	22.6	28.6	21.200	26.152

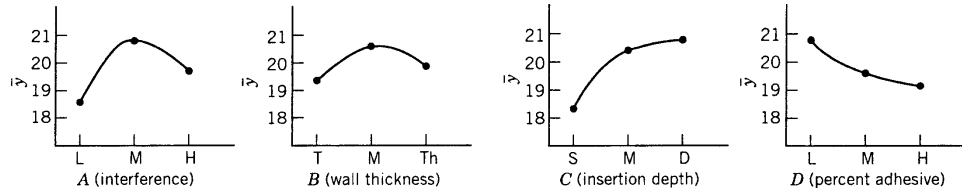


**Figure 10.5** Plot of  $\bar{y}$  against levels of control variables.

respectively. As in Example 10.1, the graphs are examined and the analysis involves a pick-the-winner approach. The following represent the optimal choices of  $A$ ,  $B$ ,  $C$ , and  $D$  according to the plots:

- $A$ : Medium
- $B$ : Medium
- $C$ : Medium or deep
- $D$ : Low

In each case, we have the levels that maximize the mean response and also maximize  $\text{SNR}_l$ . Again, these choices are made under the assumption that no interaction exists among the control factors.

Actually, when cost and other external factors were taken into account, the researchers decided to use

- $A$ : Medium
  - $B$ : Thin
  - $C$ : Medium
  - $D$ : Low
- (10.6)

The thin level for  $B$  was much less expensive. Neither of the two conditions for  $A$ ,  $B$ ,  $C$ , and  $D$  reported above was in the design. As a result, confirmatory runs were necessary. The authors report that good results were observed. The levels used in the noise variables were  $E_{\text{low}}$ ,  $F_{\text{low}}$ , and  $G_{\text{low}}$ .

### 10.3.3 Further Comments

To this point our emphasis has been on experimental design and analysis procedures suggested by Taguchi. It should be emphasized that despite criticisms put forth by statisticians concerning his approach, the methods advocated by Taguchi have been

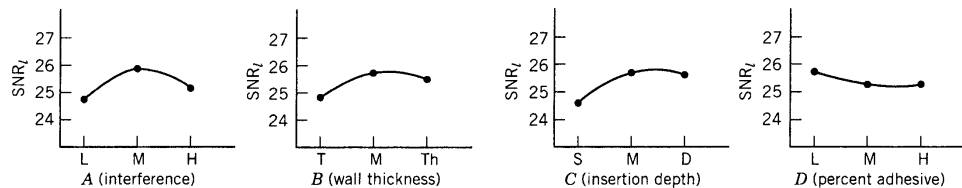


**Figure 10.6** Plot of mean  $\text{SNR}_l$  against levels of control variables.

successful, and many practitioners have used them. While there are weaknesses in the methodology as illustrated in the two previous examples, there are certainly many real-life situations in which it works well. For an excellent account of Taguchi's contributions the reader is referred to Pignatiello and Ramberg (1991). In the sections that follow, we will discuss areas where there are weaknesses and will point out situations in which these weaknesses may lead to difficulties. This is designed to motivate an emphasis on response surface methods as an alternative for solving robust parameter design problems.

**Experimental Design** The **crossed array**, or **product array**, begins with two experimental designs, one for the noise variables and one for the control variables. These designs are then crossed with each other. The two individual designs are generally quite economical because they are either saturated or near-saturated. However, the crossing of two designs often does not produce an economical design. Indeed, often the designs are huge, as in Example 10.2, where 72 runs were used to study only seven factors. As we will suggest in a subsequent section, there are more economical approaches to designing an experiment for control and noise variables.

In sections that follow we suggest economical experimental designs for handling robust design problems in which control  $\times$  control interactions are available. In addition, these designs are compatible with a response surface approach to the solution of robust parameter design problems.

**The Taguchi Analysis** Notwithstanding difficulties discussed earlier with the SNRs, the approach taken by Taguchi and described here can work very well for determining a robust product if control  $\times$  control interactions are not important. However, the marginal means approach, while placing emphasis on process optimization, does not allow the practitioner to learn more about the process. Lack of an empirical model is a major flaw in the approach. Here, the focus is on models that involve control  $\times$  control and control  $\times$  noise interactions and on the determining of separate models for the process mean and variance.

## 10.4 THE RESPONSE SURFACE APPROACH

There are several response surface alternatives for solving the RPD problem and for conducting process robustness studies. In this section we begin by emphasizing the importance of the control  $\times$  noise interactions, discuss alternative modeling and analysis strategies, and present alternatives to the Taguchi-style crossed array experimental designs. With regard to modeling strategies, it should be emphasized that, in general, process optimization may be overrated. The more emphasis is placed on learning about the process, the less important *absolute optimization* becomes. An engineer or scientist always can (and often does) find pragmatic reasons why the suggested optimum conditions cannot be adopted. A thorough study (via a response surface approach) of the control variable design space will generally provide effective alternative suggestions for operating conditions.

### 10.4.1 The Role of the Control $\times$ Noise Interaction

We have emphasized the need to model control  $\times$  control interactions. However, the control  $\times$  noise interactions are vitally important. Indeed, the structure of these interactions determines the nature of nonhomogeneity of process variance that characterizes the

**TABLE 10.5 Experimental Data in a Crossed Array**

Inner Array		Outer Array		Response Means
A	B	C = -1	+1	
-1	-1	11	15	13.0
-1	1	7	8	7.5
1	-1	10	26	18.0
1	1	10	14	12.0

parameter design problem. As an illustration consider the case of two control variables and one noise variable with data as shown in the crossed array design of Table 10.5.

Consider the plots displaying the control  $\times$  noise interactions  $AC$  and  $BC$  in Figs 10.7a and 10.7b. In viewing these interaction plots, keep in mind that while  $C$  is held fixed in the experimental design, it will vary according to some probability distribution during the process. The probability distribution may be discrete or continuous. Here it is clear that when we take this variability into account, the picture suggests that  $A = +1$  and  $B = -1$  will result in *largest product variability*, whereas  $A = -1$  and  $B = +1$  should result in *smallest product variability*. The braces on the vertical axes reflect product variability at  $A = +1$  and  $B = -1$ . Now, of course, in this simple case, the conclusion is borne out in the data themselves, but it may not be so easy to see in larger problems. In this illustration, we say that  $A$  and  $B$  are both **dispersion effects**, that is, effects that have influence on the process variance. In addition, both variables have **location effects**, namely, they have an effect on the process mean. In fact, the illustration points out the need to compromise between process mean and process variance. From the plots, the combination  $A = +1$  and  $B = -1$  produces the largest mean response, and if this is a larger-the-better case, determining the optimum conditions will involve some type of simultaneous optimization of the process mean and variance.

It should be apparent that control  $\times$  noise interactions display the structure of the process variance and relate which factors are dispersion effects and which are not. Consider the example in Table 10.6. The  $A \times C$  and  $B \times C$  interaction plots are given in Figs 10.8a and 10.8b. Here we have parallelism in the two interaction plots. There is no  $AC$  factor

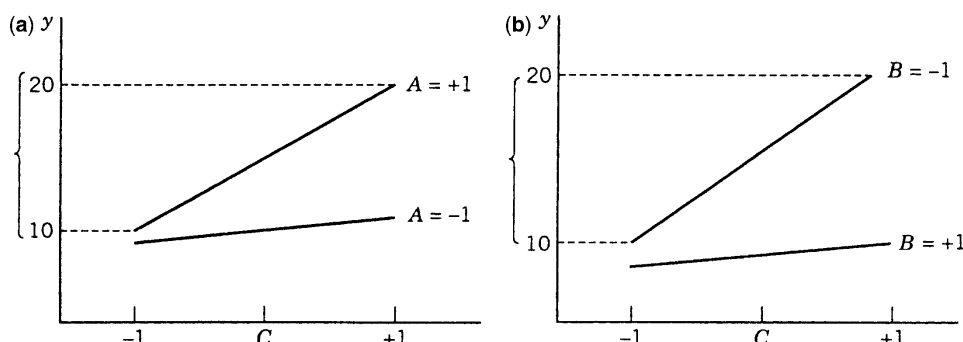


**Figure 10.7** Interaction plots for the data in Table 11.5. (a)  $AC$  interaction plot. (b)  $BC$  interaction plot.

**TABLE 10.6 Experimental Data in a Crossed Array**

Inner Array		Outer Array	
A	B	$C = C - 1$	+1
-1	-1	14.5	22.5
-1	1	19	27.5
1	-1	23.5	32
1	1	28.5	37

interaction and consequently  $A$  is *not* a dispersion effect. That is, the process variance is the same at both levels of  $A$ . There is no  $BC$  interaction, so  $B$  is *not* a dispersion effect either. The factor  $A$  has a greater location effect than  $B$ . If this is a larger-the-better case, then the combination  $A = +1$  and  $B = +1$  is optimal and there is *no robust parameter design problem*, because altering  $A$  and  $B$  has no effect on the variance produced by changing the noise variable  $C$ .

Consider a third example, for which the  $AC$  and  $BC$  interaction plots appear in Figs 10.9a and 10.9b. Figure 10.9a depicts  $A$  as a dispersion effect with  $A = +1$  representing the level of minimum variance. Figure 10.9b suggests that  $B$  is *not* a dispersion effect. Both  $A$  and  $B$  are location effects; and for a larger-the-better scenario,  $A = +1$  and  $B = +1$  represents optimum conditions. The control  $\times$  noise interactions can serve as nice diagnostic tools regarding the structure of the process variance. Note that the larger the slopes of the interaction plots, the larger the contributions to the process variance. Here we have discussed the diagnostic nature of the two-factor interactions. However, if there are three-factor interactions involving control and noise factors, these too play a role.

Consider the connector pulloff force problem in Example 10.2. Here, there are four control factors; from Fig. 10.6 factor  $A$  appears to have an effect on  $\text{SNR}_I$ , and indeed we learned that  $A$  medium is the appropriate level. In addition,  $A$  medium maximizes  $\bar{y}$ . The two-factor  $AG$  interaction plot is given in Fig. 10.10. This plot implies that  $A$  medium *minimizes the variance produced by changes in relative humidity*. It also reinforces that  $A$  medium is desirable from the point of view of the mean response.

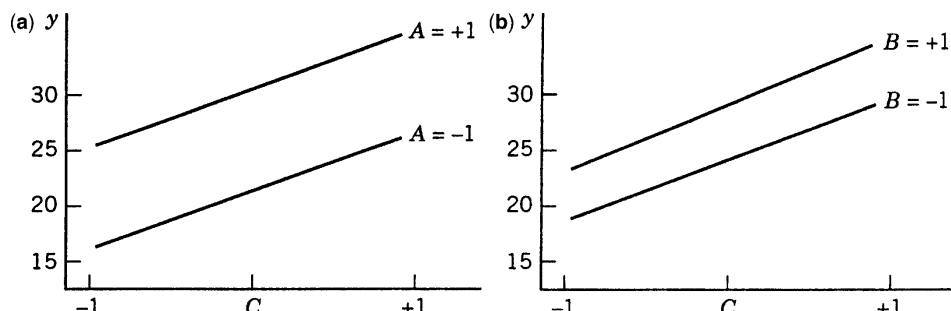


**Figure 10.8** Interaction plots for the data in Table 10.6. (a)  $AC$  interaction plot. (b)  $BC$  interaction plot.

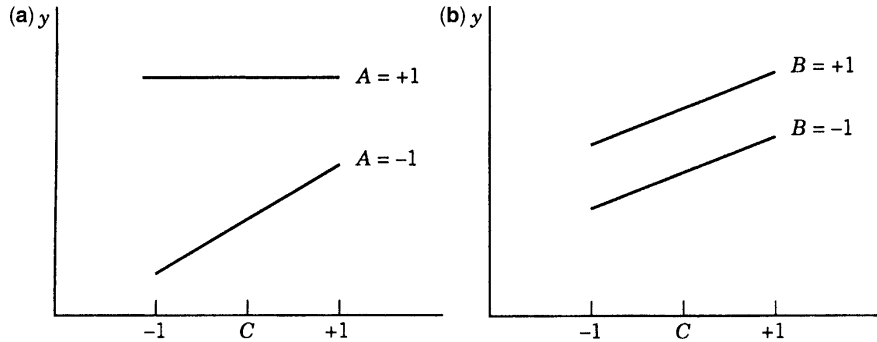


**Figure 10.9** Two-factor interaction plot. (a) AC interaction plot. (b) BC interaction plot.

As a result, it should be clear that the control  $\times$  noise interaction plot aids in the determination of which factors are dispersion effects, which are location effects, and which levels of the dispersion effects moderate the variance produced by which noise variables. For example, consider a situation in which we have three control factors ( $A$ ,  $B$ , and  $C$ ) and two noise factors ( $D$  and  $E$ ). Suppose also that interactions  $AD$  and  $BE$  are found to be significant. In addition,  $A$  is found to be insignificant while  $B$  and  $C$  are significant.

Consider the main effect and interaction plots in Fig. 10.11. The plots indicate that  $C$  has a strong location effect and  $B$  has a mild location effect. Factor  $B$  has a huge dispersion effect with minimum process variance resulting from the use of the  $-1$  level of  $B$ . *Using the  $-1$  level of  $B$  minimizes that portion of the process variance that results from changes in the noise variable  $E$ .* Despite the fact that  $A$  interacts with the noise variable  $D$ , the use of  $-1$  or  $+1$  on  $A$  results in the same process variance. However, if  $A$  is a continuous variable, there may be other levels of  $A$  that will produce a horizontal line on the  $AD$  interaction plot and thus dramatically reduce the portion of the process variance associated with changes in  $D$ . (Note the dashed line on the  $AD$  interaction plot.) Because the

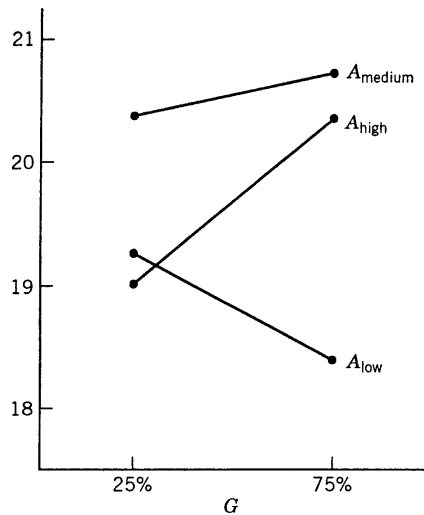


**Figure 10.10** AG interaction plot for Example 10.2.

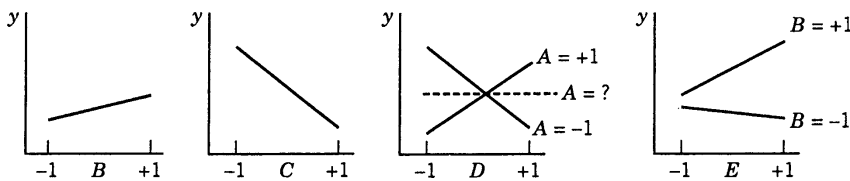


Figure 10.11 Main effect and interaction plots.

factor  $C$  does not interact with either noise factor,  $C$  cannot be used to control process variance. If one were interested in conditions that minimize mean response, say, but also result in minimizing process variance, one would choose  $B = -1$ ,  $C = +1$ , and  $A = -1$  or  $+1$ . However, if  $A$  is a continuous variable, the value of  $A$  that results in minimum process variance should be sought. This latter idea will be developed in future sections.

#### 10.4.2 A Model Containing Both Control and Noise Variables

From the discussion in the previous subsection, it becomes apparent that one may wish to make use of a model that contains main effects and interactions involving both control and noise variables. If the control variables are predominantly continuous variables, this type of model will become a very useful vehicle for the eventual formation of a **dual response surface** approach—that is, a response surface for the process mean and a response surface for the process variance. In what has preceded this section, we have assumed that control and noise factors are fixed effects. Suppose we consider  $\mathbf{x}$  and  $\mathbf{z}$ , the control and noise factors respectively. The modeling of both  $\mathbf{x}$  and  $\mathbf{z}$  in the same model has been called a **response model approach**. The following example illustrates one approach to the analysis of the response model.

**Example 10.3 The Pilot Plant Experiment** Consider the experiment described in Example 3.2, where a  $2^4$  factorial design was used to study the filtration rate of a chemical product. The four factors are temperature, pressure, concentration of formaldehyde, and stirring rate. Each factor is present at two levels. The design matrix and the response data obtained from a single replicate of the  $2^4$  experiment are repeated for convenience in Table 10.7. The 16 runs are made in random order.

Assume that temperature is hard to control. Therefore, it is the noise variable and is denoted by  $z_1$ . The other three factors are denoted  $x_1$  = pressure,  $x_2$  = concentration, and  $x_3$  = stirring rate. Because both the control factors and the noise factor are in the same design matrix, this type of design is called a **combined array design**.

Using the results from the original analysis in Example 3.2, the response model is

$$\begin{aligned}\hat{y}(\mathbf{x}, z_1) &= 70.06 + \left(\frac{21.625}{2}\right)z_1 + \left(\frac{9.875}{2}\right)x_2 + \left(\frac{14.625}{2}\right)x_3 \\ &\quad - \left(\frac{18.125}{2}\right)x_2z_1 + \left(\frac{16.625}{2}\right)x_3z_1 \\ &= 70.06 + 10.81z_1 + 4.94x_2 + 7.31x_3 - 9.06x_2z_1 + 8.31x_3z_1\end{aligned}$$

**TABLE 10.7 Pilot Plant Filtration Rate Experiment**

Run Number	Factor				Filtration Rate (gal/hr)
	$z_1$	$x_1$	$x_2$	$x_3$	
1	—	—	—	—	45
2	+	—	—	—	71
3	—	+	—	—	48
4	+	+	—	—	65
5	—	—	+	—	68
6	+	—	+	—	60
7	—	+	+	—	80
8	+	+	+	—	65
9	—	—	—	+	43
10	+	—	—	+	100
11	—	+	—	+	45
12	+	+	—	+	104
13	—	—	+	+	75
14	+	—	+	+	86
15	—	+	+	+	70
16	+	+	+	+	96

Notice that the fitted response model contains both the control and the noise factors. Let us assume that  $z_1$  is a random variable with mean zero and variance  $\sigma_z^2$ . Also, assume that  $\sigma_z^2$  is known and the high and low levels of  $z_2$  are at  $\pm\sigma_z$  in coded form. Thus,  $\sigma_z = 1$ .

Suppose that the fitted model above is adequate to allow us to assume that the true relationship between  $y$ ,  $\mathbf{x}$ , and  $z_1$  is

$$y(\mathbf{x}, z_1) = \beta_0 + \gamma_1 z_1 + \beta_2 x_2 + \beta_3 x_3 + \delta_{12} z_1 x_2 + \delta_{13} z_1 x_3 + \varepsilon$$

Because  $E(z_1) = 0$  and  $E(\varepsilon) = 0$ , a model for the **process mean** is

$$E_{z_1}[y(\mathbf{x}, z_1)] = \beta_0 + \beta_2 x_2 + \beta_3 x_3$$

Now apply a conditional variance operator across  $y(\mathbf{x}, z_1)$ . This gives

$$\begin{aligned} \text{Var}_{z_1}[y(\mathbf{x}, z_1)] &= \text{Var}_{z_1}[\beta_0 + \gamma_1 z_1 + \beta_2 x_2 + \beta_3 x_3 + \delta_{12} z_1 x_2 + \delta_{13} z_1 x_3 + \varepsilon] \\ &= \text{Var}_{z_1}[\beta_0 + \beta_2 x_2 + \beta_3 x_3 + (\gamma_1 + \delta_{12} x_2 + \delta_{13} x_3) z_1 + \varepsilon] \\ &= \sigma_z^2(\gamma_1 + \delta_{12} x_2 + \delta_{13} x_3) + \sigma^2 \end{aligned}$$

This is a model for the **process variance**. We can replace the parameters by their estimates to obtain

$$\widehat{E_z[y(\mathbf{x}, z_1)]} = 70.06 + 4.94 x_2 + 7.31 x_3$$

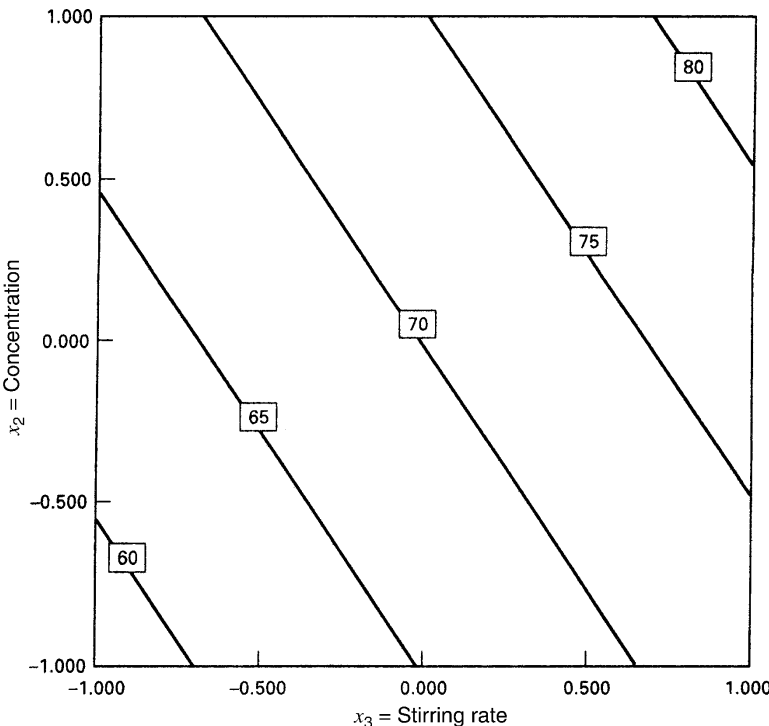
and

$$\begin{aligned}\widehat{\text{Var}_z[y(\mathbf{x}, z_1)]} &= \sigma_z^2(10.81 - 9.06x_2 + 8.31x_3)^2 + \sigma^2 \\ &= 136.42 + 82.08x_2^2 + 69.06x_3^2 - 195.88x_2 + 179.66x_3 - 150.58x_2x_3\end{aligned}$$

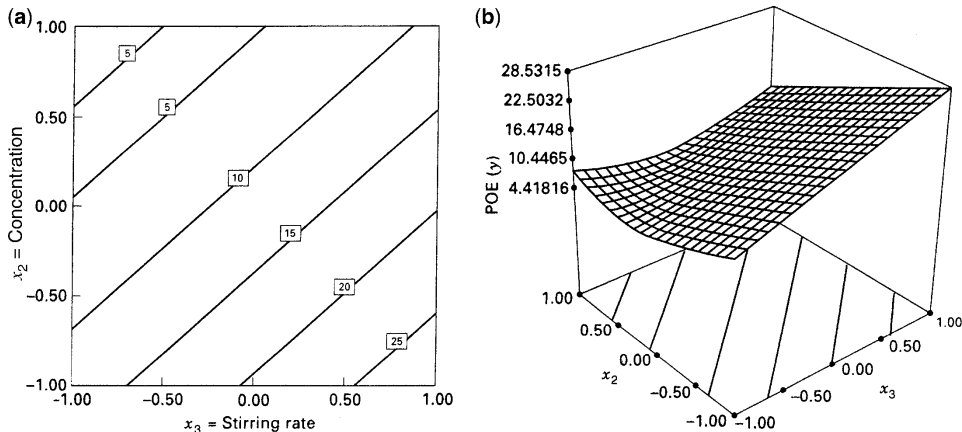
because  $\sigma_z^2 = 1$  and  $\hat{\sigma}^2 = 19.51$  (this is the residual mean square obtained by fitting the response model).

Figure 10.12 presents a contour plot of the response contours from the mean model. This plot was constructed using Design-Expert. To construct this plot, we held the noise factor (temperature) at zero and the nonsignificant controllable factor (pressure) at zero. Notice that the mean filtration rate increases as either the concentration or the stirring rate increases. Design-Expert will also construct plots automatically of the *square root* of the variance contours, which it labels **propagation of error**, or **POE**. Obviously, the POE is just the standard deviation of the transmitted variability in the response as a function of the controllable variables. Figure 10.13 shows a contour plot and a three-dimensional response surface plot of the POE, obtained from Design-Expert (in this plot the noise variable is held constant at zero, as explained previously).

Suppose that the experimenter wants to maintain a mean filtration rate about 75 and minimize the variability around this value. Figure 10.14 shows an overlay plot of the contours of mean filtration rate and the POE as a function of concentration and stirring rate, the significant controllable variables. To achieve the desired objectives, it will be necessary to hold concentration at the high level and stirring rate very near the middle level.



**Figure 10.12** Contours of constant mean filtration rate (Example 10.3) with  $z_1 = \text{temperature} = 0$ .



**Figure 10.13** Contour plot and response surface plot of propagation of error for Example 10.3, with  $z_1 = \text{temperature} = 0$ . (a) Contour plot. (b) Response surface plot.

#### 10.4.3 Generalization of Mean and Variance Modeling

The analysis in the previous subsection indicates that a *dual* response approach to the RPD problem or a process robustness study offers considerable flexibility to the analyst. Specifically:

1. It provides an estimate of the mean and standard deviation at any location of interest in the control design variables.

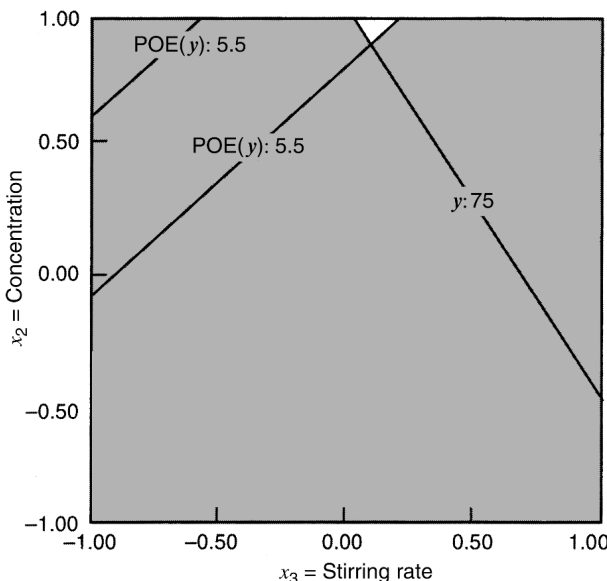


**Figure 10.14** Overlay plot of mean and POE contours for filtration rate (Example 10.3), with  $z_1 = \text{temperature} = 0$ .

2. The engineer or scientist can gain insight regarding the roles of these variables in controlling the process mean and variance.
3. It provides a ready source of process optimization via the use of a squared error loss criterion such as

$$E_z[y(\mathbf{x}, \mathbf{z}) - t]^2 = \{E[y(\mathbf{x}, \mathbf{z})] - t\}^2 + \text{Var}_z[y(\mathbf{x}, \mathbf{z})]$$

which will result in a single-number criterion appropriate for the target-is-best scenario.

4. It allows the use of a wide variety of constrained optimization techniques.

Many authors have pointed out the advantages of mean and variance modeling and illustrated its use in both RPD problems and process robustness studies. Some useful references include, Box and Jones (1989, 1992), Vining and Myers (1990), Shoemaker, Tsui, and Wu (1991), Myers, Khuri, and Vining (1992), Del Castillo and Montgomery (1993), Lucas (1994), Pledger (1996), Myers, Kim, and Griffiths (1997), Khattree (1996), Montgomery (1999), and Borror and Montgomery (2000).

The example in Section 10.4.2 involved a first-order model in the control factors. In many situations, the model in the control and noise variables may involve **quadratic**, or second-order, terms in the control variables (the  $x$ 's). Thus a plausible model would be

$$y(\mathbf{x}, \mathbf{z}) = \beta_0 + \mathbf{x}'\boldsymbol{\beta} + \mathbf{x}'\mathbf{B}\mathbf{x} + \mathbf{z}'\boldsymbol{\gamma} + \mathbf{x}'\boldsymbol{\Delta}\mathbf{z} + \varepsilon \quad (10.7)$$

In this **response model** we assume linear effects in  $\mathbf{x}$  and  $\mathbf{z}$ , two-factor interaction and pure quadratic terms in  $\mathbf{x}$  (the term  $\mathbf{x}'\mathbf{B}\mathbf{x}$ ), and the very important two-factor interactions involving control and noise variables (the term  $\mathbf{x}'\boldsymbol{\Delta}\mathbf{z}$ ).

We do not rule out the use of interactions among noise variables or even quadratic terms in noise variables. However, the model in Equation (10.17) will accommodate many real-life situations. The development of mean and variance modeling with the use of Equation 10.7 will provide the machinery for more general applications. Let  $\mathbf{z}$  in Equation 10.7 be  $r_z \times 1$ , and let  $\mathbf{x}$  be  $r_x \times 1$ . Then  $\boldsymbol{\Delta}$  is an  $r_x \times r_z$  matrix containing coefficients of the control  $\times$  noise or  $x \times z$  interactions.

**Assumptions Underlying Dual Response Development** The  $\varepsilon$ -term in Equation 10.7 plays the same role as the random error term in any response surface methodology (RSM) model discussed in Chapters 3–9. Assumptions that  $\varepsilon_i$  are NID(0,  $\sigma^2$ ) are often reasonable. It should be pointed out that the *constant variance* assumption on  $\varepsilon$  implies that any nonconstancy of variance of the process stems primarily from *inability to control noise variables*. Detection of other sources of heterogeneous variance will be addressed in Section 10.6.

The assumptions associated with the noise variables deserve special attention. As we indicated in Example 10.3, we must assume that the user possesses a reasonable amount of knowledge about the random variable  $\mathbf{z}$ . It may be assumed that in the experiment the natural levels of  $z_j$  are centered at the mean that  $z_j$  experiences in the process and that the  $\pm 1$  levels are at  $\mu_{z_j} + \sigma_{z_j}$ . As a result, the mean of the  $z$ 's in coded metric is at 0, and  $\pm 1$  levels are one standard deviation from the mean. The latter is not a hard and fast assumption. The experimenter may decide to let  $\pm 1$  correspond to  $\pm 2\sigma_z$ . Thus, we will

demonstrate a development of the process variance response surface under the assumption that  $\sigma_z$  is known, and the latter may take on values of 1,  $\frac{1}{2}$ ,  $\frac{1}{3}$  and so on, in practice. For this purpose, assume that

$$E(\mathbf{z}) = \mathbf{0}, \quad \text{Var}(\mathbf{z}) = \sigma_z^2 \mathbf{I}_{r_z} \quad (10.8)$$

Equation 10.8 implies the assumption that noise variables are uncorrelated with known variance.

**The Mean and Variance Response Surfaces** We now apply conditional expectation and variance operators to the model in Equation 10.8. Because  $E(\mathbf{z}) = 0$ , the expectation operation  $E_z$  gives the response surface model for the mean:

$$E_z[y(\mathbf{x}, \mathbf{z})] = \beta_0 + \mathbf{x}'\boldsymbol{\beta} + \mathbf{x}'\mathbf{B}\mathbf{x} \quad (10.9)$$

The conditional variance operator,  $\text{Var}_z[y(\mathbf{x}, \mathbf{z})]$  plus the error variance around Equation 10.7 gives

$$\text{Var}_z[y(\mathbf{x}, \mathbf{z})] = \text{Var}_z(\boldsymbol{\gamma}' + \mathbf{x}'\Delta)\mathbf{z} + \sigma^2$$

Here the quantity  $\boldsymbol{\gamma}' + \mathbf{x}'\Delta = \mathbf{a}'$  (say) is a vector of constants. As a result, we have to evaluate  $\text{Var}_z(\mathbf{a}'\mathbf{z})$ . Rules for applying the variance operator give

$$\text{Var}_z(\mathbf{a}'\mathbf{z}) = \mathbf{a}'\text{Var}(\mathbf{z})\mathbf{a}$$

where  $\text{Var}(\mathbf{z}) = \sigma_z^2 \mathbf{I}$  is the variance-covariance matrix of  $\mathbf{z}$ . As a result, we have

$$\text{Var}_z(\boldsymbol{\gamma}' + \mathbf{x}'\Delta)\mathbf{z} = \sigma_z^2(\boldsymbol{\gamma}' + \mathbf{x}'\Delta)(\boldsymbol{\gamma}' + \mathbf{x}'\Delta)'$$

so

$$\begin{aligned} \text{Var}_z[y(\mathbf{x}, \mathbf{z})] &= \sigma_z^2(\boldsymbol{\gamma}' + \mathbf{x}'\Delta)(\boldsymbol{\gamma}' + \mathbf{x}'\Delta)' + \sigma^2 \\ &= \sigma_z^2 \mathbf{l}'(\mathbf{x}) \mathbf{l}(\mathbf{x}) + \sigma^2 \end{aligned} \quad (10.10)$$

where  $\mathbf{l}(\mathbf{x}) = \boldsymbol{\gamma} + \Delta'\mathbf{x}$ .

Equation 10.9 is the **response surface for the process mean**, while Equation 10.10 is the **response surface for the process variance**. Equation 10.10 deserves special attention. Apart from  $\sigma^2$ , the model error variance, the process variance is  $\|\mathbf{l}(\mathbf{x})\|^2$ , where  $\mathbf{l}(\mathbf{x})$  is simply the vector of partial derivatives of  $y(\mathbf{x}, \mathbf{z})$  with respect to  $\mathbf{z}$ . In other words,

$$\mathbf{l}(\mathbf{x}) = \frac{\partial y(\mathbf{x}, \mathbf{z})}{\partial \mathbf{z}}$$

is just the **slope** of the response surface in the direction of the noise variables. This is very intuitive: the larger the vector of derivatives  $\partial y / \partial \mathbf{z}$  (the slopes), the larger the process variance. This relates very nicely to the discussion in Section 10.4.1. Recall that the flatter the  $x \times z$  interaction plots, the smaller the process variance. Clearly, *flat interaction plots result from small values of  $\partial y(\mathbf{x}, \mathbf{z}) / \partial \mathbf{z}$* . Also, note the important role of  $\Delta$ , the matrix of  $x \times z$

interaction coefficients, in the process variance response surface. If  $\Delta = \mathbf{0}$ , process variance does not depend on  $\mathbf{x}$ , and hence one cannot create a robust process by choice of settings of the control variables. In other words, the process variance is constant and thus *there is no robust parameter design problem*. In Equation 10.10 we add the model error variance. In many cases this variance will be negligible compared to the variance that is contributed by variation in the noise variables. In our development here there is an implicit assumption that the noise variables are quantitative in nature. In the case of discrete noise variables the assumption of uncorrelated noise variables is not necessarily appropriate.

Equations 10.9 and 10.10 represent the mean and variance response surfaces developed from the model (or response surface) that contains both control and noise variables Equation 10.7. Clearly the estimated response surfaces are obtained by replacing parameters by estimates found in the fitted model and

$$\hat{y}(\mathbf{x}, \mathbf{z}) = b_0 + \mathbf{x}'\mathbf{b} + \mathbf{x}'\hat{\mathbf{B}}\mathbf{x} + \mathbf{z}'\mathbf{c} + \mathbf{x}'\hat{\Delta}\mathbf{z} \quad (10.11)$$

Consequently, the estimated process mean and variance response surfaces are given by

$$\begin{aligned} \widehat{E_z[y(\mathbf{x}, \mathbf{z})]} &= \hat{\mu}_z[y(\mathbf{x}, \mathbf{z})] \\ &= b_0 + \mathbf{x}'\mathbf{b} + \mathbf{x}'\hat{\mathbf{B}}\mathbf{x} \end{aligned} \quad (10.12)$$

$$\begin{aligned} \widehat{\text{Var}_z[y(\mathbf{x}, \mathbf{z})]} &= \hat{\sigma}_z^2 \hat{\mathbf{l}}'(\mathbf{x}) \hat{\mathbf{l}}(\mathbf{x}) + \hat{\sigma}^2 \\ &= \hat{\sigma}_z^2 (\mathbf{c}' + \mathbf{x}'\hat{\Delta})(\mathbf{c} + \hat{\Delta}'\mathbf{x}) + \hat{\sigma}^2 \end{aligned} \quad (10.13)$$

Here,  $\hat{\sigma}^2$  is the mean squared error in the fitted response surface.

It is actually possible to generalize these results a bit more. We may write the response model involving the control and noise variables as

$$y(\mathbf{x}, \mathbf{z}) = f(\mathbf{x}) + h(\mathbf{x}, \mathbf{z}) + \varepsilon \quad (10.14)$$

where  $f(\mathbf{x})$  is the portion of the model that involves only the control variables and  $h(\mathbf{x}, \mathbf{z})$  are the terms involving the noise factors and the interactions between the controllable and noise factors. In Equation 10.7, the structure for  $h(\mathbf{x}, \mathbf{z})$  was assumed to be

$$h(\mathbf{x}, \mathbf{z}) = \sum_{i=1}^{r_z} \gamma_i z_i + \sum_{i=1}^{r_x} \sum_{j=1}^{r_z} \delta_{ij} x_i z_j \quad (10.15)$$

The structure for  $f(\mathbf{x})$  and  $h(\mathbf{x}, \mathbf{z})$  will depend on what type of model the experimenter thinks is appropriate. The logical choices for  $f(\mathbf{x})$  are the first-order model with interaction and the second-order model. Equation 10.15 represents a reasonable choice for  $h(\mathbf{x}, \mathbf{z})$ ; if appropriate, however, one could include more complex functions of the noise variables. If we assume that the noise variables have mean zero, variance  $\sigma_z^2$ , and covariance zero, and that the noise variables and the random errors  $\varepsilon$  have zero covariances, then the mean model for the response is just

$$E_z[y(\mathbf{x}, \mathbf{z})] = f(\mathbf{x}) \quad (10.16)$$

and the variance model for the response is

$$\text{Var}_z[y(\mathbf{x}, \mathbf{z})] = \sigma_z^2 \sum_{i=1}^r \left[ \frac{\partial y(\mathbf{x}, \mathbf{z})}{\partial z_i} \right]^2 + \sigma^2 \quad (10.17)$$

Equation 10.17 was found by expanding  $y(\mathbf{x}, \mathbf{z})$  in a first-order Taylor series about  $\mathbf{z} = 0$  and applying the variance operator (this is sometimes called the **delta method**). Equation 10.17 is also called the **transmission-of-error formula**. When the noise variables are involved linearly in  $h(\mathbf{x}, \mathbf{z})$ , Equation 10.17 will be exactly the same as Equation 10.10.

#### 10.4.4 Analysis Procedures Associated with the Two Response Surfaces

We saw a simple special case of a dual response surface analysis in Section 10.4.2. We were able to find operating conditions by overlaying the response surfaces. Another approach is to use constrained optimization, that is, select a value of  $E_z[y(\mathbf{x}, \mathbf{z})]$  that one is willing to accept. This does not imply a target on the mean but, say, a value below which one cannot accept. In fact, several of these values may be chosen in order to add flexibility. Call this constraint  $E_z[y(\mathbf{x}, \mathbf{z})] = m$ . One then chooses  $\mathbf{x}$  as follows:

$$\underset{\mathbf{x}}{\text{Min Var}_z[y(\mathbf{x}, \mathbf{z})]} \quad \text{subject to} \quad E_z[y(\mathbf{x}, \mathbf{z})] = m$$

Several values of  $m$  may be used in order to provide flexibility for the user.

There are many situations in which focus is placed entirely on the **variance** response surface. For example, there may be location effects that appear in the mean model but not in the variance model, and they can be used as tuning factors. As a result, the analysis centers around the variance model. One may be interested in determining  $\mathbf{x}$  that minimizes, or makes zero, the process variance in Equation 10.10. To that end, consider the computation of the locus of points  $\mathbf{x}_0$  for which

$$\mathbf{I}(\mathbf{x}_0) = \mathbf{0} \quad (10.18)$$

or, in terms of the fitted surface,

$$\mathbf{c} + \hat{\Delta}' \mathbf{x}_0 = \mathbf{0}$$

The condition Equation 10.18 represents  $r_z$  equations in  $r_x$  unknowns. If  $r_x > r_z$ , this result, which produces a zero estimated process variance (apart from the model error variance  $\sigma^2$ ), will result in a line or a plane. If  $r_x = r_z$ , there will be a single point  $\mathbf{x}_0$  that satisfies Equation 10.18. If  $r_x < r_z$ , Equation 10.18 may not have a solution. Of course a great deal of interest centers on whether or not the locus of points  $\mathbf{x}_0$  passes through the experimental design region in the control variables.

We now present an example involving a second-order response surface model. This example is taken from Montgomery (2005).

**Example 10.4 A Process Robustness Study in Semiconductor Manufacturing** An experiment was run in a semiconductor manufacturing facility involving two controllable

**TABLE 10.8** Combined Array Experiment with Two Controllable Variables and Three Noise Variables, Example 10.4

Run Number	$x_1$	$x_2$	$z_1$	$z_2$	$z_3$	$y$
1	-1	-1	-1	-1	1	44.2
2	1	-1	-1	-1	-1	30.0
3	-1	1	-1	-1	-1	30.0
4	1	1	-1	-1	1	35.4
5	-1	-1	1	-1	-1	49.8
6	1	-1	1	-1	1	36.3
7	-1	1	1	-1	1	41.3
8	1	1	1	-1	-1	31.4
9	-1	-1	-1	1	-1	43.5
10	1	-1	-1	1	1	36.1
11	-1	1	-1	1	1	22.7
12	1	1	-1	1	-1	16.0
13	-1	-1	1	1	1	43.2
14	1	-1	1	1	-1	30.3
15	-1	1	1	1	-1	30.1
16	1	1	1	1	1	39.2
17	-2	0	0	0	0	46.1
18	-2	0	0	0	0	36.1
19	0	-2	0	0	0	47.4
20	0	2	0	0	0	31.5
21	0	0	0	0	0	30.8
22	0	0	0	0	0	30.7
23	0	0	0	0	0	31.0

variables. The combined array design used by the experimenters is shown in Table 10.8. The design is a 23-run variation of a central composition design that was created by starting with a standard CCD for five factors (the cube portion is a  $2^{5-1}$ ) and deleting the axial runs associated with the three noise variables. This design will support a response model that has a second-order model in the controllable variables, the main effects of the three noise variables, and the interactions between the control and noise factors. The fitted response model is

$$\begin{aligned}\hat{y}(\mathbf{x}, \mathbf{z}) = & 30.37 - 2.9x_1 - 4.13x_2 + 2.60x_1^2 + 2.18x_2^2 + 2.87x_1x_2 + 2.73z_1 \\ & - 2.33z_2 + 2.33z_3 + 0.27x_1z_1 + 0.89x_1z_2 + 2.58x_1z_3 + 2.01x_2z_1 \\ & - 1.43x_2z_2 + 1.56x_2z_3\end{aligned}$$

The mean and variance models are

$$\begin{aligned}\widehat{E_z[y(\mathbf{x}, \mathbf{z})]} = & b_0 + \mathbf{x}'\mathbf{b} + \mathbf{x}'\hat{\mathbf{B}}\mathbf{x} \\ = & 30.37 - 2.92x_1 - 4.13x_1 + 2.60x_1^2 \\ & + 2.18x_2^2 + 2.87x_1x_2\end{aligned}$$

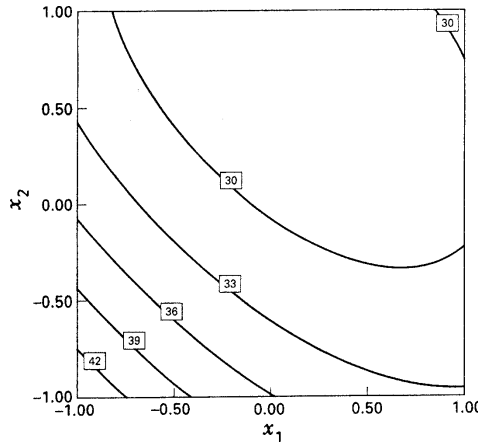


**Figure 10.15** Contour plot of the mean model, Example 10.4.

and

$$\begin{aligned}\widehat{\text{Var}_z[y(\mathbf{x}, \mathbf{z})]} &= \hat{\sigma}_z^2 \mathbf{l}'(\mathbf{x}) \mathbf{l}(\mathbf{x}) + \sigma^2 \\ &= 19.26 + 3.20x_1 + 12.45x_2 + 7.52x_1^2 + 8.52x_2^2 + 2.21x_1x_2\end{aligned}$$

where we have substituted parameter estimates from the fitted response model into the equations for the mean and variance models and assumed that  $\sigma_z^2 = 1$ . Figures 10.15 and 10.16 present contour plots of the process mean and POE (remember that the POE is the square root of the variance response surface) generated from these models.

In this problem it is desirable to keep the process mean below 30. From inspection of Figs 10.15 and 10.16 it is clear that some tradeoff will be necessary if we wish to make the process variance small. Because there are only two controllable variables, a logical way to accomplish this tradeoff is to overlay the contours of constant mean response and

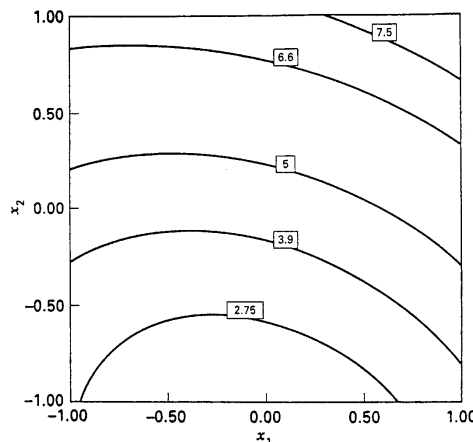


**Figure 10.16** Contour plot of the POE, Example 10.4.

constant variance, as shown in Fig. 10.17. This plot shows the contours for which the process mean is less than or equal to 30 and the process standard deviation is less than or equal to 5. The region bounded by these contours would represent a typical operating region of low mean response and low process variance.

There are other approaches to solving the robust design problem in Example 10.4. One approach would be to differentiate the fitted response model with respect to each of the noise variables  $z_1$ ,  $z_2$ , and  $z_3$  (recall that the derivatives of the response model or the slope of the response surface in the direction of the noise variables are proportional to the transmitted variance) and force these derivatives to zero while simultaneously optimizing the levels of the control variables  $x_1$  and  $x_2$ . This approach can be executed in JMP. Figure 10.18a is the output from the JMP prediction profiler showing the response  $y$  and the three derivatives for each of the noise factors after this optimization is carried out using a desirability function technique. JMP also has a simulation capability that predicts the proportion of production outside specifications on the response variable. The proportion of the response  $y$  that is predicted to be above 30 in this problem is about 25%. This indicates that the variability transmitted from the noise variables is still quite high.

In some situations it may be possible to reduce the proportion of unacceptable product by exercising some limited form of control over the noise variables. Often this control takes the form of setting the mean value of the noise variable but still having no control over the variability in the noise variable during routine process operation.

Suppose that in the situation of Example 10.4 we could set the mean of the noise variables, but they would still vary randomly around these means. How much could this additional flexibility potentially reduce the proportion of defective product (where  $y$  is above 30)? The display in Fig. 10.18b addresses this question. This display is the defect

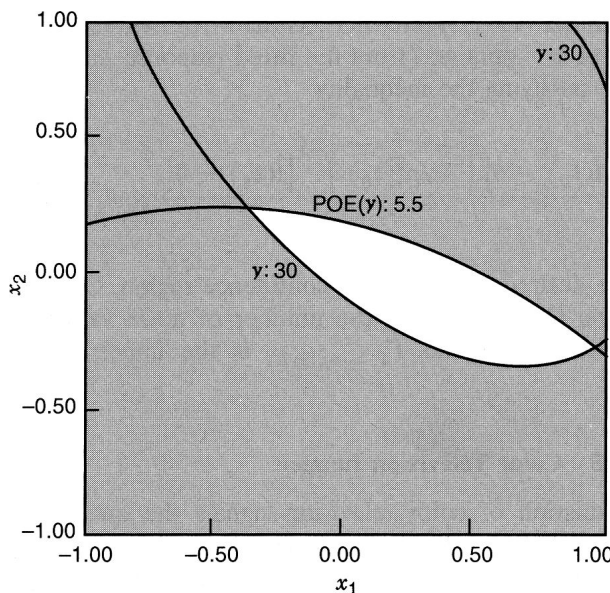


**Figure 10.17** Overlay of the mean and POE contours for Example 10.4, with the open region indicating satisfactory operating conditions for process mean and variance.

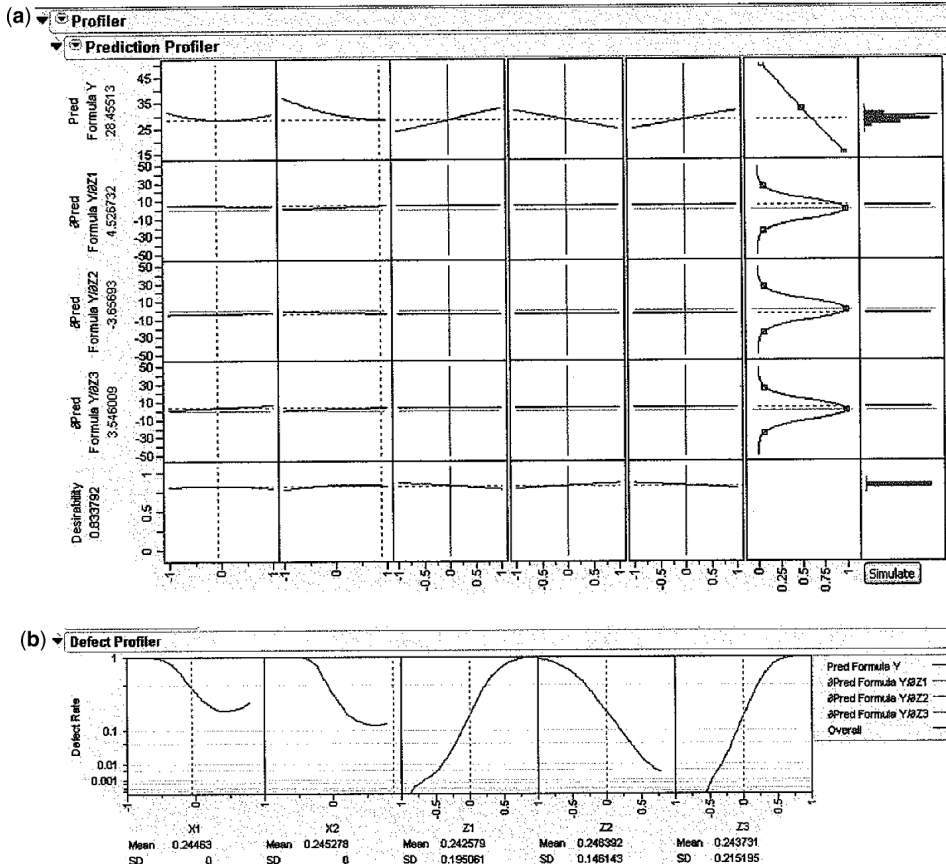


**Figure 10.18** Optimal solution to Example 10.4 using the response prediction profiler in JMP.  
**(a)** Prediction profiler output from JMP. **(b)** Defect profiler.

profiler from JMP. It provides predictions of how the defect rate is affected by changing the levels of the design factors. The output indicates that if the mean of the noise variable  $z_1$  can be moved from zero towards its low level, the defect rate will be reduced. Similarly, if the mean of the noise variable  $z_2$  can be moved from zero towards its high level and/or the mean of the noise variable  $z_3$  can be moved from zero towards  $-0.5$ , the defect rate will also be reduced. Therefore, if the experimenter has the additional flexibility of setting the mean or target level of any of the noise variables in the situation, additional improvement in process performance can be obtained.

**Confidence Regions on Minimum Process Variance Conditions** In the previous illustration we displayed a region of low process variance, where the process variance is the variability produced by the lack of sufficient control of noise variables in the process. At times, what is depicted may be a line or a plane or even a point in the space of the control variables. If minimizing process variance is important, then some characterization of the **precision** of the estimates of these conditions may also be crucial. For example, a line of minimum variance may represent a set of conditions that are unsatisfactory to the

investigator. It would be helpful then to gain some sense of how far away from the line the investigator can move and still maintain no significant difference from the minimum variance conditions. The principle here is analogous to that discussed in Chapter 6, where confidence regions were discussed for stationary points in cases where a single response surface is considered. Consider, once again, Equation 10.18 with the solution  $\mathbf{x}_0$  representing a locus of points or a single point of minimum process variance. Let  $\mathbf{t}_0$  represent the true condition of minimum variance—that is,

$$\mathbf{l}(\mathbf{t}_0) = \boldsymbol{\gamma} + \hat{\Delta}'\mathbf{t}_0 = \mathbf{0}$$

One must keep in mind that  $\mathbf{c}$  is an unbiased estimate of  $\boldsymbol{\gamma}$ , and  $\hat{\Delta}$  is an unbiased estimate of the matrix  $\Delta$ . Now, assuming normal errors around the response model containing  $\mathbf{x}$  and  $\mathbf{z}$ , we have

$$\frac{[\hat{\mathbf{l}}(\mathbf{t}_0) - \mathbf{0}]' \widehat{[\text{Var } \hat{\mathbf{l}}(\mathbf{t}_0)]^{-1}} [\hat{\mathbf{l}}(\mathbf{t}_0) - \mathbf{0}]}{r_z} \sim F_{r_z, \text{df}(E)}$$

where  $\hat{\mathbf{l}}(\mathbf{t}_0) = \mathbf{c} + \hat{\Delta}'\mathbf{t}_0$ , and  $\widehat{[\text{Var } \hat{\mathbf{l}}(\mathbf{t}_0)]^{-1}}$  is the variance–covariance matrix of  $\hat{\mathbf{l}}(\mathbf{t}_0)$  with  $\sigma^2$  replaced by the error mean square  $s^2$ . See Graybill (1976) or Myers and Milton (1991). Here  $\text{df}(E)$  is the error degrees of freedom for the estimator  $s^2$  of  $\sigma^2$  obtained from the fitted response model. As a result the conditions  $\mathbf{t}_0$  satisfying the inequality

$$\frac{[\hat{\mathbf{l}}(\mathbf{t}_0) - \mathbf{0}]' \widehat{[\text{Var } \hat{\mathbf{l}}(\mathbf{t}_0)]^{-1}} [\hat{\mathbf{l}}(\mathbf{t}_0) - \mathbf{0}]}{r_z} \leq F_{1-\alpha, r_z, \text{df}(E)} \quad (10.19)$$

represent the desired  $100(1 - \alpha)\%$  confidence region. One should note that  $r_z$  in Equation 10.19 denotes the number of noise variables that interact with control variables, and  $F_{1-\alpha, r_z, \text{df}(E)}$  is the upper percentile point of  $F_{r_z, \text{df}(E)}$ .

**Example 10.5 Color Television Images** In the transmission of color television signals the quality of the decoded signals is determined by the **PSNRs** (power signal-to-noise ratios in electronics engineering) in the image transmitted. The response here refers to the quality (coarse versus detailed) in the reception of transmitted signals in decibels. The control factors are  $x_1$  (number of tabs in a filter) and  $x_2$  (sampling frequency). These two factors form an inner array, while the noise or outer array involves  $z_1$  (number of bits in an image) and  $z_2$  (voltage applied). The design used is a  $3^2 \times 2^2$  crossed array, and the data appear in Table 10.9.

The model to be used is Equation 10.7. The  $3^2$  in the inner array allows for a second-order model in the control variables. For this specific case, the model can be written as

$$\begin{aligned} y(\mathbf{x}, \mathbf{z}) = & \beta_0 + \beta_1 x_1 + \beta_2 x_2 + \beta_{11} x_1^2 + \beta_{22} x_2^2 + \beta_{12} x_1 x_2 + \gamma_1 z_1 \\ & + \gamma_2 z_2 + \delta_{11} x_1 z_1 + \delta_{12} x_1 z_2 + \delta_{21} x_2 z_1 + \delta_{22} x_2 z_2 + \varepsilon \end{aligned} \quad (10.20)$$

**TABLE 10.9 Color TV Image Data for Example 10.5**

Factor Combination	$x_1$	$x_2$	$z_1$	Code Levels		
				-1	0	1
$x_1$ (number of tabs in a filter)				5	13	21
$x_2$ (sampling frequencies)				6.25	9.875	13.5
$z_1$ (number of bits of an image)				256	512	(bits)
$z_2$ (voltage applied)				100	200	(volts)
			$z_1$	-1	-1	1
			$z_2$	-1	1	-1
(1)	-1	-1		33.5021	41.2268	25.2683
(2)	-1	0		35.8234	38.0689	32.7928
(3)	-1	1		33.0773	31.8435	36.2500
(4)	0	-1		30.4481	41.2870	15.1493
(5)	0	0		34.8679	40.2276	27.7724
(6)	0	1		35.2202	37.1008	33.3280
(7)	1	-1		21.1553	34.1086	0.7917
(8)	1	0		27.6736	38.1477	15.5132
(9)	1	1		32.1245	38.1193	26.1673
						32.1622

The process variance is determined by taking the variance operator in Equation 10.20, namely,

$$\begin{aligned}
 \text{Var}_z[y(\mathbf{x}, \mathbf{z})] &= [\gamma_1^2 + \gamma_2^2 + \delta_{11}^2 x_1^2 + \delta_{12}^2 x_1^2 + \delta_{21}^2 x_2^2 + \delta_{22}^2 x_2^2 + 2\gamma_1(\delta_{11}x_1 + \delta_{21}x_2) \\
 &\quad + 2\gamma_2(\delta_{12}x_1 + \delta_{22}x_2) + 2(\delta_{11}\delta_{21} + \delta_{12}\delta_{22})x_1x_2]\sigma_z^2 + \sigma^2 \\
 &= [(\gamma_1 + \delta_{11}x_1 + \delta_{21}x_2)^2 + (\gamma_2 + \delta_{12}x_1 + \delta_{22}x_2)^2]\sigma_z^2 + \sigma^2 \\
 &= \left[ \left( \frac{\partial y(\mathbf{x}, \mathbf{z})}{\partial z_1} \right)^2 + \left( \frac{\partial y(\mathbf{x}, \mathbf{z})}{\partial z_2} \right)^2 \right] \sigma_z^2 + \sigma^2 \\
 &= \{[l_1(\mathbf{x})]^2 + [l_2(\mathbf{x})]^2\} \sigma_z^2 + \sigma^2
 \end{aligned} \tag{10.21}$$

Note the role of the derivatives  $l_1(\mathbf{x})$  and  $l_2(\mathbf{x})$  in the process variance function. Again, we seek  $\mathbf{x}_0$  that results in minimum process variance. Here we are assuming that the  $\pm$  levels of  $z_1$  and  $z_2$  are at  $\pm\sigma_z$ . Note that the computation of the location of estimated minimum process variance does not depend on knowledge of  $\sigma_z$ .

The least squares fit of the model in Equation 10.20 is given by

$$\begin{aligned}
 \hat{y}(\mathbf{x}, \mathbf{z}) &= 33.389 - 4.175x_1 + 3.748x_2 + 3.348x_1x_2 - 2.328x_1^2 \\
 &\quad - 1.867x_2^2 - 4.076z_1 + 2.985z_2 - 2.324x_1z_1 \\
 &\quad + 1.932x_1z_2 + 3.268x_2z_1 - 2.073x_2z_2
 \end{aligned}$$

All coefficients are significant, and the root error mean square is 0.742 dB. The slopes in the  $z_1$  and  $z_2$  directions are given by

$$\begin{aligned}\hat{l}_1(x_1, x_2) &= -4.076 - 2.234x_1 + 3.268x_2 \\ \hat{l}_2(x_1, x_2) &= 2.985 + 1.932x_1 - 2.073x_2\end{aligned}$$

Both  $x_1$  and  $x_2$  can be used to exert control on the process variance because both control  $\times$  noise interactions are significant.

The point of minimum estimated process variance is found by setting  $\hat{l}_1(\mathbf{x}) = 0$  and  $\hat{l}_2(\mathbf{x}) = 0$ . This gives the result

$$\mathbf{x}_0 = \begin{bmatrix} x_{1,0} \\ x_{2,0} \end{bmatrix} = \begin{bmatrix} -0.874 \\ 0.625 \end{bmatrix}$$

which lies in the experimental design region. For the confidence region around this value, we have

$$\widehat{\text{Var}[\hat{l}_1(\mathbf{x})]} = \widehat{\text{Var}[\hat{l}_2(\mathbf{x})]} = 0.0154 + 0.0230x_1^2 + 0.0230x_2^2$$

This result comes from the variances of the  $\hat{\delta}_{ij}$  and  $c_i$  values. Keep in mind that these estimators are uncorrelated. Thus for the confidence region, Equation 10.19 becomes

$$\frac{\hat{\mathbf{l}}(\mathbf{t})' [\widehat{\text{Var}[\hat{\mathbf{l}}(\mathbf{t})]}]^{-1} \hat{\mathbf{l}}(\mathbf{t})}{2} \leq F_{2,24,0.05}$$

which reduces to

$$\frac{(-4.076 - 2.324t_1 + 3.68t_2)^2 + (2.985 + 1.932t_1 - 2.073t_2)^2}{0.0154 + 0.0230(t_1^2 + t_2^2)} \leq 6.8056$$

Any  $(t_2, t_2)$  that satisfies the above inequality falls inside the 95% confidence region on the *location of minimum process variance*. See Fig. 10.19. Two lines  $\hat{l}_1(\mathbf{x}) = 0$  and  $\hat{l}_2(\mathbf{x}) = 0$  shows intersection at  $\mathbf{x}_0 = (+0.874, 0.625)$ , the point of estimated minimum process variance. The shaded area displays the confidence region. Also included are the contours of constant *estimated mean response*, whose response surface is obtained using the expectation operator on Equation 10.20:

$$\begin{aligned}\widehat{E_z[y(\mathbf{x}, \mathbf{z})]} &= 33.3889 - 4.1752x_1 + 3.748x_2 \\ &\quad + 3.3485x_1x_2 - 2.3277x_1^2 - 1.8670x_2^2\end{aligned}$$

The notion of a robust product here implies the choice of  $(x_1, x_2)$  that gives *large response with low variance*. Notice that the stationary point for the mean response surface is a point of estimated maximum response. This stationary point, however, does not fall inside the confidence region for the location of minimum variance. The mean response surface is fairly flat in the region of small  $x_1$  and large  $x_2$ . As a result, very little is lost on the mean if one operates at  $\mathbf{x}_0$ , the point of minimum variance. Now, consider Fig. 10.20,

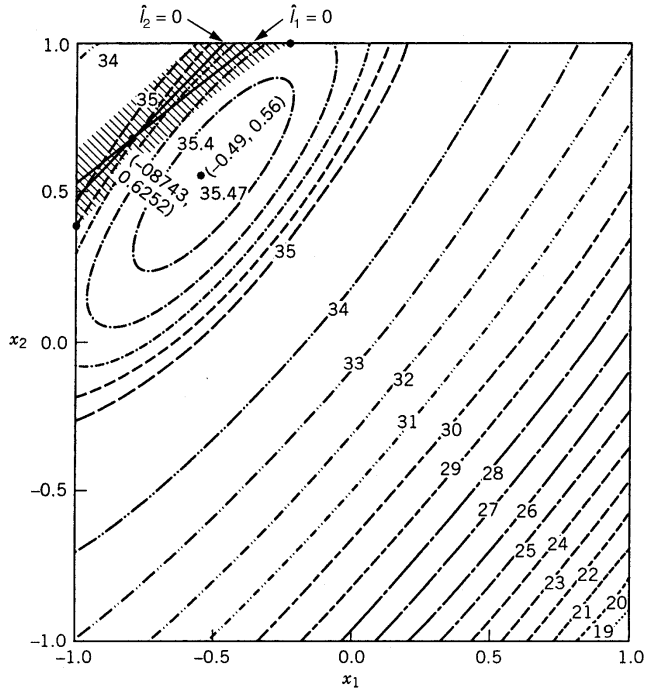


**Figure 10.19** Contours of constant mean decibels, point of estimated minimum variance, and 95% confidence region on location of process variance for Example 10.5.

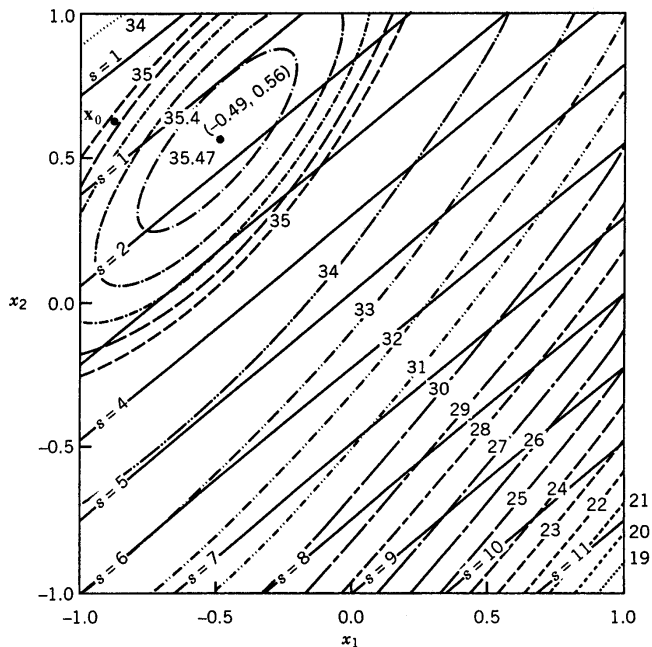


**Figure 10.20** Dual response surfaces on mean and standard deviation with points of minimum variance and maximum mean (Example 10.5).

where we have superimposed *contours of constant standard deviation*. Here,  $s$  is the estimated process standard deviation. Note that the standard deviation is stable in the upper left-hand corner. The estimated standard deviation at  $\mathbf{x}_0$  is 0.80. Note that the standard deviation becomes less stable as one moves away from the 95% confidence region.

From the display given in Figs 10.19 and 10.20, the researcher learns a great deal about the process. The most robust process will clearly be in the area of small  $x_1$  and large  $x_2$ . The trough created by the shaded area in Fig. 10.19 shows considerable flexibility as far as optimum conditions are concerned. At  $\mathbf{x}_0$ , the estimated process mean is approximately 35 dB, and the estimated process standard deviation is 0.8.

In this example the experimenter is fortunate that the intersection of  $\hat{l}_1(\mathbf{x}) = 0$  and  $\hat{l}_2(\mathbf{x}) = 0$  occurs inside the design region. If this does not occur, then one must use other response surface methods in dealing with the process variance.

#### 10.4.5 Estimation of the Process Variance

In the previous section we dealt with the use of a mean and variance response surface for learning about the influence of the control and noise design variables on the process mean and process variance. We have also discussed the use of these two response surfaces for finding robust conditions on the control variables, where some type of compromise is chosen for accommodating goals on the mean response but achieving a sufficiently small process variance. It can be argued that the two response surfaces can be dealt with in a fashion similar to that discussed in Chapter 6, where we discussed multiple response surface analysis. It is not our intention to recommend a single “best” way of blending together the mean and variance response surfaces.

In many instances the procedure of determining the conditions that produce zero value for the derivatives (i.e., values for which  $\hat{l}_1 = 0, \hat{l}_2 = 0, \dots, \hat{l}_{r_z} = 0$ ) give coordinates that are not practical. There is no assurance that this stationary point will fall inside the region of the design in the control variables. As a result, **ridge analysis** is a reasonable approach for handling both the mean and variance response surfaces. This could provide two loci of points, each locus giving constrained optimum conditions, one locus for the mean and one for the variance. In what follows we will supply a few details for the case of the variance response surface. Before we embark on this discussion we will deal with the notion of appropriate estimation of the process variance.

For the case where the noise variables are uncorrelated, the variance response surface is given by Equation 10.10. In a more general setting [say, when the noise variables are correlated and  $\text{Var}(\mathbf{z}) = \mathbf{V}$ , where  $\mathbf{V}$  is an  $r_z \times r_z$  variance–covariance matrix], the process variance is

$$\text{Var}_{\mathbf{z}}[y(\mathbf{x}, \mathbf{z})] = \mathbf{l}'(\mathbf{x})\mathbf{V}\mathbf{l}(\mathbf{x}) + \sigma^2$$

where  $\sigma^2$  is the error variance for the model of Equation 10.7. Now, if one merely replaces  $\mathbf{l}(\mathbf{x})$  by the estimator from the data, and  $\sigma^2$  by the mean squared error from the fitted model,  $s^2$ , we have as an estimator of the process variance

$$\widehat{\text{Var}_{\mathbf{z}}[y(\mathbf{x}, \mathbf{z})]} = \tilde{\mathbf{l}}'(\mathbf{x})\mathbf{V}\tilde{\mathbf{l}}(\mathbf{x}) + s^2 \quad (10.22)$$

The result in Equation 10.22 is not an unbiased estimator, because  $E[\tilde{\mathbf{l}}'(\mathbf{x})\mathbf{V}\hat{\mathbf{l}}(\mathbf{x})] \neq \mathbf{l}'(\mathbf{x})\mathbf{V}\mathbf{l}(\mathbf{x})$ . In fact,

$$E\{\widehat{\text{Var}_z[y(\mathbf{x}, \mathbf{z})]}\} = \mathbf{l}'(\mathbf{x})\mathbf{V}\mathbf{l}(\mathbf{x}) + \sigma^2\text{tr}(\mathbf{VC}) + \sigma^2 \quad (10.23)$$

where the matrix  $\mathbf{C}$  is simply  $\text{Var}[\hat{\mathbf{l}}(\mathbf{x})]\sigma^2$ . In other words,  $\mathbf{C}$  is the covariance of the  $\hat{\mathbf{l}}$ 's, apart from  $\sigma^2$ . Recall the role of this matrix in the confidence region on the location of process variance. See Equation 10.19. For standard experimental designs this matrix will be a diagonal matrix, since the  $c_i$ , and  $\hat{\delta}_{jk}$  will all be uncorrelated. However, it should be noted that the diagonal elements, that is, the variances of the  $\hat{\mathbf{l}}_i(\mathbf{x})$ , depend on  $\mathbf{x}$ . Now, from Equation 10.23 one can work out an unbiased estimator of the process variance, namely,

$$s_z^2[y(\mathbf{x}, \mathbf{z})] = \tilde{\mathbf{l}}'(\mathbf{x})\mathbf{V}\hat{\mathbf{l}}(\mathbf{x}) + s^2(1 - \text{tr } \mathbf{VC}) \quad (10.24)$$

or, for the cases that we have dealing with in this chapter, when the noise variables are uncorrelated with unit variances,

$$s_z^2[y(\mathbf{x}, \mathbf{z})] = \tilde{\mathbf{l}}'(\mathbf{x})\hat{\mathbf{l}}(\mathbf{x}) + s^2(1 - \text{tr } \mathbf{C}) \quad (10.25)$$

The estimator in Equation 10.25 will often differ only slightly from the simpler but biased estimator in Equation 10.22. In fact, we used the latter in examples in previous sections. However, there will be occasions when the difference between the two will not be negligible. This is particularly true when the process variance is being computed on or near the design perimeter, because  $\text{tr } \mathbf{C}$  becomes larger as one approaches the design perimeter. As a result, one cannot ignore  $s_z^2[y(\mathbf{x}, \mathbf{z})]$  as an estimator of process variance.

In a comparison of the biased estimator of Equation 10.22 and the unbiased estimator of Equation 10.25, it can be shown that unless the error df in the fitting of the original model in Equation 10.7 is 2 or less, the unbiased estimator in Equation 10.25 is preferable. We will not present the details of that study here. In what follows we discuss the use of the estimated process variance in a ridge-analysis-type procedure for the process variance.

**Ridge Analysis for Process Variance** The reader should recall from Chapter 6 that the purpose of ridge analysis is to produce a locus of points that are constrained optima on the response. This produces a ridge in the design space, which could give rise to future experiments, or could lead to interesting conditions that are of course confined to the experimental region. Applying the same notion to the process variance, we have

$$\min_{\mathbf{x}} \{s_z^2[y(\mathbf{x}, \mathbf{z})]\} \quad \text{subject to} \quad \mathbf{x}'\mathbf{x} = R^2 \quad (10.26)$$

That is, we will develop a locus of points that are each a point of conditionally minimum variance. The use of Lagrange multipliers as in Chapter 6 requires

$$\frac{\partial}{\partial \mathbf{x}} \left[ \tilde{\mathbf{l}}'(\mathbf{x})\hat{\mathbf{l}}(\mathbf{x}) + s^2(1 - \text{tr } \mathbf{C}) - \lambda(\mathbf{x}'\mathbf{x} - R^2) \right] \quad (10.27)$$

Now, if the experimental design renders the noise main effects independent of the control  $\times$  noise interactions, and the control  $\times$  noise interaction independent of each other, the matrix  $\mathbf{C}$  reduces to

$$\mathbf{C} = \begin{bmatrix} \mathbf{x}'\mathbf{D}_{11}\mathbf{x} + \text{Var } c_1 & & & \mathbf{0} \\ & \mathbf{x}'\mathbf{D}_{22}\mathbf{x} + \text{Var } c_2 & & \\ & & \ddots & \\ \mathbf{0} & & & \mathbf{x}'\mathbf{D}_{r_z,r_z}\mathbf{x} + \text{Var } c_{r_z} \end{bmatrix}$$

where  $\mathbf{D}_{jj}$  is an  $r_x \times r_x$  matrix containing  $\text{Var}(\hat{\delta}_{ij})/\sigma^2$  on the  $i$ th main diagonal. Here  $\mathbf{x}' = [x_1, x_2, \dots, x_{r_x}]$ . Thus  $\text{tr}(\mathbf{C})$  becomes

$$\text{tr}(\mathbf{C}) = \sum_{j=1}^{r_z} \mathbf{x}'\mathbf{D}_{jj}\mathbf{x} + \sum_{j=1}^{r_z} c_j$$

We will not supply the details in the differentiation of Equation 10.27. However, setting the partial derivatives in Equation 10.27 equal to  $\mathbf{0}$  gives

$$\left[ \hat{\Delta}\hat{\Delta}' - \sigma^2 \sum_{j=1}^{r_z} \mathbf{D}_{jj} - \mu \mathbf{I} \right] \mathbf{x} = -\hat{\Delta}\mathbf{c} \quad (10.28)$$

where  $\mathbf{c}' = [c_1, c_2, \dots, c_{r_z}]$ . To ensure that solutions are points of constrained minimum variance, values of  $\mu$ , smaller than the smallest eigenvalue of  $\hat{\Delta}\hat{\Delta}' - s^2 \sum_{j=1}^{r_z} \mathbf{D}_{jj}$  are to be used in Equation 10.28.

**Example 10.6 Application of Ridge Analysis** Consider a situation in which there are two control variables and three noise variables. The design variables  $x_1$ ,  $x_2$ ,  $z_2$ , and  $z_3$  are varied in a 23-run combined array design that is similar to the one used in Example 10.3. It is a variation of a CCD. The design and data are given in Table 10.10.

Note that as before the design is not a complete CCD. The factorial portion is a  $2^{5-1}$ , and there are no axial points in  $z_1$ ,  $z_2$ ,  $z_3$ , because we are not fitting quadratic terms in the  $z$ 's. The fitted response model is

$$\begin{aligned} \hat{y} = & 30.382 - 2.925x_1 - 4.136x_2 + 2.855x_1x_2 + 2.596x_1^2 \\ & + 2.175x_2^2 + 2.736z_1 - 2.326z_2 + 2.332z_3 \\ & - 0.278x_1z_1 + 0.893x_1z_2 + 2.574x_1z_3 + 1.999x_2z_1 \\ & - 1.430x_2z_2 + 1.547x_2z_3 \end{aligned}$$

The important derivatives in the  $z_1$ ,  $z_2$ , and  $z_3$  directions are given by

$$\hat{\mathbf{l}}(\mathbf{x}) = \begin{bmatrix} \hat{l}_1 \\ \hat{l}_2 \\ \hat{l}_3 \end{bmatrix} = \begin{bmatrix} 2.736 - 0.278x_1 + 1.999x_2 \\ -2.326 + 0.893x_1 - 1.430x_2 \\ 2.332 + 2.574x_1 + 1.547x_2 \end{bmatrix}$$

**TABLE 10.10** The Combined Array Design for Example 10.6

Observation	$x_1$	$x_2$	$z_1$	$z_2$	$z_3$	$y$
1	1	-1	1	-1	-1	30.0250
2	-1	1	-1	-1	-1	30.0007
3	-1	-1	1	-1	-1	49.8009
4	-1	-1	-1	1	-1	43.4717
5	-1	-1	-1	-1	1	44.1905
6	1	1	1	-1	-1	31.3911
7	1	1	-1	1	-1	16.0333
8	1	1	-1	-1	1	35.3823
9	1	-1	1	1	-1	30.3383
10	1	-1	1	-1	1	36.3417
11	1	-1	-1	1	1	36.1355
12	-1	1	1	1	-1	30.1289
13	-1	1	1	-1	1	41.3179
14	-1	1	-1	1	1	22.7125
15	-1	-1	1	1	1	43.2415
16	1	1	1	1	1	39.1733
17	-2	0	0	0	0	46.1502
18	2	0	0	0	0	36.0689
19	0	-2	0	0	0	47.3903
20	0	2	0	0	0	31.4659
21	0	0	0	0	0	30.8109
22	0	0	0	0	0	30.7499
23	0	0	0	0	0	30.9655

The method of ridge analysis requires the minimization of  $\hat{\mathbf{H}}\hat{\mathbf{H}} - s^2 \text{tr}(\mathbf{C})$  subject to the constraint  $\sum_{i=1}^2 x_i^2 = 2$ . Here we are assuming that the noise variables are uncorrelated with  $\sigma_z^2 = 1.0$  in the coded metric of the noise variables. In this case one needs to solve Equation 10.28 with particular values of  $\mu$ . The matrix  $\sum_{j=1}^{r_z} \mathbf{D}_{jj}$  simple becomes  $\frac{3}{16} \mathbf{I}_2$ , and  $s^2 = 0.920$  from the analysis. As a result,

$$s^2 \sum_{j=1}^2 \mathbf{D}_{jj} = \begin{bmatrix} 0.1725 & 0 \\ 0 & 0.1725 \end{bmatrix}$$

while the matrix  $\hat{\Delta}$  is the  $2 \times 3$  matrix containing the control  $\times$  noise interaction coefficients in the fitted regression. The eigenvalues of  $\hat{\Delta}\hat{\Delta} - s^2 \sum_{j=1}^{r_z} \mathbf{D}_{jj}$  turn out to be 9.995 and 5.594. As a result, we replace  $\mu$  with values smaller than 5.594. It turns out that for  $\mu = -0.486$  the solution to Equation 10.28 falls on a circle of radius  $\sqrt{2}$ . Indeed,  $(-0.0156, -1.41405)$  is the point of constrained minimum variance at radius  $\sqrt{2}$ . Figure 10.21 displays the result of the ridge analysis. All points on the path in the figure are points of constrained minimum process variance. Obviously, future experiments with  $x_1$  near zero and smaller values of  $x_2$  might be considered.

In much of what has preceded we have built mean and variance response surfaces that are generated from a single response surface that is developed from a model with noise and control variables in the same model. We now discuss alternative methods of constructing the variance model.

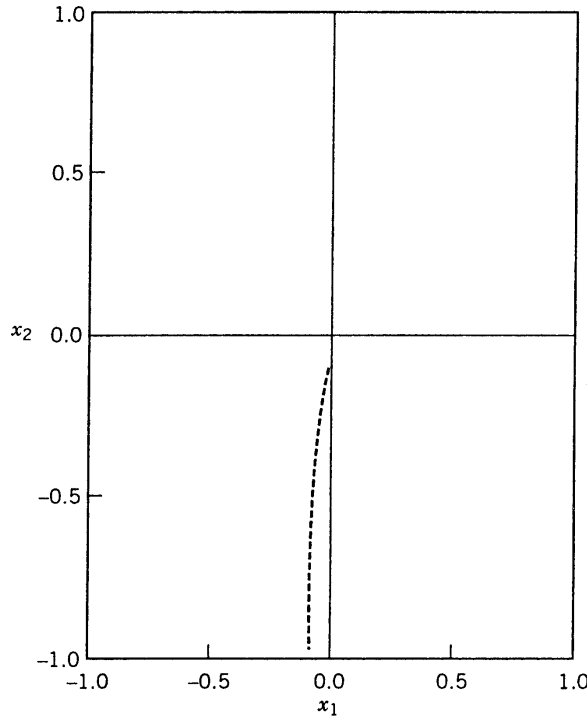


**Figure 10.21** Locus of points of minimum constrained process variance for Example 10.6.

#### 10.4.6 Direct Variance Modeling

Bartlett and Kendall (1946) in a classical paper showed that if some design points are replicated, the variance can be modeled directly without serious violation of assumptions by using a **log-linear model** of the

$$\log s_i^2 = \mathbf{x}'_i \boldsymbol{\gamma} + \varepsilon_i^*, \quad i = 1, 2, \dots, d \quad (10.29)$$

where  $s_i^2$  is a sample variance obtained from, say,  $n$  observations taken at each of  $d$  design points. The  $\mathbf{x}'_i \boldsymbol{\gamma}$  portion of the model refers to a linear model in a set of design variables. They demonstrated that if the errors are normal around the mean model; that is, if

$$y_{ij} = \mathbf{x}'_i \boldsymbol{\beta} + \varepsilon_{ij} \sigma_i, \quad i = 1, 2, \dots, d, \quad j = 1, 2, \dots, n$$

where  $\varepsilon_{ij} \sim N(0, 1)$  and  $\ln \sigma_i^2 = \mathbf{x}'_i \boldsymbol{\gamma}$ , then the use of the model in Equation 10.29 leads to approximately normal errors with constant variance. Thus ordinary least squares may be appropriate for modeling variance in a log-linear procedure. Carroll and Ruppert (1988), Engle (1992), Grego (1993), and Vining and Bohn (1998) discuss further details of variance modeling.

Taguchi revived interest in variance modeling. There are many situations where the variance can be directly modeled using the log-linear model approach. These include replicated designs (not all design points have to be replicated) and situations where

**repeat measurements** rather than true replicates are taken at the design points, Vining and Schaub (1996) discuss how one might allocate replicate runs in designs so as to obtain a variance model. In Example 3.3 we illustrated how a variance model could be built using duplicate runs. In this situation, the variance reflects **within-run variability**, but usually that is the portion of the total variability that is of most interest to the experimenter. Indeed, a crossed array design also lends itself to variance modeling.

The use of the log-linear model also often results in *simplicity*. The log transformation often reduces the effects of curvature and interaction, thereby making the results easier to interpret.

Once a log-linear variance model is fitted, the mean response surface model in the control variables can be found in the usual way as discussed in Chapter 6. Thus the dual response surface approach for finding robust or optimum conditions can be carried out. Vining and Myers discuss the approach, with illustrations, in their contribution to the panel discussion edited by Nair (1992). Also see Vining and Myers (1990).

**Example 10.7 The Wave Solder Experiment** Consider Example 10.1 where it was of interest to determine conditions on the control variables that produce a low value of response (solder defects per million joints) but also provide consistency (low variability). The data in Example 10.1 were used to develop two models, one for the mean response (standard linear regression model) and one for the variance via the log-linear variance model described here. Recall that the crossed array contains a  $2^{5-2}$  inner array design and a  $2^{3-1}$  in the outer array. Thus, four outer array points can be used for the sample variances. The fitted models, including significant terms, are given by

$$\hat{y} = 197.175 - 28.525x_1 + 57.975x_2$$

for the mean and

$$\ln(s^2) = 7.4155 - 0.2067x_1 - 0.0309x_2$$

for the variance. Here  $x_1$  is the solder pot temperature and  $x_2$  is the flux density. Figure 10.22 shows the graphical analysis involving both models. The mean and the standard deviations are plotted. The latter was found via the expression

$$s = [e^{7.4155 - 0.2067x_1 - 0.0309x_2}]^{1/2}$$

As one would expect from the analysis in Example 10.1, high temperature and low flux density minimize the mean number of errors and the variability simultaneously. However, the graphical dual response surface procedure allows the user to see tradeoffs for better understanding of the process. For the example the user may be dissatisfied with the extreme solder temperature and flux density, particularly the temperature. The graphs provide alternative conditions with resulting mean and variance estimates. It would be of interest to see the results when the variance model is computed from the **variance operator** on a model containing both control and noise variables—that is, the procedure discussed in Sections 10.4.3 and 10.4.4. See Exercise 10.25.

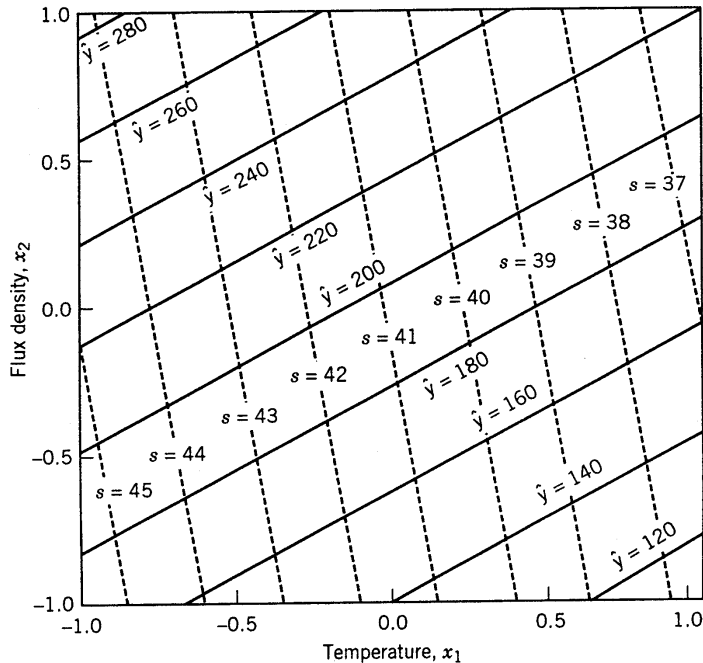


**Figure 10.22** Mean and variance models for wave soldering from Example 10.7.

#### 10.4.7 Use of Generalized Linear Models

Much of this chapter has dealt with joint modeling of the mean and variance. These two models can then be used simultaneously or jointly to arrive at candidates for operating conditions. It is instructive to discuss the role of the **generalized linear model** (GLM) in the formulation of the dual RSM procedure. We learned in Chapter 9 that GLMs are an important component in RSM modeling. Often responses are clearly nonnormal, for example, Poisson counts and binary responses. It turns out that even if the basic response is normal, the modeling of variance, either from replication or from nonreplication experiments, is an excellent example where the use of the GLM can be important. The reader will note from what follows that **iterative procedures** can easily be developed that involve two GLMs, one for the mean model and one for the variance model. We begin with the case where either a replicated experiment is made, or noise variables are involved in a crossed array.

**Case of Replicated Experiments or a Crossed Array** Let us assume initially that an experimental design allows for computation of sample variances  $s_i^2$  ( $i = 1, 2, \dots, d$ ) where  $d$  is the number of design points. The  $s_i^2$ -values come either from design replication or from variance information retrieved from an outer array. Earlier in the chapter we considered the modeling of the response  $\ln(s_i^2)$  for the **variance model**. The log transformation results in approximate homogeneity of variance, and hence ordinary least squares was considered in conjunction with a simple one-stage model development. Indeed, if the mean is to be modeled simultaneously with the variance, **weighted least squares** is an appropriate technique. Note, however, that in this approach the distribution of the  $s_i^2$  was not taken into

account. As a result the estimation procedure described in Section 10.4.6 clearly fails to exploit the distribution of the sample variance.

The random variables  $s_1^2, s_2^2, \dots, s_d^2$  are independent estimates of the variances at each design point. Consider now a typical value say  $s_i^2$ . If the responses  $y_{i1}, y_{i2}, \dots, y_{in}$  ( $n$  is the sample size at each design point) are normal, then

$$\frac{s_i^2(n-1)}{\sigma_i^2} \sim \chi_{n-1}^2$$

The  $\chi_\nu^2$  distribution is a special case of a **gamma distribution** with dispersion parameter  $2/\nu$ . Recall that the mean and variance of  $\chi_\nu^2$  are  $\nu$  and  $2\nu$  respectively. Thus a GLM fit for the variance model with a gamma distribution and known dispersion parameter is indicated. In addition, there are several attractive properties of the log-linear model for  $s_i^2$ , so a **log link** is certainly appropriate. As a result, an efficient procedure for the development of the models is as follows.

1. Use a gamma GLM on the  $s_i^2$ -responses with log link and dispersion parameter  $2/\nu$  to fit the variance model

$$\ln \sigma_i^2 = \mathbf{u}'_i \boldsymbol{\gamma} + \varepsilon_i \quad i = 1, 2, \dots, d$$

Here we use  $\mathbf{u}'_i \boldsymbol{\gamma}$  as opposed to  $\mathbf{x}'_i \boldsymbol{\beta}$  to allow for possible differences between mean model terms and variance model terms.

2. Use  $v_i = e^{\mathbf{u}'_i \hat{\boldsymbol{\gamma}}}$  as weights to compute  $\mathbf{V} = \text{diag}\{v_1, v_2, \dots, v_d\}$ . Here the  $\hat{\boldsymbol{\gamma}}$  come from the estimator in step 1.
3. Use  $\mathbf{V}$  as a weight matrix to fit the mean model

$$E(y_i) = \mathbf{x}'_i \boldsymbol{\beta}, \quad i = 1, 2, \dots, d$$

with  $\boldsymbol{\beta}$  estimated by  $\mathbf{b} = (\mathbf{X}' \mathbf{V}^{-1} \mathbf{X})^{-1} \mathbf{X}' \mathbf{V}^{-1} \mathbf{y}$  as a weighted least squares estimator.

It should be understood that the matrix  $\mathbf{X}$  contains model terms for the mean, and the model in Equation 10.29 can in fact contain a subset of these terms.

**Case of Unreplicated Experiments** For unreplicated experiments more complications arise in the case of the variance model, as was pointed out in earlier discussions in this chapter. In fact, as before, it should be noted that the quality of the variance model is very much dependent on a proper choice of the model for the mean, since the source of variability is the **squared residual**  $e_i^2 = (y_i - \mathbf{x}'_i \mathbf{b})^2$  for  $i = 1, 2, \dots, n$  design runs.

For the fundamental variance model we will still deal with the log-linear structure (Eq. 10.29). In order to motivate the use of the GLM for this case, consider the unobserved model error  $\varepsilon_i = y_i - \mathbf{x}'_i \boldsymbol{\beta}$ . As a starting point, we assume that

$$\sigma_i^2 = E(\varepsilon_i^2) = e^{\mathbf{u}'_i \boldsymbol{\gamma}} \tag{10.30}$$

where  $\varepsilon_i^2 \sim \sigma_i^2 x_i^2$ .

**Maximum Likelihood Estimation of  $\boldsymbol{\beta}$  and  $\boldsymbol{\gamma}$  Using GLM** In the dual modeling procedure for unreplicated experiments it is helpful to achieve efficiency of joint estimation

of the mean model coefficients  $\beta$  and the variance model coefficients  $\gamma$  through maximum likelihood with the GLM as the analytical tool. We can write the mean model as  $\mathbf{y} = \mathbf{X}\beta + \varepsilon$  with  $\text{Var}(\varepsilon) = \mathbf{V}_{n \times n}$  and again  $v_i = e^{\mathbf{u}'\gamma}$ . Now, the MLE for  $\beta$  is merely weighted least squares,

$$\mathbf{b} = (\mathbf{X}'\mathbf{V}^{-1}\mathbf{X})^{-1}\mathbf{X}'\mathbf{V}^{-1}\mathbf{y}$$

If we use the random vector  $\mathbf{s}' = (\varepsilon_1^2, \varepsilon_2^2, \dots, \varepsilon_n^2)$ , we have a set of independent  $\chi_1^2$  random variables with the properties shown in Equation 10.30. It is interesting, though not surprising, that if we consider maximum likelihood estimation for  $\beta$  and  $\gamma$ , two separate algorithms emerge. However, the maximum likelihood estimator of  $\beta$  involves  $\gamma$  through the matrix  $\mathbf{V}$ , and the maximum likelihood estimator of  $\gamma$  clearly involves  $\beta$ , since the data in the variance model, namely the  $\varepsilon_i$ , involve  $\beta$ . As a result, an iterative procedure is required. We will not write the likelihood function here, but details appear in Aitken (1987). Aitken also pointed out the simplicity provided by the fact that computation of the maximum likelihood estimator for both  $\beta$  and  $\gamma$  can be done with GLMs with an identity link and a normal distribution on the mean model for estimation of  $\beta$  and a log link with a gamma distribution on the variance model for estimation of  $\gamma$ . Indeed, these two procedures can be combined into an iterative procedure. The dispersion parameter for the gamma link is again equal to 2. We must use the **squared residuals**  $e_i^2 = (y_i - \mathbf{x}_i'\mathbf{b})^2$  as the data for the gamma GLM, and raw  $y_i$ -values as data for the normal GLM. The method follows:

1. Use OLS to obtain  $\mathbf{b}_0$  for the mean model  $y_i = \mathbf{x}_i'\beta + \varepsilon_i$ .
2. Use  $\mathbf{b}_0$  to compute  $n$  residuals  $e_i = y_i - \mathbf{x}_i'\mathbf{b}_0$  for  $i = 1, 2, \dots, n$ .
3. Use the  $e_i^2$  as data to fit the variance model with regressors  $\mathbf{u}$  and a log link with dispersion parameter 2. This is done via IRLS with GLM technology.
4. Use parameter estimates from step 3, namely the  $\hat{\gamma}_i$ , to form the matrix  $\mathbf{V}$ .
5. Use  $\mathbf{V}$  with weighted least squares to update  $\mathbf{b}_0$  to  $\mathbf{b}_1$ .
6. Go back to step 2 with  $\mathbf{b}_1$ , replacing  $\mathbf{b}_0$ .
7. Continue to convergence.

The entire algorithm for the model is not difficult to construct and is a useful alternative for dual estimation of the mean and variance models. However, it has the disadvantage that the estimation of the parameters in the variance model will be biased because the maximum likelihood estimation of  $\gamma$  does not allow for estimation of  $\beta$  in the formation of the residuals. A somewhat different procedure serves as an alternative. This procedure makes use of **restricted maximum likelihood** (REML), which was discussed briefly in Chapter 9. The REML procedure does adjust nicely for the bias due to estimation of  $\beta$  in the squared residuals. In addition, this procedure can also be put into a GLM framework.

**Restricted Maximum Likelihood for Dual Modeling** The source of the possible difficulties with ordinary maximum likelihood estimation as discussed above is that the response data for the variance model, namely the  $e_i^2$ , do not truly reflect  $\sigma^2$  unless the estimator  $\mathbf{b}$  is the true parameter vector  $\beta$ . As a result, one cannot expect the estimator of  $\gamma$  from the procedure to be unbiased. Of course, the amount of bias may be quite small. We will deal with this subsequently. However the IRLS procedure developed for REML is quite simple and should be considered by the practitioner.

Consider now  $E(e_i^2)$  for  $i = 1, 2, \dots, n$ . We know that for a weighted least squares procedure with weight matrix,

$$\begin{aligned} \text{Var}(\mathbf{e}) &= \text{Var} \begin{bmatrix} e_1 \\ e_2 \\ \vdots \\ e_n \end{bmatrix} = \text{Var} [\mathbf{I} - \mathbf{X}(\mathbf{X}'\mathbf{V}^{-1}\mathbf{X})^{-1}\mathbf{X}'\mathbf{V}^{-1}] \mathbf{y} \\ &= [\mathbf{I} - \mathbf{X}(\mathbf{X}'\mathbf{V}^{-1}\mathbf{X})^{-1}\mathbf{X}'\mathbf{V}^{-1}] \mathbf{V} [\mathbf{I} - \mathbf{X}(\mathbf{X}'\mathbf{V}^{-1}\mathbf{X})^{-1}\mathbf{X}'\mathbf{V}^{-1}]' \\ &= \mathbf{V} - \mathbf{X}(\mathbf{X}'\mathbf{V}^{-1}\mathbf{X})^{-1}\mathbf{X}' \end{aligned} \quad (10.31)$$

Since  $E(e_i) = 0$ , then  $E(e_i) = \text{Var}(e_i)$ . The matrix  $\mathbf{X}(\mathbf{X}'\mathbf{V}^{-1}\mathbf{X})^{-1}\mathbf{X}'$  may seem like a **hat matrix** as defined in ordinary multiple regression. However, the matrix that is most like a hat matrix for weighted regression is

$$\mathbf{H} = \mathbf{V}^{-1/2} \mathbf{X}(\mathbf{X}'\mathbf{V}^{-1}\mathbf{X})^{-1}\mathbf{X}'\mathbf{V}^{-1/2} \quad (10.32)$$

The matrix  $\mathbf{H}$  in Equation 10.32 is indempotent and plays the same role as  $\mathbf{X}(\mathbf{X}'\mathbf{X})^{-1}\mathbf{X}'$  does for standard nonweighted (OLS) regression. Now,  $\mathbf{H}$  has the same diagonal elements as  $\mathbf{X}(\mathbf{X}'\mathbf{V}^{-1}\mathbf{X})^{-1}\mathbf{X}'\mathbf{V}^{-1}$ . Thus the diagonal elements in  $\mathbf{X}(\mathbf{X}'\mathbf{V}^{-1}\mathbf{X})^{-1}\mathbf{X}'$  from Equation 10.31 are also the diagonal elements of  $\mathbf{HV}$ . As a result, if we consider only the diagonal element involvement in Equation 10.31 we have

$$E(e_i^2) = \sigma_i^2 - h_{ii}\sigma_i^2. \quad (10.33)$$

where  $h_{ii}$  is the  $i$ th hat diagonal, that is, the  $i$ th diagonal of  $\mathbf{H}$  in Equation (10.32).

From Equation 10.33 the adjustment on the response is to use  $e_i^2 + h_{ii}\hat{\sigma}_i^2$  rather than  $e_i^2$ . Here the quantity  $h_{ii}\hat{\sigma}_i^2$  is a **bias correction**. The estimation of  $\boldsymbol{\beta}$  and  $\boldsymbol{\gamma}$  are interwoven and thus an iterative scheme is used, once again with the aid of GLM. The iterative procedure is as follows:

1. Calculate  $\mathbf{b}_0$  from OLS.
2. Calculate the  $e_i$  and a set of responses  $z_{0i} = e_i^2 + h_{ii}s^2$ , where  $h_{ii}$  are the OLS hat diagonals from  $\mathbf{X}(\mathbf{X}'\mathbf{X})^{-1}\mathbf{X}'$ , and  $s^2$  is the error mean square.
3. Use the  $z_{0i}$  ( $i = 1, 2, \dots, n$ ) as responses in GLM with a gamma distribution with dispersion parameter 2 and log link to calculate the initial  $\hat{\gamma}$ , say  $\hat{\gamma}_0$ .
4. Use the  $\hat{\gamma}_0$  to produce weights from  $\hat{\sigma}_i^2 = e_i^{u_i}\hat{\gamma}_0$ , and calculate the weight matrix  $\mathbf{V}_0$ . Calculate a new estimate of the vector  $\boldsymbol{\beta}$  as  $\mathbf{b}_1 = (\mathbf{X}'\mathbf{V}_0^{-1}\mathbf{X})^{-1}\mathbf{X}'\mathbf{V}_0^{-1}\mathbf{y}$ .
5. Calculate new residuals from  $\mathbf{b}_1$  and thus new  $z_i = e_i^2 + h_{ii}\hat{\sigma}_i^2$ , where  $h_{ii}$  is the  $i$ th hat diagonal from the matrix as written in Equation 10.32. Here  $\mathbf{V}$  is diagonal with the current values  $\hat{\sigma}_i^2$  on the main diagonal.
6. Use the new  $z_i$  as responses with a gamma GLM and log link to calculate a new  $\hat{\gamma}$ . Return to step 4 with  $\hat{\gamma}$  replacing  $\gamma_0$ .

The procedure continues with variance fitted values being used for weights in the development of the mean model. The mean model continues to provide the residuals from which the  $z_i$  are developed. Upon convergence, both mean and variance models emerge.

Note the close resemblance between the iterative procedure here and the maximum likelihood estimation algorithm in the previous section. The structure is the same except that at each iteration the gamma GLM is conducted with an **adjusted response**, the adjustment coming via  $h_{ii}\hat{\sigma}_i^2$ , where  $\hat{\sigma}_i^2$  is the estimator of  $\sigma_i^2$  from the previous iteration. The procedure does maximize a **restricted log likelihood**, which is not shown here. For more details the reader should see Engel and Huele (1996). For computational details, consult Harvey (1976). For further discussion of joint modeling with two interwoven GLMs see Nelder and Lee (1991) and Lee and Nelder (1998).

Obviously the correction for bias introduced through REML may be very helpful. However, for large experiments in which  $n \gg p$  where  $p$  is the number of parameters, the bias adjustment will often be negligible.

## 10.5 EXPERIMENTAL DESIGNS FOR RPD AND PROCESS ROBUSTNESS STUDIES

Taguchi advocated the use of crossed arrays (or product arrays) in which separate designs are used for the control and noise variables, and the final design is the cartesian product of the inner array (control array) and the outer array (noise array). Consequently, crossed array designs are sometimes called **product array** designs. The impetus for the design is the SNR, which is used to provide a summary statistic for the data in the outer array. In the same vein,  $\ln s^2$ , discussed in the previous section, is a basic response for variance modeling that can be employed in the crossed array design. However, we have also indicated how, in many instances, the crossed array design can be very costly, with degrees of freedom for interaction among the control factors often being sacrificed in favor of large numbers of degrees of freedom for control  $\times$  noise interactions. If robust parameter design and process robustness studies are to be accomplished, some control  $\times$  noise interaction must be exploited. However, a more efficient type of design is needed.

### 10.5.1 Combined Array Designs

The crossed array was clearly born out of the necessity of having considerable information on which to base the SNR. However, if one is attracted to the so-called **response model** approach in which a single model is constructed for both  $\mathbf{x}$  and  $\mathbf{z}$ , with the concomitant development of a mean response surface via  $E_{\mathbf{z}}[y(\mathbf{x}, \mathbf{z})]$  and a variance response surface via  $\text{Var}_{\mathbf{z}}[y(\mathbf{x}, \mathbf{z})]$ , then the crossed array is not needed. For this approach, the so-called **combined array**, in which a design is chosen to allow estimability of a reasonable model in  $\mathbf{x}$  and  $\mathbf{z}$ , is often less costly and quite sufficient. The word “combined” implies that separate arrays are not used, but rather one array that considers a combined  $\mathbf{x}$  and  $\mathbf{z}$  is the appropriate design. We have already seen the use of combined array designs in Examples 10.3, 10.4, and 10.6. Combined array designs have been suggested by many authors, including Welch et al. (1990), Shoemaker et al. (1991), Montgomery (1991), Lucas (1989, 1994), Myers, Khuri, and Vining (1992), and Box and Jones (1989).

Combined arrays offer considerably more flexibility in the estimation of effects or regression coefficients as well as savings in run size. The designs that are chosen generally

are those that offer the concept of **mixed resolution** [see Lucas (1989)]. That is, because control  $\times$  noise interactions are so vital in modeling as well as diagnostics, the resolution of the design for these interactions is higher than that for the noise  $\times$  noise interactions, which are generally considered not as important. The resolution for the control  $\times$  control interactions may also be higher if they are known to be important. In what follows we consider situations in which models are first-order (linear effects) or first-order plus interaction in the control variables.

**Example 10.8 A Mixed Resolution Design** This example, from Shoemaker et al. (1991) shows the superiority of the combined array. Suppose there are three control factors  $x_1, x_2, x_3$  and three noise factors  $z_1, z_2, z_3$ . An obvious crossed array is as follows:

$$2_{\text{III}}^{3-1} \times 2_{\text{III}}^{3-1} \quad (\text{design 1})$$

giving a total of 16 runs. This crossed array could be viewed as a  $2^{6-2}$  combined array with defining relations  $I = x_1x_2x_3 = z_1z_2z_3 = x_1x_2x_3z_1z_2z_3$ . Clearly no interactions in the control factors can be estimated. Six main effects are estimable only if no two factor interactions are important. In addition to six main effects, nine additional degrees of freedom are available, and they are all control  $\times$  noise interactions. These interactions are estimated at the expense of control  $\times$  control interactions.

As an alternative to design 1, a combined array offers considerably more flexibility. One such design would be a  $2^{6-2}$  with defining relations

$$I = x_1x_2x_3z_1 = z_1z_2z_3 = x_1x_2x_3z_2z_3 \quad (\text{design 2})$$

This design illustrates nicely the concept of mixed resolution. The design is resolution III with regard to noise  $\times$  noise interactions and resolution IV with regard to other interactions. Indeed, the three control  $\times$  control interactions can be estimated if one is willing to assume that  $x_1z_1, x_2z_1$ , and  $x_3z_1$  are negligible. In other words, one has the option to trade control  $\times$  noise interactions for control  $\times$  control interactions if appropriate assumptions are met.

**Example 10.9 A Design for Four Control and Two Noise Factors** Consider a situation in which there are four control factors  $x_1, x_2, x_3$ , and  $x_4$  and two noise factors  $z_1$  and  $z_2$ . Assume it is known that  $x_1x_4, x_2x_4$ , and  $x_3x_4$  are important. One potential crossed array design is the 32-run design

$$2_{\text{IV}}^{4-1} \times 2^2 \quad (\text{design 1})$$

The 31 available degrees of freedom include all six main effects and 12 two-factor interactions  $x_1x_2, x_1x_3, x_1x_4, z_1z_2, x_1z_1, x_2z_1, x_3z_1, x_4z_1, x_1z_2, x_2z_2, x_3z_2$ , and  $x_4z_2$ . This represents 18 degrees of freedom. This means that 13 degrees of freedom are being used to estimate higher-order control  $\times$  noise interactions. On the other hand, a combined array  $2_{\text{VI}}^{6-1}$  with 32 runs using

$$I = x_1x_2x_3x_4z_1z_2 \quad (\text{design 2})$$

is much more appropriate. This design allows estimation of all six main effects and all 15 two-factor interactions. Thus three higher-order interactions in design 1 are being exchanged for three control  $\times$  control interactions, which will likely be more important.

An alternative combined array for this situation can be found using **computer-generated design algorithms**. In this case the model contains six main effects and 12 two-factor interactions. There are many designs with less than 32 runs available. Here we show a 22-run design from Shoemaker et al. (1991):

$$\mathbf{D} = \begin{array}{cccccc} & x_1 & x_2 & x_3 & x_4 & z_1 & z_2 \\ \left[ \begin{array}{cccccc} 1 & 1 & 1 & 1 & 1 & -1 \\ 1 & -1 & -1 & 1 & 1 & -1 \\ 1 & -1 & -1 & -1 & -1 & -1 \\ 1 & 1 & -1 & 1 & -1 & -1 \\ 1 & 1 & 1 & 1 & -1 & 1 \\ 1 & -1 & 1 & 1 & 1 & 1 \\ -1 & 1 & 1 & 1 & -1 & -1 \\ 1 & -1 & 1 & -1 & -1 & -1 \\ 1 & -1 & 1 & -1 & 1 & -1 \\ -1 & -1 & 1 & -1 & -1 & 1 \\ 1 & 1 & -1 & -1 & 1 & 1 \\ -1 & -1 & -1 & -1 & 1 & 1 \\ -1 & 1 & -1 & -1 & 1 & -1 \\ -1 & 1 & 1 & 1 & -1 & -1 \\ 1 & -1 & -1 & 1 & -1 & 1 \\ -1 & 1 & -1 & 1 & 1 & 1 \\ -1 & -1 & -1 & 1 & -1 & -1 \\ 1 & 1 & 1 & -1 & -1 & 1 \\ -1 & -1 & 1 & 1 & 1 & -1 \\ -1 & 1 & 1 & -1 & 1 & 1 \\ -1 & 1 & -1 & -1 & -1 & 1 \\ -1 & -1 & 1 & 1 & -1 & 1 \end{array} \right] \end{array}$$

This design allows efficient estimation of all important terms and leaves three degrees of freedom for lack of fit.

### 10.5.2 Second-Order Designs

The flexibility of the combined array and the use of composite designs and computer-generated designs extend nicely to the use of models that are second-order in the control variables and even second-order interactions in the noise variables. Note that the pure quadratic terms for the noise factors are typically not needed, and hence are omitted from the model. Here the mixed resolution idea for the CCD is very important. Consider, for example, a crossed array in the case of three control variables and two noise variables. The control array may be a  $3^{3-1}$  and the noise array a  $2^2$  (36 total runs) to accommodate

a second-order model in the control variables, the terms  $z_1$ ,  $z_2$ , and  $z_1z_2$ , and appropriate control  $\times$  noise interactions. A CCD containing the components

- (i)  $2^{5-1}$  using  $I = x_1x_2x_3z_1z_2$
- (ii) axial points in the directions of the control factors

$$\begin{array}{cccccc} -\alpha & 0 & 0 & 0 & 0 \\ \alpha & 0 & 0 & 0 & 0 \\ 0 & -\alpha & 0 & 0 & 0 \\ 0 & \alpha & 0 & 0 & 0 \\ 0 & 0 & -\alpha & 0 & 0 \\ 0 & 0 & \alpha & 0 & 0 \end{array}$$

- (iii) and center runs:

$$\mathbf{0} \quad \mathbf{0} \quad \mathbf{0} \quad \mathbf{0} \quad \mathbf{0}$$

contains only 22 + center runs. This design will estimate  $x_1$ ,  $x_2$ ,  $x_1^2$ ,  $x_2^2$ ,  $x_1x_2$ ,  $z_1$ ,  $z_2$ ,  $z_1z_2$ , and six linear  $\times$  linear control  $\times$  noise interactions. This leaves seven lack-of-fit degrees of freedom. Again the crossed array often invests in a large number of higher-order control  $\times$  noise interactions. The combined array is more efficient.

To better illustrate the idea of mixed resolution, consider a situation in which there are four control variables and three noise variables. Suppose it is important for the response model to contain terms that are second order in the control variables (15 terms including the intercept),  $z_1$ ,  $z_2$ ,  $z_3$ , and 12 control  $\times$  noise interactions. (Keep in mind the importance of these interactions in building the variance model.) The CCD with mixed resolution in the factorial portion is quite useful. A  $2^{7-2}$  design is appropriate for the factorial portion. Consider the defining relations

$$I = x_1x_2x_3z_1z_2 = z_1z_2z_3x_4 = x_1x_2x_3x_4z_3$$

This design, then, involves the components

- (i)  $2^{7-2}$  with the above defining relations,
- (ii) axial points in the directions of the control factors

$x_1$	$x_2$	$x_3$	$x_4$	$z_1$	$z_2$	$z_3$
$-\alpha$	0	0	0	0	0	0
$\alpha$	0	0	0	0	0	0
0	$-\alpha$	0	0	0	0	0
0	$\alpha$	0	0	0	0	0
0	0	$-\alpha$	0	0	0	0
0	0	$\alpha$	0	0	0	0
0	0	0	$-\alpha$	0	0	0
0	0	0	$\alpha$	0	0	0

- (iii) and center runs.

$$\mathbf{0} \quad \mathbf{0} \quad \mathbf{0} \quad \mathbf{0} \quad \mathbf{0} \quad \mathbf{0} \quad \mathbf{0}$$

As a result, 40 observations plus center runs are used to estimate 30 model terms. Note the careful selection of the defining relations. By definition, the factorial portion is resolution IV. However, it is of higher resolution in the control variables, because no two  $x_i x_j$  interactions are aliased. In addition, it is effectively a higher-resolution design for the control  $\times$  noise interactions, because no two-factor control  $\times$  noise interactions are aliased with each other, nor are they aliased with two-factor interactions in the control variables.

### 10.5.3 Other Aspects of Design

Because the response surface approach puts so much emphasis on efficient estimation of the appropriate response model in  $\mathbf{x}$  and  $\mathbf{z}$ , with flexibility needed in the model terms selected, the combined array is altogether appropriate. In fact, the response model approach and the combined array are quite compatible. Many times the crossed array will involve an excessive number of experimental runs as a result of higher-order control  $\times$  noise interactions. Borkowski and Lucas (1997) discuss mixed resolution combined arrays in detail and give a catalog of designs. Borror and Montgomery (2000) present an application of a mixed resolution design and compare its performance with that of a conventional crossed array design. The dissertation by Borror (1998) is an extensive study of crossed array designs for the robust design problem. She suggests that optimal designs are very appropriate as alternatives to modified versions of standard RSM designs. Borror et al. (2002) develop methodology to evaluate the predictive performance of combined array designs for both the mean model and the slope of the response model (recall the critical role played by the slope with respect to variability in  $y$  transmitted from the noise variables). They point out that the prediction variance of the response model does not tell the complete story regarding design performance and that both the prediction variance of the mean model and the variance of the slope should be evaluated. Variance dispersion graphs and fraction of design space plots introduced in Chapter 8 are an ideal way to do this.

To develop the scaled prediction error variances necessary to study the mean and variance models obtained from the response model, we first review some details concerning least squares fitting of the response model. In general, we may write the response model in the general linear model form

$$\mathbf{y} = \mathbf{X}\boldsymbol{\beta} + \boldsymbol{\epsilon}$$

where the matrix  $\mathbf{X}$  contains  $1 + 2r_x + r_x(r_x - 1) + r_z + r_x r_z$  columns representing the intercept,  $\beta_0$ , the linear effects and pure quadratic effects of the  $r_x$  control variables, the two-factor interactions among the control variables, the main effects of the  $r_z$  noise variables, and the control-by-noise variable interactions, respectively. Similarly, the vector  $\boldsymbol{\beta}$  contains the parameters from the mean model corresponding to these factors (the intercept  $\beta_0$  and the elements of  $\boldsymbol{\beta}$ ,  $\mathbf{B}$ ,  $\boldsymbol{\gamma}$ , and  $\Delta$ ). The usual least squares estimate of  $\boldsymbol{\beta}$  is

$$\hat{\boldsymbol{\beta}} = (\mathbf{X}'\mathbf{X})^{-1}\mathbf{X}'\mathbf{y}.$$

The matrix  $\mathbf{C} = (\mathbf{X}'\mathbf{X})^{-1}$  is made up of several important submatrices and can be written as in Fig. 10.23. The submatrices,  $\mathbf{C}^{kl}$  ( $k, l = 1, 2, 3$ ) represent the variance–covariance

**Figure 10.23** The structure with submatrices of  $\mathbf{C} = (\mathbf{X}'\mathbf{X})^{-1}$ .

matrices for various subsets of the model parameters. For example,  $\mathbf{C}^{11}$  represents the variance–covariance matrix for the linear, quadratic, and interactions terms involving only the control variables. The submatrix  $\mathbf{C}^{22}$  represents the variance–covariance matrix for the linear terms of the noise variables, and  $\mathbf{C}^{33}$  represents the variance–covariance matrix for the control-by-noise interactions. The off-diagonal submatrix,  $\mathbf{C}^{23}$ , plays an important role in calculations of the slope variance. Each element of the submatrix is denoted by the subscripts  $i, j$ . For example,  $C_{34}^{33}$  is the element in the third row, fourth column of the submatrix  $\mathbf{C}^{33}$ .

The fitted second-order response model for the mean is

$$\hat{E}_{\mathbf{z}, \varepsilon} [y(\mathbf{x}, \mathbf{z})] = \hat{\beta}_0 + \mathbf{x}' \hat{\boldsymbol{\beta}} + \mathbf{x}' \hat{\mathbf{B}} \mathbf{x} = \mathbf{x}^{(2)'} \hat{\boldsymbol{\beta}}_1, \quad (10.34)$$

where the regression coefficient  $\hat{\beta}_0$ , the elements of the vector  $\hat{\beta}$ , and the elements of the matrix  $\hat{\mathbf{B}}$  are contained in the vector  $\hat{\beta}_1$ . Here,  $\mathbf{x}^{(2)'} \mathbf{y}$  is a vector of the controllable variables expanded to “model form” (in this case a second-order model) containing the constant 1, the first-order terms, the second-order terms, and the control-by-control factor interactions. The vector  $\hat{\beta}_1$  contains all the regression coefficients from the variables in  $\mathbf{x}^{(2)'} \mathbf{y}$ .

Borror et al. (2002) develop a scaled prediction error variance for the mean model in Equation 10.34. The general form for the variance of the prediction error is

$$\begin{aligned} \text{Var}_{\mathbf{z}, \varepsilon} & \left[ y(\mathbf{x}, \mathbf{z}) - \mathbf{x}^{(m)'} \hat{\boldsymbol{\beta}}^* \right] \\ & = \text{Var}_{\varepsilon} \left( \mathbf{x}^{(m)'} \hat{\boldsymbol{\beta}}^* \right) + \text{Var}_{\mathbf{z}, \varepsilon} (\mathbf{z}' \boldsymbol{\gamma} + \mathbf{x}' \boldsymbol{\Delta} \mathbf{z} + \sigma^2) \\ & = \sigma^2 \left[ \mathbf{x}^{(m)'} \mathbf{C}^{11} \mathbf{x}^{(m)} \right] + \text{Var}_{\mathbf{z}, \varepsilon} [\mathbf{z}' (\boldsymbol{\gamma} + \boldsymbol{\Delta}' \mathbf{x})] + \sigma^2 \end{aligned} \quad (10.35)$$

In Equation 10.35,  $\mathbf{x}$  is a fixed set of levels of the controllable variables,  $\mathbf{z}$  is a vector of random variables, and  $\boldsymbol{\gamma} + \boldsymbol{\Delta}' \mathbf{x}$  is a vector of constants. The actual observed value of  $y$  depends on the random variables  $\mathbf{z}$  and  $\varepsilon$  and the specified values of  $\mathbf{x}$ . Now, when  $\hat{y}$  the predicted value of the response, is computed,  $\mathbf{z}$  is fixed at  $\mathbf{z} = \mathbf{0}$ . Thus, the predicted value varies due to the inherent random variability due to the error  $\varepsilon$  and the variability associated with parameter estimation.

A scaled prediction error variance is an appropriate measure to employ in making comparisons among competing experimental designs. The scaled prediction error variance is found by multiplying an expanded form of Equation 10.35 by the number of runs in the design ( $N$ ) and dividing by  $\sigma^2$  to give

$$\begin{aligned} \frac{N \text{Var}_{\mathbf{z}, \varepsilon} \left[ y(\mathbf{x}, \mathbf{z}) - \mathbf{x}^{(m)'} \hat{\boldsymbol{\beta}}^* \right]}{\sigma^2} & = N \left[ \mathbf{x}^{(m)'} (\mathbf{X}' \mathbf{X})^{-1} \mathbf{x}^{(m)} \right] \\ & + N r_2 k_1^2 + 2 N r_2 k_1 k_2 \mathbf{x}' \mathbf{1} + N r_2 k_2^2 \mathbf{x}' \mathbf{J} \mathbf{x} \end{aligned} \quad (10.36)$$

where  $\mathbf{J}$  is a matrix of 1's. Equation 10.36 is in a form that is appropriate for creating VDGs for design evaluation and comparison purposes. The constants  $k_1$  and  $k_2$  represent the contribution of the noise variables and the control-by-noise interactions, respectively. Furthermore, if there are no noise variables in the problem, then  $k_1 = k_2 = 0$ , and Equation 10.36 reduces to the scaled prediction error variance expression that is usually plotted on a VDG.

The variance model assuming  $\text{Var}(\mathbf{z}) = \sigma^2 \mathbf{I}$  is

$$\text{Var}_{\mathbf{z}, \varepsilon} [y(\mathbf{x}, \mathbf{z})] = \sigma_z^2 (\boldsymbol{\gamma}' + \mathbf{x}' \boldsymbol{\Delta}) \mathbf{V} (\boldsymbol{\gamma}' + \mathbf{x}' \boldsymbol{\Delta})' + \sigma^2 \quad (10.37)$$

The vector  $\boldsymbol{\gamma}' + \mathbf{x}' \boldsymbol{\Delta}$  is a vector of partial derivatives of the response surface with respect to the noise variables  $\mathbf{z}$  and is the slope of the response surface in the direction of the noise variables. Thus, the variance of the slope is a direct measure of the precision of estimation associated with the variance model in Equation 10.37. Furthermore, the slope variance is more directly interpretable than a variance expression for Equation 10.37 because it is in the same units as the variance for the mean model.

A general expression for the variance of the slope in direction  $i$ , ( $i = 1, 2, \dots, r_2$ ) is

$$\text{Var}_{z_i} (\text{slope}) = C_{ii}^{22} + \mathbf{x}' \mathbf{C}_i^{33} \mathbf{x} + 2 \mathbf{x}' \mathbf{C}_i^{23} \quad i = 1, 2, \dots, r_2 \quad (10.38)$$

where

$$\mathbf{C}_1^{23} = \begin{pmatrix} C_{11}^{23} \\ \vdots \\ C_{1r_x}^{23} \end{pmatrix},$$

$$\mathbf{C}_i^{23} = \begin{pmatrix} C_{i,(i-1)r_x+1}^{23} \\ \vdots \\ C_{i,r_x}^{23} \end{pmatrix} \quad \text{for } i > 1,$$

and

$$\mathbf{C}_i^{33} = \begin{pmatrix} C_{(i-1)r_x+1,(i-1)r_x+1}^{33} & \cdots & C_{(i-1)r_x+1,i r_x}^{33} \\ \vdots & \ddots & \vdots \\ C_{ir_x(i-1)r_x+1}^{33} & \cdots & C_{ir_x,i r_x}^{33} \end{pmatrix} \quad i = 1, 2, \dots, r.$$

Therefore, a VDG for the slope would be obtained by plotting the average of the slope variances computed from Equation 10.38 along with the maximum and minimum slope variance as a function of the distance of the point from the center of the design.

The VDGs constructed for the variance expressed in Equation 10.36 and Equation 10.38 can be used to make comparisons among competing designs for a process robustness study. We now present an illustration of this process.

**Example 10.10** Consider a process robustness study involving  $r_1 = 4$  controllable variables,  $r_2 = 3$  noise variables, and a design region of interest that is spherical. The designs considered by the experimenter are:

1. A “modified” central composite design or CCD ( $N = 75$  runs) with either
  - (a)  $\alpha = 2$
  - (b)  $\alpha = 2.646$   
or
  - (c)  $\alpha = 2.83$ .
2. A Box–Behnken design (BBD) with  $N = 60$  runs.
3. A modified small composite design or SCD ( $N = 33$  runs) with either
  - (a)  $\alpha = 2$
  - (b)  $\alpha = 2.646$   
or
  - (c)  $\alpha = 2.83$ .
4. A hybrid design with  $N = 48$  runs.
5. A mixed resolution design (MRD) with  $N = 43$ , and either
  - (a)  $\alpha = 2.646$   
or
  - (b)  $\alpha = 2.83$ .

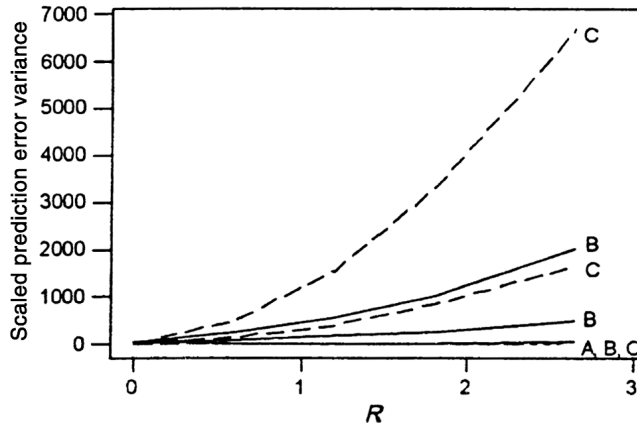


**Figure 10.24** Variance dispersion graph of scaled prediction error variance for modified CCD ( $\alpha = 2.646$ ) with  $k_1 = k_2 = 0$  (A),  $k_1 = k_2 = 0.5$  (B), and  $k_1 = 0.5, k_2 = 1$  (C).

Notice that there is considerable disparity in the number of runs for the candidate designs, and the experimenter would like to know if the extra runs in the larger designs are really beneficial. The values of  $\alpha$  were chosen based on rotatability and/or spherical properties of either the four-variable (considering only the controllable variables) or the seven-variable (considering all variables) design. The modified CCD and modified SCD are constructed from a standard CCD and SCD, respectively, by removing the axial runs for the noise variables.

The variance dispersion graphs for the scaled prediction error variance from Equation 10.36 for selected designs with various values of  $k_1$  and  $k_2$  are shown in Figs 10.24 through 10.26. The minimum, maximum, and average scaled prediction error variance and slope variance at the furthest Euclidean distance from the center for all designs of interest to the experimenter are provided in Table 10.11. As can be seen from these displays, the prediction error increases as the values of  $k_1$  and  $k_2$  increase. Also, the error increase is

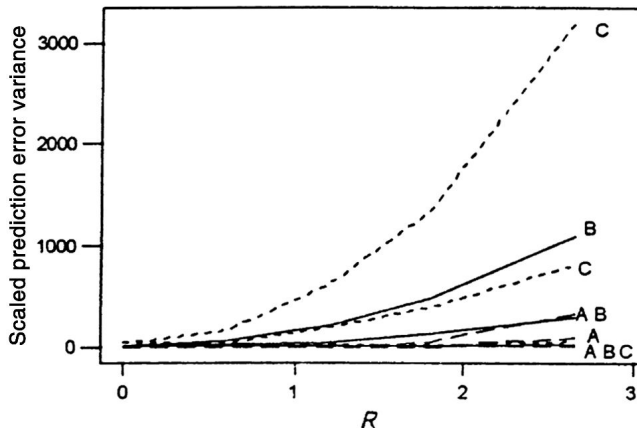


**Figure 10.25** Variance dispersion graph of scaled prediction error variance for modified SCD ( $\alpha = 2.646$ ) with  $k_1 = k_2 = 0$  (A),  $k_1 = k_2 = 0.5$  (B), and  $k_1 = 0.5, k_2 = 1$  (C).

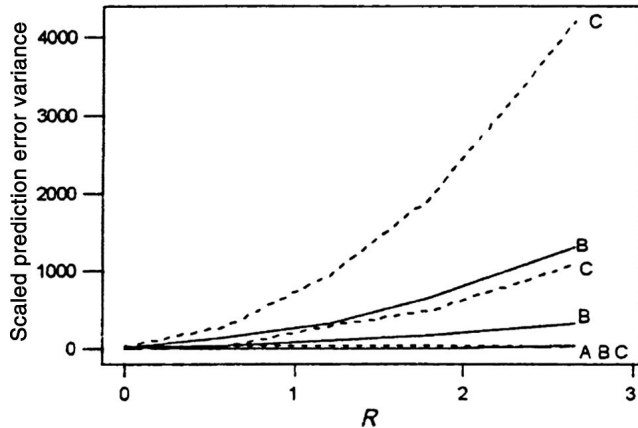


**Figure 10.26** Variance dispersion graph of scaled prediction error variance for hybrid design with  $k_1 = k_2 = 0$  (A),  $k_1 = k_2 = 0.5$  (B), and  $k_1 = 0.5, k_2 = 1$  (C).

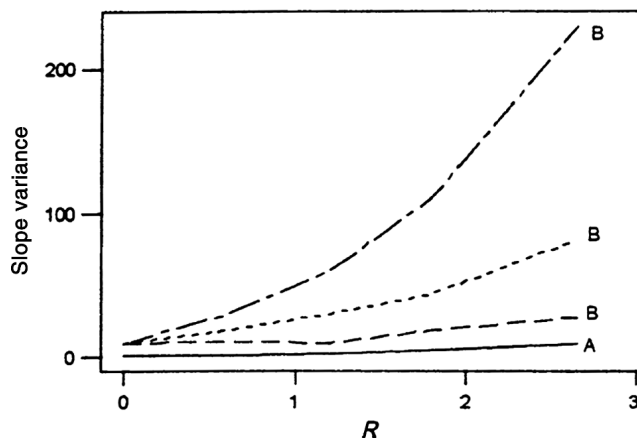
**TABLE 10.11 Scaled Prediction Error Variances and Slope Variance for Designs on Spherical Regions with Four Control Variables and Three Noise Variables**

Variance	Design	N	Scaled Prediction Error ( $k_1, k_2$ )			Var(Slope)
			(0, 0)	(0.5, 0.5)	(0.5, 1)	
Max	CCD $\alpha = 2.83$	75	38	2028	6678	9.37
	$\alpha = 2.646$	75	38	2030	6678	9.37
	$\alpha = 2$	75	64	2052	6745	9.37
	SCD $\alpha = 2.646$	33	332	1089	3193	230
	$\alpha = 2.83$	33	306	1075	3179	222
	BBD	60	204	1962	6157	50
	Hybrid	48	46	1310	4200	13.6
	MR $\alpha = 2.646$	43	33.5	1110	3650	10.75
	$\alpha = 2.83$	43	32	1116	3650	10.75
	Avg					
Avg	CCD $\alpha = 2.83$	36	484	1661	9.37	
	$\alpha = 2.646$	36	484	1660	9.37	
	$\alpha = 2$	58	507	1684	9.37	
	SCD $\alpha = 2.646$	101	299	819	82	
	$\alpha = 2.83$	94	292	811	79	
	BBD	204	564	1507	50	
	Hybrid	44	330	1080	12.2	
	MR $\alpha = 2.646$	32	290	965	10.75	
	$\alpha = 2.83$	30	288	965	10.75	
	Min					
Min	CCD $\alpha = 2.83$	35	36	40	9.37	
	$\alpha = 2.646$	35	36	39	9.37	
	$\alpha = 2$	52	55	58	9.37	
	SCD $\alpha = 2.646$	29	43	68	28	
	$\alpha = 2.83$	26	39	64	28	
	BBD	204	221	209	50	
	Hybrid	42	45	50	11.5	
	MR $\alpha = 2.646$	30	31	31	10.75	
	$\alpha = 2.83$	26	27	27.5	10.75	

affected more by the value of  $k_2$  (the factor pertaining to the control-by-noise interactions) than by the value of  $k_1$ . The variance dispersion graphs for the slope variance for the modified CCD and modified SCD are given in Fig. 10.27. We see that the modified CCD is slope-rotatable regardless of the value of  $\alpha$ ; that is, the slope variance is constant on spheres over the design region. The modified SCD is not slope-rotatable.

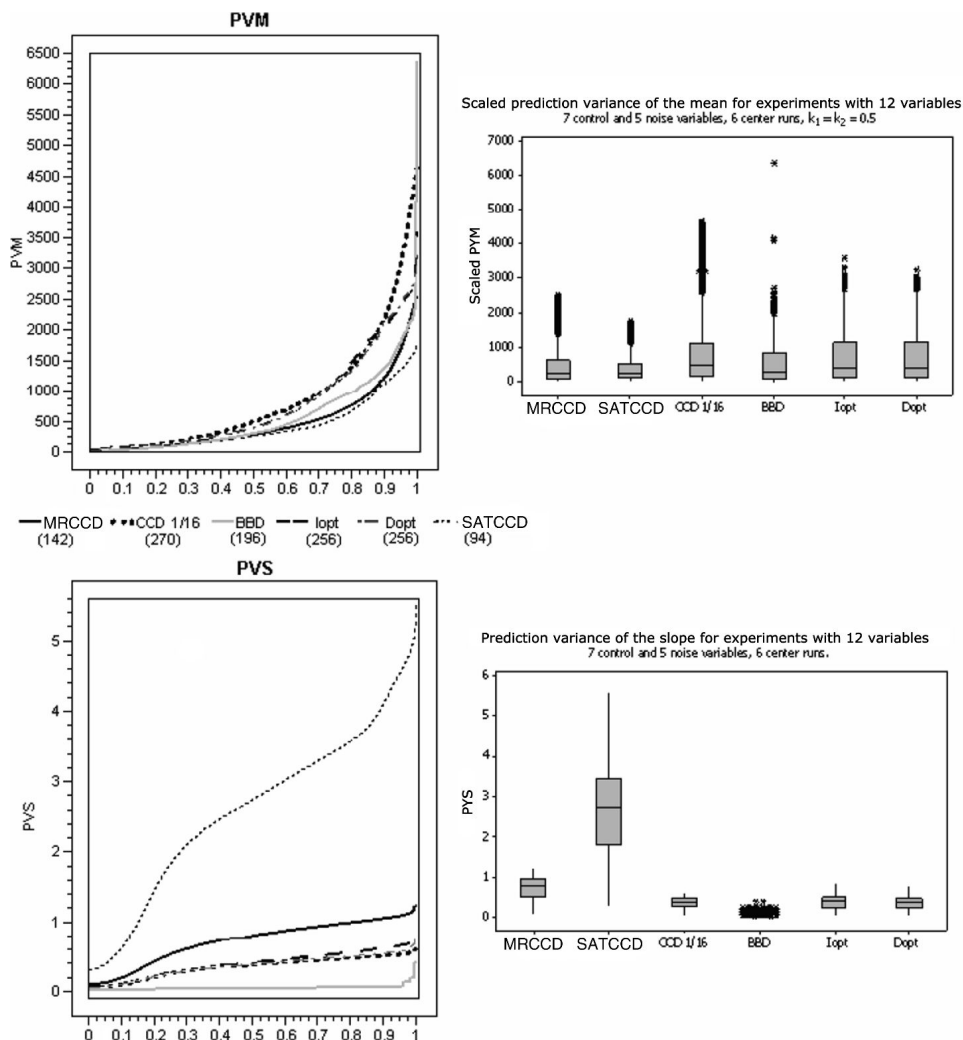
There are several important points that should be mentioned about the results in Table 10.11. The modified CCDs and the BBD have 75 experimental runs and 60 experimental runs, respectively. Consequently, these designs may be impractically large to implement. The practitioner would often rely on smaller designs such as the SCD or the hybrid. For four control variables and three noise variables, the modified SCDs have 33 experimental runs, while the hybrid design has 48 experimental runs.

Table 10.11 shows that for the situation where the noise variables do not influence the response ( $k_1 = 0, k_2 = 0$ ), the modified SCD performance is very poor compared with the modified CCD, hybrid, or mixed resolution designs. However, notice that when the noise variables are introduced into the model, the modified SCD is highly competitive with respect to scaled prediction error variance when compared with the modified CCD and the hybrid design. Because the BBD does not estimate the interaction terms as precisely as other designs, it does not perform well overall and would probably not be a good choice. Therefore, it appears that the modified SCD would be a reasonable design when run size is taken into consideration, since there is a considerable difference between  $N = 33$  for the SCDs and  $N = 75$  for the CCDs. However, before deciding that the modified SCD is the best design to use, the slope variances should be investigated. When the slope variances are taken into consideration, the modified SCD is outperformed by all other designs. Consequently, examining both the prediction error variance and the slope variance indicates that the modified CCDs, modified SCDs, hybrid, and BBD are all relatively poor performers with respect to the mean variance, slope variance, or both. In addition, we know that the small composite designs have lower  $G$ - and  $D$ -efficiencies than the other designs, and we recommend against using them. The mixed resolution design outperforms all other designs under consideration with respect to the prediction error variance, the slope variance, and the number of experimental runs. It would clearly be the recommended design in this situation if the experimenter can afford to use 43 runs.



**Figure 10.27** Slope variance for modified CCD (A) and modified SCD (B).

Fraction of design space plots are also useful in facilitating comparisons of prediction variance for the mean and slope in a robust design setting. To illustrate, suppose that we want to compare several designs for a situation where there are seven control variables and five noise variables. The designs considered are a mixed resolution CCD, a modified CCD based on a one-sixteenth fraction in the cube, a BBD, a  $D$ -optimal design, an  $I$ -optimal design, and a CCD where the cube portion of the design is a saturated resolution V fraction. Figure 10.28 shows FDS plots along with box plots of the prediction variance for the mean (PVM) and the prediction variance for the slope (PVS) for these designs. The number of runs for each design is shown in the figure and all designs have six center points. In this scenario the CCD based on a saturated fraction performs well for the mean model but



**Figure 10.28** Fraction of design space plots for the mean and slope for 12 variable designs (7 control variables, 5 noise variables).

is disastrous for the slope. The BBD is generally a good performer for the mean, except for a few outlying values of the prediction variance for the mean, and it performs very well with respect to the slope. Both optimal designs and the mixed resolution CCD are reasonable design choices.

## 10.6 DISPERSION EFFECTS IN HIGHLY FRACTIONATED DESIGNS

In this chapter we have dealt with the important notion of variance modeling where the variance is derivable from the inability to control noise variables. However, there are circumstances in which the practitioner is unable to measure noise variables or perhaps is not aware of what the noise variables are. At any rate, there is nonhomogeneous variance from one or more sources, and thus there are **both location and dispersion effects**. Detection of dispersion effects, positive or negative, is often vital, particularly if the experiment is a pilot experiment and directions are sought for future experiments. For example, consider a  $2^3$  factorial experiment with factors A, B, and C. In addition, suppose we wish to move to a different experimental region via **steepest ascent** or some other sequential procedure. Suppose the calculated effects are as follows:

$$\begin{aligned} A &: +7.5 \\ B &: +4.7 \\ C &: -3.5 \end{aligned}$$

Now, these calculated effects are **location effects**; that is, they reflect the change in the mean response as one moves from low to high. In this case, future experiments will involve an increase in A, an increase in B, and a decrease in C. However, suppose an increase in A results in a profound *increase in variance* in the response. We say that A is a **dispersion effect** as well as a location effect, and thus we are left with a mean–variance tradeoff if we are to consider moving A to the high level.

In this section the concept of a dispersion effect has not changed. In previous sections a dispersion effect was discovered in a factor if it had a certain type of interaction with a noise variable. Here we are assuming that there are not necessarily any noise variables in the problem, and yet there is a need to detect the existence of factors that influence dispersion. Plots and numerical computation of dispersion effects are useful.

### 10.6.1 The Use of Residuals

The reader should recall from Chapter 2 that much diagnostic information is gained from the use of **residuals**—that is, the values  $e_i = y_i - \hat{y}_i$ , where  $\hat{y}_i$  is the predicted or fitted value from a regression analysis. Residuals provide considerable information about unexplained variability. For example, when residuals are plotted, one expects to see random scatter around zero. Patterns in residuals suggest that some assumption that has been made is being violated. The two most prominent violations are:

1. Functional form of model mis-specified
2. Nonhomogeneous variance

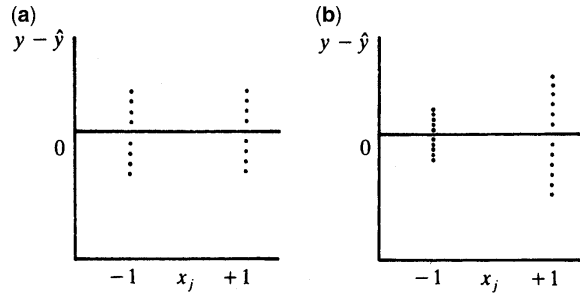


**Figure 10.29** Plots of residuals versus factor  $x_j$ .

It is violation 2 that concerns us here. It is of interest to determine if the signals from residual plots reflect a type of pattern that would identify certain factors as dispersion effects.

For example, a plot of the residuals against the levels of a factor  $x_j$  in the case of a two-level design may be as shown in Fig. 10.29a. In this case there is no evidence that factor  $x_j$  is a dispersion effect. On the other hand, suppose the plot of residuals takes the form shown in Fig. 10.29b. Now, while one must take considerable care not to read too much into residual plots for small experiments, there is certainly some evidence in Fig. 10.29b that at the high level of  $x_j$  the model error variance is larger than at the low level. While the fitted model here suggests that all three factors are location effects, it appears that  $x_j$  is a dispersion effect, with  $x_j = -1$  favored for a consistent product; that is, one with less variability in the response.

**Importance of the Fitted Mean Model** It should be understood that the use of residuals, residual plots, and other diagnostic tools for determining dispersion effects is profoundly affected by the fitted mean model, because the residuals used are the residuals from the mean model. If the mean model is not correctly specified, residuals will be clouded by model mis-specification. Thus the detection of dispersion effects depends on the presumption that the fitted model for the mean is a good one. In this regard, the detection of dispersion effects will be most successful when there are only a few well-defined effects to be used in the mean model—that is, when there is **sparsity of effects**.

### 10.6.2 Further Diagnostic Information from Residuals

It should be clear from the illustration in Section 10.6.1 that one is attempting to determine if the product or process variance depends on the design locations, rather than being homogeneous. In the example, we might conclude from the plots that the error variance is constant except when  $x_3 = +1$ . When this type of result is detected, it is hoped that the engineer or scientist has, at least in retrospect, some scientific explanation. However, there still remains the issue surrounding what is meant by a “significant change in variance.” Can we say with assurance that the plots in Section 10.6.1 indicate that  $x_3$  is a dispersion effect? Are there other diagnostic pieces of information apart from the plots?

An important diagnostic for determining if a specific factor, say factor  $i$ , is a dispersion effect is the statistic

$$F_i^* = \ln\left(\frac{s_{i+}^2}{s_{i-}^2}\right) \quad (10.39)$$

See Box and Meyer (1986). Here  $s_{i+}^2$  is the sample variance of the residuals when factor  $i$  is at the high level, and  $s_i^2$  is the sample variance of the residuals when factor  $i$  is at the low level. Obviously a value close to zero is evidence that the spread in the residuals is not significantly different for the two levels, whereas a value large in magnitude (positive or negative) is a signal that the variable has a dispersion effect. A large positive value indicates that  $\sigma_{i+}^2 > \sigma_i^2$ , whereas a large negative effect indicates  $\sigma_{i+}^2 > \sigma_i^2$ . While there should be no intention of using the  $F_i^*$ -value in Equation 10.39 as a formal test statistic, it can be a very useful diagnostic because it has been found that under  $H_0: \sigma_{i+}^2 = \sigma_i^2$ , the  $F^*$ -values are approximately normally distributed with mean 0 and common variance. This may be exploited as a numerical diagnostic, and the  $F_i^*$ -values may be studied via normal probability plots.

**Example 10.11 Dispersion Effects** In an injection molding experiment it is often important to determine conditions in which shrinkage is minimized. In the present experiment [see Montgomery (1991)] seven factors were varied in a  $2^{7-3}$  with four center runs. It was felt that there might be curvature in the system. The factors are  $x_1$  (mold temperature),  $x_2$  (screw speed),  $x_3$  (holding time),  $x_4$  (gate size),  $x_5$  (cycle time),  $x_6$  (moisture content), and  $x_7$  (holding pressure). The defining relations are

$$x_1x_2x_3x_5 = x_2x_3x_4x_6 = x_1x_3x_4x_7 = I$$

The data appear in Table 10.12. It is of interest to determine settings (within the region of the experiment) that minimize shrinkage. In addition, any dispersion effect that is found must be dealt with, because the variability in the shrinkage must also be taken into account.

**TABLE 10.12** Injection Molding Data

**TABLE 10.13 Alias Structure for the  $2^{7-3}$  Design in Table 10.12**

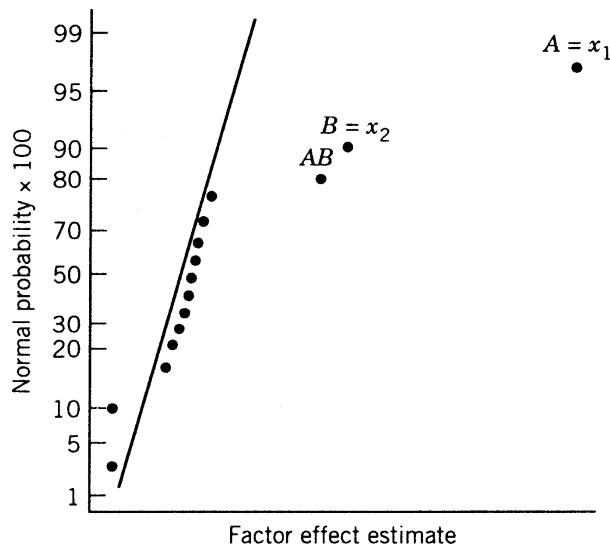
$A = BCE = DEF = CDG = BFG$	$AB = CE = FG$
$B = ACE = CDF = DEG = AFG$	$AC = BE = DG$
$C = ABE = BDF = ADG = EFG$	$AD = EF = CG$
$D = BCG = AEF = ACG = BEG$	$AE = BC = DF$
$E = ABC = ADF = BDG = CFG$	$AF = DE = BG$
$F = BCD = ADE = ABG = CEG$	$AG = CD = BG$
$G = ACD = BDE = ABF = CEF$	$BD = CF = EG$
$ABD = CDE = ACF = BEF = BCG = AEG = DEF$	

The individual location effects of interest were first placed on a normal probability plot to gain some impression of what model terms are important. Table 10.13 gives the reader a clear indication of what effects are estimable. Fifteen effects, including all main effects and two-factor interactions (and aliases), were plotted on the normal probability plot in Fig. 10.30. The  $x_1$ ,  $x_2$ , and  $x_1x_2$  effects are found to be important from the plot. All three are positive effects. The  $x_1x_2$  interaction plot in Fig. 10.31 is particularly revealing. The use of the screw speed  $x_2$  at the low level minimizes shrinkage in spite of the level of the mold temperature  $x_1$ . In addition, if the mold temperature is difficult to control in the process, the  $-1$  level of the screw speed is also a robust choice. So at this point in the analysis it would seem that  $x_2 = -1$  is absolutely necessary.

The next step in the analysis is to consider possible curvature. Table 10.14 summarizes a regression analysis with the model

$$\hat{y} = 27.3125 + 6.9375x_1 + 17.8125x_2 + 5.9375x_1x_2 \quad (10.40)$$

and an analysis of variance that reveals no evidence of curvature. The curvature term in the ANOVA is a result of center points being used in the design (only a single degree of

**Figure 10.30** Normal probability plot of location effects for Example 10.11.

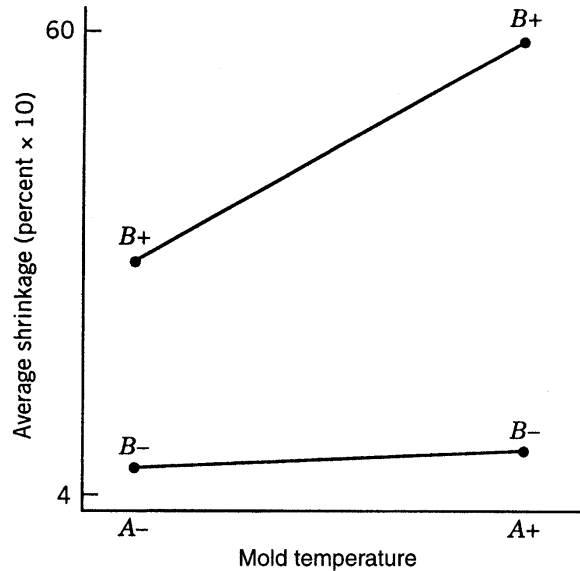


**Figure 10.31**  $AB = x_1x_2$  interaction plot for Example 10.11.

freedom). There is no actual curvature in the system. At this point it would appear that  $x_1 = -1$  and  $x_2 = -1$  are proper settings. It turns out that this would reduce the mean shrinkage by roughly 10%. But what about variability? The regression in Equation 10.40 was used to compute the residuals. The normal probability plot of residuals in Fig. 10.32 do not reveal anything out of the ordinary. However, the residuals were also plotted

**TABLE 10.14** Regression and ANOVA for Data of Example 10.11

Source of Variation	Sum of Squares	Degrees of Freedom	Mean Square	F	Probability > F
Model	6410.687500	3	2136.8958333	121.645	0.0001
Curvature	3.612500	1	3.6125000	0.206	0.6567
Error	263.500000	15	17.5666667		
Residual	248.750000	12	20.7291667		
Pure error	14.750000	3	4.9166667		
Corrected total	6677.800000	19			
Root mean squared error	4.191261		R-squared	0.9605	
Dependent mean	27.312500		Adjusted R-squared	0.9500	
CV	15.35%				
Variable	Parameter Estimate	Degrees of Freedom	Sum of Squares	t for $H_0$ : Parameter = 0	Probability >  t
Intercept	27.312500	1			
A	6.937500	1	7700.062500	6.621	0.0001
B	17.812500	1	5076.562500	17.000	0.0001
AB	5.937500	1	564.062500	5.667	0.0001

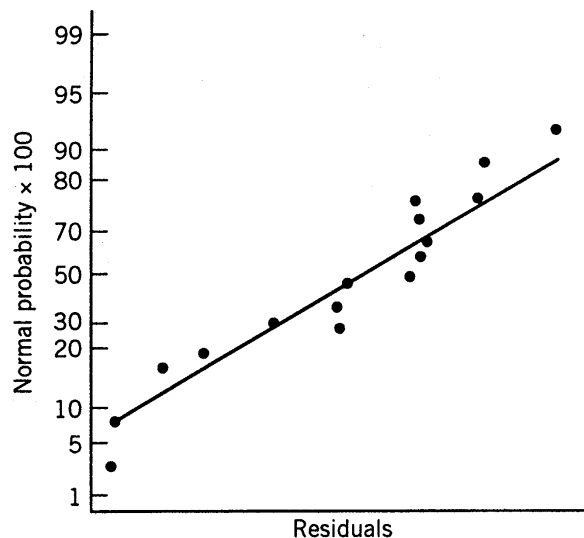


Figure 10.32 Normal probability plot of residuals for Example 10.11.

against levels of the main effects, and the residual plot involving  $x_3$  was particularly enlightening. It appears in Fig. 10.33. It seems clear that variability in the residuals is greater at high holding time than at low holding time. The  $s_{(i-)}$  and  $s_{(i+)}$  values as well as the  $F_i^*$  in Equation 10.39 were computed. They appear, along with the residuals themselves, in Table 10.15. Note that the single  $F_i^*$ -value that stands out is that of  $F^* = 2.50$ . To gain more diagnostic insight, a normal probability plot of the  $F^*$ -values appears in Fig. 10.34. Clearly,  $x_3$  stands out. It would not be unreasonable to say that  $x_3$  has a significant dispersion effect.

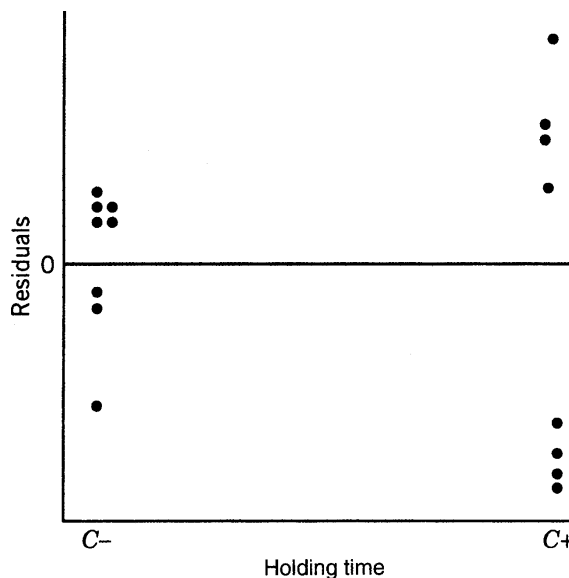
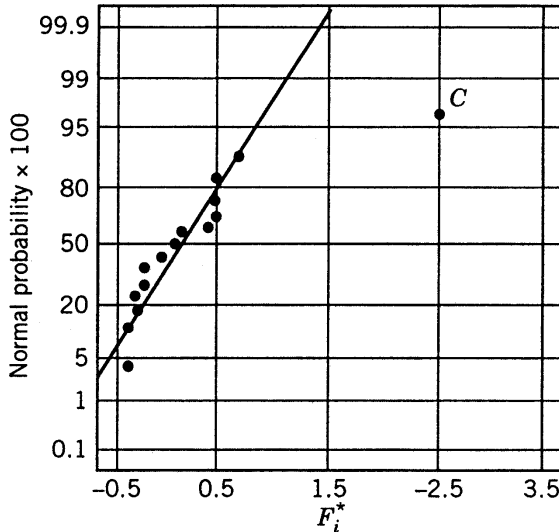


Figure 10.33 Plot of residuals against holding time for Example 10.11.

**TABLE 10.15** Residuals and  $F^*$ -values for All Effects for Example 10.11

$x_1$	$x_2$	$x_1x_2$	$x_3$	$x_1x_3$	$x_2x_3$	$x_5$	$x_4$	$x_1x_4$	$x_2x_4$	$x_1x_2x_4$	$x_3x_4$	$x_7$	$x_6$	$x_4x_5$	Residuals
-	-	+	-	+	+	-	-	+	+	-	+	-	-	+	-2.50
+	-	-	-	-	+	+	-	-	+	+	+	+	-	-	-0.50
-	+	-	-	+	-	+	-	+	-	+	+	-	+	-	+0.25
+	+	+	-	-	-	-	-	-	-	-	+	+	+	+	2.00
-	-	+	+	-	-	+	-	+	+	-	-	+	+	-	-4.50
+	-	-	+	+	-	-	-	-	+	+	-	-	+	+	4.50
-	+	-	+	-	+	-	-	+	-	+	-	+	-	+	-6.26
+	+	+	+	+	+	+	+	-	-	-	-	-	-	-	2.00
-	-	+	-	+	+	-	+	-	-	+	-	+	+	-	+0.50
+	-	-	-	-	+	+	+	+	-	-	-	-	+	+	1.50
-	+	-	-	+	-	+	+	+	-	+	-	-	+	+	1.75
+	+	+	-	-	-	-	-	+	+	+	-	-	-	-	2.00
-	-	+	+	-	-	+	+	+	-	+	+	-	-	+	7.50
+	-	-	+	+	-	-	+	+	-	-	+	+	-	-	-5.50
-	+	-	+	-	+	-	+	-	+	-	+	-	+	-	4.75
+	+	+	+	+	+	+	+	+	+	+	+	+	+	+	-6.00
$S_{i^-}$	4.59	4.41	4.10	1.63	4.52	4.33	4.25	3.59	2.75	4.41	3.51	3.50	3.65	3.12	3.40
$S_{i^+}$	3.80	4.01	4.33	5.70	3.68	3.85	4.17	4.64	3.39	4.01	4.72	3.12	3.50	3.88	4.87
$F_i^*$	-0.38	-0.18	0.11	2.50	-0.41	-0.24	-0.03	0.51	0.42	-0.18	0.52	0.51	0.23	-0.30	0.72



**Figure 10.34** Normal probability plots of dispersion effects  $F_i^*$  for Example 10.11.

It is of interest now to provide a summary picture of the mean and variability of the shrinkage response. This is particularly easy to do because there appears to be only three “main players,”  $x_1$ ,  $x_2$ , and  $x_3$ . The analysis suggests that low  $x_1$ , low  $x_2$ , and low  $x_3$  are the settings that produce, simultaneously, minimum mean shrinkage and minimum variance in shrinkage. That is, the optimum conditions are

$$x_1 = -1, \quad x_2 = -1, \quad x_3 = -1$$

### 10.6.3 Further Comments Concerning Variance Modeling

In this entire chapter we have focused on the importance of considering process variability. The major sources of process variability are often noise variables; and when this is the case, the modeling can be handled conveniently through the use of a combined array and of the resulting response surface in  $\mathbf{x}$  and  $\mathbf{z}$  and response surfaces that result for both mean and variance. Another source of variance modeling is the **log-linear model** discussed in Section 10.4.6, where  $\ln(s^2)$  becomes the response. In this context, the  $s^2$  was viewed as the sample variance associated with the outer array in a crossed array, but this need not be the case. The  $s^2$  may be computed from replicated observations or even from repeated measurements on the same experimental unit in, say, a two-level design; in other words, there may be no noise variables in the design and yet a nonconstant variance may be evident through replication ( $n$  runs at each of  $d$  design points) and the use of the model

$$\ln(s_i^2) = f(\mathbf{x}_i) + \varepsilon_i, \quad i = 1, 2, \dots, d \quad (10.41)$$

Additional levels of variance modeling and/or the computation of dispersion effects can be accomplished for cases such as Example 10.11. The experiment contains a large number of factors, and because of cost constraints the design is a highly fractionated two-level design

with no replication. Here, formal variance modeling is not necessarily a good practice, due to lack of sufficient information on variability. However, the use of residuals can highlight dispersion effects as in the example. The reader should be aware of the possibility of obtaining variance information and dispersion effects at different levels of experimentation and analysis. In addition, more discussion is needed regarding different methods of calculating dispersion effects.

**What Is a Dispersion Effect? (Case of Replicated Observations)** Box and Meyer (1986) and Nair and Pregibon (1986) discuss the notion of dispersion effects for various types of scenarios. Consider a situation in which the design is a two-level factorial or fraction and  $n$  observations appear at each data point. The fitted model may be a log–linear model with

$$\ln(s_i^2) = \gamma_0 + \gamma_1 x_{i1} + \gamma_2 x_{i2} + \cdots + \gamma_k x_{ik} + \varepsilon_i, \quad i = 1, 2, \dots, d \quad (10.42)$$

In this case, the replication variance is more reliable as process variance information than that obtained from residuals. In the latter case, the reliability of the variance information depends to a great extent on the quality of the mean model that created the residuals.

The least squares estimators of the  $\gamma_i$  in Equation 10.42 are derived from

$$\hat{\gamma} = (\mathbf{X}'\mathbf{X})^{-1}\mathbf{X}'\mathbf{e} \quad (10.43)$$

where  $\mathbf{e}$  is a vector of  $\ln s^2$  values. Because the rows of  $\mathbf{X}'$  contain  $+1$  and  $-1$  values depending on whether the specific factor is high or low, and because  $(\mathbf{B}'\mathbf{X})^{-1} = (1/d)\mathbf{I}$ , the parameter estimates for the model 10.42 become

$$\begin{aligned} \hat{\gamma}_0 &= \overline{\ln(s^2)} \\ \hat{\gamma}_i &= \frac{\sum_{j=i+} \ln s_j^2 - \sum_{j=i-} \ln s_j^2}{d}, \quad i = 1, 2, \dots, k \end{aligned} \quad (10.44)$$

Here  $\sum_{j=i+}$  implies that the sum is taken over the  $\ln s^2$  values for which the  $i$ th variable is at the  $+1$  level, while  $\sum_{j=i-}$  implies that sum is over the  $-1$  level. In addition,  $\overline{\ln(s^2)}$  is the average of the  $\ln s^2$  values over the experiment. One could, of course, extend what we know about the relationship between effects and regression coefficients for the mean model. Thus the **computed dispersion effect** for the  $i$ th variable can be written

$$(\text{Dispersion effect})_i = \left[ \overline{\ln(s^2)}_{i+} - \overline{\ln(s^2)}_{i-} \right], \quad i = 1, 2, \dots, k \quad (10.45)$$

where, obviously  $\overline{\ln(s^2)}_{i+}$  is the average  $\ln(s^2)$  value when variable  $i$  is at the high level, and  $\overline{\ln(s^2)}_{i-}$  is the same for variable  $i$  at the lower level. Now, what is done with those dispersion effects or regression coefficients? Normal probability plots can certainly be used to highlight important dispersion effects. The assumption of normality with constant variance for these effects is certainly justified. We suggested earlier that work by Bartlett and Kendall (1946) and others indicates that  $\ln(s^2)$  is approximately normal, and the averaging process strengthens the assumption. Of course, it is quite likely that in most

applications where replications are involved, the number of design points and, hence, the number of variables will not be large. As a result, there may not be many effects being studied (including interactions), so the normal probability plot may not contain a very large “sample size.” However,  $t$ - or  $F$ -tests in which lack of fit is used as the “error” for testing main effect dispersion effects will certainly supply useful information.

In addition to the dispersion effects given in Equation 10.45, another one, representing a slight variation, has been suggested. Rather than summing the log variances, the alternative dispersion effects takes sums first—that is,

$$\begin{aligned} (\text{Dispersion effect}^*)_i &= \ln \left[ \sum_{j=i+} s_j^2 \right] - \ln \left[ \sum_{j=i-} s_j^2 \right] \\ &= \ln \left[ \frac{s_{i+}^2}{s_{i-}^2} \right] \end{aligned} \quad (10.46)$$

This, of course, is closer in concept to the  $F^*$  dispersion effect discussed earlier for unreplicated experiments.

**The Unreplicated Case** We have already discussed the  $F^*$  dispersion effect calculation and illustrated it with an extensive case study in injection molding. However, it may be of interest to determine the genesis of this dispersion effect, which was developed by Box and Meyer (1986). Consider first an experiment with a two-level unreplicated factorial. Consider the mean model of  $N$  observations,

$$y_i = \mathbf{x}'_i \boldsymbol{\beta} + \varepsilon_i^* \sigma_i, \quad i = 1, 2, \dots, N \quad (10.47)$$

where the  $\varepsilon_i^*$  are independent  $N(0, 1)$  and

$$\ln(\sigma_i^2) = \mathbf{x}'_i \boldsymbol{\gamma} \quad (10.48)$$

Now, clearly the standard deviation changes as  $\mathbf{x}$  moves. The model in Equation 10.48 need not imply that all the variables in the mean model are in the variance model. In fact, the mean model often will contain interactions (or even main effects) not contained in the variance model. We noticed that in our injection molding example.

Consider now the distribution of an error in the mean model—that is, the distribution of

$$\varepsilon_i = y_i - \mathbf{x}'_i \boldsymbol{\beta}$$

We know that

$$\varepsilon_i^2 \sim \sigma_i^2 \chi_1^2$$

and thus

$$\ln \varepsilon_i^2 = \ln \sigma_i^2 + \ln \chi_1^2 \quad (10.49)$$

Thus, one could view Equation 10.49 as a model for the log of the  $i$ th squared residual. Keep in mind however, that we are assuming in Equation 10.49 that *the mean is*

known—that is,  $\varepsilon_i$  is not an observed residual  $y_i - \hat{y}_i$ , but rather  $y_i - \mathbf{x}'_i \boldsymbol{\beta}$ . As a result, one can view an *approximate* model of the log squared residual as

$$\ln e_i^2 \cong \ln \sigma_i^2 + \ln \chi_1^2$$

with  $\ln \chi^2$  representing an approximately normal random variable with mean approximately zero and constant variance. From Equation 10.49 we have

$$\ln e_i^2 = \mathbf{x}'_i \boldsymbol{\gamma} + \tilde{\varepsilon}_i \quad (10.50)$$

[it can be shown that  $\text{Var}(\ln \chi_v^2) \cong 2/v$ ], where  $\tilde{\varepsilon}_i$  has approximately mean 0 and variance 2.

At this point one should consider least squares estimation in Equation 10.50. The parameter estimates from which dispersion effects can be are given by

$$\begin{aligned}\tilde{\gamma}_0 &= \overline{\ln e^2} \\ \hat{\gamma}_1 &= \frac{\sum_{j=i+} \ln e_j^2 - \sum_{j=i-} \ln e_j^2}{N}\end{aligned}$$

As a result, an obvious dispersion effect will be  $2\hat{\gamma}_i$ , which is given by

$$(\text{Dispersion effect})_i = \left[ \overline{\ln e^2} \right]_{i+} - \left[ \overline{\ln e^2} \right]_{i-} \quad (10.51)$$

where  $\overline{\ln e^2}$  indicates the average of the log of the squared residual. Again *normal probability plotting*, once a mean model of high quality has been chosen, is certainly a reasonable diagnostic procedure. In fact, dispersion effects will be approximately normal with mean zero (assuming a zero dispersion effect) and constant variance. Thus, any dispersion effect off the straight line is diagnosed as having mean not zero and, thus, being an important dispersion effect.

From the foregoing it should be evident to the reader why  $F_i^*$ , is also a reasonable dispersion effect. As in the case with replicated factorials, the  $F_i^*$ , in Equation 10.39 is much like that in Equation 10.51 except that the  $\sum_j$  operation occurs before taking logs. In this regard, another possible dispersion effect is given by

$$F_i = \frac{\ln \sum_{j=i+} e_j^2 - \ln \sum_{j=i-} e_j^2}{N} = \ln \left[ \frac{\sum_{j=i+} e_j^2}{\sum_{j=i-} e_j^2} \right]$$

Of course this is motivated through the use of the  $e_j$  rather than the  $e_j^2$ . It is reasonable to correct the  $e_j$  for their respective means, so one is using estimates of  $\sigma_{i+}^2$  and  $\sigma_{i-}^2$ . Keep in mind that the existence of a nonzero  $\gamma_i$  in the model of Equation 10.48 presumes that the variances at  $x_i = +1$  and  $x_i = -1$  are distinct. As a result, a useful dispersion effect

is given by

$$F_i^* = \ln \left[ \frac{s_{i+}^2}{s_{i-}^2} \right]$$

which was introduced without motivation in Equation 10.39. It is important for the user to understand that the practical use of dispersion effects in unreplicated factorials or fractional factorials should include diagnostic plots (e.g., normal probability plots) and *not* formal significance testing.

## EXERCISES

- 10.1** Consider Exercise 3.11 in Chapter 3. It is of interest to maximize the etch rate. As a result, it is a larger-the-better scenario. Suppose that  $C$  (gas flow) and  $D$  (power applied to the cathode) are difficult to control in the process.
- (a) Treating  $C$  and  $D$  as noise variables, illustrate, with a drawing, that this design is a crossed array.
  - (b) Analyze the data and use the standard larger-the-better SNR. Do pick-the-winner analysis and thus determine optimum values of  $A$  (anode–cathode gap) and  $B$  (pressure in the reactor chamber).
- 10.2** Consider Example 4.2 in Chapter 4. Suppose, in this process for manufacture of integrated circuits, that the temperature is very difficult to control. There is some concern over variability in wafer resistivity due to uncontrolled variability in temperature. Consider the other factors as control variables.
- (a) From the analysis given in Chapter 4, can any of the control variables be used to exert some influence over this variability? Explain.
  - (b) It is of interest to maximize wafer resistivity and still minimize variability produced by changes in temperature. Can this be done? Explain.
- 10.3** Consider Exercise 10.2.
- (a) Give an estimate of the process variance as a function of  $x_1$ , the implant dose.
  - (b) What assumptions were made in constructing this variance function? Discuss the variance–mean tradeoff here. If we use  $\hat{\mu} - 2\sigma$  as a criterion, give optimal values of implant dose and time.
- 10.4** Consider Exercise 10.3. Because  $E$  (furnace position) and  $D$  (oxide thickness) are unimportant, reduce the design to a  $2^3$  factorial with duplicate runs. Using temperature as a single noise variable, determine the optimal values of implant dose and time. Use a Taguchi analysis with the appropriate SNR ratio for a larger-the-better situation.
- 10.5** Consider Exercise 3.9. Use the concept of dispersion effects to determine if any factors affect the process variance. Comment on your results.
- 10.6** Consider Example 10.1 dealing with solder process optimization.
- (a) Construct and edit a response model involving all control and noise variables.

- (b) Generate an estimated mean model as functions of the control variables.  
(c) Generate an estimated process variance function as a function of the control variables.
- 10.7** Consider Example 10.2. The design is criticized for not allowing interaction among the control variables to be studied.
- (a) What design would be a good candidate to replace the crossed array in this example? Do not allow your design to admit a run size any greater than the design listed in the example. Use a design that allows quadratic effects in the control factors and allows construction of a response model that can be used to generate the process mean and variance models.  
(b) Explain why your design is better than that used in the example.
- 10.8** Consider the filtration rate data in Example 10.3. Suppose that the filtration rate should be maximized. Suppose, however, that temperature must be treated as a noise variable.
- (a) What factors can be used to control the variability in filtration rate due to random fluctuation in temperature in the range  $[-1, +1]$ ?  
(b) What levels (high or low) of formaldehyde and stir rate result in minimum process variance? (Study interaction plots.)
- 10.9** Consider Exercise 10.8.
- (a) Again, consider temperature as a noise variable. Use the fitted regression model as a response model to produce a variance model assuming that one design unit in temperature is  $2\sigma_z$ , where  $\sigma_z$  is the standard deviation of temperature in the process.  
(b) What levels of  $C$  and  $D$  result in a minimum process variance?  
(c) Discuss the mean–variance tradeoff here. Give a quantitative discussion. What are reasonable levels of  $C$  and  $D$ ?
- 10.10** Consider a  $2^4$  factorial design. Suppose all six two-factor interaction effects are found to be important. Suppose, in addition, that  $A$  and  $B$  are control variables and  $C$  and  $D$  are noise variables. Suppose  $\sigma_{z_1} = \sigma_{z_2} = 1.0$ .)
- (a) Write out the form of the mean model.  
(b) Write out the form of the variance model.
- 10.11** Consider an experimental situation with  $A(x_1)$ ,  $B(x_2)$ , and  $C(z)$ —that is, two control variables and a single noise variable. Suppose the response model that is fitted is given by
- $$\hat{y} = b_0 + b_1x_1 + b_2x_2 + cz + b_{12}x_1x_2 + b_{1z}x_1z + b_{2z}x_2z + b_{12z}x_1x_2z$$
- Suppose all terms are significant in the analysis.
- (a) Write out the form of the mean model.  
(b) Write out the form of the variance model.  
(c) What assumptions are being made in the construction of the models in (a) and (b)?
- 10.12** Suppose a study is conducted with three control variables and two noise variables. A  $2^{5-1}$  fractional factorial is used as the experimental design. Only the main effects

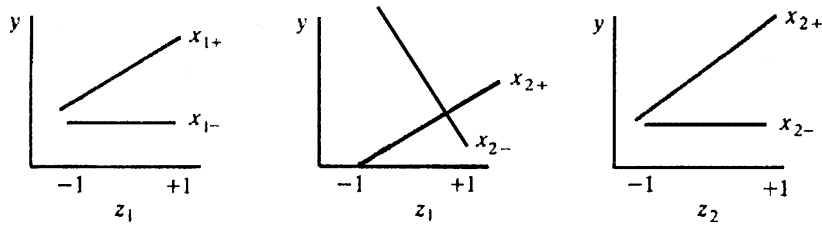


Figure E10.1 Interaction plots for Exercises 10.12 and 10.13.

and the  $x_1z_1$ ,  $x_2z_1$ , and  $x_2z_2$  interactions are found to be important. The interaction plots are shown in Fig. E10.1. The main effect plots are shown in Fig. E10.2. The purpose of the experiment is to determine condition on the control variables that *minimize mean response*.

- (a) Give approximate conditions on  $x_1$ ,  $x_2$ , and  $x_3$  that result in minimum mean response.
- (b) Give approximate conditions on  $x_1$ ,  $x_2$ , and  $x_3$  that give approximate minimum process variance.
- (c) Is there a tradeoff between optimum conditions? Explain.

**10.13** Consider Exercise 10.12. Write out the form of the variance model.

**10.14** A  $2^4$  factorial design is used to study a nitride etch process in a single-wafer plasma etcher. The response of interest is the etch rate, and the design factors are

*A*, or  $x_1$ : Spacing (gap) between anode and cathode (control factor)

*B*, or  $x_2$ : Pressure in the reactor chamber (control factor)

*C*, or  $z_1$ : Flow rate of the reactant gas (noise factor)

*D*, or  $z_2$ : Power applied to the cathode (noise factor)

The factor levels are given by

	$x_1$	$x_2$	$z_1$	$z_2$
Low(-1)	0.80	450	125	275
High(+1)	1.20	550	200	325

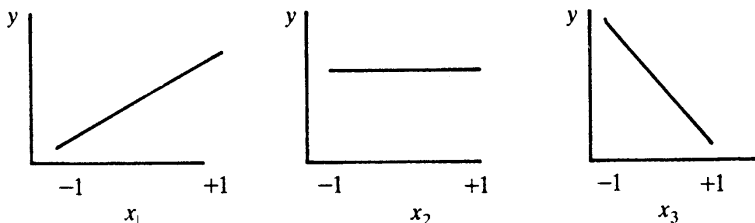


Figure E10.2 Main effect plots for Exercises 10.12 and 10.13.

**TABLE E10.1 Data for Exercise 10.14**

$A = x_1$	$B = x_2$	$C = z_1$	$D = z_2$	$y$ (etch rate, Å/min)
-1	-1	-1	-1	550
1	-1	-1	-1	669
-1	1	-1	-1	604
1	1	-1	-1	650
-1	-1	1	-1	633
1	-1	1	-1	642
-1	1	1	-1	601
1	1	1	-1	635
-1	-1	-1	1	1037
1	-1	-1	1	749
-1	1	-1	1	1052
1	1	-1	1	868
-1	-1	1	1	1075
1	-1	1	1	860
-1	1	1	1	1063
1	1	1	1	729

The design and observed results are given in Table E10.1.

- (a) Fit a response model to the etch rate data.
- (b) Find appropriate models for the mean and variance.
- (c) Suppose that it is important to keep the standard deviation of the etch rate below 150°. What operating conditions would you recommend?

- 10.15** Consider the etch rate data in Exercise 10.14. Show that the condition for minimum process variance is

$$x_1 = \frac{153.0625}{76.8125} = 1.99$$

To minimize the variance, the constraint induced by the experimental region forces the recommendation that one should operate at  $x_1 = 1.0$ .

- (a) Find a confidence region on the location (in  $x_1$ ) of minimum process variance.  
Does the region cover  $x_1 = 1.0$ ?
  - (b) Comment on your findings in (a).
- 10.16** Consider Exercise 3.9. Investigate the data set for dispersion effects by fitting a log variance model. Comment.
- 10.17** Suppose a crossed array of the type

$$2_{\text{III}}^{6-3} \times 2_{\text{III}}^{3-1}$$

is being proposed. Suppose you wish to use two levels on each variable but you wish to have access to more two-factor interactions among control variables. In

addition, you wish to fit a response model involving control and noise variables. Suggest an alternative design.

- 10.18** Consider a situation with three control variables and three noise variables. In order to construct an appropriate response model, the design should contain linear main effects, two-factor interactions among the control variables, and two-factor interactions between control and noise variables.
- What is the minimum number of design points required?
  - Give a 22-point design that is efficient for fitting this response function.
  - Give an efficient 25-point design.

- 10.19** There are situations in which two-factor interactions involving the noise variables are important, though response models involving these interactions are not emphasized in this text. Consider the fitted model

$$\hat{y} = b_0 + b_1x_1 + b_2x_2 + b_{12}x_1x_2 + c_1z_1 + c_2z_2 + c_{12}z_1z_2$$

Assume that  $\sigma_{z_1}$  and  $\sigma_{z_2}$  are both 1.0. In addition, assume that  $z_1$  and  $z_2$  are uncorrelated in the process.

- Using the notation in the above fitted model, give an estimate of the mean model.
- Give an estimate of the variance model.
- Are there any additional assumptions made in (b)?

- 10.20** Reconsider Exercise 10.18. Suppose it is known that factor A (control factor) is very likely to interact with noise variables D and E. All control variables A, B, and C are likely to be involved in two-factor interactions. Design a combined array that allows for an appropriate robust parameter design. Use 16 observations with a regular fraction of a  $2^6$ . Give appropriate defining relations.

- 10.21** Consider the data in Example 6.15 with the use of the conversion response. Suppose, in fact, that time and catalyst are control variables and temperature is a noise variable. Use a response model to produce the following:

- A process mean model
- A process variance model

What assumptions did you make in developing the above models?

- 10.22** As we indicated in Section 10.4.4, the CCD can be very useful. Suppose there are four control variables and four noise Variables. Give a CCD that is a combined array and allows for estimation of a second-order model in the control variables, all control  $\times$  noise interactions and noise main effect terms. This design should contain 64 factorial points and eight axial points, plus center runs. Use  $\alpha = 1.0$ .

- 10.23** Construct a *D*-optimal design to accommodate the constraints in Exercise 10.22. Use 45 total design points. Repeat using an *I*-optimal design. Compare the two designs.

**TABLE E10.2 Data for Exercise 10.26**

Control Variables			Noise Variables for the Following Values of $z_1$ and $z_2$					Type I Signal-to-Noise Ratio	
$x_1$	$x_2$	$x_3$	$z_1 = -1, z_2 = -1$	$z_1 = +1, z_2 = -1$	$z_1 = -1, z_2 = +1$	$z_1 = 1, z_2 = +1$	Response Average	Standard Deviation	
-1	-1	-1	118.9	65.7	95.3	92.4	93.08	21.77	29.06
+1	-1	-1	153.7	229.4	119.9	251.5	188.63	62.07	31.35
-1	+1	-1	196.7	170.9	234.2	166.6	192.10	31.06	36.44
+1	+1	-1	211.1	245.7	241.0	252.6	237.60	18.30	51.28
-1	-1	+1	145.2	132.2	167.1	137.9	145.60	15.29	45.07
+1	-1	+1	125.3	201.6	185.5	267.3	194.93	58.36	24.11
-1	+1	+1	283.0	251.1	263.4	190.4	246.98	39.94	36.44
+1	+1	+1	184.2	279.5	247.2	259.2	242.53	41.11	35.50

- 10.24** Consider a situation with the three control and two noise variables to accommodate a model that is second-order in the control variables and involves linear noise variable terms as well as all control  $\times$  noise interactions.
- (a) Give an appropriate CCD ( $\alpha = 1.0$ ) containing 22 points plus center runs.
  - (b) Give an appropriate  $D$ -optimal design.
  - (c) Give an appropriate  $I$ -optimal design.
- 10.25** Consider Example 10.1.
- (a) Fit an appropriate response model.
  - (b) Use the response model to generate a model for the process mean and a model for the process variance.
  - (c) Compare your results with those in Example 10.1 and with the direct variance modeling approach in Example 10.7
- 10.26** Montgomery (1999) describes an experiment performed in a semiconductor factory to determine how five factors influence the transistor gain for a particular device. It is desirable to hold the gain as close as possible to a target value of 200 (the specifications are actually  $200 \pm 20$ ). Three of the variables are relatively easy to control:  $x_1$  (implant dose),  $x_2$  (drive-in time), and  $x_3$  (vacuum level). Two variables are difficult to control in routine manufacturing and are considered as noise factors:  $z_1$  (oxide thickness) and  $z_2$  (temperature). The crossed array design they used is shown in Table E10.2. Conduct a Taguchi-type analysis to determine the operating conditions.
- 10.27** Reconsider the experiment described in Example 10.26. Treat the outer array runs as replicates, and fit models for the mean and variance using the control variables. Find the optimum operating conditions for the process. How do they compare with the results from the Taguchi-type analysis in Exercise 10.26?
- 10.28** Reconsider the experiment described in Exercise 10.26. Fit a response model to the data involving both the control and noise variables. Derive the mean and variance

models, and find optimum operating conditions. Compare your results with those obtained in Exercises 10.26 and 10.27.

- 10.29** The experiment in Exercise 10.26 is a  $2^3 \times 2^2$  crossed array. Viewed as a combined array, the design is a  $2^5$ . Using only the runs that correspond to a  $2^{5-1}$ , rework Exercise 10.28. Does this tell you anything useful about combined array designs?
- 10.30** Consider the experiment in Exercise 6.15. Suppose that temperature is a noise variable ( $\sigma_z^2 = 1$  in coded units). Fit response models for both responses. Is there a robust design problem with respect to both responses? Find a set of conditions that maximize conversion with activity between 55 and 60 and that minimize the variability transmitted from temperature.
- 10.31** An experiment has been run in a process that applies a coating material to a wafer. Each run in the experiment produced a wafer, and the coating thickness was measured several times at different locations on the wafer. Then the mean  $y_1$  and standard deviation  $y_2$  of the thickness measurement were obtained. The data [adapted from Box and Draper (1987)] are shown in Table E10.3.

TABLE E10.3 Data for Exercise 10.31

Run	Speed	Pressure	Distance	Mean $y_1$	Std. Dev. $y_2$
1	-1	-1	-1	24.0	12.5
2	0	-1	-1	120.3	8.4
3	1	-1	-1	213.7	42.8
4	-1	0	-1	86.0	3.5
5	0	0	-1	136.6	80.4
6	1	0	-1	340.7	16.2
7	-1	1	-1	112.3	27.6
8	0	1	-1	256.3	4.6
9	1	1	-1	271.7	23.6
10	-1	-1	0	81.0	0.0
11	0	-1	0	101.7	17.7
12	1	-1	0	357.0	32.9
13	-1	0	0	171.3	15.0
14	0	0	0	372.0	0.0
15	1	0	0	501.7	92.5
16	-1	1	0	264.0	63.5
17	0	1	0	427.0	88.6
18	1	1	0	730.7	21.1
19	-1	-1	1	220.7	133.8
20	0	-1	1	239.7	23.5
21	1	-1	1	422.0	18.5
22	-1	0	1	199.0	29.4
23	0	0	1	485.3	44.7
24	1	0	1	673.7	158.2
25	-1	1	1	176.7	55.5
26	0	1	1	501.0	138.9
27	1	1	1	1010.0	142.4

- (a) What type of design did the experimenters use? Is this a good choice of design for fitting a quadratic model?
- (b) Build models of both responses.
- (c) Find a set of optimum conditions that result in a mean as large as possible with the standard deviation less than 60.
- 10.32** In Example 10.3 we found that one of the process variables ( $B$  = pressure) was not important. Dropping this variable produces two replicates of a  $2^3$  design. The data are shown below:

$C$	$D$	A(+)	A(−)	$\bar{y}$	$s^2$
−	−	45, 48	71, 65	57.75	121.19
+	−	68, 80	60, 65	68.25	72.25
−	+	43, 45	100, 104	73.00	1124.67
+	+	75, 70	86, 96	81.75	134.92

Assume that  $C$  and  $D$  are controllable factors and that  $A$  is a noise variable.

- (a) Fit a model to the mean response.
- (b) Fit a log model to the variance.
- (c) Find operating conditions that result in the mean filtration rate response exceeding 75 with minimum variance.
- (d) Compare your results with those from Example 10.3, which used the response model approach. How similar are the two answers?



---

# 11

---

## EXPERIMENTS WITH MIXTURES

### 11.1 INTRODUCTION

In the response surface examples discussed previously, the levels chosen for any factor in the experimental design are independent of the levels chosen for the other factors. For example, suppose that there are three variables—stirring rate, reaction time, and temperature—that affect the yield of a chemical process. The levels of temperature may be chosen independently of the levels of reaction time and stirring rate, and consequently we may think of the region of experimentation as either a cube or a sphere. The experimental design will consist of an appropriate set of points over this cuboidal or spherical region (such as a factorial design or a central composite design).

A **mixture experiment** is a special type of response surface experiment in which the factors are the ingredients or components of a mixture, and the response is a function of the proportions of each ingredient. These proportional amounts of each ingredient are typically measured by weight, by volume, by mole ratio, and so forth.

For example, consider chemical etching of semiconductor wafers. The process consists of placing the wafers in a solution composed of several acids—say nitric acid, hydrochloric acid, and phosphoric acid—and observing the etch rate. In such a process, we wish to determine if a combination of these acids is more effective in etching the wafers than any of the three acids by themselves. Because the volume of the etching chamber is fixed, an experiment might consist of testing various combinations of these acids, where all mixes or blends have the same volume. If  $x_1$ ,  $x_2$ , and  $x_3$  represent the proportions by volume of the three acids, then some of the blends that might be of interest are as follows:

$$\text{Blend 1: } x_1 = 0.3, \quad x_2 = 0.3, \quad x_3 = 0.4$$

$$\text{Blend 2: } x_1 = 0.2, \quad x_2 = 0.5, \quad x_3 = 0.3$$

$$\begin{aligned} \text{Blend 3: } & x_1 = 0.5, \quad x_2 = 0.5, \quad x_3 = 0.0 \\ \text{Blend 4: } & x_1 = 1.0, \quad x_2 = 0.0, \quad x_3 = 0.0 \end{aligned}$$

Blends 1 and 2 are examples of **complete** mixtures; that is, they are made up of all three of the acids. Blend 3 is a **binary** blend, consisting of two of the three acids, and blend 4 is a mixture that is made up of 100% by volume of only one of the three acids. Each of these blends is called a **mixture**. Notice that in this example  $x_1 + x_2 + x_3 = 1$ ; and because of this constraint, the levels of the factors cannot be chosen independently. For instance, in blend 1 above, as soon as we indicate that acid 1 makes up 30% of the mixture by volume ( $x_1 = 0.3$ ) and acid 2 makes up 30% of the mixture by volume ( $x_2 = 0.3$ ), it is immediately obvious that acid 3 must make up 40% of the mixture by volume (that is,  $x_3 = 0.4$  because  $x_1 = x_2 = 0.3$  and  $x_1 + x_2 + x_3 = 1.0$ ).

In general, suppose that the mixture consists of  $q$  ingredients or components, and let  $x_i$  represent the proportion of the  $i$ th ingredient in the mixture. Then in light of the above discussion we must require that

$$x_i \geq 0, \quad i = 1, 2, \dots, q \quad (11.1)$$

and

$$\sum_{i=1}^q x_i = x_1 + x_2 + \dots + x_q = 1 \quad (11.2)$$

The constraint in Equation 11.2 makes the levels of the factors  $x_i$  dependent and this makes mixture experiments different from the usual response surface experiments we have discussed previously.

The constraints in Equations 11.1 and 11.2 are shown graphically in Fig. 11.1 for  $q = 2$  and  $q = 3$  components. For two components, the feasible factor space for the mixture experiment includes all values of the two components for which  $x_1 + x_2 = 1$ , which is the line segment shown in Fig. 11.1a. With three components, the feasible space for the mixture experiment is the triangle in Fig. 11.1b that has vertices corresponding to **pure blends**—that is, mixtures that are made up of 100% of a single ingredient—and edges

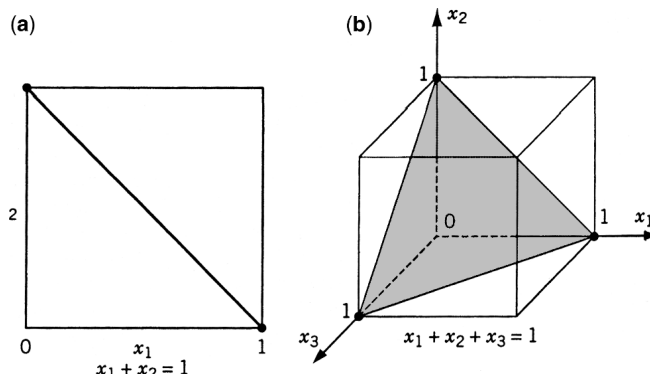


**Figure 11.1** Constrained factor space for mixtures with (a)  $q = 2$  components and (b)  $q = 3$  components.

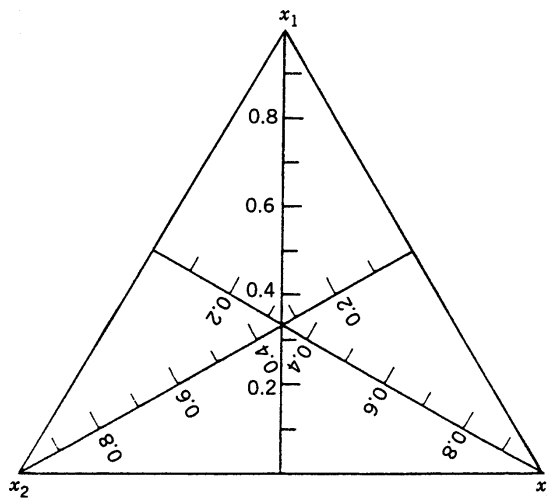


**Figure 11.2** Simplex coordinate system for three components.

that are binary blends. In general, the experimental region for a mixture problem with  $q$  components is a **simplex**, which is a regularly sided figure with  $q$  vertices in  $q - 1$  dimensions.

The coordinate system for mixture proportions is a **simplex coordinate system**. For example, with  $q = 3$  components, the experimental region is shown in Fig. 11.2. Each of the three vertices in the equilateral triangle corresponds to a pure blend, and each of the three sides of the triangle represents a binary blend mixture that has none of one of the three components (the component labeled on the opposite vertex). The nine grid lines in each direction mark off 10% increments in the respective components. Interior points in the triangle represent mixtures in which all three ingredients are present at nonzero proportionate amounts. The centroid of the triangle corresponds to the mixture with equal proportions  $x_1 = \frac{1}{3}$ ,  $x_2 = \frac{1}{3}$ ,  $x_3 = \frac{1}{3}$  of all ingredients.

Applications of mixture experiments are found in many areas. A common application is **product formulation**, in which a product is formed by mixing several ingredients together. Examples include (a) formulation of gasoline by combining several refinery products and other types of chemicals such as anticars, (b) formulation of soaps, shampoos, and detergents in the consumer products industry, and (c) formulation of products such as cake mixes and beverages in the food industry. In addition to product formulation, mixture experiments arise frequently in process engineering and development where some property of a final product depends on a mixture of several ingredients interacting with the product at a particular process stage. An example is the wafer etching process described above. Other examples include gas or plasma etching in the semiconductor industry, many joining processes such as soldering, and chemical milling or machining.

In this chapter we discuss experimental design, data analysis, and model-building techniques for the original mixture experiment defined by Equations 11.1 and 11.2. In this problem, the entire simplex region is investigated, and the only design variables are the mixture components  $x_1, x_2, \dots, x_q$ .

There are many variations of the original mixture problem. One of these is the addition of upper and lower bounds on some of the component proportions. These bounds occur

because the problem may require that at least a certain minimum proportion of an ingredient be present in the blend, or that an ingredient cannot exceed a specified maximum proportion. In some mixture problems there are **process variables**  $z_1, z_2, \dots, z_p$  in addition to the mixture ingredients. For example, in the wafer etching example above, the mixture ingredients  $x_1, x_2$ , and  $x_3$  are the proportions of the three acids, and two process variables could be the temperature ( $z_1$ ) of the etching solution and the agitation rate ( $z_2$ ) of the wafers. Including process variables in mixture experiments usually involves constructing designs that utilize different levels of the process variables via a factorial design in combination with the mixture variables. Finally, in some mixture problems the experimenter may be interested in not only the formulation of the mixture but the amount of the mixture that is applied to the experimental units. For example, the opacity of a coating depends on the ingredients from which the coating is formulated, but it also depends upon the thickness of the coating surface when it is applied. Some of these variations of the original mixture experiment will be discussed in Chapter 12.

## 11.2 SIMPLEX DESIGNS AND CANONICAL MIXTURE POLYNOMIALS

The primary differences between a standard response surface experiment and a mixture experiment are that (1) special types of design must be used and (2) the form of the mixture polynomial is slightly different from the standard polynomials used in response surface methodology (RSM). In this section we introduce designs that allow an appropriate response surface model to be fitted over the entire mixture space. Because the mixture space is a simplex, all design points must be at the vertices, on the edges or faces, or in the interior of a simplex.

Much of the work in this area was originated by Scheffé (1958, 1959, 1965). Cornell (2002) is an excellent and very complete reference on the subject.

### 11.2.1 Simplex Lattice Designs

A simplex lattice is just a uniformly spaced set of points on a simplex. A  $\{q, m\}$  simplex lattice design for  $q$  components consists of points defined by the following coordinate settings: The proportions taken on by each component are the  $m + 1$  equally spaced values from 0 to 1,

$$x_i = 0, \frac{1}{m}, \frac{2}{m}, \dots, 1, \quad i = 1, 2, \dots, q \quad (11.3)$$

and all possible combinations (mixtures) of the proportions from this equation are used. As an example, let  $q = 3$  and  $m = 2$ ; consequently,

$$x_i = 0, \frac{1}{2}, 1, \quad i = 1, 2, 3$$

and the simplex lattice consists of the following six points:

$$(x_1, x_2, x_3) = (1, 0, 0), (0, 1, 0), (0, 0, 1), \left(\frac{1}{2}, \frac{1}{2}, 0\right), \left(\frac{1}{2}, 0, \frac{1}{2}\right), \left(0, \frac{1}{2}, \frac{1}{2}\right)$$

This is a  $\{3, 2\}$  simplex lattice design, and it is shown in Fig. 11.3a. The three vertices  $(1, 0, 0)$ ,  $(0, 1, 0)$ , and  $(0, 0, 1)$  are pure blends, and the points  $\left(\frac{1}{2}, \frac{1}{2}, 0\right)$ ,  $\left(\frac{1}{2}, 0, \frac{1}{2}\right)$ , and  $\left(0, \frac{1}{2}, \frac{1}{2}\right)$  are

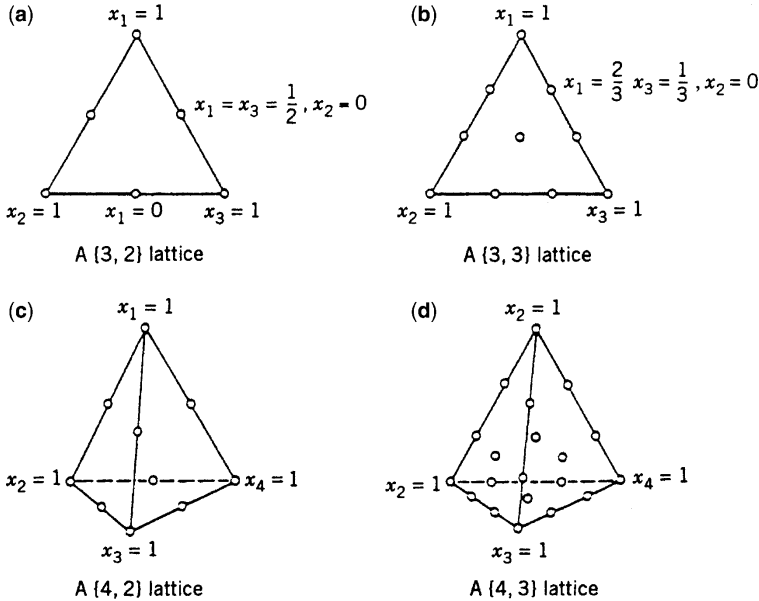


**Figure 11.3** Simplex lattice designs for  $q = 3$  and  $q = 4$  components.

binary blends or two-component mixtures located at the midpoints of the three edges of the triangle. These binary blends are made up of equal parts of two of the three ingredients. Figure 11.3 also shows the  $\{3, 3\}$ , the  $\{4, 2\}$ , and the  $\{4, 3\}$  simplex lattice designs. As we will subsequently see, the notation  $\{q, m\}$  implies a simplex lattice design in  $q$  components that will support a mixture polynomial of degree  $m$ . In general, the number of points in a  $\{q, m\}$  simplex lattice design is

$$N = \frac{(q+m-1)!}{m!(q-1)!} \quad (11.4)$$

Now consider the form of the polynomial model that we might fit to data from a mixture experiment. A first-order model is

$$E(y) = \beta_0 + \sum_{i=1}^q \beta_i x_i \quad (11.5)$$

However, because of the restriction  $x_1 + x_2 + \dots + x_q = 1$  we know that the parameters  $\beta_0, \beta_1, \dots, \beta_q$  are not unique. We could, of course, make the substitution

$$x_q = 1 - \sum_{i=1}^{q-1} x_i$$

in Equation 11.5, removing the dependence among the  $x_i$ -terms and producing unique estimates of the parameters  $\beta_0, \beta_1, \dots, \beta_{q-1}$ . Although this will work mathematically, it is not the preferred approach, because it obscures the effect of the  $q$ th component in that the term

$\beta_q x_q$  is not included in the equation. Thus, in a sense, we are sacrificing information on component  $q$ .

An alternative approach is to multiply some of the terms in the original response surface polynomial by the identity  $x_1 + x_2 + \dots + x_q = 1$  and then simplify. For example, consider Equation 11.5, and multiply the term  $\beta_0$  by  $x_1 + x_2 + \dots + x_q = 1$ , yielding

$$\begin{aligned} E(y) &= \beta_0(x_1 + x_2 + \dots + x_q) + \sum_{i=1}^q \beta_i x_i \\ &= \sum_{i=1}^q \beta_i^* x_i \end{aligned} \quad (11.6)$$

where  $\beta_i^* = \beta_0 + \beta_i$ . This is called the **canonical** or **Scheffé form** of the first-order mixture model. In general, the canonical or Scheffé forms of the mixture models (with the asterisks removed from the parameters) are as follows:

*Linear:*

$$E(y) = \sum_{i=1}^q \beta_i x_i \quad (11.7)$$

*Quadratic:*

$$E(y) = \sum_{i=1}^q \beta_i x_i + \sum_{i<j=2}^q \beta_{ij} x_i x_j \quad (11.8)$$

*Full Cubic:*

$$\begin{aligned} E(y) &= \sum_{i=1}^q \beta_i x_i + \sum_{i<j=2}^q \beta_{ij} x_i x_j + \sum_{i<j=2}^q \delta_{ij} x_i x_j (x_i - x_j) \\ &\quad + \sum_{i<j<k=3}^q \beta_{ijk} x_i x_j x_k \end{aligned} \quad (11.9)$$

*Special Cubic:*

$$E(y) = \sum_{i=1}^q \beta_i x_i + \sum_{i<j=2}^q \beta_{ij} x_i x_j + \sum_{i<j<k=2}^q \beta_{ijk} x_i x_j x_k \quad (11.10)$$

The terms in the canonical mixture polynomials have simple interpretations. Geometrically, in Equations 11.7 through 11.10, the parameter  $\beta_i$  represents the expected response for the pure mixture  $x_i = 1$ ,  $x_j = 0$ ,  $j \neq i$ , and is the height of the mixture surface at the vertex  $x_i = 1$ . The portion of each polynomial given by

$$\sum_{i=1}^q \beta_i x_i$$

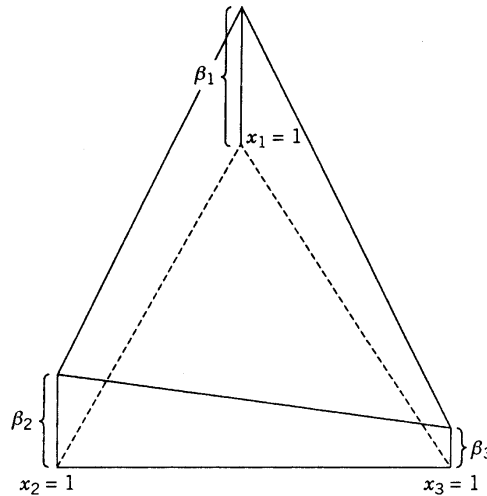


**Figure 11.4** Linear mixture model in three components with  $\beta_1 > \beta_2 > \beta_3$ .

is called the **linear blending** portion. When blending is strictly additive, then Equation (11.7) is an appropriate model. Figure 11.4 presents the case where  $q = 3$  and  $\beta_1 > \beta_2 > \beta_3$ .

Quadratic blending is illustrated in Fig. 11.5a. Notice that the quadratic term  $\beta_{12}x_1x_2$  represents the excess response from the quadratic model  $E(y) = \beta_1x_1 + \beta_2x_2 + \beta_{12}x_1x_2$  over the linear model. This is often called the **synergism (or antagonism) due to nonlinear blending**. For example, if large positive values of  $y$  are desired and if  $\beta_{12}$  is positive, synergistic blending is occurring, whereas if  $\beta_{12}$  is negative, antagonistic blending is occurring. In the cubic model, terms such as  $\delta_{12}x_1x_2(x_1 - x_2)$  enable one to model both synergistic and antagonistic blending along the  $x_1 - x_2$  edge; see Fig. 11.5b. A cubic term such as  $\beta_{123}x_1x_2x_3$  accounts for ternary blending among the three components in the interior of the simplex.

It is also helpful to consider the way in which the individual terms in a mixture model contribute to the shape of the response surface. A linear term such as  $\beta_1x_1$  only contributes to the model when  $x_1 > 0$ ; and the maximum contribution occurs at  $x_1 = 1$ , in which case the maximum effect contributed by  $x_1$  is  $\beta_1$ . The quadratic term  $\beta_{12}x_1x_2$  contributes to the model at every point in the simplex where  $x_1 > 0$  and  $x_2 > 0$ . The maximum contribution occurs at the edge joining the vertices  $x_1$  and  $x_2$  and is at the point  $x_1 = x_2 = \frac{1}{2}$ . The maximum contribution to the model from this term is  $\beta_{12}/4$ . A cubic term such as

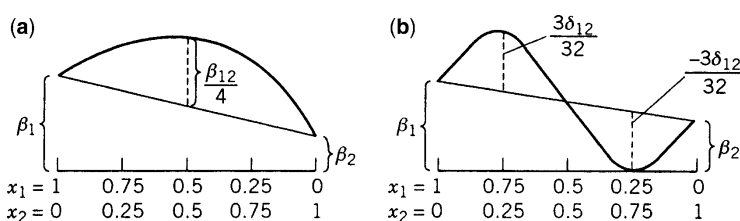


**Figure 11.5** Nonlinear blending. **(a)** Quadratic blending with  $\beta_{ij} > 0$ . **(b)** Cubic blending with  $\delta_{12} > 0$ .

$\beta_{123}x_1x_2x_3$  contributes to the model at every point for which  $x_1 > 0$ ,  $x_2 > 0$ , and  $x_3 > 0$  (in the interior of the simplex), and the maximum contribution is of magnitude  $\beta_{123}/27$  at the point  $x_1 = x_2 = x_3 = \frac{1}{3}$ .

**Example 11.1 A Three-Component Mixture** Cornell (2002) describes a mixture experiment in which three components—polyethylene ( $x_1$ ), polystyrene ( $x_2$ ), and polypropylene ( $x_3$ )—were blended to form fiber that will be spun into yarn for draperies. The product developers were interested in only the pure and binary blends of these three materials. The response variable of interest is yarn elongation in kilograms of force applied. A {3, 2} simplex lattice design is used to study the product. The design and the observed responses are shown in Table 11.1. Notice that replicate observations are run, with two replicates at each of the pure blends and three replicates at each of the binary blends. The error standard deviation can be estimated from these replicate observations as  $\hat{\sigma} = 0.85$ .

Table 11.2 shows output from the Design-Expert computer program, which was used to analyze the yarn elongation data. This program fits both the linear and quadratic mixture model to the data, and the upper panel of Table 11.2 shows the sequential  $F$ -tests for the linear blending terms and the quadratic terms. The  $F$ -test for the linear terms is significant, and the  $F$ -test for the contribution of the quadratic terms over the linear terms is also significant, indicating that a quadratic mixture model should be used. The middle panel of Table 11.2 shows a lack-of-fit test for the linear mixture model. The value of  $F = 32.32$  is very large, indicating that a linear mixture model is inadequate. Finally, the bottom panel of Table 11.2 presents several informative summary statistics for the linear and quadratic models. These statistics indicate that the quadratic model is superior to the linear model.

The  $F$ -test for the linear terms in the upper panel of Table 11.2 warrants some discussion. This is a test of the hypothesis that there is no linear blending occurring in the mixture. If there is no linear blending, then the response surface is a level plane above the simplex region; that is,  $\beta_1 = \beta_2 = \beta_3 = \beta$ . Expressed formally, the hypotheses to be tested are

$$\begin{aligned} H_0: \quad & \beta_1 = \beta_2 = \beta_3 = \beta \\ H_1: \quad & \text{At least one equality is false} \end{aligned}$$

Because from Table 11.2 the test statistic is  $F_{\text{linear}} = 4.477$  with a  $P$ -value of  $P = 0.0353$ , we would reject  $H_0$  and conclude that there is linear blending in the system.

**TABLE 11.1 The {3, 2} Simplex Lattice Design for the Yarn Elongation Problem**

Design Point	Component Proportions			Observed Elongation Values	Average Elongation Value $\bar{y}$
	$x_1$	$x_2$	$x_3$		
1	1	0	0	11.0, 12.4	11.7
2	$\frac{1}{2}$	$\frac{1}{2}$	0	15.0, 14.8, 16.1	15.3
3	0	1	0	8.8, 10.0	9.4
4	0	$\frac{1}{2}$	$\frac{1}{2}$	10.0, 9.7, 11.8	10.5
5	0	0	1	16.8, 16.0	16.4
6	$\frac{1}{2}$	0	$\frac{1}{2}$	17.7, 16.4, 16.6	16.9

**TABLE 11.2 Design-Expert Output for the Yarn Elongation Data**

Sequential Model Sum of Squares					
Source	Sum of Squares	Degrees of Freedom	Mean Square	F-Value	Probability > F
Mean	2750.0	1	2750.0		
Linear	57.6	2	28.8	4.477	0.0353
Quadratic	70.7	3	23.6	32.32	0.0001
Residual	6.6	9	0.7		
Total	2884.9	15			
Lack-of-Fit Tests					
Model	Sum of Squares	Degrees of Freedom	Mean Square	F-Value	Probability > F
Linear	70.7	3	23.6	32.32	0.0001
Quadratic	0.0	0			
Pure Error	6.6	9	0.7		
ANOVA Summary Statistics of Model Fit					
Source	Unaliased Terms	Residual Degrees of Freedom	Root Mean Squared Error	R-Squared	Adjusted R-Squared
Linear	3	12	2.54	0.4273	0.3319
Quadratic	6	9	0.85	0.9514	0.9243
					PRESS
					120.81
					18.30

Table 11.3 summarizes the quadratic model fit. The analysis of variance for the quadratic model, shown in the upper panel of Table 11.3, tests the hypothesis that the response surface is a level plane above the simplex region. Formally, this hypothesis is

$$\begin{aligned} H_0: \quad & \beta_1 = \beta_2 = \beta_3 = \beta, \quad \beta_{12} = \beta_{13} = \beta_{23} = 0 \\ H_1: \quad & \text{At least one equality is false} \end{aligned}$$

Because the test statistic is  $F = 35.2$  (with a  $P$ -value of  $P = 0.0001$ ), this hypothesis is rejected. Notice that  $t$ -tests are provided for the quadratic terms on the model because tests of the hypotheses regarding each of these individual terms (i.e.,  $H_0: \beta_{ij} = 0$ ) are meaningful. However, because similar tests on the linear blending terms are not meaningful ( $H_0: \beta_i = 0$  does not test for linear blending from component  $i$ ), these  $t$ -tests are not displayed.

The fitted quadratic mixture model is

$$\hat{y} = 11.7x_1 + 9.4x_2 + 16.4x_3 + 19.0x_1x_2 + 11.4x_1x_3 - 9.6x_2x_3$$

Because  $b_3 > b_1 > b_2$ , we would conclude that component 3 (polypropylene) produces yarn with the highest elongation. Furthermore, because  $b_{12}$  and  $b_{13}$  are positive, blending components 1 and 2 or components 1 and 3 produces higher elongation values than would be expected just by averaging the elongations of the pure blends. This is an example of **synergistic** blending effects. Components 2 and 3 have antagonistic blending effects, because  $b_{23}$  is negative.

**TABLE 11.3 Quadratic Mixture Model for the Yarn Elongation Data**

ANOVA for Quadratic Model					
Source	Sum of Squares	Degrees of Freedom	Mean Square	F-Value	Probability > F
Model	128.3	5	25.66	35.20	0.0001
Residual	6.6	9	0.73		
Corrected total	134.9	14			
Root mean squared error	0.85		R-squared	0.9514	
Dependent mean	13.54		Adjusted R-squared	0.9243	
Independent Variable	Coefficient Estimate	Degrees of Freedom	Standard Error	<i>t</i> for $H_0$ Coefficient = 0	
$x_1$	11.70	1	0.60	Not applicable	
$x_2$	9.40	1	0.60	Not applicable	
$x_3$	16.40	1	0.60	Not applicable	
$x_1x_2$	19.00	1	2.61	7.285	0.0001
$x_1x_3$	11.40	1	2.61	4.371	0.0018
$x_2x_3$	-9.60	1	2.61	-3.681	0.0051
Observation	Actual Value	Predicted Value	Residual	$h_{ii}$	Studentized Residual Cook's Distance <i>R</i> -Student
1	11.00	11.70	-0.70	0.500	-1.160 0.224 -1.185
2	12.40	11.70	0.70	0.500	1.160 0.224 1.185
3	15.00	15.30	-0.30	0.333	-0.430 0.015 -0.410
4	14.80	15.30	-0.50	0.333	-0.717 0.043 -0.696
5	16.10	15.30	0.80	0.333	1.148 0.110 1.171
6	17.70	16.90	0.80	0.333	1.148 0.110 1.171
7	16.60	16.90	-0.30	0.333	-0.430 0.015 -0.410
8	16.40	16.90	-0.50	0.333	-0.717 0.043 -0.696
9	8.80	9.40	-0.60	0.500	-0.994 0.165 -0.993
10	10.00	9.40	0.60	0.500	0.994 0.165 0.993
11	10.00	10.50	-0.50	0.333	-0.717 0.043 -0.696
12	9.70	10.50	-0.80	0.333	-1.148 0.110 -1.171
13	11.80	10.50	1.30	0.333	1.865 0.290 2.245
14	16.80	16.40	0.40	0.500	0.663 0.073 0.641
15	16.00	16.40	-0.40	0.500	-0.663 0.073 -0.641

Figures 11.6 and 11.7 present a normal probability plot of the studentized residuals from the quadratic model. These plots are satisfactory. In general, we recommend analyzing studentized residuals (in contrast to the ordinary least squares residuals) from mixture experiments, because the points in mixture designs can have substantial differences in their leverage values. Studentized residuals account for leverage through the factor  $1 - h_{ii}$  that appears in the denominator (see Eq. 2.50 in Chapter 2).

Figure 11.8 presents a contour plot of elongation and a three-dimensional response surface plot. These plots are helpful in interpreting the results. From examining the figure, we note that if maximum elongation is desired, a blend of components 1 and 3 should be chosen consisting of about 80% component 3 and 20% component 1.

Figure 11.9 presents the contours of constant standard deviation of predicted yarn elongation ( $\sqrt{\text{Var}[\hat{y}(\mathbf{x})]}$ ) over the complete mixture space. This is related to the estimated

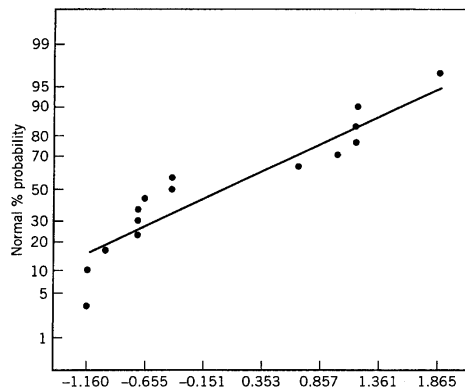


**Figure 11.6** Normal probability plot of studentized residuals for the quadratic model of yarn elongation.

prediction variance (EPV) defined in Chapter 7. Notice that the quality of prediction is better, in a variance sense, at points in the interior of the simplex than on the edges or at the vertices. However, one should be very careful about making predictions at points in the interior, because no experimental trials were performed there. The  $\{3, 2\}$  simplex lattice is a **boundary point design**; that is, all of the design points are either binary mixtures or pure mixtures. In this application the engineers were not interested in the ternary blends, so the lack of interior points is not a major concern. When one is interested in prediction in the interior, it is highly desirable to augment simplex-type designs with interior design points. We will return to this again in Section 11.2.3.

### 11.2.2 The Simplex-Centroid Design and Its Associated Polynomial

A  $q$ -component simplex-centroid design consists of  $2^q - 1$  distinct design points. These design points are the  $q$  permutations of  $(1, 0, 0, \dots, 0)$  or single-component blends, the  $\binom{q}{2}$  permutations of  $(\frac{1}{2}, \frac{1}{2}, 0, \dots, 0)$  or all binary mixtures, the  $\binom{q}{3}$  permutations of  $(\frac{1}{3}, \frac{1}{3}, \frac{1}{3}, 0, \dots, 0)$ , and so forth, and the overall centroid  $(1/q, 1/q, \dots, 1/q)$ . Figure 11.10 shows the simplex-centroid designs for  $q = 3$  and  $q = 4$  components. Note that the design

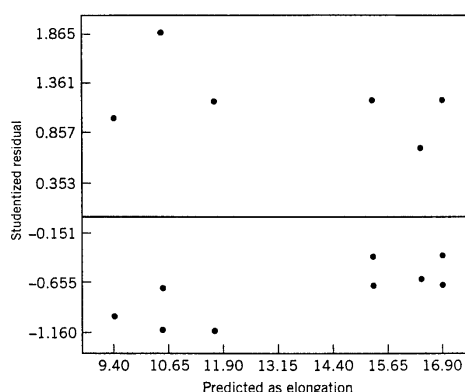


**Figure 11.7** Plot of studentized residuals versus predicted yarn elongation.

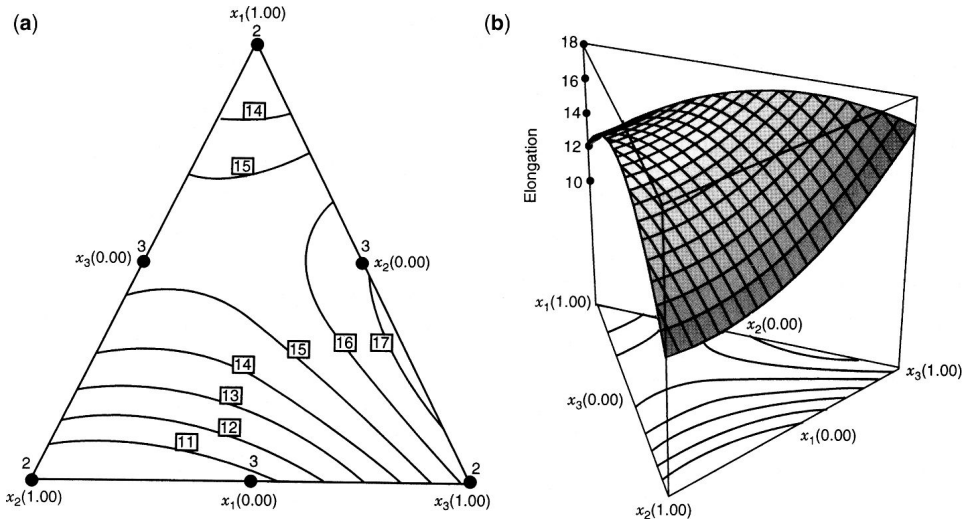


**Figure 11.8** (a) Contour plot of predicted yarn elongation. (b) Three-dimensional surface plot. The solid dots on the contour plot are the design points.

points are located at the centroid of the  $(q - 1)$ -dimensional simplex and at the centroids of all the lower-dimensional simplices contained within the  $(q - 1)$ -dimensional simplex.

The design points in the simplex-centroid design will support the polynomial

$$E(y) = \sum_{i=1}^q \beta_i x_i + \sum_{i < j=2}^q \beta_{ij} x_i x_j + \sum_{i < j < k=3}^q \beta_{ijk} x_i x_j x_k + \cdots + \beta_{12\cdots q} x_1 x_2 \cdots x_q \quad (11.11)$$

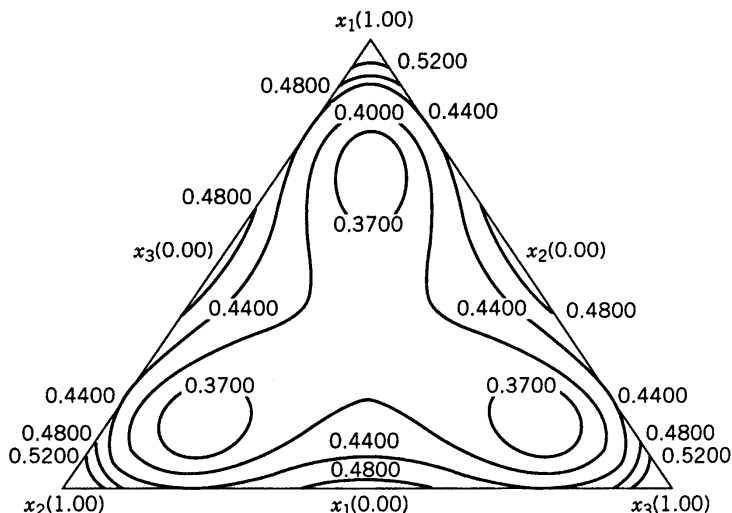


**Figure 11.9** Contours of constant standard deviation of predicted response  $\sqrt{\text{Var}[\hat{y}(x)]}$  for the quadratic mixture model for the yarn elongation data.

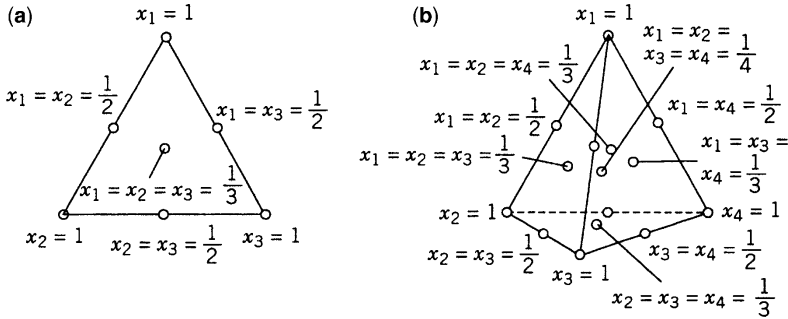


**Figure 11.10** Simplex-centroid designs with three and four components. (a)  $q = 3$ . (b)  $q = 4$ .

which is a  $q$ th-order mixture polynomial. For  $q = 3$  components, this model is

$$\begin{aligned} E(y) = & \beta_1 x_1 + \beta_2 x_2 + \beta_3 x_3 + \beta_{12} x_1 x_2 + \beta_{13} x_1 x_3 \\ & + \beta_{23} x_2 x_3 + \beta_{123} x_1 x_2 x_3 \end{aligned}$$

which is the special cubic polynomial from Equation 11.10. For  $q = 4$  components, the model is

$$\begin{aligned} E(y) = & \sum_{i=1}^4 \beta_i x_i + \sum_{i < j=2}^4 \beta_{ij} x_i x_j + \sum_{i < j < k=3}^4 \beta_{ijk} x_i x_j x_k \\ & + \beta_{1234} x_1 x_2 x_3 x_4 \end{aligned}$$

or the special cubic model with an additional quartic term. Because they are relatively efficient designs for fitting the special cubic model, simplex-centroid designs are often used when the experimenter thinks that some cubic terms may be necessary in the final model.

### 11.2.3 Augmentation of Simplex Designs with Axial Runs

The standard simplex-lattice and simplex-centroid designs are **boundary point designs**; that is, with the exception of the overall centroid, all the design points are on the boundaries of the simplex. For example, consider the  $\{3, 3\}$  lattice design shown in Fig. 11.3b. This design has ten points: the three vertices, the six points that are at the thirds of the edges, and the overall centroid. Thus there are three points that tell us something about the pure blends, six points that provide information about binary blends, and only one point that tells us anything about complete mixtures. We could say that the distribution of information about these different types of mixtures is 3 : 6 : 1.

If one is interested in making predictions about the properties of complete mixtures, it would be highly desirable to have more runs in the interior of the simplex. We recommend augmenting the usual simplex designs with **axial runs** and the overall centroid (if the centroid is not already a design point).

We define the **axis of component  $i$**  as the line or ray extending from the base point  $x_i = 0$ ,  $x_j = 1/(q-1)$  for all  $j \neq i$  to the opposite vertex where  $x_i = 1$ ,  $x_j = 0$  for all  $j \neq i$ . Figure 11.11 shows the axes for components 1, 2, and 3 in a three-component system. Notice that the base point will always lie at the centroid of the  $(q-2)$ -dimensional

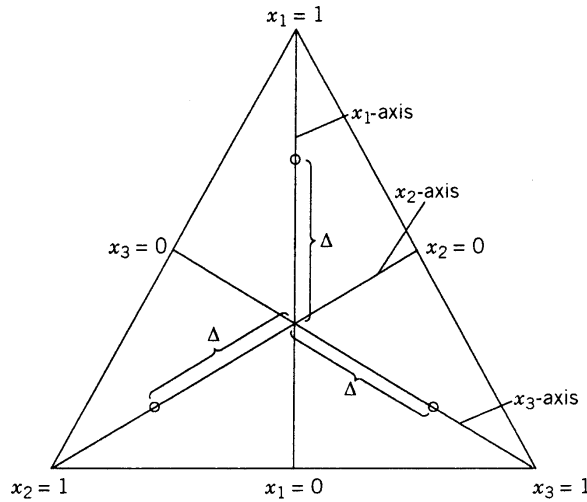


**Figure 11.11** The axes for components  $x_1$ ,  $x_2$ , and  $x_3$ .

boundary of the simplex that is opposite the vertex  $x_i = 1$ ,  $x_j = 0$  for all  $j \neq i$ . [The boundary is sometimes called a **( $q-2$ )-flat**.] The length of the component axis is one unit. **Axial points** are positioned along the component axes a distance  $\Delta$  from the centroid. The maximum value for  $\Delta$  is  $(q-1)/q$ . We recommend that axial runs be placed midway between the centroid of the simplex and each vertex, so that  $\Delta = (q-1)/2q$ . Sometimes these points are called **axial check blends**, because a fairly common practice is to exclude them when fitting the preliminary mixture model, and then use the responses at these axial points to check the adequacy of the fit of the preliminary model.

Figure 11.12 shows the  $\{3, 2\}$  simplex-lattice design augmented with the axial points. This design has 10 points, with four of these points in the interior of the simplex. Thus the distribution of information in this augmented simplex lattice is 3:3:4. Contrast this to the 10-point  $\{3, 3\}$  simplex lattice, for which the distribution of information is

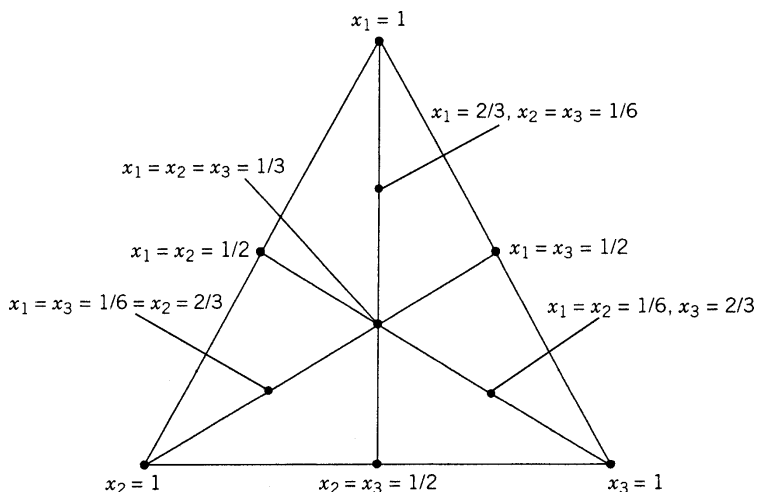


**Figure 11.12** An augmented simplex-lattice design.

$3:6:1$ . Cornell (1986) presents an extensive comparison of these two designs. He notes that the  $\{3, 3\}$  simplex lattice will support fitting the full cubic model, while the augmented simplex lattice will not; however, the augmented simplex lattice will allow the experimenter to fit the special cubic model or to add special quadratic terms such as  $\beta_{1233}x_1x_2x_3^2$  to the quadratic model. The augmented simplex lattice is superior for studying the response of complete mixtures in the sense that it can detect and model curvature in the interior of the triangle that cannot be accounted for by the terms in the full cubic model. The augmented simplex lattice has more power for detecting lack of fit than does the  $\{3, 3\}$  lattice. This is particularly useful when the experimenter is unsure about the proper model to use and also plans to **sequentially** build a model by starting with a simple polynomial (perhaps first order), test the model for lack of fit, then augment the model with higher-order terms, test the new model for lack of fit, and so forth.

**Example 11.2 Etching Wafers** Wet chemical etching is often performed on the backs of silicon wafers prior to metallization in the semiconductor industry. The etching solution is a mixture of three different acids: A, B, and C. The experimenters wish to study how the composition of this mixture affects the etch rate. The experimenters think that a quadratic mixture model might be appropriate for modeling the relationship between etch rate and the proportions of different acids. However, there is some uncertainty about the nature of this relationship, so linear and special cubic models will also be considered. The experimenters selected the augmented simplex-lattice design shown in Fig. 11.12 for the use in this study, since it is a good choice for the quadratic model, but also performs well for the linear and special cubic cases if either of these turn out to be appropriate. They decided to replicate the vertices and the overall centroid so that an internal estimate of error could be obtained. Thus the complete experimental design, shown in Table 11.4 along with the response, consists of 14 runs.

Figure 11.13 shows the fraction of design space (FDS) plot, introduced in Chapter 8, for the scaled prediction variance (SPV) for the three possible models. While previously we used the FDS plots for comparing different designs with the same assumed model, here we compare what quality of prediction we can expect depending on which final model is selected for a single design. See Ozol-Godfrey et al. (2005) for more details on assessing model robustness. As we add additional terms to the model, the SPV must necessarily

**TABLE 11.4 Augmented Simplex-Lattice Design for the Etch Rate Experiment**

Design Point	$x_1$ (Acid A)	$x_2$ (Acid B)	$x_3$ (Acid C)	Etch Rate $y$ ( $\text{\AA}/\text{min}$ )
1	1	0	0	540, 560
2	0	1	0	330, 350
3	0	0	1	295, 260
4	$\frac{1}{2}$	$\frac{1}{2}$	0	610
5	0	$\frac{1}{2}$	$\frac{1}{2}$	330
6	$\frac{1}{2}$	0	$\frac{1}{2}$	425
7	$\frac{2}{3}$	$\frac{1}{6}$	$\frac{1}{6}$	710
8	$\frac{1}{6}$	$\frac{2}{3}$	$\frac{1}{6}$	640
9	$\frac{1}{6}$	$\frac{1}{6}$	$\frac{2}{3}$	460
10	$\frac{1}{3}$	$\frac{1}{3}$	$\frac{1}{3}$	800, 850

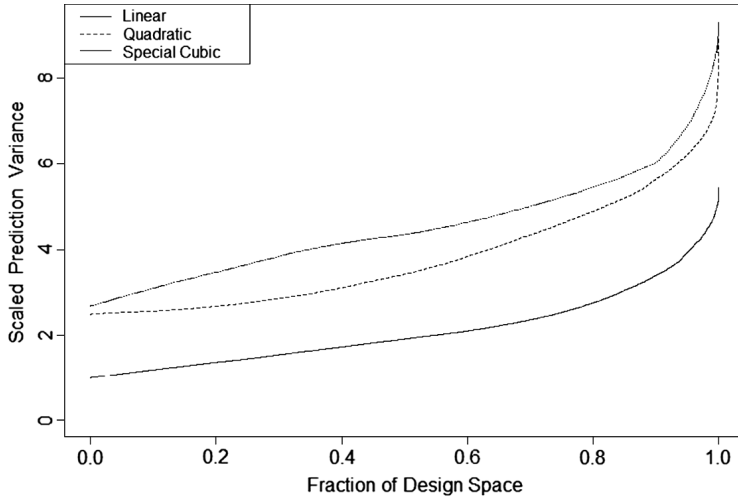


**Figure 11.13** Fraction of design space plot for the partially replicated augmented simplex-lattice design for the wafer etching example.

increase for a given design, hence the linear model has the lowest SPV throughout the region. However, if the true underlying relationship between etch rate and mixture ingredients is quadratic or special cubic, then the linear model will have large bias and will miss important features in the relationship. Hence, we wish to select the simplest model which appropriately summarizes the true relationship.

Table 11.5 presents the results of fitting linear, quadratic, special cubic, and full cubic models to the data obtained in this experiment (the computations were performed using Design-Expert). The sequential *F*-tests in this table indicate that the contribution of the quadratic terms to the model (over the linear terms) is significant, as is the contribution of the special cubic term  $\beta_{123}x_1x_2x_3$  (over the linear and quadratic terms). Furthermore, the quadratic model displays significant lack of fit, whereas the special cubic model does not; and, in addition, the special cubic model has a smaller error mean square, a larger adjusted  $R^2$ , and a smaller value of the PRESS statistic than does the quadratic model. Terms in the full cubic model are aliased and should be ignored. On the basis of this analysis, the experimenters selected the special cubic model. Table 11.6 presents the results of fitting the special cubic model. The upper portion of this table is the overall analysis of variance for this model. The *F*-test for the model is used to test the hypotheses

$$\begin{aligned} H_0: \quad & \beta_1 = \beta_2 = \beta_3 = \beta, \quad \beta_{12} = \beta_{13} = \beta_{23} = \beta_{123} = 0 \\ H_1: \quad & \text{At least one equality is false} \end{aligned}$$

Because  $F_0 = 70.23$  ( $P < 0.001$ ), the null hypothesis is rejected. The *t*-statistics on the individual model terms indicate that two of the quadratic terms,  $x_1x_3$  and  $x_2x_3$ , could be deleted; however, the experimenters decided to retain them in order to keep the model hierarchical. The *F*-statistic for lack of fit is testing for contributions of terms beyond the special cubic. This design could support three special quartic terms. The lack-of-fit test indicates that these terms are unnecessary. The diagnostic information at the bottom of Table 11.6 is generally satisfactory. The center-of-edge points in this design have relatively large leverage values

**TABLE 11.5 Sequential Model Fitting for the Etch Rate Data**

Source	Sequential Model Sum of Squares				
	Sum of Squares	Degrees of Freedom	Mean Square	F-Value	Probability > F
Mean	3,661,828.6	1	3,661,828.6		
Linear	133,755.0	2	66,877.5	2.13	0.165
Quadratic	229,364.9	3	76,455.0	5.29	0.027
Special cubic	107,877.8	1	107,877.8	96.52	0.001
Full cubic	4,240.9	2	2,120.4	2.96	0.142
Residual	3,582.9	5	716.5		
Total	4,127,850.0	14			

Lack-of-Fit Tests					
Model	Sum of Squares	Degrees of Freedom	Mean Square	F-Value	Probability > F
Linear	342,803.9	7	48,972.0	86.58	0.001
Quadratic	113,439.1	4	28,359.8	50.14	0.001
Special cubic	5,561.3	3	1,853.8	3.28	0.141
Full cubic	1,320.4	1	1,320.4	2.33	0.201
Pure Error	2,262.5	4	565.6		

ANOVA Summary Statistics of Model Fit						
Source	Unaliased Terms	Residual Degrees of Freedom	Root Mean Squared Error	R-Squared	Adjusted R-Squared	PRESS
Linear	3	11	177.1	0.2793	0.1483	516,539.9
Quadratic	6	8	120.3	0.7584	0.6073	812,042.5
Special cubic	7	7	33.4	0.9837	0.9697	80,312.0
Full cubic	9	5	26.8	0.9925	0.9805	186,374.0

(0.912), and this is responsible in part for the three large values of Cook's distance (1.453, 1.204, and 4.862) reported in the table.

The fitted special cubic model is

$$\hat{y} = 550.2x_1 + 344.7x_2 + 268.3x_3 + 689.5x_1x_2 - 9.0x_1x_3 \\ + 58.1x_2x_3 + 9243.3x_1x_2x_3$$

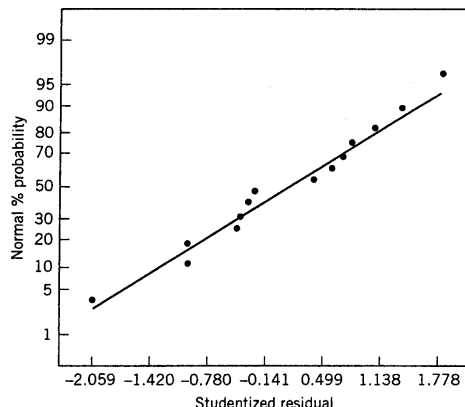
Figures 11.14 and 11.15 present the normal probability plot of the studentized residuals and a plot of the studentized residuals versus the predicted values, respectively, for this model. The plots are satisfactory, so we conclude that the special cubic model is adequate to describe the etch rate response surface.

Figure 11.16 presents plots of the etch rate response surface. In this process it is important to obtain an etch rate that is at least 750 Å/min. The contour plot in Fig. 11.16a indicates that there are several formulations that will meet that requirement.

We would like to emphasize an important point from Example 11.2. Notice that the experimenters originally intended to fit a quadratic mixture model; however, after the

**TABLE 11.6** Special Cubic Model for the Etch Rate Experiment

Source	Sum of Squares	Degrees of Freedom	Mean Square	F-Value	Probability > F		
Model	470997.6	6	78499.6	70.23	<0.001		
Residual	7823.8	7	1117.7				
Lack of fit	5561.3	3	1853.8	3.28	0.141		
Pure error	2262.5	4	565.6				
Corrected total	478821.4	13					
Root mean squared error	33.4		R-Squared	0.9837	PRESS = 80,312.0		
Dependent Mean	511.4		Adj R-Squared	0.9697			
Coefficient of variation	6.54%		Pred R-Squared	0.8323			
Component	Coefficient Estimate	Degrees of Freedom	Standard Error	<i>t</i> for $H_0:$ Coefficient = 0	Probability >   <i>t</i>		
$x_1$	550.2	1	23.2		Not applicable		
$x_2$	344.7	1	23.2		Not applicable		
$x_3$	268.3	1	23.2		Not applicable		
$x_1x_2$	689.5	1	146.5	4.71	0.002		
$x_1x_3$	-9.0	1	146.5	-0.06	0.953		
$x_2x_3$	58.1	1	146.5	0.40	0.703		
$x_1x_2x_3$	9243.3	1	940.9	9.82	<0.001		
Observation	Actual Value	Predicted Value	Residual	$h_{ii}$	Student Residual	Cook's Distance	R-Student
1	540.0	550.2	-10.2	0.483	-0.42	0.024	-0.40
2	560.0	550.2	9.8	0.483	0.41	0.022	0.38
3	330.0	344.7	-14.7	0.483	-0.61	0.050	-0.58
4	350.0	344.7	5.3	0.483	0.22	0.006	0.20
5	295.0	268.3	26.7	0.483	1.11	0.164	1.13
6	260.0	268.3	-8.3	0.483	-0.34	0.016	-0.32
7	610.0	619.8	-9.8	0.912	-0.99	1.453	-0.99
8	425.0	407.0	18.0	0.912	1.81	4.862	2.31
9	330.0	321.0	9.0	0.912	0.90	1.204	0.89
10	800.0	812.2	-12.2	0.375	-0.46	0.018	-0.43
11	850.0	812.2	37.8	0.375	1.43	0.176	1.58
12	710.0	717.4	-7.4	0.206	-0.25	0.002	-0.23
13	640.0	620.2	19.8	0.206	0.66	0.016	0.64
14	460.0	523.8	-63.8	0.206	-2.14	0.170	-3.38



**Figure 11.14** Normal probability plot of the studentized residuals.

experiment had been performed, it was clear that a higher-order model (the special cubic) would be required to adequately model the response. This happens frequently in mixture experiments: The order of the required model is higher than the one initially planned for by the experimenters. If the experimenter designs the experiment without some additional runs to measure lack of fit (and fit higher-order terms, if necessary) and the proposed model is inadequate, then he or she is in trouble. For that reason, we recommend that the experimenter should, whenever possible, make 8–10 additional runs beyond the minimum required to fit the model, with about half of these runs chosen to be replicates of some points in the design and the others chosen as new distinct points so that the lack of fit of the model can be investigated. In this example, the tentative model was the quadratic, which in three components is a six-parameter model. The use of the augmented simplex lattice automatically provided four additional distinct runs. Then the experimenters decided to replicate four runs to give an internal estimate of error. Whenever it is possible to do so, we strongly recommend this design strategy.

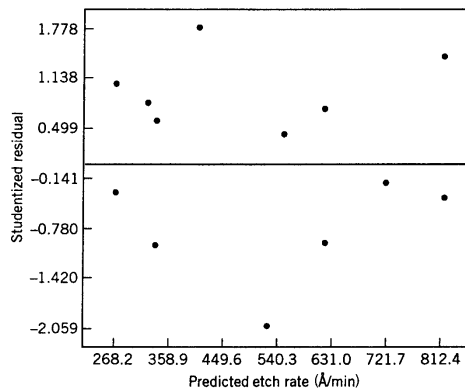


**Figure 11.15** Plot of studentized residuals versus predicted etch rate.

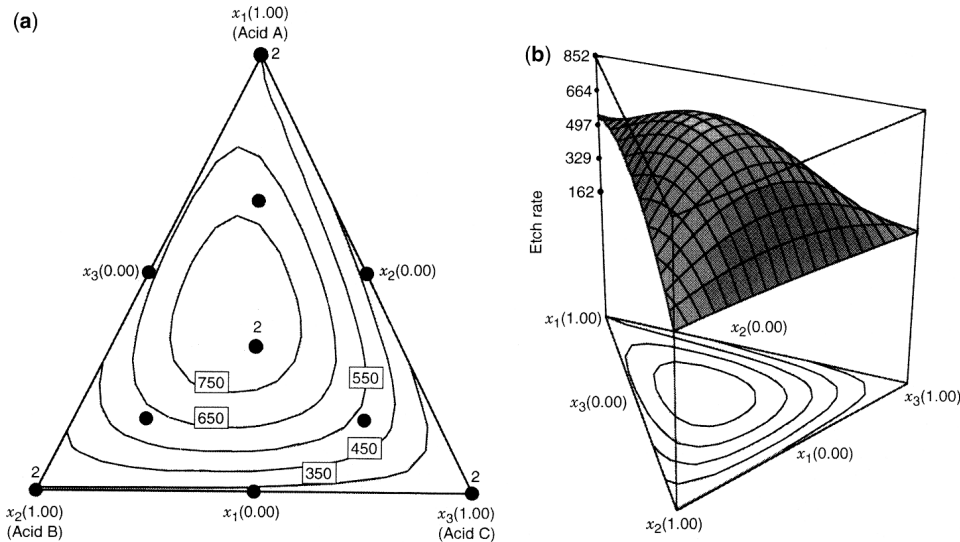


**Figure 11.16** Etch rate response surface. (a) Contour plot. (b) Three-dimensional surface plot. The solid dots in the contour plot are the design points.

### 11.3 RESPONSE TRACE PLOTS

The **response trace** is a plot of the estimated response values as we move away from the centroid of the simplex and along the component axes. More generally, we may think of the centroid as a **reference mixture** with component proportions given by  $r_i = 1/q_i$ ,  $i = 1, 2, \dots, q$  (in Chapter 12 we will discuss other choices for the proportions in the reference blend). Consider the  $i$ th component, and suppose we move away from the centroid by changing the proportion of this component by an amount  $\Delta_i$  (note that we could make  $\Delta_i$  either positive or negative). Along the  $i$ th axis, as the value of  $x_i$  either increases or decreases, the values of the other component proportions  $x_j$ ,  $j \neq i$ , either decrease or increase, but the relative proportions for these other components remain the same.

To illustrate, consider a  $q = 3$  component mixture, so that  $r_i = \frac{1}{3}$ ,  $i = 1, 2, 3$ . Suppose that component 1 is increased by  $\Delta_1 = \frac{1}{6}$  so that now  $x_1 = r_1 + \Delta_1 = \frac{1}{3} + \frac{1}{6} = \frac{3}{6} = \frac{1}{2}$ . The new proportions for components 2 and 3 are  $x_1 = x_3 = \frac{1}{4}$ . Thus the ratio of  $x_2$  to  $x_3$  is identical at the centroid ( $x_2/x_3 = \frac{1}{3}/\frac{1}{3} = 1$ ) and at the new point along the  $x_1$ -axis, because at this point  $x_2/x_3 = \frac{1}{4}/\frac{1}{4} = 1$ .

We may give a general equation for these results. If  $x_i$  is changed by an amount  $\Delta_i$  from the reference mixture, then the new proportions are

$$\begin{aligned} x_i &= r_i + \Delta_i \\ x_j &= r_j - \frac{\Delta_i r_j}{1 - r_i}, \quad j \neq i \end{aligned} \tag{11.12}$$

To construct a response surface trace plot, we choose some number of blends along each component axis, calculate the coordinates of each mixture using Equation (11.12), and then

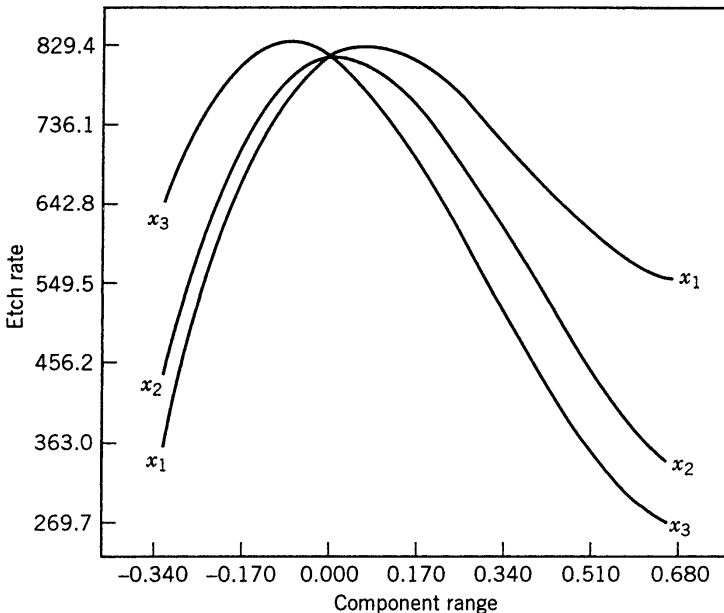


**Figure 11.17** Response trace plot of predicted etch rate along the component axes  $x_1$ ,  $x_2$ , and  $x_3$ .

substitute these coordinates into the fitted mixture model to obtain the predicted values of the response. Then these predicted responses are plotted against the changes made in the  $x_i$ ,  $i = 1, 2, \dots, q$ . There will be  $q$  of these curves, and it is customary to plot them on the same graph.

To illustrate, Fig. 11.17 is the response trace plot for the etch rate experiment described in Example 11.2. The vertical axis is the predicted etch rate, and the horizontal axis is the incremental change  $\Delta_i$  made in each component. The reference mixture, which is the overall centroid, is shown as the point 0.000 on the horizontal axis. Notice the strong nonlinear effect of all three acids on the etch rate. Also, the etch rate increases slightly and then decreases as we move along the  $x_1$ -axis from the centroid toward the  $x_1$ -vertex, and it increases as we move away from the centroid along the  $x_3$ -axis toward the base point  $x_3 = 0$ ,  $x_1 = x_2 = \frac{1}{2}$ .

In this example, the etch rate is very sensitive to changes in all three component proportions. If one or more of the response traces is a horizontal line, this indicates that these components have little effect on the response; that is, we have discovered ingredients that are **inactive**. This can have important economic consequences.

## 11.4 REPARAMETERIZING CANONICAL MIXTURE MODELS TO CONTAIN A CONSTANT TERM ( $\beta_0$ )

It is occasionally convenient to reparameterize the Scheffé mixture polynomial so that it contains a constant term, or intercept,  $\beta_0$ . This can be easily done by simply deleting one of the  $\beta_i x_i$  terms, say  $\beta_q x_q$ . Thus, instead of the linear mixture model

$$E(y) = \beta_1 x_1 + \beta_2 x_2 + \cdots + \beta_q x_q \quad (11.13)$$

we would write

$$E(y) = \beta_0 + \beta_1^* x_1 + \beta_2^* x_2 + \cdots + \beta_{q-1}^* x_{q-1} \quad (11.14)$$

and instead of the quadratic model

$$E(y) = \sum_{i=1}^q \beta_i x_i + \sum_{i < j=2}^q \beta_{ij} x_i x_j \quad (11.15)$$

we would write

$$E(y) = \beta_0 + \sum_{i=1}^{q-1} \beta_i^* x_i + \sum_{i < j=2}^q \beta_{ij} x_i x_j \quad (11.16)$$

Note that only the parameters in the linear blending portion of the canonical model are affected. Specifically, the intercept  $\beta_0$  takes on the role of the parameter  $\beta_q$  corresponding to the deleted component  $x_q$ , and the remaining parameters  $\beta_i^*$  represent the differences  $\beta_i^* = \beta_i - \beta_q$ ,  $i = 1, 2, \dots, q-1$ .

We will use the quadratic model for yarn elongation in Example 11.1 to illustrate. The fitted canonical model was

$$\hat{y} = 11.7x_1 + 9.4x_2 + 16.4x_3 + 19.0x_1x_2 + 11.4x_1x_3 - 9.6x_2x_3$$

Now fit the model in Equation 11.14 with  $q = 3$  by the method of least squares. This results in

$$\hat{y} = 16.4 - 4.7x_1 - 7.0x_2 + 19.0x_1x_2 + 11.4x_1x_3 - 9.6x_2x_3$$

That is,

$$b_0 = 16.4, \quad b_1^* = -4.7, \quad b_2^* = -7.0$$

Notice that

$$\begin{aligned} b_0 &= b_3 = 16.4 \\ b_1^* &= b_1 - b_3 = 11.7 - 16.4 = -4.7 \end{aligned}$$

and

$$b_2^* = b_2 - b_3 = 9.4 - 16.4 = -7.0$$

and that the estimates of the quadratic terms are the same in both models.

This reparameterization of the Scheffé polynomial can be useful in analyzing mixture data with standard multiple regression computer software. Most regression software packages will fit a model with the intercept term suppressed. This option will produce the correct estimates of the  $\beta$ 's in a canonical mixture model, but it will result in an incorrect value for the model or regression sum of squares, because the no-intercept option does not correct this sum of squares for the overall mean. As a result, the  $F$ -test,  $R^2$ , and the adjusted

$R^2$  will be incorrect. Reparameterizing the model as we have discussed will result in correct output for the regression or model sum of squares,  $R^2$ , and the adjusted  $R^2$ . Then the correct values of the linear blending coefficients can be calculated from

$$\begin{aligned} b_i &= b_i^* + b_0, \quad i = 1, 2, \dots, q-1 \\ b_q &= b_0 \end{aligned} \quad (11.17)$$

Another technique occasionally used in the analysis of mixture data is the **slack variable approach**. The approach differs from the previous one in that one of the mixture components is *completely eliminated* from the model. That is, if the component  $x_q$  is eliminated, then the first-order slack variable model is

$$\begin{aligned} E(y) &= \beta_0 + \beta_1^* x_1 + \beta_2^* x_2 + \cdots + \beta_{q-1}^* x_{q-1} \\ &= \beta_0 + \sum_{i=1}^{q-1} \beta_i^* x_i \end{aligned} \quad (11.18)$$

which is identical to Equation 11.13. However, the second-order slack variable model is

$$E(y) = \beta_0 + \sum_{i=1}^{q-1} \beta_i^* x_i + \sum_{i<j=2}^{q-1} \beta_{ij}^* x_i x_j + \sum_{i=1}^{q-1} \beta_{ii}^* x_i^2 \quad (11.19)$$

Note that this is a standard second-order response model in the  $q - 1$  mixture components. The slack variable version of the special cubic model is

$$\begin{aligned} E(y) &= \beta_0 + \sum_{i=1}^{q-1} \beta_i^* x_i + \sum_{i<j=2}^{q-1} \beta_{ij}^* x_i x_j + \sum_{i=1}^{q-1} \beta_{ii}^* x_i^2 \\ &\quad + \sum_{i<j<k=2}^{q-1} \beta_{ijk}^* x_i x_j x_k + \sum_{i<j=2}^{q-1} \beta_{ijj}^* x_i x_j (x_i + x_j) \end{aligned} \quad (11.20)$$

It turns out that the coefficients in the slack variable model are just simple functions of the coefficients in the original Scheffé polynomials.

Some practitioners report using the slack variable model with some success, so some software packages support it. Design-Expert is one such package. Table 11.7 is the output from Design-Expert for the yarn elongation data from Example 11.1, using  $x_3$  (component C) as the slack variable. Notice that all the terms are significant in the model. Therefore, the slack variable model is completely equivalent to the original Scheffé quadratic that we fitted to these data in Example 11.1.

Cornell (2000) points out that if we find that some terms in the slack variable model are not significant and reduce the model (say by using stepwise regression techniques such as we discuss in Appendix A), then the reduced slack variable model will not necessarily be equivalent to the Scheffé model that was also reduced by eliminating nonsignificant terms. The contour plots and hence the final conclusions from the two model can be different.

**TABLE 11.7 Design-Expect Output for the Slack Variable Model of the Yarn Elongation Data**

Response Elongation  
 \*\*\*Component C is the Slack Variable.\*\*\*

ANOVA for Slack Mixture Quadratic Model  
 Analysis of variance table [Partial sum of squares]

Source	Sum of Squares	DF	Mean Square	F-Value	Prob > F
Model	128.30	5	25.66	32.20	< 0.0001
A	4.34	1	4.34	5.96	0.0373
B	26.67	1	26.67	36.59	0.0002
$A^2$	13.92	1	13.92	19.10	0.0018
$B^2$	9.87	1	9.87	13.55	0.0051
AB	12.33	1	12.33	16.91	0.0026
Pure Error	6.56	9	0.73		
Cor Total	134.86	14			
Std. Dev.	0.85	R-Squared	0.9514		
Mean	13.54	Adj R-Squared	0.9243		
C.V.	6.31	Pred R-Squared	0.8643		
PRESS	18.30	Adeq Precision	13.890		
Component	Estimate	Coefficient DF	Standard Error	95% CI Low	95% CI High
Intercept	16.40	1	0.60	15.03	17.77
A-A	-6.70	1	2.74	0.49	12.91
B-B	-16.60	1	2.74	-22.81	-10.39
$A^2$	-11.40	1	2.61	-17.30	-5.50
$B^2$	9.60	1	2.61	3.70	15.50
AB	17.20	1	4.18	7.74	26.66

Final Equation in Terms of Pseudo Components:

Elongation =

- + 16.40
- + 6.70\*A
- 16.60\*B
- 11.40\*A<sup>2</sup>
- + 9.50\*B<sup>2</sup>
- +17.20\*A\*B

Furthermore, Cornell observes that the results one obtains can depend greatly on which variable is chosen as the slack variable. Fortunately, Design-Expert allows the user to specify the slack variable, so an experienced analyst can try different models and decide if the slack variable approach is really appropriate for his or her situation. Our own recommendation is to avoid indiscriminate use of the slack variable model in most problems and use the standard Scheffé polynomials unless there is some overriding reason to not do so. For an excellent discussion of the slack variable model and many more interesting details, refer to Cornell (2000).

**EXERCISES**

- 11.1** Three different motor fuels can be blended to form a gasoline. The miles per gallon (MPG) performance of this gasoline is the response variable. An augmented simplex-lattice design was used to study the blending properties of these three fuels, and the results are shown in Table E11.1:

**TABLE E11.1 Data for Exercise 11.1**

Design Point	Component Proportion			MPG <i>y</i>
	<i>x</i> <sub>1</sub>	<i>x</i> <sub>2</sub>	<i>x</i> <sub>3</sub>	
1	1	0	0	24.5, 25.1
2	0	1	0	24.8, 23.9
3	0	0	1	22.7, 23.6
4	$\frac{1}{2}$	$\frac{1}{2}$	0	25.1
5	$\frac{1}{2}$	0	$\frac{1}{2}$	24.3
6	0	$\frac{1}{2}$	$\frac{1}{2}$	23.5
7	$\frac{1}{3}$	$\frac{1}{3}$	$\frac{1}{3}$	24.8, 24.1
8	$\frac{2}{3}$	$\frac{1}{6}$	$\frac{1}{6}$	24.2
9	$\frac{1}{6}$	$\frac{2}{3}$	$\frac{1}{6}$	23.9
10	$\frac{1}{6}$	$\frac{1}{6}$	$\frac{2}{3}$	23.7

- (a) Fit a linear mixture model to these data. Is the model adequate?
- (b) Fit a quadratic mixture model to these data. Is this model an improvement over the linear model?
- (c) What model would you use to predict the MPG performance of the gasoline obtained by blending these three fuels?
- (d) Plot the response surface contours for the model in part (c). What blend would you use to maximize mileage performance?
- 11.2** A mixture experiment was performed to determine if an artificial sweetener could be developed for a soft drink that would minimize the aftertaste. Four different sweeteners were evaluated, and a simplex-centroid design with  $q = 4$  components was used to evaluate the different blends. The response variable is aftertaste, with low values being desirable. The data are shown in Table E11.2.
- (a) Fit an appropriate mixture model to these data. Test the model for adequacy.
- (b) Construct the response trace plot for this experiment. Provide a practical interpretation of this plot.
- (c) Construct contour plots of predicted aftertaste that would be useful to a decisionmaker in choosing a blend of these four sweeteners that minimizes the aftertaste. What blend would you recommend?
- 11.3** Consider the linear mixture model from Exercise 11.1a. Reparameterize this model to the form

$$E(y) = \beta_0 + \beta_1^* x_1 + \beta_2^* x_2$$

**TABLE E11.2 Data for Exercise 11.2**

Design Point	Component Proportions				Aftertaste <i>y</i>
	$x_1$	$x_2$	$x_3$	$x_4$	
1	1	0	0	0	19
2	0	1	0	0	8
3	0	0	1	0	15
4	0	0	0	1	10
5	$\frac{1}{2}$	$\frac{1}{2}$	0	0	13
6	$\frac{1}{2}$	0	$\frac{1}{2}$	0	16
7	$\frac{1}{2}$	0	0	$\frac{1}{2}$	12
8	0	$\frac{1}{2}$	$\frac{1}{2}$	0	11
9	0	$\frac{1}{2}$	0	$\frac{1}{2}$	5
10	0	0	$\frac{1}{2}$	$\frac{1}{2}$	10
11	$\frac{1}{3}$	$\frac{1}{3}$	$\frac{1}{3}$	0	14
12	$\frac{1}{3}$	$\frac{1}{3}$	0	$\frac{1}{3}$	10
13	$\frac{1}{3}$	0	$\frac{1}{3}$	$\frac{1}{3}$	14
14	0	$\frac{1}{3}$	$\frac{1}{3}$	$\frac{1}{3}$	8
15	$\frac{1}{4}$	$\frac{1}{4}$	$\frac{1}{4}$	$\frac{1}{4}$	12

and fit this model using least squares. Verify that this model can be converted to the linear mixture model you found in Exercise 11.1a using the method discussed in Section 11.4.

- 11.4** A thickening agent is added to a liquid soap product to control the viscosity. This agent usually makes up 10% of the soap by weight. There are three different salt compounds that are blended to make up the thickener. The product formulators have decided to investigate the combination of these ingredients using a mixture experiment. Let  $x_1^*$ ,  $x_2^*$ , and  $x_3^*$  represent the actual proportions of the three salt compounds, with  $x_1^* + x_2^* + x_3^* = 0.1$ . Notice that if we let  $x_i = x_i^*/0.1$ , then the design points can be expressed as proportions  $0 \leq x_i \leq 1$  with the standard mixture constraint  $x_1 + x_2 + x_3 = 1$ . The experiments decided to use an augmented simplex-lattice design to study the viscosity of the thickener. The design and the viscosity data are shown in Table E11.3. The centroid was replicated three times.
- (a) Fit linear and quadratic mixture models to these data. Test both models for lack of fit. Does either model seem adequate, based on this test?
  - (b) Select an appropriate mixture model for the viscosity data. Construct appropriate residual plots to check for model adequacy.
  - (c) Construct and interpret a response trace plot for this experiment.
  - (d) Construct a response surface contour plot for viscosity.
  - (e) Suppose that a desirable value for viscosity of this thickening agent is 900 centipoise. Is there a formulation that would produce the desired viscosity?
- 11.5** One of the authors (DCM) is an owner of a vineyard and winery in Newberg, Oregon. The partners that operate this business are developing a new red wine that is a blend of three different varieties of grapes: Pinot Noir–Pommard, Pinot

**TABLE E11.3 Data for Exercise 11.4**

Design Point	Component Proportions			Viscosity (centipoise)
	$x_1$	$x_2$	$x_3$	
1	1	0	0	410
2	0	1	0	880
3	0	0	1	1445
4	$\frac{1}{2}$	$\frac{1}{2}$	0	683
5	$\frac{1}{2}$	0	$\frac{1}{2}$	465
6	0	$\frac{1}{2}$	$\frac{1}{2}$	456
7	$\frac{2}{3}$	$\frac{1}{6}$	$\frac{1}{6}$	354
8	$\frac{1}{6}$	$\frac{2}{3}$	$\frac{1}{6}$	521
9	$\frac{1}{6}$	$\frac{1}{6}$	$\frac{2}{3}$	700
10	$\frac{1}{3}$	$\frac{1}{3}$	$\frac{1}{3}$	465
11	$\frac{1}{3}$	$\frac{1}{3}$	$\frac{1}{3}$	392
12	$\frac{1}{3}$	$\frac{1}{3}$	$\frac{1}{3}$	428

Noir–Wadenswil, and Gamay Noir. A three-component mixture design was used to study the blends of these three ingredients. The design is shown in Table E11.4 where  $x_1$  = proportion of Pinot Noir–Pommard,  $x_2$  = proportion of Pinot Noir–Wadenswil, and  $x_3$  = proportion of Gamay Noir in the product. Each of the 10 blends was tasted by a panel of experts and ranked on the basis of the taste-test results, with rank 1 being the best, rank 2 the next best, and so forth.

**TABLE E11.4 Data for Exercise 11.5**

Design Point	Component Proportions			Taste-Test Ranks			
	$x_1$	$x_2$	$x_3$	DCM	HPN	DLB	JPN
1	1	0	0	2	3	3	2
2	0	1	0	1	2	1	3
3	0	0	1	4	4	5	6
4	$\frac{1}{2}$	$\frac{1}{2}$	0	3	1	2	1
5	$\frac{1}{2}$	0	$\frac{1}{2}$	5	5	4	4
6	0	$\frac{1}{2}$	$\frac{1}{2}$	6	7	8	5
7	$\frac{2}{3}$	$\frac{1}{6}$	$\frac{1}{6}$	7	6	9	8
8	$\frac{1}{6}$	$\frac{2}{3}$	$\frac{1}{6}$	8	8	6	7
9	$\frac{1}{6}$	$\frac{1}{6}$	$\frac{2}{3}$	10	9	10	9
10	$\frac{1}{3}$	$\frac{1}{3}$	$\frac{1}{3}$	9	10	7	10

- (a) Fit linear and quadratic mixture models to the averages of the rank data. Test both of these models for lack of fit. Does either model seem adequate?
- (b) Select an appropriate mixture model for the average rank response. Construct appropriate residual plots to check for model adequacy.

- (c) Construct and interpret a response trace plot for this experiment.  
 (d) Construct a response surface contour plot for the average rank response. What blends of the three varieties of grapes would you recommend?
- 11.6** Reconsider the sweetener experiment in Exercise 11.2. Suppose that the experimenters are interested in a second response, the cost of the sweetener. For each of the 15 formulations of the product tested in the simplex-centroid design, the cost of the mixture of ingredients used in the formula and a manufacturing cost estimate are combined. For the design points, listed in the same order as in the original table in Exercise 11.2, these costs are as follows:
- | Design Point | Cost | Design Point | Cost | Design Point | Cost |
|--------------|------|--------------|------|--------------|------|
| 1            | 4    | 6            | 8    | 11           | 12   |
| 2            | 15   | 7            | 16   | 12           | 18   |
| 3            | 6    | 8            | 13   | 13           | 15   |
| 4            | 25   | 9            | 18   | 14           | 16   |
| 5            | 10   | 10           | 15   | 15           | 15   |
- (a) Build an appropriate mixture model for the cost response.  
 (b) Construct a response trace plot for the cost response. Interpret this graph.  
 (c) Construct a response surface contour plot of the cost response. What practical advice could you give a decision maker based on this graph?  
 (d) Consider both the response surface for cost and the aftertaste response surface developed in Exercise 11.2. Suppose that your objective is to select a blend of ingredients so that the sweetener has low aftertaste while keeping the cost of the product below 12. What blend of sweeteners would you recommend?
- 11.7 Continuation of Exercise 11.6** Reconsider the cost response surface from Exercise 11.6. Suppose that your objective was to minimize the cost of the sweetener while keeping the aftertaste below 13. What formulation of ingredients would you recommend for this product?
- 11.8** Consider the second-order polynomial in two variables:
- $$E(y) = \beta_0 + \beta_1 x_1 + \beta_2 x_2 + \beta_{12} x_1 x_2 + \beta_{11} x_1^2 + \beta_{22} x_2^2$$
- (a) Show that if the term  $\beta_0$  is replaced by  $\beta_0(x_1 + x_2)$ , if  $x_1^2$  is replaced by  $x_1(1 - x_2)$ , and if  $x_2^2$  is replaced by  $x_2(1 - x_1)$ , the canonical form of the quadratic mixture model results.  
 (b) Why are the substitutions described in (a) required in a mixture experiment?
- 11.9** When observations are collected only at the points of a  $\{q, m\}$  simplex lattice, the estimates of the parameters in the canonical polynomial are simple functions of the observed responses. Consider the  $\{3, 2\}$  lattice, let  $\bar{y}_i$  be the average of  $n_i$  observations at each vertex  $x_i = 1, x_j = 0$  for  $j \neq i$ , and let  $\bar{y}_{ij}$  be the average of  $n_{ij}$  observations at the edge midpoints or 50 : 50 binary blends  $x_i = x_j = \frac{1}{2}, x_k = 0$  for  $i < j < k = 1, 2, 3$ .

- (a) Show that on substituting  $\bar{y}_i$  and  $\bar{y}_{ij}$  for the expected response at each of the six design points, the following equations result:

$$\begin{aligned}\bar{y}_1 &= \beta_1, & \bar{y}_2 &= \beta_2, & \bar{y}_3 &= \beta_3 \\ \bar{y}_{12} &= \frac{1}{2}\beta_1 + \frac{1}{2}\beta_2 + \frac{1}{4}\beta_{12} \\ \bar{y}_{13} &= \frac{1}{2}\beta_1 + \frac{1}{2}\beta_3 + \frac{1}{4}\beta_{13} \\ \bar{y}_{23} &= \frac{1}{2}\beta_2 + \frac{1}{2}\beta_3 + \frac{1}{4}\beta_{23}\end{aligned}$$

- (b) Show that the solution to the equations given in part (a) are as follows:

$$\begin{aligned}b_1 &= \bar{y}_1, & b_2 &= \bar{y}_2, & b_3 &= \bar{y}_3 \\ b_{12} &= 4\bar{y}_{12} - 2(\bar{y}_1 + \bar{y}_2) \\ b_{13} &= 4\bar{y}_{13} - 2(\bar{y}_1 + \bar{y}_3) \\ b_{23} &= 4\bar{y}_{23} - 2(\bar{y}_2 + \bar{y}_3)\end{aligned}$$

Notice that the constants 4 and 2 in the last three equations do not depend on the number of replicates at each design point, but arise instead from the  $x_i = x_j = \frac{1}{2}$  values at each edge midpoint.

- (c) Use the equations derived in part (b) above to calculate the parameter estimates for the yarn elongation data in Example 11.1. Verify that the results obtained agree with the least squares estimates of these parameters obtained in Example 11.1.

### 11.10 Consider the quadratic mixture model

$$y = \beta_1 x_1 + \beta_2 x_2 + \beta_3 x_3 + \beta_{12} x_1 x_2 + \beta_{13} x_1 x_3 + \beta_{23} x_2 x_3 + \varepsilon$$

where  $\varepsilon$  is the usual  $NID(0, \sigma^2)$  random error term. Suppose that the  $\{3, 2\}$  lattice design as described in Exercise 11.8 above is run, and the resulting data are used to estimate the coefficients in the quadratic model.

- (a) Show that

$$E(b_i) = \beta_i$$

and that

$$E(b_{ij}) = \beta_{ij}$$

- (b) Show that

$$\text{Var}(b_i) = \frac{\sigma^2}{n_i}, \quad i = 1, 2, 3$$

and

$$\text{Var}(b_{ij}) = \frac{16\sigma^2}{n_{ij}} + \frac{4\sigma^2}{n_i} + \frac{4\sigma^2}{n_j}, \quad i < j = 2, 3$$

(c) Show that

$$\text{Cov}(b_i, b_j) = 0, \quad i \neq j$$

$$\text{Cov}(b_i, b_{ij}) = \frac{-2\sigma^2}{n_i}$$

$$\text{Cov}(b_{ij}, b_{ik}) = \frac{4\sigma^2}{n_i}, \quad j \neq k$$

- 11.11** Consider the simplex-centroid design for three components. Let  $\bar{y}_i$ ,  $\bar{y}_{ij}$ , and  $\bar{y}_{123}$  be the averages of  $n_i$  observations at the three vertices,  $n_{ij}$  observations at the edge midpoints, and  $n_{123}$  observations at the design centroid. The model of interest is

$$E(y) = \sum_{i=1}^3 \beta_i x_i + \sum_{i < j=2}^3 \beta_{ij} x_i x_j + \beta_{123} x_1 x_2 x_3$$

(a) Show that by substituting  $\bar{y}_i$ ,  $\bar{y}_{ij}$ , and  $\bar{y}_{123}$  for the expected response at each of the seven design points, the following equations result:

$$\bar{y}_i = \beta_i, \quad i = 1, 2, 3$$

$$\bar{y}_{ij} = \frac{1}{2}(\beta_i + \beta_j) + \frac{1}{4}\beta_{ij}, \quad i < j = 2, 3$$

$$\bar{y}_{123} = \frac{1}{3}(\beta_1 + \beta_2 + \beta_3) + \frac{1}{9}(\beta_{12} + \beta_{13} + \beta_{23}) + \frac{1}{27}\beta_{123}$$

(b) Show that the solution to the equation given in part (a) are

$$b_i = \bar{y}_i, \quad i = 1, 2, 3$$

$$b_{ij} = 4\bar{y}_y - 2(\bar{y}_i + \bar{y}_j), \quad i < j = 2, 3$$

$$b_{123} = 27\bar{y}_{123} - 12(\bar{y}_{12} + \bar{y}_{13} + \bar{y}_{23}) + 9(\bar{y}_1 + \bar{y}_2 + \bar{y}_3)$$

(c) What effect does the observation at the centroid have on the estimates of the linear and quadratic terms in this model?

- 11.12** Consider the special cubic model

$$\hat{y} = \sum_{i=1}^3 b_i x_i + \sum_{i < j=2}^3 b_{ij} x_i x_j + b_{123} x_1 x_2 x_3$$

(a) How large must the  $b_{ij}$ -term be if the term  $b_{12} x_i x_j$  is to contribute as much to the model at the edge midpoint as the linear term  $b_i x_i$ ?

- (b) How large must the cubic term  $b_{123}$  be if the contribution of the term  $b_{123}x_1x_2x_3$  to the model at the centroid is as large as the contribution of the quadratic term  $b_{ij}x_i x_j$ ?

**11.13** Consider the quadratic model in two components:

$$E(y) = \beta_1 x_1 + \beta_2 x_2 + \beta_{12} x_1 x_2$$

- (a) Suppose that four observations are collected at the following points:

$$\begin{aligned} y_1 &\text{ at } x_1 = 1, x_2 = 0 \\ y_2 &\text{ at } x_1 = 0, x_2 = 1 \\ y_3 \text{ and } y_4 &\text{ at } x_1 = x_2 = \frac{1}{2} \end{aligned}$$

Derive the estimates of the model coefficients for this design.

- (b) Suppose that four observations are collected at the following points:

$$\begin{aligned} y_1 &\text{ at } x_1 = 1, x_2 = 0 \\ y_2 &\text{ at } x_1 = 0, x_2 = 1 \\ y_3 &\text{ at } x_1 = \frac{1}{3}, x_2 = \frac{2}{3} \\ y_4 &\text{ at } x_1 = \frac{2}{3}, x_2 = \frac{1}{3} \end{aligned}$$

Derive the estimates of the model coefficients for this design.

- (c) Which of these two designs would you prefer, if your objective was to find minimum variance estimates of the coefficients in the quadratic model?

**11.14** Reconsider the sweetener formulation problem in Exercise 11.2. Reparameterize the problem as was discussed in Section 11.4. Fit both linear and quadratic models, and verify that they can be converted to the Scheffé models you fitted in Exercise 11.2.

**11.15** Cornell (2000) presents an example of a three-component mixture experiment used to study the tint strength of a house paint as a function of the relative proportions of two pigments ( $P_1$  and  $P_2$ ) and a solvent ( $S$ ). The volume percentages of the three ingredients are fixed at 8%, so we can write the usual mixture constraint  $x_1 + x_2 + x_3 = 1$  by letting  $x_1 = P_1/8\%$ ,  $x_2 = P_2/8\%$ , and  $x_3 = S/8\%$ , respectively. This scaling produces what are often called **real** mixture components. The data given by Cornell are supplied in Table E11.5.

Fit a second-order mixture model to the data, and find a blend that maximizes the tint strength.

**11.16** Reconsider the paint experiment in Exercise 11.15. Fit a second-order slack variable model to the data, using  $x_1$  as the slack variable. Verify that the contour plots from this model are identical to the ones obtained from the original Scheffé polynomial in Exercise 11.15. Fit another second-order slack variable model, this time using  $x_2$  as the slack variable. Obtain the contour plots. Note

**TABLE E11.5 Data for Exercise 11.15**

Blend	$x_1 (P_1)$	$x_2 (P_2)$	$x_3 (S)$	Tint Strength
1	1	0	0	1.19
2	0	1	0	0.97
3	0	0	1	-5.68
4	$\frac{1}{2}$	$\frac{1}{2}$	0	0.13
5	$\frac{1}{2}$	0	$\frac{1}{2}$	-4.02
6	0	$\frac{1}{2}$	$\frac{1}{2}$	-4.18
7	$\frac{1}{3}$	$\frac{1}{3}$	$\frac{1}{3}$	-3.36, -3.68 -3.04

that the model form is different, but the contour plots are identical to the ones from the original Scheffé polynomial.

- 11.17** Reconsider the paint experiment in Exercise 11.15. Fit a second-order slack variable model to the data using  $x_1$  as the slack variable. Eliminate the interaction term from this model, and refit. Construct a contour plot for this reduced model, and compare it with the contour plot for the full Scheffé model. Based on this analysis, how comfortable are you in general with the slack variable model approach?

---

# 12

---

## OTHER MIXTURE DESIGN AND ANALYSIS TECHNIQUES

In Chapter 11 we focused on mixture experiments for exploring the complete simplex region. We introduced simplex-lattice and simplex-centroid designs that would enable us to fit response surface models over this region. In many mixture experiments there are **restrictions**, or **constraints**, on the component proportions that prevent us from exploring the entire simplex region. Frequently these restrictions take the form of lower and/or upper bounds on the component proportions. This problem is discussed in this chapter. In addition, we also briefly discuss several other variations of the mixture problem, including the use of **ratios of components** as the design variables, the inclusion of **process variables** in mixture experiments, and **screening techniques** to identify the most important components in the mixture.

### 12.1 CONSTRAINTS ON THE COMPONENT PROPORTIONS

In many mixture experiments there are constraints on the component proportions. These are often upper- and/or lower-bound constraints of the form  $L_i \leq x_i \leq U_i$ ,  $i = 1, 2, \dots, q$ , where  $L_i$  is the lower bound for the  $i$ th component and  $U_i$  is the upper bound for the  $i$ th component. Essentially,  $L_i$  represents a minimum proportion of the  $i$ th component, and  $U_i$  a maximum proportion of the  $i$ th component, that must be present in the mixture. These constraints are usually determined by practical bounds on the relative proportion of components that produce useable results. The general form of the constrained mixture problem is

$$\begin{aligned}x_1 + x_2 + \cdots + x_q &= 1 \\L_i \leq x_i \leq U_i, \quad i &= 1, 2, \dots, q\end{aligned}\tag{12.1}$$

where  $L_i \geq 0$  and  $U_i \leq 1$  for  $i = 1, 2, \dots, q$ .

The effect of the upper- and lower-bound restriction in Equation 12.1 is to limit the feasible space for the mixture experiment to a subregion of the simplex. Therefore, experimental designs for constrained mixture problems must be limited to the feasible subregion of the simplex. In this section, we present design and analysis techniques for these constrained mixture spaces.

### 12.1.1 Lower-Bound Constraints on the Component Proportions

We now consider the case where only the lower bounds in Equation 12.1 are imposed, so that the constrained mixture problem becomes

$$\begin{aligned} x_1 + x_2 + \cdots + x_q &= 1 \\ L_i \leq x_i \leq 1, \quad i &= 1, 2, \dots, q \end{aligned} \quad (12.2)$$

To illustrate the effect that lower bounds have on the feasible mixture design space, consider a three-component example with constraints

$$0.3 \leq x_1, \quad 0.4 \leq x_2, \quad \text{and} \quad 0.1 \leq x_3$$

Figure 12.1 shows the feasible mixture space after these constraints are imposed. Notice that the imposition of lower bounds does not affect the shape of the feasible mixture space; it is still a simplex. In general this will be the case; if only lower bounds are imposed on any of the component proportions, the feasible region for the mixture experiment will be a smaller simplex inscribed inside the original (or unconstrained) region. If all lower bounds are equal ( $L_1 = L_2 = \cdots = L_q$ ), the centroid of the original simplex will also be the centroid of the smaller inscribed simplex.

Because the feasible experimental region is still a simplex, it seems reasonable to define a new set of components that will take on the values 0 to 1 over the feasible region. This will make design construction and model fitting easier over the constrained region. These redefined components are called ***L*-pseudocomponents**, or sometimes just

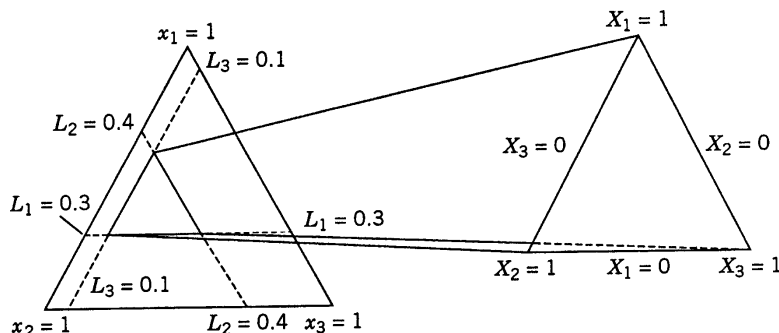


**Figure 12.1** The feasible mixture space for three components with lower bounds, and the redefinition of the region as a simplex in the *L*-pseudocomponents. [Adapted from Cornell (2002), with the permission of the publisher.]

**pseudocomponents.** The pseudocomponents  $X_i$  are defined using the following transformation:

$$X_i = \frac{x_i - L}{1 - L} \quad (12.3)$$

where

$$L = \sum_{i=1}^q L_i < 1$$

is the sum of all of the lower bounds. A value of  $X_i = 0$  now corresponds to the minimum allowable amount of the component  $i$ , while  $X_i = 1$  is the allowable maximum (obtained by setting all the other components at their minimum proportions). To illustrate, we may use the situation described previously and shown graphically in Fig. 12.1. The pseudocomponents are

$$X_1 = \frac{x_1 - 0.3}{0.2}, \quad X_2 = \frac{x_2 - 0.4}{0.2}, \quad X_3 = \frac{x_3 - 0.1}{0.2}$$

because  $L_1 = 0.3$ ,  $L_2 = 0.4$ ,  $L_3 = 0.1$ ,  $L = 0.3 + 0.4 + 0.1 = 0.8$ , and  $1 - L = 0.2$ . The factor space in terms of pseudocomponents is shown on the right-hand side of Fig. 12.1. The orientation of the  $L$ -pseudocomponent simplex is the same as the original simplex, and the height of the  $L$ -pseudocomponent simplex is  $1 - L$ .

Constructing a design in the  $L$ -pseudocomponents is easy. One simply specifies the design points in the  $X_i$  and then converts them to the settings in the original components using

$$x_i = L_i + (1 - L)X_i \quad (12.4)$$

To illustrate, suppose that we decide to use a simplex-centroid design for our experiment. Table 12.1 shows the design points in the pseudocomponents, along with the corresponding setting for the original components.

**TABLE 12.1 Pseudocomponent Settings and Original Component Settings, Simplex-Centroid Design**

Pseudocomponents			Original Components		
$X_1$	$X_2$	$X_3$	$x_1$	$x_2$	$x_3$
1	0	0	0.5	0.4	0.1
0	1	0	0.3	0.6	0.1
0	0	1	0.3	0.4	0.3
$\frac{1}{2}$	$\frac{1}{2}$	0	0.4	0.5	0.1
$\frac{1}{2}$	0	$\frac{1}{2}$	0.4	0.4	0.2
0	$\frac{1}{2}$	$\frac{1}{2}$	0.3	0.5	0.2
$\frac{1}{3}$	$\frac{1}{3}$	$\frac{1}{3}$	0.3667	0.4667	0.1666

The original component settings in Table 12.1 were calculated by using Equation 12.4. This becomes

$$\begin{aligned}x_1 &= 0.3 + 0.2X_1 \\x_2 &= 0.4 + 0.2X_2 \\x_3 &= 0.1 + 0.2X_3\end{aligned}$$

For example, consider the point  $X_1 = \frac{1}{2}$ ,  $X_2 = \frac{1}{2}$ , and  $X_3 = 0$ . In terms of the original components, this point becomes

$$\begin{aligned}x_1 &= 0.3 + 0.2\left(\frac{1}{2}\right) = 0.4 \\x_2 &= 0.4 + 0.2\left(\frac{1}{2}\right) = 0.5 \\x_3 &= 0.1 + 0.2(0) = 0.1\end{aligned}$$

as shown in Table 12.1.

We recommend using pseudocomponents to fit the mixture model. The reason for this is that constrained design spaces usually have moderately high to high levels of **multicollinearity or ill-conditioning**, and this can have serious effects on the least squares estimators of regression coefficients in that the variances of these coefficient estimators are inflated. In general, a mixture model in the pseudocomponents will have lower levels of multicollinearity than will the same model in the original component proportions. For more discussion of this point, see Montgomery and Voth (1994) and St. John (1984). It is, of course, a relatively simple matter to convert a model in the pseudocomponents into the corresponding model in the actual components.

**Example 12.1 Formulating a Propellant** We will use a three-component example from Montgomery and Voth (1994) to illustrate fitting and interpreting a model with pseudocomponents. The example includes blending fuel ( $x_1$ ), oxidizer ( $x_2$ ), and binder ( $x_3$ ) together to form a propellant used in aircrew escape systems. As in most mixture experiments, several responses are of interest, including both physical and mechanical properties of the propellant; however, we will concentrate on three responses. The first is the burning rate ( $y_1$ , cm/sec), a critical characteristic if the escape system is to perform satisfactorily. It is measured by testing several samples of propellant from the same run and reporting the average observed burning rate. The second response is the standard deviation of the observed burning rates at each run ( $y_2$ , cm/sec); low variability is desirable, implying consistent performance across different escape systems assembled from propellant grains from the same batch. The third response is a manufacturability index ( $y_3$ ) that reflects the cost and difficulty associated with producing a particular mixture. The constraints for this mixture problem are

$$\begin{aligned}x_1 + x_2 + x_3 &= 0.9 \\0.30 &\leq x_1 \\0.20 &\leq x_2 \\0.20 &\leq x_3\end{aligned}$$

Notice that the three components must make up 90% of the mixture. The remaining 10% is a fourth ingredient that is never varied. We will model this system in terms of

pseudocomponents, say

$$X_i = \frac{x_i - L_i}{\sum_{i=1}^3 L_i}, \quad i = 1, 2, 3 \quad (12.5)$$

This transformation yields pseudocomponents  $X_i$  such that  $0 \leq X_i \leq 1$ ,  $i = 1, 2, 3$ , and  $X_1 + X_2 + X_3 = 1$ . Because all the constraints in this problem are lower-bound constraints, the experimental region is a simplex. To draw this region in the usual coordinate system, we must remember that the range of each  $x_i$  on the graph is from 0 to 1. Therefore, the constraints that should be plotted on the graph are  $0.3/0.9 \leq x_1$ ,  $0.2/0.9 \leq x_2$ , and  $0.2/0.9 \leq x_3$  or

$$0.3333 \leq x_1$$

$$0.2222 \leq x_2$$

$$0.2222 \leq x_3$$

We can think of these constraints as the proportion of the flexible proportion of each component after the automatic inclusion of the mandatory 10%. This constrained region is shown in Fig. 12.2.

The experimenters decided that a quadratic mixture model would likely be adequate to describe the relationship between the responses and the three component proportions. They selected a 10-point design consisting of the simplex centroid augmented with the interior axial points located midway between the centroid and the opposed vertex. They decided to replicate each vertex twice and the centroid three times, resulting in the final 15-run design shown in Table 12.2. The relationship between the settings in the pseudocomponents and the actual component settings is

$$x_i = L_i + X_i \left( 0.9 - \sum_{i=1}^3 L_i \right)$$

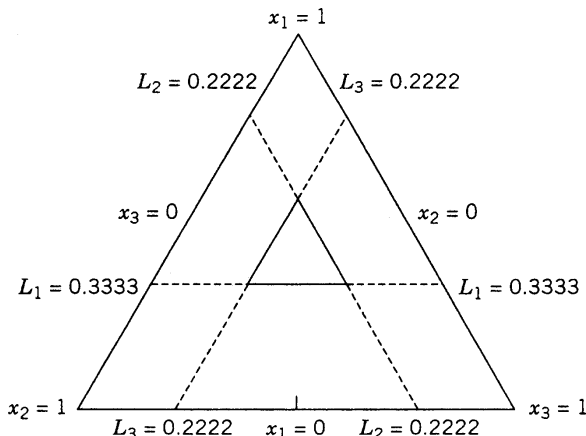


**Figure 12.2** The constrained design region for Example 12.1.

**TABLE 12.2 Data for the Propellant Example**

Observation	Pseudocomponents			Original Components			Burning Rate $y_1$	Standard Deviation of Burning Rate	Manufacturability Index
	$x_1$ (Fuel)	$x_2$ (Oxidizer)	$x_3$ (Binder)						
1	1.0	0.0	0.0	0.5	0.2	0.2	32.5	4.1	32
2	1.0	0.0	0.0	0.5	0.2	0.2	37.9	3.7	25
3	0.5	0.5	0.0	0.4	0.3	0.2	44.0	6.8	20
4	0.5	0.0	0.5	0.4	0.2	0.3	63.2	4.7	18
5	0.0	1.0	0.0	0.3	0.4	0.2	54.5	8.9	18
6	0.0	1.0	0.0	0.3	0.4	0.2	32.5	9.2	21
7	0.0	0.5	0.5	0.3	0.3	0.3	94.0	4.5	17
8	0.0	0.0	1.0	0.3	0.2	0.4	64.0	14.0	14
9	0.0	0.0	1.0	0.3	0.2	0.4	78.5	13.0	16
10	0.6667	0.1667	0.1667	0.4333	0.2333	0.2333	67.1	3.5	20
11	0.1667	0.6667	0.1667	0.3333	0.3333	0.2333	73.0	5.2	22
12	0.1667	0.1667	0.6667	0.3333	0.2333	0.3333	87.5	7.0	17
13	0.3333	0.3333	0.3333	0.3667	0.2667	0.2667	112.5	4.6	19
14	0.3333	0.3333	0.3333	0.3667	0.2667	0.2667	98.5	3.5	20
15	0.3333	0.3333	0.3333	0.3667	0.2667	0.2667	103.6	3.0	18

For the first design point in Table 12.2, where  $X_1 = 1, X_2 = X_3 = 0$  we have  $X_1 = 0.5, X_2 = 0.2$ , and  $X_3 = 0.2$ .

Table 12.3 shows the results of sequentially fitting the linear, quadratic, and special cubic models to the data in Table 12.2, using the mean burning rate response  $y_1$ . Based on the lack-of-fit test and the small  $P$ -value associated with the special cubic term, we

**TABLE 12.3 Analysis of Variance Summary and Lack-of-Fit Tests for Mean Burning Rate Response**

ANOVA Summary of Model Fit							
Source	Sum of Squares	Degrees of Freedom	Mean Square	F-Value	Probability > F	Adjusted R <sup>2</sup>	PRESS
Intercept	72,564.993	1	72,564.993				
Linear	2,395.909	2	1,197.954	2.007	0.1770	0.2507	0.1258
Quadratic	5,486.852	3	1,828.951	9.827	0.0034	0.8247	0.7274
Special cubic	1,063.615	1	1,063.615	13.92	0.0058	0.9360	0.8881
Error	611.402	8	76.425				
Corrected total	9,557.778	14					
Lack-of-Fit Tests							
Model	Sum of Squares	DF	Mean Square	F-Value	Probability > F		
Linear	6,699.757	7	957.108	10.36	0.0102		
Quadratic	1,212.905	4	303.226	3.281	0.1123		
Special cubic	149.290	3	49.763	0.5384	0.6763		
Pure error	462.112	5	92.422				

would recommend the special cubic model. Note also that the value of the PRESS statistic is smallest for the special cubic model. As noted in Chapter 2, regression models with small values of PRESS are usually good prediction equations.

In judging the relative size of PRESS, recall that it is often useful to compute the  $R^2$  for prediction based on PRESS:

$$R_{\text{prediction}}^2 = 1 - \frac{\text{PRESS}}{\text{SS}_{\text{Total}}}$$

This statistic can be thought of as a measure of the capability of the model to predict new data, and it can be compared with the usual  $R^2$  and  $R^2$ -adjusted statistics. For the special cubic model we have

$$R_{\text{prediction}}^2 = 1 - \frac{3296.975}{9555.777} = 0.6550$$

This is somewhat smaller than the other two  $R^2$ -values (see Table 12.3).

Table 12.4 contains a summary of the special cubic model. The fitted model in the pseudocomponents is

$$\begin{aligned}\hat{y}_1 &= 35.49X_1 + 42.78X_2 + 70.36X_3 + 16.02X_1X_2 \\ &\quad + 36.33X_1X_3 + 136.82X_2X_3 + 854.98X_1X_2X_3\end{aligned}$$

By substituting the definitions of the pseudocomponents into this equation, we may obtain a model for the mean burning rate in terms of the original (actual) components. However, it is usually not necessary to do this, because modern software will plot the response surface contours in either the pseudocomponents or the actual components.

From Table 12.4, notice that in the final model there are three values of the hat diagonals  $h_{ii}$  that are large (0.91); these are associated with the centers-of-edges design points. This has occurred because the  $h_{ii}$  are both model- and design-dependent, and the final model here is of higher order than the one that was initially contemplated. This happens frequently in mixture experiments and often has undesirable consequences. For example, the large  $h_{ii}$  value for design point 7 combined with a moderately large studentized residual, impacts the Cook's distance measure and the PRESS residual. The large PRESS residual dramatically reduces the  $R^2$  prediction. Hence this single observation exerts disproportionate influence on the model and its estimates.

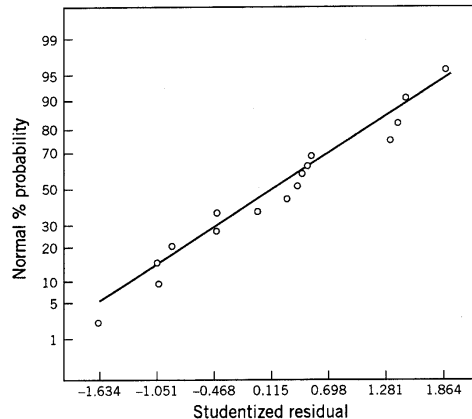
Figure 12.3 presents a normal probability plot of the studentized residuals from the special cubic model. We recommend plotting studentized residuals from mixture models, because the highly nonuniform distribution of leverage in many mixture designs results in residuals that may have very different variances. Thus, in a normal probability plot, the studentized residuals should lie approximately along a straight line. Figure 12.4 presents a contour plot for the mean burning rate response.

Table 12.5 summarizes the model-building activity for the other two responses: standard deviation of burning rate ( $y_2$ ) and manufacturability index ( $y_3$ ). In both cases, we selected the model with minimum PRESS, resulting in a quadratic model for the standard deviation of burning rate and a linear model for the manufacturability index. The values of  $R^2_{\text{prediction}}$  for those models, also shown in Table 12.5, are reasonably close to the ordinary  $R^2$ -statistic

**TABLE 12.4 Results of Fitting the Special Cubic Model for the Mean Burning Rate Response**

Variable	Parameter Estimate	Degrees of Freedom	Standard Error	$t$ for $H_0$ Parameter = 0	Probability $> t $	Observation	Actual Value	Predicted Value	Residual	$h_{ii}$	Studentized Residual	Cook's Distance	PRESS Residual
$x_1$	35.49456	1	6.07214	5.845	0.0004	1	32.50000	35.49456	-2.99456	0.482	-0.476	0.030	-5.78100
$x_2$	42.77552	1	6.07214	7.045	0.0001	2	37.90000	35.49456	2.40544	0.482	0.382	0.019	4.64371
$x_3$	70.36123	1	6.07214	11.59	0.0001	3	44.00000	43.14016	0.85984	0.910	0.327	0.154	9.55378
$x_1x_2$	16.02049	1	38.29236	0.4184	0.6867	4	63.20000	62.01159	1.18841	0.910	0.452	0.294	13.2046
$x_1x_3$	36.33478	1	38.29236	0.9489	0.3705	5	54.50000	42.77552	11.72448	0.482	1.864	0.463	22.63413
$x_2x_3$	136.82049	1	38.29236	3.573	0.0073	6	32.50000	42.77552	-10.27552	0.482	-1.634	0.355	-19.83691
$x_1x_2x_3$	854.98182	1	229.18322	3.731	0.0058	7	94.00000	90.77350	3.22650	0.910	1.227	2.165	35.85006
						8	64.00000	70.36123	-6.36123	0.482	-1.011	0.136	-12.28037
						9	78.50000	70.36123	8.13877	0.482	0.886	0.223	15.71191
						10	67.10000	67.96999	-0.86999	0.186	-0.110	0.000	-1.06878
						11	73.00000	79.98427	-6.98427	0.186	-0.886	0.026	-8.56018
						12	87.50000	95.46999	-7.96999	0.786	-1.011	0.033	-9.79114
						13	112.50000	102.22929	10.27071	0.273	1.378	0.102	14.12752
						14	98.50000	102.22929	-3.72929	0.273	-0.500	0.013	-5.12970
						15	103.60000	102.22929	1.37071	0.273	0.184	0.002	1.88543

Standard error of mean = 2.25721.



**Figure 12.3** Normal probability plot of the studentized residuals for the mean burning rate response.

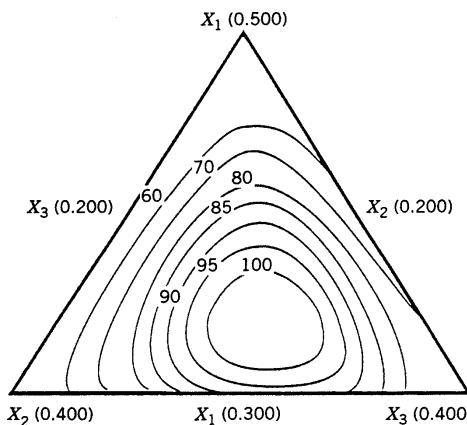


**Figure 12.4** Mean burning rate: contour plot.

**TABLE 12.5 Mixture Models for Standard Deviation of Burning Rate ( $y_2$ ) and Manufacturability Index ( $y_3$ )**

Model Form	$y_2$		$y_3$	
	$R^2$	PRESS	$R^2$	PRESS
Linear	0.4686	150.60	0.7942	39.83
Quadratic	0.9830	7.15	0.8222	69.50
Special cubic	0.9844	13.47	0.8337	140.51

$\hat{y}_2 = 3.88159X_1 + 9.03873X_2 + 13.63397X_3$   
 $- 0.19048X_1X_2 - 16.61905X_1X_3 - 27.67619X_2X_3$   
 $R^2_{\text{prediction}} = 0.9575$   
 $\hat{y}_3 = 23.13333X_1 + 19.73333X_2 + 14.73333X_3$   
 $R^2_{\text{prediction}} = 0.6456$

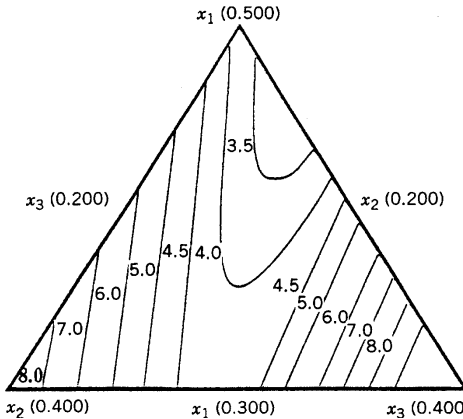


**Figure 12.5** Standard deviation of burning rate: contour plot.

for the selected model. Plots of the studentized residuals for both models were satisfactory, and the contour plots are shown in Figs 12.5 and 12.6.

As in most mixture designs, here the experimenters are interested in formulating a product that satisfies several customer requirements. Specifically, the mean burning rate must exceed 95 cm/sec, the standard deviation of the burning rate should be small (less than 4.5 cm/sec, say), and the manufacturability index should not exceed 20. Figure 12.7 presents a plot of the design region with these constraints superimposed. This graph identifies the feasible mixtures that satisfy all three response constraints. Obviously, there are many product formulations that will be satisfactory. The final choice between formulations could now be made using other supplemental criteria. For example, the conclusions here are based on predicted mean responses, and no measure of uncertainty in these predictions was evaluated. One could use confidence or prediction intervals to represent the uncertainty. Alternatively, the effects of tightening the constraints can be investigated. Figure 12.8 illustrates the effects of requiring the standard deviation of the burning rate to be less than 4 cm/sec and the manufacturability index to be less than 19. This new set of constraints has greatly reduced the feasible mixture space, and it is

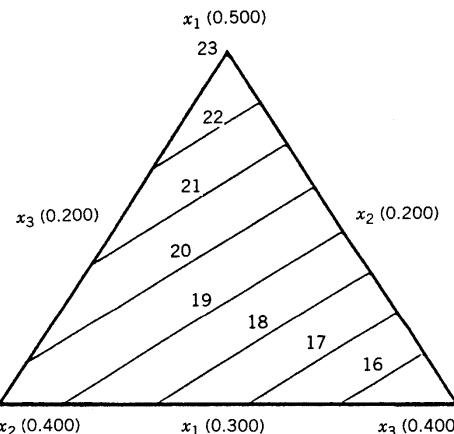


**Figure 12.6** Manufacturability index: contour plot.

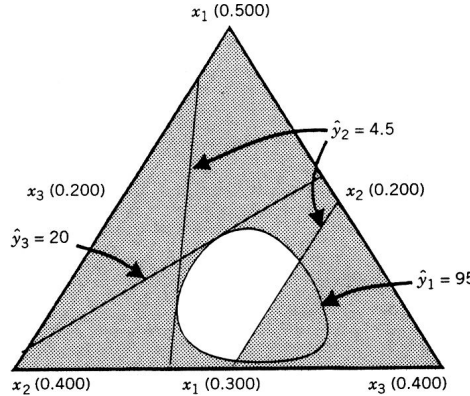


**Figure 12.7** Region of optimum solution for the propellant formulation problem.

approaching the practical limits of reduction in both variability and cost for this product if the burning rate requirement is to be met.

Finally, the effect of the influential point (design point 7) may be investigated. A simple way to do this is to withhold the point, refit the model (or models) in question, and examine the changes that occur. When this analysis is performed, similar results are obtained, but the feasible region from this refitting is somewhat smaller. It would be prudent to select a final formulation that falls in the feasible region from both models as this offers some protection from the overinfluence of design point 7.

### 12.1.2 Upper-Bound Constraints on the Component Proportions

Sometimes only **upper-bound constraints** of the form  $x_i \leq U_i$  are placed on the component proportions. In these cases, a simple modification of the simplex-lattice design consists in replacing the restricted components with mixtures consisting of combinations of the restricted components and predetermined combinations of the unrestricted components. This approach is discussed and illustrated in Cornell (2002). However, as is obvious from inspection of Fig. 12.9, where a single upper-bound constraint  $x_1 \leq U_1$  has been

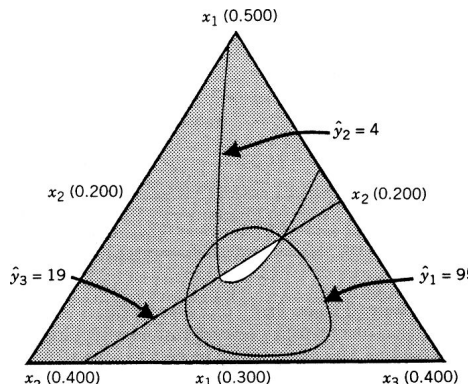


**Figure 12.8** Region of optimum solution with tighter constraints on standard deviation of burning rate and manufacturability index.

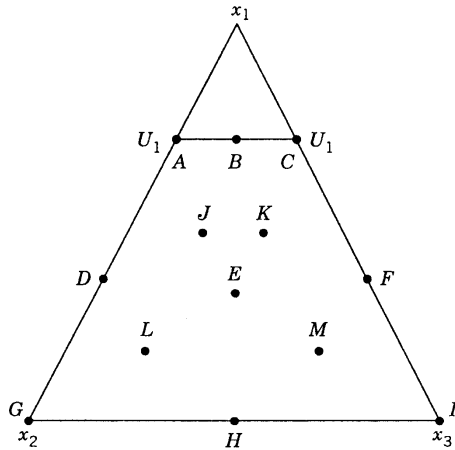


**Figure 12.9** A three-component mixture problem with an upper-bound constraint  $x_1 \leq U_1$ .

imposed, the presence of upper bounds can lead to an experimental region that is not a simplex. In such cases, **computer-generated designs** (perhaps based on the  $D$ -optimal criterion) are logical design alternatives. The points labeled  $A$  through  $K$  in Fig. 12.9 would be logical candidate points for a  $D$ -optimal algorithm to consider. Note that points  $A$ ,  $C$ ,  $G$ , and  $I$  are vertices of the constrained region,  $B$ ,  $D$ ,  $F$ , and  $H$  are centers of edges,  $E$  is the overall centroid, and  $J$ ,  $K$ ,  $L$ , and  $M$  are points that lie midway between the centroid and the vertices of the constrained region (these are somewhat analogous to the axial check blends often added to simplex-type designs).

In some cases, upper-bound constraints lead to a design space that is a simplex. For example, consider the three-component problem

$$x_1 \leq 0.4, \quad x_2 \leq 0.5, \quad \text{and} \quad x_3 \leq 0.3$$

is shown in Fig. 12.10a. Notice that the feasible region for this mixture experiment is an inverted simplex. Obviously a standard simplex-type design can be defined over

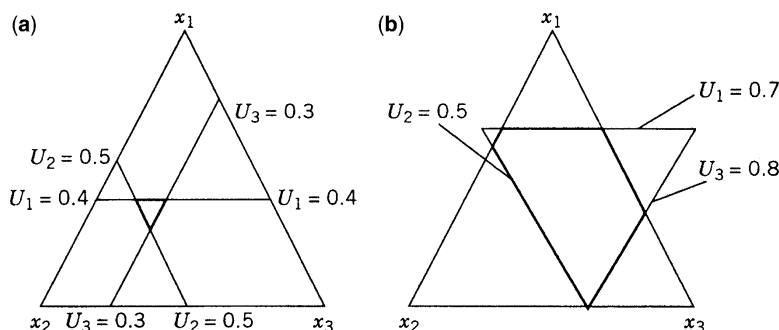


**Figure 12.10** Three-component mixture experiments. (a) The feasible region is an inverted simplex. (b) The feasible region is not a simplex.

this region Fig. 12.10b shows the feasible region for the three-component problem:

$$x_1 \leq 0.7, \quad x_2 \leq 0.5, \quad \text{and} \quad x_3 \leq 0.8$$

In this case, the feasible experimental region is not a simplex, and, once again, a computer-generated design would be a logical choice.

In general, when upper-bound constraints  $x_i \leq U_i$  are present, the feasible region will be an inverted simplex that lies entirely within the original or unconstrained simplex if and only if

$$\sum_{i=1}^q U_i - U_{\min} \leq 1 \quad (12.6)$$

where  $U_{\min}$  is the smallest of the upper bounds  $U_i$ . For example, for the situation in Fig. 12.10a we have

$$\sum_{i=1}^3 U_i = 0.4 + 0.5 + 0.3 = 1.2$$

and  $U_{\min} = 0.3$ , so

$$\sum_{i=1}^3 U_i - U_{\min} = 1.2 - 0.3 = 0.9 < 1$$

and the feasible region is an inverted simplex. On the other hand, in Fig. 12.10b we have

$$\sum_{i=1}^3 U_i = 0.7 + 0.5 + 0.8 = 2.0$$

and  $U_{\min} = 0.5$ , so

$$\sum_{i=1}^3 U_i - U_{\min} = 2.0 - 0.5 = 1.5 > 1$$

and the feasible region is not a simplex.

When two or more of the component proportions are constrained by upper bounds, Crosier (1984) suggests defining upper-bound pseudocomponents, or  $U$ -pseudocomponents:

$$u_i = \frac{U_i - x_i}{\sum_{i=1}^q U_i - 1}, \quad i = 1, 2, \dots, q \quad (12.7)$$

where

$$\sum_{i=1}^q U_i > 1$$

The region of the  $U$ -pseudocomponents is an inverted simplex; and when this inverted simplex lies entirely within the original simplex, it is easy to set up a standard simplex-type design in the  $U$ -pseudocomponents. The relationship between the settings in the original component proportions and the design points in the  $U$ -pseudocomponents  $U_i$  is

$$x_i = U_i - \left( \sum_{i=1}^q U_i - 1 \right) u_i \quad (12.8)$$

One then typically fits a model in the  $U$ -pseudocomponents. However, because the orientation of this design space is inverted, one must be careful in interpreting the coefficients in the fitted model when making inferences about the fitted surface in the original components.

### 12.1.3 Active Upper- and Lower-Bound Constraints

We now consider the case where there are both lower and upper bounds on the component proportions. In these cases, the feasible mixture region is no longer a simplex. To illustrate, suppose that we wish to formulate a shampoo in terms of three component proportions  $x_1$  = lauryl sulfate,  $x_2$  = cocamide, and  $x_3$  = lauramide, and such that

$$\begin{aligned} x_1 + x_2 + x_3 &= 0.50 \\ 0.20 \leq x_1 &\leq 0.30 \\ 0.07 \leq x_2 &\leq 0.10 \\ 0.13 \leq x_3 &\leq 0.20 \end{aligned}$$

The remaining 50% of the mixture consists of water, perfume, and coloring agents whose proportions will be held fixed. The response variable of interest is the foam height of the shampoo.

Figure 12.11 shows the feasible region for this shampoo foam experiment. Remember that in constructing this graph, the components must be scaled so that  $x_1 + x_2 + x_3 = 1$ ,

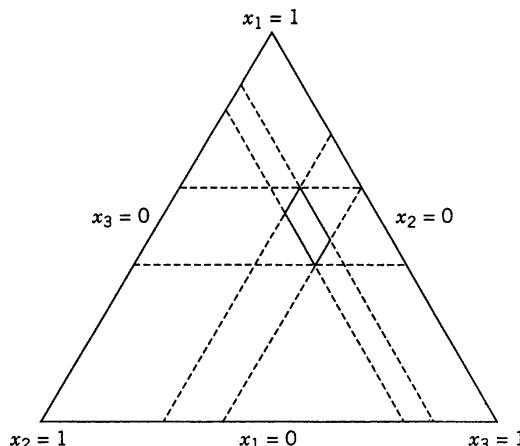


**Figure 12.11** Feasible experimental region for the shampoo foam experiment.

so the upper and lower bounds on this graph were obtained by dividing the original upper and lower bounds by 0.5. Notice that the region is not a simplex; therefore, standard simplex-type mixture designs cannot be used.

As another example, consider the flare experiment described by McLean and Anderson (1966). The objective of the experiment was to determine the formulation of a railroad flare so as to maximize the illumination level. The flare consists of four ingredients:  $x_1$  = magnesium,  $x_2$  = sodium nitrate,  $x_3$  = strontium nitrate, and  $x_4$  = binder. The constraints on the four component proportions were

$$\begin{aligned}x_1 + x_2 + x_3 + x_4 &= 1 \\0.40 \leq x_1 &\leq 0.60 \\0.10 \leq x_2 &\leq 0.50 \\0.10 \leq x_3 &\leq 0.50 \\0.03 \leq x_4 &\leq 0.08\end{aligned}$$

The constrained experimental region is shown in Fig. 12.12. Notice that the feasible region for this experiment is not a simplex, and that the actual upper bound for  $x_2$  and  $x_3$  is 0.47, since any value larger than this would combine with the other minimum values for the other components to violate the components summing to one.

In general, when both upper- and lower-bound constraints are active in a mixture experiment, the feasible design space is an irregular hyperpolytope, and usually some type of computer-generated design should be used in the experiment. We now discuss four popular criteria for constructing these designs: extreme vertices,  $D$ -optimal,  $I$ -optimal, and distance-based designs.

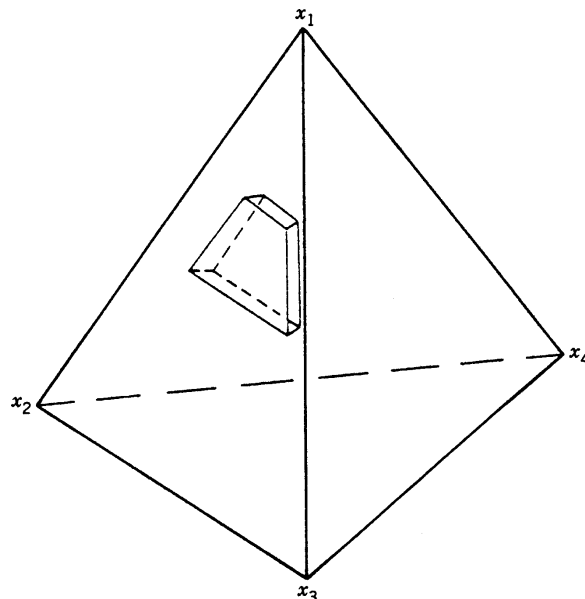


**Figure 12.12** Constrained experimental region for the flare experiment. [Adapted from Cornell (2002), with permission of the publisher.]

**Extreme Vertices Designs** The extreme vertices of the constrained region are formed by the combinations of the upper- and lower-bound constraints. In the shampoo foam study ( $q = 3$  components) there are four extreme vertices shown in Fig. 12.11, and in the flare problem ( $q = 4$  components) there are eight extreme vertices shown in Fig. 12.12. McLean and Anderson (1966) proposed using these points as the basis of a design along with a subset of the remaining centroids or points that are at the centers of the edges, faces, and so forth, including the overall centroid of the region.

McLean and Anderson (1966) demonstrated this strategy for the flare problem, assuming that a quadratic model would be adequate to describe the response. They set up a 15-point design consisting of the eight vertices, the six constraint plane centroids, and the overall centroid. This design, along with the response variable, is shown in Table 12.6.

While there are computer programs that implement the extreme vertices design strategy and this may lead to an intuitively sensible design, we feel that the other two approaches described below are generally superior. We recommend that one of these strategies be used in practice.

**D-Optimal Designs** The  $D$ -optimal criterion can be used to select points for a mixture design in a constrained region. Recall that the point exchange implementation this criterion selects design points from a list of candidate points so that the variances of the model regression coefficients are minimized. From a practical viewpoint, the points are selected so that the determinant of the matrix  $\mathbf{X}'\mathbf{X}$  is maximized.

For mixture experiments, these  $D$ -optimal design algorithms require (1) a set of reasonable candidate points from which to select the design points, (2) a convenient method for actually identifying the coordinates of these points in the constrained design space, and (3) a systematic procedure or set of rules for selecting the points. The set of candidate points to use should depend upon the order of the model the experimenter wishes to fit. Based on our practical experience, we would recommend the following:

1. **Linear Model.** The candidate points should include the vertices of the region, the edge centers, the overall centroid, and the axial points that are located halfway between the overall centroid and the vertices.

**TABLE 12.6 Extreme Vertices Design for McLean and Anderson's Flare Experiment**

Run <sup>a</sup>	$x_1$	$x_2$	$x_3$	$x_4$	y
1	0.4000	0.4700	0.1000	0.0300	145
2	0.4000	0.1000	0.4700	0.0300	75
3	0.6000	0.2700	0.1000	0.0300	220
4	0.6000	0.1000	0.2700	0.0300	195
5	0.4000	0.4200	0.1000	0.0800	230
6	0.4000	0.1000	0.4200	0.0800	180
7	0.6000	0.2200	0.1000	0.0800	350
8	0.6000	0.1000	0.2200	0.0800	300
9	0.4000	0.2725	0.2725	0.0550	190
10	0.5000	0.1000	0.3450	0.0550	220
11	0.5000	0.3450	0.1000	0.0550	260
12	0.5000	0.2350	0.2350	0.0300	260
13	0.6000	0.1725	0.1725	0.0550	310
14	0.5000	0.2100	0.2100	0.0800	410
15	0.5000	0.2225	0.2225	0.0550	425

<sup>a</sup>Vertices are runs 1–8, constraint plane centroids are runs 9–14, and the overall centroid is run 15.

2. **Quadratic Model.** The candidate points should include the vertices, the edge centers, the constraint plane centroids, the overall centroid, and the axial points.
3. **Cubic or Special Cubic Model.** The candidate points should include the vertices, the thirds of edges, the constraint plane centroids, the overall centroid, and the axial points.

There are a variety of algorithms for finding the coordinates of the vertices of a constrained region. These include the extreme vertices algorithm of McLean and Anderson (1966); the XVERT algorithm of Snee and Marquardt (1974); the modification of this by Nigam, Gupta, and Gupta (1983), called the XVERT1 algorithm; and an algorithm described by Cornell (2002) based on the  $L$ -pseudocomponents. The coordinates of the other candidate points can be expressed as linear combinations of the coordinates of the extreme vertices. Piepel (1988) presents the CONAEV algorithm for finding the centers of edge points and all other centroids.

Once an appropriate set of candidate points has been identified, a  $D$ -optimal point exchange selection algorithm can be used to select the points to be used in the design. A coordinate exchange algorithm could also be used, which would avoid the necessity of specifying the set of candidate points.

**Example 12.2 The Shampoo Foam Experiment** Consider the shampoo foam experiment described previously. Recall that

$$\begin{aligned}x_1 + x_2 + x_3 &= 0.5 \\0.2 \leq x_1 &\leq 0.3 \\0.07 \leq x_2 &\leq 0.10 \\0.13 \leq x_3 &\leq 0.20\end{aligned}$$

Figure 12.11 shows the feasible region for this experiment (with the component proportions defined as  $x_i/0.5$ ). We will construct a  $D$ -optimal design for this problem, assuming that the experimenter is planning to fit a quadratic model. We will specify as our candidate design points the four vertices of the region, the four edge centers, the overall centroid, and the four axial runs that lie midway between the centroid and the vertices of the constrained region. Table 12.7 lists these design points using the actual component proportions, the proportions defined by  $x_i/0.5$  (called “real proportions” in Table 12.7), and the  $L$ -pseudocomponents. Figure 12.13 shows the candidate points in terms of the  $L$ -pseudocomponents.

At least 6 of the 13 points in Table 12.7 must be selected in order to fit the quadratic model. We recommend that several additional runs be used in the design so that an estimate of error can be obtained and model adequacy can be checked. In general, we recommend a minimum of 7–10 additional runs, about half to be used as replicates and the other half chosen as distinct design points so that lack of fit of the model can be checked. See Snee (1985) and Montgomery and Voth (1994) for more discussion of these recommendations.

The experimenters decided to select seven additional runs, allocated as four replicate runs and three distinct points. Along with the six runs required to fit the model, this results in a design with thirteen runs. The  $D$ -optimal design was generated using the routine in the Design-Expert software package. This design is shown in Table 12.8.

**TABLE 12.7 Candidate Design Points for the Shampoo Foam Experiment, Example 12.2**

												<i>Axial Check Points</i>				
<i>Vertices</i>						<i>Edge Centers</i>										
1	Pseudo	1.0000	0.0000	0.0000	5	Pseudo	0.8500	0.1500	0.0000	9	Pseudo	0.7500	0.0750	0.1750		
	Real	0.6000	0.1400	0.2600		Real	0.5700	0.1700	0.2600		Real	0.5500	0.1550	0.2950		
	Actual	0.3000	0.0700	0.1300		Actual	0.2850	0.0850	0.1300		Actual	0.2750	0.0775	0.1475		
2	Pseudo	0.7000	0.3000	0.0000	6	Pseudo	0.6500	0.0000	0.3500	10	Pseudo	0.6000	0.2250	0.1750		
	Real	0.5400	0.2000	0.2600		Real	0.5300	0.1400	0.3300		Real	0.5200	0.1850	0.2950		
	Actual	0.2700	0.1000	0.1300		Actual	0.2650	0.0700	0.1650		Actual	0.2600	0.0925	0.1475		
3	Pseudo	0.0000	0.3000	0.7000	7	Pseudo	0.3500	0.3000	0.3500	11	Pseudo	0.2500	0.2250	0.5250		
	Real	0.4000	0.2000	0.4000		Real	0.4700	0.2000	0.3300		Real	0.4500	0.1850	0.3650		
	Actual	0.2000	0.1000	0.2000		Actual	0.2350	0.1000	0.1650		Actual	0.2250	0.0925	0.1825		
4	Pseudo	0.3000	0.0000	0.7000	8	Pseudo	0.1500	0.1500	0.7000	12	Pseudo	0.4000	0.0750	0.5250		
	Real	0.4600	0.1400	0.4000		Real	0.4300	0.1700	0.4000		Real	0.4800	0.1550	0.3650		
	Actual	0.2300	0.0700	0.2000		Actual	0.2150	0.0850	0.2000		Actual	0.2400	0.0775	0.1825		
												<i>Overall Centroid</i>				
												13	Pseudo	0.5000	0.1500	0.3500
													Real	0.5000	0.1700	0.3300
													Actual	0.2500	0.0850	0.1650

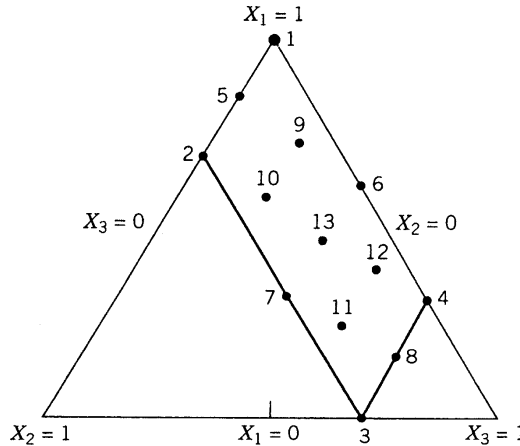


**Figure 12.13** Feasible design region using the  $L$ -pseudocomponents for the shampoo foam height experiment in Example 12.2.

The “DSN ID” column indicates which candidate points were selected, and that the vertices were also replicated. The remaining distinct design points are three edge centers (DSN ID points 5, 6, and 7), and two of the axial blends (points 9 and 12).

Table 12.9 shows the details of model fitting. Based on the relatively small value of PRESS, the adjusted  $R^2$ , and the  $P$ -value for the special cubic term, the experimenters selected the special cubic model as the best model for foam height. In terms of the pseudocomponents, this model is

$$\hat{y} = 146.74X_1 - 370.32X_2 + 94.90X_3 \\ + 745.43X_1X_2 + 183.21X_1X_3 + 876.64X_2X_3 - 524.99X_1X_2X_3$$

The analysis of variance for this model is shown in Table 12.10. Notice that all of the second-order terms and the special cubic term are statistically significant (their  $P$ -values

**TABLE 12.8 D-Optimal Design for the Shampoo Foam Experiment, Example 12.2**

Observation	DSN ID	Run Order	$X_1$	$X_2$	$X_3$	$y_1$ (Height, mm)
1	1	11	1.00	0.000	0.000	152
2	1	12	1.00	0.000	0.000	140
3	2	3	0.70	0.300	0.000	150
4	2	6	0.70	0.300	0.000	145
5	3	5	0.00	0.300	0.700	141
6	3	2	0.00	0.300	0.700	138
7	4	10	0.30	0.000	0.700	153
8	4	4	0.30	0.000	0.700	147
9	5	8	0.85	0.150	0.000	165
10	6	7	0.65	0.000	0.350	170
11	7	1	0.35	0.300	0.350	148
12	9	13	0.75	0.075	0.175	175
13	12	9	0.40	0.075	0.525	163

**TABLE 12.9 Model Fitting for the Shampoo Foam Experiment, Example 12.2**

Sequential Model Sum of Squares						
Source	Sum of Squares	Degrees of Freedom	Mean Square	F-Value	Probability > F	
Mean	303,705.3	1	303,705.3			
Linear	377.4	2	188.7	1.438	0.2825	
Quadratic	1008.0	3	336.0	7.730	0.0126	
Special cubic	153.4	1	153.4	6.103	0.0484	
Residual	150.8	6	25.1			
Lack of fit	(43.8)	2	21.9	0.8193	0.5033	
Pure error	(107.0)	4	26.8			
Total	305,395.0	13				
Lack-of-Fit Tests						
Model	Sum of Squares	Degrees of Freedom	Mean Square	F-Value	Probability > F	
Linear	1205.3	6	200.9	7.509	0.0357	
Quadratic	197.3	3	65.8	2.458	0.2026	
Special cubic	43.8	2	21.9	0.8193	0.5033	
Pure error	107.0	4	26.8			
ANOVA Summary Statistics of Models Fit						
Source	Unaliased Terms	Residual Degrees of Freedom	Root Mean Squared Error	R-Squared	Adjusted R-Squared	PRESS
Linear	3	10	11.46	0.2234	0.0681	2054.97
Quadratic	6	7	6.59	0.8199	0.6913	1035.39
Special cubic	7	6	5.01	0.9107	0.8215	657.08

are all less than 0.05). Residual plots from the model were satisfactory, and thus the special cubic equation above is the final model.

Figure 12.14 shows the shampoo foam height response surface, both as a contour plot and as a three-dimensional surface plot. The experimenters' objective was to formulate a product with foam height in excess of 170 mm. From inspection of the response surface plots we note that there are many formulations that would satisfy this objective.

Figure 12.15 is the response surface trace plot. In this plot, the centroid of the constrained region is the reference mixture, and the response trace is computed along a line connecting the centroid to the original vertex  $x_i = 1$ . This is often called **Cox's direction** (see Section 12.4 for more discussion). All three components in this trace plot exhibit strong nonlinear effects. Because all of the higher-order terms in the model were significant, this result is not unexpected.

Experimenters often select *D*-optimal designs because the concept of minimizing the variance of the regression coefficients is intuitively pleasing. However, as we have noted before, this does not necessarily guarantee that the variance of the predicted response across the region of interest is well behaved. In fact, the variance of predicted response

**TABLE 12.10 ANOVA for the Special Cubic Model, Shampoo Foam Experiment**

Source	Sum of Squares	Degrees of Freedom	Mean Square	F-Value	Probability > F
Model	1538.9	6	256.48	10.20	0.0062
Residual	150.8	6	25.14		
Lack of fit	(43.8)	2	21.92	0.8193	0.5033
Pure error	(107.0)	4	26.75		
Corrected total	1689.7	12			
Root means squared error	5.01			R-Squared 0.9107	
Dependent mean	152.85			Adjusted R-squared 0.8215	
Coefficient of variation	3.28%				
Independent Variable	Coefficient Estimate	Degrees of Freedom	Standard Error	t for $H_0$ : Coefficient = 0	Probability >  t
$X_1$	146.74	1	3.49		Not applicable
$X_2$	-370.32	1	130.14		Not applicable
$X_3$	94.90	1	15.01		Not applicable
$X_1X_2$	745.43	1	185.13	4.026	0.0069
$X_1X_3$	183.21	1	43.18	4.243	0.0054
$X_2X_3$	876.64	1	187.33	4.680	0.0034
$X_1X_2X_3$	-524.99	1	212.51	-2.470	0.0484

may be very poorly behaved. Figure 12.16 shows contours of constant standard deviation of predicted foam height from the shampoo experiment. Notice the very irregular contours of constant standard deviation of predicted response. There are some areas in which the model predicts reasonably well, and other areas nearby where the model predicts

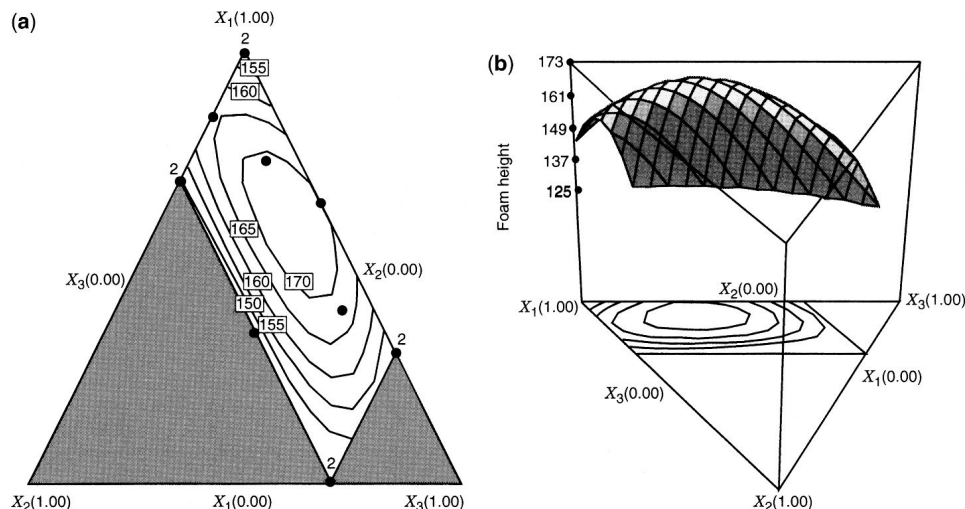


**Figure 12.14** The shampoo foam height response surface, (a) Contour plot. (b) Three-dimensional surface plot. The solid dots in the contour plot are the design points.

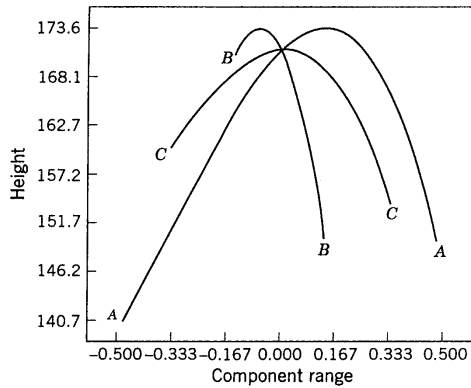


**Figure 12.15** Response surface trace plot for the shampoo foam experiment.

poorly. In particular, the model does not predict as well as one might wish near the center of the region. This is due, in part, to the tendency of the *D*-optimal criterion to **load up** the vertices of the region with design points (recall that each vertex is replicated twice in our design).

Another problem with *D*-optimal point selection is that the results obtained are often heavily dependent on the size of the design—that is, the number of runs requested. To illustrate, suppose we select a *D*-optimal design with 10 runs for the shampoo foam experiment, assuming that a quadratic model is of interest. The design selected by Design-Expert is comprised of the following DSNID numbers: 1, 2, 3, 4, 4, 5, 6, 7, 8, 13 (from Table 12.7). Notice that the algorithm selects all four vertices, all four centers of edges, and the overall centroid, and it replicates one of the vertices. This is a very different design than the one obtained in Example 12.2, and we do not think that it is as good as the 13-point design that was actually run. The 10-point design simply doesn't have enough replicate runs to give a reasonable estimate of error.

Alternate design generation strategies can be used which do not start with a set of candidate points. In this case a search strategy explores all possible points and gives the best design. For Example 12.2, the *D*-optimal design was generated in JMP for the quadratic model with 13 design points. Table 12.11 shows the selected points listed in

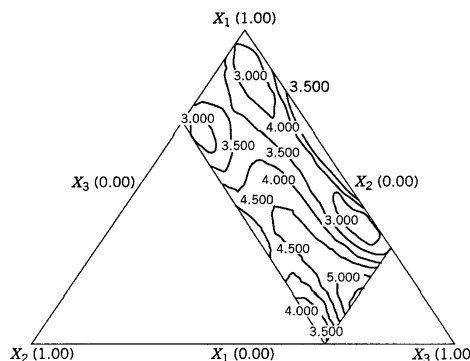


**Figure 12.16** Contours of constant standard deviation of predicted response for the shampoo foam experiment.

**TABLE 12.11 *D*-Optimal Design from JMP for the Shampoo Foam Experiment Listed in the Actual Components**

Observation	$x_1$	$x_2$	$x_3$
1	0.270	0.100	0.130
2	0.270	0.100	0.130
3	0.230	0.070	0.200
4	0.230	0.070	0.200
5	0.200	0.100	0.200
6	0.200	0.100	0.200
7	0.300	0.070	0.130
8	0.300	0.070	0.130
9	0.250	0.085	0.165
10	0.265	0.070	0.165
11	0.286	0.084	0.130
12	0.216	0.084	0.200
13	0.235	0.100	0.165

the actual coordinates. Note that this design also resulted in four replicated points (observations 1–8), even though this was not formally specified by the design selection criteria. Some of the component proportions selected have been rounded, but the reader will note that several of specified proportions look quite different from any considered in the candidate list. If there are restrictions on which proportions can be run, then a candidate list might be a more suitable approach. However, in many cases, these restrictions do not exist, and hence this more general approach to optimizing the design should be considered.

As another example of constructing *D*-optimal designs for a constrained mixture problem, consider the flare problem of McLean and Anderson (1966), described earlier. Suppose that the experimenter initially entertains a quadratic mixture model for the illumination response. Table 12.12 lists the 8 vertices, the 12 edge centers, the 6 constraint plane centroids, the 8 axial check blends, and the overall centroid for the constrained region. Because the quadratic model has 10 parameters, a reasonable design should have between 15 and 20 runs; some of the additional runs are allocated to replicates, and the others are distinct design points for checking lack of fit.

Panel A of Table 12.13 shows a 19-point *D*-optimal design for the flare problem constructed using Design-Expert. We forced the algorithm to select five replicate runs and four distinct runs for testing lack of fit, in addition to the 10 distinct runs required to fit the model. Notice that the algorithm selected six of the eight vertices, five of the eight edge centers, two of the six constraint plane centroids, and one of the eight axial check blends. The replicates were run at four vertices and one edge center. For comparison, Panel B of Table 12.13 contains a 15-point *D*-optimal design, where no restrictions were placed on how the points were selected. Notice that this design contains all eight vertices, five edge centers, and two constraint plane centroids. It shares a number of common points with the extreme vertices design of the same size, but replaces some points with edge centers.

We prefer the design in Panel A because it contains (a) enough runs to fit higher-order terms should the quadratic model be inadequate (a fairly common occurrence in mixture experiments) and (b) replicate runs so that an estimate of error can be made. Obviously, many other designs could be generated for this problem. In actual practice,

**TABLE 12.12 Candidate Design Points for the Flare Experiment**

Candidate Point	Pseudo					Actual		
<i>Vertices</i>								
1	0.0000	1.0000	0.0000	0.0000	0.4000	0.4700	0.1000	0.0300
2	0.0000	0.0000	1.0000	0.0000	0.4000	0.1000	0.4700	0.0300
3	0.5405	0.4595	0.0000	0.0000	0.6000	0.2700	0.1000	0.0300
4	0.5405	0.0000	0.4595	0.0000	0.6000	0.1000	0.2700	0.0300
5	0.0000	0.8919	0.0000	0.1081	0.4000	0.4300	0.1000	0.0700
6	0.0000	0.0000	0.8919	0.1081	0.4000	0.1000	0.4300	0.0700
7	0.5405	0.3514	0.0000	0.1081	0.6000	0.2300	0.1000	0.0700
8	0.5405	0.0000	0.3514	0.1081	0.6000	0.1000	0.2300	0.0700
<i>Edge Centers</i>								
9	0.0000	0.5000	0.5000	0.0000	0.4000	0.2850	0.2850	0.0300
10	0.2703	0.7297	0.0000	0.0000	0.5000	0.3700	0.1000	0.0300
11	0.0000	0.9459	0.0000	0.0541	0.4000	0.4500	0.1000	0.0500
12	0.2703	0.0000	0.7297	0.0000	0.5000	0.1000	0.3700	0.0300
13	0.0000	0.0000	0.9459	0.0541	0.4000	0.1000	0.4500	0.0500
14	0.5405	0.2297	0.2297	0.0000	0.6000	0.1850	0.1850	0.0300
15	0.5405	0.4054	0.0000	0.0541	0.6000	0.2500	0.1000	0.0500
16	0.5405	0.0000	0.4054	0.0541	0.6000	0.1000	0.2500	0.0500
17	0.0000	0.4459	0.4459	0.1081	0.4000	0.2650	0.2650	0.0700
18	0.2703	0.6216	0.0000	0.1081	0.5000	0.3300	0.1000	0.0700
19	0.2703	0.0000	0.6216	0.1081	0.5000	0.1000	0.3300	0.0700
20	0.5405	0.1757	0.1757	0.1081	0.6000	0.1650	0.1650	0.0700
<i>Constraint Plane Centroids</i>								
21	0.0000	0.4730	0.4730	0.0541	0.4000	0.2750	0.2750	0.0500
22	0.2703	0.0000	0.6757	0.0541	0.5000	0.1000	0.3500	0.0500
23	0.2703	0.6757	0.0000	0.0541	0.5000	0.3500	0.1000	0.0500
24	0.2703	0.3649	0.3649	0.0000	0.5000	0.2350	0.2350	0.0300
25	0.5405	0.2027	0.2027	0.0541	0.6000	0.1750	0.1750	0.0500
26	0.2703	0.3108	0.3108	0.1081	0.5000	0.2150	0.2150	0.0700
<i>Axial Check Points</i>								
27	0.1351	0.6689	0.1689	0.0270	0.4500	0.3475	0.1625	0.0400
28	0.1351	0.1689	0.6689	0.0270	0.4500	0.1625	0.3475	0.0400
29	0.4054	0.3986	0.1689	0.0270	0.5500	0.2475	0.1625	0.0400
30	0.4054	0.1689	0.3986	0.0270	0.5500	0.1625	0.2475	0.0400
31	0.1351	0.6149	0.1689	0.0811	0.4500	0.3275	0.1625	0.0600
32	0.1351	0.6149	0.1689	0.0811	0.4500	0.1625	0.3275	0.0600
33	0.4054	0.3446	0.1689	0.0811	0.5500	0.2275	0.1625	0.0600
34	0.4054	0.1689	0.3446	0.0811	0.5500	0.1625	0.2275	0.0600
<i>Overall Centroid</i>								
35	0.2703	0.3378	0.3378	0.0541	0.5000	0.2250	0.2250	0.0500

**TABLE 12.13 Two D-Optimal Designs for the Flare Experiment**

A		B		
A 19-Point Design, with Five Replicates Required <sup>a</sup>		A 15-Point Design <sup>a</sup>		
1,1	11	1	6	11
2,2	14	2	7	15
4	15	3	8	18
5	18	4	9	21
6,6	22	5	10	22
8,8	26			
9,9	27			

<sup>a</sup>The design point identification numbers refer to the points listed in Table 12.12.

we often generate several *D*-optimal designs for a problem, varying the number of replicate runs and the total number of runs on each trial. In this way, the experimenter can more clearly see any benefit associated with making a few additional runs, as well as get some idea of the total number of runs that should be made. Another strategy that we have used is to generate a *D*-optimal design with a few runs below the minimum number (but no required replicates), and then select a few points in this design for replication. For example, we might start with the 15-point design for the flare problem in Panel B of Table 12.13 and then replicate four or five of those points. We usually replicate design points that have higher leverage values whenever possible, because this generally produces smaller variance of prediction in the neighborhood of these high-leverage points, and it minimizes the effect of unusual observations or outliers that might occur at these points. For an example of this strategy applied to the flare problem, see Montgomery and Voth (1994).

***I*-Optimal Designs** The *I*-optimal criterion can also be used to create designs for constrained mixture problems. This criterion focuses on good average prediction in the design region, and can be implemented either using candidate points, or by selecting from any possible points in the design region. If we again consider the flare experiment of McLean and Anderson (1966), the *I*-optimal 15-point and 19-point designs generated by JMP using the *I*-optimal criterion are shown in Tables 12.14 and 12.15. In this case, no candidate points are provided, and the algorithm searches for the best available combinations of points which all satisfy the design region constraints. Notice that the flexibility of not specifying candidate points leads to many different settings for the each of the components. This can be both advantageous for optimizing the design, or a negative if there are restrictions on the number or values of proportions for each component which are practical.

*D*- and *I*-optimal designs focus on very different aspects of a good design, and hence likely will lead to different solutions for a given problem. Hence it is important to decide if estimation of model parameters or prediction in the design region is more important, and then choose the criterion that corresponds to the purpose of the experiment.

**TABLE 12.14 *I*-Optimal 15-Point Design from JMP for the Flare Experiment Listed in the Actual Components**

	$x_1$	$x_2$	$x_3$	$x_4$
1	0.4000	0.1000	0.4450	0.0550
2	0.4725	0.1310	0.3165	0.0800
3	0.4388	0.3480	0.1582	0.0550
4	0.5600	0.2440	0.1160	0.0800
5	0.4000	0.3070	0.2380	0.0550
6	0.6000	0.2700	0.1000	0.0300
7	0.4000	0.2280	0.2920	0.0800
8	0.6000	0.1433	0.2017	0.0550
9	0.4000	0.4200	0.1000	0.0800
10	0.4600	0.4100	0.1000	0.0300
11	0.4800	0.3650	0.1000	0.0550
12	0.4885	0.1098	0.3717	0.0300
13	0.5400	0.2025	0.2025	0.0550
14	0.4600	0.3790	0.1062	0.0548
15	0.4000	0.2850	0.2850	0.0300

**Distance-Based Designs** The distance point selection criterion attempts to spread the design points out uniformly over the feasible region. This criterion does not depend on the intended model for analysis, as it strives only to maximally spread the points. The algorithm for selecting points is very simple: Start with the point that is as close as possible to a vertex of the unconstrained region, and then add to this the point for which the Euclidean

**TABLE 12.15 *I*-Optimal 19-Point Design from JMP for the Flare Experiment Listed in the Actual Components**

	$x_1$	$x_2$	$x_3$	$x_4$
1	0.4000	0.2035	0.3415	0.0550
2	0.4227	0.4126	0.1347	0.0300
3	0.4000	0.1000	0.4700	0.0300
4	0.4600	0.3585	0.1265	0.0550
5	0.4200	0.4000	0.1000	0.0800
6	0.6000	0.1435	0.2015	0.0550
7	0.4579	0.3292	0.1579	0.0550
8	0.4968	0.3490	0.1242	0.0300
9	0.5400	0.2845	0.1205	0.0550
10	0.4000	0.1000	0.4200	0.0800
11	0.5600	0.1210	0.2890	0.0300
12	0.6000	0.1960	0.1240	0.0800
13	0.4000	0.2920	0.2280	0.0800
14	0.6000	0.2530	0.1170	0.0300
15	0.4000	0.1000	0.4450	0.0550
16	0.6000	0.2450	0.1000	0.0550
17	0.4000	0.4450	0.1000	0.0550
18	0.4720	0.1180	0.3550	0.0550
19	0.5000	0.2100	0.2100	0.0800

**TABLE 12.16 Distance-Based Designs for the Shampoo Foam Experiment**

A		B	
A 13-Point Design with Four Replicates Required <sup>a</sup>		A 10-Point Design <sup>a</sup>	
1,1	9	1	6
2,2	10	2	9
3	11	3	10
4,4	13	4	11
5,5		5	13

<sup>a</sup>The design point identification numbers refer to the points listed in Table 12.7.

distance to the first point is a maximum. All subsequent points are added similarly; that is, choose the point for which the minimum Euclidean distance to the other points in the design is maximum. The distance criterion can require a grid of candidate points or use any available points in the region, depending on the search algorithm used. If a list of candidate points is provided, we recommend the same candidate points that would be used for the *D*-optimal criterion.

To illustrate the types of designs produced by the distance criterion, consider the two distance-based designs for the shampoo foam experiment shown in Table 12.16. Panel A of this table contains a 13-point design. In constructing this design, we forced the algorithm to replicate four runs. Panel B of Table 12.16 contains a 10-point design in which we did not require any replication.

The 13-point design uses all four vertices, one of the edge centers, three of the axial points, and the overall centroid. Three of the vertices and one edge center are replicated. In general, the distance criterion will usually force more points into the interior of the feasible region than will the *D*-optimal criterion. As an illustration, compare this design with the 13-point *D*-optimal design in Table 12.8. Notice that the distance criterion placed four runs in the interior, whereas the *D*-optimal criterion placed only two runs in the interior. The 10-point distance design (Panel B of Table 12.16) also has four interior runs, whereas the 10-point *D*-optimal design has only one. Many experiments consider this **uniform** spacing of design points over the region of interest a useful feature of the distance criterion.

Table 12.17 presents two designs for the flare problem that further illustrate the distance criterion. A 19-point design in which five replicate points were forced into the design is in

**TABLE 12.17 Distance-Based Designs for the Flare Problem**

A			B		
A 19-Point Design with Five Replicates Required <sup>a</sup>			A 15-Point Design <sup>a</sup>		
1	9,9	27	1	6	27
2	18,18	28	2	9	28
3	19,19	29	3	18	29
4	20,20	30	4	19	30
5,5		35	5	20	35

<sup>a</sup>The design point identification number refer to the points listed in Table 12.12.

Panel A, and a 15-point design is in Panel B. The 19-point design contains five vertices, four edge centers, four axial runs, and the overall centroid; one of the vertices and the four edge centers are replicated. This is very different from the 19-run *D*-optimal design for this problem, which selected more of the vertices, edge centers, and constraint plane centroids. The 15-point distance design has six vertices, four edge centers, four axial runs, and the overall centroid. In contrast, the 15-point *D*-optimal design has all eight vertices, five edge centers, and two constraint plane centroids. The tendency of the distance criterion to put points in the interior of the region is clearly evident.

Generally, the distance criterion first chooses points to evenly cover the boundary of the region, and then adds interior points only when these points are further from the points already in the design than other nonincluded boundary points. As the number of variables increases, the likelihood of selecting interior points in a design with a reasonable number of points goes down, and thus for four or more components we usually prefer the *D*-optimal criterion. We have encountered cases where the distance criterion selects many low-dimensional centroids or axial check blends and relatively few vertices. Such designs would generally not be preferable to a *D*-optimal design from a variance viewpoint. Consequently, we recommend examining plots of the variance of prediction, such as variance dispersion graphs, contour plots, or the prediction profiler, over the region of interest as an aid in design selection. Fraction of design space plots would also be helpful to understand the range and distribution of the prediction variance in the region.

#### 12.1.4 Multicomponent Constraints

Sometimes in addition to upper and/or lower bounds on the individual component proportions, there are other linear constraints, such as

$$C_j \leq A_{1j}x_1 + A_{2j}x_2 + \cdots + A_{qj}x_q \leq D_j \quad (12.9)$$

for  $j = 1, 2, \dots, m$ . These types of constraints are called **multicomponent constraints**. Some of the constants  $A_{ij}$  may be zero, so that in general, not all components appear in each constraint.

When multicomponent constraints are present, they can change the shape of the feasible region for the experiment. That is, they can change the number of vertices, edges, and so on, that define the feasible space. To illustrate, consider the following example:

$$\begin{aligned} x_1 + x_2 + x_3 &= 1 \\ 0.1 &\leq x_1 \\ x_2 &\leq 0.8 \\ x_3 &\leq 0.7 \\ 0.4 &\leq x_1 + 0.8x_2 \end{aligned}$$

Figure 12.17 shows the feasible region for this design. Notice that the effect of the multicomponent constraint is to cut off part of the region that is defined by the upper- and lower-bound constraints. As a result, both the number of vertices and the number of edges in the feasible region are increased by one.

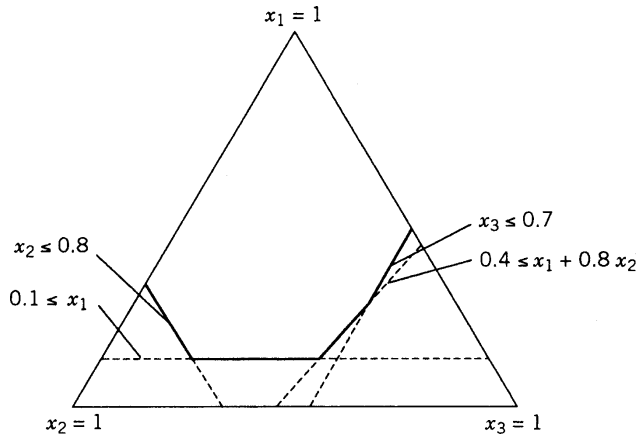


**Figure 12.17** Three-component constrained region.

Piepel (1988) has published an algorithm called CONVRT, which can locate the extreme vertices of the region when multi-component constraints are active. Both Design-Expert and JMP can handle multicomponent constraints, and generate appropriate designs for these oddly-shaped regions.

## 12.2 MIXTURE EXPERIMENTS USING RATIOS OF COMPONENTS

In some mixture experiments, the experimenter may wish to work with *ratios* of the mixture components instead of the original component proportions. For example, in formulating a detergent, it may be convenient or natural for the chemist to think of the ratio of an emulsifier to water rather than the actual proportion of each ingredient in a blend. In such an experiment, it might be natural to think of each ingredient as the ratio of the ingredient to water.

There are usually several ways to set up the ratios. For example, if there are three components, then one way to define the ratio variables is

$$r_1 = \frac{x_1}{x_3}, \quad r_2 = \frac{x_2}{x_3}$$

Another possibility is

$$r_1 = \frac{x_2}{x_1}, \quad r_2 = \frac{x_2}{x_3}$$

In general, each ratio  $r_1$  or  $r_2$  must contain at least one of the components used in the other ratio. This holds true in general: If there are  $q$  components, then we may define  $q-1$  ratios  $r_1, r_2, \dots, r_{q-1}$ , and each ratio should contain at least one of the components used in at least one of the other ratios in the set. The  $q-1$  ratio variables are *independent*; consequently any type of standard response surface polynomial can be fitted to the ratios  $r_1, r_2, \dots, r_{q-1}$ . Obviously, standard response surface designs can be used in these situations.

**Example 12.3 Gasoline Blending** Cornell (2002) presents a three-component example of blending refinery products to form gasoline. The response variable of interest is octane number. The ratios used are

$$r_1 = \frac{x_3}{x_1}, \quad r_2 = \frac{x_3}{x_2}$$

and the process currently operates at  $r_1 = 1$ ,  $r_2 = 2$  and at a composition of  $x_1 = 0.4$ ,  $x_2 = 0.2$ , and  $x_3 = 0.4$ . The region of interest is constrained by

$$\begin{aligned} 0.2 &\leq x_1 \leq 0.6 \\ 0.1 &\leq x_2 \leq 0.4 \\ 0.2 &\leq x_3 \leq 0.6 \end{aligned}$$

The feasible region is shown in Fig. 12.18. Note that for these models, the constraints are still specified in terms of the proportions of each ingredient. Hence the experimenter should track both proportions and ratios as the design is being constructed.

Suppose that the experimenter wishes to fit the quadratic model

$$y = \beta_0 + \beta_1 r_1 + \beta_2 r_2 + \beta_{12} r_1 r_2 + \beta_{11} r_1^2 + \beta_{22} r_2^2 + \varepsilon$$

in the ratio variables. Any type of response surface design in the two variables  $r_1$  and  $r_2$  could be used. Cornell chose values of the ratios equal to  $r_1 = (0.5, 1.0, 1.5)$  and  $r_2 = (1.0, 2.0, 3.0)$  and used a  $3^2$  design. The rays representing these ratios are shown in Fig. 12.18. The nine design points are at the intersections of the six rays. Table 12.18 shows the design in both the ratios and the original component proportions. The settings

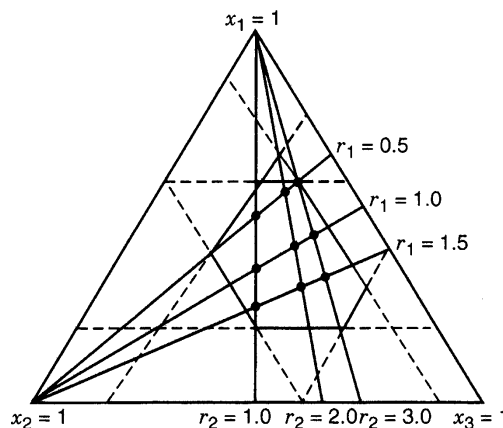


**Figure 12.18** Feasible design region for Example 12.3, along with design points in the ratio variables.

**TABLE 12.18 Octane Data for Example 12.3**

Run	$r_1 = x_3/x_1$	$r_2 = x_3/x_2$	$x_1$	$x_2$	$x_3$	Octane Number $y$
1	0.5	1.0	0.50	0.25	0.25	82.8
2	1.0	1.0	0.33	0.33	0.33	87.3
3	1.5	1.0	0.25	0.37	0.37	84.9
4	0.5	2.0	0.57	0.14	0.29	85.6
5	1.0	2.0	0.40	0.20	0.40	93.0
6	1.5	2.0	0.31	0.23	0.46	89.3
7	0.5	3.0	0.60	0.10	0.30	87.2
8	1.0	3.0	0.43	0.14	0.43	89.6
9	1.5	3.0	0.33	0.17	0.50	90.6

of the original components in terms of the ratios (which are required to run the experiment) were found by solving

$$r_1 = \frac{x_3}{x_1}, \quad r_2 = \frac{x_3}{x_2}, \quad x_1 + x_2 + x_3 = 1$$

for  $x_1$ ,  $x_2$ , and  $x_3$ , yielding

$$\begin{aligned} x_1 &= \frac{r_2}{r_1 + r_1 r_2 + r_2} \\ x_2 &= \frac{r_1}{r_1 + r_1 r_2 + r_2} \\ x_3 &= \frac{r_1 r_2}{r_1 + r_1 r_2 + r_2} \end{aligned}$$

Table 12.19 presents the analysis of variance summary for the quadratic model. The model coefficients in this table are given in terms of **coded** orthogonal variables  $z_1$  and  $z_2$ , where

$$z_1 = \frac{r_1 - 1.0}{0.5}, \quad z_2 = \frac{r_2 - 2.0}{1.0}$$

In terms of these variables, the model is

$$\hat{y} = 91.456 + 1.533z_1 + 2.067z_2 + 0.325z_1 z_2 - 3.233z_1^2 - 2.233z_2^2$$

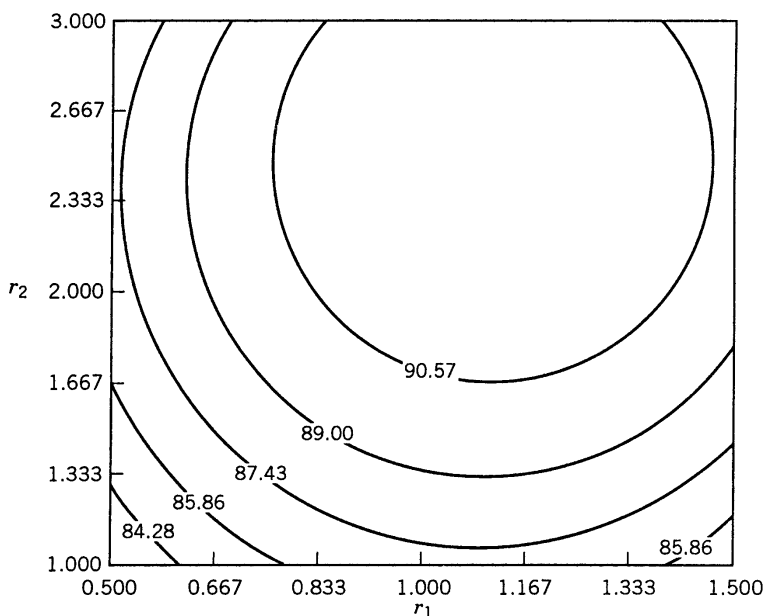
The corresponding model in terms of the ratios  $r_1$  and  $r_2$  is

$$\hat{y} = 63.689 + 27.633r_1 + 10.350r_2 + 0.650r_1 r_2 - 12.933r_1^2 - 2.233r_2^2$$

**TABLE 12.19** Analysis of Variance for the Quadratic Model in Example 12.3

Source	Sum of Squares	Degrees of Freedom	Mean Square	F-Value	Probability > F
Model	71.04	5	14.208	5.205	0.1025
Residual	8.19	3	2.730		
Corrected total	79.23	8			
Root mean square error 1.652			R-squared 0.8966		
Dependent mean 87.811			Adjusted R-squared 0.7244		
Coefficient of variation 1.88%					
Independent Variable	Coefficient Estimate	Degrees of Freedom	Standard Error	t for $H_0$ Coefficient = 0	Probability >  t
Intercept	91.456	1	1.231	74.27	
$A = z_1$	1.533	1	0.674	2.273	0.1076
$B = z_2$	2.067	1	0.674	3.064	0.0548
$A^2$	-3.233	1	1.168	-2.768	0.0697
$B^2$	-2.233	1	1.168	-1.912	0.1519
$AB$	0.325	1	0.826	0.3934	0.7203

Figure 12.19 is the octane contour plot in terms of the ratios  $r_1$  and  $r_2$ . If the experimenter wants to blend gasoline with an octane number of 89, we see from this plot that several blends will satisfy this objective. For example,  $r_1 = 1.0$  and  $r_2 = 1.33$  is a feasible set of

**Figure 12.19** Octane contour plot in terms of the ratios  $r_1$  and  $r_2$ , Example 12.3.

ratios. In terms of the original components, this point is

$$x_1 = \frac{r_2}{r_1 + r_1 r_2 + r_2} = \frac{1.33}{1.0 + (1.0)1.33 + 1.33} = 0.36$$

$$x_2 = \frac{r_1 r_2}{r_1 + r_1 r_2 + r_2} + \frac{(1.0)1.33}{1.0 + (1.0)1.33 + 1.33} = 0.36$$

$$x_3 = \frac{r_1}{r_1 + r_1 r_2 + r_2} = \frac{1.0}{1.0 + (1.0)1.33 + 1.33} = 0.28$$

The ratio variables approach is a very useful one, and we recommend it in cases where it is convenient or natural for the experimenters to work in terms of these variables. The approach does have two potential disadvantages. First, the interpretation is in terms of a function of the original component proportions (the ratios), and this may not be a natural framework for the experimenter to work in. The second disadvantage relates to how the design in terms of the ratio variables fits into the feasible mixture space. By referring to Fig. 12.18, we see that the feasible mixture space for Example 12.3 is actually larger than the region of experimentation for the  $3^2$  design in the ratios  $r_1$  and  $r_2$ . If it is important to predict the response over this entire region, then this  $3^2$  design would not be as a good a choice as a  $D$ -optimal or an  $I$ -optimal design in the original component proportions. See Piepel and Cornell (1994) for other comments on the use of ratios.

## 12.3 PROCESS VARIABLES IN MIXTURE EXPERIMENTS

### 12.3.1 Mixture-Process Model and Design Basics

**Process variables** are factors in an experiment that are not mixture components but could affect the blending properties of the mixture ingredients. For example, the effectiveness of an etching solution (measured as an etch rate, say) is not only a function of the proportions of the three acids that are combined to form the mixture, but also depends on the temperature of the solution and the agitation rate.

In general, there may be  $q$  mixture components  $x_1, x_2, \dots, x_q$  and  $p$  process variables  $z_1, z_2, \dots, z_p$ . The etching example above has  $q = 3$  mixture components and  $p = 2$  process variables. The reason we consider this as a separate class of experiment is that the mixture components are interdependent since they are constrained to sum to one, while the process variables can be varied independently.

There are two approaches to including process variables in mixture experiments. The first approach involves transforming the mixture variables into  $q - 1$  independent variables and then treating all  $p + q - 1$  factors in a conventional (nonmixture) experiment. Using ratios of the components is one transformation of the mixture variables that is widely used in practice. To illustrate, consider the etching solution described above, and let the

ratios be defined as

$$r_1 = \frac{x_1}{x_3}, \quad r_2 = \frac{x_2}{x_3}$$

The process variables are  $z_1$  = temperature and  $z_2$  = agitation rate. Then a simple model relating these factors is

$$\begin{aligned} E(y) = & \beta_0 + \beta_1 r_1 + \beta_2 r_2 + \alpha_1 z_1 + \alpha_2 z_2 \\ & + \delta_{11} r_1 z_1 + \delta_{12} r_1 z_2 + \delta_{21} r_2 z_1 + \delta_{22} r_2 z_2 \\ & + \beta_{12} r_1 r_2 + \alpha_{12} z_1 z_2 \end{aligned}$$

In this model, we may obtain information about the linear and nonlinear blending properties of the mixture components through the parameters  $\beta_1$ ,  $\beta_2$ , and  $\beta_{12}$ ; information about the main effects and interaction of the process variables through the parameters  $\alpha_1$ ,  $\alpha_2$ , and  $\alpha_{12}$ ; and information on the relation between the mixture components and the process variables through the parameters  $\delta_{ij}$ . By using the ratios the proportions of the ingredients have been expressed without constraints, and hence each of  $r_1$ ,  $r_2$ ,  $z_1$ , and  $z_2$  can be varied independently when choosing a design. In addition to the ratio approach, there are other transformations that could be used to convert the mixture components into a set of  $q - 1$  independent mixture-related variables. For a good discussion of these transformations, see Cornell (2002).

The second approach is to model the mixture components directly. This involves setting up a mixture design at each treatment combination of the factorial experiment used for the process variables. Alternatively, we can think of this as setting up a factorial in the process variables at each point in the mixture design. These two viewpoints are shown in Fig. 12.20 for the etching problem described above, assuming that a  $2^2$  factorial is used for the process variables and a simplex-centroid design is used for the three mixture components. The combined design has 28 points, and can be used to collect response data for fitting a **combined model** that includes both the mixture and the process variables. If we wish to fit a quadratic

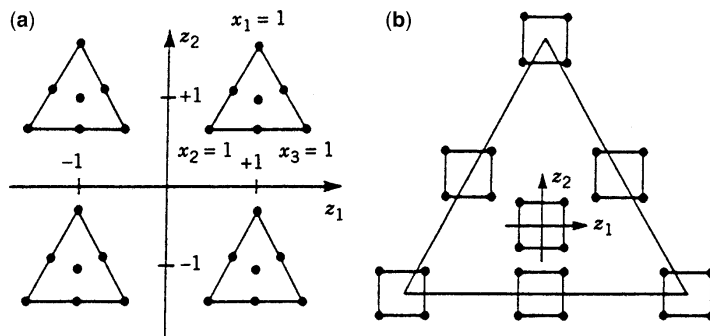


**Figure 12.20** Two different presentations of a 28-point combined design for three mixture components and two process variables. (a) The seven-point simplex centroid constructed at each of the  $2^2 = 4$  points of the factorial arrangement. (b) A complete  $2^2$  constructed at each of the seven points of the simplex centroid design. [From Cornell (2002), with permission of the publisher.]

model in the mixture variables and a model with both main effects and the two-factor interaction in the process variables, then the combined model can be written as

$$\begin{aligned}
 E(y) = & \sum_{i=1}^3 \beta_i x_i + \sum_{i<j=2}^2 \sum_{i=1}^3 \beta_{ij} x_i x_j \\
 & + \sum_{k=1}^2 \left[ \sum_{i=1}^3 \alpha_{ik} x_i + \sum_{i<j=2}^3 \alpha_{ijk} x_i x_j \right] z_k \\
 & + \left[ \sum_{i=1}^3 \delta_{i12} x_i + \sum_{i<j=2}^3 \delta_{ij12} x_i x_j \right] z_1 z_2
 \end{aligned} \tag{12.10}$$

This model has 24 parameters. Fortunately, they have relatively straightforward interpretations. The first six terms on the right-hand side of Equation 12.10 are the linear and non-linear blending portions of the model. They do not depend on the settings of the process variables. All remaining parameters measure the effects of the process variables on the linear and nonlinear blending properties of the mixture components. Note that terms involving just the process variables alone are not included in the model, since the constraint on the mixture components restrict their inclusion. See Anderson-Cook et al. (2004) for more details.

The usual approach to analyzing such a model is to fit the complete combined model and then possibly reduce the model by testing hypotheses on individual parameters or groups of parameters, using the extra-sum-of-squares method. This model would be very useful for predicting the response of a particular mixture formulation at combinations of the process variables that are not factorial design points. To predict at design points in the factorial space one could also fit individual mixture models to the mixture experiments at each factorial point. Contour plotting of the response in terms of the mixture components at each point in the factorial array is then a reasonably effective way to interpret the response surface.

As the numbers of mixture components and process variables increase, the size of these combined designs becomes very large. Several authors have suggested fractionating these combined designs, although there are no obvious best choices of the fractional design. This is a significant problem when there are constraints on the mixture components and the mixture space is a hyperpolytope. The *D*-optimal criterion is often used for generating a design for these problems. Goos and Donev (2007) provide additional details about design construction for mixture process experiments. In order to produce valid models, we caution the experimenter to be sure that there are sufficient runs in the mixture part of the experiment to support the mixture polynomial at each treatment combination in the factorial design. That is, if the combined design has too many runs, we would prefer to fractionate the process variable factorial portion of the design.

Figure 12.21 shows a design created using the *D*-optimality criterion in Design-Expert where the experimenter specified the model of Equation 12.10, a candidate set of possible points, and a total of 28 runs, where 2 runs were allocated for estimating lack of fit and 2 for pure error. The addition of the runs for  $(z_1, z_2)=(0, 0)$  are those designated for assessing lack of fit.

As with other designs, variance dispersion graphs (VDGs) and fraction of design space (FDS) plots can be used to compare the prediction performance of mixture-process

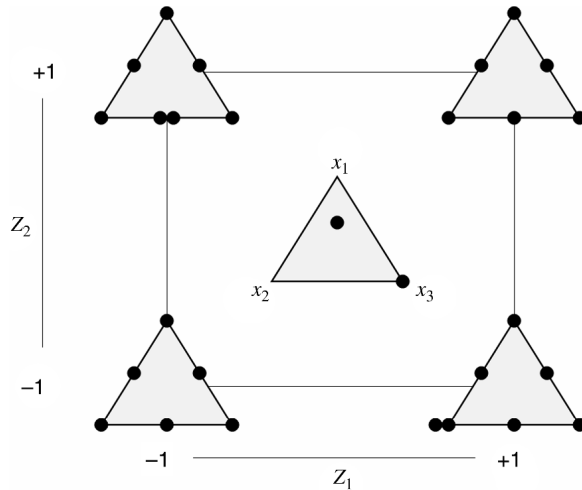


**Figure 12.21** *D*-optimal design generated by Design-Expert for model in Equation 12.10.

variables. Because we expect the performance to change differently as we move in the mixture space compared to moving in the process space, Goldfarb et al. (2004a, 2004b) developed methods for examining these features separately. Figure 12.22 shows an FDS plot for the designs considered in Figs 12.20 and 12.21. The additional lines for each plot show an FDS curve for various slices of the process space.

From the FDS plots, we can see that both designs have similar maxima and minima for SPV. Since the curves for different fixed process shrinkages are relatively flat and the different slices are separated from each other, the location in terms of the mixture components does not affect the SPV as much as the location in terms of the process variables. The

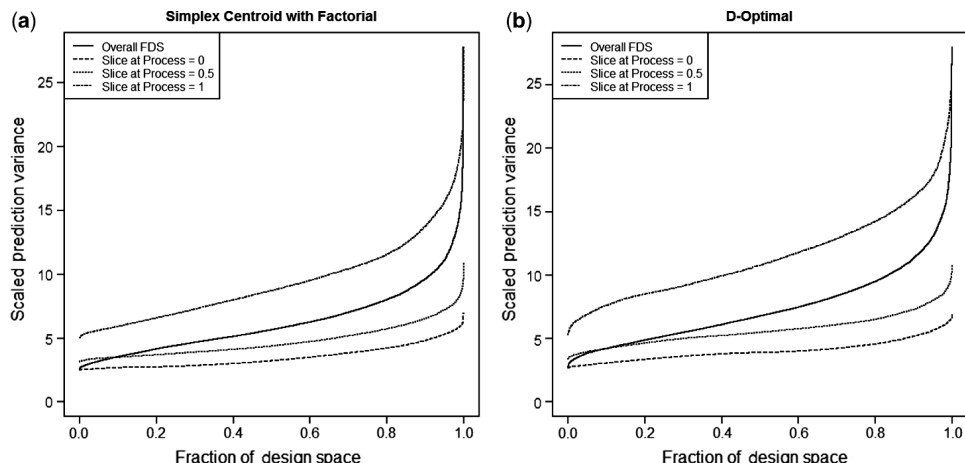


**Figure 12.22** Fraction of design space plot for designs shown in Figs 12.20 and 12.21. (a) Simplex centroid with factorial. (b) *D*-optimal.

*D*-optimal design has slightly flatter FDS curves for the majority of the design space, which makes it slightly more desirable for prediction performance. The addition of the replicates also will allow us to estimate pure error for this design.

**Example 12.4 Adhesive Formulation** An adhesive is being formulated for use in an aerospace application. The adhesive consists of a resin  $x_1$  and two crosslinkers,  $x_2$  and  $x_3$ . The mixture constraints for these variables are

$$\begin{aligned}x_1 + x_2 + x_3 &= 1 \\0.7 \leq x_1 &\leq 0.9 \\0.05 \leq x_2 &\leq 0.10 \\0.05 \leq x_3 &\leq 0.20\end{aligned}$$

The adhesive is applied to the components, and then the entire assembly is cured for 12 hr at controlled temperature and humidity. The temperature  $z_1$  and relative humidity  $z_2$  are process variables that can be controlled by the experimenter. The ranges of these process variables that the experimenters thinks are appropriate are  $40^{\circ}\text{F} \leq \text{temperature} \leq 100^{\circ}\text{F}$  and  $15\% \leq \text{relative humidity} \leq 85\%$ . The response variable of interest is the pulloff force required to separate the components after curing. It should exceed 40 pounds.

This is a three-component mixture experiment with two process variables. A reasonable model for the response is the combined model in Equation 12.10, and a design strategy similar to the one illustrated in Fig. 12.20 using a  $2^2$  factorial for the process variables, is appropriate. However, since the mixture design space is not a simplex, the experimenters cannot use a simplex-type design for the mixture components. Instead, they chose to use a *D*-optimal design, and assumed that a quadratic model would be satisfactory to represent the mixture components. The candidate set of points was taken to be the four vertices, the four edge centers, the overall centroid, and the axial check blends for the constrained mixture region at each of the four corners of the square in the process variable space. This produces a total of 52 candidate design points. The model has 24 terms, and the experimenters chose to use a design with 34 runs. There are 29 distinct design points, and five runs are replicated to provide an estimate of error. The *D*-optimal design produced by Design-Expert is shown in Table 12.20. This table contains both the actual mixture components and process variable levels, as well as their coded levels.

Table 12.21 contains the Design-Expert output that results from fitting the complete 24-term model in Equation 12.10 to the pulloff force response data. Note that there are several nonsignificant model terms. A stepwise regression algorithm was then employed, resulting in the reduced model shown in Table 12.22. There is no significant lack of fit in this model, and the residual plots are satisfactory, so we conclude that the reduced mode is adequate.

Figure 12.23 presents contour plots of the predicted pulloff force at each of the four combinations of the process variables, temperature and relative humidity. The design points are shown as circles on the plot. There are many recipes for the adhesive formulation that will produce pulloff force values in excess of 40 lb, except at low temperature and high relative humidity. The highest values of the pulloff force are obtained when temperature is high and relative humidity is low. The experimenters examined contour plots at several combinations of the process variables other than the cube corners. One of these, at

**TABLE 12.20 Design for Example 12.4 with Three Mixture Components and Two Process Variables**

Std	Run	Actual Mixture and Process Variables					Mixture Pseudocomponent			Process Variables	
		A: Resin	B: CX1	C: CX2	D: Temp (°F)	E: R.H. (%)	A ( $x_1$ )	B ( $x_2$ )	C ( $x_3$ )	D ( $z_1$ )	E ( $z_2$ )
1	26	0.90	0.05	0.05	40	15	1.000	0.000	0.000	-1	-1
2	6	0.90	0.05	0.05	100	15	1.000	0.000	0.000	1	-1
3	21	0.90	0.05	0.05	40	85	1.000	0.000	0.000	-1	1
4	8	0.90	0.05	0.05	100	85	1.000	0.000	0.000	1	1
5	5	0.70	0.10	0.20	40	15	0.000	0.250	0.750	-1	-1
6	2	0.70	0.10	0.20	100	15	0.000	0.250	0.750	1	-1
7	30	0.70	0.10	0.20	40	85	0.000	0.250	0.750	-1	1
8	24	0.70	0.10	0.20	100	85	0.000	0.250	0.750	1	1
9	17	0.75	0.05	0.20	40	15	0.250	0.000	0.750	-1	-1
10	23	0.75	0.05	0.20	100	15	0.250	0.000	0.750	1	-1
11	33	0.75	0.05	0.20	40	85	0.250	0.000	0.750	-1	1
12	9	0.75	0.05	0.20	100	85	0.250	0.000	0.750	1	1
13	11	0.85	0.10	0.05	40	15	0.750	0.250	0.000	-1	-1
14	20	0.85	0.10	0.05	100	15	0.750	0.250	0.000	1	-1
15	19	0.85	0.10	0.05	40	85	0.750	0.250	0.000	-1	1
16	22	0.85	0.10	0.05	100	85	0.750	0.250	0.00	1	1
17	10	0.80	0.07	0.13	40	85	0.500	0.125	0.375	-1	1
18	16	0.72	0.07	0.20	100	15	0.125	0.125	0.750	1	-1

19	32	0.72	0.07	0.20	40	15	0.125	0.125	0.750	-1	-1	40
20	3	0.78	0.10	0.13	40	15	0.375	0.250	0.375	-1	-1	37
21	7	0.80	0.07	0.13	100	85	0.500	0.125	0.375	1	1	46
22	29	0.78	0.10	0.13	40	85	0.375	0.250	0.375	-1	1	21
23	27	0.78	0.10	0.13	100	15	0.375	0.250	0.375	1	-1	82
24	34	0.78	0.10	0.13	100	85	0.375	0.250	0.375	1	1	43
25	15	0.82	0.05	0.13	40	15	0.625	0.000	0.375	-1	-1	32
26	1	0.82	0.05	0.13	100	15	0.625	0.000	0.375	1	-1	60
27	28	0.85	0.06	0.09	40	85	0.750	0.063	0.187	-1	1	14
28	4	0.85	0.06	0.09	100	85	0.750	0.063	0.187	1	1	38
29	14	0.83	0.09	0.09	40	15	0.625	0.187	0.187	-1	-1	45
30	13	0.78	0.10	0.13	40	85	0.375	0.250	0.375	-1	1	18
31	18	0.72	0.07	0.20	100	15	0.125	0.125	0.750	1	-1	70
32	25	0.85	0.10	0.05	40	85	0.750	0.250	0.000	-1	1	10
33	12	0.78	0.10	0.13	100	85	0.375	0.250	0.375	1	1	52
34	31	0.85	0.10	0.05	100	85	0.750	0.250	0.000	1	1	42

**TABLE 12.21 Design-Expert Output for the Full Model, Example 12.4**

Response: Force					
ANOVA for Crossed Quadratic × 2FI Model					
Analysis of variance table [Partial sum of squares]					
Source	Sum of Squares	DF	Mean Square	F-Value	Prob > F
Model	12133.68	23	527.55	24.40	<0.0001
<i>Linear</i>	<i>640.41</i>	<i>2</i>	<i>320.20</i>	<i>14.81</i>	<i>0.0010</i>
<i>Mixture</i>					
<i>AB</i>	<i>29.18</i>	<i>1</i>	<i>29.18</i>	<i>1.35</i>	<i>0.2723</i>
<i>AC</i>	<i>78.10</i>	<i>1</i>	<i>78.10</i>	<i>3.61</i>	<i>0.0865</i>
<i>AD</i>	<i>371.48</i>	<i>1</i>	<i>371.48</i>	<i>17.18</i>	<i>0.0020</i>
<i>AB</i>	<i>1044.33</i>	<i>1</i>	<i>1044.33</i>	<i>48.30</i>	<i>&lt;0.0001</i>
<i>BC</i>	<i>37.54</i>	<i>1</i>	<i>37.54</i>	<i>1.74</i>	<i>0.2170</i>
<i>BD</i>	<i>11.04</i>	<i>1</i>	<i>11.04</i>	<i>0.51</i>	<i>0.4912</i>
<i>BE</i>	<i>1.214E-003</i>	<i>1</i>	<i>1.214E-003</i>	<i>5.614E-005</i>	<i>0.9942</i>
<i>CD</i>	<i>31.91</i>	<i>1</i>	<i>31.91</i>	<i>1.48</i>	<i>0.2523</i>
<i>CE</i>	<i>8.92</i>	<i>1</i>	<i>8.92</i>	<i>0.41</i>	<i>0.5351</i>
<i>ADB</i>	<i>19.35</i>	<i>1</i>	<i>19.35</i>	<i>0.89</i>	<i>0.3665</i>
<i>ABE</i>	<i>0.55</i>	<i>1</i>	<i>0.55</i>	<i>0.026</i>	<i>0.8761</i>
<i>ACD</i>	<i>32.17</i>	<i>1</i>	<i>32.17</i>	<i>1.49</i>	<i>0.2505</i>
<i>ACE</i>	<i>3.04</i>	<i>1</i>	<i>3.04</i>	<i>0.14</i>	<i>0.7157</i>
<i>ADE</i>	<i>20.89</i>	<i>1</i>	<i>20.89</i>	<i>0.97</i>	<i>0.3488</i>
<i>BCD</i>	<i>22.32</i>	<i>1</i>	<i>22.32</i>	<i>1.03</i>	<i>0.3335</i>
<i>BCE</i>	<i>0.49</i>	<i>1</i>	<i>0.49</i>	<i>0.023</i>	<i>0.8836</i>
<i>BDE</i>	<i>4.37</i>	<i>1</i>	<i>4.37</i>	<i>0.20</i>	<i>0.6625</i>
<i>CDE</i>	<i>8.57</i>	<i>1</i>	<i>8.57</i>	<i>0.40</i>	<i>0.5431</i>
<i>ABDE</i>	<i>5.76</i>	<i>1</i>	<i>5.76</i>	<i>0.27</i>	<i>0.6171</i>
<i>ACDE</i>	<i>35.27</i>	<i>1</i>	<i>35.27</i>	<i>1.63</i>	<i>0.2304</i>
<i>BCDE</i>	<i>2.89</i>	<i>1</i>	<i>2.89</i>	<i>0.13</i>	<i>0.7221</i>
Residual	216.20	10	21.62		
<i>Lack of Fit</i>	<i>74.20</i>	<i>5</i>	<i>14.84</i>	<i>0.52</i>	<i>0.7533</i>
<i>Pure Error</i>	<i>142.00</i>	<i>5</i>	<i>28.40</i>		
Cor Total	12349.88	33			
Std. Dev.	4.65			<i>R-Squared</i>	0.9825
Mean	42.94			<i>Adj R-Squared</i>	0.9422
C.V.	10.83			<i>Pred R-Squared</i>	N/A
PRESS	N/A			<i>Adeq Precision</i>	16.103

Case(s) with leverage of 1.0000: Pred R-Squared and PRESS statistic not defined

Component	Estimate	DF	Standard Error	Coefficient	
				95% CI Low	95% CI High
A-Resin	41.11	1	2.23	36.15	46.07
B-CX1	-76.52	1	122.28	-348.99	195.94
C-CX2	42.32	1	4.99	31.21	53.43
AB	191.02	1	164.41	-175.31	557.35
AC	-27.84	1	14.65	-60.47	4.80
AD	9.23	1	2.23	4.27	14.19
AE	-15.48	1	2.23	-20.44	-10.51

(Continued)

**TABLE 12.21** *Continued*


---

Response: Force  
ANOVA for Crossed Quadratic  $\times$  2FI Model  
Analysis of variance table [Partial sum of squares]

Source	Sum of Squares	DF	Mean Square	F-Value	Prob > F
BC	214.55	1	162.81	-148.22	577.32
BD	-87.39	1	122.28	-359.86	185.07
BE	-0.92	1	122.28	-273.38	271.55
CD	6.06	1	4.99	-5.05	17.17
CE	-3.20	1	4.99	-14.31	7.91
ABD	155.53	1	164.41	-210.81	521.86
ABE	-26.29	1	164.41	-392.62	340.04
ACD	17.86	1	14.65	-14.77	50.50
ACE	-5.49	1	14.65	-38.12	27.14
ADE	-2.19	1	2.23	-7.15	2.77
BCD	165.44	1	162.81	-197.33	528.21
BCE	-24.46	1	162.81	-387.23	338.31
BDE	-55.00	1	122.28	-327.47	217.46
CDE	3.14	1	4.99	-7.97	14.25
ABDE	84.84	1	164.41	-281.50	451.17
ACDE	-18.71	1	14.65	-51.34	13.93
BCDE	59.56	1	162.81	-303.21	422.33

---

temperature 70°F and relative humidity 30%, is shown in Fig. 12.24. The experimenters selected these levels of the process variables for the final curing conditions because they were easy to maintain in the curing chamber. There are several combinations of the mixture components that will produce a pulloff force that meets or exceeds the requirements at these curing conditions.

### 12.3.2 Split-Plot Designs for Mixture-Process Experiments

Since the nature of the mixture and process variables are often very different, it is common for there to be randomization restrictions on one set of these inputs. By considering a split-plot structure, we can design an experiment which allows us to more efficiently explore the relationship between mixture and process factors on our response. This approach combines the mixture-process methodology with the split-plot concepts discussed in Chapter 9.

For example, it is sometimes convenient to make larger batches of mixtures. Then we can subdivide these batches to expose them to different process variable conditions. In this case the mixture variables are the whole plot factors, and the process variables are the subplot factors. Alternatively, in some experimental settings making up the mixtures is not time or resource intensive. Here we may wish to mix several different sets of mixtures, and then expose them in groups to different process variable conditions. Since we are running multiple sets of mixtures for each setting of the process variables, the whole plot factors in this case are the process factors, and the mixture factors and the subplots.

**Example 12.5 Vinyl Automobile Seat Covers** Kowalski et al. (2002) present an example of a split-plot mixture-process experiment for the production of automotive seat

**TABLE 12.22 Reduced Model for Example 12.4**

Response: Force

ANOVA for Crossed Quadratic  $\times$  2FI Model

Analysis of variance table [Partial sum of squares]

Source	Sum of Squares	DF	Mean Square	F-Value	Prob > F
Model	12009.06	11	1091.73	70.47	<0.0001
<i>Linear</i>	<i>640.41</i>	<i>2</i>	<i>320.20</i>	<i>20.67</i>	<i>&lt;0.0001</i>
<i>Mixture</i>					
<i>AC</i>	<i>151.08</i>	<i>1</i>	<i>151.08</i>	<i>9.75</i>	<i>0.0050</i>
<i>AD</i>	<i>460.70</i>	<i>1</i>	<i>460.70</i>	<i>29.74</i>	<i>&lt;0.0001</i>
<i>AE</i>	<i>1768.65</i>	<i>1</i>	<i>1768.65</i>	<i>114.17</i>	<i>&lt;0.0001</i>
<i>BD</i>	<i>425.88</i>	<i>1</i>	<i>425.88</i>	<i>27.49</i>	<i>&lt;0.0001</i>
<i>BE</i>	<i>210.53</i>	<i>1</i>	<i>210.53</i>	<i>13.59</i>	<i>0.0013</i>
<i>CD</i>	<i>119.78</i>	<i>1</i>	<i>119.78</i>	<i>7.73</i>	<i>0.0109</i>
<i>CE</i>	<i>91.26</i>	<i>1</i>	<i>91.26</i>	<i>5.89</i>	<i>0.0239</i>
<i>ACD</i>	<i>61.32</i>	<i>1</i>	<i>61.32</i>	<i>3.96</i>	<i>0.0592</i>
<i>CDE</i>	<i>48.32</i>	<i>1</i>	<i>48.32</i>	<i>3.12</i>	<i>0.0912</i>
Residual	340.82	22	15.49		
<i>Lack of Fit</i>	<i>198.82</i>	<i>17</i>	<i>11.70</i>	<i>0.41</i>	<i>0.9221</i>
<i>Pure Error</i>	<i>142.00</i>	<i>5</i>	<i>28.40</i>		
<i>Cor Total</i>	<i>12349.88</i>	<i>33</i>			
Std. Dev.	3.94		<i>R-Squared</i>		0.9724
Mean	42.94		Adj <i>R-Squared</i>		0.9586
C.V.	9.17		Pred <i>R-Squared</i>		0.9269
PRESS	903.20		Adeq Precision		28.424
Component	Coefficient Estimate	DF	Standard Error	95% CI Low	95% CI High
A-Resin	40.66	1	1.71	37.11	44.21
B-CX1	71.95	1	5.77	59.98	83.91

C-CX2	46.16	1	2.68	40.60	51.71
AC	-30.58	1	9.79	-50.88	-10.27
AD	9.32	1	1.71	5.77	12.86
AE	-15.49	1	1.45	-18.50	-12.49
BD	29.92	1	5.71	18.09	41.76
BE	-20.18	1	5.47	-31.53	-8.83
CD	7.43	1	2.67	1.89	12.98
CE	-4.41	1	1.82	-8.19	-0.64
ACD	19.39	1	9.74	-0.82	39.60
CDE	-2.60	1	1.47	-5.65	0.45

Final Equation in Terms of Pseudo Components and Coded Factors:

$$\begin{aligned} \text{Force} = & +40.66 * A \\ & +71.95 * B \\ & +46.16 * C \\ & -30.58 * A * C \\ & +9.32 * A * D \\ & -15.49 * A * E \\ & +29.92 * B * D \\ & -20.18 * B * E \\ & +7.43 * C * D \\ & -4.41 * C * E \\ & +19.39 * A * C * D \\ & -2.60 * C * D * E \end{aligned}$$

Final Equation in Terms of Actual Components:

$$\begin{aligned} \text{Force} = & +73.60193 * \text{Resin} \\ & -75.24237 * \text{CX1} \\ & +1247.65694 * \text{CX2} \\ & -1900.46726 * \text{Resin} * \text{CX2} \\ & -0.090433 * \text{Resin} * \text{Temp} \end{aligned}$$

**TABLE 12.22** *Continued*

Response: Force

ANOVA for Crossed Quadratic  $\times$  2FI Model

Analysis of variance table [Partial sum of squares]

Source	Sum of Squares	DF	Mean Square	F-Value	Prob > F			
	−0.48855 * Resin * Rel H							
	+4.22385 * CX1 * Temp							
	−1.16990 * CX1 * Rel H							
	−10.55458 * CX2 * Temp							
	+1.75779 * CX2 * Rel H							
	+16.2979 * Resin * CX2 * Temp							
	−9.40951E-003 * CX2 * Temp * Rel H							
Diagnostics Case Statistics								
Standard Order	Actual Value	Predicted Value	Student Residual	Leverage	Residual	Cook's Distance	Outlier t	Run Order
1	44.00	46.84	−2.84	0.534	−1.055	0.106	−1.058	26
2	70.00	65.47	4.53	0.534	1.688	0.272	1.768	6
3	19.00	15.85	3.15	0.493	1.124	0.102	1.131	21
4	33.00	34.48	−1.48	0.493	−0.528	0.023	−0.520	8
5	48.00	45.96	2.04	0.507	0.740	0.047	0.732	5
6	72.00	75.97	−3.97	0.425	−1.329	0.109	−1.354	2
7	32.00	33.15	−1.15	0.628	−0.477	0.032	−0.469	30
8	59.00	55.36	3.64	0.635	1.534	0.342	1.585	24
9	32.00	32.75	−0.75	0.417	−0.248	0.004	−0.243	17
10	58.00	59.72	−1.72	0.355	−0.545	0.014	−0.536	23
11	21.00	22.28	−1.28	0.549	−0.484	0.024	−0.475	33

12	38.00	41.46	-3.46	0.548	-1.306	0.172	-1.329	9
13	51.00	50.68	0.32	0.345	0.101	0.000	0.099	11
14	76.00	79.61	-3.61	0.380	-1.165	0.069	-1.176	20
15	22.00	17.35	4.65	0.267	1.380	0.058	1.411	19
16	49.00	46.28	2.27	0.265	0.805	0.019	0.798	22
17	17.00	15.13	1.87	0.200	0.531	0.006	0.522	10
18	69.00	67.85	1.15	0.234	0.335	0.003	0.328	16
19	40.00	39.35	0.65	0.305	0.198	0.001	0.193	32
20	37.00	41.29	-4.29	0.297	-1.300	0.059	-1.322	3
21	46.00	42.82	3.18	0.204	0.905	0.018	0.902	7
22	21.00	18.22	2.78	0.229	0.804	0.016	0.797	29
23	82.00	76.22	5.78	0.338	1.806	0.139	1.912	27
24	43.00	49.25	-6.25	0.233	-1.813	0.083	-1.920	34
25	32.00	32.76	-0.76	0.370	-0.245	0.003	-0.239	15
26	60.00	61.02	-1.02	0.383	-0.331	0.006	-0.324	1
27	14.00	13.15	0.85	0.203	0.242	0.001	0.237	28
28	38.00	38.13	-0.13	0.205	-0.036	0.000	-0.035	4
29	45.00	42.68	2.32	0.197	0.657	0.009	0.649	14
30	18.00	18.22	-0.22	0.229	-0.064	0.000	-0.063	13
31	70.00	67.85	2.15	0.234	0.625	0.010	0.616	18
32	10.00	17.35	-7.35	0.267	-2.181	0.144	-2.407	25
33	52.00	49.25	2.75	0.233	0.799	0.016	0.792	12
34	42.00	46.28	-4.28	0.265	-1.269	0.048	-1.288	31

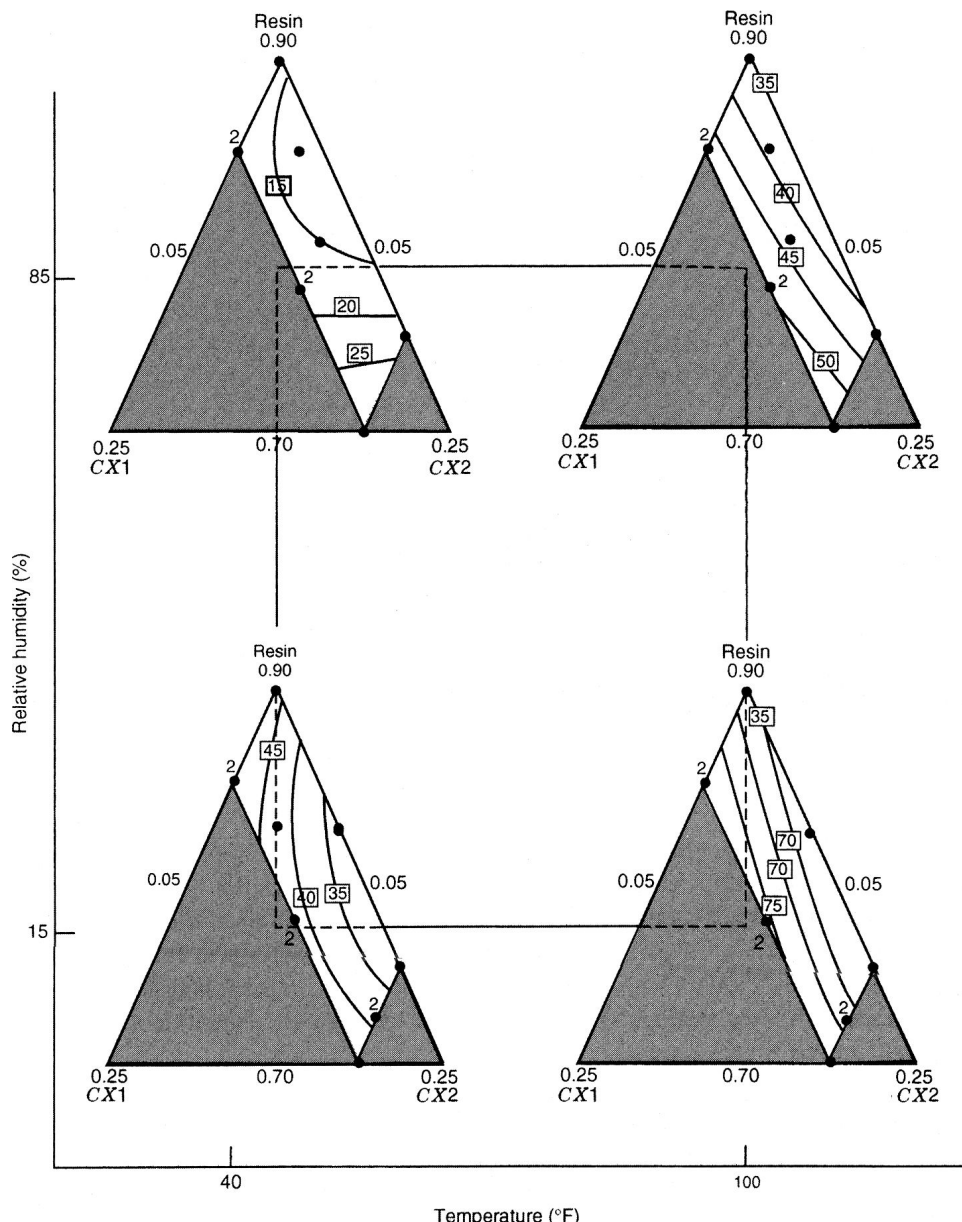


**Figure 12.23** Contour plots of predicted pulloff force for Example 12.4.

covers. Interest centers on producing vinyl with the desired thickness. The mixture components  $x_1, x_2, x_3$  are three plasticizers which can be varied from 0 to 100% of the proportion. The two process variables considered were rate of extrusion,  $z_1$ , and temperature of drying,  $z_2$ .

Based on their initial understanding of the system, the experimenters believed that a model which included a second-order model for the mixture variables with

mixture-process and process-by-process interactions. The form of the model is

$$E(y) = \beta_1 x_1 + \beta_2 x_2 + \beta_3 x_3 + \beta_{12} x_1 x_2 + \beta_{13} x_1 x_3 + \beta_{23} x_2 x_3 + \gamma_{12} z_1 z_2 \\ + \alpha_{11} x_1 z_1 + \alpha_{12} x_1 z_2 + \alpha_{21} x_2 z_1 + \alpha_{22} x_2 z_2 + \alpha_{31} x_3 z_1 + \alpha_{32} x_3 z_2 \quad (12.11)$$

Note that because of the constraint on the mixture terms, it is not possible to have linear effects for the process terms.

Since changing the rate of extrusions and temperature of drying involve reconfiguring the manufacturing environment, the experiments did not want to change this for each experimental run. Instead, the process variables were only reset seven times during the course of the experiment. Each time that the manufacturing environment had been set-up, four mixtures of the plasticizers were processed, for a total of 28 runs.

Table 12.23 shows the data from the experiment, where seven different mixture combinations were used and the process variables were varied at three levels. The design structure for the process variables was a  $2^2$  factorial design with three of the whole plots selected as center runs. The chosen mixture combinations were the pure blends of each plasticizer, two ingredient blends with equal proportions of each component, and the three component equal proportion blend.

Table 12.24 shows the JMP output for this example. Because of the split-plot structure, the standard error for the various terms of the model are dependent on the form of the model and estimates of the whole and sub-plot error terms. By using REML (REstricted or REsidual Maximum Likelihood) method of fitting mixed model, we are able to estimate the two error terms based on the data. In this case, the ratio is estimated as

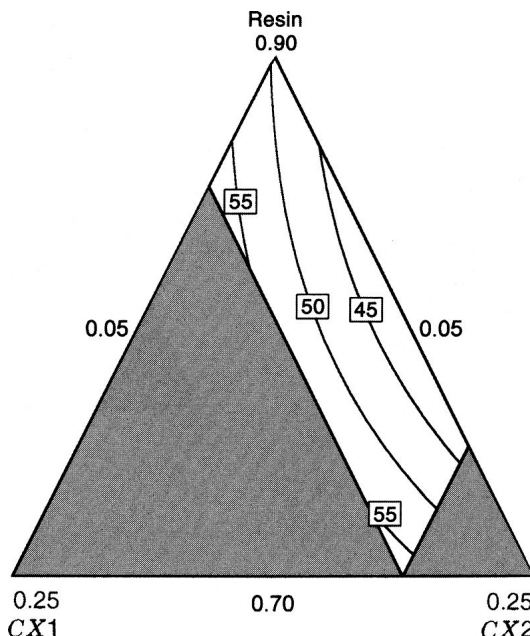


**Figure 12.24** Contour plot of predicted pulloff force when temperature = 70°F and relative humidity = 30%.

**TABLE 12.23 Design and Data for Vinyl Automotive Seat Cover Example**

Whole Plot	$z_1$	$z_2$	$x_1$	$x_2$	$x_3$	Thickness
1	−1	1	1.00	0.00	0.00	10
			0.00	1.00	0.00	8
			0.00	0.00	1.00	3
			0.33	0.33	0.33	8
2	1	−1	1.00	0.00	0.00	10
			0.00	1.00	0.00	5
			0.00	0.00	1.00	9
			0.33	0.33	0.33	9
3	1	1	0.50	0.50	0.00	5
			0.50	0.00	0.50	4
			0.00	0.50	0.50	7
			0.33	0.33	0.33	10
4	−1	−1	0.50	0.50	0.00	7
			0.50	0.00	0.50	8
			0.00	0.50	0.50	4
			0.33	0.33	0.33	7
5	0	0	0.33	0.33	0.33	8
			0.33	0.33	0.33	7
			0.33	0.33	0.33	7
			0.33	0.33	0.33	8
6	0	0	0.33	0.33	0.33	7
			0.33	0.33	0.33	8
			0.33	0.33	0.33	9
			0.33	0.33	0.33	9
7	0	0	0.33	0.33	0.33	12
			0.33	0.33	0.33	10
			0.33	0.33	0.33	9
			0.33	0.33	0.33	11

$\sigma_{WP}^2 = 0.815\sigma^2$  or  $\sigma_{WP}^2 = 0.815\sigma^2$ . The interactive Prediction Profiler in JMP, shown in Fig. 12.25 allows for exploration of the design space to determine ideal combinations of plasticizers and process inputs to optimize the seat cover thickness.

The design selected for this experiment was not an ideal choice since it does not estimate the model parameters or predict in the design space as well as possible given the constraints of the experiment. Table 12.25 gives the *I*-optimal design for this experiment with the same assumed model in Equation 12.11 which significantly improves prediction throughout the design space. However, it should also be noted that the *I*-optimal design does not allocate any degrees of freedom for estimation of the pure error for the whole plot error, nor for lack of fit of the model.

### 12.3.3 Robust Parameter Designs for Mixture-Process Experiments

Often some of the process variables cannot be fully controlled during normal production, and hence we are in a robust design setting. In this case, we are interested in determining an appropriate combination of the control factors to optimize our process when the noise

**TABLE 12.24 JMP Output from Data for Vinyl Automotive Seat Cover Example**

Summary of Fit					
RSquare	0.80174				
RSquare Adj	0.643132				
Root Mean Square Error	1.395338				
Mean of Response	7.821429				
Observations (or Sum Wgts)	28				
Parameter Estimates					
Term	Estimate	Std Error	DFDen	t-Ratio	Prob >  t
Plasticizer1(Mixture)	8.8940276	1.275453	14.45	6.97	<.0001
Plasticizer2(Mixture)	5.3940276	1.275453	14.45	4.23	0.0008
Plasticizer3(Mixture)	4.8940276	1.275453	14.45	3.84	0.0017
Extrusion Rate*Drying Temp	-1.194491	0.788355	3.534	-1.52	0.2134
Extrusion Rate*Plasticizer1	-2.007424	1.154327	11.79	-1.74	0.1081
Drying Temp*Plasticizer1	-2.008637	1.154327	11.79	-1.74	0.1079
Extrusion Rate*Plasticizer2	0.7425761	1.154327	11.79	0.64	0.5323
Drying Temp*Plasticizer2	2.2413632	1.154327	11.79	1.94	0.0765
Extrusion Rate*Plasticizer3	1.9925761	1.154327	11.79	1.73	0.1104
Drying Temp*Plasticizer3	-1.008637	1.154327	11.79	-0.87	0.3997
Plasticizer1*Plasticizer2	3.7412377	4.968701	13.83	0.75	0.4641
Plasticizer1*Plasticizer3	4.7412377	4.968701	13.83	0.95	0.3564
Plasticizer2*Plasticizer3	9.7412377	4.968701	13.83	1.96	0.0704
REML Variance Component Estimates					
Random Effect	Var Ratio	Var Component	Std Error	95% Lower	95% Upper
Block	0.8154497	1.5876555	1.7655516	-1.872826	5.0481366
Residual		1.9469694	0.7896778	1.004764	5.2623692
Total		3.5346249			100.000
-2 LogLikelihood = 62.582878702					

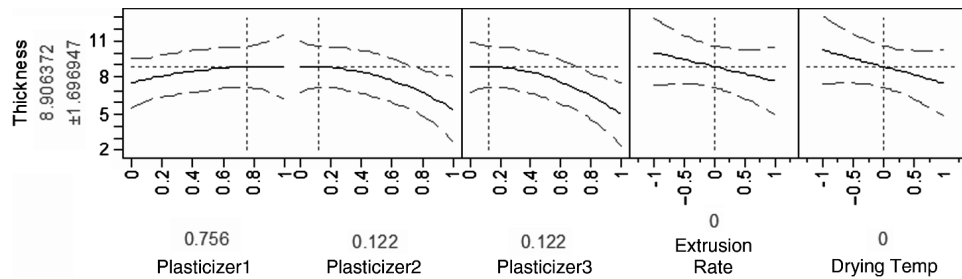


Figure 12.25 Prediction profiler for thickness of vinyl automotive seat covers.

factors vary over their natural production ranges. As discussed in Chapter 10, it is customary to fit a response model combining control and noise variables. In this case, the control variables are likely to include both mixture and process factors. We can derive models for both the mean response and for its variance. The variance model is directly related to the directional derivative or slope in the directions of the noise variables. Adaptations of the usual robust parameter designs are needed because of the constraints introduced by

TABLE 12.25 I-Optimal Design for Vinyl Automotive Seat Cover Example

Whole Plot	$z_1$	$z_2$	$x_1$	$x_2$	$x_3$
1	1	1	0	0	1
			0.5	0	0.5
			0	1	0
			1	0	0
2	-1	1	0	0	1
			1	0	0
			0	1	0
			0.5	0.5	0
3	-1	-1	0	0.5	0.5
			1	0	0
			0	1	0
			0	0	1
4	-1	1	0	0.4	0.6
			0	1	0
			1	0	0
			0.5	0	0.5
5	-1	-1	0.5	0.5	0
			0	1	0
			0.5	0	0.5
			0	0	1
6	1	1	0	0	1
			0	0.6	0.4
			0.5	0.5	0
			1	0	0
7	1	-1	0	0.5	0.5
			0	0	1
			1	0	0
			0	1	0

the mixture components. See Steiner and Hamada (1997) and Goldfarb et al. (2003) for more details.

Similar to the development in Chapter 10, the goal of the optimization is to find a combination of the control factors that is close to the desired target for the mean, while minimizing the variability transmitted to the response through the slopes in the noise factor directions.

**Example 12.6 Throughput for Soap Manufacturing** Goldfarb et al. (2003) consider an example of soap manufacturing where the goal is to maximize the amount of soap produced per hour (throughput) by the process. The soap blend is comprised of three mixture components: soap ( $x_1$ ), co-surfactant ( $x_2$ ) and filler ( $x_3$ ). There are the following restrictions on the proportions of each component:

$$0.20 \leq x_1 \leq 0.80$$

$$0.15 \leq x_2 \leq 0.50$$

$$0.05 \leq x_3 \leq 0.30$$

in addition to the usual constraint that the component proportions sum to 1.

During the manufacturing process, the first process variable, mixing time ( $w_1$ ) is considered controllable, while the plodder temperature ( $z_1$ ) is difficult to control during production, and hence is considered a noise variable. Based on understanding of the production process, the chosen model for this study involved only linear mixture components and their interactions with the controllable process and noise factors. The form of the model is

$$\begin{aligned} E(y) = & \beta_1 x_1 + \beta_2 x_2 + \beta_3 x_3 + \alpha_{11} x_1 w_1 + \alpha_{21} x_2 w_1 + \alpha_{31} x_3 w_1 \\ & + \delta_{11} x_1 z_1 + \delta_{21} x_2 z_1 + \delta_{31} x_3 z_1 + \lambda_{111} x_1 w_1 z_1 + \lambda_{211} x_2 w_1 z_1 + \lambda_{311} x_3 w_1 z_1 \end{aligned} \quad (12.12)$$

where the  $\beta$ 's are the mixture model coefficients, the  $\alpha$ 's are the interaction coefficients for the mixture and controllable process variables, the  $\delta$ 's are the interaction coefficients for the mixture and noise variables, and the  $\lambda$ 's are the interaction coefficients for the mixture, controllable process, and noise variables.

The two mixing times selected are 0.5 and 1 hour, as these cover the range common mixing times considered during production. The two plodder temperature variable levels considered are 15°C and 25°C, which is thought to cover about 70% of the variation in plodder temperature around the average value of 20°C typically observed during production. Thus the chosen values are approximately one standard deviation from the mean, and so we estimate that the mean of the noise variable is 0 and has variance  $\sigma_{z_1}^2 = 1$ .

Design-Expert was used to generate a five-run  $D$ -optimal design for the linear mixture model. The overall design was a completely randomized design where the generated mixture design was repeated for the four factorial combinations of the two process variables, for a total of 20 runs. Table 12.26 shows the design with the observed data.

**TABLE 12.26 Design and Date for the Throughput Soap Manufacturing Example**

Soap $x_1$	Co-Surfactant $x_2$	Filler $x_3$	Mixing Time $w_1$	Plodder Temperature $z_1$	Throughput
0.20	0.50	0.30	-1	-1	245.2
0.80	0.15	0.05	-1	-1	381.5
0.80	0.15	0.05	-1	-1	381.0
0.55	0.15	0.30	-1	-1	453.3
0.45	0.50	0.05	-1	-1	172.9
0.20	0.50	0.30	1	-1	285.4
0.80	0.15	0.05	1	-1	409.1
0.80	0.15	0.05	1	-1	411.7
0.55	0.15	0.30	1	-1	450.0
0.45	0.50	0.05	1	-1	245.8
0.20	0.50	0.30	-1	1	213.8
0.80	0.15	0.05	-1	1	378.4
0.80	0.15	0.05	-1	1	377.3
0.55	0.15	0.30	-1	1	408.8
0.45	0.50	0.05	-1	1	180.6
0.20	0.50	0.30	1	1	250.6
0.80	0.15	0.05	1	1	404.2
0.80	0.15	0.05	1	1	406.6
0.55	0.15	0.30	1	1	410.1
0.45	0.50	0.05	1	1	245.4

The fitted model was reduced by eliminating  $\lambda_{111}x_1w_1z_1$ , the only non-significant term (using a cutoff of 0.05) from Equation 12.12 to obtain the final model:

$$\hat{y} = 438.36x_1 - 254.01x_2 + 765.78x_3 + 34.55x_1w_1 + 263.49x_2w_1 - 203.75x_3w_1 - 0.04x_1z_1 + 5.27x_2z_1 - 18.56x_3z_1 - 3.90x_2w_1z_1 + 4.69x_3w_1z_1 \quad (12.13)$$

We can estimate the mean response surface for throughput as a function of the mixture and controllable process variables as

$$\widehat{E}(\hat{y}) = 438.36x_1 - 254.01x_2 + 765.78x_3 + 34.55x_1w_1 + 263.49x_2w_1 - 203.75x_3w_1$$

since the mean of the noise variable is assumed to be zero in the coded variables. The estimated response surface model for the throughput variance is calculated as the derivative of the overall fitted model in Equation 12.13 with respect to the noise variable. In this case it is estimated to be

$$\text{Var}(y) = \hat{\sigma}_{z_1}^2(-0.04x_1 + 5.27x_2 - 18.56x_3 - 3.90x_2w_1 + 4.69x_3w_1)^2 + \hat{\sigma}^2$$

with an estimate of  $\hat{\sigma}^2 = 1.07$ , using the mean squared error for the fitted model.

To optimize the process, we choose a combination of the mixture components and the mixing time which simultaneously maximizes the average throughout, while also minimizing the variability. Using the desirability function optimizer in Design-Expert, we obtain the following optimal conditions for production

$$\begin{aligned} \text{Soap } (x_1) &= 0.80 \\ \text{Co-surfactant } (x_2) &= 0.15 \\ \text{Filler } (x_3) &= 0.05 \\ \text{Mixing Time } (w_1) &= 1 \text{ hour (+1 in coded variables).} \end{aligned}$$

The predicted throughput at these factor settings is 408.5 with a standard deviation of 0.52.

Since robust parameter design involves simultaneously optimizing the mean and variance of the process, different tools are needed to assess the goodness of the design for this dual purpose. Goldfarb et al. (2004c) developed variations of the variance dispersion graphs and fraction of designs space plots to evaluate and compare different designs based on both of these criteria. Goldfarb et al. (2005) and Chung et al. (2007) used genetic algorithms to generate designs which perform well for both the mean and slope models. By using a desirability function to combine the prediction variance for both mean and slope, optimal designs for robust parameter design experiments can be created. Similar to the robust parameter design settings with just continuous process factors, designs that only consider the mean model may have very poor performance for the slope. However, with only small modifications, a design which is nearly optimal for the mean can often be adapted to perform well for both the mean and slope prediction variances.

## 12.4 SCREENING MIXTURE COMPONENTS

In some mixture experiments there are a large number of components, and the initial objective of the experimenter is to screen these components to identify the ones that are most important. In fact, any time there are six or more components ( $q \geq 6$ ) the experimenter should consider a **screening experiment** to reduce the number of components.

Screening is often done using the first-order mixture model

$$E(y) = \beta_1 x_1 + \beta_2 x_2 + \cdots + \beta_q x_q \quad (12.14)$$

If the experimental region is a simplex, it is usually a good idea to make the ranges of the components as similar as possible, because then the relative effects of the components can be assessed by ranking the ratios of the parameter estimates  $\beta_i$ ,  $i = 1, 2, \dots, q$ , relative to their standard errors. Obviously, important components will have large values of  $b_i/se(b_i)$ . If the effects of two or more components are equal, then the proportions of the individual components are summed and their sum is considered to be a new component.

An **axial design** in which the design points are placed only on the component axes is often recommended for screening mixture components. The simplest type of axial design has points positioned equidistant from the centroid toward each vertex. Generally, as the number of components increases, the spread of these axial points should be increased in order to increase the precision of the parameter estimates. If the vertices of the simplex are complete mixtures, as will be the case if only upper-bound constraints are active, we recommend placing the axial runs at the vertices. On the other hand, if the vertices are pure blends, some experimenters prefer to run the axial check blends as the axial design, because every run in the design will be a complete mixture.

It is, of course, still possible to examine the ratios  $b_i/se(b_i)$  in situations where the constraints form a region of experimentation that is not a simplex. We usually suggest a *D*-optimal design for the linear model (Eq. 12.14) in these cases.

To screen out unimportant components, it is necessary to measure the **effects** of the individual components. In general, we define the effect of component  $i$  as the change in the expected response from a change in the proportion of component  $i$  while holding the relative proportions of the other components constant. The largest change that we can make in component  $i$  is from 0 to 1. To keep the proportions of the other components constant, this

change must be made along the  $x_i$ -axis. The estimate of the response when  $x_i = 0$  is

$$\begin{aligned}\hat{y} &= \sum_{j \neq i}^q b_j \left( \frac{1}{q-1} \right) \\ &= (q-1)^{-1} \sum_{j \neq i}^q b_j\end{aligned}$$

Similarly, at the vertex where  $x_i = 1$ , the predicted response is

$$\hat{y} = b_i$$

If the first-order model is adequate, the **effect of component  $i$**  is just the difference in these two predicted responses:

$$(\text{effect of component } i) = b_i - (q-1)^{-1} \sum_{j \neq i}^q b_j, \quad i = 1, 2, \dots, q \quad (12.15)$$

This equation can be used for model reduction. If the true surface is linear and

$$b_i = (q-1)^{-1} \sum_{j \neq i}^q b_j$$

then the effect of component  $i$  is zero. Then the term  $\beta_i x_i$  can be removed from the model, and the component  $x_i$  is not considered further in the experiment.

When the feasible region is constrained, then often we find that the ranges of the individual components are not equal. This renders the estimate of an effect in Equation 12.15 less useful. A simple way to remedy this situation is to **adjust** the component effect estimate as follows:

$$\begin{aligned}\text{adjusted effect of component } i &= R_i \left[ b_i - (q-1)^{-1} \sum_{j \neq i}^q b_j \right], \\ i &= 1, 2, \dots, q\end{aligned} \quad (12.16)$$

where  $R_i = U_i - L_i$  is the range of component  $i$ . Notice that the adjustment essentially weights the component effect by the range of the  $i$ th component. Piepel (1982) and Cornell (2002) also discuss measuring component effects in constrained regions.

The response trace plots introduced in Chapter 11 (Section 11.3) are also very useful in screening mixture components. If one (or more) of the curves on the response trace plot is a horizontal line, then we have detected an **inactive ingredient**. In constrained regions that are not simplexes, care must be taken in defining both the reference mixture and the direction for measuring the component effect. Generally, the centroid of the constrained region is chosen as the reference mixture, and the effect of the  $i$ th component is measured along a line connecting this centroid to the vertex  $x_i = 1$ . This direction was introduced by Cox (1971) in presenting new mixture models as alternatives to those proposed by Scheffé. Consequently, this is sometimes called **Cox's direction**. The construction of the response surface trace plot for constrained regions is then identical to the procedure discussed in Section 11.3 for a simplex region of experimentation. The trace plot in Fig. 12.15 (the shampoo foam experiment, Example 12.2) uses Cox's direction. Adjusting the proportion of one component along Cox's direction results in the ratio of the other components

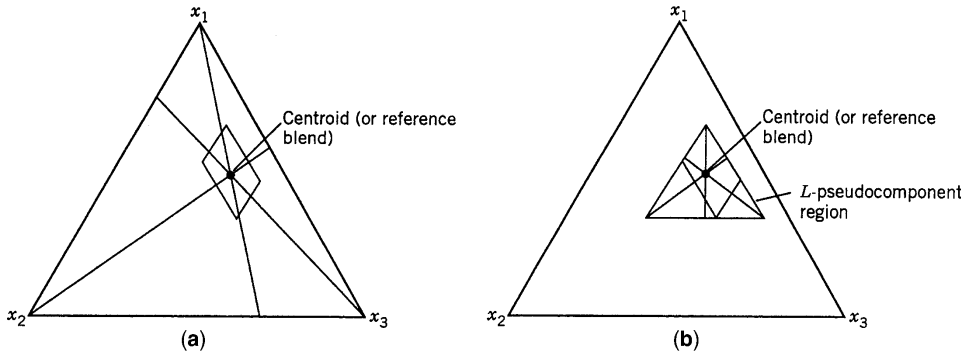


**Figure 12.26** Illustration of (a) Cox's direction and (b) Piepel's direction for the shampoo foam experiment, Example 13.1.

remaining constant. Piepel (1982) introduced another direction that could be used to construct trace plots. His direction is the line extending from a reference mixture (usually the centroid of the constrained region) to the vertices of the  $L$ -pseudocomponent region. Fig. 12.26 illustrates and compares these two directions for the shampoo foam experiment. These two directions are closely related, and usually there is little difference in the trace plots.

## EXERCISES

- 12.1** Suppose that you have fitted a second-order mixture model using  $L$ -pseudocomponents for  $q = 3$ . The fitted model is

$$\hat{y} = b_1X_1 + b_2X_2 + b_3X_3 + b_{12}X_1X_2 + b_{13}X_1X_3 + b_{23}X_2X_3$$

You wish to convert this to a model in the original components, say

$$\hat{y} = a_1x_1 + a_2x_2 + a_3x_3 + a_{12}x_1x_2 + a_{13}x_1x_3 + a_{23}x_2x_3$$

Show that the  $a$ 's can be expressed in the terms of the  $b$ 's as follows:

$$a_1 = \frac{b_{12}L_2(L_1 - 1) + b_{13}L_3(L_1 - 1) + b_{23}L_2L_3}{(1 - L)^2} + \frac{b_1 - \sum_{i=1}^3 b_iL_i}{1 - L}$$

$$a_2 = \frac{b_{12}L_1(L_2 - 1) + b_{13}L_1L_3 + b_{23}L_3(L_2 - 1)}{(1 - L)^2} + \frac{b_2 - \sum_{i=1}^3 b_iL_i}{1 - L}$$

$$a_3 = \frac{b_{12}L_1L_2 + b_{13}L_1(L_3 - 1) + b_{23}L_2(L_3 - 1)}{(1 - L)^2} + \frac{b_3 - \sum_{i=1}^3 b_iL_i}{1 - L}$$

$$a_{ij} = b_{ij}/(1 - L)^2, \quad i, j = 1, 2, 3, \quad i < j$$

**TABLE E12.1 Data for Exercise 12.2**

Design Point	$x_1$	$x_2$	$x_3$	$X_1$	$X_2$	$X_3$	Elasticity
1	0.40	0.40	0.40	1	0	0	2650
2	0.20	0.60	0.20	0	1	0	2450
3	0.20	0.40	0.40	0	0	1	2350
4	0.30	0.50	0.20	0.50	0.50	0	2950
5	0.30	0.40	0.30	0.50	0	0.50	2750
6	0.20	0.50	0.30	0	0.50	0.50	2400
7	0.27	0.46	0.27	0.333	0.33	0.333	3000
8	0.33	0.43	0.23	0.667	0.166	0.166	2980
9	0.23	0.53	0.23	0.166	0.667	0.166	2770
10	0.23	0.43	0.33	0.166	0.166	0.667	2690

- 12.2** An article in *Industrial Quality Control* (“Experiments with Mixtures of Components Having Lower Bounds,” by I. S. Kurotori, Vol. 22, 1966, pp. 592–596) describes an experiment to investigate the formulation of a rocket propellant. The propellant consists of fuel ( $x_1$ ), oxidizer ( $x_2$ ), and binder ( $x_3$ ). The restrictions on the component proportions are  $0.20 \leq x_1$ ,  $0.40 \leq x_2$ , and  $0.20 \leq x_1 \leq 0.40$ , with  $x_1 + x_2 + x_3 = 1$ . The response variable of interest is elasticity.

- (a) Draw a graph of the feasible region.
- (b) The data collected by Kurotori are shown in Table E12.1  
What type of experimental design has been used? Critique the choice of design.
- (c) Fit an appropriate model relating elasticity to the component proportions (use the pseudocomponents).
- (d) Convert the model found in part (c) to an equivalent model in the original component proportions.
- (e) Plot the contours of constant elasticity, and interpret the fitted response surface.

- 12.3** Koons and Wilt (1985) describe an experiment involving the formulation of acrylonitrile–butadiene styrene (ABS), a material used to make plastic pipe. ABS is normally made from two materials: grafted polybutadiene ( $x_1$  = graft) and styrene–acrylonitrile ( $x_2$  = SAN). Mixture experiments were performed to determine whether or not coal-tar pitch ( $x_3$  = pitch) could be added to the SAN–graft combination and form a pipe that would have physical properties that met ASTM specifications. The motive was to reduce pipe cost and utilize a by-product produced elsewhere in the plant. Experience indicated that the following constraints (on weight) should be used:

$$0.45 < x_1 < 0.70$$

$$0.30 < x_2 < 0.55$$

$$0.0 < x_3 < 0.25$$

The physical properties of interest for the ABS pipe are: Izod impact strength ( $y_1$ , ft-lb/in), deflection temperature under load ( $y_2$ , °F), and yield strength ( $y_3$ , psi).

**TABLE E12.2 Data for Exercise 12.3**

Run	$x_1$	$x_2$	$x_3$	$X_1$	$X_2$	$X_3$	$y_1$	$y_2$	$y_3$
1	0.700	0.300	0.000	1	0	0	7.4	205	4350
2	0.450	0.550	0.000	0	1	0	6.1	213	6080
3	0.450	0.300	0.250	0	0	1	0.8	183	5065
4	0.575	0.425	0.000	0.50	0.50	0	7.3	204	5280
5	0.575	0.300	0.125	0.50	0	0.50	3.9	188	5080
6	0.450	0.425	0.125	0	0.50	0.50	2.1	191	5740
7	0.535	0.380	0.085	0.34	0.32	0.34	4.4	197	5410
8	0.600	0.350	0.050	0.60	0.20	0.20	6.1	192	5035
9	0.500	0.450	0.050	0.20	0.60	0.20	4.9	202	5615
10	0.500	0.350	0.150	0.20	0.20	0.60	2.5	186	5385

- (a) Graph the feasible region for this experiment.
- (b) The response data obtained in the experiment performed by Koons and Wilt are shown in Table E12.2.
- (c) What type of experimental design has been used? Comment on the experimenter's choice of design.
- (d) Build appropriate response surface models for all three responses. Build these models using the pseudocomponents.
- (e) Convert the models found in part (d) to equivalent models in the actual component proportions.
- (f) Construct response surface contour plots for the three response variables  $y_1$ ,  $y_2$ , and  $y_3$ .
- (g) In order to produce acceptable pipe from this modified ABS material, the following response constraints must be satisfied:  $y_1 > 1 \text{ ft-lb/in.}$ ,  $y_2 > 190^\circ\text{F}$ , and  $y_3 > 5000 \text{ psi}$ . Is there a formulation of the modified ABS material that will satisfy these specifications?
- (h) If the objective is to include as much pitch in the formulation as possible and still satisfy the response specifications in part (g), what formulation would you recommend?

**12.4** The following constraints are imposed on three mixture components:

$$0.15 \leq x_1, \quad 0.25 \leq x_2, \quad 0.10 \leq x_3 \\ x_1 + x_2 + x_3 = 1$$

- (a) Draw a graph of the feasible region.
  - (b) Suppose that you could only afford to perform eight runs, and your objective is to fit a first-order mixture model. What runs would you recommend?
  - (c) Suppose that your objective is to fit a quadratic mixture model. If you can afford to perform 12 runs, what blends would you include in the design?
  - (d) List the points in the design from part (c) in terms of the  $L$ -pseudocomponents.
- 12.5** Reconsider the three component mixture problem in Exercise 12.4. What design would you recommend if the experimenter wishes to fit a special cubic model?

- 12.6** Consider the data from McLean and Anderson's flare experiment, shown in Table 12.6.
- Convert the component setting in the extreme vertices design in this table to  $L$ -pseudocomponents.
  - Fit a quadratic mixture model to the illumination response, using the  $L$ -pseudocomponents. Comment on the adequacy of this model.
  - Add the special cubic terms to the model found in part (b) above. Does the addition of these terms improve the model?
  - Construct response surface contour plots in terms of components  $x_1$ ,  $x_2$ , and  $x_3$  for various levels of  $x_4$ . Interpret the fitted surface.
- 12.7** Table E12.3 presents the actual values of the observed response from the shampoo foam height experiment in Example 12.2, the predicted response from the quadratic model, the residuals, the values of  $h_{ii}$ , and the studentized residuals.
- Construct a normal probability plot of the studentized residuals from this experiment. Interpret the plot.
  - Plot the studentized residuals versus the predicted values of foam height. What conclusions can you show about model adequacy?
  - Two points in the design (a) have relative high leverage ( $h_{10,10} = 0.874$ ,  $h_{11,11} = 0.909$ ). Where are these points located in the feasible space? Discuss the practical implications of having design points with high average.
- 12.8** A three-component mixture experiment is subject to the following constraints on the component proportions:

$$0.3 \leq x_1 \leq 0.6, \quad 0.1 \leq x_2 \leq 0.5, \quad 0.05 \leq x_3 \leq 0.45 \\ x_1 + x_2 + x_3 = 1$$

- (a) Graph the feasible region for this experiment.

TABLE E12.3 Data for Exercise 12.7

Run	Actual Value	Predicted Value	Residual	$h_{ii}$	Studentized Residual
1	152.00	146.74	5.26	0.484	1.461
2	140.00	146.74	-6.74	0.484	-1.872
3	150.00	148.16	1.84	0.466	0.501
4	145.00	148.16	-3.16	0.466	-0.863
5	141.00	139.43	1.57	0.499	0.443
6	138.00	139.43	-1.43	0.499	-0.403
7	153.00	148.93	4.07	0.473	1.119
8	147.00	148.93	-1.93	0.473	-0.529
9	165.00	164.22	0.78	0.617	0.250
10	170.00	170.28	-0.28	0.874	-0.156
11	148.00	146.95	1.05	0.909	0.698
12	175.00	171.20	3.80	0.346	0.936
13	163.00	167.83	-4.83	0.409	-1.254

- (b) Suppose that the experimenter wishes to fit a quadratic model to the response. Identify a set of candidate points that the experimenter should consider in the selected design.
- (c) Find a  $D$ -optimal design for this experiment with  $n = 14$  runs, assuming that four of these runs must be replicates.
- (d) Find an  $I$ -optimal design for this experiment with  $n = 14$  runs.
- (e) Construct an FDS plot for each of the designs in parts (c) and (d)
- 12.9** Reconsider the constrained mixture problem in Exercise 12.8.
- (a) Find a 10-point design for this experiment using the distance criterion, assuming that you are not required to replicate any points.
- (b) Find a 14-point distance-criterion design for this experiment, assuming that four of these points must be replicates.
- 12.10** Reconsider the three-component mixture experiment from Exercise 12.8. Suppose the experimenter wishes to fit a linear mixture model to the response and is willing to make  $n = 8$  runs.
- (a) Construct a  $D$ -optimal design for this problem.
- (b) Construct a distance-criterion design for this problem.
- (c) Construct an FDS plot for each design in parts (a) and (b)
- (d) Compare and contrast the designs found in parts (a) and (b). Which design would you recommend?
- 12.11** Suppose that the experimenter in Exercise 12.8 is interested in fitting a special cubic model.
- (a) Construct an FDS plot for the designs.
- (b) Compare the prediction variance for each design using the linear model, the quadratic model, and the special cubic.
- (c) Which design would you recommend?
- 12.12** A four-component mixture experiment is subject to the following constraints on the component proportions:

$$0.8 \leq x_1, \quad 0.05 \leq x_2 \leq 0.15, \quad 0.02 \leq x_3 \leq 0.10, \quad x_4 \leq 0.05 \\ x_1 + x_2 + x_3 + x_4 = 1$$

- (a) Suppose that the experimenter wishes to fit a quadratic model to the response. Identify a set of candidate points that the experimenter should consider in the selected design.
- (b) Find a  $D$ -optimal design for this experiment with  $n = 15$  runs, assuming that you are not required to replicate any points.
- (c) Find a  $D$ -optimal design for this experiment with  $n = 18$  runs, assuming that four of these runs must be replicates.
- (d) Find  $I$ -optimal designs for this experiment with  $n = 15$  and  $n = 18$  runs.
- (e) Construct an FDS plot for the four designs in parts (b), (c), and (d).
- (f) Which design would you recommend?

- 12.13** Consider the constrained mixture problem in Exercise 12.12.
- Find a 15-point design for this experiment using the distance criterion, assuming that you are not required to replicate any points.
  - Find an 18-point design for this experiment using the distance criterion. Assume that four runs must be replicates.
  - Construct an FDS plot for the designs in parts (a) and (b).
  - Which design would you recommend?
- 12.14** Consider the four-component mixture experiment from Exercise 12.12. Suppose that the experimenter wishes to fit a linear mixture model to the response and is willing to make  $n = 10$  runs.
- Construct a  $D$ -optimal design for this problem.
  - Construct a distance-based design for this problem.
  - Compare and contrast the designs in parts (a) and (b). Which design would you recommend?
- 12.15** Heinsman and Montgomery (1995) describe a four-component mixture experiment used to optimize the formulation of a household detergent. The constraints on the component proportions are:
- $$0.5 \leq x_1 \leq 1, \quad 0 \leq x_2 \leq 0.5, \quad 0 \leq x_3 \leq 0.5, \quad 0 \leq x_4 \leq 0.05$$
- $$x_1 + x_2 + x_3 + x_4 = 1$$
- The authors measured four responses:  $y_1$  = product life (in lather units),  $y_2$  = soil pellets,  $y_3$  = foam height, and  $y_4$  = total foam. The last three responses reflect the grease-cutting ability of the product. All four responses should be as large as possible. The data from the experiment they ran is shown in Table E12.4. The design used by the authors was generated by selecting some points with the distance criterion and the remaining points with the  $D$ -optimal criterion.
- Build response surface models for all four responses.
  - Plot contours of each response, and interpret the fitted surfaces.
  - What formulation of these ingredients would you recommend?
- 12.16 John Cornell's Famous Fish Patties I.** Cornell (2002) describes an experiment to optimize the texture of fish patties made from three types of fish: mullet ( $x_1$ ), sheepshead ( $x_2$ ), and croaker ( $x_3$ ). The texture is measured by the amount of force required to break the patty. Three process variables are also considered in the experiment: oven temperature (375°F, 425°F), time in oven (25 sec, 40 min), and deep fat frying time (25 sec, 40 sec). The results of this experiment are shown in Table E12.5, where  $z_1$  = oven temperature,  $z_2$  = time in oven, and  $z_3$  = deep fat frying time shown in the usual  $-1, +1$  coded units. In this problem we will consider only one of the process variables,  $z_1$  = oven temperature.
- Fit a special cubic model to the texture response at the high temperature level only. Construct a contour plot of the response surface, and interpret the results.

**TABLE E12.4 Experimental Design for Exercise 12.15**

Observation	$x_1$	$x_2$	$x_3$	$x_4$	$X_1$	$X_2$	$X_3$	$X_4$	$y_1$ (Lather Units)	$y_2$ (Pellets)	$y_3$ (Foam Height)	$y_4$ (Total Foam)
1	1.000	0.0000	0.0000	0.00000	1.000	0.000	0.000	0.0000	7.170	7.00	95.0	559.0
2	0.500	0.5000	0.0000	0.00000	0.000	1.000	0.000	0.0000	2.680	20.00	92.0	1320.0
3	0.500	0.0000	0.5000	0.00000	0.000	0.000	1.000	0.0000	3.080	3.00	44.0	275.0
4	0.950	0.0000	0.0000	0.05000	0.900	0.000	0.000	0.1000	6.990	7.00	73.0	508.0
5	0.500	0.4500	0.0000	0.05000	0.000	0.900	0.000	0.1000	2.920	20.00	105.0	1436.0
6	0.500	0.0000	0.4500	0.05000	0.000	0.000	0.900	0.1000	2.890	5.00	45.0	371.0
7	0.750	0.2500	0.0000	0.00000	0.500	0.500	0.000	0.0000	4.830	20.00	88.0	12.1
8	0.750	0.0000	0.2500	0.00000	0.500	0.000	0.500	0.0000	3.850	8.00	53.0	510.0
9	0.500	0.2500	0.2500	0.00000	0.000	0.500	0.500	0.0000	3.130	20.00	70.0	1123.0
10	0.725	0.2250	0.0000	0.05000	0.450	0.450	0.000	0.1000	4.430	20.00	80.0	1196.0
11	0.725	0.0000	0.2250	0.05000	0.450	0.000	0.450	0.1000	3.600	8.00	75.0	581.0
12	0.650	0.1500	0.1500	0.05000	0.300	0.300	0.300	0.1000	3.750	20.00	58.0	1061.0
13	0.650	0.1500	0.1500	0.05000	0.300	0.300	0.300	0.1000	3.260	20.00	59.0	1087.0
14	0.829	0.0792	0.0792	0.01250	0.658	0.158	0.158	0.0250	5.390	8.00	65.0	546.0
15	0.658	0.1583	0.1583	0.02500	0.317	0.317	0.317	0.0500	4.310	20.00	55.0	1069.0
16	0.579	0.3292	0.0792	0.01250	0.158	0.658	0.158	0.0250	2.640	20.00	80.0	1310.0
17	0.579	0.0792	0.3292	0.01250	0.158	0.158	0.658	0.0250	3.560	20.00	57.0	1011.0
18	0.804	0.0792	0.0792	0.03750	0.608	0.158	0.158	0.0750	5.230	20.00	68.0	1039.0
19	0.579	0.3042	0.0792	0.03750	0.158	0.608	0.158	0.0750	3.220	20.00	76.0	1192.0
20	0.579	0.0792	0.3042	0.03750	0.158	0.158	0.608	0.0750	3.520	20.00	59.0	1087.0

**TABLE E12.5 Fish Patty Texture for Exercises 12.16 and 12.17**

Process Factors			Mixture Composition						
$z_1$	$z_2$	$z_3$	(1, 0, 0)	(0, 1, 0)	(0, 0, 1)	( $\frac{1}{2}$ , $\frac{1}{2}$ , 0)	( $\frac{1}{2}$ , 0, $\frac{1}{2}$ )	(0, $\frac{1}{2}$ , $\frac{1}{2}$ )	( $\frac{1}{3}$ , $\frac{1}{3}$ , $\frac{1}{3}$ )
-1	-1	-1	1.84	0.67	1.51	1.29	1.42	1.16	1.59
1	-1	-1	2.86	1.10	1.60	1.53	1.81	1.50	1.68
-1	1	-1	3.01	1.21	2.32	1.93	2.57	1.83	1.94
1	1	-1	4.13	1.67	2.57	2.26	3.15	2.22	2.60
-1	-1	1	1.65	0.58	1.21	1.18	1.45	1.07	1.41
1	-1	1	2.32	0.97	2.12	1.45	1.93	1.28	1.54
-1	1	1	3.04	1.16	2.00	1.85	2.39	1.60	2.05
1	1	1	4.13	1.30	2.75	2.06	2.82	2.10	2.32

- (b) Fit a special cubic model to the texture response at the low temperature level only. Construct a contour plot of the response surface, and interpret the results.
- (c) Fit a combined model to the texture response that is a special cubic in the mixture components. Is there a simple relationship between the parameter estimates in the combined model and the parameter estimates in the two individual models built at the low and high temperature levels? Does this relationship seem reasonable?
- (d) What process conditions and recipe produces texture readings above 2.5?
- 12.17 John Cornell's Famous Fish Patties II.** Reconsider the fish patty experiment described in Exercise 12.16.
- (a) Fit a combined model to the texture response data. Can this model be **reduced** by eliminating apparently nonsignificant variables?
- (b) Construct contour plots that explain the results of your model-building efforts.
- (c) Suppose that it is desirable to have the texture above 2.5 and as close to 2.75 as possible. Find a recipe and a set of processing conditions that all satisfy these requirements.
- 12.18** An experiment was conducted to study the hardness and percentage of solids in an automotive clear coat. There are two categorial process factors: monomer type (M1 and M2), and crosslinker type (X1, X2, X3). The experimenters want to examine the effect of varying the proportions of monomer, crosslinker, and resin in a mixture process variables experiment. The constraints on the mixture components are:

Monomer	5–20%
Crosslinker	25–40%
Resin	55–70%

A *D*-optimal design with 38 runs was constructed for this experiment. The experimenters assumed that only main effects of the process variables were likely to be important, but they planned to use (up to) a special cubic model in the mixture components. The design is shown in Table E12.6.

- (a) How would you create the set of candidate points from which to construct the *D*-optimal design?

**TABLE E12.6 Data for Exercise 12.18**

Std	Run	Block	Component 1 Monomer (%)	Component 2 Crosslinker (%)	Component 3, Resin (%)	Factor 1, Vendor Type	Factor 2, Crosslinker Type	Response 1, Hardness	Response 2, Solids (%)
1	26	1	0.000	0.000	1.000	M2	X3	8.6	50.7
2	35	1	0.000	1.000	0.000	M1	X1	9.7	48.0
3	23	1	0.500	0.500	0.000	M1	X1	15.0	48.3
4	24	1	0.333	0.333	0.333	M2	X2	6.4	50.7
5	19	1	0.000	0.000	1.000	M1	X1	7.5	49.7
6	27	1	1.000	0.000	0.000	M2	X1	12.0	47.3
7	4	1	1.000	0.000	0.000	M1	X2	3.8	48.0
8	32	1	0.333	0.333	0.333	M1	X1	11.0	52.0
9	18	1	0.000	1.000	0.000	M2	X1	9.3	48.1
10	17	1	0.000	0.000	1.000	M2	X2	5.4	49.9
11	12	1	0.333	0.333	0.333	M1	X3	7.2	50.2
12	9	1	0.000	0.500	0.500	M2	X1	9.0	48.2
13	14	1	0.000	1.000	0.000	M1	X2	3.6	46.7
14	33	1	0.500	0.500	0.000	M2	X3	12.0	48.2
15	2	1	0.500	0.000	0.500	M1	X3	6.2	49.9
16	20	1	0.000	0.500	0.500	M1	X3	5.3	47.9
17	34	1	0.500	0.000	0.500	M2	X1	10.0	50.2
18	21	1	0.500	0.000	0.500	M2	X2	5.3	49.2
19	15	1	0.000	0.500	0.500	M2	X2	2.4	50.0
20	7	1	0.000	1.000	0.000	M2	X3	6.6	47.8
21	5	1	0.333	0.333	0.333	M2	X3	9.0	50.3
22	31	1	0.500	0.500	0.000	M1	X2	7.0	46.9
23	29	1	0.000	0.500	0.500	M1	X2	3.5	47.8
24	3	1	1.000	0.000	0.000	M1	X3	5.0	48.7
25	28	1	0.500	0.000	0.500	M1	X2	5.0	49.9

(Continued)

**TABLE 12.6** *Continued*

Std	Run	Block	Component 1 Monomer (%)	Component 2 Crosslinker (%)	Component 3, Resin (%)	Factor 1, Vendor Type	Factor 2, Crosslinker Type	Response 1, Hardness	Response 2, Solids (%)
26	22	1	0.000	0.000	1.000	M2	X1	7.7	50.9
27	16	1	0.500	0.500	0.000	M1	X3	8.7	48.0
28	13	1	1.000	0.000	0.000	M2	X2	6.1	49.0
29	8	1	0.000	1.000	0.000	M2	X2	5.9	47.2
30	1	1	1.000	0.000	0.000	M1	X1	11.0	47.8
31	30	1	1.000	0.000	0.000	M2	X3	10.0	47.8
32	38	1	0.000	1.000	0.000	M1	X3	6.3	46.8
33	36	1	0.500	0.500	0.000	M2	X1	14.0	46.9
34	25	1	0.000	0.500	0.500	M2	X1	9.2	50.4
35	37	1	0.000	0.000	1.000	M2	X3	7.7	49.4
36	11	1	0.333	0.333	0.333	M2	X2	6.7	50.3
37	10	1	0.000	0.000	1.000	M1	X1	7.3	50.9
38	6	1	0.000	0.000	1.000	M2	X2	5.0	49.9

- (b) Analyze the data and select appropriate models for both responses: hardness and percentage of solids.
- (c) Construct contour plots of both responses.
- (d) Can you find a recipe for the clear coat, a monomer type, and a crosslinker type for which the hardness exceeds 10 and solids exceed 50%?
- (e) Can you specify the mixture recipe so that the responses are robust to the type of crosslinker?
- (f) Can you specify the mixture recipe so that the responses are robust to the type of monomer?
- 12.19** Reconsider John Cornell's famous fish patty experiment described in Exercise 12.16. Suppose that only two of the process variables are considered important:  $z_1$  and  $z_2$ . However, it is considered necessary to fit a model that is quadratic in the process variables.
- (a) Write down an appropriate crossed model for this problem.
- (b) Set up a  $D$ -optimal design that could be used to fit the model.
- 12.20** Consider a three-component mixture experiment with the following constraints on the mixture proportions:
- $$x_1 \leq 0.5, \quad x_2 \leq 0.6, \quad x_3 \leq 0.6$$
- $$x_1 + x_2 + x_3 = 1$$
- (a) Graph the feasible region for this experiment.
- (b) Suppose that the experimenter considers a quadratic model to be adequate. What type of experimental design would you recommend? Construct the design.
- 12.21** Consider the following first-order mixture model in seven components:
- $$\hat{y} = 35x_1 + 85x_2 + 140x_3 + 77x_4 + 90x_5 + 100x_6 + 120x_7$$
- (a) Assuming that all components were varied over approximately the same ranges, calculate the effects of each component.
- (b) Is there any indication that some components can be dropped from further consideration?
- 12.22** Consider a mixture experiment with the following constraints on the component proportions:
- $$x_1 \leq 0.2, \quad x_2 \leq 0.6, \quad x_3 \leq 0.15,$$
- $$x_4 \leq 0.65, \quad x_5 \leq 0.15, \quad x_6 \leq 0.75$$
- $$x_1 + x_2 + x_3 + x_4 + x_5 + x_6 = 1$$
- (a) Suggest a screening design for this mixture experiment.

- (b) Suppose that you have obtained the following first-order model for the response.

$$\hat{y} = 20x_1 + 30x_2 + 10x_3 + 16x_4 + 45x_5 + 80x_6$$

Calculate the adjusted effects of each component. Interpret the results of this analysis.

- 12.23** Consider a mixture experiment with the following constraints on the component proportions.

$$0.05 \leq x_1, \quad 0.05 \leq x_2, \quad 0.10 \leq x_3,$$

$$0.20 \leq x_4, \quad 0.01 \leq x_5$$

$$x_1 + x_2 + x_3 + x_4 + x_5 = 1$$

- (a) Suggest a screening design for this mixture experiment.

- (b) Suppose that you have obtained the following first-order model for the response:

$$\hat{y} = 20x_1 + 65x_2 + 20x_3 + 90x_4 + 45x_5$$

Calculate the adjusted effects of each component. Interpret the results of this analysis.

- 12.24** Consider the mixture-process experiment of Example 12.6. We now assume both mixing time and plodder temperature are considered noise variables.

- (a) Find the estimated mean response surface for throughput as a function of the mixture variables.

- (b) Find the estimated variance response surface for throughput as a function of  $\sigma_{z_1}^2$  and  $\sigma_{w_1}^2$ .

- (c) Find the combination of mixture components to simultaneously maximize average throughput and minimize variability.

- 12.25** Show why the main effects for the process variables can not be included in the model given in Equation 12.10.

- 12.26** Construct a contour plot of the scaled prediction variance in the design region for the D-optimal design in Table 12.8 used for the shampoo foam experiment. Where are the worst regions for prediction? Where are the best?

---

## APPENDIX 1

---

### MOMENT MATRIX OF A ROTATABLE DESIGN

In the development that follows, it is convenient in expressing the polynomial model to make use of **derived power vectors** and **Schlaifflian matrices**. If  $\mathbf{z}' = [z_1, z_2, \dots, z_k]$ , then  $\mathbf{z}'^{[p]}$ , the derived power vector of degree  $p$ , is defined such that

$$\mathbf{z}'^{[p]} \mathbf{z}^{[p]} = (\mathbf{z}' \mathbf{z})^p$$

For example if  $\mathbf{z}' = [z_1, z_2, z_3]$ , then

$$\mathbf{z}'^{[2]} = [z_1^2, z_2^2, z_3^2, \sqrt{2}z_1z_2, \sqrt{2}z_1z_3, \sqrt{2}z_2z_3]$$

and

$$\mathbf{z}'^{[1]} = \mathbf{z}'$$

If a vector  $\mathbf{x}$  is formed from a vector  $\mathbf{z}$  containing  $k$  elements through the transformation

$$\mathbf{x} = \mathbf{H}\mathbf{z} \tag{A.1.1}$$

then the **Schlaifflian matrix**  $\mathbf{H}^{[p]}$  is defined such that

$$\mathbf{x}^{[p]} = \mathbf{H}^{[p]} \mathbf{z}^{[p]}$$

It is readily seen that if the transformation matrix  $\mathbf{H}$  is orthogonal, then  $\mathbf{H}^{[p]}$  is also orthogonal. One can write

$$\mathbf{x}'^{[p]} \mathbf{x}^{[p]} = \mathbf{z}'^{[p]} \mathbf{H}'^{[p]} \mathbf{H}^{[p]} \mathbf{z}^{[p]} \tag{A.1.2}$$

the left-hand side of Equation A.1.2 is, by definition,  $(\mathbf{x}'\mathbf{x})^p$ . Because  $\mathbf{H}$  is orthogonal,

$$(\mathbf{x}'\mathbf{x})^p = (\mathbf{z}'\mathbf{z})^p = \mathbf{z}'^{[p]}\mathbf{z}^{[p]}$$

and thus the Schlaifflian matrix  $\mathbf{H}^{[p]}$  is orthogonal. Another result that is quite useful in what follows is that, given two vectors  $\mathbf{x}$  and  $\mathbf{z}$ , each having  $k$  elements, then

$$(\mathbf{x}'\mathbf{z})^p = \mathbf{x}'^{[p]}\mathbf{z}^{[p]}$$

For a response function of order  $d$ , the estimated response  $\hat{y}$  can be written in the form

$$\hat{y} = \mathbf{x}'^{[d]}\mathbf{b} \quad (\text{A.1.3})$$

where for a point  $(x_1, x_2, \dots, x_k)$  we have

$$\mathbf{x}' = (1, x_1, x_2, \dots, x_k)$$

and the vector  $\mathbf{b}$  contains the least squares estimators  $b_0, b_1, \dots$ , for the vector  $\mathbf{x}^{[d]}$  with suitable multipliers. For example, for  $k = 2$  and  $d = 2$ ,  $\mathbf{x}' = [1, x_1, x_2]$ , and  $\mathbf{b}'$  and  $\mathbf{x}'^{[2]}$  are given by

$$\begin{aligned} \mathbf{b}' &= \left[ b_0, b_1/\sqrt{2}, b_2/\sqrt{2}, b_{11}, b_{22}, b_{12}/\sqrt{2} \right] \\ \mathbf{x}'^{[2]} &= \left[ 1, \sqrt{2}x_1, \sqrt{2}x_2, x_1^2, x_2^2, \sqrt{2}x_1x_2 \right] \end{aligned}$$

Thus, from Equation A.1.3 we obtain

$$\begin{aligned} \text{Var}[\hat{y}(\mathbf{x})] &= \mathbf{x}'^{[d]}[\text{Var}(\mathbf{b})]\mathbf{x}^{[d]} \\ &= \sigma^2 \mathbf{x}'^{[d]}(\mathbf{X}'\mathbf{X})^{-1}\mathbf{x}^{[d]} \end{aligned} \quad (\text{A.1.4})$$

where  $\sigma^2(\mathbf{X}'\mathbf{X})^{-1}$  is the variance–covariance matrix of the vector  $\mathbf{b}$ .

Consider now a *second* point  $(z_1, z_2, \dots, z_k)$ , which is the same distance from the origin as the point described by  $(x_1, x_2, \dots, x_k)$ . Denote by  $\mathbf{z}'$  the vector  $(1, z_1, z_2, \dots, z_k)$ . There is, then, an orthogonal matrix  $\mathbf{R}$  for which

$$\mathbf{z} = \mathbf{Rx} \quad (\text{A.1.5})$$

where  $\mathbf{R}$  is of the form

$$\mathbf{R} = \begin{bmatrix} 1 & 0 & \dots & 0 & \dots & \dots & 0 \\ 0 & \vdots & & & & & \\ 0 & \vdots & & & & & \\ \vdots & \vdots & & & \mathbf{H}_{k \times k} & & \\ 0 & \vdots & & & & & \end{bmatrix} \quad (\text{A.1.6})$$

and  $\mathbf{H}$  is an orthogonal matrix with the dimensions indicated in Equation A.1.6. The variance of the estimated response at the second point is then

$$\text{Var}[\hat{y}(\mathbf{z})] = \sigma^2 \mathbf{z}'^{[d]}(\mathbf{X}'\mathbf{X})^{-1}\mathbf{z}^{[d]}$$

Let  $\mathbf{R}^{[d]}$  be the Schlaifflian matrix of the transformation in Equation A.1.5:

$$\begin{aligned}\text{Var}[\hat{y}(\mathbf{z})] &= \sigma^2 \mathbf{x}'^{[d]} \mathbf{R}'^{[d]} (\mathbf{X}' \mathbf{X})^{-1} \mathbf{R}^{[d]} \mathbf{x}^{[d]} \\ &= \sigma^2 \mathbf{x}'^{[d]} [\mathbf{R}'^{[d]} (\mathbf{X}' \mathbf{X}) \mathbf{R}^{[d]}]^{-1} \mathbf{x}^{[d]}\end{aligned}\quad (\text{A.1.7})$$

because  $\mathbf{R}^{[d]}$  is orthogonal. For the design to be rotatable,  $\text{Var}(\hat{y})$  is constant on spheres, which implies that for any orthogonal matrix  $\mathbf{H}$  we have

$$\mathbf{X}' \mathbf{X} = \mathbf{R}'^{[d]} (\mathbf{X}' \mathbf{X}) \mathbf{R}^{[d]} \quad (\text{A.1.8})$$

where  $\mathbf{R}$  is of the form indicated in Equation A.1.6. The requirement in Equation A.1.8 essentially means that the moment matrix remains the same if the design is **rotated**—that is, if the rows of the *design* matrix, denoted by  $\mathbf{D}$  in the equation

$$\begin{bmatrix} 1 & \vdots \\ 1 & \vdots \\ \vdots & \vdots \\ \mathbf{D} & \vdots \\ 1 & \vdots \end{bmatrix} = \begin{bmatrix} 1 & x_{11} & x_{21} & \cdots & x_{k1} \\ 1 & x_{12} & x_{22} & \cdots & x_{k2} \\ \vdots & \vdots & \vdots & & \vdots \\ 1 & x_{1N} & x_{2N} & \cdots & x_{kN} \end{bmatrix} = \begin{bmatrix} x'_1 \\ x'_2 \\ \vdots \\ x'_N \end{bmatrix} \quad (\text{A.1.9})$$

are rotated via the transformation

$$\mathbf{z}_i = \mathbf{R}' \mathbf{x}_i$$

It is easily seen that the rotated design will have moment matrix (apart from the constant  $N^{-1}$ ) equal to the right-hand side of Equation A.1.8.

Consider now a vector  $\mathbf{t}' = [1, t_2, t_1, \dots, t_k]$  of dummy variables. The utility of these variables is in the construction of a generating function for the design moments. Consider the quantity

$$\text{MGF} = N^{-1} \mathbf{t}'^{[d]} \mathbf{X}' \mathbf{X} \mathbf{t}^{[d]} \quad (\text{A.1.10})$$

The matrix  $\mathbf{X}' \mathbf{X}$  is alternatively given by

$$\mathbf{X}' \mathbf{X} = \sum_{u=1}^N \mathbf{x}_u^{[d]} \mathbf{x}_u'^{[d]}$$

where the vector  $\mathbf{x}_u' = [1, x_{1u}, x_{2u}, \dots, x_{ku}]$  refers to the  $u$ th row of the design matrix, augmented by 1—that is, the  $u$ th row of the matrix in Equation A.1.9. Thus

$$\begin{aligned}\text{MGF} &= N^{-1} \sum_{u=1}^N \{\mathbf{t}'^{[d]} \mathbf{x}_u^{[d]} \mathbf{x}_u'^{[d]} \mathbf{t}^{[d]}\} \\ &= N^{-1} \sum_{u=1}^N \{\mathbf{t}' \mathbf{x}_u\}^{2d}\end{aligned}\quad (\text{A.1.11})$$

From Equation A.1.11, it is seen that upon expanding  $\mathbf{t}' \mathbf{x}_u$  we have

$$\text{MGF} = N^{-1} \sum_{u=1}^N \{1 + t_1 x_{1u} + t_2 x_{2u} + \cdots + t_k x_{ku}\}^{2d} \quad (\text{A.1.12})$$

When Equation A.1.12 is expanded, the terms involve moments of the design through order  $2d$ . In fact, the coefficient of  $t_1^{\delta_1} t_2^{\delta_2} \cdots t_k^{\delta_k}$  is

$$\frac{(2d)!}{\prod_{i=1}^k (\delta_i)! (2d - \delta)!} [1^{\delta_1} 2^{\delta_2} \cdots k^{\delta_k}] \quad (\text{A.1.13})$$

where  $\sum_{i=1}^k \delta_i = \delta \leq 2d$ . For a rotatable design,

$$\begin{aligned} \text{MGF} &= N^{-1} \mathbf{t}^{[d]} (\mathbf{X}' \mathbf{X}) \mathbf{t}^{[d]} = N^{-1} \mathbf{t}^{[d]} \mathbf{R}'^{[d]} \mathbf{X}' \mathbf{X} \mathbf{R}^{[d]} \mathbf{t}^{[d]} \\ &= N^{-1} (\mathbf{t}' \mathbf{R}'^{[d]} \mathbf{X}' \mathbf{X} \mathbf{R} \mathbf{t})^{[d]} \end{aligned}$$

where  $\mathbf{R}$  is the  $(k+1) \times (k+1)$  orthogonal matrix introduced in Equation A.1.6. This implies that for a rotatable design, an orthogonal transformation on  $\mathbf{t}$  does not affect the MGF. Because the MGF is a polynomial in the  $t$ 's (also involving the design moments), for a rotatable design, the MGF must be a function of  $\sum_{i=1}^k t_i^2$ . That is, it is of the form

$$\text{MGF} = \sum_{j=0}^d a_{2j} \left[ \sum_{i=1}^k t_i^2 \right]^j \quad (\text{A.1.14})$$

It is easily seen that the coefficient of  $t_1^{\delta_1} t_2^{\delta_2} \cdots t_k^{\delta_k}$  in Equation A.1.14 is zero if *any* of the  $\delta_i$  are odd. For the case where all  $\delta_i$  are even, the coefficient from the multinomial expansion of  $\left[ \sum_{i=1}^k t_i^2 \right]^j$  is given by

$$\frac{a_\delta (\delta/2)!}{\prod_{i=1}^k (\delta_i/2)!} \quad (\text{A.1.15})$$

The reader should now consider Equation A.1.15 in conjunction with Equation A.1.13, the former pertaining to the generating function for the moments *in general*, and the latter pertaining to the case of a rotatable design, with the value being zero for moments with any  $\delta_i$  odd. Upon equating the two and solving for the moment, the result is

$$N^{-1} \sum_{u=1}^N x_{1u}^{\delta_1} x_{2u}^{\delta_2} \cdots x_{ku}^{\delta_k} = \frac{\lambda_\delta \prod_{i=1}^k (\delta_i)!}{2^{\delta/2} \prod_{i=1}^k (\delta_i/2)!} \quad (\text{A.1.16})$$

for all  $\delta_i$  even, and

$$N^{-1} \sum_{u=1}^N x_{1u}^{\delta_1} x_{2u}^{\delta_2} \cdots x_{ku}^{\delta_k} = 0 \quad (\text{A.1.17})$$

for any  $\delta_i$  odd. Here,  $\lambda_\delta$  is given by

$$\lambda_\delta = \frac{a_\delta 2^{\delta/2} (\delta/2)! (2d - \delta)!}{(2d)!} \quad (\text{A.1.18})$$

If we consider Equations A.1.16 and A.1.18 for the second-order case, we have  $d = 2$ , and thus  $[i] = [ij] = [ijk] = [iij] = [iii] = 0$  for  $i \neq j \neq k$ ,  $[ii] = \lambda_2$  (fixed by scaling) and  $[iii]/[iij] = 3$ .



---

## APPENDIX 2

---

### ROTATABILITY OF A SECOND-ORDER EQUIRADIAL DESIGN

Consider first the moment of  $x_1$  of order  $\delta$  ( $\delta = 1, 2, 3, 4$ ). After multiplication by  $n_1$ , we obtain

$$\sum_{u=0}^{n_1-1} x_{1u}^\delta = \sum_{u=0}^{n_1-1} \left\{ \rho \cos\left(\theta + \frac{2\pi u}{n_1}\right) \right\}^\delta \quad (\text{A.2.1})$$

Because  $\cos \tau = [e^{i\tau} + e^{-i\tau}]/2$ , Equation A.2.1 can be written

$$\sum_{u=0}^{n_1-1} x_{1u}^\delta = \left(\frac{\rho}{2}\right)^\delta \sum_{u=0}^{n_1-1} [a\omega^u + a^{-1}\omega^{-u}]^\delta$$

where  $\omega = e^{2i\pi/n_2}$  and  $a = e^{i\theta}$ . Using a binomial expansion,

$$\sum_{u=0}^{n_1-1} x_{1u}^\delta = \left(\frac{\rho}{2}\right)^\delta \sum_{t=0}^{\delta} \binom{\delta}{t} a^{\delta-2t} \sum_{u=0}^{n_1-1} \omega^{(\delta-2t)u} \quad (\text{A.2.2})$$

An expression similar to Equation A.2.2 for the moments of  $x_2$  can be established with little difficulty. In considering the portion  $\sum_{u=0}^{n_1-1} \omega^{(\delta-2t)u}$  of Equation A.2.2 for  $t = 0, 1, 2, \dots, \delta$ , it is first noted that

$$-\delta \leq \delta - 2t \leq \delta$$

The interest here is in moments of order  $n_1 - 1$  and less, because  $n_1 \geq 5$ . If  $\delta - 2t = 0$ , then

$$\sum_{u=0}^{n_1-1} \omega^{(\delta-2t)u} = n_1$$

On the other hand, it is not difficult to show that for  $|\delta - 2t| \leq n_1 - 1$  and nonzero, we obtain

$$\sum_{u=0}^{n_1-1} \omega^{(\delta-2t)u} = 0$$

Using Equation A.2.2 for  $\delta = 1$ ,  $\delta - 2t$  takes on values  $-1$  and  $+1$  and thus  $\sum_{u=0}^{n_1-1} x_{1u} = 0$ . Likewise, for the case of  $\delta = 3$ , it is found that  $\sum_{u=0}^{n_1-1} x_{1u}^3 = 0$ . In a similar fashion, it can be shown that the odd moments of  $x_2$  are zero. For  $\delta = 2$ ,  $\delta - 2t$  does that on a zero value when  $t = 1$ . Evaluating Equation A.2.2

$$n_1[11] = \frac{n_1 \binom{2}{1} \rho^2}{4}$$

and thus

$$[11] = \frac{\rho^2}{2}$$

For  $\delta = 4$ , the nonzero contribution in Equation A.2.2 appears when  $t = 2$ . Thus the pure fourth moment is given by

$$\begin{aligned} [1111] &= \frac{\binom{4}{2} \rho^4}{16} \\ &= \frac{3\rho^4}{8} \end{aligned}$$

Similar procedures can be used for the case of  $x_2$  to show that

$$n_1[2^2] = \frac{\rho^2 n_1}{2}, \quad n_1[2^4] = \frac{\rho^4 n_1}{8}$$

At this point, consider moments of the type  $\sum_{u=0}^{n_1-1} x_{1u}^{\delta_1} x_{2u}^{\delta_2}$ , where  $\delta_1 + \delta_2 \leq 4$ . One can write

$$\begin{aligned} \sum_{u=0}^{n_1-1} x_{1u}^{\delta_1} x_{2u}^{\delta_2} &= \sum_{u=0}^{n_1-1} \left\{ \rho \cos\left(\theta + \frac{2\pi u}{n_1}\right) \right\}^{\delta_1} \left\{ \rho \sin\left(\theta + \frac{2\pi u}{n_1}\right) \right\}^{\delta_2} \\ &= \left(\frac{\rho}{2}\right)^{\delta_1 + \delta_2} \left(\frac{1}{i}\right)^{\delta_2 n_1 - 1} \{a\omega^u + a^{-1}\omega^{-u}\}^{\delta_1} \{a\omega^u - a^{-1}\omega^{-u}\}^{\delta_2} \end{aligned} \quad (\text{A.2.3})$$

where  $a$  and  $\omega$  are as before and  $i = \sqrt{-1}$ . For  $\delta_1 = 1$  and  $\delta_2 = 1$ , Equation A.2.3 is easily seen to be zero after making use of the fact that  $\sum_{u=0}^{n_1-1} \omega^{2u}$  and  $\sum_{u=0}^{n_1-1} \omega^{-2u} = 0$ . Likewise,  $n_1[112]$  and  $n_1[122]$  are found to be zero. For  $n_1[1112]$ , Equation A.2.3 becomes

$$\begin{aligned} & \left(\frac{\rho}{2}\right)^4 \left(\frac{1}{i}\right) \sum_{u=0}^{n_1-1} \{a^3 \omega^{3u} + a^{-3} \omega^{-3u} + 3a\omega^u + 3a^{-1}\omega^{-u}\} \{a\omega^u - a^{-1}\omega^{-u}\} \\ &= \left(\frac{\rho}{2}\right)^4 \left(\frac{1}{i}\right) \{-3n_1 + 3n_1\} \\ &= 0 \end{aligned}$$

Similarly  $n_1[1222]$  can be shown to be zero.

It remains now to develop the expression for  $\sum_{u=0}^{n_1-1} x_{1u}^2 x_{2u}^2$ . We can once again use Equation A.2.3 to develop the following:

$$\begin{aligned} \sum_{u=0}^{n_1-1} x_{1u}^2 x_{2u}^2 &= \left(\frac{\rho}{2}\right)^4 (-1) \sum_{u=0}^{n_1-1} \{a^2 \omega^{2u} + 2 + a^{-2}\omega^{-2u}\} \{a^2 \omega^{2u} - 2 + a^{-2}\omega^{-2u}\} \\ &= \frac{\rho^4}{16} (-1) \{n_1 - 4n_1 + n_1\} \\ &= \frac{\rho^4 n_1}{8} \end{aligned}$$

On the basis of [iiii] and [iiji] in the above developments, it is clear that the equiradial design is rotatable.



## REFERENCES

- Aitken, M. (1987), "Modeling Variance Heterogeneity in Normal Regression Using GLIM," *Journal of the Royal Statistical Society, Series C (Applied Statistics)*, 36, 332–339.
- Allen, D. M. (1971), "Mean Square Error of Prediction as a Criterion for Selecting Variables," *Technometrics*, 13, 469–475.
- Allen, D. M. (1974), "The Relationship Between Variable Selection and Data Augmentation and a Method for Prediction," *Technometrics*, 16, 125–127.
- Allen, T. T., Yu, L., and Schmitz, J. (2003), "An Experimental Design Criterion for Minimizing Meta-Model Prediction Errors Applied to a Die Casting Process Design," *Applied Statistics*, 52, 103–117.
- Ames, A. E., Mattucci, D., MacDonald, S., Szongi, G., and Hawkins, D. M. (1997), "Quality Loss Functions for Optimization Across Multiple Response Surfaces," *Journal of Quality Technology*, 29, 339–346.
- Anderson-Cook, C. M., Goldfarb, H., Borror, C. M., Montgomery, D. C., Canter, K. G., and Twist, J. A., (2004), "Mixture and Mixture Process Variables Experiments for Pharmaceutical Applications," *Pharmaceutical Statistics*, 3, 247–260.
- Anderson-Cook, C. M., Borror, C. M., and Jones, B. (2009), "Graphical Tools for Assessing the Sensitivity of Response Surface Designs to Model Misspecification," *Technometrics* (to appear).
- Anderson-Cook, C. M., Borror, C. M., and Montgomery, D. C. (2008), "Response Surface Design Evaluation and Comparison," (with discussion) *Journal of Statistical Planning and Inference* (to appear).
- Andrews, D. F. (1974), "A Robust Method for Multiple Linear Regression," *Technometrics*, 16, 523–531.
- Andrews, D. F., Bickel, P. J., Hampel, F. R., Huber, P. J., Rogers, W. H., and Tukey, J. W. (1972), *Robust Estimates of Location*, Princeton University Press, Princeton, NJ.

- Bartlett, M. S., and Kendall, D. G. (1946), "The Statistical Analysis of Variance Heterogeneity and the Logarithmic Transformation," *Journal of the Royal Statistical Society, Series B*, 8, 128–150.
- Barton, R. R. (1992), "Metamodels for Simulation Input–Output Relations," *Winter Simulation Conference*, 289–299.
- Barton, R. R. (1994), "Metamodels: A State of the Art Review," *Winter Simulation Conference*, 237–244.
- Beaton, A. E., and Tukey, J. W. (1974), "The Fitting of Power Series, Meaning Polynomials, on Band Spectroscopic Data," *Technometrics*, 16, 147–185.
- Belsley, D. A., Kahan, E., and Welsch, R. E. (1980), *Regression Diagnostics: Identifying Influential Data and Sources of Collinearity*, John Wiley & Sons, New York.
- Bettonvil, B., and Kleijnen, J. J. C. (1996), "Searching for Importance Factors in Simulation Models with Many Factors: Sequential Bifurcation," *European Journal of Operational Research*, 96, 180–194.
- Biles, W. E. (1975), "A Response Surface Method for Experimental Optimization of Multiresponse Processes," *Industrial and Engineering Chemistry—Process Design and Development*, 14, 152–158.
- Bisgaard, S. (2000), "The Design and Analysis of  $2^{k-p} \times 2^{q-r}$  Split-Plot Experiments," *Journal of Quality Technology*, 32, 39–56.
- Bisgaard, S., and Ankenman, B. (1996), "Standard Errors for the Eigenvalues in Second-order Response Surface Models", *Technometrics*, 38, 238–246.
- Bishop, C. M. (1995), *Neural Networks for Pattern Recognition*, Clarendon Press, Oxford, UK.
- Borkowski, J. J., and Lucas, J. M. (1997), "Designs of Mixed Resolution for Process Robustness Studies," *Technometrics* 39, 63–70.
- Borror, C. M. (1998), "Response Surface Methods for Experiments Involving Noise Variables," Ph.D. Dissertation, Department of Industrial Engineering, Arizona State University, Tempe, AZ.
- Borror, C. M., and Montgomery, D. C. (2000), "Mixed Resolution Designs as Alternatives to Taguchi Inner/Outer Array Designs for Robust Design Problems," *Quality and Reliability Engineering International*, 16, 117–127.
- Borror, C. M., Montgomery, D. C., and Myers, R. H. (2002), "Evaluation of Statistical Designs for Experiments with Noise Variables," to appear in the *Journal of Quality Technology*.
- Box, G. E. P. (1957), "Evolutionary Operation: A Method for Increasing Industrial Productivity," *Applied Statistics*, 6, 81–101.
- Box, G. E. P. (1963), "The Effect of Errors in the Factor Levels and Experimental Design," *Technometrics*, 6, 247–262.
- Box, G. E. P. (1988), "Signal-to-Noise Ratios, Performance Criteria, and Transformations" (with discussion), *Technometrics*, 30, 1–40.
- Box, G. E. P., and Behnken, D. W. (1960), "Some New Three-Level Designs for the Study of Quantitative Variables," *Technometrics*, 2, 455–475.
- Box, G. E. P., and Cox, D. R. (1964), "An Analysis of Transformations" (with discussion), *Journal of the Royal Statistical Society, Series B*, 26, 211–246.
- Box, G. E. P., and Draper, N. R. (1959), "A Basis for the Selection of a Response Surface Design," *Journal of the American Statistical Association*, 54, 622–654.
- Box, G. E. P., and Draper, N. R. (1963), "The Choice of a Second Order Rotatable Design," *Biometrika*, 50, 335–352.
- Box, G. E. P., and Draper, N. R. (1969), *Evolutionary Operation*, John Wiley & Sons, New York.
- Box, G. E. P., and Draper, N. R. (1971), "Factorial Designs, the  $X'X$  Criterion, and Some Related Matters," *Technometrics*, 13, 731–742.

- Box, G. E. P., and Draper, N. R. (1974), "Some Minimum Point Designs for Second Order Response Surfaces," *Technometrics*, 16, 613–616.
- Box, G. E. P., and Draper, N. R. (1975), "Robust Designs," *Biometrika*, 62, 347–352.
- Box, G. E. P., and Draper, N. R. (1987), *Empirical Model-Building and Response Surfaces*, John Wiley & Sons, New York.
- Box, G. E. P., and Draper, D. R. (2007), *Response Surfaces, Mixtures and Ridge Analyses*, Wiley and Sons, New York.
- Box, G. E. P., and Hunter, J. S. (1954), "A Confidence Region for the Solution of a Set of Simultaneous Equations with an Application to Experimental Design," *Biometrika*, 41, 190–199.
- Box, G. E. P., and Hunter, J. S. (1957), "Multifactor Experimental Designs for Exploring Response Surfaces," *The Annals of Mathematical Statistics*, 28, 195–241.
- Box, G. E. P., and Hunter, J. S. (1961a), "The  $2^{k-p}$  Fractional Factorial Designs, Part I," *Technometrics*, 2, 311–352.
- Box, G. E. P., and Hunter, J. S. (1961b), "The  $2^{k-p}$  Fractional Factorial Designs, Part II," *Technometrics*, 3, 449–458.
- Box, G. E. P., and Jones, S. (1989), "Designing Products that are Robust to the Environment," paper presented at ASA Conference, Washington, DC.
- Box, G. E. P., and Jones, S. (1992), "Split-Plot Designs for Robust Product Experimentation," *Journal of Applied Statistics*, 19, 3–26.
- Box, G. E. P. and Jones, S. (2000), "Split Plots for Robust Product and Process Experimentation," *Quality Engineering*, 13, 127–134.
- Box, G. E. P., and Meyer, R. D. (1986), "Dispersion Effects from Fractional Designs," *Technometrics*, 28, 19–27.
- Box, G. E. P., and Wetz, J. M. (1973), "Criterion for Judging the Adequacy of Estimation by an Approximation Response Polynomial," Technical Report No. 9, Department of Statistics, University of Wisconsin, Madison.
- Box, G. E. P., and Wilson, K. B. (1951), "On the Experimental Attainment of Optimum Conditions," *Journal of the Royal Statistical Society, Series B*, 13, 1–45.
- Byrne, D. M., and Taguchi, G. (1987), "The Taguchi Approach to Parameter Design," *Quality Progress*, December, 1987, 19–26.
- Carlyle, W. M., Montgomery, D. C., and Runger, G. C. (2000), "Optimization Problems and Methods in Quality Control and Improvement," (with discussion), *Journal of Quality Technology*, 31, 1–17.
- Carpenter, W. C., and Barthelemy, J. (1993), "A Comparison of Polynomial Approximations and Artificial Neural Nets as Response Surfaces," *Structural Optimization*, 5, 166–174.
- Carroll, R. J., and Ruppert, D. (1988), *Transformation and Weighting in Regression*, Chapman and Hall, New York.
- Carter, W. H., Jr., Chinchilli, V. M., and Campbell, E. D. (1990), "A Large-Sample Confidence Region Useful in Characterizing the Stationary Point of a Quadratic Response Surface," *Technometrics*, 32, 425–435.
- Cheng, B., and Titterington, D. M. (1994), "Neural Networks: A Review from a Statistical Perspective," *Statistical Science*, 9, 2–54.
- Chung, P. J., Goldfarb, H. B., and Montgomery, D. C. (2007), "Optimal Designs for Mixture-Process Experiments with Control and Noise Variables," *Journal of Quality Technology*, 39, 179–190.
- Condra, L. W. (1993), *Reliability Improvement with Design of Experiments*, Marcel Dekker, New York.
- Cook, R. D. (1977), "Detection of Influential Observation in Linear Regression," *Technometrics*, 19, 15–17.

- Cook, R. D. (1979), "Influential Observations in Linear Regression," *Journal of the American Statistical Association*, 74, 169–174.
- Cornell, J. A. (1986), "A Comparison Between Two Ten-Point Designs for Studying Three-Component Mixture Systems," *Journal of Quality Technology*, 18, 1–15.
- Cornell, J. A. (2002), *Experiments with Mixtures, Designs, Models, and the Analysis of Mixture Data*, 3rd edition, John Wiley & Sons, New York.
- Cornell, J. A. (1995), "Fitting Models to Data from Mixture Experiments Containing Other Factors," *Journal of Quality Technology*, 27, 1, 13–33.
- Cornell, J. A. (2000), "Fitting a Slack-Variable Model to Mixture Data: Some Questions Raised," *Journal of Quality Technology*, 31, 133–147.
- Covey-Crump, P. A. K., and Silvey, S. D. (1970), "Optimal Regression Designs with Previous Observations," *Biometrika*, 57, 551–566.
- Cox, D. R. (1958), *Planning of Experiments*, John Wiley & Sons, New York.
- Cox, D. R. (1971), "A Note on Polynomial Response Functions for Mixtures," *Biometrika*, 58, 155–159.
- Crosier, R. B. (1984), "Mixture Experiments: Geometry and Pseudo-components," *Technometrics*, 26, 209–216.
- Daniel, C. (1959), "Use of Half-Normal Plots in Interpreting Factorial Two-Level Experiments," *Technometrics*, 1, 311–342.
- Daniel, C. (1976), *Applications of Statistics to Industrial Experimentation*, John Wiley & Sons, Inc., New York.
- Del Castillo, E. (1996), "Multiresponse Process Optimization via Constrained Confidence Regions," *Journal of Quality Technology*, 28, 61–70.
- Del Castillo, E., Fan, S.-K. S., and Semple, J. (1997), "Computation of Global Optima in Dual Response Systems," *Journal of Quality Technology*, 29, 347–353.
- Del Castillo, E., and Montgomery, D. C. (1993), "A Nonlinear Programming Solution to the Dual Response Problem," *Journal of Quality Technology*, 25, 3.
- Del Castillo, E., Montgomery, D. C., and McCarville, D. R. (1996), "Modified Desirability Functions for Multiple Response Optimization," *Journal of Quality Technology*, 28, 347–356.
- Derringer, G., and Suich, R. (1980), "Simultaneous Optimization of Several Response Variables," *Journal of Quality Technology*, 12, 214–219.
- Donohue, J. M. (1994), "Experimental Designs for Simulation," *Winter Simulation Conference*, 200–206.
- Drain, D., Carlyle, W. M., Montgomery, D. C., Borror, C. M., and Anderson-Cook, C. M. (2004), "A Genetic Algorithm Hybrid for Constructing Optimal Response Surface Designs," *Quality and Reliability Engineering International*, 20, 637–650.
- Draper, N. R. (1963), "Ridge Analysis of Response Surfaces," *Technometrics*, 5, 469–479.
- Draper, N. R. (1982), "Center Points in Second-Order Response Surface Designs," *Technometrics*, 24, 127–133.
- Draper, N. R. (1985), "Small Composite Designs," *Technometrics*, 27, 173–180.
- Draper, N. R., and John, J. A. (1988), "Response Surface Designs for Quantitative and Qualitative Variables," *Technometrics*, 423–428.
- Draper, N. R., and Lin, D. K. J. (1990), "Small Response Surface Designs," *Technometrics*, 32, 187–194.
- Draper, N., and Sanders, E. (1988), "Designs for Minimizing Bias Estimation," *Technometrics*, 30, 319–324.

- Draper, N. R., and St. John, R. C. (1977), "Designs in Three and Four Components for Mixture Models with Inverse Terms," *Technometrics*, 19, 117–130.
- Dutter, R. (1977), "Numerical Solution of Robust Regression Problems, Computational Aspects, a Comparison," *Journal of Statistical Computation and Simulation*, 5, 207–238.
- Dykstra, O., Jr. (1966), "The Orthogonalization of Undesigned Experiments," *Technometrics*, 8, 279–290.
- Ellerton, R. R. W. (1978), "Is the Regression Equation Adequate—A Generalization," *Technometrics*, 20, 313–316.
- Engle, J. (1992), "Modeling Variation in Industrial Experiments," *Journal of the Royal Statistical Society Series C (Applied Statistics)*, 41, 579–593.
- Engle, J., and Huele, A. F. (1996), "A Generalized Linear Modeling Approach to Robust Design," *Technometrics*, 38, 365–373.
- Fan, S.-K. S. (2000), "A Generalized Global Optimization Algorithm for Dual Response Systems," *Journal of Quality Technology*, 32, 444–456.
- Fang, K. T. (1980), "The Uniform Design: Application of Number—Theoretic Methods in Experimental Design," *Acta Mathematicae Applicatae Sinica*, 3, 363–372.
- Fang, K. T., Li, R., and Sudjianto, A. (2006), *Design and Modeling for Computer Experiments*, Taylor & Francis Group, Boca Raton, FL.
- Giovannitti-Jensen, A., and Myers, R. H. (1989), "Graphical Assessment of the Prediction Capability of Response Surface Designs," *Technometrics*, 31, 159–171.
- Goldfarb, H. B., Borror, C. M., and Montgomery, D. C. (2003), "Mixture-Process Variable Experiments with Noise Variables," *Journal of Quality Technology*, 35, 393–405.
- Goldfarb, H. B., Anderson-Cook, C. M., Borror, C. M., and Montgomery, D. C. (2004a), "Fraction of Design Space to Assess the Prediction Capability of Mixture and Mixture-Process Designs," *Journal of Quality Technology*, 36, 169–179.
- Goldfarb, H. B., Borror, C. M., Montgomery, D. C., and Anderson-Cook, C. M. (2004b), "Three-Dimensional Variance Dispersion Graphs for Mixture-Process Experiments," *Journal of Quality Technology*, 36, 109–124.
- Goldfarb, H. B., Borror, C. M., Montgomery, D. C., and Anderson-Cook, C. M. (2004c), "Evaluation of Statistical Designs for Mixture-Process Variable Experiments with Noise Variables," *Journal of Quality Technology*, 36, 245–262.
- Goldfarb, H. B., Borror, C. M., Montgomery, D. C., and Anderson-Cook, C. M. (2005), "Using Genetic Algorithms to Generate Mixture-Process Experimental Designs Involving Control and Noise Variables," *Journal of Quality Technology*, 37, 60–74.
- Goos, P. (2002), *The Optimal Design of Blocked and Split-Plot Experiments*, Springer, New York.
- Goos, P., and Donev, A. N. (2007), "Tailor-Made Split-Plot Designs for Mixture and Process Variables," *Journal of Quality Technology*, 39, 326–339.
- Goos, P., and Vanderbroek, M. (2004), "Outperforming Completely Randomized Designs," *Journal of Quality Technology*, 36, 12–26.
- Graybill, F. (1976), *Introduction to the Theory of Linear Statistical Models*, Duxbury Press, Boston.
- Grego, J. M. (1993), "Generalized Linear Models and Process Variation," *Journal of Quality Technology*, 25, 288–295.
- Gunst, R. F., and Mason, R. L. (1979), "Some Considerations in the Evaluation of Alternative Prediction Equations," *Technometrics*, 21, 55–63.
- Hackney, H., and Jones, P. R. (1969), "Response Surface for Dry Modulus of Rupture and Drying Shrinkage," *American Ceramic Society Bulletin*, 46.
- Hamada, M., and Nelder, J. A. (1997), "Generalized Linear Models for Quality-Improvement Experiments," *Journal of Quality Technology*, 29, 292–304.

- Han, S. S., Ceiler, M., Bidstrup, S. A., Kohl, P., and May, G. S. (1994), "Modeling the Properties of PECVD Silicon Dioxide Films Using Optimized Back-propagation Neural Networks," *IEEE Transactions on Components, Packaging, and Manufacturing Technology—Part A*, 17, 174–182.
- Hartley, H. O. (1959), "Smallest Composite Design for Quadratic Response Surfaces," *Biometrics*, 15, 611–624.
- Harvey, A. C. (1976), "Estimation of Regression Models with Multiplicative Heteroscedasticity," *Econometrica*, 44, 461–475.
- Haykin, S. (1994), *Neural Networks: A Comprehensive Foundation*, Macmillan, New York.
- Hebble, T. L., and Mitchell, T. J. (1972), "Repairing Response Surface Designs," *Technometrics*, 14, 767–779.
- Heinssmann, J. A., and Montgomery, D. C. (1995), "Optimization of a Household Product Formulation Using a Mixture Experiment," *Quality Engineering*, 7, 583–600.
- Heredia-Langner, A., Carlyle, W. M., Montgomery, D. C., Borror, C. M., and Runger, G. C. (2003), "Genetic algorithms for the construction of D-optimal designs," *Journal of Quality Technology*, 35, 28–46.
- Heredia-Langner, A., Carlyle, W. M., Montgomery, D. C., and Borror, C. M. (2004), "Model-Robust Optimal Designs: A Genetic Algorithm Approach," *Journal of Quality Technology*, 36, 263–279.
- Hill, R. C., Judge, G. G., and Fomby, T. B. (1978), "Testing the Adequacy of a Regression Model," *Technometrics*, 20, 491–494.
- Hill, R. W. (1979), "On Estimating the Covariance Matrix of Robust Regression  $M$ -Estimates," *Communications in Statistics, Series A*, 8, 1183–1196.
- Hill, W. J., and Hunter, W. G. (1996), "A Review of Response Surface Methodology: A Literature Review," *Technometrics*, 8, 571–590.
- Himmel, C. D., and May, G. S. (1991), "Advantages of Plasma Etch Modeling Using Neural Networks over Statistical Techniques," *IEEE Transactions on Semiconductor Manufacturing*, 6, 103–111.
- Himmelblau, D. M. (1971), *Process Analysis by Statistical Methods*, John Wiley & Sons, New York.
- Hocking, R. R. (1978), "The Regression Dilemma: Variable Estimation, Coefficient Shrinkage, or Robust Estimation," paper presented at the ASQC Fall Technical Conference, Rochester, NY.
- Hoerl, A. E. (1959), "Optimum Solution of Many Variables Equations," *Chemical Engineering Progress*, 55, 67–78.
- Hoerl, A. E. (1964), "Ridge Analysis," *Chemical Engineering Symposium Series*, 60, 67–77.
- Hoerl, R. W. (1985), "Ridge Analysis 25 Years Later," *The American Statistician*, 39, 186–193.
- Hogg, R. V. (1979), "An Introduction to Robust Estimation," in *Robustness in Statistics*, edited by R. L. Launer and G. N. Wilkinson, Academic Press, New York.
- Hoke, A. T. (1974), "Economical Second-Order Designs Based on Irregular Fractions of the 3<sup>n</sup> Factorial," *Technometrics*, 17, 375–384.
- Huber, P. J. (1964), "Robust Estimation of a Location Parameter," *Annals of Mathematical Statistics*, 35, 73–101.
- Huber, P. J. (1973), "Robust Regression: Asymptotics, Conjectures, and Monte Carlo," *Annals of Statistics*, 1, 799–821.
- Hussain, A. S., Yu, X. Q., and Johnson, R. D. (1991), "Application of Neural Computing in Pharmaceutical Product Development," *Pharmaceutical Research*, 8, 1248–1252.
- Johnson, M. E., Moore, L. M., and Ylvisaker, D. (1990), "Minimax and Maxmin Distance Design," *Journal of Statistical Planning and Inference*, 26, 131–148.

- Karson, M. J., Manson, H. R., and Hader, R. J. (1969), "Minimum Bias Estimation and Experimental Design for Response Surfaces," *Technometrics*, 11, 461–475.
- Khattree, R. (1996), "Robust Parameter Design: A Response Surface Approach," *Journal of Quality Technology*, 28, 187–198.
- Khuri, A. I., and Conlon, M. (1981), "Simultaneous Optimization of Multiple Responses Represented by Polynomial Regression Functions," *Technometrics*, 23, 363–375.
- Khuri, A. I., and Cornell, J. A. (1996), *Response Surfaces*, 2nd edition, Marcel Dekker, New York.
- Khuri, A. I., Harrison, J. M., and Cornell, J. A. (1999), "Using Quantile Plots of the Prediction Variance for Comparing Designs for a Constrained Mixture Region: An Application Involving a Fertilizer Experiment," *Journal of the Royal Statistical Society Series C (Applied Statistics)*, 48, 1–12.
- Khuri, A. I., Kim, H. J., and Um, Y. (1996), "Quantile Plots of the Prediction Variance for Response Surface Designs," *Computational Statistics and Data Analysis*, 22, 395–407.
- Kiefer, J. (1959), "Optimum Experimental Designs," *Journal of the Royal Statistical Society, Series B*, 21, 272–304.
- Kiefer, J. (1961), "Optimum Designs in Regression Problems. II," *Annals of Mathematical Statistics*, 32, 298–325.
- Kiefer, J., and Wolfowitz, J. (1959), "Optimum Designs in Regression Problems," *Annals of Mathematical Statistics*, 30, 271–294.
- Koons, G. F., and Wilt, M. H. (1985), "Design and Analysis of an ABS Pipe Compound Experiment," *Experiments in Industry: Design, Analysis, and Interpretation of Results*, edited by R. D. Snee, L. B. Hare, and R. Trout, American Society in Quality Control, Milwaukee, 111–117.
- Koshal, R. S. (1933), "Application of the Method of Maximum Likelihood to the Improvement of Curves Fitted by the Method of Moments," *Journal of the Royal Statistical Society, Series A*, 96, 303–313.
- Kowalski, S. M., Borror, C. M., and Montgomery, D. C. (2005), "A Modified Path of Steepest Ascent for Split-Plot Experiments," *Journal of Quality Technology*, 37, 75–83.
- Kowalski, S. M., Cornell, J. A., and Vining, G. G. (2002), "Split-Plot Designs and Estimation Methods for Mixture Experiments with Process Variables," *Technometrics*, 44, 72–79.
- Kunugi, T., Tamura, T., and Naito, T. (1961), "New Acetylene Process Uses Hydrogen Dilution," *Chemical Engineering Progress*, 57, 43–49.
- Lee, Y., and Nelder, J. A. (1998), "Letter to the Editor: Joint Modeling of Mean and Dispersion," *Technometrics*, 40, 168–175.
- Lentner, M., and Bishop, T. (1993), *Experimental Design and Analysis*, Valley Book Company, Blacksburg, VA.
- Letsinger, J. D., Myers, R. H., and Lentner, M. (1996), "Response Surface Methods for Bi-randomization Structures," *Journal of Quality Technology*, 26, 381–397.
- Lewis, S. L. (1998), "Analysis of Designed Experiments Using Generalized Linear Models," Ph.D. Dissertation, Department of Industrial Engineering, Arizona State University (1998).
- Lewis, S. L., Montgomery, D. C., and Myers, R. H. (2001a), "Examples of Designed Experiments with Nonnormal Responses," *Journal of Quality Technology*, 33, 265–278.
- Lewis, S. L., Montgomery, D. C., and Myers, R. H. (2001b), "Confidence Interval Coverage and Precision for Designed Experiments Analyzed with Generalized Linear Models," *Journal of Quality Technology*, 33, 279–292.
- Li, J., Liang, L., Borror, C. M., Anderson-Cook, C. M., and Montgomery, D. C. (2008), "Comparing Prediction Variance Performance for Variations of the Central Composite Design Using Graphical Summaries," *Quality Technology and Quantitative Management* (to appear).

- Liang, L., Anderson-Cook, C. M., and Robinson, T. J. (2006a), "Fraction of Design Space Plots for Split-Plot Designs," *Quality and Reliability Engineering International*, 22, 275–289.
- Liang, L., Anderson-Cook, C. M., Robinson, T. J., and Myers, R. H. (2006b), "Three-Dimensional Variance Dispersion Graphs For Split-Plot Designs," *Journal of Computational and Graphical Statistics*, 15, 757–778.
- Liang, L., Anderson-Cook, C. M., and Robinson, T. J. (2007), "Cost Penalized Estimation and Prediction Evaluation for Split-Plot Designs," *Quality and Reliability Engineering International*, 23, 577–596.
- Liang, K. Y., and Zeger, S. L. (1986), "Longitudinal Data Analysis Using Generalized Linear Models," *Biometrika*, 73, 13–23.
- Lin, D. K. J., and Tu, W. (1995), "Dual Response Surface Optimization," *Journal of Quality Technology*, 27, 248–260.
- Lind, E. E., Goldin, J., and Hickman, J. B. (1960), "Fitting Yield and Cost Response Surfaces," *Chemical Engineering Progress*, 56, 62.
- Littell, R. C., Milliken, G. A., Stroup, W. W., and Wolfinger, R. D. (1996), *SAS System for Mixed Models*, SAS Institute, Inc., Cary, NC.
- Lucas, J. M. (1974), "Optimum Composite Designs," *Technometrics*, 16, 561–567.
- Lucas, J. M. (1976), "Which Response Surface Design Is Best," *Technometrics*, 18, 411–417.
- Lucas, J. M. (1989), "Achieving a Robust Process Using Response Surface Methodology," *American Statistical Association Proceedings Sesquicentennial Invited Paper Sessions 1988 and 1989*, 579–593.
- Lucas, J. M. (1994), "How to Achieve a Robust Process Using Response Surface Methodology," *Journal of Quality Technology*, 26, 248–260.
- Lucas, J. M., and Ju, H. L. (1992), "Split Plotting and Randomization in Industrial Experiments," *ASQC Quality Transactions*, Nashville, TN.
- Marquardt, D. M., and Snee, R. D. (1975), "Ridge Regression in Practice," *The American Statistician*, 29, 3–20.
- Martin, B., Parker, D., and Zenick, L. (1987), "Minimize Slugging by Optimizing Controllable Factors on Topaz Windshield Molding," *Fifth Symposium on Taguchi Methods*, American Supplier Institute, Inc., Dearborn, MI, 519–526.
- McCullagh, P., and Nelder, J. A (1989), *Generalized Linear Models*, 2nd edition, Chapman and Hall, New York.
- McKay, M. D., Beckman, R. J., and Conover, W. J. (1979), "A Comparison of Three Methods for Selecting Values of Input Variables in the Analysis of Output from a Computer Code," *Technometrics*, 21, 239–245.
- McKay, N. D., Conover, W. J., and Beckman, R. J. (1979), "A Comparison of Three Methods for Selecting Values of Input Variables in the Analysis of Output from a Computer Code," *Technometrics*, 21, 239–245.
- McLean, R. A., and Anderson, V. L. (1966), "Extreme Vertices Design of Mixture Experiments," *Technometrics*, 8, 447–454.
- Mead, R., and Pike, D. J. (1975), "A Review of Response Surface Methodology from a Biometric Viewpoint," *Biometrics*, 31, 803–851.
- Meyers, R. K., and Nachtsheim, C. J. (1988), "Constructing Exact D-Optimal Experimental Designs by Simulated Annealing," *American Journal of Mathematical and Management Sciences*, 8, 329–359.
- Mitchell, T. J., and Bayne, C. K. (1978), "D-optimal Fractions of Three-Level Factorial Designs," *Technometrics*, 20, 369–380.

- Mitchell, T. J., and Morris, M. D. (1992), "The Spatial Correlation Approach to Response Surface Estimation," *Winter Simulation Conference*, 565–571.
- Montgomery, D. C. (1991), "Using Fractional Factorial Designs for Robust Process Development," *Quality Engineering*, 3, 193–205.
- Montgomery, D. C. (1999), "Experimental Design for Product and Process Design and Development" (with comment), *Journal of the Royal Statistical Society Series D (The Statistician)*, 38, 159–177.
- Montgomery, D. C. (2005), *Design and Analysis of Experiments*, 6th edition, John Wiley & Sons, New York.
- Montgomery, D. C., Peck, E. A., and Vining, G. G. (2006), *Introduction to Linear Regression Analysis*, 4th edition, John Wiley & Sons, New York.
- Montgomery, D. C., and Runger, G. C. (1996), "Foldovers of  $2^{k-p}$  Resolution IV Designs," *Journal of Quality Technology*, 28, 446–450.
- Montgomery, D. C., and Voth, S. R. (1994), "Multicollinearity and Leverage in Mixture Experiments," *Journal of Quality Technology*, 26, 96–108.
- Montgomery, D. C., and Weatherby, G. (1979), "Factor Screening Methods in Computer Simulation," *Winter Simulation Conference*, 347–358.
- Morris, M. D. (2000), "A Class of Three-Level Experimental Designs for Response Surface Modeling," *Technometrics*, 42, 111–121.
- Myers, R. H. (1976), *Response Surface Methodology*, published by author, Blacksburg, VA.
- Myers, R. H. (1990), *Classical and Modern Regression with Applications*, 2nd edition, Duxbury Press, Boston.
- Myers, R. H. (1999), "Response Surface Methodology: Current Status and Future Directions" (with discussion), *Journal of Quality Technology*, 31, 30–44.
- Myers, R. H., and Carter, W. H., Jr. (1973), "Response Surface Techniques for Dual Response Systems," *Technometrics*, 15, 301–317.
- Myers, R. H., Khuri, A. I., and Carter, W. H. (1989), "Response Surface Methodology: 1966–1988," *Technometrics*, 31, 137–157.
- Myers, R. H., Khuri, A. I., and Vining, G. (1992), "Response Surface Alternatives to the Taguchi Robust Parameter Design Approach," *The American Statistician*, 46, 2, 131–139.
- Myers, R. H., Kim, Y., and Griffiths, K. (1997), "Response Surface Methods and Use of Noise Variables," *Journal of Quality Technology*, 29, 429–441.
- Myers, R. H., and Milton, S. (1991), *A First Course in the Theory of Linear Statistical Models*, Duxbury Press, Boston.
- Myers, R. H., and Montgomery, D. C. (1997), "A Tutorial on Generalized Linear Models," *Journal of Quality Technology*, 29, 274–291.
- Myers, R. H., Montgomery, D. C., and Vining, G. G. (2002), *Generalized Linear Models with Applications in Engineering and the Sciences*, John Wiley & Sons, New York.
- Myers, R. H., Montgomery, D. C., Vining, G. G., Borror, C. M., and Kowalski, S. M. (2004), "Response Surface Methodology: A Retrospective and Literature Survey," *Journal of Quality Technology*, 36, 53–77.
- Myers, R. H., Vining, G., Giovannitti-Jensen, A., and Myers, S. L. (1992b), "Variance Dispersion Properties of Second-Order Response Surface Designs," *Journal of Quality Technology*, 24, 1–11.
- Nair, V. N., editor (1992), "Taguchi's Parameter Design: A Panel Discussion," *Technometrics*, 34, 2, 127–161.
- Nair, V. N., and Pregibon, D. (1986), "A Data Analysis Strategy for Quality Engineering Experiments," *AT&T Technical Journal*, 74–84.
- Nalimov, V. V., Golikova, T. I., and Mikeshina, N. G. (1970), "On Practical Use of the Concept of  $D$ -Optimality," *Technometrics*, 12, 799–812.

- Nelder, J. A., and Lee, Y. (1991), "Generalized Linear Models for the Analysis of Taguchi-Type Experiments," *Applied Stochastic Models and Data Analysis*, 7, 107–120.
- Nigam, A. K., Gupta, S. C., and Gupta, S. (1983), "A New Algorithm for Extreme Vertices Designs for Linear Mixture Models," *Technometrics*, 25, 367–371.
- Notz, W. (1982), "Minimal Point Second Order Designs," *Journal of Statistical Planning and Inference*, 6, 47–58.
- Oehlert, G., and Whitcomb, P. (2002), "Small, Efficient Equireplicated Resolution V Fractions of  $2^k$  Designs and Their Application to Central Composite Designs," Paper presented at the 46<sup>th</sup> Annual Fall Technical Conference of the ASQ and ASA, Valley Forge, PA. Also available at <http://www.statease.com/>.
- Ozol-Godfrey, A., and Anderson-Cook C. M. (2007), "Fraction of Design Space Plots for Examining Mixture Design Robustness to Measurement Errors," *Journal of Statistics and Applications*, 1, 171–183.
- Ozol-Godfrey, A., Anderson-Cook, C. M., and Montgomery, D. C. (2005), "Fraction of Design Space Plots for Examining Model Robustness," *Journal of Quality Technology*, 37, 223–235.
- Ozol-Godfrey, A., Anderson-Cook, C. M., Robinson, T. J. (2008), "Fraction of Design Space Plots for Generalized Linear Models," *Journal of Statistical Planning and Inference*, 138, 203–219.
- Park, Y.-J., Richardson, D. E., Ozol-Godfrey, A., Anderson-Cook, C. M., and Montgomery, D. C. (2005), "Prediction Variance Properties of Second-Order Response Surface Designs for Cuboidal Regions," *Journal of Quality Technology*, 37, 253–266.
- Parker, P. A., Anderson-Cook, C. M., and Robinson, T. J. (2008), "Robust Split-Plot Designs," *Quality and Reliability Engineering International*, 24, 107–121.
- Parker, P. A., Kowalski, S. M., and Vining, G. G. (2006), "Classes of Split-Plot Response Surface Designs for Equivalent Estimation," *Quality and Reliability Engineering International*, 22, 291–305.
- Parker, P. A., Kowalski, S. M., and Vining, G. G. (2007), "Construction of Balanced Equivalent Estimation Second-Order Split-Plot Designs," *Technometrics*, 49, 56–65.
- Piepel, G. F. (1982), "Measuring Component Effects in Constrained Mixture Experiments," *Technometrics*, 25, 97–101.
- Piepel, G. F. (1988), "Programs for Generating Extreme Vertices and Centroids of Linearly Constrained Experimental Regions," *Journal of Quality Technology*, 20, 125–139.
- Piepel, G. F., and Cornell, J. A. (1994), "Mixture Experiment Approaches: Examples, Discussion, and Recommendations," *Journal of Quality Technology*, 26, 177–196.
- Pignatiello, Jr., J. J. (1993), "Strategies for Robust Multiresponse Quality Engineering," *IIE Transactions*, 25, 5–15.
- Pignatiello, J., and Ramberg, J. (1991), "Top Ten Triumphs and Tragedies of Genichi Taguchi," *Quality Engineering*, 4(2), 211–225.
- Plackett, R. L., and Burman, J. P. (1946), "The Design of Optimum Multifactorial Experiments," *Biometrika*, 33, 305–325.
- Pledger, M. (1996), "Observable Uncontrollable Factors in Parameter Design," *Journal of Quality Technology*, 28, 153–162.
- Pukelsheim, F. (1995), *Optimum Design of Experiments*, Chapman & Hall, New York.
- Ramsay, J. O. (1977), "A Comparative Study of Several Robust Estimates of Slope, Intercept, and Scale in Linear Regression," *Journal of the American Statistical Association*, 72, 608–615.
- Ripley, B. D. (1994a), "Statistical Ideas for Selecting Network Architecture," in *Neural Networks: Artificial Intelligence and Industrial Applications*, edited by B. Kappen and S. Gielen, Springer-Verlag, New York, 183–190.

- Ripley, B. D. (1994b), "Neural Networks and Related Methods for Classification," *Journal of the Royal Statistical Society Series B (Theory and Methods)*, 56, 409–456.
- Roquemore, K. G. (1976), "Hybrid Designs for Quadratic Response Surfaces," *Technometrics*, 18, 419–423.
- Rousseeuw, P. J., and Leroy, A. M. (1987), *Robust Regression and Outlier Detection*, John Wiley & Sons, New York.
- Rozum, M. A. (1990), "Effective Design Augmentation for Prediction," Thesis, Virginia Tech.
- Rozum, M., and Myers, R. H. (1991), "Variance Dispersion Graphs for Cuboidal Regions," paper presented at ASA Meetings, Atlanta, GA.
- Sacks, J., Schiller, S. B., and Welch, W. J. (1989), "Designs for Computer Experiments," *Statistical Science*, 4, 409–435.
- Sacks, J., and Welch, W. J. (1989), "Design and Analysis of Computer Experiments," *Statistical Science*, 4, 409–435.
- Sacks, J., Welch, W. J., Mitchell, T. J., and Wynn, H. P. (1989), "Design and Analysis of Computer Experiments," *Statistical Science*, 4, 409–423.
- Santner, T. J., Williams, B. J., and Notz, W. I. (2003), *The Design and Analysis of Computer Experiments*, Springer Series in Statistics, Springer-Verlag, New York.
- Scheffé, H. (1958), "Experiments with Mixtures," *Journal of the Royal Statistical Society, Series B*, 20, 344–366.
- Scheffé, H. (1959), "Reply to Mr. Quenoville's Comments About my Paper on Mixtures," *Journal of the Royal Statistical Society, Series B*, 23, 171–172.
- Scheffé, H. (1965), "The Simplex-Centroid Design for Experiments with Mixtures," *Journal of the Royal Statistical Society, B*, 25, 235–263.
- Schmidt, S. R., and Launsby, R. G. (1990), *Understanding Industrial Designed Experiments*, CQG Limited, Colorado Springs, CO.
- Searle, S. R., Casella, G., and McCulloch, C. E. (1992), *Variance Components*, Wiley and Sons, New York.
- Shewry, M. C., and Wynn, H. P. (1987), "Maximum Entropy Sampling," *Journal of Applied Statistics*, 14, 165–170.
- Shoemaker, A. C., Tsui, K. L., and Wu, C. F. J. (1991), "Economical Experimentation Methods for Robust Design," *Technometrics*, 33, 415–427.
- Simpson, T., and Peplinski, J. (1997), "On the Use of Statistics in Design and the Implications for Deterministic Computer Experiments," *ASME Design Engineering Technical Conference*, 1–12.
- Slaagame, R. R., and Barton, R. R. (1997), "Factorial Hypercube Designs for Spatial Correlation Regression," *Journal of Applied Statistics*, 24, 483–501.
- Snee, R. D. (1985), "Computer-Aided Design of Experiments: Some Practical Experiences," *Journal of Quality Technology*, 17, 222–236.
- Snee, R. D., and Marquardt, D. W. (1974), "Extreme Vertices Designs for Linear Mixture Models," *Technometrics*, 16, 399–408.
- Spendley, W., Hext, G. R., and Himsworth, F. R. (1962), "Sequential Application of Simplex Designs in Optimization and EVOP," *Technometrics*, 4, 441–461.
- St. John, R. C. (1984), "Experiments with Mixtures: Ill-Conditioning and Ridge Regression," *Journal of Quality Technology*, 16, 81–96.
- St. John, R. C., and Draper, N. R. (1975), "D-Optimality for Regression Designs: A Review," *Technometrics*, 17, 15–23.
- Steiner, S. H., and Hamada, M. (1997), "Making Mixtures Robust to Noise and Mixing Measurement Errors," *Journal of Quality Technology*, 29, 441–450.

- Suich, R., and Derringer, G. C. (1977), "Is the Regression Equation Adequate—One Criterion," *Technometrics*, 19, 213–216.
- Taguchi, G. (1986), *Introduction to Quality Engineering*, Asian Productivity Organization, UNIPUB, White Plains, NY.
- Taguchi, G. (1987), *System of Experimental Design: Engineering Methods to Optimize Quality and Minimize Cost*, UNIPUB/Kraus International, White Plains, NY.
- Taguchi, G., and Wu, Y. (1980), *Introduction to Off-Line Quality Control*, Central Japan Quality Control Association, Nagoya, Japan.
- Trinca, L. A., and Gilmour, S. G. (1998), "Variance Dispersion Graphs for Comparing Blocked Response Surface Designs," *Journal of Quality Technology*, 30, 314–327.
- Vining, G. (1993), "A Computer Program for Generating Variance Dispersion Graphs," *Journal of Quality Technology*, 25, 45–58.
- Vining, G. G. (1998), "A Compromise Approach to Multiresponse Optimization," *Journal of Quality Technology*, 30, 309–313.
- Vining, G. G., and Bohn, L. (1998), "Response Surfaces for the Mean and the Process Variance Using a Nonparametric Approach," *Journal of Quality Technology*, 30, 282–291.
- Vining, G. G., Cornell, J. A., and Myers, R. H. (1993), "A Graphical Approach for Evaluating Mixture Designs," *Journal of the Royal Statistical Society Series C (Applied Statistics)*, 42, 127–138.
- Vining, G. G., Kowalski, S. M., and Montgomery, D. C. (2005), "Response Surface Designs Within a Split-Plot Structure," *Journal of Quality Technology*, 37, 115–129.
- Vining, G. G., and Myers, R. H. (1990), "Combining Taguchi and Response Surface Philosophies: A Dual Response Approach," *Journal of Quality Technology*, 22, 38–45.
- Vining, G. G., and Schaub, D. (1996), "Experimental Designs for Estimating Both Mean and Variance Functions," *Journal of Quality Technology*, 28, 135–147.
- Welch, W. J. (1982), "Branch-and-Bound Search for Experimental Designs Based on D Optimality and Other Criteria," *Technometrics*, 24, 41–48.
- Welch, W. J., Yu, T. K., Kang, S. M., and Sacks, J. (1990), "Computer Experiments for Quality Control by Parameter Design," *Journal of Quality Technology*, 22, 15–22.
- Welch, W. J., Buck, R. J., Sacks, J., Wynn, H. P., Mitchell, T. J., and Morris, M. D. (1992), "Screening, Predicting, and Computer Experiments," *Technometrics*, 34, 15–25.
- Welsch, R. E. (1975), "Confidence Regions for Robust Regression," *Proceedings of the Statistical Computing Section*, American Statistical Association, Washington, DC.
- Wolfinger, R., Tobias, R., and Sall, J. (1994), "Computing Gaussian Likelihood and their Derivatives for General Linear Mixed Models," *Siam Journal on Scientific Computation*, 15, 1294–1310.
- Yates, F. (1935), "Complex Experiments," *Journal of the Royal Statistical Society, Supplement 2*, 181–247.
- Yates, F. (1937), "Design and Analysis of Factorial Experiments," Technical Communication No. 35, Imperial Bureau of Soil Sciences, London.
- Zahran, A., Anderson-Cook, C. M., and Myers, R. H. (2003), "Fraction of Design Space to Assess the Prediction Capability of Response Surface Designs," *Journal of Quality Technology*, 35, 377–386.

# INDEX

- $2^2$  factorial design, 74  
 $2^3$  factorial design, 86  
 $2^{3-1}$  fractional factorial design, 136  
 $2^k$  factorial design, 73, 96, 109  
 $2^{k-p}$  fractional factorial design, 154
- A-canonical form, 232  
Alias matrix, 284  
Aliases, 137  
Analysis of a blocked response surface experiment, 331  
Analysis of variance (ANOVA), 24, 77  
A-optimal design, 367  
Augmented simplex designs for mixtures, 569  
Average mean squared error, 421  
Average prediction variance, 422; also see *I*-optimal design  
Average squared bias, 422  
Axial runs, 49, 227
- B-canonical form, 232  
Blocking, 114, 116, 325  
Box–Behnken designs, 317  
Box–Cox method, 61  
Branch and bound, 390
- Canonical analysis, 224, 225  
Canonical link function, 450  
Canonical polynomials for mixtures, 562, 577  
Center points in the  $2^k$  design, 109, 289  
Center runs in the central composite design, 307  
Central composite design, 49, 73, 192, 225, 226, 281, 297, 306, 316, 327  
Coded variables, 2, 78  
Combined array designs, 499, 525, 527  
Completely randomized design, 121  
Computer generated designs, 386; also see optimal designs  
Conditional *D*-optimality, 387  
Confidence interval on the mean response, 33  
Confidence intervals in linear regression, 31, 33  
Confidence intervals on eigenvalues, 250  
Confidence region for direction of steepest ascent, 195  
Confidence region on the location of the stationary point, 245  
Confirmation test, 186, 492

- Confounding, 116  
 Constrained mixture experiments, 589, 590, 599, 616  
 Constrained optimization, 235, 260  
 Contour plot, 1, 232, 259  
 Contour plots of prediction variance, 374  
 Contrast, 76  
 Cook's distance, 43  
 Coordinate exchange algorithms, 390  
 Covariance matrix, 22  
 Cox's direction, 608  
 Crossed array designs, 489  
 Cuboidal regions of interest, 310  
 Curvature, 94, 109, 110
- Derived power vectors, 655  
 Design efficiencies, 371, 373  
 Design generator, 136  
 Design matrix, 86  
 Design moments, 302, 304  
 Design projection, 100, 135  
 Design resolution, 138  
 Desirability functions, 261  
 Deterministic computer models, 435  
 Dispersion effects, 496, 537, 544  
 Distance-based designs, 614  
 D-optimal designs, 365, 604  
 Double linear regression, 251  
 Dual response method, 263
- Effect of scale on steepest ascent, 193  
 Eigenvalues, 224, 250  
 Equiradial designs, 321, 661  
 Equivalent estimation split-plot designs, 474  
 Errors in design levels, 432  
 Estimated prediction variance, 310, 311  
 Even design moments, 304  
 Experimenter, 2  
 Experiments with computer models, 435  
 Extra sum of squares method, 28, 29
- Face centered cube design, 312  
 Factorial design, 73, 74  
 First-order model, 3, 182  
 First-order model with interaction, 4  
 Fitting a second-order model, 48  
 Fold-over of fractional factorials, 161, 163  
 Fraction of design space (FDS) plots, 376, 384, 529, 623  
 Fractional factorial designs, 135  
 Full model, 29
- Gaussian process model, 439, 440, 441  
 Generalized interactions, 148  
 Generalized linear models, 449, 521  
 Generating relations, 148  
 Genetic algorithms, 390  
 G-optimal design, 368
- Half-normal probability plot of effects, 100  
 Hat matrix, 38  
 Hoke designs, 350  
 Hybrid designs, 354  
 Hypothesis testing in linear regression, 24, 27, 28, 30
- Ill-conditioning in mixture experiments, 592  
 Independent variables, 1  
 Indicator variables, 55  
 Influence point, 40, 43  
 Interaction, 3  
 Interaction and curvature in steepest ascent, 189  
 Interaction effect, 75, 109  
*I*-optimal design, 369, 422, 613  
*IV*-optimal design, 369; also see  
*I*-optimal design
- Joint confidence region on regression coefficients, 32
- Koshal designs, 352
- Lack-of-fit testing, 44, 111  
 Latin hypercube designs, 437  
 Least squares normal equations, 16  
 Leverage, 42  
 Linear constraints in steepest ascent, 198  
 Linear regression analysis, 6  
 Link functions, 449, 450  
 Location effects, 496  
 Logistic regression model, 450  
 Log-linear models, 544  
 Low-order polynomials, 3  
*L*-pseudocomponents, 590
- Main effect of a factor, 75  
 Main effects model, 3  
 Mapping a response surface, 8  
 Maximum entropy designs, 437  
 Mean and variance modeling, 502  
 Metamodels, 435  
 Method of least squares, 15, 79  
 Method of maximum likelihood, 451

- Mid-course correction in steepest ascent, 182  
 Minimum bias design, 424, 427, 429, 430  
 Minimum bias estimation, 442, 444  
 Mixed resolution designs, 526  
 Mixture problems, 10, 557, 589, 621,  
     617, 636, 641  
 Model adequacy checking, 36  
 Model bias, 283, 417, 419, 422  
 Model deviance, 453  
 Model inadequacy, 282  
 Model matrix, 16  
 Model-dependent estimate of error, 23  
 Model-independent measure of error, 45  
 Moment matrix, 303, 365, 423  
 Multicomponent constraints, 616  
 Multiple linear regression, 14  
 Multiple response optimization, 253, 259,  
     260, 261, 263
- Natural variables, 2  
 Neural networks, 446  
 Noise factors, 11, 483  
 Nonlinear programming, 260  
 Normal probability plot of effects, 94
- Odd design moments, 304  
 Odds ratios, 458  
 Operability region of a process, 7, 282  
 Optimal designs, 363, 367, 368, 369, 371, 386,  
     387, 390, 391, 405, 471, 604, 613  
 Optimization of the response, 8, 9  
 Orthogonal blocking in second-order designs,  
     325, 327, 330, 331  
 Orthogonal design, 90, 285, 286, 288  
 Outliers, 38  
 Overdispersion, 454  
 Overlay contour plots, 259
- Partial *F*-test, 30  
 Path of steepest ascent, 182, 183  
 Phase one of an RSM study, 7  
 Phase two of an RSM study, 7  
 Phase zero of an RSM study, 7  
 Placket–Burman designs, 165  
 Point exchange algorithms, 390  
 Power family of transformation, 61  
 Prediction intervals, 35  
 Prediction of new observations, 35  
 Prediction  $R^2$ , 41  
 Prediction variance, 243, 294, 310  
 Predictor variables, 13  
 PRESS residuals, 40
- PRESS, 38  
 Principal fraction, 148  
 Process robustness studies, 484  
 Process variables in mixture experiments,  
     621, 629  
 Projection of fractional factorials, 140, 155  
 Projection principle, 135  
 Propagation of error, 501
- Qualitative factors, 74, 114, 398  
 Qualitative regressor variables, 55  
 Quantitative factors, 74, 110
- Randomized complete block design, 115  
 Ratios of mixture components, 617  
 Reduced model, 29  
 Reference mixture, 576  
 Region moments, 423  
 Region of experimentation, 8, 282  
 Region of interest, 8  
 Regression coefficients, 14  
 Regression model, 13; also see multiple  
     linear regression  
 Regressors, 13  
 REML, 470, 523  
 Replication, 45  
 Residual plots, 37  
 Residuals, 17, 37, 38, 39, 41  
 Resolution III design, 138, 158  
 Resolution IV design, 139, 167  
 Resolution V design, 139, 167  
 Response, 1  
 Response model, 499  
 Response surface designs, 6  
 Response Surface Methodology (RSM), 1  
 Response trace plots, 576  
 Ridge analysis, 235, 236, 237, 238, 515  
 Ridge systems, 228  
 Rising ridge, 228  
 Robust parameter design for mixture-process  
     experiments, 636  
 Robust parameter design, 10, 11, 483, 636  
 Rotatability, 55, 302, 305, 306, 655, 661  
*R*-student, 41
- Saddle point, 221, 239  
 Saturated design, 159, 349, 362  
 Scaled prediction variance, 295, 310  
 Scaled residuals, 38  
 Scheffé polynomials, 560  
 Schlaifflian matrices, 655  
 Screening experiment, 6, 73, 135, 641

- Screening mixture components, 641  
 Second-order model, 3, 4, 14, 48, 192, 219  
 Sequences of fractional factorials, 140  
 Sequential experimentation, 6, 140, 437  
 Signal-to-noise ratios, 486, 488  
 Simplex centroid designs, 567  
 Simplex coordinate system, 559  
 Simplex design, 291  
 Simplex lattice designs, 560  
 Simulated annealing, 390  
 Single-factor fold-over, 163  
 Small composite designs, 358  
 Space-filling designs, 437  
 Sparsity of effects principle, 96, 135  
 Sphere-packing designs, 437  
 Spherical design region, 315, 317, 321, 429  
 Split plot factor, 124  
 Split-plot design and steepest ascent, 202  
 Split-plot design, 121, 168, 202, 466, 474, 629  
 Split-plot designs for mixture-process experiments, 629  
 Split-plot designs for second-order models, 466, 469  
 Split-plot fractional factorial designs, 168  
 Standard error of predicted response, 243  
 Standard order, 78  
 Standardized residuals, 38  
 Stationary point, 221, 223, 245  
 Stationary ridge, 228  
 Statistical error, 2  
 Steepest ascent, 73, 83, 181, 189, 194, 195, 198, 202  
 Stochastic computer models, 435  
 Studentized residuals, 39  
 Subplot factor, 124  
 Subplots, 124  
 Synergistic blending, 563, 565  
 Taylor series, 6  
 Test for significance of regression, 24  
 Tests on groups of regression coefficients, 28  
 Tests on individual regression coefficients, 27  
 Transformation, 58  
 Unbiased estimator, 22  
 Uniform designs, 437  
 Unreplicated  $2^k$  design, 96  
 Unscaled prediction variance, 310  
 Variance dispersion graphs (VDGs), 375, 384, 529, 623  
 Variance modeling, 105  
 Variance modeling, 519, 544  
 Variance of the predicted response, 33  
 Variance optimal design, 286  
 Variance stabilizing link, 463  
 V-optimal design, 369  
 Whole plot, 122  
 Whole plot factors, 122  
 Word in a design generator, 136

## WILEY SERIES IN PROBABILITY AND STATISTICS

ESTABLISHED BY WALTER A. SHEWHART AND SAMUEL S. WILKS

Editors: *David J. Balding, Noel A. C. Cressie, Garrett M Fitzmaurice,  
Iain M. Johnstone, Geert Moenberghs, David W. Scott, Adrian F. M. Smith,  
Ruey S. Tsay, Sanford Weisberg*  
Editors Emeriti: *Vic Barnett, J. Stuart Hunter, Jozef L. Teugels*

The *Wiley Series in Probability and Statistics* is well established and authoritative. It covers many topics of current research interest in both pure and applied statistics and probability theory. Written by leading statisticians and institutions, the titles span both state-of-the-art developments in the field and classical methods.

Reflecting the wide range of current research in statistics, the series encompasses applied, methodological and theoretical statistics, ranging from applications and new techniques made possible by advances in computerized practice to rigorous treatment of theoretical approaches.

This series provides essential and invaluable reading for all statisticians, whether in academia, industry, government, or research.

- † ABRAHAM and LEDOLTER · Statistical Methods for Forecasting  
AGRESTI · Analysis of Ordinal Categorical Data  
AGRESTI · An Introduction to Categorical Data Analysis, *Second Edition*  
AGRESTI · Categorical Data Analysis, *Second Edition*  
ALTMAN, GILL, and McDONALD · Numerical Issues in Statistical Computing for the Social Scientist  
AMARATUNGA and CABRERA · Exploration and Analysis of DNA Microarray and Protein Array Data  
ANDĚL · Mathematics of Chance  
ANDERSON · An Introduction to Multivariate Statistical Analysis, *Third Edition*  
\* ANDERSON · The Statistical Analysis of Time Series  
ANDERSON, AUQUIER, HAUCK, OAKES, VANDAELE, and WEISBERG · Statistical Methods for Comparative Studies  
ANDERSON and LOYNES · The Teaching of Practical Statistics  
ARMITAGE and DAVID (editors) · Advances in Biometry  
ARNOLD, BALAKRISHNAN, and NAGARAJA · Records  
\* ARTHANARI and DODGE · Mathematical Programming in Statistics  
\* BAILEY · The Elements of Stochastic Processes with Applications to the Natural Sciences  
BALAKRISHNAN and KOUTRAS · Runs and Scans with Applications  
BALAKRISHNAN and NG · Precedence ~ Type Tests and Applications  
BARNETT · Comparative Statistical Inference, *Third Edition*  
BARNETT · Environmental Statistics  
BARNETT and LEWIS · Outliers in Statistical Data, *Third Edition*  
BARTOSZYNSKI and NIEWIADOMSKA-BUGAJ · Probability and Statistical Inference  
BASILEVSKY · Statistical Factor Analysis and Related Methods: Theory and Applications  
BASU and RIGDON · Statistical Methods for the Reliability of Repairable Systems  
BATES and WATTS · Nonlinear Regression Analysis and Its Applications  
BECHHOFER, SANTNER, and GOLDSMAN · Design and Analysis of Experiments for Statistical Selection, Screening, and Multiple Comparisons  
BELSLEY · Conditioning Diagnostics: Collinearity and Weak Data in Regression

†Now available in a lower priced paperback edition in the Wiley—Interscience Paperback Series.

\*Now available in a lower priced paperback edition in the Wiley Classics Library.

- † BELSLEY, KUH, and WELSCH · Regression Diagnostics: Identifying Influential Data and Sources of Collinearity
- BENDAT and PIERSOL · Random Data: Analysis and Measurement Procedures, *Third Edition*
- BERRY, CHALONER, and GEWEKE · Bayesian Analysis in Statistics and Econometrics: Essays in Honor of Arnold Zellner
- BERNARDO and SMITH · Bayesian Theory
- BHAT and MILLER · Elements of Applied Stochastic Processes, *Third Edition*
- BHATTACHARYA and WAYMIRE · Stochastic Processes with Applications
- BILLINGSLEY · Convergence of Probability Measures, *Second Edition*
- BILLINGSLEY · Probability and Measure, *Third Edition*
- BIRKES and DODGE · Alternative Methods of Regression
- BISWAS, DATTA, FINE, and SEGAL · Statistical Advances in the Biomedical Sciences: Clinical Trials, Epidemiology, Survival Analysis, and Bioinformatics
- BLISCHKE AND MURTHY (editors) · Case Studies in Reliability and Maintenance
- BLISCHKE AND MURTHY · Reliability: Modeling, Prediction, and Optimization
- BLOOMFIELD · Fourier Analysis of Time Series: An Introduction, *Second Edition*
- BOLLEN · Structural Equations with Latent Variables
- BOLLEN and CURRAN · Latent Curve Models: A Structural Equation Perspective
- BOROVKOV · Ergodicity and Stability of Stochastic Processes
- BOULEAU · Numerical Methods for Stochastic Processes
- BOX · Bayesian Inference in Statistical Analysis
- BOX · R. A. Fisher, the Life of a Scientist
- BOX and DRAPER · Response Surfaces, Mixtures, and Ridge Analyses, *Second Edition*
- \* BOX and DRAPER · Evolutionary Operation: A Statistical Method for Process Improvement
- BOX and FRIENDS · Improving Almost Anything, *Revised Edition*
- BOX, HUNTER, and HUNTER · Statistics for Experimenters: Design, Innovation, and Discovery, *Second Edition*
- BOX and LUCEÑO · Statistical Control by Monitoring and Feedback Adjustment
- BRANDIMARTE · Numerical Methods in Finance: A MATLAB-Based Introduction
- † BROWN and HOLLANDER · Statistics: A Biomedical Introduction
- BRUNNER, DOMHOF, and LANGER · Nonparametric Analysis of Longitudinal Data in Factorial Experiments
- BUCKLEW · Large Deviation Techniques in Decision, Simulation, and Estimation
- CAIROLI and DALANG · Sequential Stochastic Optimization
- CASTILLO, HADI, BALAKRISHNAN, and SARABIA · Extreme Value and Related Models with Applications in Engineering and Science
- CHAN · Time Series: Applications to Finance
- CHARALAMIDES · Combinatorial Methods in Discrete Distributions
- CHATTERJEE and HADI · Regression Analysis by Example, *Fourth Edition*
- CHATTERJEE and HADI · Sensitivity Analysis in Linear Regression
- CHERNICK · Bootstrap Methods: A Guide for Practitioners and Researchers, *Second Edition*
- CHERNICK and FRIIS · Introductory Biostatistics for the Health Sciences
- CHILÈS and DELFINER · Geostatistics: Modeling Spatial Uncertainty
- CHOW and LIU · Design and Analysis of Clinical Trials: Concepts and Methodologies, *Second Edition*
- CLARKE and DISNEY · Probability and Random Processes: A First Course with Applications, *Second Edition*
- \* COCHRAN and COX · Experimental Designs, *Second Edition*
- CONGDON · Applied Bayesian Modelling

†Now available in a lower priced paperback edition in the Wiley—Interscience Paperback Series.

\*Now available in a lower priced paperback edition in the Wiley Classics Library.

- CONGDON · Bayesian Models for Categorical Data
- CONGDON · Bayesian Statistical Modelling
- CONOVER · Practical Nonparametric Statistics, *Third Edition*
- COOK · Regression Graphics
- COOK and WEISBERG · Applied Regression Including Computing and Graphics
- COOK and WEISBERG · An Introduction to Regression Graphics
- CORNELL · Experiments with Mixtures, Designs, Models, and the Analysis of Mixture Data, *Third Edition*
- COVER and THOMAS · Elements of Information Theory
- COX · A Handbook of Introductory Statistical Methods
- \* COX · Planning of Experiments
- CRESSIE · Statistics for Spatial Data, *Revised Edition*
- CSÖRGÖ and HORVÁTH · Limit Theorems in Change Point Analysis
- DANIEL · Applications of Statistics to Industrial Experimentation
- DANIEL · Biostatistics: A Foundation for Analysis in the Health Sciences, *Eighth Edition*
- \* DANIEL · Fitting Equations to Data: Computer Analysis of Multifactor Data, *Second Edition*
- DASU and JOHNSON · Exploratory Data Mining and Data Cleaning
- DAVID and NAGARAJA · Order Statistics, *Third Edition*
- \* DEGROOT, FIENBERG, and KADANE · Statistics and the Law
- DEL CASTILLO · Statistical Process Adjustment for Quality Control
- DEMARIS · Regression with Social Data: Modeling Continuous and Limited Response Variables
- DEMIDENKO · Mixed Models: Theory and Applications
- DENISON, HOLMES, MALLICK and SMITH · Bayesian Methods for Nonlinear Classification and Regression
- DETTE and STUDDEN · The Theory of Canonical Moments with Applications in Statistics, Probability, and Analysis
- DEY and MUKERJEE · Fractional Factorial Plans
- DILLON and GOLDSTEIN · Multivariate Analysis: Methods and Applications
- DODGE · Alternative Methods of Regression
- \* DODGE and ROMIG · Sampling Inspection Tables, *Second Edition*
- \* DOOB · Stochastic Processes
- DOWDY, WEARDEN, and CHILKO · Statistics for Research, *Third Edition*
- DRAPER and SMITH · Applied Regression Analysis, *Third Edition*
- DRYDEN and MARDIA · Statistical Shape Analysis
- DUDEWICZ and MISHRA · Modern Mathematical Statistics
- DUNN and CLARK · Basic Statistics: A Primer for the Biomedical Sciences, *Third Edition*
- DUPUIS and ELLIS · A Weak Convergence Approach to the Theory of Large Deviations
- EDLER and KITSOS · Recent Advances in Quantitative Methods in Cancer and Human Health Risk Assessment
- \* ELANDT-JOHNSON and JOHNSON · Survival Models and Data Analysis
- ENDERS · Applied Econometric Time Series
- † ETHIER and KURTZ · Markov Processes: Characterization and Convergence
- EVANS, HASTINGS, and PEACOCK · Statistical Distributions, *Third Edition*
- FELLER · An Introduction to Probability Theory and Its Applications, Volume I, *Third Edition*, Revised; Volume II, *Second Edition*
- FISHER and VAN BELLE · Biostatistics: A Methodology for the Health Sciences
- FITZMAURICE, LAIRD, and WARE · Applied Longitudinal Analysis
- \* FLEISS · The Design and Analysis of Clinical Experiments
- FLEISS · Statistical Methods for Rates and Proportions, *Third Edition*

\*Now available in a lower priced paperback edition in the Wiley Classics Library.

†Now available in a lower priced paperback edition in the Wiley—Interscience Paperback Series.

- † FLEMING and HARRINGTON · Counting Processes and Survival Analysis
- FULLER · Introduction to Statistical Time Series, *Second Edition*
- † FULLER · Measurement Error Models
- GALLANT · Nonlinear Statistical Models
- GEISSER · Modes of Parametric Statistical Inference
- GELMAN and MENG · Applied Bayesian Modeling and Causal Inference from Incomplete-Data Perspectives
- GEWEKE · Contemporary Bayesian Econometrics and Statistics
- GHOSH, MUKHOPADHYAY, and SEN · Sequential Estimation
- GIESBRECHT and GUMPERTZ · Planning, Construction, and Statistical Analysis of Comparative Experiments
- GIFI · Nonlinear Multivariate Analysis
- GIVENS and HOETING · Computational Statistics
- GLASSERMAN and YAO · Monotone Structure in Discrete-Event Systems
- GNANADESIKAN · Methods for Statistical Data Analysis of Multivariate Observations, *Second Edition*
- GOLDSTEIN and LEWIS · Assessment: Problems, Development, and Statistical Issues
- GREENWOOD and NIKULIN · A Guide to Chi-Squared Testing
- GROSS and HARRIS · Fundamentals of Queueing Theory, *Third Edition*
- \* HAHN and SHAPIRO · Statistical Models in Engineering
- HAHN and MEEKER · Statistical Intervals: A Guide for Practitioners
- HALD · A History of Probability and Statistics and their Applications Before 1750
- HALD · A History of Mathematical Statistics from 1750 to 1930
- † HAMPEL · Robust Statistics: The Approach Based on Influence Functions
- HANNAN and DEISTLER · The Statistical Theory of Linear Systems
- HEIBERGER · Computation for the Analysis of Designed Experiments
- HEDAYAT and SINHA · Design and Inference in Finite Population Sampling
- HEDEKER and GIBBONS · Longitudinal Data Analysis
- HELLER · MACSYMA for Statisticians
- HINKELMANN and KEMPTHORNE · Design and Analysis of Experiments, Volume 1: Introduction to Experimental Design, *Second Edition*
- HINKELMANN and KEMPTHORNE · Design and Analysis of Experiments, Volume 2: Advanced Experimental Design
- HOAGLIN, MOSTELLER, and TUKEY · Exploratory Approach to Analysis of Variance
- \* HOAGLIN, MOSTELLER, and TUKEY · Exploring Data Tables, Trends and Shapes
- \* HOAGLIN, MOSTELLER, and TUKEY · Understanding Robust and Exploratory Data Analysis
- HOCHBERG and TAMHANE · Multiple Comparison Procedures
- HOCKING · Methods and Applications of Linear Models: Regression and the Analysis of Variance, *Second Edition*
- HOEL · Introduction to Mathematical Statistics, *Fifth Edition*
- HOGG and KLUGMAN · Loss Distributions
- HOLLANDER and WOLFE · Nonparametric Statistical Methods, *Second Edition*
- HOSMER and LEMESHOW · Applied Logistic Regression, *Second Edition*
- HOSMER, LEMESHOW, and MAY · Applied Survival Analysis: Regression Modeling of Time-to-Event Data, *Second Edition*
- † HUBER · Robust Statistics
- HUBERTY · Applied Discriminant Analysis
- HUBERTY and OLEINIK · Applied MANOVA and Discriminant Analysis, *Second Edition*
- HUNT and KENNEDY · Financial Derivatives in Theory and Practice, *Revised Edition*

†Now available in a lower priced paperback edition in the Wiley—Interscience Paperback Series.

\*Now available in a lower priced paperback edition in the Wiley Classics Library.

- HURD and MIAMEE · Periodically Correlated Random Sequences: Spectral Theory and Practice
- HUSKOVA, BERAN, and DUPAC · Collected Works of Jaroslav Hajek—with Commentary
- HUZURBAZAR · Flowgraph Models for Multistate Time-to-Event Data
- IMAN and CONOVER · A Modem Approach to Statistics
- † JACKSON · A User's Guide to Principle Components
- JOHN · Statistical Methods in Engineering and Quality Assurance
- JOHNSON · Multivariate Statistical Simulation
- JOHNSON and BALAKRISHNAN · Advances in the Theory and Practice of Statistics: A Volume in Honor of Samuel Kotz
- JOHNSON and BHATTACHARYYA · Statistics: Principles and Methods, *Fifth Edition*
- JOHNSON and KOTZ · Distributions in Statistics
- JOHNSON and KOTZ (editors) · Leading Personalities in Statistical Sciences: From the Seventeenth Century to the Present
- JOHNSON, KOTZ, and BALAKRISHNAN · Continuous Univariate Distributions, Volume 1, *Second Edition*
- JOHNSON, KOTZ, and BALAKRISHNAN · Continuous Univariate Distributions, Volume 2, *Second Edition*
- JOHNSON, KOTZ, and BALAKRISHNAN · Discrete Multivariate Distributions
- JOHNSON, KEMP, and KOTZ · Univariate Discrete Distributions, *Third Edition*
- JUDGE, GRIFFITHS, HILL, LÜTKEPOHL, and LEE · The Theory and Practice of Econometrics, *Second Edition*
- JUREČKOVÁ and SEN · Robust Statistical Procedures: Asymptotics and Interrelations
- JUREK and MASON · Operator-Limit Distributions in Probability Theory
- KADANE · Bayesian Methods and Ethics in a Clinical Trial Design
- KADANE and SCHUM · A Probabilistic Analysis of the Sacco and Vanzetti Evidence
- KALBFLEISCH and PRENTICE · The Statistical Analysis of Failure Time Data, *Second Edition*
- KARIYA and KURATA · Generalized Least Squares
- KASS and VOS · Geometrical Foundations of Asymptotic Inference
- † KAUFMAN and ROUSSEEUW · Finding Groups in Data: An Introduction to Cluster Analysis
- KEDEM and FOKIANOS · Regression Models for Time Series Analysis
- KENDALL, BARDEN, CARNE, and LE · Shape and Shape Theory
- KHURI · Advanced Calculus with Applications in Statistics, *Second Edition*
- KHURI, MATHEW, and SINHA · Statistical Tests for Mixed Linear Models
- KLEIBER and KOTZ · Statistical Size Distributions in Economics and Actuarial Sciences
- KLUGMAN, PANJER, and WILLMOT · Loss Models: From Data to Decisions, *Second Edition*
- KLUGMAN, PANJER, and WILLMOT · Solutions Manual to Accompany Loss Models: From Data to Decisions, *Second Edition*
- KOTZ, BALAKRISHNAN, and JOHNSON · Continuous Multivariate Distributions, Volume 1, *Second Edition*
- KOVALENKO, KUZNETZOV, and PEGG · Mathematical Theory of Reliability of Time-Dependent Systems with Practical Applications
- KOWALSKI and TU · Modern Applied U-Statistics
- KROONENBERG · Applied Multiway Data Analysis
- KVAM and VIDAKOVIC · Nonparametric Statistics with Applications to Science and Engineering
- LACHIN · Biostatistical Methods: The Assessment of Relative Risks
- LAD · Operational Subjective Statistical Methods: A Mathematical, Philosophical, and Historical Introduction
- LAMPERTI · Probability: A Survey of the Mathematical Theory, *Second Edition*
- LANGE, RYAN, BILLARD, BRILLINGER, CONQUEST, and GREENHOUSE · Case Studies in Biometry

†Now available in a lower priced paperback edition in the Wiley—Interscience Paperback Series.

- LARSON · Introduction to Probability Theory and Statistical Inference, *Third Edition*  
 LAWLESS · Statistical Models and Methods for Lifetime Data, *Second Edition*  
 LAWSON · Statistical Methods in Spatial Epidemiology  
 LE · Applied Categorical Data Analysis  
 LE · Applied Survival Analysis  
 LEE and WANG · Statistical Methods for Survival Data Analysis, *Third Edition*  
 LEPAGE and BILLARD · Exploring the Limits of Bootstrap  
 LEYLAND and GOLDSTEIN (editors) · Multilevel Modelling of Health Statistics  
 LIAO · Statistical Group Comparison  
 LINDVALL · Lectures on the Coupling Method  
 LIN · Introductory Stochastic Analysis for Finance and Insurance  
 LINHART and ZUCCHINI · Model Selection  
 LITTLE and RUBIN · Statistical Analysis with Missing Data, *Second Edition*  
 LLOYD · The Statistical Analysis of Categorical Data  
 LOWEN and TEICH · Fractal-Based Point Processes  
 MAGNUS and NEUDECKER · Matrix Differential Calculus with Applications in Statistics and Econometrics, *Revised Edition*  
 MALLER and ZHOU · Survival Analysis with Long Term Survivors  
 MALLOWS · Design, Data, and Analysis by Some Friends of Cuthbert Daniel  
 MANN, SCHAFER, and SINGPURWALLA · Methods for Statistical Analysis of Reliability and Life Data  
 MANTON, WOODBURY, and TOLLEY · Statistical Applications Using Fuzzy Sets  
 MARCHETTE · Random Graphs for Statistical Pattern Recognition  
 MARDIA and JUPP · Directional Statistics  
 MASON, GUNST, and HESS · Statistical Design and Analysis of Experiments with Applications to Engineering and Science, *Second Edition*  
 McCULLOCH, SEARLE, and NEUHAUS · Generalized, Linear, and Mixed Models, *Second Edition*  
 McFADDEN · Management of Data in Clinical Trials, *Second Edition*  
 \* McLACHLAN · Discriminant Analysis and Statistical Pattern Recognition  
 McLACHLAN, DO, and AMBROISE · Analyzing Microarray Gene Expression Data  
 McLACHLAN and KRISHNAN · The EM Algorithm and Extensions, *Second Edition*  
 McLACHLAN and PEEL · Finite Mixture Models  
 McNEIL · Epidemiological Research Methods  
 MEEKER and ESCOBAR · Statistical Methods for Reliability Data  
 MEERSCHAERT and SCHEFFLER · Limit Distributions for Sums of Independent Random Vectors: Heavy Tails in Theory and Practice  
 MICKEY, DUNN, and CLARK · Applied Statistics: Analysis of Variance and Regression, *Third Edition*  
 \* MILLER · Survival Analysis, *Second Edition*  
 MONTGOMERY, JENNINGS, and KULAHCI · Introduction to Time Series Analysis and Forecasting  
 MONTGOMERY, PECK, and VINING · Introduction to Linear Regression Analysis, *Fourth Edition*  
 MORGENTHALER and TUKEY · Configural Polysampling: A Route to Practical Robustness  
 MUIRHEAD · Aspects of Multivariate Statistical Theory  
 MULLER and STOYAN · Comparison Methods for Stochastic Models and Risks  
 MURRAY · X-STAT 2.0 Statistical Experimentation, Design Data Analysis, and Nonlinear Optimization  
 MURTHY, XIE, and JIANG · Weibull Models

\*Now available in a lower priced paperback edition in the Wiley Classics Library.

- MYERS and MONTGOMERY · Response Surface Methodology: Process and Product Optimization Using Designed Experiments, *Second Edition*
- MYERS, MONTGOMERY, and VINING · Generalized Linear Models. With Applications in Engineering and the Sciences
- † NELSON · Accelerated Testing, Statistical Models, Test Plans, and Data Analyses
- † NELSON · Applied Life Data Analysis
- NEWMAN · Biostatistical Methods in Epidemiology
- OCHI · Applied Probability and Stochastic Processes in Engineering and Physical Sciences
- OKABE, BOOTS, SUGIHARA, and CHIU · Spatial Tesselations: Concepts and Applications of Voronoi Diagrams, *Second Edition*
- OLIVER and SMITH · Influence Diagrams, Belief Nets and Decision Analysis
- PALTA · Quantitative Methods in Population Health: Extensions of Ordinary Regressions
- PANJER · Operational Risk: Modeling and Analytics
- PANKRATZ · Forecasting with Dynamic Regression Models
- PANKRATZ · Forecasting with Univariate Box-Jenkins Models: Concepts and Cases
- \* PARZEN · Modern Probability Theory and Its Applications
- PEÑA, TIAO, and TSAY · A Course in Time Series Analysis
- PIANTADOSI · Clinical Trials: A Methodologic Perspective
- PORT · Theoretical Probability for Applications
- POURAHMADI · Foundations of Time Series Analysis and Prediction Theory
- POWELL · Approximate Dynamic Programming: Solving the Curses of Dimensionality
- PRESS · Bayesian Statistics: Principles, Models, and Applications
- PRESS · Subjective and Objective Bayesian Statistics, *Second Edition*
- PRESS and TANUR · The Subjectivity of Scientists and the Bayesian Approach
- PUKELSHEIM · Optimal Experimental Design
- PURI, VILAPLANA, and WERTZ · New Perspectives in Theoretical and Applied Statistics
- † PUTERMAN · Markov Decision Processes: Discrete Stochastic Dynamic Programming
- QIU · Image Processing and Jump Regression Analysis
- \* RAO · Linear Statistical Inference and Its Applications, *Second Edition*
- RAUSAND and HØGYLAND · System Reliability Theory: Models, Statistical Methods, and Applications, *Second Edition*
- RENCHER · Linear Models in Statistics
- RENCHER · Methods of Multivariate Analysis, *Second Edition*
- RENCHER · Multivariate Statistical Inference with Applications
- \* RIPLEY · Spatial Statistics
- \* RIPLEY · Stochastic Simulation
- ROBINSON · Practical Strategies for Experimenting
- ROHATGI and SALEH · An Introduction to Probability and Statistics, *Second Edition*
- ROLSKI, SCHMIDLI, SCHMIDT, and TEUGELS · Stochastic Processes for Insurance and Finance
- ROSENBERGER and LACHIN · Randomization in Clinical Trials: Theory and Practice
- ROSS · Introduction to Probability and Statistics for Engineers and Scientists
- ROSSI, ALLENBY, and McCULLOCH · Bayesian Statistics and Marketing
- † ROUSSEEUW and LEROY · Robust Regression and Outlier Detection
- \* RUBIN · Multiple Imputation for Nonresponse in Surveys
- RUBINSTEIN and KROESE · Simulation and the Monte Carlo Method, *Second Edition*
- RUBINSTEIN and MELAMED · Modern Simulation and Modeling
- RYAN · Modem Engineering Statistics
- RYAN · Modem Experimental Design

<sup>†</sup>Now available in a lower priced paperback edition in the Wiley—Interscience Paperback Series.

\*Now available in a lower priced paperback edition in the Wiley Classics Library.

- RYAN · Modern Regression Methods
- RYAN · Statistical Methods for Quality Improvement, *Second Edition*
- SALEH · Theory of Preliminary Test and Stein-Type Estimation with Applications
- \* SCHEFFE · The Analysis of Variance
- SCHIMEK · Smoothing and Regression: Approaches, Computation, and Application
- SCHOTT · Matrix Analysis for Statistics, *Second Edition*
- SCHOUTENS · Levy Processes in Finance: Pricing Financial Derivatives
- SCHUSS · Theory and Applications of Stochastic Differential Equations
- SCOTT · Multivariate Density Estimation: Theory, Practice, and Visualization
- † SEARLE · Linear Models for Unbalanced Data
- † SEARLE · Matrix Algebra Useful for Statistics
- † SEARLE, CASELLA, and McCULLOCH · Variance Components
- SEARLE and WILLETT · Matrix Algebra for Applied Economics
- SEBER · A Matrix Handbook for Statisticians
- † SEBER · Multivariate Observations
- SEBER and LEE · Linear Regression Analysis, *Second Edition*
- † SEBER and WILD · Nonlinear Regression
- SENNOTT · Stochastic Dynamic Programming and the Control of Queueing Systems
- \* SERFLING · Approximation Theorems of Mathematical Statistics
- SHAFER and VOVOK · Probability and Finance: It's Only a Game!
- SILVAPULLE and SEN · Constrained Statistical Inference: Inequality, Order, and Shape Restrictions
- SMALL and McLEISH · Hilbert Space Methods in Probability and Statistical Inference
- SRIVASTAVA · Methods of Multivariate Statistics
- STAPLETON · Linear Statistical Models
- STAPLETON · Models for Probability and Statistical Inference: Theory and Applications
- STAUDTE and SHEATHER · Robust Estimation and Testing
- STOYAN, KENDALL, and MECKE · Stochastic Geometry and Its Applications, *Second Edition*
- STOYAN and STOYAN · Fractals, Random Shapes and Point Fields: Methods of Geometrical Statistics
- STREET and BURGESS · The Construction of Optimal Stated Choice Experiments: Theory and Methods
- STYAN · The Collected Papers of T. W. Anderson: 1943–1985
- SUTTON, ABRAMS, JONES, SHELDON, and SONG · Methods for Meta-Analysis in Medical Research
- TAKEZAWA · Introduction to Nonparametric Regression
- TANAKA · Time Series Analysis: Nonstationary and Noninvertible Distribution Theory
- THOMPSON · Empirical Model Building
- THOMPSON · Sampling, *Second Edition*
- THOMPSON · Simulation: A Modeler's Approach
- THOMPSON and SEBER · Adaptive Sampling
- THOMPSON, WILLIAMS, and FINDLAY · Models for Investors in Real World Markets
- TCIAO, BISGAARD, HILL, PEÑA, and STIGLER (editors) · Box on Quality and Discovery: with Design, Control, and Robustness
- TIERNEY · LISP-STAT: An Object-Oriented Environment for Statistical Computing and Dynamic Graphics
- TSAY · Analysis of Financial Time Series, *Second Edition*
- UPTON and FINGLETON · Spatial Data Analysis by Example, Volume II: Categorical and Directional Data

\*Now available in a lower priced paperback edition in the Wiley Classics Library.

†Now available in a lower priced paperback edition in the Wiley—Interscience Paperback Series.

- VAN BELLE · Statistical Rules of Thumb
- VAN BELLE, FISHER, HEAGERTY, and LUMLEY · Biostatistics: A Methodology for the Health Sciences, *Second Edition*
- VESTRUP · The Theory of Measures and Integration
- VIDAKOVIC · Statistical Modeling by Wavelets
- VINOD and REAGLE · Preparing for the Worst: Incorporating Downside Risk in Stock Market Investments
- WALLER and GOTWAY · Applied Spatial Statistics for Public Health Data
- WEERAHANDI · Generalized Inference in Repeated Measures: Exact Methods in MANOVA and Mixed Models
- WEISBERG · Applied Linear Regression, *Third Edition*
- WELSH · Aspects of Statistical Inference
- WESTFALL and YOUNG · Resampling-Based Multiple Testing: Examples and Methods for *p*-Value Adjustment
- WHITTAKER · Graphical Models in Applied Multivariate Statistics
- WINKER · Optimization Heuristics in Economics: Applications of Threshold Accepting
- WONNACOTT and WONNACOTT · Econometrics, *Second Edition*
- WOODING · Planning Pharmaceutical Clinical Trials: Basic Statistical Principles
- WOODWORTH · Biostatistics: A Bayesian Introduction
- WOOLSON and CLARKE · Statistical Methods for the Analysis of Biomedical Data, *Second Edition*
- WU and HAMADA · Experiments: Planning, Analysis, and Parameter Design Optimization
- WU and ZHANG · Nonparametric Regression Methods for Longitudinal Data Analysis
- YANG · The Construction Theory of Denumerable Markov Processes
- YOUNG, VALERO-MORA, and FRIENDLY · Visual Statistics: Seeing Data with Dynamic Interactive Graphics
- ZELTERMAN · Discrete Distributions—Applications in the Health Sciences
- \* ZELLNER · An Introduction to Bayesian Inference in Econometrics
- ZHOU, OBUCHOWSKI, and McCLISH · Statistical Methods in Diagnostic Medicine

\*Now available in a lower priced paperback edition in the Wiley Classics Library.